LAND SUBSIDENCE

SYMPOSIUM

SUBSIDENCE TERRESTRE

IAHS-AISH Publication No. 121

Proceedings of the Second International Symposium on Land Subsidence, held at Anaheim, California, 13–17 December 1976

Actes du Deuxième Colloque International sur la Subsidence Terrestre, a eu lieu à Anaheim, Californie, 13–17 décembre 1976

Published by the International Association of Hydrological Sciences 1977
and printed by LithoCrafters, Ann Arbor, Michigan.

Table of contents
Table des matières

Preface

The Second International Symposium on Land Subsidence was attended by engineers and scientists from 19 countries, attesting to the worldwide interest in this subject. The symposium papers sessions were held on December 13-17, 1976, at the Inn at the Park, Anaheim, California, USA. The symposium was sponsored by the International Association of Hydrological Sciences (IAHS), International Association of Hydrogeologists (IAH), International Society for Soil Mechanics and Foundation Engineering (ISSMFE), the U.S. National Committee for Scientific Hydrology (USNC/SH), and the United Nations Educational, Scientific, and Cultural Organization (UNESCO). The American Geophysical Union (AGU) administered all business affairs for the symposium, and UNESCO and the USNC/SH provided some financial support.

This symposium was organized within the framework of the International Hydrological Program, which succeeded the International Hydrological Decade in 1975. The subject of land subsidence was included among the research problems forming the program of the International Hydrological Decade, resulting in the First International Symposium on Land Subsidence held during September 1969 in Tokyo, Japan. The 64 technical papers presented at the symposium were published in IAHS Publication No. 88 and 89. It was at the Tokyo symposium that Chief U.S. Delegate A. I. Johnson proposed (IAHS Publication No. 88, pp. 10-11) that the second international symposium on land subsidence be held in the United States at least 6 years from the date of this first symposium. After several years of effort, the plans for this second symposium were approved by the IAHS Bureau at its 1971 meeting in Moscow.

The purpose of the Second International Symposium was to bring together international specialists on land subsidence, to present the results of research and practice related to cause, effect, and control, and to take stock of the advance in knowledge taking place in the subject since the 1969 symposium. Intensive development of water, oil, gas, and minerals to meet the needs of a more and more highly industrialized world has resulted in an increasingly wider interest in the land subsidence that frequently results from such development. Increased recognition of land subsidence in many corners of the world lent urgency to the holding of this symposium on the subject, especially on the means for preventing, decreasing, or at least controlling land subsidence.

The technical papers presented at the symposium discussed subjects ranging from mathematical modeling studies through broad descriptions of project progress and subsidence case histories to legal and economic aspects of subsidence. The program was very broad in scope, including land surface sinking resulting from such causes as withdrawal of water, oil, or gas, dewatering of organic deposits, hydrocompaction, extraction of solids by mining, and collapse of limestones. This proceedings volume contains 60 of the papers submitted for the technical sessions and also contains the opening remarks presented by the representative of the host state, California, and by representatives of cosponsoring organizations, IAH, ISSMFE, and USNC/SH. Opening remarks on behalf of IAHS and its International Commission on Ground Water, presented by A. I. Johnson and S. Yamamoto, respectively, are incorporated in this preface. Also included, at the end of this proceedings volume, are the summaries of three Russian papers on subsidence for which the full papers were not received in time for publication.

The General Cochairmen for the symposium were A. I. Johnson of the U.S. Geological Survey, Reston, Virginia, and S. Yamamoto of the Tokyo University of Education, Tokyo, Japan. J. F. Poland (U.S. Geological Survey, Sacramento, California) served as Vice Chairman for Technical Programs; D. R. Allen (Department of Oil Properties, City of Long Beach, California) was Vice Chairman for Local Arrangements and Chairman for the short field trip; B. E. Lofgren (U.S. Geological Survey, Sacramento, California) was Chairman for the long field trip and representative of IAH. In addition, the Symposium Organizing Committee also included R. T. Bean (Consulting Geologist, La Crescenta, California), Representative of IAH; G. Springall (President, Sociedad Mexicana de Mecánica de Suelos, Coyoacan, Mexico, D. F.) and Pierro Sembenelli (Electroconsult, Milano, Italy), representatives of ISSMFE; S. N. Davis (University of Arizona, Tucson, Arizona), representative of USNC/SH; H. L. Koning (Laboratory for Soil Mechanics, Delft, Netherlands); R. O. Castle (U.S. Geological Survey, Menlo Park, California); J. C. Stephens (U.S. Agricultural Research Service, Ft. Lauderdale, Florida); and R. R. Parizek (Pennsylvania State University, University Park, Pennsylvania).

The symposium was preceded by a 2-day field trip by bus, leaving from San Francisco, California, early on December 9 and ending on the evening of December 10 at Anaheim. The tour covered points of subsidence, hydrologic, geologic, historical, agricultural, and sociological interest in the Santa Clara and San Joaquin Valleys--areas with the greatest diversity of causes, largest magnitude, and most widespread man-induced subsidence presently known in the world. A field trip guide, containing detailed road logs and several technical papers on subsidence in the areas covered by the trip, was prepared by the Guide Book Committee consisting of B. E. Lofgren, R. L. Ireland, and Margaret Farmer, all of the U.S. Geological Survey in Sacramento, California. On the third day of the 5-day symposium a short field trip covered the Long Beach, California, area. This trip included a bus tour of the Wilmington subsidence area (subsidence about 33 feet) resulting from pumping of oil, a boat trip to one of the artificial islands created for the oil wells and for the injection wells used to prevent further subsidence, lunch aboard the ship Queen Mary, and a tour of the Los Angeles County Flood Control District's injection well barrier project.

On behalf of IAHS and the cosponsoring organizations, we express gratitude to the members of the Symposium Organizing Committee, the session chairmen, AGU staff personnel, and the many others who assisted with the many organizational tasks. Also acknowledged with appreciation are the contributions of the many authors who gave of their time, effort, and knowledge to produce a good program. It is hoped that the interdisciplinary nature of the program and of the sponsorship will encourage multidisciplinary efforts to solve the many problems related to land subsidence.

Arnold I. Johnson
First Vice President
International Association
of Hydrological Sciences

S. Yamamoto
President
International Commission
on Ground Water, IAHS

Préface

Des ingénieurs et des savants de dix-neuf pays se sont réunis au Deuxième Symposium International sur l'Affaissement des Terrains, témoignant ainsi de l'intérêt mondial a ce sujet. Les présentations des communications ont eu lieu du 13 au 17 décembre 1976 à l'Inn at the Park, Anaheim, Californie (Etats-Unis). L'Association Internationale des Sciences Hydrologiques (AISH), l'Association Internationale des Hydrogéologues (AIH), l'International Society of Soil Mechanics and Foundation Engineering (ISSMFE), l'U.S. National Committee for Scientific Hydrology (USNC/SH), et l'United Nations Educational, Scientific, and Cultural Organization (UNESCO) ont patronné le symposium. L'Union Américaine de Géophysique (AGU) s'est chargée de tous les arrangements pour le symposium, et l'UNESCO et l'USNC/SH l'ont partiellement subventionné.

Le symposium était organisé dans le cadre du Programme Hydrologique International, qui a succédé en 1975 à la Décennie Hydrologique Internationale. Le sujet de l'affaissement des terrains était l'un des problemes de recherche du programme de la Décennie Hydrologique Internationale. Cet intérêt a mené au Premier Symposium International sur l'Affaissement des Terrains, qui a eu lieu à Tokyo (Japon) en septembre 1969. Les soixante-quatre communications techniques présentées à ce symposium ont été publiées comme Publications AISH 88 et 89. Lors de la réunion à Tokyo, le chef de la délégation des Etats Unis, A. I. Johnson, a proposé (Publication AISH no. 88, pp. 10-11) qu' un deuxime symposium international sur l'affaissement soit tenueaux Etats Unis dans six ans au moins de la date du premier symposium. Après plusieurs années de travail, le Bureau de l'AISH a approuvé, lors de sa réunion à Moscou en 1971, les projets pour le deuxième symposium.

Le but du deuxième symposium international était de réunir des spécialistes internationaux, d'echanger des informations et des données d'experience sur les questions de cause, de conséquences, et de limitation de l'affaissement, et de faire l'inventaire des progres depuis le symposium de 1969. Le développement intensif des ressources en eau, pétrole brut, gaz naturel, et minéraux pour subvenir aux besoins d'un monde de plus en plus industralisé a fait croître l'intérêt a l'affaissement, qui est souvent le résultat d'un tel développement. L'attention accrue donnée à l'affaissement des terrains dans le monde rendait plus urgent un symposium sur ce sujet, surtout sur les moyens d'empêcher, de diminuer, ou, tout au moins, de limiter l'affaissement.

Les communications présentées au symposium ont traité des sujets variant des études de modèles mathématiques aux descriptions générales des progrès des projets et des cas d'espèce de l'affaissement jusqu'à ses aspects légaux et économiques. L'étendue du programme était vaste, comprenant l'abaissement de la surface par suite de l'extraction de l'eau, du pétrole brut ou du gaz naturel, de l'exhaure des sols organiques, de l'hydrocompaction, de l'extraction des solides par exploitation des mines, et de l'affaissement karstique. Ce volume de comptes-rendus contient soixante des communications soumises pour les sessions techniques aussi bien que les allocutions des representants de l'état de Californie et des organisations patronnes du symposium, l'AIH et l'ISSMFE. Cette préface comprend les allocutions au nom de l'AISH et de sa Commission Internationale des Eaux de Surface, présentées respectivement par A. I. Johnson et S. Yamamoto. A la fin du volume se trouvent les précis de trois communications russes sur l'affaissement; leurs textes complets sont arrivés trop tard pour être publiés ici.

Les présidents généraux du symposium étaient A. I. Johnson (U.S. Geological Survey, Reston, Virginie) et S. Yamamoto (Université d'Education, Tokyo, Japon). J. F. Poland (U.S. Geological Survey, Sacramento, Californie) exerçait la fonction de vice président des programmes techniques; D. R. Allen (Department of Oil Properties, Ville de Long Beach, Californie) était vice président pour les arrangements locaux et organisateur de la courte excursion. B. F. Lofgren était organisateur de la longue excursion et représentant de l'AIH. Le Comité d'Organisation comprenait également R. T. Bean (Consulting Geologist, La Crescenta, Californie), representant de l'AIH; G. Springall (Président, Sociedad Mexicana de Mecánica de Suelos, Coyoacan, Mexique, D.F.) et Pierro Sembenelli (Electroconsult, Milan, Italie), representants de l'ISSMFE; S. N. Davis (Université d'Arizona, Tucson, Arizonie), représentant de l'USNC/SH; H. L. Koning (Laboratoire de la Mécanique des Sols, Delft, Pays Bas); R. O. Castle (U.S. Geological Survey, Menlo Park, Californie); J. C. Stephens (U.S. Agricultural Research Service, Ft. Lauderdale, Floride); et R. R. Parizek (Pennsylvania State University, University Park, Pennsylvanie).

Le symposium était précédé d'une excursion en autobus de deux jours, partant de bonne heure de San Francisco, Californie, le 9 décembre et terminant à Anaheim le soir du 10 decémbre. Le tour a parcouru des points d'affaissement et des lieux d'intérêt hydrologique, géologique, historique, agricole, et sociologique dans les vallées de Santa Clara et San Joaquin. Ces régions ont l'affaissement le plus sévère et l'étendue la plus grande du monde, résultat d'une grande diversité de causes, anthropogéniques et autres. Le Comité du Guide, dont les membres étaient B. E. Lofgren, R. L. Ireland, et Margaret Farmer, tous de l'U.S. Geological Survey, Sacramento, Californie, a préparé un guide de l'excursion. Le guide comprend un journal détaillé de la route et plusieurs articles techniques sur l'affaissement dans les regions visitées par le tour. Le troisième jour du symposium, qui a duré 5 jours, une courte excursion dans la région de Long Beach, Californie, a eu lieu. Cette excursion comprenait un tour en autobus de la région d'affaissement à Wilmington (affaissement d'à peu près trente-trois pieds) où l'affaissement est le résultat de l'extraction du pétrole brut; un voyage en bateau à une île artificielle créée pour les puits de pétrole et les puits d'injection utilisés pour empêcher l'avance de l'affaissement; le dejeuner à bord du paquebot Queen Mary; et une visite à la barrièr des puits d'injection du District de Contrôle des Inondations de Los Angeles.

Au nom de l'AISH et des organisations patronnes, nous voudrions exprimer nos remerciements aux membres du Comité d'Organisation du symposium, aux présidents des seances, au personnel de l'AGU, et a tous ceux qui nous ont aidés ã accomplir tant de tâches d'organisation. Nouns voudrions aussi remercier les auteurs qui ont donné leur temps, leurs efforts, et leur science pour produire un bon programme. Il est à esperer que la nature interdisciplinaire du programme et de son patronage encouragera les efforts multidisciplinaires pour résoudre les nombreux problèmes de l'affaissement des terrains.

Arnold I. Johnson
Premier Vice Président
Association Internationale des Sciences Hydrologiques

S. Yamamoto
Presidént
Commission Internationale des Eaux Souterraines, IAHS

Publication n°121 of the International Association of Hydrological Sciences
Proceedings of the Anaheim Symposium, December 1976

WELCOMING REMARKS

Ronald B. Robie, Director
California Department of Water Resources
Sacramento, California, USA

Ladies and gentlemen, on behalf of California, I welcome you to our State--the place where the Sun sinks slowly in the west and where, unfortunately, so does our land.

We are very pleased you are here. This is probably one of the most appropriate places in the world to hold a symposium on land subsidence. California has always been on the move, figuratively and literally. The Sierra Nevada, which traverses much of California's eastern border, is a young range of mountains and they are still going up. Our great Central Valley, which many of you saw yesterday, bordered by the Sierra on the east and the coast range on the west, has many areas in its southern portion which are slowly going down.

These are the facts. The fiction is even worse. For those of you who may have seen the movie Earthquake, its alleged setting was a comparatively few kilometres from here. With respect to that Hollywood-created disaster, we certainly acknowledge the possibility--perhaps the probability--of an earthquake, but we would like to think that our dam engineers and our structural engineers did a better job than implied by the film. Even more catastrophic events for our golden State have been prophesied by various pseudo-scientific persons. One of the most mind boggling was the prediction a few years ago that the occurrence of a severe earthquake would cause much of the State to break off and disappear into the Pacific Ocean. Fortunately, it was the predication that was faulty and we came through unshaken.

In a more serious vein, however, I think it would be appropriate if I commented on some of the subsidence problems which we have here in California. Most of you are probably aware that our State has experienced the maximum subsidence in the United States--9 metres (29 feet) in the San Joaquin Valley. You are also probably aware that, as far as known, Mexico City is the only foreign locality that has experienced subsidence of that amount. I could add, somewhat facetiously, that since Mexico City has an elevation of nearly 2,240 metres (7,350 feet), it has more room to subside than the San Joaquin Valley. The San Joaquin Valley, including the Tulare Lake Basin, is roughly 400 kilometres (250 miles) long, ranging from a few metres to about 100 metres above sea level. The San Joaquin River system with its relatively flat gradient, drains much of this area from south to north, eventually flowing through the Sacramento-San Joaquin Delta, on through the Carquinez Straights into San Francisco Bay, and thence to the Pacific Ocean. It doesn't take too much imagination to picture what would happen if the floor of the San Joaquin Valley and the river bed were to sink sufficiently to put it below sea level with a direct connection to the Pacific Ocean. We already have one famous valley in California below sea level--that is Death Valley. We hope it will remain the original and the only one.

Our 715-kilometre (444-mile) California Aqueduct traverses much of the San Joaquin Valley and was designed with a gradient of about 5 centemetres per kilometre (3 inches per mile). Recognizing the many geologic and seismic problems that the California Aqueduct and the California State Water Project in general involved, the Department of Water Resources made an unprecedented use of earth scientists during all stages of design and construction. During the peak period, 134 earth scientists were employed. Many of these people were involved with the San Joaquin subsidence problems associated with design and construction of the California Aqueduct. Cliff Lucas of our staff was with you when you took the tour during the last couple of days and he will have a paper on this subject on Friday's program.

In general, the Department's San Joaquin Valley subsidence program involved detection of potential areas of subsidence, estimating ultimate settlements, determining causes and mechanics, and developing effective countermeasures. Four types of land subsidence were recognized in the regions proposed to be crossed by the aqueduct. These included subsidence caused first by ground-water extraction--a deep subsidence. I might add that during last week, I was visiting the San Joaquin Valley and in view of our very serious drought of this last year, we have had very substantial reductions in ground-water levels in San Joaquin Valley. In many instances there has been new subsidence and one person advised me that the water level had gone down about 2 metres (6.5 feet). Subsidence has been effected this year as the ground-water pumping levels have been drawn down farther than in normal times. The second kind of subsidence is hydrocompaction--the shallow subsidence. The third is subsidence from oil and gas production, and the fourth is from tectonic activity. With respect to ground-water extraction and deep subsidence, the Department, working cooperatively with the U.S. Geological Survey, had already been investigating the phenomenon for some 18 years. The development of a compaction recorder by the U.S. Geological Survey assisted greatly in developing an understanding of the mechanics of subsidence and its relationship to hydrogeology.

Shallow subsidence, as you well know, is a somewhat more simple concept--put water on the ground and it subsides. Our solution or countermeasure was to precompact by putting water on the ground and into the ground along the alinement until the subsidence stopped. For those of you who visited the Mendota Test Plot location where the subsidence was tested, I want you to know of one of the side effects of such a test. That side effect is to be left with a test area after you're through with no way to sell it--so if anyone would like to buy a used subsidence test area, we have one that worked very well.

There were 493 oil fields in California and subsidence due to production has occurred at 27 of these. The California Aqueduct crosses six of these producing oil fields and passes within 1.6 kilometres (1 mile) of 11 others. One of our current concerns is the matter of the Navy's Elk Hills reserve field which for many years has been an oil reserve owned by the U.S. Navy. In view of the serious energy problems the United States is facing, the Congress authorized the use of oil from that field. It is going into production status and we will be monitoring the effects there very closely to make certain that it does not have adverse impact on our aqueduct. The aqueduct is now delivering large quantities of water on a regular basis and cannot be out of operation for any period of time without inconveniencing and perhaps causing serious difficulties.

The tectonic activity is something I expect we will always be concerned with and worry about, particularly the rapid movement related to earthquakes. In general, we have accepted possible effects on the aqueduct of this movement as an intangible risk. We would hope that you people in a symposia such as this will advance technology to enable better prediciton of extent and frequency of this hazard.

As a matter of interest, since your first symposium of this group was held in Japan, I couldn't help but draw parallels between some problems in Japan and the United States. In addition to subsidence, we are also mutually concerned about earthquakes, about tsunamis, and we even have an active volcano in California, Mount Lassen, which had an erruption as recently as 1915. The several problems of nature that we share with the Japanese and the subsidence problems we have in common with Mexico City are truly exemplary of the fact that these are not Japanese nor Mexican nor California problems, but rather problems of the world. It is, therefore, highly appropriate that such problems be addressed by the scientists of the world as you are doing here today and this week.

I am very impressed with the assemblage of technical expertise represented here. We are very pleased that you had the opportunity to come to our State for this meeting. I am certain that you will contribute much toward solving the solvable problems and that collectively, through meetings such as this, solutions can come more quickly. In this very technical area in which you are working, I, with my educational background being primarily legal, will defer to you. While there are legal problems related to subsidence, it is seldom that you can stop subsidence with an injunction.

In closing this morning, I again would welcome you, and wish you a successful and productive meeting. I hope that you're not involved with conference entirely throughout your visit here and that you will take an opportunity to enjoy yourself. With Disneyland, Knotts Berry Farm, Magic Mountain, and other attractions so close by, and with this incredibly beautiful weather that we have had continuously for a year and a half, no one could fault you for slipping away for a few hours while you let further consideration of these earth-shaking problems subside. Thank you and welcome again.

Publication n°121 of the International Association of Hydrological Sciences
Proceedings of the Anaheim Symposium, December 1976

REMARKS ON BEHALF OF THE INTERNATIONAL ASSOCIATION OF HYDROGEOLOGISTS

L. A. Heindl
Office of International Activities
U.S. Geological Survey
Reston, Virginia, USA

Abstract

As Chairman of the U.S. National Committee for the International Association of Hydrogeologists (IAH) it is a great honor and a pleasure to say a few words about the Association and its interest in subsidence. The IAH is somewhat differently oriented than the International Association of Hydrological Sciences (IAHS) and these differences may be of interest to you. The IAHS is concerned with hydrological problems principally from the physical, chemical, and engineering points of view. In keeping with this, the IAHS adheres to the International Union of Geodesy and Geophysics. In contrast, the International Association of Hydrogeologists approaches most hydrological matters from the geological point of view. Because of this orientation, IAH is associated with the International Union of Geological Sciences. Also pertinent, is the fact that IAH is an association that is not made up of societies--it is an association that is made up of individuals. Perhaps that is because it is a little more difficult to regiment geologists than most other groups of scientists.

The IAH has been concerned with subsidence for some time because it is deeply involved in the study of limestone and carbonate terranes of the world. It has an active Commission on this subject, which also was the subject of IAH's twelfth international congress, held in Huntsville, Alabama, just about nine months ago. Although the Commission is more concerned with subsidence in carbonate terranes, the Association is concerned with all types of subsidence including those considered here.

At this point, I would like to digress for a moment from the International Association of Hydrogeologists, and the problems with which we are concerned directly at this symposium. It is well-known and obvious to all of you that subsidence involves not only the hard sciences but also is very much a social, economic, and political event. It is involved in the day-to-day living of millions of people around the globe. Many of us in the International Association of Hydrogeologists believe that this human aspect of our geological studies needs to be investigated much more fully. As geologists and hydrologists we should be more alert to the social, economic, and political aspects of subsidence. After all, here is an environmental problem that is probably much more fully studied by our own profession than by any other. We thus have a responsibility to present its humanistic aspects to the public as well as those of our particular discipline. These humanistic aspects, however, have long been considered to be outside of our ken. Thus it will take deliberate action by our professional groups and by our universities to provide the background in education and research we all need to respond to this new responsibility. Particularly we need research in the interrelationships of scientific events and their social impacts so that we as scientists can do the job expected of us by the society in which we live.

On behalf of the International Association of Hydrogeologists, President Stevenson Buchan of England, First Vice President Phil LaMoreaux and the other officers of the Association's Council, I wish you a pleasant, interesting, stimulating, and provocative symposium.

Publication n°121 of the International Association of Hydrological Sciences
Proceedings of the Anaheim Symposium, December 1976

REMARKS ON BEHALF OF THE INTERNATIONAL SOCIETY FOR SOIL MECHANICS AND FOUNDATION ENGINEERING

German E. Figueroa Vega, Director
Aquas Subterraneas y Superficiales
Comision de Aquas del Valle de Mexico
Mexico, D.F.

It is a great honor for the International Society for Soil Mechanics and Foundation Engineering to participate together with other international organizations at this Second International Symposium on Land Subsidence, as promoted by the International Association of Hydrological Sciences. The number of areas affected by subsidence increased alarmingly in different regions of the world, mainly due to human needs such as pumping of water and exploitation of oil, gas and minerals.

The behavior of large and deep soil masses is one of the most interesting subjects in soil mechanics. Subsidence caused by the action of natural agents or by man may normally go unnoticed while the amount doesn't reach a magnitude large enough to create damage to structures and other installations, especially in urban areas. However, classical examples of large amounts of subsidence cannot go without recognition, such as that in Mexico City, for example. The subsidence has been as great as 8.7 meters in 80 years. This fact caused an endless amount of damage, as well as flooding risks that can only be controlled through very extensive engineering works. The great danger that threatens the city of Venice also is well known. Of no less importance are the cases of Long Beach and San Joaquin Valley.

An exception to the general rule of subsidence causing damage is a special case in which settlement produced by man acts for his benefit. It is the creation of reservoirs by consolidation of high compressibility within the limi of the ancient Texcoco Lake near Mexico City. The importance of the phenomenon of subsidence and of its consequences, contributes to the need for increased studies of large soil mass behavior, expecially in prediction and control. It is believed that the information and knowledge provided by the authors of the more than 60 papers presented at this symposium will surely contribute to the advance of this subject area.

On behalf of the International Society for Soil Mechanics and Foundation Engineering, and of its President, Professor Jean Kerisel, I express best wishes for a successful symposium, and I congratulate the co-chairmen and the members of the organizing committee for their fine work.

Publication n°121 of the International Association of Hydrological Sciences
Proceedings of the Anaheim Symposium, December 1976

REMARKS ON BEHALF OF THE U.S. NATIONAL COMMITTEE FOR SCIENTIFIC HYDROLOGY

J. S. Cragwall, Jr., Chief Hydrologist
U.S. Geological Survey
Reston, Virginia, USA

As chairman of the U.S. National Committee for Scientific Hydrology, it is a real pleasure for me to be with you to talk about U.S. participation in the International Hydrological Program (IHP), with emphasis on subsidence. Particularly, it gives me an opportunity to thank the International Association of Hydrological Sciences (IAHS) and its Commission on Ground Water and its cosponsors, not only for organizing this symposium, but also for the many years and the many ways in which IAHS and its commissions have cooperated with the international programs of the Decade and IHP.

In nearly 15 years since the beginning of the Decade, hydrology has come a long way, and this symposium is representative of the many changes that have taken place. Where once an international hydrological symposium concentrated on one aspect or another of the movement and occurrence of water, today its sessions are more broadly based and certainly more problem oriented. They are interdisciplinary and multidisciplinary. They consider, as Dr. Heindl has mentioned, the political, social, and economic relationships, and in many cases like this one, are certainly international in scope.

Land subsidence is a phenomenon that involves a noticeably rapid, in terms of earth movement, and sometimes catastrophically certain, lowering or settling of the Earth's surface. It can occur naturally, or under the impact of a wide variety of human activities, and it is with the latter that we are most concerned. This is true of the programs of the U.S. Geological Survey (USGS) and of IHP in this subject area, and is the focus of most of the papers to be presented at this symposium.

But, as a little aside to this, I think we might mention that we in the water resources program of the Geological Survey have played a continuing role in the studies of land subsidence, not merely because of the hazards and economic losses associated with it, but also because the fluid withdrawal is an important engineering aspect of this whole phenomenon. The compaction processes that lead to the subsidence help us to better understand the operation of the ground-water system. For example, the water accounted for by compaction in the San Joaquin Valley, our experts tell us, represents a major part of that withdrawn in the subsiding areas. A hydrologic model developed without accounting for these impacts of compaction would certainly be erroneous and fall short of the mark. So, subsidence is important in understanding hydrologic systems and in water-resources planning, even though the resulting land settlement might constitute little hazard or economic loss. One reason for the breadth of concern and interest in subsidence is that in many of the regions where it most expensively affects human activities, it is suspected if not absolutely proven, that it is caused by human activities. Therefore, it should be capable of being slowed, corrected, stopped, or mitigated by man's technology and good management. That is why you are here and that is what this symposium is all about. Moreover, subsidence is not confined to any one continent or region. In one form or another it occurs in most, if not all, countries. Thus, it is particularly appropriate that progress in understanding subsidence should be both the subject of an international symposium and also a great matter of interest to IHP.

Many of you have heard of IHP in general terms. Let me take a few moments to be a bit more specific about the program itself and also the role and nature of U.S. participation. I believe this will be of interest to those of you who are representing the U.S. scientific community and those of you from elsewhere as well. IHP is an outgrowth of the International Hydrological Decade. Like its predecessor, it is under the aegis of UNESCO. IHP now involves about 80 countries, and its activities are guided by an intergovernmental council made up of representatives of 30 member countries. These members generally rotate.

The Decade's outstanding contribution to international hydrology was the boost it gave to the hydrological services, especially in the developing countries. The scientific and technical objectives set by this prestigious international body were used by hydrologists to upgrade the institutional and administrative, as well as the scientific, capabilities of their domestic programs to the ultimate benefit of the country and its people. IHP seeks to continue this function so that eventually all countries may be able to cope with their individual and collective water problems.

U.S. participation in IHP is under the guidance of the U.S. National Committee for Scientific Hydrology. This Committee was formed by USGS at the request of the Department of State and with the endorsement of the water-concerned Federal agencies. The responsibilities of the National Committee are not restricted to IHP, although for all practical purposes this international program has been its main focus up to now. Our Committee may also be called upon to concern itself with other international hydrological programs and, in a way, is also quite active in the operational-hydrology program of the World Meteorological Organization.

The functions of the National Committee are (1) to formulate the U.S. program of participation in IHP; (2) to serve as a channel of communication among those involved; (3) to promote international hydrological activities; (4) to help the Department of State prepare U.S. positions in the realm of water; and (5) to arrange for U.S. activities as related to other countries' requests, insofar as we can do so. The Committee now has 15 members. It may have as few as 10 or as many as 20. The Chief Hydrologist of USGS serves as Chairman, and representatives of eight other Federal agencies and six non-Federal organizations assist him in this work. The Committee's day-to-day business is conducted by a parttime Executive Secretary of great experience, Leo Heindl, who came from IHD, and some administrative support, which he says is never quite enough. The Federal agencies now on the Committee besides USGS are the National Weather Service of NOAA, Corps of Engineers, Bureau of Reclamation, Office of Research and Technology, Tennessee Valley Authority, Environmental Protection Agency, and the Energy Research and Development Administration. The Department of State and the National Science Foundation sit ex-officio on this Committee. As for the non-Federal sector, the universities are represented by the Universities Council on Water Resources and the technical societies are represented by the Hydrology Section of the American Geophysical Union, the Hydrogeology Division of the Geological Society of America, and the Hydraulics Division of the American Society of Civil Engineers. The social, economic, and political interests are represented by the American Water Resources Association and the National Academy of Sciences.

IHP derives from that of the Decade. Its program is made up of five major categories of activities: (1) the scientific part, which includes studies of the hydrological cycle, assesment of water resources, and the evaluation of the influence of man's activities on water resources; (2) promotion of education and training in hydrology; (3) enhancement of exchange of information in hydrology; (4) technical assistance; and (5) enlargement of regional cooperation. The overall responsibility for the content of the international program lies with the IHP Intergovernmental Council, which I've previously mentioned, and this operates through the IHP Secretariat in UNESCO. Much of the actual work is done by members of the Secretariat, supplemented by the working groups and rapporteurs appointed by the Council. In addition, the Council is advised by two committees concerned respectively with the affects of man's activities on the hydrological cycle and with education, training, and technical assistance. The United States holds membership on both committees and has also supplied four rapporteurs and members to eight working groups in the scientific program.

The general IHP program is planned in six-year stages. Every two years, to coincide with UNESCO's budgetary system, the Council meets to plan the detailed program for the succeeding intersessional two-year period and to adjust the longer range objectives as needed. The Council next meets in June 1977.

I note with interest that this conference is the site of a meeting of the IHP working group on land subsidence. This working group is composed of members from Belgium, Japan, Mexico, and the United States, and I am really pleased that Joe Poland, who has spent many years with USGS working on problems of land subsidence in this part of the United States, is the U.S. representative on this work group. I note with interest, too, that the working group has set a worthy goal of undertaking the very challenging task of preparing a case book on land subsidence in a way that it will serve as a guide to research and practice in developing countries.

One other activity in the international area I would like to touch on. Land subsidence, as a phenomenon affecting many aspects of human endeavors in many parts of the globe, undoubtedly will be discussed at the U.N. Water Conference, which will be held in Mar del Plata, Argentina, in March 1977. This is not the usual type of water conference, however, because it is addressed to policymakers. Primarily, the conference is intended to promote the need for nations to prepare themselves individually and collectively to avoid water crises in the next few decades. Hopefully, the policymakers will improve their awareness of subsidence in water planning, and I am very hopeful that the activities taking place here, Ivan, will make some contributions in this regard.

In closing, I would like to extend the best wishes of both the U.S. Geological Survey and the U.S. National Committee for Scientific Hydrology to IAHS and the organizers of the meeting for a successful and stimulating meeting. The problems of land subsidence are so widespread and so diverse that they can best become understood by conscious and continuous efforts to exchange information, concepts, and points of view nationally, regionally, and internationally. I certainly wish you a most successful meeting, and I certainly thank you for allowing me to be a part of your introductory session.

Publication n°121 of the International Association of Hydrological Sciences
Proceedings of the Anaheim Symposium, December 1976

RECENT TREND OF LAND SUBSIDENCE IN JAPAN

Soki Yamamoto
Inst. of Earth Science, Univ. of Tsukuba
Japan

Abstract

The number of subsiding areas in Japan is still increasing and has now reached 40. In most of the well known existing subsidence areas, such as Tokyo, Chiba, Kanagawa (Yokohama and Kawasaki), Osaka, and Niigata, artesian pressures have recovered as much as several meters in a year and the rates of subsidence have decreased considerably. Moreover, the land surface has rebounded, creating many new problems. The maximum amount of recorded rebound is 30 mm in one year (1974-1975) at a point in Kawasaki. These phenomena are mostly the result of the countermeasure of legal prohibition of ground-water withdrawal in each area.

Recently, calculation and prediction of the amount of subsidence in several areas has been tried, by means of a mathematical simulation model utilizing the relation between compaction and ground-water withdrawal. However, complications that severely affect the quality of the results are (1) the inaccuracy of available data on withdrawals, and (2) the problem of trying to obtain representative piezometric pressures from deep wells screened in multi-layered aquifer systems.

Introduction

A scientific study on land subsidence in Japan dates back to the time of early 1900's in Tokyo and of 1930 in Osaka. The papers presented at the First International Symposium on Land Subsidence in 1969 in Tokyo were based on statistical data collected to the end of 1966. Since that time, land subsidence in Japan has shown remarkable change of aspects in its area and character so the author wants to review these recent trends and point out some problems concerning countermeasures and studies.

Land Subsidence Area and Its New Trends

According to the recent study of the Ministry of Construction's Geographical Research Institute[1/] and the Environmental Protection Agency[2/] there are many land subsidence areas besides Tokyo (including Chiba, Saitama and Kanagawa), Osaka (including Amagasaki and Kobe), and Niigata (fig. 1). They made analysis of precise leveling data with geodesically high accuracy in Japan and pointed out the areas with a rate of subsidence more than 20 mm per year. These areas (fig. 2) are Kanaura (Akita), Naoetsu (Niigata), Kujikuri (Chiba), Mikawa Plains (Aichi), Nobi Plains (including Aichi, Mie and Gifu prefectures), Tottori Plain (Tottri), Saga Plain (Saga), Aomori City, Nanao City, Yamagata City, and Haranomachi City.

Recent land subsidence areas in Japan have increased remarkably in number to 46, and to 7,380 Km^2 in area. Among these, the area that is below mean sea level amounts to about 1,200 Km^2. These areas are equipped with compaction recorder (extensometer) and companion water-level recorder. Details of the land subsidence aspects at Tokyo and the Nobi Plain will be described by other authors of this symposium (M. Ishii, F. Kuramochi, and T. Endo; K. Iida, K. Sazanami, T. Kuwahara, and K. Ueshita; and T. Kuwahara, K. Ueshita, and K. Iida).

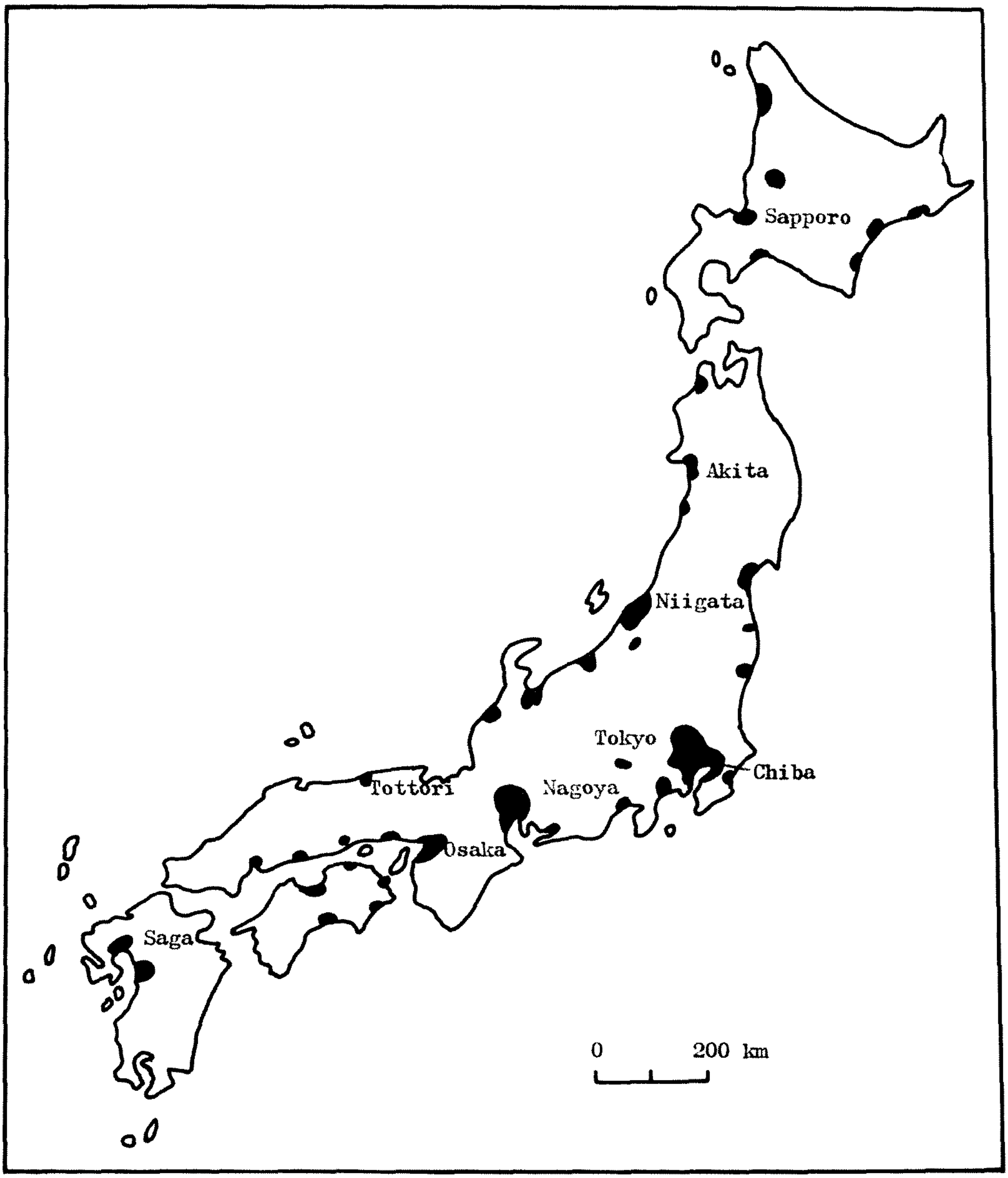

Figure 1.—Land Subsidence Areas in Japan, 1965 (Soki Yamamoto, after G S I)

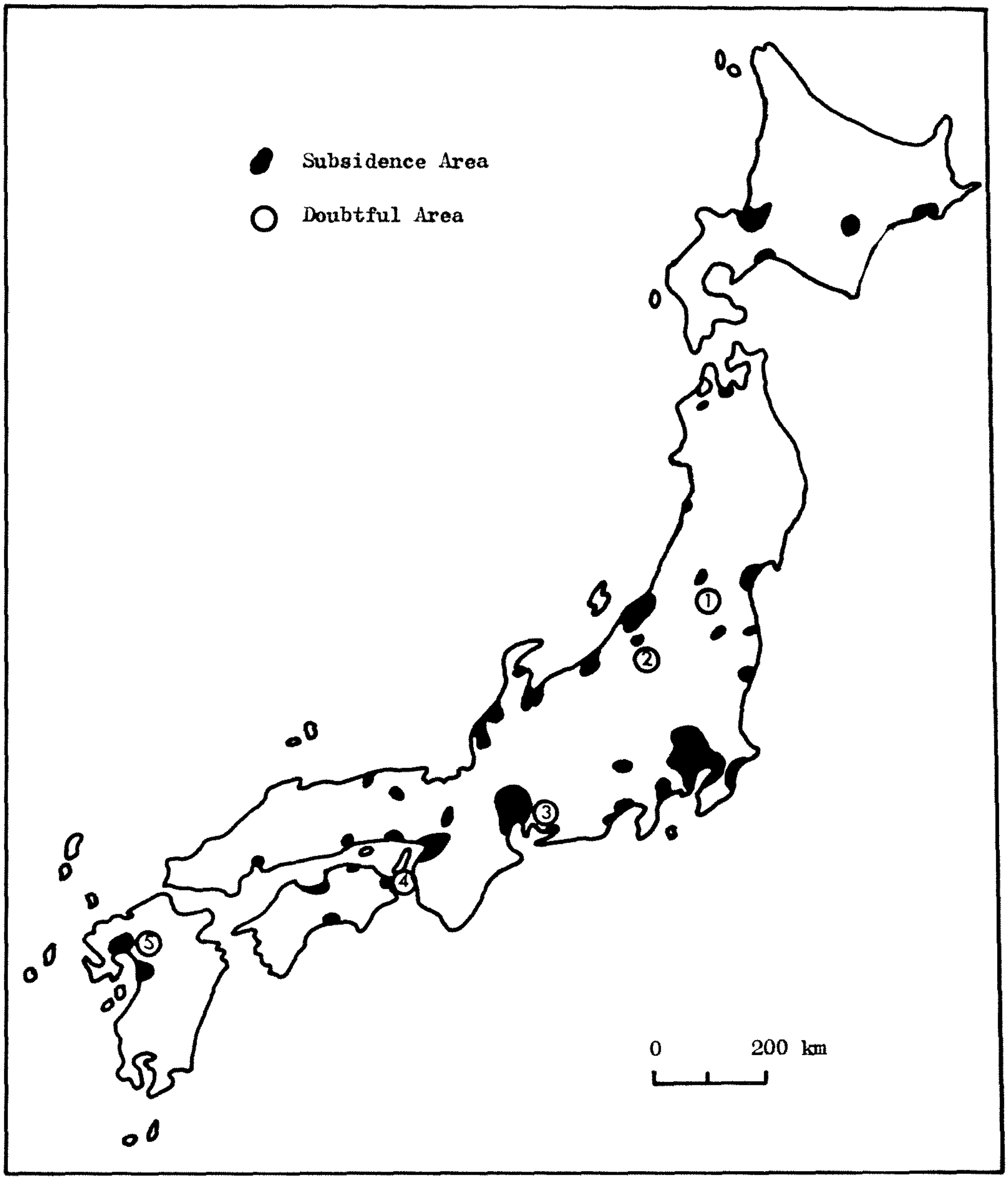

Figure 2.--Land Subsidence Areas in Japan, 1975 (Soki Yamamoto, after G S I)

Land subsidence in Japan is man-made, caused by overdrafting of ground water in an area. The main purposes of ground water pumpage in the earlier period (table 1) were for industrial and municipal (excluding drinking water) uses and gas exploitation, but recently (table 2) usage increased for drinking, agricultural, and snow melting (winter period in Japan) purposes.

Large scale geothermal exploitation has been undertaken in some areas but its effect on land subsidence is not yet clarified. New subsiding areas, such as Yamagata, Saga and Haranomachi areas belong to the agricultural pumpage areas; Nanao and Aomori to the withdrawal areas for drinking water supply; and Nanaura and Kujukuri to the gas exploitation ones.

In contrast to these, the subsidence rate has decreased drastically in existing famous subsiding areas (table 3) such as Osaka, Kawasaki, suburb of Tokyo, and Chiba. In these areas, subsidence slowed or stopped and remarkable rebound has occurred because of the rapid rise in artesian head due to the decrease in ground water draft resulting from legal prohibition. This kind of rebound in a long term subsidence area provides new problems for construction, reconstruction works, and others, such as in Kawasaki where the maximum amount of recorded rebound is 30 mm in one year (1974-1975) and it has been mistaken as a sign of earthquake attack in the near future.

Table 1. Total amount of groundwater utilization in Kanto district, 1960, m^3/day

	Drinking	Industrial	Agricultural	Miscellaneous	Total
Tokyo Proper	178,500	900,000	0	1,215,000	2,293,500
Tokyo Suburb	319,500	166,000	4,000	196,000	685,500
Chiba	117,000	222,000	23,000	99,000	461,000
Kanagawa	42,000	348,000	3,000	64,500	457,500
Saitama	171,000	302,000	10,000	81,000	564,000
Tochigi	19,500	46,000	16,000	21,000	102,500
Gunnia	72,000	108,000	2,000	28,500	210,500
Ibaraki	76,500	86,000	155,000	48,000	365,500
Total	996,000	2,178,000	213,000	1,753,000	5,140,000

Table 2. Total amount of groundwater Utilization in Kanto district, 1970, m^3/day

	Drinking	Industrial	Agricultural	Miscellaneous	Total
Tokyo	763,233	902,356	21,000	461,805	1,938,394
Proper	179,186	425,906		227,296	
Suburb	584,047	266,450		234,509	
Chiba	404,556	437,843	514,000	68,927	1,425,326
Kanagawa	257,082	541,160	13,000	—	811,242
Saitama	820,360	564,192	1,150,000	15,843	2,550,395
Tochigi	257,802	309,339	9,290,000	—	9,857,141
Gunnia	302,173	216,604	1,368,000	—	1,886,777
Ibaraki	270,534	240,545	2,044,000	—	2,555,079
Total	3,075,740	3,002,039	14,400,000	546,575	21,024,354

Table 3. Change of subsidence in selected areas

	Tokyo		Osaka		Nagoya	Niigata	
Subsiding area approx. (Km^2)	200 (1958)	230 (1974)	120 (1960)	20 (1975)	290 (1973)	2000 (1959)	70 (1974)
Past maximum subsidence rate (cm/year)	Up. 0	22*	20	0*	-	X	X
	Lo. 38	13	14	2*	16	45*	1

Up.=upland, Lo.=lowland * rebounding is seen in some area (1976)

Countermeasure and its problems

At the first symposium in Tokyo, the author proposed the necessity of rational forcasting based on a scientific basis, suggesting the start of a mathematical simulation model study and carrying on of artificial recharge of ground water in Japan. The author is still skeptical about the strengthening of the legal control and/or prohibition of ground-water extraction as he believes that it contains some fundamental and philosophical problems about making ground water a natural resource. "No use is the best use" does not hold true on ground water utilization in the world.

As for the control of ground-water withdrawal, the Osaka city authorities secured their control of the pumping of ground water for building use in 1962. The Industrial Water Law of 1957 became effective and was later applied in Tokyo, Yokohama, and others since 1961. In addition to this, Municipal Ground Water Laws for Building and Public Disaster Prevention Regulation by local governments were also established since that time in many places. In the case of Tokyo 3/, the Industrial Water Law was applied over the Koto District in 1961, but there still was ground-water withdrawal of 650,000 m^3/day and a subsidence area of 75 km^2 where the subsidence rate exceeded 10 cm/year. Even after the application of the Building Ground Water Law in 1963, Tokyo still continued to have pumpage amounts of 500,000 m^3/day and a subsidence area of 20 km^2. This is mostly due to the difficulty of applying such a law to existing facilities with no substitution of water and to gas exploitation facilities, which are controlled by Mining Law. Recently, legislation on prohibition of ground-water pumpage by local Prefectural Government, cities and towns is growing popular in Japan, (fig. 3) and on the other hand a Council of Self-control and Coordination of Groundwater Usage in a district is going on at several industrial regions.

The author and his collaborator had started on the basic hydrological study on the vertical movement of water through unsaturated zone with neutron moisture meter and estimation of recharge rate by tritum contents in ground water with a proper simulation model. I. Kayane has shown that land subsidence occurred on the area where pumpage amounts exceeded more than 1 mm/day/km^2 which might be the average maximum recharge amount in Japan.

Recently, calculation and predictions of the amount of subsidence in several areas has been tried by T. Shibasaki, A. Kamata, and their group by means of mathematical simulation model utilizing the relationship between compaction and ground water withdrawal. However, basic complications that severely affect the quality of such results are (1) the

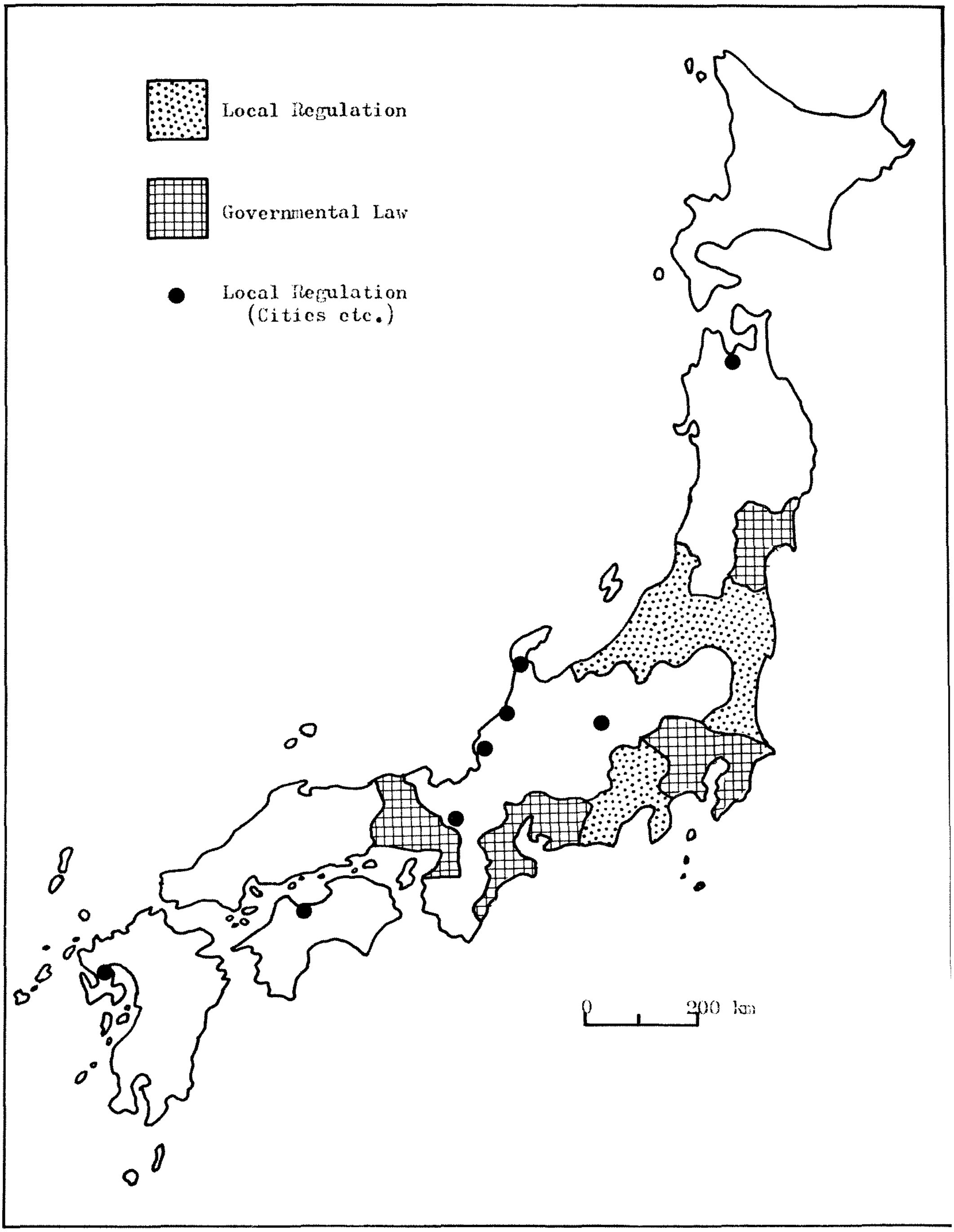

Figure 3.--Ground water controlled areas in Japan

inaccuracy of available data on withdrawals, and (2) the problem in trying to obtain representative water levels from deep wells screened in all parts of multi-layered aquifer systems.

Unfortunately, **some** fundamental mistakes are made. For example, in applying so called "vertical two dimentional multi-aquifer model", the following equations have been used:

$$K_{xx}\frac{\partial^2 h}{\partial x^2}+K_{zz}\frac{\partial^2 h}{\partial z^2} = S_s\frac{\partial h}{\partial t} + Q(x,z,t) \qquad (1)$$

$$Q(x,z,t) = L_E + S_q + A_r - Q_d \qquad (2)$$

$$L_E = \frac{K'}{d'}(h-H) \qquad (3)$$

$$S_q = K'\frac{\partial h'}{\partial z}\Big|_{z=d'} \qquad (4)$$

where A_r = recharge, and Q_d = discharge

In equation (2), the first term of right side, L_E, should be deleted. The famous leakage term expressed by Eq.(3) is a part of squeeze term S_q. Consequently, the calculated subsidence amount is always overestimated because it is assumed that subsidence amount is directly proportional to the amount of head decrease.

References

(1) Tomori, G. and Kato, T., 1971, Survey on land subsidence in Japan: Geographical Survey Institute.
(2) 1976, Data on land subsidence in Japan: Environmental Protection Agency.
(3) Yamamoto, S., Kayane, I., Aoki, S., and Fuji, S., 1971, Simulation of groundwater balance as a basis of considering land subsidence in the Koto Delta, Tokyo: Int. Assoc. Scientific Hydrol. Pub. No. 88, pp. 215-224.

Publication n°121 of the International Association of Hydrological Sciences
Proceedings of the Anaheim Symposium, December 1976

LAND-SURFACE SUBSIDENCE IN THE HOUSTON-GALVESTON REGION, TEXAS

R. K. Gabrysch
U.S. Geological Survey
Houston, Texas

Abstract

Development of ground water in the region began in the 1890's. Pumping of ground water from the Chicot and Evangeline aquifers for municipal supply, industrial use, and irrigation was about 23 cubic meters per second by 1974. Pumping of large amounts of ground water has resulted in water-level declines during 1943-73 of as much as 61 meters in wells completed in the Chicot aquifer and as much as 99 meters in wells completed in the Evangeline aquifer. The declines in artesian pressures have resulted in pronounced regional subsidence of the land surface.

The center of subsidence is east-southeast of Houston at Pasadena, where as much as 2.3 meters of subsidence occurred between 1943 and 1973. The maximum amount of subsidence during 1964-73 was about 1.1 meters. The area in which subsidence is 0.3 meter or more has increased from about 906 square kilometers in 1954 to about 6,475 square kilometers in 1973.

Water from Lake Livingston on the Trinity River, about 97 kilometers east of Houston, will become available in 1976. As a result, it is estimated that ground-water pumping will decrease by about 3.1 cubic meters per second in the area of maximum artesian-pressure decline and subsidence. The recovery of water levels is expected to decrease the rate of subsidence substantially.

Introduction

The Houston-Galveston region, which occupies a featureless coastal plain of low altitude, borders on Galveston and Trinity Bays and the Gulf of Mexico. Downtown Houston is at an altitude of about 15 meters above mean sea level, and the Johnson Space Center south of Houston is at an altitude of about 5.2 meters. Land-surface subsidence has caused critical problems of inundation by normal tides, and much of the region may be subject to catastrophic flooding by hurricane tides. Hurricanes resulting in tides of 4.6-6.1 meters above sea level strike the Texas coast on the average of once every 10 years.

Land-surface subsidence caused by the lowering of pressure heads due to pumping of water and oil has been recognized in the Houston-Galveston region for many years. Reports describing the magnitude and causes of subsidence date back to 1926 when Pratt and Johnson (1926) reported on the subsidence of the Goose Creek oil field. They attributed subsidence to the withdrawal of oil, gas, water, and sand. Pratt and Johnson concentrated their study on the oil field itself, but localized subsidence may have occurred in the vicinity of a few centers of ground-water development.

Studies in the Texas coastal subsidence area indicate a large degree of preconsolidation load. Foundations engineers indicate a preconsolidation load equivalent to 18 meters of overburden. The land surface is a depositional surface rather than an erosional surface, and it may be more logical to account for the preconsolidation load in terms of sea-level recession. Nevertheless, to overcome preconsolidation loads of 18 meters of overburden, artesian pressures must be lowered about 38 meters.

Therefore, during the first several tens of feet of decline in artesian pressure, the compaction of the fine-grained materials would be in the elastic range and would result in only a small amount of land-surface subsidence. In addition, the pumping centers were generally remote from Galveston Bay, and in the absence of other indicators such as the determination and redetermination of elevations, subsidence was not apparent.

The next area in the Houston-Galveston region where land-surface subsidence became evident probably was at Texas City in the southern part of Galveston County (fig. 1). Subsidence in Texas City began in the late 1930's, and by 1943, as much as 0.49 meter of subsidence had occurred in the industrial area. The tabulations in the American Oil Company report (1958, section A, table 1, p. 6) show that during 1943-52, the rates of subsidence at four bench marks in the industrial area ranged from 0.065 to 0.102 meter per year. Subsidence was attributed to the withdrawal of fresh ground water and the resulting lowering of artesian pressure.

It was not until the early 1950's that a report on the regional nature of land-surface subsidence was prepared. Winslow and Doyel (1954) in their description of changes in elevation stated as follows:

"The United States Coast and Geodetic Survey has established extensive nets of first- and second-order level lines covering most of the region. The first leveling in the region was the first-order line from Smithville to Galveston, which was run in 1905 and 1906. The next was in 1918 when a first-order line was run from Sinton, Texas, to New Orleans, Louisiana. During that period between 1932 and 1936 several other first- and second-order lines were run and the two original lines were releveled.

"In 1942 and 1943 a large number of second-order lines were established in the region and most of the old lines were releveled. At this time subsidence in the Houston area was noted from the results of leveling, although the actual amount of subsidence was not determined because of changes in datum."

Development of Ground Water in the Houston-Galveston Region

Development of ground water in the region began in the 1890's by pumping from the Chicot and Evangeline aquifers. The geologic and hydrologic setting has been described by several authors and will not be redescribed in this report. However, it is important to repeat that the aquifers are composed of unconsolidated lenticular deposits of sand and clay under artesian conditions. Pumping of ground water for municipal supply, industrial use, and irrigation approximates 46 percent, 33 percent, and 21 percent, respectively, of the total of 23 cubic meters per second pumped in 1972. The principal areas of pumping in each area are shown on figure 1. Pumpage in 1974 for all uses was 23 cubic meters per second.

Pumping of large amounts of ground water has resulted in water-level declines during 1943-73 of as much as 61 meters in wells completed in the Chicot aquifer and as much as 99 meters in wells completed in the Evangeline aquifer (figs. 2 and 3). The maximum average annual rates of water-level decline for 1943-73 were 2.0 meters in the Chicot aquifer and 3.3 meters in the Evangeline aquifer. During 1964-73, the maximum rates were 3.0 meters in the Chicot and 5.4 meters in the Evangeline.

Subsidence of the Land Surface

The center of the greatest amount of subsidence coincides with the center of artesian-pressure decline east-southeast of Houston at Pasadena. Figure 4 shows that as much as 2.3 meters of subsidence occurred between 1943 and 1973. It should be noted that within the region of subsidence, more than one center of subsidence occurs, as indicated by the closed contours. Some of the centers may be associated with oil-field production and some may be associated with ground-water production. Further complications in analysis result from varying thicknesses of individual

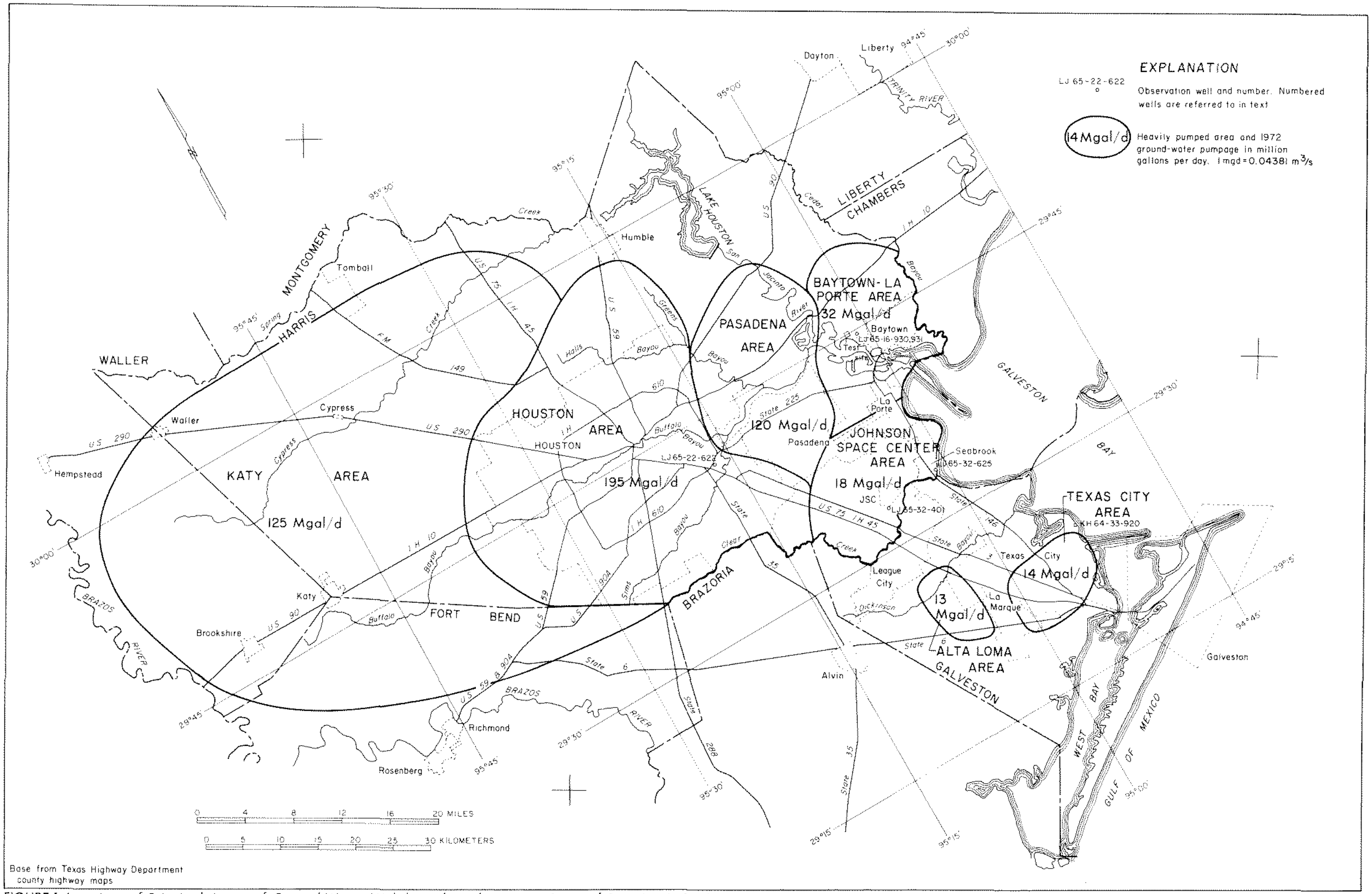

FIGURE 1 Locations of Principal Areas of Ground-Water Withdrawals and Average Rates of Pumping in 1972

FIGURE 2.-Approximate Declines of Water Levels in Wells Completed in the Chicot Aquifer, 1943-1973

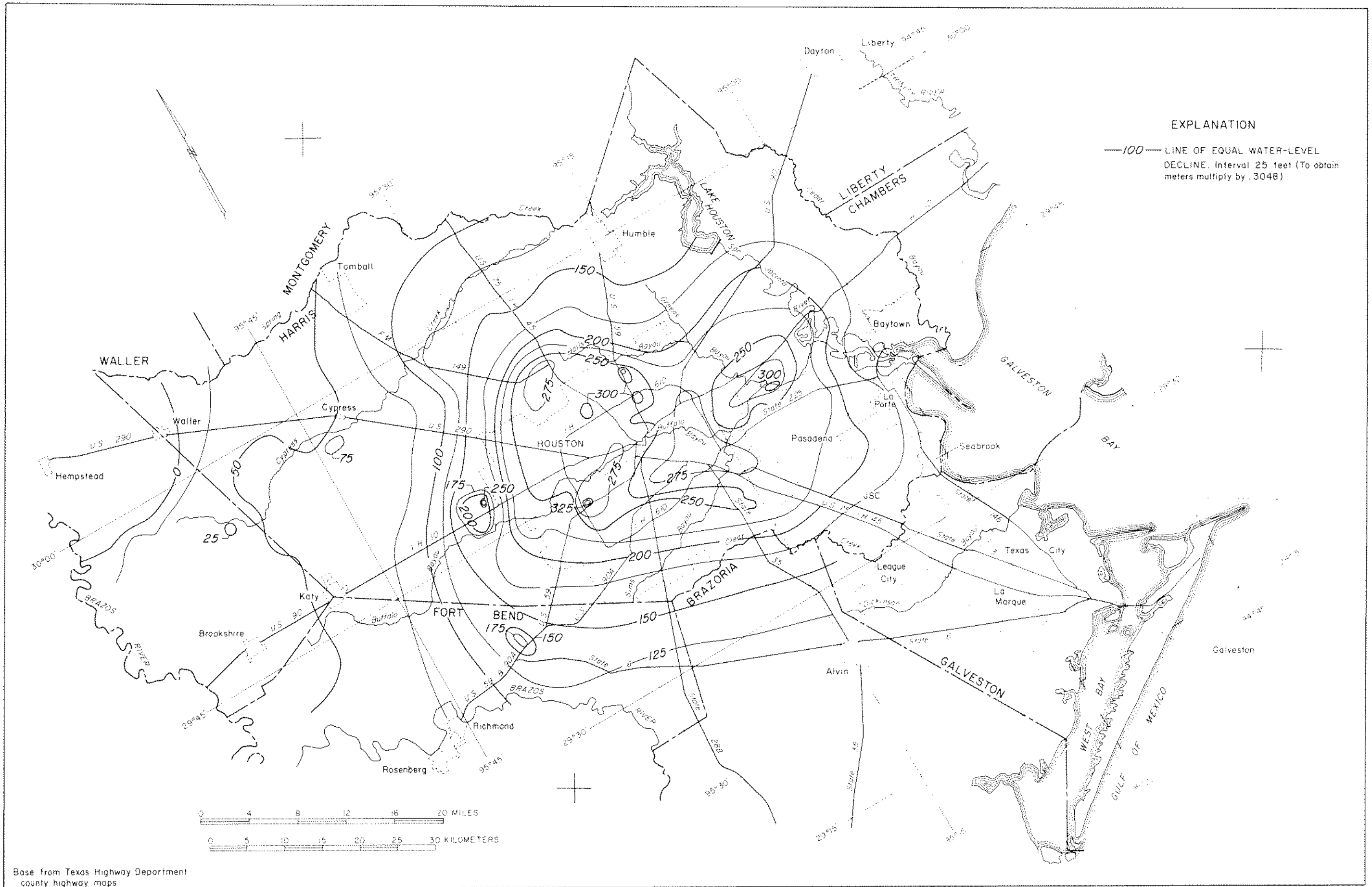

FIGURE 3.-Approximate Declines of Water Levels in Wells Completed in the Evangeline Aquifer, 1943-1973

beds of fine-grained material, the varying total thickness of fine-grained material, the vertical distribution of changes in artesian head, and the relation of compressibility to depth of burial.

As an example of the latter, about 55 percent of the subsidence in the southern part of Harris County is due to compaction in the Chicot aquifer, which is the upper one-fourth of the estimated compacting interval. More than 0.3 meter of subsidence occurred at Pasadena between 1906 and 1943.

Figure 5 shows subsidence for 1964-73. The maximum amount of subsidence during the period was about 1.1 meters. The indicated average maximum rate for the 9-year period is about 0.12 meter per year as compared to the maximum average of 0.08 meter per year for the 30-year period 1943-73. Thus, during the last part of the 1943-73 period, the rate of subsidence has accelerated. In addition, the area of subsidence is increasing. The area in which subsidence is 0.3 meter or more has increased from about 906 square kilometers in 1954 to about 6,475 square kilometers in 1973.

Where total clay thicknesses of similar unit compressibility exist, gross compressibility for a given amount of head decline should be comparable. In addition, where individual bed thicknesses and rates of head decline are similar, the rates of subsidence should be comparable. If so, field data obtained in the Houston area may have transfer value to yet undeveloped areas of the Texas Gulf Coast. Some effort has been made to relate subsidence to head decline and clay thickness for a specified time. At Seabrook, on Galveston Bay midway between Houston and Galveston, it is estimated that for each 0.3 meter of average water-level decline, 0.3 meter of clay will compact 0.0094 millimeter and 7.56 millimeters of subsidence will occur.

It has been suggested that some, if not all, of the numerous faults in the Houston-Galveston region are activated by man-caused land-surface subsidence. Attempts have been made to relate the fault activity to subsidence, but because of a lack of data, the relationships are not clear. It has also been hypothesized that the numerous faults act as barriers to ground-water flow and therefore control subsidence; however, data on artesian-pressure fluctuations in the area do not support this hypothesis.

Future Subsidence in the Region

Water from Lake Livingston on the Trinity River, about 97 kilometers east of Houston, will become available in 1976. Voluntary commitments to purchase surface water have been made by all major industries using ground water in the southern half of Harris County. As a result, it is estimated that ground-water pumping will decrease by about 3.1 cubic meters per second in the area of maximum artesian-pressure decline and subsidence. An analog-model study of the decrease suggests a maximum water-level recovery of 30 meters in the center of the bowl of subsidence. Data are not sufficient to determine the head recovery necessary to stop subsidence, but the rate of subsidence is expected to decrease substantially.

The Harris-Galveston Coastal Subsidence District was created by the Texas Legislature in 1975 to "provide for the regulation of the withdrawal of ground water within the boundaries of the district for the purpose of ending subsidence which contributes to or precipitates flooding, inundation, or overflow of any area within the district, including without limitation rising waters resulting from storms or hurricanes." The district plans to monitor the stress-strain relationships with additional compaction monitors and piezometers designed for installation prior to the expected voluntary decrease in ground-water pumping. The data collected will be the basis for controlling pumpage through well permits.

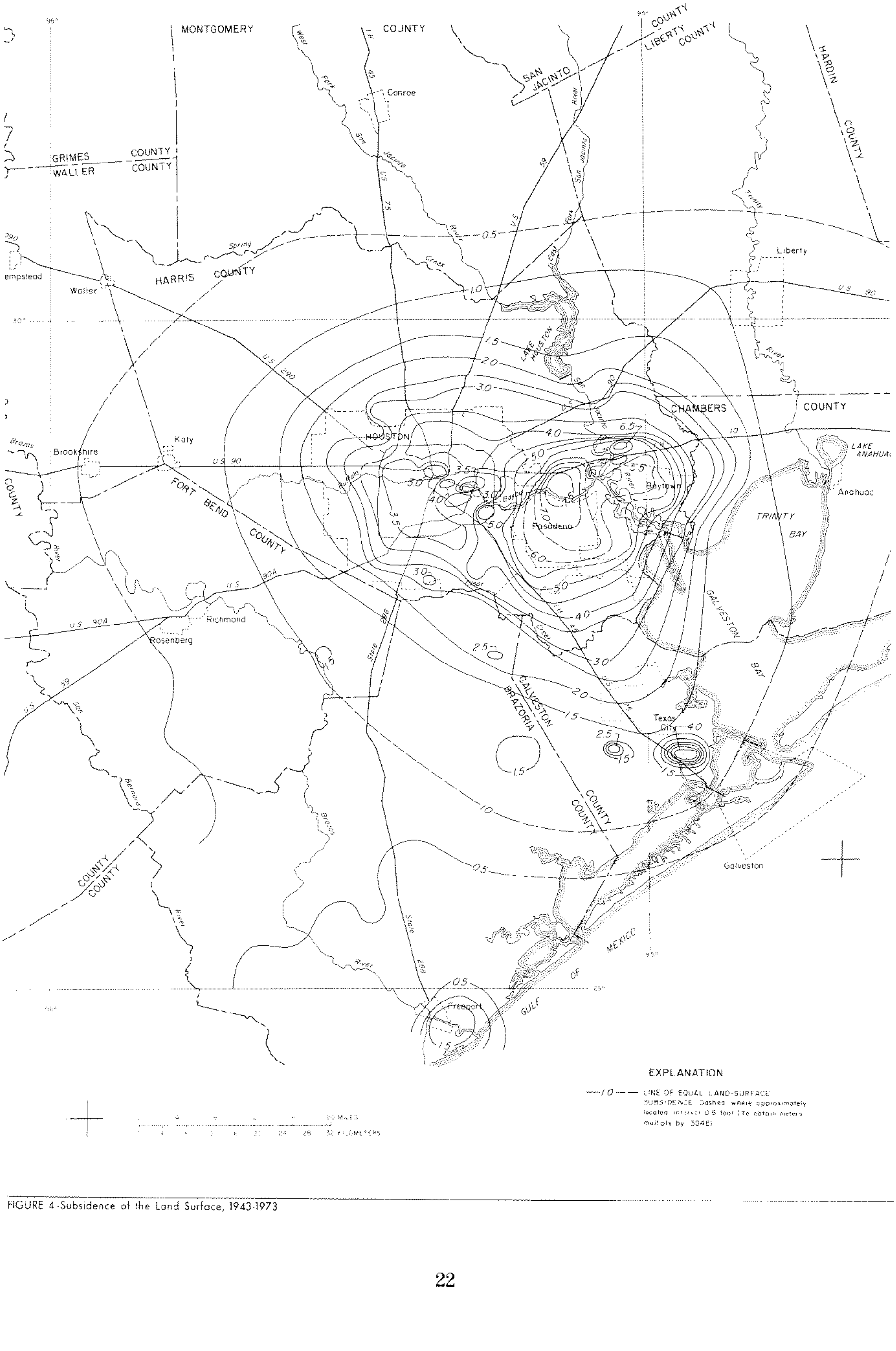

FIGURE 4-Subsidence of the Land Surface, 1943-1973

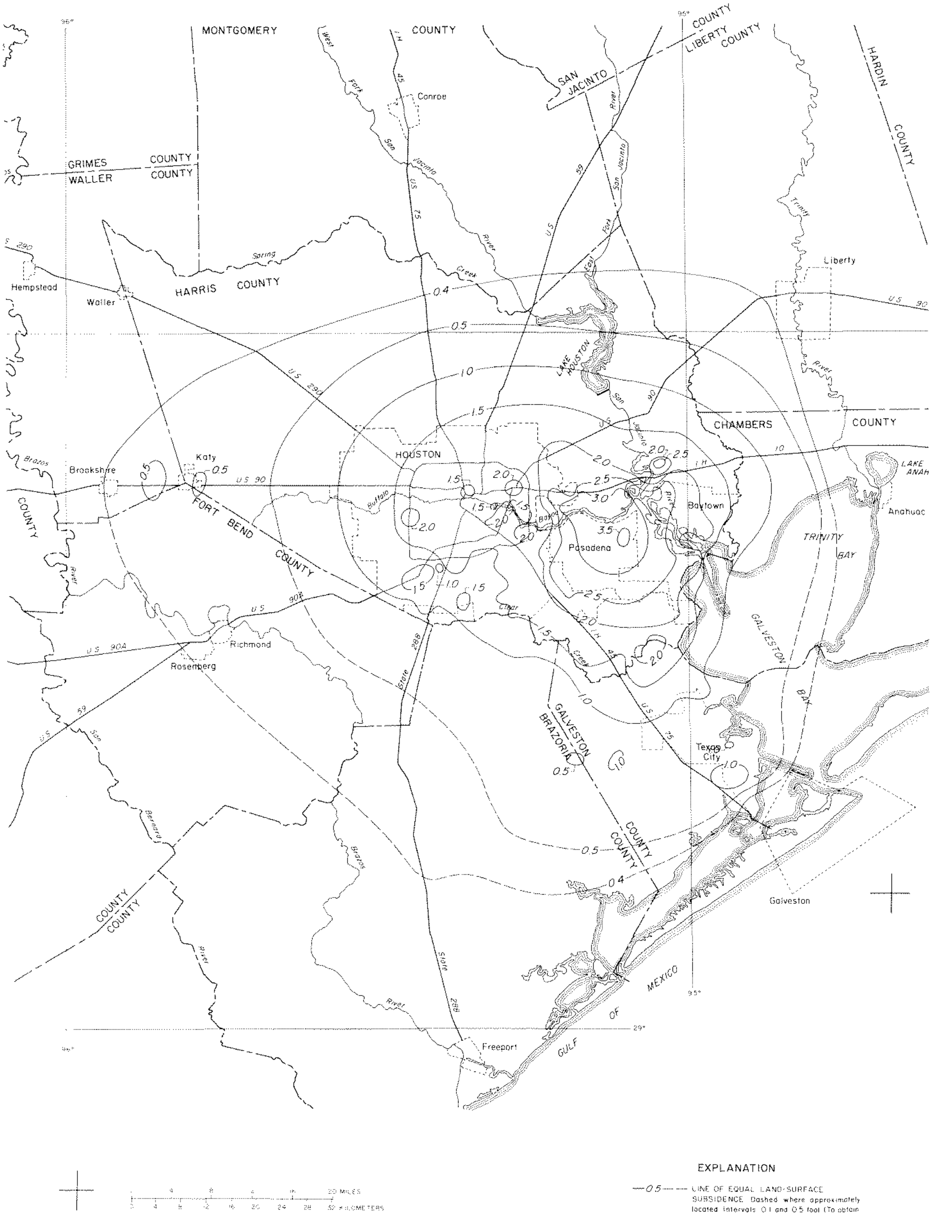

FIGURE 5. Subsidence of the Land Surface, 1964-1973

References

American Oil Company, 1958, Refinery Ground Subsidence: Plant Engineering Dept., Texas City, Tex., 58 p.

Gabrysch, R. K., and Bonnet, C. W., Land-Surface Subsidence in the Houston-Galveston Region, Texas: Tex. Water Devel. Board Rept. 188, 19 p.

Pratt, W. E., and Johnson, D. W., 1926, Local Subsidence of the Goose Creek Oil Field: Jour. Geology, v. XXXIV, no. 7, pt. 1, p. 578-590.

Winslow, A. G., and Doyel, W. W., 1954, Land-Surface Subsidence and Its Relation to the Withdrawal of Ground Water in the Houston-Galveston Region, Texas: Econ. Geology, v. 49, no. 4, p. 413-422.

Publication n°121 of the International Association of Hydrological Sciences
Proceedings of the Anaheim Symposium, December 1976

RECENT TENDENCIES OF THE LAND SUBSIDENCE IN TOKYO

M. Ishii, F. Kuramochi and T. Endo
Institute of Civil Engineering, Tokyo Metropolitan Government
1-1-18, Kōnan, Minato-Ward, Tokyo

Abstract

In the east area of Tokyo, the groundwater level has been dropped to about 60m due to the surplus withdrawal of the groundwater from various aquifers. The cumulative land subsidence since the early 1900's is 4.57m in 1975. The water level and land subsidence, however, have taken a favorable turn during several years as follows:

1. The groundwater level recovered to 10-30m since 1971 and the annual land subsidence is 1-2cm in the alluvial lowland in 1975.
2. The upheaval of land surface was measured at various places to conform with decrease of the land subsidence.
3. The water level is recovering due to the restriction of the groundwater withdrawal, but alluvial soft clay layer is still compacting. On the other hand, sand rich diluvium deposit is expanding in the whole area of Tokyo according to recovery of water level.
4. With the recovery of the water level, chlorine ion in ground water is reduced, and tritium ratio is increased.

1. Introduction

The large cities in Japan have been developed in seaside plains by means of the topographical factor. The development of the land subsidence occurred in some areas of Tokyo, where particularly population is highly being increased, is a serious problem in respect of the flood control and environmental programs.

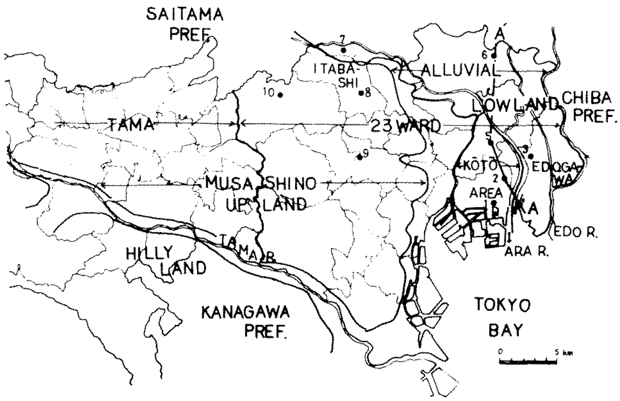

Fig.-1 Map showing the area discussed in this paper.
Note, •:Observation station (1: Minamisuna. 2: Kameido. 3: Shinedogawa. 4: Kojima. 5: Azuma. 6: Shinmeiminami. 7: Todabashi. 8: Itabashi. 9: Sinjuku. 10: Nerima.)
A-A': Section line of Fig.-12.

Table-1 Transition of the subsidence area more than 10cm, a year (in square kilometer)

Year	Area	Index number
1959	43	100
1960	53	123
1961	74	174
1962	64	149
1963	69	160
1964	42	98
1965	24	56
1966	12	28
1967	18	42
1968	30	70
1969	20	47
1970	33	77
1971	16	37
1972	4	9
1973	15	35
1974	6	14
1975	0	-

Half a century is about to pass since the subsidence of the lowland in Tokyo has been considered due to groundwater withdrawal. The maximum subsidence rate during this period is 4.57m in Kōtō ward. The leveling network of the land subsidence measured till 1930 and so was less, and the distribution state being unknown. The cumulative subsidence at lowland area from 1938 to 1975, the survey of the land subsidence on a full-scale was commenced in 1938, is about 3m in Kōtō area as shown on Fig.-2.

Such a land subsidence was limited in Kōtō area enclosed with the Sumida and Ara rivers in the early days. However, with the magnification of industrial zone after the Second World War, the subsidence area became magnified in order, and in the latter half of 1950's, the southern part of Kantō plain forming a large subsidence area.

The degree of the land subsidence of making a center of alluvial lowland in Tokyo was annually increased since 1950, and in 1961 the area to be subsided in more than 10cm per year becoming 74km^2 (Table-1). To prevent such a land subsidence, newly providing well was not allowed in Kōtō area since January, 1961 and in 23 wards area of Tokyo from July, 1963. After that, in Kōtō area the restriction on groundwater withdrawal was put in practice after substitute water for industrial use was supplied. But regardless of having restricted using the groundwater near the estuary of the Ara river, the subsidence of 20cm was succeed through the year. For the time being, it was considered that concerning this matter, the water soluble natural gas, which had been extracted in this area since 1951, had given a big effect to the land subsidence in addition to such as thick soft clay layer being deposited near the estuary of the Ara river and the insufficient restriction of groundwater withdrawal. Fig.-3 shows the land subsidence developed in 1968, and that being the one in most violent time.

After that, in northern part of alluvial lowland, the restriction on the groundwater withdrawal was started in December, 1971 and extracting the water soluble natural gas near the estuary of the Ara river was banned in December, 1972. By means of such a series of the restriction of the groundwater withdrawal, the water levels in 23 wards area of Tokyo were recovered and the tendency of the land subsidence being annually reduced since 1972.

On the other hand, in the west area, called Tama area, newly providing deep wells for industrial and building use is prohibited but the

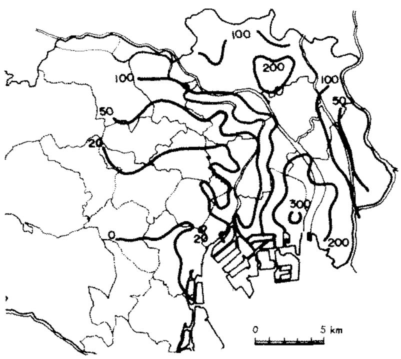

Fig.-2 Cumulative subsidence of land surface, 1938-1975 (in cm).

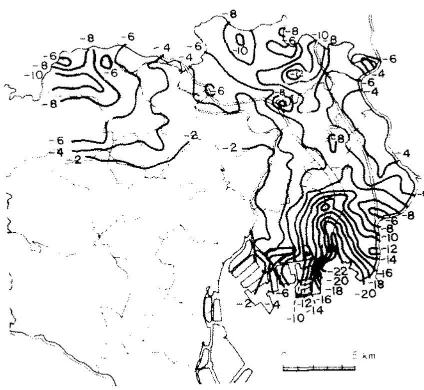

Fig.-3 Subsidence of land surface, 1968 (in cm).

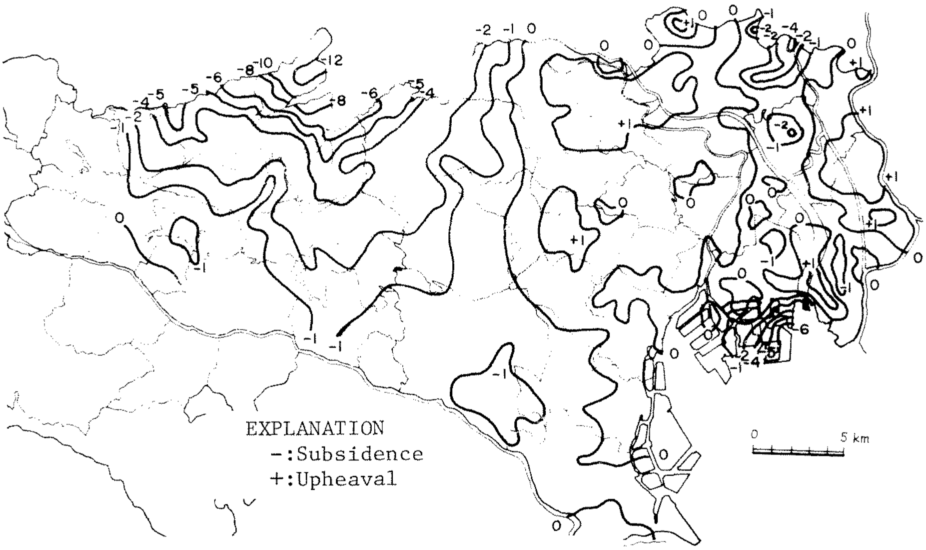

Fig.-4 Change of land surface, 1974 (in cm).

groundwater withdrawal from existing well has not been executed. The groundwater of this area is mainly used as domestic water, and quantity of withdrawal about 500,000m^3/day is being continued. The water level is yearly dropped 3-4m by this reason, and finding subsiding area over 10cm per year till 1974. However, in view of the fact that the restriction of the groundwater withdrawal was carried out in 23 wards area adjacent to

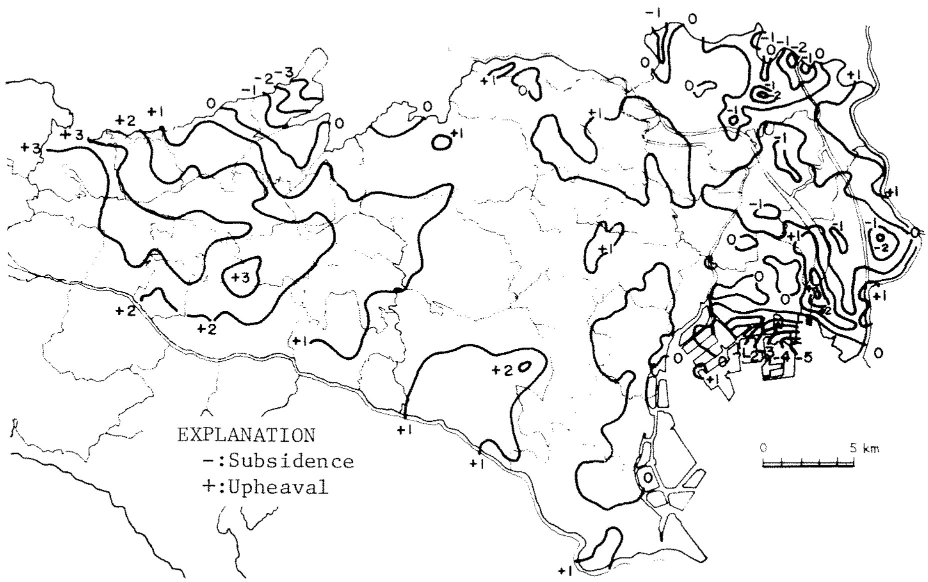

Fig.-5 Change of land surface, 1975 (in cm).

the west area and the southern part of Saitama Prefecture. The water level has been almost recovered from its equilibrium state. Fig.-4 shows the change of the land surface for the year of 1974,and Fig.-5 indicating that of 1975.

The land subsidence in Tokyo was rapidly reduced during several years. In 1975, the upheaval of the land surface was recognized over the extensive areas. This report is clarified depending on the records of observation wells mainly in regard with the latest tendencies of the land subsidence in Tokyo.

2. Hydrogeologic Setting

Tokyo Metropolis is located in the southern part of Kantō plain. In its west side, The Kantō Mountains having outcroped rocks composed with the Pre-Tertiary deposit are developed. The hilly regions are developed in its mountain foot and the south side of the Tama river. Musashino upland is developed in the north part of the Tama river, and alluvial lowland comparatively high in about 20m being distributed in the east side. The subsidence area in Tokyo comprise Musashino upland and alluvial lowland. The stratum in the area is shown on Table-2 classified by the unit of geology.

Among these, strata forming the aquifer system of artesian water are in the Tokyo Group and the Kazusa Group in upland area, and the Tokyo Group in the lowland area. The compaction accompanied with lowering of the water level is caused over the whole strata except volcanic ash layer and terrace gravel layer.

3. Land Subsidence Investigation System in Tokyo

The basis of the land subsidence investigation consist of both first order leveling and measurement of compaction of soil layer and water level. As in October, 1976, the investigated area measured by the leveling is $900km^2$, and that being made once a year. The compaction rate of the soil layer is carried out by 68 observation wells belonged to the observation stations, and the water level being measured by automatic recorder.

On the other hand, for analysing the compaction mechanism of soil layers, the change of pore water pressure, which is accompanied with the change of water level of the aquifer, is being measured by the pore water pressure gauge. This is made to use the automatic recorder at five places

Table-2 Stratigraphic succession in the Tokyo area

Region / Age	Musashino upland	Alluvial lowland	Thickness in meter	Facies
Holocene		Yūrakuchō Form.	10- 30	Soft clay
Pleistocene		Nanagochi Form.	10- 30	Sand,clay
	Tachikawa loam Tachikawa gravel Musashino loam Musashino gravel		10- 15	Volcanic ash Terrace gravel Volcanic ash Terrace gravel
	Tokyo Group		50-450	Sand, clay gravel
Pliocene	Kazusa Group		1000+	Upper: Sand Lower: Sandy mud

of the alluvial lowland from April, 1970 to adopt the soil layers of 10-50m under each ground surface as the object. Further, surveying the quality of the groundwater at the observation wells and general wells is executed once annually, and the analysis of flow mechanism of the artesian groundwater being carried out.

4. Correlation of Quantity of Withdrawal and Groundwater Level

It is said that the utilization of the groundwater was prosperous in about 1920 in Tokyo. After that, according to the increment of the pumpage, the groundwater level of flowing water in the northern part of the alluvial lowland in 1920 and so was dropped till -63.94m in August, 1971.

The change of the water level of the representative observation well which is under the Institute of Civil Engineering is shown on Fig.-6. In accordance with this, the lowering of the water level was continued till 1965 in Kōtō area and 1971 in the other area, and after that being recovered. Such a recovery of the water level agreed with the period when the extraction of the groundwater from existing wells was banned in the observation area and its environs.

The relation between such reduction of the groundwater withdrawal and the recovery of the water level in detail will be as follows: Fig.-7 shows the quantity of the withdrawal in Itabashi ward of northern part of alluvial lowland and the change of water level at Todabashi No.1 observation well (depth of strainer, 256-268m), which is located in the same ward. In this area, using deep well, less than 160m in depth was prohibited before December, 1971, and also deep well, more than 160m being done before May, 1974. In that result, about 90,000m^3/day, quantity of groundwater withdrawal in 1971 was reduced to about 10,000m^3/day in May, 1974. On the other hand, the water level was remarkably recovered to conform with reducing the quantity of withdrawal from the latter half of 1971 and the middle of 1974. The coefficient of correlation between the quantity of groundwater withdrawal and water level from January, 1971 to December, 1974 is 0.966.

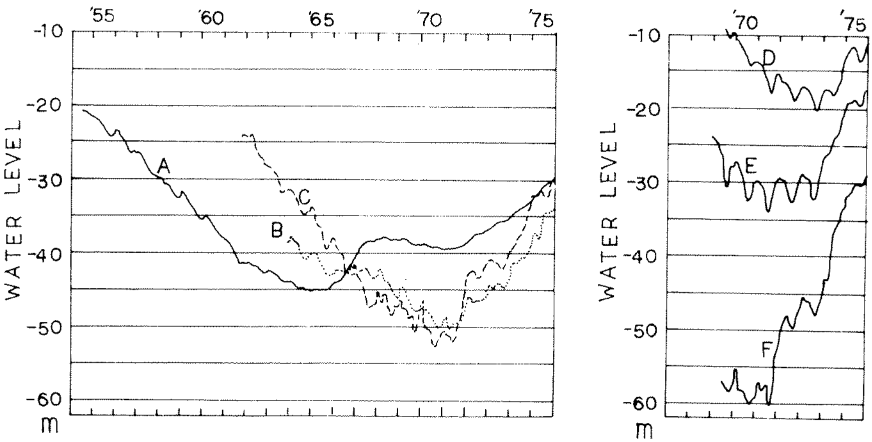

Fig.-6 Annual change of groundwater levels at observation wells.
A:Kameido O.W., B:Shinedogawa O.W., C:Todabashi O.W., D:Nerima O.W., E:Shinjuku O.W., F:Itabashi O.W.

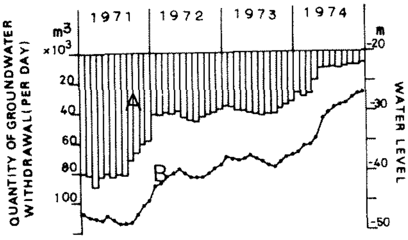

Fig.-7 Relation between quantity of groundwater withdrawal in Itabashi Ward (A) and water level of Toda-bashi No.1 o.w.(B).

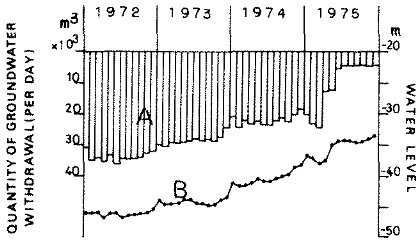

Fig.-8 Relation between quantity of groundwater withdrawal in Edogawa Ward (A) and water level of Shinedogawa No.2 o.w.(B).

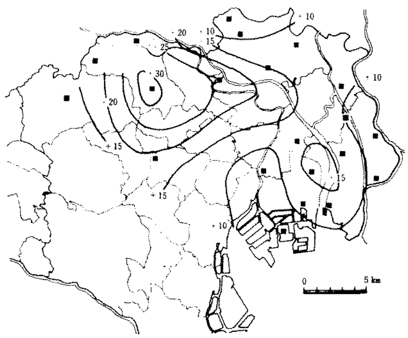

Fig.-9 The total recovery of water level.

Fig.-8 shows the quantity of withdrawal in Edogawa ward located in the southern part of the alluvial lowland and the change of water level at Shinedogawa No.2 observation well (depth of strainer, 129-150m) in the same ward. In this area, the restriction of groundwater withdrawal was completed in March, 1975. About 30,000m^3/day of the quantity of withdrawal in 1972 was reduced to about 4,000m^3/day in June, 1975. The coefficient of correlation between the quantity of groundwater withdrawal and water level from January, 1972 to December, 1975 is 0.956.

Water level which was raised due to the restriction of the groundwater withdrawal is about 30m in Itabashi ward as shown on Fig.-9.

5. Change of Pore Water Pressure

In near the estuary of the Ara river in the southern part of alluvial lowland, some 20cm of the subsidence had been continued in the past, but the subsidence rate was rapidly decreased since 1973. This means that Tokyo Metropolitan Government purchased the mining right of the water soluble natural gas that is reserved in more than 450m below the surface in this area, and extracting the gas was banned at the end of December, 1972.

The relation of the quantity of compaction of soil layer and the water level at Minamisuna observation station in natural gas collection area is shown on Fig.-10. Some 60m of the alluvial soft clay is deposited in the area. The quantity of compaction of this layer has been annually reduced since 1961 when newly installing wells was prohibited. On the contrary, the compaction of the soil layer having more than 70m in depth was maintained to conform with the fluctuation of the water level. However the expansion of 2-3cm has been kept since 1973.

The change of the pore water pressure in such alluvial soft layer with the progress of the recovery of the water level of the aquifer system

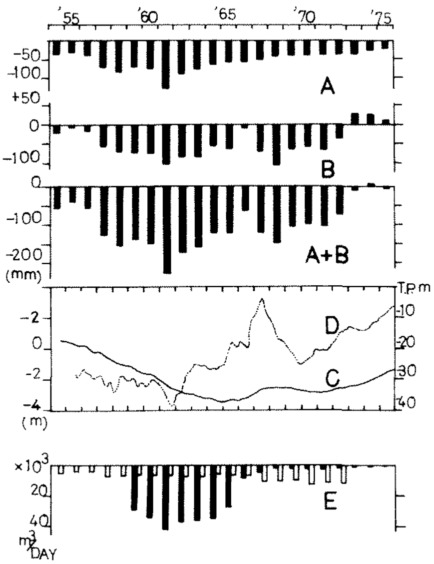

EXPLANATION
A:Compaction of soil layer from surface to -70m (in mm)
B:Compaction or Expansion of soil layer below -70m (in mm)
A+B:Change of land surface (in mm)
C:Water level (in mean sea water level)
D:Difference of water level (compared with the year before)
E:Quantity of groundwater withdrawal
▬ :Groundwater
▭ :Gas water

Fig.-10 Relation between compaction or expansion rate of soil layer and water level at Minamisuna o.w. (Depth, 70m).

will be as follows: The pore water pressure gauges are provided to install these in 20, 30m in the alluvial clay layer and 50m in sandy layer of the Nanagochi Formation under the surface at the Minamisuna observation station. The pore water pressure gauge are connected with standard pipes. The quantity of compaction in respective depth can be measured.

Table-3 shows the annual change of the compaction or expansion rate of the soil layer concerning the standard pipes for surveying the pore water pressure and the land subsidence observation wells.

Table-3 Annual change of the compaction or expansion rate of soil layer at Minamisuna observation station (in mm).

Year / Depth(m)	1971	1972	1973	1974	1975
0-20	-29.3	-14.1	-16.3	-11.3	-9.1
20-30	-13.5	-17.5	-16.8	-13.8	-10.5
30-50	+2.5	-5.2	+0.6	-3.4	-1.7
50-70	+0.3	+0.6	-3.4	+1.3	-0.1
70-130	+2.2	+2.5	+1.2	+0.9	+2.0
130+	-69.1	-37.5	+26.4	+21.0	+22.0

Note, -:Compaction, +:Expansion

Fig.-11 shows the water level from the surface converted from pore water pressure at each depth. The water level of aquifer was recovered to about 24m under the surface in December, 1975, but the pore water pressure in the clay layer of the Yūrakuchō Formation in 30m under the surface is still dropped, and the compaction of the soil layer being continued. On the other hand, the pore water pressure of the Nanagochi Formation in 50m under the surface dropped till 1972, but after that being recovered.

In the Tokyo Group, the expansion which is caused by the increase of the pore water pressure is recognized by the recovery of the water level of the aquifer, but the compaction is continued in the alluvial deposit which the recovery of the pore water pressure is not noticed.

Such a tendency was found whole area of 23 wards in Tokyo since 1975. In near the estuary of the Ara river where extracting the water soluble

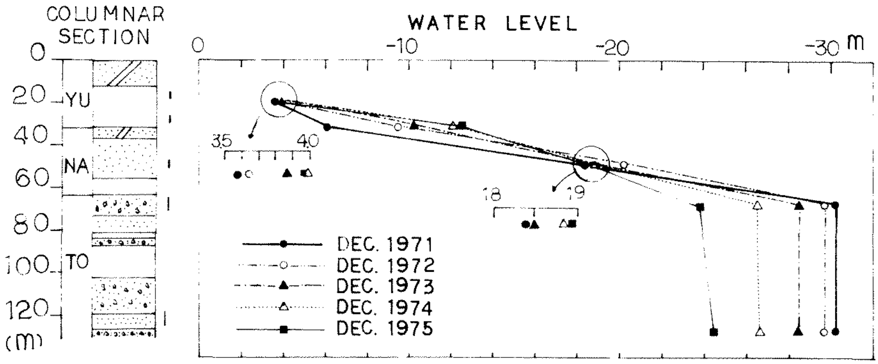

Fig.-11 Annual change of pore water pressure and water level at Minamisuna observation station.

natural gas was made and where the depth of the alluvial deposit is thin and in the area of Musashino upland, the upheaval of the land surface can be seen. Such an upheaval is considered to be a rebound phenomenon of the land subsidence (Allen & Mayuga, 1969).

6. Quality of Groundwater

The land subsidence is a compaction phenomenon of soil layer due to lowering water pressure of aquifer system, and that the dehydration of the pore water happen in such a process being acknowledged. A consideration is paid on the effect which such pore water will give to the quality of groundwater.

Fig.-12 shows the water quality distribution in the alluvial lowland. According to this graph, the chlorine ion content is more than 100 ppm along Tokyo Bay, and in the inland being rapidly decreased. In 1972, the chlorine ion content and the conductance are distributed as to close toward Tokyo Bay, but being altered as to be open toward Tokyo Bay since 1973 when the restriction of groundwater withdrawal and the ban of extracting the water soluble natural gas were made. The tritium ratio is little in less than about 3 T.R. till 1973, and nearly showing the same value. But along Tokyo Bay and in the northern part of the alluvial lowland, these are being rapidly increased.

Corresponding to the alteration of the quality of groundwater with the water level will be as follows: In the lowering period of the water level, the chlorine ion content is increased and the tritium ratio is decreased. On the contrary, in case of the recovering period of the water level, the opposite phenomenon is happened in 1-2 years after the recovery of the water level in the alluvial lowland, but, that occures nearly at the same time with the recovery of the water level in Musashino upland (Fig.-13).

Chlorine ion content is increased in the lowering period of the water level has been considered becoming salinity by the intrusion of sea water in the past. The tritium ratio of the sea water is about 30 T.R. in Tokyo Bay (Kasida & Inoue, 1976). If becoming salinity by the sea water, the tritium ratio should be increased. And the border between the area of high chloride groundwater of 100 ppm and over in the chlorine ion content and the area of fresh water is remain unchanged regardless of the water level having been lowered since 1930. On the other hand, in the obser-

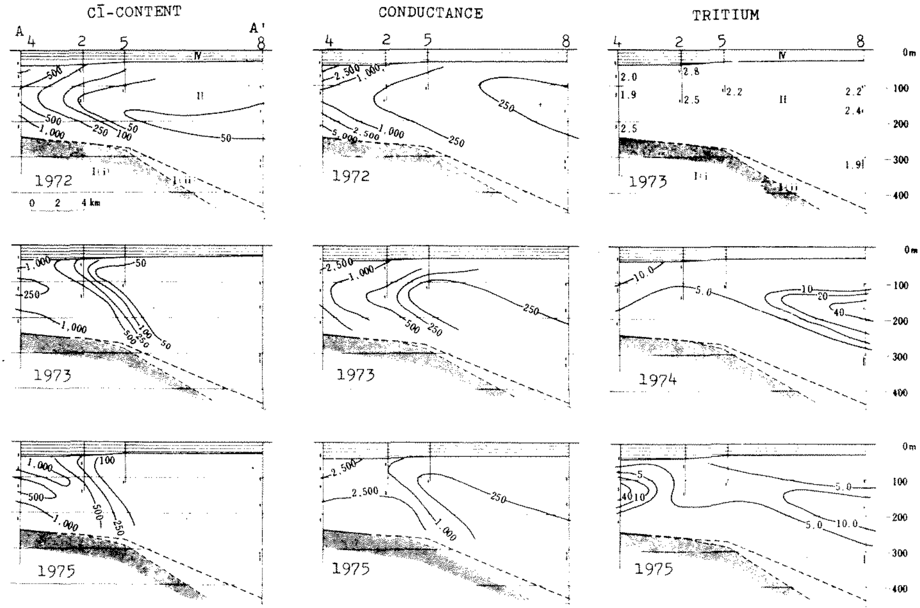

Fig.-12 Vertical distribution of groundwater quality in alluvial lowland (Section line is shown on Fig.-1).
Note, I(i):Mud facies of Kazusa G., I(ii):Sand facies of Kazusa G., II:Tokyo G., IV:Nanagochi F. and Yūrakuchō F..

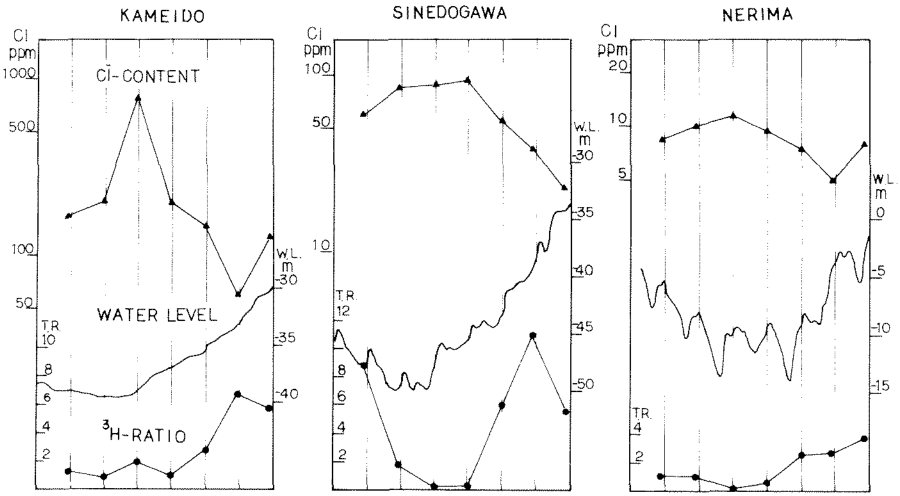

Fig.-13 Annual change of groundwater quality.

vation well on Musashino upland where is outside of the area of high chloride groundwater and also far from tidal river, the increase of the chlorine ion content and the decrease of tritium ratio are noticed at the lowering period of the water level. It is better to consider that by the reason of the tritium ratio being reduced, the supply of the groundwater is being made by squeezing out the pore water than considering that cause by the reason of the chlorine ion being increased at the lowering period of the water level to be due to the vertical permeation of the surface water which was artificially polluted.

As stated above, the lowering period of the water level, namely, the period when the compaction of the soil layer is kept will indicate that the pore water moving to the vertical direction has been eminent than circulating groundwater which is moving the aquifer in horizontal direction. Specially as the southern part of the alluvial lowland has no supply of fresh water on the geological structure and the tritium ratio is small value, zero, it is considered that the groundwater has been mostly supplied by squeezing out the pore water. But due to the squeezing out the pore water having been stopped after the restriction of groundwater withdrawal, the quality of the groundwater is considered to become gradually showing the quality of circulating groundwater.

Conclusion

Land subsidence in Tokyo, which has continued half a century, rapidly taken a favorable turn during several years by means of restrictions of groundwater withdrawal. As a result of this fact, the rebound phenomenon was recognized over the extensive area. The following became clear after the analysis of the observation records.

1. The groundwater level is recovered subsequent to the reduction of the groundwater withdrawal. The relation between the quantity of the groundwater withdrawal and water level is approximately shown in a simple equation.

2. The expansion phenomenon can be noticed in the deep soil layer such as the Tokyo Group and Kazusa Group due to the recovery of the water level in the aquifer system, but the compaction being still continued in the alluvial clay layer.

3. The groundwater was supplied by squeezing out the pore water during the lowering period of the water level. After the restriction of the groundwater withdrawal, the water level become recovered, and causing so that the quality of groundwater may indicate the circulative groundwater.

References

Allen, D.R. and Mayuga, M.N., 1969,The Mechanics of Compaction and Rebound, Wilmington Oil Field, Long Beach, California, U.S.A.: Land Subsidence, Vol.II, Publ. No. 89. IASH-Unesco-WMO, p.410-423.

Kashida, Y. and Inoue, Y., 1976,Survey Data on Tritium Concentration in Environment: The 16th Abstract of Survey Data of Radioactivity. Science and Technology Agency of Japan. p.55-59.

Publication n°121 of the International Association of Hydrological Sciences
Proceedings of the Anaheim Symposium, December 1976

SUBSIDENCE OF THE CITY OF MEXICO; A HISTORICAL REVIEW

Germán E. Figueroa Vega
Comisión de Aguas del Valle de México, S.R.H. México

Abstract

Subsidence due to groundwater pumpage has been one of the main problems of Mexico City. Maximum measured subsidence, of the order of 9 m has made sewage disposal expensive and risky.

The phenomenon, which began during the past century, was discovered in 1925 by Roberto Gayol through comparison of two precision levelings of 1877 and 1924 and has been recorded up to 1973, together with piezometric measurements in the clayey strata and more recently, in the underlaying aquifer.

A mathematical model, based on a correspondence principle, has been developed to simulate the entire phenomenon, although its calibration has been impaired because data pertaining to the aquifer are relatively scarce. Some preliminary results are presented.

The subsidence of Mexico City, built on highly compresible clays, is, for its magnitude, one of the most remarkable cases in the world.

At the beginning of this Century, Roberto Gayol, author of the sewage project of the city and Director of its construction, was blaimed for the subsidence of the hydraulic structure of San Lazaro, located at the beginning of the main sewage channel of the city. He demonstrated before the Association of Engineers and Architects of Mexico City, in 1925, that the behaviour of the structure was the result of the general sinking of the bottom of the Valley, presenting as evidence two precision levelings, performed in 1877 and 1924 of a monument located near the Cathedral.

Gayol attributed the phenomenon to the draining effect of the recently built sewage system.

Twenty-three years later, in 1948, Nabor Carrillo demonstrated, based on Terzaghi's consolidation theory, that the subsidence of the city was due to the extraction of groundwater for domestic, industrial and municipal uses. He achieved a fairly good comparison of actual and theoretical piezometric evolutions at shallow depth computed from observed subsidence rates.

The city of Mexico was built over lacustrine deposits constituted by a clayey layer of variable thickness overlaying a sand and a gravel aquifer.

Originally, fresh water was provided to the city from springs located at the lower part of the western mountains; by 1860 the first deep well was drilled to provide water for a public swimming pool and thereafter drilling became common all over the city. Accordingly, it is probable that the subsidence of Mexico City began at the same time. This conclusion is supported by the fact that all the wells of the city were flowing wells at the beginning of this century. Also, the nearest springs located at the Chapultepec forest practically disappeared by 1890, pointing to the generalized groundwater drawdown responsible for the subsidence.

The quantitative history of the subsidence of the city of Mexico has been recorded since 1891 through several succesive precision levelings. However, measurements were limited to the area covered by the city in that year. Since 1952, levelings have been extended to include the rest of the city.

TABLE 1. MEXICO CITY PROBABLE ORDERS OF MAGNITUDE OF GROUNDWATER PUMPAGE

Year	Pumping Rate
1860	0.0 m^3/s
1910	0.5 m^3/s
1930	1.5 m^3/s
1940	6.0 m^3/s
1950	9.0 m^3/s
1960	9.0 m^3/s
1970	9.0 m^3/s

As an average, the older part had a subsidence rate of 4.5 centimeters per year from 1891 to 1938, 7.6 centimeters per year from 1938 to 1948, reaching a maximum of 44 centimeters per year from 1948 to 1950 and 46 centimeters per year from 1950 to 1951.

Since then, the subsidence rate has been diminishing, being presently of the order of 5 centimeters per year.

As for the total area covered by the city, the average subsidence rate of 14 centimeters per year corresponding to the period 1952-1959 has also diminished to the order of 6 centimeters per year in 1970-1973.

Protruding casings are also another means of observing the subsidence at different parts of the City. In general it has been observed that protrusion of casings is of the same order as the measured subsidence, with plus or minus differences.

The maximum observed subsidence has taken place within the older

TABLE 2. MEXICO CITY (OLDER PART)

From-To	Total Subsidence (m)	Average (m/ year)
1891 - 1938	2.12	0.045
1938 - 1948	0.76	0.076
1948 - 1950	0.88	0.440
1950 - 1951	0.46	0.460
1951 - 1952	0.15	0.150
1952 - 1953	0.26	0.260
1953 - 1957	0.68	0.170
1957 - 1959	0.24	0.120
1959 - 1963	0.22	0.055
1963 - 1966	0.21	0.070
1966 - 1970	0.28	0.070
1970 - 1973	0.17	0.051

TABLE 3. MEXICO CITY (TOTAL AREA)

From-To	Total Subsidence (m)	Average (m/ year)
1952 - 1959	1.014	0.140
1959 - 1963	0.440	0.110
1963 - 1966	0.254	0.080
1966 - 1970	0.260	0.065
1970 - 1973	0.203	0.059

TABLE 4.

Well	Protrusion 1970 - 1973 (m)	Subsidence 1970 - 1973 (m)
San Juan de Aragón Campamento	0.304	0.440
Czda. Guadalupe	0.130	0.172
Sta. Isabel Tola	0.259	0.320
Monumento a la Revolución Frontón México	0.179	0.200
Jardín de los Angeles No. 2	0.076	0.145
Insurgentes Norte 1407	0.199	0.283
Penitenciaría Jardín	0.233	-
Gómez Farías No. 61	0.113	0.140
Monumento a la Revolución Procuraduría	0.323	-
Jardín de los Angeles No. 3	0.100	0.145
Jardín de los Angeles No. 1	0.146	0.150

limits of the city, and has reached slightly more than 8.5 meters; however, this does not mean that this is the absolute maximum.

Damages derived from subsidence are of several types: damages to buildings, pavements and fresh water and sewage nets. However, the most important is the potential damages of a sewage water flooding, since sewage water must be now pumped to the main channel, which formerly was below the general elevation of the city.

Although this risk has been diminished by the recent construction of a deep sewage tunnel, the danger is still present because the main sewage channel must be kept in service, at least until the year 2000.

Besides, future subsidence may endanger the recently built deep tunnel and the also new subway. For these reasons, it is necessary to be able to predict the future evolution of the entire phenomenon, in order to take decisions about the future exploitation of the aquifer.

Since 1972, two models have been developed to simulate the subsidence of the city of Mexico on the basis of a previous work (Herrera and Figueroa Vega, 1969). The central idea of these models is to reduce the system of partial differential equations representing the behaviour of the main aquifer and the consolidating layer to one integrodifferential equation for the main aquifer, which includes the consolidation inputs through convolution, or memory terms.

If memory terms are kept withouth modifications, the model is exact; if they are simplified, the model is less precise. Simplifications are introduced to reduce computing time and to take account of the storage memory capacity of the available computer. Obviously, in such case, errors are introduced also.

Each model has 203 cells (the clayey zone is covered by 82 of them) and provides on, year by year, groundwater and soil surface levels.

Preliminary results indicate that with both kinds of models the simulation is feasible, within limitations introduced by simplifications, if any (Figueroa Vega, 1973). Recently the effort, has been focused on the calibration of both, and this part is the most difficult one, because historic data are relatively scarce, with the possible exception of subsidence itself.

References

Herrera, Ismael and Figueroa Vega, Germán E., 1969, A correspondence principle for the theory of leaky aquifers: Water Resources Research, v. 5, no. 4, pp. 900-904.

Figueroa Vega, Germán E., 1973, Aquifer and subsidence model for Mexico City: 85th annual meeting of The Geological Society of America, v. 5 no. 7, p. 620.

Publication n°121 of the International Association of Hydrological Sciences
Proceedings of the Anaheim Symposium, December 1976

DEVELOPMENT OF ARTIFICIAL RESERVOIRS BY INDUCING LAND SUBSIDENCE

Ismael Herrera* and Jesus Alberro
IIMAS* and Institute of Engineering
National University of Mexico.

Roberto Graue and Juan J. Hanel
S. de Recursos Hidráulicos
Mexico City, Mexico.

Abstract

In the project Lago de Texcoco four lakes are being built using pumping of groundwater to produce land subsidence. Mexico City as well as neighbouring Texcoco Lake subsoils, constitute leaky aquifer systems. Groundwater hydrology can be used to predict ground settlements and therefore to plan and control the corresponding works. In this paper the studies that in this manner have been carried out at Texcoco, Mexico, are briefly described.

Introduction

In the Proyecto Texcoco (1969) two lakes are being built in the first stage of its development and two more will be built in the second one. To construct them groundwater is being pumped in order to produce land subsidence 8m deep. Mexico City as well as neighbouring Texcoco Lake subsoil constitute leaky aquifer systems, and surface settlements are sensibly equal to the volume of extracted water. Thus, well hydraulics has been used to predict land subsidence.

The studies carried out in the period 1973-75 covered two aspects: the applicability of leaky aquifer theories; and the settlement analysis for the "Proyecto Texcoco". The applicability of the theories, as it is presently understood, was the subject of a previous report (Herrera, 1974). This paper describes the second part of the study (Herrera et al, 1974) in which many data and observations gathered in previous work (Proyecto Texcoco, 1969) were used. The main purpose of the analysis was to determine the feasibility of the project and to detect unforeseen problems that could endanger its successful completion. The description given here will be restricted to one of the lakes, called Texcoco Sur.

Relations between soil mechanics and well hydraulics

Well hydraulics is from the point of view of soil mechanics a consolidation problem. Some relations between the notations used in both of these sciences is given in this section (Terzaghi, 1956; Walton, 1970).

Consolidation coefficient C_v and permeability K, are related by:

$$K = C_v M_v \gamma_w \tag{1}$$

where γ_w is the specific weight of water and M_v the compressibility index. On the other hand:

$$C_v = \alpha = \frac{K}{S_s} = \frac{T}{S} \tag{2}$$

Here, S_s and S are the specific and total storage coefficients, respectively, and T is the transmissivity. Consider two aquifer separated by an aquitard of thickness b'; then, the pumping time t required for the interaction between the aquifers to be perceptible satisfies (Herrera, 1974):

$$\alpha' t/b'^2 = T_u/4 = t_u H^2/4C_v = \frac{1}{6} \tag{3}$$

Here, 2H=b', t_u is the time required to achieve a u^0/o degree of consolida-

*Institute for Research in Applied Mathematics and Systems.

tion under conditions of unidimensional flow, T_u is Terzaghi's time factor and the primes refer to aquitard properties.

Description of the study

To test the method of construction an experimental field was pumped for a period of 10 months (October, 1967 through July, 1968) (Proyecto Texcoco, 1969). In this place many soundings were made, particularly three deep soundings (Marsal, 1969). In order to verify the stratigraphy, a standard penetration test at a depth of 60m, was carried out. The mechanical properties of the aquifers were determined by means of several pumping tests. The piezometric heads were registered during the entire 10 months pumping period. Later, similar soundings and tests were made at the actual area of construction, before pumping was started.

A hydraulic model was developed for the experimental field which was calibrated using the measurements taken during its pumping. This model was later adjusted on the basis of Texcoco Lake conditions. Settlement predictions for this site were made under design, as well as actual operation conditions.

The hydraulic model

The field and laboratory observations imply in view of the range of applicability of the theories (Herrera, 1974), the following hydraulic model for the experimental field:

a) The subsoil constitutes a leaky aquifer system (fig 1), which has two main aquifers: the upper one called "hard layer" and the lower one called "deep deposits". The hard layer is limited above and below by aquitards called the upper and lower clay formations respectively; the deep deposits are limited below by an impervious stratum. All the layers are homogeneous.

b) The flow is vertical in the aquitards.

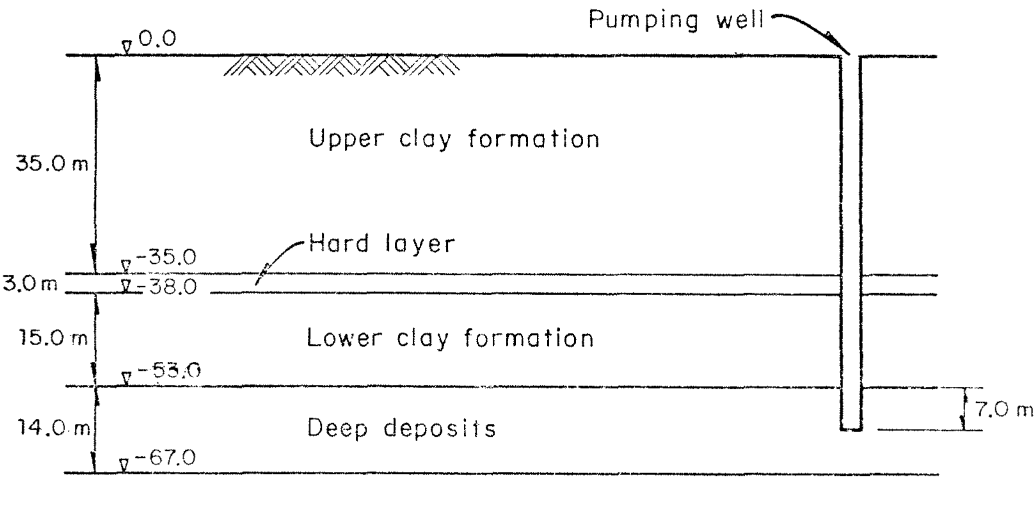

Fig. 1 Stratigraphy of the experimental field.

TABLE 1. PROPERTIES AT THE EXPERIMENTAL FIELD

Stratum	Thickess, b, in m	Permeability, K, in m/day	Transmissivity, T, in m^2/day	Storage Coefficient, S	$C_v = \nu = T/S$, in m^2/day	Specific storage Coefficent, S_s, in m^{-1}
Upper Clay	$b' = 35$ (1)	$K' = 0.47 \times 10^{-3}$	$T' = 1.64 \times 10^{-2}$	$S' = 1.82$	$C_v' = 9 \times 10^{-3}$ (1)	$S' = 5.2 \times 10^{-2}$
Hard Stratum	$b_1 = 3$	$K_1 = 6$ (1)	$T_1 = 18$	$S_1 = 1.65 \times 10^{-4}$	$C_{v_1} = 1.08 \times 10^{+5}$	$S_{s_1} = 5.5 \times 10^{-5}$ (1)
		$K_1 = 8$ (2)	$T_1 = 24$ (2)	$S_1 = 2.65 \times 10^{-4}$ (2)	$C_{v_1} = 9.05 \times 10^{+4}$ (2)	$S_{s_1} = 8.83 \times 10^{-5}$ (2)
Lower Clay	$b' = 15$	$K'' = 1.44 \times 10^{-5}$ (1)	$T'' = 2.16 \times 10^{-4}$	$S'' = 0.24$	$C_v'' = 9 \times 10^{-4}$ (1)	$S_s'' = 1.6 \times 10^{-2}$
Deep Deposits	$b_2 = 7$ (1)	$K_2 = 7.8$ (1)	$T_2 = 42$	$S_2 = 3.85 \times 10^{-4}$	$C_{v_2} = 1.08 \times 10^{+5}$	$S_{s_2} = 5.5 \times 10^{-5}$ (1)
	$b_2 = 14$ (2)	$K_2 = 7.5$ (2)	$T_2 = 105$ (2)	$S_2 = 1.24 \times 10^{-3}$ (2)	$C_{v_2} = 8.47 \times 10^{+4}$ (2)	$S_{s_2} = 8.83 \times 10^{-5}$ (2)

(1) Herrera et al, 1974

(2) Values yielded by calibration

c) There is no significant interaction between the main aquifers; thus, they work independently.

d) Each of the main aquifers is governed by the theory for small values of time (Herrera, 1974).

e) The strata are unlimited in the horizontal directions.

f) The volume of the lake created, is sensibly equal to the water extracted from the formations.

Table 1 gives the dimensions and properties of the strata at the experimental field. To apply this model to Texcoco Sur it was necessary to make the changes implied by table 2. An important change in the

TABLE 2. PROPERTIES AT TEXCOCO SUR

Stratum	Thickess, b_1, in m	Permeability, K, in m/day	Transmissivity, T_1, in m^2/day	Storage Coefficients, S	Coefficent C_v, in m^2/day	Specific storage Coefficient, S_s, in m^{-1}
Upper Clay	32	0.47×10^{-3}	1.5×10^{-2}	1.66	9×10^{-3}	5.2×10^{-2}
Hard Stratum	2	8	16	1.77×10^{-4}	$9 \times 10^{+4}$	8.8×10^{-5}
Lower Clay	16.5	1.44×10^{-5}	2.38×10^{-4}	0.26	9×10^{-4}	1.6×10^{-2}
Deep Deposits	8.5 or infinity	7.5	63	7.33×10^{-4}	$8.5 \times 10^{+4}$	0.9×10^{-4}

stratigraphy is that horizontal variations were too big to be ignored (fig 2).

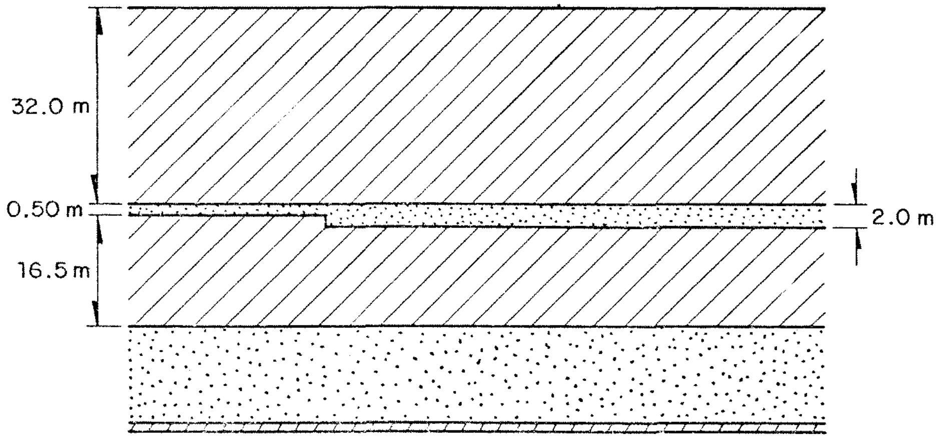

Fig. 2 Stratigraphy of Texcoco Sur Lake.
Measures, in meters.

Calibration of the model

The knowledge of the range of applicability of the theories, permitted to obtain reliable results and to keep the possible error sources under effective control. It was then possible to explain observed discrepancies and make adjustments in the model to remove them (Herrera et al, 1974). The basis for the calibration was comparison of calculated drawdowns and ground settlements with those observed (fig 3).

The drawdown observations used as basis for the comparison were taken at piezometric station EP1, which worked normally during the ten month period. The details of the computations are given by Herrera et al (1974).

The pumping period was divided in the manner shown in table 3. Satisfactory agreement was found between observed and computed piezometric heads when the property values shown in table 1 were used and a discharge distribution of 18% at the hard layer and 82% at the deep deposits was assumed. Many wells were closed on December 1968 which apparently produced a discharge redistribution; after this date 20% of the discharge came from the hard layer and 80% from the deep deposits.

After the model had been calibrated on the basis of drawdowns, overall comparison of the predicted and observed land settlements was made. The observations consisted of levelings of the area, carried out at several dates during the pumping period. For a pumping period as long as the one preformed at the experimental field, it was found that an important proportion of the water extracted, comes from points outside the area of interest and which were not covered by the levelings. Restricting the predictions to the area of interes, table 4 was obtained.

To simplify the computations, the total extraction was assumed to occur at the geometrical center of the field.

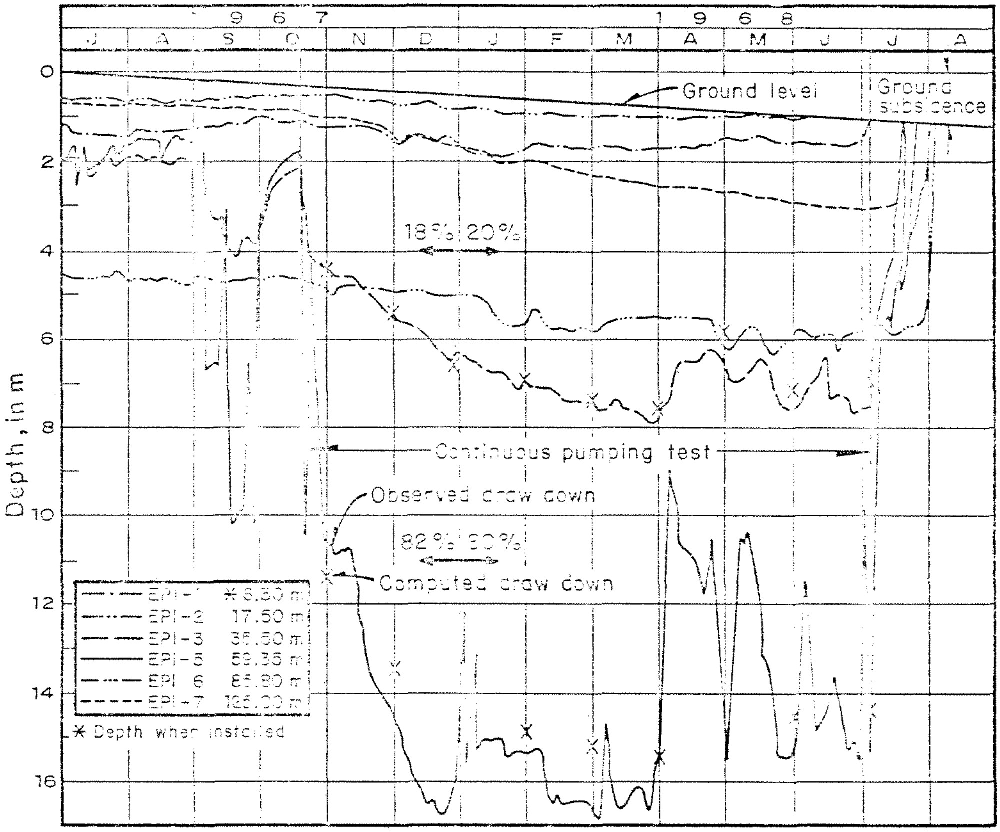

Fig. 3 Observed and computed drawdowns at EP1 station.

TABLE 3. PUMPING PERIODS

Period	Starting date			Final date			Duration in days	Days Accumulated
	Day	Month	Year	Day	Month	Year		
1	21	October	1967	30	November	1967	41	41
2	1	December	1967	28	December	1967	28	69
3	29	December	1967	31	January	1968	34	103
4	1	February	1968	29	February	1968	29	132
5	1	March	1968	31	March	1968	31	163
6	1	April	1968	30	April	1968	30	193
7	1	May	1968	31	May	1968	31	224
8	1	June	1968	4	July	1968	34	258

TABLE 4. PREDICTED Vs OBSERVED EFFICIENCY

Days	Efficiency (%)	
	Computed	Observed
69	24.8	28.0
150	21.1	26.5
224	20.5	14.0
270	19.4	--
1 800	13.0	--

Therefore, the actual efficiency has to be smaller than the one predicted, because many wells are closer to the field limits than its geometrical center.

Application to Texcoco Sur

When the calibration of the model was finished one of the main limitations of the project was a possible drastic reduction of the efficiency, which could render impossible to obtain the foreseen discharges. For the pumping period of the project (5 to 8 years), the maximum admissible drawdowns can be insufficient to yield the required discharges. On the other hand, at first it was thought that probably a large proportion of the land subsidence in Texcoco Sur was to occur outside the area of interest, because the envisioned pumping period is much larger than for the experimental field. However, due to the much larger dimensions of Texcoco Sur it was found that is not the case.

When computing the land settlements at Texcoco Sur, it was necessary to keep the head constant at some wells instead of imposing the more usual condition of constant discharge. This was due to the fact that the limiting drawdown values were reached. Also, because some stratigraphic features were not sufficiently clear, it was feared that the deep deposits could have a thickness practically unlimited in some area (fig 4); however, observations made once the pumping was started proved this suspicion to be false. The details of the computations are given in reference (Herrera et al., 1974).

Conclusions and recommendations

The main conclusions and recommendations were as follows:

i) The adopted hydraulic model was satisfactory to describe the land settlements on sections 1, 2 and 3 (fig 4).

ii) At sections 4 and 5 there are unforeseen soil formations which apparently consist of thin pervious strata which lie in the lower clay formation. These formations do not endanger the success of the project, because they considerably increase the speed of land subsidence and the pumping efficiency.

iii) It will be possible to achieve volume of soil settlements required for the project completion.

iv) To avoid important differential settlements, it was

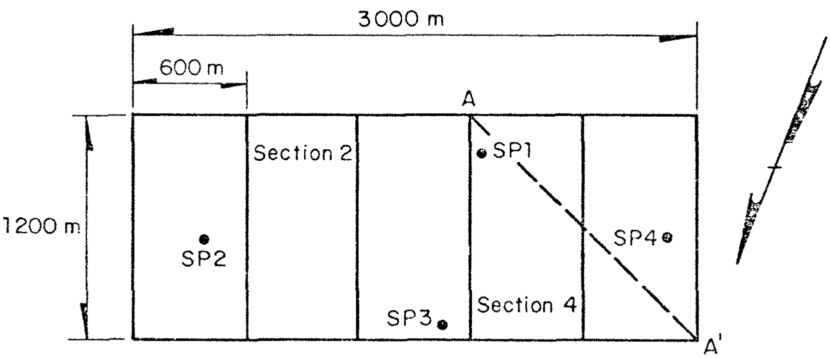

Fig. 4 Lago de Texcoco Sur. Dotted line limits area where thickness of deep deposits apparently was unlimited.

recommended to extract three times as much water from section 2 than from section 4.

References

Herrera, I., 1974, Integrodifferential equations for systems of leaky aquifers and applications. Part 2. Error analysis of approximate theories, Water Resources Research, v. 10, no. 4, pp. 811-820.

Herrera, I., J. Alberro, J.L. León and B. Chen, 1974, Análisis de asentamientos para la construcción de los Lagos del Plan Texcoco, Instituto de Ingeniería, 340.

Marsal, R.J., 1969, Desarrollo de un lago por la consolidación de arcillas blandas, inducida con bombeo, Volumen Nabor Carrillo, Secretaría de Hacienda y Crédito Público, México, D.F., pp. 229-266.

Proyecto Texcoco, 1969, Memoria de los trabajos realizados y conclusiones, Secretaría de Hacienda y Crédito Público, México, D.F.

Terzaghi, K., 1956, Theoretical Soil Mechanics, John Wiley.

Walton, C.W., 1970, Groundwater Resources Evaluation, McGraw-Hill.

Publication n°121 of the International Association of Hydrological Sciences
Proceedings of the Anaheim Symposium, December 1976

SUBSIDENCE OF THE NŌBI PLAIN

K.Iida, Professor, Aichi Institute of Technology, Yakusa-cho, Toyoda
K.Sazanami, Director, Chūbu Branch, G.S.I., Ministry of Construction
T.Kuwahara, Professor, Meijo University, Tenpaku-ku, Nagoya
K.Ueshita, Professor, Nagoya University, Chikusa-ku, Nagoya, Japan

Abstract

The Nōbi plain underlain by younger sediments is situated in the central part of Japan and is about 1300 km^2 in area. The yearly rates of subsidence in this area were 1.4 - 1.8 mm before 1925, 2 - 5 mm during the period from 1925 to 1950, 10 - 20 mm during the period from 1950 to 1960, 20 - 40 mm during the period from 1960 to 1965 and more than 100 mm at places having severe subsidence recently. The major cause of this increasing subsidence is the increasing withdrawal of ground water for industrial, agricultural and other purposes. As a result of such subsidence, an area of 250 km^2 subsided below the mean sea level. The drainage during and after heavy rainfalls has been becoming difficult day by day, and the potential danger of tidal flood under a typhoon has been increasing year by year. Against such subsidence of the Nōbi plain, investigations are being done by officials of central and prefectural governments and professors of universities in this area. Based on the investigations, withdrawal of ground water in this plain is now being controlled by regulations of the authorities concerned.

The Nōbi plain underlain by younger sediments is situated in the central part of Japan as shown in Fig. 1 and is about 1300 km^2 in area. The land surface subsided 237 cm in 87 years from 1888 to 1975 at Yatomi (a place in this plain).

This area faces the Ise bay, where Ibi, Nagara, Kiso and Shōnai rivers find their ways, and is composed of alluvial fans, flood plains, deltaic plains, terraces, reclaimed lands and filled-up grounds as shown in Fig. 2.

The west-east profile of the southern part of this area is illustrated in Fig. 3. The basement block in the Nōbi plain area bounded by Yōrō fault has tilted and is covered with sediments dipping westwards. The strata from a depth of about 2000 m to the ground surface in

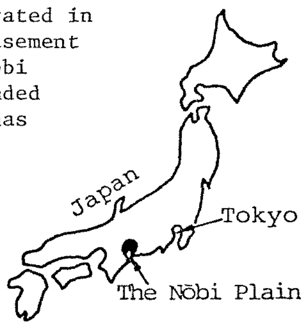

Fig. 1 The Nōbi Plain

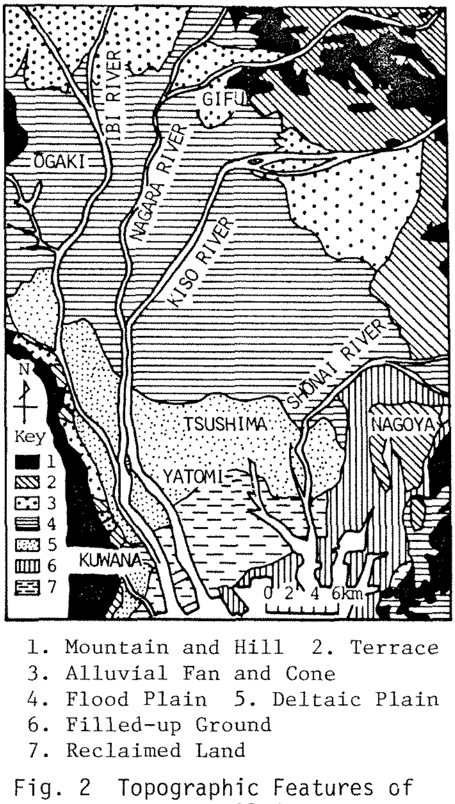

1. Mountain and Hill 2. Terrace
3. Alluvial Fan and Cone
4. Flood Plain 5. Deltaic Plain
6. Filled-up Ground
7. Reclaimed Land

Fig. 2 Topographic Features of the Nōbi Plain

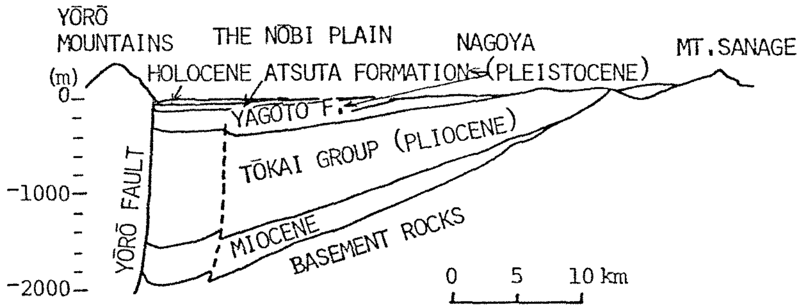

Fig. 3 West-East Profile of the Nōbi Plain

the western margin of the tilting block are sediments since the Pliocene. The average rate of displacement of the basement, based on the geological profile, was estimated only about 1 mm/year at Yatomi as shown in Table 1 (Kuwahara, 1968). Therefore, the recent subsidence of more than a few cm per year in this area is caused by consolidation of younger sediments, in which the pore water pressure has been decreasing by increasing withdrawal of ground water.

Formerly, this plain was mainly farming lands. But recently, a large number of textile mills and many kinds of factories using great quantities of ground water have been located and many residential quarters have also been developed. Since 1963, there have been developed several hot-spring resorts pumping up hot water from depths of more than 1000 m.

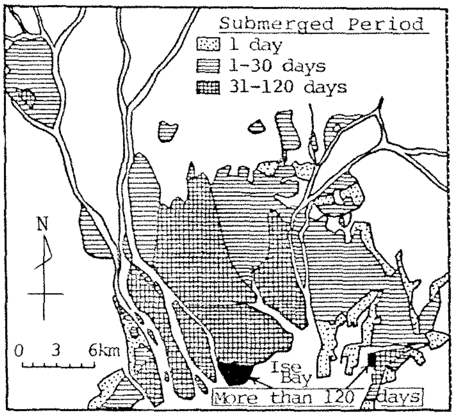

Fig. 4 Submerged Area of the Nōbi Plain after a Typhoon on 26 Sept.1959

Since old times, people of this plain often suffered damages from floods. Especially, they suffered severely from the flood caused by a typhoon which passed this plain in the northeast direction from Ise bay on the 26th of September, 1959. By this typhoon, 5,122 persons were put to death, 15,384 persons were wounded, 127,625 houses were destroyed completely or partly, and 3,846 houses were washed away in the whole of Japan. But the Nōbi plain suffered most of the damages. After this typhoon, considerably wider area of this plain was submerged for a long time as shown in Fig. 4. It was known by this submersion that there was an area of 186 km^2 below the

Table 1 Geological Displacement of the Nōbi Plain

Item / Target	Age $\times 10^4$ years B.P.	Inclination	Displacement at Yatomi	Ave. Rate of Displacement
Atsuta Surface	3.5	2.5×10^{-3}	60m	1.7mm/year
Yagoto Surface	30 ~ 70	4×10^{-3}	300m	1~0.4mm/year
Base of Tōkai Group	400± (200±)		2000m	0.5± (1.0±) mm/year

mean sea level at that time.

The history of ground subsidence in this area is shown in Fig. 5 by the use of three bench marks, the locations of which are given in Figs. 6 and 7. During the period from 1950 to 1973, the subsidence increased exponentially and some places subsided more than 20 cm/year in 1973.

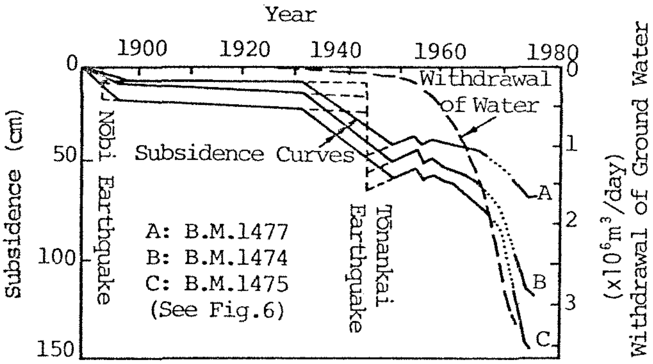

Fig. 5 Subsidence of Bench Marks and Withdrawal of Ground Water in the Nōbi Plain

Fig. 6 shows the comparison between the area subsided more than 2 cm/year from Feb.1961 to Feb.1962 and the one from Nov.1972 to Nov.1973. This figure explains how the subsiding area in this plain enlarged from 1961 to 1973.

The subsidence of this plain for about 15 years from Feb.1961 to Nov. 1975 is shown in Fig. 7. The southern part of Nagashima facing the Ise bay settled 147 cm during these 15 years. The total subsiding area is 1140 km^2 (Environment Agency, Japan, 1976). By 1973, 363 km^2 has become lower than the mean high-sea level (1.1 m higher than the mean sea level), 248 km^2 lower than the mean sea level and 37 km^2 lower than the mean low-sea level (1.4 m lower than the mean sea level) as shown in Fig. 8. The area below the mean sea level enlarged from 186 km^2 in 1961

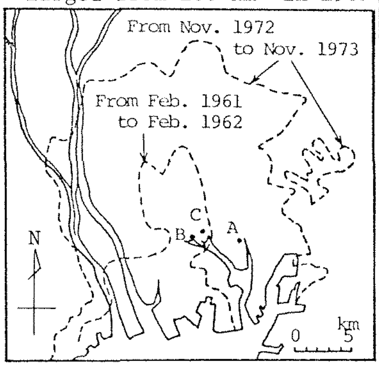

Fig. 6 Enlargement of the Area subsided more than 2 cm/year

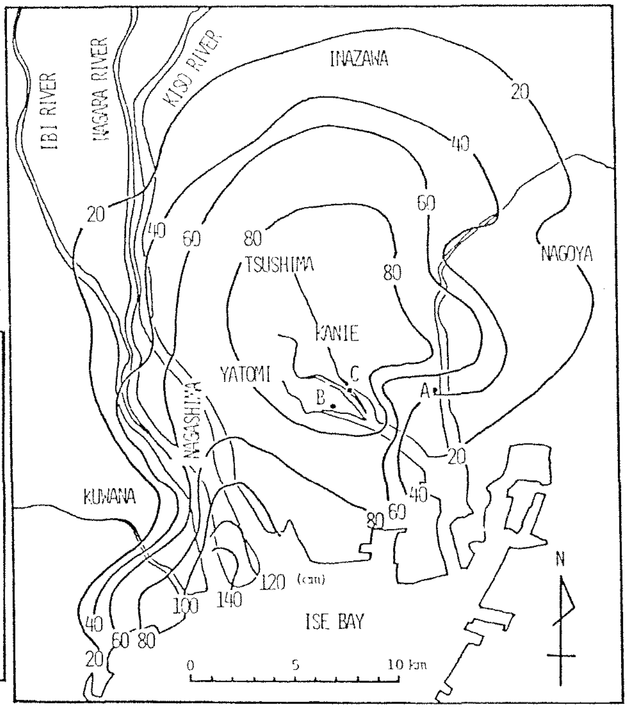

Fig. 7 Subsidence for 15 Years from Feb.1961 to Nov.1975 in the Nōbi Plain (cm)

to 248 km^2 in 1973.

The increasing withdrawal of ground water in the Nōbi plain is shown in Table 2 and Fig. 5. The use of ground water is shown in Table 3. The use for industry amounts to 60 per cent of the total.

The recent yearly withdrawal of ground water in the Nōbi plain is equal to the volume of 32 per cent of the yearly rainfall on this plain. This volume is much larger than the natural recharge of ground water. Therefore, the withdrawal of ground water must be reduced to arrest the subsidence of this plain (Ueshita, 1976).

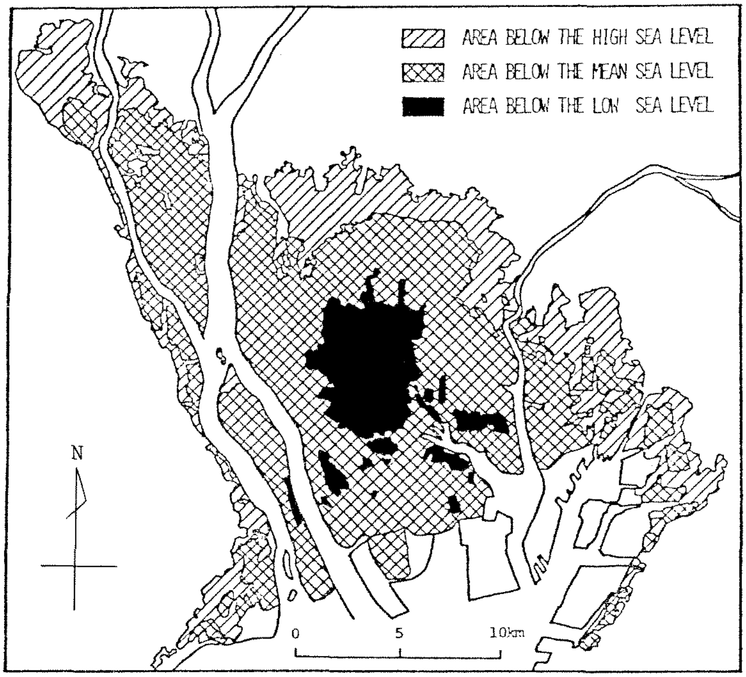

Fig. 8 Area below the Sea Levels in the Nōbi Plain

In the 1920's, the piezometric levels of confined aquifers were higher than the ground surface in the most part of this plain. In the 1940's, flowing wells were still observed in Ōgaki, Kanie and Kasugai districts as shown in Fig. 9. But the piezometric levels fell down corresponding to the increase in number of artesian wells. The piezometric level of the 2nd confined aquifer (G_2) was already lowered as shown in Fig. 10 (see Kuwahara et al, 1976).

In order to arrest the subsidence of the Nōbi plain, the Tōkai Three-Prefecture Investigation Committee on Land Subsidence was organized in 1971 and reorganized to strengthen in 1975, and many investigations have been done by officials of central and prefectural governments and professors of universities in this area. Based on the investigations, the withdrawal of ground water in this plain is now controlled by regulations of the authorities

Table 2 Withdrawal of Ground Water in the Nōbi Plain

Year	m^3/day
1925	1 638
1945	129 088
1950	154 040
1955	360 301
1960	849 338
1965	1 552 764
1970	3 002 128
1973	3 514 195

Table 3 Use of Ground Water for Each Purpose in the Nōbi Plain (1973)

Item	Total	Industry	Buildings	Water Supply	Agriculture
Withdrawal of Ground Water (m^3/day)	3 802 293	2 290 015	343 025	477 028	692 225
Percentage	100	60	9	13	18

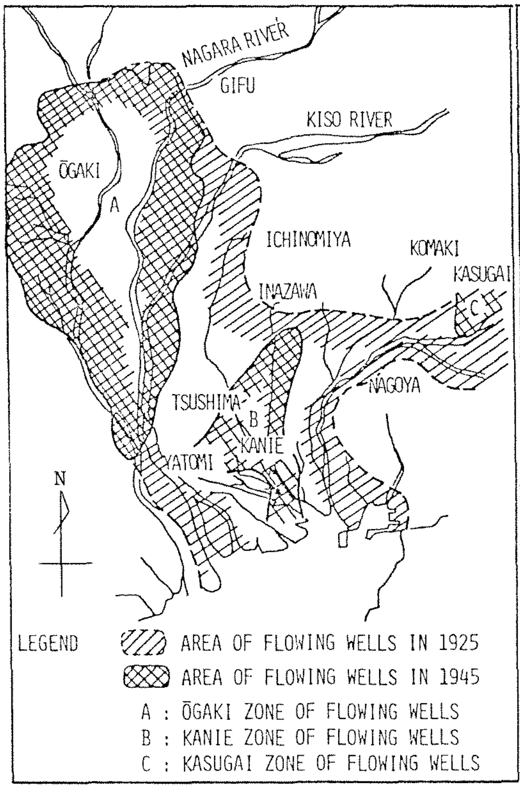

Fig. 9 Area where Flowing Wells existed in the Past

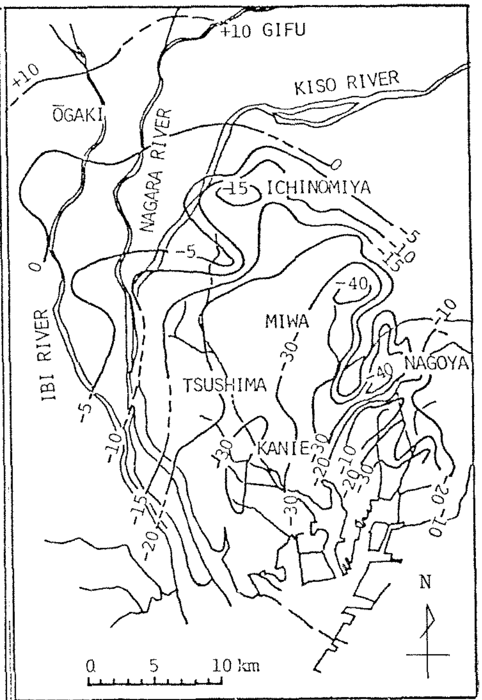

Fig. 10 Piezometric Level of the 2nd Confined Aquifer (G_2) in 1973 (measured in Meter based on the Mean Sea Level)

concerned as shown in Fig. 11.

Regulations of withdrawal of ground water in the Nōbi plain are as follows:

The Industrial Water Law (established in 1956)

The areas designated by the Industrial Water Law are supplied with

Table 4 Regulations for the Areas designated by the Industrial Water Law

Area	Zone (See Fig.11)	Allowed Depth of Strainer	Inside Area of Discharge Pipe
Southern Industrial Area of Nagoya designated in 1960	N_1	deeper than 80 m	less than 46 cm^2
		deeper than 300 m	greater than 46 cm^2
	N_2	deeper than 90 m	less than 46 cm^2
		deeper than 180 m	greater than 46 cm^2
Industrial Area of Yokkaichi designated in 1957 and 1963	Y_1	deeper than 100 m	less than 21 cm^2
		deeper than 230 m	from 21 cm^2 to 46 cm^2
	Y_2	deeper than 50 m	less than 21 cm^2
		deeper than 150 m	from 21 cm^2 to 46 cm^2

industrial water from surface sources instead of restriction on pumping up of ground water. The regulations for these areas are shown in Table 4.

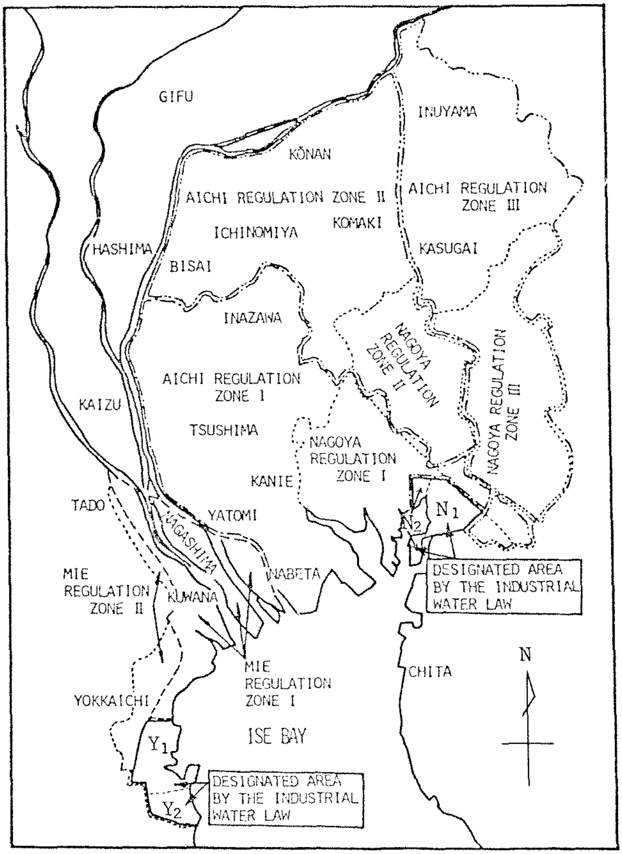

Fig. 11 Restriction of Withdrawal of Ground Water in the Nōbi Plain

<u>Regulations by Ordinance of Aichi Prefecture</u>

(1) Aichi Regulation Zone I (enforced on 30 Sept. 1974)

This regulation zone was decided considering the rate of subsidence greater than 5 cm/year in 1972 and/or 1973. In this zone, a newly bored well must have the following conditions;

a) The depth of strainer should not be greater than 10 m.
b) The inside area of discharge pipe should be less than 19 cm^2.
c) The power of motor should be less than 2.2 kW.
d) Total discharge should be less than 350 m^3/day.

Concerning the wells that existed before the regulation, flow meters were installed to them and the discharge records are reported to the Prefectural office every year. Since the 1st of January, 1976, the withdrawal of ground water from existing wells was restricted within 80 percent of the discharge in the past.

(2) Aichi Regulation Zones II and III (enforced on 1 April 1976)

The regulations for newly bored wells and existing wells are the same as those for Zone I, excepting that for the existing wells in Zone II, the withdrawal from the 1st of April, 1977 is going to be restricted within 80 percent of the discharge in the past, and for the existing wells in Zone III, the withdrawal in future is going to be restricted within the discharge in the past.

Table 5 Dealing with Existing Wells in the Case where the strainers are deeper than 10 m in Nagoya

Zone	Wells for Buildings	Wells for Industry
I	Changed to use city water since 16 Nov. 1975	Change to the industrial water supply as soon as possible
II	Changed to use city water since 16 Nov. 1976	
III	Increasing of withdrawal is forbidden.	

<u>Regulations by Ordinance of Mie Prefecture</u> (enforced on 1 April 1975)

The regulations for newly bored wells and existing wells are the same as those explained for Aichi Regulation Zones II and III, where Mie Regulation Zones I and II correspond to Aichi Regulation Zones II and III, respectively.

<u>Regulation by Ordinance of Nagoya City</u> (enforced on 16 November 1974)

According to the ordinance of Nagoya City, a new well can be allowed only in the case where the strainer is not deeper than 10 m and the inside area of discharge pipe is less than 19 cm^2. Existing deep wells are being treated as shown in Table 5. The regulation zones of Nagoya City are overlapped by the regulation zones of Aichi Prefecture. Therefore, the withdrawal of ground water in Nagoya is controlled by ordinances of Nagoya City and Aichi Prefecture.

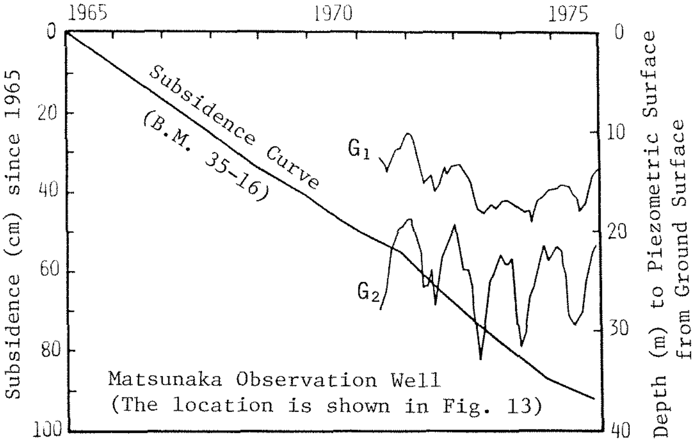

Fig. 12 Subsidence and Ground Water Condition at Nagashima during Recent Years

Fig. 12 shows the subsidence of Nagashima during the recent ten years and the piezometric levels of the 1st confined aquifer (G_1) and the 2nd confined aquifer (G_2) measured by Matsunaka observation well during the recent five years. The confined aquifers G_1 and G_2 are located at depths between 40 m to 60 m and 100 m to 115 m respectively at the observation site. Concerning the piezometric levels, seasonal changes are superposed on total trends of ground water levels. The seasonal drops of piezometric levels are caused by the increase of pumpage for cooling and irrigation in summer. The piezometric level of the deeper confined aquifer is lower than the one of the shallower confined aquifer, because ground water of better quality is pumped up in plenty from the deeper aquifer.

The piezometric levels of aquifers are having recovering trends since 1974. Corresponding to this phenomenon, the rate of subsidence reduced in 1975. Reflecting this favorable turn in ground water

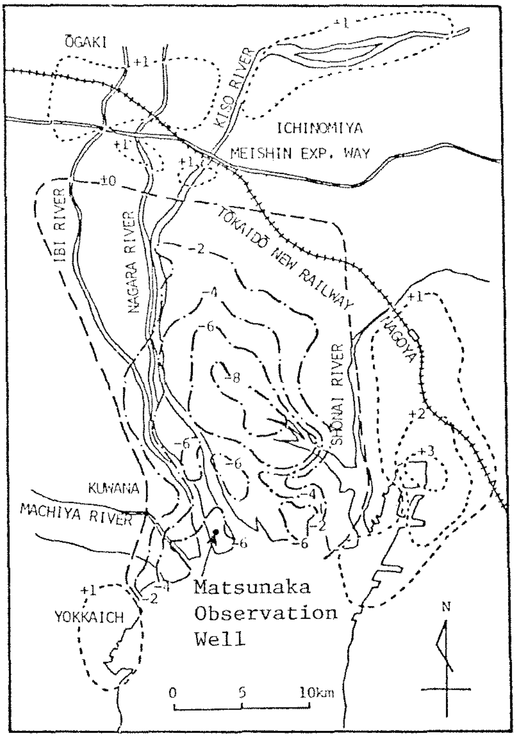

Fig. 13 Subsidence and Rebound of the Nōbi Plain from Nov.1974 to Nov.1975 (Unit: cm/year)

situation, the subsiding area became smaller and the rate of subsidence decreased for the period from Nov.1974 to Nov.1975 as shown in Fig. 13. Moreover, there appeared several rebounding areas around the area having reduced subsidence.

The organs and persons concerned are still directing their efforts to stop the subsidence of this plain completely.

In conclusion, the authors would like to express their hearty gratitude to the members of the Tōkai Three-Prefecture Investigation Committee on Land Subsidence and to the organs and persons concerned, especially the Ministry of Construction, Aichi and Mie Prefectures for their cooperation and their agreement in presenting this paper at the Second International Symposium on Land Subsidence. The research grants from the Ministry of Education are also acknowledged.

The authors are thankful to Professor M.S.I.Khan for his helpful advice on English expression of this paper.

References

Environment Agency, Japan, 1976, White Paper on the Environment: Printing Bureau, Ministry of Finance, Tokyo, p. 431.

Kuwahara, T., 1968, The Nōbi Basin and Its Fault Block Movements: The Quaternary Research (Dai-yonki Kenkyū), v. 7, pp. 235-247(in Japanese).

Kuwahara, T., Ueshita, K. and Iida, K., 1976, Analysis of Land Subsidence in the Nōbi Plain: Proc. 2nd Int. Symposium on Land Subsidence.

Ueshita, K., 1976, Land Subsidence and Regulation on Withdrawal of Ground Water in the Nōbi Plain: Journal of Japan Society of Civil Engineers, v. 61, no. 4, pp. 31-36(in Japanese).

Publication n°121 of the International Association of Hydrological Sciences
Proceedings of the Anaheim Symposium, December 1976

ANALYSIS OF LAND SUBSIDENCE IN THE NOBI PLAIN

Tooru Kuwahara, Professor, Meijo University, Tenpaku, Nagoya
Kano Ueshita, Professor, Nagoya University, Chikusa, Nagoya
Kumizi Iida, Professor, Aichi Institute of Technology, Toyoda, Japan

Abstract

The land subsidence in the Nobi Plain, central Japan, was examined in relation to groundwater level declining. The authors tried to examine, using several thousands of borehole materials, the complicated system in the groundwater basin which involves the subsurface stratigraphy, soil properties and so on, and to explore pumping amounts of groundwater and the declining process of the groundwater levels from data of water wells during a past few decades in the plain.

Using the above results, the authors successfuly obtained the numerical solution appropriate to the land subsidence up to the present, and they estimated the future land subsidence in the plain.

1 Underground Conditions of the Nobi Plain

There existed, during the Pliocene and early Pleistocen, a large sedimentary basin called Lake Tokai in the area which covers the present Nobi Plain, Ise Bay and their environs, central Japan. The tilting movements of the Nobi Plain Tectonic Block started to develop at the early stage of the middle Pleistocene. The movements have formed a westward dipping sedimentary sequence over 350 m in thickness. It overlies unconformably the sediments of Lake Tokai which is more than 1,000 m in thickness.

The subsurface stratigraphy of these sediments in the plain has been explored on the basis of borehole material obtained from several thousands of water wells and test borings. The geological succession of these sediments is shown in Table 1, and geological cross sections in Fig. 1.

The middle Pleistocene sediments and the younger are composed of an alternation of clay, sand and gravel beds. Change in sedimentary environments and climatic fluctuations of these sediments have been studied by means of the microfossil analyses of numerous boring core samples (Nobi Plain Quarternary Resarch Group, 1976).

Semiconsolidated fresh water lacustrine clay beds and fluvial sand and gravel beds are interbeded in the lower horizon of the Pleistocene sediments

Table-1 The Subsurface Stratigraphy in the Nobi Plain

		(Thickness)
HOLOCENE	NANYO FORMATION (H) *(loose upper sand bed and very soft marine clay bed)*	10- 60 m
PLEISTOCENE	NOBI FORMATION (N) *(alternation of sand and silt bed)*	10- 20 m
	DAIICHI GRAVEL BED (G1)	10- 30 m
	ATSUTA FORMATION (D3) *(upper sand and clay beds and unconsolidated lower marine clay bed)*	10-100 m
	DAINI GRAVEL BED (G2)	5- 30 m
	AMA FORMATION GROUP *(alternations of semiconsolidated sand, clay and gravel beds)*	30-100 m
	PRE-AMA FORMATION GROUPS *(alternations of semiconsolidated sand, clay and gravel beds)*	30- 70 m
PLIOCENE	TOKAI GROUP *(alternations of semiconsolidated clay, sand and gravel beds)*	200-1000 m
	M I O C E N E S E R I E S	
	P R E - T E R T I A R Y B A S E M E N T R O C K S	

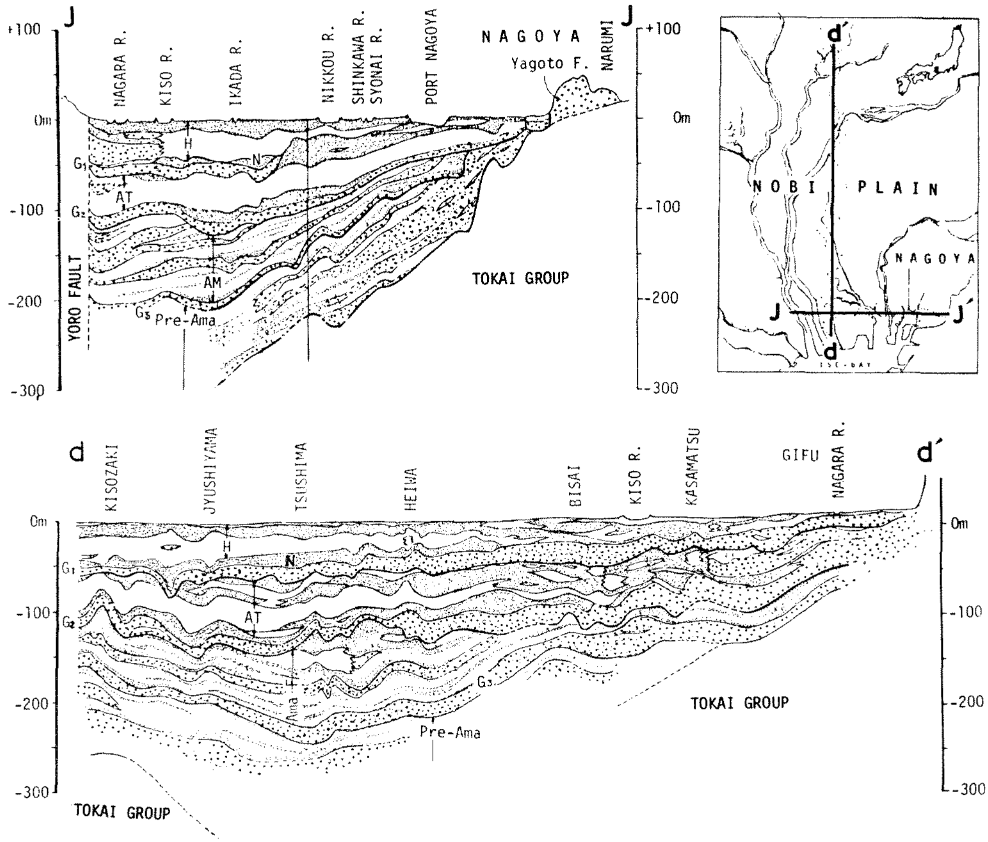

Fig. 1 Geologic Cross Sections of the Nobi Plain
H : Nanyo Formation (Holocene), N : Nobi F., AT : Atsuta Formation,
Dotted : gravels, Fine dotted : sand, Blank : clay.

called Pre-Ama Formation Groups. Ama Formation Group and the younger sediments are composed of alternations of fluvial sand or gravel beds and unconsolidated marine clay beds, deposited under inner bay conditions. Each of these marine clay beds shows a sedimentary cycle from transgressive to regressive phase, and represents a relatively warm period, interglacial epock or interstadial. In colder periods, the gravel beds have been deposited as either terrace or river-bed gravels in the valleys formed during the period of low sea level falling. The river-bed gravel deposited in the bottom of the valleys during a maximum stage of sea level falling reaches 20 m or more in thickness. The terrace gravel beds are generally thinner than the valley bottom gravel beds. These two types of gravel beds are distributed under the almost whole area of the Nobi Plain. Buried topography such as hills, terraces and valleys formed in the lowering process of sea level is depicted in the base contour map of these gravel beds (in Fig. 2). These buried topography and types of gravel bed effect groundwater yield in this plain. The marine clay beds overlying the gravel beds have attained to more than 30 m in thickness in the valleys, and spread far and wide under the plain area except for the alluvial fan area, where the clay beds are thinning out and grading into sand or gravel beds (Fig. 3).

In the alluvial fan area, precipitation and surface water percolate downward through these permeable sand and gravel beds, and recharge groundwater in the Nobi Plain. Superficial sand bed, the upper member of Nanyo Formation, attaining to 15 m in thickness contains unconfined groundwater which is recharged directly from precipitation and infiltration of surface water. The gravel beds, interbeded in clay beds, G_1, G_2, and others, are artesian aquifers and supply a large quantity of groundwater. Before the pumping is largely developed, many flowing wells tapping into these gravel beds were found in most of all area of the Nobi Plain (Iida et al, 1976).

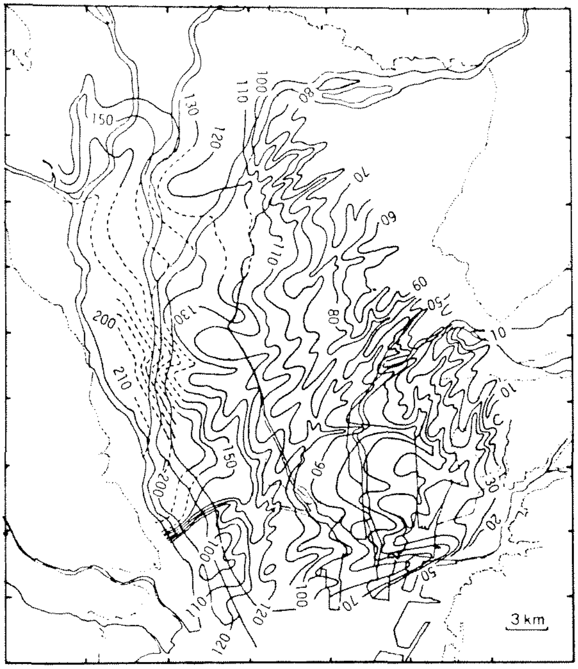

Fig. 2 Buried Topography Beneath G_2 Aquifer (contour lines below sea level in meter)

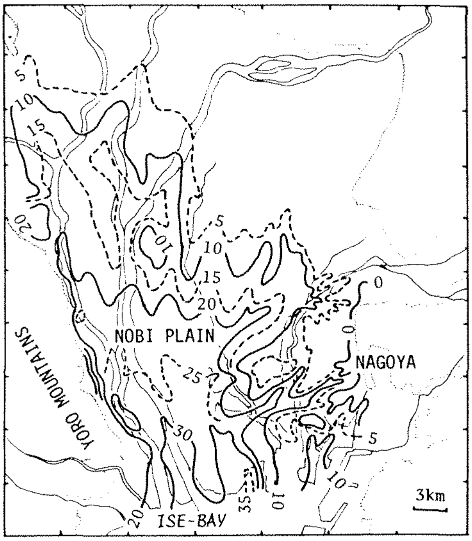

Fig. 3a Distribution of Thickness of the Holocene Marine Clay Bed, AL. (in meter)

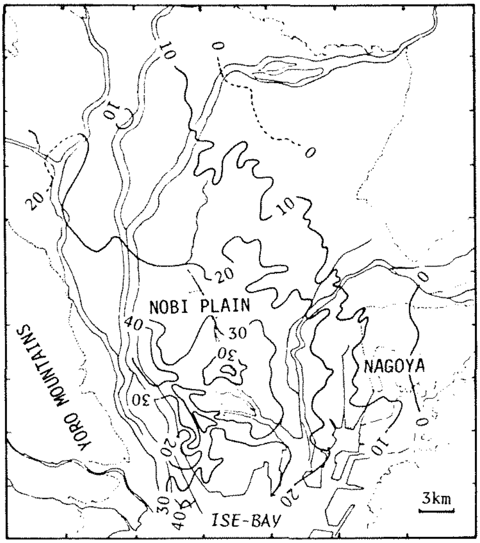

Fig. 3b Distribution of Thickness of the Lower Marine Clay Bed,D3L, in the Atsuta Formation (in meter)

2 The Increased Pumping of Groundwater and Downward Trend of the Groundwater Levels in the Nobi Plain

As the use of groundwater has grown in the Nobi Plain area, the wells tapping the artesian aquifers have been enormously multiplied during the last two decades, and recently about ten thousands and more wells are supplying over 3.7 million tons of water per day.

The pumping intensity, namely the pumping amount in a certain unit area which is a rectangle of 4.4 km^2 in this case, has been enlarged in the marginal zone (except for the western part) of this plain where urbanization and industrialization have been advancing (Fig. 4). In Ogaki, one of the industrial cities, located in the northern area of this plain, daily pumping intensity amounts to 100 thousands ton per 4.4 km^2. Fig. 5 explains increasing amounts of water supplied from each aquifer unit in recent years. The pumping amount from each aquifer in Fig. 5 was conveniently estimated in proportion to the thickness of each aquifer because many production wells are usually open to more than one aquifer. During the period from 1961 to 1965, the largest quantity of

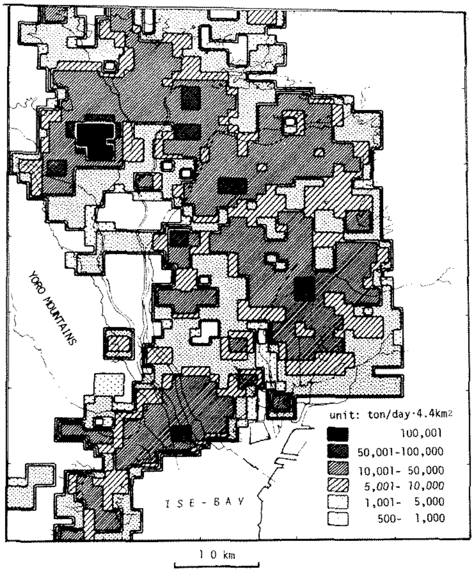

Fig. 4 Pumping Intensity from the Whole Aquifers in the Nobi Plain in 1973

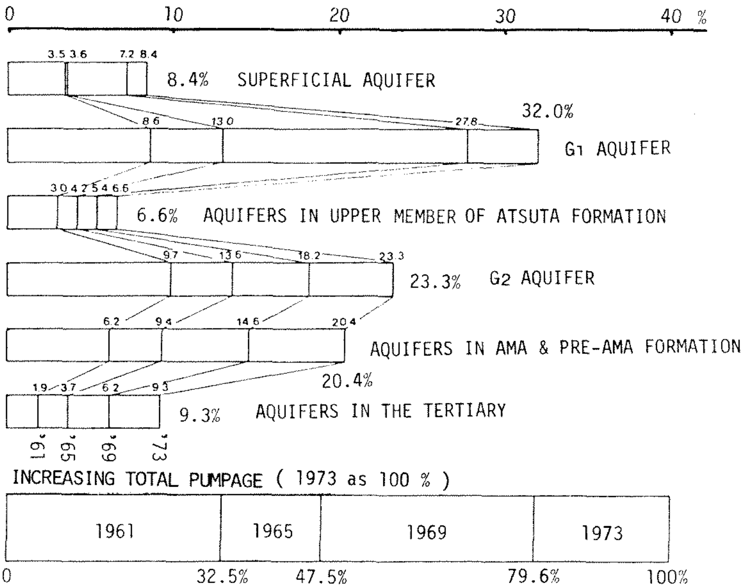

Fig. 5 Increasing Total Pumpage and Extraction Rate from Each Aquifer Unit in the Nobi Plain from 1961 to 1973

pumpage in this plain was from G_2 aquifer, and from 1965 to 1969 the largest supplying source was replaced by the shallower productive G_1 aquifer. The proportions of the pumping amount from each source, in 1973, are as follows, 8.4 % from superficial unconfined aquifer, 32.0 % from G_1 aquifer, 6.6 % from upper sand bed of Atsuta Formation, 23.3 % from G_2 aquifer, 20.4 % from

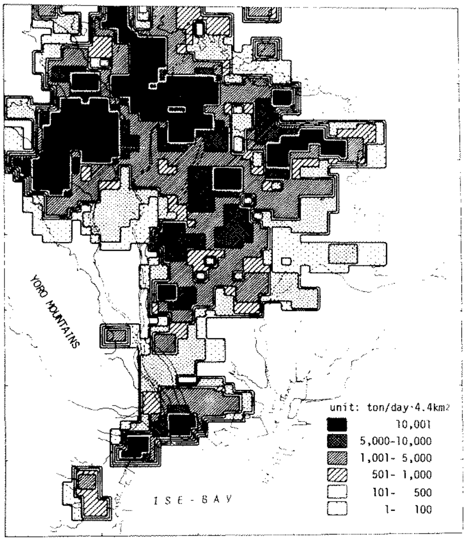

Fig. 6 Pumping Intensity from G_1 Aquifer in 1973

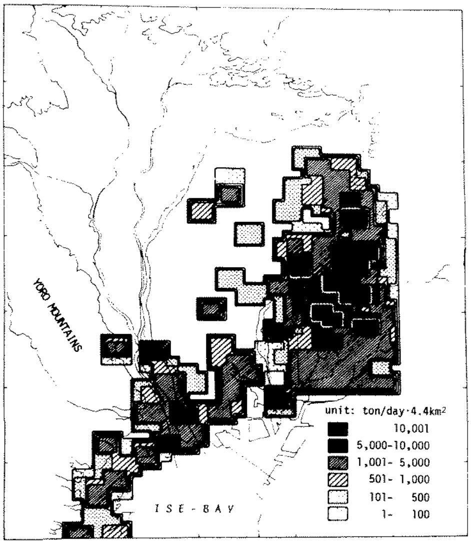

Fig. 7 Pumping Intensity from the Tertiary Aquifers in 1973

Ama and Pre-Ama Formation and 9.3 % from aquifers in the Tertiary. About 70 % of total pumpage in this plain, therefore, was withdrawn from the aquifers shallower than G_2.

Figs. 6 and 7 indicate the areal distribution of pumping intensity from each aquifer unit. The groundwater is intensively extracted from the shallower aquifers, namely superficial and G_1, in northern areas of the plain where they have a high recharge rate and where industrialization has increasingly developed recently. Fig. 6 shows pumping intensity of G_1 aquifer. The deeper aquifers than G_2 are used as the main water source in the south-eastern area of this plain. The use of Tertiary aquifers is shown in Fig. 7. G_2 aquifer is the source of the groundwater supply throughout the whole plain area. Deeper wells, exceeding 1,000 m in depth, tap the aquifers in the Pliocene or the underlying Miocene which is interbeded with clay, sand and gravels. Higher temperature water used for spas is extracted from these deeper wells.

As pumping water increases, the piezometric surfaces which were above the land surface before the World War II, have declined continuously except alluvial fan areas. The piezometric surfaces are lowered 40 m below sea level in intensively declined areas with the rate of 2 m per year (Kuwahara, 1976a).

The land subsidence occurs in the area where unconsolidated thick clay beds lie and intense declining of piezometric surfaces is observed. The subsidence rate ranges from 2 to 20 cm per year, and the total amount of subsidence during the period from 1961 to 1975 attains to 147 cm in an area of maximum subsidence (Iida et al, 1976). No appreciable subsidence has occured in areas where piezometric surface declining is little and/or coarse materials predominate.

3 The Analysis of Land Subsidence due to Groundwater Withdrawals

Data from the observation wells have indicated that the compaction of unconsolidated sediments above G_2 contributed largely (70-80 %) to the subsidence of land surface. Since the compaction rate of these sediments is closely related to the rate of decline of piezometric surfaces, the reduction of the artesian pressure evidently causes the land subsidence in the Nobi Plain. A reduction of artesian pressure results in an increase of grain-to-grain or effective stress on the skeleton system of the sediments which may cause compaction. The subsidence, therefore, depends upon the subsurface lithology and upon the magnitude and rate of artesian pressure reduction.

The processes of compaction of sediments due to the artesian pressure reduction were calculated based on the Terzaghi Consolidation Theory. We excluded the deeper sediments underlying G_2 from the calculation, because the details of artesian pressure reduction are not too clear in the deeper part and also the compaction in this part contributes only a little to the surface subsidence. The compaction of sand and gravel beds among the sediments overlying G_2 is also excluded from the calculation because both of these beds have much smaller coefficient of volume compressibility than clay beds. Unconsolidated soft marine clay beds, namely the lower member of Nanyo Formation (AL) and the lower member of Atsuta Formation (D3L), therefore, are taken into consideration.

Depth and thickness at any point of these clay beds are depicted by the subsurface information from thousands of materials of water wells and test borings. Fig. 3 shows isopack maps of clay beds. The data obtained from many undisturbed soil samples proved that most of these clay beds are normally consolidated, while the deeper beds are almost over-consolidated.

Compression index, Cc, varies vertically and horizontally in these clay beds and the values are closely related to the sedimentary facies. The value is the largest in the middle horizon which deposited in the maximum phase of transgression and is composed of finer materials. Lateral distribution of the mean Cc value calculated by averaging vertical variations, as shown in Fig. 8, reflects the sedimentary environment of clay bed.

Natural void ratio of clay, e_0 , has a close relation with the contents of clay fraction, sedimentary environments and the geological history of the sediments (Kuwahara, 1966). There are remarkable corelations between e_0 and Cc, as follows:

$$Cc = 0.5(e_0 - 0.5)$$

for AL (Kuwahara and Horiuchi, 1966, Ueshita and Nonogaki, 1970),

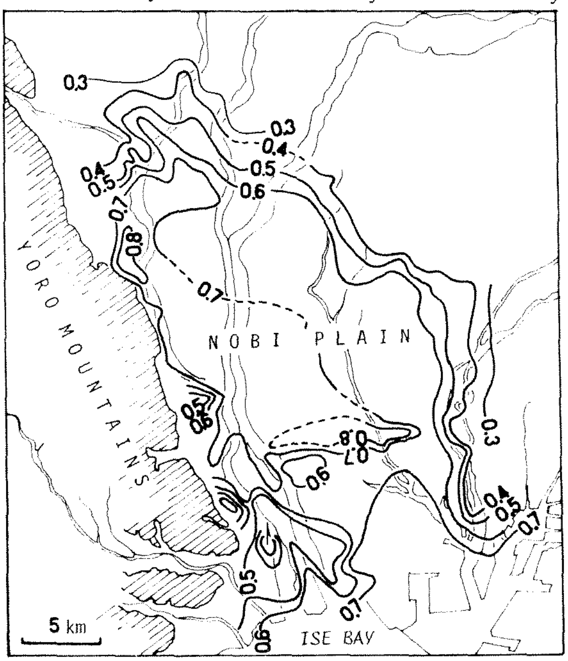

Fig. 8 Distribution of the Mean Cc Value in the Holocene Marine Clay, AL

$$Cc = e_0 - 0.5$$

for D3L (Kuwahara, 1976b).

The ultimate consolidation of the clay bed, S, is computed by equation (1);

$$S = \frac{Cc \cdot H}{1 + e_0} \cdot \log \frac{P + \Delta P}{P} \qquad (1)$$

where H : thickness of clay bed,
P : effective stress before the artesian pressure reduction,
ΔP : increase in effective stress by the artesian pressure reduction.

The value of e_0 in each clay bed used in the equation is computed from the corelations with Cc mentioned above.

Considering the increasing effective stress due to the continuous artesian pressure reduction, the rate of consolidation of the clay bed must be solved by the following consolidation equation under incremental loading (Schiffman, 1985 and Lumb, 1963);

$$\frac{\partial u}{\partial t} = Cv \cdot \frac{\partial^2 u}{\partial z^2} + R\ (z,\ t) \qquad (2)$$

where u : pore pressure at time t,
Cv : coefficient of consolidation,
z : distance from the surface of clay bed,
R : rate of incremental loading.

Equation (2) is not solvable unless the load increment is linear. In the case of non-linear load increment (non-linear artesian pressure reduction), the solution may be approximated by superposing two or more linear incremental conditions.

The process of artesian pressure reduction of each aquifer in the past, at various locations, is estimated from the recorded water levels in each artesian well (Kuwahara, 1976a).

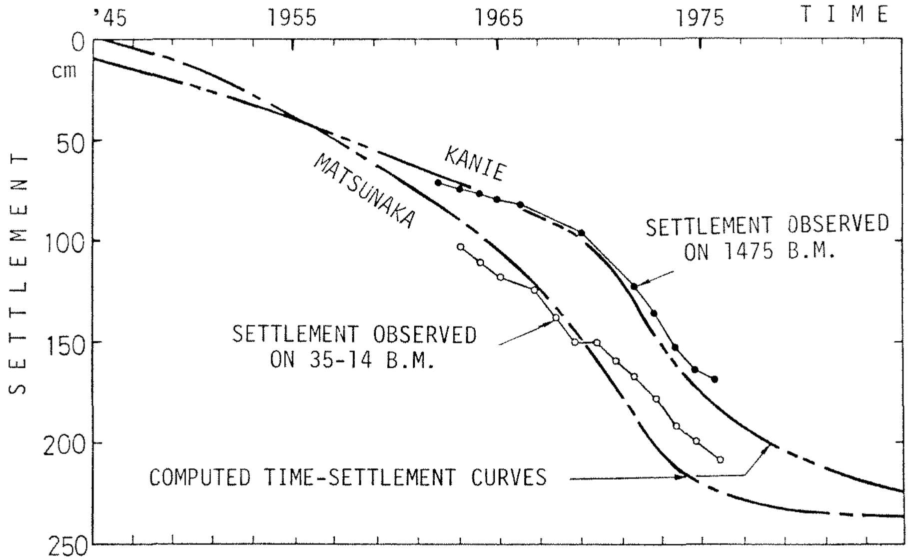

Fig. 9 Computed Rate of the Settlement of the Clays above G_2, Observed Settlement also Plotted

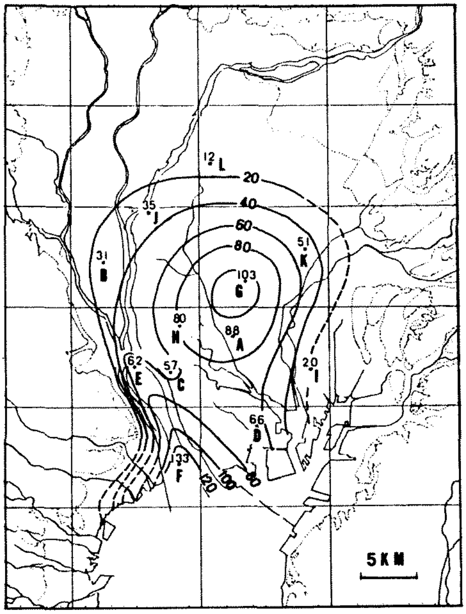

Fig. 10 Distribution of the Amount of Settlement Computed for the Clay Beds above G_2 from 1961 to 1973 (in cm)

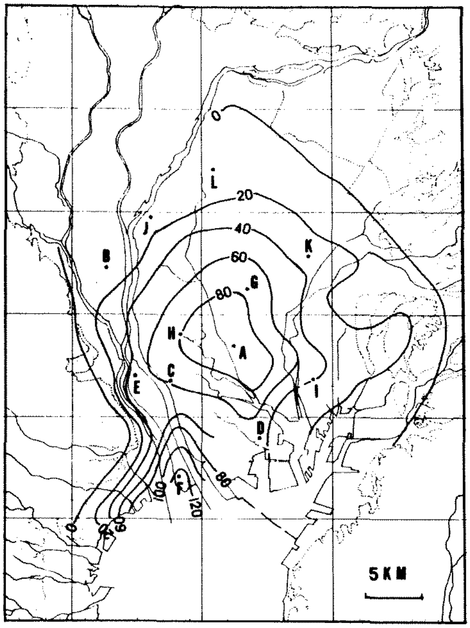

Fig. 11 Land Subsidence Observed from 1961 to 1973 (in cm)

The computed rates of consolidation at certain points where the informations of subsurface lithology, soil properties and the process of artesian pressure reduction are given, coinside with the results of repeated precise levelings of the bench marks on or near the computed points, as the examples in Fig. 9. It may be said that the computing method in this paper is effective to the analysis of land subsidence in the Nobi Plain.

The areal distribution of computed rate of settlement during the period from 1961 to 1973 (Fig. 10) is compatible with that observed (Fig. 11) during the same period in the Nobi Plain. The computed rate at point G is somewhat larger than the observed one, probably because of the incorrect records of the water level declining there.

The areal distribution of the computed settlement in this plain during the period from the year when all piezometric surfaces were at the ground level to 1973 is shown in Fig.12.

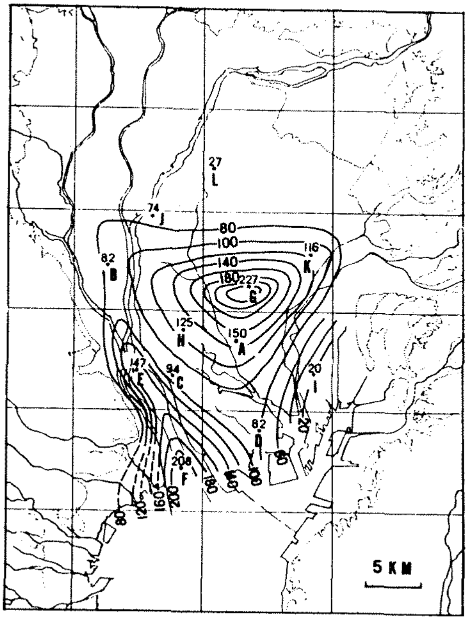

(in cm)

Fig. 12 Distribution of the Computed Settlement during the Period from the Year When Piezometric Surfaces were at the Ground Level to 1973

The settlement in core area of subsidence amounts to 2 m. These computed amounts are not inconsistent with the results from the leveling surveys in the past.

The same method is used to estimate the further subsidence in this plain under the several presupposed artesian pressure reduction conditions. The conditions are as follows: the groundwater levels are fixed in the 1973's levels in each aquifer (rate=0), the levels continue to lower in the same rates as in 1973 (rate=1), the lowering rate will decrease to 3/4 (rate= 3/4), decrease to 1/2 (rate=1/2) and decrease to 1/4 (rate=1/4).

The computed results, as given in Table 2, show that the residual settlement due to the time delay required for consolidation will attain to 70 cm in another decade, even if the artesian surfaces can be fixed at the 1973's levels.

Table 2 Computed Further Settlement of Clay Beds above G_2 from 1973 (in m)

Point \ R	TO 1978					TO 1983					SETTLEMENT TO ULTIMATE WATER LEVEL
	0	1/4	1/2	3/4	1	0	1/4	1/2	3/4	1	
A	0.465	0.619	0.756	0.884	0.981	0.697	1.105	1.370	1.462	1.586	3.419
B	0.062	–	–	–	–	0.110	–	–	–	–	4.320
C	0.172	0.195	0.219	0.240	0.264	0.276	0.340	0.408	0.466	0.530	3.852
D	0.235	0.301	0.324	0.365	0.403	0.372	0.552	0.613	0.725	0.831	3.325
E	0.180	0.198	0.220	0.236	0.248	0.291	0.340	0.403	0.449	0.480	3.960
F	0.216	0.356	0.492	0.612	0.724	0.257	0.605	0.944	1.244	1.526	3.829
G	0.087	0.113	0.132	0.154	0.175	0.116	0.183	0.239	0.289	0.342	1.112
H	0.176	0.209	0.249	0.286	0.323	0.266	0.368	0.470	0.566	0.665	5.300
I	0.045	0.073	0.101	0.127	0.151	0.047	0.116	0.182	0.246	0.304	4.337
J	0.005	0.029	0.039	0.057	0.071	0.011	0.057	0.097	0.142	0.178	1.733
K	0.001	0.030	0.057	0.086	0.111	0.001	0.070	0.135	0.199	0.258	0.386
L	0.000	0.010	0.018	0.027	0.036	0.000	0.022	0.043	0.063	0.082	0.586

The Table 2 also shows that the maximum settlement will reach 160 cm in the next decade, if the same rate of the surface lowering continues. If the artesian surfaces in main aquifers decline to the ultimate state, the further settlement resulted only from the sediments above G_2 will attain to 3 or 4 m in the southern and western areas of this plain.

In order to prevent the land subsidence in the Nobi Plain, it is indispensable to regulate the use of the groundwater without delay. To promote the regulation, the limit of groundwater use must be precisely computed from groundwater balance between discharge and recharge in this plain. The optimum policy must be taken to prevent the disasters induced by the subsidence and to maintain the groundwater resource. We are now computing the groundwater balance using the finite element method (Ueshita et al, 1976) as well as the finite difference method (Kamata et al, 1975).

Acknowledgments

In concluding this report, the authors would like to express their heartly gratitude to members of the Tokai Three-Prefecture Investigation Committee on Land Subsidence, the organs and persons concerned, especially the Ministry of Construction, Aichi Prefecture and Mie Prefecture for their willing co-operations and their kind agreement on this report. Also

research grants for the Ministry of Education are acknowledged.

References

Iida, K., Sazanami, K., Kuwahara, T. and Ueshita, K., 1976, Subsidence of the Nobi Plain, Proc. 2nd Int. Symposium on Land Subsidence.

Kamata, A., Fuzisaki, K. and Kuwahara, T., 1975, Simulation of the Land Subsidence in the Nobi Plain, Proc. 82th Annual Conf. Geol. Soc. Japan, p. 351.*

Kuwahara, T., 1966, Engineering Property and Its Significance of Alluvial Clayey Deposits, The Quaternary Research (Dai-yonki Kenkyu), v.5, pp. 121-138.**

Kuwahara, T., 1976, Groundwater Use and Its Conditions, Rep. on the Land Subsidence and Its Counterplan, v.2, Aichi Prefecture, pp. 33-75.*

Kuwahara, T., 1976, Computed Further Land Subsidence in the Nobi Plain, ibid, pp. 109-149.*

Kuwahara, T. and Horiuchi, T., 1968, Soil Technological Investigation of Soft Clayey Deposits in the Southern Area of Nagoya City, Rep. Faculty of Science and Technology, Meijo Univ. No. 7, pp. 34-59.**

Lumb, P., 1963, Rate of Settlement of Clay Layer due to a Gradually Applied Load, Civil Eng. Wrs. Rev., v. 58, pp. 315-317.

Nobi Plain Quaternary Research Group, 1976, Stratigraphy and Microfossil Analysis of Quaternary Sedimens in the Nobi Plain, Central Japan, Memoirs Geol. Soc. Japan. (in press)**

Schiffman, R.L., 1958, Consolidation of Soil under Time Dependent Loading and Varying Permeability, Proc. H.R.B., pp. 584-617.

Ueshita, K. and Nonogaki, K., 1970, Considerations on the Unified Soil Classification of Fine-Grained Soils and Sandy Soils in the Tokai District, Japan, Trans. Japan Soc. Civil Eng., v.2, pp. 313-316.

Ueshita, K., Itabashi, K. and Tanahashi,H., 1976, Analysis of Land Subsidence in the Nobi Plain, Proc. 38th Annual Conf. Japan Soc. Civil Eng. v.3, pp. 183-184.*

* in Japanese, ** in Japanese with English abstract.

Publication n°121 of the International Association of Hydrological Sciences
Proceedings of the Anaheim Symposium, December 1976

NEW TREND IN THE SUBSIDENCE OF VENICE

Laura Carbognin, Paolo Gatto and Giuseppe Mozzi
National Research Council, S. Polo 1364, Venice - Italy
Giuseppe Gambolati
IBM Scientific Center, S. Polo 1364, Venice - Italy
Giuseppe Ricceri
Department of Soil Mechanics, University of Padua - Italy

Abstract

Following a brief review of the hydrogeology and physical characteristics of the confined aquifer system underlying the Venetian area, the history of the water withdrawals and the resulting land subsidence until 1975 is reported.

Geodetic surveys indicate that the settlement has been about 14 cm in Marghera and 10 cm in Venice from 1952 to 1969. In the corresponding period the average piezometric decline has been recorded as being 13 m in Marghera and 5 m in Venice.

New recordings show that the industrial pumpage has been reduced by 60% and the flow field beneath Venice is recovering at an appreciable rate. Simultaneous geodetic levelling shows that the subsidence in Venice has been arrested and a rebound of about 2 cm has occurred.

The application of the hydrologic subsidence model previously developed, shows a good agreement between the latest observations and the predictions provided earlier by the model.

1. Introduction

Many areas of Italy are affected by land subsidence. Among these, the area of Venice (fig. 1) has caused the greatest concern. Its sinking in fact, in spite of the relatively small rate, could be fatal, due to the low level of the city in relation to the sea. The well known floods (or "acque alte", a local idiom meaning high waters), essentially caused by weather and astronomical factors, are indirectly enhanced by subsidence both in amplitude and in frequency. When the studies were started, it became quite clear that, out of the various factors responsible for the sinking, the withdrawals of underground water was the main one. Thus, after a preliminary analysis, the research effort was mainly directed to hydrogeology.

In 1969, the Italian Consiglio Nazionale delle Ricerche (CNR, National Research Council) constituted a working group for the Venice problem. Starting that year an accurate inventory was made of the data already available but widely scattered. They were filed according to lithostratigraphy, hydrology, geotechnique and geodesy. During their processing, specific experimental tests were performed, to validate and supplement the preliminary reconstructions.

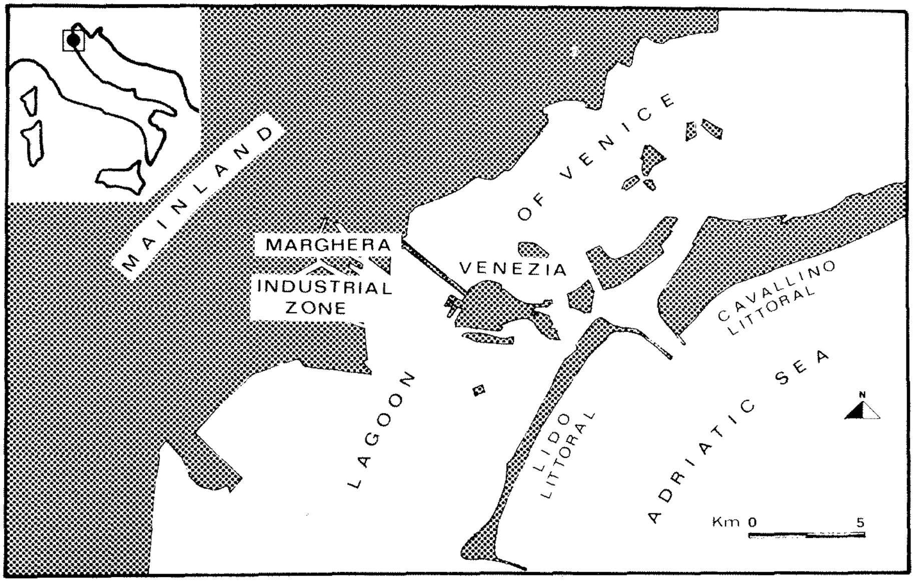

FIGURE 1 - Map of the Venetian area under investigation.

The analysis was given two major aims: first, to describe the physical environment where the phenomena under study occur; next, to describe their evolution, to investigate their mechanism and to make predictions with numerical models. The final results of the research confirm the dependence of the subsidence on the artesian withdrawals, the possibility of stopping the settlement of the city and even of obtaining a slight rebound by naturally recharging the depleted aquifer system.

2. The Physical Environment

The Venice confined system, down to 1000 m depth (Quaternary basement),is constituted by sand layers (aquifers) bounded by silt and clay layers (aquitards). Moving North-West, towards the foothills of the Alps, the sedimental structure tends to change. Materials are more and more coarse, while the aquitards become thinner, and, at a certain point, they disappear. In the foothill belt the unconsolidated mantle is a whole homogeneous system of sand and gravel. For the hydrologist, it represents the reservoir supplying the aquifer-aquitard system extending beneath Venice and even further.

The Venetian aquifer system has been investigated in detail by taking information from both the existing artesian wells (Alberotanza et al.,1972) and a new deep test borehole, VE 1 CNR, where continuous samples of the Quaternary series were taken (Consiglio Nazionale Ricerche, 1971). Thousands of

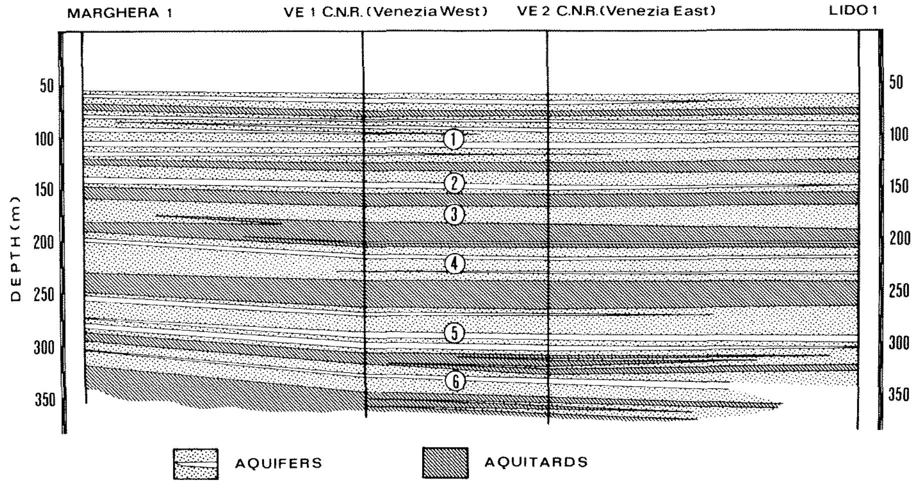

FIGURE 2 - Hydrogeological map of the confined aquifer system updated using the electric logs recorded in deep test boreholes.

analyses were performed on the borehole samples, and a complete physiography of the local subsurface formations was obtained. From this drilling a more complete interpretation of the scattered information was made possible. Moreover, the starting point was available for the definition of the hydrogeological stereogram of the region. Figure 2 is a map of the upper 350m, where the aquifers are pumped (after Gambolati et al., 1974 , slightly modified). Six aquifers appear, four of which are extensively exploited (2^{nd}, 4^{th}, 5^{th} and 6^{th}).

Permeability, grain size and clay chemistry of aquifers and aquitards are reported in tables 1, 2 and 3, whose values were obtained by analyzing the cores of the VE 1 CNR and two other test boreholes LIDO 1 and MARGHERA 1.

Permeability (table 1) was defined by laboratory tests performed only on clean sand for aquifers and silt clay for aquitards.

The prevailing fraction (table 2) is silt, followed by sand and clay.

The illite is dominant (table 3); instead the most plastic one, montmorillonite, is in general rather scarce, and its relative abundancy grows towards the historical center and Lido.

Some details of the mechanical properties of these soils are given here (see a recent and more complete paper by Ricceri and Butterfield , 1974). The values of the compressibility coef

TABLE 1. Average permeability of samples taken from VE 1 CNR Borehole (placed in Venice), from laboratory tests.

DEPTH (meters)	AQUIFERS (average horyzontal permeability)	AQUITARDS (average vertical permeability)
74 - 81		3×10^{-5} cm/sec
81 - 124	1×10^{-3} cm/sec	
124 - 132		7×10^{-8} cm/sec
132 - 153	1×10^{-3} cm/sec	
153 - 163		3×10^{-6} cm/sec
163 - 181	4×10^{-5} cm/sec	
181 - 203		5×10^{-7} cm/sec
203 - 235	6×10^{-4} cm/sec	
235 - 260		6×10^{-7} cm/sec
260 - 302	2×10^{-4} cm/sec	
302 - 318		6×10^{-6} cm/sec
318 - 340	10^{-6} cm/sec (°)	

(°) The 6th aquifer is exploited only at Marghera, since at Venice its permeability is too low.

TABLE 2. Summary of grain size analysis as measured in the laboratory on samples taken from the VE 1 CNR borehole (after Gambolati et al., 1974).

DEPTH (meters)	L I T H O T Y P E S Coarse fraction	Sands	Silts	Clays
0 - 50	0.3	38.0	41.7	20.0
51 - 100	0.7	50.0	35.0	14.3
101 - 150	-	46.2	42.2	11.6
151 - 200	0.4	33.6	48.2	17.8
201 - 250	-	26.0	54.0	20.0
251 - 300	5.6	38.4	34.8	21.2
301 - 350	-	13.5	61.6	24.9
Average	1.0	35.1	45.4	18.5

TABLE 3. Percentages of various clay-types in the core samples taken from MARGHERA 1, VE 1 CNR, and LIDO 1 test bore holes (after Mozzi et al., 1975).

Clay Minerals	MARGHERA	VENICE	LIDO	Average
Illite	48.75	48.45	48.00	48.40
Chlorite	33.75	28.00	30.00	30.58
Kaolinite	11.25	12.80	9.00	11.02
Montmorillonite	6.25	10.75	13.00	10.00

ficient ($m_v=(\Delta e/\Delta p)(1/1+e_o)$) versus depth (fig.3) have been computed by oedometric tests at the actual "in situ" pressure (p_o) in the loading (m_{v1}) and unloading (m_{v2}) curves. The maximum load attained in these tests was 5÷20 times p_o for the samples coming from the upper 100 meters and twice the values of p_o for the others. In figure 3, solid lines connect the values m_{v1} and m_{v2} for each sample; dashed lines refer to oedometric tests where loads were increased up to slightly above p_o and then gradually reduced to zero. The two coefficients decrease with increasing depth. In particular, m_{v2} seems rather insensitive to the maximum load applied in the test, and its average value is about 20% of m_{v1}.

The reader is referred to the bibliography for further information about the physical aspects of the Venetian formations.

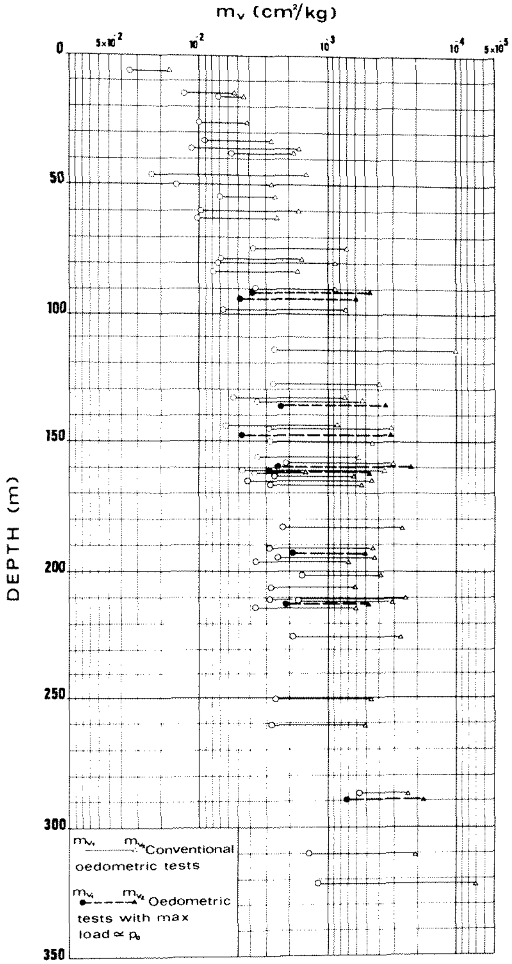

FIGURE 3 - Coefficients of compressibility m_{v1} and m_{v2} versus depth.

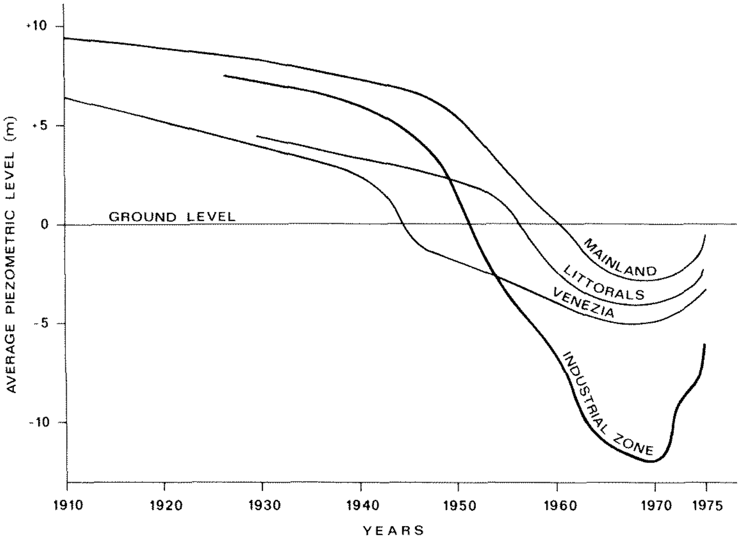

FIGURE 4 - Average piezometric levels from 1910 to 1975.

3. <u>History of the Phenomena</u>

By comparing the development of the artesian exploitation and of subsidence, three periods appear distinguishable: the first before 1952, the second from 1952 to 1969 and the last afterwards.

In figure 4 the average piezometric level in different places of the Venetian area is plotted versus time.

<u>Period before 1952</u>. When the artesian exploitation was not very intensive, subsidence was due only to natural causes; its rate was about one millimeter per year (Leonardi, 1960; Fontes and Bortolami, 1972).

The extraction of the artesian water began around 1930 when the first factories were established in Marghera. The piezometric level remained above the ground level, except in Venice, where it became lower since the time of World War II. The average decrease was slow all over the area, up to the fifties, when an intensive exploitation started, due to the industrial development (fig. 4).

<u>Period between 1952 - 1969.</u> After 1950 the changes became more evident. Artesian water was very actively withdrawn (Serandrei Barbero, 1972) and in the fifties all the hydraulic heads declined below the surface. In the industrial area the average rate reached 0.70 m/y, which is definitely higher than in any other part of the area (fig. 4). The observed minima were attained in 1969; in Marghera the fourth and fifth aquifers went down to 16 m below surface and in Venice the third and fifth

went to 7 m below. From 1952 to 1969, as an average in the industrial zone, a hydraulic head loss of more than 12 m was recorded. In Marghera the withdrawal occurred in about 50 wells, and it was about 460 l/sec in 1969; in Venice there were about 10 active wells, but in fact only one (10 l/sec) represented the whole extraction of the city. A significant ratio of 1 to 50 existed between the exploitation in the historical center and in Marghera.

In the period 1952-1968 geodetic surveys showed an average subsidence of 6.5 mm/y in the industrial area and 5 mm/y in the city. The most alarming figures appeared between 1968 and 1969, where maxima were observed of more than 17 mm in Marghera and 14 mm in Venice (Caputo et al., 1971)(fig. 5). Overall between 1952 and 1969 the local average subsidence was over 11 cm in the industrial zone and about 9 cm in the city, with local maxima of 14 and 10 cm respectively (fig. 5).

Years between 1969 - 1975. These years are characterized by a great number of experimental data and theoretical studies worth describing.

After drilling the deep test hole, VE 1 CNR, previously mentioned, two important steps were carried out: the annual repetition of the geodetic survey for controlling the ground movement in the area and the installation of a network of 112 piezometers (24 of which were continuously recording) for controlling the six exploited aquifers (fig. 6). Therefore it was possible to annually reconstruct the altimetric profiles and the

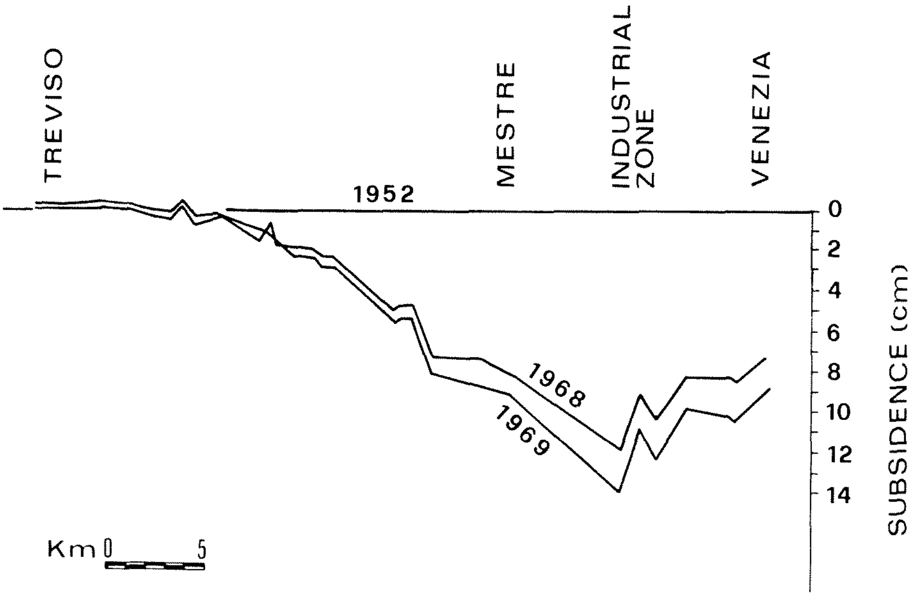

FIGURE 5 - Comparative plot of the levellings in 1968 and 1969 as referred to 1952.

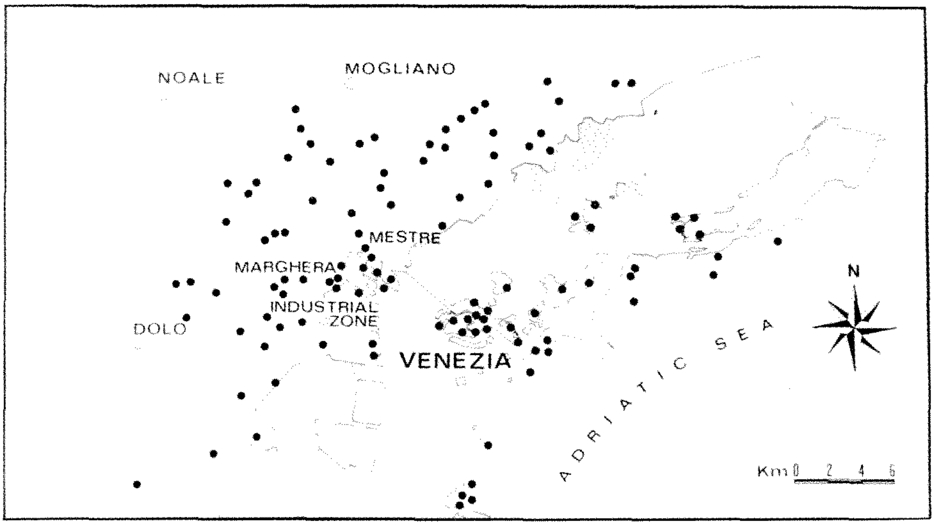

FIGURE 6 - Map of the 112 piezometers.

maps of the equipotential lines (e.g. see fig. 7 which refers to the 5^{th} aquifer for 1975. Similar behaviour holds true for the previous years).

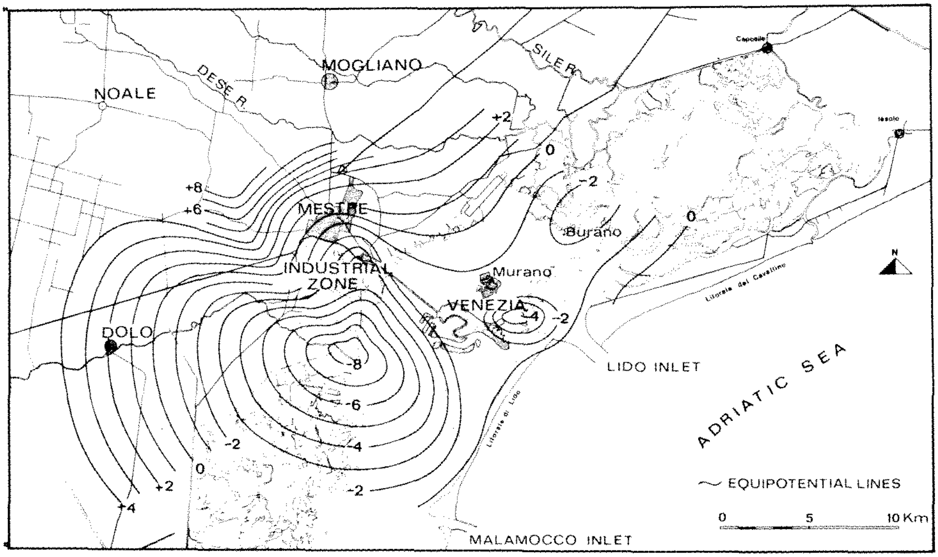

FIGURE 7 - Piezometric surface of the 5^{th} aquifer in 1975. Equipotential lines are given in meters a.s.l.

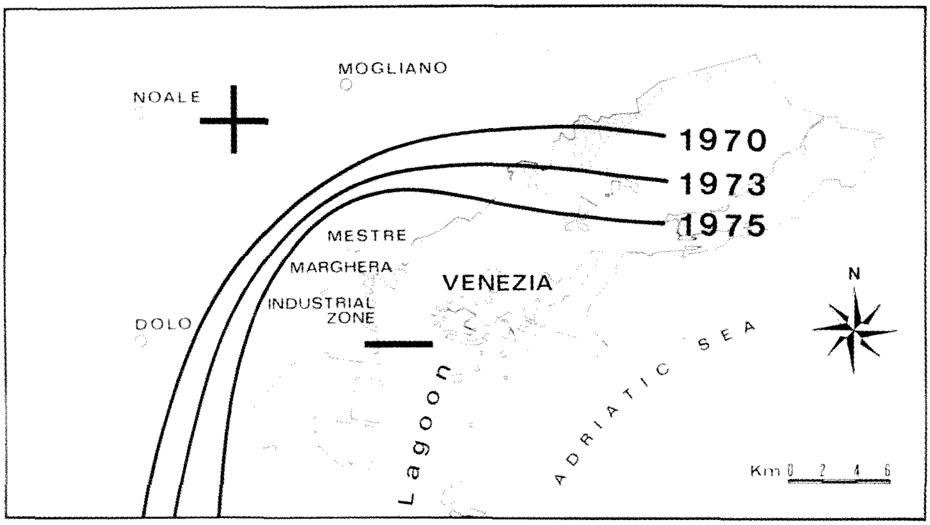

FIGURE 8 - Boundary of the areas where average piezometric level is above (+) or below (-) the ground level in 1970, 1973 and 1975.

In general, after the minima recorded in 1969, one can observe a gradual and remarkable improvement in the piezometric surfaces. In 1975, the average recovery in the industrial area reached a maximum of over 8 m, and in Venice more than 3 m. This new behaviour can be seen in figure 4 and it is also well shown in figure 8, where the the progressive reduction of the depressurized area in recent years is evident.

Similarly to what happened when piezometric levels were declining, a ground surface rebound is now accompanying the piezometric recovery. After a stability period, which is evident from the 1973 survey (Folloni et al., 1974),the 1975 levelling shows a rebound of the land which, in the historical center, is more than 2 cm with respect to 1969 (fig. 9). Even taking into account the range of the errors affecting the altimetric curve (Gubellini and DeSanctis Ricciardone, 1972), the variation of the ground level in this area remains positive. This is consistent with what appears in the tidal records in Rovinj and Bakar (on the Yugoslavian coast, which is taken to be stable) and those in Venice. Until 1969,the average annual sea level recorded at Venice was apparently increasing with respect to that of the other two stations. In recent years this did not occur any more (Tomasin A., private communication based on official data).

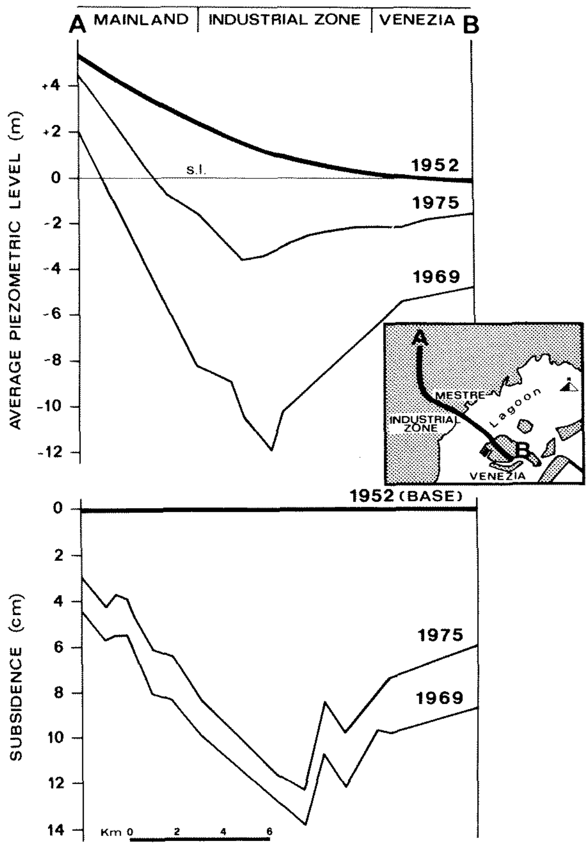

FIGURE 9- Comparison of the average piezometric levels and ground levels over mainland (A) and Venice (B).

4. Discussion

Analysis of Experimental Data. We will now analyze the most recent data, i.e. the period when the phenomena show a reverse trend.

Looking at the isopiezometric maps , we noted that:

- the piezometric surfaces of the aquifers in the Venetian area show strong depression, assuming the shape of an inverted asymmetrical cone typical of localized pumpage (Mozzi et al.,1975);
- the maximum drawdown in all the aquifers occurs in the Marghera area, which appears as the main withdrawal center. Minor discrepances are seen in the islands of Murano, Burano, Le Vignole and Lido;
- the greatest depressurization is found in the 4^{th} and 5^{th} aquifers;
- the development of the equipotential lines show that pumpage at Marghera affects the natural hydraulic balance of the aquifers also in the historical center, where the local withdrawals do not account for the observed drawdown;

- the distance between equipotential lines gets smaller landward. Figure 7 also suggest that a no flux boundary condition exists seaward. This is in keeping with the reconstructed geology.

The aquifer recovery is due to a decrease in the water exploitation. Since 1970, some areas in the district have been supplied by the public aqueduct. The industrial activity of Marghera has been reduced. Above all, well drilling was prohibited in the Venetian plain. In January 1975, the new industrial aqueduct, supplied by the Sile River, was put into operation (a 60% reduction in the number of active wells was observed in Marghera from 1969 to 1975, when the withdrawal was estimated to be about 200 l/sec).

The raising of the hydraulic levels is certainly not due to the increased recharge of the aquifers, since in the last decade the natural water supply in the recharge area is diminishing (Carbognin et al., in press).

The levellings, as already stated, show the stop of the subsidence and a certain rebound. The close connection between withdrawal and subsidence is evident in figure 9, where the altimetrical variations and the average piezometric level variations are given for the periods 1952-'69 and 1969-'75, along the same section from the mainland to Venice. Graphical comparison visualizes the presence of minima in the industrial zone, and similar behaviour of the processes during exploitation and recovery. In the rebound phase, however, we notice that while at Marghera a strong recovery determines a slight altimetrical rebound, at Venice a minor piezometric recovery causes a greater rebound. This can be ascribed to the diverse nature of the cohesive soils at Marghera and Venice.

The assumption of the interdipendence between the piezometric and the altimetric variations was statistically verified. In fact, the linear correlation coefficient, with a 95% probability, is between 0.70 and 0.92. The connection between the two variables is therefore expected to be extremely high. Consequently, the coefficient of determination indicates that the piezometric variations account for 70% of the altimetric ones, in terms of variance and in the limiting hypothesis of linear behaviour. The residual variance must be explained by other factors, such as natural subsidence and loading by buildings, but also errors in measurements and deviation from the linear hypothesis.

The interpretation of the subsidence to piezometric variations ratio ($R=\eta/\Delta h$) is also interesting. Its trend in the years 1952-'69 (fig. 10-A) is progressively rising from the industrial zone (1/109) towards the historical center (1/54). This variation can be attributed to the already noted gradual increase towards Venice of the more compressible soils. It explains why in Venice, where less water was pumped than in Mar-

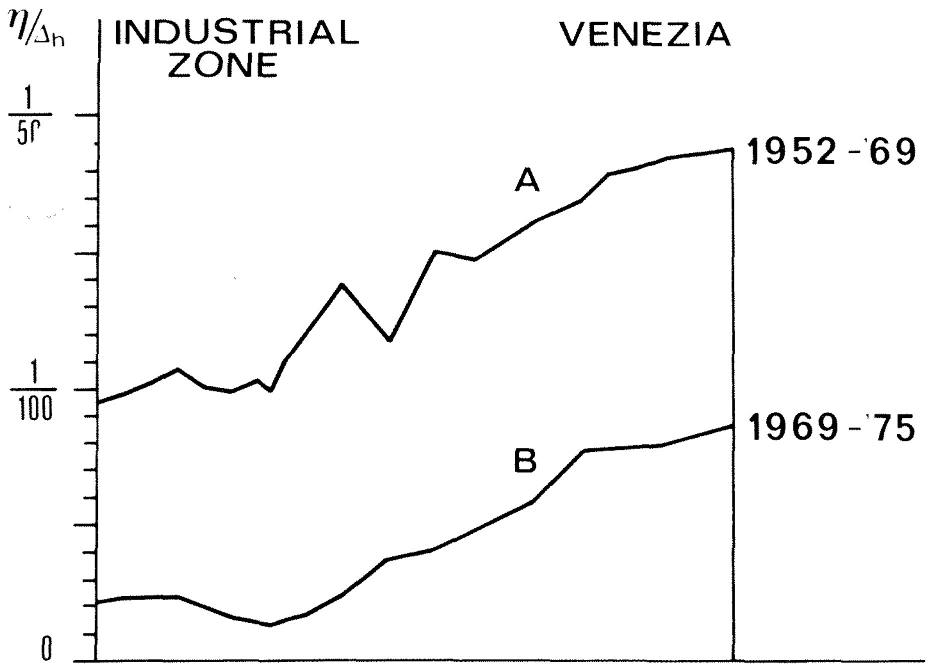

FIGURE 10 - The ratio of subsidence to piezometric variations from the industrial zone to Venice; A-settlement and B-rebound.

ghera, a subsidence of the same magnitude was observed. A similar behaviour is found in the rebound phase (fig. 10-B) between 1969 and 1975. However in this period, the curve lies definitely below the other one, thus confirming that the elasticity of the system is very limited.

<u>Predictive Simulations with the New Records.</u> Recently, a numerical model based on the classical diffusion equation and one-dimentional vertical consolidation has been used to simulate the past behaviour of the Venice subsidence and to predict the future settlement of the city (Gambolati and Freeze, 1973; Gambolati et al., 1974; Gambolati et al., 1975). A complete description of the approach together with an extensive discussion of the underlying assumptions may be found in the works cited.

The model has been applied again by using the new records to check its ability to reproduce the complex event at hand and to verify "a posteriori" its predictive capacity.

To date the pumpage at Marghera has been reduced to 40% of its maximum value (460 l/sec in 1969) and this change in the withdrawal rate has been assumed to occur in 1970 for it is apparent from figure 4 that the flow field recovery in Marghera started in 1970. Permeability distribution is the same as that used in the previous simulation (Gambolati et al., 1974) while the soil compressibility in rebound has been increased up to 20% of the corresponding values in compression, as is evidenced by the most recent laboratory tests summarized in figure 3. Therefore, the new results are slightly different from the early predictions given in figures 21 and 22 of the paper by Gambolati et al., 1974.

Figure 11 and figure 12 show the piezometric decline in the first aquifer (where the largest amount of data is available) and the Venice subsidence respectively versus time as provided by the mathematical model using the updated records. For the benefit of the reader the behaviour during the calibration period has been reported as well. The comparison with the experimental observations indicate a fairly good agreement, and especially so, if one considers the degree of uncertainty which is inevitably related to physical events of such a great complexity. This is further evidence of the adeguacy of the above model to reliably predict the settlement of Venice. At the same time the results allow the conclusion that the numerical models can be useful tools to investigate and keep under control land subsidence caused by subsurface fluid removal.

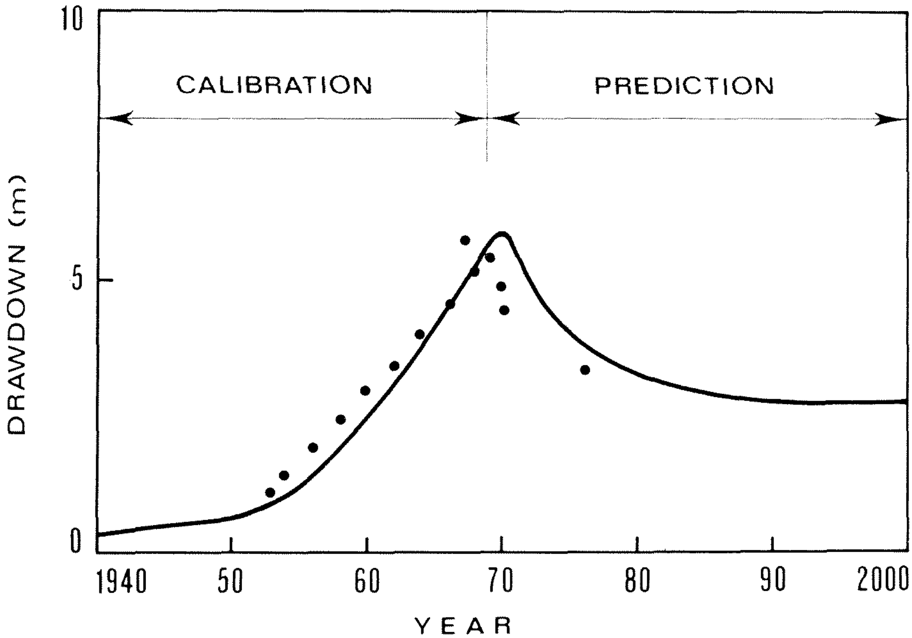

FIGURE 11 - Piezometric decline versus time in the first aquifer. The closed circles represent experimental records and the solid line gives the response of the model using the new data in our possession.

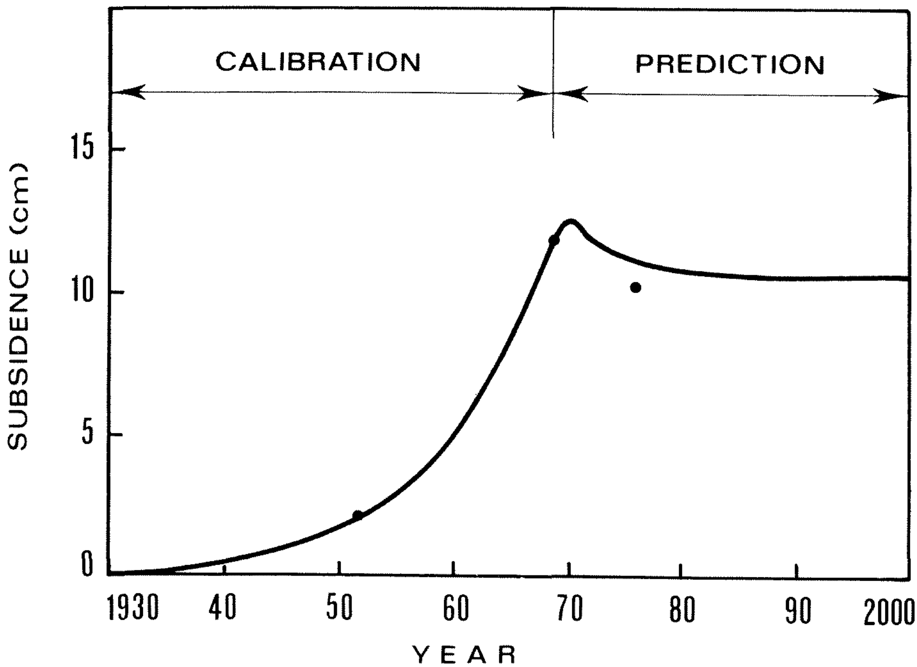

FIGURE 12 - Subsidence in Venice versus time as provided by the model using the new data in our possession. The experimental records (•) are indicated.

5. Conclusions

The results of the experimental research have confirmed that also in the case of Venice, the sinking was caused by the artesian withdrawals. Also statistical analysis attributes 70% of land subsidence occurring between 1952 - 1969 to the withdrawal of the underground water.

The experimental data showed that the pumpage performed at Marghera has greatly altered the natural flow field under the historical center and that the effects of the resulting subsidence are not uniformly distributed. In fact, for every meter of piezometric decline, the subsidence in the industrial area and in Venice was respectively one and two centimeters. This is connected to the relative increment towards Venice of the clay-type soils, which are more compressible making the level of the city more dependent on the piezometric situation.

Soil deformations related to hydraulic head variations occur in a relatively short time due to the fact that aquitards are mainly silty and each of them is interrupted by thin sandy layers which facilitate the drainage.

But the most significant fact that arises from our investigation remains in any case the sudden rise of the piezometric levels recorded in the whole area since 1970, and related to a significant reduction of the artesian withdrawals in the last years. It is also important that there is a parallel surface rebound (2 cm in Venice), that ensures that land subsidence has been arrested. This result is in agreement with the predictions from the mathematical model.

Since a more careful use of the underground waters give a very quick recovery, one can trust that a complete re-establishment of the natural hydraulic balance can be obtained, maybe with further intervention against wasting water (which can be estimeted to be about 4.5 m^3/sec due to the spontaneous spilling in the adjacent areas which influence the Venetian aquifer system).

Recovery will not however bring back the land to the original position as it has demonstrated that the reversibility of the compaction of the aquitards is possible for only 20% (which would correspond to a rebound of about 3 cm).

In spite of its serious responsability in the sinking of the ground, we do not see the necessity of stopping the extractions in the future.

Because of the unstable situation of Venice, it is necessary to continue the control of the piezometric levels of the aquifers and the ground altimetry. This is the only system by which we can evidence possible future variations from the present trend.

Bibliography

Alberotanza,L., Favero,V., Gatto,P., Masutti,M., Mozzi,G., Pianetti, F., and R. Serandrei, 1972, Catasto Pozzi del Comune di Venezia: Cons. Naz. Ric., Lab. Din. Gr. Mas., Tech. Rep. 23, 5 vols., Venezia, 1168 p.

Benini,G., 1971, Relazione fra Emungimenti ed Abbassamenti del Suolo:Ministero Lavori Pubblici, Comitato Difesa Venezia, III Gruppo, Padova, 97 p.

Caputo,M., Folloni,G., Gubellini,A., Pieri,L., and M. Unguendoli, 1972, Survey and Geometric Analysis of the Phenomena of Subsidence in the Region of Venice and its Hinterland: Riv. Ital. di Geofisica, Milano, v. XXI, n.1/2, pp.19-26.

Carbognin,L., Gatto,P., and G. Mozzi, 1974, Situazione Idrogeologica nel Sottosuolo di Venezia: Cons. Naz. Ric., Lab.Din. Gr. Mas., Tech. Rep. 32, Venezia, 29 p.

Carbognin,L., and P. Gatto, 1976, A Methodology for Hydrogeological Data Collection in the Venetian Plain: IBM Seminar on "Regional Groundwater Hydrology And Modeling", Venezia, 24 p.

Carbognin,L., Gatto,P., and G. Mozzi, 1976, Movimenti del suolo a Venezia e variazioni piezometriche negli acquiferi artesiani: Cons. Naz. Ric., Lab. Din. Gr. Mas., Tech. Rep. 67, Venezia, in press.

Consiglio Nazionale delle Ricerche, 1971, Relazione sul Pozzo

VE 1 CNR: Cons. Naz.Ric., Lab. Din. Gr. Mas.,Tech. Rep. 14 - 21, Venezia;

Consiglio Nazionale delle Ricerche, 1975, Livellazione Geometrica di precisione Rua di Feletto-Venezia: unpublished report of the Lab. Din. Gr. Mas., Venezia.

Favero,V., Alberotanza,L., and R. Serandrei/Barbero, 1973, Aspetti paleoecologici, sedimentologici e geochimici dei sedimenti attraversati dal pozzo VE 1 bis CNR: Cons. Naz. Ric., Lab. Din. Gr. Mas., Tech. Rep. 63, Venezia, 51 p.

Folloni, G., De Sanctis Ricciardone, and A. Gubellini, 1974, Evoluzione recente del fenomeno di subsidenza nella zona di Venezia e del suo entroterra: Ist. di Topografia e Geodesia, Università di Bologna, 16 p.

Fontes,J. Ch., and G. Bortolami, 1972, Subsidence of the area of Venice during the past 40.000 years: Cons. Naz. Ric., Lab. Din. Gr. Mas., Tech. Rep. 54, Venezia, 11 p.

Gambolati,G., and R.A. Freeze, 1973, Mathematicam Simulation of the Subsidence of Venice, 1st Theory: Water Resource Research, v. 9, n° 3, pp.721-733.

Gambolati,G., Gatto,P., and R.A. Freeze, 1974, Mathematical Simulation of Subsidence of Venice, 2nd Results: Water Resource Research, v. 10, n° 3, pp. 563-567.

Gambolati,G., Gatto,P., and A.R. Freeze, 1974, Predictive Simulation of the Subsidence of Venice: Scienze, v. 183, pp. 849-851.

Gubellini,A., and G. De Sanctis Ricciardone, 1972, Analisi dei risultati di due livellazioni eseguite nella zona di Venezia nel 1970 e nel 1971: Cons. Naz. Ric., Lab. Din. Gr., Mas., Tech. Rep. 41, Venezia, 18 p.

Leonardi, P., 1960, Cause Geologiche del Graduale Sprofondamen-to di Venezia e della sua Laguna: Ist. Ven. Sc. Lett. e Arti, Venezia, 21 p.

Ministero dei Lavori Pubblici, 1973, Pozzi LIDO 1 e MARGHERA 1: Comitato Difesa Venezia, III Gruppo, Relazione AGIP, S.Donato Milanese.

Ministero dei Lavori Pubblici, 1974, Catasto dei Pozzi Artesiani: Comitato Difesa Venezia, IV Gruppo, n° 1, Fasc.n° 18, 35 p.

Mostertman,L.J., and J.F. Poland, 1969, Reconnaissance investigation of the subsidence of Venice and suggested steps toward its control: UNESCO report, Paris, 24 p.

Mozzi,G., Benini,G., Carbognin,L., Gatto,P., and M. Masutti, 1975, Evoluzione delle pressioni di strato negli acquiferi artesiani, Cons. Naz. Ric., Lab. Din. Gr. Mas., Tech. Rep. 66, Venezia, 38 p.

Neglia,S., 1972, Pozzi VE 1 e VE 1 bis CNR, Analisi geochimiche sulle carote argillose: Cons. Naz. Ric., Lab. Din. Gr. Mas., Tech. Rep. 56, Venezia, 16 p.

Ricceri,G., and R. Butterfield, 1974, An Analysis of Compressi bility Data from a Deep Borehole in Venice: Géotechnique, v. 24, n° 2, London, pp. 175-192.

Rowe,P.W., 1973, Soil Mechanics Aspects of the Cores of the deep borehole VE 1 CNR in Venice: Cons. Naz. Ric., Lab. Din. Gr.Mas., Tech. Rep. 57, Venezia, 53 p.

Serandrei Barbero R., 1972, Indagine sullo sfruttamento artesiano nel Comune di Venezia, 1846-1970: Cons. Naz. Ric., Lab. Din. Gr. Mas., Tech. Rep. 31, Venezia, 97 p.

Publication n°121 of the International Association of Hydrological Sciences
Proceedings of the Anaheim Symposium, December 1976

THE USE OF MUD-JACKING FOR THE UPHEAVING OF URBAN ZONES. COMPUTER CONTROL OF THE WORKS. EXPERIMENTAL APPLICATION TO THE PROBLEM OF VENICE.

Dott. Ing. Santiago Marchini
Vice President Ing. G. RODIO & C. S.p.A.
Casalmaiocco (Milano) - Italy

Dott. Ing. Andrea Tomiolo
Ing. G. RODIO & C. S.p.A.

Abstract

The upheaving of urban zones, even of quite large extent, by means of mud-jacking process is discussed.

A proper application of this method implies the fulfilment of certain conditions. On one hand the upheaval must be permanent, even if an incidental reintegration might be possible. On the other hand the sequence of the operations must permit limiting the differential upheaval to a fixed quantity. Finally the injected materials must comply with the environmental conditions from the physical, chemical and biological points of view.

It is difficult to establish a computable correlation between the upheaval of a point and the parameters of the injection which has caused it. A tentative numerical analysis of the problem has however been tried out and introduced in a computer program. The data recorded during the first site operations are statistically analysez allowing probabilistic predictions. Subsequent site operations are selected in accordance with the computed results.

This operational approach was meant for tests carried out by the authors in the Venice area.

Foreward

This paper deals with a case of induced negative subsidence aimed at counteracting a much larger phenomenon of land subsidence.

Grouting is usually employed either to improve mechanical soil characteristics or for reducing soil permeability.

Sometimes bad execution of the works may cause surface upheaving damaging the existing structures. These upheavings are normally caused by inclusion of a continuous grout layer in the soil fractured by grouting pressure (figure 1). They are normally considered as an accident to be avoided, hence a special technique to control them has been developed.

A fairly similar technique can be employed in order to obtain a desired upheaving instead of avoiding it. This technique consists of grouting under high pressure special compounds having very high viscosity as compared with the low permeability and grain size distribution of soils.

This technique was first carried out, with a most encouraging result, to heave a building in Rotterdam (The Netherlands) and was reported by Cambefort and Puglisi in 1971.

A more extensive application of this principle was carried out in Venice in an experimental field. This paper describes the test and a new approach to the general problem of safeguarding Venice against the effects of recurring floods.

A special chapter is devoted to computer controls intended to limit

Grouting for the upheving

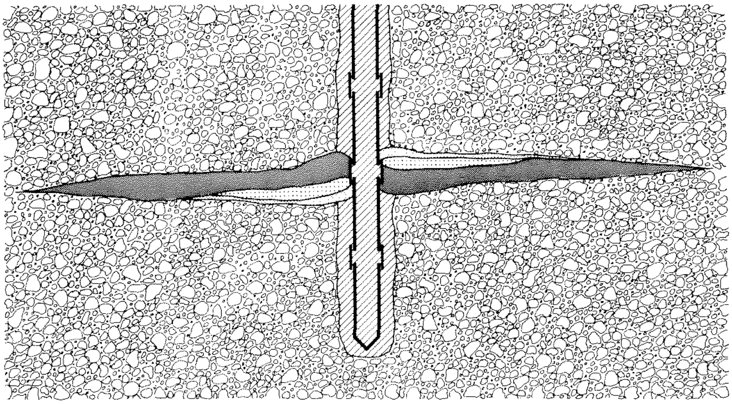

Normal grouting

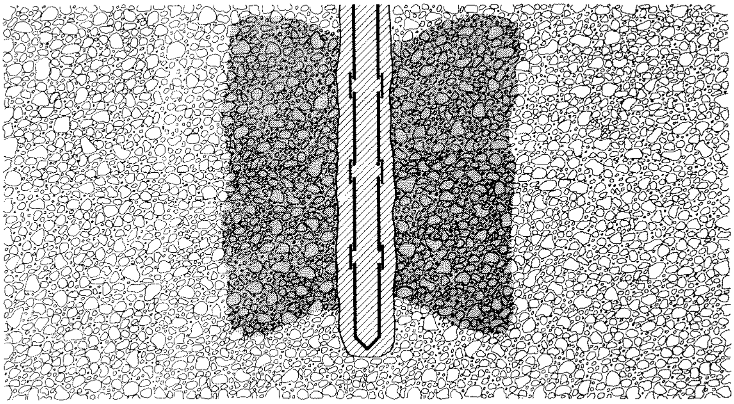

Fig. 1

the differential heaving of the various points of the existing structures.

The problem of Venice

The problem of Venice arises essentially from the subsidence of the lagoon and the periodic "high waters".

The general subsidence of the lagoon area and the town was estimated at about 5 mm per year, from 1952 to 1962, and tends to increase. The main causes of the subsidence are :

- general subsidence of tectonic origin
- natural process of consolidation of sedimentary deposits
- lowering of piezometric levels due to pumping in deep strata, which causes further consolidation of the upper layers
- rise in the average sea level.

The term high waters refers to the abnormal rising of the water wi-

Subdivision and yearly duration of the sea levels

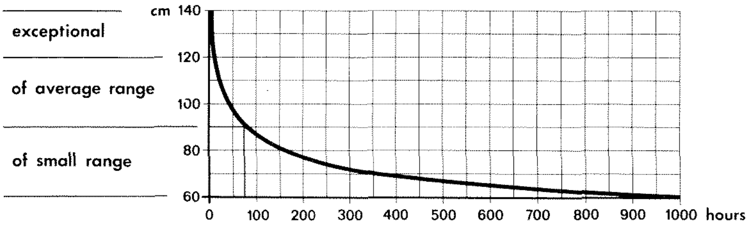

from the CNR report of 1970, data supplied by Punta Salute tide station

Fig. 2

thin the lagoon owing to the simultaneous action of :
- tides
- low pressures and winds
- local oscillation of the water caused by the shape of the basin.

Figure 2 shows the distribution of high water in one year.

In figure 3 the grey zones indicate which parts of the town are affected by a high water of 90 cm.

The only method of protecting Venice against high waters is that of regulating the flow into the lagoon during the tides by means of gated structures.

However this protection against high sea level within the lagoon causes remarkable consequences of an environmental and hygienic nature to the necessary water circulation. Another very important consequence is economical and concerns the commercial and industrial activity of the harbour.

The time during which gates must be kept closed to prevent the water in the lagoon from rising to levels exceeding 90 cm is less than 100 hours per year.

Nevertheless flooding of some areas in the historical center will occur even if tides are limited to heights of average range. These areas are of rather small extent but some of them are among the most significant for their architecture and urban structure. A project aiming at a permanent upheaval of these zones constitutes a logical completion of the overall reclamation project which permits attainment of the two essential requirements : to reduce shut-off by gates to a minimum corresponding to exceptionally high waters and provide the entire city, and in particular the most precious zones, with equal safety protection against the effects of recurring floods.

The magnitude of the average necessary upheaval to be induced may be roughly assumed as being 20 cm. In fact 10 cm is the difference of level between the zones subjected to flooding at lagoon water level +90 cm. The other 10 cm is the estimated amount of ground settlement which will occur within the next 50 years owing to geological subsidence and rising of average sea level. The solution is valid provided that in the meantime all the necessary measures are taken to eliminate reasons for subsidence connected with industrial activities (i.e. pumping water from deep strata).

The experiment carried out

The experiment was carried out on a portion of Poveglia Island near Venice, where an upheaval of 10 cm was induced over a 900 sq.m. test area, including two small old building

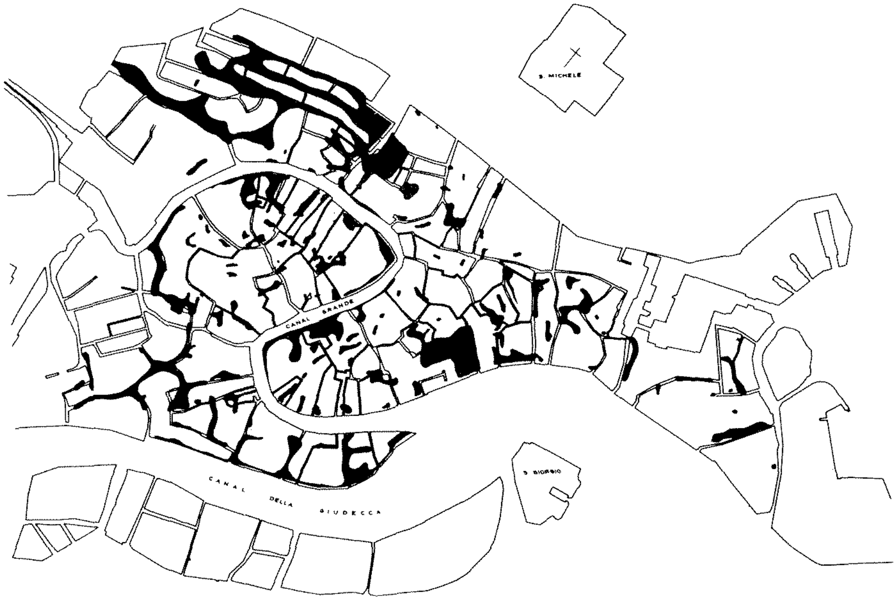

Areas submerged by low sea levels (less than 90 cm)

0 500

Fig. 3

Grouting was carried out at a depth where a very high ratio of horizontal to vertical permeability had been detected, constituting the most favourable condition for the formation of horizontal grout lenses, as shown in figure 1.

The superposition of these lenses enabled the formation of a continuous and firm layer of mortar of thickness sufficient to obtain the desired upheavals at various points (figure 4).

The soil down to 20 m was a typical lagoon sedimentary soil with alternations of fine sands and silty-clays layers.

The grouting material consisted of a cement-clay mix with the addition of inexpensive additives having a long term resistance of about 20 kg/cm^2.

In figure 5 the lay-out of the grouting holes and the points of upheaving control are shown. In the same figure the two small existing buildings are also shown. Figure 6 shows the amount of grout necessary to obtain un upheaval of 10 cm.

The distance between the holes was 5 metres while at the periphery this distance was reduced to 2,5 metres in order to win the shear resistance along the perimeter and get better control of the heavings.

The choice of level where grouting was to be carried out was mainly dictated by the following considerations :

- to obtain good distribution of pressure in the upper layers
- to limit the volumes of grout necessary
- to enable use of a network of holes large sufficiently

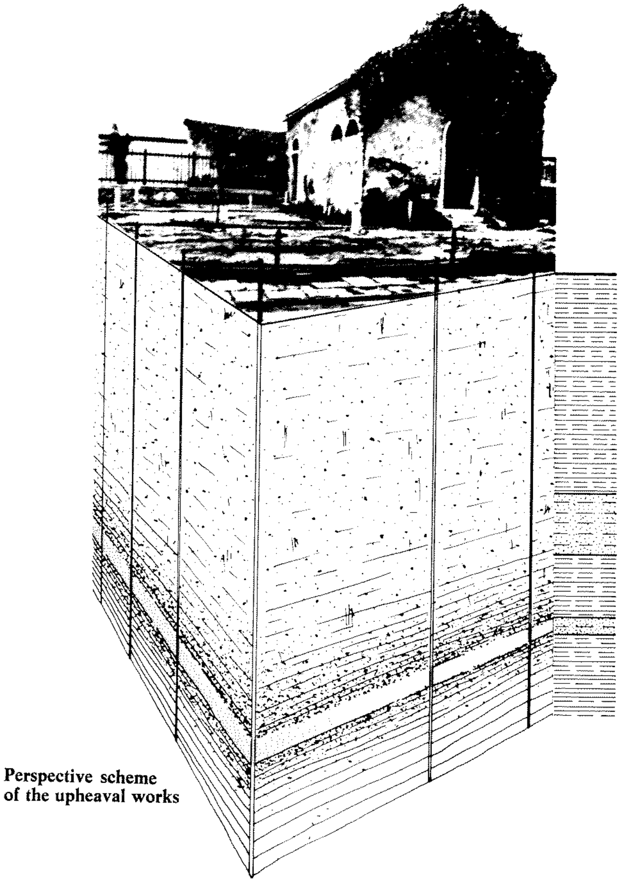

Fig. 4

Lay-out of grout holes and upheaving control

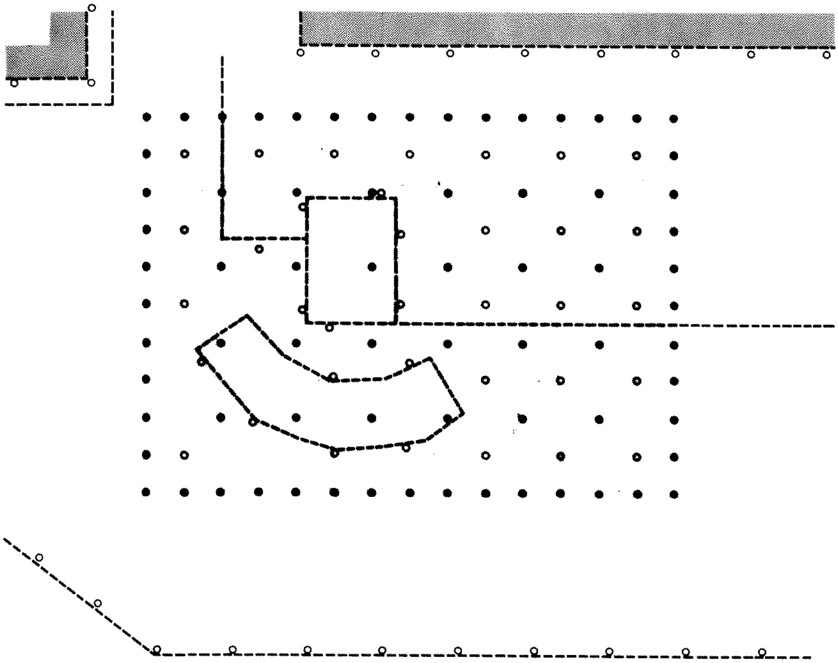

• grout holes

o upheaving control

Fig. 5

Curves of equal grout quantities in cubic metre per hole

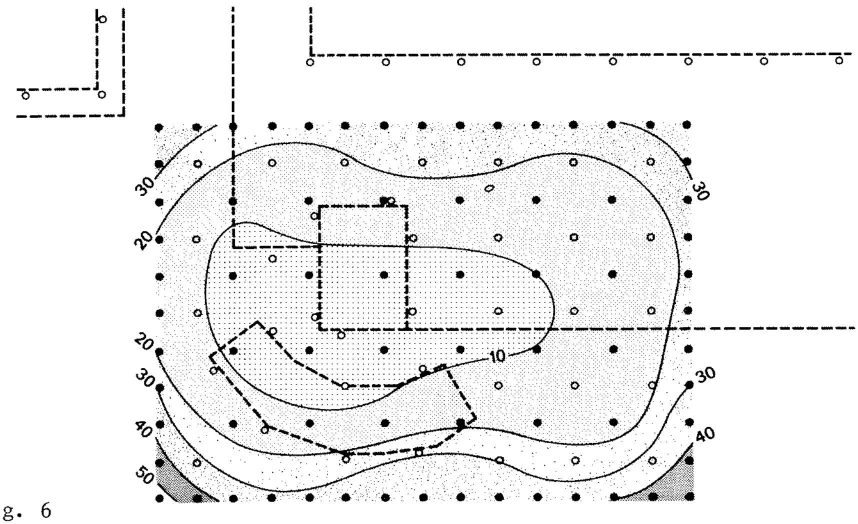

Fig. 6

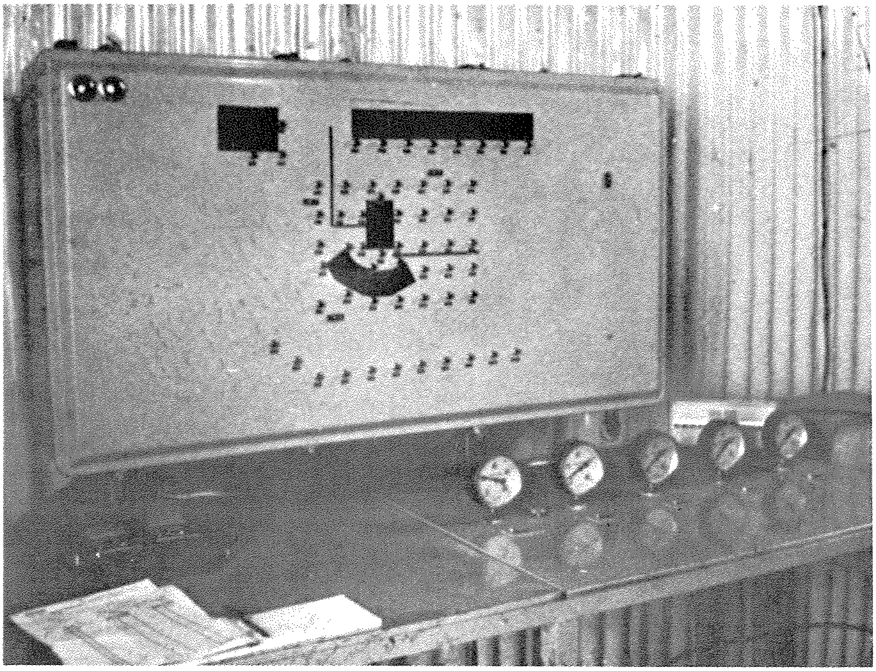

Fig. 7 - Control board

Fig. 8 - General view of the site

Fig. 9 - Grout operations

- to take advantage of the presence of a thin sandy layer interbedded between two clay layers at a depth of about 10 metres which could act as confining boundaries to the grouted material forcing it to expand only in a horizontal direction.

Uplifts were controlled by means of a specially designed system of electric cells.

The experiment, which matched quite closely the design forecast, required particular ingenuity in its practical implementation and showed that :

- upheaval can be obtained according to the predetermined phases, by keeping to the specified differences of level between the different points
- it is possible to control the uplifting operation since the effects can be limited to the testing area without affecting the surroundings
- a system for monitoring the absolute and differential upheavals among the various points within a given area is available
- tests and precision levelling repeated systematically during a period of one year prove that final uplift is permanent
- the quantities of grouted material and the cost of the entire operation compare well with the cost of the damage avoided to land and property produced by floods.

Grouting control

The magnitude of upheaving in each point of the surface is a function of a very large number of parameters. Thus it is practically impossible to establish an analytical law correlating surface uplift and grouting details.

For this reason a statistical model has been set up. This model takes into account the results obtained with the early grouting performed in the area and permits probabilistic predictions for further operations. It is a dynamic model which is continuously supplied with the latest results obtained and enables the problem of how to heave a given area in the most uniform and economic way to be solved.

In practice the model simulates further grouting in advance and indicates the operations necessary to achieve the required results.

Correlation between grouting and upheaving

The general law correlating grouting at a point J and the upheaving w of the area S_i can be written in the following form :

$$1)\quad w_{ij} = c_{ij} \frac{V_j}{S_i} \frac{R_v}{R_{cj}}$$

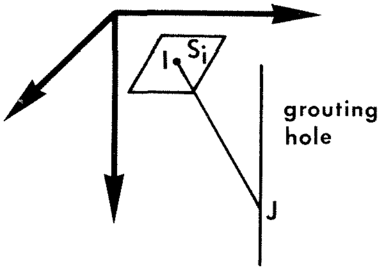

Fig. 10

where

w_{ij} is the average upheaving of the area S_i caused by grouting at point J

c_{ij} is the coefficient of grouting correlation between points J and i

V_j is the grouted volume in J

S_i is the area represented by point I

R_v is the ratio between the grouted volume and the volume actually inserted in the soil

R_{cj} is the factor of precompression effectiveness at point J. It depends essentially on the depth of J, on the preexisting stress situation in the vicinity of J and on grout characteristics (volume rate of discharge, pressure, etc....)

Some of these factors can be quantitatively defined for a given site. In particular S_i and R_v can be treated as constants after the initial phase of the works. Thus only the coefficient c_{ij} can be considered as a variable fully representing the cause-effect correlation.

Equation 1) enables the correlation between the coefficient c_{ij} with the predicted or measured upheaving $\overline{w}_{ij}$ to be established.

A system consisting of m upheaving measuring points and n grouting points can be represented in a correlation matrix $[C]$.

$$C = \begin{bmatrix} c_{11} & \cdots & c_{1n} \\ \vdots & c_{ij} & \vdots \\ c_{m1} & \cdots & c_{mn} \end{bmatrix}$$

Fig. 11

In this matrix each element c_{ij} represents the influence on heaving at point i of introducing a given volume of grout at point J.

Such a model can be used to deal with two different types of problem:

a) to lift up one or more zones S_i

b) to equalise different heavings.

In these cases the model indicates the optimum for :

- the location of points J to be grouted

- the volumes to be introduced into the soil at various points
- the expected heavings.

The optimization obtained with the model allows the number of operations and grout volumes to be minimized.

Initial matrix

Practical applications require that an initial matrix of correlation be established. The more approximate the initial matrix the faster and more reliable is the model in its earlier phases. The authors elected to fill the matrix [C] by approximating the grouting correlation coefficients to vertical forces acting at each point J, rather than with random figures.

Surface heaving can be evaluated by Mindlin's formulae concerning the action of a force F acting in a semi infinite space.

The results of the application of Mindlin's formulae show that heaving w (x) is a function of the elastic characteristics of the media.

The heaving of the four corners k, l, m, n, of the area S_i can be calculated so that an average value can be formulated :

Fig. 12

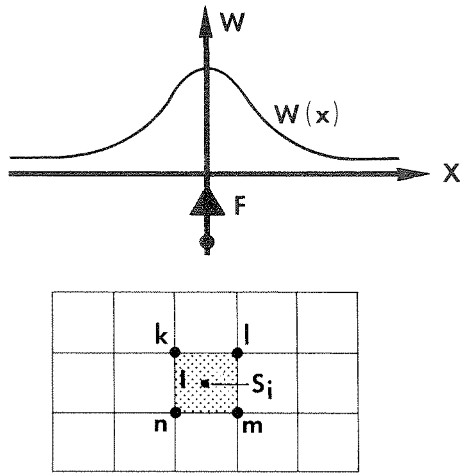

$$w_i = \frac{w_k + w_l + w_m \; w_n}{4}$$

The average volume heaved is represented by $w_{ij} \; S_i$ and the total volume for the n areas is

$$P = \sum_{1}^{n}{}_i \; w_{ij} \; S_i$$

The correlation coefficient can be defined as :

$$c_{ij} = \frac{w_i \; S_i}{\sum_{1}^{n}{}_i \; w_{ij} \; S_i}$$

This matrix has the following characteristic :

- it is a rectangular matrix of m lines representing the holes and n columns representing the number of areas
- the sum of the coefficient c_{ij} of each column is equal to 1
- when grouting is simultaneous in several holes the coefficient of correlation can be added.

Evolution of the model

After the initial matrix is fed in the model develops as follows :

- it determines the coefficient R_{cj}
- it determines the coefficient c_{ij}

The probable heavings produced by grouting at a point J have the following total volume :

$$P = V_j \frac{R_v}{R_{cj}}$$

After grouting operation, according to computer indication, site measurements give : actual heavings $\overline{w}_{ij}$, total actually heaved volume P and the total volume grouted Q.

From these values the true value of R_{cj} can be found :

$$R_{cj} = \frac{Q}{P} R_v$$

This value of R_{cj} will be fed back to the program and used in further runs.

In a similar way the value of c_{ij} can be obtained by introducing the measured values of $\overline{w}_{ij}$ in equation 1) :

$$\overline{w}_{ij} = c_{ij} \frac{Q}{S_i} \frac{R_v}{R_{cj}}$$

Equation 1) represents variations of the heavings w_{ij} corresponding to the volume V_j at point J. In this equation R_v, R_{cj}, V_j and S_i can be considered as given variables, while the variable w_{ij} can be considered as a Gaussian variable. As a consequence also the variable c_{ij} becomes a Gaussian variable.

It is possible to back figure the values of c_{ij} based on the in situ measurements by equation 1) and to place them in a Gauss distribution for c_{ij} so that the most probable values for c_{ij} can be used in further probabilistic applications of the model.

Practical use of the model

A computer terminal is installed at the site and it is connected with the grouting and upheaving measurement equipments.

The input of the quantities data is direct and their values are recorded on magnetic tape.

The sequence of operations is the following :

1) goal definition (for instance : heaving zone A without heaving zone C)
2) instructing the computer
3) determining, by the computer, the points where grouting must be applied
4) grouting
5) monitoring of pressure, heaving, etc. and direct feed-in to the computer
6) processing of the measured quantities through the dynamic model and updating the model matrix.

Symbols

C = matrix of coefficients of correlation
c_{ij} = coefficients of correlation
I = point of measurement of upheavings
J = point of grouting

S_i = area represented by point I
P = total heaving caused by grouting
Q_j = total volume grouted at point J
R_{cj} = factor of precompression effectiveness
R_v = volume effectiveness of grout volume
V_j = volume to be grouted at point J
w_{ij} = upheaving at point I caused by grouting in point J
$\bar{w}_{ij}$ = measured upheavings

References

Cambefort H., 1967, Injection des Sols : Eyrolles Editeur - Paris, 2 vol. 393 p., 177 p.

Cambefort H., Puglisi R., 1971, Soulèvement d'un Bâtiment par Injection du Sol : Ann. Inst. Techn. Bât. Trav. Publ., n. 281, p. 27 - 36.

Publication n°121 of the International Association of Hydrological Sciences
Proceedings of the Anaheim Symposium, December 1976

LAND SUBSIDENCE IN CENTRAL ARIZONA

Carl C. Winikka and Paul D. Wold
Administrator, Arizona Resources Information System, Phoenix, Arizona
Geologist, U.S. Bureau of Reclamation, Phoenix, Arizona

Abstract

Land subsidence and earth fissures occurring in parts of central Arizona are related to water-level declines caused by large-scale groundwater withdrawal. Differential land subsidence and earth fissures have damaged Picacho Reservoir, agricultural lands, water-distribution systems, water wells, buildings, interstate highways, county roads and streets, and have necessitated rerouting of a proposed major aqueduct. Earth fissures, probably associated with the land subsidence, were first reported in 1927, and land subsidence was first measured in 1948.

The maximum documented subsidence from 1948 to 1967 was 2.29 m near the town of Eloy. Since 1967, more than 0.9 m of subsidence has been measured along Interstate Highway 10 near Picacho.

Between 1948 and 1967, in the lower Santa Cruz Basin, about 570 square kilometers have subsided more than 0.15 m, and about 155 square kilometers have subsided more than 0.9 m in the Casa Grande-Eloy area. In the Stanfield-Maricopa area, approximately 200 square kilometers have subsided more than 0.3 m.

In the Salt River Valley, the land surface has subsided as much as 1.16 m near Queen Creek, 0.64 m west of Luke Air Force Base, and 1.13 m east of Mesa, between 1948 and 1967. Between 1971 and 1975, approximately 0.3 m of subsidence was measured southeast of Mesa.

By 1964, large-scale pumping, principally for irrigation, had lowered water levels more than 110 m in parts of the area, and numerous earth fissures were observed. Since 1964, water levels have declined more than 24 m in local areas. Compaction-recorder data indicate long-term water-level declines correspond with land subsidence. Seasonal water-level fluctuations correspond with seasonal sediment compaction and expansion; however, the amount of compaction greatly exceeds the expansion. Between April 1965 and April 1974, measured compaction in the upper 253 m of sediment in the Santa Cruz Basin near Eloy accounts for 0.41 m (63%) of the 0.65 m total surface subsidence at the compaction-recorder site.

Earth fissures, as much as 13.8 km long, occur in the alluvial sediments on the periphery of the subsiding areas, transect natural drainageways, and act as drains. The fissures intercept surface runoff in undeveloped areas, and capture irrigation water traversing cultivated lands. Downward and lateral water movement in the fissures causes rapid near-surface widening--partly by slumping but mainly by erosion of the sides.

In 1976, renewed fissuring near the Picacho and Santan Mountains and several areas of previously unmapped fissures were mapped on orthophoto quads using a helicopter. New and renewed fissuring, measured water-level declines and sediment compaction, together with the limited leveling data available indicate land subsidence continues to occur over large areas of central Arizona.

Introduction

Major dams constructed on rivers in central Arizona provide the water necessary for extensive agricultural and industrial development. This development coupled with a mild, dry, sunny climate have made Arizona an increasingly more desirable place to live and development has continued at a rapid pace. From 1970 to 1975, Arizona's increase in population was over 25 percent, the highest growth rate of any State in the Nation.

To meet water requirements of this growing area, ground water is being pumped in addition to that supplied through the reservoir system. The volume of ground water withdrawn now greatly exceeds the rate of recharge. Land subsidence and earth fissures occurring in parts of central Arizona are related to water level declines caused by large-scale ground-water withdrawal (Figure 1).

Ground-water withdrawal in Arizona now exceeds the recharge by 2,700 cubic hectometers per year. The Central Arizona Project is expected to lessen this overdraft by approximately 1,500 cubic hectometers of water per year beginning in the 1980's. In the meantime, substantial subsidence and the intensification of earth fissuring in subsiding central Arizona basins is continuing. The Central Arizona Project, new highway construction, and flood control projects will all be affected by this continuing subsidence process. Residential, industrial, and commercial expansion which follow will also be affected not only by the physical hazards involved but also by the depreciation effect earth fissures have on property when occurring in or near development (Figure 2) or irrigated farmland (Figure 3).

At present, the extent to which declining ground water levels, subsidence, and related earth fissures constitute environmental hazards is minimal. Subsidence effects are gradual and take place generally in agricultural or undeveloped desert areas.

While fissures normally occur in natural desert areas they have also occurred across interstate highways, in irrigated fields, across pipelines, and frequently across unpaved local roads. In two known instances, earth fissures are in residential areas. Subsidence has caused the collapse of well casings and in some places apparent extrusion of well casings from the ground surface. Subsidence has thus required well replacement or modification.

The subsidence process in Arizona transects both the scope and geographical extent of agency responsibilities. As a result, the total effects are not known and any assessment of the effects on future projects requires a considerable data gathering effort. Records of subsidence are scarce and existing level lines must be carefully evaluated prior to use for subsidence measurements. A continuity of elevation change measurements is made increasingly difficult due to the destruction of bench marks and the rising cost of field surveys.

Earth fissures not shown on existing maps were discovered during studies for the Bureau of Reclamation's Central Arizona Project. Other interested Federal and State agencies, with a common need for this information, joined the Bureau of Reclamation in mapping all visible earth fissures in the 2,000 square kilometer area in three major basins south and east of Phoenix, Arizona (Figure 1).

This paper reports on a joint effort by several agencies to update and bring together information to better understand the interrelationship between ground-water declines, subsidence, and earth fissures.

Techniques

Mapping of the earth fissures was done in two stages. First, 1:24,000 and larger scale color infrared aerial photographs were taken of all known fissure areas. A total of 144 aerial photographs were obtained. The aircraft and camera were provided by Arizona Department of Transportation and the film by the U.S. Geological Survey. All identified fissures, as well as probable fissures, were transferred from this photography to 1:24,000

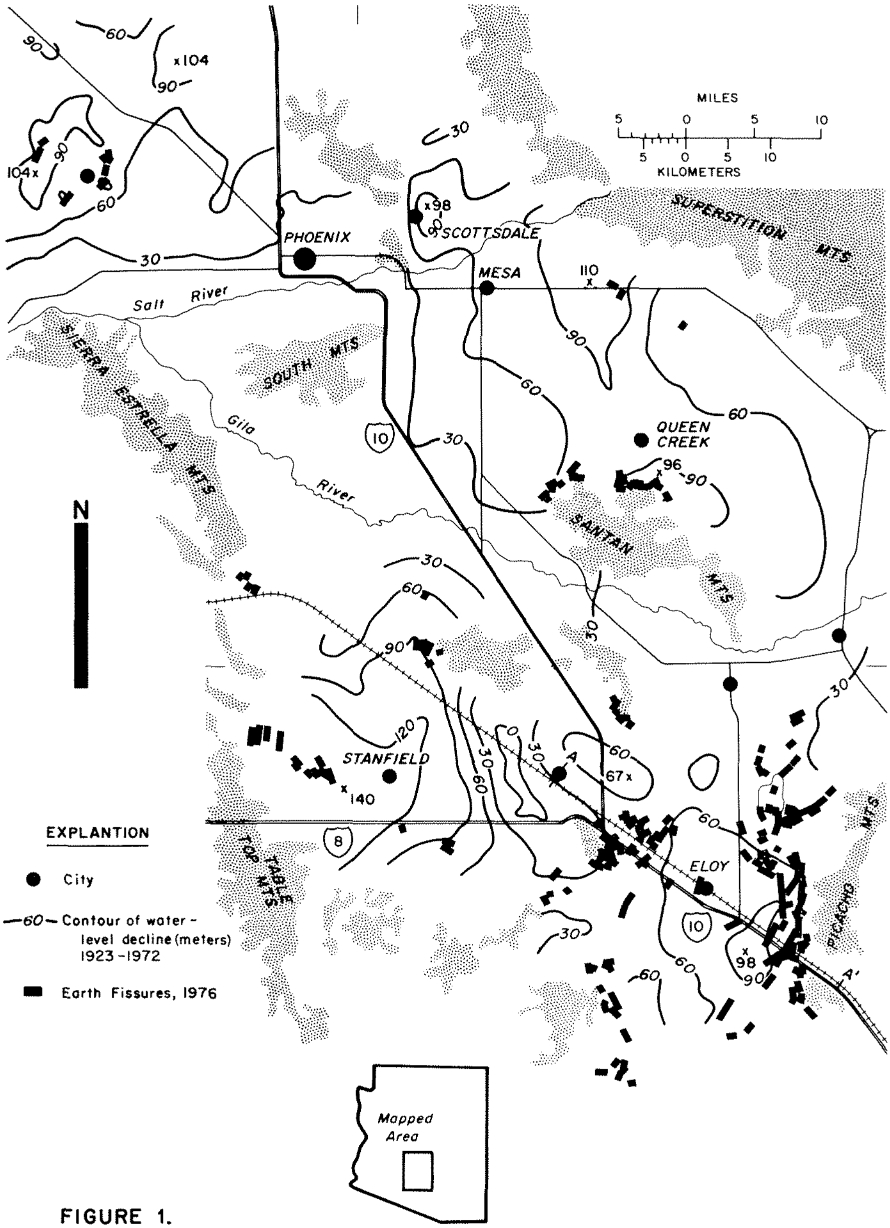

FIGURE 1.

LOCATION OF WATER-LEVEL DECLINES AND EARTH FISSURES IN CENTRAL ARIZONA.

Figure 2 - New earth fissure heading toward housing development south of the Sacaton Mountains.

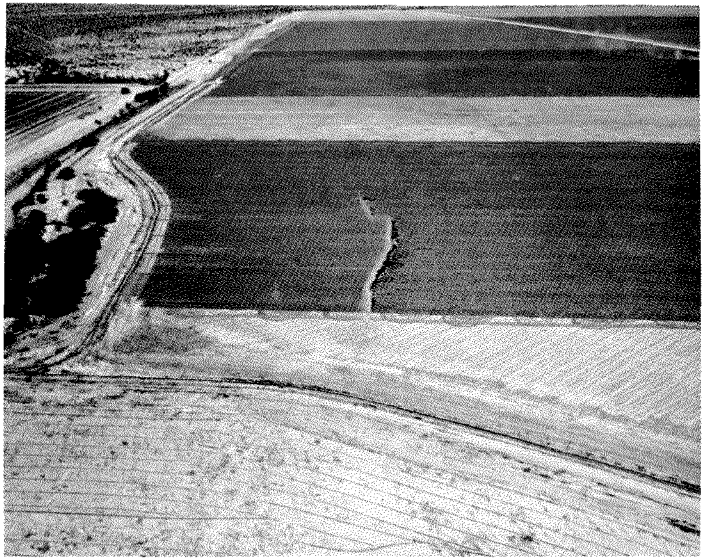

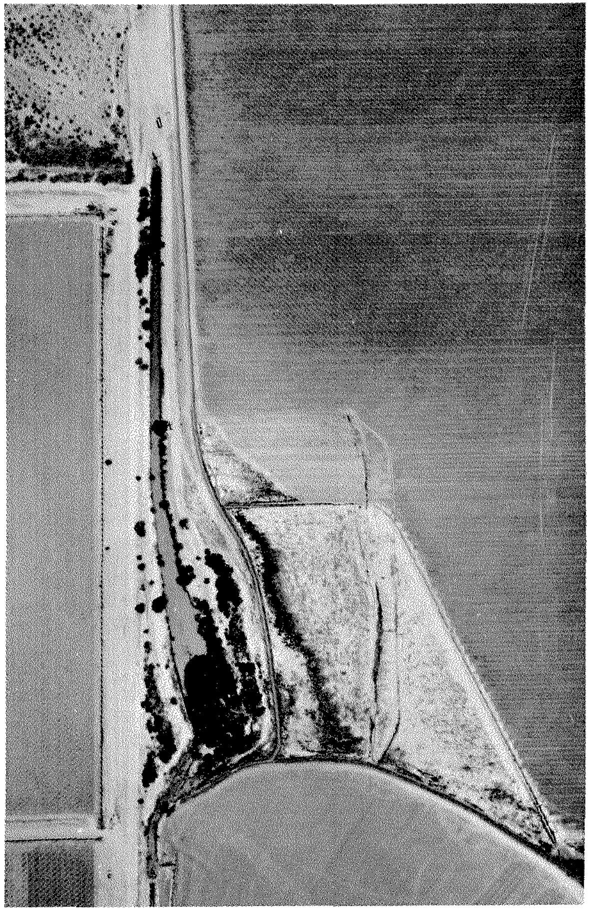

Fig. 3. Oblique aerial view (above) of earth fissure in agricultural land photographed in April 1970, 3 days after fissure appeared during irrigation. The same fissure (right) in a vertical aerial photograph taken in June 1974. Note land taken out of production and extension of fissure toward top of photograph.

scale orthophotoquads (Winikka-Morse 1974) furnished by the Arizona Resources Information System.

Second, these fissures were checked and the entire area of approximately 2,000 square kilometers was searched by two observers and a recorder in a four place helicopter. Fissures were spotted from the air and checked on the ground. Locations were determined by using the orthophotoquads as base sheets. This procedure took three days for a total of about 15 hours flying time.

Ground-water decline and measured subsidence information was gathered from State and Federal agency records. Recent information was found to be available from the U.S. Geological Survey and the Arizona Department of Transportation.

Water-Level Declines

Substantial water-level declines are continuing in a number of ground-water dependent areas in central Arizona (Laney-in preparation). While these areas are predominantly agricultural, urban areas are not excluded (Figure 1). Maximum values of water-level decline are 140 meters near Stanfield, 110 meters east of Mesa, 98 meters southeast of Eloy, south of Queen Creek, and at Scottsdale. The decline at Scottsdale is recent, having occurred since 1952 (USBR-in preparation). In all of the above areas declines are increasing in magnitude and in total area affected.

Subsidence

Land subsidence in Arizona related to ground-water withdrawal (Poland-Schumann 1969) is continuing. Subsidence has a relationship to ground-water declines in the Casa Grande-Picacho section of Pinal County (Figure 4). When declines and subsidence are plotted against time, a strong linear relationship is found at Picacho (Figures 5 and 6).

Information available on four bench marks in the Toltec-Eloy area of Pinal County shows subsidence of these marks from 1960 to 1975 to range from 0.44 m to 0.69 m. In the Picacho area several marks have subsided more than 0.70 m from 1967 to 1975 with the result that the area of maximum measured subsidence has shifted approximately 6 kilometers southeasterly along the Casa Grande-Picacho Peak profile since 1967 (Figure 4). The maximum known subsidence measured in Arizona between 1967 and 1975 has occurred at Picacho where a 1967 National Geodetic Survey Bench Mark, X363, subsided 0.93 m. During that same time period, other marks in the area subsided by amounts exceeding 0.70 m, as illustrated in Figures 4 and 6.

The longest earth fissure in Arizona, 13.8 kilometers in length, which also has a vertical displacement (Figure 4), crosses Interstate Highway 10 between bench marks B and C. The southeastern side of this fissure is now subsiding at the same rate as the northwestern side, 0.09 m per year. An intensified fissure pattern is developing north and south of Interstate Highway 10 within 3 kilometers of the existing long fissure.

The subsiding areas of central Arizona are substantial as shown by Schumann 1974. In Pinal County within the lower Santa Cruz Basin from 1948 to 1967, an area of about 570 square kilometers subsided more than 0.15 m and about 155 square kilometers of this area has subsided more than 0.9 m. In the Stanfield-Maricopa area approximately 200 square kilometers has subsided more than 0.3 m.

Earth Fissures

Earth fissures have existed in parts of Arizona for many years (Schumann-Poland 1969) and (Schumann 1974). The new mapping of these fis-

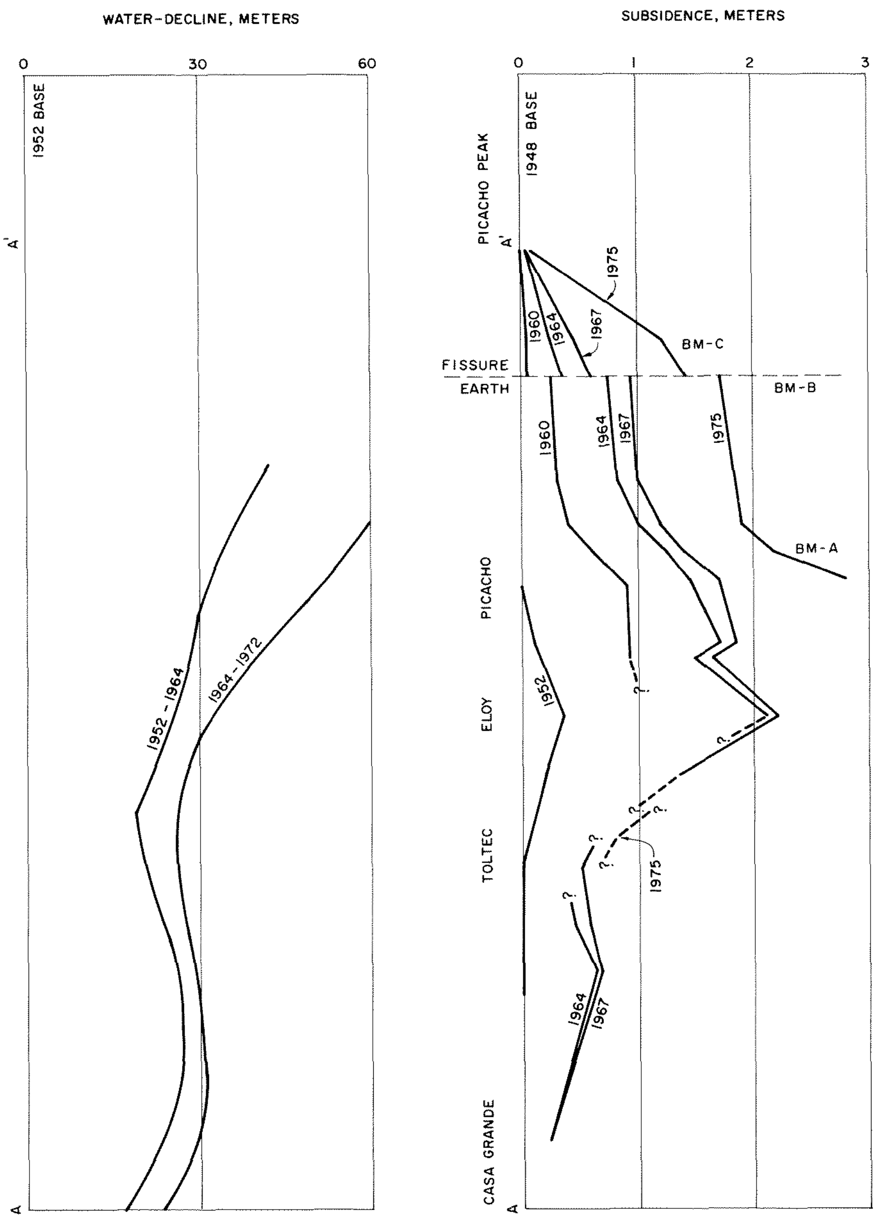

FIGURE 4. PROFILES OF WATER-LEVEL DECLINES AND SUBSIDENCE IN PINAL COUNTY.

FIGURE 5. WATER-LEVEL DECLINE IN PICACHO VICINITY 1952-1972

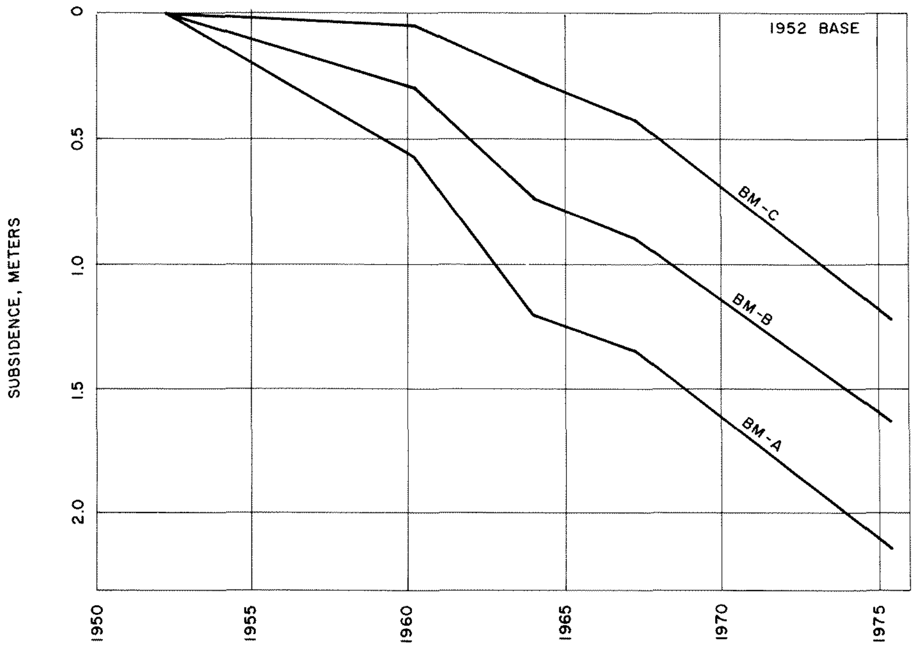

FIGURE 6. TOTAL SUBSIDENCE AT THREE BENCH MARKS IN PICACHO VICINITY. 1952-1975. (FOR LOCATION SEE FIGURE 4)

sures confirms the fact that they are continuing in or near areas of substantial subsidence (Figure 1). Three forms of intensification were noted during the mapping. First, fissures have occurred in new areas, second, fissures are developing en echelon with or parallel to older fissures, and third, older fissures have reopened. These forms of intensified fissuring are expected to continue unless stabilized ground-water levels are achieved.

Conclusions

The coincidence of areas of continued ground-water declines, continued subsidence, and increased earth fissuring support the view that there is a causal relationship begun by ground-water declines. These phenomena are having an adverse impact on habitation and agriculture.

The full significance of ground-water withdrawal, subsidence, and earth fissuring is relatively unknown at this time. Much additional information, primarily costly field surveying, is needed to adequately define this potentially severe problem.

The ground-water withdrawal, subsidence, and earth fissuring occurring in Arizona are broader in scope than existing agencies are able to address.

Acknowledgments

Data presented were collected by persons from several agencies. The following assisted in mapping: Robert L. Laney and Thomas L. Holzer of the U.S. Geological Survey; Edward A. Nemecek and Phillip C. Briggs of the Arizona Water Commission. Robert L. Laney and his staff prepared the water-level declines maps. Richard H. Raymond of the Bureau of Reclamation was of much assistance in all phases of gathering and interpreting data. Herbert H. Shcumann of the U.S. Geological Survey furnished valuable background information.

References

Laney, R.L. (in preparation): Water-level Decline, Land Subsidence and Earth Fissures in South-Central Arizona. Twentieth Annual Watershed Symposium Proceedings-Arizona Water Commission.

Schumann, H.H. (1974): Land Subsidence and Earth Fissures in Alluvial Deposits in the Phoenix Area, Arizona, U.S. Geological Survey Miscellaneous Investigations Map I-845-H.

Schumann, H.H. and Poland, J.F. (1969): Land Subsidence, Earth Fissures and Groundwater Withdrawal in South Central Arizona, U.S.A., International Symposium on Subsidence, Tokyo, pp-295-302.

U.S. Bureau of Reclamation (in preparation): Geology and Ground-Water Resources Report, Central Arizona Project, Arizona Projects Office, Phoenix, Arizona.

Winikka, Carl C. and Morse, Samuel A., Jr. (1974): Orthophotoquads for Arizona Land-Use Mapping and Planning, Journal of the Surveying and Mapping Division, ASCE, Vol. 100, Proc. Paper 10525, May 1974, pp. 1-6.

Publication n°121 of the International Association of Hydrological Sciences
Proceedings of the Anaheim Symposium, December 1976

LAND SUBSIDENCE IN NIIGATA

S. Aoki
Niigata University
Niigata, Japan

Abstract

This paper deals with recent features of land subsidence in and around Niigata City with reference to the injection of water into gas-reservoirs. Since 1973, the pumping water of about 110,000 cubic meters per day, from which natural gas was separated, has been injected into the several underground aquifers. Since October of 1973, the groundwater level has been rising rapidly and the uplift or rebound of the ground surface has been recognized. The uplift of the surface, measuring 2.8 cm per year in maximum, seems to be temporary and be caused by the expansion of the subsurface strata which lie under these aquifers.

Introduction

Recently several land subsidence areas in Japan have become to decrease rapidly at the rate of subsidence as a result of control of groundwater withdrawal. This paper deals with the case of the land subsidence area in and around Niigata City with reference to the injection of water into the natural gas reservoirs.

I wish to express my thanks to the members of the Niigata Prefectural Geverments and of the Agricultural Ministry for their kind discussions and encouragements during this research.

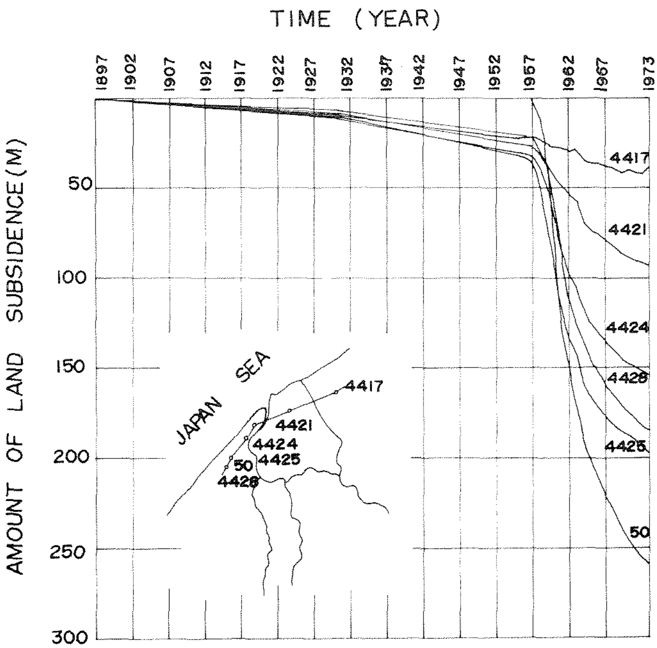

Figure 1. Integrated land subsidence in Niigata.

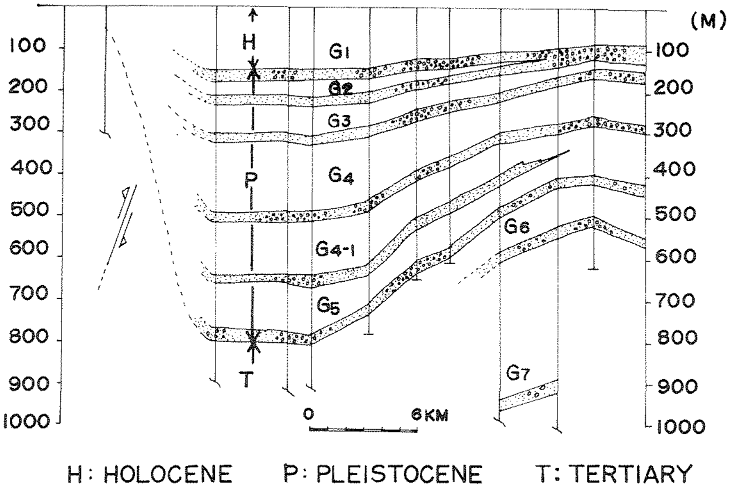

Figure 2. Geological Profile.

Outline of land subsidence in and around Niigata City

Since 1956, the area in and around Niigata City has been suffered a severe land subsidence as shown in figure 1. The maximum rate of surface subsidence was measured 50 cm per year in 1959 at Yamanoshita in Niigata City. From about 1957 to 1959, many reports of investigation were published especially as to the causation and countermeasures.

The results obtained from the records by the observation wells showed that the layers at the depth from 380m to 610m were remarkably contracting. This fact suggested that the subsidence might be attributed to the drop in the hydraulic pressure of the confined aquifers, accompanying natural gas mining which has been rapidly developed since about 1953 in the area considered.

The subsurface geology of this area consists mainly of Holocene, Pleistocene and Neogene Tertiary deposits from upper to lower as shown in figure 2.

The majority of gas reservoirs in the Niigata gas field belongs to the Pleistocene Uonuma Group which is characterized by the alternation of clay, sand and gravel beds. Gas reservoirs, i.e. confined aquifers consisting of sand and gravel, are filled by brackish to saline water.

For the purpose of the development of these natural gas, the producing wells have become to increase rapidly in the area near the mouth of the Shinano River or along the coast of Japan Sea as shown in figure 3. With increase of the amount of groundwater withdrawal from gas wells, the rapid lowering of the groundwater level was recognized.

Although there were many different opinions concering the causation of the subsidence, a long term regulation of their own has enforced towards control of groundwater withdrawal in association with natural gas for industrial use. Then, the speed of subsidence in the area along the Japan Sea

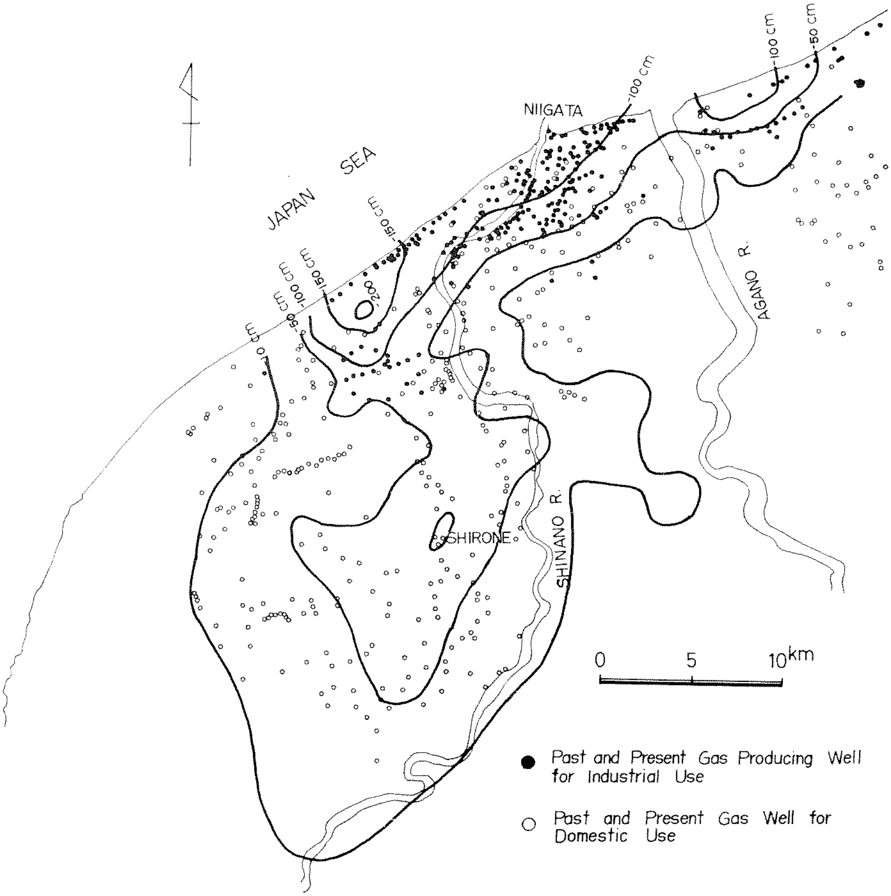

Figure 3. Distribution of gas wells and total amount of land subsidence during 1959～1974.

coast reduced to a few centimeters per year. (Momotake, M. and Miyazawa, K., 1976).

Another type of surface subsidence had occurred in the inland area of the Niigata plain, southern part of Niigata City (Takeuchi, S. et al 1969). In 1959 the center of the subsidence located near Shirone Town, it was measured about 14 cm per ten months. Based on the data from observation wells, the most of observers have concluded that the compaction was located in the zone shallower than 120m depth, which is correlated with the Holocene and younger Pleistocene deposits. As shown in figure 3, about 10,000 wells of natural gas for domestic use are distributed in this area. The amount of the groundwater withdrawal from these wells was calculated to be approximately 60,000 cubic meters per day in 1960. Since 1960, the control of the groundwater withdrawal has been undertaken by putting under the ban of drilling of new well in this area. After then, the volume of groundwater withdrawal began to the tendency toward a decrease, and also has been observed to decrease at the same rate as one of subsidence.

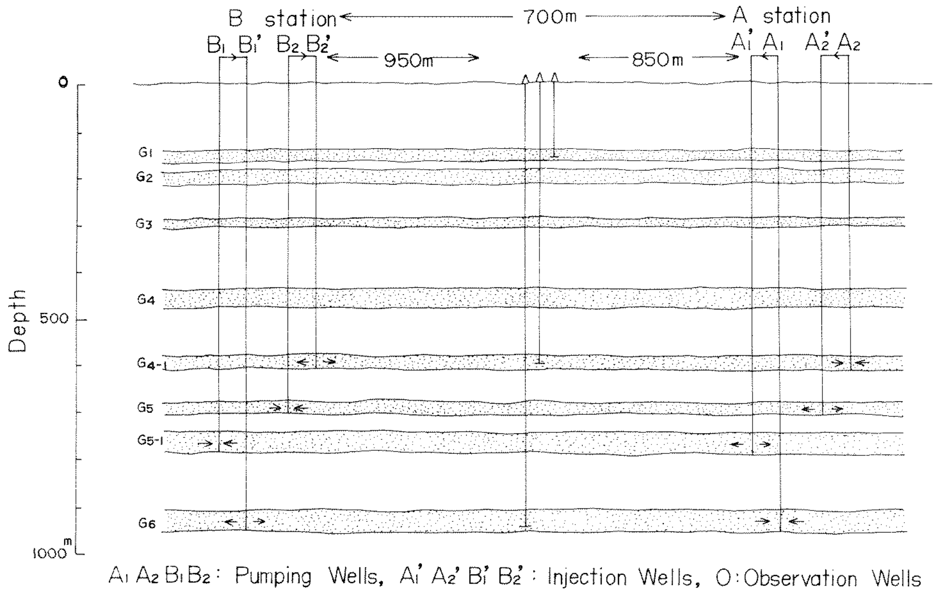

Figure 4. Profile of water injection experimental station (at Kurosaki).

Artificial recharge and land subsidence

Since 1960 or so, the Goverment and group of mining companies had plan to promote experiment of artificial recharge in this land subsidence area, because a few centimeters subsidence had yet been continuing in spite of long-term control of groundwater withdrawal.

The first experiment of water injection into the gas reservoirs were cariied out in Niigata City from 1960 to 1963. The summary of these results is as follows: (Ishiwada, 1969)

a) Permeability of the main reservoirs range from 10 to 50 darcys,
b) Injectiveity index is, in general, less than a quarter of productivity index,
c) Back-washing at adequate time intervals is necessary to long-term injection.

The second step of experiments was started from 1965, in order to investigate whether the re-developments of gas resources is compatible with prevention of land subsidence or not. The injection system was composed of one set of pumping and injection wells in two stations as shown in figure 4. Total amount (about 3,000 ubic meters per day) of the pumped water drained from closed gas-water separater has been all injected into the four aquifers. The change of the groundwater levels of the aquifers and compactions of the subsurface layers have been observed at the observation wells located near experimental stations. The results of experiments from 1965 to 1973 showed that the continuous injection and withdrawal of groundwater seem to have little influence for the surrounding land subsidence.

Based on the results mentioned above, injection wells for artificial recharge were bored in the vicinity of producing wells in three areas as shown in figure 5. Since 1973, all amount of the pumping water of about 110,000 cubic meters per day, from which natural gas was separated, has been injected into the gas reservoirs through the injection wells.

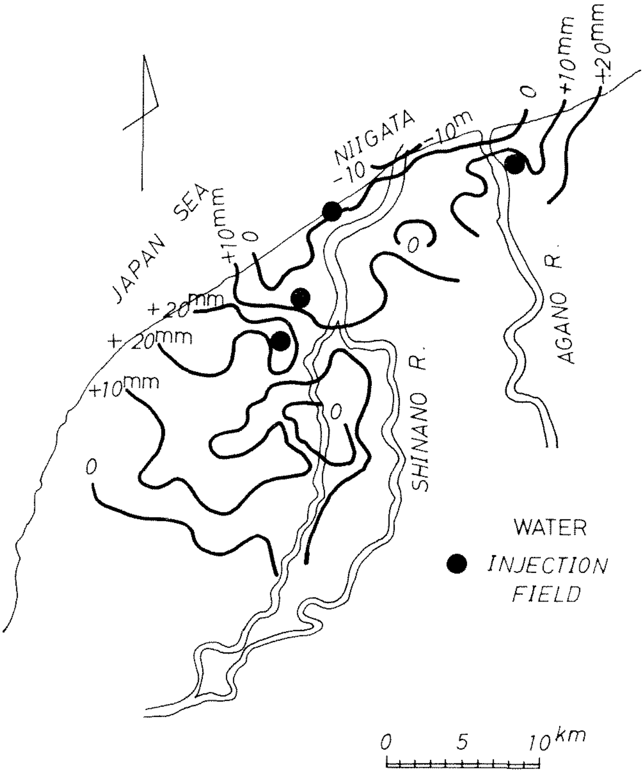

Figure 5. Land subsidence during 1973 ~ 1974.

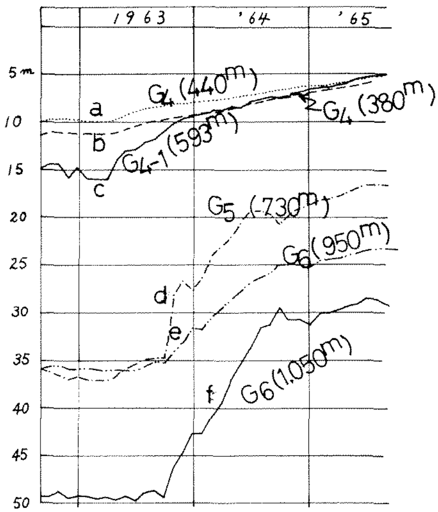

Figure 6. Change in groundwater levels at observation wells (Kurosaki -Shirone area).

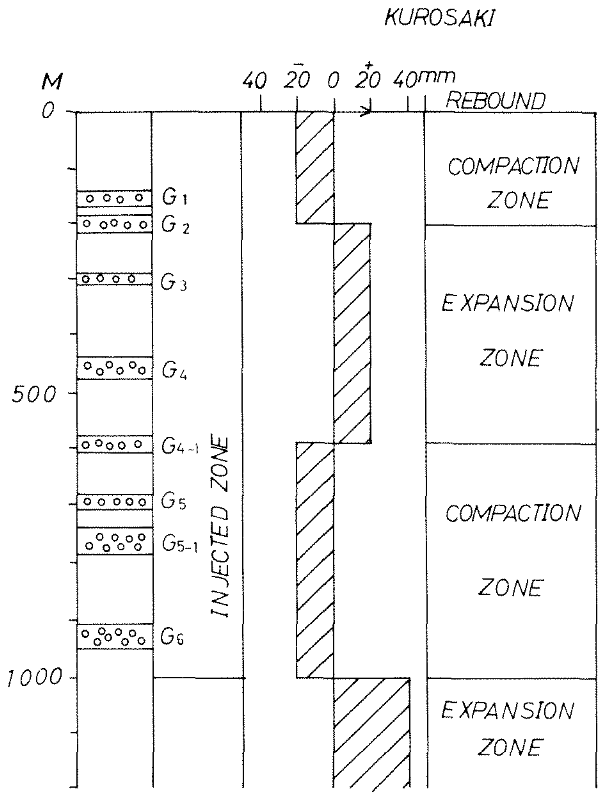

Figure 7. Columnar section showing the position of expansion and compaction layers at Kurosaki.

After then, the land surface response from water injection was recognized as shown in figure 5 in three area near the main injection fields. The maximum rebound of the land surface recorded was 2.8 cm at Uchino during 1973 to 1974. The rising of the groundwater levels of the aquifers was remarkable at Nishikanbara with the rate of 20m per year as shown in figure 6. The observation wells within the rebounded area recorded that the most expanded zone of the strata was located under the injected auifers as shown in figure 7. Injected and pumped up zone of the water was not expanded but slightly compacted. Two years later, the surface rebound from the injection seems to change to subside as shown in figures 8 and 9.

From the results mentioned above, it is considered at present that more investigation and observation will be neccessary before judging whether the method of artificial recharge undertaken in Niigata is completely useful for both of prevention of land subsidence and for re-development of natural gas resources.

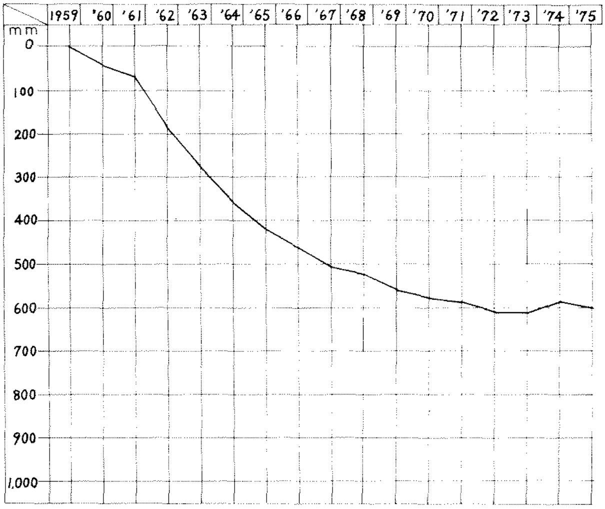

Figure 8. Integrated subsidence of a bench mark in Kurosaki water injection field.

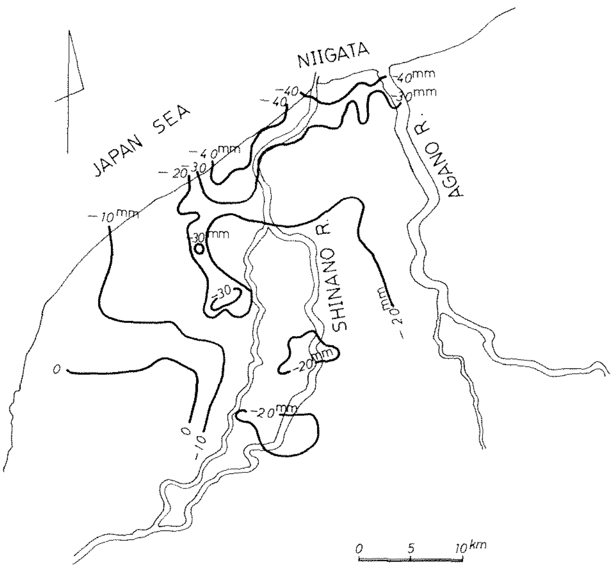

Figure 9. Land subsidence during 1974 ～ 1975.

References

Ishiwada, y., 1969, Experiments on water injection in the Niigata gas field: I.A.S.H. -Unesco, p. 629-634.

Momotake, M. and Miyazawa, K. 1976, A study of the land subsidence in the vicinity of Niigata Cigy: Professor Shoichi Nishida memorial volume, Geological and Mineralogical Institute of Niigata University, P. 349 -356.

Takeuch, S., Kimoto, S., Wada, M., Shiina, H. and Mukai, K., 1969, Geological and Geohydrogical properties of the land subsided area: I.A.S.H. -Unesco, p. 232-241.

Publication n°121 of the International Association of Hydrological Sciences
Proceedings of the Anaheim Symposium, December 1976

HYDROGEOLOGIC EFFECTS OF SUBSIDENCE, SAN JOAQUIN VALLEY, CALIFORNIA

B. E. Lofgren
U.S. Geological Survey
Sacramento, California

Abstract

Subsidence has slowed in most of the San Joaquin Valley, Calif., site of the maximum (shared with Wilmington, Calif., oilfield; and Mexico City, ground-water withdrawal) and most extensive manmade subsidence in the world. After 40 years of ground-water overdraft, canal imports have generally reversed declining water-level trends. As of 1976, artesian heads have recovered toward presubsidence levels, and subsidence rates have decreased from an earlier maximum 0.5 m/yr to near zero in much of the valley. Increasing irrigation demands, however, particularly during years of deficient precipitation, pose the threat of increased pumping and another cycle of widespread land subsidence. Because of significant hydrogeologic changes during the 1930-70 overdraft period, however, the ground-water basin will respond differently during a second cycle of overdraft.

The close correlation between water-level decline, compaction of the aquifer systems, and land subsidence has been precisely monitored in the San Joaquin Valley for 2 decades. From these data, both the elastic and the "virgin" inelastic stress-strain characteristics of the unconsolidated valley deposits and the response of the aquifer system to prolonged cyclic pumping overdraft have been determined.

Subsidence is caused by the compaction of the water-yielding deposits and is directly related to increased effective stresses induced by the head decline. Subsidence represents "water of compaction" squeezed from the compressible deposits, and represents a permanent change in the aquifer system. Because the change occurs primarily within the fine-grained aquitards, the capability of the aquifers with reference to withdrawal or recharge of ground water is only slightly decreased. During a second cycle of prolonged pumping overdraft, whenever this might occur in the valley, water levels should decline much more rapidly than during the first. Subsidence, however, should be minimal until pumping levels again approach their former lows and preconsolidation stresses are again exceeded.

Introduction

Widespread land subsidence in the San Joaquin Valley, California, represents one of the great environmental changes man has imposed on the environment. Roughly half the entire valley, representing about 13,500 km^2 (5,200 mi^2) of irrigable farmland, has been affected by subsidence, and maximum subsidence exceeds 8.8 m (29 ft). Throughout most of the area, subsidence has occurred so slowly and uniformly over such a broad area that its effects have been largely unnoticed by most residents. Locally, however, the subsidence has been abrupt and nonuniform. This has resulted in severe problems in the design and maintenance of canals and waterways, the expenditure of millions of dollars in repair and replacement cost of deep irrigation wells, and changes in irrigation and other farming practices.

The San Joaquin Valley is a broad alluviated intermontane structural trough (fig. 1), constituting the southern two-thirds of the Central Valley of California (see insert). It is about 400 km (250 mi) long and from 40 km (25 mi) to 90 km (55 mi) wide. Figure 1 shows pertinent geographic features of central and southern San Joaquin Valley and areas affected by subsidence. All the major streams enter the valley from the Sierra Nevada on the east; almost no stream runoff is available for irrigation on the western and southern margins of the valley.

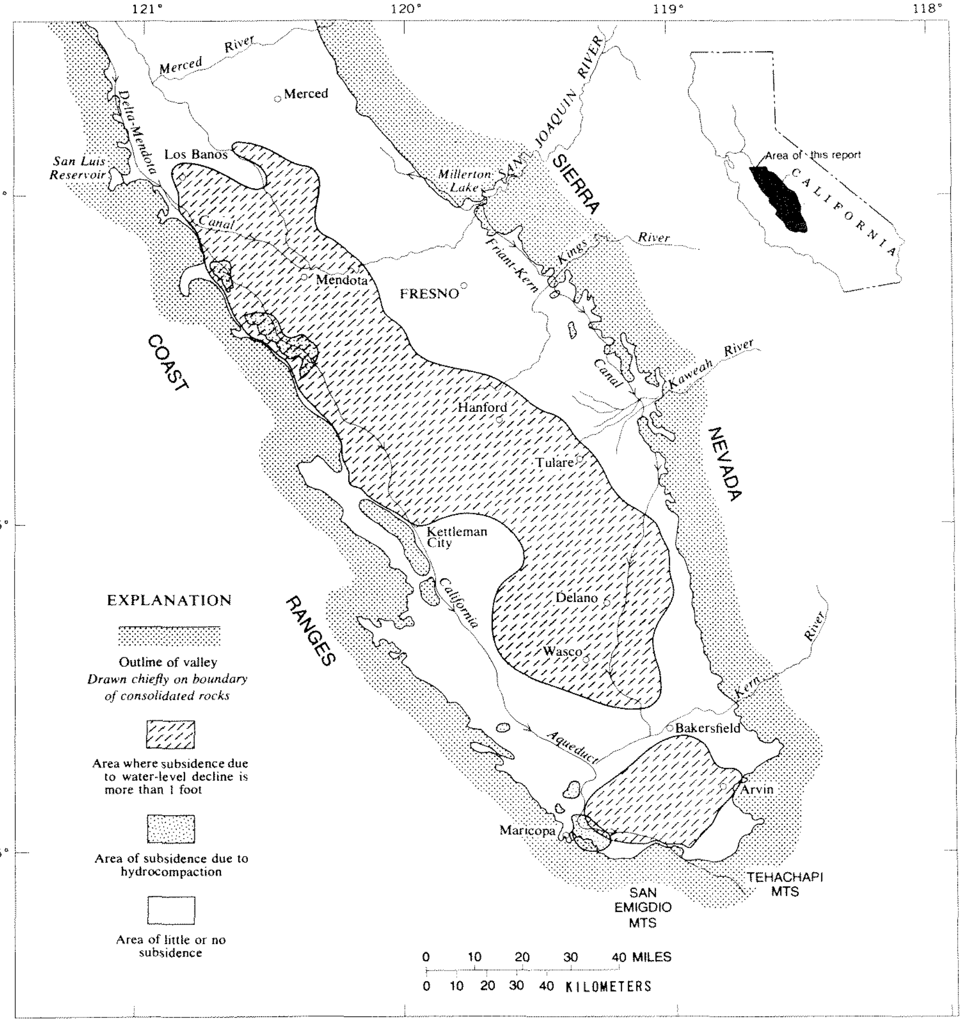

Figure 1.--Pertinent geographic features of central and southern San Joaquin Valley and areas affected by subsidence. (From Poland, Lofgren, Ireland, and Pugh, 1975, fig. 1.)

Surface streams supply most of the irrigation needs in the northeastern part of the valley. South of Kings River, however, and throughout the west side of the valley, natural runoff ranges from inadequate to negligible. Prior to the construction of major canals, many of the valley's western and southern areas were irrigated by thousands of large and deep irrigation wells.

Three quite unrelated man-induced processes are causing land subsidence in the San Joaquin Valley (Poland, Lofgren, Ireland, Pugh, 1975). In descending order of areal extent, these are (1) subsidence due to the compaction of aquifer systems caused by the intensive pumping of ground water, (2) subsidence due to the compaction of moisture-deficient deposits when water is first applied--a process known as hydrocompaction, and (3) local subsidence caused by the extraction of fluids from producing zones in several oilfields. Figure 1 delineates the principle areas affected by (1) and (2).

In addition to the artificial changes, tectonic adjustments--principally the slow uplift of the southern and western mountains and the very slow settlement of the valley trough--are recognized. Also, in the delta area of the Sacramento and San Joaquin Rivers at the north end of the San Joaquin Valley, the oxidation of organic soils caused by farming practices results in a lowering of the land surface.

Hydrogeologic Setting

The San Joaquin Valley is a major structural trough, whose main axis trends northwest-southeast somewhat west of the valley's drainage axis. Throughout Late Cretaceous and much of Tertiary time thousands of feet of shallow-water marine sediments were deposited in this down-warping geosyncline. Overlying these marine deposits are continental deposits of late Tertiary and Quaternary age. In aggregate, these marine and continental deposits form an immense wedge which thickens from east to west and also from north to south. At the extreme south end of the valley the thickness of Cenozoic sediments exceeds 8,500 m (28,000 ft).

The present form of the valley is chiefly a result of tectonic movement during late Tertiary and Quaternary time, which included major westward tilting of the Sierra Nevada. Quaternary deformation has been principally along the south and west borders of the valley, where marine and continental rocks are tightly faulted and folded and stream terraces are conspicuously elevated.

Ground water in the San Joaquin Valley occurs under confined and unconfined conditions. Three distinct ground-water bodies are present in much of the western, central, and southeastern parts of the valley. In downward succession, these are (1) a body of unconfined and semiconfined fresh water in alluvial deposits overlying a widespread lacustrine confining bed--the Pleistocene Corcoran Clay Member of the Tulare Formation, (2) an extensive reservoir of fresh water confined beneath the Corcoran Clay Member in alluvial and lacustrine deposits of late Pliocene and Quaternary age, and (3) a body of saline water contained in marine sediments of middle Pliocene or older age, which underlies the freshwater body throughout the area. In much of the eastern part of the valley, especially in the areas of the major streams, the Corcoran Clay Member is not present and ground water occurs as one freshwater body to considerable depth.

Recharge to the ground-water body is by infiltration from streams, canals, and ditches, underflow entering the valley from tributary stream canyons, infiltration of rainfall, and by infiltration of excess irrigation water. In much of the valley, however, the annual rainfall is so low that little penetrates through the soil zone, and soil-moisture deficiency is perennial. Infiltration from stream channels and canals is the principal source of recharge.

Subsidence Due To Hydrocompaction

Loose, dry, low-density deposits that compact when they are wetted for the first time--a process known as hydrocompaction--are located on the western margin of San Joaquin Valley (fig. 1). These deposits are restricted to a belt of Quaternary alluvial detritus shed eastward and northward into the valley in the form of steep alluvial fans. Being in the rain shadow of the Coast Ranges during the prevailing winter storms, these areas receive only 13-18 cm (5-7 in) of precipitation annually. Summers are long, hot, and dry. Native vegetation is sparse. Winter storms are usually of high intensity and short duration, and runoff to the valley occurs principally as infrequent torrential floods from normally dry arroyos.

Two types of streams characterize the southwestern margin of the valley: (1) major streams that extend far back into the mountainous hinterland, with large watershed areas and fairly large seasonal runoff; these have built broad, gentle fans far onto the valley floor, and (2) secondary ephemeral streams that have small frontal watershed areas of less than 80 km^2 (30 mi^2); these have built short, steep alluvial fans that form coalescing aprons between the fans of the major streams. Deposits that subside on wetting are restricted to the steeper fans of the secondary streams, where mudflow-type deposits predominate

The destructive effects of hydrocompaction on the west side of the San Joaquin Valley were recognized as early as 1915 when a newly constructed pumping plant began to tilt and crack soon after lawns were planted. Today probably 650 km^2 (250 mi^2) is affected by hydrocompaction, with abrupt differential settlements commonly varying from 1 m (3 ft) to 5 m (16 ft). Areas of severe subsidence, surface cracks, sunken ditches, undulating fields and roads, tilted buildings and structures, all evidences of hydrocompaction, are readily apparent even to the casual observer. Today, many of the farmers have resorted to sprinkler irrigation practices to irrigate their uneven fields. Also, thorough prewetting of susceptible deposits usually precedes the building of engineering structures in these areas. As much as 120 km (75 mi) of the large California Aqueduct crossed areas susceptible to hydrocompaction (see fig. 1) and required expensive preconsolidation before construction began. The cost of precompacting 89 km (55 mi) of alinement was estimated at $20 million ("Land subsidence along the California Aqueduct as related to environment," Clifford V. Lucas, 1964, Calif. Dept. Water Resources, unpub. written commun.). Ponding and prewetting of susceptible deposits in areas of new development are continuing along secondary distribution lines from the aqueduct, and may be seen in scattered areas of construction.

Subsidence Due To Ground-Water Withdrawal

Ground-water pumping has been intense in the San Joaquin Valley, especially since World War II. During the 1950's more than one-quarter of all ground water pumped for irrigation in the United States was used in the San Joaquin Valley. Widespread pumping began about 1900 and increased at an accelerated rate from the early 1940's to mid-1960's. Pumping extractions increased from 3.7×10^9 m^3 (3×10^6 acre-ft) in 1942 to at least 12.3×10^9 m^3 (10×10^6 acre-ft) in 1964. An estimated 40,000 large wells were in operation at the height of pumping, with depths generally ranging from 40 m (130 ft) to over 900 m (2,900 ft) and discharge from 0.8 m^3/min (0.5 ft^3/s) to over 7 m^3/min (4 ft^3/s). In the early 1960's pumping lifts frequently exceeded 150 m (500 ft). On the average, these wells were idle about three-quarters of the time during the year.

Ground-water overdraft has prevailed in much of the San Joaquin Valley since the 1930's. The declining trend of water levels was well established long before the problems or the causes of subsidence were recognized. Few areas, however, had sufficient leveling control to reveal subtle changes of the land surface. Subsidence apparently began in centers of overdraft in the 1920's and became of widespread concern in the late 1940's. During the 1950's and early 1960's, water levels declined at an unprecedented rate in much of the area. Pumping lifts became inordinately high, well casings failed at an alarming rate, and differential settlement of the land surface caused numerous problems.

Importation of surface water to areas of serious overdraft began in the northern part of the Friant-Kern Canal (fig. 2) service area in 1950 by

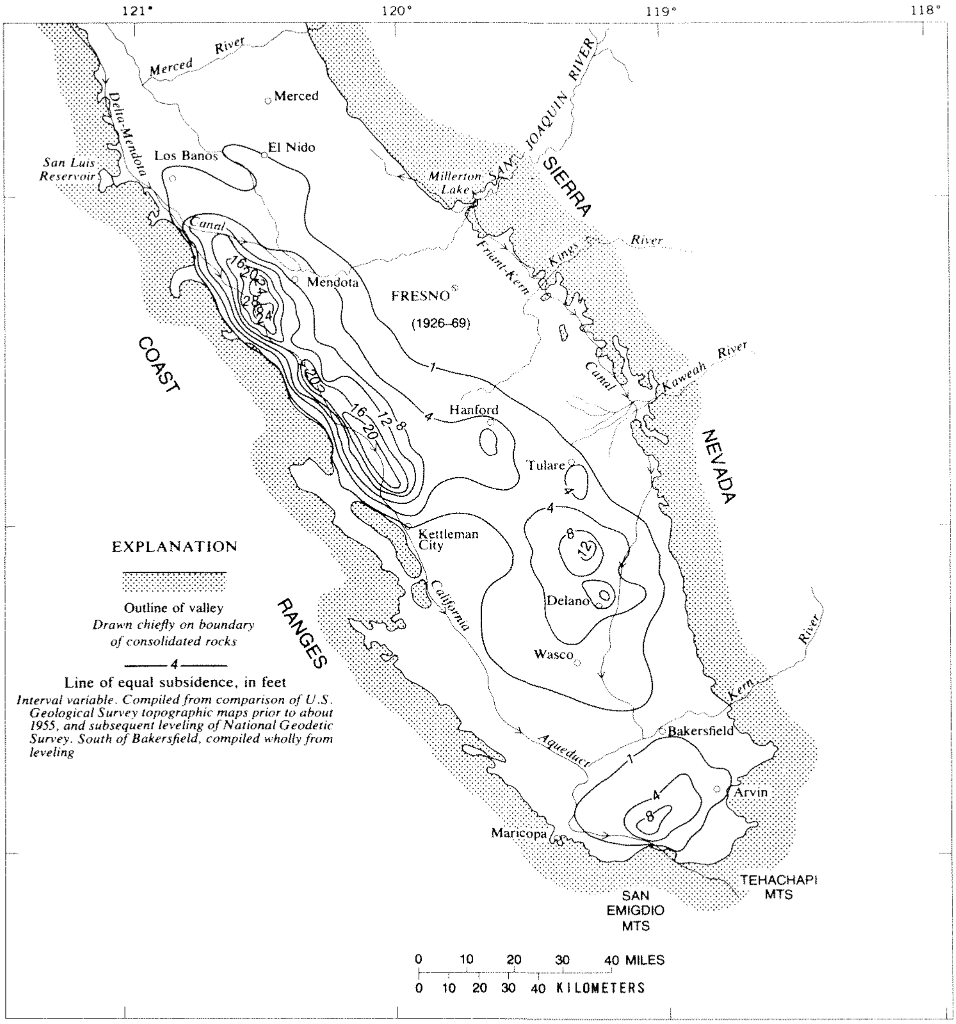

Figure 2.--Land subsidence due to ground-water withdrawal, 1926-70. (From Poland, Lofgren, Ireland, and Pugh, 1975, fig. 5.)

diverting water from the San Joaquin River. Canal deliveries progressed south as construction advanced; by 1966 diversions had reached the Arvin area. Canal imports to the west side of the valley via the Delta-Mendota Canal began in the early 1950's. Additional imports to deficient areas via the California Aqueduct began on the west side of the valley in 1968. By 1970, aqueduct imports had extended southward to the Tehachapi Mountains.

As a result of the large volume of surface-water imports, pumping of ground water has been reduced, and the rapid decline of artesian head has been reversed in parts of the areas of overdraft. By the end of 1972, many hundreds of irrigation wells were idle and subsidence trends were leveling out as stresses on the deposits were reduced. Today, after three decades of overdraft much of the overdrawn area of the San Joaquin ground-water basin is returning to a stable water budget. Artesian pressures are recovering toward their presubsidence levels.

Figure 2 shows the magnitude and areal extent of subsidence in the San Joaquin Valley from 1926 to 1970, caused by the excessive pumping of ground water. As shown, there are three centers of major subsidence: (1) a long narrow trough west of Fresno, referred to as the Los Banos-Kettleman City area, with a maximum subsidence of over 8.8 m (29 ft). (2) a central subsidence bowl between Tulare and Wasco with more than 3.6 m (12 ft) of settlement, and (3) a southern depression south of Bakersfield, commonly referred to as the Arvin-Maricopa area. with maximum subsidence of about 2.7 m (9 ft). For additional detail on the causes and effects of subsidence in these areas, see the annotated bibliography in Poland and others, 1975, Land subsidence in the San Joaquin Valley as of 1972, U.S. Geol. Survey Prof. Paper 437-H (p. H5-H7).

Subsidence due to ground-water pumping began in the middle 1920's, but the cumulative volume of subsidence (fig. 3) remained small until after World War II. By 1970, the total volume of subsidence in the valley was 19.3 x 10 m (15.6 x 10 acre-ft), having doubled since 1957. Roughly 11.1 x 10 km (4,300 mi) of farm land had subsided more than 1 foot. Although damages to wells, canals, and drainage systems represent many millions of dollars, few of the effects of this subsidence are spectacular or even evident to the casual observer. Because of the vastness of the area and the subtle land-surface changes, it is difficult to demonstrate in the field either the magnitude of the changes or the impact these changes have had on the farming practices in the valley.

Not all of the effects of subsidence are negative. Three beneficial effects are worthy of mention. First, water of compaction released to wells as subsidence progressed represented a major source of water. Therefore, water levels declined more slowly and pumping lifts were less than if

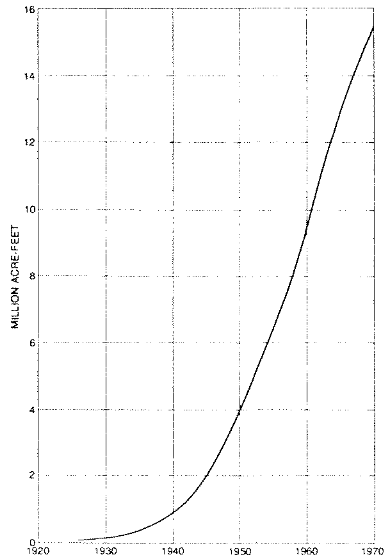

Figure 3.--Cumulative volume of subsidence in the San Joaquin Valley, 1926-70. (From Poland, Lofgren, Ireland, and Pugh, 1975, fig. 6.)

comparable volumes had been withdrawn from a less compressible aquifer system. Second, the deposits of the ground-water basin are now largely "preconsolidated" to their mid-1960 stressed conditions, thus the basin can be managed for cyclic storage nearly to the historical low levels without the threat of serious future subsidence. Third, the basin has provided a field laboratory for testing compression characteristics of complex aquifer systems, in situ, and for measuring mechanical and storage parameters of aquifer systems under a wide range of loading stresses.

Hydraulic Stresses Cause Subsidence

Land subsidence in areas of intense water-level declines is attributed to the compaction of the subsurface water-yielding deposits. Compaction results from an increase in effective loading stress on the deposit, caused by the water-level change.

Depending on the nature of the deposits, compaction may be (1) largely elastic--that is, stress proportional to strain, largely recoverable, and independent of time, or (2) principally inelastic, resulting from a rearrangement of the granular structure and causing a permanent volume decrease and density increase of the deposits. In general, if the deposits are coarse sand and gravel, the compaction will be small and largely elastic, whereas if they contain fine-grained interbeds, or even small amounts of clay, the compaction will be much greater and chiefly inelastic--that is, largely permanent. In either case the compression of the deposits is largely vertical, resulting in subsidence of the land surface.

As described by Lofgren (1968), effective stresses in an aquifer system are changed in two principal ways: (1) water-table fluctuations change the buoyant support of the grains in the zone of the change, and (2) a change of water table or of artesian head, or both, may induce vertical hydraulic gradients and seepage stresses in the deposits. The stress changes are additive in their effect with gravitational stresses and generally are the principal cause of compaction of the compressible deposits.

Stress-strain characteristics

Figure 4 shows a typical relationship between (1) water-level fluctuations in two aquifer systems--a deep confined system (16N3) and a shallow semiconfined system (16N4), (2) change in effective stress, as calculated from these hydrographs (Lofgren, 1968), (3) compaction of two depth intervals, as measured by extensometer (Lofgren, 1969, figs. 7 and 8), and (4) subsidence of the land surface. For convenience, stress changes are expressed in equivalent units of water head (1 ft of water equals 0.433 lb/in^2). Subsidence of bench mark Q945 was determined by spirit leveling from a distant stable bench mark. These records are for a 13-year period at the Pixley recorder site near the center of maximum subsidence in the Tulare-Wasco area (fig. 2). During this period, measured compaction to a depth of 232 m (760 ft) was 75 percent of the total subsidence. Thus, 25 percent of the vertical shortening was due to compaction below 232 m (760 ft).

Comparison of the compaction rate with fluctuations in water level in the semiconfined and confined aquifer systems indicates that compaction began each year during the period of rapid head decline in the aquifer system, continued through the pumping season, and ceased during the early stages of head recovery. Although the correlation between compaction and artesian-head change in the confined aquifer system is good, the correlation with changes in effective stress in the confined aquifer system is closer.

A special computer program is available whereby the relationships of figure 4 are calculated and graphed by computer. Field data from the deep and shallow water-level and compaction recorders are supplied to the computer

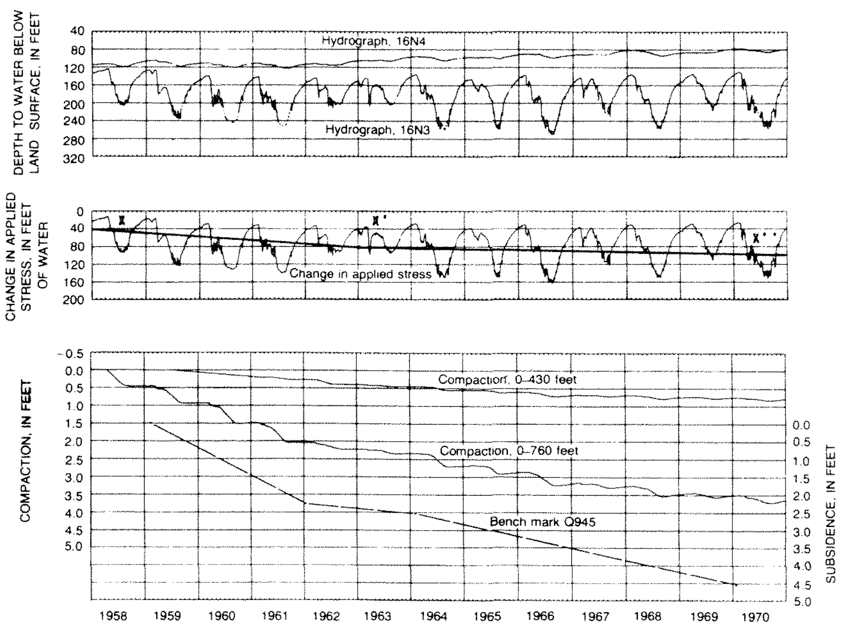

Figure 4.--Hydrographs, calculated change in applied stress, compaction of two depth intervals and subsidence at the Pixley recorder site, 1958-70.

in digital form, and from these various stress-strain parameters are obtained.

Of particular interest is the position of the X-X'-X" line drawn across the effective-stress graph. Most of the compaction occurred when effective stresses were below this line (that is, stresses were greater). Above the X-X'-X" line deposits respond elastically--that is, they have low compressibility and the compaction is recoverable. Below the X-X'-X" line deposits undergo much greater compression which is largely nonrecoverable. Elastic storage parameters generally are 1 to 2 orders of magnitude less than the nonrecoverable parameters.

The X-X'-X" line demarks the preconsolidation stress in the aquifer system; its level is determined largely by the nature of the deposits and the history of water-level declines. In an aquifer system that has had a long record of declining water levels, the preconsolidation stress is usually found to be somewhere between the seasonal highs and lows of the annual fluctuations during the lowest years of the hydrograph. This is an important concept. It applies to compressible aquifer systems everywhere. Subsidence occurs primarily during the first cycle of prolonged pumping drawdown; little subsidence occurs during the second or subsequent cycles. Not until water levels are drawn down to their preconsolidation stresses, will appreciable subsidence resume.

Figure 5 is a computer plot of the stress-strain characteristics of the principal pumped zone of the confined aquifer system at the Pixley site, using the data of figure 4. Stress, calculated from the two hydrographs (fig. 4A), increases upwards; strain, calculated from the two extensometer graphs (fig. 4C), increases to the right. Each pumping year begins with an

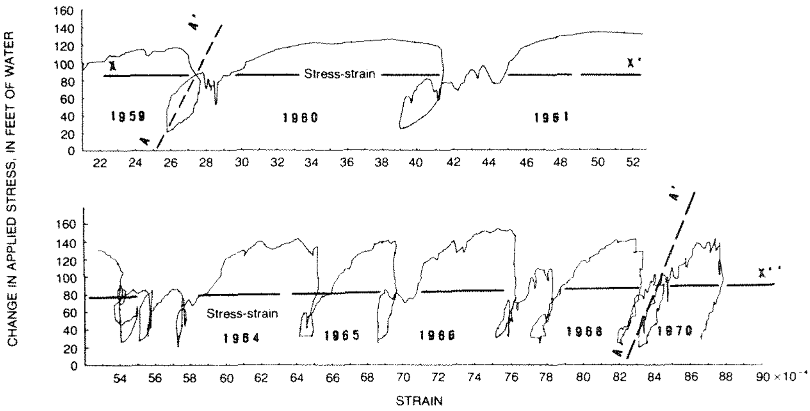

Figure 5.--Stress-strain plot of the 430-760-foot depth interval, Pixley recorder site.

upward-trending curve of increasing stress and increasing strain. It closes with a downward trend of decreasing stress and decreasing compaction. The characteristic hysteresis loop separating one year from the next roughly defines the elastic parameters of the measured portion of the aquifer system. The slope of line A-A' on the hysteresis loop of the stress-strain curve (fig. 5) is a measure of the elastic compressibility of the water-yielding deposits whereas the broad span between the seasonal hysteresis loops is a rough measure of the gross virgin compression parameter. Elastic parameters derived from short-term pumping tests at stresses less than preconsolidation give no clue of the response of the system at stresses greater than preconsolidation. All nonrecoverable compaction occurs when stresses are greater than the preconsolidation X-X'-X" line. At stresses less than preconsolidation, the water-bearing deposits deform elastically--with a very low coefficient of compressibility.

It is significant that in the elastic range, not only is the compaction recoverable, but the rate of compaction per foot of stress change is one to two orders of magnitude lower than in the inelastic, nonrecoverable range. Typically, throughout the subsidence areas of the valley, the storage coefficient for stresses greater than preconsolidation is 10 to 100 times the elastic storage coefficient at stresses less than preconsolidation. Water levels, therefore should decline much more rapidly during a second cycle of prolonged pumping drawdown.

Hydrogeologic Changes Caused by Pumping Overdraft

Many permanent changes have occurred in the San Joaquin Valley as a direct result of the 1930-70 ground-water overdraft. The most obvious relate directly to effects of subsidence of the land surface--disrupted gradients of natural streams, canals, and drainages; irrigation ditches that flow west instead of east; the damage or collapse of thousands of deep well casings; topographic maps out-of-date before publication, and so forth. Other changes are less obvious, affecting the hydrogeologic characteristics of the subsurface ground-water reservoir. Three closely interrelated changes that have occurred in the response of aquifer systems in the valley to imposed pumping stresses are discussed briefly below.

First, with water levels now high (1976), little subsidence should occur in the valley during a second period of pumping drawdown, in marked contrast to the 1930-70 period. As noted earlier, the maximum preconsolidation stress imposed on an aquifer system (line X-X'-X", fig. 4) is established during the period of lowest ground-water levels. Generally, it falls somewhere between the highs and lows of the seasonal stress cycle. Subsidence should be minimal until pumping levels approach their former lows and preconsolidation stresses are again exceeded.

Second, with the compressible deposits of the aquifer systems now preconsolidated, both the compressibility and the storage coefficient of the aquifer systems are in the elastic range of stressing rather than in the inelastic or virgin range of prior times. For this reason, water levels will decline much more rapidly now, for a given rate of pumping.

Third, since water of compaction is a one-time mining of pore water from the compressible aquifer system, this supply would not be available during a second extended period of drawdown. During 40 years of overdraft on the west side of the San Joaquin Valley, the volume of subsidence (fig. 6) was roughly one-third of the total pumpage. Water of compaction therefore, a one-time source of water, represented one-third of the total water pumped. During a second drawdown episode this supply would not be available.

The areal distribution of the subsidence-pumpage ratio for the south end of the valley is shown in figure 7. To prepare this map, the subsidence-pumpage ratio was calculated on a quarter-township basis, and these data then contoured. As shown, the proportion of the total pumpage derived from water of compaction varies from 1 percent at several points on the perimeter of the subsidence area to more than 40 percent in the area of maximum subsidence. The remainder of the pumpage comes each year from recharge.

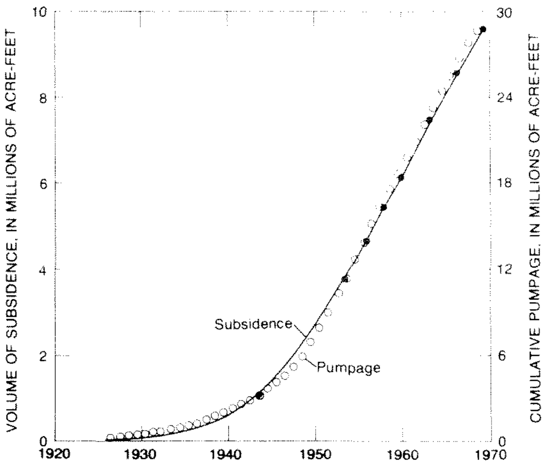

Figure 6.--Cumulative volumes of subsidence and pumpage, 1926-69, Los Banos-Kettleman City area. Points on subsidence curve indicate times of leveling control.

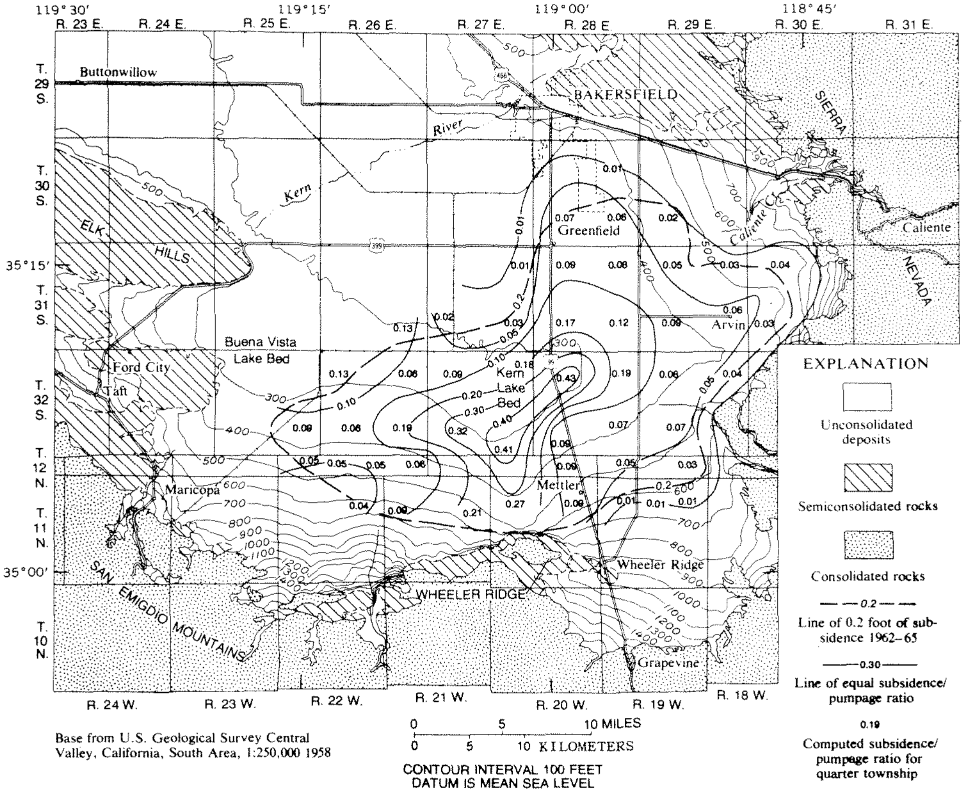

Figure 7.--Proportion of pumpage derived from water of compaction, 1962-65, in the Arvin-Maricopa area.

References

Lofgren, B. E., 1960, Near-surface land subsidence in western San Joaquin Valley, California: Jour. Geophys. Research, v. 65, no. 3, p. 1053-1062.

_____1968, Analysis of stresses causing land subsidence, in Geological Survey research 1968: U.S. Geol. Survey Prof. Paper 600-B, p. B219-B225.

_____1969, Field measurement of aquifer-system compaction, San Joaquin Valley, California, USA, in Tison, L. J., ed., Land subsidence, v. 1: Internat. Assoc. Sci. Hydrology, Pub. 88, p. 272-284.

Poland, J. F., Lofgren, B. E., Ireland, R. L., and Pugh, R. G., 1975, Land subsidence in the San Joaquin Valley as of 1972: U.S. Geol. Survey Prof. Paper 437-H, 78 p.

Publication n°121 of the International Association of Hydrological Sciences
Proceedings of the Anaheim Symposium, December 1976

LAND SUBSIDENCE STOPPED BY ARTESIAN-HEAD RECOVERY, SANTA CLARA VALLEY, CALIFORNIA

J. F. Poland
U.S. Geological Survey
Sacramento, California

Abstract

From 1916 to 1966 in the San Jose area of Santa Clara Valley, California, generally deficient rainfall and runoff was accompanied by a fourfold increase in withdrawals of ground water. In response, the artesian head declined 55-75 m (180-250 ft). As a direct result of the artesian-head decline, the land surface subsided as much as 3.9 m (12.7 ft) in San Jose, due to compaction of the fine-grained compressible aquitards as their pore pressures decreased. The subsidence resulted in flooding of lands bordering the southern part of San Francisco Bay; the compaction of the sediments caused compressional failure of well casings in several hundred wells. The gross costs of subsidence to date are estimated to be $15-20 million.

The recovery of artesian head since 1967 has been dramatic. In downtown San Jose, the artesian head in two index wells recovered about 30 m (100 ft) in the 8 years from 1967 to 1975. Recovery of water levels was due to a fivefold increase in surface-water imports from 1965 to 1975, favorable local water supply, decreased withdrawal, and increased recharge.

In 1960, the Geological Survey installed extensometers in core holes 305 m (1,000 ft) deep in San Jose and Sunnyvale. Measurements of compaction of the confined aquifer system obtained from these extensometers demonstrate the marked decrease in rate of compaction in response to the major head recovery since 1967. In San Jose the rate decreased from about 30 cm (1 ft) in 1961 to 7.3 cm (0.24 ft) in 1967 and to 0.3 cm (0.01 ft) in 1973. Net expansion (land-surface rebound) of 0.6 cm (0.02 ft) occurred in 1974.

The subsidence has been stopped throughout the extent of the confined system as of 1974-75 by raising the artesian head in the aquifers until it equaled or exceeded the maximum pore pressures in the aquitards. However, the subsidence will recommence if the artesian head is drawn down appreciably below the levels of 1971-73.

Introduction

In 1969, at the first International Symposium on Land Subsidence in Tokyo, I presented a paper on the status of subsidence in the Santa Clara Valley (Poland, 1969). At the time that paper was prepared (1968), resurveys of bench-mark elevations in 1963 and 1967 had indicated that downtown San Jose was still subsiding at an average rate of 0.12 m/yr (0.4 ft/yr). In the succeeding 8 years, the water-management practices of the Santa Clara Valley Water District have raised the artesian head sufficiently to stop the subsidence as of 1974-75.

The Santa Clara Valley is a long narrow structural trough that extends about 145 km (90 mi) southeast from San Francisco. San Francisco Bay occupies much of its northern third. The discussion in this paper is limited to the densely populated central third of the valley, which extends southeastward about 48 km (30 mi) from Redwood City and Niles to Coyote, at the bedrock narrows about 16 km (10 mi) southeast of downtown San Jose. As shown by figure 1, most of this central area experienced 0.3 to 2.4 m (1 to 8 ft) of subsidence from 1934 to 1967.

The water-bearing deposits forming the ground-water reservoir in this central reach of the valley are chiefly of Quaternary age. They are principally alluvial, and range from coarse gravel to silt and clay. Near the

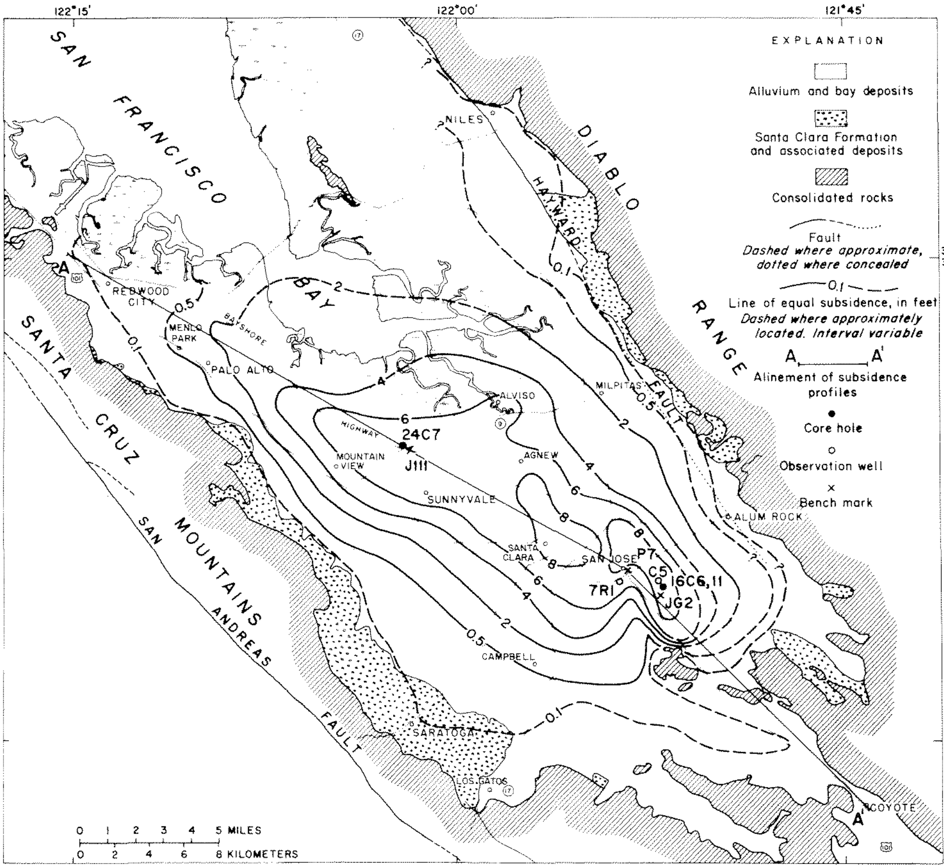

Figure 1.--Land subsidence from 1934 to 1967, Santa Clara Valley, California. Compiled from leveling of National Geodetic Survey in 1934 and 1967.

Valley margin, coarse-grained deposits predominate. Near the Bay, however, as much as 80 percent is silt and clay. The deposits are tapped by many hundreds of productive water wells to depths of 150 to 365 m (500-1,200 ft) (California Dept. Water Resources, 1967, pl. 4).

In the central two-thirds of the valley below a depth of about 60 m (200 ft) ground water is confined. The confinement extends northward from the southern part of San Jose to Palo Alto and Milpitas and beneath the Bay. In most of the area of confinement, wells more than 200 feet deep flowed in the early years of development. The confined aquifer system is as much as 245 m (800 ft) thick. Around the valley margins, ground water is unconfined and most of the natural recharge to the ground-water reservoir percolates from stream channels crossing alluvial-fan deposits.

Decline of artesian head, 1916-66

In the spring of 1916, the artesian head in index well 7R1 in San Jose stood 3.7 m (12 ft) above land surface. By the autumn of 1966, the level was 55 m (180 ft) below land surface. The principal factors in this major 50-year decline of 58 m (192 ft) are shown in figure 2. The upper line is

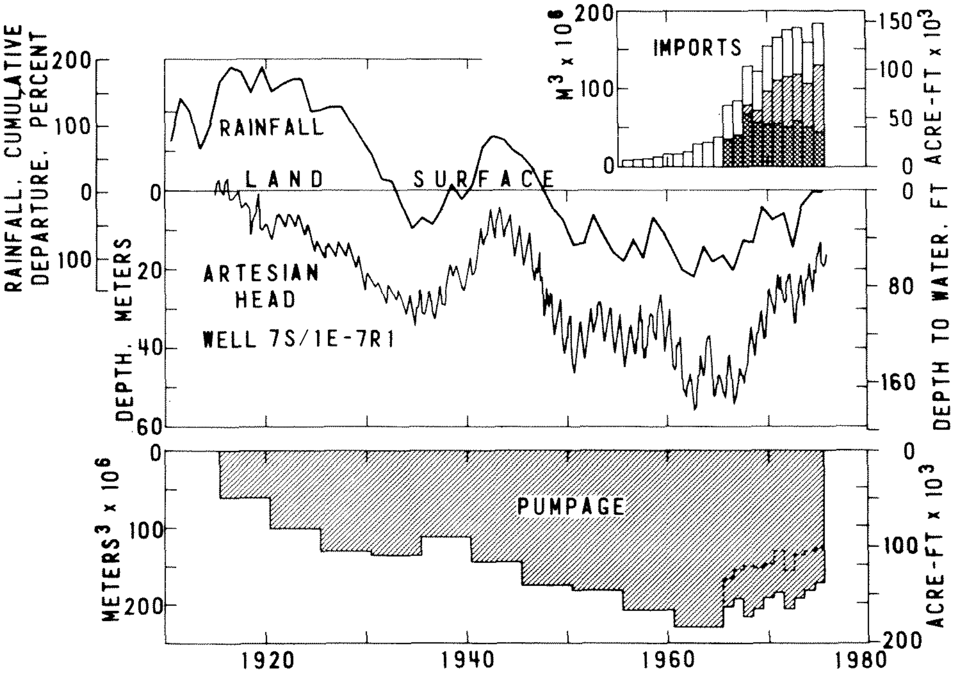

Figure 2.--Artesian-head change in San Jose in response to rainfall, pumpage, and water imports.

a plot of the cumulative departure, in percent, of the seasonal rainfall at San Jose from the State's 50-year seasonal mean, 1897-98 to 1946-47 (California State Water Resources Board, 1955, p. 26). The 50-year mean is 34.85 cm (13.72 in). Except for the 6-year wet period 1936-42, the departure in the 50 years 1916 to 1966 was generally negative and the cumulative departure was about 300 percent, equal to a cumulative deficiency of about 104 cm (41 in).

The bottom graph of figure 2 shows the estimated pumpage for the 60 years 1915-75. Estimates to 1965 are based chiefly on electric-power consumption for agricultural use; since then virtually all pumpage has been metered. Total yearly pumpage increased nearly fourfold from 1915-20 to 1960-65--from 60 to 228 hm^3 (49,000 to 185,000 acre-ft) a year (1 cubic hectometer, $hm^3 = 1 \times 10^6\ m^3$ = 810.7 acre-ft).

The 50-year decline in artesian head plainly was caused by generally deficient rainfall and constantly increasing pumping draft. The curve of artesian-head decline conforms remarkably well with the cumulative departure curve of the seasonal rainfall at San Jose.

Land Subsidence

Land subsidence was first noted in 1932 when bench mark P7 in San Jose, established in 1912, was resurveyed and found to have subsided nearly 1.2 m (4 ft). As a result, a valleywide network of bench marks was established in 1934 (Poland and Green, 1962, fig. 3). From 1934 to 1967 the National Geodetic Survey (formerly the U.S. Coast and Geodetic Survey) resurveyed the network from "stable" bedrock ties a dozen times to determine changes in elevation of the bench marks; the latest full survey of the network was in

1967. During the 33-year period 1934-67, subsidence ranged from 0.3 to 1.2 m (1 to 4 ft) under the Bay to 2.4 m (8 ft) in San Jose (fig. 1). The volume of subsidence (pore-space reduction) in this period was about 617 hm^3 (500,000 acre-ft).

The subsidence record for bench mark P7 in San Jose is plotted in figure 3, together with the artesian head in nearby well 7R1, taken from

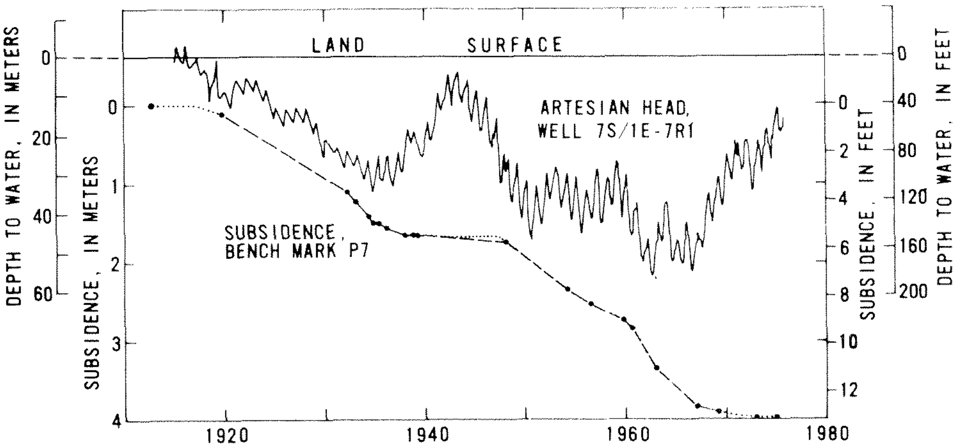

Figure 3.--Artesian-head change and land subsidence, San Jose.

figure 2. The fluctuation of artesian head represents the change in stress on the aquifer system and the subsidence is the resulting strain. Subsidence at bench mark P7 began about 1918 and was 1.6 m (5.4 ft) by 1938. From 1938 to 1947 subsidence stopped during a period of artesian-head recovery but resumed in 1947 coincident with rapidly declining head. By 1967 bench mark P7 had subsided 3.86 m (12.67 ft). Releveling of this bench mark in 1969 showed a small increased settlement to 3.93 m (12.88 ft).

Figure 4 shows land-subsidence profiles along line A-A' from Redwood City to Coyote from 1912 through 1969 (for location, see fig. 1). The 1934 leveling was used as a reference base because this was the first complete leveling of the net. Note that from 1934 to 1967, maximum subsidence of 2.6 m (8.6 ft) was near bench mark W111, 4.8 m (3 mi) northwest of bench mark P7; also that from 1934 to 1960 the greatest subsidence along line A-A' was 1.7 m (5.7 ft) at bench mark J111 in Sunnyvale. Changes in the rate and magnitude of artesian-head decline doubtless have caused such geographic variations in subsidence rate and magnitude with time.

Subsidence Problems

The subsidence has created several major problems. Lands adjacent to San Francisco Bay have sunk 0.6 to 2.4 m (2 to 8 ft) since 1912, requiring construction and raising of levees to restrain landward movement of the saline Bay water onto 44 km^2 (17 mi^2) of land now below high-tide level. Also, flood-control levees have been built and maintained near the bayward ends of the depressed stream channels. About $9 million of public funds has been spent to 1974 on flood-control levees on the streams entering the Bay to correct for subsidence effects, according to Lloyd Fowler of the Santa Clara Valley Water District. In addition, a major salt company has spent an unknown but substantial amount maintaining levees on 78 km^2 (30 mi^2) of salt ponds and the landward chain of dikes, to counter as much as 2.4 m (8 ft) of subsidence. Several hundred water-well casings have been ruptured by the compaction of the sediments. The cost of repair or replacement of such

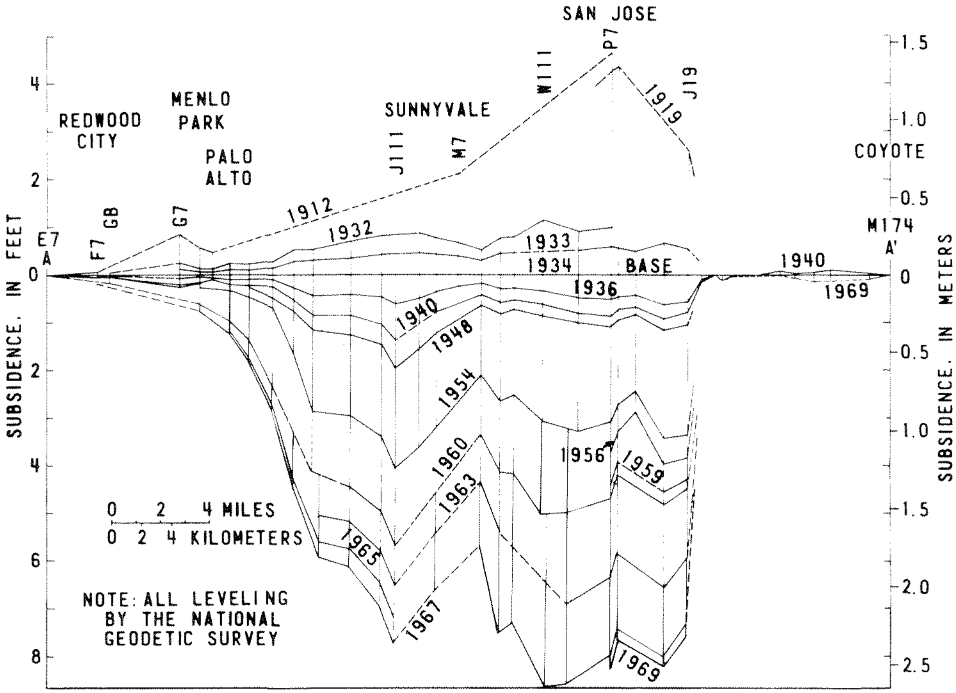

Figure 4.--Profiles of land subsidence, Redwood City to Coyote, Calif., 1912-69.

damaged wells has been estimated as at least \$4 million (Roll, 1967). Including funds spent on maintaining the salt-pond levees, establishing and resurveying the bench-mark net, repairing railroads, roads, and bridges, and making private engineering surveys, the gross costs of subsidence must have been \$15-20 million to date.

Detention Reservoirs to Salvage Flood Waters

Local agencies have been working since the 1930's to conserve and obtain water supplies adequate to stop the ground-water overdraft and raise the artesian head. Their program has involved (1) salvage of flood waters from local streams that would otherwise waste to the Bay and (2) importation of water from outside the valley. In 1935-36 five storage dams were built on local streams to provide detention reservoirs with combined storage capacity of about 62 hm^3 (50,000 acre-ft) to retain flood waters and permit controlled releases to increase streambed percolation (Hunt, 1940). The storage capacity of detention reservoirs was increased to 178 hm^3 (144,000 acre-ft) by the early 1950's (California State Water Resources Board, 1955, p. 51).

Recovery of Artesian Head, 1967-75

The recovery of water level since 1967 has been dramatic. By 1975, the spring high water level at index well 7R1 (fig. 2) was 32 m (104 ft) above that of 1967, and about equal to the level in this well in 1925. This major recovery of artesian head was due to several factors, including increased imports of water, favorable local water supply, decreased pumpage, and increased recharge (fig. 2). The most important factor was the increase in imports.

The import of surface water to Santa Clara County began about 1940 when San Francisco began selling water imported from the Sierra Nevada to several municipalities. This import increased to 15 hm^3 (12,000 acre-ft) in 1960 and to 54 hm^3 (44,000 acre-ft) by 1975 (see blank segments of yearly bars, upper right graph, fig. 2). Surface water imported from the Central Valley through the State's South Bay Aqueduct first became available in 1965; by 1974-75, the Aqueduct import was 128 hm^3 (104,000 acre-ft) (see cross-hatched plus diagonally-ruled segments of yearly bars, upper right graph, fig. 2). As a result, total imports to Santa Clara County increased five-fold from 1964-65 to 1974-75--from 37 to 183 hm^3 (30,000 to 148,300 acre-ft) per year.

The average seasonal rainfall at San Jose was 13 percent above normal in the period 1966-75. The cumulative departure graph (fig. 2) indicates a positive increase of 120 percent or about 41 cm (16 in) in the 9-year period.

The average yearly pumpage of ground water, which had reached its peak of 228 hm^3 (185,000 acre-ft) in 1960-65, decreased to 185 hm^3 (150,000 acre-ft) in 1970-75. A principal reason for this 19-percent decrease is the tax on ground-water pumpage applied since 1964 for water extracted from the ground-water basin. In 1970-71, for example, the ground-water tax was levied at $8 per acre-ft for ground water extracted for agricultural purposes and at $29 per acre-ft for ground water extracted for other uses. For water delivered on the surface in lieu of extraction the cost was $10.50 per acre-ft for water used for agriculture and $31.50 per acre-ft for water used for other purposes. The economic advantage of using surface water where available is obvious.

Recharge from stream channels and percolation ponds to the ground-water reservoir has been augmented since 1965 by water from the South Bay Aqueduct that could not be delivered directly to the user. The yearly quantity diverted to recharge areas (cross hatched segment of yearly bars, upper right graph, fig. 2) in the 10 years has averaged about 51 hm^3 (41,000 acre-ft) a year and represents 56 percent of the total import from the South Bay Aqueduct. This additional recharge can be considered as an equivalent reduction in net pumpage (see dashed line, 1965-75, in pumpage graph of figure 2). For 1970-75 this recharge in effect reduced the net yearly pumpage to about 42 percent below the average gross pumpage of 1960-65.

Extensometers to Measure Compaction

Extensometers (compaction recorders) were installed by the Geological Survey in 1960 in the 305-m (1,000-ft) cased core holes at the centers of subsidence: 16C6 in San Jose and 24C7 in Sunnyvale (fig. 1). They have recorded compaction of the confined aquifer system for 16 years. When first installed, the extensometers consisted of an anchor (subsurface bench mark) emplaced in the formation below the bottom of the well casing, attached to a cable that passed over sheaves at the land surface, and counterweighted to maintain constant tension (fig. 5, A). A recorder connected to the cable yields a time graph of the movement of land surface with respect to the anchor--that is, the compaction or expansion of the sediments within that depth range. To reduce the friction problem and increase the accuracy of measurement, the installations were modified in the early 1970's by replacing the anchored cable with a "free-standing pipe" of 3.8 cm (1 1/2-in) diameter (fig. 4, B). Records from these instruments show that the compac-

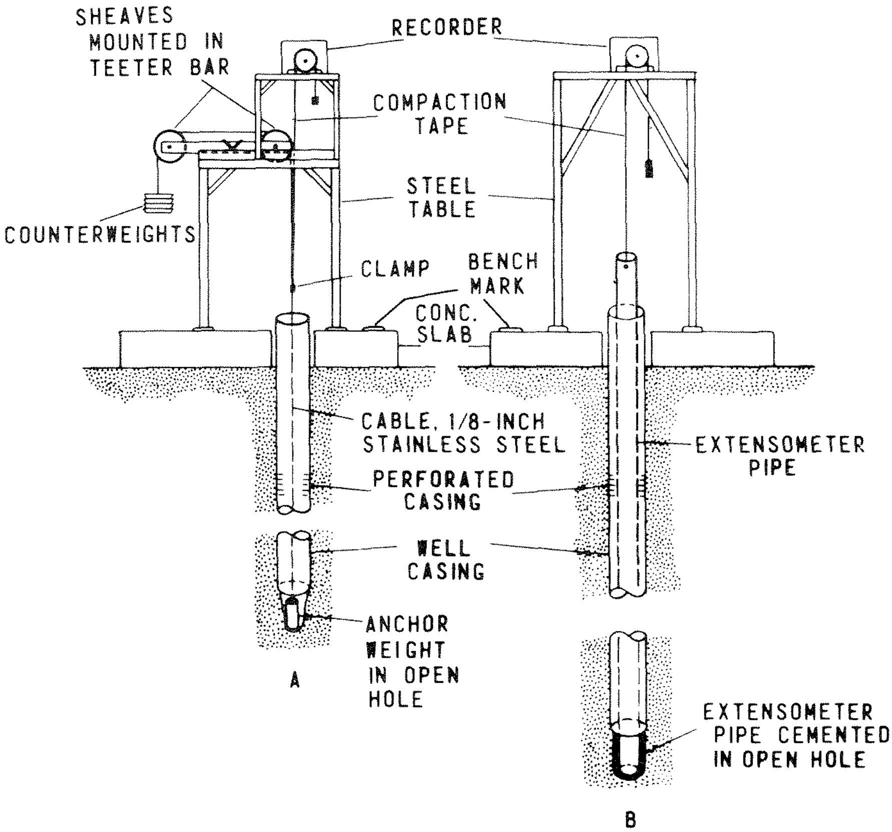

Figure 5.--Recording extensometer installations. A, Cable assembly; B, Pipe assembly.

tion measured to a depth of 305 m (1,000 ft)--nearly the maximum depth of water wells--is about equal to the land subsidence as measured periodically by leveling of the bench-mark net. Therefore, these instruments function as continuous subsidence recorders at their respective locations.

Figure 6 is a time plot of the measured compaction in the 305-m (1,000-ft) well in San Jose (well 16C6, 11), and the compaction and artesian-head fluctuation (change in applied stress) in adjacent unused well 16C5, through 1975; also the subsidence of adjacent bench mark JG2 from 1960 to 1969. Measured compaction of the confined aquifer system to the 305 m depth from July 1, 1960, to December 31, 1975, was 1.4 m (4.7 ft). The rapid 18-m (60-ft) decline of artesian head from 1959 to 1962 caused rapid compaction of the aquifer system in those years but the rate decreased during the relatively consistent head fluctuation from 1962 to 1967. From 1967 to 1975, the artesian head recovered about 30 m (100 ft) at well C5.

The marked decrease in rate of subsidence in response to the dramatic head recovery since 1967 is demonstrated graphically by the compaction records from the two deep extensometers in San Jose and Sunnyvale (fig. 7). The rate of compaction in well 16C6, 11, in San Jose decreased from about 30 cm (1 ft) per year in 1961 to 7.3 cm (0.24 ft) in 1967 and to 0.3 cm (0.01 ft) in 1973. Net expansion (land-surface rebound) of 0.6 cm (0.02 ft)

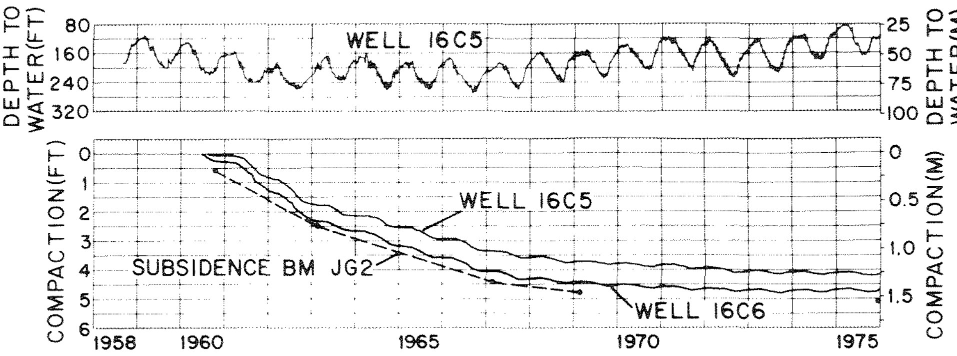

Figure 6.--Measured water-level change, compaction, and subsidence in San Jose.

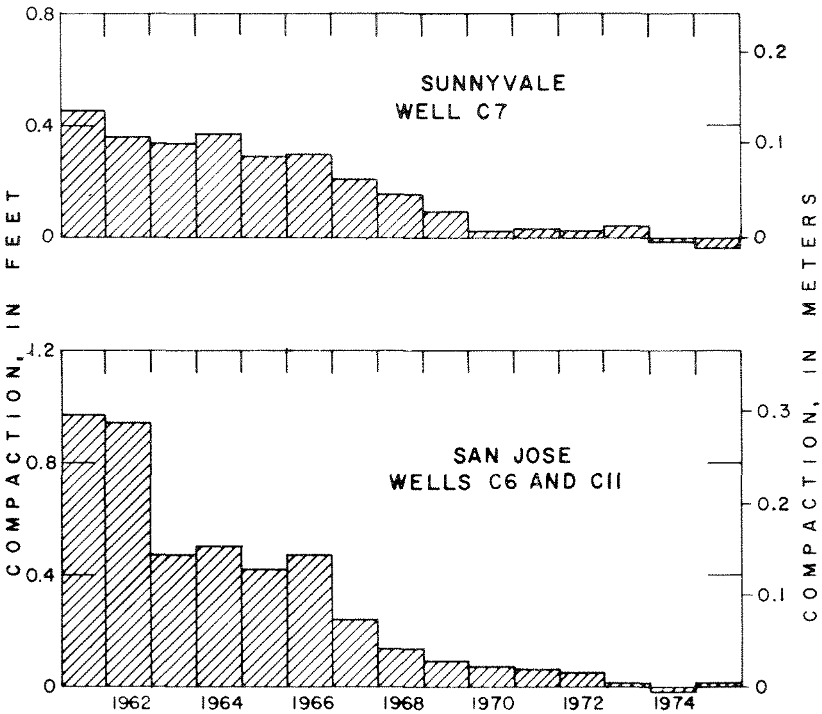

Figure 7.--Measured annual compaction to 1,000-foot depth.

occurred in 1974. In Sunnyvale, compaction of the sediments above the 305-m anchor in well 24C7 decreased from about 15 cm (0.5 ft) per year in 1961 to 1.2 cm (0.04 ft) in 1973; net expansion of 0.5 cm (0.016 ft) and 1.1 cm (0.04 ft) occurred in 1974 and 1975, respectively.

Both the cause of subsidence and the means of its control are known. The evidence given here and in other studies by the Geological Survey proves that the subsidence is caused by decline of the artesian head and the resulting increase in effective overburden load or grain-to-grain stress on the water-bearing beds in the confined system. The sediments compact under the increasing stress and the land surface sinks. Most of the compaction occurs in the fine-grained clayey beds (aquitards) which are the most compressible but have low permeability. Therefore, the escape of water (decay of excess pore pressure) and the increase in effective stress are slow and time-dependent, but the ultimate compaction is large and chiefly permanent.

The subsidence has been stopped by raising the artesian head in the aquifers until it equaled or exceeded the maximum pore pressures in the aquitards. The compaction and water-level records being obtained by the Geological Survey indicate that if the artesian head can be maintained 3 to 6 m (10 to 20 ft) above the levels of 1971-73, subsidence will not recur. On the other hand, subsidence will recommence if artesian head is drawn down as much as 6 to 9 m (20 to 30 ft) below the 1971-73 levels.

References

California State Water Resources Board, 1955, Santa Clara Valley Investigation: Bull. no. 7, 154 p.

California Department of Water Resources, 1967, Evaluation of ground-water resources, South Bay: Bull. No. 118-1, Appendix A, Geology, 153 p.

Hunt, G. W., 1940, Description and results of operation of the Santa Clara Valley Water Conservation Districts project: Am. Geophys. Union Trans., pt. 1, p. 13-22.

Poland, J. F., 1969, Land subsidence and aquifer-system compaction, Santa Clara Valley, California, USA, in Tison, L. J., ed., Land Subsidence, Vol. 1: Internat. Assoc. Sci. Hydrology, Pub. 88, p. 285-292.

Poland, J. F., and Green, J. H., 1962, Subsidence in the Santa Clara Valley, California--A progress report: U.S. Geol. Survey Water-Supply Paper 1619-C, 16 p.

Roll, J. R., 1967, Effect of subsidence on well fields: Am. Water Works Assoc. Jour., v. 59, no. 1, p. 80-88.

Publication n°121 of the International Association of Hydrological Sciences
Proceedings of the Anaheim Symposium, December 1976

NUMERICAL MODEL FOR LAND SUBSIDENCE IN SHALLOW GROUNDWATER SYSTEMS

T. N. Narasimhan and P. A. Witherspoon
Lawrence Berkeley Laboratory and Department of Materials Science & Engineering
University of California
Berkeley, California 94720

Abstract

A numerical model is presented to simulate compaction of shallow groundwater systems. The model combines a general three-dimensional fluid flow field with a one-dimensional deformation of the porous medium. The governing equation is solved with an Integrated Finite Difference Method using a mixed explicit-implicit iteration scheme for advancing in the time domain. The model can handle heterogeneous flow regions with complex geometry, and with time dependent variation of material properties and boundary conditions. Five illustrative examples are provided to demonstrate the applicability of the model to problems of relevance in studying land subsidence.

Introduction

The purpose of this paper is to present a numerical model for simulating the compaction of a groundwater reservoir caused by withdrawal of water. As used here, the term groundwater reservoir includes those parts of the groundwater system which release water from storage in order to directly compensate for the water withdrawn. If the reservoir occurs at a shallow depth, all the deformations associated with the compaction may be expressed at ground surface as land subsidence. If the reservoir is buried at considerable depths, the effects of compaction may undergo more or less attenuation in being transmitted to the land surface through the overburden. The propagation of the effects of reservoir compaction through the overburden is outside the scope of this paper. Conceptually, the model combines a general three-dimensional fluid flow field with a one-dimensional, vertical, deformation of the porous medium. The first part of the paper deals with the theory and the salient features of the model. In the second, five illustrative examples are given to demonstrate the applicability of the model to problems that are relevant in studying land subsidence.

Theory

The equation governing saturated-unsaturated flow in a deforming porous medium can be expressed in an integral form as (Narasimhan and Witherspoon, 1976b)

$$G + \int_{\Gamma} \bar{\rho}_w \bar{K} \nabla (z+\psi) \bullet \vec{n} \, d\Gamma = M_c \frac{D\psi}{Dt} \qquad (1)$$

in which Γ is the surface of an appropriately small volume element fixed in the solid phase of the porous medium, D/Dt is a material derivative and M_c, the fluid mass capacity of the volume element defined by

$$M_c = V_s \rho_w \, [\underbrace{eS\gamma_w \beta}_{\substack{\text{expansion}\\ \text{of}\\ \text{water}}} + \underbrace{S\gamma_w \chi' a_v}_{\substack{\text{change in}\\ \text{pore}\\ \text{volume}}} + \underbrace{e\frac{dS}{d\psi}}_{\substack{\text{change in}\\ \text{saturation}}}] \qquad (2)$$

M_c denotes the mass of water which the volume element can release from storage due to an unit change in the mean value of ψ.

Restricting ourselves, in this paper, to a saturated flow region and neglecting small changes in ρ_w, (1) reduces to

$$G + \int_{\Gamma} \rho_{wo} \bar{K}\nabla(z+\psi)\bullet\vec{n}\, d\Gamma = \rho_{wo} V_s \gamma_w [e\beta+\chi' a_v] \frac{D\psi}{Dt} \tag{3}$$

As opposed to (3) it is more customary in hydrogeology literature to write the governing equation in the form

$$G + \int_{\Gamma} \rho_{wo} \bar{K}\nabla(z+\psi)\bullet\vec{n}\, d\Gamma = \rho_{wo} V \gamma_w [n\beta+m_v] \frac{\partial\psi}{\partial t} \tag{4}$$

The quantity, $\gamma_w[n\beta + m_v]$ is often referred to as specific storage, S_s.

In dealing with reservoir compaction, the treatment of the deformation parameter is critical. As pointed out by Helm [1974], it is necessary to distinguish between recoverable (elastic) and non-recoverable (non-elastic, virgin) components of compaction. This distinction can be implemented in the present model by using different values of a_v (in equation 3) or S_s (in equation 4) for the elastic and virgin compression ranges. Alternatively, one could replace a_v in (3) by c_c/σ' or c_s/σ'.

The governing equations (3) and (4) are subject to appropriate initial and boundary conditions. The equations are in general non-linear since K and M_c are both functions of the dependent variable ψ. To numerically solve the equations, an Integrated Finite Difference Method (Narasimhan and Witherspoon, 1976a) has been employed, using a mixed explicit-implicit iterative procedure to advance in time. The details of the algorithm can be found in Narasimhan (1975) and will be published elsewhere.

In general, the model can simulate a heterogeneous three dimensional flow region with complex geometry. Anisotropy can be taken into account by orienting the elemental interfaces normal to the principal axes of anisotropy. The source term as well as the boundary condition can be dependent on time or on ψ. The total stress may be prescribed to vary with time. The initial state of ψ and preconsolidation stress may be arbitrary. The material properties, K, e, a_v, m_v, n and S_s may vary with effective stress. A choice is available either to use (3) or (4) as the governing equation, although, (3) is technically preferable, especially when the material properties are stress dependent.

Probably the chief limitation of the model is that it ignores lateral deformations. For hydrogeological systems with large lateral dimensions, ignoring lateral deformations appears to be valid in the light of the recent work by Helm (1975). Perhaps the only way to realistically simulate lateral displacements is to solve a second governing equation for stress-strain, suitably coupled with the flow equation (3). This necessarily leads to increased effort and increased requirement of refined field data. Such a coupled model may be especially needed if there is a significant overburden between the reservoir and the land surface.

Illustrative Examples

In order to verify the model, the five problems listed below were solved:

1. One-dimensional, homogeneous clay column. Step-change in total stress, followed by drainage.
2. One-dimensional, heterogeneous clay, column. Step-change in total stress, followed by drainage.
3. One-dimensional, homogeneous clay column. Constant total

stress. Cyclic variation of hydraulic head at the boundary.

4. Two-dimensional, homogeneous region. Time-dependent total stress with drainage.
5. Axi-symmetric, leaky aquifer system. Constant total stress. Pumpage from a well.

Example 1. There are 100 doubly-draining beds of clay, normally consolidated and under hydrostatic conditions. At t = 0 a step-load equal to 3.05 m of water is applied at the boundary of each bed, resulting in the development of 3.05 m of excess pore-pressure within each-bed. The clay has $K' = 9.67 \times 10^{-12}$ m/sec and $S_s = 3.28 \times 10^{-4}$ m^{-1}. It is required to compute total compaction as a function of time. The problem was solved numerically using a mesh spacing of 6.096×10^{-2} m. An analytic solution for the problem can be found in Taylor (1948). A comparison of the analytical and the numerical solutions show excellent agreement (Figure 1).

Example 2. Schiffman and Gibson (1964) reasoned that for realistic settlement calculations due consideration must be given to the variability of permeability and compressibility with depth in thick clay columns. To establish their hypothesis, they considered a 30.48 m column of London Blue clay (Figure 2) with depth-dependent material properties (Figure 3). Treating K and m_v as continuous functions of depth and using a finite difference model they computed compaction as a function of time. The same problem was solved by our numerical model, by dividing the column into 10 materials with step-wise change in properties (Figure 3) and 100 volume elements. A comparison of the results is shown in Figure 4. The agreement appears reasonable and the small differences seen after two years is probably attributable to the different techniques employed for handling the spatial variation of material properties.

Example 3. The subsidence of land surface as well as the associated fluctuation in piezometric heads near Pixley, California has been carefully measured over several years by the U. S. Geological Survey (Lofgren and Klausing, 1969). Recently, Helm (1975) successfully modeled observed subsidence at Pixley for a 12-year period from 1958, treating the observed piezometric fluctuations as the causative mechanism. Within the alluvial sediments at Pixley there exist 21 compacting clay beds of varying thickness, aggregating 85 m and separated by hydraulically continuous, highly permeable sand beds. In accordance with Helm's findings, the Pixley system was treated in the present study as equivalent to 17 doubly draining clay beds, each 4.877 m thick. Because of symmetry, only one half of a bed need be modeled. The column was discretized into 20 elements, 0.1219 m thick. The following material properties were used: $K' = 2.9 \times 10^{-11}$ m/sec; $(S_s)_{virgin} = 7.54 \times 10^{-4}$ m^{-1}; $(S_s)_{elastic} = 1.51 \times 10^{-5}$ m^{-1}. The boundary conditions consisted of day by day hydrographs of the piezometric variations in the aquifer. The simulation was carried out for 4000 days from October 21, 1958. The initial distribution of pore pressure was assumed hydrostatic while that of the preconsolidation stress was assumed to vary parabolically from the bottom to the center of the clay bed.

A comparison between the observed and computed compactions presented in Figure 5 shows a reasonable agreement, with a maximum deviation of about 7 percent in early 1964. A similar accuracy was also obtained by Helm (1975). For the period, 1966-1968, Helm obtained slightly better agreement than is seen in Figure 5. In this regard it may be pointed out that Helm plotted

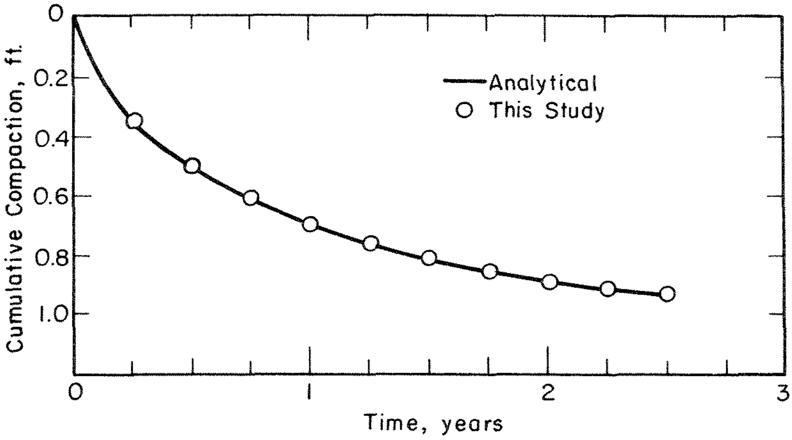

Fig. 1. Compaction of homogeneous clay beds: comparison of analytical and numerical results.

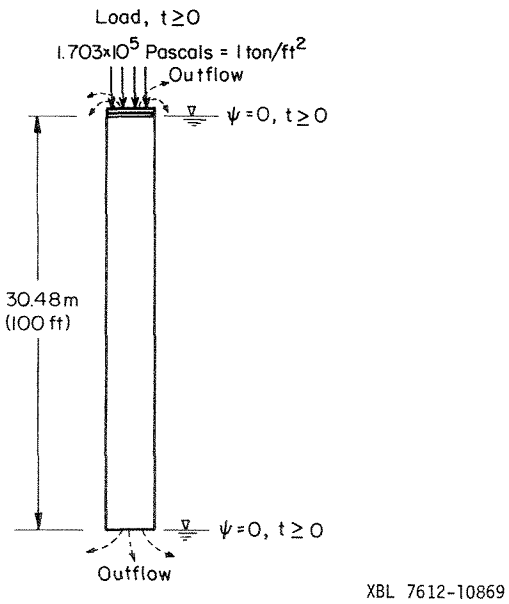

Fig. 2. Compaction of non homogeneous clay column: initial and boundary conditions.

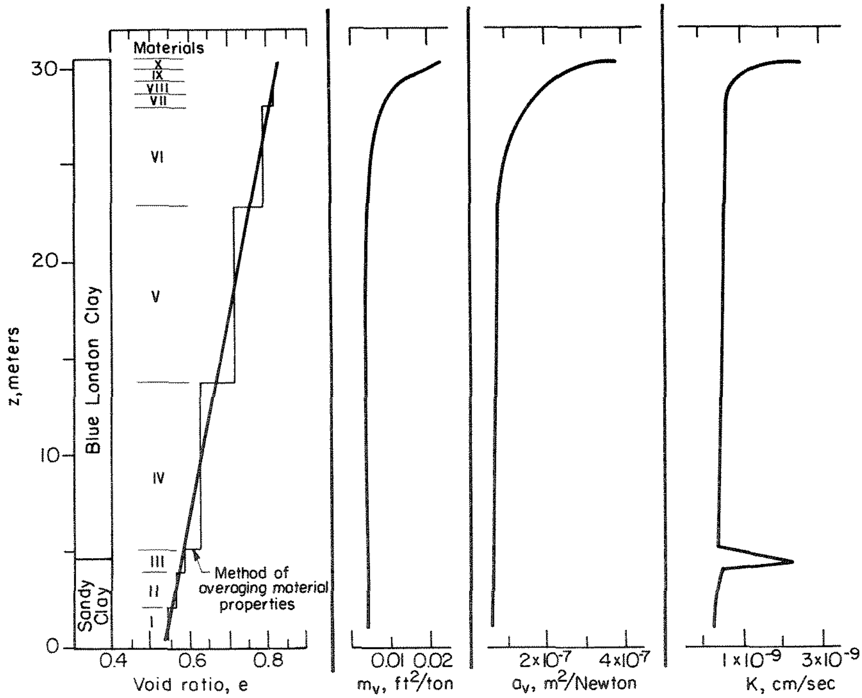

Fig. 3. Compaction of non homogeneous clay column: variation of material properties with depth.

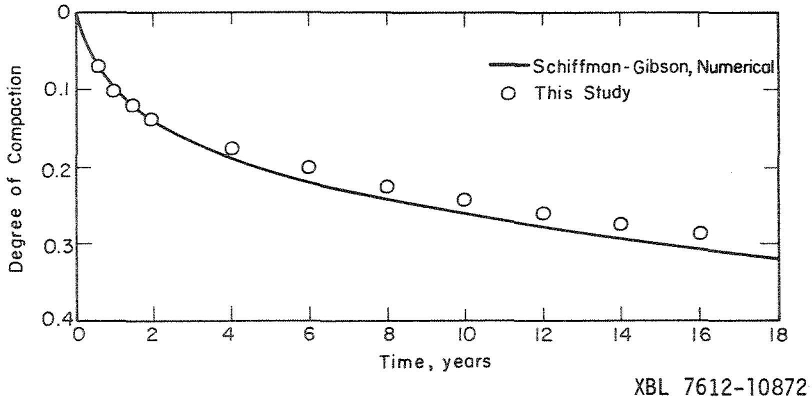

Fig. 4. Compaction of non homogeneous clay column: comparison of numerical results.

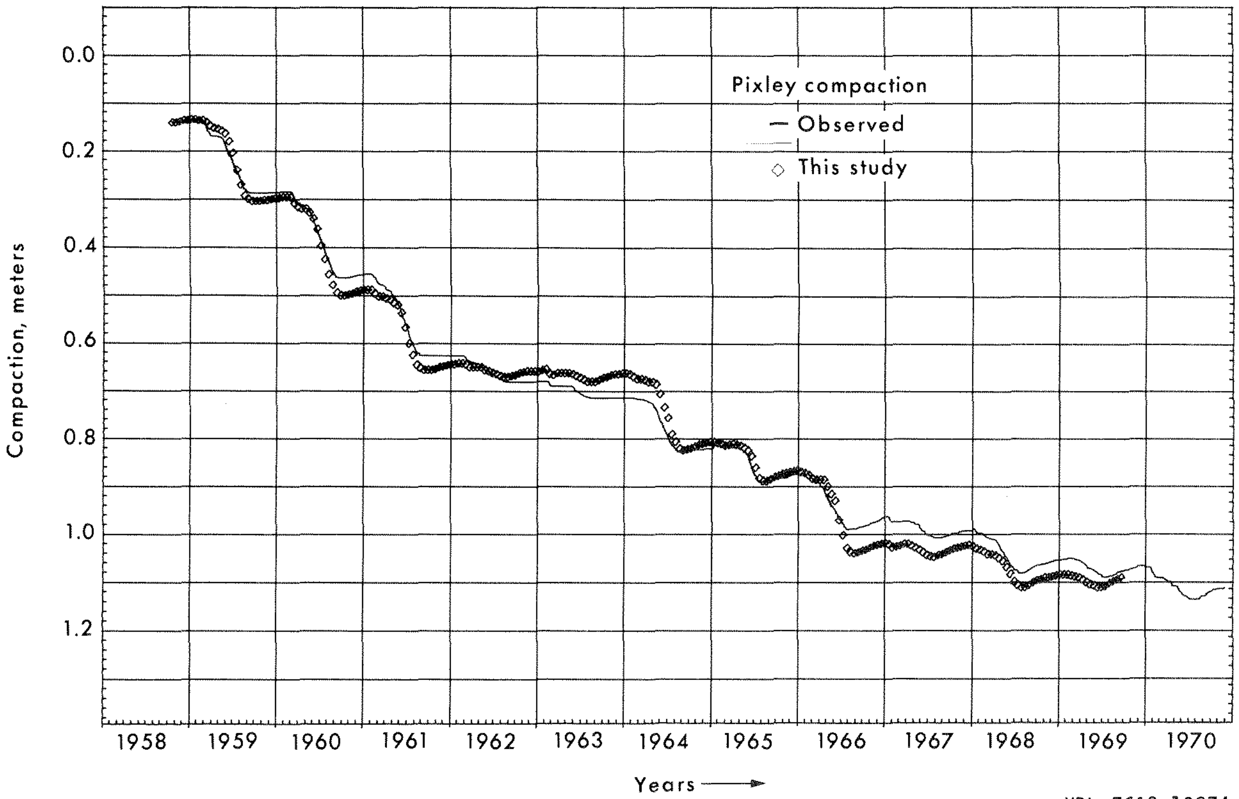

XBL 7612-10874

Fig. 5. Land subsidence at Pixley, California: comparison of observed and computed compactions.

the cumulated compaction of 21 different beds of variable thickness while Figure 5 relates to 17 equivalent beds of the same thickness.

Example 4. In the foregoing examples, σ was considered invariant with time. However, there may be cases in which σ is indeed a function of time. One would suspect that in hydrogeological systems the time-scale of such a variation of σ will be very large as compared to that of the drainage phenomenon of interest. To demonstrate how variable total stress could be mathematically modeled, a hypothetical example is chosen from the field of soil mechanics.

A doubly-draining clay layer (Figure 6) is normally consolidated and has $K' = 9.81 \times 10^{-10}$ m/sec and $S_s = 5 \times 10^{-3}$ m^{-1}. A strip-load, 10^5 N/m^2, is gradually applied on a segment of the upper boundary, with the loading being completed after 90 days. It is required to compute compaction during the loading period.

To handle this problem we need to know, a priori, the rate of pore pressure generation caused by the variable load. Note that pore-pressure is generated at constant σ' and compaction takes place only when the generated pore pressure dissipates. Hence, as pore pressure is generated, the total stress is also to be increased by an equal amount.

In this problem, the generation of pore pressure was calculated using the elastic equations (Poulos and Davis, 1974) for uniform strip-loading, assuming that the magnitude of pore pressure generated is equal to the increase in octahedral stress. The ultimate pore pressures so generated are shown contoured in Figure 7. The time-rate of pore pressure generation is equal to the ultimate value divided by the duration of loading. The problem was numerically solved using 280 elements of variable size. The computed compaction profiles at various times are shown in Figure 8.

Example 5. Subsidence caused by withdrawal water by pumping wells is an important field problem. The present mathematical model can, in general, simulate reservoir compaction due to one or more wells producing from a multiple aquifer-aquitard system under arbitrary initial and boundary conditions. For purposes of illustration we consider a simple example.

A one-meter radius well fully penetrates a 20-meter aquifer with $K = 9.8 \times 10^{-6}$ m/sec and $S_s = 1 \times 10^{-5}$ (Figure 9) and overlain by 10-meter aquitard with $K' = 2.9 \times 10^{-10}$ m/sec and $S_s = 7.54 \times 10^{-4}$ m^{-1}. The well

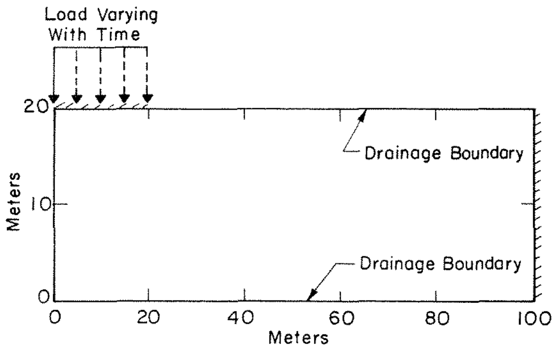

Fig. 6. Compaction due to time-dependent loading: initial and boundary conditions.

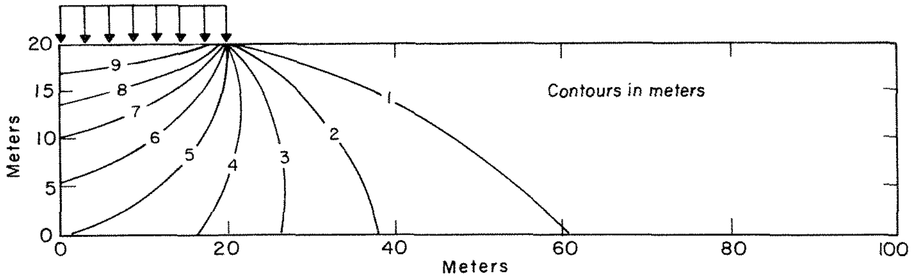

Fig. 7. Compaction due to time-dependent loading: contours of ultimate pore-pressures generated.

produces at a constant rate of 0.02 m^3/sec. It is required to compute the changes in hydraulic head within the system and the compaction as functions of time.

The axisymmetric system was discretized into 421 volume elements with the aquitard divided vertically into 20 zones, each 0.5 m thick. The simulation was carried out for 200 days. Hantush (1960) derived an analytical expression for the drawdown changes within the aquifer in a leaky aquifer system described above. A comparison of the computed results with Hantush's solution is presented in Figure 10, at a point in the aquifer, 125 m away from the well. The computed profiles of compaction are presented in Figure 11. In addition, the computer program also calculates volume strains and strain-rates for each volume element in the system. The contours of equal cumulated strains at the end of 200 days are presented in Figure 12. A mass balance check showed that the volume of water pumped from the aquifer-aquitard system agreed with the total volume change of the system with an error very much less than one percent.

<u>Nomenclature</u>

a_v	coefficient of compressibility	[LT^2/M]
C_c	compression index	[1]
C_k	slope of e versus log K straight line	[1]
C_s	swelling index	[1]
e	void ratio	[1]
G	mass generation rate from a volume element	[M]
K, $\bar{K}$	hydraulic conductivity; mean hydraulic conductivity	[L/T]
M_c	fluid mass capacity	[M/L]

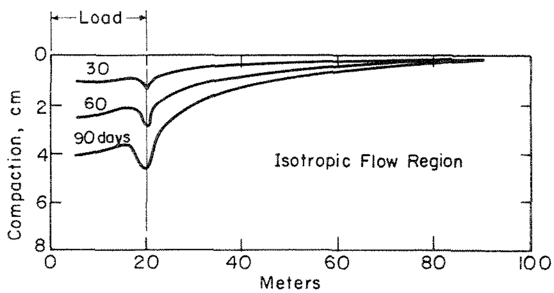

XBL 7612-10873

Fig. 8. Compaction due to time-dependent loading: profiles of compaction at different times.

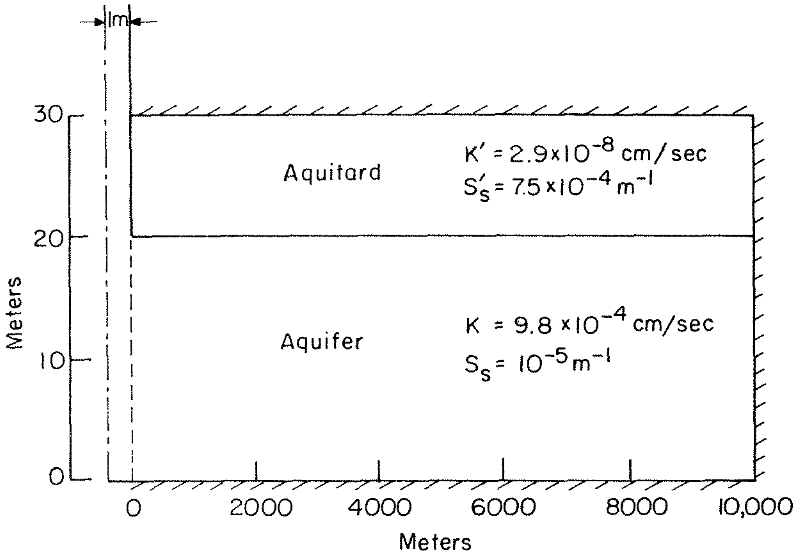

Fig. 9. Leaky aquifer system: boundary conditions.

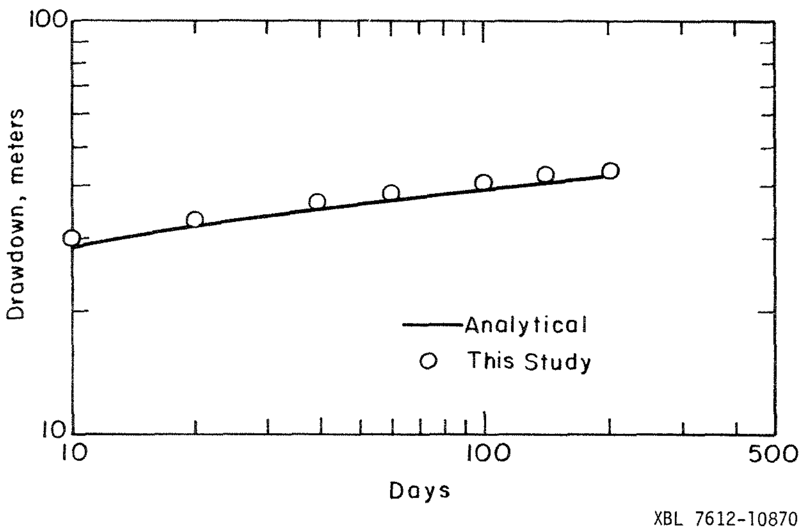

Fig. 10. Leaky aquifer system: comparison of analytical and numerical results at r = 125 m in the aquifer.

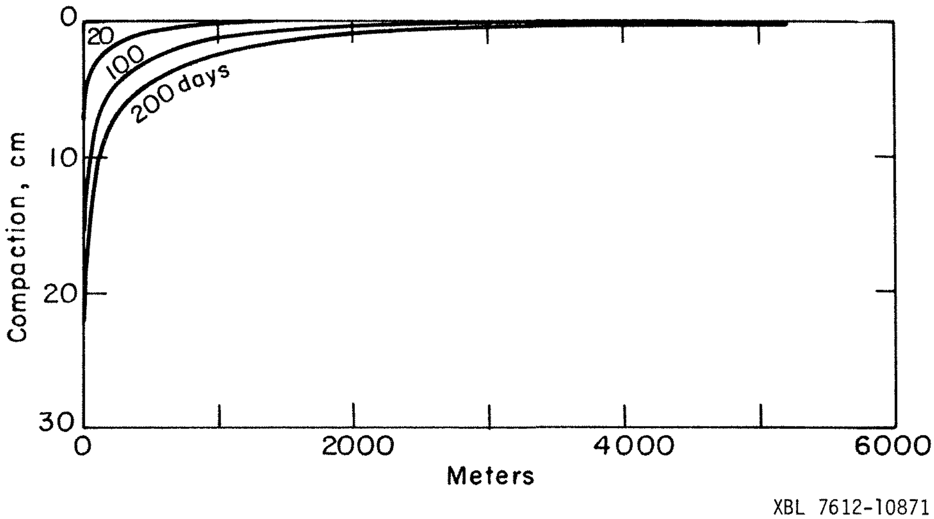

Fig. 11. Leaky aquifer system: profiles of compaction at different times.

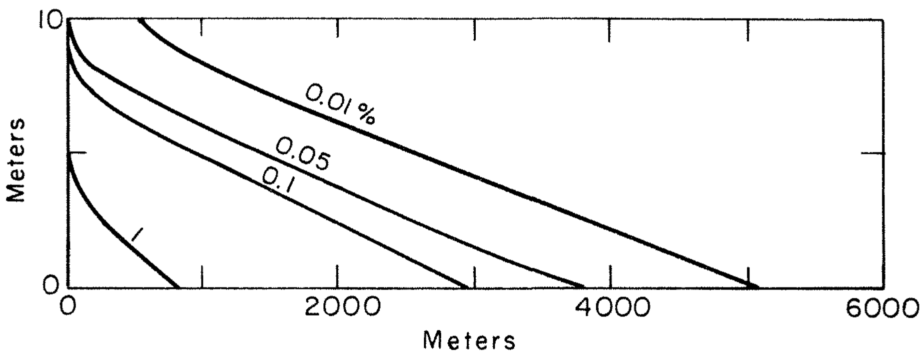

Fig. 12. Leaky aquifer system: contours of equal cumulated strain in the aquitard after 200 days pumping.

m_v	coefficient of volumetric compressibility	$[LT^2/M]$
n	porosity	$[1]$
$\vec{n}$	unit outer normal	$[1]$
S	saturation	$[1]$
S_s	coefficient of specific storage	$[1/L]$
t	time	$[T]$
V_s	volume of solids	$[L^3]$
V	bulk volume	$[L^3]$
z	elevation above arbitrary datum	$[L]$
β	compressibility of water	$[LT^2/M]$
Γ	boundary surface of volume element	$[L^2]$
γ_w	specific weight of water	$[ML/T^2]$
$\rho_w, \bar{\rho}_w, \rho_{wo}$	density, mean density and reference density of water	$[M/L^3]$
σ	total stress	$[M/LT^2]$
σ'	effective stress	$[M/LT^2]$
χ'	coefficient relating pore pressure change to effective stress change	$[1]$
ψ	pressure head	$[L]$

Acknowledgement

This work was done with support from the U. S. Energy Research and Development Administration.

References

Hantush, M. S., 1960, Modification of the theory of leaky aquifers, J. Geophys. Res., v. 65, no. 11, p. 3713-3726.

Helm, D. C., 1974, Evaluation of stress-dependent aquitard parameters by simulating observed compaction from known stress history, Ph.D. thesis, Univ. of California, Berkeley, 175 pp.

Helm, D. C., 1975, One-dimensional simulation of aquifer system compaction near Pixley, California, 1. Constant parameters, Water Resources Res., v. 11, no. 3, p. 465-478.

Lofgren, B. E. and R. L. Klausing, 1969, Land subsidence due to groundwater withdrawal, Tulare-Wasco area, California, U. S. Geol. Surv. Prof. Paper 437-B, 103 pp.

Narasimhan, T. N., 1975, A unified numerical model for saturated-unsaturated groundwater flow, Ph.D. thesis, Univ. of Calif., Berkeley, 244 pp.

Narasimhan, T. N. and P. A. Witherspoon, 1976a, An integrated finite difference method for analyzing fluid flow in porous media, Water Resources Res., v. 12, no. 1, p. 57-64.

Narasimhan, T. N. and P. A. Witherspoon, 1976b, Numerical model for saturated-unsaturated flow in deformable porous media, Water Resources Res., to be published.

Poulos, H. G. and E. H. Davis, 1974, Elastic Solutions for Soil and Rock Mechanics, John Wiley and Sons, New York, 411 pp.

Schiffman, R. L. and R. E. Gibson, 1964, Consolidation of non homogeneous clay layers, Am. Soc. Civil Eng., J. Soil Mech. and Found. Eng., v. 90, no. SM5, p. 1-30.

Taylor, D. W., 1948, Fundamentals of Soil Mechanics, John Wiley and Sons, New York, 700 pp.

Publication n°121 of the International Association of Hydrological Sciences
Proceedings of the Anaheim Symposium, December 1976

ESTIMATING PARAMETERS OF COMPACTING FINE-GRAINED INTERBEDS WITHIN A CONFINED AQUIFER SYSTEM BY A ONE-DIMENSIONAL SIMULATION OF FIELD OBSERVATIONS

D. C. Helm
U.S. Geological Survey
Sacramento, California

Abstract

A one-dimensional mathematical model that calculates idealized aquifer-system compaction and expansion has been applied to observed water-level fluctuations and to the resulting observed transient compaction-and-expansion behavior of a total thickness interval at one site in the San Joaquin Valley and at several sites in the Santa Clara Valley. Values for total cumulative thickness b'_{sum} of fine-grained interbeds within the confined aquifer system, the weighted-average thickness b'_{equiv} of these interbeds, recoverable vertical compressibility S'_{ske}, and the initial distribution of preconsolidation pressure $p'_{max}(z, 0)$ must be approximated from field data independently of any subsequent simulation process. Only values for vertical components of hydraulic conductivity K' and nonrecoverable compressibility S'_{skv} are adjusted by trial-and-error to fit calculated to observed compaction history. The estimated values for K' at the sites studied range from 1.7×10^{-7} to 3.8×10^{-6} m/day, those for S'_{skv} range from 4.6×10^{-4} to 4.3×10^{-3} m^{-1}, and those for S'_{ske} range from 7.2×10^{-6} to 5.2×10^{-5} m^{-1}. For established values of b'_{sum}, b'_{equiv}, and $p'_{max}(z,0)$, it is demonstrated that carefully evaluated values of K' and S'_{skv} can be used to predict aquifer-system behavior with reasonable accuracy over periods of several decades.

A major problem facing hydrologists is how to predict land subsidence. Developing a reliable method for evaluating aquitard parameters for modeling purposes is a key to solving this problem. A field method of aquitard parameter evaluation has advantages over laboratory methods. For example, parameters estimated from direct macroscopic field measurements represent mechanical properties of large-scale behavior in situ. By contrast, after laboratory consolidation data have been analyzed the vertical distribution in the field of mechanical properties of soil-specimen behavior must be estimated statistically.

If pumping rates at the center of a well field are measured or projected, then for a computational model of skeletal (matrix) behavior to be considered reliable it must accurately account for both transient radial fluid flow (and the corresponding cumulative radial displacement of the skeletal matrix) and transient vertical fluid flow (and the corresponding cumulative vertical displacement of the skeletal matrix). Alternatively, if water-level fluctuations in the coarse-grained part of a confined aquifer system are directly measured or projected, the conceptual and computational problems are greatly simplified. For this second alternative a one-dimensional model of vertical deformation of the matrix is both sufficient and reliable.

A one-dimensional model of vertical deformation has been developed (Helm, 1975, 1976) that essentially uses Terzaghi's theory of consolidation. Using the concept of preconsolidation pressure developed in soil mechanics allows nonrecoverable compaction of fine-grained beds to be distinguished numerically from recoverable compaction and expansion. Computation of vertical deformation patterns is thereby simplified.

Extensometers in the field (Riley, 1969) measure the vertical behavior of a total thickness interval. According to standard convention, it is assumed that the nonrecoverable component of observed compaction occurs within fine-grained deposits. Hence the term b'_{sum} will represent only the cumulative thickness of the fine-grained component of a total thickness interval. Because the depth intervals of interest are generally beneath the overlying semiconfining bed, the behavior of such a bed was not modeled. For simplicity of calculation, all deformation is assumed to occur within idealized doubly draining clay interbeds characterized by no-flow midplanes (aquitards).

For simulating field compaction the two parameters S'_{skv} and K' (nonrecoverable vertical specific storage and vertical hydraulic conductivity, respectively) are of critical importance. For macroscopic behavior S'_{skv} is intimately related to total thickness of fine-grained compacting beds b'_{sum} and to ultimate nonrecoverable compaction $\Delta b'_{ult}$ of the total thickness. In other words, S'_{skv} equals $\gamma_w(\Delta b'_{ult}/b'_{sum})/\Delta p'_{max}$ where γ_w is the unit weight of water. The use of $\Delta b'_{ult}$ implies that a specified increase in past maximum effective stress (preconsolidation pressure) $\Delta p'_{max}$ has progressed _in situ_ throughout b'_{sum} from one equilibrium distribution of p'_{max} to another.

Unfortunately, because values for K' of fine-grained interbeds are small and because water levels within adjacent coarse-grained material vary with time, $p'_{max}(z, t)$ seldom if ever reaches a new equilibrium distribution within thicker clay interbed members of a confined aquifer system. Correspondingly, observed compaction $\Delta b'_{sum}(t)$ is transient in the field and seldom reaches its theoretical ultimate value $\Delta b'_{ult}$ in response to boundary $\Delta p'_{max}$ observed in the coarse-grained material (aquifers).

The rate of observed compaction $d(\Delta b'_{sum})/dt$ is significant in evaluating K'. Rate of compaction depends essentially on three things: (1) the number N and thickness b'_i of individual fine-grained compacting beds, (2) the effective value K_i for each i-_th_ bed, and (3) the history of boundary stress values at all the 2N aquitard-aquifer interfaces. It is not possible in the field to measure $d(\Delta b'_i)/dt$ independently for each bed, nor thereby to estimate a distinct value of K_i for each i-_th_ bed. Because rate of compaction is observed in the field for a total aggregate of coarse- and fine-grained material, only a single K' value (or function) for cumulative observed behavior at a site can be approximated.

Helm (1975) tested the computational appropriateness and efficiency of using a weighted-average clay-bed thickness b'_{equiv} in simulating an observed rate of compaction of a series of 21 doubly draining clay interbeds within a single confined aquifer system near Pixley, California. Instead of calculating each $\Delta b'_i(t)$ and assuming an identical K' and S'_{skv} for each i-_th_ bed and then summing over i, $\Delta b'_{equiv}(t)$ was calculated and multiplied by a constant of proportionality N_{equiv}; this change in procedure reduced computation time by more than an order of magnitude. In other words, considerable computer time was saved, and observed $\Delta b'_{sum}(t)$ was as closely approximated by calculating $N_{equiv}\,\Delta b'_{equiv}(t)$ as it would have been by calculating $\sum_{i=1}^{N} \Delta b'_i(t)$ where near Pixley N_{equiv} equals 18 and N equals 21.

A third parameter of importance is a vertical recoverable specific storage parameter S'_{ske}. Its value can be estimated from field data only where vertical expansion is observed. Although $S'_{ske} << S'_{skv}$, Helm (1976) has shown that S'_{ske} noticeably affects stress/strain behavior in the field, not only when current effective stress $p'(z, t)$ is less than the past maximum effective stress, as expected, but also when $p'(z, t)$ equals $p'_{max}(z,t)$. In other words, the influence of S'_{ske} is not completely masked by S'_{skv} even when stresses reach preconsolidation levels.

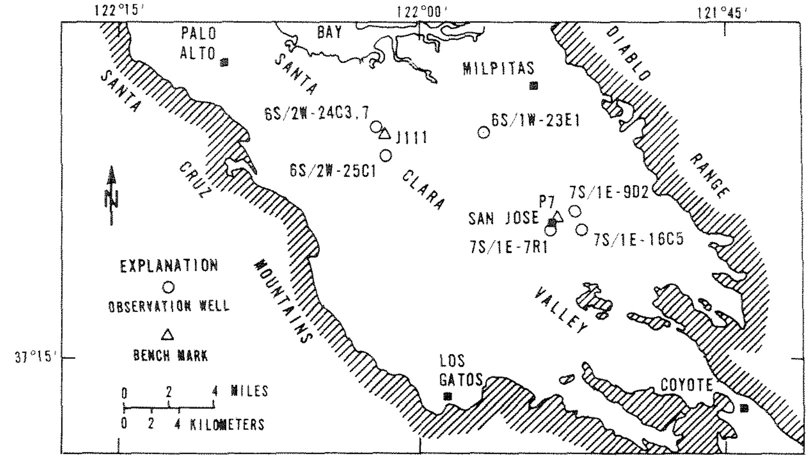

Figure 1.--Location of selected wells in Santa Clara Valley, California

Before the calculation process begins, it is necessary to estimate the initial value of $p'_{max}(z, t)$, at every nodal point within the model. The observed stress at which only net vertical expansion is actually measured *in situ* gives an indication of a preconsolidation pressure at the midplane of the thickest aquitard within the measured depth interval. This information, and measurement of stress history within coarse-grained material, allow one to estimate an initial distribution of preconsolidation pressure $p'_{max}(z, 0)$ within an idealized or model aquitard.

The procedure used by the author to evaluate system-behavior parameters from observed water-level fluctuations and compaction is to match calculated to observed compaction and expansion by trial-and-error adjustment of parameters. The model has been applied to field data from six sites in the Santa Clara Valley (fig. 1) and one site (Pixley) in the San Joaquin Valley, Calif. The location of the Pixley site is shown by Lofgren and Klausing (1969) and by Helm (1975). The model has also been applied to two additional sets of field data in the Santa Clara Valley where infrequently collected observations cover periods of 54 and 60 years.

Table 1 lists the values for b'_{sum}, b'_{equiv}, K', S'_{skv}, and S'_{ske} that were used to simulate observed compaction and expansion at selected sites (fig. 1). Table 1 also lists periods of record of field data at these sites. Wherever possible, the value for S'_{ske} was estimated directly from rebound field data. After values for b'_{sum}, b'_{equiv}, S'_{ske} and the initial distribution of p'_{max} had been approximated for a site, they were not changed. Only values for K' and S'_{skv} were adjusted in order to simulate observed compaction history as closely as possible. The history of transient effective stress at the idealized aquitard-aquifer interface is estimated directly from observed water-level fluctuation within the confined aquifer by a method developed by Lofgren (Lofgren and Klausing, 1969, p. B64-B68). Using boundary stress fluctuations, a thickness value, and constant parameter values in a manner described by Helm (1975), compaction values can be calculated for each site.

Figure 2 shows model results for a San Joaquin Valley site near Pixley, Calif., using parameters estimated by Riley (1969) (table 1). The solid line in figure 2A represents calculated compaction; the dotted line

TABLE 1.--VALUES OF PARAMETERS USED FOR SIMULATING OBSERVED COMPACTION AT SELECTED SITES IN SANTA CLARA AND SAN JOAQUIN VALLEYS, CALIFORNIA

SITE OF WATER-LEVEL DATA	PERIOD OF RECORD (YEARS)		ESTIMATED THICKNESS (METERS)		ESTIMATED VALUES OF PARAMETERS		
	WATER-LEVEL DATA	COMPACTION DATA	TOTAL b'_{sum}	WEIGHTED AVERAGE b'_{equiv}	K' $\frac{METER}{DAY} \times 10^{-6}$	S'_{skv} $\frac{1}{METER} \times 10^{-4}$	S'_{ske} $\frac{1}{METER} \times 10^{-6}$
SANTA CLARA VALLEY							
6S/1W-23E1	1958-72	1958-72	57.6	4.6	0.36	4.6	24.6
6S/2W-24C3	1960-72	1960-72	77.7	5.5	0.17	43.0	13.0
6S/2W-24C7	1960-72	1960-72	128.6	16.2	3.8	11.0	8.5
6S/2W-25C1	1960-72	1960-72	77.7	5.5	0.23	10.7	52.0
6S/2W-25C1	1921-74	1932-74	77.7	5.5	0.22	10.8	--
7S/1E-7R1	1915-74	1916-74	145.4	5.5	0.57	7.38	--
7S/1E-9D2	1958-72	1960-63, 1965-72	78.6	5.5	0.25	20.0	26.0
7S/1E-16C5	1958-72	1960-72	145.4	5.5	1.0	7.55	7.2
SAN JOAQUIN VALLEY							
23S/25E-16N3	1952-71	1959-71	84.7	4.9	2.5	7.55	15.0

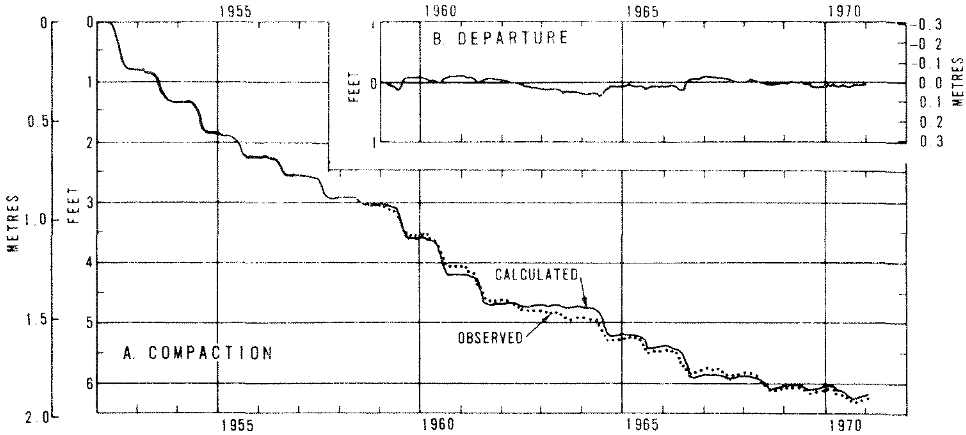

Figure 2.---Simulation of compaction based on water-level data for well 23S/25E-16N3 (1952-71) and on the difference in compaction observed in wells -16N3 and -16N1. (From Helm, 1975, Figure 8.)

represents observed compaction. Figure 2B shows the difference between calculated and observed compaction from 1959 to 1971. Transient boundary effective stress values were plotted and discussed by Riley (1969) and Helm (1975, 1976) and are not repeated here.

Figures 3 through 10 show simulation results for sites in Santa Clara Valley (fig. 1) using parameter values listed in table 1. As mentioned earlier, measured and continuously changing depth-to-water values are used at each site in order to estimate transient boundary effective stress values

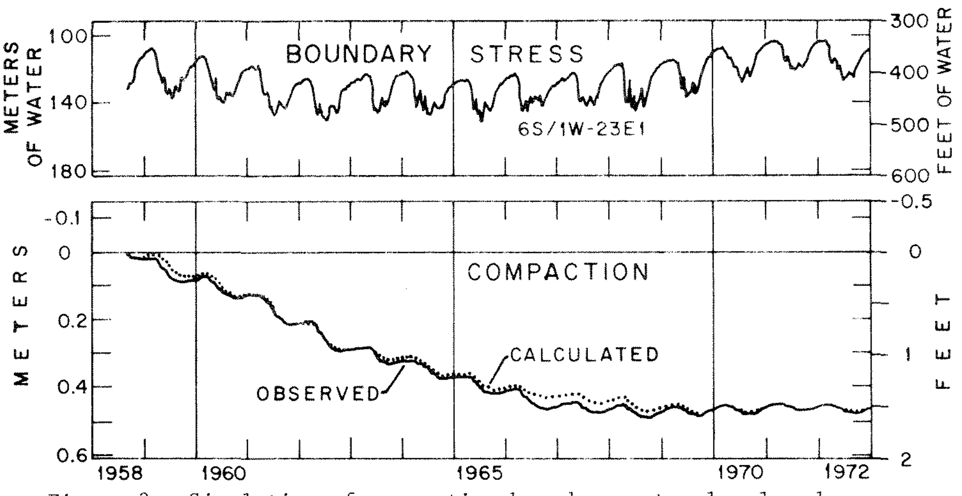

Figure 3.--Simulation of compaction based on water-level and compaction data for well 6S/1W-23E1 (1958-72).

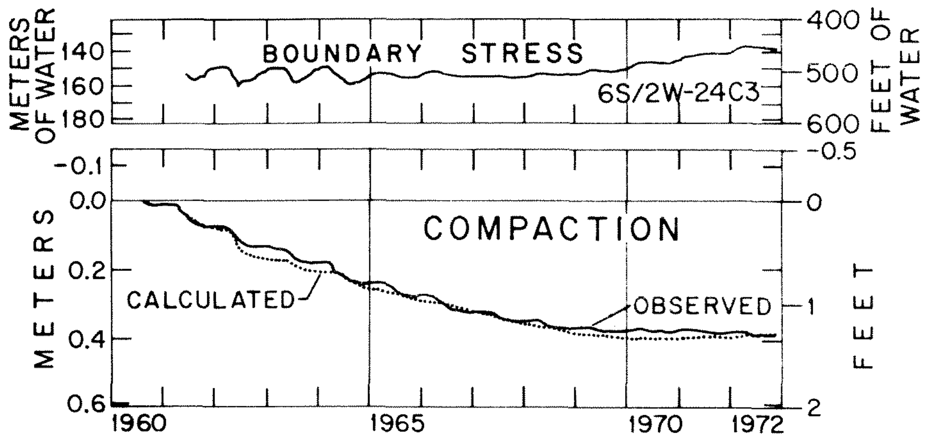

Figure 4.--Simulation of compaction based on water-level and compaction data for well 6S/2W-24C3 (1960-72).

at the top of figures 3 through 10 that are needed for calculating compaction. Observed compaction in figures 2 and 5 represent compaction of a lower depth interval at two sites. Hence a difference in observed compaction in two wells at each site is used in figures 2 and 5. Calculated compaction does not differ greatly from observed compaction at any site (figs. 3-10). Estimated values for K' in the Santa Clara Valley range from 1.7×10^{-7} to 3.8×10^{-6} m/day; estimated values for S'_{skv} range from 4.6×10^{-4} to 4.3×10^{-3} m^{-1}; and estimated values for S'_{ske} range from 7.2×10^{-6} to 5.2×10^{-5} m^{-1}.

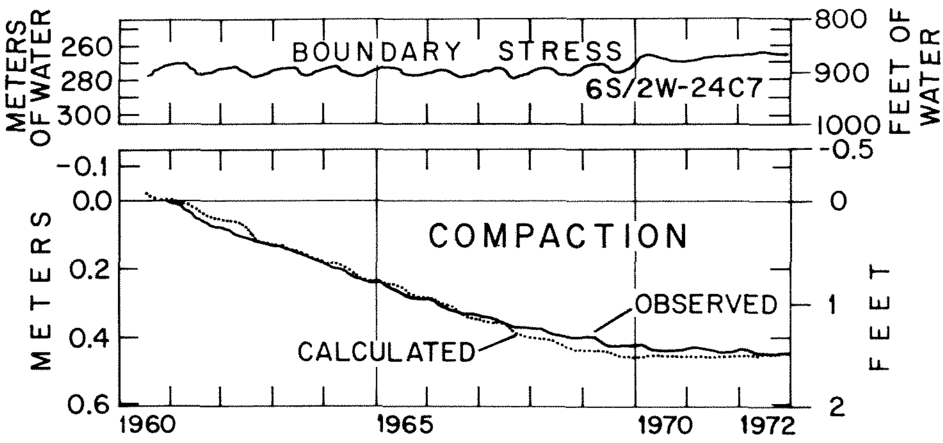

Figure 5.--Simulation of compaction based on water-level data for well 6S/2W-24C7 (1960-72) and on the difference in compaction observed in wells -24C7 and -24C3.

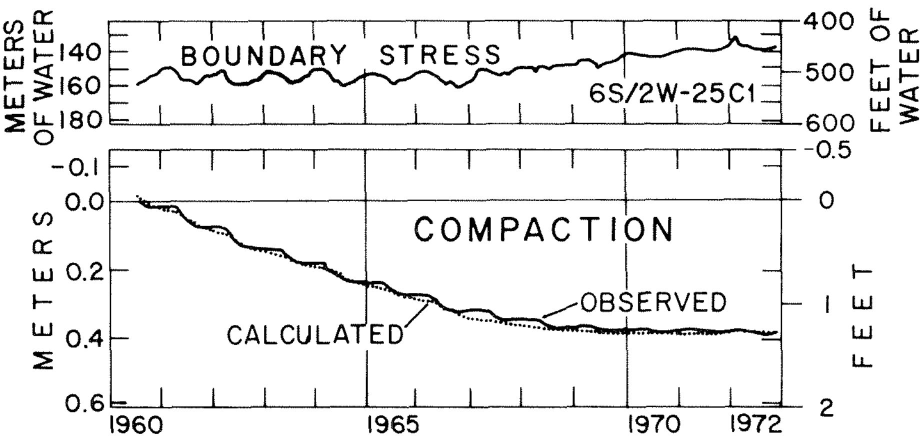

Figure 6.--Simulation of compaction based on water-level data for well 6S/2W-25C1 (1960-72) and compaction data observed in well -24C3.

It is instructive to discuss nonuniqueness of estimated parameter values and thereby the degree of confidence in selecting a single set of parameter values (or functions) as a predictive tool. If at any site (fig. 1) the value for either total compacting aquitard thickness b'_{sum} or equivalent aquitard thickness b'_{equiv} were changed, from the value listed in table 1, different values of S'_{skv} and K' would also have to be found in order for calculated compaction to fit observed compaction accurately. This interdependence is evident because for known compaction history and predetermined bed-thicknesses, S'_{skv} is related inversely to b'_{sum} and K' is

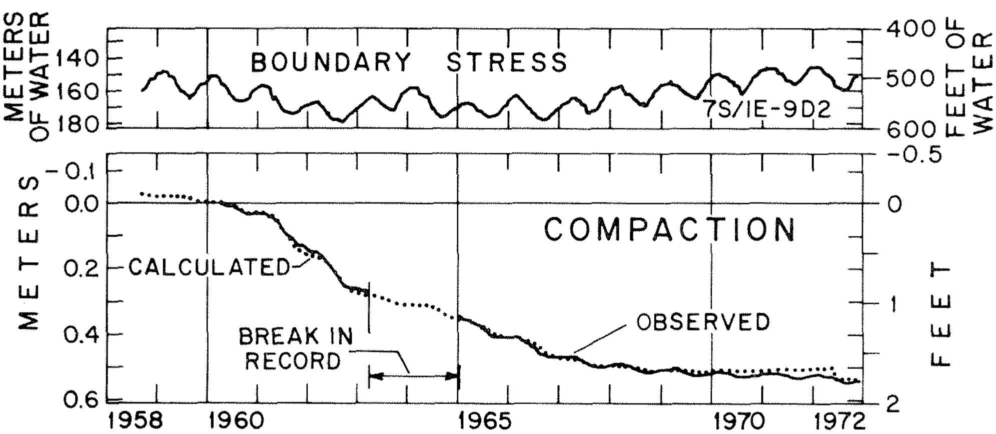

Figure 7.--Simulation of compaction based on water-level data (1958-72) and compaction data (1960-72) for well 7S/1E-9D2.

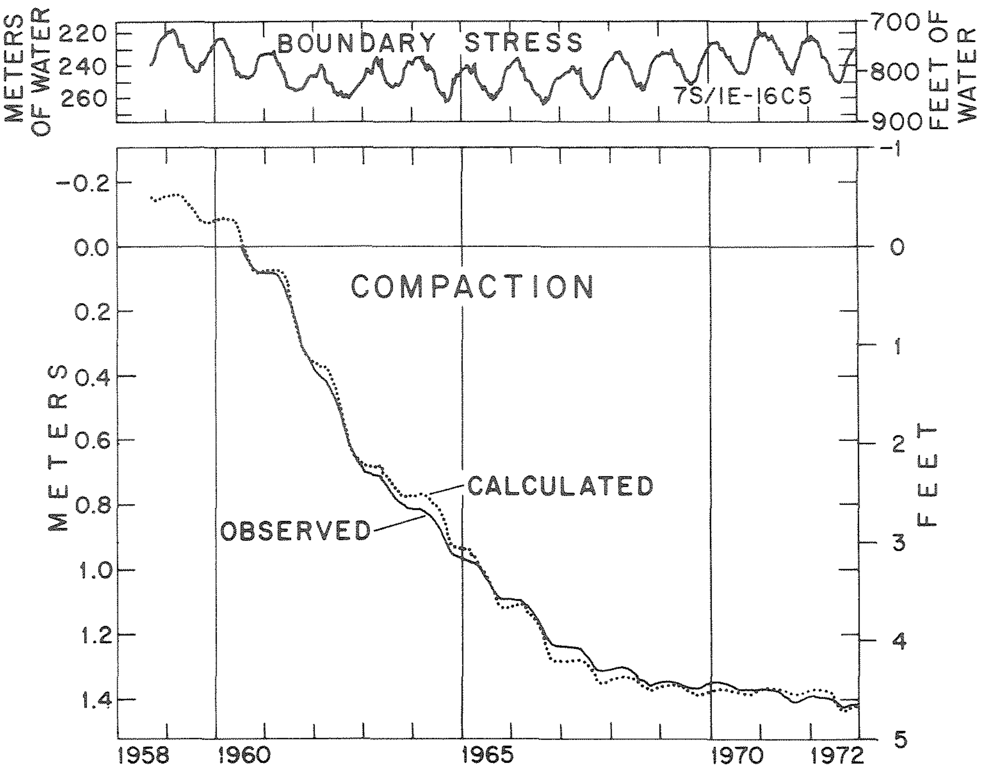

Figure 8.--Simulation of compaction based on water-level data for well 7S/1E-16C5 (1958-72) and on compaction data observed in wells -16C6 and -16C11.

related approximately to b'_{equiv}. Therefore, values of b'_{sum} and b'_{equiv} must be estimated unambiguously by geophysical or other field measurement and statistical methods. In the Santa Clara Valley such estimates have been made (J. F. Poland, written commun., 1973-76) for depth intervals of interest from the best available geophysical data.

A second problem of nonuniqueness is the initial distribution of $p'_{max}(z, t)$. This distribution in effect implies an assumed average degree of consolidation U of fine-grained material in the field at the beginning of simulation. This initial preconsolidation stress condition affects all subsequent computations of compaction and hence affects the estimated values of K' and S'_{skv} that are needed to duplicate observed compaction. Changing $p'_{max}(z, 0)$ for any subsequent computer run will require searching anew for appropriate model values of K' and S'_{skv}.

A third more subtle problem of nonuniqueness will be discussed here in some detail (fig. 11). Using any set of values for K' and S'_{skv} on the dashed line in figure 11 (or on extensions of the dashed line) within the computational model will give the correct net compaction at 6S/1W-23E1 (fig. 3) between the two dates March 1959 and December 1972. However, the calculated rate of compaction between these two dates also varies according

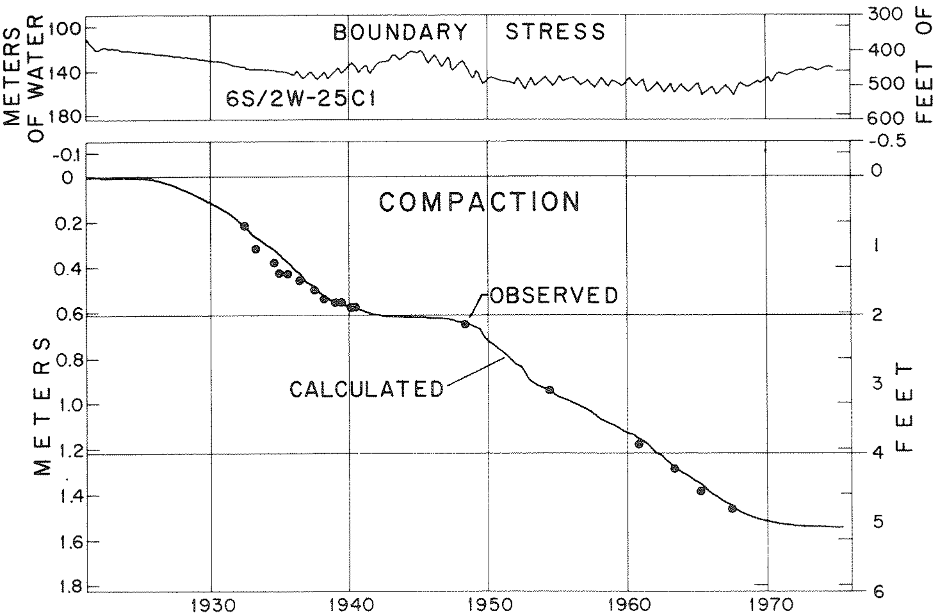

Figure 9.--Simulation of compaction based on water-level data for well 6S/2W-25C1 (1921-74) and on compaction estimated as a portion of subsidence measured at bench mark J111.

to choice of parameter values. In contrast, using any set of K' and S'_{skv} values on the solid line in figure 11 gives the correct net compaction between the two dates March 1959 and December 1963. Similarly, using parameter values on the dotted line will duplicate net observed compaction between the two dates March 1959 and December 1966. To simulate observed compaction closely throughout the entire 1959-72 period, however, the choice of appropriate parameter values becomes more limited, namely near the area where these three zero error lines (dashed, solid, and dotted) tend to converge or cross. Solid circles in figure 11 represent some of the parameter values for which computer runs have been made. Each set of three values in parentheses is associated with parameter values at each solid circle. For each of the three indicated time periods a corresponding value in parentheses gives the departure of calculated compaction from observed compaction in percent of net observed compaction (namely, in percent of 0.45 m compaction observed between March 1959 and December 1972). For example: using parameter values for 6S/1W-23E1 (table 1), figure 11 indicates that the calculated compaction (fig. 3) between March 1959 and December 1963 is 2 percent less than the above-mentioned observed compaction, is 6 percent less between March 1959 and December 1966, and is 0.07 percent less between March 1959 and December 1972. In order to estimate parameter values from field data with sufficient confidence to make the method a predictive tool it is essential to know, to calculate, and to reproduce accurately the rate of compaction as well as the net observed compaction between two specified dates.

Regarding the problem of model calibration, if for example one uses measurements of March 1959 and December 1963 alone to estimate parameter values, the solid line in figure 11 (and its extension) can be considered a zero-error calibration line. The choice of (3.4×10^{-7} m/day, $5.6 \times 10^{-4} m^{-1}$) or ($6 \times 10^{-7}$ m/day, 3.3 m^{-1}) for (K', S'_{skv}) would be as appropriate for such a calibration as using values given in table 1 for 6S/1W-23E1 and

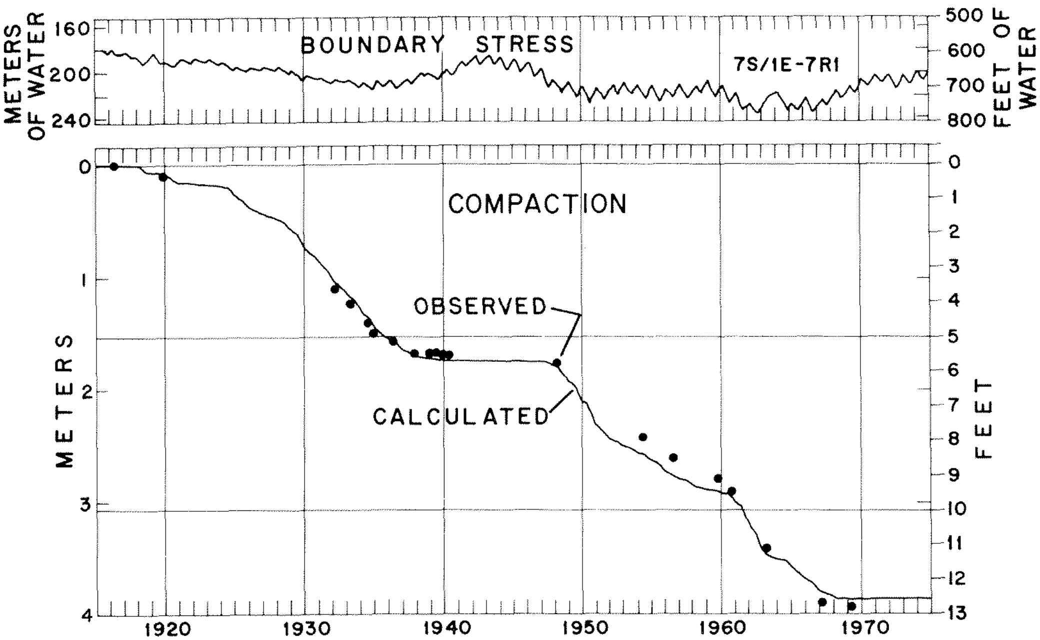

Figure 10.--Simulation of compaction based on water-level data for well 7S/1E-7R1 (1915-74) and on subsidence measured at bench mark P7.

discussed in the previous paragraph. However, according to figure 11, predicting observed behavior at this site through 1972 would be in error (5 percent too much in the one case and 13 percent too little in the other case). Simulation error for the 1959-72 period is even greater for parameter values lying on extensions of the solid line in figure 11.

The final question to be addressed in the present paper is whether constant values of K' and S'_{skv} can be used to predict compaction at a site over an extended period of time. Attention is called to figure 6 where compaction at site 6S/2W-25C1 is computed (dotted line) using daily values of water-level data (transformed into boundary stress in figure 6) from 1960 through 1972, and also to figure 9 where compaction is computed (solid line) using periodic water-level measurements at the same site (collected into the boundary stress line in figure 9) from 1921 through 1974. Each solid circle in figure 9 represents a compaction value on a particular day which has been estimated from first-order leveling from a stable datum to nearby bench mark J111 at land surface. The solid line (and its extension in either direction) in figure 12A shows what values of K' and S'_{skv} are needed to compute net observed compaction correctly between two specific dates, spring 1932 and spring 1939. The dashed line in figure 12A similarly shows appropriate parameter values for accurately simulating net observed compaction between the two dates spring 1932 and spring 1967. The upper left solid circle in figure 12A indicates parameter values (table 1) which were used for calculating compaction (solid line) in figure 9. The numbers in parentheses in figure 12A indicate that by using 2.2×10^{-7} m/day for K' and 10.8×10^{-4} m^{-1} for S'_{skv} the net calculated compaction between Spring 1932 and spring 1939 is 2 percent larger and between spring 1932 and spring 1967 is 0.8 percent larger than net observed compaction of 1.2 m between spring 1932 and spring 1967. The numbers in parentheses near the lower right solid circle indicate

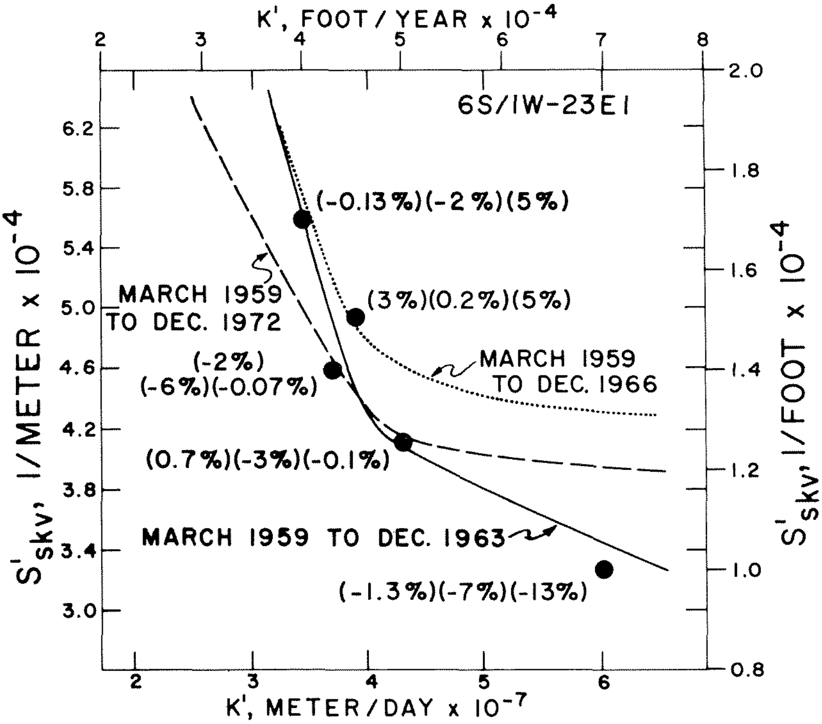

Figure 11.--Zero-error curves for simulation at well 6S/1W-23E1.

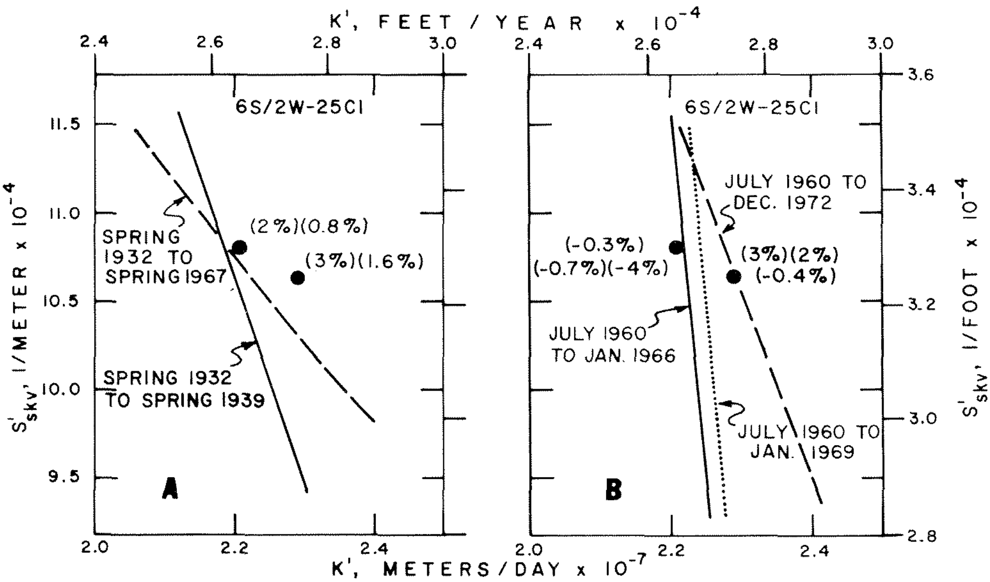

Figure 12.--Zero-error curves for simulation at well 6S/2W-25C1.

that by using 2.3 x 10^{-7} m/day for K' and 10.7 x 10^{-4} m^{-1} for S'_{skv} the net calculated compaction between spring 1932 and spring 1939 is 3 percent larger and between spring 1932 and spring 1967 is 1.6 percent larger than the aforementioned net observed compaction. These latter parameter values were used (table 1) for computing compaction at 6S/2W-25C1 from 1960 to 1972 (fig. 6). Hence the use of the 1960-to-1972-based parameters to duplicate compaction for several decades leads to very small error.

Figure 12B is also a plot of zero-error curves for site 6S/2W-25C1 between specified dates. Figure 12B is related to figure 6 as figures 11 and 12A are related to figures 3 and 9. Considering the difficulties of model calibration discussed earlier and the sparseness of stress and compaction data at 6S/2W-25C1 prior to 1960, examination of figures 12A and 12B suggests that carefully evaluated values of K' and S'_{skv} can be used to predict both rate of compaction and total compaction with reasonable accuracy over periods of several decades.

References

Helm, D. C., 1975, One-dimensional simulation of aquifer-system compaction near Pixley, California. 1, Constant parameters: Water Resources Research, v. 11, no. 3. p. 465-478.

______1976, One-dimensional simulation of aquifer-system compaction near Pixley, California. 2, Stress-dependent parameters: Water Resources Research v. 12, no. 3, p. 375-391.

Lofgren, B. E., and Klausing, R. L., 1969, Land subsidence due to ground-water withdrawal, Tulare-Wasco area, California: U.S. Geol. Survey Prof. Paper 437-B. 103 p.

Riley, F. S., 1969, Analysis of borehole extensometer data from central California, in Tison, L. J., ed., Land Subsidence, v. 2: Internat. Assoc. Sci. Hydrology, Pub. 89, p. 423-431.

Publication n°121 of the International Association of Hydrological Sciences
Proceedings of the Anaheim Symposium, December 1976

COMPACTION PROCESSES AND MATHEMATICAL MODELS OF LAND SUBSIDENCE IN GEOTHERMAL AREAS

E. John Finnemore and Mary L. Gillam*
Systems Control, Inc.
Palo Alto, California

Abstract

Several occurrences of geothermal subsidence, up to 4.7 m, indicate the need for a better understanding of compaction processes in hydrothermal reservoirs and for improved modeling capabilities.

Three processes are thought to cause compaction in hydrothermal reservoirs. Intergranular pore compaction is considered to be the major compaction process in hydrothermal areas, as in hydrocarbon and groundwater areas, but many of the contributing factors differ. The most important differences may reflect temperature effects, fluid phase relationships, and a wider variety of reservoir materials with more variable deformation properties. Fracture closing may be significant in cemented rock. Thermal contraction is minor.

A summary of twenty-two subsidence models of different types compares their characteristics, capabilities, and site applications. These models are of various complexities and incorporate different constitutive relations for simulating material deformations. Only three simulate temperature changes, indicating the early stage of geothermal subsidence model development. No model has yet been verified by application to geothermal areas. Continuing development is under way, using various approaches. Unique hydrothermal features should be incorporated wherever possible. Further work is particularly needed to increase our knowledge of in-situ material deformation behavior, and so make possible its improved simulation.

Introduction

Among geofluids whose extraction may cause land subsidence, geothermal fluids have received relatively little attention due to the recency of geothermal development. However, the occurrence of subsidence at several geothermal fields indicates the need for concern.

This paper surveys two aspects of geothermal subsidence research: compaction processes and their simulation with mathematical models. The information presented here is summarized from a longer report (Atherton and others, 1976), to which the reader is referred for more detail and for additional reference citations. That report also includes extensive discussions of simplified subsidence models, potential environmental effects of geothermal subsidence, subsidence prediction methods, and sensitivity analysis of subsidence models.

Only a few geothermal fields are known to have subsided as a result of fluid production. However, the magnitude of the ground deformations may be significant, as indicated by the behavior of three liquid-dominated fields in New Zealand (Stilwell and others, 1975). Wairakei, the earliest and most extensively developed, has experienced maximum ground motions of 4.7 m vertically and 0.8 m horizontally from 1956 to 1974. The other fields, Broadlands and Kawerau, have subsided much less. At The Geysers vapor-dominated field in California, a few centimeters of subsidence, attributed in part to steam production, occurred from 1972 to 1974 (Lofgren, oral communication, 1976).

*M. L. Gillam is now with Woodward-Clyde Consultants, San Francisco, Calif.

On the basis of these preliminary indications and the behavior of other geofluid reservoirs, researchers have attained a general consensus on the potential for fluid-withdrawal subsidence in different types of geothermal areas. The anticipated amounts of subsidence vary, but are quite large for certain types of hydrothermal systems.

At vapor-dominated fields, fluid withdrawal is expected to cause at most a slight amount of subsidence because of the vapor state of the fluids and the relatively well indurated reservoir rock (White, 1973; Lofgren, 1973).

At liquid-dominated systems near hydrostatic fluid pressure, subsidence is considered a definite hazard unless injection is practiced to prevent widespread reductions in fluid pressure. White (1973) considers subsidence particularly likely where these reservoirs consist in part of clay, silt, or shale which may de-water into adjacent sands. Lofgren (1973) considers subsidence in the Imperial Valley a definite risk unless adequate precautions are taken.

Subsidence over geopressured systems in Texas and Louisiana may be severe. The reservoir sands in these areas are well cemented, but significant drainage is expected from undercompacted shales. Subsidence predictions of 5-7 m and 0.3 m to more than 10 m have been made (Papadopulos and others, 1975; Kreitler and Gustavson, 1976).

Subsidence predictions such as these are not exact, but provide a broad indication of risk. Only experience will show how certain types of geothermal fields respond to changes in effective stress. However, the considerable threat of subsidence in some areas demonstrates the need for research on subsidence processes and prediction procedures at this early stage of geothermal development.

Compaction Processes in Geothermal Areas

Previous experimental work and continuing investigations of geothermal areas provide a basis for conjecture about potential differences in the behavior of geothermal and other fluid resource fields.

Three kinds of induced ground movements may occur in geothermal areas (Lofgren, 1973): subsidence or rebound of the land surface due to fluid pressure changes; horizontal movements caused by induced fluid pressure gradients; and vertical movements attributed to thermal expansion or contraction of the reservoir rock. Fluid pressure controls two compaction processes: loss of intergranular pore space and fracture closing. These processes and thermal contraction are discussed below, with emphasis on their nature and potential severity in geothermal areas.

A fourth process, natural tectonic deformation, may cause substantial ground movements in many geothermal areas because of their common location in tectonically active zones. Movements of a few millimeters or centimeters per year are now occurring at the four Americal geothermal sites--Imperial Valley, Raft River, Geysers, and Long Valley--for which repeat levelling data are available (Lofgren, 1974, 1975). Such movements must be differentiated from the impacts of geothermal resource development.

Intergranular Pore Compaction

The loss of intergranular pore space, resulting from increased effective stress, is widely believed to be the major subsidence process in all areas of fluid extraction. Most subsidence models simulate only this process.

Bulk compaction is the result of several processes acting on a grain-to-grain scale. The amount of compaction is a function of many properties of the reservoir and overburden, in addition to the change in fluid pressure.

The processes causing compaction vary in relative importance with pressure and other factors, but may be summarized as follows (Atherton and others, 1976). Clays compact primarily by the development of preferred particle orientation, elastic distortion of single particles and flocs, destruction of flocs, and removal of chemically bound water. Sands compact by grain rearrangement, elastic distortion, grain fracturing, plastic deformation, and grain solution at contact points. At the greater depths and temperatures encountered in geothermal systems, sands may account for a greater proportion of total compaction than in shallower groundwater aquifers. Plastic deformation and grain solution are expected to be relatively more important.

The severity and extent of subsidence at geothermal areas may be influenced by several characteristics of geothermal systems, including high temperature, fluid phase relationships, different reservoir materials, restricted natural recharge, and relatively impermeable reservoir boundaries.

<u>Temperature</u> - Although the temperature encountered in deep oil wells may approach 200°C, such temperatures are found in geothermal areas at much shallower depths. The average reservoir temperature at producing geothermal fields ranges from 170° to 250°C and exceeds 300°C at the Salton Sea field. Such high temperatures promote compaction by decreasing grain strength, increasing mineral solubility, and decreasing the length of time required for rock to readjust to changes in effective stress (Maxwell, 1960). Deformation properties also vary slightly with temperature changes induced by production and injection.

<u>Fluid phase relationships</u> - The proportions of water, oil, and gas in hydrocarbon fields are affected only by differential mobilization and by variations in the mutual solubility of oil and gas (Finol and Farouq Ali, 1975). However, geothermal fields undergo a natural thermodynamic evolution, marked by a progressive phase change from water to steam, which is accelerated by production. The initial phase of geothermal fluids and the occurrence of flashing (boiling) affect compaction in several ways. Most obvious are the smaller buoyant support and decreased lubricating power of steam. Flashing also buffers the loss of fluid pressure in two-phase geothermal systems. For equivalent enthalpy production, the pressure decline is fastest in all-liquid reservoirs, intermediate in steam reservoirs, and slowest in two-phase reservoirs.

The change in fluid pressure during the lifetime of a geothermal field depends on initial reservoir conditions, management practices, and the enthalpy input requirements of the utilization system. Potential changes in pressure are 25 kg/cm^2 for vapor-dominated systems near 240°C; 100-200 kg/cm^2 for liquid-dominated systems from 150-300°C, assuming average reservoir depth of 2 km and complete flashing; and 240-420 kg/cm^2 for geopressured systems near 140-185°C, using the production scheme of Papadopulos and others (1975). These values compare with the following changes in fluid pressure at subsiding areas: 7-14 kg/cm^2 in groundwater aquifers and 140-280 kg/cm^2 in hydrocarbon reservoirs (Poland and Davis, 1969).

<u>Different reservoir materials</u> - Subsiding groundwater, oil, and gas areas are located in unconsolidated silt, sand, and clay sequences deposited in alluvial fan, lacustrine, deltaic, or shallow marine environments. Geothermal resources, however, may occur in a much wider variety of geologic settings. Some hydrothermal areas contain unconslidated sands (for example, some strata in the Imperial Valley). Others contain sandstone (The Geysers) and interlayered volcanic flows, tuffs, and tuffaceous sediments (Long Valley and Valles Caldera). These materials may have very different deformation properties from unconsolidated epiclastic sediments. Hydrothermal alteration and cementation are likely to have indurated the reservoir rock or reservoir margins in irregular patterns governed by

temperature and permeability variations. The highly angular rock fragments which form tuffs are particularly susceptible to mechanical fracturing. In general, geothermal areas are quite variable lithologically and it is likely to be impossible to generalize behavior from one site to another.

Natural recharge - In geothermal areas, rates and patterns of natural recharge can be expected to vary greatly. However, recharge must be low in vapor-dominated systems, which are underpressured and otherwise would fill with water. Recharge may be localized or slow in self-sealing systems, in which silica is deposited at the cooler reservoir margins and top.

Reservoir boundaries - The small areal extent of most geothermal reservoirs (typically less than 100 km^2) and the relative permeability of faulted or hydrothermally cemented reservoir boundaries may restrict subsidence to a small area.

Seismic activity - Earthquake shaking, common in geothermal areas because of their genetic relationship to tectonically active crustal zones, promotes adjustment to changed effective stress by facilitating grain rearrangement. This effect has been documented at Wilmington oil field (Poland and Davis, 1969).

Fracture Closing

The full or partial collapse of fluid-filled fractures, in response to changed effective stress, may be a significant process of compaction in geofluid reservoirs. The extent of fracture closing depends on total fracture volume; shape and orientation of individual fractures; change in fluid pressure; and deformation properties of the reservoir rock. Most geothermal reservoirs have high fracture porosity due primarily to tectonic stresses, but also perhaps due in part to heat waves associated with magmatic intrusion and sudden increases in fluid pressure associated with seismic shock waves.

At the present time, the only means for evaluating the net change in reservoir thickness which may result from fracture closing is by testing samples of the reservoir rock. Unfortunately, few such studies have been performed. Using the axial fracture strain measured by Batzle and Simmons (1976) for cemented rock from the Raft River and Salton Sea geothermal areas, thickness changes were computed for a variety of conditions (Atherton and others, 1976). For a geothermal reservoir 1 km thick, experiencing a uniform change in fluid pressure of 50 kg/cm^2, the maximum predicted strain due to microfracture closing is 1.6 cm. Although small, this value is a minimum because it does not reflect the behavior of numerous larger fractures. Fractures closing may have an appreciable impact if larger fractures contribute significantly to the total deformation.

Experiments show that fracture porosity is more compressible than intergranular porosity (Batzle and Simmons, 1976). Thus, ideally the two processes should be treated separately in mathematical models.

Thermal Contraction

The contribution of thermal contraction to total subsidence at geothermal areas is minor because of the small value of thermal expansion coefficients (typically one part in 10^5 or 10^6) and small changes in average reservoir temperature which result from production. For example, the average temperature at The Geysers declined only 3-6°C from 1970 to 1976 (D. McMurdie, oral communication, 1976), while at Wairakei the change was 10°C from 1957 to 1969 (Bolton, 1970).

Order of magnitude calculations, using an average thermal expansion coefficient for sandstone, indicate that uniformly cooling a geothermal reservoir 1 km thick by 20°C would produce 20 cm of shortening. However, such widespread cooling is unlikely. Cooling may be locally more extreme near injection wells.

Geothermal Subsidence Models

Mathematical models attempt to simulate subsidence processes so that the impacts of fluid extraction may be predicted. In addition, models may be used to clarify the nature and behavior of a producing field, investigate schemes for subsidence mitigation, identify most crucial data needs, or extrapolate to unknown conditions. Several agencies now require subsidence susceptibility appraisals prior to drilling.

Alternatives to models for predicting land subsidence fall into two major categories. Other analysis methods use compaction coefficients, core compression tests, and stress calculations. Analogy methods make comparisons with other subsidence sites and base estimates on the similarities found. Ideally, both methods should be used for a given site, in an interactive and dynamic manner as additional information is obtained. The capability of analogy methods to provide some accounting for unique features which are hard to analyze, such as tectonic and seismic activity in geothermal areas, is particularly important.

Differing levels of physical complexity and different numerical solution procedures have been combined to produce a large variety of subsidence models. For the physically complicated models, problems of data availability and computational tractability arise. Models of different complexity should be used in a hierarchical fashion, employing more advanced models only when their need has been demonstrated by less advanced ones.

Simplified subsidence models, not dependent upon large computers, complement advanced models in important ways. Their necessary simplicity facilitates understanding of the subsidence process by non-experts, and their independence from large computer programs provides inexpensive means for making first estimates of subsidence. Furthermore, the limited data which they require is much more likely to be available.

The simplest compaction model, illustrating the fundamentals of compaction, computes compaction from the product of the reservoir thickness, the reduction in pore fluid pressure, and a compaction coefficient. The compaction coefficient must be determined from compression tests on cores or from prior subsidence. In the former case this simple model does not account for the response of the overburden, and hence the ground surface, to reservoir compaction. In the latter case major errors may result if significantly different time delays in the aquifer and the overburden are represented in the observed subsidence. This model is also limited to ultimate, one-dimensional movements, and does not compute reductions in pore pressure.

A generally applicable, computerized geothermal subsidence model must be very complex to account for all of the significant physical processes and quantities. Such a model must be capable of solving for the unsteady flow of heat and fluid through a deformable porous medium in up to three dimensions. The heat may flow by conduction and convection. The fluid may exist in any or all of the fully saturated, partially saturated, and vapor conditions; the addition of two-phase flow capability will at least double a model's complexity. Various laws may be prescribed to govern the porous media deformations, but laws valid at one scale of observation may not be valid at another. The media properties may vary with position, direction, temperature, and time.

An advanced geothermal subsidence model must combine four or five component models. First, a wellbore model is needed to predict downhole pressures from the usually controlling wellhead conditions. Next, interactive reservoir flow and material deformation models are required to compute the time-varying pressure distributions and resulting compaction. These models must be interactive because compaction affects flow via reservoir permeability. A deformation model for clays in hydraulic communication with the reservoir must compute the greater but much delayed compactions which occur in these materials. Finally, an overburden deformation model is required to simulate the transmission of strain from the reservoir to the surface. The overburden can usually be treated as elastic because it will experience mainly tension. However, clays and the reservoir itself must be modeled inelastically to provide irreversibility.

Many intermediate levels of models lie between the extremes discussed above, depending for example upon the number of dimensions and fluid phases to be simulated, the material stress-strain relationships, and the data needs and use costs.

Basic information on seven simplified and fifteen advanced subsidence models is given in Table 1. Models of all types are included because isothermal models have provided, and will continue to provide, a basis for the development of more complex geothermal models.

The first subsidence models were developed in the 1950's. In the 1970's, the increased availability of large computers and greater concern for our environment encouraged the development of advanced, computerized models. The less complex and more widely applicable oilfield and groundwater subsidence models were developed first; subsidence models not listed are known to have been developed by oil companies. Advanced goethermal subsidence models, with their added ability to simulate temperature effects and in some cases two fluid phases, were first reported in 1975. By late 1976, five groups in industry and the universities had such models in various stages of development. A user's manual is available only for FLOWCP.

Underground stress changes are determined in most of the tabulated models by fluid flow simulators. Models that do not incorporate fluid flow therefore require the stress changes to be prescribed input. While the latter approach has certain advantages, it also makes such models much more difficult to use with future production schemes, particularly if flow/deformation interaction is significant.

The all-important constitutive (stress/strain) relations, which govern material deformations, have been handled in a number of ways. Many of the oilfield and earlier models employed elastic and poro-elastic deformation, which yield complete rebound upon stress recovery, obviously incorrect for most cases of significant subsidence. Several of the groundwater subsidence models are based on either Terzaghi's theory of vertical consolidation or simple vertical compressibility. Being limited to one dimension, these methods are unable to simulate the lateral ground movements which have frequently accompanied land subsidence (up to 3.6 m at Wilmington, 0.8 m at Wairakei). Deformation irreversibility was provided in a number of these models by incorporating two different compressibility values for each material, one for virgin compaction (preconsolidation) and another, about one-tenth as large, for expansion (rebound) and recompression. This two-compressibility approach is meaningful only for one-dimensional deformation. Kosloff and Scott at the California Institute of Technology recently incorporated into their model the strain-hardening plastic behavior of soils, with multi-dimensional deformation, by basing their constitutive relations upon the plastic cap model of DiMaggio and Sandler (1971). However, this improvement increased computation time five-fold. Few models employ stress and strain tensors and material moduli. AGRESS, developed for geothermal applications, does, and therefore is able to handle non-linear pore collapse mechanisms and elastic-plastic

Table 1. Summary of Subsidence Models for Pore Fluid Withdrawal

Developers (date)	Subsidence Type	Fluid Phases	Dimensions Flow	Dimensions Deform.	Numer. Method Flow	Numer. Method Deform.	Computer Model?	Model Name	Constitutive Relations	Applications Sites	Applications Verified?
McCann & Wilts (1951)	Oilfield	None	-	3	-	N/A	No	-	Elastic	Wilmington	No
Geertsma (1957, 1966)	Oil or Gas	None	-	2-3	-	N/A	No	-	Poro-elastic	None	No
Gambolati (1972a)	Oil or Water	Liquid	-	3	N/A	N/A	No	-	Poro-elastic	None	No
Geertsma & van Opstal (1973)	Oil or Gas	None	-	2-3	-	F.Elem.	Yes	ASKA	Elastic	None	No
	Oil or Gas	None	-	2-3	-	N/A	No	-	Elastic	Groningen	No
Frazier (in Riney, 1973) & Archambeau (1974)	Oilfield	Liquid	2	2	F.Elem.	F.Elem.	Yes	FRI	Elastic	Wilmington	Yes
Finol & Farouq Ali (1975)	Oilfield	Oil & Gas	2	1	F.Diff.	F.Diff.	Yes	-	Poro-elastic*	Venezuela	(Yes)
de Ferrer & Farouq Ali (1975)	Oilfield	Oil & Water	2	1	F.Diff.	F.Diff.	Yes	-	Poro-elastic*	None	No
Kosloff & Scott	Oilfield	None	-	2-3	-	F.Elem.	Yes	PANDORA	Plastic Cap Model	Wilmington	Yes
Sandhu & Wilson (1970)	Isothermal	Liquid	2	2	F.Elem.	F.Elem.	Yes	FLOWCP	Elastic	None	No
Sandhu & Liu (1976)	Isothermal	Liquid	2	2	F.Elem.	F.Elem.	Yes	VISCON	Viscoelastic	None	No
Jacquin & Poulet (1970)	Natural G.W.	Liquid	2	1	N/A	N/A	Yes	-	Porosity/depth	None	No
Mitchell (1976)	Permafrost	Thaw	-	2	-	F.Elem.	Yes	-	Poro-elastic	Prudhoe Bay	(Yes)
Gambolati (1972b)	Groundwater	None	-	1	-	N/A	No	-	Compressibility	Venice, Italy	No
Gambolati and others (1973, 1974)	Groundwater	Liquid	2	1	F.Elem.	F.Diff.	Yes	-	Compressibility*	Venice, Italy	No
Helm (1975, 1976)	Groundwater	Liquid	(1)	1	F.Diff.	F.Diff.	Yes	COMPAC	Terzaghi*	California	Yes
Narasimhan (1975)	Groundwater	Liquid	2-3	1	Integrated F.D.		Yes	TRUST	Terzaghi*	Pixley	Yes
Safai & Pinder	Groundwater	Liquid	2	2	F.Elem.	F.Elem.	Yes	-	Viscoelastic	None	No
Papadopulos (1975)	Geopressured (Isothermal)	Liquid	2	1	N/A	N/A	No	-	Elastic sand, plastic clay	Hidalgo County, Texas	No
Brownell, Garg & Pritchett (1975)	Geothermal	Two	2-3	2-3	F.Diff.	F.Elem.	Yes	AGRESS	Elastic-plastic	Wairakei, N.Z.	No
Lippmann, Narasimhan & Witherspoon (1976)	Geothermal	Liquid	2-3	1	Integrated F.D.		Yes	CCC	Terzaghi*	None	No
Atherton and others(1976)	Geothermal	Two	0	0	-	-	No	-	Compaction coef.	None	No

N/A: Numerical methods not applicable. *: Two different compressibilities, for irreversibility (see text).

shear responses in multiple dimensions. Other approaches for modeling constitutive relations may be presented at this symposium.

Only three geothermal subsidence models have been completed. Undoubtedly because of their recent development and the scarcity of the site data such models require, none have yet been verified in specific applications. Verification is here taken to mean the successful prediction of independently obtained subsidence data with the previously calibrated model. Besides the three surveyed geothermal subsidence models, development of others is known to be under way or planned at three different institutions: CIRES and the Department of Mechanical Engineering at the University of Colorado; Intercomp Resource Development and Engineering, Inc., of Houston, Texas; and the Department of Civil Engineering at Princeton University.

Geothermal subsidence models may be developed from scratch or by modification of existing models. For example, the groundwater model TRUST was extended to non-isothermal capabilities to produce the CCC model. Future geothermal subsidence models may be developed by adding deformation to existing reservoir models (surveyed by Atherton and others, 1976).

To summarize, subsidence models in general are in a very early stage of development. Few have been verified in applications to specific sites and their three-dimensional capabilities have not been adequately tested. The preferable constitutive relations have not yet been determined, while the development of models employing plastic deformation is just beginning.

By comparison, geothermal subsidence models are still in their infancy. Only one model (Brownell and others, 1975) simulates compaction processes other than primary pore collapse. None of the three operational models have yet been verified. Even the porous reservoir models have only recently reached the application stage.

Future Research Needs

Efforts to model subsidence are hampered by poor understanding of compaction processes and by the difficulty of representing these processes mathematically. Much research is needed to improve subsidence prediction procedures.

To better define deformation processes, additional experimental work and in-situ observations of macroscopic behavior are required. The physical principles governing lateral displacements must be investigated. We must also determine whether standard theory of flow in porous media and Terzaghi's consolidation theory are applicable to the fissured rock, temperature, and depth of geothermal reservoirs. Preliminary studies indicate, for clays, that a number of differences in deformation behavior are obtained from standard soil mechanics laboratory compaction tests (rapidly increasing external loads) and from tests specially designed to simulate in-situ stress conditions (gradually decreasing internal support) (Delflache, 1974). Improved methods of core testing must be developed to provide adequate input data for the models.

To improve existing models, future research should determine the best way to model compaction/fluid flow interactions, develop numerical methods to improve the computational tractability of multi-dimensional simulators, and assess model uncertainties with sensitivity analysis. Perhaps most challenging is the development of more realistic procedures for simulating material deformation. Wherever possible, geothermal subsidence models should be modified to include unique features such as convection cells and self-sealing caps, variations in rock properties associated with fissuring and faulting, and potential difficulties with reinjection schemes.

All these efforts are needed to attack our next major objective: to make a number of field applications with geothermal subsidence models. These efforts will require modelers to work more closely with laboratory and field workers. It is extremely important that modeling sophistication be guided by field observations. This need is apparent from the frequently unexpected behavior of subsurface materials and from the tendency to rely too strongly on laboratory observations.

Acknowledgements

Support for this study was provided by the National Science Foundation. Many of the cited modelers and other researchers have contributed through their helpful discussions. The first coauthor of this paper contributed mainly to the review of mathematical models, while the second provided the discussion of compaction processes.

References

Archambeau, C. B., 1974, Final Report, 1971-1973, ARPA-USGS Fluid Injection-Waste Disposal Research Program: Calif. Inst. Tech., Pasadena, 340 p.

Atherton, R. W., E. J. Finnemore, M. L. Gillam, A. E. DeGance, G. P. Grimsrud, and R. B. Schainker, 1976, The Analysis of Subsidence Associated with Geothermal Development: Systems Control, Inc., Palo Alto, California, NTIS Accession Nos. NSF/RA-760414/5/6, 3 v., 1134 p.

Batzle, M. L., and G. Simmons, 1976, Microfractures in Rocks from Two Geothermal Areas: Earth and Planetary Science Letters, v. 30, p. 71-93.

Brownell, D. H., S. K. Garg and J. W. Pritchett, 1975, Computer Simulation of Geothermal Reservoirs: Paper No. SPE 5381, presented at 45th Ann. Calif. Regional Mtg. of the SPE of AIME, at Ventura, Calif., 9 p.

de Ferrer, M. P., 1975, Two-phase Oil-Water Two Dimensional Flow in a Compacting Reservoir, and the Resulting Land Subsidence: M.S. thesis, Pennsylvania State Univ., University Park, 87 p.

Delflache, A. P., 1975, Control of Land Subsidence in the Texas Gulf Coast Area: 3rd semi-annual progress report to NSF, Dept. of Civil Eng., Lamar Univ., Beaumont, Texas.

DiMaggio, F. L., and I. Sandler, 1971, Material Model for Granular Soils: J. Eng. Mech. Div., Proc. ASCE, p. 935-950.

Finol, A., and S. M. Farouq Ali, 1975, Numerical Simulation of Oil Production with Simultaneous Ground Subsidence: J. Soc. Pet. Eng., v. 15, no. 5, p. 411-424.

Gambolati, G., 1972a, A Three-dimensional Model to Compute Land Subsidence: Bull. Internat. Assoc. Hydrological Sciences, v. 17, no. 2, p. 219-226.

Gambolati, G., 1972b, Estimate of Subsidence in Venice Using a One-dimensional Model of the Subsoil: IBM J. Research and Development, v. 16, no. 2, p. 130-137.

Gambolati, G., and R. A. Freeze, 1973, Mathematical Simulation of the Subsidence of Venice, 1: Theory: Water Resources Research, v. 10, no. 3, p. 563-577.

Geertsma, J., 1966, Problems of Rock Mechanics in Petroleum Production Engineering: Proc. 1st Congr. Internat. Soc. Rock Mechanics, Lisbon, Portugal, v. 1, p. 585-594.

Geertsma, J., and G. van Opstal, 1973, A Numerical Technique for Predicting Subsidence above Compacting Reservoirs, Based on the Nucleus of Strain Concept: Verhandelingen Kon. Ned. Geol. Mijnbouwk. Gen., v. 28, p. 63-78.

Helm, D. C., 1975, One-dimensional Simulation of Aquifer System Compaction Near Pixley, California: 1. Constant parameters: Water Resources Research, v. 11, no. 3, p. 465-478.

Helm, D. C., 1976, One-dimensional Simulation of Aquifer System Compaction Near Pixley, California: 2. Stress-dependent Parameters: Water Resources Research, v. 12, no. 3, p. 375-391.

Jacquin, C. and M. T. Poulet, 1970, Study of the Hydrodynamic Pattern in a Sedimentary Basin Subject to Subsidence: Paper No. SPE 2988, presented at 45th Annual Fall Meeting of the SPE of AIME, Houston, Texas.
Kreitler, C. W. and T. C. Gustavson, 1976, Geothermal Resources of the Texas Gulf Coast--Environmental Concerns Arising from the Production and Disposal of Geothermal Waters: Proc. 2nd Geopressured Geothermal Energy Conf., Univ. of Texas, Austin, v. V, 55 p.
Lippmann, M. J., T. N. Narasimhan and P. A. Witherspoon, 1976, Numerical Simulation of Reservoir Compaction in Liquid Dominated Geothermal Systems: Proc. 2nd Internat. Symp. on Land Subsidence, Anaheim, Calif.
Lofgren, B. E., 1973, Monitoring Ground Movement in Geothermal Areas: Specialty Conf. Proc., Hyd. Div., ASCE, 21st Ann. Meeting, p. 437-447.
Lofgren, B. E., 1974, Measuring Ground Movement in Geothermal Areas of Imperial Valley, California: Proc. Conf. on Research for the Development of Geothermal Energy Resources, Jet Propulsion Laboratory, Calif. Inst. Technology, Pasadena.
Lofgren, B. E., 1975, Land Subsidence and Tectonism, Raft River Valley, Idaho: U. S. Geol. Survey Open-File Report 75-585, 21 p.
Maxwell, J. S., 1960, Experiments on Compaction and Cementation of Sand: Geol. Soc. America Memoir 70, p. 105-132.
McCann, G. D. and C. H. Wilts, 1951, Mathematical Analysis of the Subsidence in the Long Beach-San Pedro Area: Calif. Inst. Tech., Pasadena, 117 p.
Mitchell, R. F., 1976, A Mechanical Model for the Permafrost Thaw-Subsidence: Paper No. 76-Pet-54, presented at ASME 31st Annual Petroleum Mech. Eng. Conf., Mexico City, 4 p.
Narasimhan, T. N., 1975, A Unified Numerical Model for Saturated-Unsaturated Groundwater Flow: Univ. of Calif., Berkeley, Ph.D. thesis, 244 p.
Papadopulos, S. S., 1975, The Energy Potential of Geopressured Reservoirs - Hydrogeologic Factors: Proc. 1st Geopressured Geothermal Energy Conf., University of Texas, Austin, p. 173-192.
Papadopulos, S. S., R. H. Wallace, Jr., J. B. Wesselman and R. E. Taylor, 1975, Assessment of Onshore Geopressured-geothermal Resources in the Northern Gulf of Mexico Basin: USGS Circular 726, p. 125-146.
Poland, J. F. and G. H. Davis, 1969, Land Subsidence Due to Withdrawal of Fluids: in D. J. Varnes and G. Kiersch (eds.), Reviews in Engineering Geology II, Geol. Soc. America, Boulder, Colo., p. 187-269.
Riney, T. D., and others, 1973, Constitutive Models and Computer Techniques for Ground Motion Predictions: Systems, Science and Software Report No. SSS-R-73-1490, La Jolla, Calif.
Sandhu, R. S., H. Liu and K. J. Singh, 1976, Computer Programs for Plane Strain and Axisymmetric Soil Consolidation: Geotech. Eng. Report No. 4, Dept. of Civil Eng., Ohio State Univ., Columbus.
Sandhu, R. and E. L. Wilson, 1970, Finite Element Analysis of Land Subsidence: in Land Subsidence, Proc. Tokyo Symposium, IASH-Unesco, Gentbrugge, Belgium, and Paris, France, v. 2, p. 393-400.
Stilwell, W. B., W. K. Hall and J. Tawhai, 1975, Ground Movement in New Zealand Geothermal Areas: Proc. 2nd U. N. Symposium on the Development and Use of Geothermal Resources, San Francisco, Calif.
White, D. E., 1973, Characteristics of Geothermal Resources: in P. Kruger and C. Otte (eds.), Geothermal Energy, Stanford Univ. Press, Stanford, Calif., p. 69-94.

Publication n°121 of the International Association of Hydrological Sciences
Proceedings of the Anaheim Symposium, December 1976

DETERMINATION OF SOIL SUBSIDENCE DUE TO WELL PUMPING BY NUMERICAL ANALYSIS

Abdel-Aziz I. Kashef and Kou-Roung Chang
Civil Engineering Department
North Carolina State University
Raleigh, North Carolina 27607, U.S.A.

Abstract

A numerical solution is developed to determine the land subsidence due to groundwater pumping from an unconfined aquifer overlying an aquitard. It is assumed that the water well completely penetrates the aquifer and is pumped at a constant rate. The changes in pore water pressures within the aquitard due to pumping from the upper unconfined aquifer are considered. The time-dependent flow pattern in the aquifer-aquitard system is determined by a suggested approach eliminating most of the currently used approximations in the available procedures. The actual well radius, the outflow surface, and the storativity of the aquitard are all taken into account. The formulated mathematical model with moving free surface is solved numerically by the "Alternating Direction Implicit (ADI)" method in dimensionless form. The total land subsidence resulting from the compressibility of both the aquifer and the aquitard is determined in the vertical directions by a time-dependent summation procedure based on the consideration of the pressure head diagram along these directions. The numerical analysis has been checked with available solutions by solving special cases to accommodate the approximations made in these solutions. The presented analysis proved to be highly convergent and stable. Selected results are presented together with a solved example.

Introduction

Overexploitation of groundwater is the main cause of the recorded cases of land subsidence and associated problems. The zones of subsidence coincide generally with the zones of heavy groundwater withdrawal as evidenced in Mexico City, Venice, Houston and Galveston Bay, Santa Clara Valley, Baton Rouge and other areas. Meinzer and Hard (1925) were probably the first to recognize the compressibility of artesian aquifers due to the decline in water pressures. Jacob (1940) analyzed analytically the aquifer and aquitard response to water withdrawal from an artesian aquifer. His results were later used by Lohman (1961) in determining the extent of elastic compression. The solution of Jacob (1946) for leaky artesian aquifers neglected the aquitard compressibility. Moreover, it was assumed that the flow in the aquitard was vertical. This assumption is valid when the contrast between the permeabilities of the aquifer and the aquitard is very large. Hantush (1960) modified the differential equation for flow in leaky artesian aquifers (Hantush and Jacob, 1955) taking into account the storage of the aquitard but assuming that the flow direction in the aquitard is vertical. He concluded that the percentage of water derived from leaky sources with respect to the total withdrawal would be considerable. Hantush (1964) developed also an approximate general equation for the flow in a sloping unconfined aquifer resting on an aquitard. Aravin and Numerov (1965) investigated a similar system. In both investigations, the aquitard storage was neglected, and

Dupuit's assumptions were adopted. In the proximity of the well, these assumptions would result into the dislocation of the free surface and the elimination of the outflow surface. The assumption of incompressible aquifer used by Boulton (1954) and Dagan (1967) for analyzing unconfined aquifers, limited the application of their results to large values of time. Polubarinova-Kochina (1962) derived a non-linear equation for the free surface on the assumption that it was slightly curved over and above an average height and that the horizontal velocity was independent of the vertical direction.

The proposed numerical approach in this paper determines the time dependent free surface in a leaky aquifer-aquitard system without resorting to Dupuit's approximations. Moreover, the actual well radius, the coefficient of storage of the aquitard, and the drawdown of the free surface have all been taken into account. The formulated mathematical model is solved numerically by the alternating direction implicit method (ADI). The application of the method to non-leaky unconfined aquifers shows good agreement with Neuman's (1975) analytical solution at small pumping rates. The presented solution proved to be stable and convergent.

At early stages of pumping, the numerical solution of the presented system fall fairly close to the early time Theis drawdown curve, indicating that water is released from storage. At intermediate stages, gravity drainage and water leakage from the aquitard become dominant and at final stages, the effects of elastic storage vanish. The numerical solution indicated also that the linear relationship between pumping rates and water pressure changes is valid only for low pumping rates; it is non-linear for large rates contradicting other investigators.

The increase in the intergranular stress at a specific point within the flow system at a certain time is equal to the difference between the decrease in the water pressure and the decrease in the total stress at the same point. Thus, the total settlement is determined along a vertical direction by a summation procedure based on the behavior of these time dependent stresses. Settlements due to multiple-well system are also investigated in an illustrated example of common practical conditions.

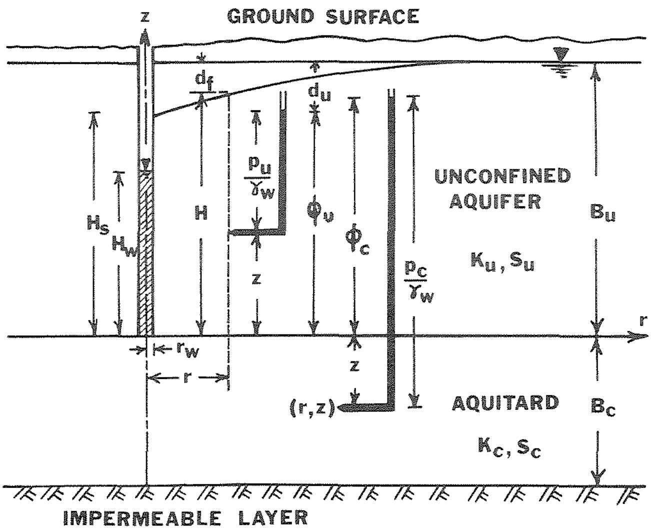

Figure (1): Diagrammatic Sketch of the Investigated System

Theoretical Formulation

Consider a leaky unconfined homogeneous and isotropic aquifer of infinite lateral extent underlain by a homogeneous and isotropic aquitard (Figure (1)) with constant storage coefficients. The capillary fringe in the aquifer is neglected and the pumped well completely penetrates the aquifer and discharges at a constant rate Q. The subsidence of the system is considered to take place in the vertical direction only neglecting any lateral deformation. Accordingly, the following governing equations are developed (Chang, 1976). The equation of motion of the free surface is:

$$(1/r)\partial P/\partial r + \partial^2 P/\partial r^2 + (K_c/K_u)(\partial\phi_c/\partial z)\big|_{z=0} = (S_y/K_u)\partial H/\partial t, \qquad \ldots(1)$$

where $P = \int_o^H (h_u/\gamma_w)dz$; other symbols are listed at the end of the paper. The equation governing the flow at any point within the flow medium of the unconfined aquifer is:

$$(1/r)\partial\phi_u/\partial_r + \partial^2\phi_u/\partial r^2 + \partial^2\phi_u/\partial z^2 = (S_u/T_u)\partial\phi_u/\partial t, \qquad \ldots(2)$$

The equation governing the flow in the aquitard is:

$$(1/r)\partial\phi_c/\partial r + \partial^2\phi_c/\partial r^2 + \partial^2\phi_c/\partial z^2 = (S_c/T_c)\partial\phi_c/\partial t \qquad \ldots(3)$$

The boundary conditions are given in Eqs. (4), (5), and (6) as follows:

$$\phi_u(\infty,z,t) = B_u,\ \phi_c(\infty,z,t) = B_u: \qquad \ldots(4)$$

$$\phi_u(r_w,z,t) = H_w \text{ at } 0 \leqslant z \leqslant H_w;\ \phi_u(r_w,z,t) = z \text{ at } H_w \leqslant z \leqslant H_s; \qquad \ldots(5)$$

$$\phi_u(r,o,t) = \phi_c(r,o,t);\ K_u(\partial\phi_c/\partial z) = K_c(\partial\phi_c/\partial z) \text{ at } z = o;\ (\partial\phi_c/\partial z) = 0 \text{ at}$$

$$z = -B_c;\ (\partial\phi_c/\partial r) = 0 \text{ at } r = r_w \text{ and } 0 \geqslant z \geqslant -B_c \qquad \ldots(6)$$

The constant rate of pumping Q is expressed as:

$$Q = 2\pi r_w K_u \int_o^H (\partial\phi_u/\partial r)dz + \pi r_w^2(\partial H_w/\partial t) \qquad \ldots(7)$$

It may be noticed that Boussinesq equation is obtained if Dupuit's assumptions are introduced in Eq. (1).

The increase in the intergranular stress due to pumping at a certain point is equal to the difference between the decrease in water pressure and the decrease in total stress of the soil-water system due to water withdrawal. Accordingly, the total settlement at any time t is expressed as (Chang, 1976):

$$\rho_t = \int_o^{B_u}\{(S_u/B_u\gamma_w)-S_y\beta_o\}(d_u-S_y d_f)\gamma_w dz + \int_o^{B_c}\{(S_c/B_c\gamma_w)-m_2\beta_o\}(d_c-S_y d_f)\gamma_w dz \qquad \ldots(8)$$

The subsidence of land surface due to groundwater pumping from a multiple gravity well system cannot be based on the same principle of superposition commonly used in multiple artesian wells. The summation of the individual effects of ϕ cannot be justified due to the continuously changing flow domain in gravity wells. Kashef (1970) established a modified procedure of superposition for gravity wells based on the superposition of the decrements in the P diagram. The settlement at any point (x,y) is therefore a function of the decrease in the resultant area of the P diagram across the vertical section passing through that point.

Accordingly, the subsidence of the vertical section through point (x,y) due to pumping from a multiple well system is:

$$\rho_{x,y,t} = \{(S_u/B_u\gamma_w)-(S_y\beta_o)\}\sum_{i=1}^{n}\int_o^{B_u}(d_{u,i}-S_y d_{f,i})\gamma_w dz +$$

$$\{(S_c/B_c\gamma_w)-(m_2\beta_o)\}\sum_{i=1}^{n}\int_o^{B_c}(d_{c,i}-S_y d_{f,i})\gamma_w dz \qquad \ldots(9)$$

Numerical Analysis

Pinder and Bredehoeft (1968) showed that the ADI method proposed by Peaceman and Rachford (1955) could save tremendous computing time as compared to Crank-Nicolson (1947) method. Rushton and Tomlinson (1971) made also a critical study of the efficiency of the ADI method in solving groundwater flow problems. In order to apply the ADI method in this study, several adjustments have been made to account for the changing free surface which forms the upper curved boundary, and the non-uniform mesh spacings. The finite difference equations in dimensionless forms are as follows (noting that the symbols with primes are the dimensionless form of their equivalents given in the previous equations):

$$\beta\,\frac{H_{i,t+\Delta t}-H_{i,t}}{\Delta t'} = \frac{1}{\Delta r'_{i-1}(\Delta r_{i-1,j}+\Delta r'_{i,j})}\left(\frac{\Delta r'_{i-1,j}}{r'_i}+2\right)P'_{i+1}$$

$$-\frac{1}{\Delta r'_{i-1,j}(\Delta r'_{i-1,j}+\Delta r'_{i,j})}\left(\frac{\Delta r'_{i,j}}{r'_i}-2\right)P'_{i-1}$$

$$-\frac{1}{\Delta r'_{i-1,j}\Delta r'_i}\left(\frac{\Delta r'_{i-1,j}-\Delta r'_{i,j}}{r'_i}+2\right)P'_i + \theta\,\frac{\phi'_{c,i,j}-\phi'_{c,i,j-1}}{\Delta z'_{i,j-1}}\Bigg|_{z=0} \qquad \ldots(10)$$

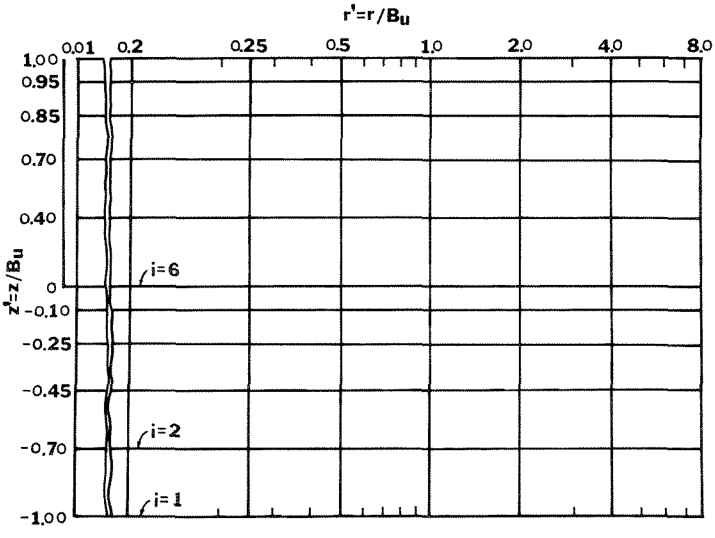

Figure (2): Mesh Size Used in the Numerical Solution

$$\text{and } \left(C_{ur,i}\phi'_{u,i-1,j}+D_{ur,i}\phi'_{u,i,j}+E_{ur,i}\phi'_{u,i+1,j}\right)_{t+\frac{1}{2}\Delta t} = \left(F_{ur,i}\right)_t \quad \ldots(11)$$

$$\text{where: } C_{ur,i} = -\frac{\Delta r'_{i,j}-2r_i}{r'_i\Delta r'_{i-1,j}(\Delta r'_{i-1,j}+\Delta r'_{i,j})};\ D_{ur,i} = -\frac{\Delta r'_{i-1,j}-\Delta r'_{i,j}+2r_i}{r'_i\Delta r'_{i-1,j}\Delta r'_{i,j}}$$

$$-\frac{2}{\Delta t'};\ E_{ur,i} = \frac{\Delta r'_{i-1,j}+2r_i}{r'_i\Delta r'_{i,j}(\Delta r'_{i-1,j}+\Delta r'_{i,j})};\ \&\ F_{ur,i,t} =$$

$$\frac{-2}{\Delta z_{i,j-1}\Delta z'_{i,j}(\Delta z'_{i,j-1}+\Delta z'_{i,j})}\{\Delta z_{i,j-1}\phi'_{u,i,j+1}+\Delta z_{i,j}\phi'_{u,i,j-1}$$

$$-\left((\Delta z'_{i,j-1}+\Delta z'_{i,j}) - \frac{\Delta z'_{i,j-1}\Delta z'_{i,j}(\Delta z'_{i,j-1}+\Delta z'_{i,j})}{\Delta t'}\right)\phi_{u,i,j}\}_t$$

$$\left(C_{uz,j}\phi'_{u,i,j-1}+D_{uz,j}\phi'_{u,i,j}+E_{uz,j}\phi'_{u,i,j+1}\right)_{t+\Delta t} = \left(F_{uz,j}\right)_{t+\frac{1}{2}\Delta t}\Big| \quad \ldots(12)$$

$$\text{where: } C_{uz,j} = \frac{2}{\Delta z'_{i,j-1}(\Delta z'_{i,j-1}+\Delta z'_{i,j})};\ D_{uz,j} = -\left(\frac{2}{\Delta z'_{i,j-1}\Delta z'_{i,j}}+\frac{2}{\Delta t'}\right);$$

$$E_{uz,j} = \frac{2}{\Delta z'_{i,j}(\Delta z'_{i,j-1}+\Delta z'_{i,j})};\ \&\ \left[F_{uz,j}\right]_{t+\frac{1}{2}\Delta t} = -\frac{\Delta r'_{i-1,j}+2r'_i}{r'_i\Delta r'_{i,j}(\Delta r'_{i-1,j}+\Delta r'_{i,j})}\times$$

$$\phi'_{u,i+1,j}+\frac{(\Delta r'_{i,j}-2r'_i)\phi_{u,i-1,j}}{r'_i\Delta r'_{i-1,j}(\Delta r'_{i-1,j}+\Delta r'_{i,j})}+\left\{\frac{\Delta r'_{i-1,j}-\Delta r'_{i,j}+2r'_i}{r'_i\Delta r'_{i-1,j}\Delta r'_{i,j}}-\frac{2}{\Delta t'}\right\}\phi'_{u,i,j}\Big)_{t+\frac{1}{2}\Delta t}$$

Eqs. (10), (11), and (12) are respectively the finite difference forms of Eq. (1), Eq. (2) in the radial direction and Eq. (2) in the vertical direction. Two finite difference equations similar to Eqs. (7) and (8) can be written for Eq. (3) replacing ϕ_u by ϕ_c and S_u/T_u by S_c/T_c.

At the boundary between the unconfined aquifer and the aquitard, the finite difference equations must be reevaluated to account for the discontinuity in the hydraulic heads. Thus two imaginary horizontal planes with imaginary potentiometric heads are introduced, one in the aquifer and the other in the aquitard (Abbott, 1960). The finite difference forms of Eqs. (2), (3), and (6) written in terms of the real and imaginary potentiometric heads at the boundary are then combined into one set by eliminating the imaginary potentiometric heads (Chang, 1976).

Computer Program

A computer program was written in Fortran language to execute the proposed numerical analysis. It consists of a main program and a subprogram (ADI). Five combinations of mesh spacings and time steps were studied to check the accuracy of the numerical method. It was found that values of $\Delta t = (1.5+t)(0.1)^2$ and a mesh size as shown in Fig. (2) gave satisfactory results. The selected time step is sufficiently small to account for the rapid changes in the potentiometric heads during the early pumping periods thus minimizing the truncation errors resulting

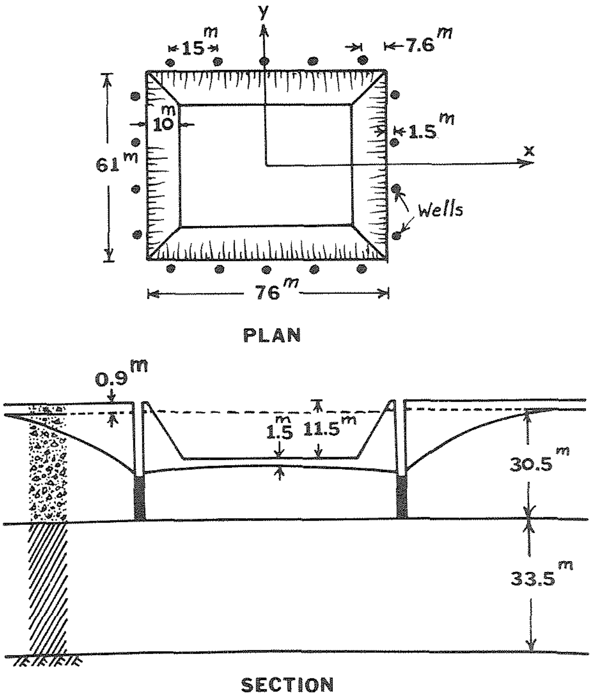

Figure (3): Layout of Solved Example

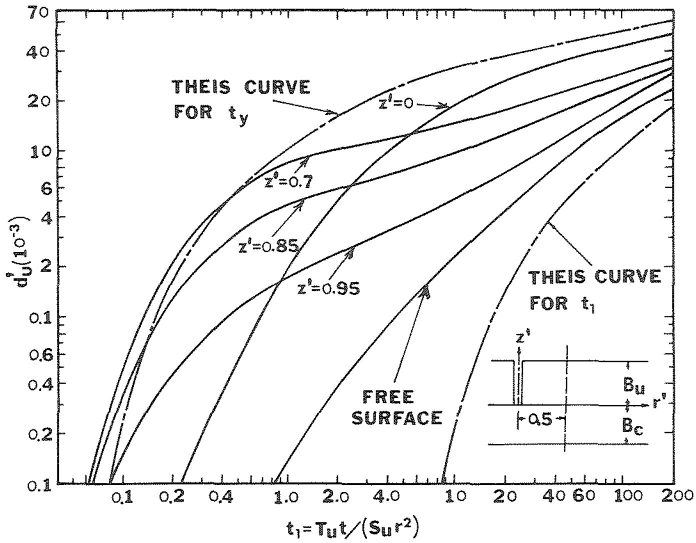

Figure (4): Curves d'_u versus t_1 at $r' = 0.5$ for indicated z' values (log-log scale): $Q' = 2.0$, $\alpha = 10^3$, $\beta_u = 10^2$ and $\theta = 10^{-2}$.

from the approximation. Larger time increments can be used during the late pumping periods when the changes in head decrease. A non-leaky unconfined aquifer was solved in order to compare the results with those of Neuman's analytical solution at small pumping rates. The comparison shows good agreement (Chang, 1976) justifying the reliability of the selected mesh spacing and time step. The numerical solution proved also to be convergent and stable.

The main program includes the following operations: At the beginning of each time step, the water height in the well, H_w, is assumed. Values of ϕ at the well periphery are assigned in such a way that the conditions given by Eqs. (4) and (5) are satisfied. Eqs. (2), (3), and (6) written in their finite difference forms are then used to calculate the ϕ values for all nodal points below the free surface. Eq. (10) can thus be used to calculate the free surface elevations, H_i, except for H_s at r_w. This is calculated by the following polynomial equation from the values of H_2, H_3, ... H_n, the elevations of the free surface at r_2, r_3, ... r_n computed by the Lagrangian interpolating formula (Conte and De Boor, 1972):

$$H_r = \sum_{j=2}^{n} K_j(r) H_j \qquad \ldots(13)$$

$$\text{where } K_j(r) = \frac{(r-r_2)(r-r_3)\ldots.(r-r_{j-1})(r-r_{j+1})\ldots.(r-r_n)}{(r_j-r_2)(r_j-r_3)\ldots.(r_j-r_{j-1})(r_j-r_{j+1})\ldots.(r_j-r_n)}.$$

If $r = r_w$, $H_r = H_s$ can be evaluated from Eq. (13). The nodal spacings between the newly calculated free surface and the uppermost nodal points below the free surface are then stored in the computer memory to replace the preceding values. The inflow into the well plus the water pumped from the well storage, $Q^{(n)}$, is calculated from Eq. (7) and compared with the designated pumping rate Q. If $|Q-Q^{(n)}| > 1\%\ Q$, then a new trial for H_w is made. Assuming further a linear relationship between H_w and $Q^{(n)}$, then:

$$\{H_n^{(n+1)}-H_w^{(n-1)}\}/\{Q-Q^{(n-1)}\} = \{H_w^{(n)}-H_w^{(n-1)}\}/\{Q^{(n)}-Q^{(n-1)}\},$$

$$\text{or: } H_w^{(n+1)} = H_w^{(n-1)} + \{H_w^{(n)}-H_w^{(n-1)}\}\{Q-Q^{(n-1)}\}/\{Q^{(n)}-Q^{(n-1)}\} \qquad \ldots(14)$$

where n denotes the iteration number; $H_w^{(n-1)}$ and $H_w^{(n)}$ are the assumed water levels in the pumped well; and $Q^{(n-1)}$ and $Q^{(n)}$ are the calculated pumping rates in the last two iterations. After selecting a new value for H_w, the ϕ values at the well periphery are adjusted in accordance with Eqs. (4) and (5). The calculations are repeated for all nodal points below the free surface until the condition $|Q-Q^{(n)}| < 1\%\ Q$ is satisfied. The subsidence of the ground surface is calculated after completing the operation of each time step. A listing of the complete computer program with instructions for data input is already available (Chang, 1976).

Applications

The presented numerical approach is applied to a typical example of a well group in an aquifer-aquitard system. Eighteen completely penetrating wells (in the aquifer only) are arranged in a rectangular pattern 62.5 x 77.5 m and spaced at 15.20 m around the site of a planned excavation 76.00 x 61.00 m in plan and 11.50 m deep [Fig. (3)]. The following data have been predetermined: B_u = 30.50 m, B_c = 33.50 m, $S_u = 2 \times 10^{-3}$,

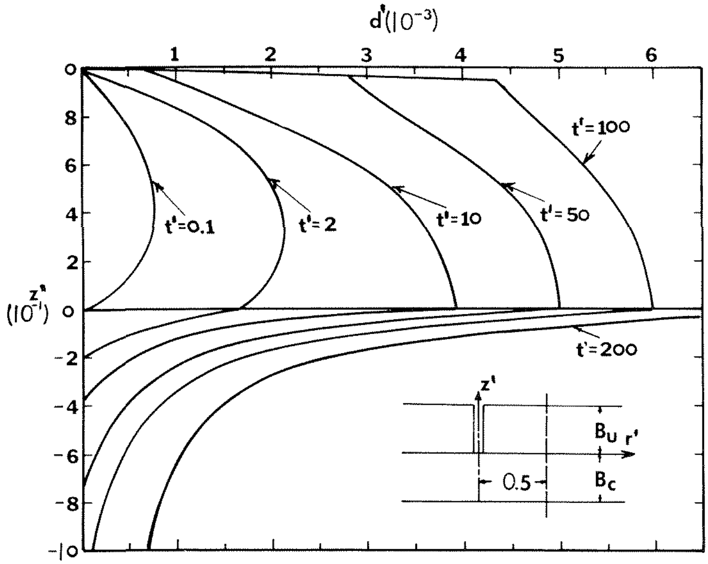

Figure (5): Curves d' versus z' at r' = 0.5 for indicated t' values (Natural Scale): Q' = 2.0, $\alpha = 10^3$, $\beta_u = 10^2$ and $\theta = 10^{-2}$

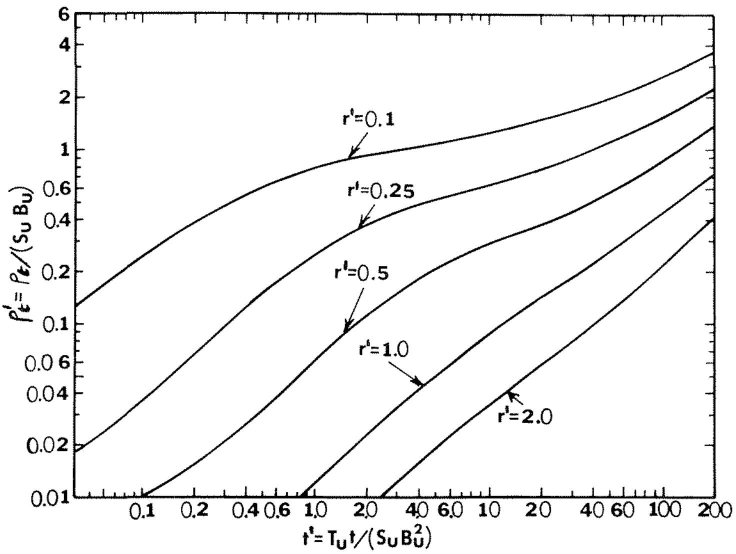

Figure (6): Curves ρ_t' versus t' for indicated r' values (log-log scale): Q' = 2.0, $\alpha = 10^3$, $\beta_u = 10^2$ and $\theta = 10^{-2}$

$S_c = 0.2$, $S_y = 0.2$, $K_u = 5 \times 10^{-5}$ m/sec and $K_c = 5 \times 10^{-7}$ m/sec. It is required to lower the water table 12.20 m below the center of the planned excavation in order to keep its level beneath the bottom of the excavation by 1.5 m or lower. The design of the well system should include the time required to lower the water table to the specified level and the resulting anticipated land subsidence.

Dimensionless solutions for various values of pumping rates Q' have been worked out (Chang, 1976) for a single well. Typical results for Q' = 2.0 are given in Figs. (4), (5), and (6). The changes in the hydraulic heads with log(t') for various values of z' are given in Fig. (4). The vertical profiles of these changes in heads are given in Fig. (5). The relationships between the land subsidence and time are shown in Fig. (6) in dimensionless form. The group of eighteen wells in this example can be reduced to one equivalent well with a radius $r_w = \{62.5 \times 77.5/\pi\}^{1/2} = 39.20$ m, according to Leonard (1962). It was found that such an equivalent well would lower the water level 12.20 m after 15 days and thereafter if Q' = 2.0, i.e., when the pumping capacity Q = 71.6 m^3/min. Accordingly, each well in the planned well system would be pumped at 71.6/18 ≃ 4 m^3/min and each well can thus have an internal diameter of 25 cms (Leonard, 1962). Thus for the equivalent single well, the results given in Figs. (3), (4), and (5) are valid ($\alpha = 10^4$, $\beta = 10^2$, and $\theta = 10^{-2}$ in the illustrated example). Fig. (7) indicates the drawdown contours of the water table for the equivalent well as well as a comparison with Neuman's (1975) approach where he assumed $K_u = S_u = 0$ (Other parameters are kept the same). The land subsidence is determined for the illustrated example, Fig. (7), for both the equivalent well and the planned group of wells. In the latter case, the modified procedure of superposition has been applied (Kashef, 1970).

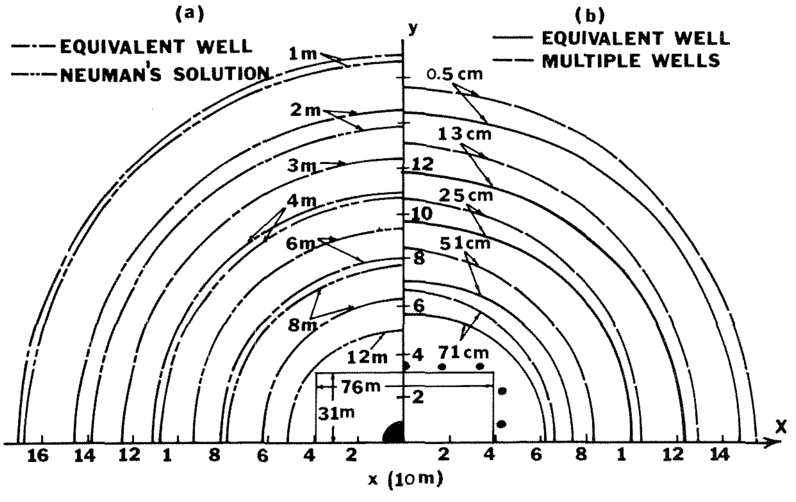

Figure (7): Land Subsidence and Drawdowns of the Solved Example:

a) Contours of Drawdowns in meters for the Equivalent Well by the Proposed Method Compared with Neuman's Solution

b) Contours of Land Subsidence in Centimeters by the Proposed Method Considering both the Actual Multiple Well System and the Equivalent Well

Conclusions

The results of the illustrated example are typical of other cases of different parameters. At the early stages of pumping, the curves corresponding to various z' values, Fig. (4), fall fairly close to the early time Theis drawdown curve, indicating that the water is derived mainly from storage. At the intermediate stages of pumping, gravity drainage and leakage from the aquitard become more dominant; thus the curves fall below Theis curve. At later stages, the water is derived mainly from leakage and ultimately the effect of elastic storage vanishes. The curves at these stages would therefore become closer to the late time Theis drawdown curve [Fig. (4)]. These same conclusions are also apparent in Fig. (5). When the ratio of the hydraulic conductivities between the aquitard and the unconfined aquifer increases, the explained trend would naturally become less pronounced.

In Neuman's (1975) solution, the unconfined aquifer is considered as compressible while the drawdowns of the water table are assumed negligible. His results would therefore be practically valid for low rates of pumping. A comparison is shown in Fig. (7) between Neuman's solution and the presented approach applied for the illustrated example. Most of the common assumptions made by Neuman (1975) and others are eliminated in this approach. It has been found the relationship between the pumping rates and the changes in the water pressures is not linear as reported in most of the available solutions. Using the suggested approach for low rates of pumping the linear relation is established only due to the insensitivity of the resulting low values of the changes in water pressures.

Land subsidence in the vertical direction depends upon the geometric and hydraulic boundaries of the aquifer-aquitard system as well as the physical characteristics of water and its media. Land subsidence due to a discharge well has an analogous pattern to the drawdown of water table [Fig. (7)] thus leading to severe uneven settlements which are more detrimental than those produced by structural loads. The settlements obtained from a multiple well system [Fig. (7)] exceed those computed for an equivalent well.

Notations

B_u : initial thickness of saturated zone (aquifer)
B_c : thickness (aquitard)
d_c, d_u : respectively change in total head at any point in the aquitard and aquifer
d_f : drawdown of water table
$d' = d/B_u$ (d may be d_c or d_u)
H : height of water table
$H' = H/B_u$,
H_s : height of water table at r_w
H_w : height of water level within well
K_c, K_u : respectively hydraulic conductivity of aquitard and aquifer
m_c, m_u : respectively porosity of aquitard and aquifer
Q : constant rate of pumping,
$Q' = 100\ Q/(4\pi T_u B_u)$
r_w : radius of well
$r' = r/B_u$
S_c, S_u : respectively storage coefficient of aquitard and aquifer
S_y : specific yield of aquifer,
T_c, T_u : respectively transmissivity of aquitard and aquifer
$t_1 = T_u \cdot t/(S_u r^2)$
$t' = T_u \cdot t/(S_u \cdot B_u^2)$

$z' = z/B_u$
$\alpha = K_u S_c/(K_c S_u)$,
$\beta = S_y/S_u$
β_o = water compressibility
γ_w : unit weight of water
$\theta = K_c/K_u$
ρ_t : settlement at time t
$\rho_t' = \rho_t/(S_u B_u)$
ϕ_c, ϕ_u : respectively total head at any point in aquitard and aquifer
$\phi_u' = \phi_u/B_u$
$\phi_c' = \phi_c/B_u$

References

Aravin, V. I., and Numerov, S. N., 1965, Theory of Fluid Flow in Undeformable Porous Media:Program for Scientific Translation, Clearinghouse for Federal Scientific and Technical Information, Springfield, Va.

Abbott, J., 1960, One-dimensional Consolidation of Multi-layered Soils: Geotechnique, v. 10, p. 151.

Boulton, N. S., 1954, The Drawdown of the Water Table under Non-steady Conditions Near a Pumped Well in an Unconfined Formation:Proc. Inst. Civil Eng., part 3, p. 564.

Conte, S. D., and De Boor, C., 1972, Elementary Numerical Analysis:2nd ed., McGraw-Hill Book Co., N. Y.

Chang, K. R., 1976, Determination of Soil Subsidence due to Well Pumping by Numerical Analysis:Ph.D. dissertation, Dept. Civil Engineering, North Carolina State University.

Crank, J., and Nicolson, P., 1947, A Practical Method for Numerical Evaluation of Solutions of Partial Differential Equations of the Heat Conduction Type:Proc. Camb. Phil. Soc., v. 43.

Dagan, G., 1967, A Method of Determining the Permeability and Effective Porosity of Unconfined Anisotropic Aquifers:Water Res. Res., v. 3, no. 4, p. 1059.

Hantush, M. S., 1960, Nonsteady Flow to Flowing Wells in Leaky Aquifers: J. Geophys. Res., v. 65, p. 1043-1052.

Hantush, M. S., 1964, Hydraulics of Wells:In Advances in Hydroscience, v. 1, (V. T. Chow, editor) Academic Press, N. Y.

Hantush, M. S., and Jacob, C. E., 1955, Nonsteady Radial Flow in an Infinite Leaky Aquifer:Trans. Am. Geophys. Union, v. 36, p. 95-100.

Jacob, C. E., 1940, On the Flow of Water in an Elastic Artesian Aquifer: Trans. Am. Geophys. Union, v. 21, p. 559-569.

Jacob, C. E., 1946, Radial Flow in a Leaky Artesian Aquifer:Trans. Am. Geophys. Union, v. 27, p. 198-205.

Kashef, A. I., 1970, Multiple Gravity Wells under Transient States of Flow:Water Res. Res., v. 6, no. 6, p. 1729-1736.

Lohman, S. M., 1961, Compression of Elastic Artesian Aquifers:U.S.G.S. prof. paper 424-B, p. B47-B49.

Meinzer, O. E., and Hard, H. A., 1925, The Artesian Water Supply of the Dakota Sandstone:U.S.G.S. Water Supply Paper, no. 520-E, p. 73-95.

Neuman, S. P., 1975, Analysis of Pumping Test Data from Anisotropic Unconfined Aquifer Considering Delayed Gravity Response:Water Res. Res., v. 11, no. 2, p. 329-342.

Peaceman, D. W., and Rachford, H. H., 1955, The Numerical Solution of Parabolic and Elliptic Differential Equations:J. SIAM, v. 3., p. 28-41.

Pinder, G. E., and Bredehoeft, J. D., 1968, Applications of the Digital

Computer for Aquifer Evaluation:Water Res. Res., v. 4, no. 5, p. 1069-1094.
Polubarinova-Kochina, P. Ya., 1961, Theory of Groundwater Movement: English Translation from Russian (1952), Princeton Univ. Press.
Rushton, D. R., and Tomlinson, L. M., 1971, Digital Computer Solutions of Groundwater Flow:J. of Hydrology, v. 12, no. 4, p. 339-362.

Publication n°121 of the International Association of Hydrological Sciences
Proceedings of the Anaheim Symposium, December 1976

NUMERICAL SIMULATION OF RESERVOIR COMPACTION IN LIQUID DOMINATED GEOTHERMAL SYSTEMS

Marcelo J. Lippmann, T. N. Narasimhan and P. A. Witherspoon
Lawrence Berkeley Laboratory
University of California
Berkeley, California 94720

Abstract

Recently much attention has been focused on the development of geothermal systems. A large number of geothermal fields are of the hot water type, dominated by circulating liquid that transfers most of the heat and largely controls subsurface pressures. During the exploitation of such systems, a reduction of pressures is inevitable which, in some areas may lead to land subsidence.

A numerical model is introduced which simulates the effects of fluid production as well as reinjection on the vertical deformation of water dominated geothermal reservoirs. This program, based on an Integrated Finite Difference technique and Terzaghi's one-dimensional consolidation model, computes the transport of heat and water through porous media, and resulting pore volume changes. Examples are presented to show the effects of reservoir heterogeneities on the compaction of these hot water systems, as well as the effects of different production-injection schemes. The use of isothermal models to simulate the deformation of non-isothermal systems is also investigated.

Introduction

The production of fluids from geothermal systems may result in ground surface displacements due to the lowering of pressures in the reservoir and surrounding rocks. These displacements may not only affect installations directly related to the geothermal field (e.g., well casings, steam transmission lines, power plant) but also nearby roads, buildings, and irrigation canals. Therefore it is important to foresee the magnitude and location of the so-called "subsidence bowl" as soon as adequate data on the geologic structure, stratigraphy, rock properties, and proposed development program become available. A number of models to simulate the vertical and horizontal ground deformations in geothermal systems have been or are being developed. These are reviewed in another paper presented at this meeting (Finnemore and Gillam, 1976).

Here, we introduce a mathematical model to simulate the transport of heat and water through a porous geothermal system, including the vertical deformations produced by effective stress changes. This code named "CCC" (for Conduction-Convection-Consolidation) is restricted to one-phase water dominated geothermal fields. At the present time, these systems have the largest potential for developing geothermal energy for electrical and non-electrical uses. They are characterized by circulating liquid that transfers most of the heat and largely controls subsurface pressures (Renner, et al., 1975).

A number of examples are presented below to illustrate some of the capabilities of our computer program. We shall demonstrate the effect of geologic heterogeneities on the behavior of the geothermal system as well as the effect of the location of production and injection wells. A comparison of results will also be made when the system is analyzed under isothermal and non-isothermal conditions.

Method and Governing Equations

Program CCC is based on the numerical models SCHAFF (Sorey, 1975) for mass and heat transport through saturated porous media, and TRUST (Narasimhan, 1975) for one-dimensional isothermal consolidation. The code can simulate one, two or three-dimensional, heterogeneous, isotropic, non-isothermal systems. Deformation parameters may be non-linear and non-elastic; the thermal and hydraulic properties can be temperature and/or pressure dependent.

An integrated finite difference method (Narasimhan and Witherspoon, 1976) is used to solve the energy and fluid flow equations. In integral form the flow equation for a slightly compressible fluid (e.g., water) is given by:

$$\frac{\partial}{\partial t}\int_V \frac{\rho}{1+e}\left(e\kappa + \frac{de}{d\sigma'}\right) P dV = \int_S \frac{k\rho}{\mu}(\nabla P - \rho\bar{g})\bullet \bar{n} dS + \int_V Q dV \qquad (1)$$

and the energy equation is given by:

$$\frac{\partial}{\partial t}\int_V (\rho c)_M T dV = \int_S K_M \nabla T \bullet \bar{n} dS - \int_S \rho c_F \delta T \bar{v}_d \bullet \bar{n} dS + \int_V q dV \qquad (2)$$

where, t is time, ρ fluid density, e void ratio, κ fluid compressibility, σ' effective stress, P pore pressure, V volume, k intrinsic permeability, μ viscosity, $\bar{g}$ gravitational acceleration, $\bar{n}$ outward unit normal on surface S, Q mass injection rate per unit volume, $(\rho c)_M$ heat capacity per unit volume of the solid-fluid mixture, K_M thermal conductivity of the solid-fluid mixture, c_F fluid specific heat capacity at constant volume, δT difference between the mean temperature within the volume element and that on the surface element dS, $\bar{v}_d$ Darcy velocity, and q heat injection rate per unit volume. Details of the method used to solve these equations are given by Sorey (1975) and Narasimhan (1975), and will not be repeated here.

Concurrent with the mass and energy flow, the vertical deformation of the geothermal system is simulated based on the one-dimensional consolidation theory of Terzaghi. The void ratio at each nodal point is computed by using "e-log σ'" curves (Figure 1). According to the preconsolidation and effective stresses at the point, the program calculates the void ratio by using either the virgin curve (of slope C_c) or swelling-recompression curves (of slope C_s). The model neglects the hysteresis between swelling and recompression curves. While the pore volume changes with effective stress, the solid volume is defined to remain constant; the thermal expansion of the rock skeleton is not considered. Because of

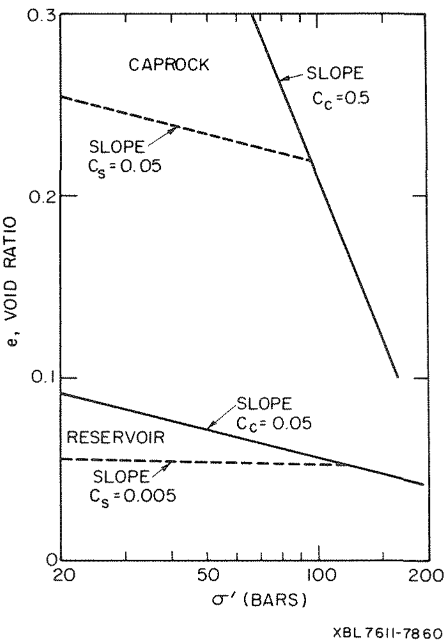

Figure 1. Plot of void ratio (e) versus effective stress (σ') for caprock and reservoir of example 4.

the one-dimensional nature of the consolidation model the pore volume changes caused by void ratio changes are directly reflected in a vertical deformation of the individual volumetric nodes.

The deformations computed by this model are restricted to those of the reservoir and neighboring saturated formations which release water from storage to partly or wholly compensate for the fluid withdrawn. These vertical displacements may or may not be directly expressed at the ground surface. The external loading of the overburden, caused by the vertical deformation of the deeper geothermal system, may result in displacements at the surface that may be different in magnitude and direction. Future versions of this model will include the computation of vertical and horizontal displacements at the ground surface itself.

The flow and energy equations (1) and (2) are interconnected by (a) the second order equation of state for the fluid,

$$\rho = \rho_o[1 - \beta(T-T_o) - \gamma(T-T_o)^2] \tag{3}$$

where, β and γ are coefficients of thermal expansion, and ρ_o and T_o are the reference density and temperature, respectively, for the fluid, (b) the Darcy velocity used in the convection term of the energy equation, and (c) the temperature and/or pressure dependence of certain parameters.

Because these interrelations, equations 1 and 2 are solved alternatively by interlacing their solutions in time; this is shown schematically on Figure 2. The flow equation solves for P, $\bar{v}_d$ and e assuming that the temperature dependent properties of the fluid and rock remain constant. Then, the energy equation is used to obtain T assuming that $\bar{v}_d$ and pressure dependent properties remain constant. Since the temperature varies much more slowly than the pressure, much smaller time steps have to be taken in the flow cycles than in the energy cycles (Figure 2) in order to compute pressure variations accurately.

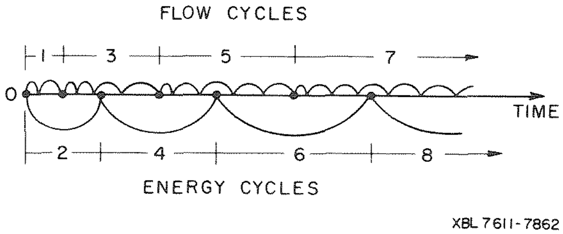

Figure 2. Interlacing of flow and energy calculations

Examples and Results

Four examples are presented below. In all cases it is assumed that, (a) the systems are normally consolidated (i.e., initial effective stresses and preconsolidation stresses are equal), (b) total stresses do not change in time, and (c) the intrinsic permeability (k), thermal conductivity (K_M), and heat capacity of the rock (c_R), as well as the compressibility (κ) and coefficients of thermal expansion (β,γ) of the water are constant. These assumptions are made to simplify the examples presented here, although the program can consider more complex conditions and relationships. The fluid density (ρ), heat capacity (c_F) and viscosity (μ) are temperature dependent, while the void ratio (e) is dependent on pore pressure and previous stress history.

Example 1. System with caprock of variable thickness

This case shows a totally penetrating well placed at the center of an axisymmetric system which has a caprock of variable thickness. The well withdraws 2.8×10^6 kg/day of water uniformly along the thickness of the reservoir. Figure 3 shows the dimensions, boundary conditions and initial temperature distribution for this system. At t = 0, only heat conduction occurs between the boundaries, since the Rayleigh number (Ra) in the reservoir is less than 20. This dimensionless number is equal to the ratio between the buoyant and viscous forces acting in the reservoir, and at this low Ra, free convection is not expected to occur.

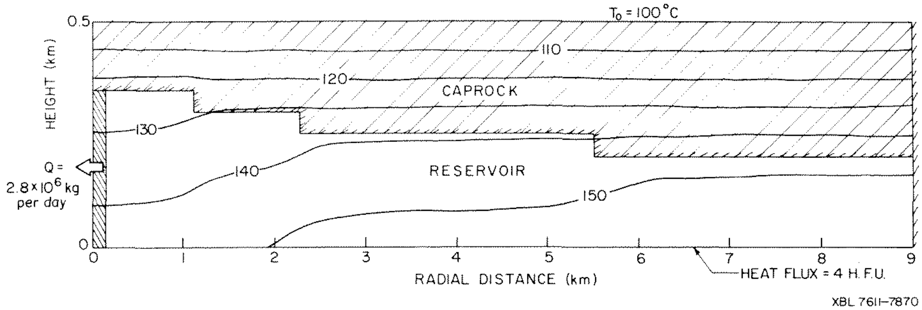

Figure 3. Example 1. Geometry, initial temperature and boundary conditions

The shape of the initial isotherms reflects the non-uniform thicknesses of materials of different thermal conductivities under the prevailing boundary conditions. The lower boundary is impermeable with a constant influx of 4×10^{-6} cal cm^{-2} sec^{-1} (4 H.F.U.). The upper boundary is isothermal (100°C) and impermeable. The outer radial boundary is closed both to heat and fluid flow. The overburden (not shown) is 1000 m thick and its average density is 2.5 g cm^{-3}. The rock and fluid properties used in this example are given in Tables 1 and 2.

When production starts, water in the reservoir flows essentially radially towards the well and vertically downward in the caprock. The resulting consolidation after 2400 days is shown on Figure 4. Near the well a maximum compaction of 29.2 cm was determined, of which about 70% occurred in the caprock.

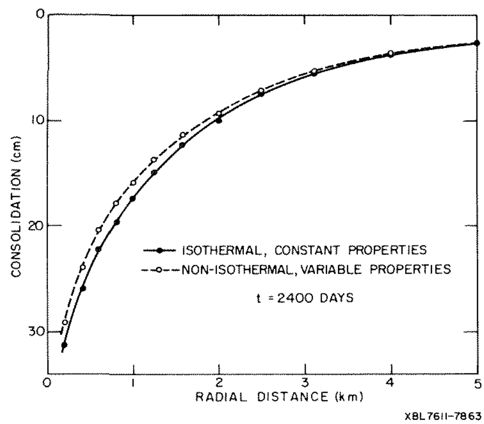

Figure 4. Example 1. Consolidation versus distance under isothermal and non-isothermal conditions.

The same system was also investigated under isothermal

Table 1. Material properties of rocks used in examples 1 to 3

	Caprock	Reservoir
Thermal conductivity (K_M) ($mcal\ cm^{-1}\ sec^{-1}\ °C^{-1}$)	2.52	6.64
Rock heat capacity (c_R) ($cal\ g^{-1}\ °C^{-1}$)	0.222	0.232
Rock density (ρ_R) ($g\ cm^{-3}$)	2.70	2.65
Intrinsic permeability (k) (cm^2)	1×10^{-12}	5×10^{-10}
Reference void ratio (e_o)	0.250	0.053
Reference effective stress (σ'_o) (bars)	185	185
Slope of virgin curve (C_c)	0.5	0.05
Slope of swelling-recompression curve (C_s)	0.05	0.005

Table 2. Fluid properties of water used in all examples

Compressibility (κ)	5.5×10^{-5} $bars^{-1}$
Coefficient of thermal expansion (β)	3.17×10^{-4} $°C^{-1}$
Coefficient of thermal expansion (γ)	2.56×10^{-6} $°C^{-2}$
Reference temperature (T_o)	25°C
Reference density (ρ_o)	0.997 $g\ cm^{-3}$
Viscosity (μ) and heat capacity (c_F)	f(T) for P = 100 bars

conditions using fluid properties corresponding to 135°C, which is the average temperature for example 1. In this case, the consolidation within 2 km from the well was between 7 and 9% larger than under non-isothermal conditions (Figure 4). The larger computed compaction for the isothermal case is apparently to be attributed to the viscosity effects; in the isothermal system a constant viscosity of 0.284 cp was used, whereas in the non-isothermal case the viscosity varied between 0.202 cp and 0.315 cp across the system.

From this example, we conclude that in order to use an isothermal model to simulate the behavior of a non-isothermal system, periodic adjustments of model properties may have to be made to account for the temperature variations that can occur as the simulation progresses in time.

Example 2. System with low permeability lens in reservoir

The system considered here differs from that of example 1 in that a lens of the same material as the caprock has been incorporated into the reservoir. This lens increases the tortuosity of the flow lines, resulting in more pressure drop near the well and less drop further away. This is shown on Figure 5 where lines of equal pressure reduction at t=2400 days are plotted for examples 1 and 2. The effects of these differences in pore pressure change produce different consolidation patterns as shown on Figure 6. These results indicate that it is possible to have a larger compaction away from the producing well due to a heterogeneity in the

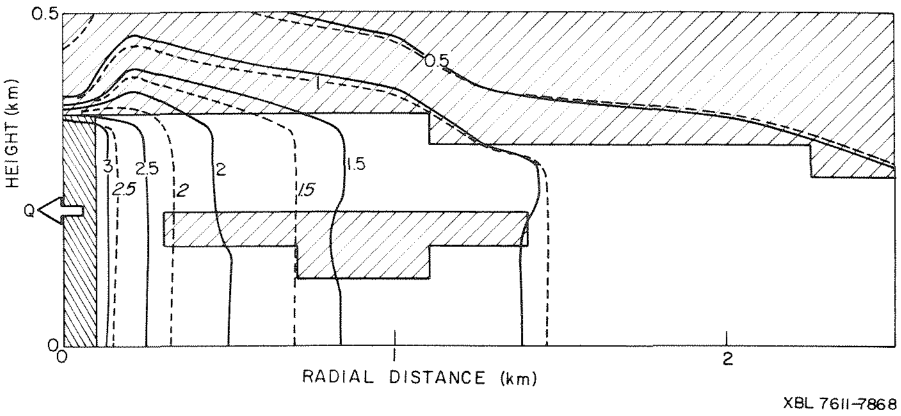

Figure 5. Pore pressure drop, in bars, after 2400 days of water withdrawal. Dashed lines: Example 1 (without lens); Solid lines: Example 2 (with lens).

reservoir. The lens provides a larger volume of more compressible material at locations where large pressure changes are occurring.

This type of heterogeneity in the reservoir could explain why in the Wairakei geothermal field of New Zealand, the maximum ground displacements occur in an area distant from the more intensively developed well field (Stillwell et al., 1976). This idea needs further investigation using three dimensional systems with non-uniform caprocks and differently shaped lenticular structures.

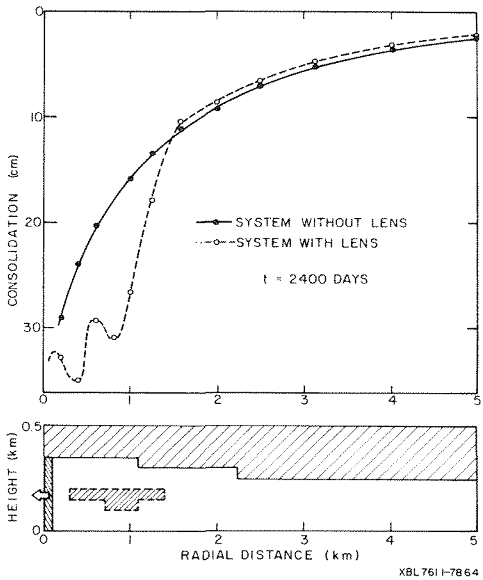

Figure 6. Consolidation versus distance after 2400 days of water withdrawal. Solid lines: Example 1; Dashed lines: Example 2

<u>Example 3. System with intercalated layer in reservoir</u>

This example is intended to show that even when all the produced water is reinjected, some amount of compaction cannot be avoided. The geometry, properties, initial and boundary conditions used here are similar to those of example 1. A layer of the same material as the caprock is intercalated in the reservoir as shown in Figure 7. The layer might be an aquitard partially dividing the reservoir in two parts. The separation is not complete since the layer only extends radially 1750 m from the well. A production rate of 1.2 x 10^6 kg/day of hot water is maintained from the upper 150 m of the reservoir. The same mass is reinjected into the lower 100 m of the reservoir, but the temperature of the injected water is only 25°C. The total pressure changes after 15 years of simulation time are shown in Figure 8. Note that pressures decrease in the upper part and increase in the lower part. As shown in Figure 7, the consolidation of the system is restricted to the first 1500 m out from the well. Negligible effects occurred beyond this distance from the well which agrees with the location of the curve for zero pressure change (see Figure 8). The development of consolidation with time is depicted on Figure 7. At the beginning, the compaction rate of the system is significant, but it falls off rapidly with time.

Because of the injection of colder waters, the lower part of the reservoir slowly cools. After 15 years, the thermal front separating the colder and warmer waters is located at a radial distance of about 175 m from the well. The hydrodynamic front, indicating the position of the reinjected water which largely has been warmed up by the heat stored in the reservoir rock skeleton, has advanced to about 650 m from the well. The approximate location of the hydrodynamic front has been calculated by assuming that the water has flowed only radially away from the injection well. This is only a simplification since some of the water actually has seeped upward through the layer separating the reservoir.

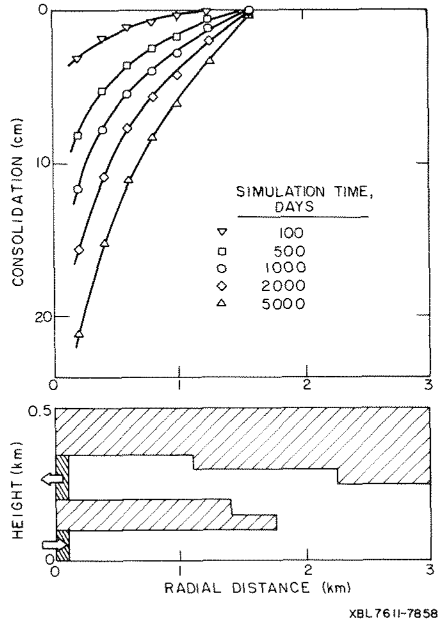

Figure 7. Example 3. Geometry and consolidation versus time and distance.

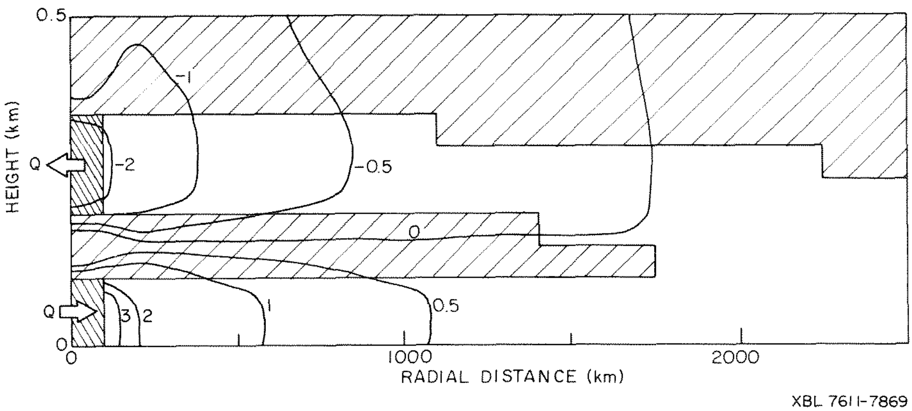

Figure 8. Example 3. Pressure changes, in bars, after 15 years of simulation.

Due to the colder temperature near the well and the higher mass flow rate per unit injected area of the well, large increases of pressure occur in the lower part of the reservoir, which are greater in magnitude than the pressure reductions in the upper reservoir. Even under these conditions, a net compaction still occurs around the well. This suggests that it may be necessary to have rates of reinjection that are larger than the production rates in order to minimize the effects of consolidation. Further work along these lines is needed.

Example 4. Convecting system with three layers

This last example is intended to describe the response of a free convecting system to two different production and reinjection schemes. The system is a parallelepiped 550 m high, 750 m wide and 50 m deep and contains three different layers (Figure 9). The caprock and reservoir are deformable, their "e-log σ'" curves are given in Figure 1, but the baserock is incompressible. Tables 2 and 3 list the fluid and material properties used in this example. Because of the large temperature difference between the top and bottom boundaries (260°C), the heat flow across this system is much larger than in the previous cases. It is approximately 37 H.F.U. The Rayleigh number for the reservoir is about 93, which exceeds the critical Ra ≃ 40. Indeed, free convection is established in the reservoir as is shown schematically in Figure 9 by the dashed circles and reflected by the shapes of the isotherms. Two production-injection schemes were considered. In both cases a total of 4 x 10^4 kg/day of water were produced and 3.2 x 10^4 kg/day of 100°C water were reinjected

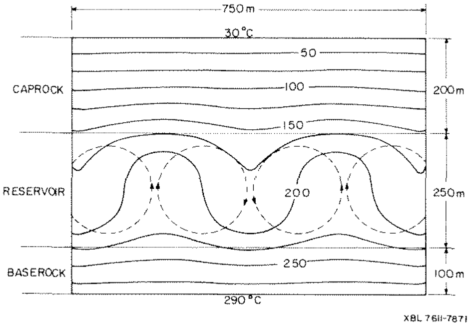

Figure 9. Example 4. Geometry and initial temperature distribution. Dashed circles: Convection cells (schematic representation).

Table 3. Material properties of rocks used in example 4

	Caprock	Reservoir	Baserock
Thermal conductivity (K_M) (mcal cm^{-1} sec^{-1}°C^{-1})	4.98	4.98	5.53
Rock heat capacity (c_R) (cal g^{-1}°C^{-1})	0.222	0.232	0.222
Rock density (ρ_R) (g cm^{-3})	2.70	2.65	2.70
Intrinsic permeability (k) (cm^2)	1 x 10^{-12}	5 x 10^{-10}	1 x 10^{-13}

(80% reinjection). The amount of water involved is rather small, and the rates used in this example were such as to avoid "overpowering" the natural convection cells, each of which transported about 7000 kg/day of water through the system. In the first case (example 4a) water is removed at the top of the ascending columns of convection and injection is at the bottom of the descending columns (Figure 10A). In example 4b water is removed at the bottom of the ascending columns and injection is at the top of the descending columns (Figure 11A). A symmetrical arrangement of sources and sinks was used to retain the symmetry implied by the impermeable side boundaries.

Figures 10B and 11B show the resulting temperature distribution for both cases after 20 years of simulation. A general cooling of the system is observed. There was no significant difference in the amount of consolidation occurring in either case. A difference might possibly be detected after longer period of time because the cooling patterns are not the same in both cases. The consolidation is fairly uniform across the system being slightly larger (2%) over the pumping areas. Figure 12 shows the development of consolidation in time for example 4a. The compaction increases almost linearly with time, and the contribution of the reservoir to the total consolidation is important only at early time. Later, most of the compaction occurs in the caprock. This may be explained by the delayed lowering of pore pressure in the caprock (see Figure 13).

For comparison purposes, example 4a was also modelled as a 175°C isothermal system. Pore pressures, total and preconsolidation stresses were the same. The resulting compaction was 4-6% higher than that of the non-isothermal case. When pressure changes are compared (Figure 14), it is evident that in the isothermal system, the pore pressure decreased more in the upper part of the caprock and less in the lower part as well as in the reservoir.

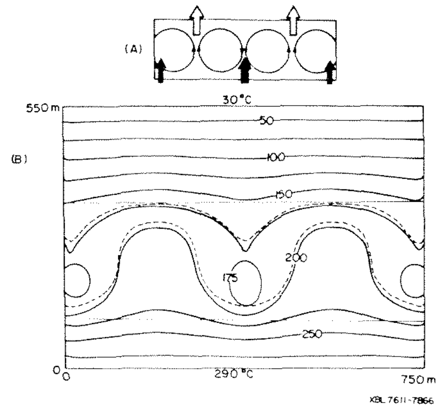

Figure 10. Example 4a. (A) Dark arrows: injection; light arrows: production. (B) Temperature distribution after 20 years of simulation. Dashed lines: initial 175° and 200°C isotherms.

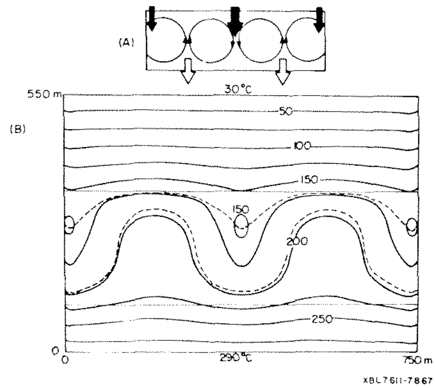

Figure 11. Example 4b. (A) Dark arrows: injection; light arrows: production. (B) Temperature distribution after 20 years of simulation. Dashed lines: initial 175° and 200°C isotherms.

As in example 1, the unequal response to the withdrawal of fluids can be attributed to the viscosity differences in the two cases. In the isothermal system, the viscosity is uniform (0.212 cp), but in the non-isothermal case it varies from 0.150 cp at the bottom of the reservoir, to 0.446 cp at the top of caprock. The differences in the distribution of fluid density in the isothermal and non-isothermal cases will also have similar effects on pressure distribution and compaction as the viscosity variation, but the magnitudes will be smaller relative to viscosity effects.

The final example suggests that compaction of water dominated geothermal fields with large temperature differences and complex fluid patterns will be difficult to model as isothermal systems. This is especially the case if one is interested in the pressure and compaction history at particular parts of the system.

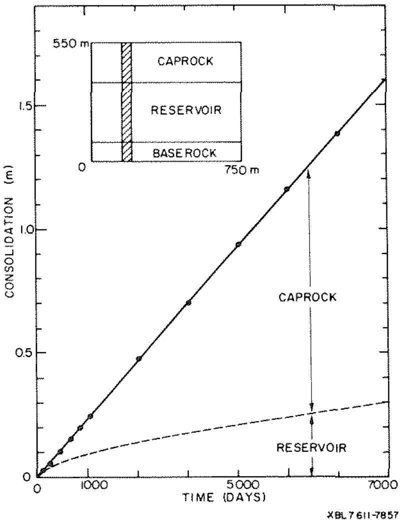

Figure 12. Example 4a. Consolidation versus time (corresonds to the column indicated in the insert).

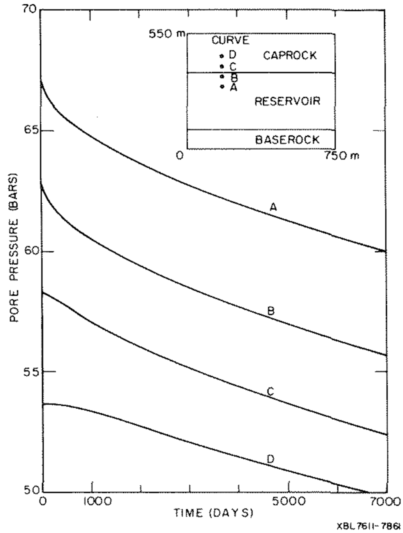

Figure 13. Example 4a. Pore pressure change with time at different points in the caprock and reservoir.

References

Finnemore, E. J. and M. L. Gillam, 1976. Compaction processes and mathematical models of land subsidence in geothermal areas: Proc. 2nd Int. Symp. Land Subsidence, Anaheim, Ca., Dec. 13-17, 1976.

Narasimhan, T. N., 1975. A unified numerical model for saturated -unsaturated groundwater flow: Ph.D. thesis, Univ. California, Berkeley, 244 p.

Narasimhan, T. N. and P. A. Witherspoon, 1976, An integrated finite difference method for analyzing fluid flow in porous media: Water Resour. Res., 12(1), p. 57-64.

Renner, J. L., D. E. White and D. L. Williams, 1975. Hydrothermal convection systems: U. S. Geol. Survey Circ. 726, p. 5-57.

Sorey, M. L., 1975. Numerical modeling of liquid geothermal systems: Ph.D. thesis, Univ. California, Berkeley, 65 p.

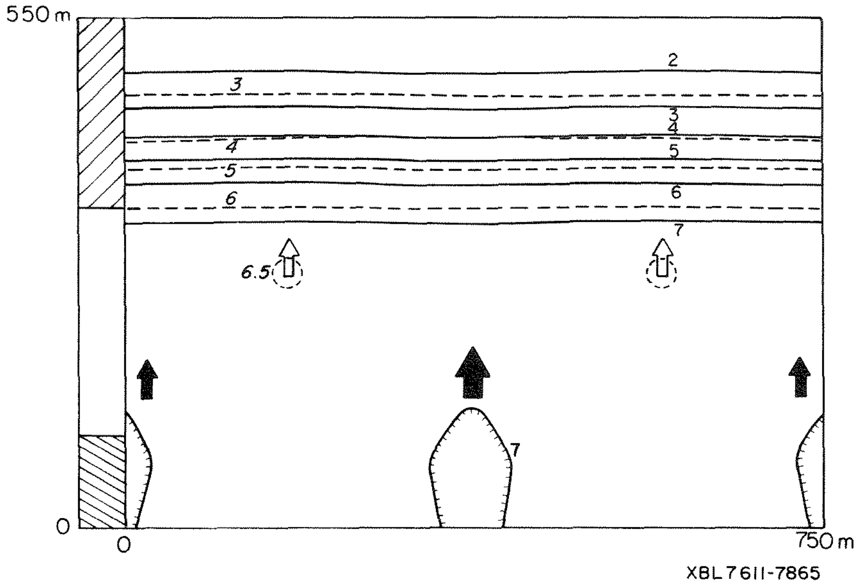

Figure 14. Example 4a. Pressure drop, in bars, after 20 years of simulation. Solid lines: non-isothermal case; Dashed lines: isothermal case; Dark arrows: injection; Light arrows: production (not to scale).

Stilwell, W. B., W. K. Hall and J. Tawhai, 1976. Ground movement in New Zealan geothermal fields: Proc. 2nd U. N. Symp. Development and Use of Geotherma Resources, San Francisco, Ca., May 20-29, 1975, p. 1427-1434.

Acknowledgement

This work was done with support from the U. S. Energy Research and Development Administration.

Publication n°121 of the International Association of Hydrological Sciences
Proceedings of the Anaheim Symposium, December 1976

MATHEMATICAL MODELLING OF LEAKY AQUIFERS WITH RHEOLOGICAL PROPERTIES

Yavuz Corapcioglu
Dept. of Engineering Sciences
Middle East Technical University
Ankara, Turkey

Abstract

The compression mechanism of a leaky aquifer was linked to the flow equation through a viscoelastic stress-strain relation for the porous material and the analytical solution was given. Also, the equation was given for a rate-independent plastic porous material as an alternative.

Introduction

In many areas of the world, groundwater pumping is a very essential way of obtaining water. In the coming years, the need for water will increase to meet the demands of an increasing population and associated agricultural and industrial development, which bring many subsidence problems resulting from exploitation of groundwater resources.

Change in stress due to groundwater pumping becomes effective in changing the thickness of the fine grained beds in the aquifer. The amount of compaction that an aquifer can have is a function of its compressibility and soil characteristics. The compaction of an aquifer has two components as mentioned by Poland et al.,(1972): "an inelastic component that is not recoverable upon decrease in stress and a recoverable elastic component".

A compressible aquifer can either be confined or semi-confined depending on the hydraulic conductivity of its confining bed. There are only a few absolutely confined aquifers most of them being to some extent "leaky". So, the effect of leakage has to be considered in formulations. Flow of water in leaky aquifers has been extensively studied by many authors especially by Hantush(1956).

In this study, the compression mechanism of a leaky aquifer will be linked to the flow equation through a rheological constitutive equation.

Basic Equations of Porous Media

The compaction of aquifers is a deformation process of a porous media saturated with water. The theory of porous solids saturated by fluids is of interest in various fields of engineering and technology. Therefore, it has been the subject of numerouos investigations dating back to the experimental observations of Darcy. An account of the main body of these efforts can be found in the publications of Paria(1963), Suklje(1969), and Scheidegger(1974).

Significant improvement in the theory of porous media was made by Biot(1941, 1955,1972) who appears to have been the first researcher to consider the deformation of the porous media. The equations given by Biot were drived based on purely mechanical considerations and in a somewhat intuitive way. On the other hand, the works of Terzaghi(1925) and Heinrich and Desoyer(1961) in soil mechanics on consolidation of saturated soils have also influenced the studies on this field. The compressibility of aquifers has been first included in the formulation of groundwater flow by Jacob(1940). Verruijt(1969) has shown that Biot's theory reduces to Jacob's theory when the horizantal deformations are disregarded with respect to the vertical deformations.

A more systematic derivation of the equations of fluid saturated porous media has been given following the formulations used in continuum mechanical theories of binary mixtures(Trusdell and Toupin, 1960) and irreversible thermodynamics(Groot and Mazur, 1962). The former attempt was undertaken by Raats and Klute(1968a, 1968b), Ramirez(1971), Ahmadi and Farshad(1974) and Auriault(1975), the latter by Groenevelt and Bolt(1973). The similarities and differences between these approaches are given by Groenevelt and Bolt(1973).

Now, we will give the basic equations of porous media which are the equations of balance of mass, linear momentum, and moment of momentum for the fluid saturated porous medium. These equations are arrived at by using the equations proposed by Raats and Klute(1968a, 1968b).

1- Balance of Mass: The balance of mass equation is postulated in differential form for water

$$\partial(n\theta_w)/\partial t = -\partial(\theta_w\ \partial W_j/\partial t)/\partial x_j + L \tag{1}$$

and for solid

$$\partial[(1-n)\theta_s]/\partial t = -\partial[\theta_s(1-n)\ \partial U_j/\partial t]/\partial x_j \tag{2}$$

where n denotes the porosity, θ_w and θ_s the density of the fluid and solid phase respectively, and W and U the displacements of the fluid and solid parts respectively relative to their initial position. Fluid displacement is defined such that the displaced fluid volume is obtained when W is multiplied by the total cross sectional area of porous material. L denotes the time rate of supply of mass of water per unit volume. In leaky aquifers, the inflow of water through the confining bed is represented by this term. When the solid part is incompressible, eq.2 becomes

$$\partial n/\partial t = \partial[(1-n)\ \partial U_j/\partial t]/\partial x_j \tag{3}$$

The strain components of the solid are defined as

$$\epsilon_{ij} = (\partial U_j/\partial x_i + \partial U_i/\partial x_j)/2 \tag{4}$$

The dilatation for solid part is

$$\epsilon = \nabla . U = \epsilon_{ii} \tag{5}$$

The relevant strain of the fluid is also the dilatation

$$\epsilon_w = \nabla . W \tag{6}$$

If compression is assumed to be strictly vertical without any horizantal displacement as in the case of most land subsidence problems

$$\epsilon = \epsilon_{xx} \tag{7}$$

2- Balance of Linear Momentum: A differential form can be given for the solid matrix in terms of effective stresses σ_{ij} for quasi-static case

$$\partial(\sigma_{ij} - p\delta_{ij})/\partial x_j = 0 \tag{8}$$

where p is the fluid pressure. The stresses in eq.8 are incremental stresses, therefore the body forces do not appear.

The deformations of the porous medium are caused by the effective stresses which are transmitted through the grain to grain contacts of the porous medium. In accordance with the usual sign convention in the theory of elasticity, the normal stress σ_{ii} is taken to be positive under tension. The pore pressure p is taken positive for compression, in accordance with the usual sign convention in the theory of flow through porous media.

The part of the stress tensor due to pore pressure has been found experimentally and theoretically as $(-pn\delta_{ij})$ by Nur and Byerlee(1971). But, when grain compressibility can be neglected , it reduces to form $(-p\delta_{ij})$ as suggested by Terzaghi(1925).

The basic assumption in our problem regarding the stresses is that any changes in vertical compressive stress on the porous medium are balanced by equal and opposite changes in fluid pressure. Therefore, we obtain

$$\sigma_{ij} = p\delta_{ij} \tag{9}$$

3- Balance of Angular Momentum: The law of balance of angular momentum leads to the conclusion that stress tensors are symmetric tensors

$$\sigma_{ij} = \sigma_{ji} \tag{10}$$

Constitutive Equations

The behaviour of specific materials is introduced in the constitutive equations, in which various ideal materials are defined in terms of concepts introduced in the balance equations. The main restriction on the constitutive equations is that they satisfy the principle of material indifference as mentioned by Truesdell and Toupin(1960). The proposed constitutive equations should be in terms of physically measureable quantities- i.e., pore pressure, porosity, hydraulic conductivity, etc.

A saturated consolidating porous medium requires three constitutive equations,

1- The first constitutive equation is related to the compressibility of fluid phase(water). Under the assumption of elastic fluid, we may write

$$\partial\theta_w/\partial t = \beta\theta_w\ \partial p/\partial t \tag{11}$$

where β denotes the compressibility of water which is assumed to be constant during consolidation.

2- The second constitutive equation is a generalization of Darcy's law. Darcy's law relates the flux of fluid at a point per unit cross sectional area of porous material to pore pressure gradient. In treatment of the problem of flow through compressible porous media, one cannot separate the motion of the fluid from that of the bulk of the porous mass. Now, as the porous matrix also moves during consolidation, the real average velocity of the fluid should be replaced by the relative velocity of the fluid with respect to solid to satisfy the principle of material indifference. Biot(1955) used this treatment in his formulation. Thus, Darcy's law reads

$$[(1/n)\ \partial W_i/\partial t - \partial U_i/\partial t] = -k_{ij}/(n\gamma_w)\ \partial p/\partial x_j \tag{12}$$

where k_{ij} is the hydraulic conductivity and γ_w is the specific weight of water. It has been shown by Bear(1972) that k_{ij} is a symmetric tensor and in an isotropic medium

$$k_{ij} = k\ \delta_{ij} \tag{13}$$

3- For consolidating porous materials the system requires another constitutive equation to describe the deformation of the solid matrix(aquifer). It is assumed that the solid phase(grains) of porous material is incompressible. This constitutive equation will be expressed in terms of rheological elements. Rheology investigates and expresses the relationship between stresses and strains. Thus, the general form of rheological equation is

$$R(\ \epsilon_{ij},\ \dot{\epsilon}_{ij},\ \sigma_{ij},\ \dot{\sigma}_{ij}\ ) = 0 \tag{14}$$

where a dot over a variable indicates time differentiation. There are many rheological materials. Elastic, viscoelastic, and plastic materials are the most widely used ones. The linear relationship between the components of the stress and strain tensor are characteristics of a Hookean elastic material which is represented with an elastic spring. Plastic materials have irreversible stress-strain relations, but that relation does not consider the influence of rate effects. Viscoelastic materials comprise those in which time and rate effects play an important role in their response to stress. In this section, first a time dependent stress-strain relation will be given and later rate-independent plastic constitutive equations will be given as an alternative.

3.A- Choice of Viscoelastic Model and Derivation of Viscoelastic Constitutive Equations: The compaction of aquifers can be considered in two phases which are called primary and secondary. In the primary consolidation the soil skeleton is compressed because of linear coupling of solid and fluid components. During this phase, the viscous behavior of the soil skeleton which is related to the microscopic structure of the soil-water system is not considered. During this phase soil can be likened to a system of rigid particles connected by springs as mentioned by Biot(1941). By this assumption the elastic response of the soil skeleton is isolated.

Investigations on the structure of fine grained soils such as clay and peat have shown that the soil skeleton is composed of an assemblage of very small segments; between the segments connecting in edge to face contact, there is a thin layer of adsorbed water which binds up the segments. Segments in the skeleton are assumed to bind themselves by interparticle force (Coulomb and London-Van Der Waals forces) as mentioned by Tan (1959). It is this skeleton structure which is assumed to be responsible for the secondary phase of consolidation. The viscous response which characterizes this phase has a nature that approaches a stable limit with time.

A review of viscoelastic soil mechanics in the light of these observations shows that Merchant's(1939) model is a realistic device to explain the compaction of aquifers. Therefore it will be used to express the stress-strain relation of the aqifer material under compression.

Merchant assumes that primary and secondary consolidation start simultaneously. It can be shown that Merchant's differential equation corresponds to that obtainable for a body consisting of a Hookean spring placed in series with a Kelvin body; a Kelvin body consists of a linear spring placed in parallel with a linearly viscous dashpot. The kelvin body was assumed to represent the behaviour of the soil under secondary consolidation whereas the Hookean element was assumed to describe behaviour during primary consolidation. For the compression phase of the displacement, the total strain of this system is

$$Eq''_o \epsilon + Eq''_1 \partial\epsilon/\partial t = (q''_o+E)\, p + q''_1 \partial p/\partial t \qquad (15)$$

where E and q''_o are the elasticity modulu of the Hookean spring and of the spring of the Kelvin body, respectively. q''_1 is the viscosity of the model. This equation can be solved by the Laplace transformation for any known function p of time as described by Brutsaert and Corapcioglu(1976). So the solution is as follows when the body initially is free of stress and strain

$$\epsilon(t) = \alpha_1\, p(t) + (1/q''_1) \int_0^t p(\nu) \exp(-1/[\alpha_2 q''_1]\,[t-\nu])\, d\nu \qquad (16)$$

where $\alpha_1=1/E$ and $\alpha_2=1/q''_o$. α_1 and α_2 denote primary and secondary compressibilities. Eq. 16 is the viscoelastic constitutive equation of the porous material during compression. Since the porous material is assumed to be a continuum, the force acting on the spring and on the Kelvin body is actually the stress moreover, as the displacement is in the vertical only, on account of eq.9 this stress equals the incremental fluid pressure p. For recovery phase of the loaded aquifer,

$$\begin{aligned} \epsilon &= 0 && \text{for} \quad p_{ex} < p < 0 \\ \epsilon(t) &= \alpha_1 p(t) && \text{for} \quad 0 \le p \end{aligned} \qquad (17)$$

where p_{ex} is the maximum stress reached during compression. Zero level would indicate the original equilibrium stress prior to loading. As seen, during recovery, material shows elastic behaviour. The strain of the Kelvin body is irreversible.

3.B- Rate-independent Constitutive Equation

In the previous section, a time dependent equation was given. In this section an alternative equation will be suggested for a porous material with plastic rate-independent properties.

Assume first that the strains are the sum of elastic and plastic components in the usual way

$$\epsilon_{ij} = \epsilon_{ij}^{e} + \epsilon_{ij}^{p} \qquad (18)$$

and that elastic strains are related to the effective stresses thru Hooke's law and they constitute the reversible part of the consolidation. The stress-strain relation for plastic materials is given by the flow rule

$$d\epsilon_{ij}^{p} = \lambda\ \partial f/\partial\sigma_{ij} \qquad (19)$$

where λ denotes the proportionality constant, and $d\epsilon_{ij}^{p}$ plastic strain increments. f is the yield function which is a locus of points bounding the elastic region of the stress plane. All combinations of the stresses on the yield locus cause irreversible plastic strains. Therefore, a yield function defines the state of stress under which the plastic flow may begin. There have been many attempts in the past to obtain a yield criterion considering the volume change of porous materials during compression. A review of these attempts are given by Corapcioglu (1976). As seen in this review, the yield function for a porous material is basicly a function of the first and second invariants of the stress tensor.

$$J_1 = \sigma_{ii} \quad ; \quad J_2' = (1/2)\ S_{ij}\ S_{ij} \quad \text{where} \quad S_{ij} = \sigma_{ij}-(J_1/3)\delta_{ij} \qquad (20)$$

In a conventional fully-dense material, yielding is a function only of J_2'. The yield criterion of Kuhn and Downey(1971) has been borrowed from powder metallury for this purpose, with some modifications. The yield function of Kuhn and Downey(1971) is

$$Y = \left[(2+2\mu)\ J_2' + (1-2\mu)/3\ J_1^2\right]^{\frac{1}{2}} \qquad (21)$$

where μ is Poisson ratio and Y is the yield stress of the material in simple compression test. Y is a function of porosity for porous materials. μ can be related to porosity as

$$\mu = 0.5(1-n)^m = 0.5\bar{\theta}^m \qquad (22)$$

Kuhn and Downey give m=1.92 experimentally. In this study, we will assume m=2. The strain increments are obtained in terms of principal stresses by using eq.19.

$$d\epsilon_1 = (\lambda/Y)\ [\sigma_1 - \mu(\sigma_2+\sigma_3)] \qquad (23)$$

$$d\epsilon_2 = (\lambda/Y)\ [\sigma_2 - \mu(\sigma_3+\sigma_1)] \qquad (24)$$

$$d\epsilon_3 = (\lambda/Y)\ [\sigma_3 - \mu(\sigma_1+\sigma_2)] \qquad (25)$$

From eqs.24 and 25, $\sigma_2 = \sigma_3 = \sigma_1 \mu/(1-\mu)$ (26)
by considering only vertical deformation(eq.7). Therefore, the density change is

$$-d\overline{\theta}/\overline{\theta} = d\epsilon_1 \quad \text{which gives} \quad \epsilon_1 = \ln(\theta_o/\overline{\theta}) \tag{27}$$

where $\overline{\theta}$ is the relative density which is ratio of the density of the soil skeleton to solid density and θ_o is the initial relative density. ϵ_1 is defined as the true strain which is equal to ln of 1+conventional strain. So eq.22 becomes $\mu=0.5\theta_o^2/(1+\epsilon)^2$ (28)
Eq.21 takes the following form by inserting eqs.26 and 28 and by making use of eq.9

$$p = Y(n)/[(1-\theta_o^2/(1+\epsilon)^2)(1+0.5\theta_o^2/(1+\epsilon)^2)/(1-0.5\theta_o^2/(1+\epsilon)^2)]^{\frac{1}{2}} \tag{29}$$

Derivation of Groundwater Flow Equation

The equation governing the pore pressure distribution can be obtained by combining the stress-strain relationship (either viscoelastic or plastic) with generalized Darcy's law and continuity equations together with the assumptions for strain and stress.

The displacement of the fluid can be eliminated first by multiplying eq.12 by θ_w, then taking the divergence and substituting eq.1. The resulting equation is reduced to a simpler form by disregarding the second order terms and using eqs.3 and 11. The details of the derivation are given in Brutsaert and Corapcioglu(1976). Finally, we obtain,

$$\partial\epsilon/\partial t + (\beta n)\, \partial p/\partial t - L = (k/\gamma_w)\, \nabla^2 p \tag{30}$$

Eq.30 represents the flow of water in porous media together with the constitutive equation which is either eq.16 or eq.29.

Flow Equation for a Viscoelastic Consolidating Porous Media

By substituting eq.16, eq.30 takes the following form in terms of drawdown. The drawdown in a well can be calculated simply by dividing the pressure by the specific weight of water. It is true, although the compressibility of water is considered. Since any observation well behaves like a manometer and the water in the well is not under compression. So, for a leaky aquifer

$$(k/\gamma_w)\, \nabla^2 s - k_1\, s/(bb_1\gamma_w) = (n\beta+\alpha_1)\, \partial s/\partial t + (1/q_1'').$$
$$\partial[\int_0^t s(\nu)\, \exp(-[t-\nu]/[\alpha_2 q_1''])\, d\nu]/\ t \tag{31}$$

In leaky aquifers, the term for leakage flow thru its top end is directly related to leakance (k_1/b_1) where k_1 is the hydraulic conductivity and b_1 is the thickness of the confining layer. Eq.31 is the groundwater flow equation in a viscoelastic, saturated, homogeneous leaky aquifer with one dimensional displacement of soil skeleton which has the stress-strain relation of eq.16. Note that for an elastic porous material with compressibility α_1, eq.31 reduces to the Hantush and Jacob(1955) equation. When water is drawn at a steady rate of flow, Q, thru a single fully penetrating well, in an extensive leaky aquifer of uniform thickness b, eq.31 is subject to the following conditions

$$\lim_{r\to 0} [r\ \partial s/\partial r] = -Q/(2\pi kb) \quad ; \quad s(\infty,t) = 0 \quad ; \quad s(r,0) = 0 \tag{32}$$

By using the solution technique of Brutsaert and Corapcioglu(1976) governing equation can be reduced by the Laplace transformation and the convolution theorem to an ordinary equation, whose solution can be inverted by applying Schapery's (1961) approximate method. The resulting solution is

$$s = [Q/(2\pi kb)]\ K_o[r\ [\gamma_w(n\beta + \alpha_1 + 2k_1t/(bb_1\gamma_w) + 2\alpha_2 t/[q_1''\alpha_2 + 2t])/(2kt)]^{-\frac{1}{2}}] \tag{33}$$

where K_o is the zero order modified Bessel function of the second kind. The application of eq.33 requires the determination of 5 parameters. (kb) and $(bb_1k/k_1)^{\frac{1}{2}}$ can be determined by the method of Hantush(1956). As shown by Brutsaert and Corapcioglu(1976) α_1, α_2 and q_1'' can be obtained from subsidence data.

In the recovery phase, the drawdown can be described by the Hantush and Jacob's(1955) solution, that is

$$s = [Q/(4\pi T)]\ W(u, r/(bb_1k/k_1)^{\frac{1}{2}}) \tag{34}$$

where $W(u,r/B)$ is the well function for leaky aquifers with $u= r^2S/(4Tt)$, $T=kb$, the transmissivity and $S=b\gamma_w(n\beta+\alpha_1)$ the storage coefficient.

The amount of subsidence and recovery can be calculated by using eqs.16 and 17 respectively.

Flow Equation for a Plastic Consolidating Porous Media

Eq.30 can be solved by using stress-strain equation given by eq.29 with conditions in eqs.32. An analytical solution seems impossible. But a numerical solution could be obtained. The numerical technique of Rushton and Booth(1976) might be useful to apply the problem in radial coordinates. The yield stress Y, has to be determined from simple compression tests in the laboratory.

Plasticity theory for fluid saturated porous media is at a very early stage of development. Further theoretical and experimental work is required.

Conclusion

Prediction of subsidence by use of the viscoelastic model requires practical evaluation of the parameters under the conditions existing in the field. This field approach by considering the aquifer as a whole instead of by analyzing a large number of individual layers in it, is preferable. The latter method is expensive and time consuming because of extensive data collection and laboratory tests. This approach should consider the average properties of soil layers in the aquifer. By using the viscoelastic modelling an important characteristic of clay layers existing in the aquifer systems is represented. An applicat-

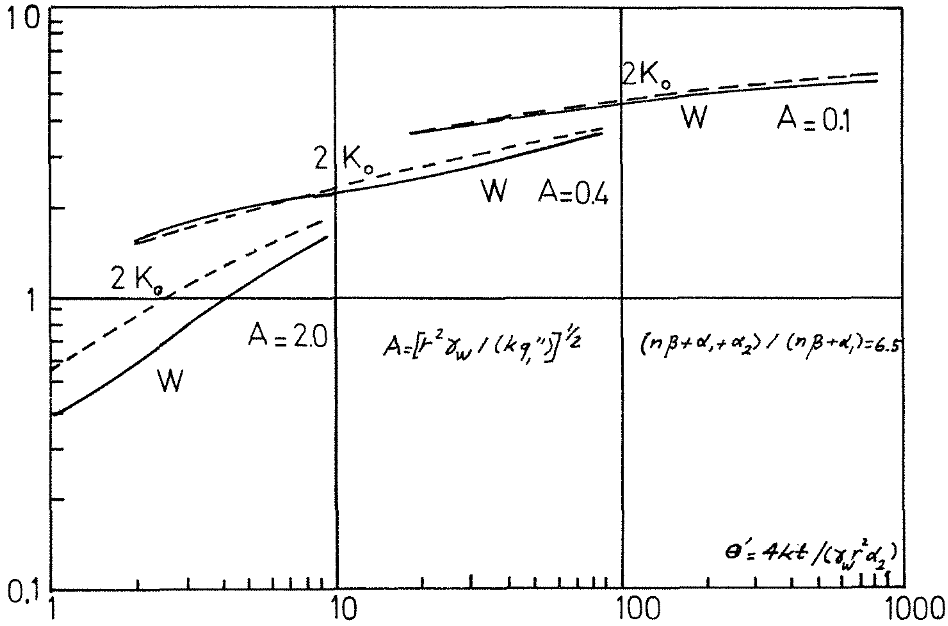

Figure 1- Comparison of exact and approximate solutions for a confined aquifer.

ion of the model by Corapcioglu and Brutsaert(1976) gave satisfactory results for the subsidence in the San Joaquin Valley in California. In the case of rate-independent aquifer materials as mentioned by Helm(1976), the proposed plastic model of eqs. 29 and 30 might give an alternative approach. But, the application of this model require laboratory tests for determination of the yield stress.

To estimate the accuracy of the Schapery's(1961) approximate inversion it may be some interest to consider the case of confined aquifer with same viscoelastic model for which the exact solution is available by making an analogy to Boulton's(1963) equation. A comparison between W(exact solution) and K_0(approximate solution) reveals that both solutions are quite close within practical limits.

References

Ahmadi, G., and Farshad, M., 1974, On the Continuum Theory of Solid-Fluid Mixture: Ind. J. Tech., v. 12, p.195-198.

Auriault, J. L., 1975, Sur la Rheologie d'un Milieu Poreux Sature Consolidant: Arch. Mech., v. 27, p. 363-370.

Bear, J., 1972, Dymamics of Fluids in Porous Media: American Elsevier Co. New Yory, N. Y., 139 p.

Biot, M. A., 1941, General Theory of Three-dimensional Consolidation: J. App. Phys., v. 12, p.155-164.

Biot, M. A., 1955, Theory of Elasticity and Consolidation for a Porous Anisotropic Solid: J. App. Phys., v. 26, p.182-185

Biot, M. A., 1972, Theory of Finite Deformations of Porous Solids Indiana Univ. Math. J., v.21, p. 597-620

Boulton, N. S., 1963, Analysis of Data from Nonequilibrium Pumping Tests Allowing for Delayed Yield from Storage: Proc. Inst. Civil Eng., v. 26, p. 469-482
Brutsaert, W., and Corapcioglu, M. Y., 1976, Pumping of Aquifer with Viscoelastic Properties: Proc. ASCE, HY11, v.102.
Corapcioglu, M. Y., 1976, Yield Criterions of Porous Materials: (submitted to Powder Technology)
Corapcioglu, M. Y., and Brutsaert, W., 1976, Viscoelastic Aquifer Model Applied to Subsidence Due to Pumping(to be published in Water Resour. Res.)
Groenevelt, P. H., and Bolt, G. H., 1973, Theory of Transport in Solis: Ecological Studies, v.4, Springer, Berlin, 43 p.
Groot, S. R., and Mazur, P., 1962, Nonequilibrium Thermodynamics: North- Holland Pub. Co. Amsterdam.
Hantush, M. S., 1956, Analysis of Data from Pumping Tests in Leaky Aquifers: Trans. Ame. Geophy. Un., v.37, p. 702-714.
Hantush, M. S., and Jacob, C. E., 1955, Steady Three-Dimensional Flow to a Well in a Two-Layered Aquifer: Trans. Ame. Geophy. Un., v.36, p. 286-292.
Heinrich, G., and Dsoyer, K., 1961, Theorie of Dreidimensionnaler Setzungsvorgaenge in Tonnschichten: Ing. Arch., v.300
Helm, D., 1976, Personal Communication.
Jacob, C. E., 1940, The Flow of Water in an Elastic Artesian Aquifer: Trans. Ame. Geophys. Un., v. 21, p. 574-586.
Kuhn, H. A., and Downey, C. L., 1971, Deformation Characteritics and Plasticity Theory of Sintered Powder Materials: Int. J. Powder Met., v. 7, p. 15-25.
Merchant, W., 1939, Some Theoretical Considerations on the One-Dimensional Consolidation: S.M. Thesis, M.I.T.
Nur, A., and Byerlee, J. D., 1971, An Exact Effective Stress Law for Elastic Deformation of Rocks: J. Geophys. Res., v.76.
Paria, G., 1963, Flow of Fluids Through Porous Solids: App. Mech. Rev., v. 16, p. 421-423.
Poland, J. F., Lofgren, B. E., and Riley, F.S., 1972, Glossary of Selected Terms..........: U.S.G.S. Water Supply P.2025
Raats, P. A. C., and Klute, A., 1968a, Transport in Soils: The Balance of Mass: Soil Sci. Soc. Ame. Proc., v.32,p.161-166
Raats, P. A. C., and Klute, A., 1968b, Transport in Soils: The Balance of Momentum: Soil Sci. Soc. Ame. Proc., v.32,p.167
Ramirez, A. G., 1971, Constitutive Equations for the Flow of Incompressible Fluids: Israel J. Tech., v.9, p.411-425.
Schapery, R. A., Approximate Methods of Transform Inversion for Viscoelastic Stress Analysis: 4th U.S. Nat. Cong. of Mech.
Scheidegger, A.E., 1974, The Physics of Flow Through Porous Media: 3th Ed., Toronto Univ. Press, Toronto.
Suklje, L., 1969, Rheological Aspects of Soil Mechanics: Wiley-Interscience, London.
Tan, T. K., 1959, Structure Mechanics of Clays: Scientica Sinica, v. 8, p. 83-97.
Terzaghi, K., 1925, Erdbaumechanik auf Bodenphysikalischer Grundlage: Deuticke, Wien.
Truesdell, C., and Toupin, R. A., 1960, The Classical Field Theories, Handbuch der Physik, III/1:226-793, Springer, Berlin.
Verruijt, A., 1969, Elastic Storage of Aquifers, in Flow Through Porous Media, Academic Press, New York, N.Y., p.331-376.

Publication n°121 of the International Association of Hydrological Sciences
Proceedings of the Anaheim Symposium, December 1976

ANALYSIS OF LAND SUBSIDENCE BY THE VERTICAL TWO DIMENSIONAL MULTI-AQUIFER MODEL

Akira Kamata*, Kazuhiko Harada* and Hisashi Nirei**
*Kokusai Aerial Surveys Co., Ltd. **Chiba Prefectural Institute for Enviromental Pollution, Japan

Abstract

The settlement in the deep stratum was studied by the digital simulation model. The simulation model was constructed along the main geological cross section of the land subsidence area.

The basic groundwater flow equation introduced to the model assumed that flow is two dimensional in the vertical plane (X-Z plane).

The hydrogeological profile was subdivided into square unit area (cell) as a digital form in the model. And the actual water balance calculation was made at the unit cell neglecting water flow in the y-direction.

The solution of the water balance equation was obtained by A.D.I. method. And then, the compression of unit cell was calculated by the following equation.

$$\Delta m = \Delta Z \cdot m_v \cdot \gamma w \cdot \Delta h$$

where Δm: the compression of each unit cell, ΔZ: vertical length of each unit cell, γ_w: unit weight of water, Δh: change of groundwater head at each cell, m_v: coefficient of volume compressibility.

The aggregate compression in each column which corresponds to the settlement of land subsidence M is expressed as

$$M = \Sigma(m_v \cdot \gamma_w \cdot \Delta h \cdot \Delta Z)$$

The calculated settlement and groundwater head distribution were in satisfactory agreement with the observed value.

Introduction

The land subsidence phenomena which is resulting from overdevelopment of groundwater and natural gas resources is spreading in many urban areas in Japan. Moreover, settlement of deep stratum, such as Pleistocene and Pliocence deposits which have relatively low compressibility, appeared with the progress of the development of deeper aquifers.

The problem on the settlement of deep stratum is not fully discussed because of a few information on underground geology and characteristics of rock mechanics in the land subsidence area of Japan.

In order to obtain a definite policy for the countermeasure of land subsidence and groundwater basin management, a simulation study carried out by the authors and the staffs of Chiba Prefectural Research Institute for Enviromental Pollution in 1972. The purpose of this paper is to show the way of land subsidence analysis from the previous work briefly.

Groundwater Balance Model

On the cubic cell shown in Fig. 1, if water flow in the y direction is neglected, water volume through the area ABCD is expressed by Darcy's law

$$q_2 = K_{xx} \frac{h_2 - h_0}{\Delta x} \Delta y \cdot \Delta z \tag{1}$$

where K_{xx} is the coefficient of permeability in x direction, h_2 and h_0 are

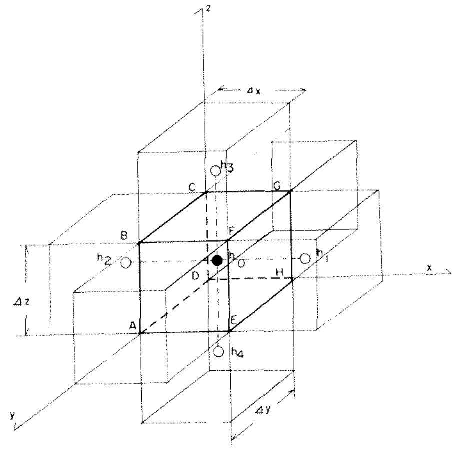

Fig. 1 Groundwater Balance in Unit Cubic Cell

groundwater head at the center of the unit cubic cells, Δx, Δy and Δz are the unit length of the cell in x, y, and z direction respectively. Same equations are obtained to the groundwater flow through other areas,

$$q_1 = K_{xx} \frac{h_1 - h_0}{\Delta x} \Delta y \cdot \Delta z \tag{2}$$

$$q_3 = K_{zz} \frac{h_3 - h_0}{\Delta z} \Delta x \cdot \Delta y \tag{3}$$

$$q_4 = K_{zz} \frac{h_4 - h_0}{\Delta z} \Delta x \cdot \Delta y \tag{4}$$

where k_{zz} is the coefficient of permeability in z direction.

Total groundwater volume flowing through four areas must be equal to the change of storage in and discharge from or recharge to the central unit cell. Thus,

$$K_{xx} \frac{h_1 + h_2 - 2h_0}{\Delta x} \Delta y \Delta z + K_{zz} \frac{h_3 + h_4 - 2h_0}{\Delta z} \Delta x \Delta y$$

$$= S_s \frac{\partial h}{\partial t} \Delta x \Delta y \Delta z + W \tag{5}$$

where S_s is the specific storage and W is the source or sink term.

Dividing by Δx, Δy, Δz and assuming that time increment is Δt, Eq.(5) becomes

$$K_{xx} \frac{\bar{h}_1 + \bar{h}_2 - 2\bar{h}_0}{\Delta x^2} + K_{zz} \frac{\bar{h}_3 + \bar{h}_4 - 2\bar{h}_0}{\Delta z^2}$$

$$= S_s \frac{\bar{h}_0 - h_0}{\Delta t} + \frac{W}{\Delta x \Delta y \Delta z} \tag{6}$$

If $\bar{h}$ is unknown, the above equation is the implicit finite difference apporoximation of two-dimensional groundwater flow equation.
The solution of Eq.(6) can be obtained by A.D.I method which was devised by

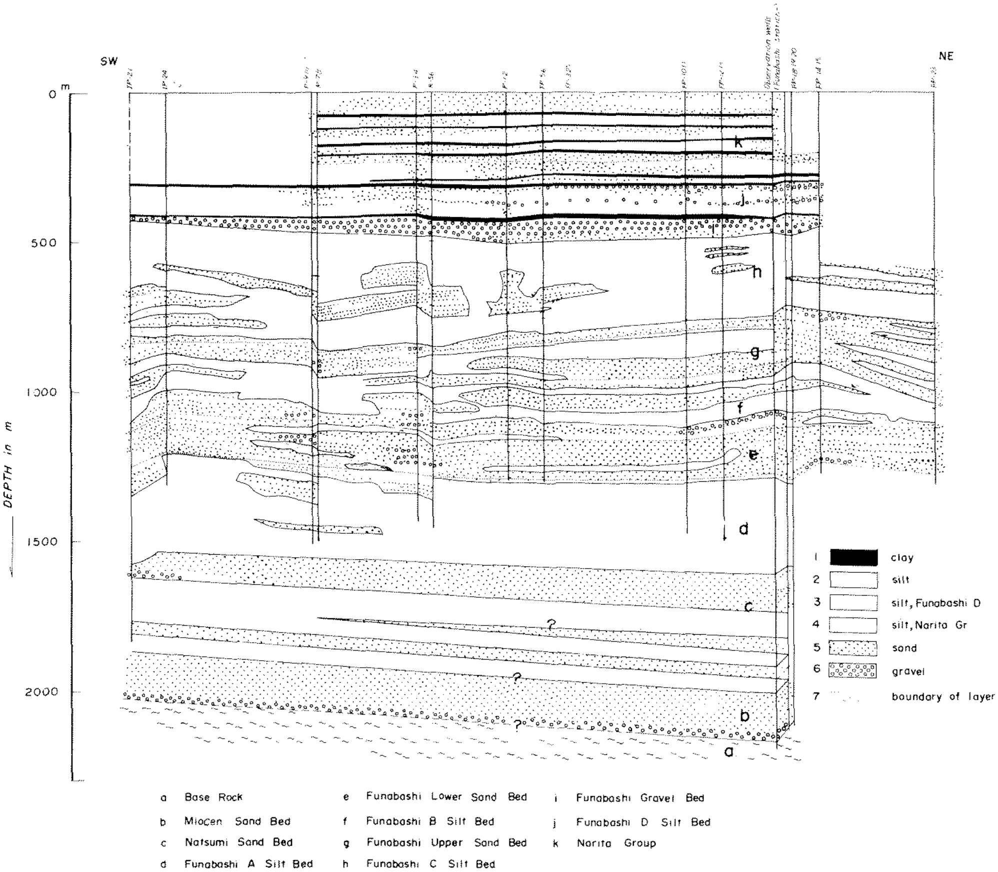

Fig. 2 Geological Cross Section of Funabashi Basin

Peaceman and Rachford (1955) under the arbitrary initial and boundary conditions.

The obtained result shows the groundwater head at each cubic cell. The change of groundwater head in time increment Δt is shown as

$$\Delta h_{ij}^{k} = h_{ij}^{k+1} - h_{ij}^{k} \tag{6}$$

where i and j are the subscript of nodal spacing, k is the subscript of time increment.

Compression of Stratum

By Lohman (1961), the deformation of an aquifer caused by the lowering of groundwater pressure is shown as

$$\Delta m = \alpha m \Delta p \tag{7}$$

where Δm is volume change of the aquifer in vertical direction, α is the vertical compressibility, m is the original thickness of aquifer, and Δp is the change of groundwater pressure.

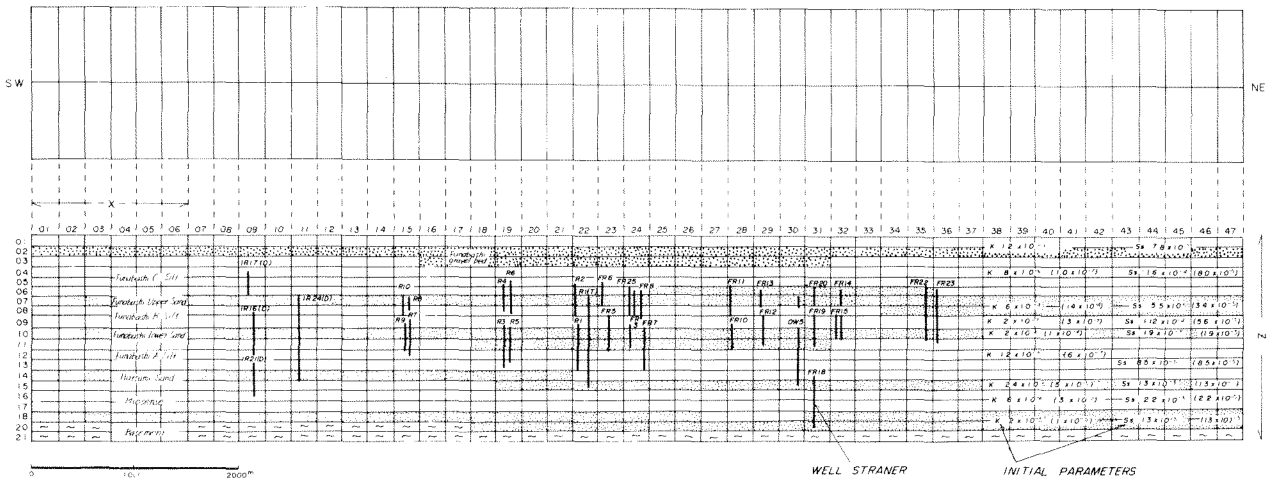

Fig. 3 Finite Difference Network of Funabashi Basin

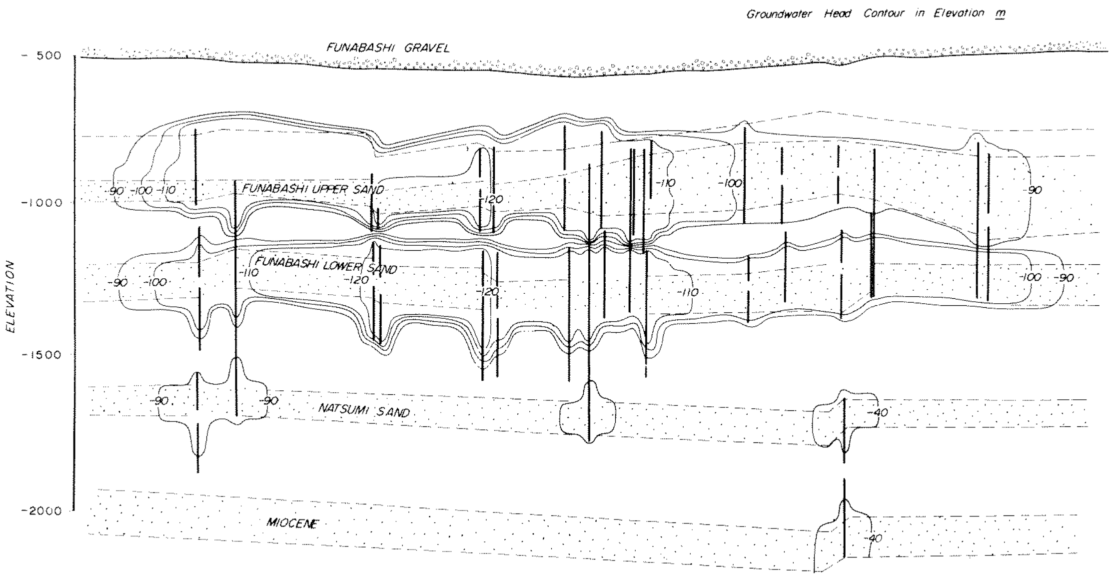

Fig. 4 Distribution of Groundwater Head in 1970

By the definition, specific storage S_s can be written as

$$S_s = \rho wg(\alpha + n\beta) \quad (8)$$

where ρw is the density of water, g is the accelation due to gravity, n is the porosity and β is the compressibility of water.

Assuming that β equals to zero, then Eq. (7) becomes

$$\Delta m = \frac{S_s}{\rho wg} m\Delta P$$

$$= m_v \cdot m \cdot \gamma w \cdot \Delta h \quad (9)$$

where m_v is the coefficient of volume compressibility, γw is the unit weight of water and Δh is the change of groundwater head.

The groundwater head decline in an unit cell which caused by pumping is obtained by the solution of water balance equation. Therefore, compression of each unit cell is expressed as

$$\Delta m_i = m_v \cdot \Delta Z_i \cdot \gamma w \cdot \Delta h_i \quad (10)$$

where i denotes the subscript of cell number in vertical direction (column), ΔZ_i is the vertical original length of unit cell.

The aggregate compression in each column which corresponds to the settlement of land subsidence M is expressed as

$$M = \Sigma\ (m_v \cdot \gamma_w \cdot \Delta h_i \cdot \Delta Z_i) \quad (11)$$

Aquifer System

The studied area, Funabashi gas field, is about 50 km^2 alluvial lowland which is located along the north-eastern coast of Tokyo Bay.

The geologic formation underlying the studied area is classified into 12 layers. A generalized section clarified by well log is as follows.

Geologic Age		Named Rock Unit and Lithology	Depth m
Recent	1	Alluvial deposit	
Pleistocene	2	Narita Group (sand, gravel, clay)	215
	3	Funabashi D Silt Bed	403
	4	Funabashi Gravel Bed	454
	5	Funabashi C Silt Bed	840
Pliocene	6	Funabashi Upper Sand Bed	930
	7	Funabashi B Silt Bed	1,090
	8	Funabashi Lower Sand Bed	1,250
	9	Funabashi A Silt Bed	1,720
	10	Natsumi Sand Bed	1,920
Miocene	11	Not named (gravel, sand, silt)	2,149
	12	Base Rock (shist)	

A shematic profile is shown in Fig. 2.

The layer 1 and 2 have unconfined or confined groundwater.
The layer 3 to layer 11 have confined groundwater containing natural dissolved gas. The development of natural gas resource carried out from 1955 to 1971 by 1,000 - 1,500 m deep wells. The total amount of withdrawal reached 12.2 x 10^6 m^3 through 12 years.
There are regulary carried out geodetic measurements for investigation of land subsidence since 1963. Results of this investigation show that the maximum recorded value is 120 cm at Minato-cho, Funabashi in the period from 1963 to 1971.

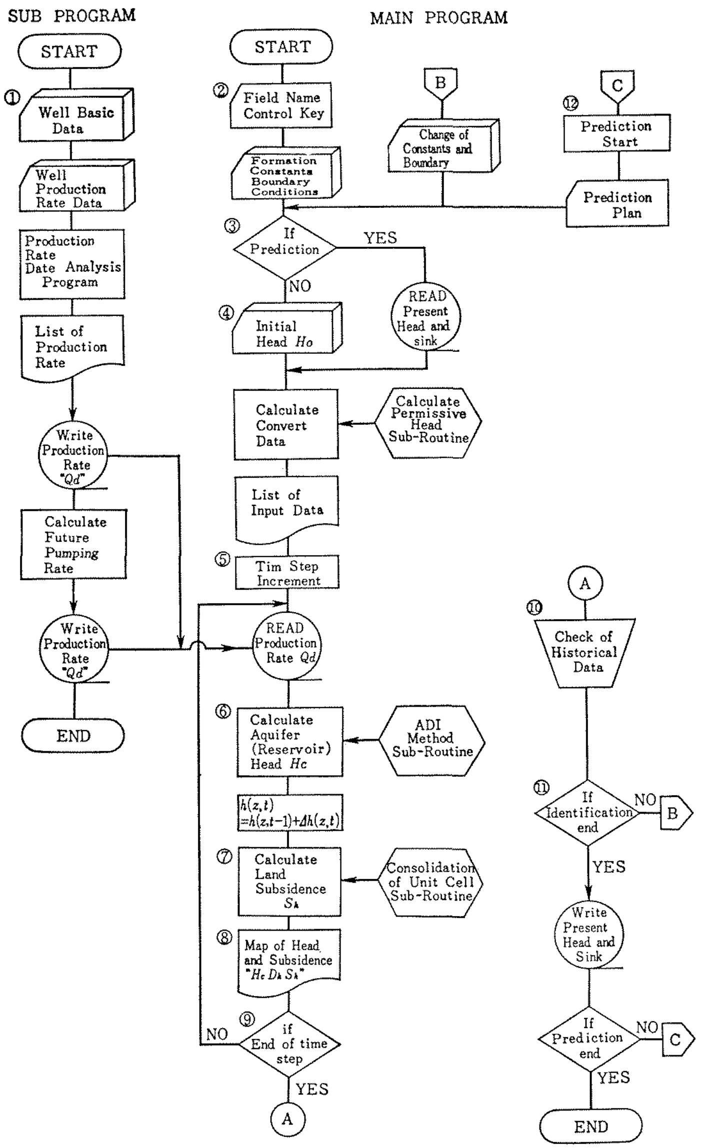

Fig. 5 Simplified Flow Chart of Simulation Procedure

Modeling of Groundwater Basin

The hydrogeological profile is divided into rectangular unit cell as digital form. Fig. 3 shows the finite difference network in vertical cross section of Funabashi gas field. The size of each cell is same on a column in the x or z direction. The profile was subdivided into 1034 cells and

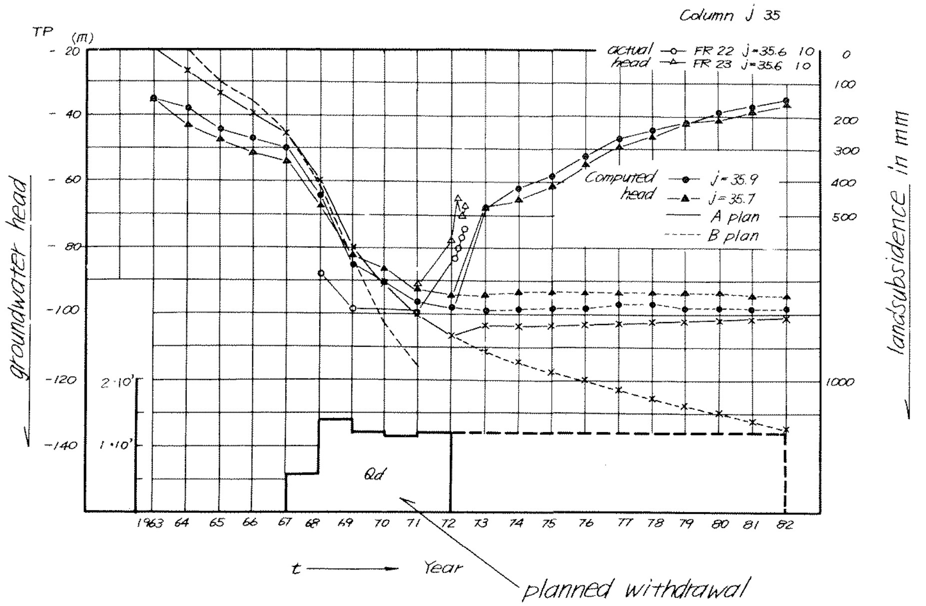

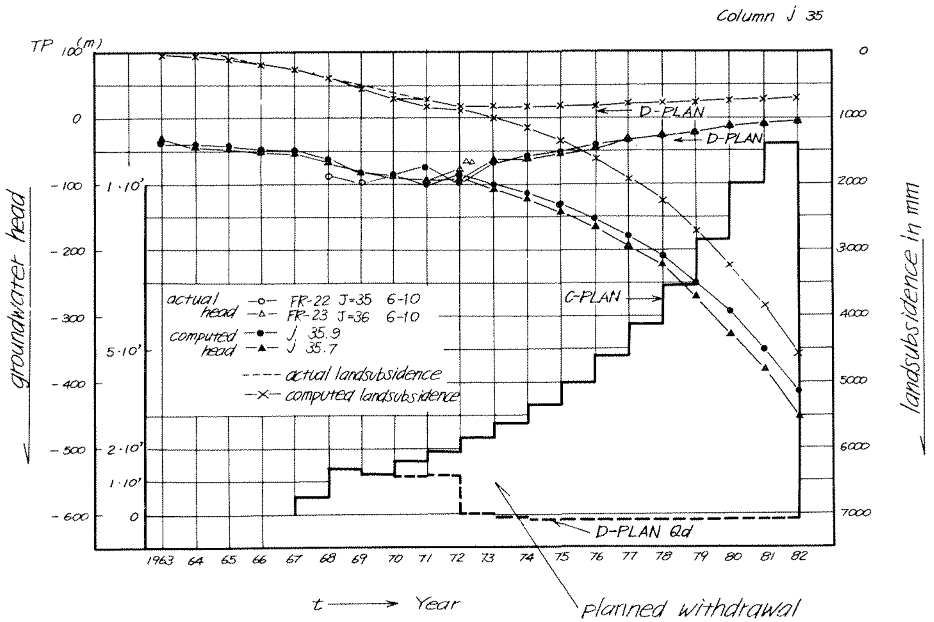

Fig. 6 Prediction of the Grounwater Head and Land Subsidence

Δx was 250m and Δz was 100m.

The groundwater flow in the vertical cross section is two dimensional, however, the model for the caluculation has width Δy. The actual water balance calculation is made at the unit cell neglecting groundwater flow in the y direction. Δy is set into both sides from the section line of the profile with the width of $\Delta y/2$ respectively. Δy of the studied model is 1,500m.

Groundwater Head and Landsubsidence

The lowering of groundwater head due to extraction of groundwater is shown in Fig. 4. This iso-groundwater head line on the profile is made by plotting the screen position and their groundwater head at the same period of the wells located in the zone with the width Δy. These contour maps are made according to the change of groundwater head through years. The groundwater head in each unit cell in each period can be taken as digital by reading the above iso-groundwater head lines superimposing the profile.

Initial and Boundary Condition

The groundwater head distribution at the least development stage in the above process is put into the model as the initial condition.

The boundary conditions are treated as follows.

(1) Closed boundary: If the upper most cells or bottom cell are formed of the impermeable bed where no recharging flow is expected, this condition is applied.

(2) Constant groundwater head: When the upper most unit area are formed of water table aquifer or closed to river, lake or pond with constant water level where recharging flow into deeper aquifer is expected, this condition is applied to the model.

The boundary conditions introduced to the Funabashi model were as follows.

(a) Upper most boundary: Column No. J=16∿31 (constant groundwater head), J=1∿15 and 31∿50 (closed)

(b) Lower boundary: Closed

(c) Both sides: Constant groundwater head (except I=12∿20 of left side)

Aquifer Parameters

The initial values for the parameters applied to the layers were taken from the laboratory consolidation tests of core samples. These parameters are inspected through the test operation of the simulation model by observing the response.

The final values for the parameters applied to the model were as follows.

	Layer	Permeability Coefficient (cm/s)	Specific Storage (1/m)
1	Funabashi gravel	1.2×10^{-3}	7.8×10^{-5}
2	Funabashi C Silt	8.0×10^{-6}	1.6×10^{-4}
3	Funabashi Upper Sand	6.0×10^{-4}	5.5×10^{-5}
4	Funabashi B Silt	2.0×10^{-5}	1.12×10^{-4}
5	Funabashi Lower Sand	2.0×10^{-4}	1.9×10^{-5}
6	Funabashi A Silt	1.2×10^{-5}	8.5×10^{-5}
7	Natsumi Sand	2.4×10^{-5}	1.3×10^{-5}
8	Miocene (Silt)	6.0×10^{-6}	2.2×10^{-5}
9	Miocene (Sand)	2.0×10^{-5}	1.3×10^{-5}

Identification of the Model and Prediction

The model was operated through the year 1963 to 1970.
The simplified flow chart of the simulation procedure is shown in Fig. 5.

The parameters are adjusted by correlating the calculated responses to the recorded historical data until an acceptable conformation is achieved. The groundwater head change of an unit cell and the aggregate shrinkage in a column which corresponding to the land subsidence are used for the inspection of interpolation of the model.

The adjustment of aquifer parameters are made in each geologic facies, not one by one in each unit cell for the quick and effective conformation.

The results of computation by using two-dimensional multi-aquifer model are plotted together with the actual values in Fig. 6. Good agreement with the actual groundwater head and landsubsidence can be seen at the identification phase.

After the parameters and the boundary conditions are fixed on the model, the planned withdrawal placed to study its response of future groundwater head decline and the future settlement.

Result of the prediction in Funabashi gas field by this model are as follows.

(1) If the withdrawal in future will be kept the same as it has been since 1971, the land subsidence in 1981 will be estimated to be 10 cm larger.
(2) If the withdrawal was completely ceased in the period from 1972 to 1981, the modest rebound of 2-3 cm can be expected.

Conclusion

The settlement of deep stratum can be analyzed by the vertical two dimensional multi-aquifer model in cross section. This model should be helpful in the observation of the response of the land subsidence and groundwater head decline according to the change of withdrawal of groundwater in each aquifer. For example, the behavior of both shallower stratum and deeper stratum can be examined by the model operation, in which the withdrawal in the shallow aquifers is controlled in the designed depth.

One of the purpose of the simulation is find out the withdrawal plan which cause zero aggregate settlement of land subsidence. The simulation technique will be useful for the estimation of the reduction of withdrawal.

There are some problems remaining unsolved in this model. As a tool of groundwater basin management, three-dimensional model will be required in future to study.

Acknowledgement

The authors wish to thank Dr. T. Shibasaki for offering many helpful comments throughout the study. The authors also wish to thank Messrs. S. Higuchi, Y. Hara and K. Furuno, staffs of Chiba Prefectural Research Institute for Enviromental Pollution, who provide us some technical advise.

References

Chiba Prefectural Research Institute for Enviromental Pollution, 1973, On the Mechanism of Landsubsidence and Consolidation at great Depths in Funabashi Gas Field Japan, Project Report No.1, 129 p.

Lohman, S.W., 1961, Compression of Elastic Artesian aquifers, U.S. Geol. Surv., Profess. Papers, 424-B p. 47-48

Peaceman, D.W., and H.H. Rachford, 1955, The numerical solution of Parabolic and Elliptic Differential Equations, Jour. Soc. Indust. Appl. Math., V3, p. 28-41

Publication n°121 of the International Association of Hydrological Sciences
Proceedings of the Anaheim Symposium, December 1976

LAND SUBSIDENCE RESEARCH AND REGIONAL WATER RESOURCE PLANNING OF THE NANAO BASIN

M. Murakami and Y. Takahasi
Nippon Koei Co., LTD. and Department of Civil Engineering, University of Tokyo
Tokyo, Japan

Abstract

The purpose of this research is to develop realistic methodology and regional water resource planning for artesian groundwater basin of land subsidence area. The Nanao Basin is one of the typical land subsidence area in Japan. The results of the 7 years (1970-1976) obervation wells and simulation study are summerlized in this paper and make a comparative study of the three types of mathematreal simulation models. Based on the predicted simulation results, water resource planning of the Nanao Basin was studied.

The Nanao Basin of an area of 20' Km^2 is roughly rectangular in shape with the long axis of about 10 Km length orientated in an north-west direction. All the running water in the river-channel are used for agriculture and so domestic, industrial and municipal use of water are obliged to depend on the artesian groundwater. Pumping discharge rate of the Nanao Coastal Basin amounts to about 6,500 m^3/ day / km^2.. This excess pumping discharge causes the land subsidence. The maximum subsidence rate amounts to 24 cm/ year, in 1973.

1. Hydrogeology of the basin

Hydrogeological structure of the Nanao Basin coincides with the geological structure of the northern part of Oochi graven which is the largest graven in Japan. Geology of the basin consists of semi-confining layer of allunial silty clay [alluvium I(1)], aquifer of middle quarternary "Okuhara" sand-silt layer [diluvium I(2)], lower quarternary "Tokuda" sand-gravel layer [diluvium II (3)], middle miocene "Akaura" coarse sand layer [tertiary 1(4)] and impermeable basement of creaceous granitic rocks or lower miocene andesite rocks. Thickness of the alluvial silty clay layer is 5 - 20 meters, and aquifer of [diluvium I(2)] 30 - 70 meters, [diluvium II (3)] 40 - 80 meters, [tertiary I(4)] 100 - 250 meters in descending order. So the sediment of the basin is not so thick about 200 - 300 meters and the boundary condition of the basin is simple, that the Nanao basin is suitable for computer simulation modeling.

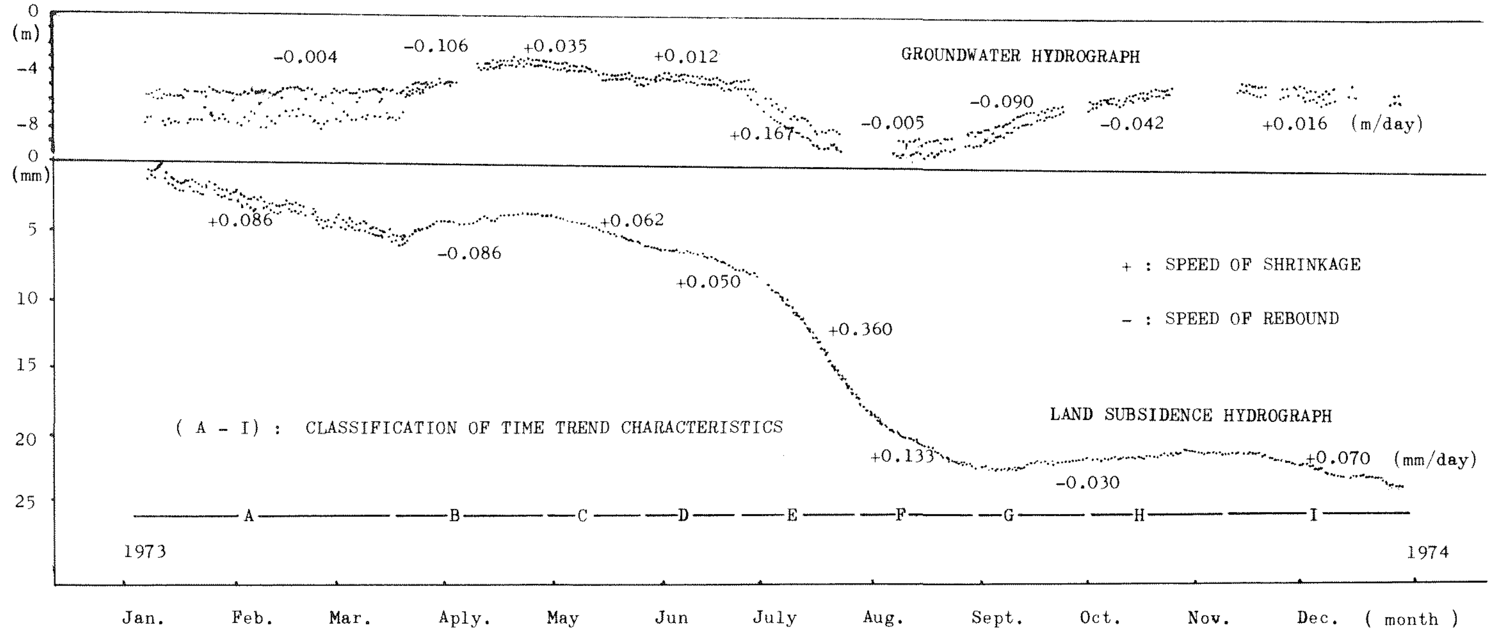

Figure - 1 Hydrograph of Groundwater and Land Subsidence (1973 - 1974)

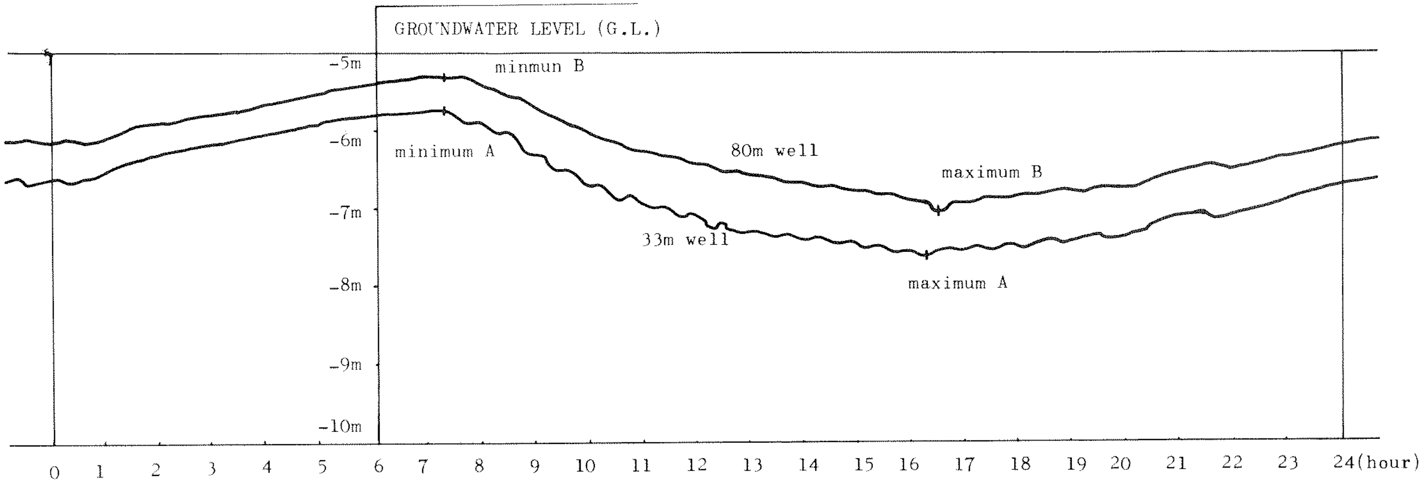

Figure - 2 Daily cyclic Groundwater Level Change of Observation Wells (1973. 2.25)

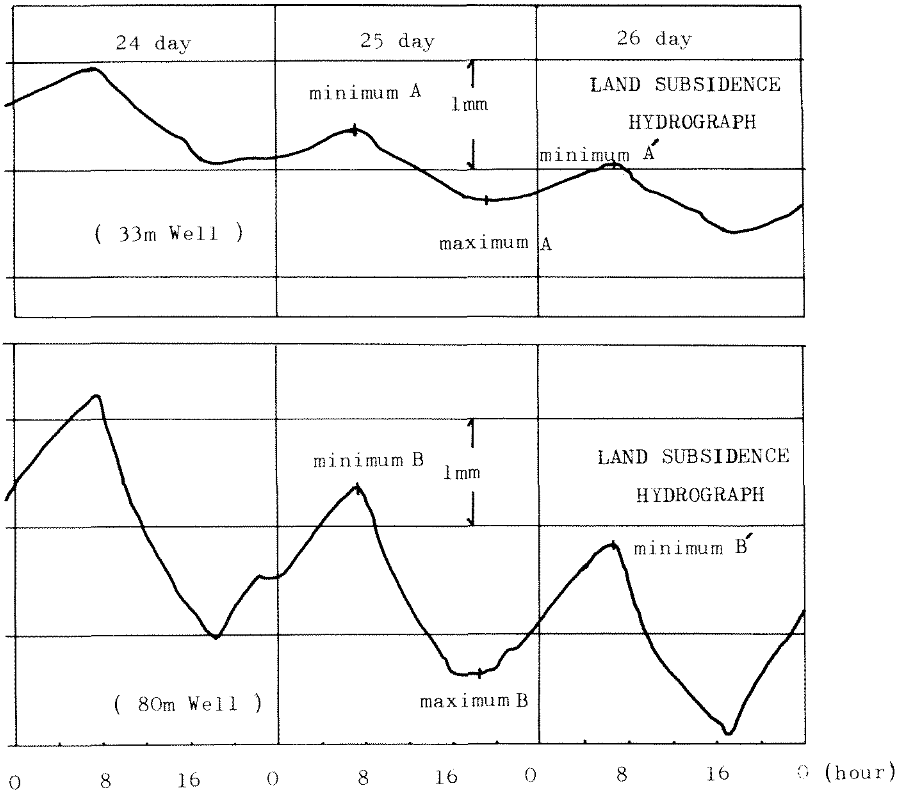

Figure - 3 Daily Cyclic Land Subsidence Rate Change (1973. 2.)

2. Groundwater Basin Simulation

Based on the geohydrological research, digital computer models were used to simulate the unsteady state effects of pumping diacharge on artesian groundwater level and subsidence rate. The alternating direction implicit numerical procedure was used in solving the finite difference approximations of the partial differential equation of groundwater flow.

As the geohydrologic data and the computer storage required for a numerical solution are insufficient, the solution of three-dimensional problems of groundwater hydrology are generally difficult. Then writers combined two models: horizontal (x, y) and vertical (x, z) two dimensional simulation models.

In the horizontal (x, y) model, hydrologic system is composed of two aquifer systems: semi-confining layer of aquitard and main aquifer. Under the condition of clear contrast in permeability between main aquifer and adjacent aquitard, the flow can be assumed to be vertical in the aquitard and horizontal in the aquifer. It is possible to evaluate the squeeze from ftorage in the semi-confining layers and the leakage through adjacent semi-pervious strata in this quasi-three dimensional aquifer model. This model is adopted to the land subsidence analysis of the Nanao Coastal Basin.

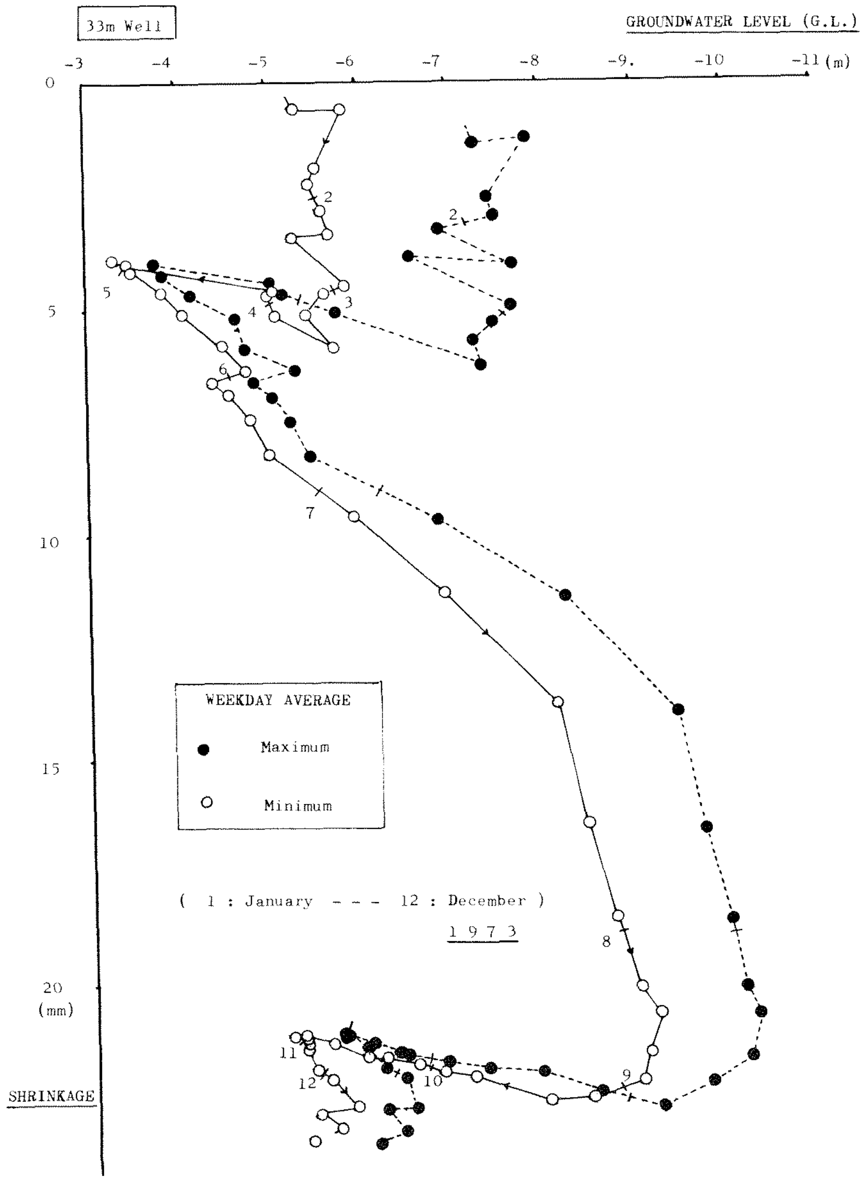

Figure - 4 Correlation Diagram of Groundwater level and Land subsidence Rate

In the vertical (x, z) model, hydrologic system is composed of multi-layered aquifers: semi-confining layer (alluvium I (1)) and aquifer (diluvium I (2), diluvium II (3), tertiary I (4)). Through the geohydrologic research and field testing, it is evident that the geological stratigraphic classification of the aquifer of the stratum is in clear relation to the physical classification of aquifer. This model has an advantage to simulate the macroscopic movement of regional groundwater flow.

Table-1 Classification of aquifer

formation	lithology	k (cm/sec)	Ss (1/m)	Thickness (m)
alluvium I(1)	silty clay	4.0×10^{-4}	2.0×10^{-3}	5 - 20
diluvium I(2)	silty sand	4.0×10^{-3}	9.1×10^{-4}	30 - 70
diluvium II (3)	silt, sand, gravel	2.6×10^{-2}	4.7×10^{-4}	40 - 80
tertiary I(4)	coarse sand	2.0×10^{-2}	6.0×10^{-4}	100 - 250

3. Mathematical models of the two aquifer systems

Two dimensional horizontal (x, y) groundwater flow equation is as follows:

$$\partial^2 h/\partial x^2 + \partial^2 h/\partial y^2 = S/T\, \partial h/\partial t + W(x, y, t) \quad \ldots\ldots (1)$$

$$W(x, y, t) = L(x,y,t) + Sq(x,y,t) + Ar(x, y, t) - Qd(x, y, t) \quad \ldots (2)$$

$$L(x, y, t) = K'/b' \,(\, h(t) - H(t)\,) \quad \ldots\ldots\ldots\ldots\ldots (3)$$

$$Sq(x, y, t) = K' \cdot \partial h'/\partial Z\Big|_{z=b'} = (K' - \Delta h)/b'(\pi k' t/b'^2 Ss)^{1/2} \{1 + 2\sum_{n=1}^{\infty} \exp[-n^2/(k' r/b'^2 S's)]\} \quad \ldots\ldots\ldots (4)$$

Where, h is confined water head, S is storage coefficient of main aquifer, T is transmissibility of main aquifer, W(x, y, t) is recharging or discharging rate, L(x, y, t) is leakage, Sq(x, y, t) is squeeze, Ar(x, y, t) is artificial recharge, Qd(x, y, t) is discharge, K' is permeability of semi-confining layer of silty clay, b' is thickness of silty clay, h(t) is confining water head, H(t) is unconfined water head, h' is excess water head in semi-confining layer and S's is specific storage of semi-confining layer, respectively. Two dimensional vertical (x, z) groundwater flow equation is as follow:

$$[\ Kxx\, \partial^2 h/\partial x^2]_1 + [\ Kzz\, \partial^2 h/\partial z^2]_1 = [\ Ss \partial h/\partial t]_1 + W(x, z, t) \quad \ldots . (5)$$

Where, [ ] means the properties of the lth number of layer in the multi-aquifer system. Analytical solution of the squeeze (4) is replaced by the following partial differential equation.

$$\partial^2 h'/\partial z^2 = S's/k' \times \partial h'/\partial t \quad \ldots\ldots\ldots (6)$$

Then the partial differential equations (1), (5) and (6) are replced by finite difference form of ADI method.

4. Evaluation of the two models

The simulation results of the groundwater level coincidence with the historical time trend data, but the land subsidence rate is not so good as the water level. In case of water table rise, these two models can not evaluate the rebound rate without any adjustment rebound parameter (R) which is decided empirically case by case in the model.

5. Analysis the Mechanism of land subsidence

After the simulation five ovsernation mells were setted in each depth of the aquifer (33 m, 50 m, 80 m, 100 m, 150 m) to analysis the mechanism

Table - 1 Rebound Response Coefficient of Land Subsidence (Rr)

33m WELL	MONTH (1973)											
DAY	1	2	3	4	5	6	7	8	9	10	11	12
1				120	70	0	0	6	0	80	60	22
2	66	42	61	100	0	220	0		108	67	22	267
3	42	85	143	33	0	89	0		42	78	120	17
4	52	85	138	69	17	100	0		100	90	267	0
5	85	93	63	150	40	89	0	50	120	200		0
6	80	108	73	80	0	50	0	32	83	54	50	0
7	116			163	0	0	0	11	100		43	0
8	90				160	0	0	60	111	120	89	0
9	36	49	64		40	150	0	12	133	100	0	0
10		46	62	325	0	0	0	55	143	100		0
11		128	110		7	57	0	21	80	100		78
12	42	75	87	43	0	0	0	0	400	100	600	38
13	52	100	59		0	0	0	11	1300		45	25
14	75				0	40	0	12	300	130	114	125
15	67				0	0	0	50	233	114	57	300
16	80	73	68		23	0	0	57	100	129		0
17		88	41	66	0	0	0	0		200	57	114
18		96	79	117	0	0	0	5		138	100	117
19	60	84	71	167	0	0	0	29		43	8	0
20	78	70	128		0	0	0	60	138		83	100
21	86				0	0	0	25	100		18	0
22	79				56	0	0	0	433		14	0
23	105				11	0	0	114	80	143	38	0
24	88	36	144		70	0	0	100	125	138	50	0
25		52	133	57	0	0	0	43	200	57	0	0
26	52	88	450	50	0	91	0	94	100	100	80	0
27	66	133		10	0	67	15	38	167	950	0	0
28	77			50	75	0	0	75	60	175	0	
29	102		1300	33	0	0	10	30	183	60	67	0
30	72				0	0	0	30	1000	88	200	0
31	33		125		0		18	75		29		0

of land subsidence. The purposes of the observation mells are to analysis the correlation between groundwater head change and landsubsidence rate and to determine the parameters of each aquifer system by field pumping test and laboratory soil mechanical test. The result of the field and laboratory tests had summerlized in the " 76' report of the land subsidence research at the coastal plain along the Nanao bay, ISIKAWA prefecture " by Dr. Y. Kaseno, Dr. T. Sibasaki, Mr. K. Nakagawa, Mr. N. Masuhara and

Table - 2   Rebound Response Coefficient of Groundwater Level (Rgw)

DAY	33m WELL		MONTH									(1973)
	1	2	3	4	5	6	7	8	9	10	11	12
1					83	195	101		72			97
2		98	95	100	103	154	76		162			114
3		99	113	88	79	135	80		106			87
4		109	108	100	100	97	95		129			66
5		99	88		81	60	63		100	73		119
6		108	101		108	106	113		80	152		98
7					76	93	60		153	413		56
8	98				110	107	83		115	96		116
9	104	102	93		95	296	128		93		108	133
10		102	101		103	85	48	93	115	103		99
11		96	107		91	103	119	94	120	95		97
12	84	93	99	67	76	86	77	79	128	91		
13	96	104	96	167	74	77	112	99	143	36		
14	103			116	95	143	92	99	109	470		
15	95			79	63	74	86	112	123	160		
16	101	97	89	235	96	106	78	110	109	97	150	
17		97	93	88	89	96	74	55	109	181	84	
18		102	99	141	76	96	82	132	96	127	105	
19	94	98	94	120	87	83	113	104	92	111	88	
20	75	93	101	92	103	80	99	107	133	102	95	
21	130	97		115	120	83	106	103	89	129	98	
22	98			133	91	102	106	92	176	120	94	
23	103	97		69	128	90	97	130	98	100	104	
24	103	80	111	143	134	80	85	114	123	105		
25		86	78	78	53	86		94	102	91		
26	90	110	89	138	65	96			121	126		
27	95	109	106	75	79	102				118		
28	97		115	95	126	55						
29	102		67	106	91	98				94		
30	95		100	75	109	94				122	105	
31			100		96			111			59	

et. all. Purpose of this section is to analyse the mechanism of landsubsidence and the standard pressure problem which had pointed out by Dr. K. Wadatsu in 1939. The analytical results of the ovservation mells are as follows:

1. Variations of groundwater level and land subsidence are cyclic and divided into four time categories: yearly, seasonaly, weekly and daily.

2. Annual land subsidence rate of alluvial silty clay [Alluvial I(1)] layer is ten times or more as large as the aquifer of sand [diluvium I(2)], diluvium II (3), tertiary I(4)] layers.
3. Daily rebound response coefficient Rr (Rr = (swelling (mm)/shrinkage (mm))x100%) of silty clay layer is smaller than the aquifers of sand, so the rebound response characteristic of silty clay layer is plastic and sand layer is elastic. Table-1 shows the daily rebound response coefficient of land subsidence for silty clay layer and table-2 also show the rebound response coefficient of groundwater level.
4. Daily cyclic groundwater level change (maximum 2.5m) is dynamic except sunday and extremly larger than the annual cyclic groundwater level change. Because the annual cyclic change is nearly equal to zero from 1973 to 1976 and sometimes show the yearly groundwater recovery.
   Figure-1 plots the daily maximum and minimum value alternatively on the yearly hydrograph. Figure-2 and figure-3 show the daily hydrograph for the cyclic groundwater level change and land subsidence rate.
5. Although the groundwater level is constant in winter season, the land subsidence rate gradualy increase to 0.086 mm/day.
6. Land subsidence rate greatly increase to 0.36 mm/day when the groundwater table below the -8 ~ -10 meters. Correlation between the land subsidence rate and standard pressure (Po) is recognized, but their relationship is not simple. Because the standard pressure for the subsidence rate (Pos) is not linear but nonlinear dynamic parameters. Figure-4 shows the correlation diagram of groundwater level and land subsidence rate and table-3 shows the daily specific land subsidence coefficient (Ssg) for unit groundwater level change in 1973. Where minus (-) means rebound, and Ssg is calculated by: Ssg = (land subsidence of daily maximum - land subsidence of daily minimum)/(groundwater level of daily maximum - groundwater level of daily minimum), and vise versa.
7. Time trend characteristics of the correlation between groundwater level and land subsidence rate are also shown in figure - 1.

Based on the above results, the third simulation model is completed. Quasi-three dimensional aquifer model is adopted again. The distinctive features of this model are as follows :

1. Select the time dimension(Δt) to one day in order to analyse the rebound effect. Because the land subsidence phenomena is the hysteretic accumulations of daily cyclic hysteresis of the aquifers.
2. Plastic - elastic model is adopted to analyse the land subsidence effect by lowering or increasing of groundwater level (pressure). Solution of the elastic model for aquifer of sand fundamentally depend on the Hook's Law and Lohman's formula.

   $\Delta m = ((S/\rho g) - n\beta m)\Delta P$ . . . . . (7)

   Solution of the plastic model for aquifer of silty clay layer which is not completely plastic includes the Po problem, standard pressure for subsidence rate(Pos) and time lag effects for consolidation process(U) is

   $\Delta \mathring{m} = ((S/\rho g) - n\beta m)\Delta P \cdot U$ . . . . . (8)

   Where, $\Delta \mathring{m}$ is volume change of the aquifer in vertical direction, S is strativity of the aquifer, n is porocity of the aquifer, Table - 3 Specific Land Subsidence Coefficient for Unit Groundwater Level (Ssg)

DAY	33m WELL — MONTH (1973) 1	2	3	4	5	6	7	8	9	10	11	12
1									-0.06			-0.07
						0.20			0.08			0.14
2									0			-0.03
		0.43	0.40			0.21			0.18			0.06
3		-0.18	-0.26			-0.30			-0.12			-0.14
		0.37	0.20			0.37	0.12		0.19			0.17
4		-0.31	-0.26			-0.23			-0.07			-0.03
		0.34	0.27	0		0.19	0.31		0.14			0.16
5		-0.27	-0.35		-0.06	-0.20			0.11	-0.20		0
		0.33	0.36		0.23	0.19	0.17		0.12	0.27		0.10
6		-0.31	-0.26		-0.11	-0.29			-0.14	-0.75		
		0.27	0.32		0.36	0.65	0.31		0.13	0.62		0.05
7		-0.27	-0.23		-0.11	-0.30			-0.14	-0.22		
		0.23	0.29		0.06	0.13	0.17		0.16	0		0.24
8	-0.31				0	0			-0.11	-0.42		
	0.28				0.16	0.20	0.33		0.12	0.18		0.27
9	-0.26				-0.23	0			-0.12	-0.26		
	0.39	0.38	0.37		0.26	0.09	0.28		0.12	0.29		0
10	-0.14	-0.18	-0.25		-0.11	-0.04			-0.18	-0.27		
		0.10	0.32		0.20	0.17	0.21	0.09	0.22	0.22		0.10
11		-0.05	-0.20		0			-0.05	-0.27	-0.22		
		0.21	0.27		0.44	0.18	0.38	0.12	0.17	0.22		0.14
12		-0.28	-0.28		-0.03	-0.10		-0.03	-0.11	-0.23		-0.11
	0.43	0.30	0.29		0.27	0.18	0.30	0.11	0.06	0.22		0.14
13	-0.21	-0.25	-0.25		0			0	-0.18	-0.24		
	0.40	0.31	0.35		0.30	0.30	0.29	0.19	0.02	0.05		
14	-0.22	-0.30	-0.22		0			-0.02	-0.20	0		
	0.33	0.26	0.36		0.38	0.17	0.28	0.16	0.06	10.00		
15	-0.24				0	-0.05		-0.02	-0.16	-0.28		
	0.30				0.12	0.17	0.25	0.08	0.11	0.28		
16	-0.22				0			-0.04	-0.20	-0.20	-0.11	
	0.31	0.35	0.36		0.29	0.19	0.38	0.07	0.17	0.19		
17	-0.25	-0.26	-0.27		-0.07			-0.04	-0.16	-0.25	-0.07	
	0.30	0.29	0.48		0.24	0.13	0.31	0.04		0.16	0.13	
18	-0.18	-0.27	-0.21					0		-0.17	-0.09	-0.12
		0.32	0.27		0.26	0.16	0.38	0.24		0.27	0.07	0.08
19		-0.30	-0.21					-0.01		-0.29	-0.07	
	0.36	0.35	0.37		0.08	0.38	0.42	0.18		0.20	0.20	
20	-0.23	-0.30	-0.24					-0.05		-0.08	-0.02	
	0.44	0.33	0.24		0.34	0.15	0.25	0.18	0.19	0.09	0.10	
21	-0.46	-0.24	-0.31					-0.10	-0.20	0	-0.09	
	0.47	0.30	0.27		0.40	0.28	0.31	0.27	0.18		0.17	
22	-0.31		-0.42					-0.07	-0.20		-0.03	
	0.39				0.27	0.19	0.29	0.22	0.10		0.20	
23	-0.31				-0.16			0	-0.25		-0.03	
	0.34				0.31	0.14	0.35	0.11	0.19		0.15	
24	-0.35	-0.24			-0.03			-0.10	-0.15	-0.23		
	0.20	0.37			0.29	0.18	0.21	0.14	0.17	0.20		
25		-0.17			-0.15			-0.12	-0.17	-0.26		
	-0.18	0.35		0.16	0.17	0.09	0.32	0.26	0.12	0.13		
26		-0.21		-0.11				-0.12	-0.24	-0.08		
	0.39	0.33		0.19	0.16	0.21			0.16	0.12		
27	-0.23	-0.26		-0.24		-0.20			-0.13	-0.10		
	0.36	0.23		0.23	0.25	0.10			0.22	0.05		
28	-0.25	-0.29		-0.03		-0.07				-0.41		
	0.37	0.32		0.16	0.26	0.15						
29	-0.29			-0.08	-0.15						0	
	0.32			0.09	0.15	0.37					0.09	
30	-0.32			-0.03							-0.06	0
	0.35				0.20	0.32					0.04	0
31	-0.27							-0.03				0
	0.26				0.19			0.09				0.23

ΔP is the change of groundwater pressure, U is the time lag coefficient, ρ is specific gravity of the aquifer and g is acce - lation of gravity.

Then the formula(8) is replaced by the next formula.

$$m = mv' \cdot m \cdot \Delta P \cdot U \quad . \ . \ . \ . \ . \quad (9)$$

Where, mv is the coefficient of volume compressibility which is estimated by figure - 4 as mv'.

6. Cyclic daily analysis and standard pressure

The ΔP of the formula(9) is defined as follow: (Refer the figure2,3)

$$P = K1(PminA(t) - PmaxA(t+\tfrac{1}{2})) + K2(PmaxA(t+\tfrac{1}{2}) - PminA'(t+1)) \quad . \ . \ . \ . \ . \ . \ (10)$$

Where, K1 is shrinkage coefficient, K2 is rebound coefficient and U is the time lag coefficient which is the function of the pumping discharge duration time. *If $Pmax(t+\frac{1}{2})$ is less than Po, both coefficients of K1 and K2* assumed to be zero : this is the standard pressure problem(Po). And if $PmaxA(t+\frac{1}{2})$ is larger than Po, K1 and K2 are defined by the function of water pressure(level). Then the K1 and K2 are

$$K1 = 1 \ . \ . \ . \ . \ . \ (11) \qquad K2 = (Pos - PmaxA(t+\tfrac{1}{2}))/(Pos - Po) \ . \ . \ . \ . \ (12)$$

In this model Po and Pos are estimated by figure - 4 of 2.5 and 8.5 meters. The plastic - elastic model simulate the historical time trend of rebound characteristics of the aquifer of silty clay and sand well, and adequete simulation results were obtained.

7. Groundwater basin management and regional water resource planning

Based on the seven years land subsidence research of hydrogeological survey, observations and three steps of the digital computer simulations, controlling method of the groundwater basin management and realistic methodology for regional water resources planning were studied. The study consists of the artificial groundwater recharge effects for groundwater basin reservoir using the river water of non-irrigation season and correlation effects between the regulation of groundwater resources and new development of the river water resources encompassing the mountain ranges.

8. Conclusion

Purpose of the groundwater simulation is not to simulate the mathematical simulation models, but to proffer the fundamental data for the water resources planning. *However, the final model includes some untested and* soluved important problems yet ; dynamic standard pressure problem, time lag effects and etc.,for example. Then the furthermore land subsidence research will be planned and proceed, and better water resources planning will be completed. This is our best wish hope.

9. Acknowledgements

The work on which this article is based was supported by the committee of the research group of land subsidence along the Nanao Bay, Isikawa Prefecture. We also thank the committee that provided unpublished basic data and, in particular, we would like to thank Dr. T.Sibasaki, Dr. Y. Kaseno, Mr. K. Nakagawa, Mr. Kamata, Mr. K. Harada and Mr. N. Masuhara, because of without whose approval and cooperation this article could not have been completed. The authers express their sincere thanks for professor Dr. H. Kano, Akita University, who first indicated the applied geological study and all the members of the study room of river engineering Department of Civil Engineering University of Tokyo.

Publication n°121 of the International Association of Hydrological Sciences
Proceedings of the Anaheim Symposium, December 1976

ANALYSIS OF LONG TERM OEDOMETER TEST RESULTS

S. Ohmaki
Disaster Prevention Research Institute, Kyoto University
Gokasho, Uji City, Kyoto Prefecture, Japan

Abstract

The long term oedometer test results under various sets of consolidation pressure p_0 and pressure increment ratio $\Delta p_0/p_0$ are shown for three kinds of normally consolidated, fully saturated clay. Based on these results, a one dimensional model to describe the mechanical and rheological behavior of soil skelton is proposed, in which the instant and total strains are calculated from the e - log p relationship shown by Bjerrum (1967) and a rheological model with the modified Eyring viscosity by Murayama and Shibata(1956) is used to describe the rheological behavior of soil skelton.

The way to determine the parameters of this model is also explained in detail. The influences of p_0 and $\Delta p_0/p_0$ on these parameters from experiments are investigated and the empirical relationships between these parameters and stress conditions are shown.

Finally regarding clay as two phase material consisting of incompressible pore water and clay skelton of which mechanical and rheological behavior is shown by this model, time dependent deformation behaviors of these clay samples under various p_0 and $\Delta p_0/p_0$ are calculated by the finite difference method. Good agreement is obtained between the calculated and experimental results over wide range of p_0 and $\Delta p_0/p_0$.

Introduction

Many investigators have studied the one dimensional compressibility of saturated clays because it is the most fundamental condition in deformation of clay. Studies by Terzaghi were the beginnings in this field. Thereafter the detailed experimental and theoretical studies have been carried out (Murayama and Shibata,1956, Leonards and Girault,1961, Crawford,1964, Davis and Raymond,1965, etc.). Recently upon these experimental and theoretical treatments, many studies are published in which nonlinear compressibility and permeability of clay during consolidation, effect of overconsolidation, nonlinear viscosity of soil skelton, effect of load increment ratio are considered (Barden,1965, Bjerrum,1967, Berre and Iversen,1972, Lowe,1974, etc.).

In this paper, the long term oedometer test results for three kinds of normally consolidated, fully saturated clay with various sets of consolidation pressure and pressure increment ratio are investigated. Based upon these results, a one dimensional model to describe the mechanical and rheological behavior of clay will be proposed and the way to determine these parameters from experimental results will be given. Relationships between these parameters thus obtained from experiments and their stress conditions are examined. Finally regarding clay as two phase material consisting of clay skelton described by this model and incompressible pore water, time dependent behaviors of strains of these clay samples under various stress conditions are calculated by the finite difference method and compared with experimental results.

Theoretical consideration on one dimensional compression of clay

A one dimensional mechanical and rheological model of soil skelton is shown in Fig.1. In Fig.1(a), a family of e - log p curves with loading period as a parameter is shown, in which they are parallel with each other and straight with a slope of compression index C_c. The t_0 curve is the hypothetical instant curve which is linear with log p for large pressure increment ratio $\Delta p_0/p_0$ and nonlinear for small $\Delta p_0/p_0$ where t_0 is an infinitely short period (Bjerrum, 1967).

We will consider the case in which pressure increment Δp_0 is applied to the specimen at a point $A(e_0,p_0)$ on the t_1 line where the specimen has been loaded with consolidation pressure p_0 for t_1 period (Fig.1(a)). If we consider the clay specimen as an imaginary one which has no pore water but has the same structure as fully saturated one, the application of Δp_0 instantaneously moves the state point A of clay to C on the t_0 curve (in the case of Δp_0 being small, to the point B), and then to the point E on t_2 line (Δp_0 being small, to the point D) at t_2 period after the start of test. Now we consider the case in which its state path in Fig.1(a) goes from A to E through C. Then the slope of AC and AE is given by eqs.(1) and (2) respectively.

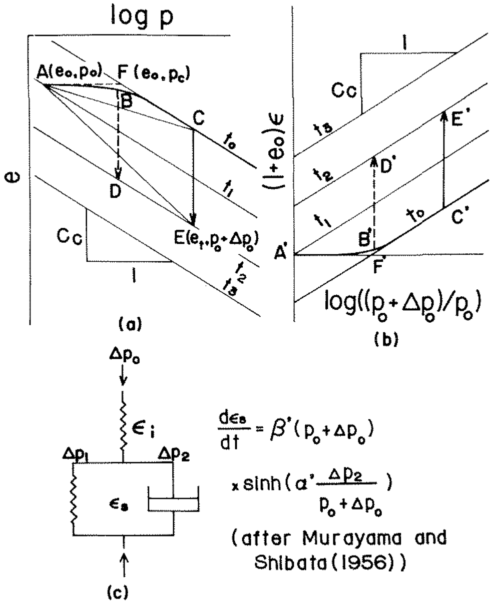

Fig.1 A one dimensional model of clay skelton

$$C_{ci} = C_c - \frac{\Delta e_i}{\log_{10}((p_0+\Delta p_0)/p_0)} \quad \text{......(1)}$$

$$C_{ct} = C_c + \frac{\Delta e_t}{\log_{10}((p_0+\Delta p_0)/p_0)} \quad \text{......(2)}$$

In these equations, C_c is the compression index which is obtained from the standard oedometer test, Δe_i is a longitudinal distance between t_0 and t_1 lines and Δe_t is also a distance between t_1 and t_2 lines (Fig.1(a)). It may be noted that when $t_1 \lesseqgtr t_2$, $\Delta e_t \gtreqless 0$ respectively. In Fig.1(b) is shown a relationship between $(1+e_0)\varepsilon$ and $\log((p_0+\Delta p_0)/p_0)$, in which the points A' - F' correspond to A - F in Fig.1(a) respectively. The t_0, t_1, t_2, ... lines in Fig.1(b) also correspond to those in Fig.1(a) respectively and they have also the same slope of C_c, where t_1 line goes through the origin. Δe_t in eq.(2) is the intercept of t_2 line on the $(1+e_0)\varepsilon$ axis and $(-\Delta e_i)$ is that of a straight portion of t_0 curve. Accordingly, Δe_t is dependent on both loading periods t_1 and t_2 and Δe_i is t_1 only. In Fig.1(c) is shown a rheological model of soil skelton. We assume the strain of a top spring and the total strain in this model are represented by eq.(3) when $t \to \infty$,

$$\left.\begin{aligned} \varepsilon_i &= \frac{C_{ci}}{1+e_0} \log_{10} \frac{p_0+\Delta p_0}{p_0} \\ \varepsilon_\infty &= \frac{C_{c\infty}}{1+e_0} \log_{10} \frac{p_0+\Delta p_0}{p_0} \end{aligned}\right\} \quad \text{......(3)}$$

where C_{ci} is given by eq.(1) and $C_{c\infty}$ by eq.(2) when $t \to \infty$. Then final strain of the Voight model in Fig.1(c) when $t \to \infty$ is represented as follows.

$$\varepsilon_s = \varepsilon_\infty - \varepsilon_i = \frac{C_{c\infty} - C_{ci}}{1 + e_0} \log_{10} \frac{p_0+\Delta p_0}{p_0} \quad \text{......(4)}$$

Now we employ the following equation to represent a rheological behavior of a dash pot in this model (Murayama and Shibata, 1956),

$$\frac{d\varepsilon_s}{dt} = \beta' \, (p_0+\Delta p_0) \sinh \left(\alpha' \frac{\Delta p_2}{p_0+\Delta p_0}\right) \quad \text{......(5)}$$

where α' and β' are rheological parameters and Δp_2 is such pressure increment as shown in Fig.1(c). Then by using an alternative variable s instead of ε_s as eq.(6), we obtain eqs.(7) and (8) to describe the rheological behavior of the Voight model in Fig.1(c).

$$s = \exp \frac{(1+e_0)\,\varepsilon_s}{C_{c\infty}' - C_{ci}'} \quad \text{......(6)}$$

$$t = \frac{C_{c\infty}' - C_{ci}'}{(1+e_0)\,\beta'\,(p_0+\Delta p_0)} f\left(\alpha', \frac{\Delta p_0}{p_0}, s\right) \quad \text{......(7)}$$

$$f\left(\alpha', \frac{\Delta p_0}{p_0}, s\right) = \int_1^s \frac{ds}{s \sinh \left\{\alpha' \left(1- \frac{p_0 \, s}{p_0+\Delta p_0}\right)\right\}} \quad \text{......(8)}$$

where $C_{c\infty}' = 0.434\ C_{c\infty}$, $C_{ci}' = 0.434\ C_{ci}$.

In Fig.2 are shown the calculated ε - log t curves with α' and β' as parameter using eqs.(6), (7) and (8) where $\varepsilon = \varepsilon_i + \varepsilon_s$. This figure shows that the slope of ε - log t curves decreases with increase of α' and ε - log t curves move parallel towards negative direction to log t axis with increase of β'. From these characteristics, we are possible to determine graphically the rheological parameters α' and β' from test results. That is, if we could determine ε_i and ε_∞ by some way, we obtain ε_1 and ε_2, for example, defining as $\varepsilon_1 = \varepsilon_i + 0.1\ (\varepsilon_\infty - \varepsilon_i)$, $\varepsilon_2 = \varepsilon_i + 0.8\ (\varepsilon_\infty - \varepsilon_i)$.
Corresponding to these strains ε_1 and ε_2, we obtain t_1 and t_2 from ε - log t curves which are different from those in Fig.1 and s_1 and s_2 from eq.(6). Then α' and β' are written as a function of Δlog t with various pressure increment ratio $\Delta p_0/p_0$ as follows,

$$\Delta \log t = \log \frac{t_2}{t_1} = \log \frac{f(\alpha', \Delta p_0/p_0, s_2)}{f(\alpha', \Delta p_0/p_0, s_1)} = F\left(\alpha', \frac{\Delta p_0}{p_0}\right) \quad \text{......(9)}$$

$$\frac{(1+e_0)\ \beta'\ (p_0+\Delta p_0)\ t_2}{C_{c\infty}' - C_{ci}'} = f\ (\alpha',\ \frac{\Delta p_0}{p_0},\ s_2) = G\ (\Delta \log\ t,\ \frac{\Delta p_0}{p_0}) \quad \cdots\cdots(10)$$

since from eqs.(3) and (6),

$$s_1 = \left(\frac{p_0+\Delta p_0}{p_0}\right)^{0.1} , \quad s_2 = \left(\frac{p_0+\Delta p_0}{p_0}\right)^{0.8} .$$

In Fig.3(a) and (b) are shown the results calculated from eqs.(9) and (10) with $\Delta p_0/p_0$ as parameter, from which we can determine the rheological parameters α' and β'.

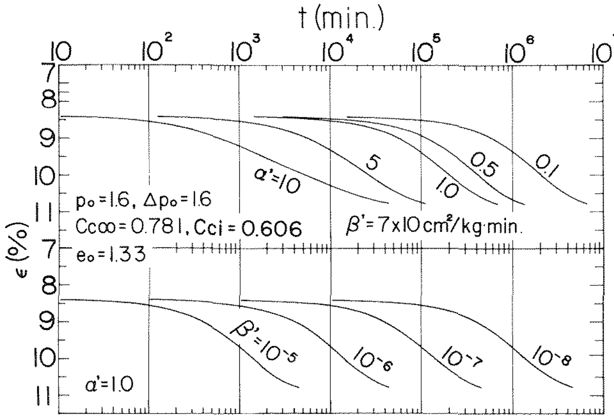

Fig.2 Effect of α' and β' on ε - log t curves

Samples and test procedures used in oedometer tests

Three kinds of clay named Sample No.1, No.2 and No.3 are used. Sample No.1 is an undisturbed one which is obtained from Akoh City, Hyogo Pref. in Japan at depth of 10 m below the ground level. Sample No.2 is a remoulded and reconsolidated one to a final pressure, 0.5 kg/cm^2, for about a month from slurry at about 120 percent water content. Sample No.3 is an undisturbed one which is

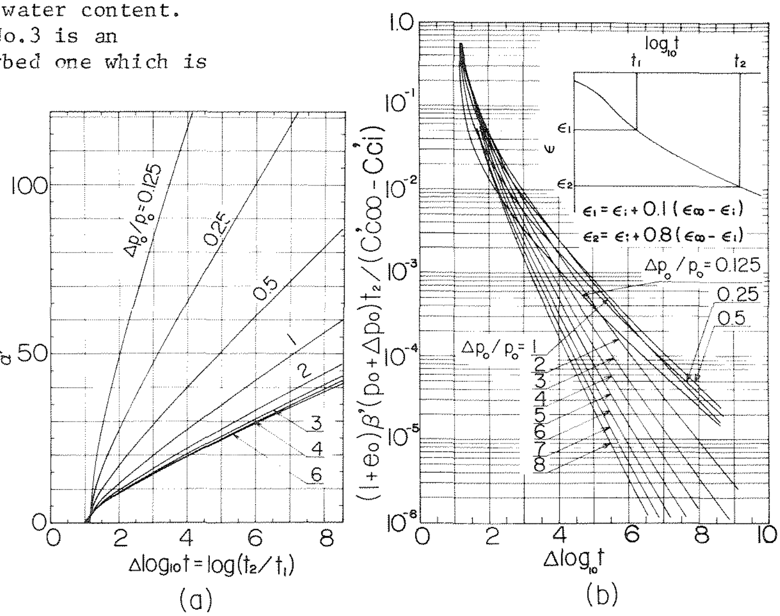

Fig.3 Graphs used to determine the rheological parameters α' and β'

obtained from Kurashiki City, Okayama Pref. in Japan at depth of 12 m under the ground level. Physical properties of these samples are listed in Table 1. In all tests, the fixed ring type consolidometers with double drainage condition are used. The inside of rings is lubricated with silicone grease in order to decrease the side friction. Diameter and height of the specimen are 6 and 2 cm respectively. Loading procedure used in the present tests is as follows. For Sample No.1, double loading system with 24 hours interval is used from consolidation pressure, 0.05 kg/cm^2, to p_0 which is greater than preconsolidation pressure, and specimens are consolidated for 25 - 48 days at consolidation pressure $p_0+\Delta p_0$, that is, t_1 in Fig.1 is equal to one day and t_2 is equal to 25 - 48 days. For Sample No.2, after doubling loading with 24 hours interval by the similar procedure to Sample No.1 except that consolidated at pressure p_0 for about 16 days, each specimen is consolidated for about 16 days at pressure $p_0+\Delta p_0$, that is, t_1 and t_2 in Fig.1 are both equal to about 16 days. Fresh specimens are used for all tests for Sample No.1 and No.2. For Sample No.3, loading procedure is not the same each other and their loading duration at consolidation pressure p_0 and $p_0+\Delta p_0$ is 16 - 60 days. All these tests are performed in the temperature controlled room at 20 $\pm$ 0.5 degree. The strain ε in this paper is defined as a value of a vertical displacement by pressure increment Δp_0 devided by the thickness of a specimen just before loading Δp_0.

Table 1 Physical properties of clays

Sample	LL	PL	PI	<5μ	G_s
No.1	95.5	38.0	57.5	54.0 %	2.673
No.2	55.0	34.0	21.0	48.2	2.648
No.3	37.6	21.4	16.2	22.2	2.753

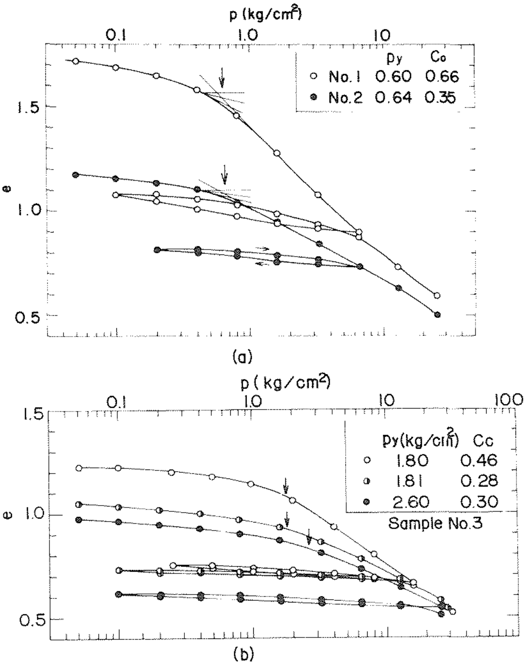

Fig.4 e - log p curves for samples used

Test results

The e - log p curves from the standard oedometer tests for three samples with pressure increment ratio $\Delta p_0/p_0$ of unity and loading period of 24 hours are represented in Figs.4(a) and 4(b), in which the preconsolidation pressure p_y and the compression index C_c for each sample are also presented. In Fig.5, ε - log t curves for all tests of Sample No.1 are represented, which shows that secondary compression tails of these curves are approximately linear and their shapes varies from Type 1 to Type 3 curves with decrease of $\Delta p_0/p_0$ (Leonards and Girault, 1961). In Fig.6,

$(1+e_0)\varepsilon$ at 100 percent consolidation, 10^5, 10^6 and 10^7 min for three samples are plotted against $\log((p_0+\Delta p_0)/p_0)$. For the tests which pressure increment ratio $\Delta p_0/p_0 \geqq 1$, the strain at 100 percent consolidation ε_{100} is determined by the so called log t method and for those which $\Delta p_0/p_0 < 1$, it is determined as the strain corresponding to such t_{100} on ε - log t curves that the value of $(k\ t_{100}\ /\ h_0{}^2)$ is equal to the mean value of $(k\ t_{100}\ /\ h_0{}^2)$ for tests which increment ratio $\Delta p_0/p_0 \geqq 1$, where h_0 is a thickness of a specimen. A coefficient of permeability k for tests with $\Delta p_0/p_0 < 1$ is determined from the e - log k curves from the tests with $\Delta p_0/p_0 \geqq 1$.

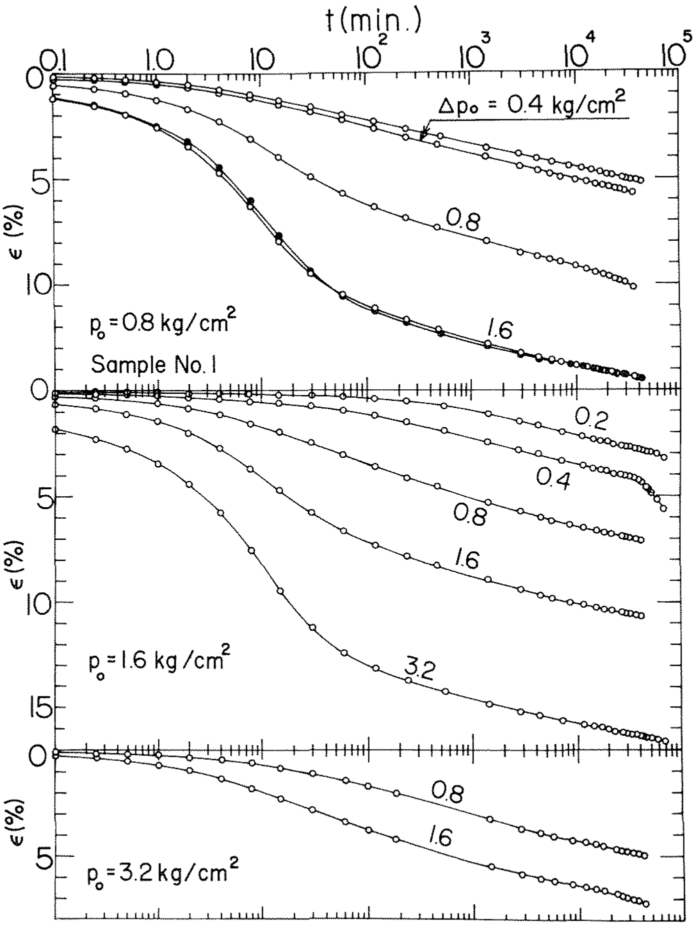

Fig.5 ε - log t curves (Sample No.1)

Strains at 10^5, 10^6 and 10^7 min in Fig.6 are obtained by extending the secondary compression portions of ε - log t curves linearly to the respective times. Solid lines in this figure are those which have the slope of C_c for each sample indicated in Fig.4 where 0.3 is used as C_c for Sample No. 3. Hereafter we regard as t_0 curve in Fig.1(a) and (b) approximately the solid one at 100 percent consolidation in Fig.6, which has the nonlinear portion for small $\Delta p_0/p_0$, since an ideal t_0 curve is impossible to determine correctly for clayey soil for the sake of the time lag due to the dissipation of excess pore water pressure.

In Fig.7, the rheological parameters α' and β' are plotted against $p_0/\Delta p_0$ and $p_0/(p_0+\Delta p_0)^2$ respectively which are determined by the way indicated in Fig.3 where ε_{100} and ε at 10^6 min in Fig.6 are used as ε_i and ε_∞ respectively. From this figure, we obtain the following empirical equations.

$$\left.\begin{aligned} \alpha' &= \alpha_1 + \alpha_2\ p_0/\Delta p_0 \\ \beta' &= \beta\ p_0/(p_0+\Delta p_0)^2 \end{aligned}\right\} \qquad \cdots\cdots\cdots (11)$$

The value of constants α_1, α_2 and β for three samples are also indicated in this figure.

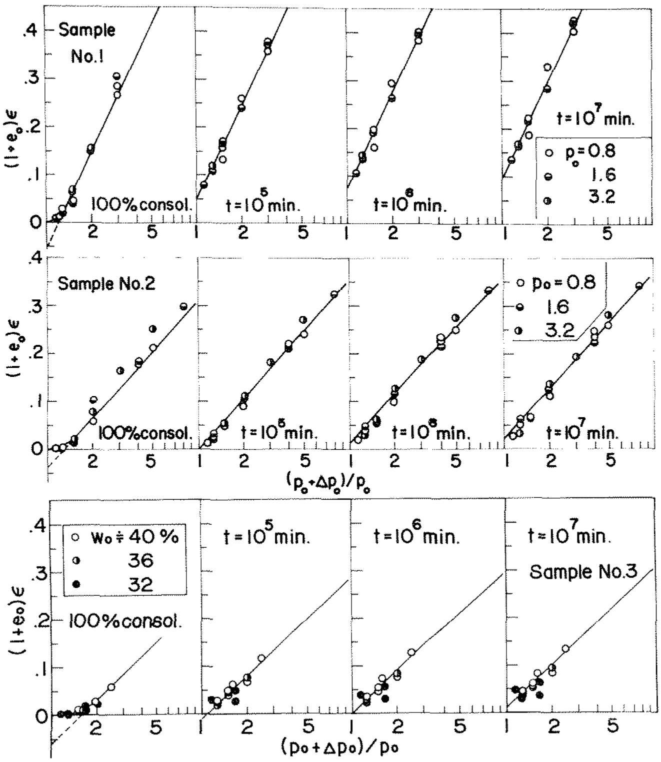

Fig.6 $(1+e_0)\varepsilon$ - $\log((p_0+\Delta p_0)/p_0)$ plots

<u>Theoretical equations of one dimensional consolidation of saturated clays</u>

We will consider the one dimensional consolidation problem in which a uniform load $\Delta p_0(t)$ is distributed all over the ground (Fig.8). We use as a constitutive relation the beforementioned rheological model (Fig.1 (c)). If we replace Δp_0 in this model with $(\Delta p_0 - u_e)$ and use eq.(11) instead of α' and β', then the equation of equilibrium is expressed as eq.(12). In this equation, $\Delta p_0(t)$ is assumed to be constant with time. We use eq.(13) as e - log k relation where e_e, C_k and k_e are constant.

$$\frac{\partial \varepsilon}{\partial t} + \frac{C_{ci}'}{1+e_0}\,\frac{1}{p_0+\Delta p_0-u_e}\,\frac{\partial u_e}{\partial t} = \frac{p_0\,\beta}{p_0+\Delta p_0-u_e}\sinh\left[\left(\alpha_1+\alpha_2\frac{p_0}{\Delta p_0-u_e}\right)\cdot\left\{1-\frac{p_0}{p_0+\Delta p_0-u_e}\exp\frac{(1+e_0)\varepsilon - C_{ci}'\ln((p_0+\Delta p_0-u_e)/p_0)}{C_{c\infty}'-C_{ci}'}\right\}\right] \quad \cdots\cdots(12)$$

$$e = e_e + C_k \log_{10}(k/k_e) \quad \cdots\cdots(13)$$

For simplicity, we assume that void ratio e in eq.(13) is represented as $e_0 + U\,\Delta e_i$, where U is a degree of consolidation, then a coefficient of permeability k is written as follows.

$$k = k_e \exp\frac{e_0 - e_e - U\,C_{ci}'\ln((p_0+\Delta p_0)/p_0)}{0.434\,C_k} \quad \cdots\cdots(14)$$

If we assume a coefficient of permeability k is dependent only on time and independent on depth, then the welknown equation of continuum for the one dimensional consolidation is given as eq.(15).

$$\frac{\partial \varepsilon}{\partial t} + \frac{k}{\gamma_w}\frac{\partial^2 u_e}{\partial z^2} = 0 \quad \cdots\cdots(15)$$

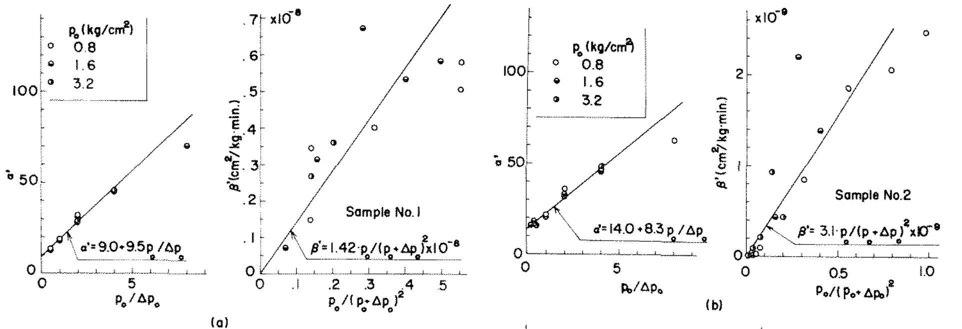

Fig.7 α' - $p_0/\Delta p_0$ and β' - $(p_0/(p_0+\Delta p_0)^2)$ relations

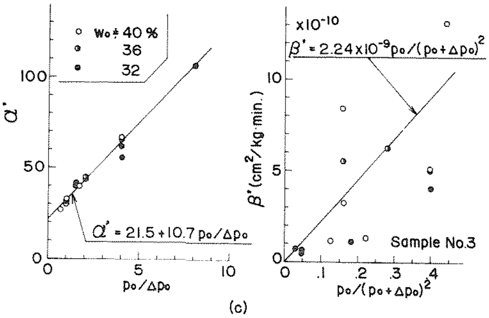

Numerical assessment of one dimensional consolidation and settlement

In this paragraph, calculated results of one dimensional consolidation and creep from eqs.(12) and (15) with using eq.(14) by the finite difference method are presented and compared with experimental ones. In Fig.9 is given a comparison of analytical results under various sets of p_0 and $\Delta p_0/p_0$ with experimental ones for Sample No.2. Values employed in calculation are as follows; $C_c = 0.35$ (from Fig.4), $\Delta e_\infty = 0.01$, $\Delta e_i = 0.04$ (Fig.6), $\alpha_1 = 14.0$, $\alpha_2 = 8.3$, $\beta = 0.31 \times 10^{-8}$ /min (Fig.7), $k_e = 10^{-6}$ cm/min, $C_k = 0.417$, $e_e = 0.821$. The satisfactory agreement is gained between both results over the wide range of p_0 and $\Delta p_0/p_0$.

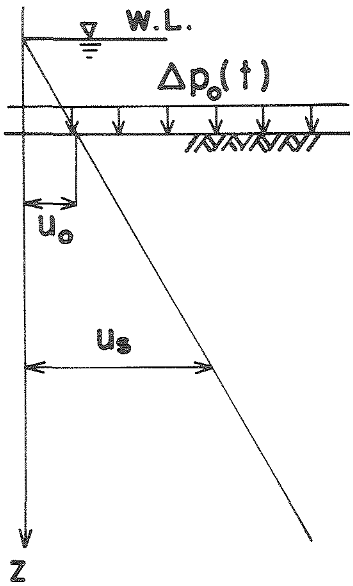

Fig.8 Clay stratum

Conclusions

The author has shown the results of long term oedometer tests which are performed under various sets of consolidation pressure and pressure increment ratio, and proposed a one dimensional model of clay skelton which is composed of a nonlinear Voight model connected with a nonlinear top spring in series. Thereafter rheological characteristics of the model are discussed comparing with test results. From these, the following conclusions are obtained.

1. $(1+e_0)\varepsilon$ at the time when the sufficient time is elapsed since the start of test can be plotted linearly against log $((p_0+\Delta p_0)/p_0)$ which slope is equal to the compression index C_c. $(1+e_0)\varepsilon_{100}$ for the tests with $\Delta p_0/p_0$ greater than about 0.5 are also plotted linearly against log $((p_0+\Delta p_0)/p_0)$

with the slope C_c although this relation becomes non-linear for small $\Delta p_0/p_0$.

2. When the proposed model is used, its rheological parameters can be determined graphically from the test results. Empirical relationships between the rheological parameters α', β' by this way and p_0, Δp_0 are given as eq.(11).

3. Good agreement is obtained between calculated strains and experimental ones over the wide range of p_0 and $\Delta p_0/p_0$, regarding clay as two phase material consisting of incompressible pore water and clay skelton of which mechanical and rheological behavior is described by this model.

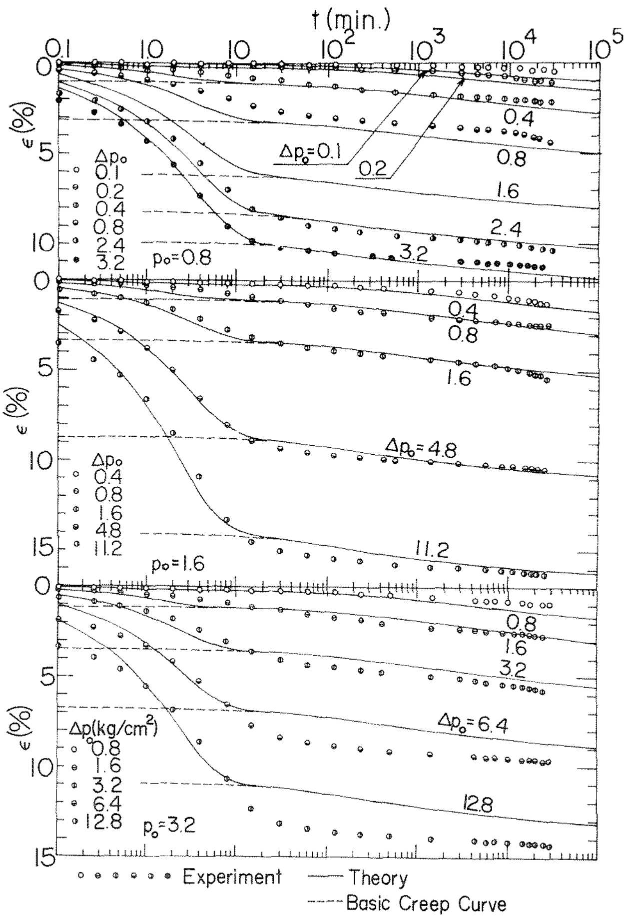

Fig.9 Comparison of ε − log t curves with experimental results (Sample No.2)

Acknowledgement

The work described in this paper was carried out at Kyoto University under the supervision of Professor T. Shibata. The author wishes to express his deep appreciation to Professor T. Shibata for his guidance and encouragement throughout the present study. The author carried out the oedometer tests described in this paper together with Mr. H. Shimizu and Mr. T. Sueoka at Disaster Prevention Research Institute, Kyoto University, to whom the author is grateful. The author also expresses his gratitude to Mr. M. Tominaga and Mr. C. Suematsu for their offering a part of samples used in this work. It is also acknowledged that the related computations were carried out by using the digital computer Facom 230 - 75 at the Data Processing Center, Kyoto University.

References

Barden, L., 1965, Consolidation of Clay with Nonlinear Viscosity: Geotech., v.15, p.345 - 362.

Berre, T. and K. Iversen, 1972, Oedometer Tests with Different Specimen

Heights on a Clay Exhibiting Large Secondary Compression: Geotech., v.22, p.53 - 70.

Bjerrum, L.,1967, Engineering Geology of Norwegian Normally-Consolidated Marine Clays as Related to Settlement of Buildings: Geotech., v.17, p.81 - 118.

Crawford, C. B., 1964, Investigation of the Consolidation Tests: Proc. ASCE, v.90, No.SM5, p.87 - 102.

Davis, E. H. and G. P. Raymond, 1965, A Non-linear Theory of Consolidation: Geotech., v.15, p.161 - 173.

Leonards, G. A. and P. Girault, 1961, A Study of the One-dimensional Consolidation Tests: Proc. 5th ICSMFE, v.1, p.213 - 218.

Lowe, J. 1974, New Concepts in Consolidation and Settlement Analysis: Proc. ASCE, v.100, No.GT8, p.574 - 612.

Murayama, S. and T. Shibata, 1956, On the Rheological Characteristics of Clay: Trans. of JSCE, No.40, p.1 - 31. (in Japanese)

Publication n°121 of the International Association of Hydrological Sciences
Proceedings of the Anaheim Symposium, December 1976

RECENT ELEVATION CHANGE IN SOUTHERN CALIFORNIA

S. R. Holdahl
National Geodetic Survey
National Ocean Survey, NOAA
Rockville, Maryland

Abstract

Velocities of elevation change for two time periods have been determined from Southern California leveling data. Two periods were selected for study: 1906 through 1962 and 1959 through 1976. The study area extends from San Pedro north to latitude 35°.5, and between longitudes 117° and 119°.5. The shape of the fitted velocity surface for the latter epoch agrees with the original uplift established by Castle et al. (1976) with the exception that no eastern termination is evidenced within the study area. The velocity surface for the earlier time period shows negligible subsidence of 1 mm/yr at Palmdale, increasing to 9 mm/yr at Bakersfield. The 11 mm/yr maximum uplift velocity determined for the period 1959 through 1976 is approximately twice the corresponding standard deviation. Weighted velocities, extracted from tidal records at six stations on the coast, were used to provide input for absolute height change.

Introduction

Because of the concern associated with crustal uplift in Southern California, an attempt has been made by the National Geodetic Survey (NGS) to obtain the best estimates possible of its character, magnitude, and areal extent. Tide gage records and repeated leveling surveys have been combined in a least-squares adjustment, using a computerized program, SURFACE, to accomplish this task. SURFACE solves for heights of selected points at a selected reference time and for coefficients of a polynomial which expresses height change as a function of latitude and longitude.

Castle et al. (1976) suggest that the uplift began around 1960. For this reason the analysis described in this report is given in two parts. The first part concerns tide gage and leveling data existing prior to late 1962; the second part treats data originating after early 1959.

The NGS investigation of Southern California elevation change had the following specific objectives:

1. Test the early conclusion that insignificant aseismic vertical deformation had taken place prior to 1960.
2. Test the early conclusion that significant aseismic vertical deformation began after 1960.
3. Determine a velocity (of elevation change) surface for each study period to describe the pattern of characteristic motion.
4. Isolate locations which exhibit nonlinear vertical movements during the recent study period.

The geographical limits of the study area are shown in figure 1, along with the locations of tide gages and major faults. Figure 2 shows the locations of levelings used in the investigation.

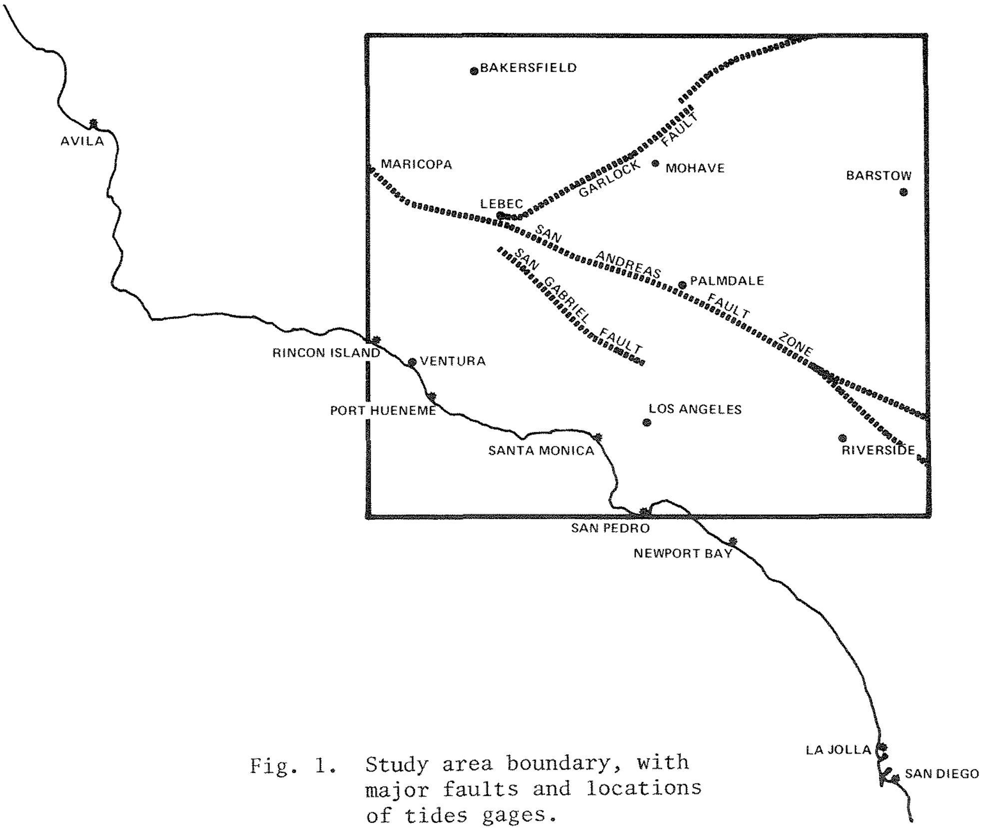

Fig. 1. Study area boundary, with major faults and locations of tides gages.

Leveling Data

Most levelings in Southern California naturally fall into epochs which have lasted several years. During this time, surveying activity would be intense. Then, typically, a period would follow in which leveling activity would be minimal. The oldest levelings used in this investigation date back to 1906. A great many original levelings, and some relevelings, were accomplished between 1926 and 1929. A significant releveling effort was made in 1946, but it was not extended northward beyond San Fernando. Although levelings were accomplished in a time-scattered manner for the next 14 years, another major releveling of the study area was not accomplished until 1959-62.

Extensive network relevelings were performed in the epochs 1968-69 and 1973-74, with individual net segments being acquired at various intermediate and later times.

Two adjustments were performed to evaluate the preliminary conclusions mentioned in the introduction. Levelings made prior to 1962 have been used in adjustment I to estimate the magnitude, pattern, and constancy of movement for the early period. The 1959-62 epoch levelings were also used, with the 1968-69 and 1973-74 epoch measurements in adjustment II to determine corresponding information for the more recent period.

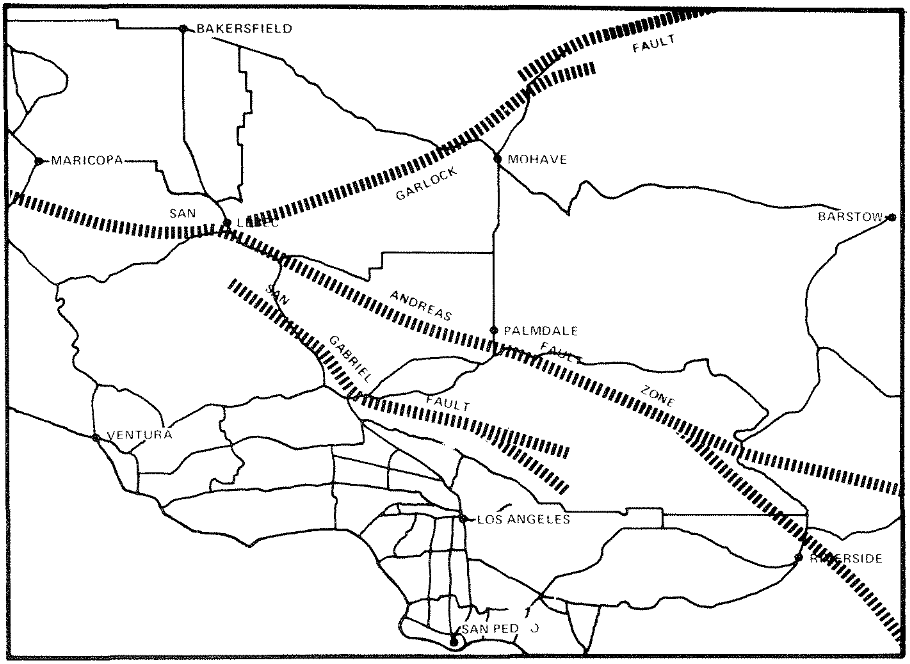

Fig. 2. Locations of level lines used to estimate uplift.

All of the leveling data used in adjustments I and II are first-order measurements, i.e., they are of the highest precision.

Tidal Data

The locations of the tide gages which were used in the analyses are shown in figure 1. Specific details concerning the stations are summarized in table 1.

Estimates of absolute velocities have been extracted from the tidal records by assuming that the secular change in sea level relative to the tidal bench mark has two basic components: (1) the eustatic or world-wide rise in sea level, and (2) the apparent change in sea level due to local and regional vertical movement of the land. The eustatic rise was taken as +1.0 mm/yr. The height change velocities at the locations of the tide gages were derived by fitting straight lines through plots of annual mean sea levels (see fig. 3). The slopes of these lines are considered to represent the velocities at which the sea was rising with respect to the land at each tide station. By reducing the slope to account for the eustatic rise of sea level, and changing the sign, a value was obtained for the velocity at which the land moves vertically with respect to a stable reference. The standard deviations of the slopes of the fitted lines were taken as the standard deviations of the corresponding velocities of elevation change at the tidal bench marks.

The annual mean sea level (MSL) values that were used in the study were not corrected for meteorological or other conditions. Wherever possible, two velocities (corresponding to the pre-62 and post-59

Table 1.--Tide Gage Stations in Southern California
(Velocities of Elevation Change are given in mm/yr)

	Adjustment I			Adjustment II		
Gage Name	Velocity	Standard Deviation	Series	Velocity	Standard Deviation	Series
San Diego	-1.33	0.41	1926-62	+2.80	1.19	1957-75
La Jolla	-0.65	0.40	1925-62	+1.63	1.43	1957-75
Newport Bay				+1.38	1.22	1956-74
San Pedro	0.00	0.39	1924-62	+3.44	1.08	1957-75
Santa Monica	-2.16	0.65	1933-62			
Port Hueneme	-4.04	1.05	1941-62			
Rincon Is.				-5.62	2.67	1962-74
Avila	-1.87	1.02	1946-70	-1.87	1.02	1946-70

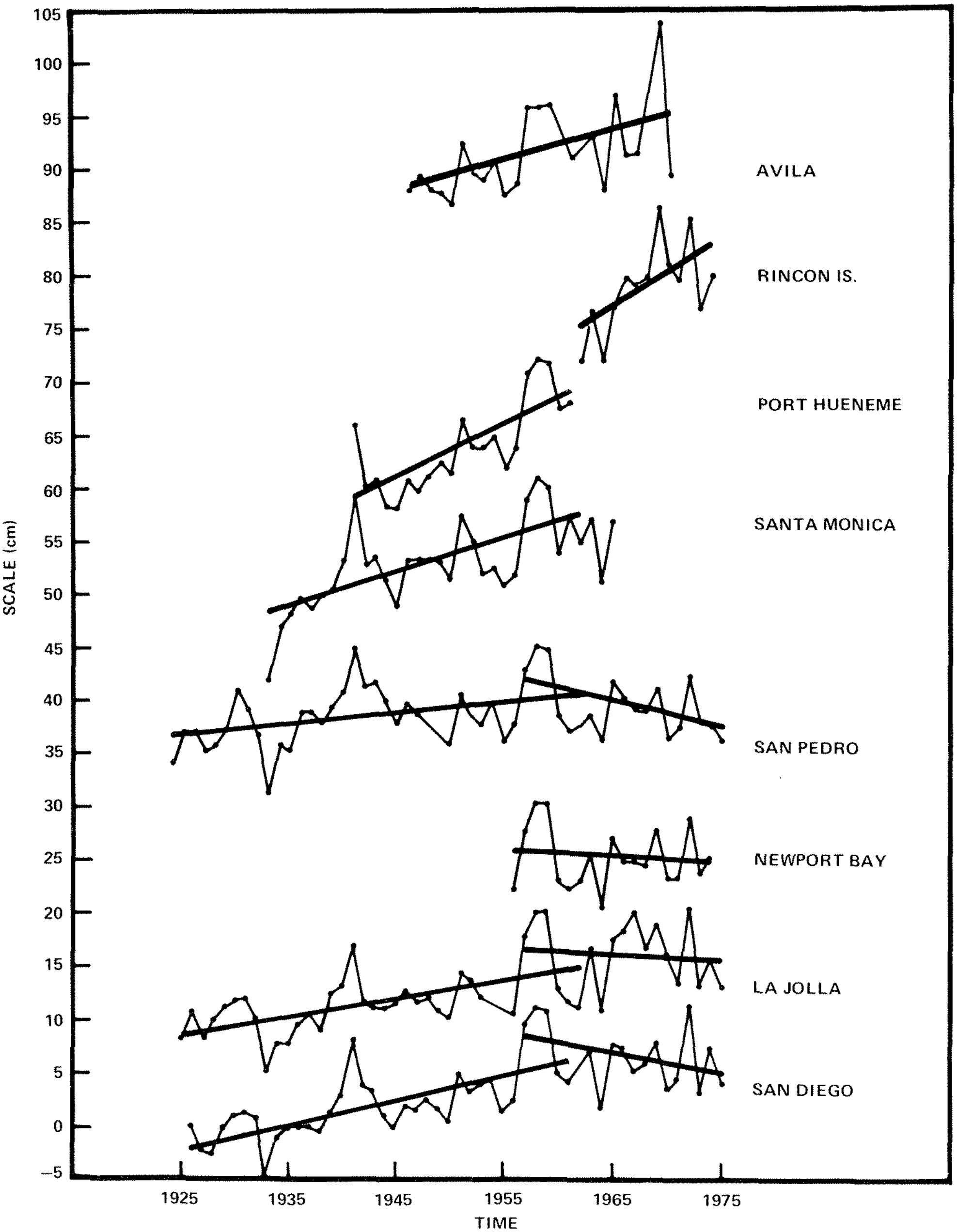

Fig. 3. Variation of mean sea level.

periods) were determined for input to the surface fitting process. For adjustment II, the annual MSL values from 1957 to 1975 were used. This eliminated bias that might have been introduced when using data which did not extend over an 18.6 year astronomical cycle.

The direct estimation of velocity at each tide gage provides the only absolute information in adjustments I and II. Analysis of leveling data without these direct estimates can provide the shape of the deformed surface, but contour labels would only be meaningful in the relative sense. Weights given to the tide gage velocities were inversely proportional to the square of their standard deviations.

Adjustment Method

For any bench mark, A, in a study area, the following expression gives its height at time t_i:

$$h_{a,i} = h_{a,o} + V(x_a, y_a)\,(t_i - t_o) \tag{1}$$

where, for example,

$$V(x_a, Y_a) = c_0 + c_1 X_a + c_2 Y_a + c_3 X_a Y_a + c_4 X_a^2 + \ldots \tag{2}$$

In equation 1, $h_{a,o}$ is the height of point A at the selected reference time, t_o, $V(x_a, y_a)$ is the velocity at location x_a, Y_a. The unknowns in the adjustment are the height at each point corresponding to time t_o, and the coefficients c_k, k = 1, 2, 3, . . . m which define the velocity surface. If u is the number of unknown junction heights, then the total number of unknowns is u + m. The number m of coefficients is arbitrary and is limited only by the number of redundant observations. In adjustment volving the Palmdale area data, 24 coefficients were used. Note that the constant term in equation (2) drops out when the observation equation is formed:

$$R_{b-a,i} = h_{b,i} - h_{a,i} - \Delta h_{b-a,i} \tag{3}$$

In (3) above, $R_{b-a,i}$ is the correction (residual) for the observed height difference $\Delta h_{b-a,i}$ made at time t_i, between points A and B.

The development of this computational approach was motivated by the need for a flexible adjustment program to deal with vertical motion of bench marks in a level network (Holdahl 1975), and the need to obtain automated graphic display of vertical deformation and velocity error sources.

The merit in fitting a velocity surface to time-scattered and repeated leveling may not be obvious if elevation change is likely not to be occurring at constant rates. Actually, a variety of benefits results from the "surface fitting" type of leveling adjustment, when the leveling data are adequately redundant:

- The adjustment determines a surface, the shape of which reflects the accumulated deformation over the time range of the leveling observations.
- The average velocities of elevation change are determined for each locality in the study area.
- The linearity or constancy of the movement is evaluated statistically.

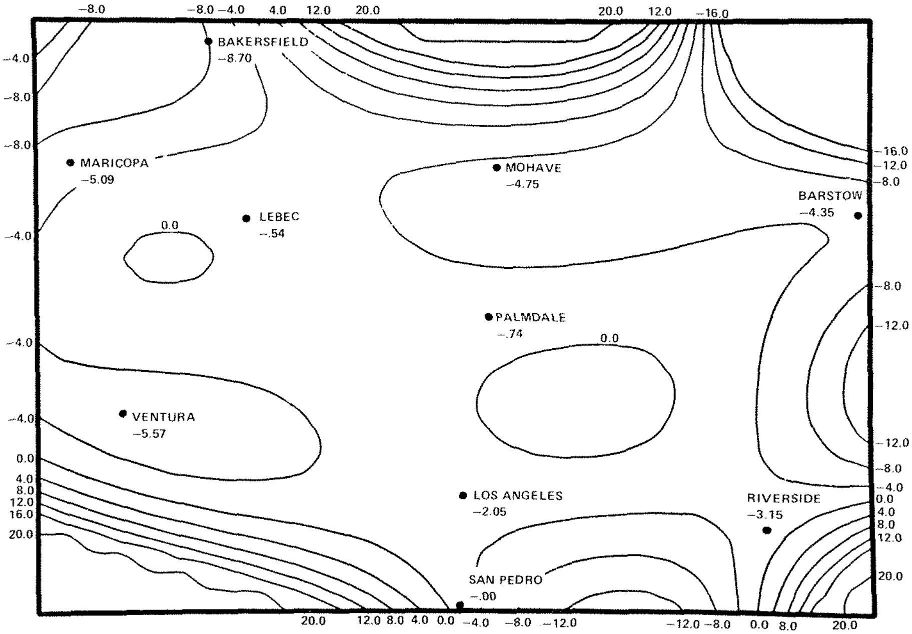

Fig. 4. Velocity contour map of Palmdale vicinity, 1906 - 1962 (units in mm/yr).

o Locations of abnormally nonlinear movements are isolated by the model.

The first benefit, determination of the shape of the deformed surface, is useful information regardless of whether the movement occurred episodically or uniformly. The estimated velocities are meaningful only if the model fits adequately. Adequate fit is evidenced by a small sum of weighted squared residuals. Adequate model fit means that movement is reasonably close to being constant with time over most of the study area.

In the adjustment each observation takes a correction. Observations taking large corrections may form a geologically meaningful pattern when plotted over the study area. A large residual is one which is several times the size of its standard deviation. The standard deviation of a residual can be computed rigorously, or can be approximated by, for example, the a priori standard deviation of the observation.

Summary of Results

Figures 4 and 5 are contour and 3-dimensional representations of the velocity surface resulting from adjustment I. Figures 6 and 7 are the corresponding contour and 3-dimensional illustrations of the velocity error surface. It is important to view figures 4 through 7 together, so that conclusions can be made about the significance and reliability of the velocities. For example, it should be obvious from looking at figures 6 and 7 that lack of data in the Pacific Ocean, west of San

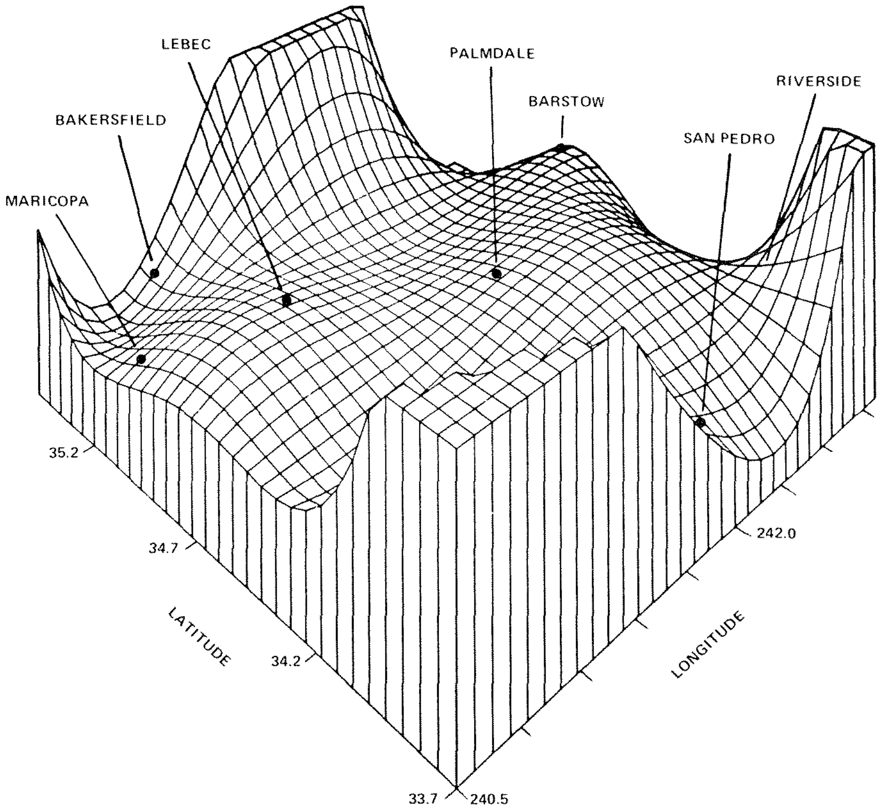

Fig. 5. Veolcity surface in Palmdale vicinity 1906 to 1962.

Pedro, and in the desert north of Barstow, make velocities computed there very unreliable.

Figures 4 through 7, corresponding to the 1906-62 data analyzed in adjustment I, show that little vertical movement had accumulated during that period. Palmdale and Lebec exhibited negligible movement, while Maricopa and Bakersfield showed subsidence, which was most likely attributable to water withdrawal for agriculture. This general pattern of movement tends to verify the conclusions of Castle et al.(1976) that the study area did not exhibit broad aseismic motion prior to 1960.

Figures 8 through 11 were generated from adjustment II, using the data from 1959 through 1976. Comparison of figures 4 and 8 shows how striking the uplift has been during the later period. The new uplift velocities at Maricopa and Mohave are more significant when it is understood that these locations were previously moving downward. The only point which has preserved its pre-1962 velocity was Ventura. The velocity standard deviations in the fastest moving areas are about half as large as the velocities. This means the uplift should be regarded as a real phenomenon.

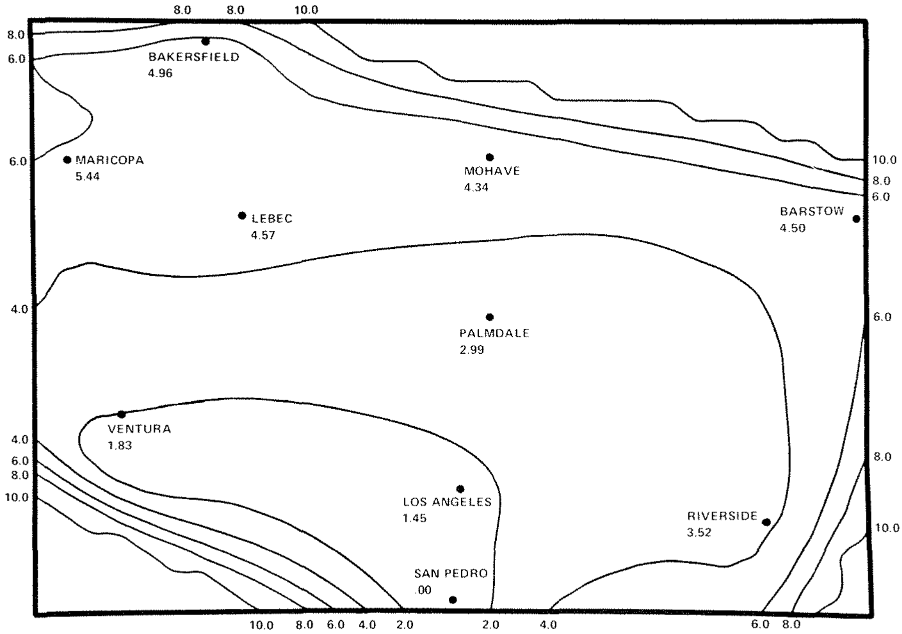

Fig. 6. Surface of velocity standard deviations in Palmdale vicinity, 1906 to 1962 (units in mm/yr).

From the "goodness of fit" standpoint, neither adjustment I nor adjustment II was particularly successful. The standard deviation of an observation of unit weight from each adjustment was 12.6 mm and 8.2 mm, respectively. An observation of unit weight in these adjustments refers to a double-run measurement, one kilometer in length, performed according to first-order specifications. It might have been possible to achieve a better model fit if the number of coefficient used to describe the velocity surface had been increased. However, poor fit was more likely caused by the use of some junction bench marks that were not outside the area affected by the 1952 Arvin-Tehachapi earthquake (adjustment I) and outside the area affected by the 1971 San Fernando earthquake (adjustment II). This latter suspicion is justified in figure 12, which shows the locations of observations taking large corrections in adjustment II.

Many of the plotted observations cluster near San Fernando. The plotted observations have residuals six times as large as their a priori standard deviations. It must also be acknowledged that a significant percentage of the aseismic vertical movement taking place in Southern California does not occur at constant rates. In fact, knowing where episodic aseismic movement is taking place may be of major importance to the seismologist. With this in mind, figure 12, or any similar illustration, should be studied carefully.

Figures 8 and 9 agree reasonably well with results first presented by Castle et al. (1976). The velocities given here indicate only 16.3 cm of

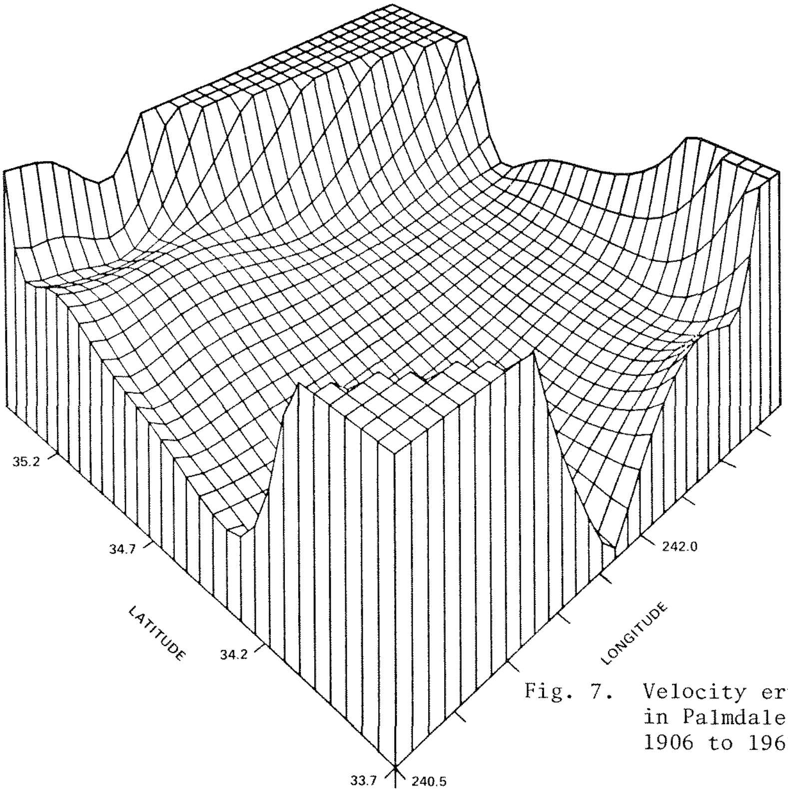

Fig. 7. Velocity error surface in Palmdale vicinity 1906 to 1962.

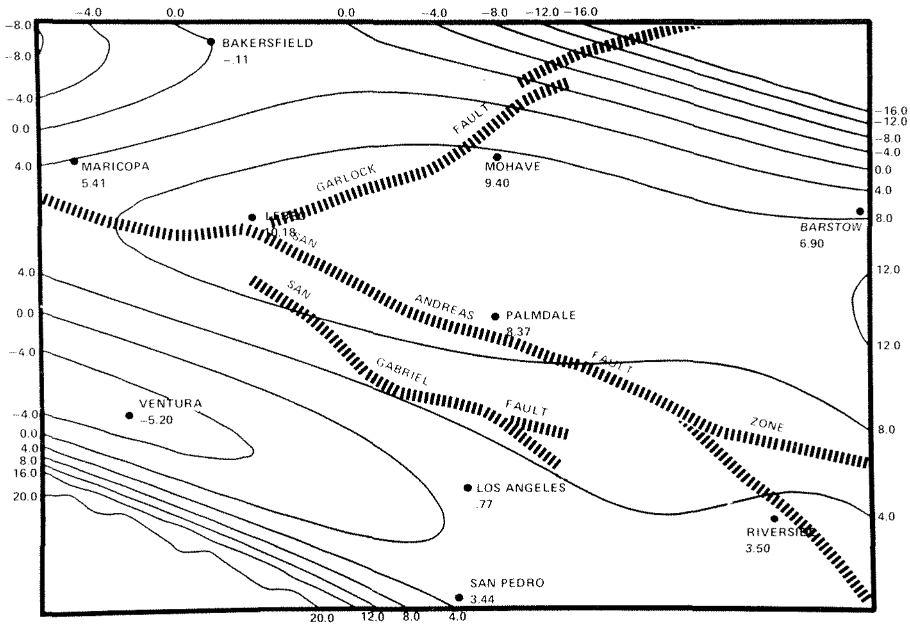

Fig. 8. Velocity contour map for Palmdale vicinity, 1959 to 1976 (units in mm/yr.).

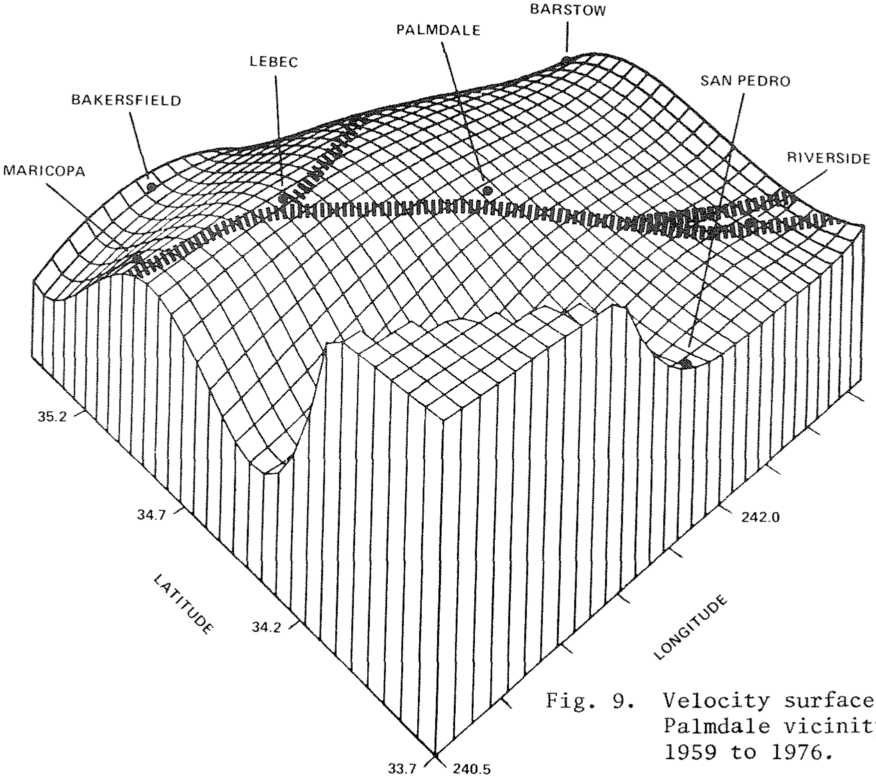

Fig. 9. Velocity surface for Palmdale vicinity, 1959 to 1976.

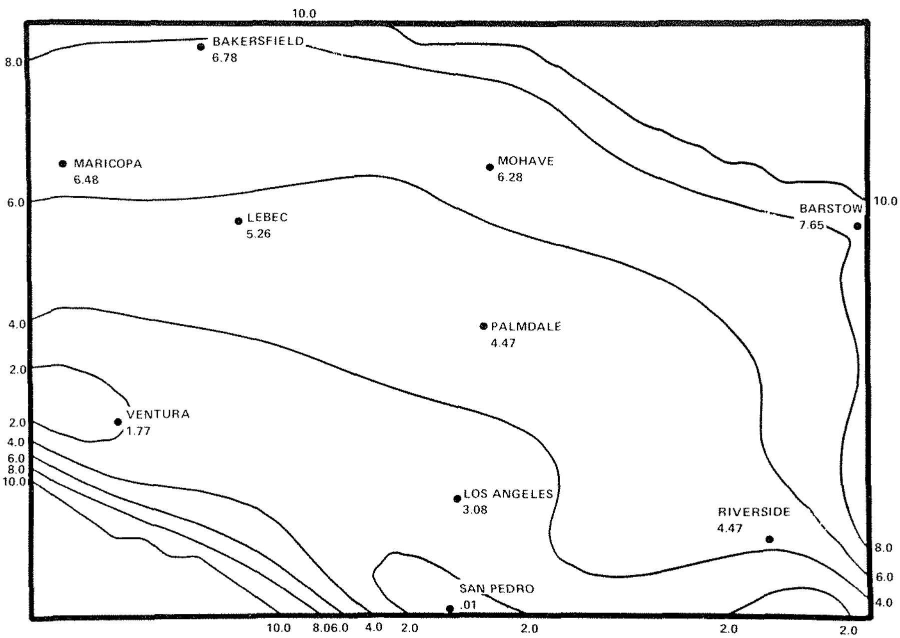

Fig. 10. Surface of velocity standard deviations for Palmdale vicinity, 1959 to 1976 (units in mm/yr).

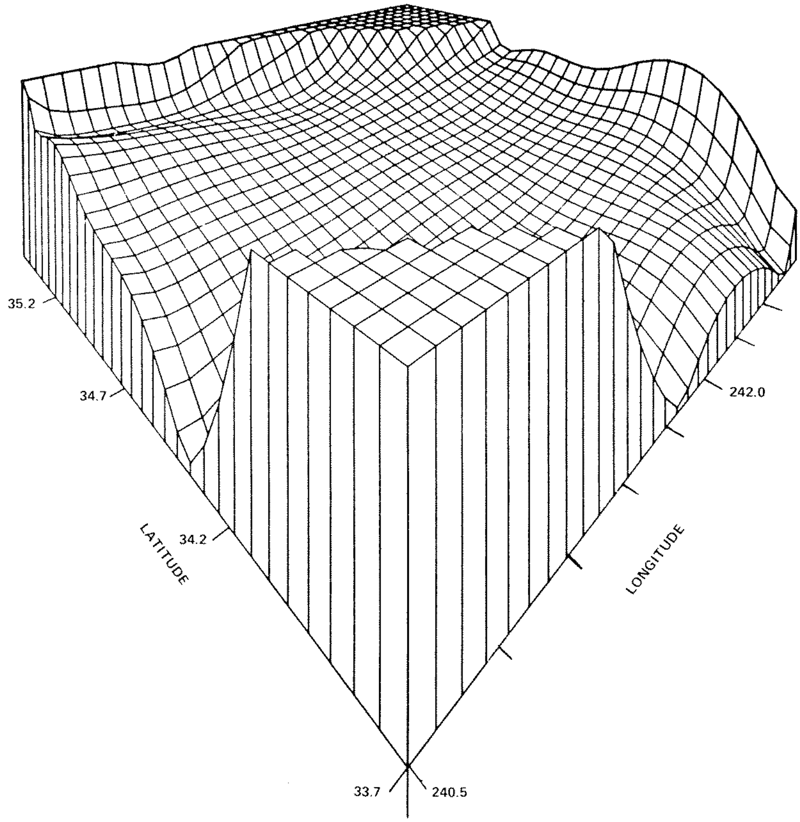

Fig. 11. Velocity error surface for Palmdale vicinity, 1959 to 1976.

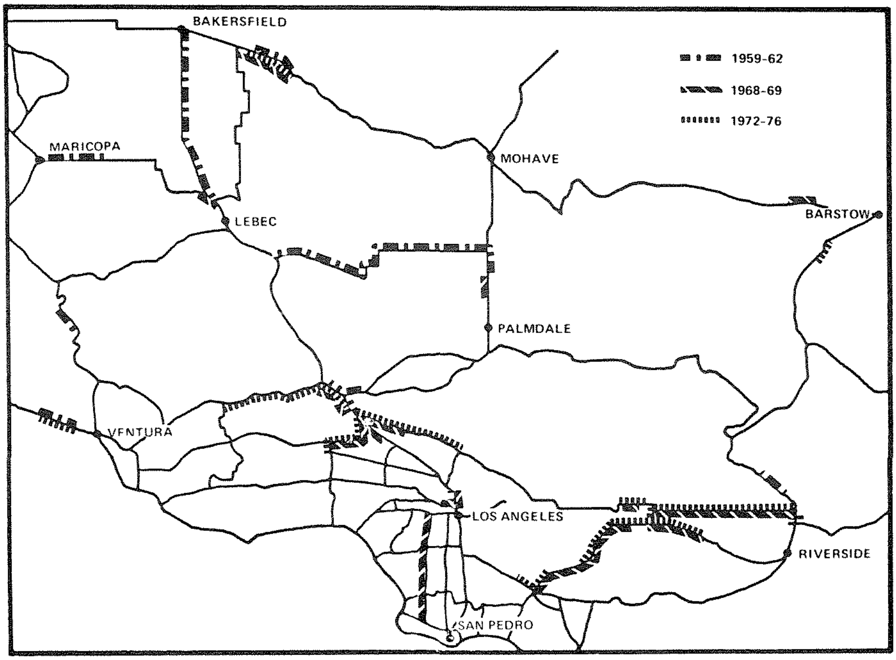

Fig. 12. Observations having excessive residuals.

uplift during the last 16 years, rather than the 25 cm first presented. However, when the NGS investigation was first performed, it included only the tidal record at San Pedro and none of the others. In that first analysis, higher uplift velocities were obtained, the maximum being 13.1 mm/yr at Lebec. Thus in some respects, the two analyses agreed more favorably prior to the introduction of additional tidal data. The zone of uplift determined here is somewhat to the north of the original maximum estimated to be at Palmdale, and no eastern terminus of the uplift is evidenced within the study area.

References

Castle, R. O., Church, J. P., and Elliot, M. R., 1976, Aseismic Uplift in Southern California: Science, v. 192, p. 251-253.

Holdahl, S. R., 1975, Models and Strategies for Computing Vertical Crustal Movements in the United States. Presented to XVI General Assembly of the International Association of Geodesy, International Union of Geodesy and Geophysics, Symposium on Recent Crustal Movements, Grenoble, France, August 25 - September 6, 10 pp: Collected Reprints 1975 National Ocean Survey, National Oceanic and Atmospheric Administration, U. S. Department of Commerce, Rockville, Md., p. 173-187.

Publication n°121 of the International Association of Hydrological Sciences
Proceedings of the Anaheim Symposium, December 1976

DETECTABILITY OF LAND SUBSIDENCE FROM SPACE

W. D. Kahn and F. O. Vonbun
Goddard Space Flight Center
Greenbelt, Maryland 20771

Abstract

Earth surface motions on the order of one to several cm per year have been observed. These motions could be due to land subsidence (i. e. the gulf coast of Texas subsides about 5 to 10 cm year; likewise, similar values hold for portions of the Flordia coast), crustal uplift (e.g. dilatancy which is a phenomena observed to precede earthquakes primarily along thrust faults), and loading (i.e. due to large dams, etc.). Knowledge of these motions is of practical importance to government and local agencies.

A possible technique of ranging from a spacecraft to a number of ground reflectors is considered for the accurate (i.e. to within fractions of cm/yr) detection of these motions. It is shown that over a six day period, assuming a 50% cloud cover, utilizing spaceborne precision ranging systems, intersite distances on the order of 5 to 25 km (dependent mostly on the beam width of the laser) can be determined in the vertical and horizontal components with errors in the 0.5 to 1.5 cm range. These errors are almost independent of ground survey errors up to 0.25 meters and orbit errors up to 200 meters.

The results shown make such a system very attractive as a new tool for monitoring very small earth surface motions.

INTRODUCTION

In many geographic areas of the globe, extremely small motions on the earth's surface have to be studied and monitored. Land subsidence, is such a relatively slow process that may continue for several decades, as shown by Tank (1973) and Legget (1973). Subsidence may produce conditions that trigger some instantaneous event such as for example, the failure of a dam or a levee. A classical example for land subsidence is that experienced in Long Beach, California. In the latter city, an area of about 52 square km. subsided about 30 to 35 cm over a twenty year period. This corresponds to a average annual rate of subsidence of 1.75 cm/yr. A precision laser ranging system in orbit and corner cube retroreflectors distributed on the ground can be used to monitor small motions near or on large dams, major construction sites, shore facilities, and structures, etc.

I. SYSTEM CONCEPT

In order to observe small motions such as those that are associated with land subsidence, arrays of laser retroreflectors are to be distributed over the subsidence region as shown in Figure 1. The smallness of the motions to be observed over several years requires the use of a rather specific ranging and/or tracking systems concept. In essence, one wants to determine very accurately (cm-range) a distance

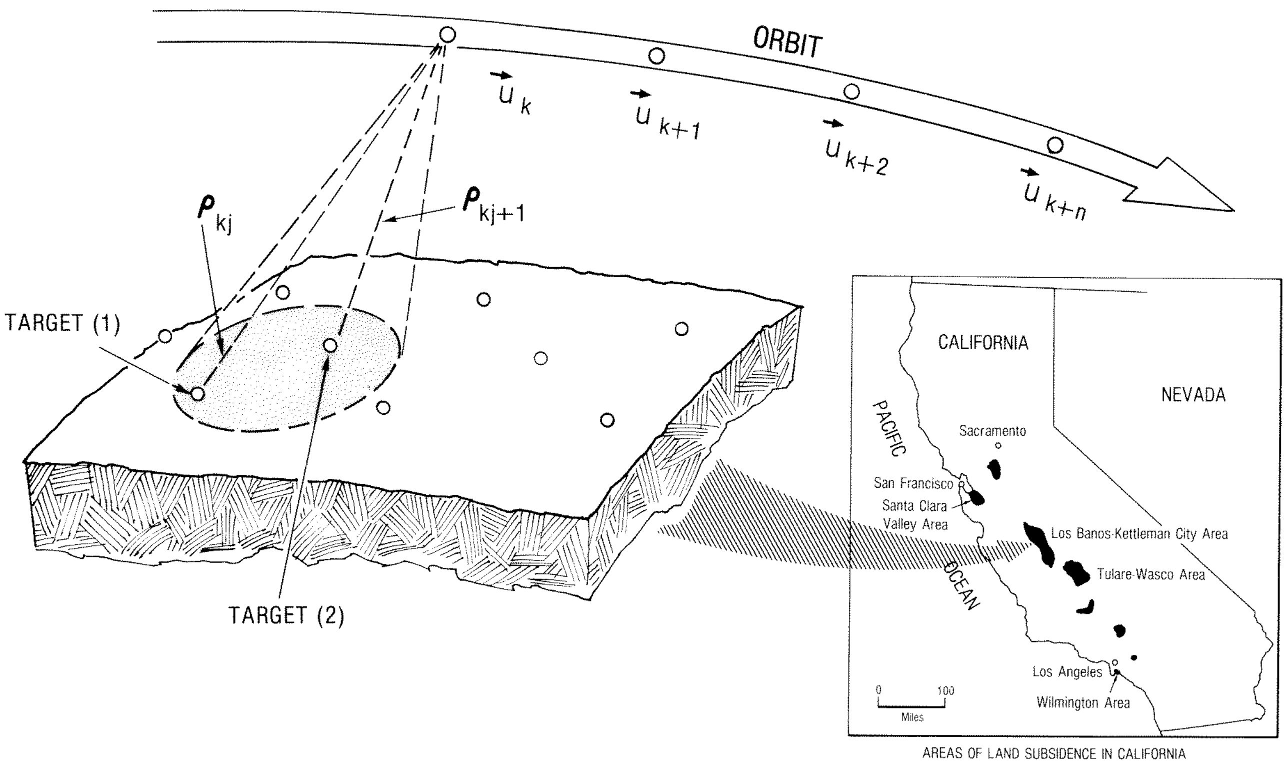

Figure 1. Land Subsidence Monitoring from Space

$|\vec{D}|$ or better, its changes between two ground points using satellite technology. In general, there are three major obstacles or error sources to overcome if one wishes to compute extremely accurate vector distances of 5 to 20 km, that is accurate to 0.5 to 1.5 cm from a spacecraft. These are:

1. Orbital errors of the spacecraft
2. Bias errors in the ranging system
3. Atmospheric propagation errors

These can be eliminated to first order by using range differencing. Practically, this means sending one pulse from the spacecraft to two or more ground stations, subtracting these measurements and using only their "differences" to compute $|\vec{D}|$, the distance between neighboring ground stations (i.e. transponders or laser corner cubes). It is thus evident by studying Figure 2 that the above mentioned error sources will not play any major role (only second order) since

$$\begin{aligned} \Delta\rho_{kj} &\doteq (\rho_{kj} + \delta\rho_{kj}) - (\rho_{kj+1} + \delta\rho_{kj+1}) \\ &\doteq (\rho_{kj} - \rho_{kj+1}) + (\delta\rho_{kj} - \delta\rho_{kj+1}) \\ &= (\rho_{kj} - \rho_{kj+1}) \end{aligned}$$

For bias errors in the ranging system

$$\delta\rho_{kj+1} = \delta\rho_{kj}$$

because both the j^{th} and $(j+1)^{th}$ reflectors are interrogated by the same signal (within the beam). For orbital errors and atmospheric refraction,

$$\delta\rho_{kj+1} = \delta\rho_{kj} + (\text{second order terms})$$

In summary, using range differences as the basic "measured" quantity eliminates all first order errors in the determination of the distance $|\vec{D}|$.

Using one pulse to cover more than one corner cube (or transponder) unfortunately raises a power problem. From a signal to noise ratio vantage point it is preferable to send a single beam out at a time to one ground station. This does, however, create a problem by introducing the effects of errors 1 and 2 mentioned before. For instances a two second time interval between pulses means their origin (spacecraft position) has separated in space by say 15 km. This means the orbit error introduced by those 15 km along the orbit pass will now increase the error in the determination of $|\vec{D}|$. The bias error in range, from firing to one cube and the subsequent firing to the other cube will further directly influence the determination of $|\vec{D}|$. Thus the control of bias errors in the ranging system and the orbit error becomes an important systems design factor. A detailed analysis of this second possibility will subsequently be published.

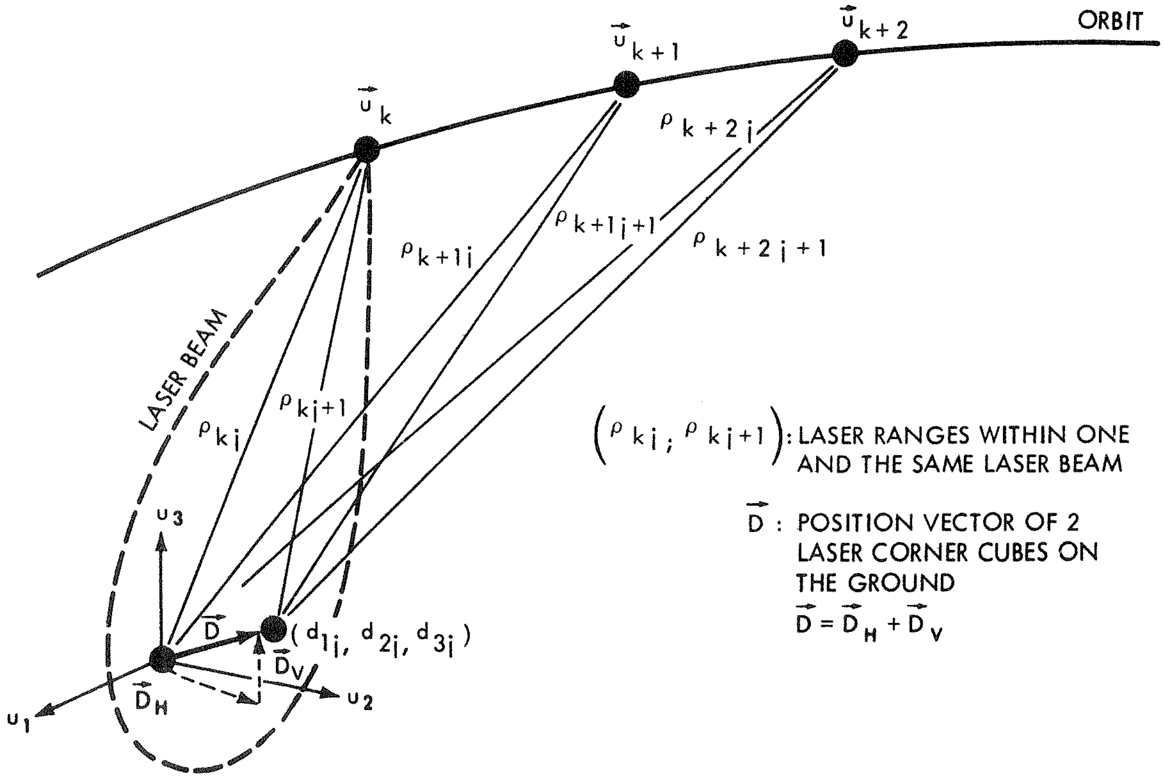

Figure 2. Schematic Spaceborne Ranging System Measurement Geometry

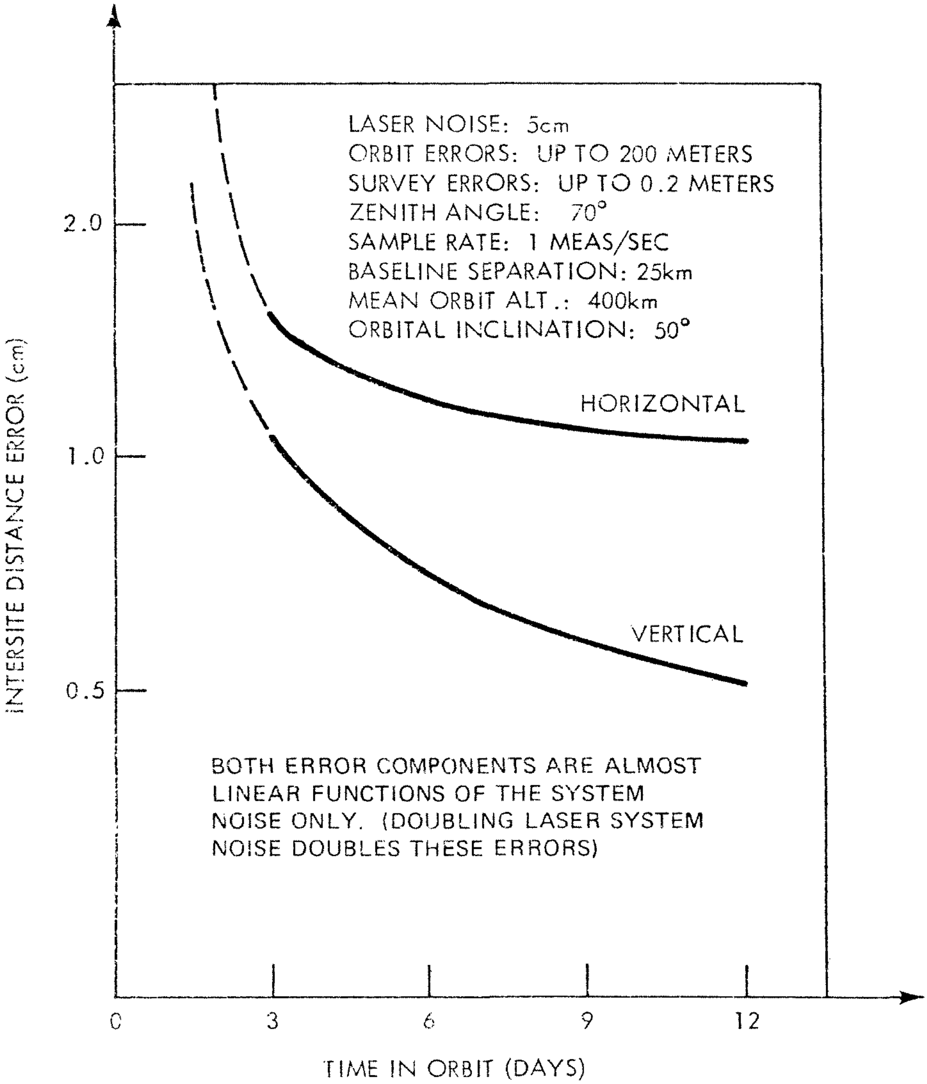

Figure 3. Intersite Distance Errors vs. Time in Orbit

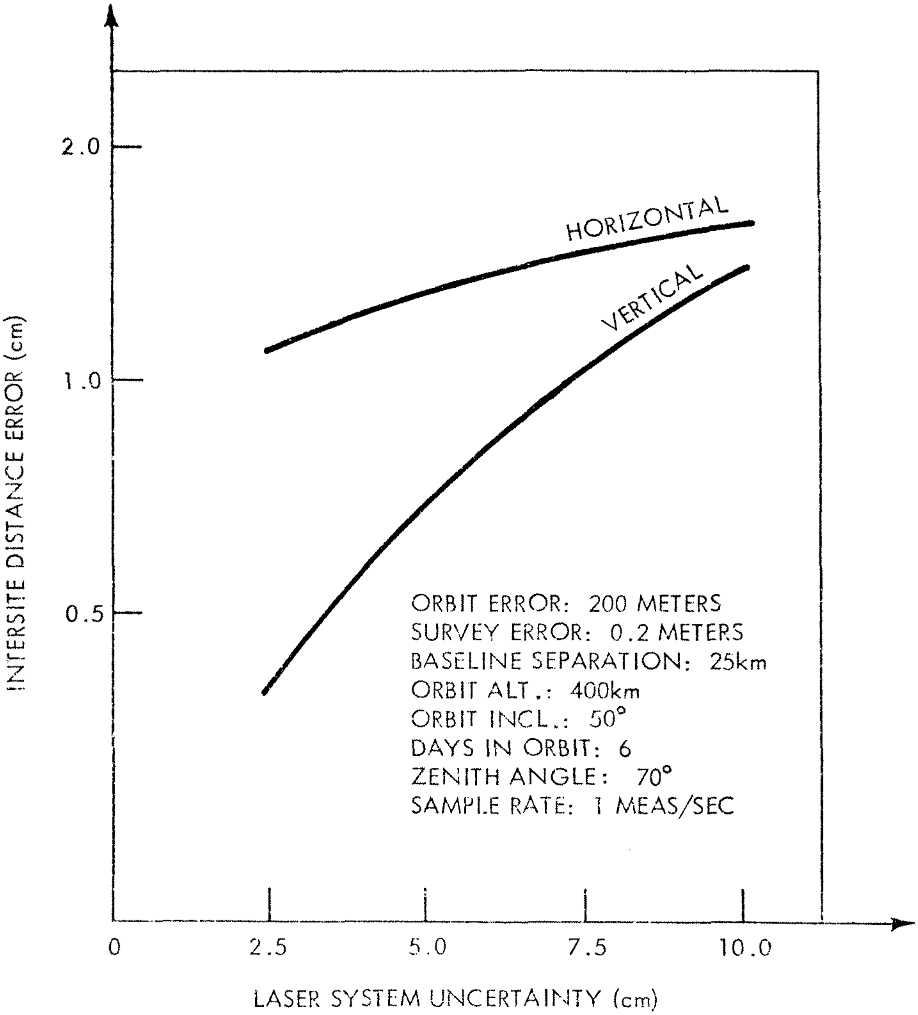

Figure 4. Intersite Distance Errors vs. Laser System Uncertainty

II. MATHEMATICAL MODELS

1. DIRECT BASELINE ESTIMATION USING SIMULTANEOUS RANGING

The variation in $|\vec{D}|$ is the quantity needed to determine small (cm-range) horizontal and vertical displacements in the earth's upper crust. This quantity represents the magnitude of the vector $\vec{D}$.

The vector $\vec{D}$ is to be computed from range difference measurements which are scalar quantities. The basic measurement, slant range ρ, from the ground stations to the spacecraft or vice versa can be expressed in matrix notation as follows:

$$\rho = (Z^T Z)^{1/2} \tag{1}$$

where

$$Z^T Z = U^T U + S^T S - 2S^T U$$

and

$$(U^T U)^{1/2} = \text{geocentric distance to spacecraft}$$
$$(S^T S)^{1/2} = \text{geocentric distance to ground station}$$

By assuming that at time t_k, a signal is sent out by the ranging system onboard the spacecraft and received at the j^{th} and $(j+1)^{th}$ station. The range at each station is by (1) expressed as follows:

$$\rho_{kj} = [(U^T U)_k + (S^T S)_j - 2S_j^T U_k]^{1/2} \tag{2a}$$

$$\rho_{kj+1} = [(U^T U)_k + (S^T S)_{j+1} - 2S_{j+1}^T U_k]^{1/2} \tag{2b}$$

with similar expressions as (2a) and (2b) resulting for times $t_{k+1}, t_{k+2}, \ldots,$

The range difference measurement is obtained by subtracting equation (2b) from (2a) which then represents the fundamental observation equation, that is:

$$\begin{aligned}(\rho_{kj} - \rho_{kj+1}) = {} & [(U^T U)_k + (S^T S)_j - 2S_j^T U_k]^{1/2} \\ & - [(U^T U)_k + (S^T S)_{j+1} - 2S_{j+1}^T U_k]^{1/2}\end{aligned} \tag{3}$$

In arriving at equation (3), the assumption made is that both stations, the j^{th} and $(j+1)^{th}$ simultaneously observe the laser pulse at time t_k.

Since the range difference measurement is subject to errors as all measurements are, and since $\vec{D}$ is derived from these measurements, $\vec{D}$ is also subject to errors. We estimate the errors of $\vec{D}$ due to errors in the range difference measurements $(\rho_{kj} - \rho_{kj+1})$. To do so, standard linear estimation theory, as shown by Deutsch (1965), is used for a set of k observations of the same cubes. That is, by varying (3) and using first order terms of the Taylor expansion one obtains:

$$\tilde{y}_{(k\times 1)} = A_{(k\times 6)} \underset{(6\times 1)}{\tilde{x}_0} + B_{(k\times 3)} \underset{(3\times 1)}{\tilde{s}_j} + C_{(k\times 3)} \underset{(3\times 1)}{\tilde{s}_{j+1}} + \varepsilon_{(k\times 1)} \tag{4}$$

where

$$\tilde{y}_{(k\times 1)} = \delta(\rho_{kj} - \rho_{kj+1})_{(k\times 1)}$$

$$A_{(k\times 6)} \equiv \left\{\frac{1}{\rho_{kj}} [U_k - S_j]^T - \frac{1}{\rho_{kj+1}} [U_k - S_{j+1}]^T\right\} \left[\frac{\partial U_k}{\partial U_0}\right]$$

$$\underset{(6\times 1)}{\tilde{x}_0} \equiv \underset{(6\times 1)}{\delta U_0}$$

$$B_{(k\times 3)} \equiv -\frac{1}{\rho_{kj}} [U_k - S_j]^T$$

$$\underset{(3\times 1)}{\tilde{s}_j} \equiv \delta S_j$$

$$C_{(k\times 3)} \equiv \frac{1}{\rho_{kj+1}} [U_k - S_{j+1}]^T$$

$$\underset{(3\times 1)}{\tilde{s}_{j+1}} \equiv \delta S_{j+1}$$

2. INTERSITE DISTANCE DETERMINATION AND ITS ACCURACY

An estimation of the intersite distance between two ground emplaced corner cube and their errors is obtained from range difference measurements by using the standard least squares estimation technique as shown by Deutsch (1965), Lynn (1974), and Reference 5. In order to minimize the effects due to geopotential uncertainties, multiple short orbital arcs of 1 to 1-1/2 revolutions are used. In the least squares process, estimates are to be obtained simultaneously for each orbital arc's state vecto as well as the coordinates of the corner cubes. The intersite distances and their erroı are computed by a least sqaures solution. A mathematical description of the estimatio process now follows.

The generalized matrix equation which represents all the observation equations obtained from simultaneous ranging from the spacecraft to two ground emplaced laser retroreflectors reads as follows:

$$\tilde{Y}_{\ell\times 1} = \Gamma_{\ell\times(6r+6)} \, T_{(6r+6)\times 1} + V_{\ell\times 1} \tag{5}$$

where

r = number of different orbital arcs for which the state vector is to be estimated r = 1, 2, . . . p;

$$p \geq 1$$

$\ell \equiv \sum_{i=1}^{r} k_i$; k_i ≡ total number of observations associated with each orbital arc.

$$\ell >>> (6r + 6)$$

The estimate of the vector T is obtained from ℓ range difference measurements with $\ell >> 1$ and a priori information about the state of each orbital arc and station survey. That is:

$$\mathbf{T}_{(6r+6)\times 1} = \underset{(6r+6)\times(6r+6)}{[\Gamma^T W^{-1}\Gamma + W_{T_0}^{-1}]^{-1}} \quad \underset{(6r+6)\times 1}{[\Gamma^T W^{-1}\tilde{\mathbf{Y}} + W_{T_0}^{-1} T_0]} \tag{6}$$

where

$W^{-1} \equiv$ A priori covariance matrix associated with system accuracy.

$W_{T_0}^{-1} \equiv$ A priori covariance matrix associated with orbit accuracy and station survey for each retroreflector.

The errors associated with the estimate of $T_{\ell\times 1}$ are obtained from the covariance matrix given by the following equations

$$E(\mathbf{T}\mathbf{T}^T) \equiv (\Gamma^T W^{-1}\Gamma + W_{T_0}^{-1}]^{-1}_{(6r+6)\times(6r+6)} \tag{7}$$

Equations (6) and (7) are now used to (a) compute the intersite distance and (b) its errors. The intersite distance, that is, the difference between the corner cube position vectors $(\tilde{s}_j - \tilde{s}_{j+1})$ is obtained by a coordinate transformation of the vector T. This transformation reads as follows;

$$\vec{D} \equiv (\tilde{\mathbf{s}}_j - \tilde{\mathbf{s}}_{j+1})_{3\times 1} = Q_{3\times(6r+6)}\, \mathbf{T}_{(6r+6)\times 1} \tag{8}$$

where

$$\mathbf{Q} \equiv [\mathbf{0}_{(3\times 6r)} \,|\, \mathbf{I}_{(3\times 3)} \,|\, -\mathbf{I}_{(3\times 3)}]_{3\times(6r+6)}$$

$\mathbf{0} \equiv$ a null matrix

$\mathbf{I} \equiv$ the identity matrix

The error in the intersite distance is now given by the covariance matrix of the intersite distances, that is:

$$E[(\tilde{\mathbf{s}}_j - \tilde{\mathbf{s}}_{j+1})(\tilde{\mathbf{s}}_j - \tilde{\mathbf{s}}_{j+1})^T]_{(3\times 3)} = \{\mathbf{Q}E(\mathbf{T}\mathbf{T}^T)\,\mathbf{Q}^T\}_{(3\times 3)} \tag{9}$$

which upon introducing Equation (7) finally reads:

$$E[(\tilde{s}_j - \tilde{s}_{j+1})(\tilde{s}_j - \tilde{s}_{j+1})^T]_{(3\times 3)} = \{\mathbf{Q}[\Gamma^T W^{-1}\Gamma + W_{T_0}^{-1}]^{-1}\,\mathbf{Q}^T\}_{(3\times 3)} \tag{10}$$

Equation (10) represents the intersite distance error, and is the basic equation used for spaceborne laser ranging system error analysis. Numerical results using (10) are depicted in Figures 3 and 4.

III. ERROR ANALYSIS RESULTS

Figures 3 and 4 describe the results of a covariance error analysis in which the former figure provides an estimate of the precision with which the intersite vector components can be determined for a 5-element, 25-km grid as a function of time in orbit and the latter figure relates intersite vector component precision to the spaceborne laser ranging system. For this analysis, very moderate systems errors were assumed.

Although orbital errors up to 200 meters were used in the error analysis, their contribution to the intersite vector's components (i. e., vertical and horizontal) consistently remained negligible. In a similar fashion, survey errors associated with the location of the retroreflectors also do not significantly change the errors in the vertical and horizontal components of the intersite vector.

In Figure 4 however, there is linear dependency indicated for both the vertical and, to a lesser extent, horizontal components of the intersite vector to the spaceborne lasers system precision. As can be seen, a 5-cm system is adequate, producing errors in the 0.7 and 1.3-cm ranges, respectively. Ground laser ranging systems having precision of ±5 cm are now operational at Goddard Space Flight Center, thus no difficulties are forseen in achieving this same level of precision for a spaceborne laser system.

IV. PRACTICAL APPLICATIONS

The spaceborne laser ranging system can be developed as a payload for the shuttle applications program. The typical mission duration would be 7 days with a nominally circular 400-km orbit. Orbital inclination would be between 50 and 57 degrees.

A breadboard model of the spaceborne laser system is under development at GSFC as shown by Minott (1975). Such a system can be utilized to detect small variations in the earth's upper crust in the 0.3 to 0.5-cm/yr range. Monitoring, is thus possible, of land subsidence as it occurs in the coastal regions of California, Texas, and Florida, as well as construction sites such as dams and even large buildings.

V. CONCLUSIONS

This paper and earlier Vonbun, Kahn, et al., have shown that a spaceborne laser ranging system can be used to determine intersite distances up to 25 km, depending only on the beamwidth or beam splitting of a spaceborne laser system within a 6-day shuttle mission to a precision 0.5 cm to 1.5 cm (assuming 50% cloud coverage). Covariance error analyses have shown that (a) orbital errors up to 200 meters, (b) survey errors up to 0.25 meters, and (c) range bias errors (many meters) do not significantly influence the accuracy with which the intersite vector can be determined. In fact, the latter error sources are second order effects. Consequently, the spaceborne laser ranging system as envisaged, has potentially many practical applications where small relative motions are to be monitored.

REFERENCES

Deutsch, Ralph, "Estimation Theory" Prentice Hall, 1965.

Legget, T. R., "Cities and Geology", 1973, McGraw Hill, Inc.

Lynn, J. J., "NAPCOV Program Documentation". Old Dominion Systems, Inc. November 1973 (revised May 1, 1974).

Minott, P. O., "Design of a Ground Based Laser Retroreflector Array for Space to Ground Geodey", Unpublished Report, Revised March 1975.

Old Dominion Systems, Inc., "User's Guide to Data Preparation, Navigation Analysis Program (NAP 3.1)," April 1974.

Tank, R. W., "Focus on Environmental Geology", Oxford University Press, 1973.

Vonbun, F. O., Kahn, W. D., et al., "Spaceborne Earth Applications Ranging System — SPEAR," Goddard Space Flight Center Preprint, December 1975.

Publication n°121 of the International Association of Hydrological Sciences
Proceedings of the Anaheim Symposium, December 1976

SUBSIDENCE IN THE BOLIVAR COAST

O. Nuñez and D. Escojido
Maraven, S.A., Venezuela

Abstract

The greater part of the eastern shore of Lake Maracaibo, the Bolivar Coast, extends over an area of low ground and swamp. Compaction is presently the principal production mechanism for oil recovery from the Bolivar Coast heavy oil reservoirs. In 1929 the first signs of subsidence were observed and by 1930 a system of bench marks was installed and precise levelling taken at regular intervals.

Laboratory studies carried out on cores of the Bolivar Coast showed that the compressibility of loose sand was of the same order as that of the clay and therefore the clay and sand compaction were the main causes of the subsidence.

Subsidence is observed over a total area of 452 sq. km. As subsidence continued, it became necessary both to protect the area from flooding and construct a drainage system. The coastal dykes are built in succesive steps and are raised according to the forecasted subsidence. This forecast is based on the extrapolation of the linear relationship observed between fluid withdrawal and measured subsidence together with an estimate of future gross production from the reservoirs.

History

The greater part of the eastern edge of Lake Maracaibo, known as the "Bolivar Coast" (Fig. 1), extends over an area of low ground and swamp. Before the start of oil field operations in 1926 these swamps were separated from the Lake by a comparatively narrow strip of land slightly higher than mean Lake water level, but these strips of land became inundated during high tides and storms with strong onshore winds. A number of shallow gutters connected the swamps to the Lake and during the dry season water flowed from the Lake into the swamp, while during the rainy season this flow would be reversed.

During several years, oil field operations were limited to the coastal strip of land in the Tía Juana, Lagunillas and Bachaquero fields, and small earthen dykes were built by hand labor along the shore, using the vegetation on the foreshore as a breakwater. On account of the subsidence, to which the attention was drawn for the first time by a dyke break in 1929 and subsequent flooding of one camp, the foreshore became permanently submerged and the vegetation started to whither away, leaving the earthen dyke exposed to wave action. In the beginning the hope existed that the subsidence phenomenon would be of a temporary nature and therefore it was tried to protect the earthen dykes against erosion by the use of local materials such as corrugated iron sheets and junk tank plates, making a breakwater of any type of junk material laid at the toe of the dyke. This additional protection had some beneficial effects locally and in shallow water, but required continuous supervision and maintenance. Several other types of protection such as clay facing on the earth dyke and a palisade close to the toe of the dyke, grooved wooden sheet piling made of pine boards, a facing of gravel and bitumen emulsion etc. were failures. It was soon realised that these temporary structures had to be replaced by a more permanent protection (at least over the part of the coast with considerable subsidence). Therefore a concrete dyke was constructed while a drainage system was also built to protect the area from inundations.

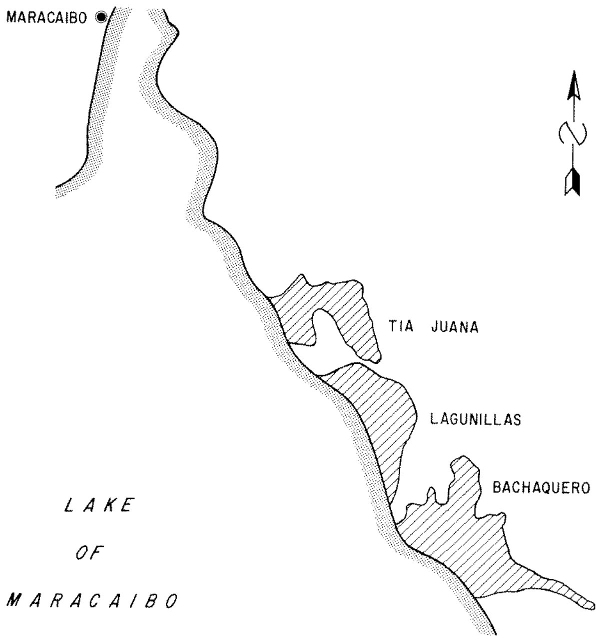

Fig. 1

Oil Reservoirs

The main heavy oil reservoirs found on the "Bolivar Coast", initially contained some 35 billion bbl of oil in place (in Maraven acreage which covers the land areas but the reservoirs extend under the Lake) with gravities in the range of 10 to 15 °API. The reservoirs are characterized by moderate depth (generally 1,000 to 4,000 ft.), good formation properties such as net oil sand thickness (50 to 600 ft.), high porosity (30 to 40 percent), permeability (1 to 8 darcies), oil saturation (initially about 80 percent) and high oil viscosity (100 to 10,000 cp. in situ). The three fields, Tía Juana, Lagunillas and Bachaquero, are drilled up with some 5300 wells in a triangular pattern, with a basic well spacing of 231 meters (10 acres/well).

The reservoirs consist of unconsolidated sands, interspersed with clay lenses. The average sand/clay thickness ratio for Tía Juana, Lagunillas and Bachaquero is approximately 1.8:1, 1:1 and 1:1 respectively. These values are not uniform throughout the reservoirs and could not be used for compaction calculations. For the calculations, not only the total amount of clay is needed, but also the clay distribution. Since the compaction factor depends greatly on the thickness of the clay beds, a subdivision into beds of different thickness is required. Such studies were performed for the three fields.

Development of the Lagunillas field started as early as 1926 and already by 1929 first signs of subsidence were observed. Development of Tía Juana and Bachaquero fields started around the mid thirties and also subsidence was soon observed. Only after the second world war. considerable surface subsidence above the three fields occurred as a result of a sharp increase in offtake.

Subsidence in the Bolivar Coast fields had been ascribed to the compaction of soft clay layers in and adjoining the producing sand layers. An analysis showed that this concept led to discrepancies between calculated and observed subsidence. Four wells were continuously cored to obtain precise information on the distribution of sand and clay in the producing intervals and to carry out compression experiments on representative sand samples in order to establish the contribution of sand compaction.

Compression Experiments

The compression experiments on clay and sand as reported by van der Knaap (1967) revealed that under conditions prevailing in the Bolivar Coast reservoirs, the final compressibility of the two materials is of the same order of magnitude. This means that the total reduction in thickness of an interval from which fluids have been produced is insensitive to the ratio in which sand and clay layers occur. This is only partially correct, because upon fluid withdrawal, the pressure in the permeable sand drops more rapidly than that in the almost impermeable clay. This results in a delayed compaction of the clay layers. This effect is naturally more marked when the clay layers are thick.

With the compaction of the clay layers, water is pressed into the oil bearing sands, thus creating a weak water drive. An estimate of the water production to be expected in compacting oil reservoirs should therefore include a subsurface study of the total clay thickness and its distribution.

The cores obtained from the wells were also examined for clay-mineral and granular composition. Differences in clay composition were found to be small. The clay is mostly of an illite/kaolinite type. The sands are angular and fine to medium fine. Despite large distances separating the cored wells no significant differences in clay mineral composition or angularity and size of the sand grains were observed. This implies that a uniform compaction behaviour over the area may be expected.

Compaction Mechanism

Compaction of porous sands and clays is caused by an increase in the effective pressure, expressing the net load on the rock matrix and defined as the overburden pressure minus the fluid pressure in the pores. In the field the reservoir is loaded and compacted due to decrease of the reservoir pressure, while overburden pressure remains constant. Reservoir fluid pressure has to drop in some cases below a definite value or threshold value before compaction and hence subsidence occurs. Such is the case of Bachaquero as reported by Merle et al (1975). The compaction characteristics of Bachaquero, evident from plots of compaction (as a percentage of initial gross reservoir thickness) against pressure drops derived from field data, are illustrated in Fig. 2 for four reservoir blocks at different depth. It is seen that negligible compaction occurs until a certain effective pressure has been exceeded, that the magnitude of this threshold value increases with reservoir depth, and that formation compressibility, as reflected by the slope of the compaction curves, becomes smaller at greater depths.

Based on observations in loading/unloading/reloading experiments on Bolivar Coast sand samples, it has been concluded that Bachaquero compaction behaviour is probably due to the reservoir having been subjected in its geological history to a higher effective pressure (larger load) than that existing at the start of the production.

The interpreted compaction history of a given part of the reservoir since its deposition is shown in Fig. 3. After deposition the formation is loaded by sediments until some maximum depth has been reached. Subsequently, the reservoir is unloaded due to uplift and erosion of overlying

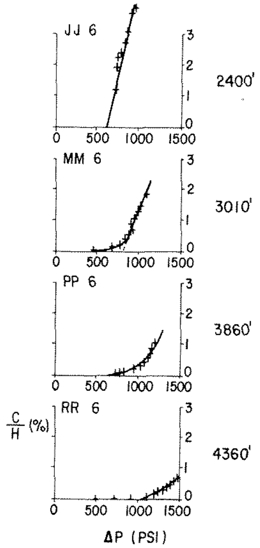

Fig. 2

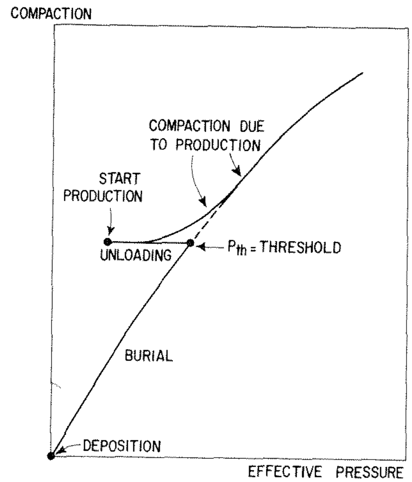

Fig. 3

sediments or due to overpressuring of the reservoir fluid or due to both. During this unloading, expansion of the formation is minimal since sand compaction is almost irreversible. Decreasing the reservoir fluid pressure due to withdrawal of oil results in reloading of the reservoir. Initial compaction remains small until the previous maximum load (threshold) has been exceeded by a few hundred psi, upon which the original compaction curve is followed again.

Liner failure, casing collapse and the necessity for dykes to contain the Lake are some of the problems arising from the subsidence. On the other hand, it should not be forgotten that compaction is a very effective recovery mechanism particularly in heavy oil reservoirs. The volume of the surface sink represents at least part of the oil produced.

In studies of the overall field performance of the Bolivar Coast reservoirs it has been found that during the more recent production history incremental subsurface volumes of produced oil, gas and water approximately equals incremental surface subsidence volumes. From these observations it may be concluded that, following the initial production period when there was an active solution gas drive, formation compaction becomes the main production mechanism. By the end of 1975 compaction drive accounted for some 60% to 80% of total oil produced.

Summarizing, it has been found that for strongly subsiding oil fields, a straight line relationship exists between subsidence and reservoir withdrawal after an initial period of low subsidence when the principal producing mechanism was solution gas drive (Fig. 4).

Evaluations

Formation compaction, surface subsidence and the contribution made by compaction to oil recovery have been investigated by radioactive bullets, ground level measurements and material balance analysis respectively which are now discussed: 1) Over the period 1956-1964 nine wells of the Bolivar Coast fields were shot with radioactive bullets. The purpose was to provide

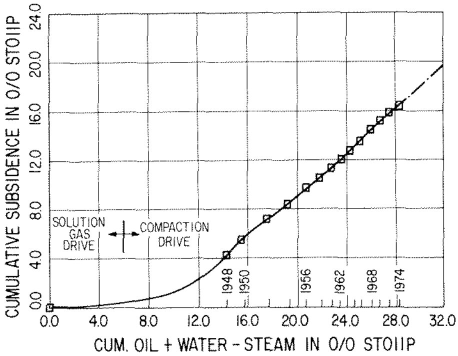

Fig. 4

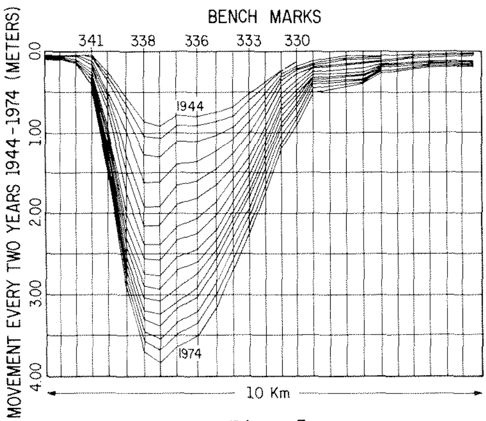

Fig. 5

markers for observation of changes in subsurface thickness resulting from compaction. Bullets in the overburden were spaced approximately 100 ft. apart and bullets over the productive interval at 10 ft. intervals. Subsequent measurements of the bullet depth yield information on changes in reservoir and overburden thickness. On each measurements the following was recorded: a gamma ray curve, a casing collar log, the cable magnetic marks, time marks every 4 seconds and cable tension increments. Results in general show compaction over the productive sand intervals while the clays appear to have expanded. This apparent lengthening may be attributed to the presence of a systematic error, possibly in the cable marking process. The value obtained for the compaction of the reservoir after removing the assumed systematic error is close to surface subsidence measured by the movement of the well head. However, the accuracy of the radioactive bullet surveys did not prove completely satisfactory. 2) In 1929 the first signs of subsidence were observed and by 1930 a system of bench marks was installed and precise levelling taken at regular intervals in order to check further ground movements. The surveys are presently carried out every two years. The subsiding areas are in the form of a bowl and coincide with the productive areas (Fig. 5). As stated previously a linear relationship is observed between volumetric subsidence and fluid withdrawals. In May 1932 a check levelling was carried out which showed a maximum of 43 cm. of difference with the first levelling; subsequent measurements showed a progressive subsidence. In the period between 1930 and 1939 the yearly rate at the point of maximum subsidence along the coast was about 22 cm. Observations in subsequent years have been carried out and in 1976 the total cumulative maximum subsidence is 410 cm. At present, a system of 1244 bench marks exists in the three main fields of the Bolivar Coast. 3) Material balances indicate that formation compaction contributes significantly to oil production. The material balance equation may also be used to predict the recovery from a compacting field for a given pressure drop and the ultimate compaction at abandonment pressure. Results are such that for complete pressure depletion total compactions in the range of 7-13% of NOS may be expected, leading to recoveries of 15-25% of STOIIP.

Dyke and Drainage Systems

The subsidence is observed over a total area of 452 sq. km., 189 sq. km. under Lake Maracaibo and 263 sq. km. along its eastern shore. As subsidence continued, it became necessary both to protect the area from flooding and construct a drainage system. This protection consists of 44 km. of coastal dyke whose main function is to avoid floods by Lake Maracaibo and 58 km. of interior dykes to create a protection against rain water draining down from higher ground (Fig. 6).

Dyke System

The present dykes are built by steps and have the following characteristics: 1) The height of the dyke is determined by the water level and the wave run-up, all in accordance with the expected subsidence. It is known that waves generated by wind are irregular in height and length. During wave attack some waves reach the crest and some do not; as a criterion for the height of the dyke it has been assumed that not more than 2% of the numbers of waves during a storm should reach the crest. The Delft Hydraulics Laboratory has carried out studies and model tests with water depths of 2.8 m. or more and a dyke with a smooth slope and a gradient of 1:3. The conclusion from this work was the necessity of a dyke height of at least 3.75 m. above the mean low lake level (MLLL). This height may be reduced to 1.8 m. above the MLLL by application of a layer of rip rap 1.25 m. thick. For water depths of less than 2.8 m., the waves are lower and consequently the wave run-up is reduced so a lower dyke would suffice; nevertheless a minimum dyke height of 1.8 m. above the MLLL is generally required. 2) The Delft Soil Mechanics Laboratory has studied the stability of the dykes based on soil investigations and the results showed that for a dyke with a height of 10-12 m. on a subsoil of silty sand an outer slope is required not steeper than 1:2.5 and an inner slope not steeper than 1:3. For lower dykes on the same subsoil, a somewhat steeper inner slope could be accepted. The outer slope of low dykes, however, should not be increased. For the stability of the outer slope a shallow sliding plane is critical, while for the stability of the inner slope a deep one is determinant. On a subsoil of sandy silt, the inner slope of a dyke with height of 10-12 m. requires an even gentler slope. However, for lower dykes in general a slope of 1:3 is still acceptable. The gradients of 1:2.5 and 1:3 as mentioned above are only permissible if the material of the dyke body has friction properties at least corresponding to an angle of internal friction of 25° and a cohesion of 2.2 kg. per cm^2 with good drainage near the inner toe. 3) The revetment of the outer slope generally consists of concrete slabs, supported at the toe of the dyke by a sheet piling. This sheet piling is also of concrete, except in some few places where wooden piles have been used. In 1966, movements of the concrete slabs were observed over a length of about 400 m.; these movements caused permanent dislocation in some areas and for this reason the use of concrete slabs was discontinued and it was replaced by a flexible revetment. This consisted of a layer of stones each weighting between 10 and 120 kg. while the lowest 20 cm. of the layer should be penetrated with asphalt mastic. To apply the asphalt mastic, as well as to prevent a viscous flow after application, the slope should not be steeper than 1:3. On this revetment a layer of rip rap should be dumped with a thickness of 1.25 m. on the slope and of 1.0 m. on the berm when it exist. The weight of the stones of the rip rap on a slope of 1:2.5 to 1:3 should be between 300 and 800 kg. with an average of 500 kg. The inner slope is protected with a grass-lining (corocillo) (Fig. 7). 4) Three type of soils are used in the construction of the dykes. The permeability of these soils is increased from the outer slope toward the inner slope (Table I).

The progressive raising of the dyke is determined by the rate of subsidence. However, it cannot be predicted exactly and therefore it is advis-

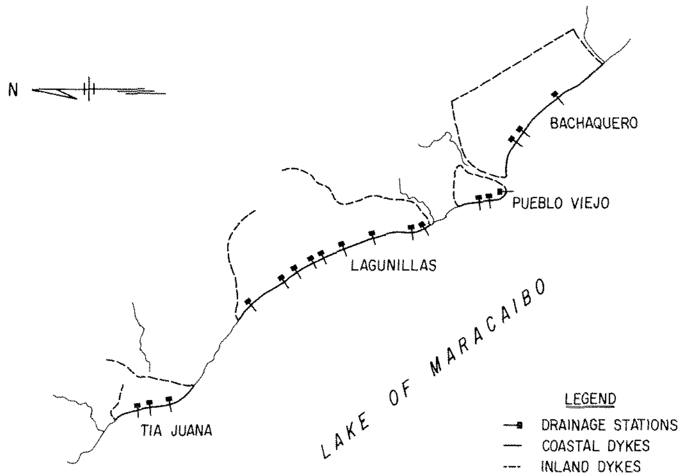

Fig. 6

able to raise the dykes in steps. This prevents construction of dykes higher than will be ultimately required (Fig. 8). In general, a ditch is present at varying distances behind the dykes. If a relatively permeable layer under the dyke has to be drained, this can be done by connecting the ditch with this layer.

Drainage System

For the drainage of the field area small pumps (each of capacity of 1350 m^3/hr) were installed in 1939, with sufficient capacity to handle the run-off water of a 3 in. rainfall in 24 hours.

At present, the drainage system in the Bolivar Coast Area consists of 22 drainage stations with a total of 55 pumps. The drainage capacity is 104,445 m^3/hr and the total ditch length is 345 km. All the drainage stations are located near the Coast and the water is pumped to the Lake via steel pipeline (Fig. 6).

Prediction of Subsidence

The prediction of future subsidence has been achieved through extrapolation of the volumetric subsidence/cumulative gross production trends for individual production blocks in conjunction with a production forecast in line with Maraven's long term estimate of future activities. The migration pattern existing between production blocks can be studied by comparing the field trend with the individual production block trend. If no migration occurs, both trends are the same; efflux (migration >0) from the block causes the block trend to be higher whereas trends for blocks with a cumulative influx (migration <0) will be lower than the field trend.

Results of the subsidence prediction at the bench marks along the dyke in the Lagunillas field for 1976 were compared with measured values. The difference did not exceed 1.3 cm. (Table II).

Costs

Up to 1976 costs of construction and maintenance of the dyke and drainage systems amounted to 35 million dollars. It is estimated that future spending on the systems will amount to 5 million dollars per year.

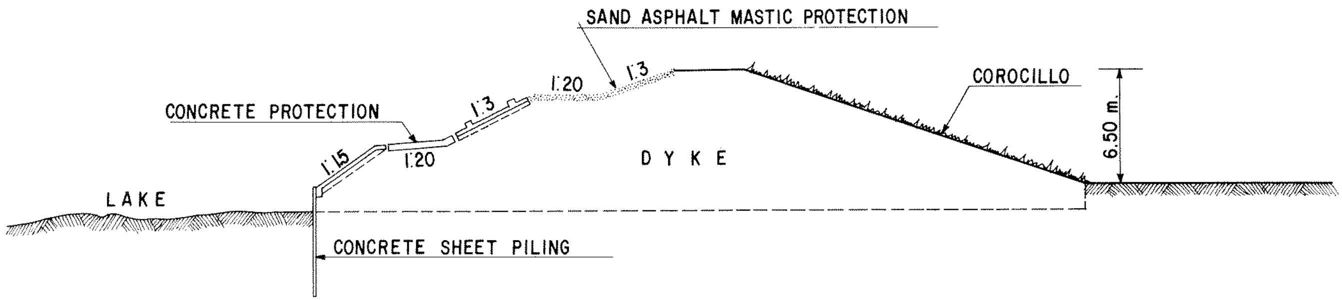
SAND ASPHALT MASTIC PROTECTION
CONCRETE PROTECTION
COROCILLO
1:3
1:20
1:3
1:20
1:15
6.50 m.
D Y K E
LAKE
CONCRETE SHEET PILING

Fig. 7

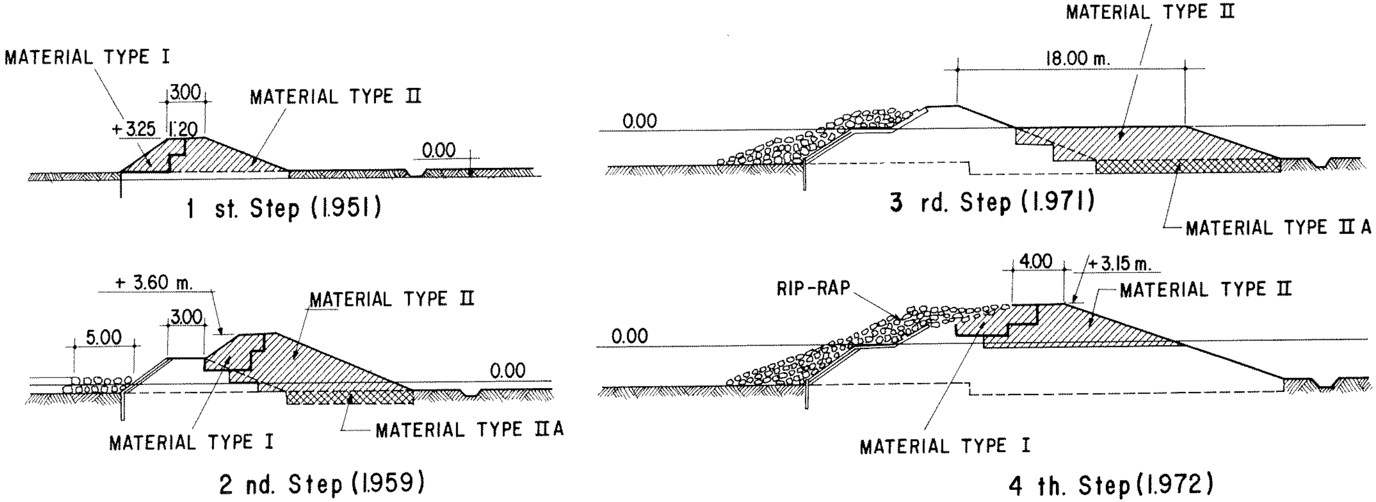
MATERIAL TYPE I
3.00
+3.25
1.20
MATERIAL TYPE II
0.00
1 st. Step (1.951)
+ 3.60 m.
3.00
5.00
MATERIAL TYPE II
0.00
MATERIAL TYPE I
MATERIAL TYPE II A
2 nd. Step (1.959)
MATERIAL TYPE II
18.00 m.
0.00
3 rd. Step (1.971)
MATERIAL TYPE II A
4.00
+3.15 m.
RIP-RAP
MATERIAL TYPE II
0.00
MATERIAL TYPE I
4 th. Step (1.972)

Fig. 8

Conclusions

1. Subsidence has been observed in the three main fields of the Bolivar Coast.
2. Reservoir fluid pressure has to drop in some cases below a definite value or threshold value before compaction and hence subsidence occurs.
3. Compaction is a very effective recovery mechanism particularly in heavy oil reservoirs.
4. Under conditions prevailing in the Bolivar Coast reservoirs, the compressibility of the sand and clay is about the same.
5. A good system of bench mark is required to carry out precise levelling at regular intervals and predict future subsidence.
6. The height of the dykes is determined by the water level and the wave run up, all in accordance with the expected subsidence.
7. A good drainage system is required to avoid floods.
8. A straight line relationship is observed between volumetric subsidence and fluid withdrawals. The prediction of future subsidence is based on the extrapolation of this line.
9. It is estimated that 5 million dollars per year will be spent on maintenance of the present dyke and drainage systems.

TABLE I

TYPE OF SOILS USED IN THE DYKE

	Particles < 5 μ	Particles > 60 μ
Type I	40 - 60%	max. - 25%
Type II	15 - 30%	30 - 60%
Type IIA	15 - 23%	40 - 60%

TABLE II

ESTIMATED AND MEASURED SUBSIDENCE OF BENCH MARKS ALONG THE DYKE OF THE LAGUNILLAS FIELD

Bench Mark	SUBSIDENCE, 1976 Estimated (cm)	Measured (cm)	Difference (cm)
AA	393.6	394.9	-1.3
D	376.0	377.2	-1.2
T	36.5	35.3	1.2
U	32.6	31.4	1.2
10	246.6	246.6	0.0
12	216.0	216.6	-0.6
18	88.2	88.1	0.1
81	366.8	367.2	-0.4
87	320.0	320.6	-0.6
126	39.0	38.7	0.3

References

Merle, H.A., Kentie, C.J.O., van Opstal, G. and Schneider, G.M.C., 1975, The Bachaquero Study-A Composite Analysis of the Behavior of a Compaction Drive/Solution-Gas Drive Reservoir, paper presented at the 50th annual Fall Meeting of the Society of Petroleum Engineers of AIME, Dallas, Texas, p. 1-7.

van der Knaap, W. and van der Vlis, A.C., 1967, On the Cause of Subsidence in Oil Producing Areas, Proc., 7th World Pet. Cong., Mexico City, p. 85-95.

Publication n°121 of the International Association of Hydrological Sciences
Proceedings of the Anaheim Symposium, December 1976

LAND SUBSIDENCE AS A RESULT OF GAS EXTRACTION IN GRONINGEN, THE NETHERLANDS

J. B. Schoonbeek
Nederlandse Aardolie Maatschappij B.V.
Assen, The Netherlands

Abstract

The Groningen gas field, one of the largest in the world, was discovered in 1959, but its size was not recognised until 1963. It extends over an area of approximately 900 km2. The sandstone reservoir is situated at a depth of about 2900 m, and has an average thickness of some 150 m.

The large reservoir size, together with the expected pressure drop of 300 kg/cm2 led to the expectation that appreciable subsidence might occur. An intensive study of the compaction behaviour of the reservoir was initiated. Numerous measurements on core material were made and a mathematical model was developed. Both combined resulted in subsidence prognoses up to the year 2050 where a maximum subsidence of 1 m was predicted.

A number of measuring systems were set up to monitor the subsidence phenomena to allow early adjustments to the predictions:
- conventional levelling surveys
- measurements of young sediment compaction near the surface. This is accomplished by measuring the 'movement' of a cable in a well held under constant tension by an anchor weight at a depth of 400 m and counter weights at the surface
- measurements of reservoir compaction by monitoring the relative displacement of radio-active bullets shot into the formation at regular distances.

From levelling surveys it has been proved that subsidence indeed takes place, however, at a degree which is considerably less than predicted. After refinement of the original mathematical model, the calculated spatial distribution of subsidence corresponds well with that obtained from the levelling surveys.

Based on subsidence/pressure behaviour in time and on geological considerations it is concluded that the compaction measurements in the laboratory are not representative for the reservoir in-situ.

Considerable difficulties have hampered the measurements in the deep observation wells. After several improvements now an accuracy with an mean error of 1 cm per 100 m has been attained.

From the first measurements it appears that the compaction is in accordance with the measured subsidence.

An excellent history match could be obtained for the subsidence behaviour up to 1974. Prognoses based on this history match now result in a figure of 30 cm for the final maximum subsidence.

Measurements up to 1976 are in agreement with the prognoses.

Introduction

The Groningen gas field in the Netherlands was discovered in 1959, but its large size was not recognised until 1963. The field is now known to extend over an area of approximately 900 km2. The sandstone reservoir belongs to the Permian Rotliegend formation. Its depth of burial is approximately 2900 m. The gross thickness increases from 70 m in the south to 240 m at the northern boundary. The in-situ weighted

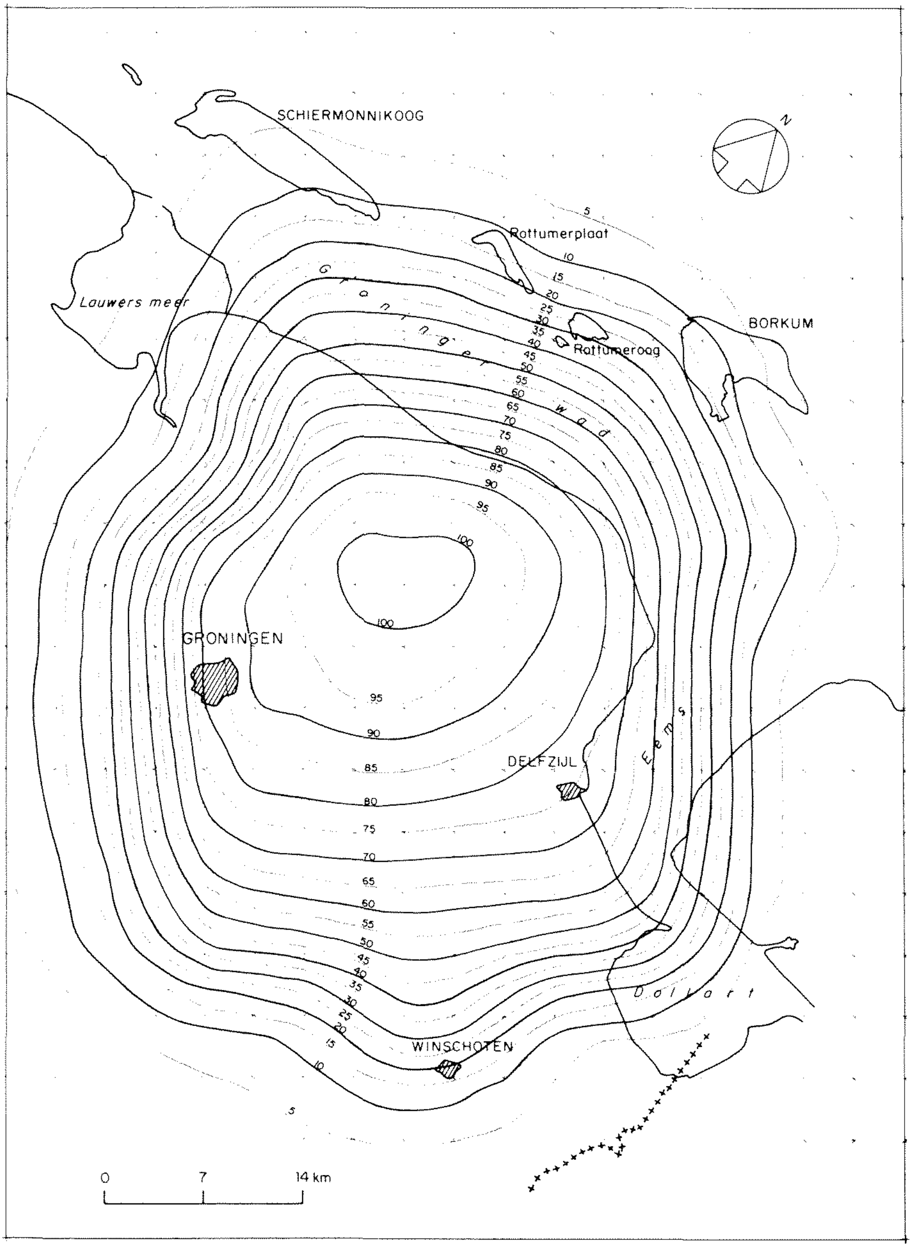

Fig. 1. Subsidence 2050.

average well porosity ranges from 16 to 20 percent, the permeability from 0,1 mD to a few Darcies.

At the time of the discovery, when only a fraction of the reservoir was discovered, there seemed to be hardly any reason to expect notable subsidence, since known cases of subsidence are all related to shallow reservoirs, consisting of unconsolidated material. However, when the actual size of the field was recognised, it was realised that appreciable subsidence might still occur, as the drop in reservoir pressure is expected to be approximately 300 bar.

These considerations led to an intensive study of the compaction behaviour of the Groningen reservoir (Teeuw, 1973; Van Kesteren, 1973). A mathematical model based on an elastic concept was developed by Geertsma and Van Opstal (1973) to be able to give subsidence predictions in an early stage of the development of the field. The results of the subsidence calculations were presented as contour maps for subsequent years, as demonstrated in figure 1 for the year 2050 with a maximum subsidence of about 1 m.

The validity of the predictions is largely dependent upon the compaction measurements on formation samples. It is questionable if these measurements on highly disturbed core material are representative for the behaviour of the reservoir in-situ.
It was therefore considered of prime importance to introduce a number of measuring systems to monitor the subsidence phenomena to allow early adjustments to the predictions:
- measurements of surface subsidence by means of conventional levelling surveys. The total length of the levelling network is 1250 kms and contains 1300 benchmarks (fig. 2).
- measurements of young sediment compaction near the surface, either natural or caused by human activities. The principle, as applied elsewhere in the world, is to measure the 'movement' of a cable, which is held under constant tension by means of an anchor weight at the bottom of a well and counterweights at the surface, thus permitting the relative movement of the surface with respect to the bottom of the well to be established (De Loos, 1973; fig. 3).
- measurements of reservoir compaction. This is accomplished by measuring the relative displacement of radio-active bullets shot into the formation at regular distances of about 10 m (De Loos, 1973, fig. 4) with a gamma ray sonde containing three detectors.

Shallow and deep observation wells are evenly spread over the field (fig. 5). The combination of these three measuring systems should give a complete insight in the compaction/subsidence behaviour due to gas production.

Results of measurements

1. Precision levelling surveys

Since 1964, regular precision levelling surveys have been carried out to establish the amount of subsidence taking place at the surface. Details of the surveys of 1964/1965 and 1968/1969 have already been published by the Survey Department of the Department of Public Works and Water control (1973).

For the repeat survey in 1972, the levelling survey network was considerably enlarged, giving a total length of about 1250 km. The network now covers almost the entire province of Groningen and parts of adjacent provinces.

To obtain a more detailed indication of the rate of subsidence, a further small-scale survey was carried out in 1973. This latter survey covered a number of lines across the centre of the gas field following routes also covered by the full surveys which are made every three years (fig. 2).

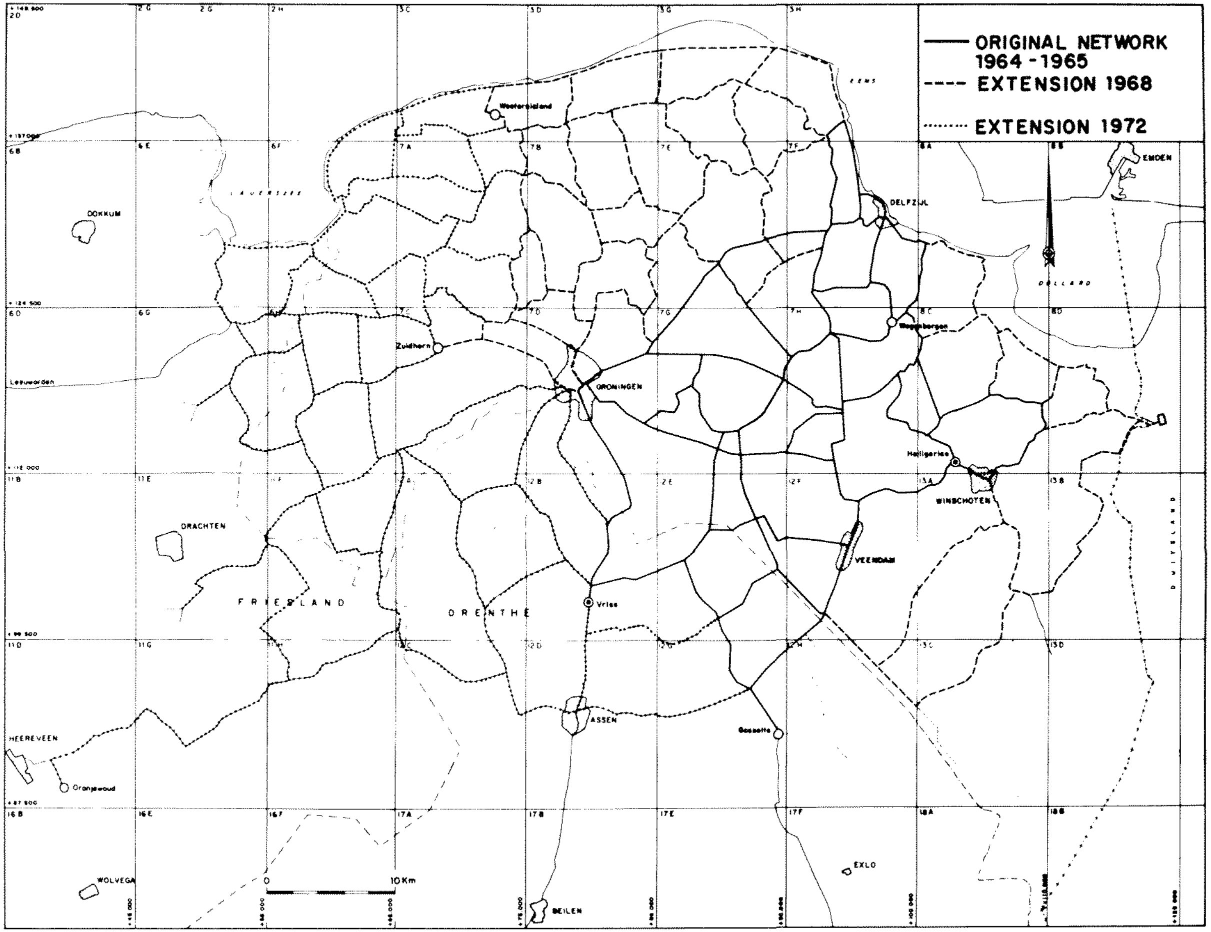

Fig. 2. Groningen levelling network.

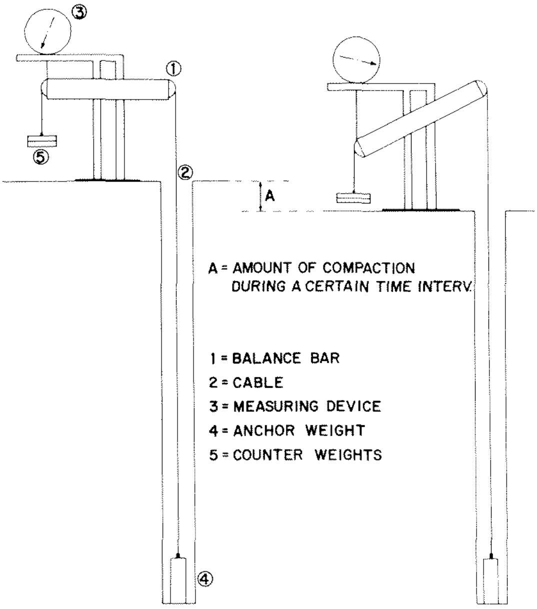

Fig. 3. Principle of cable measurement method.

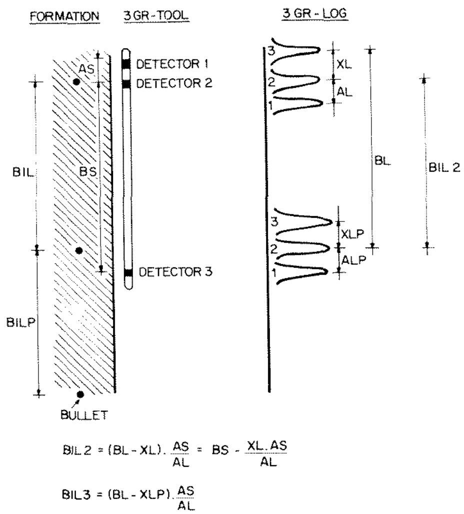

Fig. 4. Formation, 3 gr tool, 3 gr log.

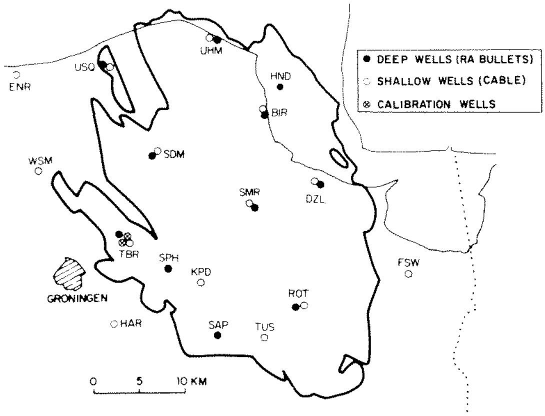

Fig. 5. Compaction observation wells in Groningen.

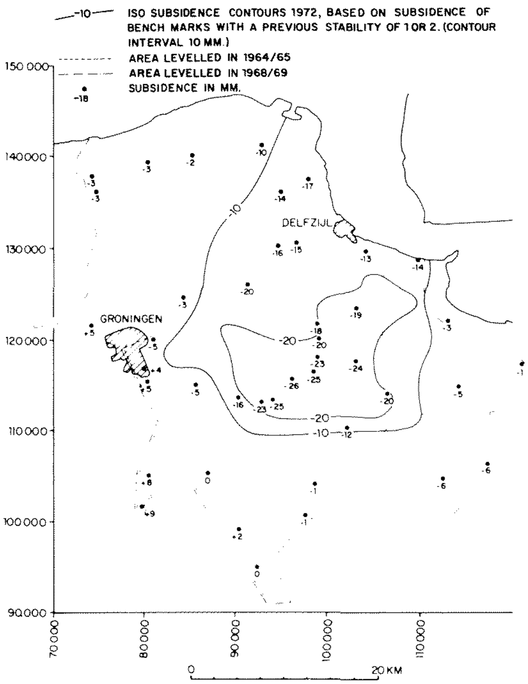

Fig. 6. Subsidence 1964/65-1972.

The Survey Department prepared a contour map from the results of the 1972 survey, using the heights calculated from the 1964/1965 surveys as a reference (fig. 6). To eliminate less reliable benchmarks, this map is based exclusively on the subsidence of benchmarks which are known for their good stability in the past. The report of the Government Surveying Department from which this map originates, indicates that the contour lines should not be taken too strictly. It is also not inconceivable that points which were formerly very stable have become unstable due to local disturbances such as a lowering of the water table.

By incorporating all the measured benchmarks, a contour map results which clearly shows some areas of exceptionally large subsidence (fig. 7).

The existence of such areas with local rates of settlement of around 6 mm a year has long been known (e.g. the region to the east of Schildmeer lake). Due to the water level in many polders having been lowered and the control of water being much improved in recent years, there is a strong possibility that more areas of accelerated settlement will be revealed by future levelling surveys.

A section drawn between Gasselte and a point midway between Gieten and Bareveld (fig. 8) is indicative of the accuracy of the levelling surveys. In view of the fact that there is no indication that this part of the route is subject to subsidence due to either exploitation of the gas field or due to any significant natural compaction of the surface layers, the scatter in the results gives a good indication of the accuracy achieved. This scatter indicates that a difference in height of less than about 7 mm cannot be considered significant (ref. 7).

2. Shallow observation wells - surface compaction measurements

Measurements of the compaction of the upper Quaternary sediments (i.e. from surface to 400 m), are made up of two components:

1. Continuous measurement of the change in the thickness of the sediments from a depth of 400 m to the foot of the piles beneath the measurement buildings (cable measurements).
2. Measurement of the compaction taking place between the surface and the foot of the piles by levelling between frost-free points around these buildings.

The algebraic sum of these two measurements give the compaction taking place in the Quaternary sediments.

Figure 9 shows the results of these measurements obtained from the various observation wells over recent years. In a number of cases the foundations of the measurement buildings have settled, necessitating the application of a negative correction factor to the cable measurements (see, for example, Stedum).

These results show that, in general, compaction of the top 400 m varies between 0,2 mm and 2 mm a year, with a few localized areas showing much greater instability (e.g. Schildmeer, Roode Til and Finsterwolde, which have rates of compaction up to 9 mm a year (fig. 10)).

An attempt has been made to present the results of the measurements in the shallow observation wells in the form of a contour map (fig. 11). The extent of the unstable areas around Schildmeer, Roode Til and Finsterwolde has been obtained by observing the behaviour of the benchmarks surrounding the wells.

As the differences in height are, in general, small, the actual line taken by the contours over a large part of the area covered by the survey network may deviate somewhat from that given. However, a comparison of figures 11 and 7 clearly indicates that the areas of more extreme subsidence are a result of compaction of the uppermost Quaternary sediments.

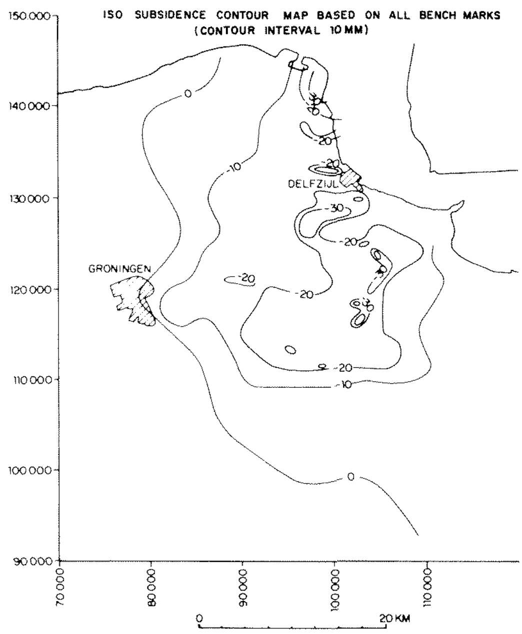

Fig. 7. Levelling survey results 1964/65-1972.

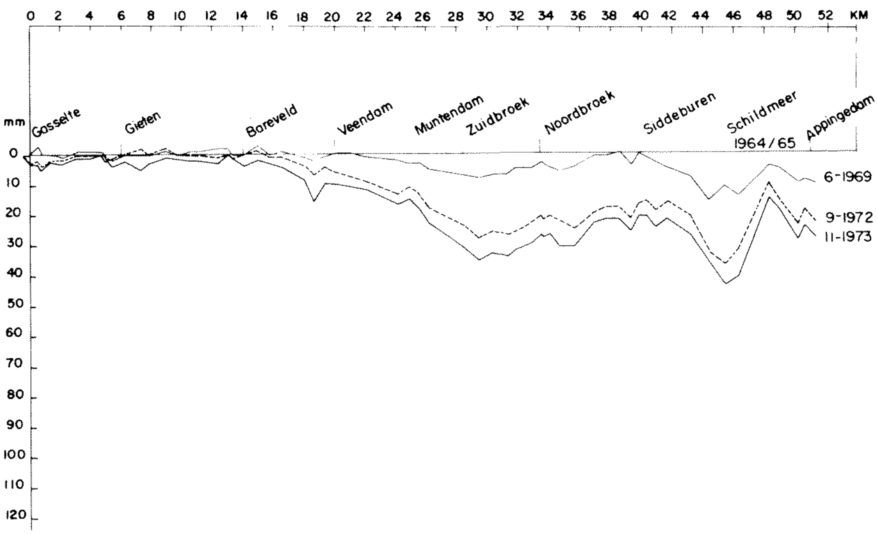

Fig. 8. Differences in elevation of bench marks 1964/65-1973.

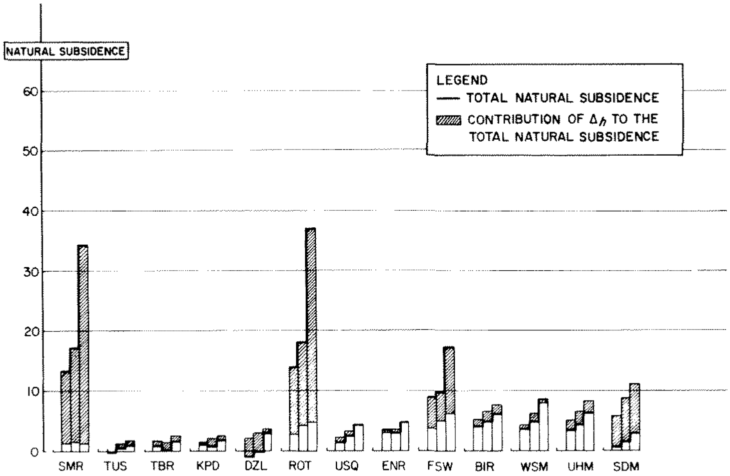

Fig. 9. Subsidence due to natural compaction and other surface phenomena over the years 1972, 1973 and 1974 (reference year 1970) (From shallow observation well measurements).

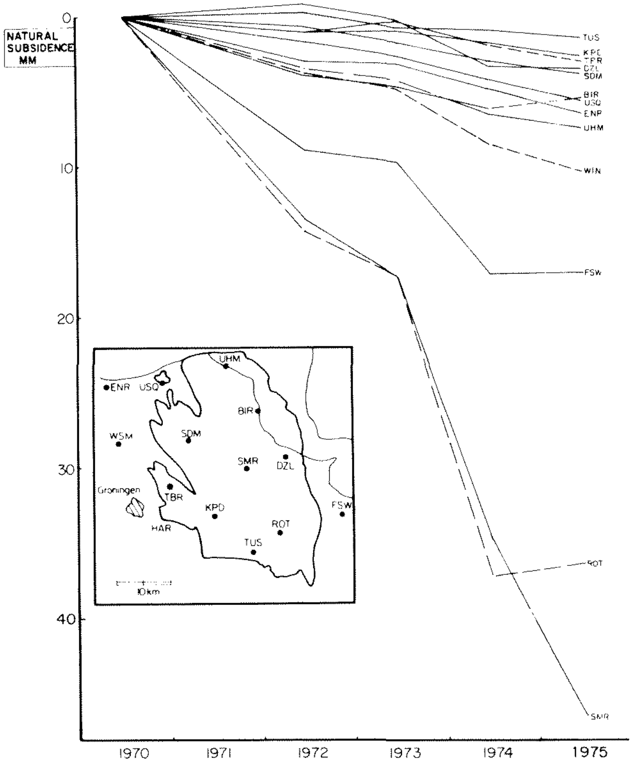

Fig. 10. Subsidence due to natural compaction and other surface phenomena (From shallow observation wells).

3. Deep observation wells - precise depth measurements

The object of the measurements is to monitor the in-situ compaction of the reservoir and so verify the value of Cm, the compaction coefficient* used in the subsidence prediction calculations. The method used (De Loos, 1973) involves the periodic measurement of the distance between radio-active bullets which have been shot into the formation.

Since publication of the subsidence predictions in 1971 (Geertsma, 1973) sufficient time has elapsed to be able to expect to have obtained reliable figures for comparison.

However, it has now been proved that the measurement system initially used does not give the desired degree of accuracy. In some cases the observations even showed an expansion of the reservoir. After a considerable amount of research several modifications were made to the system in both the measurement and computation procedures.

Inaccuracies in the past arose from two main sources:

1. The inability to check the tool calibration immediately before and after each survey and so detect any malfunctioning of the instrument at an early stage.
2. The inability of the computation procedure to identify and delete automatically those intervals affected by tension variations occurring during the measuring survey.

These tension variations can adversely affect the measurements.

In order to remove the first source of error a new tool calibration system was developed. In place of the old system whereby the instruments were calibrated in a special well every three or four months, the new method uses a horizontal surface calibrator which enables calibration before and after each survey.

The calibrator (fig. 12) consists of a tube of material with a very low coefficient of expansion (invar) into which radio-active markers have been introduced at accurately determined distances.

During the calibration, the measuring tool is moved back and forth in a tube which is clamped beneath the invar tube. This system enables a large number of calibration measurements to be obtained in a short space of time.

During investigations into the sources of error it was found that the most vulnerable parts of the measurement probes were the detector crystals themselves which were probably susceptible to damage before, during and after measurements. These crystals have now been replaced by recently developed sintered types which are considerably more robust.

The effect of the errors resulting from variations in cable tension have been reduced by modifications to the computer programs and by paying greater attention to the cleaning of the wells before taking measurements. Experiments have also been carried out to find the most ideal bottom hole fluid.

The accuracy of the new system is demonstrated by figure 13. After a thorough cleaning, four surveys were made using two different tools in the well Roode Til. Both instruments were calibrated before and after taking measurements. With this arrangement, it was possible to calculate eight independent interval lengths. By statistical analysis it was found that the mean error of these measurements was 1 cm in 100 m of measured interval.

Attempts to use the results of the pre-1974 measurements by comparing the old and new calibration methods have so far met with no success.

---

*Compaction per unit stress.

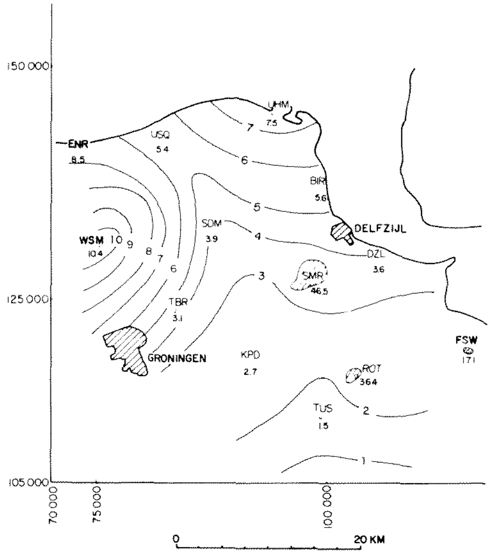

Fig. 11. Subsidence(mm) due to surface compaction and other surface phenomena 1970-1975 (From shallow observation wells).

In view of the degree of accuracy obtained compared with the predicted amount of compaction, it is unlikely that significant results in all observation wells will be obtained before the year 1977.

New subsidence predictions

1. General

Since the publication in 1971 of the maximum amount of subsidence which could be expected above the Groningen gas field, new ideas have gradually developed regarding the subsidence mechanism.

The mathematical model has now been modified in order to incorporate certain established features and input data of greater accuracy has become available on both the reservoir engineering and geological

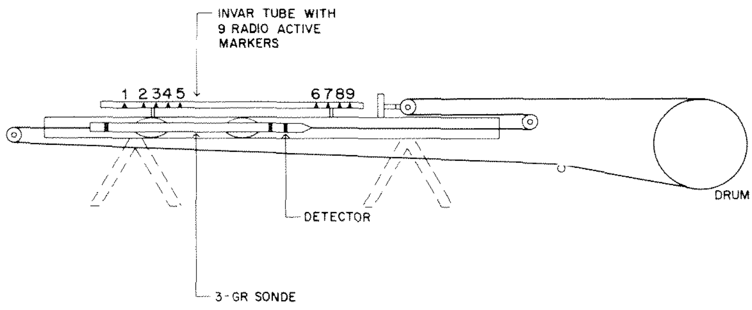

Fig. 12. Surface calibrator.

front. In addition, production plans have undergone repeated changes since 1971 with commensurate effects on the expected pressure distribution.

The original model developed by Geertsma and Van Opstal (1973) was based on the assumption that both the reservoir rock and the strata lying above and below had a homogeneous structure. One of the results of this assumption was that it was predicted that the base of the reservoir would actually drop, resulting in a greater subsidence.

The unlikelyhood of a homogeneous structure was confirmed by measurements of the deformation of core material from a deep exploration well. The model has now been modified so that an elasticity contrast can be introduced between the reservoir and the beds beneath (Van Opstal, 1974; Williamson 1974).

In previous predictions a compaction coefficient of $1,45 \times 10^{-5}$ bar^{-1} had been assumed for the entire field (Van Kesteren, 1973). This value, deduced from the laboratory tests was found to be about 10% too high because a conversion factor had been omitted.
Moreover, laboratory measurements have shown that a relationship exists between the compaction coefficient and porosity. As a further refinement this dependence on porosity has been incorporated in the model on the basis of data obtained from petrophysical measurements in the wells.

In order to obtain an idea of the effect of these refinements, a subsidence prediction for 1st January 1974 was made using the pressure drops actually measured. The resulting predicted subsidence for 1st January 1974 (fig. 14) shows an excellent agreement, as far as the pattern is concerned, with the contour map obtained from the 1972 levelling survey (fig. 6). This becomes even more apparent from a comparison of the sections, drawn on the basis of figure 14, with the profiles obtained using all measured points from the various levelling surveys along a number of routes across the gas field (fig. 15, 16, 17). The similarity between both the various levelling survey sections and the predicted section is remarkably good and gives considerable confidence in the more refined mathematical model. The measured values of the subsidence (max. 3, 5 cm) are, however, considerably less than the predicted values (more than 11, 0 cm), for the 1st January 1974.

The question that arises is whether or not this trend will continue in the future.

In other words, what is the cause of this rather large discrepancy?

Supplementary investigations during recent years have yielded the following new knowledge:

- The deformation behaviour of the strata overlying the reservoir has been subjected to closer scrutiny. The only layer that might be expected to behave uniquely is a relatively thin layer of potassium and magnesium salts which occurs locally sandwiched within thick rock salt deposits. Using the results of measurements on core material made under appropriate conditions of pressure and temperature, a specially developed mathematical model has shown that levelling effects of this salt would only be noticeable over periods of 10 000 - 100 000 years.
- The occurrence of "creep" in the reservoir rock (i.e. delay between loading and compaction) appears unlikely in view of the type of material.
- Cases have been known in which the compaction rate is greater at a later stage than initially. This strange behaviour of the compaction coefficient as a function of pressure can occur when a reservoir has

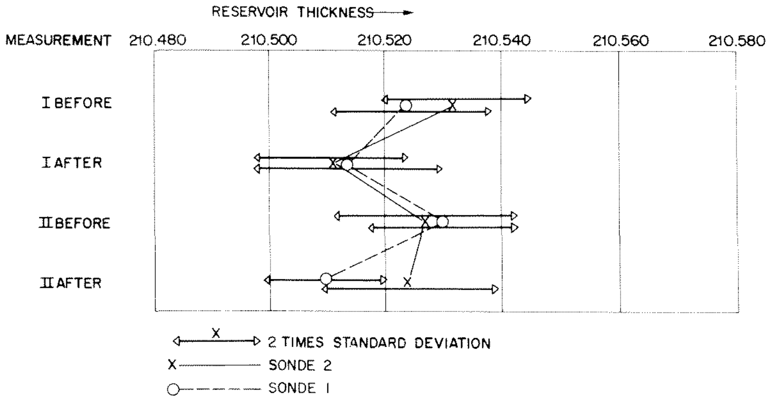

Fig. 13. Roode Til Repeatability test January 1975.

been burried at a considerably greater depth in the geological past than it does at present. This situation can best be illustrated schematically by figure 18, which represents a rock that has been successively loaded, unloaded and reloaded. Whilst under load (sedimentation on top of the future reservoir) both elastic and non-elastic deformation (e.g. crushing of grains) occurs (AB). When the load decreases (erosion of the overburden) the rock recovers only from the elastic deformation (BC). Re-application of the load along the same line re-introduces predominantly elastic compaction with a smaller compaction coefficient (CB).

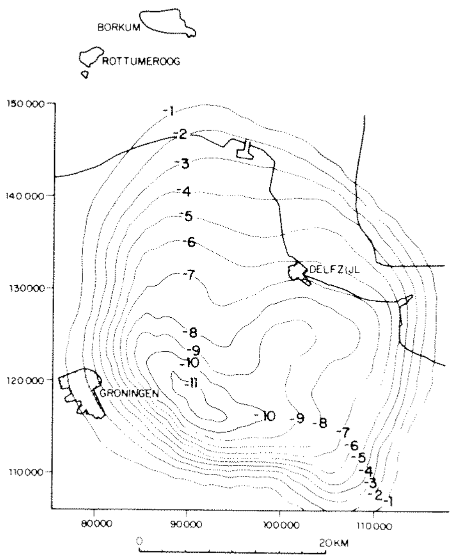

Fig. 14. Subsidence prediction Groningen 1974 in cm. (Lab. determined cm.)

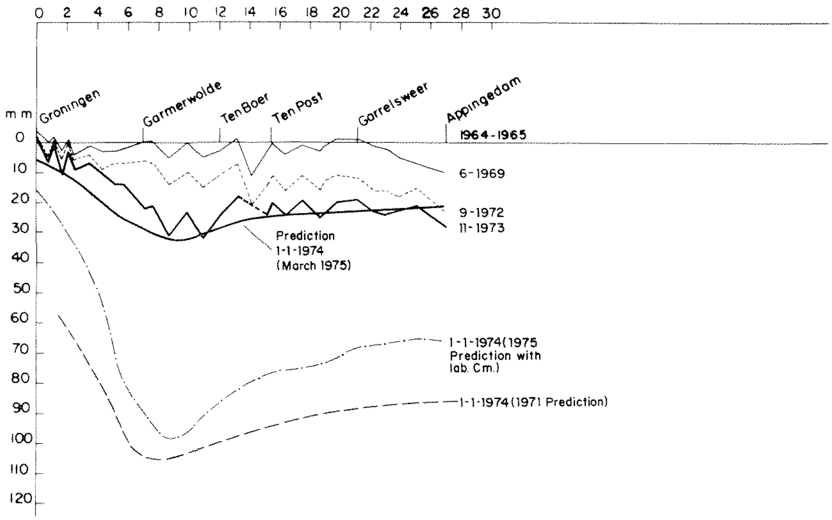

Fig. 15. Differences in elevation of bench marks 1964/65-1973.

The accelerated compaction (BD) can only take place if the greatest pressure the material has ever previously been subjected to is exceeded. This phenomenon will therefore only be able to manifest itself if, at an early geological time, the reservoir was situated deeper than it does now. If the reservoir was never buried any deeper, then as the load increases (owing to production from the reservoir), the line AD will apply during the entire gas production phase. In this

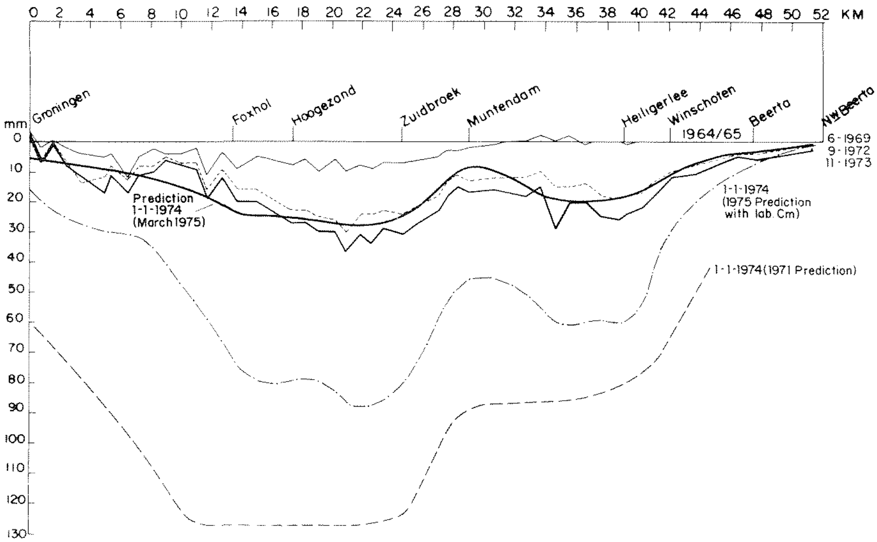

Fig. 16. Differences in elevation of bench marks 1964/65-1973.

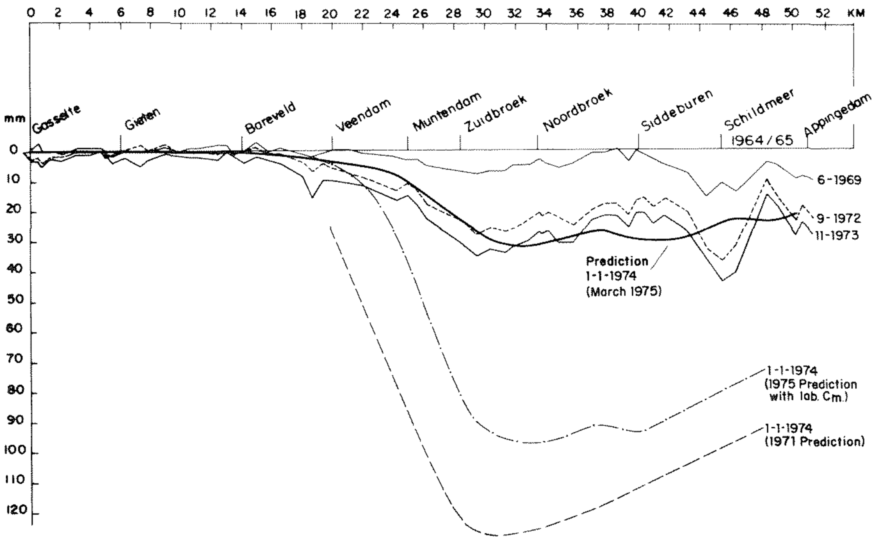

Fig. 17. Differences in elevation of bench marks 1964/65-1973.

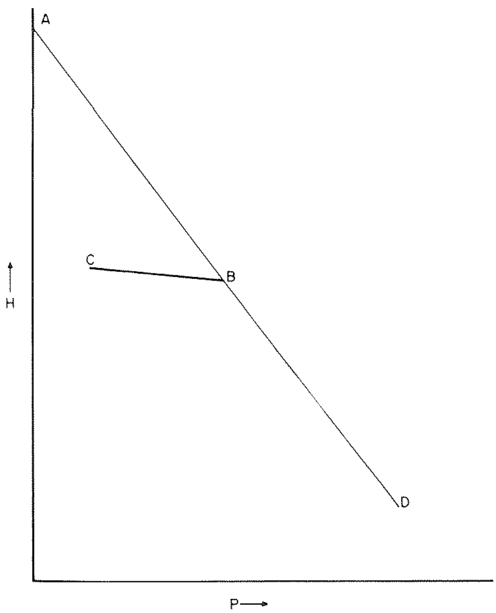

Fig. 18. Cyclic loading of rock.

theory a linear relationship is assumed between pressure drop and compaction. This has, to a first approximation, been confirmed by observation in the laboratory.
On the basis of geological considerations it is unlikely that the Groningen gas reservoir has ever been any deeper than its present depth and, in consequence, it is considered unlikely that a more rapid rate of compaction will occur in the future. Confirmation of this assumption can be found by studying the subsidence behaviour so far measured. Figure 19 is a plot of subsidence measured in successive levelling surveys plotted against pressure drop for four different locations in the field. It can be seen that so far there is no evidence of acceleration in the rate of compaction, despite the fact that the pressure drop by November 1973 amounted to 75 bar.

The above factors combined with our latest knowledge obtained from theory and observation indicate that the compaction coefficient is, in practice, most likely only about a third of the value deduced from laboratory measurements. The main reason for this discrepancy may be that the core material on which the laboratory measurements were carried out was so disturbed by the relief of pressure, drilling, coring and transport that its compaction properties were no longer representative of the behaviour of the in-situ formation. This possibility was recognised at an early stage in the laboratory investigations (Teeuw, 1973) and was one of the principal considerations leading to the introduction of the radio-active measurements in deep observation wells.

2. Predictions

Subsidence predictions now have been made using the revised mathematical model. The relationship used to calculate the compaction coefficient from porosity was obtained by combining the results of a laboratory investigation on core material with a history match between predicted and actual subsidence as measured by levelling surveys. The porosity data was obtained from the petrophysical field evaluation. The use of this compaction coefficient relationship for the year 1974, together with the actual pressure drops (fig. 20), results in a striking correlation with the levelling survey results, as can be seen from the sections in figures 15, 16 and 17.

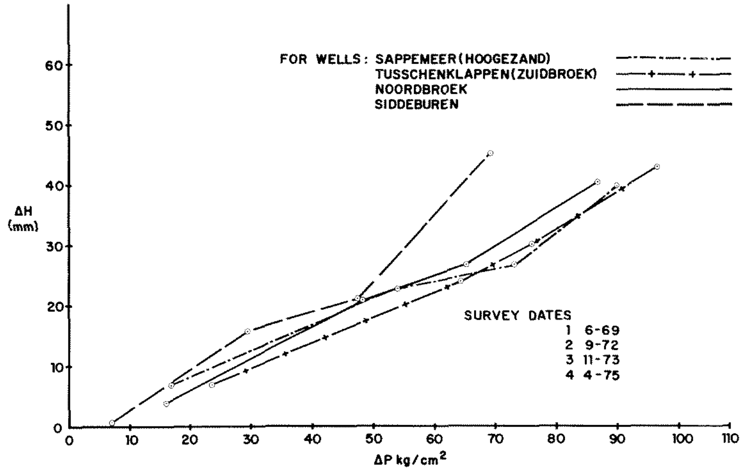

Fig. 19. Subsidence since 1964/65 vs. pressure drop.

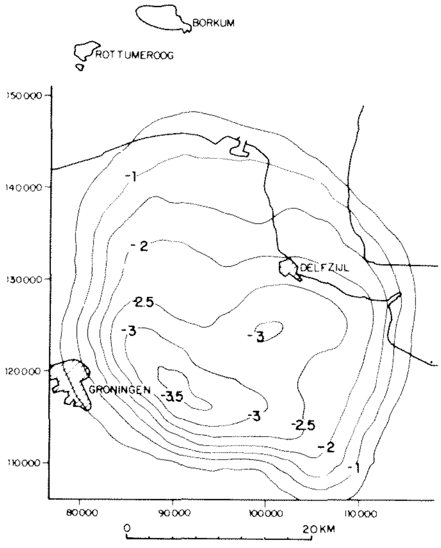

Fig. 20. Subsidence prediction Groningen 1974 in cm.

The pressures used for the subsidence predictions were based on the gas offtake plan. For this prediction the influence of the aquifer has been taken into account in the predicted pressure behaviour, as deduced from recent reservoir studies.

The greatest part of the subsidence will take place before 1990,

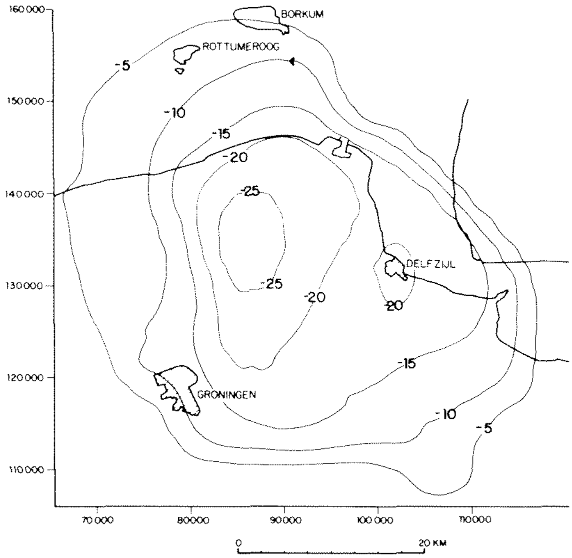

Fig. 21. Subsidence prediction Groningen 2025 in cm.

after which there will be relatively little change. The maximum amount of subsidence, about 30 cm, will be attained by 2025 (fig. 21).

Assuming that the assumptions mentioned in III-1 are correct, then the prediction accuracy of the maximum subsidence (27 cm) seems to be largely determined by the accuracy of the new value of the compaction coefficient.
Since this value is deduced from direct subsidence measurements, its accuracy is estimated to be similar to that of the levelling surveys; i.e. an error of the order of $\pm$ 10% can be expected.

As the gas production continues, more data will become available from both the reservoir and the measuring systems which, together with possible new ideas, will lead to a further refinement of the prognosis.

References

Geertsma, J. "A basic theory of subsidence due to reservoir compaction: the homogeneous case". Verhandelingen Kon. Ned. Geol. Mijnbouwk. Gen. Volume 28, 1973, p. 43.

Geertsma, J. and Opstal van, G. "A numerical technique for predicting subsidence above compacting reservoirs, based on the nucleus of strain concept". Verhandelingen Kon. Ned. Geol. Mijnbouwk. Gen. Volume 28, 1973, p. 63.

Kesteren van, J. "Estimate of compaction data representative of the Groningen field". Verhandelingen Kon. Ned. Geol. Mijnbouwk. Gen. Volume 28, 1973, p. 33.

Loos de, J.M. "In-situ compaction measurements in Groningen observation wells". Verhandelingen Kon. Ned. Geol. Mijnbouwk. Gen. Volume 28, 1973, p. 79.

Meetkundige Dienst Rijkswaterstaat. (Levelling surveys). "Rapport over de NAM-waterpassing van 1972 over het gasveld Groningen". Delft, October 1973.

Meetkundige Dienst Rijkswaterstaat. (Levelling surveys). "Rapport over de NAM-waterpassing van 1968-1969 over het gasveld Groningen". Delft, October 1973.

Opstal van, G. "The effect of base rock rigidity on subsidence due to compaction". Proceedings of the third congress of the international society for rock mechanics, Denver, Colorado, September 1/7/1974. Volume II, part B, National Academy of Sciences, Washington, D.C., 1974.

Teeuw, D. "Laboratory measurement of compaction properties of Groningen reservoir rock". Verhandelingen Kon. Ned. Geol. Mijnbouwk. Gen. Volume 28, 1973, p. 19.

Williamson, A.S. "Volumetric subsidence - compaction ratio for a layered elastic half-space". Proceedings of the third congress of the international society for rock mechanics, Denver, Colorado, September 1/7/1974. Volume II, part B, National Academy of Sciences, Washington, D.C., 1974.

Publication n°121 of the International Association of Hydrological Sciences
Proceedings of the Anaheim Symposium, December 1976

SUBSIDENCE CONTROL AND URBAN OIL PRODUCTION - A CASE HISTORY BEVERLY HILLS (EAST) OIL FIELD, CALIFORNIA

R. C. Erickson
Standard Oil Company of California
San Francisco, CA

Abstract

The City of Los Angeles has permitted Urban oil producing operations for the past 20 years in the belief that the risk of significant oilfield subsidence is negligible and in the knowledge that should slight negative changes in the surface elevations be noted at or near the outset of production measures can be taken to abate the condition before damage to surface improvements could occur. Soon after the Beverly Hills (East) Oilfield had been discovered in December 1964, it became apparent that a major hydrocarbon reserve had been found in an urban area. Early in the life of the field it was determined that pressure maintenance operations would prove economically attractive and water injection was begun in December 1969. A cooperative venture to monitor precisely the ground elevations over the field area was initiated in 1966 by establishing a network of benchmarks to add detail to those benchmarks previously established by the City of Los Angeles. Because a history of ground movement existed in the Beverly Hills area prior to first production and so little rock physics or reservoir data were available, the operators constructed an empirical model to aid in the prediction of the potential for surface subsidence. By gathering the essential data to apply in the model, the operators concluded that the potential for surface subsidence from oilfield operations would be negligible. The operators also developed a procedure for evaluating the survey records in order to separate oilfield related ground movements from other possible causes.

Introduction

The City of Los Angeles, situated on top of one of the great petroleum provinces of the world, has been dealing with oilfield subsidence since 1945. So dramatic was the classic case at Wilmington that oil production in urban areas is no longer permitted without reasonable assurance that similar events will not occur. In 1964, after the Beverly Hills (East) Oilfield had been discovered in two separate core holes drilled by the Standard Oil Company and the Occidental Petroleum Company, both operators and the City Government recognized a potential problem. Working together under the existing city oil ordinance, a workable solution was devised for monitoring for oilfield subsidence which permitted oil development to move ahead in a densely populated urban area.

Oilfield History

The Beverly Hills (East) Oilfield is located within an East-West trending elongate complexly folded and faulted anticline situated on the Northwesterly rim of the Los Angeles Basin at the common boundaries between the Cities of Beverly Hills and Los Angeles (Figure 1). Productive limits eventually encompassed approximately 848 acres within which 6,200 individuals are currently receiving royalty payments. Depth of the productive formations ranges from 3,200 feet below the surface at the structural crest to over 8,000 feet in the deepest zones. A simplified structure contour map drawn at the top of the main zone is represented by Figure 2.

Table 1. Beverly Hills (East) Reservoir Data.

BEVERLY HILLS (EAST) RESERVOIR DATA			
Zone	Repetto	Miocene Main	Miocene Deep
Year of First Production	1967	1966	1967
Reservoir Area (Acres)	–	840	-
Depth to Top of Zone (ft.)	3200	5350	6750
Maximum Width (ft.)	2000	3300	2300
Ratio of Depth/Width*	1.6	1.6	2.9
Net Sand Thickness at Crest (ft.)	535	455	425
Average Porosity (% bulk volume)	28.6	23.1	20.3
Average Permeability (millidarcies)	265.0	108.0	22.0
Interstitial Water (% pore space)	22.0	22.7	26.0
Original Oil in Place (barrels/acre–feet)	1349	990	710
Original Solution Gas–Oil Ratio (standard cubic feet/barrel)	500	665	1040
Initial Formation Volume Factor (volume[1]/volume)	1.283	1.40	1.64
Original Reservoir Pressure (psig)	2200	2850–2920	3300
Saturation Pressure (psig)	2200	2680–2975	3300
Datum (feet subsea)	4700	5700	7000
Reservoir Temperature (^{o}F)	170	200	215
A P I. Gravity of Oil (^{o})	30–35	22–30	40–45

*Ratio of Depth/Width at Wilmington Ranger Zone 2300/15000 – 15

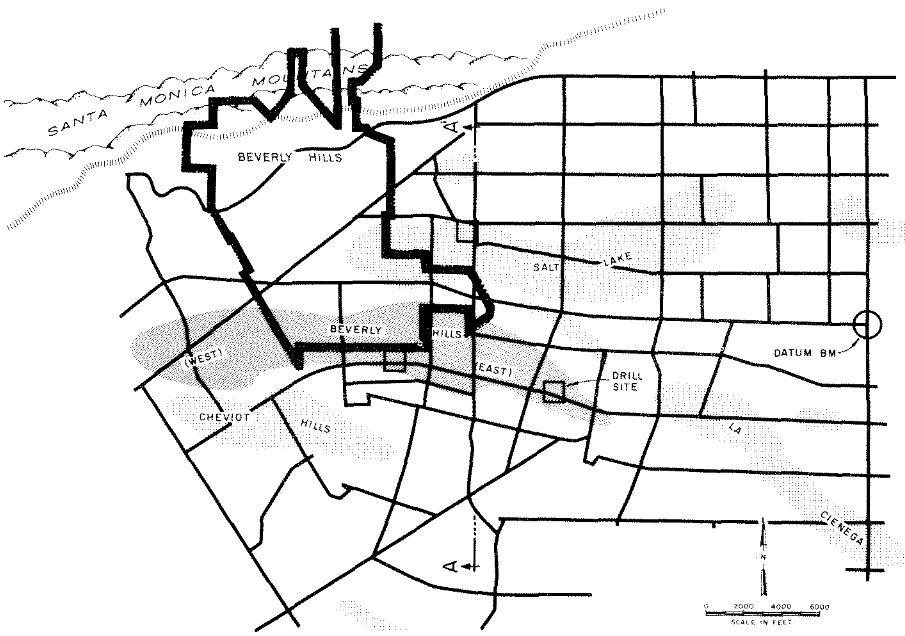

Fig. 1. Oilfield Location and Survey Traverse Line Map.

This structure is noteworthy in that the Southerly flank is vertical to overturned and is characterized by an active natural water drive within the field. Cross Section A-A', (Figure 3) is drawn North-South from the Santa Monica Mountains to the Inglewood Fault and passes through the middle of the Beverly Hills (East) Field. The Santa Monica Fault is on the North end of the cross section and separates the intrusives and metamorphic rocks from the basinal rocks to the South. The Southerly acting crustal pressure has also generated a complex series of en echelon folds, some of which have ruptured due to the intensity of folding and have developed thrustal faults similar to the Santa Monica Fault. As is indicated on the cross section, these faults are not major faults as they become obscure higher in the section and are apparently limited to the Miocene formations. The field has produced a net voidage of oil, water and gas from all reservoirs through December 1975 of approximately 234,000,000 barrels. Maximum daily production reached 34,000 barrels of oil per day during September of 1968 from 62 producing wells.

History of Earth Movements

Southern California has long been known as a tetonically restless province. In connection with oil production from an urban area, it is therefore essential that the history of earth movements be reviewed and understood before substantial production is permitted. Fortunately, the record of such movements is both extensive and has been thoroughly investigated (Grant 1939). Since 1934, the City and the County of Los Angeles have leveled over an extensive network of precise level lines (Figure 1). These survey records were used as part of the earth movement evaluation by Occidental and Standard for the Beverly Hills (East) Field. Although the available leveling records in the area of study go back to the 1920's, their erratic coverage did not allow for the construction of good regional ground movement maps; but by 1949, the density of these traverse lines in this area was such that one could begin to construct regional maps using the 1949 data. Figure 4 shows the annual rate and distribution of ground movement that was occurring in the area for the period 1949 to 1963. This is prior to any fluid extraction from the Beverly Hills (East) Oilfield. In addition to reviewing this information, Occidental and Standard decided to establish their own leveling network over the area of indicated oil accumulation prior to any fluid extraction. With this background in hand, Occidental and Standard set about analyzing and describing the various possible causes of pre-production ground movement that are apparent in Figure 4.

Possible Causes of Ground Movement

Standard and Occidental have used an empirical approach for predicting potential subsidence wherein each of the possible contributing factors have been considered, weighed and, as necessary, received further evaluation. Many of the factors causing earth movement are not perfectly known. With sufficient data, however, it has become possible to isolate certain components and determine which may be contributing to the movement. Whenever there are multiple causes, difficulty naturally arises in estimating the quantitative effect of each. Those variables which the author considered important in the evaluation of earth movements -- particularly oilfield related -- have been organized into the following empirical model and were applied to the Beverly Hills (East) Field prior to production in order to estimate the oilfield subsidence potential.

1. Tectonic Activity.
2. Compaction of Sediments Due to Earth Surface Loading or Wetting.

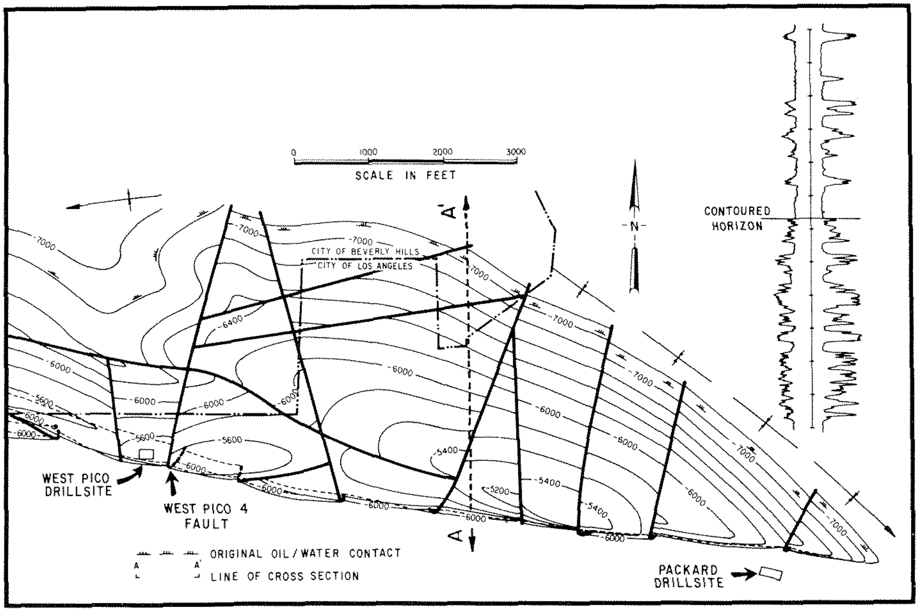

Fig. 2. Beverly Hills (East) Oilfield, structure contour map on top Miocene Main Zone.

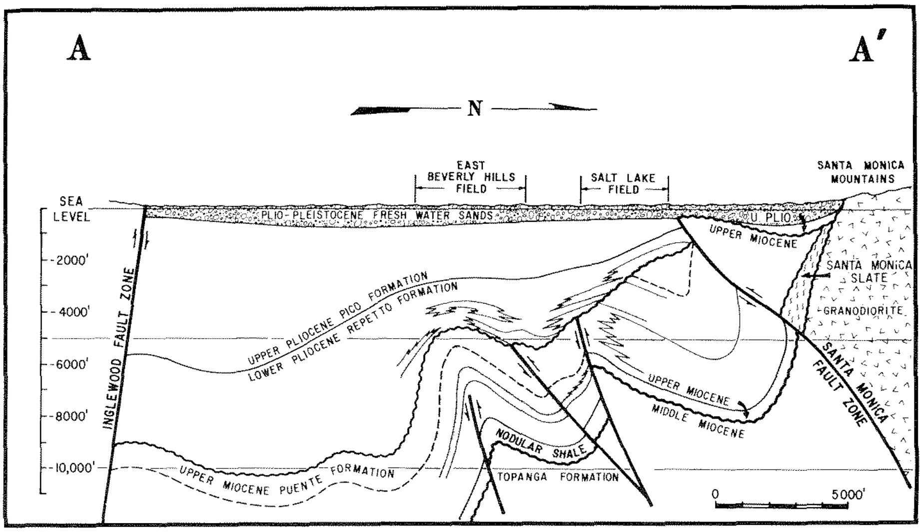

Fig. 3. Inglewood to Santa Monica mountains cross section.

3. Compaction and Consolidation Due to Vibration.
4. Subsurface Solution or Cavitation.
5. Subsurface Pore Pressure Reduction.
    a. Controlling Geological Characteristics.
        (Note: These may be applied to all of the foregoing items.)
        (1) Regional Structural Conditions.
            (a) Geological Structure.
            (b) Depth of Production.
            (c) Breadth and Length of Accumulation.
            (d) Thickness of Productive Zones.
        (2) Physical Properties of Producing Zones.
            (a) Porosity.
            (b) Lithology.
            (c) Preconsolidation and Cementation.
        (3) Formation Temperature Changes or Thermal Properties.

In the Beverly Hills (East) Area, variations in recorded ground movement were too great and too complex to be explained by only one or two causes listed above. By analyzing these recorded ground movements in light of each of the possible causes, it can be shown that in this area the movements were resulting from the combined effects of tectonism, near-surface fresh-water fluid withdrawals and, to a slight extent, the recently deeper oilfield fluid withdrawals. For this empirical approach to be effective, it has become necessary to rely on correlation techniques wherein the survey records are used as the base to which all other factors are compared on a time-of-occurrence basis (i.e., formation pressure decline, earthquake instance, the lowering of fresh water tables, etc.). Figure 5, a graphic display of surface changes in elevation at a benchmark near the center of the Beverly Hills (East) Oilfield and fluid level changes in a shallow water well located nearby should be referred to for the history of ground movements in the Beverly Hills Area since 1935.

Tectonic Activity

That the Beverly Hills-Hollywood area is, and has been, tectonically active is readily apparent from the existing, folding, faulting and sedimentary patterns. Also, recorded seismic activity (Figure 6), surface physiographic features and the fault displacements of quarternary sediments testifies to the restlessness of the region. How much, where and at what rate the earth has moved as a result of this activity has been revealed by the recourse to proper monitoring systems. For example, surface movements have been measured by precise surveying techniques and the seismic activity has been recorded by the seismographs.

Compaction of Sediments Due to Either Surface Loading or Wetting

There are no indications that any significant part of the present-day earth movements in the immediate area of the Beverly Hills (East) Field have resulted from surface loading or wetting. The fact that the water table was, at one time, at or near the present surface precludes shallow compaction from surface wetting in the area (Mendenhall, 1905, and Ebert, 1921).

Compaction and Consolidation Due to Vibration

The only events capable of causing subsidence by vibration are earthquakes, although some very minor local movements may be occurring as a result of surface traffic. Recent leveling traverses East of the Beverly Hills (East) Oilfield and along Pico Boulevard showed a marked acceleration and subsidence between level runs in October 1970 and March 1971. It is

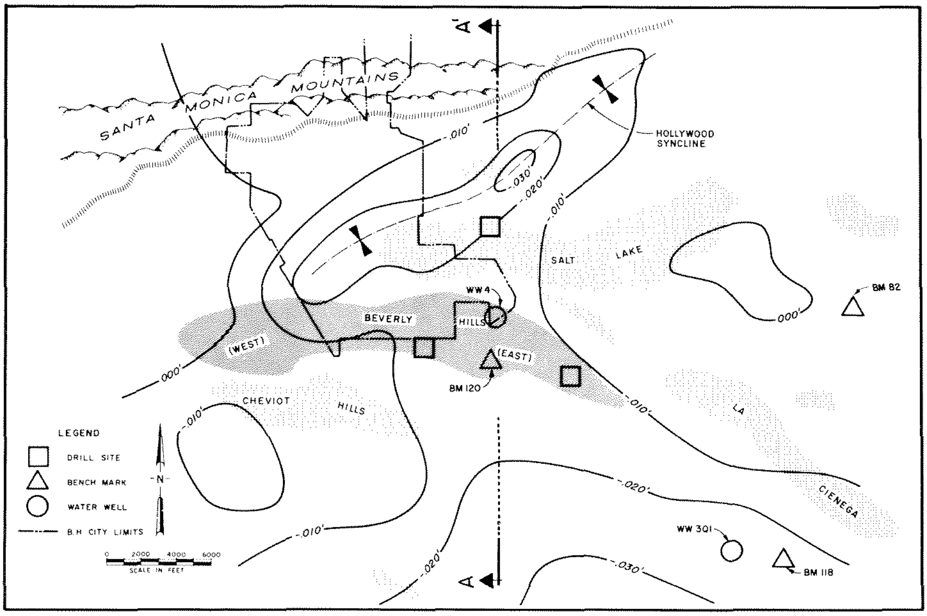

Fig. 4. Annual rate of earth movement for the period 1949 to 1963.

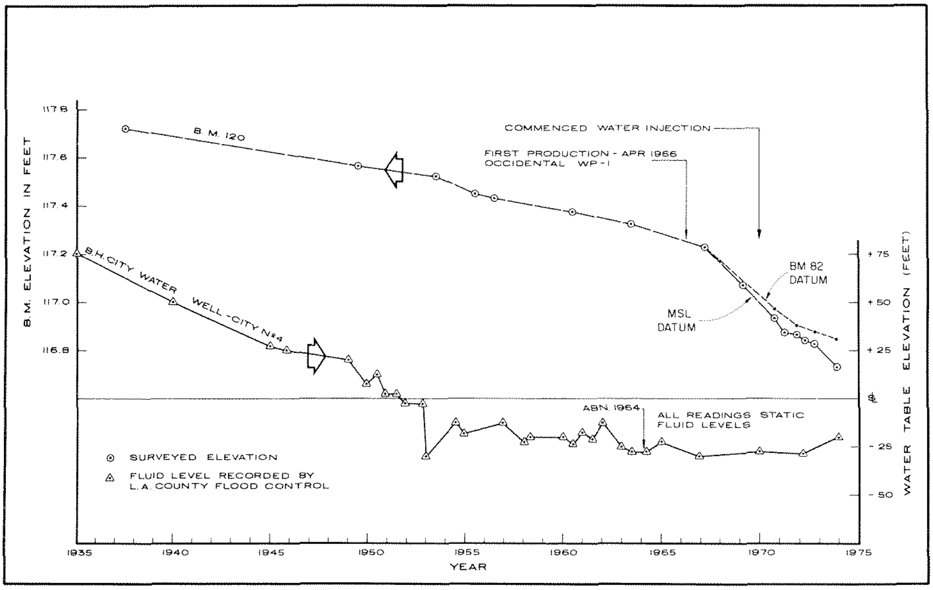

Fig. 5. Graph of surface change in elevation at B.M. 120 and hydrograph of fluid levels at B.H. City water well No. 4.

believed that this acceleration resulted from vibratory subsidence set up within the shallow fresh water aquifiers by the February 9, 1971, magnitude 6.4 San Fernando Earthquake.

Subsurface Solution or Cavitation

There is no evidence that any of the subsidence in the Beverly Hills Area has resulted from subsurface solution or cavitation.

Subsurface Pore Pressure Reduction (Fluid Withdrawal)

One of the most important criteria related to oilfield subsidence is the reduction or change in pore pressure within the subsurface formations undergoing depletion. When the formation pressure is either reduced or increased deformation within the particular reservoir will occur. Such a change in formation pressure will result in a load transfer from the fluid phase to the solid matrix, or the reverse. The magnitude of the resulting deformation is dependent upon several other variables which interact with each other. Because of the difficulty in adequately defining each of these variables at the time of first hydrocarbon discovery, a rigorous mathematical analysis of the eventual magnitude of deformation is impossible. An early assessment of the potential compaction can, however, be made by using the empirical approach mentioned earlier.

Studies discussed earlier have revealed the fact that some of the subsidence in the area is related to shallow fresh water withdrawals. The same controlling geologic characteristics discussed in considerable detail under Oilfield Related Subsidence can also be applied to shallow fresh water aquifers. To determine the extent to which shallow groundwater withdrawals were contributing to subsidence in the area, the distribution and thickness of the acquifers were mapped (Figure 7). The changes in the water table elevations within this aquifer system were then compared to the overlying ground movement measurements (Figures 3, 5 and 8).

Subsidence which might be attributed to oilfield production is depicted on Figures 5, 9 and 10. To further evaluate this ground movement, a bench mark within the survey system but removed from the influence of fluid withdrawals was selected as a constant datum. In this case, Bench Mark No. 82 at the corner of Western Avenue and Wilshire Boulevard was selected because of its historical stability.

Figure 11 shows the amount of movement based on mean sea level datum that have occurred in the area of Bench Mark No. 82 between 1967 and 1973, as the possible result of tectonic movement, surveying error, and minor local building or traffic disturbances. All of the elevation changes shown in Figure 10 were adjusted based on Bench Mark 82 as a datum to produce Figure 12. This new map (Figure 12) probably represents the rate and areal distribution of subsidence related to oilfield fluid withdrawals during this period. A rate and amount too small to be considered serious. Figure 13, an annual rate of earth movement map based on Bench Mark 82 as datum for the period October, 1972 to October, 1973, shows the arresting affect of both the water injection project and the declining production, on the rates of subsidence in the oilfield area. The total field production history can be seen on Figures 9 and 14.

Controlling Geologic Characteristics of Beverly Hills (East) Oilfield Subsidence

Each of the controlling geologic characteristics listed in the empirical model were set forth prior to oilfield production and reviewed again during the progress of field development and production. Numerical values for some of these characteristics are set out in Table 1. It can be seen on analyzing the amount of subsidence that occurred that there were some very definite reasons why the amount of subsidence was not large. First, the regional structural conditions for the Beverly Hills

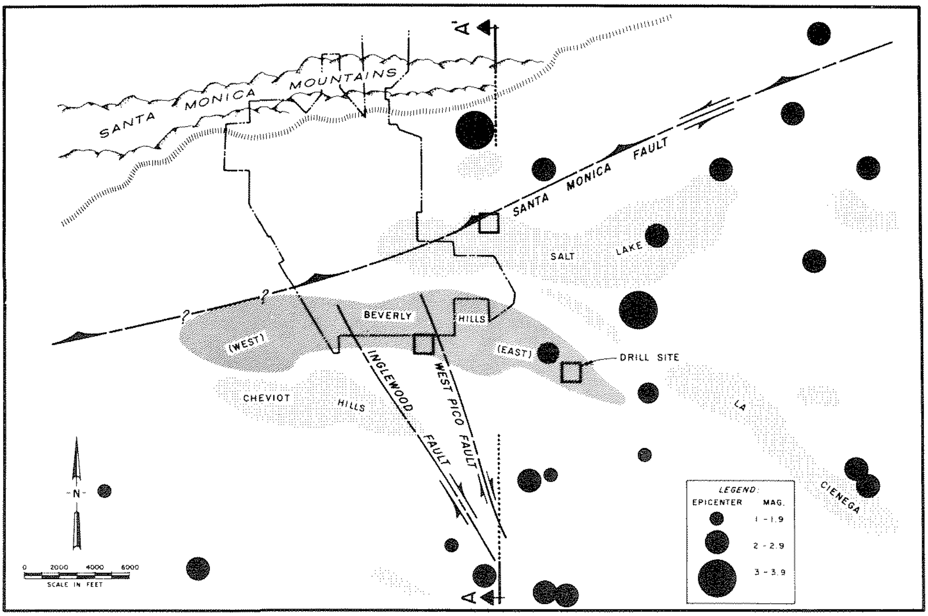

Fig. 6. Earthquake epicenter map for the period 1934 to 1974, data from California Institute of Technology and USC Geophysical Lab.

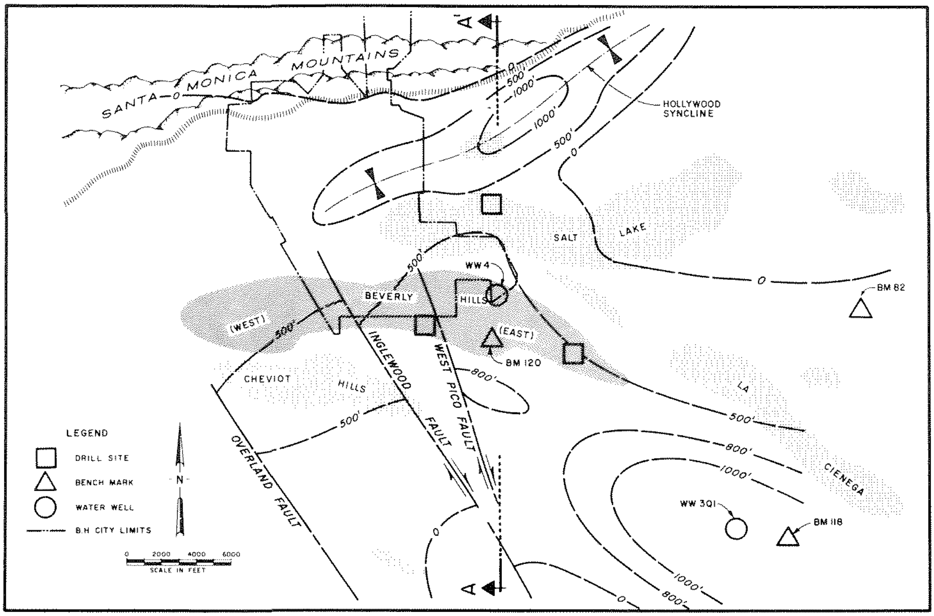

Fig. 7. Isochore map of fresh water aquifers. Refer to Fig. 3 for stratigraphic position.

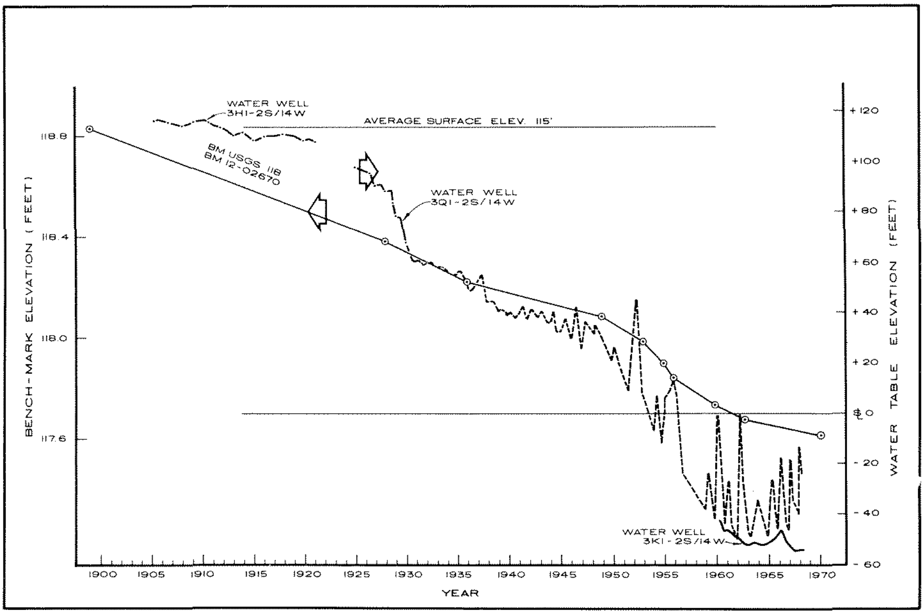

Fig. 8. Graph of surface movement at B.M. USGS 118 and hydrograph of water wells located in Section 3-T2S/R14W.

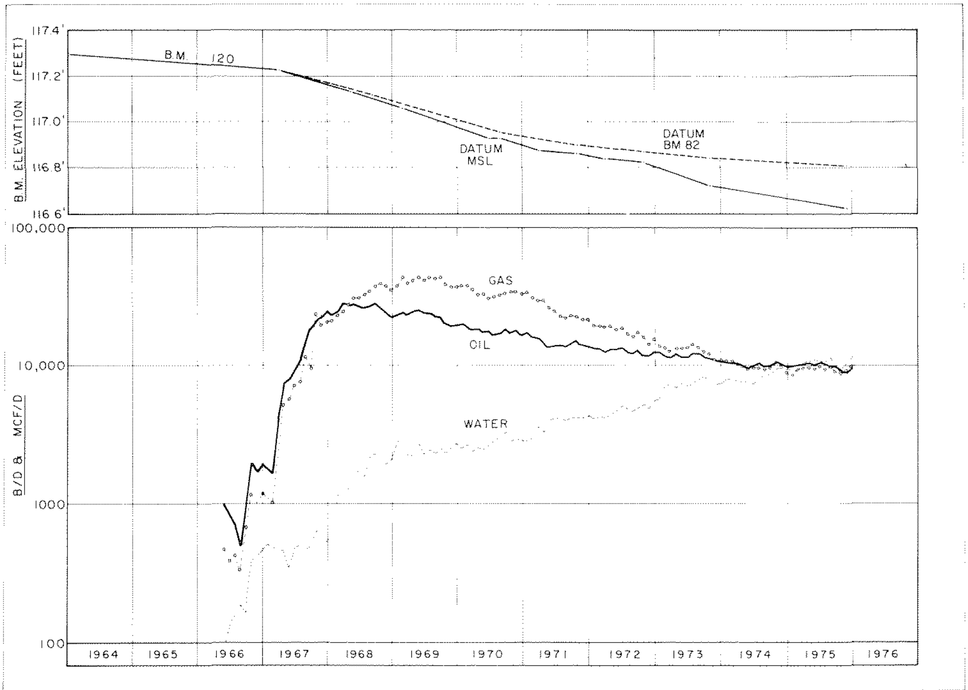

Fig. 9. Graph of surface movement at B.M. 120 and daily production rates from the Beverly Hills (East) Oilfield.

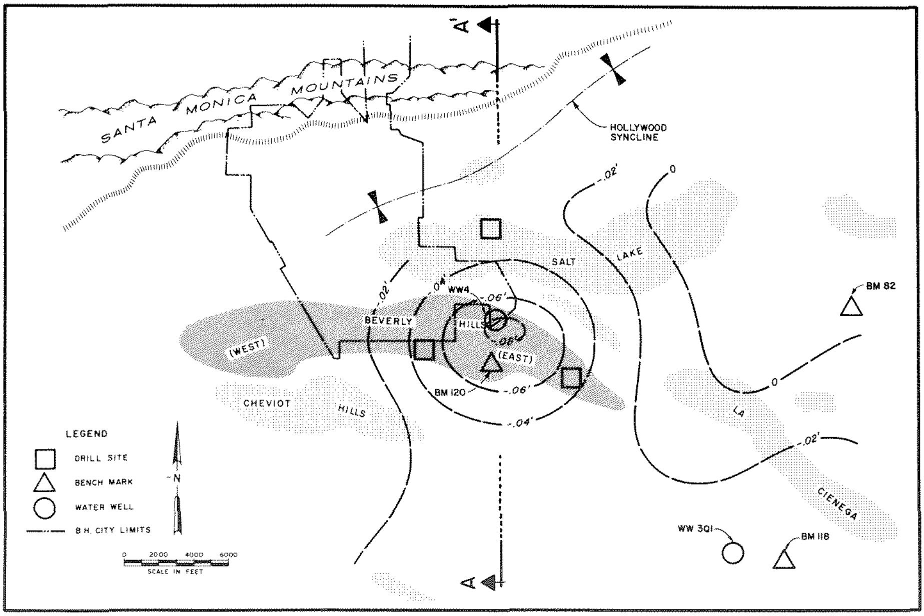

Fig. 10. Annual rate of earth movement for the period March 1967 to March 1971, based on a mean sea level datum.

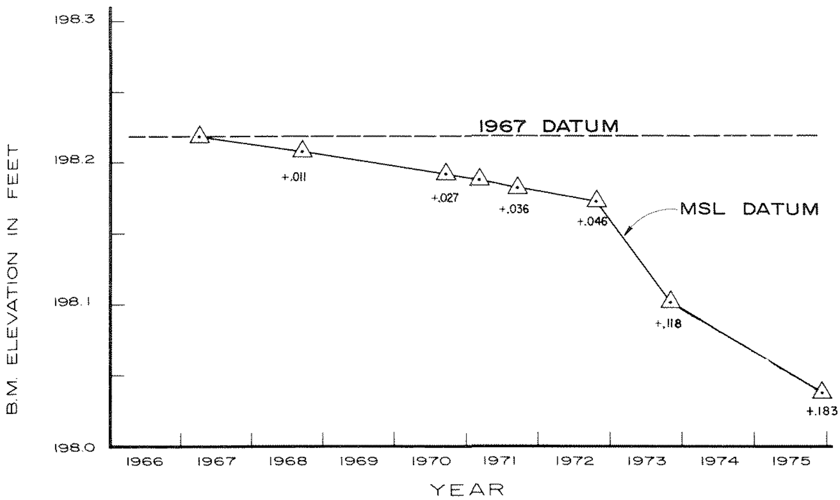

Fig. 11. Adjustment of B.M. No. 82 to a constant datum as of March 1967.

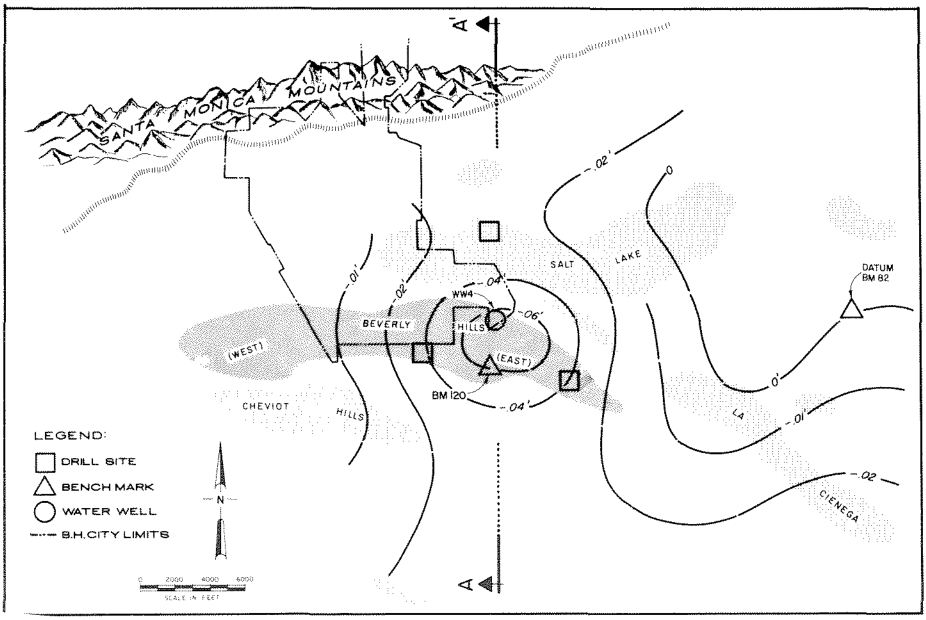

Fig. 12. Annual rate of earth movement for the period March 1967 to March 1971, based on B.M. No. 82 as datum.

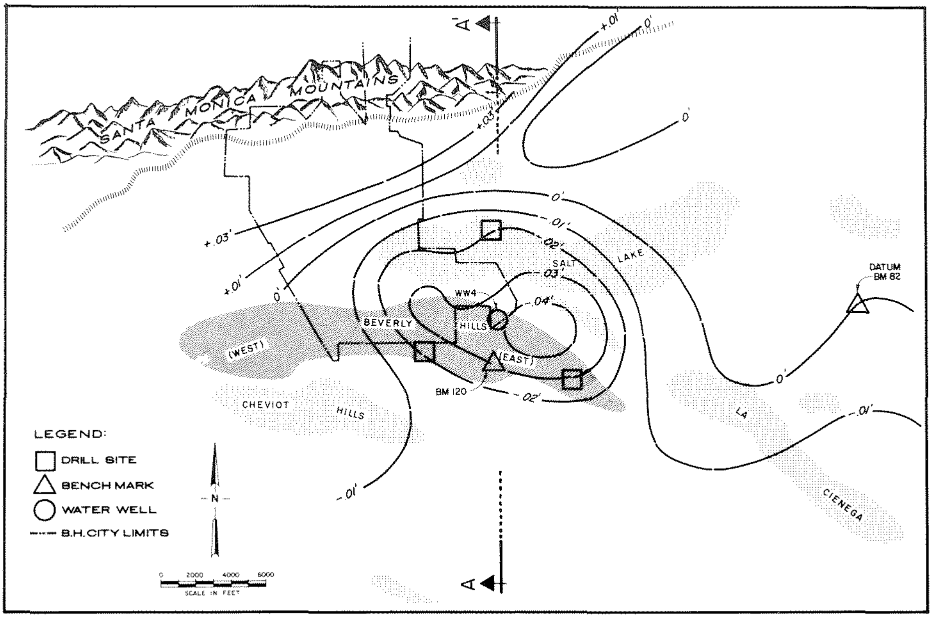

Fig. 13. Annual rate of earth movement for the period October 1972 to October 1973, based on B.M. No. 82 as datum.

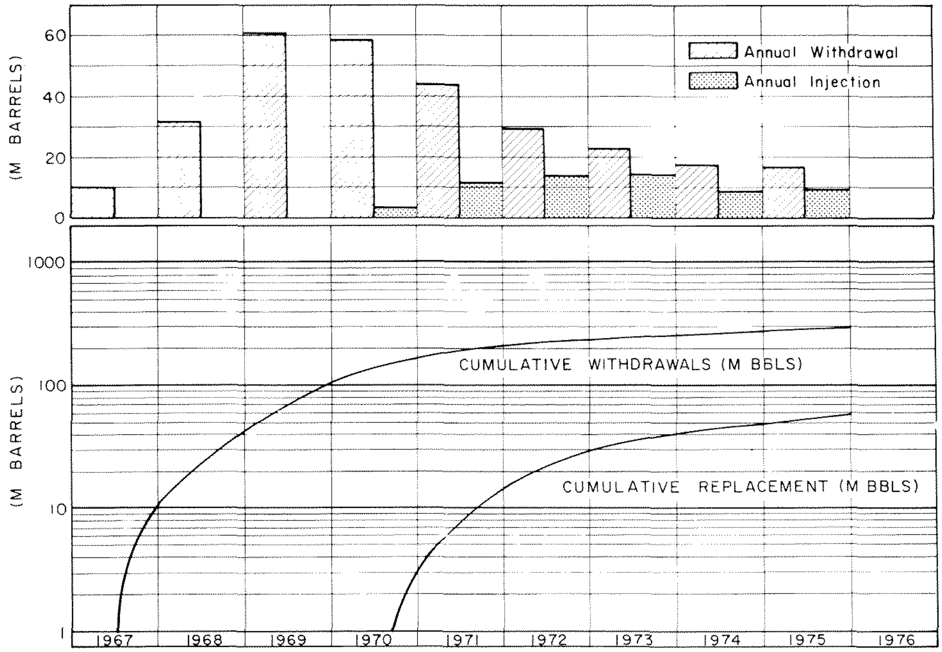

Fig. 14. Beverly Hills (East) Oilfield, total barrels of reservoir voidage and injection.

(East) Field vary from a tight asymmetrical fold within deep Miocene sediments to a broad gentle fold in the shallower lower Pliocene rocks. The significant oil accumulation occurs within the deep, tightly folded section which reflects, along with the associated thrust faulting, strong north-south compression. This configuration should furnish arch support within both the producing intervals and the overlying capping rock (Figure 3).

The ratios of the breadth of accumulation to depth for each significant zone are listed in Table 1. Thickness of the oil productive main section is impressive on the south flank, where the beds are standing nearly vertical. Oil productive thickness on this flank ranges up to 1,000 feet, whereas, on the north flank, which is more gently dipping, the productive section averages about 650 feet in thickness. There is also the strong likelihood that these deeper Miocene reservoirs are more resistive to consolidation due to retained tectonic prestressing.

Second, the physical properties of the producing zones have a bearing on the degree of consolidation which may occur when and if a sizeable load transfer from the fluid phase to the rock matrix occurs. Of the rock characteristics that exert some control in the Beverly Hills (East) Field, the lithology and preconsolidation and cementation probably are the most effective. From ditch samples, cores and sidewall samples, it was determined that the reservoir rock is a firm clastic with intergranular porosity. The porosity in the main producing horizon and shallow zones is quite good, ranging from 20 to 30%.

The third property, formation temperature changes that may result in contraction or expansion of the reservoir rock, does not appear to apply in this instance.

Conclusions

1. Regulations of the City of Los Angeles have been effective in controlling oil well drilling and production within the city.

2. The Beverly Hills (East) oilfield is situated in an area undergoing regional subsidence as a consequence of tectonic forces. Imprinted upon this regional downwarping are subsidence components arising from shallow water production and deeper oilfield fluid withdrawals. Singly or in combination, these forces produce subsidence measurable in no more than a few hundredths of a foot per year.

3. Precise leveling surveys conducted by Standard Oil Company of California and Occidental Petroleum Corporation have been effective in detecting and monitoring surface elevation changes over the Beverly Hills (East) oilfield. Similarly, these surveys have demonstrated that subsidence attributable to oilfield operations is being arrested by subsurface reservoir pressure maintenance based on water injection.

4. Oilfield subsidence, which in rare cases has been extremely damaging, can be detected at an early date following the advent of production by precise leveling surveys. Corrective measures can be instituted to arrest subsidence before damage to surface structures or wells occur.

5. Oilfield subsidence may be due to a wide assortment of causes, chiefly geologic in nature, and, therefore, its prediction may not be quantitatively accomplished. From a qualitative point of view, however, the construction of a model using impirical components may be extremely helpful in forecasting subsidence prospects and estimating their magnitude. Subsurface geologic data, coupled with other related information, are indispensable in the accuracy of such forecasts.

Acknowledgements

The author wishes to express his appreciation to the Standard Oil Company of California for permission to prepare and publish this paper, and to Messrs. A. O. Spaulding and I. I. Dagan for their valuable suggestions and discussion.

References

Allen, Dennis R. -- 1970, "Surface Subsidence Possibilities in the Beverly Hills, Salt Lake, Las Cienegas and Los Angeles Downtown Oil Fields, City of Los Angeles, California," Report prepared for the City of Los Angeles.

California Department of Water Resources -- 1965 to 1970, Bul. 130-64 through 130-68 Series, Hydrologic Data, Southern California

Ebert, F. C. -- 1921, "Records of Water Levels in Wells in Southern California," USGS Water-Supply Paper No. 468, 156p.

Grant, U.S. and Sheppard, W. E. -- 1939, "Some Recent Changes of Elevation in the Los Angeles Basin, Southern California, and Their Possible Significance," Bul. of the Seismological Society of America, Vol. 29, No. 2, pp. 224-326.

Los Angeles City -- 1963, Bureau of Engineering Survey Division Published Precise Bench Mark Index.

Meade, R. H. -- 1968, "Compaction of Sediments Underlying Areas of Land Subsidence in Central California," USGS Prof. Paper 497-D, p. 39.

Mendenhall, W. C. -- 1905 "Western Coastal Plain Region of Southern California," USGS Water-Supply Paper No. 139, 103p.

Pafford & Associates -- 1972, Unpublished Precise Level Survey Records, Beverly Hills Area.

Spaulding, Arthur O. -- 1971, "Oil and Los Angeles - An Environmental Triumph," Paper No. SPE 3616, presented at SPE 46th Annual Fall Meeting, New Orleans, Oct. 3-6.

Publication n°121 of the International Association of Hydrological Sciences
Proceedings of the Anaheim Symposium, December 1976

CALCULATED HORIZONTAL MOVEMENTS AT BALDWIN HILLS, CALIFORNIA

Kenneth L. Lee
Professor, School of Engineering and Applied Science
University of California, Los Angeles, California

Abstract

The paper demonstrates that a linear elastic finite element calculation can provide a good indication of the ground surface subsidence and horizontal movements caused by fluid removal from an oil field. The case history used for comparison purposes was the Inglewood Oil Field, Los Angeles, California, which included the site of the Baldwin Hills dam failure in 1963, believed by many to be related to the oil field induced ground movements.

Sommaire

L'article démontre comment l'utilisation des éléments finis en élasticité linéaire peut donner une bonne indication des tassements en surface et des déplacements horizontaux provoqués par l'extraction de fluide dans un champ de pétrole. Le cas considéré pour illustration est le champ de pétrole Inglewood à Los Angelès, California qui englobe le site du barrage de Baldwin Hills, dont la rupture en 1963 est considérée par beaucoup comme lieé aux mouvements de surface causés par le champ de pétrole.

Introduction: This paper reports the results of a study to check the validity of using a linear elastic finite element approach for calculating the nature and magnitude of horizontal ground movements to be expected from subsidence due to fluid withdrawal from a confined oil field. Geotechnical engineering abounds with examples of horizontal ground surface movements which develop in association with vertical subsidence. The best known examples involve mining operations, but other examples include soil consolidation and pumping of fluids (oil and water) from underground reservoirs. Many methods have been proposed for quantifying the amount of vertical and horizontal movements that will develop under various natural and man imposed conditions, of which the finite element method is thought to be the newest and most versatile. It has been shown to give reasonably good checks against field case history data for some model tests and dam settlement (Lee and Shen, 1969), salt mine collapse (Lee and Strauss, 1969) and subsidence due to oil pumping at Long Beach, California (Lee, 1975).

An additional case history comparison between observed and computed ground movements caused by oil pumping from an underground reservoir is presented herein. This case history is particularly significant because of the failure of an important earth dam which was located in the subsidence bowl. Although many detailed engineering investigations have been conducted and expert opinions expressed on factors pertaining to this dam failure, there still appears to be no consensus of opinion as to whether or not the failure was caused predominantly by the oil field operations (Casagrande et al, 1972; Castle and Youd, 1972; Hudson and Scott, 1965; Investigation, 1964; Jansen et al, 1967; Leps, 1972). This paper does not intend to indicate blame for the dam failure, but rather to investigate the ability of the calculation technique to reproduce the observed ground movements. The dam failure merely adds an interesting and perhaps instructive aspect to the discussion.

Case History Description: Details of the Baldwin Hills area, the underlying Inglewood Oil Field and the dam are readily available so that only a brief summary need be repeated here. The Baldwin Hills area lies within the city of Los Angeles, midway between the International Airport and Downtown. Oil was discovered in 1924 and significant oil production has continued from that time to the present.

A water storage reservoir was constructed during the years 1948 to 1951 by excavating into a hilltop and building an earth dam across a small valley with the excavated soil. On Dec. 14, 1963, the dam failed by eroding a V-notch through the embankment. The ensuing flood damaged a large portion of the city to the north below the reservoir to the extent of about 15 million dollars and killed 5 people.

The ground conditions at Baldwin Hills consist of interbedded shales and sandstones which extend to a depth in excess of 20,000 ft. This sedimentary rock material is similar to that at Long Beach, where some engineering property data are available (7). These Long Beach data were also used in this study because the sedimentary rock was believed to be similar.

The major oil producing zones at Baldwin Hills occur within a depth range of about 1000 to 1500 ft below the surface, but some smaller amounts of oil are produced at depths ranging up to 10,000 ft. Good records of oil reservoir pressures are unavailable (Castle and Yerkes, 1969), but such data as exist suggest that prior to any oil production, the initial pore fluid pressure, u_o, in Southern California oil fields increases hydrostatically with depth, D, below the surface according to the equation, $u_o = \gamma_w D$, where $\gamma_w = 64$ lb per cu ft, the unit weight of sea water. It is further estimated (Investigation, 1964) that the reservoir pressure in the zone of major production reduced to about 30 psi (4.3 ksf) as the oil was removed.

The exact magnitudes of ground subsidence and horizontal movements in the Baldwin Hills area are somewhat uncertain. Two original surveys were conducted in 1911 and 1917 respectively, before oil was discovered. The next surveys were not until after oil production began and considerable movements had developed causing shifts in the basic bench marks. The ground movements presented herein are believed to be approximately correct, at least within sufficient accuracy for the purposes of this paper.

A plan of subsidence rate contours in the Baldwin Hills area (as of 1961) is shown in Fig. 1. The available data do not permit drawing contours of total subsidence. However, the data do define a tpyical bowl shaped subsidence pattern. Vectors of measured total horizontal movements for a known period of time are also shown. As typical in all subsidence cases, the direction of the horizontal movements is toward the center of the subsidence bowl. This leads to extension strains (with the possibility of ground cracks) at the outer edges of the bowl and compression near the center. Indeed, there are numerous ground cracks at the edges of the Baldwin Hills

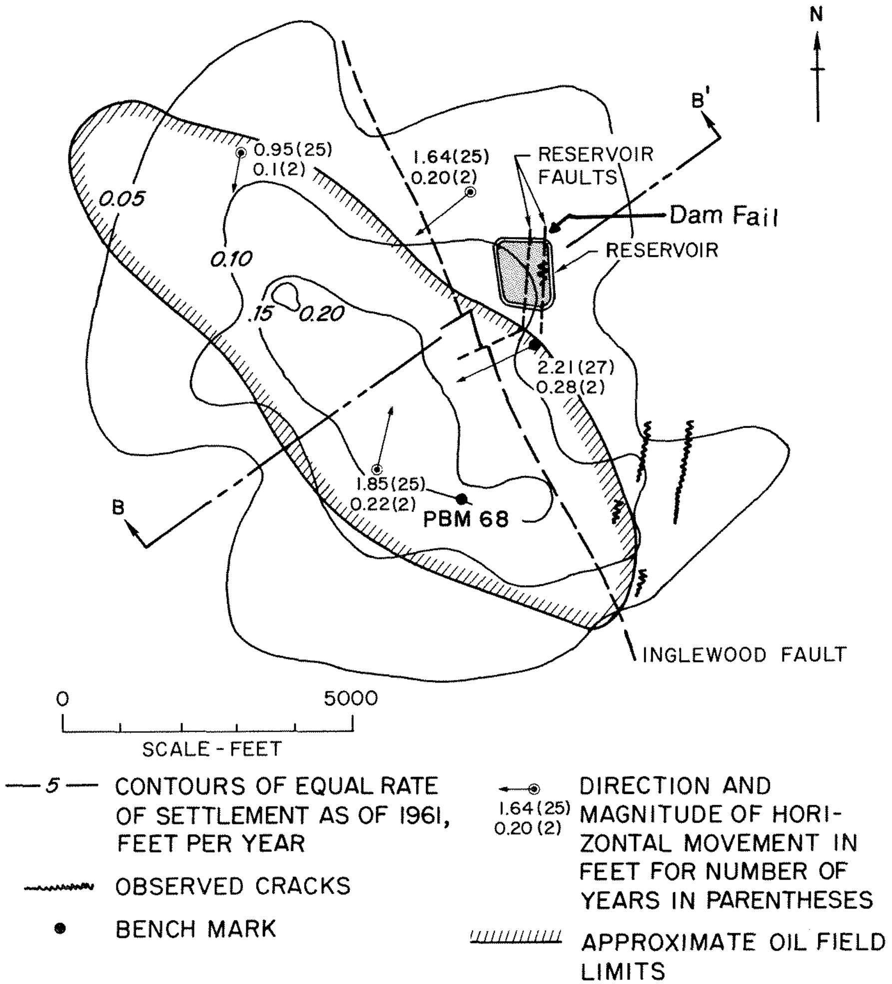

Fig. 1. Horizontal Movements and Subsidence Rates in Baldwin Hills Area

subsidence bowl. The crack pattern is complicated however, by the existence of several pre-existing old near vertical tectonic faults. Two of these faults pass through the Baldwin Hills Dam, and the seepage piping failure of the dam occurred at the location of one of these faults.

One hypothesis (Casagrande et al, 1972) for the cause of the dam failure is that the lining of the reservoir was inadequate and that the material within the fault zone was highly erodable. Thus, when seepage water penetrated through the asphalt lining of the reservoir it then washed out the material along the fault, accelerating with time to produce a complete piping failure of the dam. This action is viewed as being independent of any subsidence induced horizontal extension strains at the fault. An alternate hypothesis

(Leps, 1972) favors the opinion that subsidence led to extension strains at the fault which initiated the above described erosion process.

A photograph looking from south to north over the Baldwin Hills reservoir and dam after failure is shown in Fig. 2. With the water drawn down, a crack could be traced through the reservoir from the V-notch at the top of the photograph to the pavement at the construction joint in the parapet wall at the bottom of the photograph. This crack followed the pre-existing fault trace shown in Fig. 1. Certainly the weak soil in the pre-existing tectonic fault zone contributed to the failure, but the question still remains whether or not the fault opened to develop a crack in the foundation as a result of oil field subsidence induced horizontal ground motion.

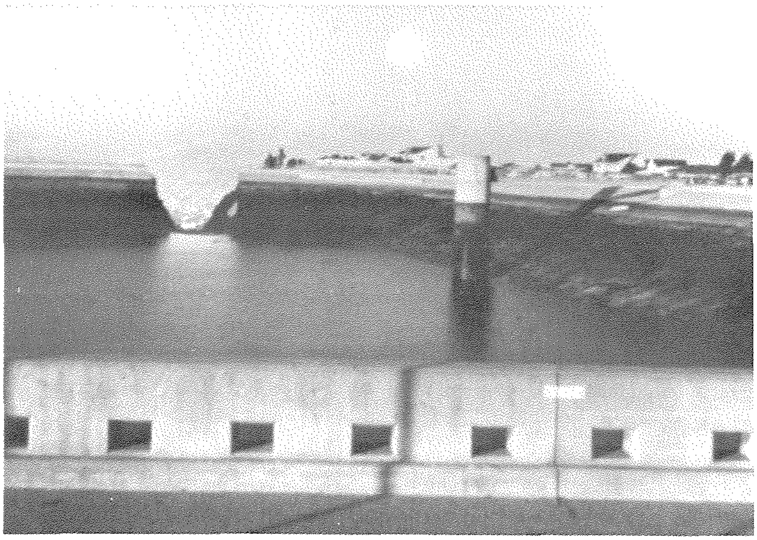

Fig. 2 Photograph of Failed Baldwin Hills Dam Looking North Along Reservoir Faults. Construction Joint has opened and Pavement in Front has Cracked Recently.

A chronological history of significant ground movements and related events at the Baldwin Hills area is shown in Fig. 3. Note the well defined relation between reservoir pressure drop, oil production and ground movements. The data in Fig. 3d are particularly interesting in that they show the widening of a crack in an inspection tunnel which crossed the fault through the reservoir. This extension strain movement continued progressively with the oil production and ground subsidence up to the time of failure. The reservoir pressures (Fig. 3a) were obtained at one of the producing wells. It is expected that the average pressure in the field away from the well would not have reduced as fast as at the well (Castle and Yerkes, 1969).

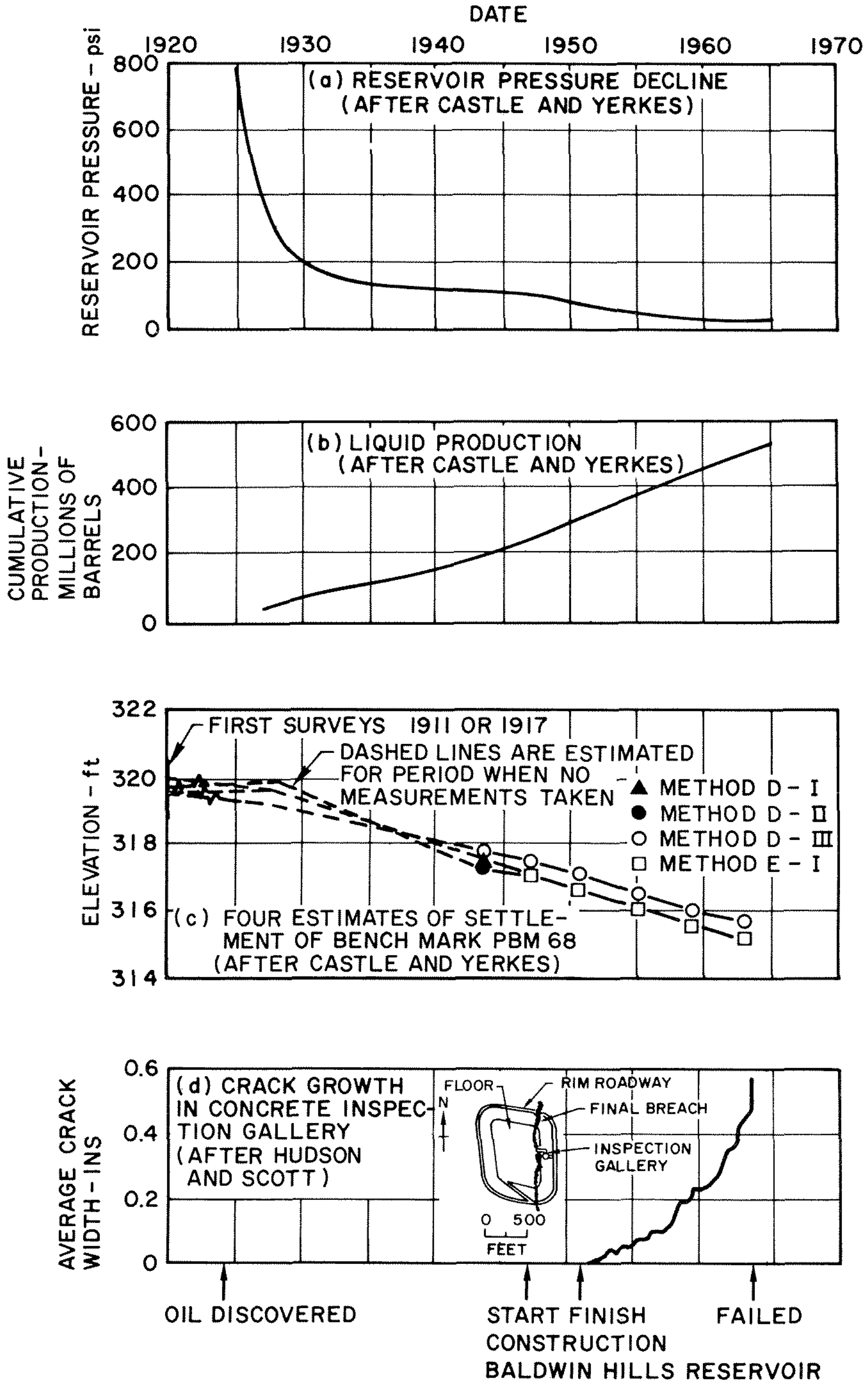

Fig. 3 . Oil Production and Subsidence at the Inglewood Oil Field

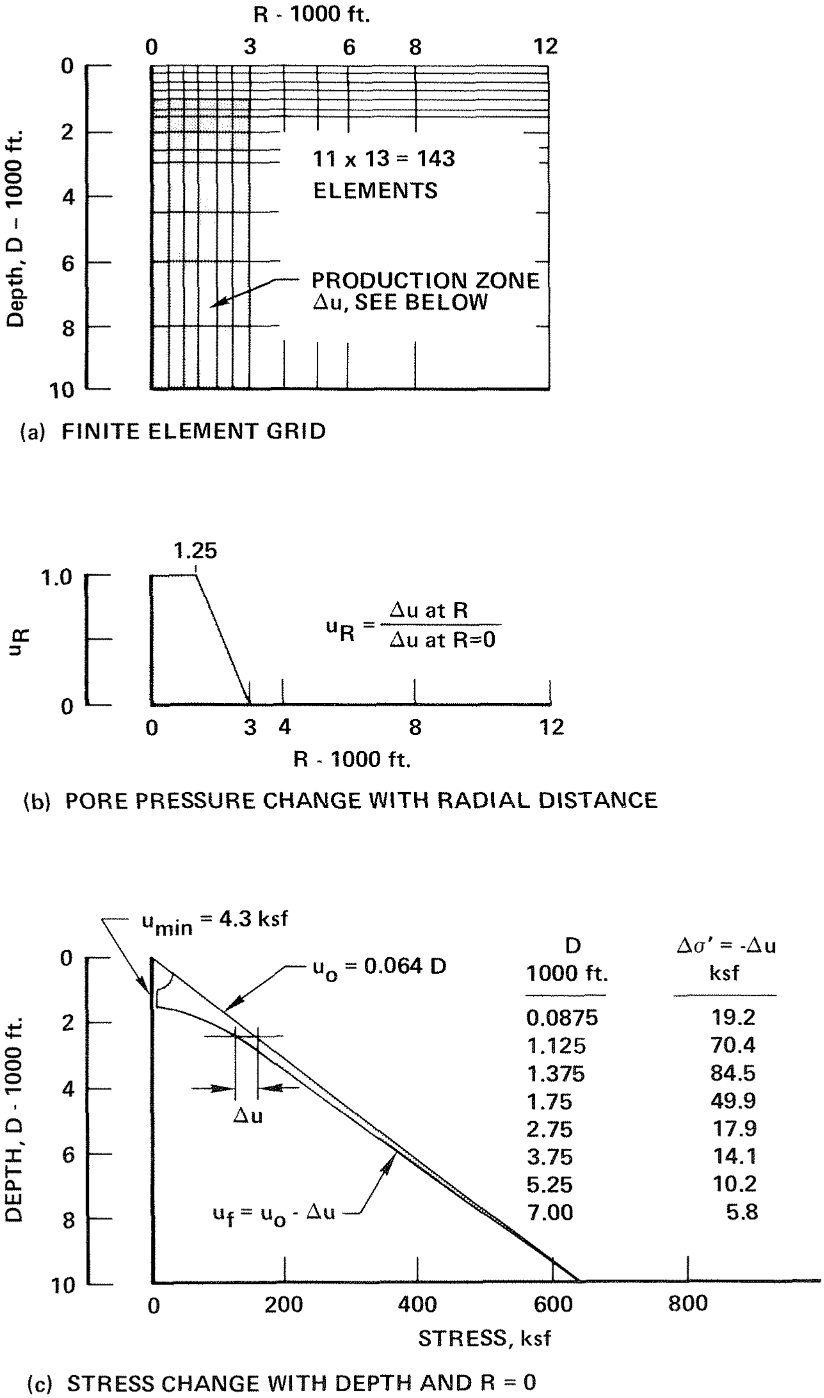

Fig. 4. Finite Element Grid and Stress Distribution

Finite Element Model: The element modeling technique used herein was essentially the same as used by Lee (1975) in a similar study of the movements at the Wilmington Oil Field in Long Beach. The model and the pressure changes are shown in Fig. 4.

The finite element program was a standard axis-symmetric, linear elastic program written by the writer. From the Lee (1975) data, Poisson's ratio was taken to be 0.1 and Young's modulus was assumed to vary with depth (D ft) according to the equation

$$E = 500\ D^{0.5}\ \text{psf} \qquad (1)$$

The loading used to simulate the oil removal was defined in terms of changes in pore pressure throughout the producing zone shown by the shaded areas in Fig. 4. The three dimensional extent and the magnitude of these pore pressure changes were estimated from the known limits of the oil field (Fig. 1) along the Section BB', and the other information described above. No data were available for pore pressure changes in the deep zones, but since the deep zones were not the source of major oil production, it was reasoned that it would likewise not by a zone of major pore pressure change.

Following the basic principle of effective stress and as described by Lee (1975), the only net loading that need be considered in the analysis is the isotropic change in effective stress which is equal and opposite to the change in pore water pressure, $\Delta\sigma' = -\Delta u$. No other loading changes occurred, and the calculations were intended to define the movements caused by only this change in loading. Therefore, the appropriate values of $\Delta\sigma'$ at the center of each element within the shaded producing zone (Fig. 4) were converted to nodal point forces as the sole source of loading.

It should be noted that the extent of the oil producing zone and the pore pressure reduction used in the analysis correspond to the 25 year period, 1937–1962, because the data available to the writer pertained to this period. Note also that the oval shaped producing zone (Fig. 1) has been approximated in the calculations by a circle of radius, R = 2000 ft with an assumed linear transition zone of pore pressure reduction beginning at R = 1250 ft and extending to R = 3000 ft where $\Delta u = 0$.

Calculated Ground Surface Movements: The computer output from a finite element calculation provides detailed information concerning deformations, strains, and stresses at every location within the grid system. For this study, only the movements at the ground surface were of interest, since this was the only location where actual observed field data were available. Note however, that in a previous similar study by Lee (1975), the calculated results at various vertical as well as horizontal locations were of interest since they could be compared with field measured data within the ground as well as at the ground surface.

The calculated ground surface movements at the Baldwin Hills area are shown in Fig. 5 along with field measured data points. In considering a comparison between measured and calculated movements, a few brief comments on the measured data are appropriate. The horizontal movement data over the periods shown in Fig. 1 are believed to be fairly reliable. The three points closest to Sec. BB' have been transferred to this section and are shown in Fig. 5. The vertical subsidence profile follows the shape of the subsidence rate contours in Fig. 1, with magnitude interpolated on the basis of the measured vertical subsidence at bench mark PBM 68 (Fig. 1 and 3) which Castle and Yerkes (1969) believe to be the most correct. The single strain data point was obtained from a measured extension of 0.4 ft in the 1100 ft long NE-SW diagonal of the Baldwin Hills water reservoir between the 13 year period 1950-1963. Assuming that the stretching would be proportional to the measured subsidence at PBM 68 back to 1937, a value of horizontal extension strain of 0.1 percent was obtained for the 25 year period at this location. As can be seen in Fig. 5, there was excellent agreement between the calculated and the observed field ground surface movements along the section BB'.

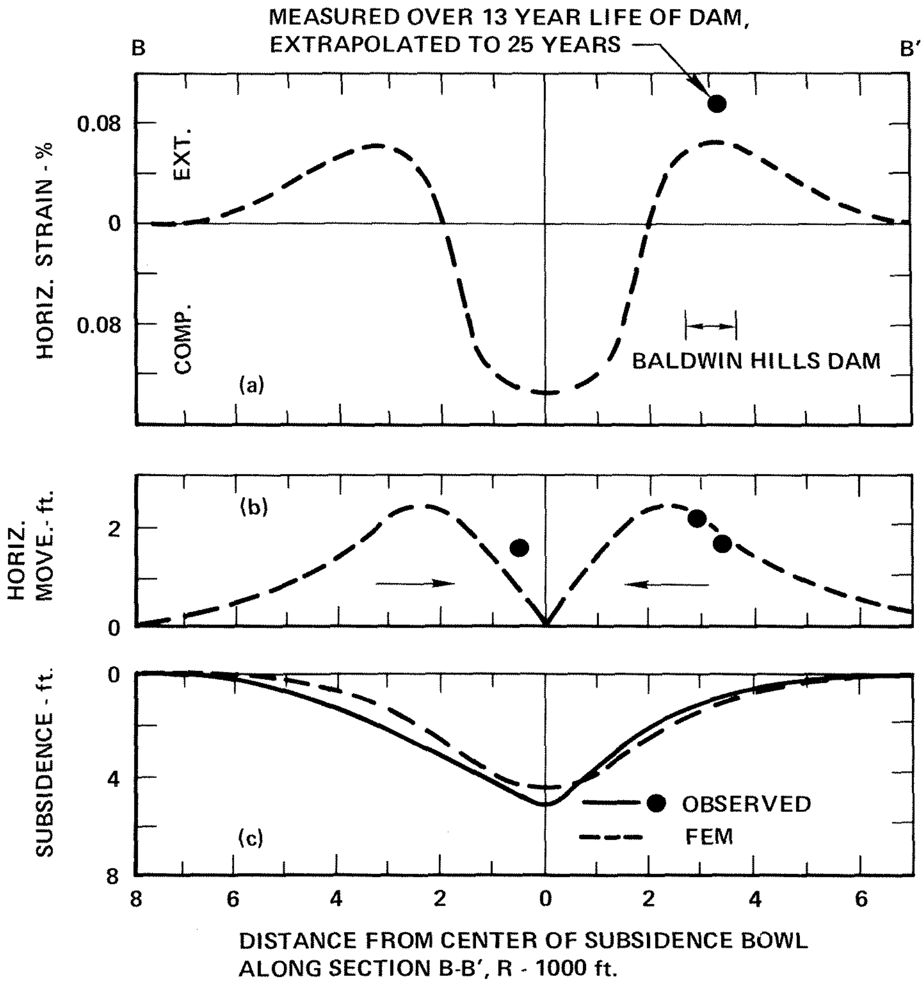

Fig. 5. Observed and Computed Ground Surface Movements at Baldwin Hills Area for 25 Year Period; 1937-1962.

Concluding Comments: A simple linear elastic finite element calculation has been used to calculate ground surface vertical and horizontal movements for comparison with measured field data. The purpose of this study was to check whether this method of calculation would be able to reproduce the observed movements, and therefore would it be reasonable to use the method for future studies of similar problems. The results suggest an affirmative answer to each of these questions. Furthermore, the reader is referred to the cited previous similar studies by the writer which have also produced similar confirming results. Taken together, it would appear that the technique described herein should provide a useful method for predicting in advance the nature of ground surface movements likely to be associated with subsurface fluid withdrawal.

Of course, the accuracy of the predictions depends greatly on the accuracy of the boundary and loading conditions used in the analytical formulation. Nevertheless, the results from this and the previous similar study at the Wilmington field, suggest that with estimates of boundary and loading conditions that should be possible to make in advance, useful results can be obtained. Alternatively, the technique can provide a means of studying the effect of boundary or loading conditions that might be possible to control, such as the extent of the underground fluid zones that are produced and the amount of fluid pressure reduction allowed without resorting to auxiliary fluid pressure injection.

Since the geographical study area for this paper involved the site of the Baldwin Hills Dam, perhaps a brief comment on the application of the results to the dam failure would also be appropriate. The ground strain data (Fig. 5) and the plan view (Fig. 1) illustrate that the dam was situated in the most inappropriate location and orientation from the point of view of ground surface movements caused by fluid removal from the underlying oil field. The dam was located toward the edge of the subsidence bowl where the largest extension strains developed. The embankment was oriented in an approximate radial direction, so that the extension strains in the ground would have the maximum adverse affect by stretching the axis, which would be favorable to crack development. Had the dam been turned by about 90 degrees, the axis would have been parallel to the subsidence contours, which would have led to compressive axial strains as described by Lee (1975) for the Commodore Heim Lift Bridge in the Wilmington field.

Finally, it was unfortunate that the ground contained a weak fault zone also located unfavorably across the dam foundation where the subsidence alone would produce fairly large extension strains. Assuming that the fault was weaker than the surrounding rock foundation, it follows that the extension strains would tend to concentrate at the fault where a crack would develop, as was actually observed.

It is beyond the scope of this paper to speculate on what might have happened without any subsidence or without a pre-existing fault or to suggest responsibility for the failure. The results of the study do indicate however, that the subsidence could be expected to produce substantial extension strains along the axis of the dam, which would be unfavorable to its stability. Thus, had an analysis such as this been performed prior to the dam construction, it would have shown this unfavorable situation and probably led to precautionary or alternative procedures with regard to a water storage facility in the area. Unfortunately, the finite element method had not been invented in 1948 when construction began on the dam.

References

Casagrande, A., Wilson, S. D. and Schwantes, E. D., 1972, The Baldwin Hills Reservoir Failure in Retrospect: Performance of Earth and Earth Supported Strctures, Proceedings of Specialty Conference, ASCE, p. 551-558.

Castle, R. O., and Yerkes, R. F., 1969, A Study of Surface Deformations Associated with Oil-Field Operations: Report of the U.S. Geological Survey, Menlo Park, California.

Castle, R. O. and Youd, T. L., 1972, The Baldwin Hills Reservoir Failure: Discussion: Proc. Specialty Conference on Performance of Earth and Earth Supported Structures, ASCE, v. iii, Purdue University, p. 91-102.

Hudson, Donald E., and Scott, Ronald F., 1965, Fault Motions at the Baldwin Hills Reservoir Site: Bulletin of the Seismological Society of America, v. 55, No. 1, p. 165-180.

Investigation of Failure, Baldwin Hills Reservoir, 1964, Department of Water Resources, Sacramento California.

Jansen, Robert B., Dukleth, Gordon W., Gordon, Bernard B., James, Laurence B. and Shields, Clyde E, 1967, Earth Movements at Baldwin Hills Reservoir: Journal of the Soil Mechanics and Foundations Division, ASCE, v. 93, No. SM4, p. 551-575.

Lee, Kenneth L., 1975, A Mechanism for Subsidence Earthquakes at the Wilmington, California Oil Field : Paper presented at the First International Symposium on Induced Seismicity, Banff, Alberta, Canada.

Lee, Kenneth L. and Shen, C. K., 1969, Horizontal Movements Related to Subsidence: Journal of the Soil Mechanics and Foundations Division, ASCE, Vol. 95, No. SM1, p. 139-166.

Lee, Kenneth L. and Strauss, Michael E., 1969, Prediction of Horizontal Movements Due to Subsidence over Mined Areas: Proc. International Symposium on Land Subsidence, held in Tokyo, Publication No. 88, Vol. II, IASH-UNESCO, p 512-522.

Leps, Thomas M., 1972, Analysis of Failure of Baldwin Hills Reservoir; Performance of Earth and Earth-Supported Structures, Proc. of Specialty Conference, ASCE, p. 507-550.

Publication n°121 of the International Association of Hydrological Sciences
Proceedings of the Anaheim Symposium, December 1976

SUBSIDENCE SUSCEPTIBILITY: METHODS FOR APPRAISAL

Dennis R. Allen
City of Long Beach, Department of Oil
Properties, Long Beach, Ca. 90801

Abstract

Subsidence is an evironmental problem around the world today; but particulary in California, U.S.A., due to the requirements for environmental impact reports prior to undertaking virtually any major construction and development project. Appraisals of man induced subsidence susceptibility can be classified into two broad categories, (1) the comparative-empirical and (2) the analytical methods. The comparative-empirical method depends primarily upon a geological comparison between the area being appraised and known areas of subsidence. The analytical method attempts to quantify subsidence by the application of soil mechanics and other theorems using approaches such as either a finite element grid or a sophisticated equation. Several papers have been published in the past few years using one or both of the above methods of appraisal. When data are available some combination of the two methods is best.

As applied to oil fields, the pertinent factors are structural integrity, type of faulting, pressure drops in the reservoir, width/depth ratio of the structure, cementation, consolidation, compressibility and the insitu stress fields.

The most elusive element in subsidence forecasting is the time-rate response, due to "lag time" (a displacement in time relative to the causative factors); many other variables also enter into the problem. Three types of time-rate response have been identified in oil field subsidence; i.e., (1) the bell-shaped frequency curve, (2) the two-rate or "threshold break" curve and (3) a linear time-rate relationship.

Introduction

"Stop pollution! Protect our environment; develop a balanced ecology." These are the demands of today's society. A surge of public awareness has encompassed the United States and to some degree many countries around the world. "Spaceship Earth" which has become a favorite phrase of environmentalists, often ignores the fact that many of earth's scars are self-healing. Even though nebulous, the danger of subsidence often must be addressed in preliminary planning. Environmental impact studies are often required. Subsidence is only one item that must be covered in any environmental impact report; however, it assumes a position of importance due to widespread publicity given to such areas as Wilmington Field, California and Tokyo, Japan. Significant oil field subsidence, defined as that which causes damage, is relatively rare, although small amounts have been documented many times. All types should be reviewed in an environmental appraisal.

Types of Subsidence

When examining an area for either potential subsidence or to define the cause of documented subsidence, many factors must be evaluated, particularly those that could lead to an improper assessment of cause. For ease of investigation, subsidence should first be divided into two basic categories; (1) geological ("natural") subsidence, and (2) induced subsidence (caused by mans activities).

Geological subsidence includes: (1) natural consolidation and/or compaction caused by the overburden weight, diagensis of sediments, etc.; and

(2) tectonic movements, which includes localized elevation changes along active faults and regional downwarping.

Induced subsidence is that either caused by or related to man's activities. It is usually associated with the removal of a subsidence, either a fluid such as water, oil or gas, or a solid such as coal or salt. One major exception to the above is subsidence caused by "hydro-compaction", which is a loss in volume of dessicated, high porosity sediments caused by the addition of water.

Susceptibility Analysis

Subsidence predictions can be divided into two techniques; (1) the comparative-empirical, and (2) the analytical.

In method one, all relevant data from the area in question are compared with data from areas that have had subsidence. A judgement then is made, based on geological similarity, as to the probability of subsidence in the area being investigated. Method number two includes all mathematical approaches that utilize compressibility and other test data from cores and other sources. Some modified combination of the above methods is best. Many investigators in the past, have tended to view the subsidence problem from a narrow viewpoint. Several recent studies have been made that utilize a multiple discipline approach as should be done.

Comparative Approach

Figure 1 is a critical element chart of the causes of subsidence. It shows the major causes that should be investigated, with an expansion of elements related to oil field subsidence. A similar expansion could be made for subsidence due to any other cause. In the expanded portion of the chart, the solid lines indicate features that tend to contribute to subsidence susceptibility, the dotted lines those that tend to contribute to surface stability.

Studies of subsided areas caused by fluid extraction of all types have revealed a number of common factors. These are: (1) sand reservoirs with a thick vertical section: (2) the sands are unconsolidated; (3) porosities of of 25-40%; (4) reservoir sands are interbedded with clays, siltstones, etc.; (5) large fluid production and (6) large drops in fluid levels.

Oil producing reservoirs have additional common features: (1) relatively shallow burial (top of uppermost zone is less than 1,000 meters $\pm$; (2) the overburden is composed of unconsolidated sediments; (3) reservoir beds have gentle dips; (4) tension faulting common, graben blocks formed; (5) miocene and younger ages and (6) the subsidence is associated with oil field development by location and by time of occurrence.

Water producing areas also have common features: (1) shallow, flat-lying aquifers covering large areas; (2) subsidence rate is cyclic and controlled partially by seasonal fluid level fluctuations; (3) pliocene and younger ages; (4) clay interbeds and (5) fine-grained aquifers.

No one of the features listed above or on Figure 2 is a mandatory item; however, a preponderance certainly points to subsidence susceptibility. In oil field subsidence, the question always arises, why did not field "X" subside because it fits all of the items on Figure 1. The answer often has to be "I don't know". However, two items that must rate high when explaining the non-susceptibility of an area are: (1) cementation of the intergranular structure and the degree and type of sand packing (cementation may be the prime contributor to a structure's self supporting ability); and (2) preconsolidation, a related item that corresponds to the deepest burial to which a formation has been subjected. Data from two oil fields that have had destructive subsidence are shown on Figures 2 and 3.

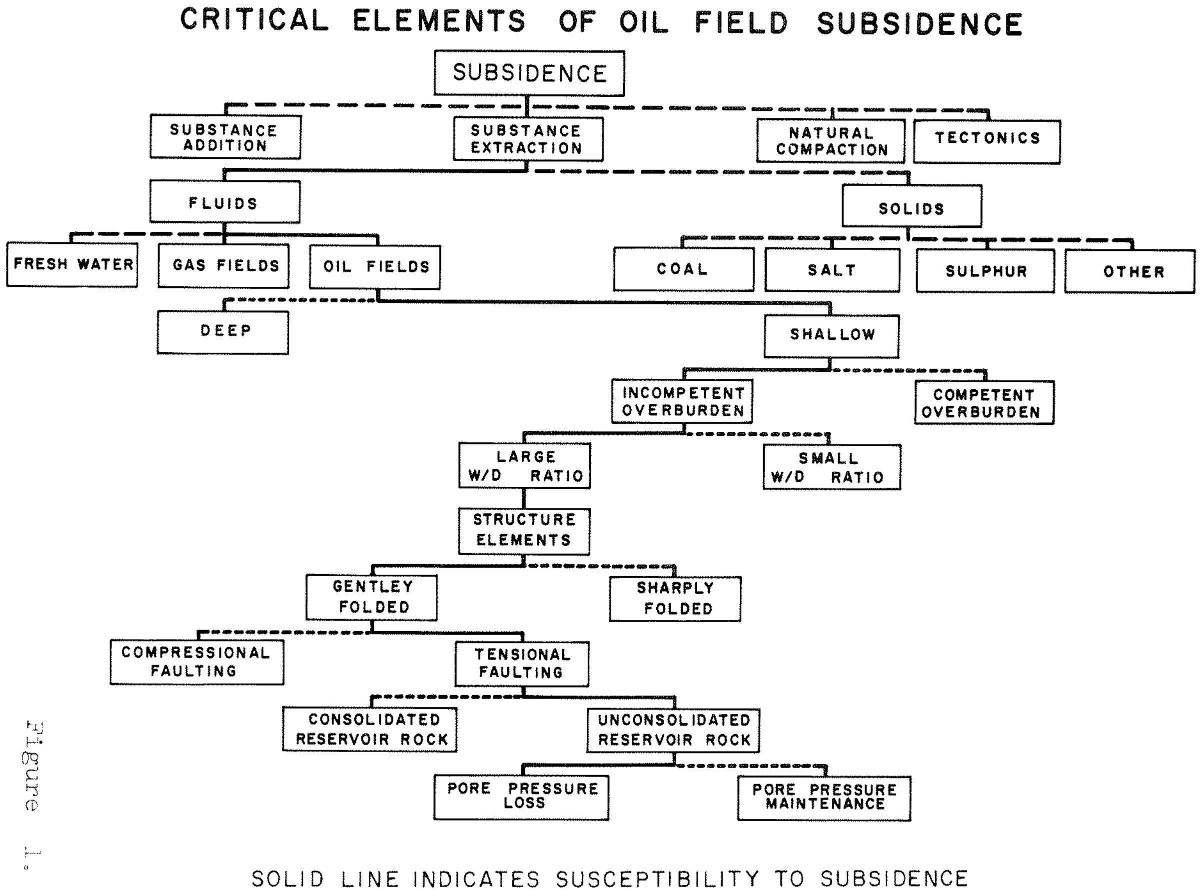
CRITICAL ELEMENTS OF OIL FIELD SUBSIDENCE
SUBSIDENCE
SUBSTANCE ADDITION
SUBSTANCE EXTRACTION
NATURAL COMPACTION
TECTONICS
FLUIDS
SOLIDS
FRESH WATER
GAS FIELDS
OIL FIELDS
COAL
SALT
SULPHUR
OTHER
DEEP
SHALLOW
INCOMPETENT OVERBURDEN
COMPETENT OVERBURDEN
LARGE W/D RATIO
SMALL W/D RATIO
STRUCTURE ELEMENTS
GENTLEY FOLDED
SHARPLY FOLDED
COMPRESSIONAL FAULTING
TENSIONAL FAULTING
CONSOLIDATED RESERVOIR ROCK
UNCONSOLIDATED RESERVOIR ROCK
PORE PRESSURE LOSS
PORE PRESSURE MAINTENANCE
SOLID LINE INDICATES SUSCEPTIBILITY TO SUBSIDENCE

Figure 1.

The Analytical Approach

The analytical method for estimating subsidence susceptibility is basically a mathematical approach. The usefulness of any predictive equation is measured by its ability to duplicate history in an area that has had subsidence. Due to empirically derived constants that are used, a formula that works in one area often will not work in another. In many cases special tests must be made. The same data used in the comparative method may be used, however, an effort is made to quantify each variable. That is, mathematical expressions for rock compressibility, "beam" strength, structure width, depth, material density, fluid pressure, rate of loading transfer and insitu stress fields are applied.

Geertsma and Van Opstal (1973) used an analytical approach in quantifying possible subsidence for the Groningen Gas Field, The Netherlands. They predicted about one meter of subsidence and stated that none had been measured at the date of prediction. The overall approach was similar to that recommended in this paper in that they reviewed the properties of subsiding areas, used core compressibility tests and determined that a range of 50 to 200cm of compaction could be expected. It was noted that reservoir rock compressibility was approximately the same as good concrete. Based on the preliminary calculations, a detailed analytical study was then made. A complex (to this observer) formula was used to calculate both vertical and horizontal displacement. It included Poisson's ratio, the depth of burial of the strain center, the radius of the strained area and rock compressibility. They also presented tables of Bessel functions that relate the depth of burial and width of the reservoir to reservoir compaction and surface subsidence. It was noted that such a sophisticated approach is not always justified. They concluded "that oil reservoirs of the depletion type in loose sands, and extremely large gas reservoirs in either loose or friable rock types, are most sensitive to subsidence".

Based on a comparison of features common to subsidence prone areas, the unknown structural stress and the elastic and cataclastic dilation of pore space that must occur to some extent above such a deep compacting reservoir (3,000 meters), it would be difficult for this observer to predict the occurrence of surface subsidence. It is the writers understanding that a slight amount of subsidence has been measured subsequently. In any event, this paper was a superior effort. With the exception of unknown subsurface stress fields, this approach included all significant features.

Analytical calculations are strongly dependent upon the insitu mechanical properties of the reservoir and overburden rocks, and such properties are virtually impossible to obtain from the unconsolidated core specimens that are characteristic of most subsiding areas.

Various other writers have suggested that the "finite element method" be used for both subsidence and horizontal movement calculations. This method requires that the area in question be divided into a large number of discrete elements and that an inter-related solution be made for each. It also requires the use of a computer, which tends to limit its use, particularly in a preliminary survey.

Influence of Structure

Structural strength is a factor that must be considered in any type of subsidence susceptibility study.

The principles, as related to known subsiding areas, are (1) broad structures with flat lying anticlinal crests, maximum flank dips of 25 degrees or less and tensional faulting are susceptible to subsidence and (2) narrow or tightly folded structures with dips greater than 25 degrees are less susceptible, which is particularly true if faulting is caused by compressional forces.

GEOLOGIC STRUCTURE	Faulted anticline, flat overburden on eroded crest. Tensional faulting, graben at center. Dips flat to about 20°, upper zones.
DEPTH OF BURIAL	2,000' to top of upper zone.
DESCRIPTION AND STRENGTH OF RESERVOIR	Sand reservoirs, vary from massive to thin-bedded. Uncemented, resemble beach sand, contain fine silt and clays, often inter-bedded with siltstones and shales. Materials are incompetent and deform easily.
DESCRIPTION AND STRENGTH OF OVERBURDEN	Overburden is composed of uncemented sands and soft siltstones which grade to clays towards the surface. Very little apparent strength. Faulting does not penetrate overburden.
POROSITY	About 33 to 38% in the upper four zones.
GEOLOGIC AGE	Pliocene and Miocene
SUBSIDENCE	About 30' since 1938, covers 20 square miles. Upper four oil zones compacted, measured by casing deformation. Subsidence rate and cumulative total agreed with fluid production rates.
CAUSATION	Reduction in reservoir fluid pressure caused subsurface compaction and surface subsidence.
CURRENT STATUS	Subsidence essentially halted. Large area recovering elevation due to repressuring.

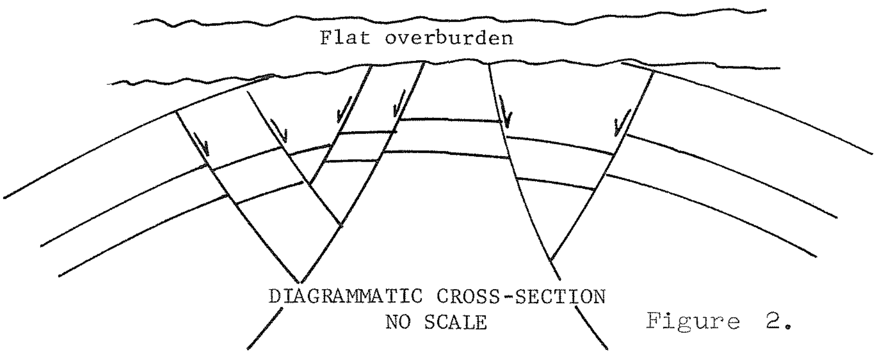

DIAGRAMMATIC CROSS-SECTION
NO SCALE

Figure 2.

GEOLOGIC STRUCTURE	Faulted anticline. Fold and faults extend to surface. Faulting right lateral, normal, graben near center. Dips flat to 20° upper zones.
DEPTH OF BURIAL	1,000' to upper zones.
DESCRIPTION AND STRENGTH OF RESERVOIR	Sand reservoirs. Thick and massive to interbedded, uncemented. Interbedded shales soft, overall incompetent.
DESCRIPTION AND STRENGTH OF OVERBURDEN	Soft sands and interbedded siltstones and shales. Shales incompetent.
POROSITY	About 35% in upper zones, 15-20% deeper zones.
GEOLOGIC AGE	Pliocene and Miocene.
SUBSIDENCE	About 5' definite, estimates to 12', extent about 12 sq. mi. Subsurface compaction very probable as indicated by well failures. Area and shape related to field outline. Subsidence not linear to pressure decline.
CAUSATION	Reduction in reservoir fluid pressure caused subsurface compaction and surface subsidence.
CURRENT STATUS	Subsidence rate slowed, probably still continuing. Water injection program may be current influence. Possible cause of surface-cracking.

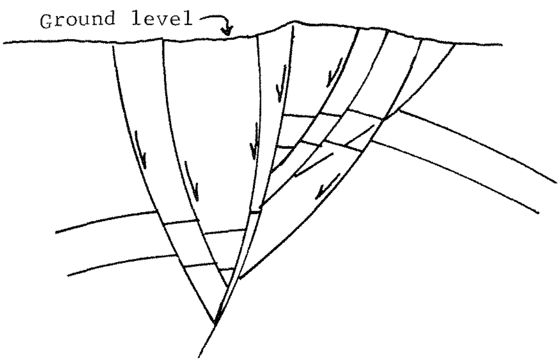

DIAGRAMMATIC CROSS-SECTION
NO SCALE

Figure 3.

Both Wilmington and Long Beach Oil Fields, which are only a few miles apart, have produced large volumes of oil from similar formations. Wilmington had a subsidence of nearly 10 meters, Long Beach less than one meter. Wilmington, the "type" field is shown in Figure 4. It is wide, the producing zones are relatively shallow, the sands are uncemented, the fold is gentle, dips are nearly flat at the crest, and tension faulting with a graben indicates that the sediments are in a relaxed state. Assuming that vertical stress equals one, then horizontal stress is about one-third vertical.

The Long Beach Field, Figure 5, is a narrow fold and has high-angle reverse faulting; all other factors are similar. Figure 6, which is transverse to both anticlines, compares the two fields. The load response in Wilmington is analogous to a set of bed springs (coil) and in Long Beach Field to dual leaf springs. Within reasonable limits, equal loads on the coil springs cause equal deformations. In the case of the leaf springs, as long as material failure is not reached, equal increases in load causes a diminishing deformation because the structural configuration of the springs tends to resist the additional load. The original deformation or "set" taken by the leaf springs is believed to be analogous to the small amount of subsidence documented over many fields. The load transfer did not cause much compaction because of the greater structural integrity of the narrow fold, which was aided by the insitu horizontal stress field. It can be seen intuitively that a broad, flat structure does not have the inherent "slab" effect support of a narrow structure. As an example, a steel beam supported at both ends will fail from its own weight if the end supports are far enough apart. This analogy also is effected by the thickness of the suspended beam. A thick beam of a specified length is less subject to failure from vertical stress than a thin beam of the same length and material.

Prediction of Subsidence Rate

A most elusive factor in subsidence forecasting is the rate at which it might occur. Terzaghi and Frolich formulated a time-rate relationship for clay consolidation in 1936 (in Terzaghi and Peck, 1967), that has been widely used by soil scientists. This concept states that as clays dewater due to loading, they do so at a rate dependent upon the length of the drainage paths and permeability. They developed percent of consolidation vs. dimensionless time graphs that could be used in conjunction with laboratory tests data for predicting settlement times of structures. Similar formulas have been developed by other workers using different variables. The problems of predicting oil field subsidence are the same for rate as they are for amount; i.e., neither the effective transfer of load (stress) nor the structure's ability to resist such a transfer are known until such time as experience makes these data no longer pertinent. A complicating factor is that multiple modes of compaction may exist, each with a different time-rate. Allen and Mayuga (1969), based on subsurface measurements in Wilmington Field, described varying rates of compaction in several oil zones, plus two rates (sands and shales) in each zone. Three distinct time-rate relationships have been noted in three oil fields that have a well documented subsidence. These are: (1) Wilmington Field, California, which had an increasing and then decreasing rate of subsidence with a relationship to fluid production (bell-shaped); (2) Lake Maracaibo, Venezuela, where the subsidence rate was minor until what appeared to be a reservoir pressure threshold was reached, at which time subsidence rate increased dramatically for a period of time (two distinct rates); and (3) Inglewood Field, California, which appeared to have a more-or-less constant rate (straight-line subsidence).

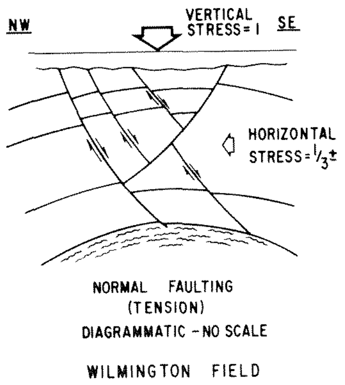

Figure 4.

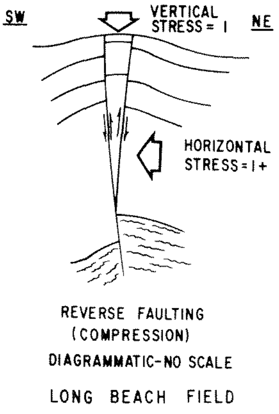

Figure 5.

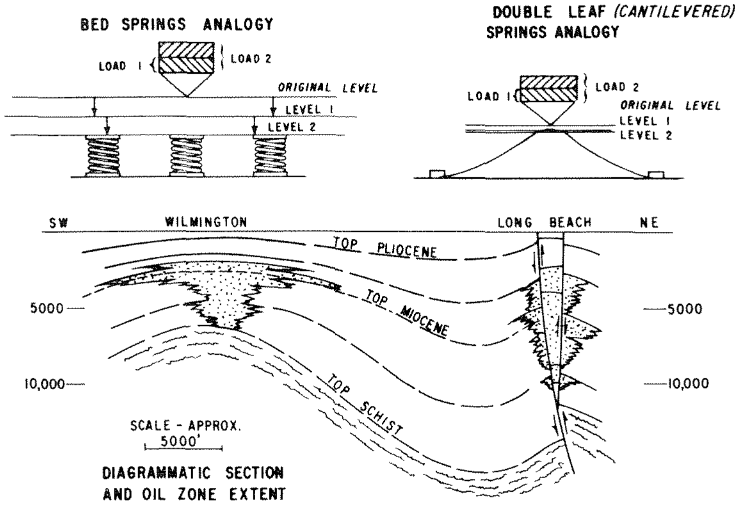

Figure 6.

Yerkes et al. (1969) investigated these same fields plus Huntington Beach Field, California, and found what they termed "a crudely developed relationship between cumulative net-liquid production and one or more measures of subsidence". The generally accepted theory is that subsidence is related to reservoir pressure drop and only indirectly to fluid production. A primary problem is the "lag", which is the displacement in time of the effect relative to cause. Structural competency, cumulative fluid production, width/depth ratio of the structure, etc. all enter into this problem.

For most subsidence susceptibility evaluations, rate predictions are best avoided. Both rate and total amount of subsidence were predicted by a number of writers during the early stages of Wilmington subsidence. None was accurate until about three-fourths of the ultimate subsidence had run its course.

References

Allen, D. R. and Mayuga, M. N., 1969, "The Mechanics of Compaction and Rebound, Wilmington Oil Field, Long Beach, Ca.", in Land Subsidence, Vol. II, Publ. No. 89: LASH-Unesco-WMO, pp. 410-423.

Geertsma, J., and Van Opstal, G., 1973, "A Numerical Technique for Predicing Subsidence above Compacting Reservoirs Based on the Nucleus of Strain Concept", in, The Analysis of Surface Subsidence Resulting from Gas Production in the Groningen Area, The Netherlands, Ed., Nederlandse, Aardolie Maatschappy B.V.: K.N.G.M.G., Mijnbouwstraat 20, Delft, The Nederlands.

Hubbert, M. K., and Rubey, W. W., 1959, "Role of fluid pressure in mechanics of overthrust faulting", I: Geo. Soc. Amer. Bull., Vol. 70, Feb, 1959.

Law, Jan, Seal Beach, Ca., Personal Communications.

Poland, J. F., 1972, "Subsidence and its control", in, Underground Waste Management and Environmental Implications, Ed., Cook, T.D.: Amer. Assoc, Pet. Geol. Memoir 18.

Terzaghi, K. and Peck, R., 1967, Soil Mechanics in Engineering Practice, 2nd Ed.: John Wiley and Sons, New York.

Yerkes, R. F., and Castle, R. O., 1969, "Surface deformation associated with oil and gas field operations in the United States:, in Land subsidence, Vol. I, Publ. No. 88: LASH-Unesco-WMO, pp. 55-65.

Publication n°121 of the International Association of Hydrological Sciences
Proceedings of the Anaheim Symposium, December 1976

PROBLEMS IN INJECTION OF WATERS IN WILMINGTON OIL FIELD, CALIFORNIA

G. L. Gates, W. H. Caraway, and H. J. Lechtenberg
US ERDA, Fossil Energy Programs, Oakland, California

Abstract

Extensive subsidence in the Wilmington oil field has been controlled by injecting large volumes of water. To prevent plugging of the pores of the petroleum-bearing reservoir rocks suspended solids in the waters must be controlled by chemical and physical treatment. In 1975 over 85 million cubic meters(500 million barrels) of water were injected to 1) control subsidence, 2) produce 10 million cubic meters(66 million barrels) of oil and, 3) utilize 67 million cubic meters(422 million barrels) of water produced with the petroleum.

Increasing injection pressures were observed and study by US ERDA revealed that suspended solids in the waters were oil-coated iron sulfide, barium sulfate, calcium carbonate, clay, sand, and bacteria. Sulfide as high as 90 milligrams per liter, was apparently the metabolic product of sulfate-reducing bacteria found throughout the water systems. Injection of ocean water for over 20 years increased the sulfate content of the produced waters from about 3 to 250 milligrams per liter enhancing the growth of bacteria. The waters were supersaturated with barium sulfate.

Research is in progress to find suitable methods for making secondary sanitary sewage effluent suitable for injection into petroleum reservoir rocks.

Subsidence has been observed in the Long Beach, California region since 1928. Rapid growth in production of petroleum and water from the Wilmington oil field starting about 1937 was associated with rapid increase in subsidence in the Wilmington-Long Beach harbor area. Development of a subsidence bowl has been described previously(1). The deepest part of the subsidence bowl, which was located approximately above the crest of the oil-bearing structure, sank about 9 meters(29 feet) between 1928 and 1968.

Water injection has stopped subsidence throughout the Wilmington field. Repressuring of the oil-bearing reservoir rocks by controlled water injection not only stopped subsidence but has resulted in rebounding or recovery of bench mark elevations over 30 cm(1 foot) in some locations.

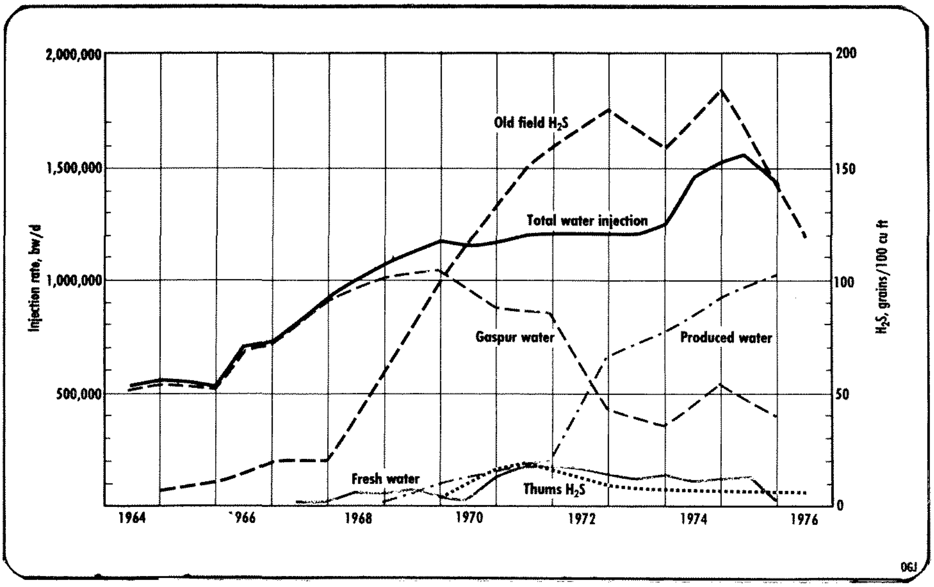

Fig. 1. Water Injection Wilmington Oil Field.

The volumes and rates of withdrawl and injection of fluids from the Wilmington field are shown in table 1.

Table 1

1975

Liquids Produced and Injected

Oil Produced	10.5 million m^3(66 million bbl)
Water Produced	67.1 million m^3(422 million bbl)
Water Injected	88.7 million m^3(558 million bbl)
Water Injected	0.24 million m^3/D(1.5 million bbl/D)

The injection of the large volumes of water required careful treatment of the waters because suspended solids in the water plugged the pore channels of the petroleum-reservoir rock restricting injection and causing high injection pressures.

Careful study of the suspended particles and the waters was made to insure the continued success of the water injection program(2)(3). Results of the study indicated two major problems: 1) suspended particles must be removed and 2) sulfate reducing bacteria which produced hydrogen sulfide must be controlled.

As shown in table 1 all of the water produced with petroleum was treated and injected into the petroleum-bearing sandstones. In addition supplemental waters, 21.6 million m^3(136 million barrels) were treated and injected into the rocks. Supplemental waters were obtained from the Gaspur zone which outcrops on the ocean floor. This water was similar to ocean water and to petroleum reservoir water except that it was very high in sulfate and much lower in barium. Waters produced with petroleum were low in sulfate but relatively high in barium content.

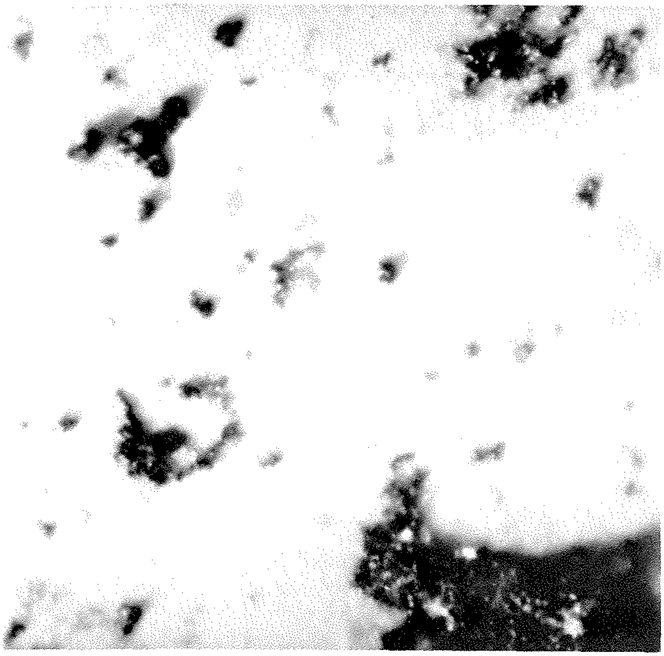

Fig. 2. Solids Filtered From Injection Waters (x80).

Nineteen injection plants were used to inject the 0.24 million m^3(1.5 million barrels) of water per day. Decreasing injection rates and increasing injection pressures threatened the success of the injection program to control subsidence, recover additional petroleum and utilize the large volume of salt water produced each day.

The waters produced with petroleum were found to contain suspended particles consisting of iron sulfide, barium sulfate, calcium carbonate, clays, silt, sand and or silica. Most of the solids were oil coated. To reduce the suspended particle concentration millions of dollars were spent in treating plants consisting primarily of free-water separators, heaters, wash tanks, skim tanks, gas flotation units, rapid mixed-media sand filters and holding tanks.

Evidence of the plugging effect of the suspended matter was obtained from a sand filter in a water treatment plant. The sand filter had an area of 7.25 m^2(78 ft^2) and a thickness of 1.5 m(5 ft). The filter rate was 3,500 m^3(22,000 bbl)/day. In 5 hours the pressure drop across the filter increased from 0.08(0.25) to 4.8 m(15.8 ft) of water.

Analyses of the waters produced with petroleum showed an increase in sulfate from about 3 to 250 milligrams per liter during the period between 1953 and 1973 when increasing volumes of ocean water were injected. Produced waters contained about 40 milligrams per liter barium indicating a high degree of supersaturation. Previous studies showed at equilibrium the waters contained 4 milligrms of barium

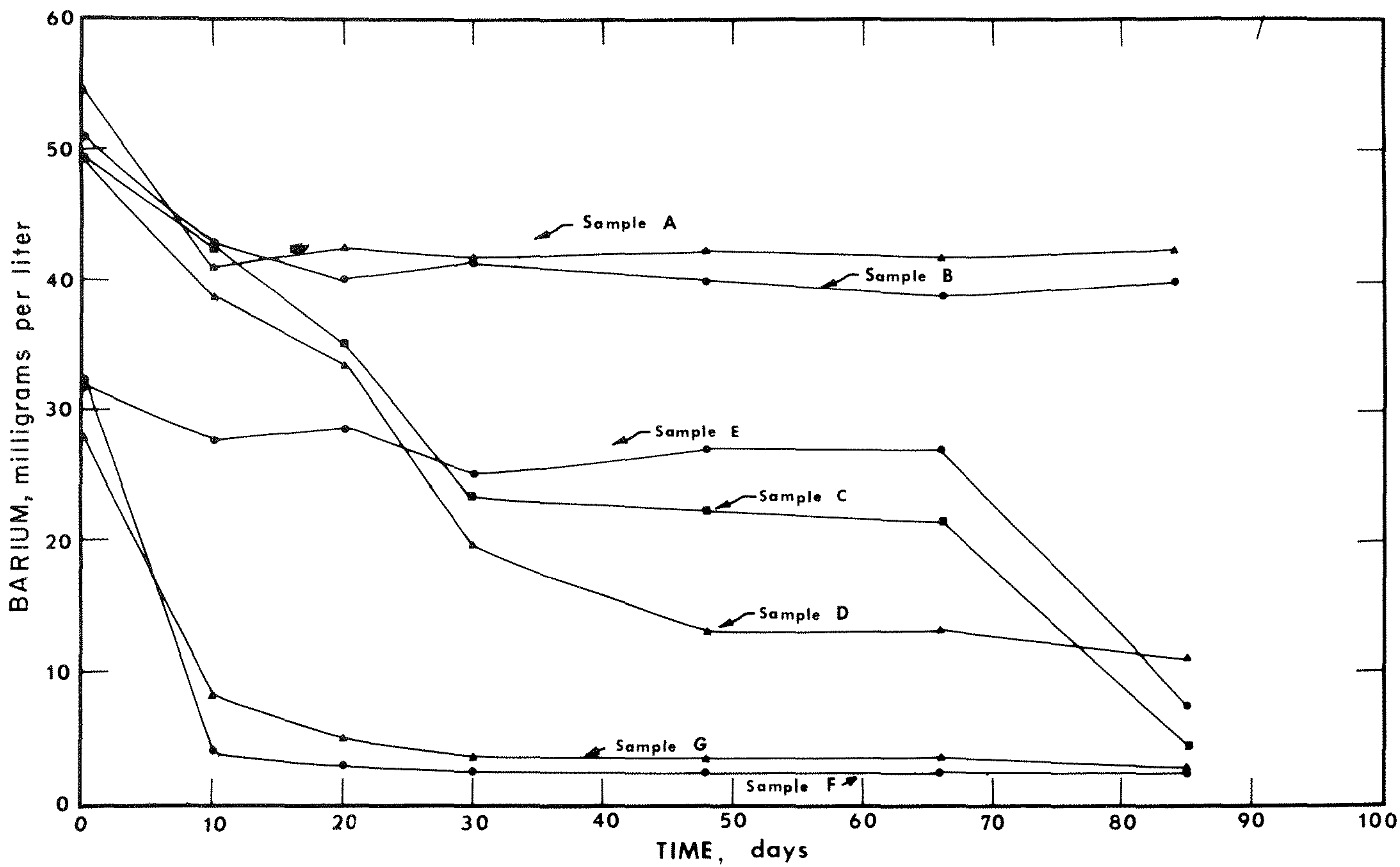

Fig. 3. Barium Sulfate Instability in Produced Waters.

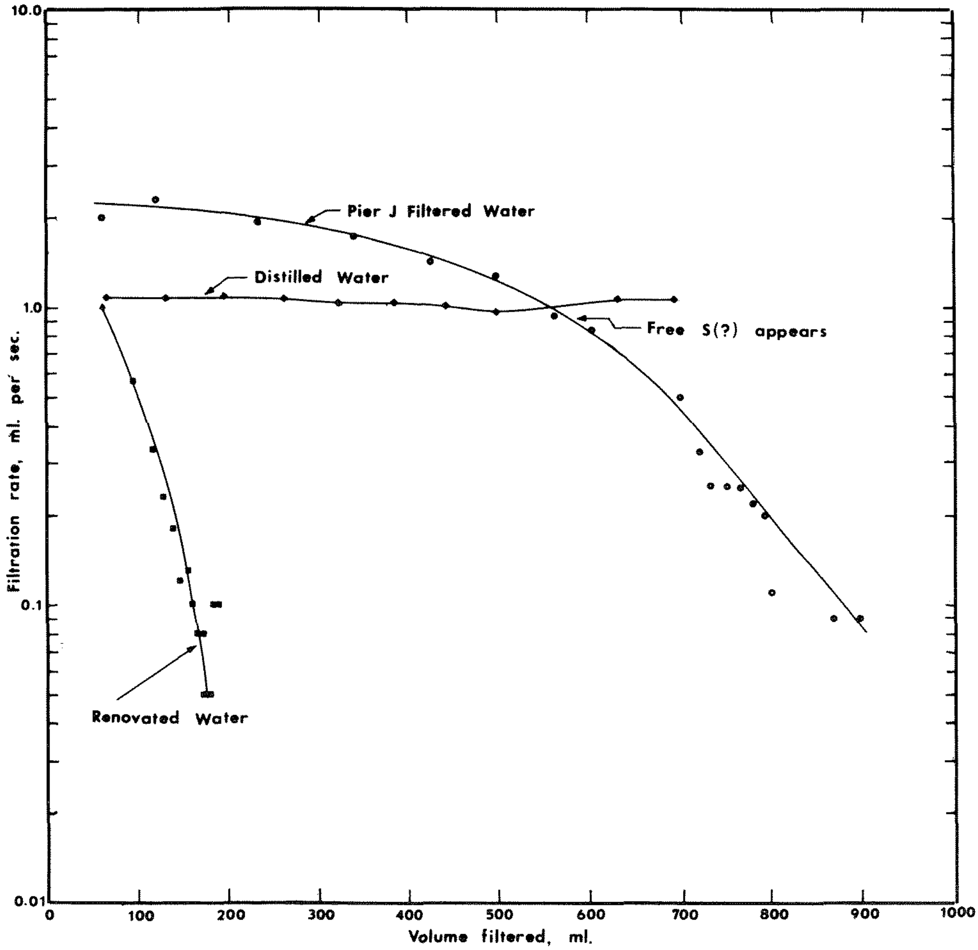

Fig. 4. Filter Properties of Injection Waters.

sulfate or about 2 milligrams of barium per liter. Barium sulfate precipitated from solution slowly at room temperature standing quietly in the laboratory. Formation of barium sulfate solids has been inhibited in the field by adding complex phosphates, figure 3.

Qualitative tests identified sulfate-reducing bacteria, desulfovibrio desulfuricans, present in nearly all of the water systems from the producing wells, through the treating plants and the injection plants. Black iron sulfide was observed throughout the water systems. Sulfide was found in most waters in concentrations as high as 90 milligrams per liter. Gas and water produced from this field were free of sulfide prior to 1953, but simultaneously with increasing sulfate content of the water the sulfide content increased correspondingly. The results indicate that sulfate-reducing bacteria increased in number thereby increasing the sulfide as a product of biological metabolism. The hydrogen sulfide content of the gas increased at a compound growth rate of 50 percent per year. Wells that produced the most water also produced the most hydrogen sulfide gas. Bactericides have been used to control bacterial growth with local short-time success.

Treatment of produced and supplemental water has used 41 chemicals, including 13 corrosion inhibitors, 5 oxygen scavengers, 4 coagulents, several biocides and others called flocculents.

Sulfide in the water formed suspended solids by combining with iron to form slightly soluble black iron sulfide. In contact with oxygen or other oxidizers sulfide is oxidized to elemental sulfur which plugs filters as shown in figure 4.

Water from secondary sewage plants in the Los Angeles Sanitation district was studied to obtain additional injection water required in the injection program. Results of the study showed(figure 4) that renovated water (secondary plant effluent) plugged filters rapidly although the suspended solids concentration was only about 10 milligrams per liter. Most of the solids appeared to be gelatinous amorphous organic material. By the use of deep filters to meet rigorous requirements for bacteria and virus removal the suspended solids can be reduced to 1 - 3 ppm. Thus only a "polishing" oxidation such as ozone treatment is needed to obtain suitable filter properties. The economics of the treatment appear favorable. Large volumes of sewage effluent are available.

References

1. Mayuga, M. N. and D. R. Allen, 1969, Subsidence in the Wilmington Oil Field, Long Beach, California, U.S.A. Presented at Symposium on Land Subsidence (International Hydrological Decade), September 17-22, 1969, Tokoyo, Japan.
2. Gates, G. I., W. H. Caraway, and H. J. Lechtenberg, 1975, Source of Solids in Injection Waters, Wilmington Field, California: U. S. Bureau of Mines, Report of Investigations 8031, 23 p.
3. Gates, George L. and C. F. Parent, 1976, Water Quality Control Presents Challenge in Giant Wilmington Field: Oil and Gas Journal, Vol. 74, No.33, pp. 115, 116, 118, 123-126.

Publication n°121 of the International Association of Hydrological Sciences
Proceedings of the Anaheim Symposium, December 1976

INJECTION WELL OPERATION AND MAINTENANCE

J. A. Rancilio
Supervising Civil Engineer I
Water Conservation Division
Los Angeles County Flood Control District
Los Angeles, California

Abstract

Injection wells are one means of accomplishing artificial recharge of ground-water reservoirs. Because of the high cost of recharge by this method, injection wells are usually used where some other benefit is derived as well. Injection wells are sometimes used for waste water disposal, including storm water, cooling water, and reclaimed waste water. They are also used to control land subsidence. The Los Angeles County Flood Control District has operated injection wells for the past 20 years to create a freshwater pressure barrier to protect the coastal ground-water basins of Los Angeles County from sea-water intrusion. The nature of the sea-water intrusion barrier requires that injection be maintained continually. The District currently has 180 operational injection wells located at 150 sites.

Over the 20 years of operating experience, the District has never had to permanently cease operation of an injection well because of loss of operating efficiency. The District's experience indicates that with a reasonable level of maintenance and for the operating conditions existing at the barrier projects, an injection well should continue to operate efficiently for at least 20 years and probably longer.

Information is presented describing injection well characteristics, typical designs of injection wells, operational considerations, clogging, redevelopment, and well construction costs.

WELL CHARACTERISTICS

In the following discussion consideration is given only to those wells reaching ground water. Thus, the injection wells discussed herein are differentiated from pit-type wells where injection occurs by infiltration into an unsaturated formation. It should be stressed that a thorough geologic understanding of the underground formations is a prerequisite to obtaining the best results. In addition to an analysis of available data to assist in selection of the drilling site, it is desirable to drill a test hold in the vicinity of one or more proposed injection wells. In any event, a detailed log should be taken during drilling to assist in the most effective completion of the well.

Type of Well

The type of well chosen for a given location would likely be similar to that which would be chosen for a pumping well. Depending on the nature of the formation, the injection well would be of the gravel pack or the non-gravel pack type. The gradation of the gravel pack would be chosen to control the migration of fines from the formation, just as in a pumping well.

Drilling Methods

Injection wells can be drilled with any of the three common drilling methods, cable tool, rotary, or reverse-rotary. The cable tool method has been used considerably because of the relatively clean nature of the resulting drill hole. Drilling by the cable tool method encounters expensive difficulties as the holes deepen. Also, drilling by the cable tool method limits the choice of well casing to those materials which have high compressive strength, notably the common steel casing.

The rotary drilling method has not been used extensively for injection wells because of the possibility that the mud cake, which is an essential feature of this drilling method, may not be completely removed from the walls of the drilled hole in the well development process. Should the mud cake not be removed, it is likely that the remaining fine particles will eventually be eroded by the injected water and forced into the formation, thus adding to the clogging problems of the well. It is likely that by careful and thorough development techniques, the fine materials associated with the drilling fluid and the mud cake could be completely removed and the injection well be quite satisfactory. However, the risk and the factor of not being able to see or test the completeness of the development generally has led to the choice of other drilling methods.

The reverse-rotary method has been tried as a compromise with the regular rotary method. In the reverse-rotary method clay is usually not added to the drilling fluid, because the cuttings from the bottom of the hole are forced upward through the drill stem at high enough velocities such that the carrying ability of dense drilling mud is not required. Sometimes when highly-permeable strata are encountered, clay is added to reduce the loss of drilling water. This method, together with the careful placement of the gravel packing and a careful development procedure, results in a satisfactory injection well. Drilling by this method provides the opportunity to use other types of well casing besides steel; which may be particularly significant if corrosion problems exist.

Well Diameter

The considerations for choosing a well diameter for an injection well are quite similar to those used for pumping wells. The larger the diameter of the well, the better are the hydraulic characteristics in the adjacent formation. Consideration must be given to the velocity of outward flow in the immediate vicinity of the injection well casing, in the same way that consideration of the velocity is made for a pumping well. The injection well casing must be large enough to accept the conductor pipe and other facilities which might be placed in the well and to provide ample room for the redevelopment procedures. Of course, the larger the well casing, the greater the cost. For the Los Angeles County barrier projects, injection wells have been standardized at a nominal 30 cm in diameter.

Depth Limitations

Similar limitations to depth arise with injection wells as control pumping wells; that is, generally the cost of the well per metre of depth rises as the well deepens. Certain drilling methods are limited in depth or become considerably more costly as the depth limitations are reached.

There is no apparent reason to indicate that the injection technique should be limited on account of greater depths of injection wells. On the other hand, the deeper the injection well, the more closely it resembles injection wells used in the oil industry where the nature of the formation and the thick overburden allow high injection pressures. High allowable injection pressures would result in reduced frequency of well redevelopment and lower maintenance costs. Redevelopment is discussed in more detail further on.

Well Casing

Well casing can be the usual types of steel used in regular pumping well construction. However, it has been found that the barrier injection wells have a highly corrosive environment caused by intruded sea water. At the barrier projects the corrosivity is enhanced by high dissolved oxygen in the injection water. To minimize corrosion problems, wells have been cased with such non-corrosive materials as asbestos-cement pipe and stainless steel.

Well Perforations

Perforations are adjusted to the formation in a similar way as pumping wells. The size of perforations is related to the size of the gravel pack or the natural formation. Minimum spacing must be related to the strength of the casing. Total area of perforations should be large enough to reduce flow velocity to reasonable levels at the expected injection rate. If the thickness of the formation allows, considerable additional perforation area should be provided to minimize well clogging effects.

Conductor Pipe

An essential feature of an injection well is the conductor pipe required to carry the injection water into the well to a point beneath the water surface inside the well casing. This pipe is required so that the injected water will not plunge into the well casing and cause turbulence which may entrain air bubbles and carry them into the gravel packing of the well and the aquifer formation beyond.

A full flow in the conductor pipe can be assured by designing the size of the pipe so that friction loss is comparable to the distance the water must drop. However, this procedure limits the range of flows which may be used.

Another method is to place a back-pressure valve at the bottom of the conductor pipe. A number of different designs for such a valve can be used. One that was found to be the most successful in the barrier projects involved a round plate which was placed in a horizontal plane and moved vertically within a cylinder which had triangular-shaped holes in the wall with the point of the triangle at the top. The plate was actuated by a stem reaching to the top of the well so that the size of the triangular opening could be varied. The cylinder was seated at the base of the conductor pipe in such a way that the injected water was forced into the cylinder and through the variable-sized triangular holes in the cylinder wall. Because of the corrosion factor, it was found necessary to construct these valves from stainless steel, but even so, considerable operating difficulties were encountered.

Another method is to use a conductor pipe which does not provide for a flowing full condition but which does provide for the exclusion of a continuous supply of air by being constructed airtight. Thus, when the initial body of air is evacuated from the conductor pipe by the flow of the injected water, no additional air is available to become entrained within the flow. Although there are theoretical considerations of dissolved fractions being released from the water under the influence of the reduced pressures, the experience in operating the barrier projects show that this type of conductor pipe is satisfactory, and is the system now used on all operating wells.

Clay Cap

In those formations which are under pressure, the injection well will have penetrated one or more confining layers of fine materials often called the clay cap. In the vicinity of the well penetration of this layer of materials, a structural weakness exists. This weakness is a matter of concern for two reasons. One is that it may provide a channel for considerable leakage of native water or of injected water from the pressure aquifer to overlaying materials, where it may be of little or no value or where it might cause problems such as high ground water. Another concern is that, under the high pressures which exist during injection in the vicinity of the injection wells, movement of water through the area of weakness may cause erosion of the fine materials and eventually a structural failure at this point.

It appears from the experience of the barrier projects that, by a minimum amount of care during construction in the area of the confining member, the potential problems can be minimized.

TYPICAL DESIGN OF BARRIER INJECTION WELL

Following is an example of the typical design of an injection well patterned after those now used for the barrier projects. Basically the well can be described as a gravel packed, asbestos-cement casing well.

This type of well must be drilled by the rotary method, preferably the reverse-rotary method. A 90 cm protective casing is placed which reaches a number of metres into fairly stable soils. The reverse-rotary hole is then drilled approximately 80 cm in diameter to the depth desired. Then perforated, asbestos-cement pipe casing is lowered into the hole with the string of pipe supported upon a steel plate which is attached to the drilling stem with a reverse threaded drill collar. Suitable spacers are connected to the casing at 4 metre intervals (each section of pipe) so that the casing will remain centered in the drilled hole. When the complete string of casing has been placed, the drill stem is disengaged from the left-hand threaded drill collar and plate which remain in the hole.

Next, a tremie pipe is lowered through the drilling fluid remaining in the hole between the casing and the drilled hole so that gravel can be introduced directly at the bottom of the hole. The tremie pipe is slowly withdrawn as the gravel fills the annular space, never being more than 3 metre above the gravel. Just below the confining member (clay cap), the gravel packing is topped with a 30 cm layer of sand,and a 2:1 cement-grout mixture is then placed in the annular space through the zone of the confining member and up to the ground surface. Prior to the placing of the sand layer and the grout mixture, two 10 cm plastic tremie pipes are set permanently extending from the surface to the gravel envelope, so that gravel can be introduced as needed into the annular space below the confining member.

After the grout mixture is placed, development of the well begins by surging within the well casing with the drill stem in such a manner as to remove the fines from the gravel layer and the formation in the vicinity of the well casing. Sometimes a more violent surging is obtained by using a swab, which consists of a leather ring, supported between steel plates and connected to the drill stem, and which has a minimum clearance within the well casing. During swabbing water may be circulated down through the gravel-pack and up through the drill stem to remove the drilling fluid and the fines from the well casing. As fines are withdrawn from the gravel packing, additional gravel is added as needed through the permanent tremie pipes. After surging is completed, the well is developed by pumping. During pumping, gravel is added to the annulus, as needed.

In these wells, conductor pipes are made of 7.5 cm plastic pipes. With this design, no corrosive materials exist in the drilled well to come in contact with the injected water.

OPERATIONAL CONSIDERATIONS

Operation of injection wells requires a normal configuration of connector pipes, fittings, and regulating valves. For maintenance purposes, it has been found necessary to install two valves on the pipeline servicing each recharge well: (1) a valve for on and off operation and (2) a valve for regulation. Experience at the barrier projects indicates that a butterfly valve is probably the preferable valve for on and off operation. All regulating valves on the barrier projects' injection wells were originally globe-type valves, and their operation has proven satisfactory. Possible use of butterfly valves for regulation purposes is being investigated, and preliminary results indicate that they may also be satisfactory. A meter or flow rate measuring device should be included for each well. For operational control of the barrier projects, it is not necessary to record the total quantity of water entering a well, therefore, only a flow rate measuring device has been installed at each well. Both orifice plates and venturi-type measuring devices have been used at the barrier projects. Experience indicates that orifice plates provide sufficient accuracy and offer fewer maintenance problems. Provision should be made for measuring the water level (or pressure or vacuum) in the conductor pipe, within the injection well casing, and within the gravel-pack tremie pipes. These various points of data are valuable in interpreting operational characteristics and problems. A small tap for collecting samples of the injection water has been found useful.

Control of operations for the barrier projects can be accomplished with data from the injection wells once a week. The amount of personnel required depends upon the number of injection wells in the project, the amount and complexity of equipment to be maintained, the degree that the facilities are automated, the relative hazard to adjacent property if failures occur, and the relative economy of close control on the rate of injection versus need for the injection water. Depending on specific conditions, the cost of operating and maintaining an injection well can vary from as low as $1,000 to as high as $6,000 per year.

Injection Rate

The rate at which water may be recharged through a well is dependent on several factors such as injection head, quality of injected water, ground water levels, temperature of water, geologic conditions, well construction, and area of perforations. Clogging, which will be discussed later, also affects the injection rate; generally, all other factors affecting the injection rate remaining constant, the ability to inject water will decrease with time due to clogging.

At the barrier projects, operational injection heads vary from 9 metres to 61 metres, and the transmissibility of the aquifers varies from 0.0002 m^2/s to 0.0018 m^2/s. For wells where a low transmissibility exists and a low operational injection head has been established, the injection rate over a yearly period averages about 0.0085 m^3/s for a year.

The primary consideration controlling the injection rate for the barrier project injection wells is the water requirements for maintaining the required pressure mound to prevent sea-water intrusion. Injection rates for the 180 barrier injection wells vary from 0.0057 m^3/s to 0.028 m^3/s. For the majority of the wells, it is not necessary to operate them at their maximum injection capability.

The operating procedure for the barrier injection wells calls for changes in injection rate to be at a rate no greater than 0.0071 m^3/s every 4 hours. This is necessary to give an opportunity for pressure equalization within the immediate vicinity of the recharge wells. The gradual change is especially important when decreasing the injection rate. One barrier injection well had to be destroyed due to damage caused by a rapid shutoff of the injection rate.

Injection Head

The term "injection head" is used to describe the condition of an injection well with respect to its ability to distribute water into the underground formations. The term is somewhat analogous to a pumping well's drawdown. The injection head may be defined as the height of the column of water within the injection well casing, above that level representing the injection mound, required to overcome friction losses encountered as the water moves into the aquifer. Obviously, the limitation on injection head will vary greatly depending upon the structural integrity of the overlying clay cap, the absence or presence of the clay cap, the amount of hazard to surface installations, and other special considerations at each location. For wells at the barrier projects, the limitations on injection head vary from a low of 9 metres for some wells to a high of 61 metres for other wells.

Injection Water

Because of the filter bed nature of injection wells, water to be used for injection must be highly treated for the removal of suspended matter. The dissolved constituents must be reasonably compatible with the native underground water and the soils of the water-bearing formation. At the barrier projects, injection water is taken from an imported source prepared for municipal and industrial purposes. The suspended solids of this water are generally less than 1 mg/l and the TDS is approximately 290 mg/l. Prior to October of 1974, the TDS was approximately 780 mg/l.

It has been found that water prepared for municipal and industrial purposes having a relatively-balanced calcium carbonate content may create problems when it moves through the gravel packing and aquifer immediately adjacent to the well casing. Apparently, this is because of the nature of calcium carbonate deposition where the tendency to deposit is increased in the presence of greater surface area for such deposition. Thus, by the nature of the travel of water in underground formations, a maximum opportunity is presented for the deposition of calcium carbonate. It is suspected that as the deposition continues the interstices of the formation become clogged, and the injection head required for a given injection rate becomes larger and larger.

CLOGGING

Clogging of injection wells is one of the most serious maintenance problems encountered. Well clogging is believed to occur in the perforations, in the gravel pack, at the interface where the gravel pack contacts the aquifer, and possibly within the aquifer itself.

Clogging may occur in recharge wells because of one or more of the following reasons: (1) biological, (2) mechanical, or (3) chemical. Due to the inaccessibility of the areas of clogging, it is difficult to determine the exact causes; but for the barrier project injection wells, it is suspected that a combination of a build-up of materials brought in by the injection water and chemical changes brought about by the injection water are the primary causes of clogging.

The cause of clogging is further obscured by the fact that some injection wells clog faster than others under "apparently" identical operating conditions. Where one well may clog within several months after redevelopment, an adjacent well may take several years. Some wells have never required redevelopment.

Construction methods and the initial well development appear to be primary factors in determining how a well will react to clogging.

Another factor which obscures the clogging process is the characteristic of an injection well to require less injection head for a given injection rate without any "apparent" outside measures being taken. In other words, a well may exhibit a tendency to "unclog" as well as to clog. This tendency is usually observed following a period of injection rate reduction or shutdown but also has been observed for a well during a period of prolonged continuous injection.

Biological

Dissolved materials, both organic and inorganic, may promote biological growth. These growths may occur inside or outside the casing and perforations, at the aquifer face or in pores of aquifers some distance from the well. The most troublesome is the slime-forming type. The growth may be from new organisms introduced by injection or may be due to stimulation of previously dormant micro-organisms within the formation. Clogging may be due to the slime growths themselves or from chemical products resulting from bacterial activity.

Mechanical

There are clogging mechanisms which are related to the different kinds of well drilling equipment utilized. If the rotary process is used, a hazard of clogging exists if clearing of drilling mud is not complete. There are factors inherent in the type of well construction. Improper design or installation of perforations are examples, as well as the possibility of careless gravel packing. The development method is important. Development must be sufficient, but not excessive as the possibility often exists of exposing layers of fine-grained materials to erosion.

Minute particles carried in the injected water may cause clogging either in the gravel pack, at the interface between the gravel pack (or the well casing) and the natural formation materials, or within the interstices of the formation itself. Depending upon the size of the particles, the gradation of the formation, and the flow velocity, particles may filter out within a fraction of an inch of the face of the well or may be carried on into the formation. The fine-grained, clogging material may have been introduced by the injected water or may be eroded particles from residual layers of drilling fluid on the sides of the drilled hole or may be eroded particles from within the formation itself. There may be re-orientation of the formation particles into a denser, less permeable pattern. In some types of soils, expansion of clay minerals may occur upon contact with a water with new chemical characteristics.

Chemical

Admission of free air as bubbles in the injected water may cause binding in the formation. Gas binding in the aquifer may result from gas coming out of solution when the temperature of the injected water is lower than the temperature of the underground formation.

Chemical clogging may occur at the casing perforations, at the formation face, or in the aquifer itself. Chemical clogging may be caused by: (a) precipitated metabolic products of autotrophic bacteria, including hydroxide of iron, ferrous bicarbonate, metal sulphides, or calcium carbonate, particularly in the presence of high concentrations of dissolved oxygen or chlorine; (b) chemical interaction of the dissolved chemicals in the injected water and in the soil itself; (c) contact of injected water and native underground water or different chemical characteristics yielding precipitates; (d) solution and redeposition of gypsum; and (e) reaction of high sodium water with soil particles causing deflocculation of the soil.

Such factors of the formation itself as its permeability and its porosity may have a significant affect on the clogging. With respect to clogging, the local characteristics of these factors are more important than the more general characteristics.

REDEVELOPMENT OF INJECTION WELLS

When the injection head in an injection well is at the maximum desirable level or the limit of available injection water pressure, it is necessary to do some type of redevelopment so that the well may remain in service at the desired injection rate.

The procedure used for the first well redevelopments at the barrier projects was to disassemble the well and redevelop it by a combination of mechanical bailing, swabbing, surging, and turbine pumping. Over the years of field experience, improvements have been made in the redevelopment method. Today the injection wells are redeveloped by airlift pumping with a dual packer assembly, and occasionally mechanical bailing is used for the removal of fill materials.

The dual packer airlift redevelopment allows for high velocity, low flow rate pumping, and surging. It also enables each section of the perforated interval to be developed to its maximum. This method has proven to be very successful in maintaining the operating efficiency of the injection wells.

The cost of injection well redevelopment varies depending on the length of perforations and individual well characteristics. The average length of perforated interval for the barrier project injection wells is 43 metres. Redevelopment of one of the wells takes an average of 5 days and costs an average of about $1,700 per redevelopment.

TABLE I

Comparative Construction Costs of Injection Wells

Type of Well (1)	Cost per Metre (2)	Average Depth, Metre (3)	Number of Wells (4)	Date Drilled (5)
Cable tool, 30 cm, steel cased, non-gravel packed	$ 57.25	81	8	1952-53
Cable tool, 30 cm, steel cased, gravel packed	106.75	75	2	1953-54
	106.52	94	4	1957-58
Reverse-rotary, 30 cm, asbestos-cement, gravel packed	121.44	82	1	1960
	167.17	124	12	1963
	139.35	122	19	1964
	142.03	173	17	1964
	117.24	113	9	1966
	121.24	185	5	1966
	118.66	99	11	1967
	120.58	127	8	1968
	113.42	68	17	1970
	112.95	117	12	1971
	232.02	218	11	1975
Reverse-rotary, 30 cm, stainless steel, gravel packed	123.88	86	14	1965
	197.47	134	3	1967

CONSTRUCTION COSTS

Costs of contructing injection wells are presented in Table I giving comparative cost information on several types of wells constructed for the barrier projects. Some of the early wells were built by force account and some by contract. Since 1963 all wells have been constructed by contract. The dates of construction have been indicated, but no attempt has been made to equalize the cost data on the basis of construction cost indices. The cost figures shown include the cost of drilling, casing, gravel packing, and installation of necessary piping and valves at each well. The costs of the water supply system, surface enclosure for a well, and contract administration are not included.

Publication n°121 of the International Association of Hydrological Sciences
Proceedings of the Anaheim Symposium, December 1976

SUBSIDENCE OF ORGANIC SOILS AND SALINITY BARRIER DESIGN IN COASTAL ORANGE COUNTY, CALIFORNIA

James B. Fairchild and Karl H. Wiebe
Orange County Water District and
James M. Montgomery, Consulting Engineers, Inc.

Abstract

Lenticular deposits of peat and organic sediment accumulated widely across the coastal plain of Orange County during the Holocene epoch. Dewatering of these organic sediments resulted in initial shrinkage of the materials and subsequent oxidation and decomposition.

Agricultural drainage of coastal marshy lands and later extractions of ground water resulted in lowered levels of saturation. Decline in ground water levels was accompanied by localized subsidence of areas underlain by peat. Continued decline also resulted in the invasion of saline ocean waters into the coastal aquifers. Intrusion was most pronounced in the Santa Ana Gap area of Huntington Beach, and by 1964 increased chloride ion concentrations had progressed about 4 miles (6.4 km) inland from the coast.

In order to preserve the coastal ground water basin, a salinity barrier was constructed following extensive studies by the California Department of Water Resources and the Orange County Water District. The hydraulic barrier consists of a line of extraction wells near the coast and a parallel line of injection wells located farther inland. The dual concept was adopted to minimize the decline of water levels and the resulting local dewatering of organic materials, while at the same time reducing the likelihood of excessive waterlogging of the surface soils along the injection ridge. Water for the injection wells is a combination of tertiary treated waste water and demineralized water blended to meet public health requirements.

Introduction

Subsidence has long constituted a serious problem in the reclamation and development of peat lands in many parts of the world. The purposes of this paper are to present information on the origin, character and location of peat and to describe the nature of peat subsidence in coastal Orange County and its effect upon salinity barrier construction. The study area is shown on Figure 1.

The study included review of pertinent published and unpublished reports, collection of geologic, hydrologic, and elevation survey data, and field observation of peaty areas. Additional information was obtained through consultation with local firms and public agencies at the City, County, State and Federal level and with numerous long-time residents in the Fountain Valley area.

Nature of Peat and Organic Soils

Peat and organic soils form in water-saturated environments where incomplete decomposition occurs due to prevailing anaerobic conditions. In Orange County, environments favorable to luxuriant growth of peat-forming plants include undrained depressions, plains or river deltas, and fresh water swamps. Poor drainage is essential in the formation of peat. The elevation relationship between surface water or ground water and land surface must remain relatively constant for long periods of time if significant quantities of peat are to accumulate and be preserved. Within the coastal plain of Orange County, logs of many water wells and soil borings indicate that these conditions have long been prevalent.

In the Quaternary period, near the end of late Pleistocene time, sea level declined to about 300 feet (90 m) below its present level. During

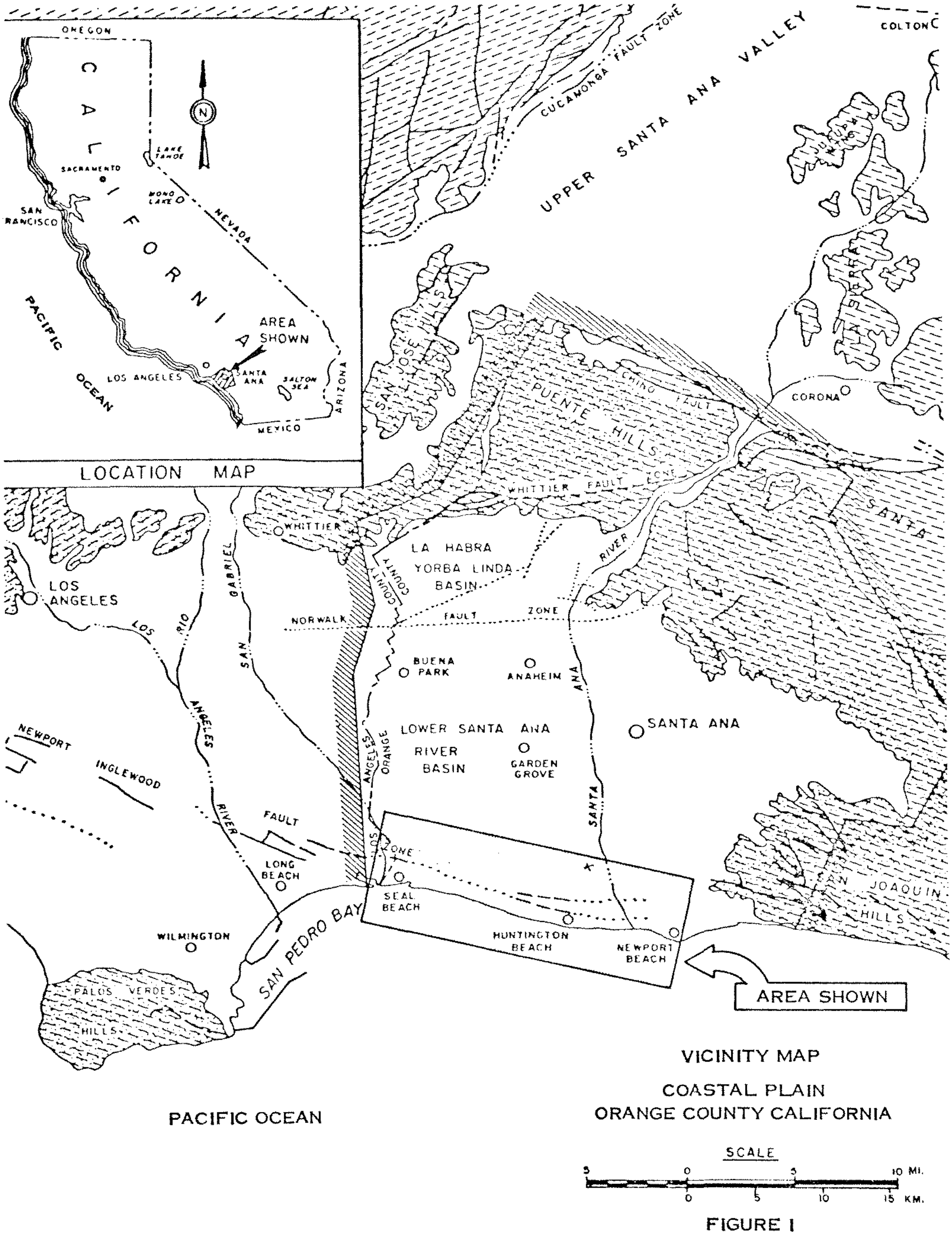

VICINITY MAP

COASTAL PLAIN
ORANGE COUNTY CALIFORNIA

FIGURE 1

that period, an ancient Santa Ana River eroded deep valleys across the coastal plain to the receding base level. With a subsequent rise in sea level during early Holocene time, these valleys were backfilled, first with coarse alluvial debris. Later, the rate of sea level rise decreased, and the ancestral Santa Ana River appears to have deposited finer-grained materials in the valleys or gaps. While periodic shallow marine embayments occurred in portions of the gaps, the area was generally very slightly above sea level. It was during this period that extensive deposits of peat accumulated. Resulting general geologic features are shown on Figure 2.

The geologic history of the area suggests that not only were repeated flooding, ponding and burial significant factors in accumulation of peat, but also that continued upward flow of artesian ground water from the underlying coarse alluvial materials was important. Locally, upwelling ground waters and resultant "peat springs" must have remained in a relatively constant location. Logs of several water wells show that peat deposits extend from the surface downward to the top of the coarse alluvium. According to pioneer, T. B. Talbert, springs and general swampy conditions persisted until the time of agricultural development. He states that upon his arrival in 1897, (Talbert, 1952, P. 37) "This area...was so full of peat springs and artesian wells which flowed the year around that it was quite inaccessible. It had a growth of willows, sycamore, tules, ...and other vines, grasses and shrubs that made it almost an impenetrable thicket."

Location of Peat Deposits

Delineation of peat deposits in the coastal plain was originally made from a review of all available soil boring logs, water well drillers' logs, old maps, and through personal communication with local residents. This information was updated through review of information developed by Messrs. J. Evans and R. Munson for the cooperative mapping program of the County of Orange and the California Division of Mines and Geology. The historic locations of major bodies of organic sediment are shown on Figure 2.

It is interesting to note that within approximately 1 mile (1.6 km) of the present coastline, significant quantities of peat have not been encountered. Generally, conditions are not favorable for the luxuriant growth of peat-forming plants in coastal areas which are subject to frequent incursions of saline ocean water. Prior to residential development, the coastal area was interlaced by tidal sloughs, and surface soils were encrusted with salts. If these saline conditions persisted throughout late Holocene time, it is not likely that any major peat deposits will be found near the present coastline.

Subsidence Rates

Subsidence of organic soils in the Fenland area of England was first noted in 1806 (Okey, 1918), after initial drainage of the area for agricultural uses. The famous HOLME POST, sunk solidly into clays underlying the peat at Holme Fen in 1848, is probably the oldest authenticated record of peat subsidence in existence. Measurements at that site show a lowering of the ground surface of 10 feet (3 m) in a 65-year period. Although subsidence rates were probably not constant, these records indicate an average subsidence of 1.9 inches (4.8 cm) per year.

Subsidence in the Everglades region of Florida, the Delta region of California, and an area of peat springs in Huntington Beach have been observed and noted following drainage or change in overall levels of saturation. Subsidence in these areas has been estimated to range from about 2 to slightly over 3 inches (5 to 7.6 cm) per year.

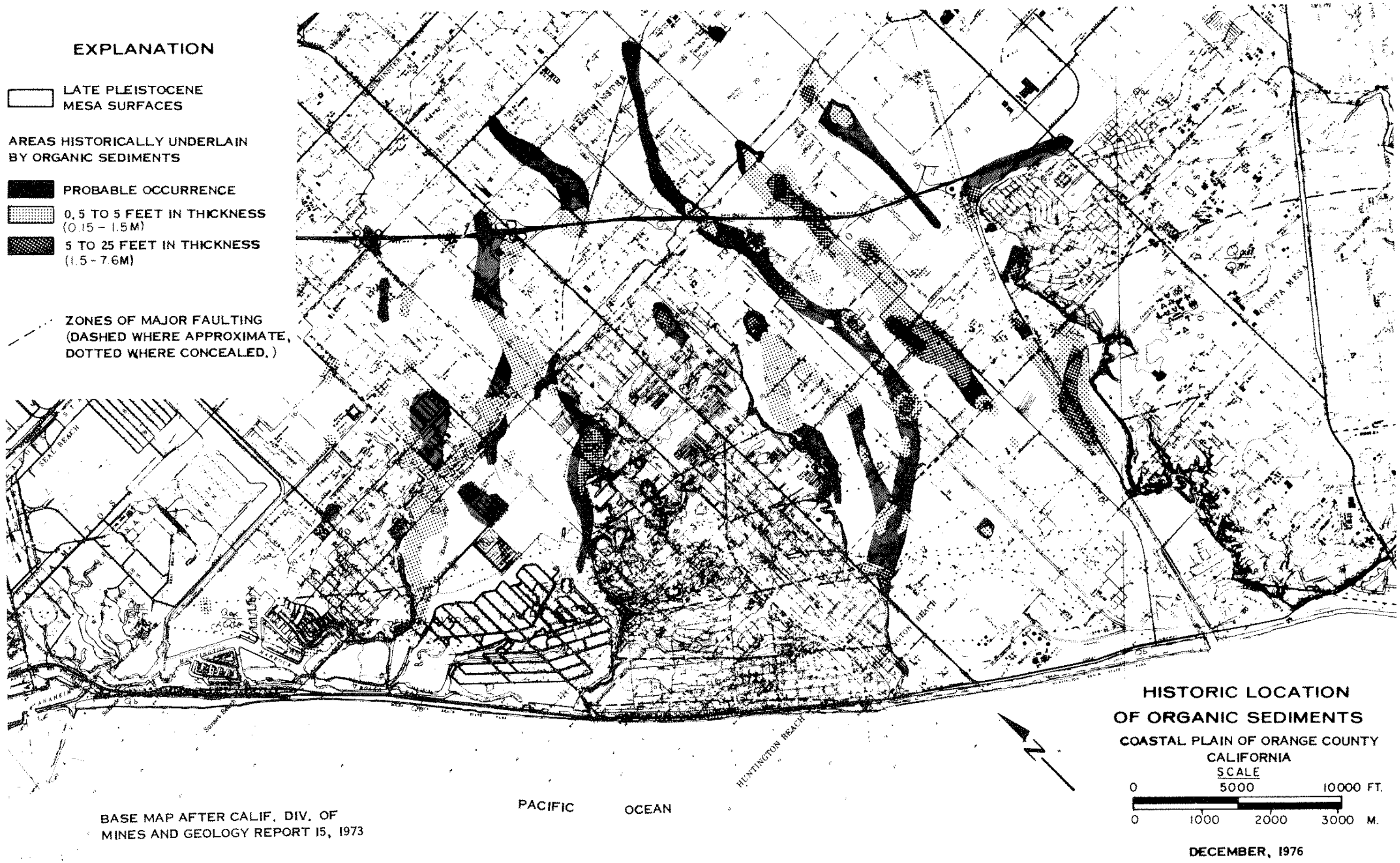
EXPLANATION
LATE PLEISTOCENE MESA SURFACES
AREAS HISTORICALLY UNDERLAIN BY ORGANIC SEDIMENTS
PROBABLE OCCURRENCE
0.5 TO 5 FEET IN THICKNESS (0.15 - 1.5M)
5 TO 25 FEET IN THICKNESS (1.5 - 7.6M)
ZONES OF MAJOR FAULTING (DASHED WHERE APPROXIMATE, DOTTED WHERE CONCEALED.)
COSTA MESA
HUNTINGTON BEACH
PACIFIC OCEAN
N
BASE MAP AFTER CALIF. DIV. OF MINES AND GEOLOGY REPORT 15, 1973
HISTORIC LOCATION OF ORGANIC SEDIMENTS
COASTAL PLAIN OF ORANGE COUNTY CALIFORNIA
SCALE
0 5000 10000 FT.
0 1000 2000 3000 M.
DECEMBER, 1976

FIGURE 2

Although no actual records of annual peat subsidence were kept in the Orange County area, it is considered that the elevations of peat land in the City of Fountain Valley were at or above prevailing ground surface prior to 1897. By 1949, elevation contours suggest subsidence averaging 10 to 14 feet (3 to 4.3 m) in areas underlain by major bodies of peat. In a few locations, up to 20 feet (6 m) of subsidence had occurred. Based upon these estimates, subsidence has averaged 2.3 to 3.2 inches (5.8 to 8.1 cm) per year.

Causes of Subsidence

The most important causes of peat subsidence include wind erosion, burning, compaction by tillage machinery, shrinkage resulting from reduction in moisture content, and decomposition and decay. Another more obvious factor is simply the cessation of peat deposition. Some peats, especially sedimentary types, probably consolidate as they are deposited. Continuous formation tends to keep pace with the consolidation. However, the supply of new material is curtailed when the cycle is interrupted by surface development.

Continuous submergence of organic soils during formation prevented or greatly retarded oxidation. A reducing environment allowed significant thickness of peat to accumulate and be preserved. Drainage of peat lands not only results in shrinkage of soils, but greatly stimulates the subsequent loss of soil mass by allowing oxidation from biochemical action. Considering past events and conditions of drainage, oxidation is considered to be the major cause of peat subsidence in the Orange County Coastal Plain.

Effect of Water Level Fluctuations on Orange County Peats

Peat soils may shrink as much as 60 percent when the moisture content is reduced to about 35 percent. From studies in other areas, it appears that with the lowering of water saturation levels, shrinkage occurs first and is followed by relatively continuous decomposition or oxidation of the dewatered organic material.

Local areas of the Orange County Coastal Plain were developed for agricultural purposes on a large scale in 1898. Springs were first drained and later drainage ditches were dug to the tidal inlets and channels. By 1901 tile drains had been installed in a major portion of the area. Personal communications with early settlers suggest that subsidence adjacent to the "peat springs" occurred almost immediately after drainage of the land had been started, and that by 1915, the major part of localized subsidence throughout the area had occurred.

In an attempt to document the conclusions of long-time residents, the authors collected useful historic elevation and surface contour data. The few historic traverses for which records exist were run primarily along section line roads. As local subsidence occurred, fill was repeatedly placed on the roadbeds and no bench marks were established in these subsiding areas. A number of early elevations were obtained for the town intersection of Talbert Avenue and Bushard Street. These indicate that the intersection has remained relatively constant in elevation since 1898, at about 24 feet (7.3 m) above mean sea level.

The most valuable historic elevation data on subsidence were obtained from successive U.S.G.S. quadrangles and from surveys made for the Talbert Drainage District. For analysis, a suitable site adjacent to a known body of sedimentary and fibrous peat was selected, and all surface elevation and water level data available for this location were plotted against time. These data are shown on Figure 3. Historic water levels for the underlying alluvial materials were obtained from a composite of records of wells 5S/10W-28B1, 6S/10W-5B5 and -6L2. The initial elevation of a nearby subsurface drain is

SURFACE SUBSIDENCE AND GROUND WATER LEVELS

1895 TO 1976

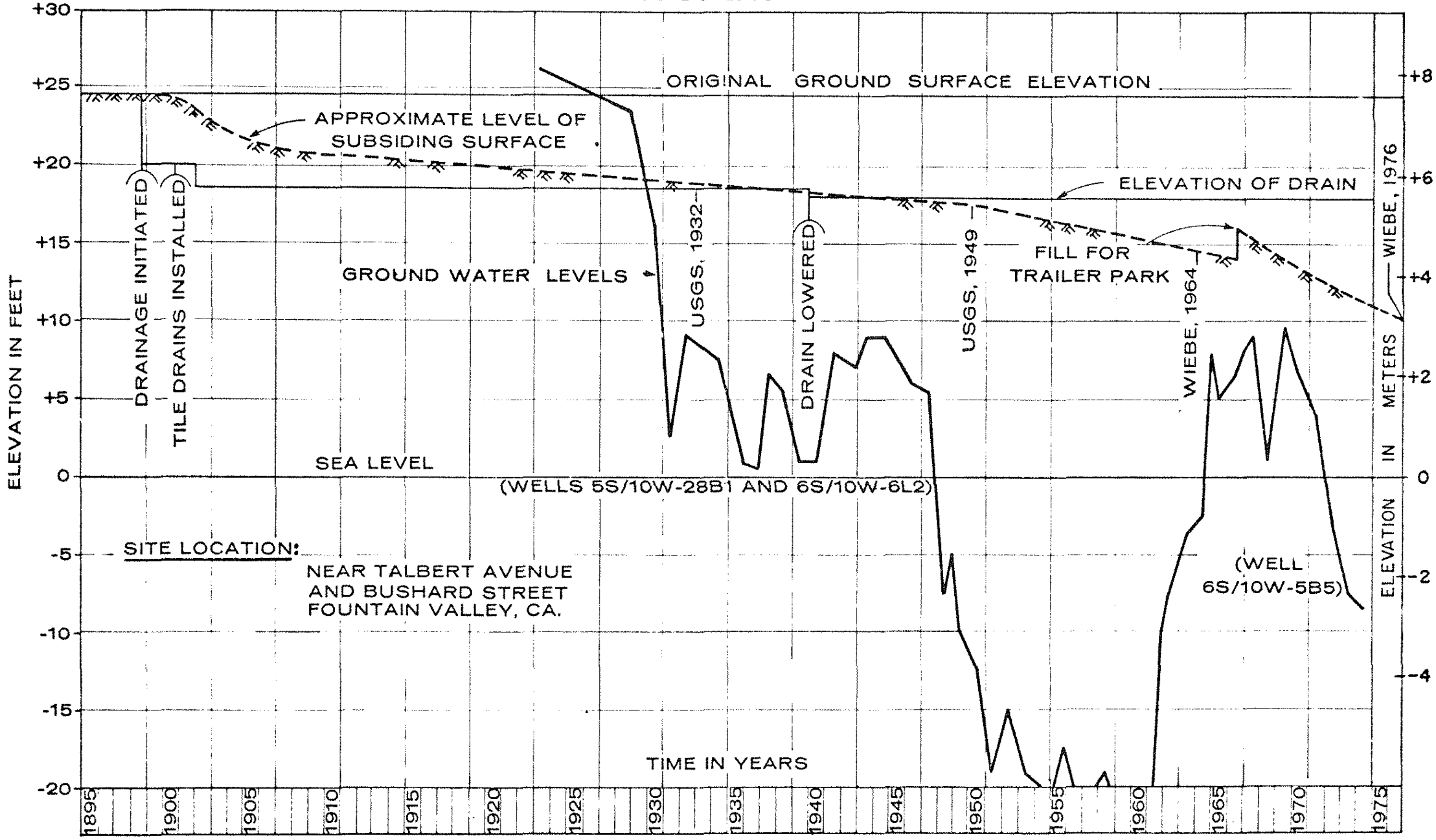

FIGURE 3

depicted by a straight line. The apparent subsidence at the location totaled 10 feet (3 m) from 1898 to 1964. In 1966, the location and surrounding area were partly backfilled for the construction of a mobile home park. However, the location has continued to subside, and by 1976, subsidence totaled about 14 feet (4.3 m). It is reasonable to assume that initial subsidence occurred relatively quickly after drainage. Thereafter, subsidence is projected on Figure 3 at an almost uniform rate until 1950.

By the mid-1920's, pumping of wells perforated in the underlying alluvium lowered pressure levels to below prevailing ground surface and the few remaining springs ceased to flow. By about 1930, pressure levels had declined to elevations below both the peat soils and the drains at the reference site.

By 1946, the soils themselves had subsided below the initial level of the subsurface drains at the reference site. At this time, a truer perspective of the influence of the major underlying aquifer began to develop. Peats continued to subside, suggesting that semiperched waters in the peats and surrounding materials were draining downward to the underlying aquifer, because the drains were locally above the zone of saturation. From 1947, the elevation of the piezometric surface in this aquifer declined rapidly, reaching levels of about 40 feet (12.2 m) below the peat surface in 1957. Starting about 1950, an increase in the rate of surface subsidence may be noted on Figure 3.

By 1964, the peat surface at the reference site had subsided 3-1/2 feet (1.07 m) below the level of adjacent subsurface drains. From 1964 to 1966, subsidence continued, but in August of that year the site was backfilled in part. From 1966 to 1976, the surface continued to subside at a somewhat accelerated rate.

Land Use

Land use in areas of the coastal plain where relatively thick organic sediments have not been removed has been undertaken locally with imagination and creativity. Some remaining wet or swampy areas have been developed as drainage channels, water hazards, wild life refuges, architectural lagoons and fishing lakes. Dryer areas of organic soil are being used for driving ranges, golf courses, playing fields, parks and recreational areas, parking lots, mobile home parks and drive-in movies.

Sea Water Intrusion

Sea water intrusion has occurred in what is locally referred to as the Santa Ana Gap. This is the area where the Santa Ana River, during late Pleistocene time, eroded a deep channel into the older inland dipping deposits. The subsequent backfilling of this channel with coarse-grained deposits created a permeable aquifer in contact with the ocean which allows the landward movement of sea water if the water levels in the basin fall below sea level. The Talbert aquifer, as this Holocene age deposit is named, is approximately 3 miles (4.8 km) wide. The relationship of the Talbert aquifer and the older aquifers which are subject to intrusion is shown in the cross section, Figure 4. The Newport-Inglewood fault system extends along to the coastline and acts as a barrier to saline intrusion in all aquifers except the Talbert.

Historically, the area had a high piezometric surface with many springs and flowing artesian wells. Subsequent development and increased use of well water throughout the ground water basin lowered the piezometric surface to such an extent that sea water intrusion occurred and, by 1964, extended inland approximately 4 miles (6.4 km) from the coast. This saline intrusion posed a serious threat to the quality of the water in the remainder of the basin. The ground water basin underlies an area of approximately 200,000 acres (81,000 hectares) and at its deepest point, there is fresh water to a

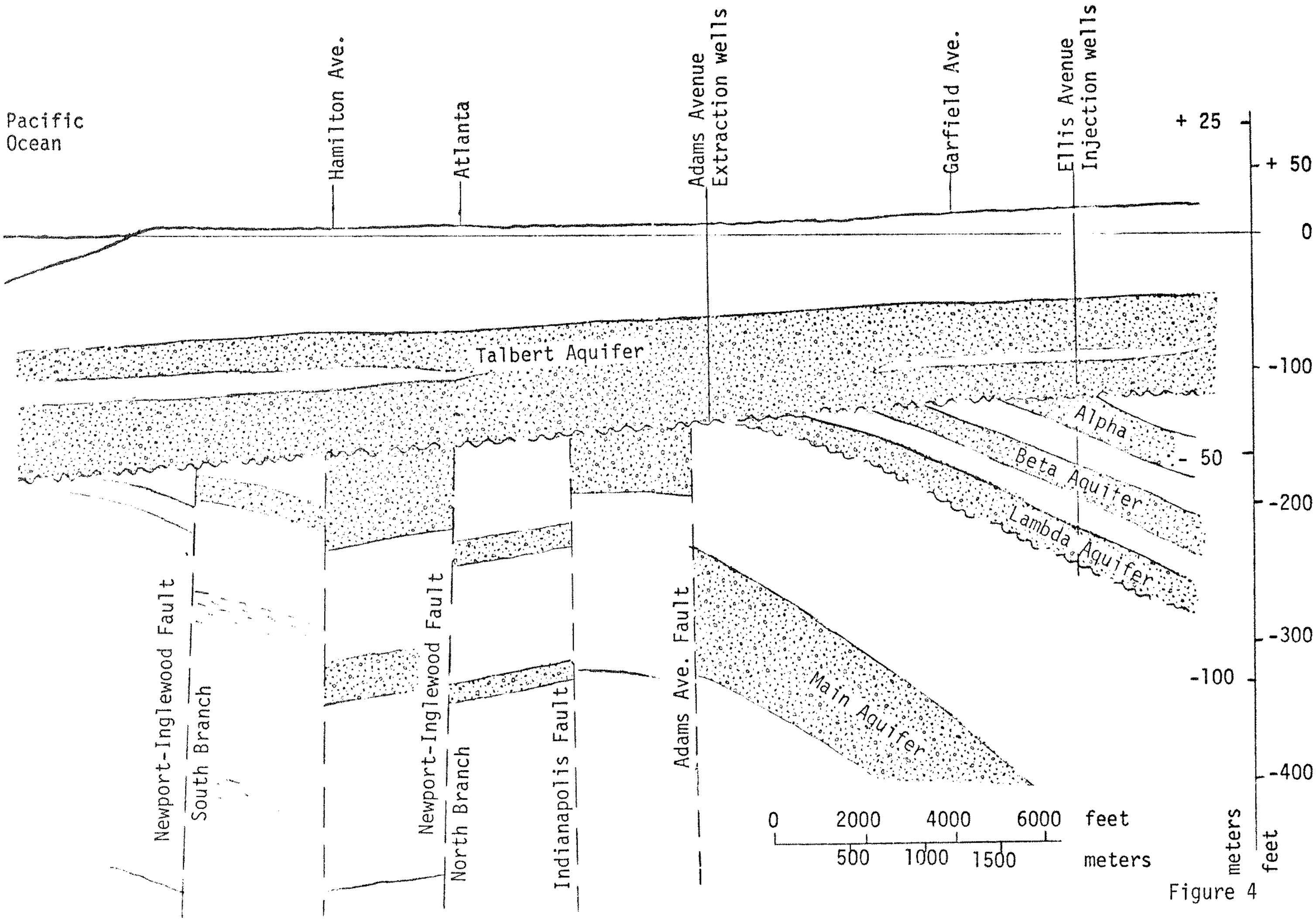

Pacific Ocean
Hamilton Ave.
Atlanta
Adams Avenue Extraction wells
Garfield Ave.
Ellis Avenue Injection wells
Talbert Aquifer
Alpha
Beta Aquifer
Lambda Aquifer
Main Aquifer
Newport-Inglewood Fault South Branch
Newport-Inglewood Fault North Branch
Indianapolis Fault
Adams Ave. Fault
+ 25
+ 50
0
-100
- 50
-200
-300
-100
-400
meters
feet
0
2000
4000
6000
feet
500
1000
1500
meters

Figure 4

depth in excess of 3,000 feet (915 m). The water in storage in the basin has been estimated to be as much as 40 million acre-feet (4.93 million hectare meters)(DWR, 1967). The annual pumping draft on the basin is approximately 225,000 acre-feet (27,743 hectare meters).

Detailed information regarding the subsurface geology and hydrology of the area was developed in several studies performed by the State of California Department of Water Resources. This information was used as a basis for the design of the barrier project which is being implemented by the Orange County Water District.

Salinity Barriers

The design of hydraulic barriers to stem the invasion of saline ocean waters in the coastal plain has been modified to a significant degree because of the occurrence of sensitive organic sediments. For example, a pumping trough barrier requires lowering of levels to elevations below inland operational water levels. Organic materials could then be dewatered, shrink, and become compressed. Subsequently, a massive reduction in volume would occur as the peats oxidize.

Because of their mode of origin, peat deposits are moderately permeable. The design of a pressure recharge barrier could entail raising ground water levels to elevations higher than ground surface. This action could result in upward leakage through the organic materials, and the local re-establishment of historic springs and swampy areas.

A combined injection-extraction barrier facility includes some of the advantages, but not the major disadvantages, of either system acting alone. For example, if operation levels at the injection ridge portion were maintained at about sea level, and extraction trough levels at about 5 feet (1.5 m) below sea level, a seaward gradient could be maintained, and the adverse effects of both peat subsidence and water-logging would be minimized.

Because of uncertainties regarding the future availability of imported water for injection in the barrier, and the close proximity of a source of secondary treated waste water, the Orange County Water District undertook an investigation to determine the feasibility of using reclaimed waste water for injection. During the period 1966 to 1970, pilot studies were carried out to investigate the various parameters necessary for the design of the barrier project. The pilot project included a small-scale water treatment plant, 3 injection wells and 12 observation wells. During this study, various water treatment methods were evaluated to determine the method most suitable for the available waste water. Treated waste water was injected in the 3 wells in order to explore the required well spacing and the necessary rates of injection for various conditions of basin overdraft.

The barrier project as finally designed consists of 7 extraction wells, 23 injection wells, a water treatment plant and a network of 29 observation wells for monitoring ground water conditions and the effects of injection.

Injection Wells

The alignment of the injection wells is along Ellis Avenue which coincides with the front of intruded saline water (Figure 5). The wells are designed to inject into each of the 4 aquifers which are subject to saline intrusion. Because of differences in aquifer transmissivity and the effects of local ground water extraction, it was considered desirable to be able to control the injection rate into each aquifer separately. In order to accomplish this, each injection site consists of up to 4 separate casings, each perforated in a different aquifer and controlled individually at the surface.

To construct the wells, a 30-inch (0.76 m) diameter hole was drilled to the required depth, using the reverse rotary drilling method. A 6-inch

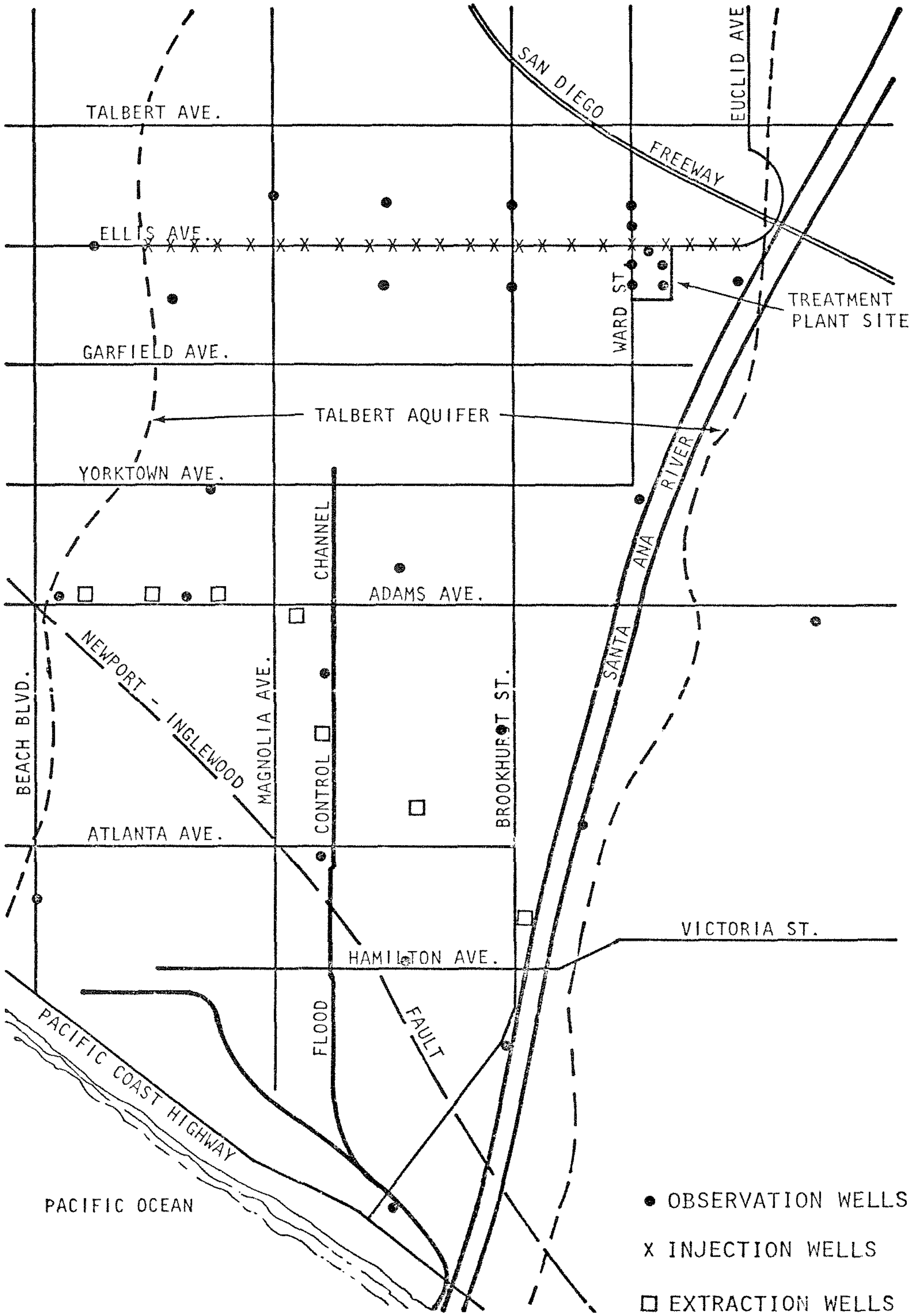
TALBERT AVE.
SAN DIEGO
FREEWAY
EUCLID AVE
ELLIS AVE.
WARD ST.
TREATMENT
PLANT SITE
GARFIELD AVE.
TALBERT AQUIFER
YORKTOWN AVE.
RIVER
ANA
SANTA
CHANNEL
CONTROL
FLOOD
ADAMS AVE.
NEWPORT - INGLEWOOD
FAULT
BEACH BLVD.
MAGNOLIA AVE.
BROOKHURST ST.
ATLANTA AVE.
VICTORIA ST.
HAMILTON AVE.
PACIFIC COAST HIGHWAY
PACIFIC OCEAN
● OBSERVATION WELLS
X INJECTION WELLS
□ EXTRACTION WELLS

Figure 5

(15.2 cm) diameter, pre-perforated, mild stainless steel casing was installed for each aquifer. After installation of the casings, gravel pack was emplaced adjacent to each aquifer and a cement grout plug was placed in the clay strata between aquifers for hydraulic separation. Figure 6 is a diagram showing a typical 4-casing installation. For clarity, the casings are shown side by side; in practice they are arranged in a square.

There are 23 injection well sites spaced approximately 600 feet (183 m) apart and located in the street right-of-way on Ellis Avenue. Because the wells had to be located in the street or sidewalks, it was necessary to enclose all the surface facilities in underground vaults. Each well casing has a control valve, a pressure gage and a flow measuring device. The pressure and flow rate is telemetered to a computer in the central control building at the treatment plant site. The computer can be programmed to print out the flow and pressure of each casing as often as desired or on demand by the plant operator. The data collection is done by telemetry but control of the flow rate is done manually.

Water Supply

The supply water for the injection barrier is tertiary treated waste water. Secondary treated wastewater that would normally be discharged through the ocean outfall sewer is obtained from the Sanitation Districts of Orange County and given tertiary treatment and demineralization to produce a product water that meets the drinking water standards of the Department of Public Health. The tertiary treatment consists of lime flocculation and sedimentation, ammonia stripping, recarbonation, sand filtration, carbon adsorption, and chlorination. After this treatment, the water meets all requirements except for total dissolved solids (TDS). In order to meet the TDS requirements of 500 mg/l, the water must be blended in the proper proportion with a low TDS water. The low TDS water will be provided by a 5 million gallon per day (18,900 cm per day) reverse osmosis plant, now under construction, which will take a portion of the tertiary treated water and reduce the dissolved solids content to approximately 100 mg/l. This demineralized water will be blended with the tertiary treated water to provide a product water of the required quality. The quantity of water required, based on the pilot study calculations, could vary from 5 million to 30 million gallons (18.9 to 113.6 million liters) per day depending on the condition of the basin overdraft. The capacity of the present treatment plant is approximately 15 million gallons (56,800 cm) per day.

Extraction Wells

The 7 extraction wells are located in a line roughly parallel to the coast and seaward of the areas where the Talbert aquifer is in hydraulic continuity with the older, landward dipping aquifers. These wells are conventional gravel-packed, 10-inch (25.4 cm) diameter casings, perforated in the Talbert aquifer, and equipped with deep well turbine pumps. Pumping rates can be controlled up to a maximum of approximately 1,000 gpm (63 l/sec). The saline water pumped from these wells is wasted to nearby flood control channels which drain to the ocean.

Observation Wells

There are approximately 30 observation wells in the area which are used to monitor ground water conditions. Fifteen of these wells are intended to be used for monitoring the effects of injection in each of the separate aquifers. The design of these wells is similar to the injection wells with a separate casing installed for each aquifer. Instead of stainless steel, the casings are 4-inch (10.2 cm) diameter plastic pipe.

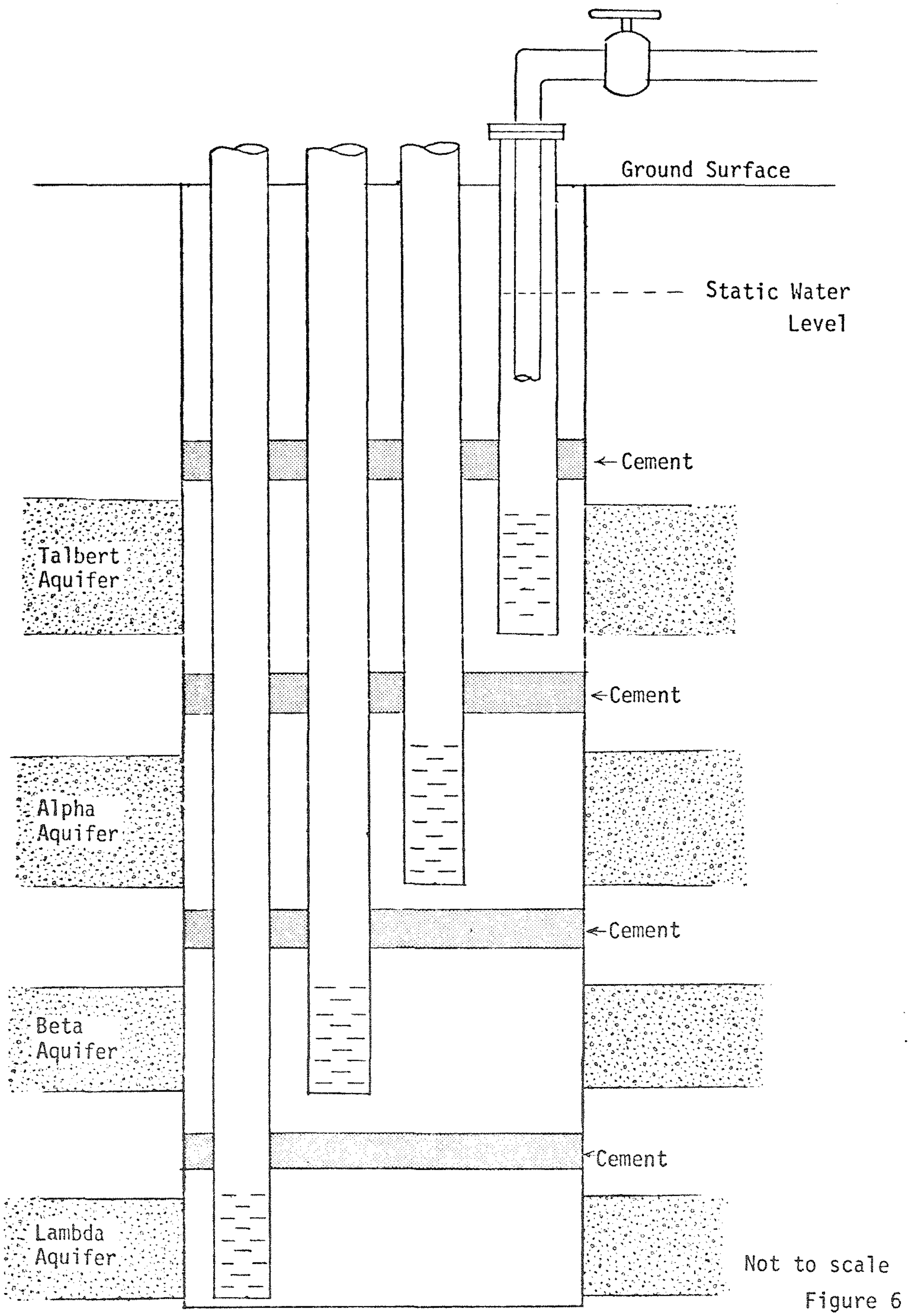
Ground Surface
Static Water Level
Cement
Talbert Aquifer
Cement
Alpha Aquifer
Cement
Beta Aquifer
Cement
Lambda Aquifer
Not to scale
Figure 6

Operations

Construction has been completed and the treatment plant is now operating full time at a reduced rate of production. Before full scale operations begin, water will be injected at each well site individually and the effects will be monitored at the observation wells. The data from this test procedure will be used to determine the injection characteristics of each well casing and to evaluate any variations in aquifer transmissivities along the barrier. Full scale operations are scheduled to begin in March of 1977.

References

California Department of Water Resources, 1966, "Santa Ana Gap Salinity Barrier, Orange County", Bulletin No. 147.1.

California Department of Water Resources, 1967, "Progress Report on Ground Water Geology of the Coastal Plain of Orange County".

Dachnowski, A. P., 1926, "Factors and Problems in the Selection of Peat Lands for Different Uses", U. S. Department of Agriculture, Bulletin No. 1419.

Okey, C. W., 1918, "The Subsidence of Muck and Peat Soils in Louisiana and Florida", Transactions of the American Society of Civil Engineers, v. 82.

Poland, J. F., Piper, A. M. and Others, 1956, "Ground Water Geology of the Coastal Zone, Long Beach-Santa Ana Area, California", U. S. Geological Survey Water-Supply Paper 1109.

Talbert, T. B., 1952, "My Sixty Years in California", Huntington Beach News Press.

Weir, W. W., 1950, "Subsidence of Peat Lands of the San Joaquin Delta", Hilgardia, v. 20, No. 3.

Publication n°121 of the International Association of Hydrological Sciences
Proceedings of the Anaheim Symposium, December 1976

FURTHER EXAMINATION OF SUBSIDENCE AT SAVANNAH, GEORGIA, 1955-1975

George H. Davis and Harlan B. Counts, U.S. Geological Survey, Reston, VA, and Atlanta, GA, and Sandford R. Holdahl, National Ocean Survey, Rockville, MD

Abstract

Land subsidence resulting from head declines in the past, reported earlier in the Savannah area has continued at a maximum rate of about 4 millimeters per year from 1955 to 1975. The area of maximum artesian head decline has shifted to the west and southwest of Savannah thus inducing subsidence in some areas that previously were stable. Although the decline in the area of maximum decline as of 1955 has virtually ceased since 1963, subsidence has continued there unabated, suggesting that the cause of subsidence is slow drainage of fine-grained sediments in response to previous head decline in the principal artesian aquifer, a Tertiary limestone sequence. Initiation of subsidence during 1955-75 in previously stable areas, suggests that a threshold stress equivalent to 15 meters of head decline is required to produce subsidence in much of the Savannah area.

Introduction

The first formal reporting of land subsidence at Savannah, Georgia was a paper by Davis, Small, and Counts (1963) based on precise leveling in 1918, 1933, 1935, and 1955. Releveling in 1975 by the National Ocean Survey over parts of the lines surveyed in 1955 offered an opportunity to determine further land-surface change and to test hypotheses presented in the 1963 paper.

At the outset it should be noted that land subsidence at Savannah has not been sufficient to be recognized as a serious engineering problem, rather it is of interest more as a consideration in precise leveling and as a complicating factor in quantitative modeling of ground-water systems. Moreover, the geology of the aquifer system underlying Savannah is rather typical of the South Carolina-Georgia-Alabama Coastal Plain and much of the Florida Peninsula, where ground water is widely developed for municipal, industrial, and agricultural use. Thus, a similar response to large artesian head declines might occur elsewhere in the southeastern coastal plain under hydrogeologic conditions analogous to those at Savannah.

Geology, ground-water conditions, and land subsidence as of 1955 leveling at Savannah were described by Davis and others (1963, p. 2-3). To recapitulate briefly; Savannah, one of the largest ports of the southeastern United States is on the Savannah River in a tidal reach some 23 km upstream from the Atlantic Ocean (fig. 1). The City of Savannah is on gently rolling low hills that rise sharply from sea level at the riverbank to about 13 m above sea level. Much of the area surrounding Savannah is low-lying swampy land near or only slightly above sea level.

Underlying the Savannah area are several thousand meters of sedimentary rocks, chiefly of marine origin, ranging in age from Late Cretaceous to Holocene. The sedimentary rocks dip seaward and also thicken in that direction. At Savannah the principal artesian aquifer comprises a limestone sequence ranging in age from middle Eocene to Miocene. It consists of soft, granular, commonly highly porous limestone, but includes also beds of sand and marl, and sandy, clayey, cherty, and dolomitic limestone. The principal aquifer is overlain and confined by silty non-calcareous sediments of the Miocene Hawthorn Formation. Weaver (1969), in describing regional mineral facies of the southeastern coastal plain, noted that montmorillonite is the principal clay mineral of fine-grained sediments of Paleocene through Miocene age; this mineral

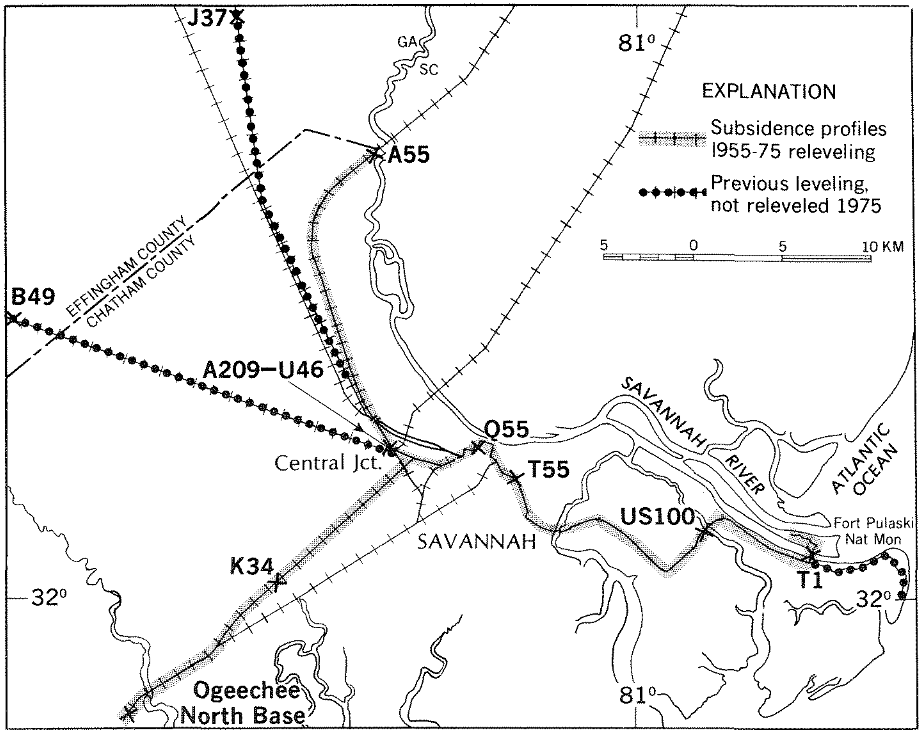

Fig. 1 Location map showing level lines, key bench marks

association is not incompatible with the occurrence of compaction elsewhere in the world. At Savannah the principal aquifer is at a depth of about 50 m, and is about 150 m thick.

Artesian wells have been used for municipal water supply at Savannah since 1887 when 14 flowing wells were put into use. By 1955 withdrawals averaged 216,000 cubic meters per day (fig. 2). Pumping increased to 276,000 m^3 per day by 1963 when it more or less stabilized in the immediate area of Savannah. However, increasing demand caused an increase in the average rate of ground-water pumpage in the Savannah area to 288,000 m^3 per day from 1971-73.

Artesian head declines which corresponded closely to changes in rates of withdrawals, showed marked acceleration in the mid-1930's, a leveling off during the mid-1940's, acceleration from 1953 to 1963, and stability thereafter. The early period of withdrawal was largely confined to Savannah and its immediate environs and by 1955 a sharp cone of depression had developed extending to 35 m below sea level at its center, (fig. 4). Since 1955, however, pumpage outside the City of Savannah, particularly to the west and southwest, has caused a broadening of the cone of depression and of the area subject to significant subsidence.

Precise leveling in 1918, 1933, 1935, and 1955, mainly by the U.S. Coast and Geodetic Survey (the predecessor of the National Ocean Survey) indicated that subsidence of as much as 100 mm had occurred, mostly since 1933. By 1955

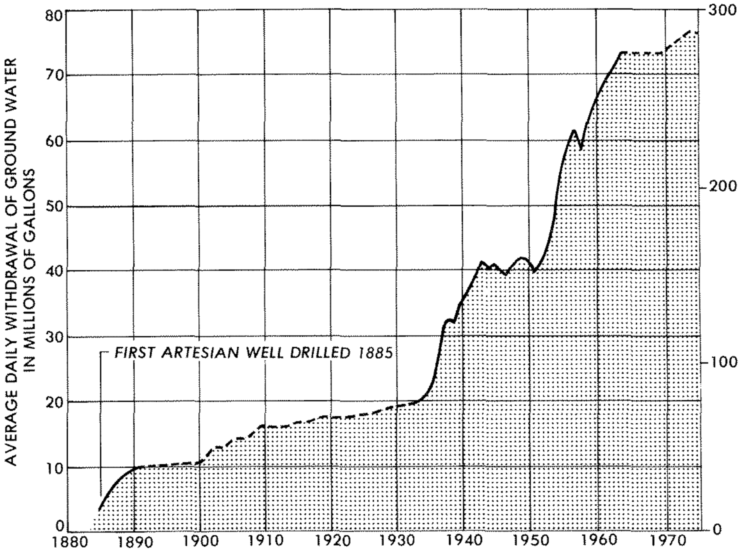

Fig. 2 Ground-water withdrawal, vicinity of Savannah, Ga. 1855-1975

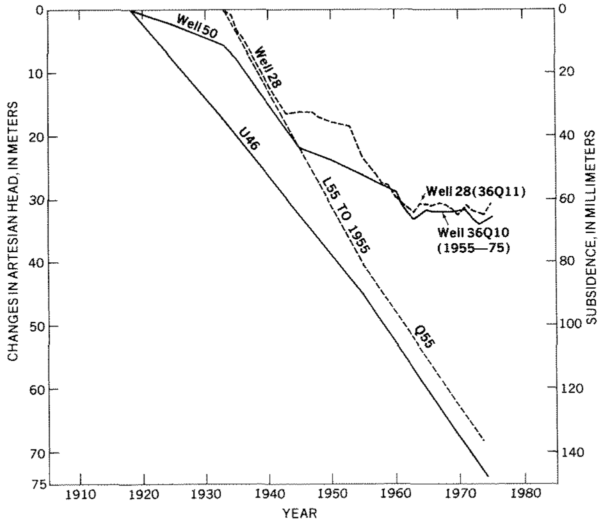

Fig. 3 Subsidence at selected bench marks and decline of artesian head at nearby wells, 1918-75

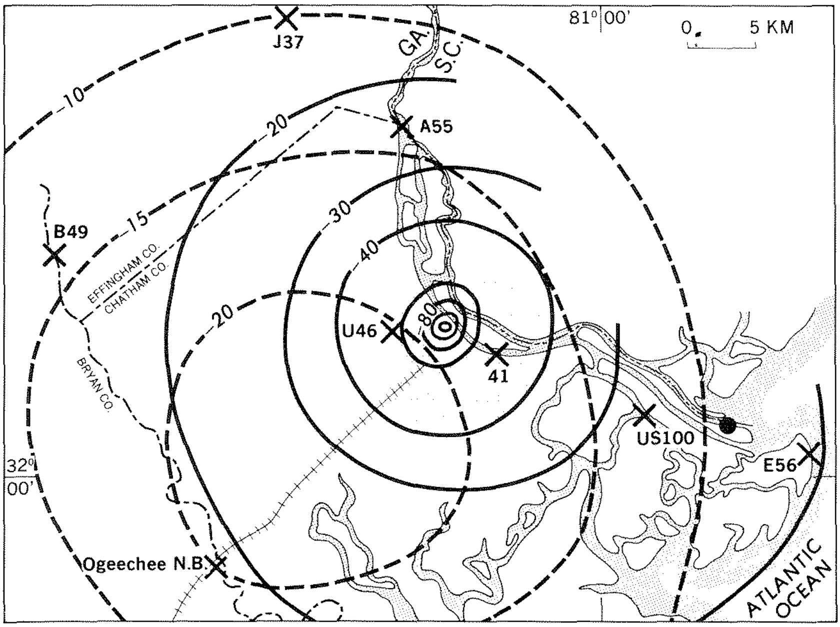

Fig. 4 Lines of equal decline of head, Savannah area, 1933-55 (solid lines) and 1955-75 (dashed lines) in feet; area of more than 20 mm subsidence 1933-55 (shaded); mareograph (heavy dot). (Modified after Davis and others, 1963, fig. 1) 1 meter = 3.2808 feet.

more than 130 km^2 had subsided at least 20 mm. Davis and others (1963) postulated that subsidence was related to decline in head in the principal artesian aquifer, which by 1955 had reached 50 m; of which more than 40 m had occurred between 1933 and 1955. They surmised that the limestone beds of the principal artesian aquifer were not necessarily compacting; rather that compaction more likely was occurring in interbedded clay and marl and/or in silt and clay of the overlying confining unit, the Hawthorn Formation.

Subsidence

Leveling of 1918 through 1955 and the method of analysis of land-surface change was described in detail by Davis and others (1963, p. 3). Briefly, analysis of unadjusted field observations along leveling lines radiating out from Savannah in four directions (fig. 1) indicated that Savannah had subsided relative to distant points on all the lines. Subsidence of 20 mm or more was observed as far as 11 miles northwest and 12 miles west of Savannah. The area in which subsidence appeared to have exceeded 20 mm over the period 1933-55 was roughly 130 km^2; however, the area in which subsidence exceeded 50 mm during the same period was limited to the City of Savannah and the surrounding industrial and suburban districts, about 40 km^2. The maximum change observed at a single bench mark was 90 mm at BM U46 (fig. 1) from 1918 to 1955, however, extrapolation suggested that some newer bench marks may have subsided

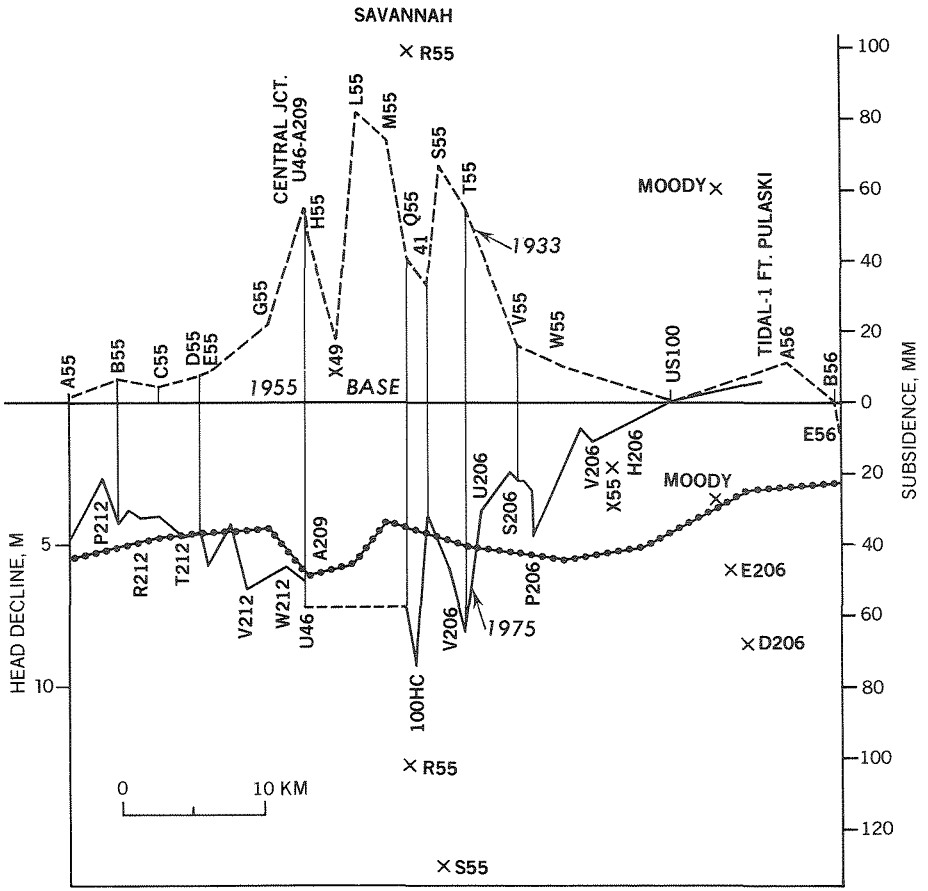

Fig. 5 Profile of land subsidence BM A55 to Fort Pulaski, Ga. 1933-55-1975, and head decline 1955-75 (dotted line)

as much as 110 mm over the longer period. Further extrapolation based on comparison of subsidence rate to head decline in the areas of maximum head decline, where leveling control was lacking, suggested that as much as 200 mm of subsidence may have occurred there.

Leveling in 1975 over previously leveled lines (fig. 1) extended from Fort Pulaski on the Savannah River, 17 km southeast of Savannah, through the city to Central Junction, thence northward along the former Atlantic Coast Line Railroad (now Seaboard Coast Line) to its crossing of the Savannah River at BM A55. Another line from Ogeechee North Base, 30 km to the southwest and which was leveled in 1955 connected with this line at Central Junction.

Not all bench marks were honored in drawing the profiles. Bench marks indicated by leveling parties as having been disturbed were honored only when

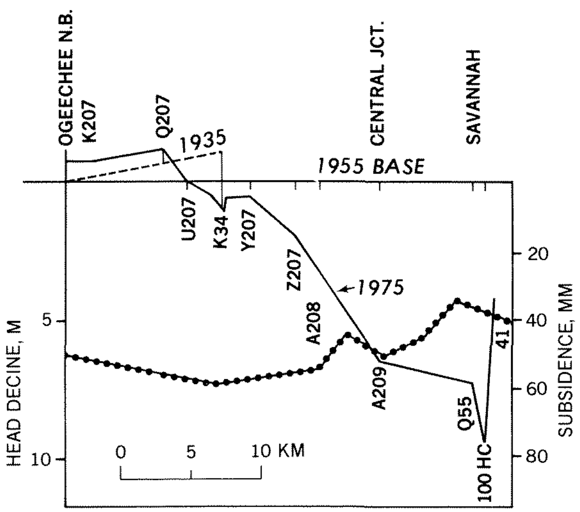

Fig. 6 Profile of land subsidence Savannah to Ogeechee North Base, and decline of artesian head 1955-75 (dotted line)

their records showed good agreement with nearby marks. Bench marks affixed to buildings were commonly erratic and are suspect because of the possibility that they may have been mechanically disturbed, or that differential sinking may have occurred due to superimposed loads of the buildings. Several standard concrete-post-type bench marks in swampy ground also appear erratic (i.e. D206, E206, and Moody, fig. 5) and were not honored in drawing the profiles but are shown for comparison nonetheless.

A comparison of leveling of 1933, 1955, and 1975 over the line from Fort Pulaski through Savannah to BM A55 is shown on fig. 5, using the 1955 leveling as a basis for comparison. In this comparison BM US100, which appears relatively stable and is common to all three levelings, is held fixed. Leveling of 1955 and 1975 over the line extending southwest from Central Junction is illustrated in fig. 6 also using 1955 as the basis for comparison. As in the other comparison, BM US100 is held fixed, that is, the same change from 1955 to 1975 as in fig. 5 at BM A209 was used as a starting point. This results in an apparent minor rise of about 2 mm at BM Ogeechee North Base, which is not significant in light of potential cumulative errors over the distance from BM US100 to Ogeechee N.B. A short line of leveling of 1935 from BM K34 to BM Ogeechee N.B. is common to the leveling of 1955 and 1975; however, as the connection to 1933 leveling in the vicinity of Savannah is very tenuous this record serves only to confirm that BM K34 subsided with respect to BM Ogeechee N.B. during the period 1935-55 as well as from 1955-75. All leveling used in this analysis was of first-order precision; the standard deviation for these levelings is less than 1 mm for a single kilometer.

While the leveling of 1975 was not as extensive as that of 1955 and earlier periods it confirms continuing subsidence at Savannah, and indicates that the area subject to subsidence has expanded. It also provides further information concerning rate of subsidence with respect to artesian head decline as will be discussed further on. The most significant features of the records illustrated on figs. 5 and 6 are that additional subsidence of as much 70 mm has occurred since 1955, that BM A-55, which was stable over the period 1933-1955, subsided 40 mm from 1955-77, and that the area in which subsidence exceeded 20 mm in the 20-year period 1955-75 is estimated to encompass at least 330 km^2 as compared to 150 km^2 over the previous period (1933-55).

The subsidence reported here is not to be confused with crustal movements of regional scale as reported by Holdahl and Morrison (1974) and Brown and Oliver (1976). The subsidence due to decline of head is a local effect superimposed on such regional tilting effects. In any event, Savannah is close to the line of zero elevation change as reported by Holdahl and Morrison (1974, fig. 5). A point of some interest with respect to the regional change is that the mareograph at Fort Pulaski is a key anchor for the leveling network used in regional analysis. In this regard, it is of special interest that bench marks Tidal 1 and Tidal 2 at Fort Pulaski agree closely with BM US100, that is, they indicate no subsidence due to decline in head. All three of these marks are on concrete highway bridge structures which offer better stability than standard bench marks located in swampy soils nearby (see fig. 5).

Decline of artesian head

Davis and others (1963) showed a close correlation between decline in head and land subsidence as indicated by changes in the piezometric surface from 1933 to 1955 (table 1 and figs. 4 and 5). In the area of maximum subsidence a uniform ratio of subsidence to head decline of 0.0033 was noted. Despite changes in patterns of pumping and stabilization of ground-water pumping in the Savannah area beginning in 1963, the head has declined significantly over the period 1955-75 although the area of the greatest decline has shifted southwestward in agreement with changed pumpage distribution (fig. 4). It is notable that the decline shown at BM A55, a little more than 5 m is only exceeded slightly by the 6 m decline near BM U46 which is near the area of maximum decline for the period 1933-1955 (Davis and others, 1963, fig. 5). In that paper it was noted that decline in head of as much as 6.7 m had not resulted in measurable subsidence in much of the Savannah area and it was postulated that a threshold stress of at least this magnitude had to be exceeded before significant compaction begins. Information now available suggests that the threshold stress to be exceeded before subsidence begins may be about 15 m decline of head. This is based on the observation that BM A55 and W55 now show significant subsidence in areas, where total head decline from the virgin condition of 1885 has been 20 m and 17 m respectively, whereas BM T1 and T2 at Fort Pulaski and Ogeechee N.B. exhibit negligible subsidence, where total head decline has been 13 m and 14 m, respectively.

Comparison of subsidence of bench marks as of 1955 to head decline at nearby wells (Davis and others, 1963, table 1) indicated a rather uniform ratio of 0.0033 near Savannah. Regrettably, most of the bench marks in the area between downtown Savannah and Central Junction, were obliterated in construction of Interstate Highway 16 prior to 1975. Moreover, most of the old wells in that area no longer are available for measurement. Thus, of the bench marks used for the 1955 calculation of ratio of subsidence to head decline only BMs U46, Q55 and T55 are suitable for a similar calculation for the period 1955-75. At each of those bench marks subsidence continued at about the same rate as during 1933-55 or at a greater rate despite a general flattening of the head-decline curve after 1963, consistent with stabilized pumping at Savannah. Accordingly, the ratio of subsidence to head decline from 1955 to 1975 (calculated from fig. 5) near BM Q55 and BM T55 increased to 0.013. Elsewhere in the area the comparable ratio is 0.01 near BM U46 and 0.007 near A55, and values between 0.007 and 0.016 are characteristic throughout the area of maximum subsidence. As subsidence declines toward zero in the direction of BM US100 and toward Ogeechee N.B., of course, the ratio approaches zero. Composite graphs showing subsidence of selected bench marks and decline in head at nearby wells are shown in fig. 3.

These changes in ratios from about 0.0033 in the period prior to 1955 to much larger numbers in the succeeding period are not in conflict with, and indeed, offer strong support for the concept that subsidence is causally related to slow drainage of water from fine-grained marl, clay, and silt to the permeable limestones of the principal aquifer. Once a head gradient is established a fine-grained bed continues to drain and compact slowly until a new equilibrium is reached, despite the fact that decline in head in the permeable adjacent bed may have ceased. Such effects have been recognized elsewhere (Poland and Davis, 1969). The time required to reach a new equilibrium condition is a function of the thickness and permeability of the fine-grained strata. To go further than this qualitative explanation would require extensive and expensive coring of the compacting section and laboratory testing of cores.

Summary

Releveling in 1975 indicates that subsidence has continued at Savannah despite major changes in the amount and areal distribution of decline of artesian head in the principal artesian aquifer. In the vicinity of the area of maximum head decline and maximum subsidence for the period prior to 1955, subsidence has continued at about the previous rate of about 4 mm per year despite virtual cessation of head decline since 1963. This offers strong support for the earlier conclusion that subsidence is caused by compaction of fine-grained sediments through slow drainage rather than by compaction of limestone in the principal artesian aquifer.

A shift in the area of maximum head decline to the west and southwest of its former location is reflected by initiation of subsidence in areas that previously were stable and by more than doubling of the area subject to more than 20 mm of subsidence. Data now available suggest that in much of the Savannah area, a threshold stress equivalent to 15 m of head decline is required to initiate subsidence. Thus the key mareograph at Fort Pulaski can be expected to start subsiding as regional head decline continues. Also the entire Savannah area can be expected to continue subsiding slowly in response to head changes of 1885-1963 until a new equilibrium is reached barring further substantial head declines. To arrive at a better quantitative analysis of the situation would require additional specialized leveling, test drilling and extensive laboratory analysis of core materials, and operation of subsidence recorders.

References

Brown, L. D., and Oliver, J. E., 1976, Vertical Crustal Movements from Leveling Data and Their Relation to Geologic Structure in the United States: Reviews of Geophysics and Space Physics, v. 14, no. 1, p. 13-35.

Davis, G. H., Small, J. B., and Counts, H. B., 1963, Land Subsidence Related to Decline of Artesian Pressure in the Ocala Limestone at Savannah, Georgia: Geol. Soc. Amer. Engr. Geology Case Histories, no. 4, p. 1-8.

Holdahl, S. R., and Morrison, N. L., 1974, Regional Investigations of Vertical Crustal Movements in the U.S., Using Precise Relevelings and Mareograph Data: Tectonophysics, v. 23, p. 373-390.

Poland, J. F., and Davis, G. H., 1969, Land Subsidence Due to Withdrawal of Fluids: Geol. Soc. Amer. Reviews in Engr. Geology, v. II, p. 187-269.

Weaver, C. E., 1968, Mineral Facies in the Tertiary of the Continental Shelf and Blake Plateau: Southeastern Geology, v. 9, no. 2, p. 57-63.

Publication n°121 of the International Association of Hydrological Sciences
Proceedings of the Anaheim Symposium, December 1976

GROUND WATER AND LAND SUBSIDENCE IN BANGKOK, THAILAND

Charoen Piancharoen
Director of the Ground Water Division, Department of Mineral Resources, Bangkok, Thailand

Abstract

Bangkok is in the Lower Central Plain of Thailand and is only 25 kilometers north of the Gulf of Thailand. The plain has been filled with clastic sediments more than 2,000 m thick, the upper 300 meters of which form principal artesian aquifers at present yielding about 700,000 m^3/day of ground water for domestic and industrial use in the Bangkok Metropolis. The pumpage is in excess of sustained yields as evidenced by a decline in the piezometric heads of 3-4 meters a year. The fall in piezometric pressures in the aquifer system is suspected to cause surface settlement as a result of consolidation compression of the clay strata, especially the normally consolidated Bangkok Clay on which the city is constructed. Evidence of land subsidence is, however, not apparent, and insufficient data exist at present for an adequate investigation. An attempt has been made to predict the degree of settlement as a function of water level drawdowns for four sites in Bangkok. The computation indicated that a maximum subsidence of about 0.82-1.04 meters could be expected as a result of consolidation in the Bangkok Clay alone. Further calculation predicted that the lowering of the piezometric heads of 2 meters in the sand immediately beneath the Bangkok Clay would result in land subsidence of about 0.10 meter. Consolidation tests of the Bangkok Clay at two sites in Bangkok revealed that the clay is compacted under additional loads exerted on the ground surface. An external loading of 3-5 tons per square meter caused maximum compaction of 0.40-0.56 meter in the clay at one place and 0.85-1.24 meters at another.

Observation and measurement of the piezometers in the Bangkok Clay and the underlying sand layer during the last three years indicated that the rates of lowering of water levels are 0.065 and 0.106 meter annually. The relative settlement of the land surface in the observed area is 0.02-0.06 meter, but the cause of subsidence is still far from conclusive as the result of deep well pumping. Since Bangkok can not tolerate land subsidence because its average elevation is only 1.00-1.50 meters above mean sea level, three 4-year programs of scientific investigation related to levelling, subsidence, and ground water management are now being proposed to the Government for implementation with the total budget of about $1.5 million.

Resume

Bangkok se trouve à la plaine basse centrale de Thailande, 25 km au nord de La Golfe de Thailande. La plaine a été remplie des sédiments clastiques qui ont une épaisseur de 2000 m dont les 300 m supérieurs forment des eaux juveniles principales qui donnent à present 700,000 m^3 de l'eau souterraine par jour pour les usages domestiques et industriels à Bangkok. Le décroissement des charges piézométriques de 3-4 m par an prouve que l' extraction excède le rendement soutenu. On croit que la diminution des pressions piézométriques dans la couche aquifère cause l'affaissement par compaction par suite de l'affermissement des couches d'argile, particulièrement de l'Argile de Bangkok normalement endurcie sur laquelle la ville est bâtie. L'évidence de la subsidence du terrain n'est pourtant en apparence et il manque des données à présent pour une investigation suffisante. On a essayé de prédire l'affaissement par compaction comme fonction de la baisse de la surface de l'eau à quatre terrains à Bangkok. Les calculs ont montré qu'une subsidence maximum d'à peu près 0.82-1.04 m pourrait être attendu comme suite de l'affaissement par compaction dans l'

Argile de Bangkok à lui seul. On a calculé aussi qu'une décroissement de 2 m des charges piézométriques dans le sable au dessous de l'Argile de Bangkok donnerait une subsidence du terrain de 0.10 m. L'épreuve de la consolidation de l'Argile de Bangkok à deux endroits à Bangkok a montré aussi que l'argile sera endurcie comme suite des charges supplémentaires sur la surface de la terre. Deux telles charges de 3 et de 5 tonnes la metre carrée ont donné une compaction maximum de l'argile de 0.40-0.56 m dans une localité et de 0.85-1.24 m ailleurs.

L'observation et le mesurage des piézomètres dans l'Argile de Bangkok et dans le sable en dessous pendant les trois derniers ans ont indiqué que les taux de l'abbaissement de la surface de l'eau sont 0.065 et 0.106 m par an respectivement. L'affaissement rélatif de la surface de la terre sur le terrain observé était 0.02-0.06 m mais on n'a pas déterminé la cause exacte de l'affaissement à cause du pompage des puits profonds. Depuis que Bangkok ne peut tolérer l'affaissement avec son altitude moyenne de 1.00-1.50 m au dessus du niveau moyen de la mer, trois recherches scientifiques durant 4 ans qui concernent le nivellement, la subsidence et la gestion de l'eau souterraine avec un budget total de U.S. $1.5 m sont en train d'être proposées au gouvernement.

Introduction

Bangkok is in the Lower Central Plain of Thailand and is situated on the flood plain and delta of the Chao Phraya river which originates from 4 main tributaries which join some 250 kilometers to the north and drains into the Gulf of Thailand 25 kilometers to the south. The Bangkok Metropolis covers an area of about 700 square kilometers with a population of 4.2 million.

The general land surface of Bangkok is relatively flat and local flooding occurs after heavy rain storms. The elevation is only 1.00-1.50 meters above mean sea level or only tens of centimeters above the river water level during high tide. The natural drainage of Bangkok is the Chao Phraya river, whose depth is about 15 meters, and its complex system of natural and manmade canals.

Geologic formations and ground water

The Lower Central Plain, approximately 120 kilometers in width and 200 kilometers in length, was originally formed by the accumulation of clastic sediments more than 2,000 meters thick in the fault/flexure depression since Tertiary time. The original deposition might have occurred under the fluvial environment and consisted mainly of alternating meander belt sands and flood-basin clays. The raising and lowering of the sea level to the present standstill probably began in Pleistocence time. During the transgression period, the sea might have extended as far as 175 kilometers north of the present Gulf of Thailand. With the subsequent regression of the sea level the Chao Phraya river system built its deltaic plain, consisting of brackish to saline clays and sands,to its present position (Figure 1).

The ground surface of Bangkok is entirely underlain by blue to gray marine clay up to 30 meters thick, known as the Bangkok Clay. The upper 15 meters of the Bangkok Clay, generally called the Bangkok Soft Clay, is very soft and highly compressible. The lower part, referred to as the Bangkok Stiff Clay, which is rather stiff and less compressible extends to an average depth of 25-30 meters. The water in these clays is very saline and salty.

The water bearing formations of Bangkok consist mainly of sands and

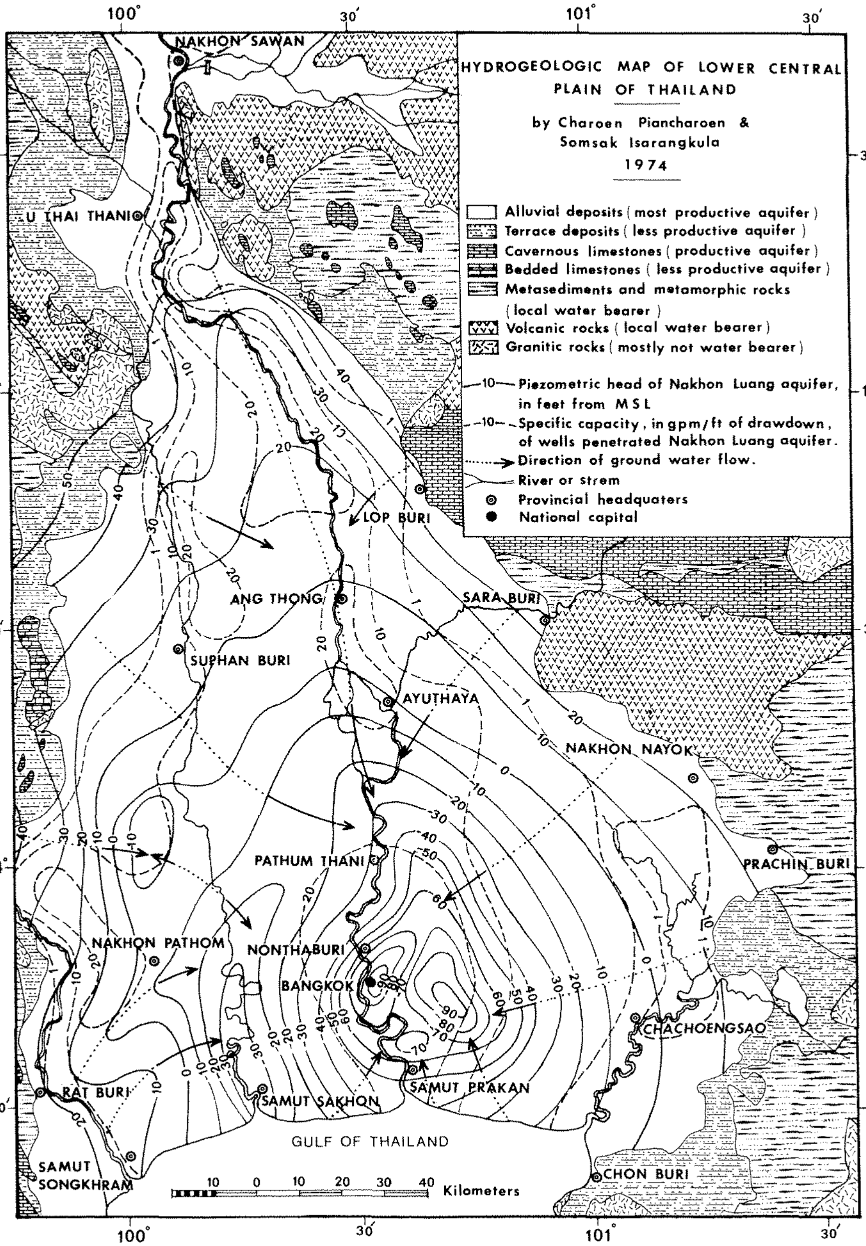

FIGURE 1. — Hydrogeologic map of the Lower Central Plain of Thailand.

FIGURE 2.–HYDROGEOLOGIC NORTH–SOUTH SECTION OF THE LOWER CHAO PHRAYA DELTA SHOWING PRINCIPAL AQUIFERS OF BANGKOK METROPOLIS

(CORRELATED BY ELECTRIC AND GAMMA-RAY LOGS)

By Charoen Phiancharoen & Somkid Buapeng

1973

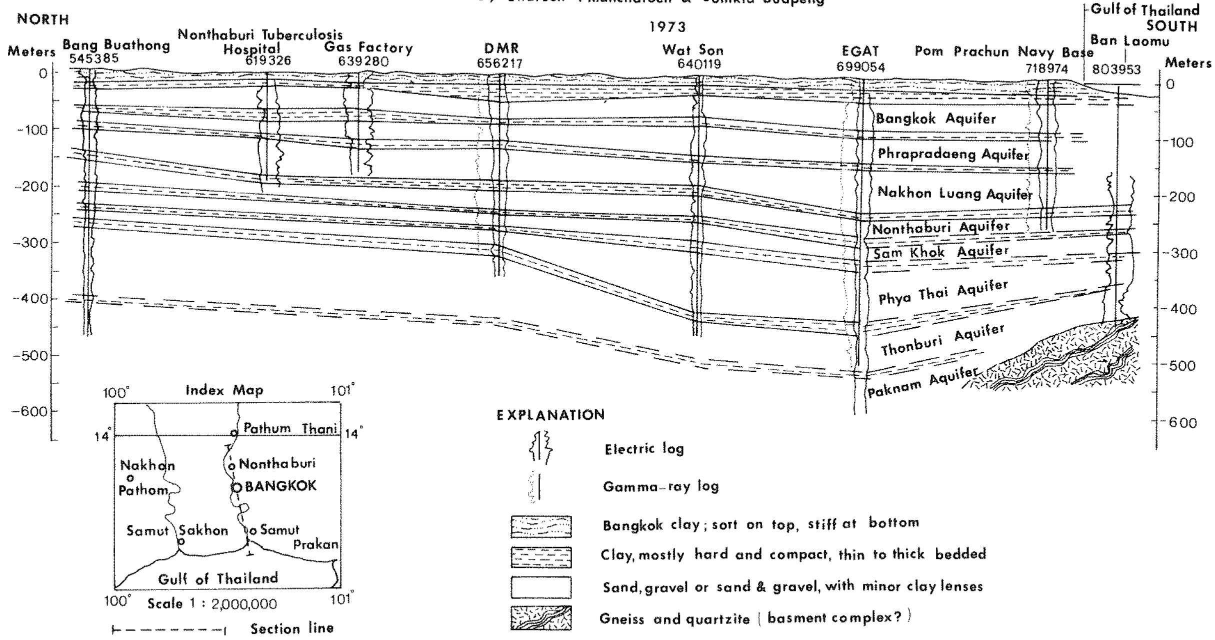

gravels with minor clay lenses *(Piancharoen and Chuamthaisong, 1976)*. They are similar in occurrence and composition but can be zoned according to the geoelectrical properties (Figure 2) into 8 principal artesian aquifers, separated by thick confining clay or sandy clay layers; namely: 50-meter zone (the Bangkok Aquifer), 100-meter zone (the Phra Pradaeng Aquifer), 150-meter zone (the Nakhon Luang Aquifer), 200-meter zone (the Nonthaburi Aquifer), 300-meter zone (the Sam Khok Aquifer), 350-meter zone (the Phaya Thai Aquifer), 450-meter zone (the Thon Buri Aquifer), and 550-meter zone (the Pak Nam Aquifer). These aquifers generally extend the full width and length of the Plain. Most wells in Bangkok penetrate the second, third and fourth aquifers because they are highly productive, with a Coefficient of Transmissibility of 40-130 m^2/hr (150,000-250,000 gallons per day per foot), and yield water of relatively excellent quality. The first aquifer, immediately beneath the Bangkok Clay, gives saline water whereas the fifth and sixth aquifers are not popular due to their greater depths and water of inferior quality. The seventh and the eighth have been proved to yield fresh water but have been tapped by only few wells. The sediments at depths from 650 meters to the metamorphic basement rocks at about 2,000-3,000 meters have been indicated by electric well logging to yield brackish to saline water. In the northern part of the Lower Central Plain, however, fresh ground water could be obtained from the first aquifer.

Ground water has been exploited for domestic supply in Bangkok for the past six or seven decades, but heavy utilization began in 1957 when the surface water for domestic and industrial use could not meet demand. For many years, about one third of the total public water supply in Bangkok has come from the aquifers (Table 1).

Table 1: Ground water pumpage for public water supply in Bangkok.1/

Year	Pumping rate (m^3/day)	Year	Pumping rate (m^3/day)
1965	84,314	1971	331,966
1966	199,170	1972	318,276
1967	316,963	1973	362,738
1968	342,963	1974	370,032
1969	310,027	1975	350,000
1970	307,540	1976	345,000

1/ *Source of data: Bangkok Metropolitan Water Works Authority.*

Is is estimated that the present total pumpage for domestic and industrial use is as high as 700,000 m^3/day. This pumping rate exceeds the safe yield and brings about an acute problem of water level decline *(Piancharoen, 1974)*. At an early stage of development, the water level was about the ground surface but it gradually fell until cones of depression developed in many areas. In 1958-1959 the water level in the center of Bangkok was about 8-9 meters from the ground surface while that in the suburbs was 4.5-6 meters. Since 1967 a remarkable change of water level could be observed. During 1968-1969 the depth to water level in heavily pumped area was 22-25 meters and 10-12 meters in the suburbs. At present the general depth to water level is 30 meters while that at the center of the cone of depression is in excess of 33 meters (Figure 3). The annual rate of decline in the water level is now as high as 3-4 meters for the 100-meter, 150-meter and 200-meter aquifers. In the 50-meter aquifer the water level is also falling about 1 meter a year due to the interception of recharging water at the northern part of the Plain. The consequences of heavy pumpage are not only the over-draft of aquifers but

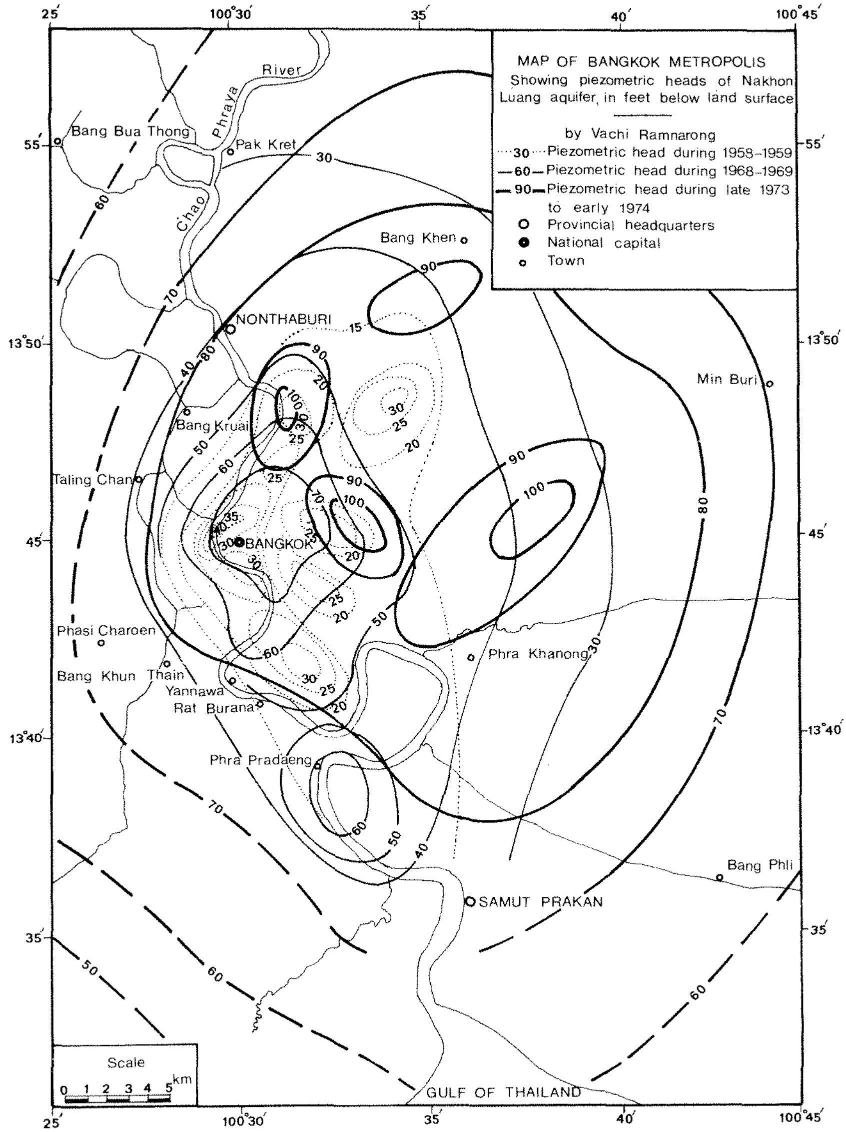

FIGURE 3.– Water level map of the Nakhon Luang Aquifer.

also the salt water encroachment into the southern part of the Bangkok Metropolis and the possibility of land subsidence.

Problems of land subsidence

There is no serious damage due to land subsidence in Bangkok at the present time although flooding in localized areas is believed to be a result of a reduction in the altitude of the ground surface. However, the possibility of land subsidence due to the effect of deep well pumping has been spoken of by soil scientists for many years but no definite scientific proofs could be issued. No systematic investigation or observation leading to a reliable quantitative expression of subsidence behavior has been made to date. Soil engineers, particularly those of the Asian Institute of Technology, are of the opinion that the extraction of water from the deep aquifers underlying Bangkok is causing declines in the piezometric pressure in the normally consolidated Bangkok Clay. As the piezometric pressure in an aquifer system decreases, surface settlement normally results from (1) compaction and elastic compression of the aquifers themselves, and (2) consolidation compression of the many clay strata. The compaction and elastic compression of the aquifers are belived to be slight but the consolidation compression of the Bangkok Clay is causing concern. To support the hypothesis, an estimation of the degree of settlement of the clay has been made based on scant field data, laboratory tests, and some assumption. Brand and Paveenchana (1971) outlined two hypothetical modes of settlement by assuming the long term piezometric pressure declines in the Bangkok Clay to occur either when the water level drops but the clay remains saturated or when the water level remains unchanged but the piezometric pressure in the sand layer at the base of the clay declines. The calculation for four selected sites indicates that a settlement for each mode of assumption is the same and the maximum subsidence of about 0.82-1.04 meters could be experienced as a result of consolidation in the Bangkok Clay alone. The computation also indicates that to control the subsidence within 10 centimeters limit the drawdowns must be limited to 0.5-1.3 meters for the former mode and 1.9-3.7 meters for the latter. In conclusion, the lowering of piezometric head in the sand by 2 meters would result in land subsidence of about 10 centimeter. (see table 2)

Table 2: Maximum settlements and tolerable drawdowns for four sites. 2/

Sites	Maximum Settlement, m	Drawdown for Settlement of 10 cm, m	
	Mode I & II	Mode I	Mode II
Municipal building	0.87	1.3	2.5
Lumpini Park	0.82	1.4	3.7
Rama IV Road	1.04	0.5	1.9
Chulalongkorn Univ.	1.00	0.5	1.9

2/ *Source of data: Brand and Paveenchana (1971)*

Haley & Aldrich (1969) also conducted a consolidation test of the Bangkok Clay and suggested that the Soft Bangkok Clay is somewhat overconsolidated throughout its length. If so, the load on the clay *(resulting from declines of piezometric pressure)* could be increased from that at present before reaching a critical stress level. Beyond the critical stress level, the clay would consolidate in a virgin compression and the subsidence would develop. Using the result of the test and assuming the maximum past pressure or load to be 3-5 tons per square meter (tms) greater than the existing overburden stress, the increase in stress of 3 to 5 tms (or the in*crease in load to reach the critical stress) will result in settlement* from re-compression of 0.05 to 0.07 meter. The increase in stress in the clay by a value twice that required to reach the critical stress would result in settlement about 10 times greater than settlement due to re-compression. Since lowering the piezometric level in the clay will result in an increase in effective stress, the rate of drawdown of 0.3 meter per year in the clay at a depth of 12 meters would take from 10 to 15 years to increase the average stress level by 3 to 5 tms.

Observation and measurement of three piezometers by the Ground Water Division of the Department of Mineral Resources indicated that the annual rates of decline in water levels in the lower part of the Soft Bangkok Clay (at a depth of 12 meters) and in the sand layer just beneath the Bangkok Stiff Clay (at a depth of 20 meters) are 6.5 and 106 centimeters, respectively, for the last three years (31 March 1973 - 31 March 1976) while that in the 100-meter aquifer at the same location is 103.65 centimeters. *Land settlement in the area observed has caused the pump's concrete foundation to overhang the ground by 6 cm and the piezometer casing to protrude an additional 2-6 cm.* This type of settlement occurs in many areas, the maximum measured being 15 centimeters. This evidence is still not conclusive as the result of deep well pumping since other consolidation tests suggest alternative causes. Sitthichaikasem (1975) reported that the Soft Bangkok Clay is generally 65-75% water saturated, hence it is very soft and highly compressible. Under additional loads exerted on the ground surface, the clay will be compacted. Consolidation tests of the clay at two sites as listed in Table 3 revealed that under external loading of 3-5 tms the maximum magnitudes of compaction was 0.40-0.56 meter at one place and 0.85-1.24 meters at another. The compaction rate, however, decelerates as time progresses. For example; at the site of maximum compaction of 1.24 meters under a load of 5 tms, the settlement after 1, 5, 10, 20, 50 and 80 years would be 0.20, 0.43, 0.62, 0.86, 1.09 and 1.15 meters, respectively. The external loads at present are earth-fills and buildings whose piles are short or still in the soft clay. Other additional loads are mainly public utilities; i.e., highways, water mains and the sewage system. It is calculated that earth-fills one meter high exert 2 tms load on the original ground surface and 3, 4, 5 and 6 tms are figures for the highways, two-three-and four-storey buildings, respectively. Under these loads it[3/] was

Table 3: Maximum settlement due to external loading for 2 sites.

External Load (tms)	Maximum Settlement, m	
	at Makkhawan Bridge	at Phlapphlachai
2.0	0.30	0.62
3.0	0.40	0.85
4.0	0.48	1.06
5.0	0.56	1.24

3/ Source of data: Sitthichaikasem (1975) predicted that in the vicinity of a highway system maximum subsidence of about 0.85 meter could be expected, while 1.06 meters would be possible in residential areas. If these figures are correct, an earth-fill of one meter above the ground level for two-storey building would eventually bring the ground floor to the original ground level by the compaction of the Bangkok Soft Clay.

Investigation programs

Since the tests and accompanying evidence are far from conclusive, the problem of land subsidence and whether Bangkok is sinking is still debatable. Many geologists and hydrologists believe that the present deep well pumpage, mostly below 150 meters, has no effect on land subsidence, and if there is any subsidence external loads are to blame. Local flooding is also believed to be due to poor drainage in Bangkok. Since Bangkok could not tolerate major subsidence, the National Environment Board and the National Research Council were asked to look into the matter. The Asian Institute of Technology, Chulalongkorn University, and the Ground Water Division of the Department of Mineral Resources were then requested by the Board, with the support of the Council, to draw up a program of investigation. Three projects are now being submitted for consideration; namely, the levelling in the Bangkok Metropolitan Area for the investigation of land subsidence, the investigation of land subsidence caused by deep well pumping, and the development and management studies of ground water resources in the Bangkok area. The program of levelling work includes the establishment of temporary and permanent benchmarks outside and inside the Bangkok area, one of which will be driven into the shallowest bedrock. The absolute value of elevations of the benchmarks shall be transferred from the stable benchmarks some 100-150 kilometers out of Bangkok. Several levelling tests will be done so that subsidence rates can be computed. The investigation of land subsidence includes determination of soil properties, measurement of piezometric pressures, measurement of soil compression, establishment of a subsidence model to be used for forecasting. The ground water resources study will include an analysis of the aquifer system by mathematical models while proper management of ground water resource development will be recommended. These program will be interrelated and aimed for completion within 4 years with a total budget of about 1.5 million U.S. dollars. The proposals have not been officially accepted since the financial problems are anticipated *(at least at the time this report was prepared in April 1975)*. However, the Government also adopted in principle the draft Ground Water Act as proposed by the Department of Mineral Resources to control ground water drilling and pumping in Bangkok. The Act is expected to come into effect after approval by Parliament not before 1977.

References

Brand, E.W. and Paveenchan, T., 1971, Deep-well pumping and subsidence in the Bangkok area: Proc. 4th Asian Regional Conference on Soil Mechanics and Foundation Engineering, Bangkok, Vol. 1, pp. 1-7.

Haley & Aldrich, Inc., 1970, Effect of deep well pumping on land subsidence in Bangkok: in Master Plan, Water Supply and Distribution, Metropolitan Bangkok, Thailand, Vol. 4; as prepared by Camp, Dresser & McKee Consulting Engineers.

Piancharoen, C., 1974, Ground water resources of the Lower Central Plain of Thailand: Proc. 1st Technical Conference of Thailand Water Works Assoc., Bangkok. (text in Thai)

Piancharoen, C. and Chuamthaisong, C., 1976, Ground water of Bangkok Metropolis, Thailand: Paper presented at the Inter. Hydrological Con-

ference on Hydrogeology of Great Sedimentary Basins, Budapest, 31 May-5 June 1976.
Sitthichaikasem, S., 1975, Bangkok subsidence, too late for tomorrow: Technical article in the Prachachart daily newspaper, Bangkok, 27 October 1975, (text in Thai).

Publication n°121 of the International Association of Hydrological Sciences
Proceedings of the Anaheim Symposium, December 1976

SOIL COMPRESSIBILITY AND LAND SUBSIDENCE IN BANGKOK

Edward W. Brand, Professor of Geotechnical Engineering
A.S. Balasubramaniam, Associate Professor of Geotechnical Engineering,
Asian Institute of Technology, Bangkok, Thailand

ABSTRACT Bangkok is situated on more than 1000 m of unconsolidated deposits, and extensive ground water pumping in the Bangkok area is causing subsidence. The hydrogeological conditions are reviewed in the paper, and the mechanism of subsidence is discussed. An approximate method is described for the prediction of subsidence, and brief mention is made of the approach now being adopted to develop a sophisticated two-part model capable of predicting *rates* of subsidence for any pattern of future water extraction from the eight aquifers. Approximate predictions of ultimate subsidence are presented based on all the available data.

RESUME La ville de Bangkok est située sur des sédiments non consolidés a plus de 1000 m d'épaisseur et le pompage exagéré des eaux souterraines provoque des affaissements dans cette région. Cet article présente les conditions hydrogéologiques ainsi que le mécanisme de ces affaissements. La discussion porte également sur une méthode approximative pour la prédiction des problèmes de l'affaissement et sur une nouvelle conception présentement adoptée pour développer un modèle à deux phases en vue de préduire le taux d' affaissement due à l'extraction de l'eau provenant des huit nappes. Finalement, une estimation des affaissements basée sur les données existantes, est présentée.

INTRODUCTION

The city of Bangkok is situated about 40 km from the sea on either side of the Chao Phraya River which runs through the large flat deltaic plain of the same name. The elevation of the city is generally only 1 to 1.5 m above mean sea level. It has been found expedient to extract water from hundreds of metres of 'unconsolidated' deposits beneath the Chao Phraya Plain (Fig. 1) at an ever-increasing rate with the result that there are now the serious hydrological and geotechnical problems of (1) depletion of aquifers, (2) deterioration of water quality, and (3) general land subsidence. This paper reviews the problem of land subsidence only and discusses the problems involved in predicting its magnitude. The paper is complementary to that by *Piancharoen* (1976), which deals largely with the hydrogeological aspects of the problem.

There are several publications which are directly relevant to the subject of this paper. The available data on the ground water resources of Bangkok have been compiled in reports by *Camp, Dresser & McKee* (1969), *Piancharoen* (1972) and *Ramnarong* (1974) and summary pictures have been given by *Brand & Arbhabhirama* (1973), *Piancharoen & Chumthaisong* (1976) and *Piancharoen* (1976) as the available data have increased. The question of land subsidence in Bangkok was first raised by *Haley & Aldrich* (1970) and was first investigated by *Brand & Paveenchana* (1972). Crude predictions of its possible magnitude were made by *Brand* (1974), and these predictions were subsequently refined by *Worayingyong* (1976).

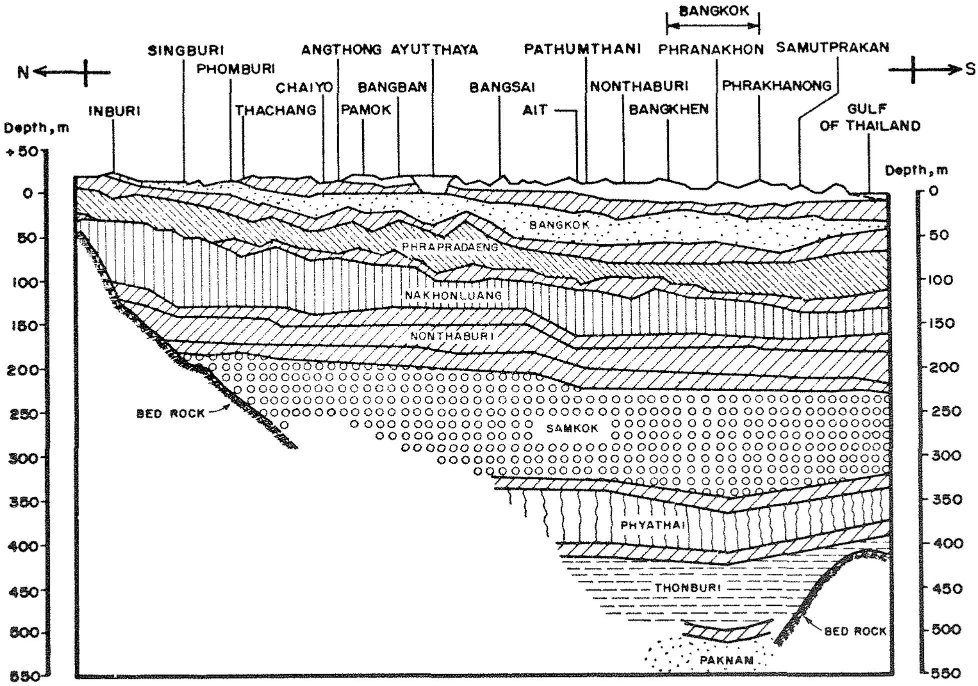

Fig. 1 System of Aquifers under the Chao Phraya Plain

GROUND WATER RESOURCES OF BANGKOK

The Chao Phraya Plain consists of a broad deep basin filled with sedimentary soil deposits which form alternate layers of sand, gravel and clay. The profile of the surface of the bedrock is still undetermined, but its depth in the Bangkok area is known to be between about 550 m and 2000 m. The aquifer system beneath the city area is undoubtedly very complex. The available geological, hydrological and geophysical evidence suggests that there exist eight confined aquifers separated by virtually impervious strata of clay.

At the present time, about two-thirds of the city's water supply for both domestic and industrial use is obtained from more than 1,500 wells tapping the aquifers beneath the Chao Phraya Plain. The net production rate from wells in Bangkok is estimated to be about 700,000 m^3/day (193 million gal/day).

All the problems associated with the development of the ground water resources are a direct result of overpumping the production aquifers. Excessive pumping has caused large drawdowns in the piezometric surface in the main production aquifers, which has resulted in the installation of deeper and deeper wells. The main production aquifers at present are the Phrapradaeng, Nakhonluang and Nonthaburi Aquifers. The Phrapradaeng Aquifer is gradually being abandoned because of salt water encroachment, and the Nonthaburi Aquifer, which was little used until recently, is becoming important.

A decrease in piezometric pressure in a soil will result in an increase in the 'effective' stress, and a compression will take place. As these pressure decreases take place in an aquifer system such as exists beneath Bangkok, surface settlements result from (1) instantaneous compaction of the aquifers, (2) instantaneous elastic compressions of the aquifers, (3) instantaneous elastic compressions of the clay layers, and (4) time-dependent consolidation compressions of the clay layers. The magnitude of the settlement of the ground surface is controlled by the piezometric pressure decline and the total compressibilities of the soil strata over the total depth affected by the pumping. It can usually be expected that the compressibilities of the soil layers will decrease with depth, and the resulting compressions of deep strata for a given effective stress decrease will be relatively small.

The surface settlement caused by aquifer compressions (combined compaction and grain compression) can be shown to be given by (*Brand*, 1974):

$$\delta_a = \Sigma\, S.\Delta u \qquad \ldots\ldots \quad (1)$$

where S is the storage coefficient. It may be assumed that this settlement occurs without appreciable time lag, i.e. it occurs at the same rate as the piezometric pressure declines in the aquifers.

For deep clay strata, vertical compressions will take place by drainage from the soil voids to either of the bounding aquifers. The simplest case will be where the pressure changes in the two aquifers are equal; the change in effective stress, $\Delta\sigma_v$ (= Δu), would then be constant throughout the clay stratum for a particular time interval.

For the surface deposit of 'Soft Bangkok Clay', measurements presented below (see Fig. 5 later) show that the level of the ground water has remained virtually unchanged while a decline in the piezometric pressure in the underlying aquifer has resulted in a decrease in the effective stress in the clay which might ultimately increase linearly with depth (Fig. 2). This model gives a simple expression for the vertical effective stress increase, $\bar{\sigma}_v$, at any depth z below the original water table as:

$$\Delta\bar{\sigma}_v = \frac{z}{D}.\Delta u_a \qquad \ldots\ldots \quad (2)$$

where D is the saturated thickness of the clay layer and Δu_a is the pressure decline in the underlying aquifer. This idealized situation represents only the condition after all excess pressures in the clay have dissipated and compressions have ceased. It therefore predicts the *ultimate* subsidence.

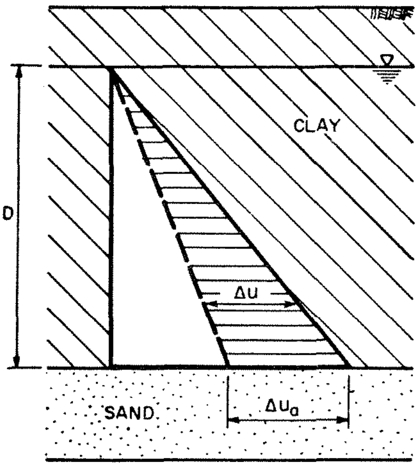

Fig. 2 Model for Surface Clay Deposit

The total consolidation compression, δ_c, in a clay layer can be calculated for the assumed conditions by the application of the well-known expression for one-dimensional consolidation;

$$\delta_c = \Sigma\, m_v.\Delta\bar{\sigma}_v.h \qquad \ldots\ldots \quad (3)$$

where $\Delta\bar{\sigma}_v$ is the change in effective stress at the centre of a thin slice of thickness h which has a coefficient of compressibility m_v. This would enable only primary consolidations to be predicted, however, and some account *might need to be taken of secondary compressions.*

Predictions of *rates* of compression for the clay layers (and hence, rates of subsidence) are much more difficult, and certainly much more important, than the estimations of the ultimate magnitudes. The rate of settlement of the ground surface is governed by (1) the net rate of extraction of water from the ground (which is the amount by which the extraction of water at any time exceeds the aquifer recharge), and (2) the rate of 'excess' pressure dissipation in the clay layers. The manner in which the piezometric pressure declines in a permeable aquifer is fairly well understood and is governed by well hydraulics. The manner of drainage of the intervening clay layers, however, presents a much more difficult situation, since this is controlled by the rapidly changing conditions at the upper and lower surfaces of each layer as the bounding aquifers are pumped. This results in a time-dependent process which is out of phase with the piezometric pressure changes in the sand aquifers. For given boundary conditions, the drainage of a clay layer is governed by the process of consolidation, in which the most important factors are the compressibility, permeability and thickness of the clay stratum.

Since the question of subsidence is inextricably linked to the ground water hydrology of the Chao Phraya Basin, it is necessary to develop a dynamic model capable of predicting the subsidence at any instance on the basis of input data describing an assumed history of ground water extraction. The model must be sufficiently flexible, therefore, to handle a wide range of future possible patterns of well pumping. For this purpose, a finite difference model is now being established at the Asian Institute of Technology. The two components of this are (1) a quasi-three-dimensional aquifer model, and (2) a one-dimensional soil consolidation model. These two components have already been used successfully to reproduce accurate numerical solutions to the problems of (1) single and multiple well pumping in a confined aquifer (*Theis* solution), and (2) consolidation of a clay layer under single multiple stage loading (*Terzaghi* solution). Although this work is in a fairly early stage, there is optimism among those concerned with it that this will result in a sophisticated tool for subsidence prediction.

DATA AVAILABLE FOR SUBSIDENCE PREDICTIONS

The study of land subsidence in the Bangkok area has always been, and still is, hampered by the lack of the necessary data. Good predictions, based on a suitable theoretical model require data on (1) the properties of the 'unconsolidated' deposits and (2) the distribution of water extraction, both horizontal and vertical, and its variation with time.

Data on the distribution and rate of pumping is probably the easiest of the data to collect, but no systematic attempt has so far been made to do this. Although the available data is sufficient for an approximate division of the profile into separate confined aquifers, very little quantitative information is available. Pumping tests have been carried out only at a few locations in the Phrapradaeng and Nakhonluang Aquifers, and the results can be regarded as very approximate only. These tests have yielded storage coefficients of about 1×10^{-4} (*Brand & Arbhabhirama*, 1973).

The nature of the sediments in the vicinity of Bangkok can be judged from Fig. 3, where a section of the subsurface profile has been accurately reconstructed from some available borehole data. Many layers and lenses of clay are interbedded with the sand and gravel of the aquifer beds. It can also be seen that a thick deposit of soft clay is present from the ground surface to a depth of about 20 m. This clay is a marine sediment which was probably deposited during the Late Recent period. It has been named the 'Soft Bangkok Clay' and, because of its engineering importance, it has been fairly extensively investigated (*Moh et al*, 1969). This clay is normally consolidated or lightly overconsolidated and, therefore, plays an important part in considerations of regional subsidence.

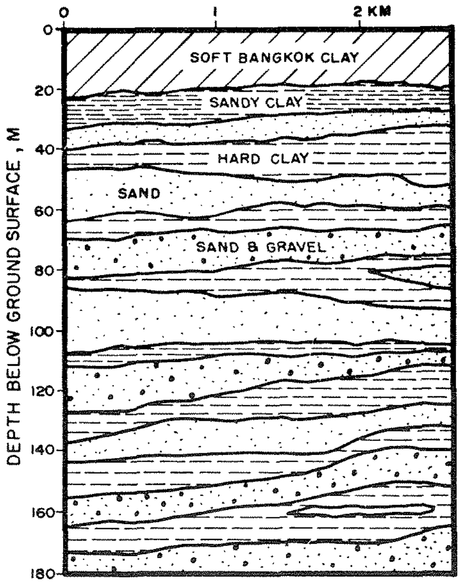

Fig. 3 Typical Shallow Profile

The many deep clay deposits in the Bangkok area have received very little attention, and information about their geotechnical properties appears to have been published only by *Brand* (1971) and *AIT* (1976) whose investigations were limited to a depth of less than 100 m. These limited data show that the deep clay deposits are overconsolidated (OCR = 3-5), with water contents decreasing from about 30% at 30 m to about 15% at 100 m.

Typical void ratio-pressure relationships are shown in Fig. 4 for the clays from various depths in Bangkok. The compressibility of the Soft Clay is clearly of a different order of magnitude from the deeper clays, and its importance in the considerations of subsidence cannot be overemphasized. The very great combined thickness of the hard clay layers, however, is such that the total compression of these resulting from pressure declines in the aquifers is likely to be evern more significant (see below).

A theoretical model designed to predict the subsidence process must link the categories of data listed above. An intermediate step in the solution must be the prediction of the distribution of the piezometric pressure throughout the aquifer system which results from any assumed pattern of pumping. This stage of the model can then be calibrated by comparing the actual pressure distribution with the predictions based on the recent pumping pattern. At the present time, very little information exists as to the piezometric pressure declines in all the Bangkok aquifers, but in the Phrapradaeng, Nakhonluang and Nonthaburi Aquifers, declines are reported to be occurring at the rate of as much as 4 m per year (*Brand & Arbhabhirama*, 1973;

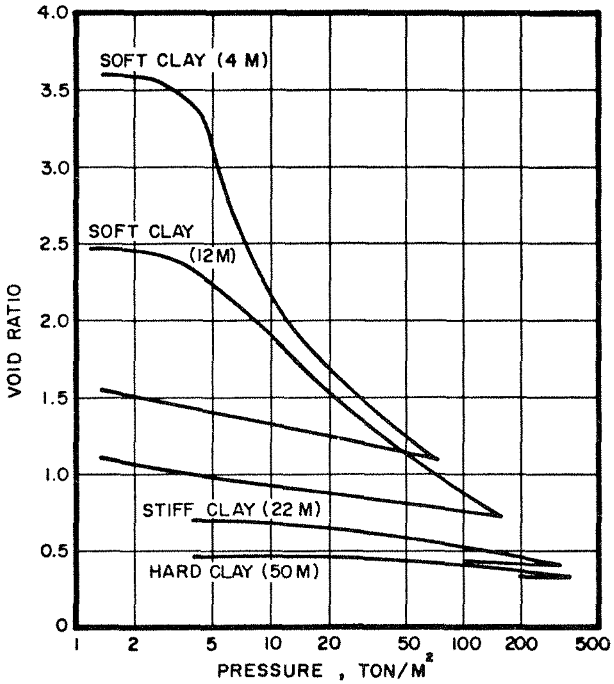

Fig. 4 Typical Clay Compressibilities

Piancharoen, 1976). A clear picture of the current situation in the Nakhonluang Aquifer has been presented by *Piancharoen* (1976); the piezometric surface changed dramatically between 1959 and 1968, and a recognisable cone of depression has now formed with its centre located on the area of the most intensive pumping. The maximum decline is now in excess of 30 m. Depletions of the Phrapradaeng and Nonthaburi Aquifers are similar but are centred on Phrapradaeng to the south of Bangkok itself.

Piezometers have been installed only recently at only a few locations at shallow depths in the city area, and none of these records the pressures in a deep clay layer. Of particular importance in this respect are the pressures in the surface deposit of Soft Bangkok Clay. Figure 5 shows some recent piezometer measurements at three sites in the Bangkok area, where it can be seen that the piezometric pressures are now well below the hydrostatic levels. The pressures in the Soft Bangkok Clay are controlled by those in the Bangkok Aquifer, and although its high salinity precludes its use for water supply, it appears that this aquifer behaves in a semi-leaky manner and transmits water vertically to the aquifer below. It is probable, therefore, that the Phrapradaeng Aquifer (which is heavily pumped) controls, at least partly, the pressures in the Bangkok Aquifer. It might be feasible, however, to prevent further compressions of the Soft Clay by recharging the Bangkok Aquifer.

Once the ground water stage of the theoretical model has been calibrated against field measurements of changes in aquifer pressures, it is then necessary to develop the second stage which predicts the rates of pressure change in the many clay layers and, hence, the consolidation rates. For this purpose, laboratory values of compressibility and permeability can only be a first approximation, since they cannot possibly represent the mass characteristics of the clays. It is essential, therefore, that this second stage of the model is calibrated by comparing the predicted and measured subsidences over a wide area and over several years. In addition, compression indicators installed at a number of depths will indicate the relative compressions of the soil strata. The model parameters can then be adjusted to give coincidence of the predicted and measured subsidence contours. The complete model can then be used with confidence to predict the results of any future pattern of pumping.

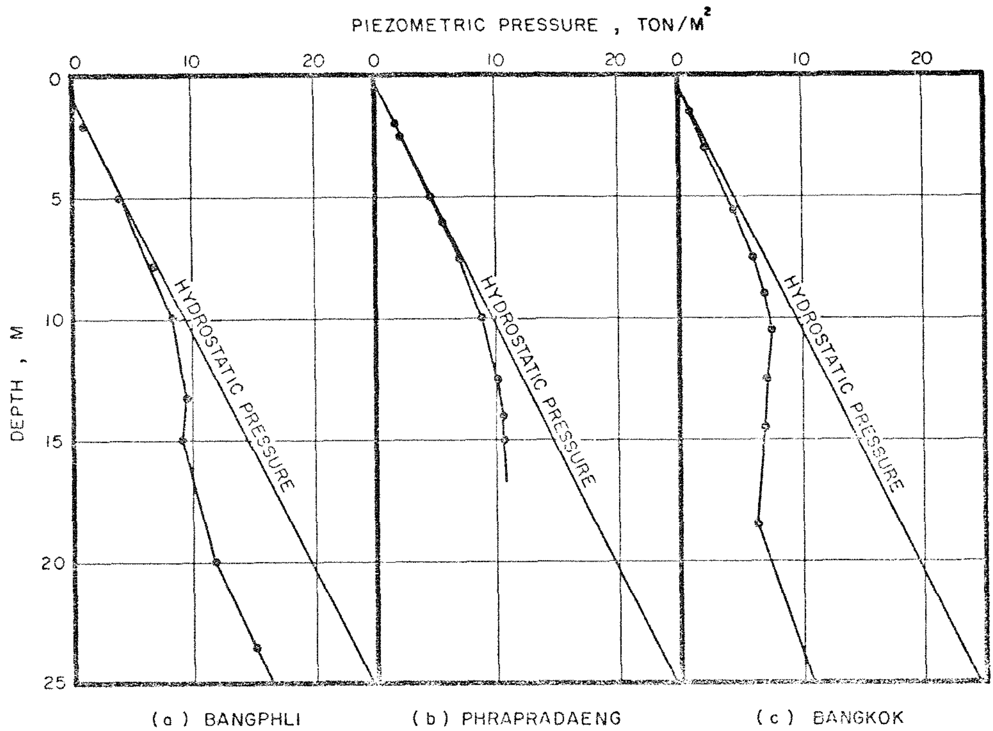

Fig. 5 Piezometric Pressure Drops in the Soft Bangkok Clay

PREDICTIONS OF ULTIMATE SUBSIDENCE

No predictive model has yet be devised to enable even good guesses to be made of the likely rate of subsidence under a given pattern of ground water pumping. The best that can be attempted at this stage, therefore, is estimates of the order of magnitude of the *ultimate* subsidence that is likely to result from a particular piezometric pressure decline. It is not even possible at the present time to relate this pressure to the rate and distribution of water extraction.

In their early paper, *Brand & Paveenchana* (1971) estimated the compressions of the Soft Bangkok Clay at four sites in the Bangkok area for a range of pressure declines in the Bangkok Aquifer beneath the clay. Later, further predictions were made to estimate the orders of magnitude of the compression of the aquifers themselves and of the many hard clay layers throughout the geological profile on the Chao Phraya Plain (*Brand*, 1974). For this purpose, it was assumed that the hard clay layers comprised 25% of the total thickness of the soil profile, and that the bedrock was at a depth of 600 m. The compressibilities of the hard clays were estimated from available pressure-compression relationships obtained on samples from depths of 50-100 m (*Brand*, 1971). The results of these crude predictions indicated that the Soft Clay would contribute the major part of the subsidence and that the aquifer compressions were unlikely to be significant.

Since 1971, attempts have been made at the Asian Institute of Technology to collect and analyse all the available data with a view to improving the predictions of subsidence. A start has also been made on the establishment of a two-part dynamic predictive model, as mentioned above. The method of approach adopted to refine the ultimate subsidence analysis was to establish 'model' relationships between void ratio and pressure for the Soft Clay (assumed as 25 m thick) and the hard clays on the basis of the available data (*Worayingyong*, 1975). Total compressions were then computed for each stratum, as revealed by well drill holes going as deep as 600 m, to obtain the 'minimum probable', 'most probable' and 'maximum probable' subsidence.

Figure 6 shows the range of predictions of the *ultimate* compressions of the Soft Bangkok Clay based on the simple model depicted on Fig. 2. These are based on a large amount of available compression test data and are likely to be reliable. Predictions of the range of ultimate subsidence for the Bangkok area are shown in Fig. 7, and Fig. 8 shows the breakdown of the 'most probable' subsidence into its various components. The results in Figs. 7 & 8 were obtained on the assumption that an equal pressure decline occurs throughout the entire 600 m of soil deposits, which is a highly unlikely event in reality.

The latest predictions of subsidence, represented by Fig. 8, do not differ much in magnitude from the earlier crude estimates made without much available data (*Brand*, 1974). It appears, however, that the likely compressions of the Soft Bangkok Clay were greatly overestimated in 1971 and that those of the hard clays were greatly underestimated. It is clear that the compression of the deep hard clay layers, under the right circumstances of ground water extraction, could be the main cause of land subsidence in Bangkok.

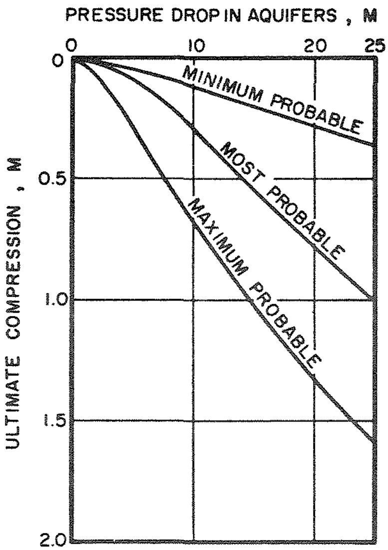

Fig. 6 Predicted Compressions of Soft Bangkok Clay

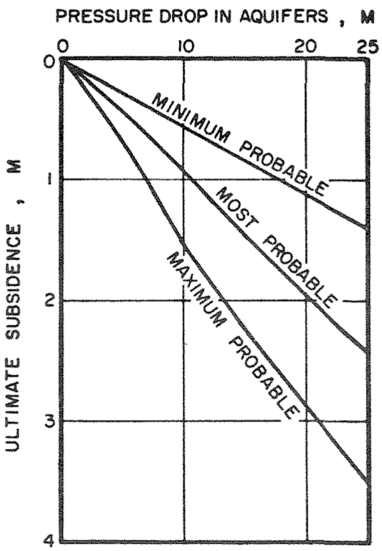

Fig. 7 Predicted Ultimate Subsidence of Bangkok

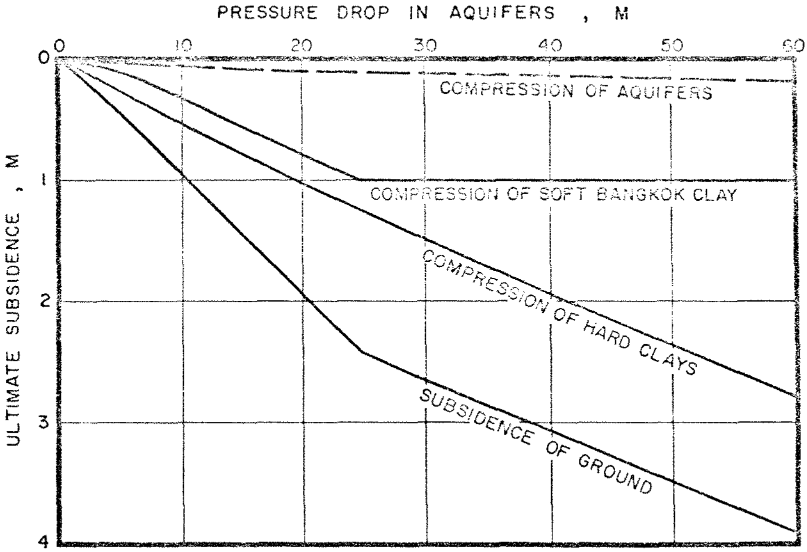

Fig. 8 Predicted Components of Ultimate Subsidence

MEASUREMENTS OF SUBSIDENCE

It it important to understand that no measurements of subsidence have ever been made in the Bangkok area, although there are some visual signs and other indications that a general subsidence is taking place. It is particularly noticeable, for example, that large areas of the city now suffer flooding for several months of the year. The particular difficulty associated with making settlement measurements in Bangkok is the absence of a suitable reference level. No benchmark has been established from which to monitor the subsidence, because the compressible soil strata extend to depths in excess of 1000 m (see Fig. 1). In addition, the nearest outcrop of bedrock is more than 100 km from the city.

Accurate measurements of subsidence are required for the calibration of the second stage of the two-part dynamic model, as discussed earlier. A datum level must, therefore, be established in the near future, and it has been suggested that this will be feasible only by using a tension member or an optical method from the deep bedrock (*Brand*, 1974). Much thought has been given to this question recently by *Hothmer* (1977), however, and he sees no hope of obtaining absolute measurements of ground settlement except on the basis of the stochastic analysis of accurate mean sea level readings over a large number of years. This is a debatable question, and some expert opinion in Bangkok suggests that two recently installed steel casings for oil drill holes will be adequate as datum levels for the subsidence measurements.

REFERENCES

Asian Institute of Technology (1976), Investigation of the Geotechnical Engineering Aspects of Phra Pathom Chedi, *Asian Institute of Technology, Report*, submitted to Public Works Department, Bangkok.

Brand, E.W. (1971), Subsurface Investigation at the Site of Memorial Bridge, Bangkok, *Asian Institute of Technology, Report* submitted to Public Works Department, Bangkok.

Brand, E.W. (1974), Predictions of Subsidence in the City of Bangkok, *Proc. 2nd Int. Conf. Eng. Geology*, Sao Paulo, Vol. 1, pp. III-21.1-III-21.10.

Brand, E.W. and Arbhabhirama, A.(1973), The Ground Water Resources of Bangkok, *Proc. Int. Symp. Development of Ground Water Resources*, Madras, Vol. 3, pp. V43-V51.

Brand, E.W. and Paveenchana, T. (1971), Deep-well Pumping and Subsidence in the Bangkok Area, *Proc. 4th Asian Reg. Conf. Soil Mech. Found. Eng.*, Bangkok, Vol. 1, pp. 1-7.

Camp, Dresser & McKee Inc. (1969), Ground Water Resources of the Bangkok Metropolitan Area, *Interim Report* to the Metropolitan Water Works Authority, Bangkok.

Haley & Aldrich Inc. (1970), Effect of Deep Well Pumping on Land Subsidence in Bangkok, *part of* "Master Plan, Water Supply and Distribution, Metropolitan Bangkok, Thailand", Vol. 4, *Report by Camp, Dresser & McKee Inc.*, submitted to Metropolitan Water Works Association, Bangkok.

Hothmer, J. (1977), Measurement of Absolute Subsidence of the Soft Clay Area of Bangkok, *Proc. Specialty Session on Geotechnical Engineering and Environmental Control, 9th Int. Conf. Soil Mech. Found. Eng.*, Tokyo, (in press).

Moh, Z.C., Nelson, J.D. and Brand, E.W. (1969), Strength and Deformation Behaviour of Bangkok Clay, *Proc. 7th Int. Conf. Soil Mech. Found. Eng.*, Mexico City, Vol. 1, pp. 287-296.

Piancharoen, C. (1972), Ground Water of Bangkok, *Ground Water Open-File Report No. 73, Department of Mineral Resources*, Bangkok.

Piancharoen, C. (1976), Ground Water and Land Subsidence in Bangkok, *Proc. 2nd Int. Symp. Land Subsidence*, Anaheim, California, (in press).

Piancharoen, C. and Chumthaisong, C. (1976), Ground Water of Bangkok Metropolis, Thailand, *Proc. Int. Hydrological Conf. Hydrogeology of Great Sedimentary Basins*, Budapest, (in press).

Ramnarong, V. (1974), Piezometric Map of the Phrapradaeng Aquifer in Bangkok Metropolis during Late 1973 and Early 1974, *Ground Water Div., Department of Mineral Resources*, Bangkok.

Worayingyong, K. (1975), Preliminary Predictions of Subsidence in the Bangkok Area, *M.Eng. Thesis, Asian Institute of Technology*, Bangkok.

Publication n°121 of the International Association of Hydrological Sciences
Proceedings of the Anaheim Symposium, December 1976

LAND SUBSIDENCE IN SWEDEN DUE TO WATER-LEAKAGE INTO DEEP-LYING TUNNELS AND ITS EFFECTS ON PILE SUPPORTED STRUCTURES

by Bengt B. Broms and Anders Fredriksson, Royal Institute of Technology, Stockholm.
Leif Carlsson, Chalmers University of Technology, Gothenburg.

Abstract

Extensive damage on buildings and other structures have been caused in Sweden by a lowering of the groundwater level due to water-leakage into deep-lying tunnels in rock. Other factors such as deep excavations, large trees, changes of the climatic conditions have affected the groundwater level as well as the reduced recharge of water when streets, sidewalks and parking-lots are paved.

Buildings supported in timber piles have been damaged when the piles are exposed above the groundwater level and start to decay. Subsidences can increase the load in piles below a building due to negative skinfriction, since the piles will carry part of the surrounding soil. This increase of the load can be so large when the compressible strata are thick that the compressive strength of the piles is exceeded.

Batter or raked piles are frequently used in Sweden to resist lateral loads. Even a moderate subsidence can increase the maximum bending moment in the piles just below the pile cap so that the yield strength of the reinforcement is exceeded. Subsidence has also caused pile failures due to the lateral displacement of the soil under a building.

Different methods can be used to decrease or to eliminate the subsidence, e.g. preloading of the soil, pregrouting of the tunnels or injection of water.

Underground construction in Sweden

Sweden has old traditions in mining and underground construction. Internationally Sweden is one of the leading nations with respect to the volume of excavated rock per capita. The total volume exceeded 26 Mm^3 in 1974. The mines accounted for about 85% (23 Mm^3). Each year more than 35 km of tunnels are constructed in urban areas for traffic, service lines (water, sewage etc) and to a certain extent for storage (Jansson and Winqvist, 1976). Fig. 1 shows the tunnel-system in the region of Stockholm.

The tunnels have in many cases caused extensive subsidence due to a lowering of the groundwater. Subsidences of 20 to 40 cm are common. Especially deep-lying tunnels have caused serious problems.

Geological conditions

About 95% of the bedrock in Sweden consists of crystalline rock, which in general is very favourable for underground constructions because of its high strength and the fact that the loose and weathered parts at the surface have been removed by the ice during the glaciation. Depressions in the rock surface are in most places indications of tectonic zones in the underlying rock which have been eroded and deepened by the land-ice.

After the latest glaciation parts of Sweden were covered with water, fig. 2. During this time clay and silt were deposited partly as products from the melting land-ice, partly from redeposited and outwashed material during the land upheaval. The clays and silts were deposited in many places over a thin layer of till or sand and gravel on the surface of the bedrock. The areas covered by clay are rather small as shown in fig. 2, but the urban regions in Sweden are to a great extent situated in these areas.

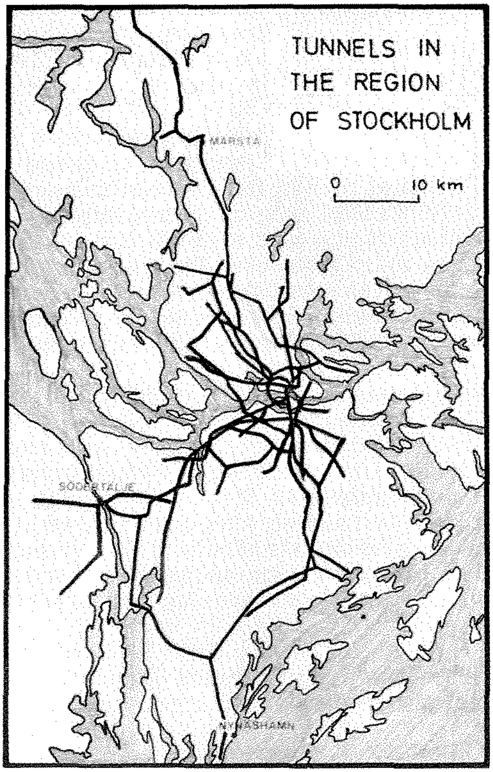

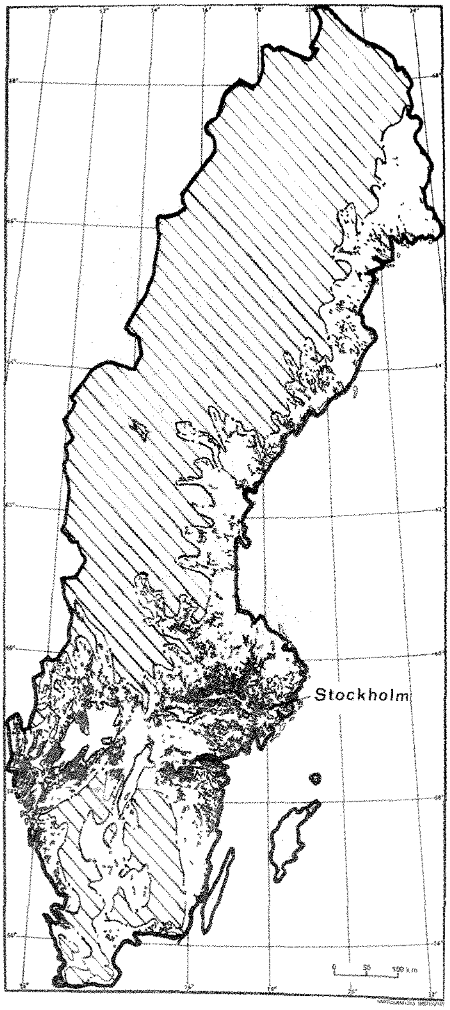

Fig. 1 (above). Map over the tunnel system in the region of Stockholm, Sweden (Morfeldt, 1976).

Fig. 2 (right). Areas in Sweden covered by water after the latest glaciation (with exceptions of ice-dammed lakes in the Caledonian mountains) and areas with sedimentary clay deposits.

Hydrogeological conditions

A section through a clay-filled valley is illustrated in fig. 3. Deep-lying tunnels act as drains, particularly in tectonic zones which lower the pore water pressure first in the pervious bottom layers (confined aquifer), and then gradually in the overlying clay layer. The permeability and storage coefficient of the aquifer is usually about 10^{-6} to 10^{-5} m /s and 10^{-5} to 10^{-4}, respectively. The leakage rate varies but is in general small. However, the total volume can with time be large as well as the area affected by the lowering of the groundwater table. The size of the affected area (500 m^2 to 1 km^2) depends on the topography and the lateral extent of pervious layers.

The initial pore water pressure in the soil before the construction of a deep-lying tunnel increases normally linearly with depth. The groundwater level for the surface layers is normally the same as for the pervious bottom layers as illustrated in fig. 3a.

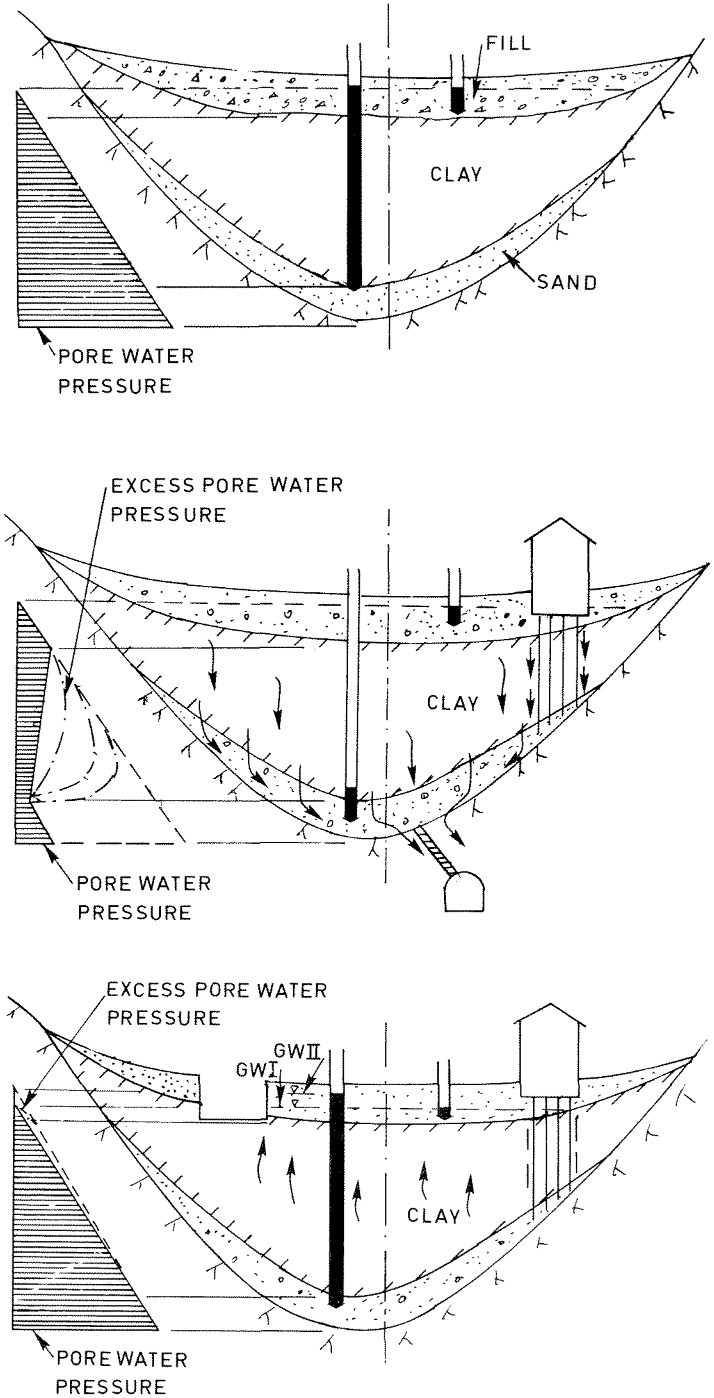

a. *Initial pore pressure distribution.*

b. *Pore pressure distribution after lowering of the groundwater level in the bottom layers.*

c. *Pore pressure distribution after lowering of the groundwater level in the surface layers.*

Fig. 3. Effect of a lowering of the groundwater level on the pore pressure in a deep clay layer.

In general, this groundwater level is not affected since these layers are normally not in direct contact with the pervious bottom layers. The resulting high excess pore water pressures in the clay will gradually decrease with time as indicated in fig. 3b. Ten to thirty years may be required before the excess pore water pressures have fully dissipated, when the thickness of the clay layer is relatively large and the clay does not contain any continuous sand or silt seams.

The effective stress in the clay and the subsidences gradually increases when the pore water pressure and the water content of the clay decrease. The shaded area to the left in fig. 3b indicates the pore pressure distribution after several years when the excess pore water pressures in the clay have dissipated. The change of the pore water and of the effective pressure in the clay layer will be large. A flow rate of only a few millimeters per year in the clay from the surface layers can be expected. In fig. 3c, the groundwater level has been lowered in the surface layers, e.g. by pumping from a deep excavation. This will only have a moderate effect on the pore water pressure in the clay in comparison with a deep-lying tunnel. The subsidences will in general be relatively small. The shaded area to the left in fig. 3c indicates the pore pressure distribution after equilibrium has been reached and the excess pore water pressures in the clay have fully dissipated. A leakage from the pervious bottom layers through the clay up to the surface layers will be the result.

The effects of a lowering of the groundwater level have been studied by Torstensson (1975a) for different boundary conditions. The change of the pore water pressure with time has been calculated in fig. 4 for a 15 m thick clay layer which is located on a pervious sand layer. The groundwater level has been lowered 6 m. The indicated isochrones have been calculated for one-dimensional flow.

Evaluation of subsidence

The glacial and postglacial clays in Sweden are comparatively young. They are normally consolidated to slightly overconsolidated. The water content of the clays is high ($>60\%$), while the shear strength is low, often less than 20 to 30 kPa. The compressibility is high and even a relatively small change of the piezometric level can cause large subsidences.

The groundwater level in Sweden can vary appreciably between different years as well as during one year, depending on hydrometeorological and geological factors.

The groundwater level in the surface layers is in general at its highest in the spring during the thawing period and reaches its lowest level early in the spring just before the thawing period. The yearly variations of the groundwater level can vary from a few centimetres to several meters. Numerous structures were damaged in Sweden during the dry summers in 1947 and 1955 because of the exceptionally low groundwater level (Hellgren, 1959). Also in 1976 the damage was extensive.

The subsidence can be calculated from the change of pore water pressure or of the piezometric head and the compressibility of the soil. Pore pressure sounding instruments have been developed as well as improved pore pressure gauges, so that the effects of a lowering of the groundwater level can be calculated (Torstensson, 1975a). Pumping and injection testing methods , which can be used to analyse the hydraulic properties of aquifers (Carlsson, 1973, Carlsson and Kozerski, 1976), and the deformation properties of deep-lying clay layers (Alte, 1976) fig. 5 have been improved. Numerical models are used to evaluate the influence of different factors and the effectiveness of various methods which can reduce or eliminate the subsidence.

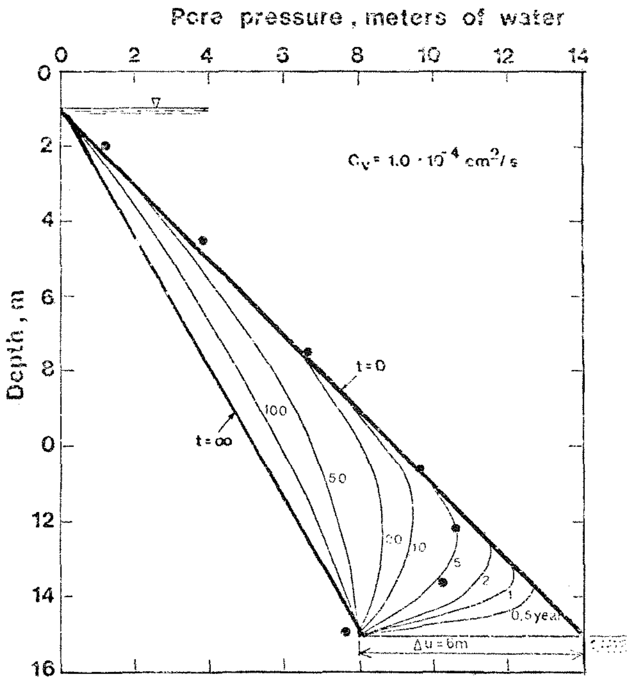

Fig. 4. Pore pressure distribution in a 15 m thick clay layer at different times after a 6 m lowering of the groundwater level.
• = measurement after four years (Torstensson, 1975a).

A decrease of the groundwater level has the same effect as an externally applied load. The subsidence from a 1.0 m thick fill will be about the same as that from a 2.0 m lowering of the groundwater level. Examples of subsidence calculations are shown in fig. 6 for different thicknesses of the compressible layer (Torstensson, 1975a).

The subsidence rate depends to a large extent on the permeability and the thickness of the different strata. Ten to thirty years are normally required before the consolidation has stopped, due to the low permeability of the clay (10^{-10} to 10^{-11} m/s).

Continuous pervious sand or silt layers in the clay will affect the rate of the subsidence. The real subsidence rate is in general considerably higher than that calculated, mainly because of the difficulties to evaluate correctly the drainage conditions. A pervious sand or silt layer, located at the center of an impervious clay layer, will increase the subsidence rate four times and the time required to reach a given subsidence and degree of consolidation will only be 25% of the time estimated without this pervious layer at the center. It is not certain that sand or silt layers will affect the settlement rate, since it may be entirely enclosed in the clay and has no contact with the pervious bottom layers.

Overconsolidated clays are frequently fractured which will also affect the consolidation rate. The rate of subsidence in organic soils, especially peat, is often considerably lower than that estimated from oedometer tests due to creep (secondary consolidation).

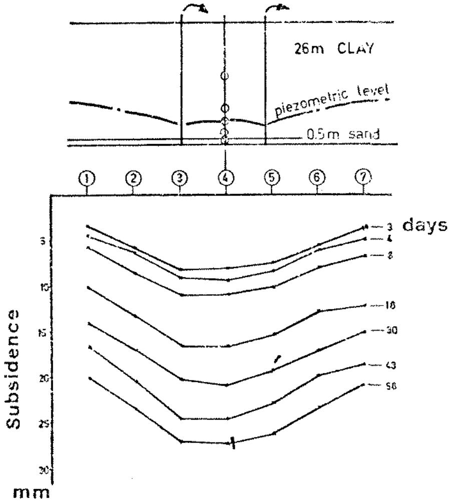

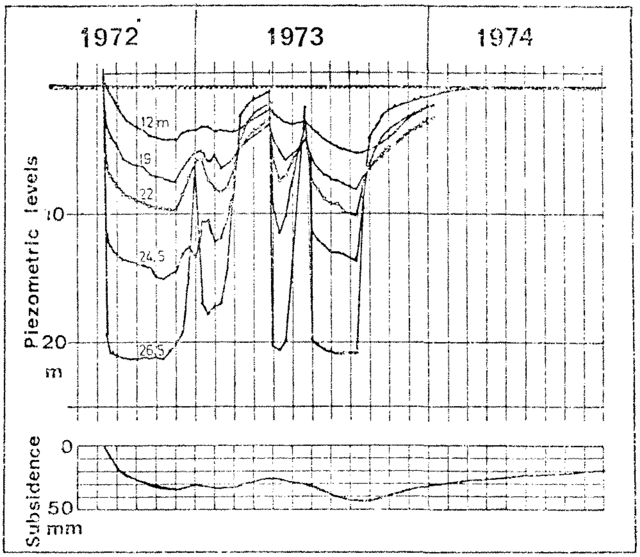

Fig. 5. Changes in piezometric levels in clay and subsidences during a pumping test in the Angered area, Gothenburg (Alte, 1976).

The groundwater level can be lowered by other factors than leakage to tunnels. The rebound after the glaciation (land upheaval) has resulted in an apparent lowering of the goundwater level which has caused problems in the Old Town ("Gamla Stan") in Stockholm. Also the reduced recharge of rain water, when streets, sidewalks and parking-lots are paved, affect the groundwater as discussed e.g. by Hellgren (1969) and Gustafson (1970). The groundwater level is also influenced by growing trees, deep excavations, drain pipes and sewer lines.

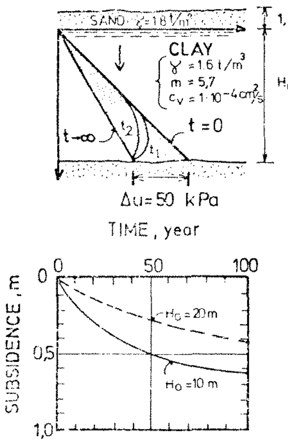

Fig. 6. Calculated subsidence versus time for different thickness of a clay-layer (Torstensson, 1975b).

Damage caused by subsidence

Lindskoug and Nilsson (1974) have investigated the damage from subsidence during the years 1966 to 1973 due to leakage to tunnels. Buildings are for example damaged when the differential settlement exceeds 1:200 à 1:500. Water and sewer lines rupture when the total subsidence is larger than about 15 to 30 cm (Broms, 1966, 1973). The damage caused by differential subsidences depends not only on the magnitude, but also on the rate of the subsidence and on the building material. Wooden houses as well as brick buildings, where lime has been used in the joints, can tolerate relatively large differential subsidences without damage (1:200 à 1:300). Brick structures, where cement mortar has been used can be severly damaged even by moderate differential settlements (1:300 à 1:500). Doors and windows become difficult to open and it is possible to "feel" that a floor is not level when the slope is larger than about 1:150. High rise buildings are often affected even when the differential subsidences are small, 1:500 to 1:100.

Uneven subsidence also changes the load and moment distribution in statically indeterminate structures as has been studied e.g. by Beigler (1976). The maximum bending moment in beams and columns can increase several hundred percent by differential subsidences. Even the direction of the moments can change. Timber piles and wooden grillages start to rot when they are exposed above the groundwater level. (Broms, 1973, Lindskoug and Nilsson, 1974). The bearing capacity of timber piles can be reduced already after a few months of exposure, particularly in areas where the ground temperature is high, e.g. below furnaces and where the groundwater has been polluted by sewage.

The load in the piles below a pile supported structure increases when the surrounding soil subsides (Broms, 1973). The piles will also carry part of the surrounding soil. This increase of the load in the piles, due to negative skinfriction, depends among other factors on the magnitude of the subsidence, the shear strength of the surrounding soil and on the thickness of the compressible layers. Test data indicate that the negative skinfriction for cohesive soils can be up to 20 to 25% of the effective overburden pressure. This means that the load increase due to negative skinfriction can be as large as 400 to 500 kN (40 to 50 Mp) for a 30 x 30 cm point bearing precast concrete piles driven through a 20 m clay layer, with the groundwater level located at 2.0 m below the ground surface. The axial load in a pile can thus be more than doubled due to negative skinfriction when the length exceeds 20 to 25 m.

Measurements on two instrumented precast concrete piles, which have been driven through a 40 m deep clay layer at Bäckebol about 20 km north-east of Gothenburg, indicate that the axial load in the piles has increased by 400 kN (40Mp) after six months because of negative skinfriction. The subsidence of the surrounding soil was small (2 to 3 mm). After two years, the increase was 550 to 600 kN (55 to 60 Mp) (Fellenius and Broms 1969, and Fellenius, 1971). After eight years, when a fill was placed around the piles, the negative skinfriction had increased to 800 kN (80 Mp).

Mainly the piles at the periphery of a structure are affected by negative skinfriction. The increase of the load in the center piles of a pile group will be small, when the piles are closely spaced, since the weight of the soil enclosed by the group is distributed between several piles. When the strength of a pile is exceeded at the pile point due to negative skinfriction, the behaviour changes from that of a point bearing to a friction pile. The subsidence of the pile will be approximately the same as that of the surrounding soil. The supported structure can then be damaged by the resulting differential subsidences.

Batter piles (raked piles), which are not vertical, can be damaged and may fail when the surrounding soil settles. Such piles are frequently used below road embankments to resist the lateral earth pressures in the embankments or below buildings or other structures to resist for example wind loads. Since the lateral resistance of a pile in soft clay is low, the lateral deflection of the pile will correspond to the subsidence of the surrounding soil. The maximum bending moment in the pile can be so large that the yield strength of the reinforcment is exceeded even when the subsidence is moderate as shown by Broms and Fredriksson (1976). Batter piles should be avoided when large subsidences are expected. Any lateral loads acting on a building can be resisted, for example by a concrete skirt which extends into the soil below the building.

Extensive damage on existing structures has been observed in Stockholm and in the surrounding suburbs as illustrated in fig. 7. At the Maria Square ("Mariatorget") in Stockholm (Tyrén and Sund, 1970), the groundwater level has been lowered with about 3 m since the turn of the century. This decrease of the groundwater level has been caused by water leakage to deep-lying tunnels and by reduced rechange water.

The subsidence that has occurred at Karlaplan in Stockholm is an example of moderate leakage into a deep-lying tunnel, causing extensive lowering of the groundwater level (Morfeldt et al, 1967). There a thin layer of sand and moraine is located at the bottom of a through in the bedrock which functions as a drain for the overlying up to 30 m thick layer of clay. Many of the structures, which were built in the area at the turn of the century, have been damaged. Water and sewer lines have ruptured. It has therefore been necessary to reconstruct the streets and the side walks.

A lowering of the groundwater level of up to 5 m has been observed around the Municipal Court Building ("Rådhuset") in Stockholm (Tyrén, 1968, Sund, 1970) which has partly been caused by deep-lying tunnels. The total leakage to the tunnels is about 70 m^3/day which corresponds to a theoretical subsidence of 20 cm/year from consolidation, if there is no infiltration of rain water.

Large subsidences have also been observed at Huddinge Center, located about 10 km south of Stockholm, which have been caused partly by a lowering of the groundwater level and partly by a fill which was placed over the

Fig. 7. Damage caused by subsidence.

area before the construction of the center. The height of the fill has gradually been increased in order to maintain the initial elevation of the ground surface. When the weight of the fill exceeds a critical value, which depends on the shear strength of the underlying soft clay, the soil and the piles below a building are laterally displaced, as illustrated in fig. 8. This occurs when the weight of the fill at foundation level exceeds 5.5 c_u, where c_u is the undrained shear strength of the soft clay as determined e.g. by vane or unconfined compression tests. A lowering of the groundwater level affects the settlements, not only outside a pile supported building, but also below the building so that a void is created below the basement floor.

Damage due to the lateral displacements of the subsoil can be prevented by using light backfill material, e.g. expanded shale ("Leca") or by supporting the fill on separate piles around the perimeter of the structure. These embankment piles will also reduce the negative skinfriction on the main structural piles below the building.

Prevention of subsidence

The factors which affect the subsidence and methods which can be used to prevent subsidences caused by water leakage into tunnels have been studied intensively in Sweden during the last ten years as well as the legal aspects of the problem (Jansson and Winqvist, 1976).

Precautionary measures can be taken: a) before the construction of a tunnel by avoiding areas which can be affected by subsidence, b) during the construction by e.g. pregrouting, c) after the construction of a tunnel by grouting in order to reduce the leakage or by artificial infiltration of water to maintain the pore water pressure in the compressible layers.

It is often possible to decrease the subsidences in soft clays by preloading. A fill is then placed over the area and is removed when the

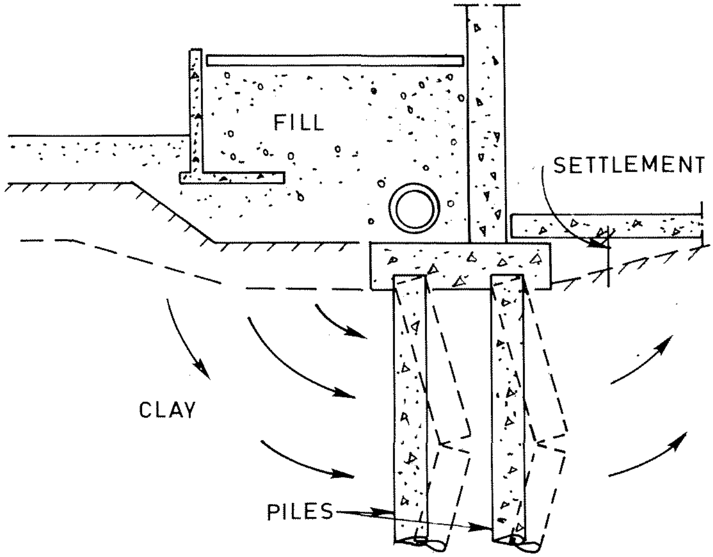

Fig. 8. Failure of piles at Huddinge Center due to lateral displacements.

subsidences have stopped which may require several years. The additional settlements from a lowering of the groundwater level will then be small as long as the increase of the load from the lowering of the groundwater level is less than the weight of the fill. Preloading can only be used where the compressible layers are relatively thin or the soil is stratified so that the subsidences occur relatively rapidly.

It is also possible to preload the compressible layers in advance by temporarily lowering the groundwater level by pumping from deep wells.

Subsidences due to a lowering of the groundwater level can also be reduced by removing part of the soil above the groundwater level. This method has been used for example in Linköping.

The leakage that can be allowed in a tunnel depends primarily on the landuse within the area affected by the lowering of the groundwater level. The maximum rate is often limited to one litre per second and kilometre of tunnel. Even this low rate can be excessive in sensitive areas. Experiences with tunnels in Gothenburg indicate that pregrouting in combination with postgrouting using cement can reduce leakage to only 0.2 litre per second and kilometre (Lysén and Palmquist, 1976). Good results have also been obtained with silica, lignin and plastic grouts (Bergman et al, 1975).

Attempts have been made to inject water into the pervious bottom layers through wells where a lowering of the groundwater level has occurred (Gedda and Riise, 1976). Fig. 9 shows the effect of tunneling and water injection on the piezometric level in an area in Gothenburg. Water has also been injected through boreholes into the fissured rock beneath the pervious bottom layers from pressurized tunnels (Bergman, 1976). This method has proved very effective.

It has been possible to control the groundwater level in a one-square kilometre large area at Botkyrka, located close to Stockholm, by injecting 3 litres of water per second through a 2-inch perforated steel tube.

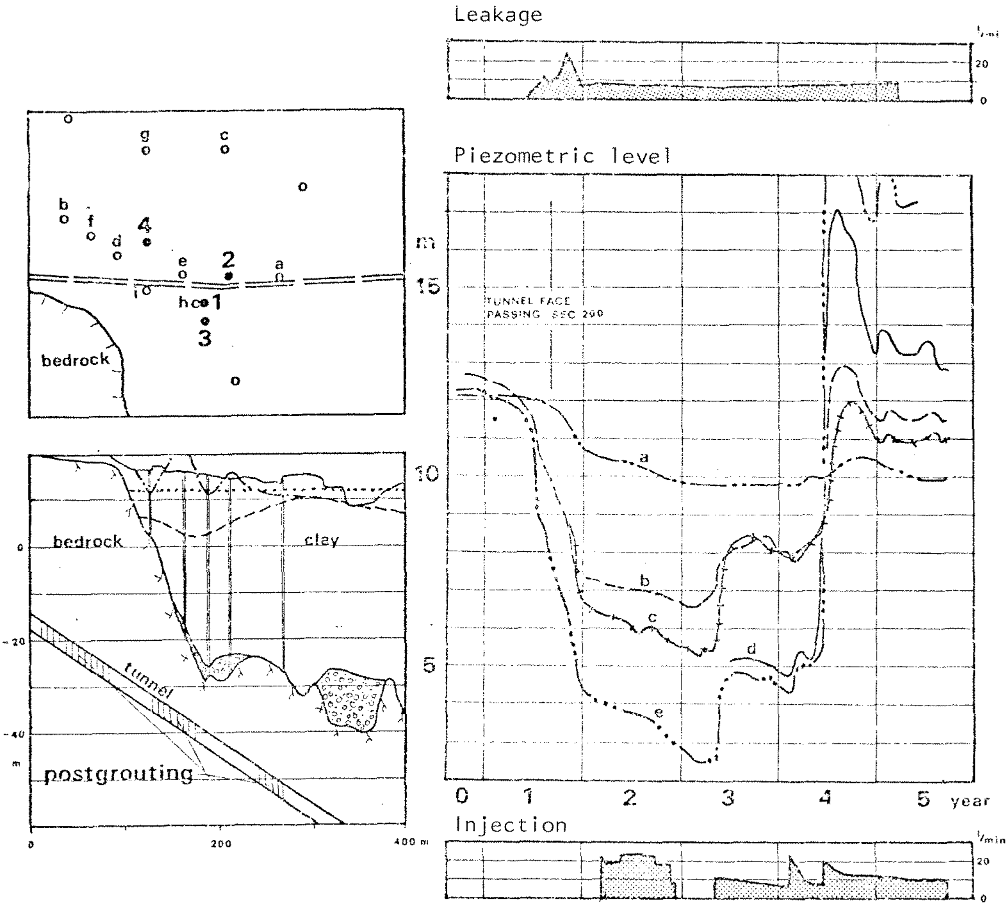

Fig. 9. Change in piezometric levels due to leakage to a tunnel and due to injection of water (Gedda and Riise, 1976).

a. Map and section over the area (1,2,3 and 4 are injection wells).
- - - - groundwater level before tunneling
— — — - " - before injection
—·—· - " - during injection.

b. Leakage into the tunnel, piezometric levels and injection capacities.

Clogging in and around injection wells has been observed. Both the injection rate and piezometric head in the aquifer are thereby reduced.

Tunnels have also been used as injection galleries. The piezometric level in the bottom layers can hereby be closely controlled through boreholes which are connected with a water reservoir. In one area, the total costs of a tunnel, when used as an injection gallery, was approximately one tenth the estimated costs of underpinning due to the subsidence (Andréasson et al, in print).

Reference areas are required in order to evaluate whether a change of the groundwater level is caused by a change of the climatic conditions or by a deep-lying tunnel, adjacent excavations or service lines etc. Such reference areas ("groundwater crosses") have been established close to Stockholm and Gothenburg which are representative of the virgin conditions within the regions.

For the planning of a region or a municipality it is necessary to have extensive information of the initial soil and groundwater conditions from boring and observation wells, so that the effects of a lowering of the groundwater level can be evaluated. It is essential that detailed engineering-geological and hydro-geological maps are available. A recent development in Sweden is land and foundation cost index maps, which show the relative cost in an area for different types of foundations. These maps are very useful in the different planning stages (Johansson and Lindskoug, 1971, Lindskoug and Nilsson, 1974).

References

Alte, B., 1976, Determination of compression properties in deep clay layer by controlled groundwater lowering. (In Swedish): Swedish Council for Building Research, Report R12:1976.

Andréasson, L., Svensson, G., Svensson, P-L., in print, Geohydrological activities in urban areas for environmental control: To be published at the 9th Int. Conference on Soil Mechanics and Foundation Engineering in Tokyo, July 1977.

Beigler, S-E., 1976, Soil-structure interaction under static loading, Thesis: Dept. of Geotechnical Engineering, Chalmers University of Technology, Gothenburg, Sweden 1976.

Bergman, G., 1976, Artificial recharge into rock. (In Swedish): Byggmästaren 1976, No 3.

Bergman, S.G.A., Lindman, K., Lundström, L., Söderman, P., Ullerud, S., 1975, Grouting of tunnels to prevent small-scale infiltration. (In Swedish): Swedish Council for Building Research, Report R25:1975.

Broms, B.B., 1966, Damage on structures due to settlements: Byggnadskonst, Vol. 58, No 8, pp 367-375, Stockholm. (In Swedish).

Broms, B.B., 1973, Subsidence - causes, consequences and precautionary measures: Royal Academy of Engineering Sciences, Report No 56, Stockholm. (In Swedish).

Broms, B.B., Redriksson, A., 1976, Failure of pile-supported structures caused by settlements: Proc. 6. European Conf. on Soil Mech. and Found. Engineering, Vol. 1. 2., pp 383-386, Vienna.

Carlsson, L., 1973, Evaluation of the hydraulic diffusivity in aquitards. (In Swedish): Chalmers University of Technology, Dept. of Water Supply and Sewerage, Publ. B 1973:3.

Carlsson, L., Kozerski, B., 1976, Injection of water into wells for investigation of limited aquifers: Nordic Hydrological Conference, Reykjavik 1976, p III-40 - III-51.

Fellenius, B.H., 1971, Negative skin friction on long piles driven in clay: Proc. Swedish Geotechnical Institute, No 25, 38 pp, Stockholm.

Fellenius, B.H., Broms, B.B., 1969, Negative skin friction for long piles driven in clay: Proc. 7. Int. Conf. Soil Mech. and Found. Engineering, Vol. 2, pp 93-98.

Gedda, C., Riise, P., 1976, Deep-infiltration of water into soil. (In Swedish): Report to the Swedish Council for Building Research, 1976-04-22.

Gustafsson, Y., 1970, Effects of the urbanization on the ground water balance: Nordisk Hydrologisk Konferens, Stockholm, Aug. 27-29 1970, Vol. 3, pp 91-99. (In Swedish).

Hellgren, A., 1959, Damage from changes of the ground water level: Stadsbyggnad, No 5, pp 117-123, Stockholm. (In Swedish).

Hellgren, A., 1969, Problems caused by a lowering of the ground water level: Svensk Naturvetenskap, Stockholm, pp 243-249. (In Swedish).

Jansson, B., Winqvist, T., 1976, Plannings of subsurface use: Swedish Council for Building Research, Document S 10:1976.

Johansson, B., Lindsloug, N-E., 1971, Land and foundation cost index maps. (In Swedish): Swedish Council for Building Research, Information B12:1971.

Lindskoug, N-E., Nilsson, L-Y., 1974, Ground water and urban planning. Report from STEGA 1966-73. (In Swedish): Swedish Council for Building Research, Report R20:1974.

Lysén, L., Palmqvist, K., 1976, Grouting of rocktunnels. (In Swedish): Swedish Council for Building Research, Report R4:1976.

Morfeldt, C-O., 1976, Rock-cavity and tunnels. (In Swedish): Swedish Council for Building Research, Report R15:1976.

Morfeldt, C-O., Nordin, P-O., Roosaar, H., 1967, Engineering geology with respect to the geological equilibrium: Byggmästaren, Vol. 46, No 6, pp 245-267, Stockholm. (In Swedish).

Sund, B., 1970, Lowering of the ground water level at "Rådhuset" in Stockholm: Byggmästaren, Vol. 49, No 6, pp 20-22, Stockholm. (In Swedish).

Torstensson, B-A., 1975a, Measurement of the pore pressure in the clay gives information of subsidences. (In Swedish): Byggmästaren, No 8, pp 15-19, 1975.

Torstensson, B-A., 1975b, Pore pressure sounding instrument: ASCE Speciality Conf. on In Situ Measurement of Soil Properties, Raleigh, North Carolina, 1975.

Tyrén, S., 1968, Problems with ground water in urban areas: Byggforskning 68, Swedish Council for Building Research, pp 87-99. (In Swedish).

Tyrén, S., Sund, B., 1970, Lowering of the ground water level at "Mariatorget" in Stockholm: Byggmästaren, Vol. 49, No 6, pp 17-19. (In Swedish).

Publication n°121 of the International Association of Hydrological Sciences
Proceedings of the Anaheim Symposium, December 1976

GROUNDWATER DEPLETION AND LAND SUBSIDENCE IN TAIPEI BASIN

Chian-Min Wu
Water Resources Planning Commission
Taipei, Taiwan, Republic of China

Abstract

In the previous paper presented at Tokyo Symposium on land subsidence (Hwang and Wu, 1969), the plots of subsidence against decline in artesian head and feedback computations of subsidence by Terzaghi's one dimensional consolidation model were used to verify that the decline in artesian pressure was the major cause of subsidence of the land surface in the Taipei Basin.

In 1968, a regulatory measure was implemented to limit the groundwater pumpage. As a result of this enforced groundwater use, the pumping center was shifted from the east side to the west side of the basin. Because of this shifting, both the groundwater depression center and the sharp subsidence-area moved correspondingly. This further suggests that the decline in artesian pressure was the major cause of the subsidence.

After the Tokyo symposium (1969), the subsidence of Taipei Basin has progressed considerably. This paper describes the subsidence conditions of the basin up to the year of 1976, and presents the state of knowledge of the land subsidence in the Taipei basin with special stress on the reliability of predicted subsidence which was forecasted in 1969. Through 5 years of subsidence observations it was possible to verify the magnitude of subsidence forecasted in 1969. As a result of this analysis, it was concluded that declines in piezometric pressure occur over a very large area such as the Taipei Basin, the simplest one dimensional Terzaghi's consolidation model may offer a reliable forecasting of the future subsidence.

Introduction

In many areas of the world, land subsidence has been observed to accompany extensive drawdown by excessive pumping from confined aquifers. The cause of the phenomenon is as yet well understood; however, it is believed that reduction of hydrostatic pressure in the aquifer increases the stress on confining clay layers, resulting in their being compressed. Several investigations indicated that the magnitude of land subsidence was controlled by the stratigraphic, and mechanical properties of the soil formation, state of preconsolidation, underground structure of the geological formation, change in the elastic or other physical properties of soils, clay mineral compositions and tectonic movement, etc. In the previous paper presented at Tokyo Symposium on Land Subsidence (Hwang and Wu, 1969), Plots of subsidence against decline in artesian head and feedback computations of subsidence by Terzaghi's one-dimensional consolidation model were used to verify that the decline in artesian pressure was the major cause of the subsidence of the land surface in the Taipei Basin, Fig. 1.

In 196ↄ, a regulatory measure was implemented to limit the groundwater pumpage. As a result of the imposition of strict limitation, the extracted center was shifted from the east part to the west side of the basin. Because of this shifting, both the groundwater depression center and the sharp subsidence area moved correspondingly.

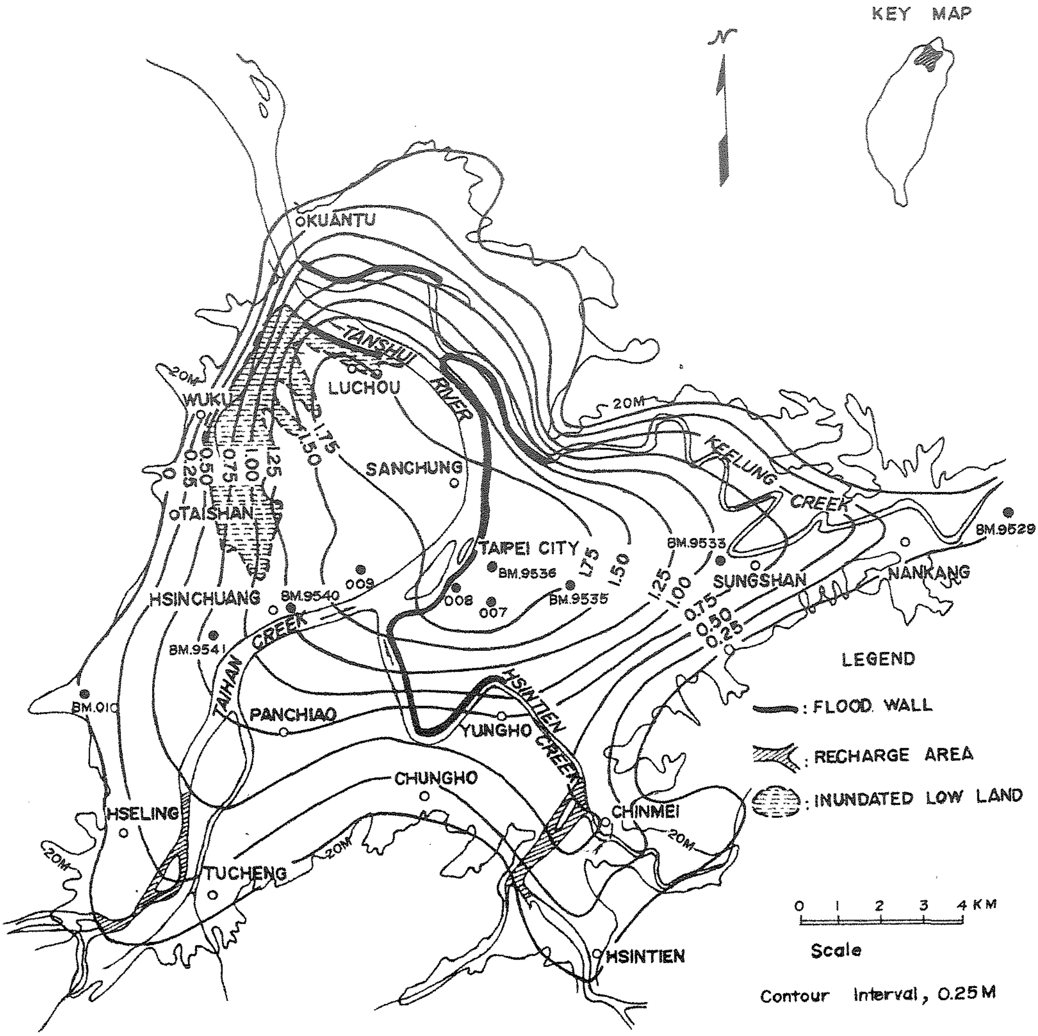

FIG. 1. LOCATION AND SUBSIDENCE IN TAIPEI BASIN, AREA CONTOURED ON DIFFERENCES IN SUBSIDENCE IN METER, 1957-1974

This again demonstrates that the pressure decline was the major cause of the subsidence.

After the Tokyo symposium in 1969, the subsidence of the Taipei Basin has progressed considerably. This paper describes the subsidence of the Taipei Basin up to the year of 1976, and presents the state of knowledge on the land subsidence with special stress on the reliability of predicted subsidence which was forecasted in 1969.

BASIN GEOLOGY

The basin is described as of tectonic origin associated with a downfaulted structure. Unconsolidated sediments of alternating layers of sand, gravel, clay and silt occupy the basin to depths of 280 m. The basin sediments are classified into four formations, the lowermost being the Tanawan formation (consisting of clay), followed in successive order by the Linkou formation, the Sungshan formation and an upper alluvium of recent age. The Linkou formation is made up of alluvial deposits, generally 90 to 130 m thick. It is divided into three units, the upper one is made up of mostly gravel, and the middle and lower units contain clay with intercalated sand and gravel layers. An impervious lateritic cover ranging from 0 to 3 m thick, forms an impervious copping on top of the Linkou formation.

The Sungshan formation is 40 to 60 m thick and consists mostly of clay, silt and fine sand with subordinate layers of coarse grained sediments. A recent alluvium overlies the Sungshan formation and underlies the land surface to a depth of up to 3 m and consists of sand and gravel.

The most extensive water bearing zone is found in the upper part of the Linkou formation at depths generally below 50 m from the land surface. Sand, gravel and cobble beds ranging from about 20 to 30 m thick are commonly associated with the upper part of the Linkou formation, while at lower depths the proportion of finer to coarse tends to increase. Although predominantly fine grained, three water bearing zones have also been identified in the Sungshan formation. The lowermost zone consists of an irregularly distributed sand and gravel, 0 to 13 m thick, and is believed to be hydraulically interconnected with the upper Linkou formation and with it they form the principal aquifer in the Taipei Basin. The intermediate and upper water bearing zones are found at depths of 30 to 40 m and 10 to 30 m below land surface respectively. They are made up mostly of fine to medium sand, and are widely distributed within the central part of the basin.

With the exception of the coarse grained sediments in the Linkou and lower sand and gravel unit of the Sungshan formation, which make up the principal aquifer, the overlying water bearing zones are estimated to have a limited potential of groundwater resources. The top of the principal aquifer occurs near or above sea level in the Hsintien Creek, Tahan Creek and Huang Creek areas. It becomes progresively deeper toward the central and northwestern parts of the basin where it reaches a depth of 70m or more below sea level. A reduction of aquifer thickness from over 50 m to less than 10 m is also evident toward the northwestern part of the basin. Locations having a maximum thickness and higher elevation indicate the source of the aquifer's sediments to be principally from the drainage area of Tahan and Hsintien Creeks and are coincident to the intake areas in which most of the aquifer's recharge originates.

The principal aquifer is largely made up of highly permeable sediments which are capable of yielding up to 4.5 m^3/min to an individual well. The values for the coefficient of permeability range from 30 to 420 m/day, and those for transmissibility from 1,000 to 7,800 m^2/day. The coefficient of storage is estimated to be 0.2 for unconfined and 1×10^{-4} for confined aquifer.

The compressibility of Taipei clay was mainly investigated on the undisturbed samples obtained from deep borings of Shungshan formation and its physical and engineering properties were given in the previous paper (Hwang and Wu, 1969; Wu 1973).

Pumpage

Wells have been used for domestic water supply in Taipei Basin since about 1895. Uncontrolled large scale development of groundwater started after 1957. In 1957 there were only 240 cased wells, 1765 open pits and 330 bamboo wells with total pumpage of 9 million m^3/yr. Since then the groundwater utilization has increased rapidly and reached an estimated maximum pumpage of 435 million m^3/yr from 3,846 wells in 1970. As a result of an imposition of strict limitation, the extracted water was reduced to 249 and 212 million m^3/yr in 1972 and 1974 respectively. Table 1 shows the estimates on pumpage by various use since 1964. The cooling use for air conditioning was once estimated to be 128 million m^3/yr or 29 percent of the total pumpage in 1970, but the said amount was reduced to 57 million m^3/yr in 1971 by installation of cooling towers. The basin has been developed into a metropolitan area containing the Taipei city as the center on the east half and the Taipei Hsien as a satellite community on the west half. The pumpages were originally concentrated in the Taipei City. Since 1970 the pumping center has moved from the Taipei City to the west part of the basin. Table 2, shows the area distribution of extracted water and the shifting of groundwater use since 1964.

Table 1. Type of Uses of Groundwater Pumpage (million m^3/yr)

year	Cooling	Industrial	Public Supply	Others	Total
1964	66(20%)	215(66%)	46(14%)	-	327
1970	128(29%)	109(25%))	110(25%)	88(21%)	435
1971	57(18%)	129(40%)	65(20%)	70(22%)	321
1972		114(46%)	65(26%)	70(28%)	249
1973		102(46%)	94(42%)	28(12%)	224
1974		82(39%)	84(40%)	46(21%)	212

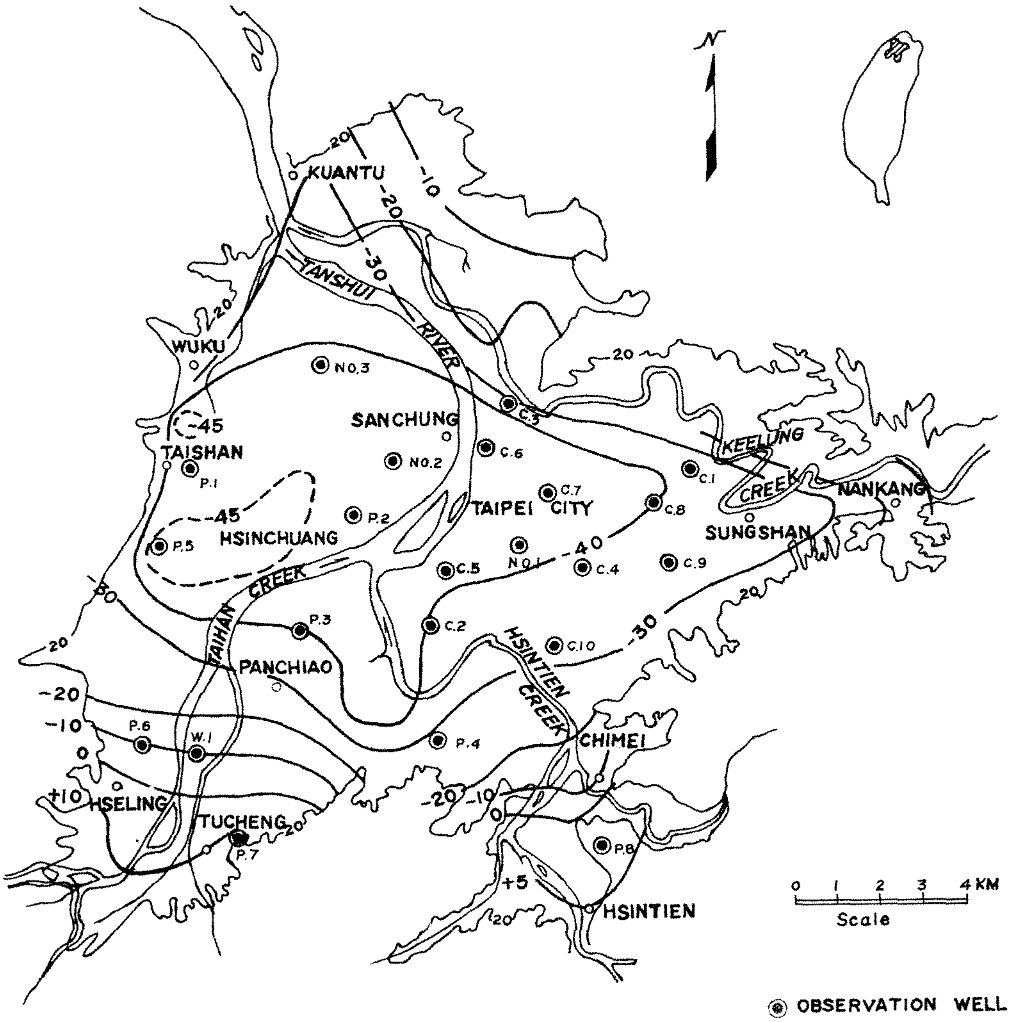

FIG.2. PIEZOMETRIC WATER LEVELS IN METER (MSL), IN TAIPEI BASIN, 1974

Decline of Artesian Head

In the Taipei Basin, the water table in the middle water bearing zone is mainly governed by the fluctuations of the stream flow, but has had little change from its initial position. On the contrary, the heavy pumping has lowered the piezometric head in the lower water bearing zone as much as 47 meters since 1957. In 1957, the piezometric head in the whole basin was within the range of +2.0 to +0.0 meters (MSL). It was reported that even the artesian wells could be seen in some parts of

Table 2. Area Distribution of Groundwater Pumpage (million m^3/yr)

Year	Taipei City Wells	Taipei City Pumpage	Satellite Community Wells	Satellite Community Pumpage	Total for basin	Total From Principal Aquifer
1964	1,158	187(57%)	1,097	140(43%)	327	295
1970	3,408	320(75%)	438	115(25%)	435	392
1971	1,233	118(37%)	1,630	203(63%)	321	289
1972	966	91(36%)	1,384	158(64%)	249	186
1973	756	51(22%)	1,246	173(78%)	224	-
1974	814	41(19%)	1,246	171(71%)	212	188

the basin. However, the increasing withdrawal of groundwater caused a continuous lowering of the artesian head. From 1961 to 1964, the artesian head declined from 11 m to 22 m below sea level with an average annual rate of -4m. In 1968, the static level was at the elevation of -30 m, forming a cone of depression under the city. From 1970 to 1974, because of shifting groundwater use, the cone of depression expanded and deepened to the depth of 45 m below the mean sea level, Fig. 2. The center of the cone of depression was moved to the western border and established two small closed depression centers with their elevation of -45 m.

In recent years, except at the western border area, the rate of artesian head decline has been gradually reduced due to the reduction in pumpage (Table 3.)

Subsidence Survey

The subsidence of Taipei Basin first was found through the 1955 releveling of a 1950 first-order level line. *It indicated that several centimeters of settlement had*

Table 3. Lowering of Piezometric Heads of Selected Wells, 1971-1974

Wells	* Piezometric Heads in 1974 below Sea Level(m)	Total Lowering From 1968 to 1974(m)	Annual Lowering in m. 1971	1972	1973	1974
No. 1	-37.94	-10.34	-3.63	-0.91	-0.10	+0.97
2	-42.97	-13.50	-5.40	-1.03	-2.64	+0.57
3	-42.24	-13.24	-5.80	-1.27	-2.43	+0.26
4	-41.11	-11.11	-2.30	-1.53	-2.35	-0.04
5	-44.50	-12.60	-3.50	-2.22	-2.35	-0.33
6	-46.41	-21.41	-4.55	-3.94	-2.32	-0.95
7	-46.99	-21.99	-4.63	-3.78	-3.81	-1.18
8	-46.84	-26.84	-4.17	-2.00	-5.22	-1.62
9	-40.14	-	-	-0.03	-3.82	-3.39
10	-32.52	-	-	-10.62	-5.43	-3.23

* Remark : Wells No. 1 to 3 are located in the Taipei city and the rest in the Taipei Hsien.

occurred in the Taipei City area. In order to determine the area of known and suspected subsidence, the first-order bench mark system established in 1950 was relevelled at least once in a year, releveled 15 times from Nov. 1955 to Oct. 1976. The accuracy of the results of releveling was tested by analyzing the probable error of the disclosures between forward and backward sighting from one bench-mark to another. Curve fitting of the frequency data shows that the problable error of recent releveling (1973 and 1975) is equal to $\pm$ 1.8 mm for a single observation, or the Gaussian constant h^2 is equal to $0.070\overline{2}$. The constant h can be defined by the error function

$$f(\xi) = \frac{h}{2\sqrt{\pi}} e^{-h^2\xi^2} \qquad (1)$$

An analysis of recorded subsidence in the Taipei Basin shows that the maximum daily subsidence between two adjoining bench marks may reach 0.3 mm. Since the local conditions limit the speed of observations, twenty-day interval is required for a series of releveling. The height-difference may consequently deviate by about 6 mm. Hence the probable error of the disclosure (± 1.8 mm.), for a single observation is considered to be adequate for the subsidence survey in the Taipei Basin. The volume of subsidence from 1957 to 1974 was 190 x 10^6 m^3, equivalent to nearly 5% of estimated gross pumpage in that period. Thus about 5% of ground-water pumpage in the 17-year period was obtained from compaction of the confined aquifer system. This represents reduction in the pore volume of the ground-water reservoir, but the reduction has been principally in the fine-grained aquitards, hence it should not affect appreciably the storage capacity or flow characteristics of the sand and gravel aquifers.

Subsidence.

The general pattern of the land subsidence in the Taipei City could be characterized as a sharp bowl with the bottom at the center part of the basin, Fig. 1. The most rapid rates of 28 cm/yr and 24 cm/yr at the stations of BM 9535 (East side) and No. 009 (West side) were observed in 1968, and their total depths of subsidence reached 1.17 m and 0.9 m respectively (1957-1974). In response to the change of pumpage distribution and enforced groundwater use, the rate of subsidence has gradually reduced and the center of the sharps subsidence area moved westward. In 1974 the largest rate of subsidence was 14 cm/yr located at western border where about 470 hectares of the low farm land has become perennially inundated, Fig. 1.

Prediction of Land Subsidence

The mechanism of land subsidence is complicated. However, consolidation theory may provide a framework for prediction of probable future subsidence under presumed conditions. The physical phenomenon of land subsidence in the Taipei basin is three-dimensional. However, it is believed that declines in piezometric pressure occur over a very large area and the changes of effective stress are essentially one-dimensional. Hence the result of the one-dimensional analysis is a good approxomation to the problem.

As was stated in the previous paper (Huang and Wu, 1969), a study was made to predict the future subsidence of the Taipei Basin due to groundwater depletion. In computing the ultimate subsidence, the consolidation equation

$$S = \frac{Cc}{1 + e_o} \ HoLog \ \frac{Po + \triangle P}{Po} \qquad \text{———————} \quad (2)$$

was used, where S is the amount of the ultimate subsidence, Ho is the initial thickness of soil layer, e_o is the initial void ratio, Po is the initial overbarden pressure, $\triangle P$ is the change in effective pressure and Cc is the compression index. Using the graphical method proposed by Terzaghi and Frohlich, the computed ultimate subsidence was further distributed to determine the relation-ship between the elapsed time and the degree of consolidation. Table 4 showsa typical result of the subsidence computations using well log data of Ambassador Hotel, about 1 km north of BM9536, and the recorded rate of piezometric head change. As was stated in the previous report, the graphs of computed subsidence is about 75% less than the actual. This was expected because subsidence in the cohesiveless strata was not taken into consideration. Again, other causes such as loading at land surface, vibrations at or near land surface, compaction due to seepage water and tectonic movement might contribute appreciably to the overall land-subsidence. As subsidence due to these factors can not be determined quantatively in 1969-prediction, the ratio of the computed subsidence to the observed subsidence has been used to adjust the magnitude of the computed future subsidence. This over-all calibration, though is not backed up by any theory, is considered to be justified. Following surveys in 1971 to 1976 showed that the forecasted values were fairly close to the observed values, the differences were is the range of ± 2 cm, (see Table 4).

When the prediction was made in 1969, the piezometric head at the center of the basin was only 10 ± 5 meters above the top of the confined aquifer. It was assumed that the drawdown would continue until the piezometric head fell below the top of the aquifer. Since then, continued drawdown would interfere with pumping operations, and the peizometric head in the confined aquifer would stablize itself

Table 4. Comparison of forecasted and observed subsidence

Year	forecasted subsidence m	observed subsidence m	Difference m
1961	0.00	-	-
1970	1.32	-	-
1971	1.48	1.50	0.02
1972	1.59	1.60	0.01
1973	1.64	1.65	0.01
1974	1.73	1.72	-0.01
1975	1.77	1.78	0.01
1976	1.83		
1981	2.20		
Ultimate	2.30		

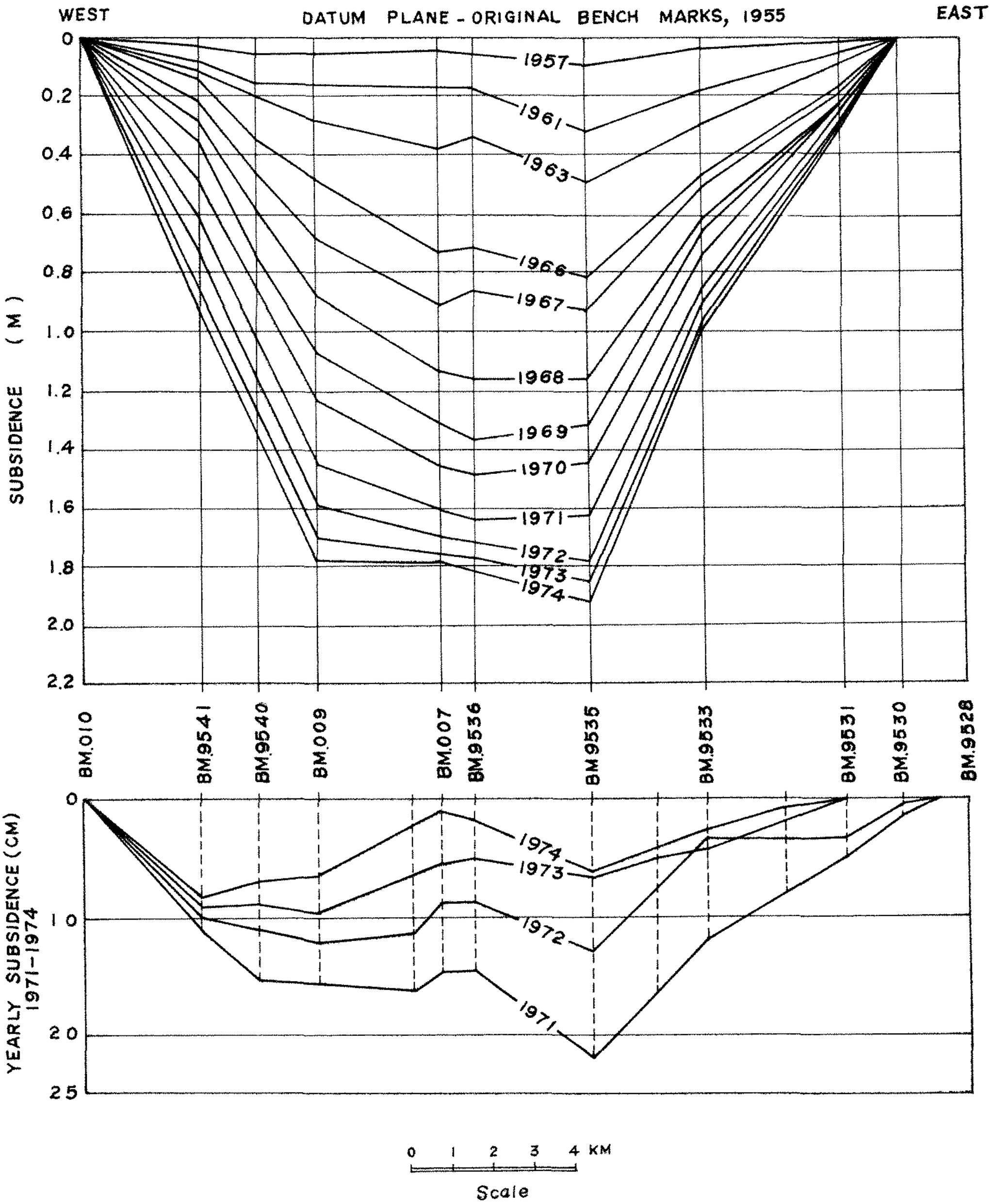

FIG.3. PROFILE ACROSS BENCH MARKS IN TAIPEI BASIN

automatically. Atomospheric pressure would be prevailed between the lower face of the aquitard and the water table in the aquifer. With these assumptions, it was estimated that the additional amount of subsidence due to groundwater drawdown may reach 50 to 80 cm over a period of 10 years for the downtown Taipei and 80 to 200 cm for the surrounding area respectively. Even if the drawdown of the confined aquifer were to cease, the land subsidence would continue to settle for several years.

In the paper entitled "Groundwater Depletion and Land Subsidence in Taipei Basin" in 1969, the subsidence due to cohesiveless materials was neglected. Though this difference might be covered by the model calibration, however, comparison of the volume of subsidence and the total pumpage during the period from 1957 to 1974 showed that only 5% of ground water pumpage was obtained from the compaction of the confined aquifer. Hence the reduction in the pore volume could be neglected. This again shows that the settlement has been principally in the fine-grained compressible aquitards. In the Taipei basin, though further predictions of future subsidence by two dimensional and three-dimensional models were performed by various authors, however, historical data were not long enough for verifcation. Hence on the basis of presently available data it may be concluded that the simplified one-dimensional model may be used to estimate the location, rate, and magnitude of future subsidence of the land surface with the applications of the laboratory physical properties of well logs and field drawdown data.

References

J.M. hwang and C. M. Wu, "Land Subsidence Problems in Taipei Basin", Proc. Intnl. Symposium on Land Subsidence, Tokyo, 1969.

C. M. Wu "Groundwater Depletion and Subsidence Problems in Taipei Basin", Proc. Intnl. Symposium on Development of Ground Water Resources, Vol. 1. 1973 pp II-b 17-28

Publication n°121 of the International Association of Hydrological Sciences
Proceedings of the Anaheim Symposium, December 1976

LAND SUBSIDENCE RELATED TO BROWN COAL OPEN CUT OPERATIONS LATROBE VALLEY, VICTORIA, AUSTRALIA

Claus Sax Gloe
Principal Geologist
State Electricity Commission of Victoria

Abstract

The winning of brown coal for the production of electrical energy in Victoria has involved the development of large and deep open cuts in the Latrobe Valley. The brown coal occurs as thick seams beneath a thin cover of sands and clays in the Tertiary Gippsland basin, one of the coastal artesian basins of Australia. In order that the coal may be excavated under safe operating conditions, it is necessary to reduce the piezometric levels of aquifers beneath the coal seams.

The normal ground movements associated with open cuts, particularly in relatively unconsolidated sediments, have been experienced, but, in addition, widespread subsidence has taken place. The field evidence indicates that the increased effective stresses resulting from the widespread lowering of artesian pressures and of groundwater levels adjacent to open cuts have induced consolidation of strata and so have been responsible for the regional subsidence.

Introduction

The Gippsland basin covers an area of some 40 000 km^2. Four-fifths of this area is located off-shore and the remaining fifth in the Gippsland region of south-eastern Victoria. The off-shore area contains a number of oil and gas fields, while the on-shore portion includes an area of some 800 km^2, known as the Latrobe Valley Depression, where major deposits of brown coal occur beneath a thin cover of overburden.

During 1975/76, about 85% of Victoria's electrical energy requirements were derived from power stations burning brown coal won from open cuts in the Latrobe Valley. Over that period, coal production reached 28 000 000 tonnes while 6 500 000 m^3 of overburden was removed. The development of each of the open cuts has been accompanied by significant vertical and horizontal movements, both within the excavations as well as in surrounding areas.

Investigations of these movements and of the factors responsible have been carried out for many years. In 1970, the investigations were intensified at Morwell, the second and largest of the major open cuts being operated in the Latrobe Valley, in collaboration with Golder, Brawner and Associates Ltd of Vancouver.

The area affected by subsidence is now regional in extent and has been influenced by the reduction in artesian and groundwater pressures found necessary to achieve stability within and around the open cut.

Geology

The Gippsland basin developed in the off-shore area in Upper Cretaceous times with the deposition of largely lacustrine and fluviatile clays and sands with a number of brown coal seams. The subsiding area gradually moved westwards and lithologically similar sediments were deposited in the on-shore area in Lower Tertiary times (Fig 1).

Within the Latrobe Valley Depression, up to 700 m of Tertiary sediments, including thick brown coal seams and some volcanics towards the base, were deposited (Gloe, 1975). Over most of the area, these strata, named the Latrobe Valley Coal Measures, overlie Lower Cretaceous arkoses and shales. The coal measures include three groups of major coal seams. Separating and underlying the seams are clays and sands. The sands carry artesian waters - in fact the Gippsland basin is one of the coastal artesian basins of Australia.

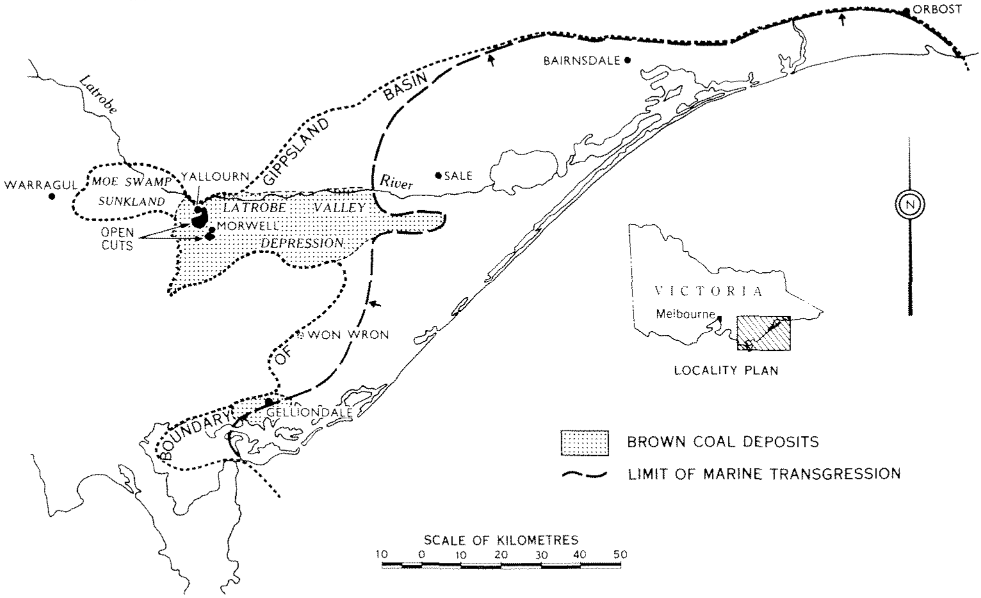

Fig. 1 Gippsland Basin

The oldest seams belong to the Traralgon Formation, but occur only in the eastern half of the depression. They are overlain by the Morwell Formation which includes a complex system of thick coal seams. In the Morwell area, individual seams are up to 165 m thick, while at Loy Yang, combinations of Morwell seams reach 230 m in thickness. The Yallourn Formation includes the youngest or uppermost coal seams. The main seam has a maximum thickness of 100 m and is overlain in downwarped areas by up to 100 m of clays.

In Late Tertiary times, the deposits were tilted, folded and faulted. Extensive erosion followed, virtually to the stage of peneplanation. In Plio-Pleistocene times, a thin cover of mainly clays and silts was deposited on the eroded surface.

The earth movements caused the development of a number of major monoclinal structures considered to reflect faulting in the basement rocks. Only minor faulting has been observed within the coal measures, but each open cut has shown the coal to be strongly jointed. The faults and joints provide conditions of potential instability in permanent batters and operating faces.

In the Yallourn open cut, the Yallourn seam averages 60 m in thickness and underlies some 10 to 15 m of younger overburden. Beneath the Yallourn seam are some 120 to 150 m of sands and clays overlying a further thick coal seam.

The Morwell 1 seam is being excavated in the Morwell open cut. Its average thickness ranges from 90 to 130 m, with a cover of 12 to 15 m of overburden (Fig 2). Underlying the coal seam are 15 to 23 m of sands and clays followed by the Morwell 2 coal seam, which is up to 50 m thick in this area. A further sequence of clays and sands, including an almost completely weathered layer of basalt and a thick basal silty gravel, totalling some 140 m in thickness, underlie the Morwell 2 seam and rest unconformably on Lower Cretaceous basement.

A reconstruction of the stratigraphic sequences considered to have existed prior to peneplanation indicates that considerable thicknesses of sediments were eroded in some areas. It is estimated that 120 to 150 m of clays and coal were eroded from above the present top of the Yallourn seam at Yallourn open cut, while, in the area of the Morwell open cut, 240 to 300 m of clays, sands and brown coal were eroded (Fig 2).

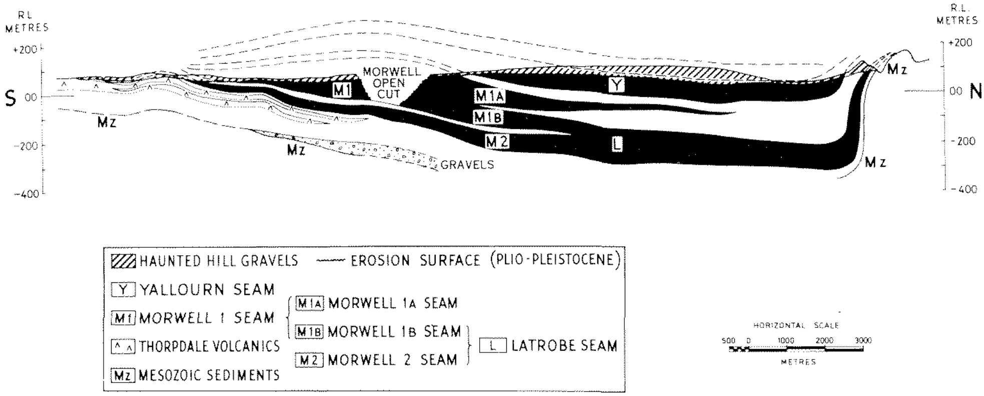

Fig. 2 Reconstruction of pre - erosional stratigraphy

Underground Water

Unconfined groundwaters are present over most of the area, but quantities are mainly small and the quality brackish. These waters are in contact with the joint or fracture waters in the uppermost coal seam and are therefore also under atmospheric pressure.

Confined or pressure waters are found in the sands separating or underlying coal seams, and in fresh basalt flows. Prior to the development of Morwell open cut, waters struck in bores in low-lying areas flowed at the surface, sometimes under considerable head.

Strong flows of water were encountered at depths exceeding 60 m below the Yallourn seam in the Yallourn open cut. In general, thick clays and sandy clays underlie the seam, and, although up to 2 m heaving of the floor occurred, the weight of clays overlying the aquifers was sufficient to withstand the hydrostatic pressures.

Some 8-9 m of medium to coarse-grained, poorly sorted and highly permeable sands, known as the Morwell 1 aquifer, occur below the Morwell 1 seam (Barton, 1971). The sands are irregular and typical sheet deposits. Along the northern edge of the open cut, the original piezometric levels of the Morwell 1 aquifer stood at +60 AHD, a height some 150 m above the level of the aquifer in that area.

The Morwell 2 aquifer is made up of several irregular zones of sand beds down to a depth of some 35 m below the Morwell 2 seam. The sands are stratigraphically interconnected, but vertical "leakage" between sand layers also occurs. There is also evidence of vertical leakage between the Morwell 2 and Morwell 1 aquifers - partly due to numerous boreholes and to the fracturing which accompanied heaving of the floor of the open cut, but also naturally as part of a leaky aquifer system.

Before open cut operations commenced, it had been calculated that the weight of coal and clay would be unable to withstand the artesian pressures, once a working level had been established to an area 300 m across at a depth of some 65 m below the original surface. As this still left some 50 m of coal above the base of the seam, it was clear that Morwell 1 aquifer levels would need to be progressively lowered as the open cut was developed in depth (Gloe, 1967).

The main program of lowering piezometric pressures, frequently called dewatering, commenced in 1960. By initial use of free-flow bores and subsequently pumping bores, pressure levels were lowered as the open cut was deepened. On several occasions, large scale heaving, accompanied by uncontrolled breakthrough of water from below, took place in the floors of newly opened up levels.

Subsequent investigations established that the pressures from the Morwell 2 aquifers, although already substantially reduced through leakage, would require further lowering to ensure safe operating conditions. This reduction was achieved, again initially through free-flow bores, and then pumping bores with capacities of up to 160 lps.

The maximum rate of pumping from the Morwell 2 aquifers was 1160 lps at which time the total pumping rate was 1320 lps. Once piezometric levels of both aquifers had been reduced to a safe level, pumping rates were reduced to a rate which would just maintain "operational target levels". The present yield from bores is 1055 lps of which 925 lps is derived from Morwell 2 aquifers and 130 lps from Morwell 1 aquifer. These rates have been maintained for one year, but will need to be increased as the open cut develops to the west. The total quantity of artesian water pumped from Morwell open cut up to June 1976 was 200 000 Ml.

Water levels in observation bores, generally westwards from Morwell open cut, are measured at regular intervals. No Morwell 1 aquifers were found to the east and south-east of the cut and the interseam sands gradually cut out towards the north.

The piezometric surface of the Morwell 1 aquifer, as at June 1976, is shown on Fig 3. The Morwell 2 aquifer levels have a generally similar pattern. The levels should be compared with an original gently sloping surface with values of +60 AHD at Morwell open cut and rising to about +65 AHD in the west. Along portion of the Morwell anticline, south-west from the cut, the piezometric level has now dropped below the level of the Morwell 1 aquifer and bores suck air when the dry sands are encountered.

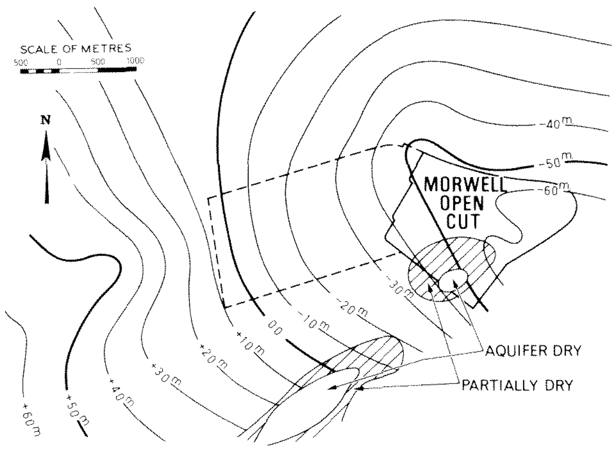

Fig. 3 Piezometric surface of Morwell 1 aquifer

Investigations of recharge and intake areas have included carbon dating of water samples. The youngest water from near the edge of the basin was found to be 2200 years old, while the water pumped from Morwell open cut gave values of up to 23 500 years for Morwell 1 aquifer water and 13 800 years for Morwell 2 aquifer. These ages conform with the concept of a multi-aquifer and aquitard, or leaky aquifer system, which has a large volume of water in storage, but in which the upper aquifers at least are not replenished by rapid infiltration of rainwater in intake areas. It is considered that much of the water pumped from Morwell 1 aquifer has been derived through leakage from lower aquifers, with some water derived from the compaction of aquitards.

Mechanical Properties of Brown Coal and Associated Strata

Properties of these strata were described by Gloe, James and McKenzie (1973). Brown coal was shown to be a highly preconsolidated organic material with a low bulk density (1.13 g/cc) and very high moisture content (up to 200% as expressed on an engineering basis).

For purposes of calculating consolidation settlements where the consolidation pressures were less than 1300 kPa, the following values of coefficient of volume decrease (m_v) were assigned:

Morwell 1 seam 0.2 sq cm/kN at top of seam to 0.1 sq cm/kN at base of seam. Morwell 2 seam 0.1 sq cm/kN.

The Morwell 1 aquiclude is a layer 3 to 13 m thick of stiff grey preconsolidated silty clay with a bulk density of 1.8 g/cc and m_v 0.2 sq cm/kN.

The Morwell 1 aquifer ranges from coarse sand with fine gravel to silty fine sand. It is dense to very dense and relatively incompressible. In the area of the open cut, the Morwell 2 aquifer sands are generally thicker and hence have a higher transmissibility than those of the Morwell 1 aquifer. In other respects, the sands are very similar.

The Morwell 2 aquiclides and aquitards are mainly silty clays and silts with properties similar to those of the Morwell 1 aquiclude.

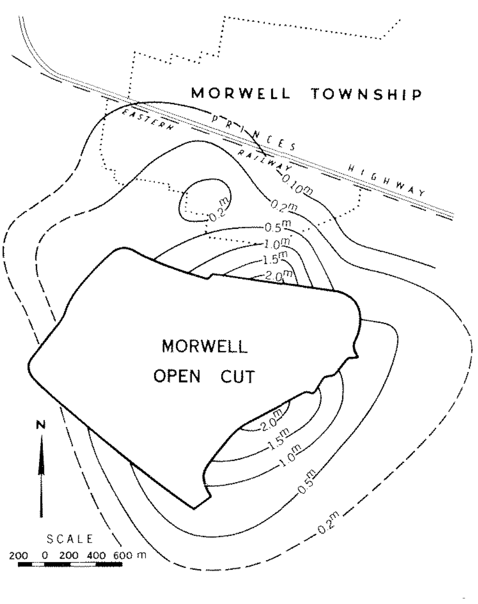

Fig. 4 Horizontal displacement adjacent to Morwell open cut

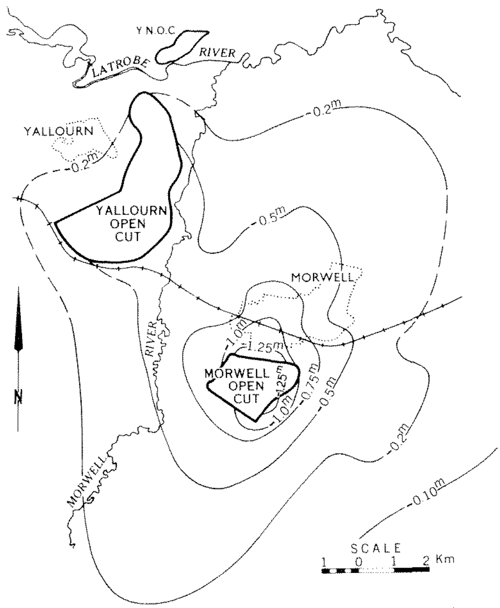

Fig. 5 Regional subsidence in the Yallourn - Morwell area

Extent of Movements

Surface movements, both inside and outside the Yallourn and Morwell open cuts, have occurred ever since excavation commenced. Regular surveys are carried out to determine the amounts of these movements.

Block movements in the permanent batters and outside the Yallourn open cut were largely overcome by flattening the originally relatively steep permanent batters. The maximum movements of survey marks along the edge of the open cut amounted to 1 m horizontally and 1 m subsidence.

Movements at Morwell exceed those at Yallourn open cut, mainly because of the dewatering operations and greater depth of the open cut. At the top of the northern and eastern batters, the horizontal movement has reached as much as 2.3 m and the vertical 2.0 m.

The movements on the boundaries of the open cuts have gradually spread outwards, with subsidence now affecting the whole of the Yallourn-Morwell area and extending eastwards into the Loy Yang area, some 20 km east of Morwell. Contours of horizontal movements in the Morwell area and of subsidence in the Yallourn-Morwell area are shown on Figs 4 and 5 respectively. The pattern of horizontal movement is roughly concentric about the floor of the open cut, and the 20 cm contour is at present stationary and approximately 1050 m northwards and 1000 m eastwards from the edge of the open cut. By March 1976, the 20 cm and 50 cm subsidence contours were located 7.8 km and 4.5 km, respectively, north of Morwell open cut and the 50 cm contour embraced much of Morwell township.

The C line of survey marks passes through the southern portion of Morwell township at right angles to the northern edge of the open cut. Horizontal displacement and subsidence profiles along the C line are shown on Fig 6.

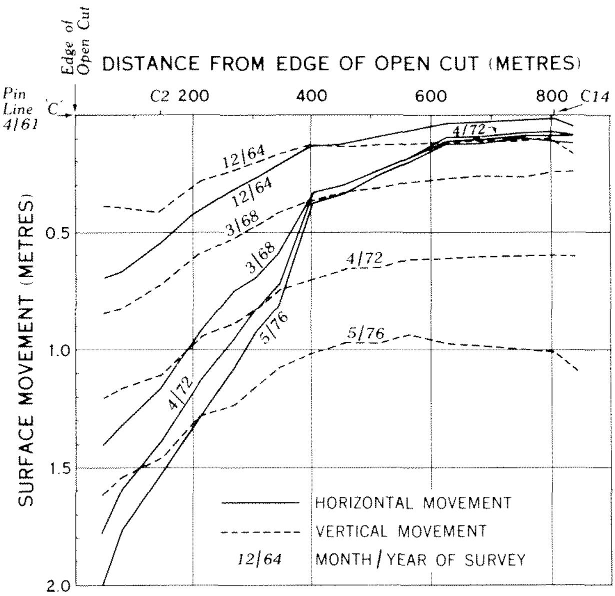

Fig. 6 Horizontal displacement and subsidence profiles on the C - line

By 1976, the total southerly displacement of a point adjacent to the edge of the open cut was 2.0 m, but at a distance of 400 m from the cut was only 0.35 m. Beyond that distance, horizontal movements are relatively small. Similar patterns of movements are found on other pin lines. Horizontal ground strains are greatest at the southern fringe of Morwell township (300 to 400 m from the edge of the cut). Values do not generally exceed 0.5%, but locally reach 0.7%. At distances of 600 m from the open cut, the strains are less than 0.05%.

At the edge of the open cut, subsidence commenced at a slower rate and at one stage was little more than half that of horizontal movement. However, the steady rate of subsidence has been maintained while horizontal movements are decreasing as the floor of the open cut extends westwards. At 200 m from the northern edge of the cut, vertical and horizontal movements are now roughly equal, while at 800 m vertical movements exceed horizontal by 0.9 m (Fig 6).

Causes of Movement

Factors contributing to earth movements were discussed by Gloe, James and Barton (1971). Apart from geometry of the open cut and geological structure, the significant factors influencing movements in the area around Morwell open cut are pressure relief and reduction in artesian and groundwater pressures. Pressure relief movements consist of uplift of the floor of the open cut accompanied by an inward and downward movement of the permanent batters. Uplift is increased when excess water pressures exist in aquifers below the floor.

Pressure relief is responsible also for movements outside the Morwell open cut. As stated above, the major horizontal movements occur within a distance of 400 m from the edge of the open cut. It is concluded that within this zone horizontal movements are due to pressure relief as well as to response to differential subsidence. Outside the 400 m zone, the movements are considered to have resulted from the slope of the subsidence profile.

The *reduction in artesian and groundwater pressures* has been in progress since 1960. The piezometric levels of the Morwell 1 (Fig 3) and Morwell 2 aquifers have been lowered within the open cut by 125 and 120 m respectively and are being held at those levels.

The groundwater table has been lowered simultaneously, mainly by natural drainage through joints intersecting batters, aided by horizontal bores up to 250 m long drilled at the toes of permanent batters. It is estimated that this lowering of the water table extends for distances up to 600 m from the edge of the Morwell open cut.

The relationship between surface movement and piezometric levels is shown on Fig 7. The Morwell 1 aquifer levels in bore 1388 M dropped at a steady rate of 13 m per year between 1964 and 1972, with only minor changes in level to 1976. Although virtually no water was extracted from the Morwell 2 aquifer until 1970, water levels had dropped by over 40 m by that time, presumably through leakage into Morwell 1 aquifer. After 1970, water levels in Morwell 2 aquifer dropped by 15 m per year until 1975 and have since remained steady.

Fig 7 indicates that vertical and horizontal movements at Pin C2 (150 m north of the open cut) follow a generally similar pattern. However, at C14 (800 m north of the open cut and beyond the influence of pressure relief), horizontal movement remains minimal, while steady subsidence parallels that occurring at C2 and is considered to reflect the lowering of artesian water pressures.

At a point about 5 km north of the open cut, while no horizontal movement has been discerned, steady subsidence at the rate of 0.04 m per year has occurred since 1970, with total settlement since 1960 of 0.5 m.

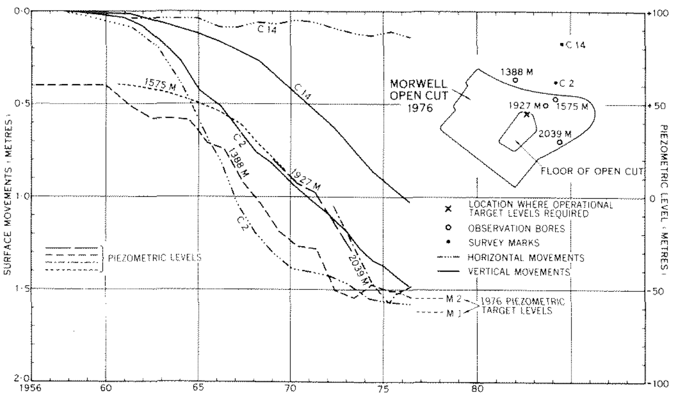

Fig. 7 Relationship of piezometric levels and surface movements on the C - line

Predicted Future Movements

Allowing for the effects of geometry of the open cut and geological structure, it is concluded from the pattern of horizontal and vertical movements that (a) horizontal movements are basically due to pressure relief and are mainly confined to a zone up to 400 m wide surrounding the open cut; (b) the increased effective stresses resulting from the widespread lowering of artesian pressures and of groundwater levels adjacent to open cuts have induced consolidation of strata and so been responsible for the regional ground subsidence taking place in the Latrobe Valley.

Areas of major land subsidence due to groundwater extraction listed by Poland (1970) all contained compacting deposits which were presumed to be normally consolidated. The sediments in the Morwell area have been overconsolidated. Laboratory tests have indicated that the effective stresses resulting from the reduction of aquifer pressures will not exceed the preconsolidation pressures. Consolidation, therefore, is taking place on the recompression portion of the field consolidation curve. The resulting subsidence is only partially complete and will continue for many years.

With the full development of Morwell open cut, ultimate settlement values are predicted to reach approximately twice those which have occurred to 1976 in the main Morwell township area. Values of up to 3 m are expected at the southern edge of the town and 1 m at the northern boundary. Present subsidence contours will increase towards the west and the 3 m contour will be located west of the Morwell River (about 3.5 km west of the present floor of the open cut).

Subsidence will not extend beyond the limits of the Latrobe Valley depression as basement consists of strong and largely incompressible rocks. However, some subsidence may extend into the Moe Basin, a probable intake area, as well as to the east. At Loy Yang, where the next major open cut will be located, and where evidence of subsidence has already been observed, high pressure waters occur in fine sands separating the several coal seams involved in this project. The designed depth of the open cut is 200 m and the required lowering of piezometric levels is likely to result in even greater settlements than will occur at Morwell. Ultimately, the settlement basins at Morwell and Loy Yang are likely to coalesce.

Acknowledgements

The author wishes to thank the State Electricity Commission of

Victoria for permission to publish this paper, and also the many people involved in the compilation of data presented.

References

Barton, C M, 1971: The Morwell Interseam Sands. J Geol Soc Aust, 17, pp 191-204.

Gloe, C S, 1960: The Geology of the Latrobe Valley Coal Field. Proc Australas Inst Min Metall, 194, pp 57-125.

Gloe, C S, 1967: The Lowering of the Artesian Water Pressure Surface in the Vicinity of the Morwell Open Cut. Inter Assoc Hydrogeol Cong, Hannover 1965, vii, pp 193-196.

Gloe, C S, James, J P, and Barton, C M, 1971: Geotechnical Investigations for Slope Stability Studies in Brown Coal Open Cuts. Proc 1st Aust-NZ Conf Geomech, 1, pp 329-336.

Gloe, C S, James J P, and McKenzie, R J, 1973: Earth Movements Resulting from Brown Coal Open Cut Mining - Latrobe Valley, Victoria. Subsidence in Mines, 4th Ann Symp, Illawarra Branch, Australas Inst Min Metall, 8, pp 1-9.

Gloe, C S, 1975: Latrobe Valley Coal Field, in Economic Geology of Australia and Papua-New Guinea. 2 Coal Australas Inst Min Metall, pp 345-359.

Poland, J F, 1970: Status of Present Knowledge and Needs for Additional Research on Compaction of Aquifer Systems. Land Subsidence, Proc Tokyo Symp 1969, IASH-Unesco, Vol 1, pp 11-21.

Publication n°121 of the International Association of Hydrological Sciences
Proceedings of the Anaheim Symposium, December 1976

THE CHARACTERISTICS OF SUBSIDENCE DUE TO UNDERGROUND COAL MINING AT NEWCASTLE, NEW SOUTH WALES

W. A. Kapp,
Research Engineer,
Rock Mechanics and Strata Control,
The Broken Hill Proprietary Co. Ltd./Australian Iron & Steel Pty. Ltd.,
Wollongong,
New South Wales.

Abstract

Ground movements occur when fluids or minerals are mined from beneath the surface and a subsidence bowl or trough subsequently forms over the extraction. The characteristics of all subsidence bowls and troughs include the vertical and horizontal displacements of points on the surface, the change in the slope of the surface and the tensile and compressive strains. The magnitudes and development of these elements vary with the depth of cover, the geological environment and with the extent and rate of mineral extraction.

Subsidence surveys are being carried out over areas of underground coal extraction in the Newcastle district, 160 km north of Sydney. The investigations in one area showed the development of the subsidence, slope and strain at the surface as the extracted area increased. The maximum principal strains were determined at various stages of extraction.

The characteristics of the subsidence trough over coal extraction were similar to those of the subsidence bowl over extraction of oil at Long Beach, even though the maximum subsidence at Long Beach was 8 times greater.

Introduction

A gradual subsidence basin forms at the surface when ground water, gas or oil is extracted. The mining of coal or other tabular deposits where the seam thickness is small in relation to the depth of cover also causes gradual subsidence movements. The surface does not necessarily fracture or fissure.

A subsidence basin has certain characteristics which can be related to particular geometries of extraction and geological conditions. A program of subsidence investigations is being carried out in the Newcastle and in the Southern Coalfields, New South Wales. The aim is to investigate the nature of subsidence and its effects on the surface and to enable coal extraction to be planned to produce the desired subsidence effects on the surface, and to take into account any surface structures requiring protection.

Subsidence surveys are made along lines of stations over the extracted area at regular time intervals. One line of stations was over pillar extraction from a seam 2.0 m thick with a depth of rock cover of 116 m. The maximum subsidence was 1.1 m and the maximum strains were 4.0 mm/m tension and 5.8 mm/m compression. Associated with these strains were the changes in slope and the curvatures. The development of the principal strains and their directions was related to the progress of mining. The value of strain calculated varies with the measured distance on which the calculation is based.

The maximum subsidence due to oil extraction at Long Beach was 9 m. Although Newcastle coal extraction does not produce such gross subsidence, comparison of profiles should indicate if controls are similar.

Characteristics of Trough Subsidence

a) General features

When an underground seam of coal is mined over a wide area the immediate roof will collapse. Movement is transferred through to the surface and increases to a finite limit as the ratio of the width of the extracted area w to the depth of cover h increases to a certain value.

Subsidence is a three dimensional phenomenon which is usually simplified in two dimensions. The characteristic elements associated with the geometry of a subsidence trough are shown diagramatically in Fig. 1a. The main features of subsidence are vertical displacement, change in ground slope, and the strains which develop at the surface.

The different profiles which represent surface movements over coal extraction from a horizontal or near horizontal seam are shown in Fig. 2 (Kapp and Williams, 1972). The values shown are typical but they vary widely according to the extraction geometry, geology and mining practice.

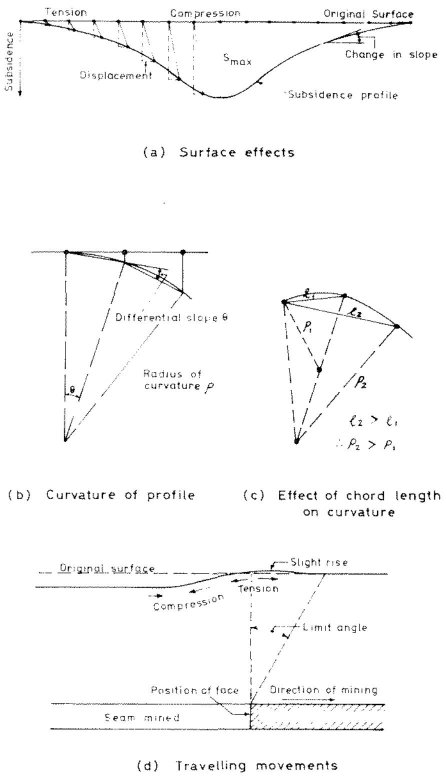

FIG.1 ELEMENTS OF SUBSIDENCE

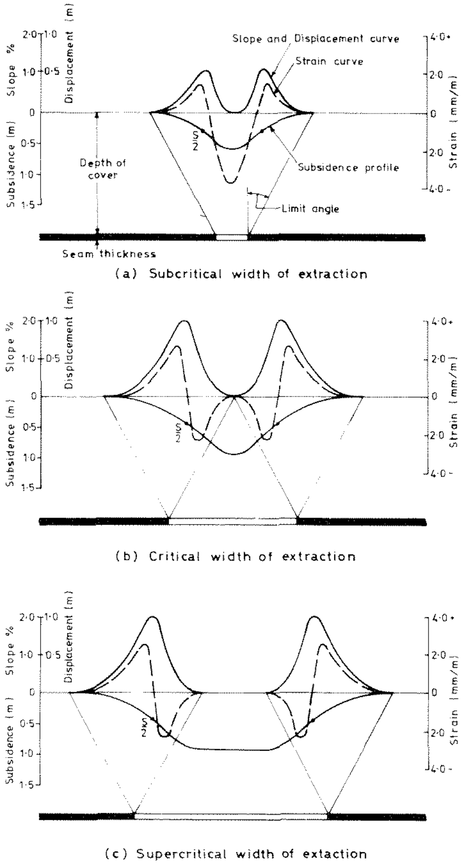

FIG. 2 TROUGH SUBSIDENCE

As the extracted area becomes wider the amount of subsidence increases until the maximum subsidence S_{max} is reached when the area of extraction is at or above a critical value. This occurs when the w/h ratio reaches a figure of about 1.1 to 1.4. At values of w/h less than critical the maximum subsidence is less than the critical subsidence and is termed subcritical (Fig. 2a). When coal is extracted beyond the critical area the maximum subsidence does not increase but the area over which it occurs becomes greater (Fig. 2c). This is called supercritical extraction. The ratio of S_{max} to the mining height m is termed the subsidence factor a. The value of a depends on the nature of the strata and on the percentage of coal recovered in the area mined.

Mining by using the layout of the panel and pillar system requires leaving barriers of coal in place between panels of subcritical width which are mined (Orchard, 1964). The method results in a series of overlapping subcritical subsidence curves with low values of w/h. The subsidence is considerably less than that associated with critical or supercritical extraction and this method of mining is currently being used under residential areas in the Newcastle district.

An imaginary line joining the limit of underground extraction (or goaf edge) with the limit of detectable surface movement makes an angle with the vertical which is termed the 'limit angle' or sometimes 'angle of draw'.

The subsidence of a horizontal ground surface appears as an increasing slope around the edges of the basin. If the ground is originally sloping then the slope of the surface would either increase or decrease depending on the relationship of the underground workings to the surface topography.

A change in ground slope indicates that the surface has developed some curvature and this is expressed as either a differential slope θ or a radius of curvature ρ (Fig. 1b). The radius of curvature of a portion of a subsidence profile depends on the distance between adjacent points on the profile since the minimum radius of curvature may be masked by an excessive chord length ℓ as shown in Fig. 1c (National Coal Board, 1975).

The movement of a point on the surface towards the centre of the subsidence trough is known as the displacement. The horizontal displacement increases from zero beyond the edge of the subsidence trough to a maximum at the point of maximum slope and then decreases to zero over the centre of the trough (Fig. 2).

Points on the surface are displaced both vertically in relation to each other and horizontally towards the centre of the subsidence trough (Fig. 1a). The relative vertical and horizontal movements combine to produce the surface strains which develop as the subsidence trough forms. Near the edge of a subsidence trough there is an extension of the surface as the ground sags and in the central part of a subcritical subsidence basin the surface is in compression. In the strain profile the change from tension to compression occurs at or near the transition point (or point of inflexion) where the subsidence is half the maximum.

b) Calculation of the elements of subsidence

The subsidence of a station is the difference between its reduced level at a particular date and its initial reduced level. The slope developed is calculated from the difference in subsidence between adjacent stations and the horizontal distance between those stations. The change in slope from Station A to Station B is given by $\frac{b - a}{\text{distance AB}}$ where a and b are the subsidence values at A and B.

The ground curvature developed along a subsidence profile between Stations A, B and C is calculated from the relationship $\frac{(b - a) \quad - \quad (c - b)}{(\text{distance AB} \times \text{distance BC})}$. The calculated curvature is shown multiplied by a factor of 10^{-4} to enable a direct comparison with the strains which are then of the same numerical order of magnitude, and with a change of sign the curvature and strain profiles can be compared directly. The inverse of the curvature is simply the radius of curvature.

The strain developed along the surface between any two successive stations is the change per unit length of the distance between those stations. The strain is the ratio of the change in slope distance to the original slope distance and is expressed in millimetres per metre.

c) Travelling movements

Points on the surface begin to move when they come within the influence of the extracted area. As the workings advance, a wave of subsidence moves along in association with the face. The travelling wave of subsidence is accompanied by travelling strain profiles. The effects on the surface caused by an advancing extraction are shown in Fig. 1d.

As the subsidence profile advances, the surface is first subject to tensile strains and then to compressive strains, the magnitude of the strains being greater where the depth of cover is less. The strains accompanying an advancing face are less than the final movements (Wardell, 1953-54) and the maximum tension of the travelling strain decreases with increasing rate of advance (Brauner, 1973).

As final subsidence occurs, the slope of the subsidence profile increases due to movements in the strata above the broken roof rock which forms the goaf. The increase in the slope results in an increase in curvature at the edge of the subsidence basin with an associated increase in the tensile strains.

d) Some aspects of the measurement of strain

The distance over which the strain is measured is termed the bay length. Because of the curvature of the subsidence profile the strains calculated on measurements made over long bay lengths are smaller than those calculated on measurements over shorter bay lengths. In fact, if the ratio of the bay length to the depth of cover decreases from 0.15 to 0.10 the measured strain will increase by approximately 20 per cent (National Coal Board, 1975). More investigation is required but the National Coal Board has recommended that the bay length should be 0.05 of the depth of cover. With shorter distances the number of observations would become excessive and the effects of survey errors would be increased.

The strain calculated over a bay length is in the same direction as the distance measured. The strain should be observed in three directions to determine the magnitudes and directions of the principal strains.

A convenient procedure is to consider the strain e on each side of a triangle. The directions and magnitudes of the principal strains developed at the surface at each triangle are discussed by Leeman (1965). The shear strain is given as γ_{xy}.

$$e_\phi = e_x \sin^2\phi + e_y \cos^2\phi + \gamma_{xy} \sin\phi \cos\phi$$

For each triangle there are three equations, one for each value of ϕ which is the orientation of the maximum principal strain relative to the direction of e_y and for the corresponding value of e_ϕ. The equations are solved for e_x, e_y and γ_{xy}.

The principal strains are then found from the relationship:

$$E_{p,q} = \tfrac{1}{2}\left[e_x + e_y + \text{or} - \sqrt{(e_x - e_y)^2 + \partial_{xy}^{\;2}}\,\right]$$

The orientation of the maximum principal strain relative to the direction of e_y is given by: $\tan \phi = (E_p - e_y) / \partial_{xy}$ where ϕ is measured from the direction of e_y to that of E_p. The direction of E_q is always perpendicular to the direction of E_p.

Subsidence Investigations at Newcastle

a) General introduction

The work described in this report forms part of one of the subsidence investigations being carried out 10 km south of the City of Newcastle. A plan of the mining district is shown in Fig. 3. Pillars were formed in the development workings to a height of 2.0 m and then extracted from the north west. Mining continued in a south westerly direction beneath the line of subsidence survey stations. Pillar extraction commenced in the panel on 10th September, 1970 and was completed on 30th April, 1971. The subsidence phenomena were investigated as the extraction face passed beneath the subsidence line.

Above the seam are other coal seams and beds of conglomerate, sandstone and shale of varying thicknesses. A generalised geological section is shown in Fig. 3. Some minor faulting occurred in the area but was not of sufficient magnitude to affect the investigations.

The investigations are over the area of pillar extraction in an undeveloped area of light timber cover so that the characteristics of the development of subsidence could be observed. The surface is gently undulating with a varying depth of sandy soil on the surface. The depth of cover from the top of the seam was from 110 m to 128 m, the average depth being taken as 116 m. The average full extraction width is 183 m giving a supercritical width to depth ratio of 1.6.

b) Survey procedures and data processing

The line of stations shown in Fig. 3 is part of the subsidence grid which in turn forms part of an overall program including several subsidence grids.

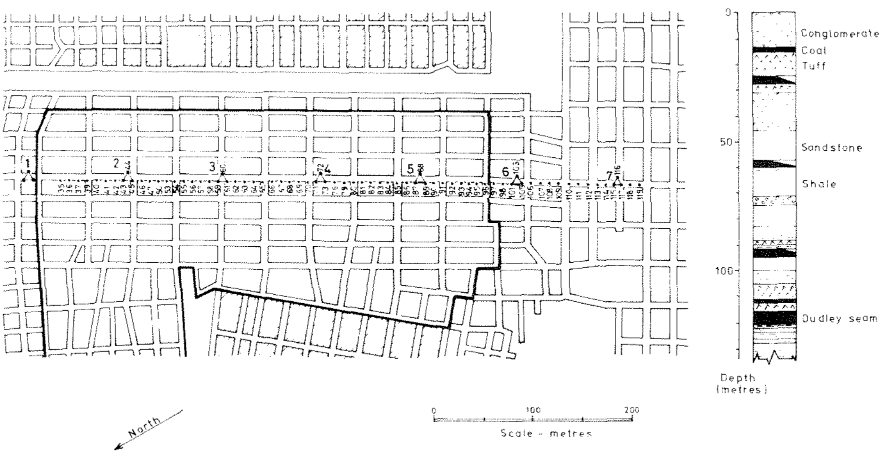

FIG.3 PILLAR EXTRACTION AREA

The line of stations numbered 53 to 119 was established in May 1970 before the extraction took place. The bench mark was established well outside the extraction area and was unaffected by mining. The stations were steel Y-bars hit to refusal and cut off just above the surface. Observations of levels and distances on all stations were at regular time intervals. Stations forming a number of approximately equilateral triangles were established along the line to enable the magnitudes and directions of maximum surface strains to be determined.

The spacing of stations recommended by the National Coal Board (1975) for the calculation of strain is 0.05 of the depth of cover. The average depth of cover is 116 m which would mean a station interval of 6 m. To minimise the survey work an interval of 9 m was adopted here and generally in the Newcastle District. At some locations stations were established at intervals of from 3 m to 18 m to enable the relationship between strains and the distance on which the strains were calculated to be studied. The initial survey was in May 1970 and then at regular intervals of time until final subsidence had occurred.

Because of the large number of subsidence grids established, several computer programs were designed to handle the calculations and the filing and data manipulation from the field booking sheets to the presentation of calculated results from the computer.

The computer printouts show the dates and results calculated from the observations and list the following information:

1. total subsidence at a particular station for each date of observation and the incremental subsidence since the previous observation,
2. total and incremental strains for both slope and horizontal distances for each distance measured, and
3. maximum and minimum principal strains in magnitude and direction for each strain triangle.

The derived elements of slope and curvature along a subsidence profile were calculated by using a Hewlett-Packard 9810 model programmable desk calculator.

c) Features of subsidence and related profiles

The topographic section is shown in Fig. 4a. The surface slopes gently away from a sand dune which is above the start of extraction. The section along the seam shows the positions of the line of extraction at progressive dates. The depth of cover from the top of the seam to the surface decreases from 128 m to a consistent 110 m.

The development of the subsidence and the associated profiles, related to the advances of the line of extraction, illustrate the various phenomena associated with the travelling and final subsidence profiles. The vertical dashed lines relate the elements of subsidence to each other at corresponding dates (Fig. 4).

The first subsidence profile is for 27th October, 1970. The corresponding face position is shown in Fig. 4a and the mining layout at that date is shown in Fig. 5a. The maximum subsidence of 427 mm occurred at Station 39 with zero slope at the bottom of the subsidence trough (Fig. 4c) where the compression had a maximum value C_1 of 2.9 mm/m. The maximum tension T_1 of 1.8 mm/m occurred towards the edge of the subsidence trough at Station 54 where the slope was half the maximum.

As the area of extraction increased with the advance of the face to 12th January, 1971, the maximum subsidence increased to 914 mm at Station 45. The curvatures and strains are both negative in this area and are somewhat erratic. The sand dune dips steeply with a maximum slope of 25° and a combination of vertical and horizontal movements due to subsidence appears to have caused differential movements of

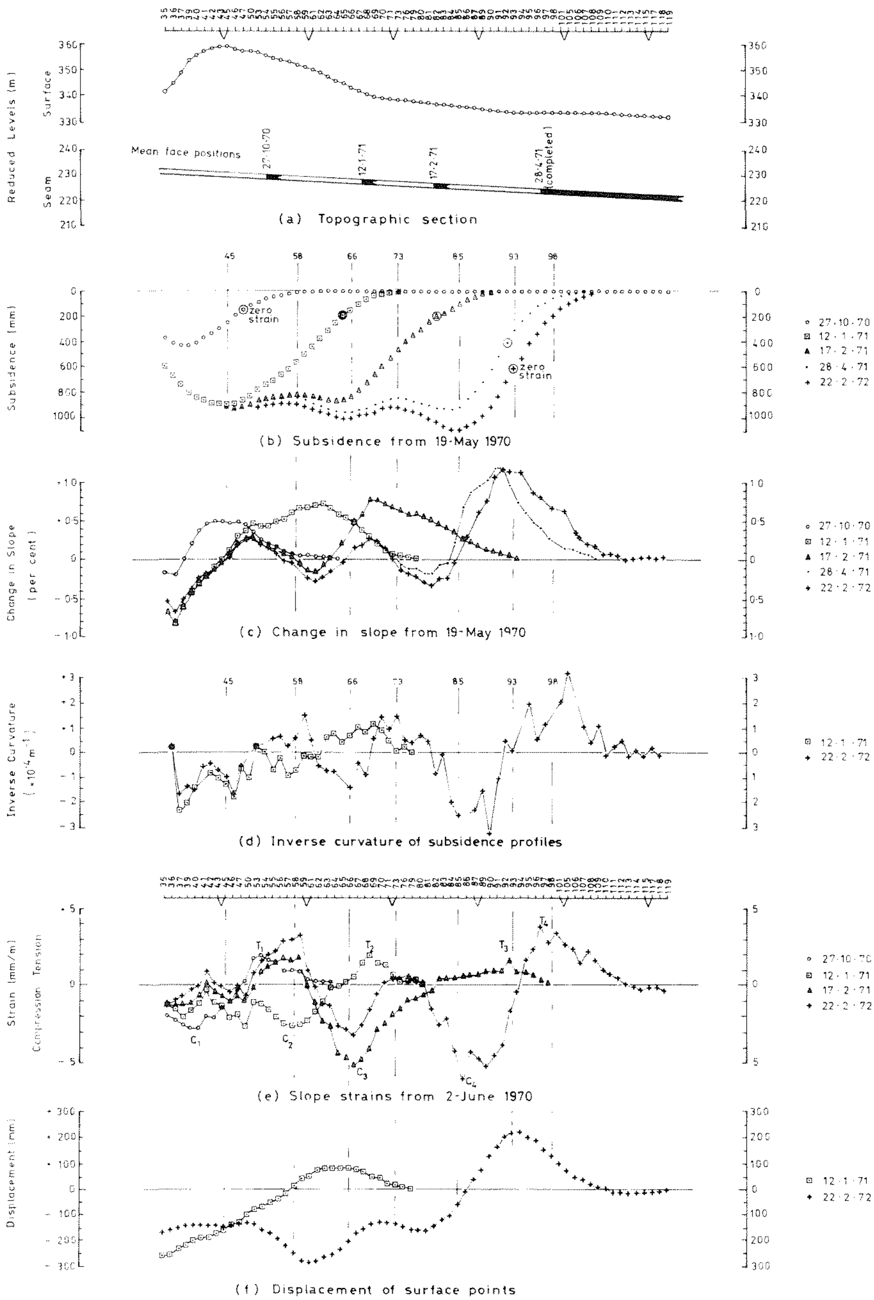

FIG.4. PROFILES OF ELEMENTS OF SUBSIDENCE

stations down the slope. The maximum tension T_2 of 1.8 mm/m occurred between Stations 68 and 69 where the maximum inverse curvature was $1.2 \times 10^{-4}m^{-1}$, which is equivalent to a minimum radius of curvature of 8,720 m. The maximum displacement away from the stable end of the line was 90 mm (Fig. 4f) caused by an extension of the surface due to the accumulation of the tensile strain effects. Thereafter the total length decreased due to the development of the compressive strains towards the bottom of the trough.

The profiles of the elements of subsidence continued to change with the advance of the line of extraction until subsidence was complete. The profiles selected to represent the final subsidence effects are at 22nd February, 1972. The profile at 28th April, 1971 is at the date when extraction was complete. Final subsidence occurred over the earlier extraction while subsidence was continuing over the more recently extracted area. After mining finished there was an additional subsidence of 168 mm to a maximum of 1100 mm, this additional subsidence occurring at a decreasing rate. The humps in the bottom of the final subsidence profile are due to irregularities in the extraction of coal pillars. Associated with these humps are tensile strains, and compressive strains are associated with the troughs. The small humps of only 90 mm which occur in the bottom of the final subsidence trough cause significant changes in strain, where with a flat bottomed subsidence trough it would be expected that the strain would reduce to zero (Fig. 2c). At Station 93, typical characteristics of a critical subsidence trough occur. At the point of half maximum subsidence, the slope is a maximum, both the curvature and strain are zero and the displacement is a maximum.

The maximum slope of the travelling subsidence profile of 0.75 per cent increased to 1.2 per cent as the subsidence profile slowed to its final shape (Fig. 4c). Associated with the change in slope is the calculated curvature of the subsidence profile which is shown plotted for two dates chosen to illustrate the change in the curvature (Fig. 4d). At the leading edge of each subsidence profile the corresponding maximum travelling tensile strains all approximate 1.8 mm/m (T_1, T_2, T_3). When final subsidence occurred, the maximum tensile strain increased to 4.0 mm/m (T_4) which is equivalent to a maximum positive curvature of $2.6 \times 10^{-4}m^{-1}$, or a minimum radius of curvature of 3800 m.

Similarly compressive strains are associated with the trough of the travelling subsidence profile. The values of 2.8 mm/m (C_1, C_2) increased to 5.1 mm/m (C_3) on 22nd February 1971 due to the slight rise which developed at Station 57 in the subsidence profile rather than it remaining as a flat bottomed trough. The mean value of the final maximum compressive strain (C_4) is 5.8 mm/m and corresponds to the maximum negative curvature of $2.8 \times 10^{-4}m^{-1}$, or a minimum radius of curvature of 3600 m.

Slope displacements were calculated from the survey distance measurements. The surface is flat from Station 119 at least to Station 85 (Fig. 4a) where a horizontal displacement profile would be almost identical with the slope displacement profile. The final slope displacement profile on 22nd February 1972 shows an increase in the length of the surface from Station 112 which reaches a maximum at Station 93 of 240 mm (Fig. 4f) with the accumulation of the effects of the tensile strains. After Station 93 the effects of compression strains reduce the displacements until a value of zero is reached at Station 85, the point of maximum subsidence. Where maximum subsidence occurs horizontal displacements become zero as shown in Fig. 2. Changes in the

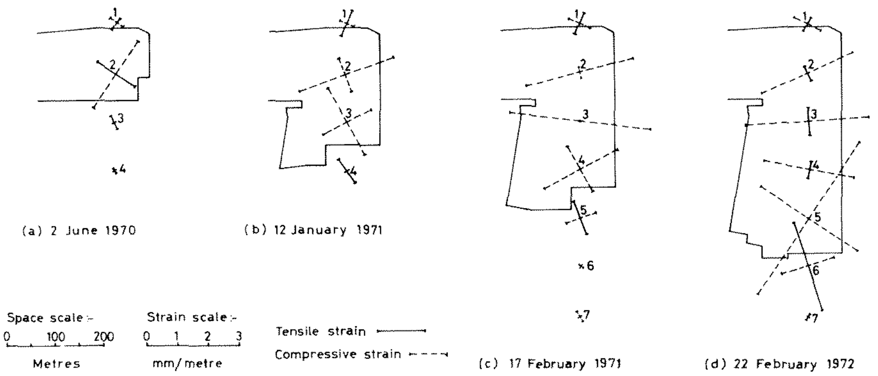

Fig.5 Principal Strains

slope displacement profiles in Fig. 4f can be related to changes in the corresponding strain profiles in Fig. 4e. On 12th January 1971 the displacement increased from a stable point to a maximum value of 85 mm then decreased to zero at Station 58 which is not where the maximum subsidence occurs because of the effects of the natural ground slope (Fig. 4a).

d) Strain triangles

Triangles were established for the calculation of the magnitudes and directions of the maximum and minimum principal strains. The triangles were placed along the line of subsidence survey stations and were made approximately equilateral.

The series of plans in Fig. 5 shows the changes in the principal strains in relation to the extracted area of coal pillars as the line of extraction advanced. The principal strains are located at the triangles numbered 1 to 7 shown in Fig. 3. The plans selected show the pattern of ground movement for the dates on which the strain profiles in Fig. 4e were drawn. In each case the three dimensional nature of the subsidence trough can be visualised by associating the subsidence and strain profiles in Fig. 4 with the plans in Fig. 5.

For example, on 30th October 1970, the principal strains of +0.5 mm/m and -0.2 mm/m at Triangle 3 changed to -2.5 mm/m and -1.8 mm/m on 14th January 1971 as the line of extraction passed beyond the triangle, causing it to come within the compression zone in the subsidence trough (Fig. 4b, 4e). With the further development of subsidence, the principal strains became zero and -4.6 mm/m on 22nd February 1971 and +0.9 mm/m and -4.0 mm/m on 22nd February 1972. At the location of the triangle the hump on the subsidence profile (Fig. 4b) is associated with a change from tensile to compressive strains in a longitudinal direction which is in the direction of mining (Fig. 4e). However the subsidence trough in a lateral direction resulted in the corresponding high compressive strains (Fig. 5d).

The differences in the magnitudes of the two principal tensile strains at Triangles 1 and 6 of 0.5 mm/m and 3.1 mm/m respectively is due to the flatter ground slope at Triangle 1. The maximum principal compressive strains are 6.1 mm/m and 3.8 mm/m respectively and occur near the point of maximum subsidence (Fig. 4b).

e) <u>Characteristics of subsidence and their relationships to mine geometry</u>

The amount of subsidence which occurs over an extracted area of coal increases to a finite value as the ratio of the width of extraction w to the depth of cover h increases. In the area of maximum subsidence at Station 85 (Fig. 4b), w = 213 m and h = 110 m so that w/h = 1.94, a supercritical value. Also S_{max} = 1.10 m and the mining height m = 2.0 m so that the subsidence factor a = S_{max}/m = 0.55. The subsidence is not equal to the full height mined because only about 80 per cent of the coal is recovered in the mining process. After fracturing, the strata above the seam occupy a greater bulk volume than the rock in its original state before being disturbed, which further reduces the subsidence.

An estimate was made of the limit angle from the final subsidence profile in Fig. 4b. The subsidence became zero at Station 111, the tensile strain at that point being 0.5 mm/m. The distance in plan of Station 111 from the goaf edge was 87 m giving a limit angle of 38°. There is a reasonable depth of sandy soil on the surface which contributes to an increase in the limit angle and causes some strain to be present at the point of zero subsidence.

The curvatures calculated from each subsidence profile correspond to the measured strains (Fig. 4). There was a general trend in the relationship between the corresponding maximum values in each profile. In both the tension and compression zones, the strain increased with increased curvature.

At locations along the line of subsidence investigations, stations were placed at intervals of from 3 m to 18 m. These distances were measured at each date a subsidence survey was carried out and the strains were calculated. The results indicated that for bay lengths of between 3 m and 18 m the measured strain, whether in a tensile or compressive zone, decreased by about 0.1 mm/m for every 3 m increase in bay length.

<u>Subsidence due to Oil Extraction at Long Beach</u>

a) <u>Summary of the subsidence phenomena</u>

The extraction of oil causes a reduction of fluid pressure in the strata. The surface subsides to form a depression which will develop into a subsidence bowl. The maximum subsidence and area affected depend on the nature and extent of the deposit and on the geological environment. This subsidence can be arrested if fluid pressure is restored.

Subsidence has occurred over Wilmington oil field which is located under the industrialised port of Long Beach, California, and under a United States Navy shipyard. There has been subsidence of more than 9 m associated with the oil production (Allen, 1971) and the subsidence bowl which formed covered an area of approximately 8 km by 4 km (Fig. 6a). The median depth of production was about 1000 m (Yerkes and Castle, 1969).

Profiles of subsidence, displacement and strain to 1970 across the subsidence bowl along Section AB are shown in Fig. 6b (Allen, 1971). The differences in total lateral displacements of surface points result in surface strains which were estimated to have a maximum value of 1.4 mm/m along Section AB. The strains, combined with the tilting effects, have produced severe damage in long structures. The correlation of subsidence damage and surface strains is generally in agreement with experience in the United Kingdom which is discussed in the Subsidence Engineers' Handbook (National Coal Board, 1975).

b) Comparison with subsidence over coal extraction

A study of surface movements associated with oil and gas field operations showed that the horizontal displacements of surface points vary from zero at the edge of the subsidence bowl to a maximum at the point of maximum developed slope and return to zero at the centre of the subsidence bowl. The maximum tensile strains develop in the outer parts of the subsidence bowl and the maximum compressive strains develop at or near the centre of the subsidence bowl (Yerkes and Castle, 1969). The profiles in Fig. 6b follow the general trend of the corresponding profiles which relate to subsidence over coal extraction for a sub-critical width of extraction shown in Fig. 2a.

A subsidence profile was drawn along the minor axis of the subsidence bowl, across the steepest part of the subsidence basin shown as Section CD in Fig. 6a. The displacement and strain profiles along this axis to 1962 (Yerkes and Castle, 1969) are similar to those in Fig. 6b. The maximum values are shown in Table 1. The displacement becomes zero at the centre of the profile where the section crosses the centre of the subsidence bowl. The slopes and curvatures along the subsidence profile were calculated according to the methods applied to the calculations over coal extraction areas and the maximum values were tabulated.

A comparison is made between the maximum values of the elements associated with the final subsidence profiles (Table 1). Although the maximum subsidence at Wilmington of 9 m is more than 8 times the maximum subsidence over coal extraction in the Newcastle example, the line of the section is approximately 12 times longer. It would thus be expected that there would be similarities in the maximum magnitudes of the various phenomena, depending on the shapes of the profiles. The accompanying table compares these values. The curvatures, strains and displacements were compared only for the tension zone, not for the compression zone. At Wilmington a true bowl is formed whereas at Newcastle the subsidence profile flattens out in the bottom of the subsidence trough. At Wilmington the strains were calculated from the measured displacements from a fixed station outside the subsidence bowl

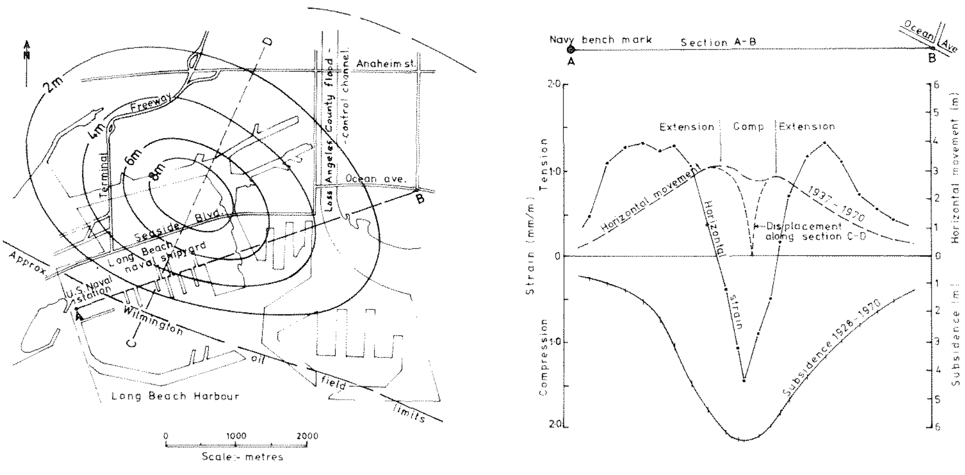

(a) Subsidence from 1928 to 1970

(b) Profiles of subsidence phenomena

FIG 6. SUBSIDENCE AT LONG BEACH

Subsidence area	Max. subs. (m)	Length of half section (m)	Max. slope (per cent)	Tensile zone Max. curv. ($x10^{-4}$ m^{-1})	Min. rad. of curv. (m)	Max. strain (mm/m)	Max. displ. (mm)
Wilmington	9.2	3050	0.7	0.1	152,400	2	3050
Newcastle	1.1	244	1.2	2.6	3,800	4	240

Table 1. Comparative values from subsidence profiles

and at Newcastle the displacements were calculated as the sum of the differences in measurements of individual distances. Thus the different methods of calculating the strains and displacements could affect the confidence in making direct comparisons between corresponding values.

The subsidence at Wilmington is more than 8 times greater than that in the example chosen from the Newcastle district and the maximum slope of the subsidence profile is of the order of half that at Newcastle. Since the change in slope takes place over much greater distance the calculated curvature is very small. At Wilmington the maximum measured displacement was 3 m over 3 km whereas at Newcastle the maximum calculated displacement was 240 mm over a distance of 101 m. From these values of displacement it could be calculated that the 'average' strain over the tensile zone would be 3 to 4 times greater at Newcastle than that at Wilmington. The maximum tensile strain at Wilmington along Section CD is 2 mm/m (Yerkes and Castle, 1969). The maximum measured tensile strain at Newcastle is 4 mm/m (Table 1), twice the corresponding value at Wilmington.

Final Comments

The characteristics of surface movements due to extraction of fluids and of coal are similar. Associated with subsidence due to the mining of both coal and oil are the slope, curvature, displacement and strain profiles. Survey techniques enable these elements of subsidence and their development with increasing subsidence to be defined in some detail.

The techniques and methods of evaluation of the results used in the investigation of subsidence due to underground coal mining have an application in the investigation of the phenomena associated with subsidence due to oil extraction.

Acknowledgements

The results of the subsidence investigations are published with the permission of The Broken Hill Proprietary Company Ltd. The efforts and work of the survey staff and other officers who have assisted with the investigations are acknowledged.

References

Allen, D.R., 1971. Horizontal movement and surface strain due to rebound: Report prepared for The Department of Oil Properties, City of Long Beach, California, 6 p. August.

Brauner, G., 1973. Subsidence due to underground mining: U.S.

Department of the Interior, Bureau of Mines Information Circular 8572, 53 p.
Kapp, W.A. and Williams, R.C., 1972. Extraction of coal in the Sydney Basin from beneath large bodies of water: Annual Conference, Aust. Inst. Min. & Met. May, p. 77-87.
Leeman, E.R., 1965. The measurement of stress in rock: Journal of the South African Inst. Min. & Met., April-June, p. 248-284 (Symposium on Rock Mechanics and Strata Control in Mines: Johannesburg).
National Coal Board, 1975. Subsidence Engineers' Handbook: National Coal Board - Mining Department, 111 p.
Orchard, R.J., 1964. Partial extraction and subsidence: The Mining Engineer, April, p. 417-430.
Wardell, K., 1953-54. Some observations on the relationship between time and mining subsidence: Transactions Institution of Mining Engineers, v. 113, p. 471-483.
Yerkes, R.F. and Castle, R.O., 1969. Surface deformation associated with oil and gas field operations in the United States: Symposium on Land Subsidence, September, v.1, p.55-56: International Association of Scientific Hydrology, Tokyo, Japan.

Publication n°121 of the International Association of Hydrological Sciences
Proceedings of the Anaheim Symposium, December 1976

GROUND FAILURE IN AREAS OF SUBSIDENCE DUE TO GROUND-WATER DECLINE IN THE UNITED STATES

Thomas L. Holzer
U.S. Geological Survey
Menlo Park, California 94025

Abstract

Ground failure related to the extraction of ground water occurs in several areas of land subsidence in the United States--Arizona, California, Raft River Valley (Idaho), Houston-Galveston (Texas), and Las Vegas Valley (Nevada). The nature of the ground failure ranges from fissuring (formation of an open crack) to faulting (differential offset of the opposite sides of the failure plane parallel to the plane). A few open cracks with vertical offset also have been observed. The temporal and areal correlation between earth fissures and large ground-water overdrafts in basins that are subsiding strongly suggests that fissuring is produced by lowering ground-water levels or the associated subsidence. Moreover, in some areas such as central Arizona, San Jacinto Valley (California), and Las Vegas Valley (Nevada), the number of fissures has increased significantly as declines of ground-water levels and associated subsidence have continued. Only one active surface fault, the Picacho fault in central Arizona, has been documented to have been caused by ground-water extraction. The documentation consists of the demonstration of coincidence in time between surface faulting and subsidence, agreement between observed vertical displacements and those predicted by an analytical model of a fault active only within the zone of compaction, lack of conclusive evidence for recent tectonic faulting, and seasonal periodicity of faulting. By comparison with this fault, some surface faults in California and Texas appear compatible with a mechanism associated with ground-water extraction.

Introduction

Ground failure associated with land subsidence caused by the withdrawal of ground water was first recognized in 1949 in central Arizona, and consisted of earth fissures which are large, open cracks (Feth, 1951; Robinson and Peterson, 1962; Schumann, 1974). Other areas in which earth fissures subsequently have been reported include southeastern Arizona (Eaton, 1972), Raft River Valley, Idaho (Lofgren, 1975), Las Vegas Valley, Nevada (Mindling, 1974), San Jacinto Valley, California (Morton, 1977), and the San Joaquin Valley, California (Lofgren, 1971). Almost simultaneously with Feth's (1951) observations, investigators in the Texas Gulf Coast suspected a relationship between surface faulting and land subsidence caused by ground-water withdrawal (Lockwood, 1954). Because of the difficulty of distinguishing between tectonic faulting and subsidence-associated faulting, ambiguity concerning the cause of faulting exists for most faults which have been attributed to ground-water withdrawal. Only the Picacho fault in central Arizona has been documented to have been caused by ground-water extraction (Holzer and others, in press). On the basis of this documentation, some faulting in California and Texas appears compatible with a cause related to ground-water extraction.

Earth fissures and faults will be discussed separately because of their strikingly different appearance and behavior. Earth fissures are open, vertical cracks which typically have lengths measured in hectometers and depths in excess of 10 meters. Movement of blocks adjacent to a fissure usually is perpendicular to the plane defined by the fissure and typically is less than three centimeters. The term fault is used to characterize failure on a discrete plane (or zone) in which a significant component of the relative displacement of blocks adjacent to the failure plane is parallel to the plane. Vertical components of offset exceeding 15 centimeters are common. The lengths of the fault traces commonly are measured in kilometers. The distinction between faults and fissures may be somewhat arbitrary, however, because faults and fissures are areally associated in some places and a few fissures have shown significant vertical offset.

Earth Fissures

The temporal and areal correlation between earth fissures and large ground-water overdrafts in basins that are subsiding strongly suggests that fissuring is produced by lowering ground-water levels or the associated subsidence (table 1). In some areas such as central Arizona, San Jacinto Valley, and Las Vegas Valley the number of fissures has increased significantly as declines of ground-water levels and associated subsidence have continued (Mindling, 1974; Morton, 1977; Winikka and Wold, 1977). Moreover, when adjacent areas without ground-water development but with similar hydrogeologic settings are examined, no fissures are found. A word of caution, however, is in order. A few fissures have been observed which appear to have been formed by natural processes, *i.e.*, the area is unaffected by ground-water development (Leonard, 1929; Robinson and Peterson, 1962; U.S. Geological Survey, 1976). Hence fissures apparently can be both artificially and naturally induced.

The distinguishing characteristics of earth fissures are their length and depth. Lengths exceeding a kilometer are known, and lengths exceeding three hectometers are common (*e.g.*, Morton, 1977; Winikka and Wold, 1977). Reported depths of fissures are biased because fissures typically do not have external drainage, and hence behave as sinks for sediment. Hence, the lowering of a weighted probe into a fissure, the usual method of measurement, only indicates the minimum depth of the original fissure. Depths based on this technique of measurement commonly exceed 10 meters. The deepest confirmed depth of a fissure is 16 meters measured near Pixley, California (Los Angeles Department of Water and Power, 1974). The depth is based on the logging of a bucket auger boring. The boring stopped before encountering the base of the fissure.

Displacements associated with fissures are small and usually perpendicular to the fissure where detectable. No surveyed measurements of displacement associated with the initial opening of fissures have been published, but a variety of field observations are pertinent. Horizontal openings, perpendicular to the plane of the fissure, ranging from hairline cracks to three centimeters have been measured across fissures in Las Vegas Valley where the fissures fracture indurated caliche. Where fissures have intersected paved roads in Arizona, California, and Nevada, the horizontal opening typically is much less than two centimeters. Because many of the fissures in central Arizona occur in areas of undisturbed desert, plant roots commonly extend across the fissure. Although commonly taut, the roots are seldom broken. On one fissure, north of the West Silver Bell Mountains, Arizona, the trunk of a mesquite tree was split and opened horizontally 6.4 centimeters by a fissure. This is the largest offset across a fissure known to the author. Investigations based

TABLE 1.--SUMMARY OF FISSURES ASSOCIATED WITH SUBSIDENCE CAUSED BY GROUND-WATER EXTRACTION
(COMPILED FROM PUBLISHED AND UNPUBLISHED SOURCES AND FIELD WORK BY THE AUTHOR 1975-76)

LOCATION	SUBSIDENCE MAX. MEASURED (M)	DATES	MAX. WATER-TABLE DECLINE (M)	(DATES) 1/	NO. OF FISSURES	DATE OF FIRST OCCURRENCE	MAX. LENGTH (KM)
ARIZONA							
CENTRAL	2.67	1905-74	114	(1915-71)	>75	1949 2/	1.68
SOUTHEASTERN	0.21	1952-60	?		> 2	<1962	5.20
CALIFORNIA							
TULARE-WASCO	4.27	1926-70	30	(1920-59)	3	1969	0.64
SAN JACINTO VALLEY	0.71 3/	1939-59	?		>15	<1953	0.70
YUCAIPA	?		?		1	1952	0.61
IDAHO							
RAFT RIVER VALLEY	0.80	1934-74	?		1	±1962	5.18
NEVADA							
LAS VEGAS VALLEY	1.02	1935-73	30	(1955-73)	>33	<1960	0.76

1/ BASED ON WATER-LEVEL DECLINES OF SHALLOW WELLS.

2/ FIRST REPORTED FISSURE OCCURRED IN 1927 (LEONARD, 1929).

3/ INCLUDES A COMPONENT OF TECTONIC SUBSIDENCE.

on trenches to depths of six meters across fissures confirm the conclusions concerning the magnitude and sense of displacement based on surface observations.

Fissures in arid areas often are enlarged by erosion. In fact, this may be the principal hazard associated with them. The enlargement also may provide a clue to their depth since field observations indicate that the sediment eroded from the upper portion of fissures is washed down and deposited deeper within the fissure. The volume of the unfilled portion of the fissure at the surface, therefore, may be used to estimate the depth of the fissure if the average opening or width of the original fissure is assumed. Because of the long lateral extent of fissures, the problem can be treated two dimensionally by considering a cross section perpendicular to the plane of the fissure. Cross-sectional areas of the upper part of fissures, the unfilled portions, commonly exceed 3.5 square meters. If an average initial width of 2.5 centimeters is assumed for the fissure, the depth of fissure is estimated to be in excess of 140 meters. Although the calculation is approximate, the conclusion that at least some fissures extend to considerable depth is difficult to refute.

Fissures occur suddenly. In central Arizona, an area of desert, they usually are observed after heavy rains. Detailed surface observations preceding the occurrence of fissures are rare. Field observations by the author and others indicate that the surface appearance of some fissures may be preceded by minor depressions in the land surface. Many fissures in central Arizona appear to have propagated upwards from depth. Within a year or two of forming, most fissures appear to be inactive. For example, field investigations by the author of fissures formed over six years ago indicate they are passively being filled in with sediment. In a few instances, new fissures have formed in close proximity to older fissures.

Individual fissures commonly are not continuous, but consist of series of segments along the same trend. Occasionally segments form an en echelon pattern, but this is the exception. Segments are not connected at the surface. Occasionally a zone, defined by several closely spaced parallel fissures, occurs, the width of which is on the order of 30 meters. Fissures also commonly have secondary cracks associated with them. These cracks develop subparallel to the main fissure and usually are only a few dekameters long. They occur at distances up to 15 meters from the fissure. The geometry of fissure traces ranges from linear to curvilinear forms. The intersection of fissures is a common occurrence and the angle of intersection is variable. Orthogonal intersections are the most common, but a variety of angles are observed. Fissures do not cut through other fissures, i.e., only triple junctions are observed

The locations of many fissures appear to be either lithologically or structurally controlled. In alluvial basins in which bedrock crops out, many fissures commonly parallel the bedrock-alluvium contact at the ground surface and are closely adjacent to the contact (Morton, 1972; Winikka and Wold, 1977). Feth (1951) suggested that fissures not near bedrock outcrops occur over shallow bedrock irregularities. Sauck (1975), however, did not find geophysical evidence for irregularities beneath some fissures on the north side of the Santan Mountains, Arizona. In Las Vegas Valley, Nevada, fissures are associated with faults of geologic origin (Mindling, 1974).

Causes of Earth Fissures

Three different mechanisms have been proposed for the formation of earth fissures: (1) horizontal strains associated with differential subsidence (Feth, 1951); (2) tension caused by horizontal seepage forces (Lofgren, 1972); and (3) tensile failure caused by horizontal contraction in the zone drained by water-table declines (Holzer and Davis, 1976). Some leveling data, particularly in Las Vegas Valley (Mindling, 1974), support a differential subsidence mechanism. A fissure which occurred in central Arizona in 1949, however, indicates that fissures can occur with negligible subsidence. Differential subsidence in 1949 of less than 0.15 meter is indicated by two bench marks 8.6 kilometers apart on opposite sides of the fissure (fig. 1). Moreover, most of this differential subsidence probably was not localized in the vicinity of the fissure but was associated with regional land subsidence. The occurrence of fissures near the center of cones of depression (e.g., Domenico and others, 1964) is incompatible with the proposed role of horizontal seepage forces in the formation of fissures since this area is predicted by this mechanism to be a zone of compression rather than tension. Support for the contraction-tensile failure mechanism consists principally of the correlation of fissures with water-table declines, the estimate that fissures extend from the surface to drained zone, and the conclusion that many fissures appear to have propagated upwards. Horizontal contraction at depth also is suggested by the adjacent, semi-closed patterns formed by some fissures (fig. 2).

Faults

The Picacho fault in central Arizona (table 2) is the only fault which has been documented to have been caused by ground-water extraction (Holzer and others, in press). The principal argument is based on a precise and well-documented coincidence in time between surface faulting and subsidence attributable to ground-water pumping. The possibility of a

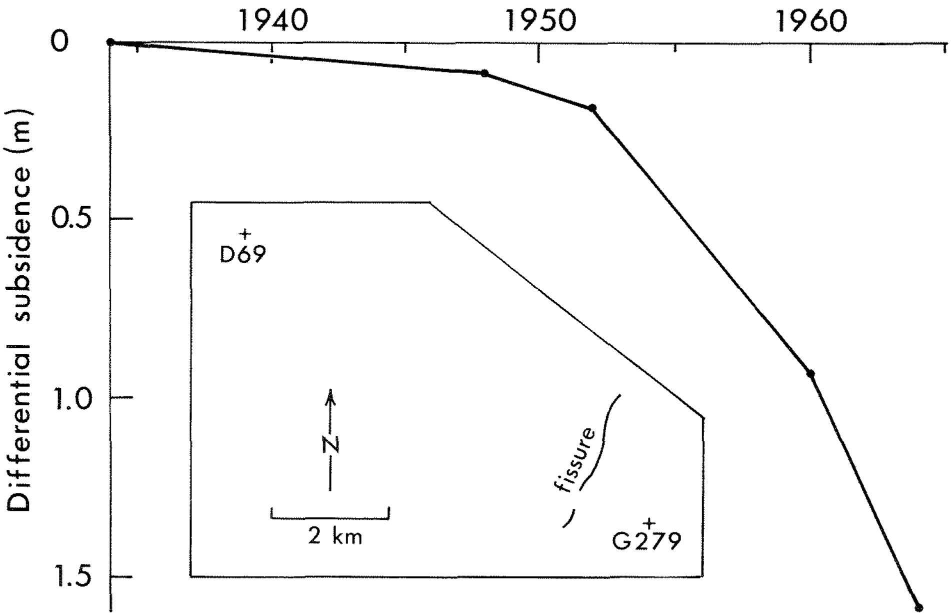

Figure 1.--Differential subsidence of bench mark D69 relative to G279, 1934-1964, near Picacho, Arizona. Map insert shows location of bench marks and earth fissure which occurred in 1949. Subsidence of G279 prior to 1960 is negligible. Center of subsidence bowl is northwest of D69.

fortuitous coincidence of tectonic faulting and subsidence, the nemesis of most subsidence-associated fault investigations, was excluded based on agreement between vertical displacements observed at the surface and those predicted by modeling of a fault active only within the zone of compaction. The argument is reinforced by a lack of evidence for prehistoric but geologically recent faulting. Surface faulting on the Picacho fault was interpreted to have been preceded by differential subsidence over a narrow zone, i.e., a flexure. The fault scarp developed in the center of the flexure. Fault scarp height presently ranges from 0.2 to 0.6 meter along the length of the fault. Significant land subsidence has occurred on both sides of the fault scarp. Fault movement appears to vary seasonally, with most of the annual movement occurring over a three-month period based on the data from 1964 to 1965 (fig. 3A). No cessation or reversal in the sense of fault movement has been detected. Fault offset, based on the modeling of the vertical displacements, is in a normal sense. Ground-water level declines on the downthrown side of the fault when the scarp began to develop were approximately 40 meters. Water-level data on the upthrown side of the fault are unavailable. Subsurface data are too incomplete to demonstrate that the Picacho fault connects at depth to a fault of geologic origin but such an interpretation is compatible with borehole, gravity, and magnetic data.

Rogers (1967) suggested that surface faulting on the Busch fault, 9.7 kilometers northwest of Hollister, California, may have been caused by ground-water extraction (table 2). His suggestion was based on the anomalous structural geologic setting of the Busch fault. The Busch fault is

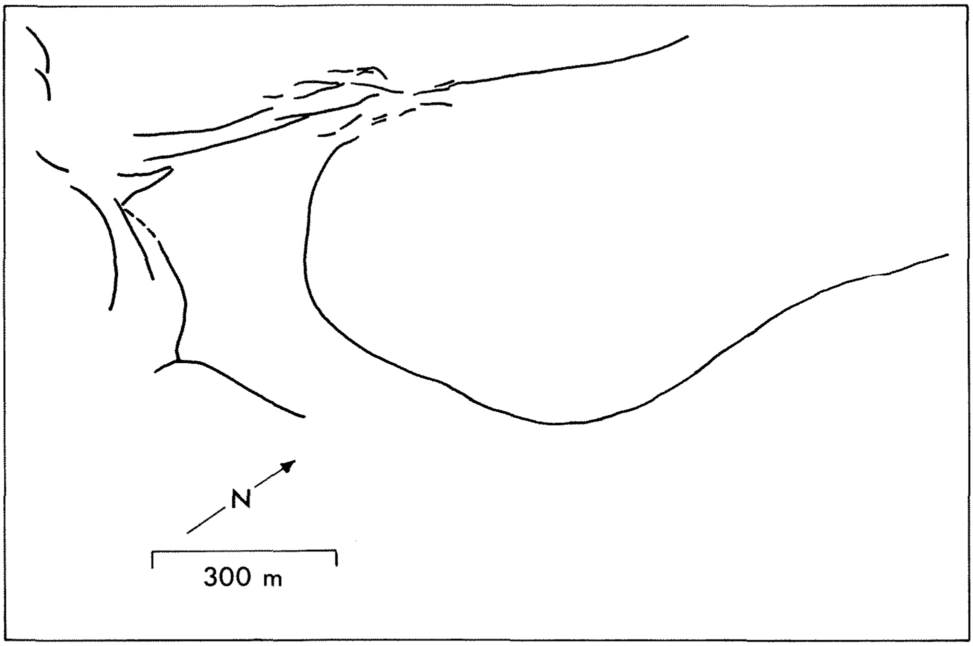

Figure 2.--Semi-closed, adjacent "polygons" formed by earth fissures on the eastern margin of Eloy-Picacho, Arizona subsidence bowl.

in an alluvial basin from which heavy ground-water withdrawals have occurred. Ground-water declines exceeded 30 meters near the fault as of 1975. No geodetic surveys in the vicinity of the fault have been run, and only a few surveys to determine changes of elevations in the general area have been repeated. Available data, however, suggest subsidence has exceeded 0.60 meter in Hollister. Because of extensive agricultural activity the fault scarp has been disturbed along most of its trace. At the driveway to the Busch ranch, the scarp height presently exceeds 0.17 meter. Creep on the fault, measured since 1970 by a tiltbeam established across the fault (Nason and others, 1974; Nason, 1977), is remarkably periodic with an average annual vertical displacement of 0.86 centimeter (fig. 3B). Negligible creep occurs until September or October of each year, and then most of the annual creep occurs over the next three months. The annual initiation of creep occurs about at the end of the pumping season and precedes the beginning of seasonal rainfall, usually in November.

Active surface faulting on the Pond-Poso Creek fault near Pond, California may be another example of subsidence-associated faulting. The active portion of this fault is in the Tulare-Wasco subsidence bowl described by Lofgren and Klausing (1969). The fault was thoroughly explored as part of the site investigation for the San Joaquin Nuclear Project (Los Angeles Department of Water and Power, 1974) and the movement was assumed in that investigation to be tectonic. Approximately 15 centimeters of vertical offset occurs on two roads, 1.6 kilometers apart, which cross the active trace. According to county highway maintenance personnel (H. Silva, oral communication, 1976), road offset was not noticed until sometime between 1956 and 1966, many years after subsidence began. The

TABLE 2.--SUMMARY OF SURFACE FAULTS ASSOCIATED WITH SUBSIDENCE CAUSED BY GROUND-WATER EXTRACTION (COMPILED FROM PUBLISHED AND UNPUBLISHED SOURCES AND FIELD WORK BY THE AUTHOR 1975-1976)

FAULT NAME	LOCATION (NEAREST TOWN)	SUBSIDENCE MAX. MEASURED (M)	DATES	SURFACE FAULTING LENGTH (KM)	SURFACE FAULTING DISPLACEMENT (M)	AV. RATE OF DISPLACEMENT (CM/YR)	(DATES)	TYPE[1]
ARIZONA								
Picacho fault	Picacho	2.67	1905-1974	12.8	0.47	3	(1961-76)	Hn
CALIFORNIA								
Busch fault	Hollister	0.80	1948-1972	0.74	>0.17	0.86	(1970-75)	H
Pond-Poso Creek fault	Pond	4.27	1926-1970	>2.22	0.15	1	(1956-74)	Hn
TEXAS								
(Over 50 faults)	Houston-Galveston[2]	2.59	1906-1973	12.97[3]	1.04[3]	3.3	(?)	Hn

[1] H, high angle; N, normal

[2] Probably includes active faults not caused by ground-water extraction.

[3] Maximum values reported (van Siclen, 1967).

principal argument that faulting is caused by ground-water extraction, apart from the coincidence of faulting with subsidence, is based on the assumption that differential compaction is the cause of the faulting. The level of ground-water on the upthrown side of the fault is 9.1 meters above the level on the downthrown side. The subsidence to head-decline ratio in the vicinity of the fault is approximately .044 (Lofgren and Klausing, 1969). Based on the 9.1 meter difference of ground-water levels, predictured differential compaction across the fault is 40 centimeters, exceeding the measured fault displacement by 25 centimeters. Comparison of the average geologic rate of the vertical component of fault offset with the historic rate of displacement also supports a subsidence-associated mechanism although the argument ignores the possibility of episodic geologic movements. The average geologic rate of vertical displacement is less than 1.8 x 10^{-3} cm/year based on 10.7 meters of vertical offset of the Corcoran clay member of the Tulare Formation, which is dated as older than 600,000 years (Miller and others, 1971). The historic rate of vertical displacement is approximately 1 cm/year, which is comparable to rates of subsidence in that area.

More than 50 discrete, active faults with an aggregate length of more than 220 kilometers have been discovered in the Houston-Galveston, Texas subsidence bowl (Reid, 1973). Because of the concentration of known active surface faults in the subsidence bowl and the lack of pre-subsidence fault-line scarps on some presently active faults, a relation between ground-water extraction and surface faulting has been suspected for more than 20 years (Lockwood, 1954; van Siclen, 1967; Kreitler, 1976), However, since some fault-line scarps antedate significant man-induced subsidence, the relation between faulting and ground-water extraction is ambiguous (van Siclen, 1967). Demonstration of a relation between faulting and ground-water pumping is further complicated by surface faulting possibly caused by petroleum extraction (Pratt and Johnson, 1926; Yerkes and Castle, 1971). Reid (1973) observed seasonal creep on some faults which he monitored continuously from 1971 to 1972 (figs. 3C and 3D) and concluded that both tec-

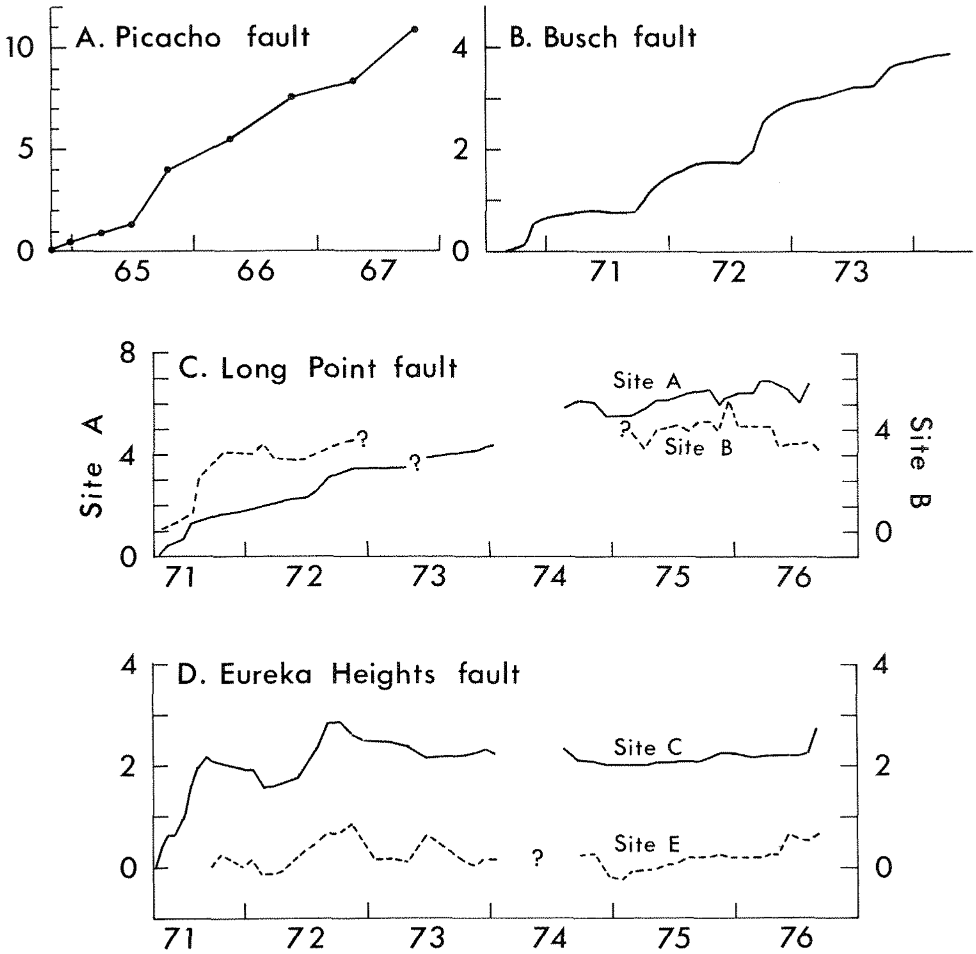

Figure 3.--Records of differential vertical displacement (in centimeters) across active surface faults in subsidence bowls: A. Picacho fault, Arizona (Holzer and others, in press); B. Busch fault, California (Nason, 1977); C. Long Point fault, Houston, Texas; and D. Eureka Heights fault, Houston, Texas. Texas data from Reid (1973) and Gabrysch (written communication, 1976). Question mark indicates loss of reference datum.

tonic forces and mechanisms related to ground-water extraction were operative. Continued monitoring of the same creepmeters by the U.S.G.S. (R. K. Gabrysch, written communication, 1976), however, has not yielded results comparable to Reid's in that seasonal fault creep has not been observed (figs. 3C and 3D). In general, surface fault movement has not occurred at a constant rate, and some faults which have moved in historic times may have ceased moving (Gray, 1958; van Siclen, 1967). Most investigators have concluded that the active surface faults connect to geologic faults at depth (van Siclen, 1967; Kreitler, 1976). Borings drilled for Brown and Root, Inc., in connection with an investigation of an active surface fault in Pasadena, Texas confirmed such a relationship for this one fault (Woodward-Lundgren and Associates, 1974).

Causes of Faults

The preferred mechanism for faulting in subsidence bowls is differential compaction (Castle and Youd, 1972; Reid, 1973). The principal uncertainty is the relevant distance over which the differential compaction occurs. Castle and Youd (1972) argued that the surface faulting is caused by changes in the horizontal stress at the fault attributable to differential compaction across the entire subsidence bowl. Surface faulting on preexisting faults occurs because the preexisting faults are planes of weakness. Reid (1973) argued that the relevant differential compaction is localized at the fault. He suggested that localization of differential compaction in the Houston-Galveston area may be caused by faults acting as partial ground-water barriers. The behavior of the Picacho fault, particularly the formation of the flexure, is more supportive of Reid's (1973) argument than the argument of Castle and Youd (1972). The close agreement between predicted surface faulting based on the observed ground-water differential across the Pond-Poso Creek fault and the observed magnitude of faulting also supports Reid's (1973) argument. The seasonal creep on subsidence-associated faults is compatible with both hypotheses since both regional and localized differential subsidence can vary seasonally.

Summary

Both surface faults and earth fissures can be related to ground-water extraction or the associated land subsidence caused by the ground-water extraction. The temporal and areal correlation between earth fissures and large ground-water withdrawals in basins that are subsiding strongly suggests that fissuring is produced by lowering ground-water levels or the associated subsidence. Fissures are associated with water-table declines, and apparently can occur before significant land subsidence associated with water-level declines begins. Only the Picacho fault in central Arizona has been documented to have been caused by ground-water extraction. This documentation gives credence to the possibility that other occurrences of surface faulting in California and Texas are related to ground-water extraction.

Acknowledgments

I am indebted to numerous individuals for discussions and cooperation, particularly J. K. Boling, Jr., M. C. Carpenter, S. N. Davis, R. K. Gabrysch, C. W. Kreitler, B. E. Lofgren, R. Patt, R. H. Raymond, and C. C. Winikka.

References

Castle, R. O., and Youd, T. L., 1972, Discussion: The Houston fault problem: Assoc. Eng. Geologists Bull., v. IX, no. 1, p. 57-68.

Domenico, P. A., Stephenson, D. A., and Maxey, G. B., 1964, Ground water in Las Vegas Valley: Nevada Univ., Desert Research Inst., Tech. Rept. no. 7, 53 p.

Eaton, G. P., 1972, Deformation of Quaternary deposits in two intermontane basins of southern Arizona, U.S.A.: Internat. Geol. Cong., 24th Montreal, 1972, sec. 3, p. 607-616.

Feth, J. H., 1951, Structural reconnaissance of the Red Rock quadrangle, Arizona: U.S. Geol. Survey open-file report, 32 p.

Gray, E. V., 1958, The geology, ground water, and surface subsidence of the Baytown-LaPorte area, Harris County, Texas: Unpub. M.S. Dissert. Texas A & M Univ., College Station, 66 p.

Holzer, T. L., and Davis, S. N., 1976, Earth fissures associated with water-table declines: Geol. Soc. America, Abs. with Programs, v. 8, no. 6, p. 923-924.

Holzer, T. L., Davis, S. N., and Lofgren, B. E., _____, Faulting caused by ground-water extraction: Science (in press).

Kreitler, C. W., 1976, Lineations and faults in the Texas Coastal Zone: Texas Univ., Bur. of Econ. Geology, Rept. Inv. no. 85, 32 p.

Leonard, R. J., 1929, An earth fissure in southern Arizona: Jour. Geology, v. 37, p. 765-774.

Lockwood, M. G., 1954, Ground subsides in Houston area: Civil Eng., v. 24, p. 370-372

Lofgren, B. E., 1971, Field measurement of aquifer-system compaction, San Joaquin Valley, California, U.S.A. in Land Subsidence: Internat. Assoc. Sci. Hydrology-UNESCO Pub. no. 88, v. 1, p. 283.

_____, 1972, Sensitive response of basin deposits to regional stress changes: Geol. Soc. America, Abs. with Programs, v. 5, no. 7, p. 715-716.

_____, 1975, Land subsidence and tectonism, Raft River Valley, Idaho: U.S. Geol. Survey open-file report 75-585, 21 p.

Lofgren, B. E., and Klausing, R. L., 1969, Land subsidence due to ground-water withdrawal Tulare-Wasco Area, California: U.S. Geol. Survey Prof. Paper 437-B, 103 p.

Los Angeles (City) Department of Water and Power, 1974, San Joaquin Nuclear Project Early Site Review, v. I & II.

Miller, R. E., Green, J. H., and Davis, G. H., 1971, Geology of the compacting deposits in the Los Banos-Kettleman City subsidence area, California: U.S. Geol. Survey Prof. Paper 497-E, 46 p.

Morton, D. M., 1972, Geology of the Lakeview and Perris (7½') quadrangles, Riverside County, California: California Div. Mines and Geology Map Sheet 19.

_____, 1977, Surface deformation in part of the San Jacinto Valley, Southern California: U.S. Geol. Survey Jour. Research, v. 5, no. 1, p. 117-124.

Mindling, A. L., 1974, Effects of ground-water withdrawal on I-15 Freeway and vicinity in North Las Vegas, Nevada: Nevada Univ. Center for Water Resources Research, Desert Research Inst., Proj. Rept. Series no. 33, 37 p.

Nason, R. D., 1977, Instrumentally measured fault movements due to subsidence: Internat. Symp. Land Subsidence, 2nd, Anaheim, California, 1976.

Nason, R. D., Philippsborn, F. R., and Yamashita, P. A., 1974, Catalog of creepmeter measurements in central California from 1968 to 1972: U.S. Geol. Survey open-file report 74-31, 287 p.

Pratt, W. E., and Johnson, D. W., 1926, Local subsidence of the Goose Creek oil field (Texas): Jour. Geology, v. 34, no. 7, p. 577-590.

Reid, W. M., 1973, Active faults in Houston, Texas: unpub. Ph.D. Dissert. Texas Univ., Austin, 122 p.

Robinson, G. M., and Peterson, D. E., 1962, Notes on earth fissures in southern Arizona: U.S. Geol. Survey Circ. 466, 7 p.

Rogers, T. H., 1967, Active extensional faulting north of Hollister near the Calaveras fault zone: Seismol. Soc. America Bull., v. 57 no. 4, p. 813-816.

Sauck, W. A., 1975, Geophysical studies near subsidence fissures in central Arizona: Am. Geophys. Union Trans., v. 56, no 12, p. 984-985.

Schumann, H. H., 1974, Land subsidence and earth fissures in alluvial deposits in the Phoenix Area, Arizona: U.S. Geol. Survey, Misc. Geol. Inv. Map I-845-H.

U.S. Geological Survey, 1976, Field trip to Nevada Test Site: U.S. Geol. Survey open-file report 76-313, p. 27-30.

van Siclen, D. C., 1967, The Houston fault problem: American Inst. Geologists, Proc. 3rd Ann. mtg., Texas Sec., Dallas, 1967, p. 9-31.

Winikka, C. C., and Wold, P. D., 1977, Land subsidence in central Arizona: Internat. Symp. Land Subsidence, 2nd, Anaheim, California, 1976.

Woodward-Lundgren and Associates, 1974, Detection and Evaluation of Differential Surface Displacement in the Texas Gulf Coastal Region: Consulting report to Brown and Root, Inc., p. 1-41.

Yerkes, R. F., and Castle, R. O., 1971, Surface deformations associated with oil and gas field operations in the United States in Land Subsidence: Internat. Assoc. Sci. Hydrology-UNESCO Pub. no. 88, v. 1, p. 55-66.

Publication n°121 of the International Association of Hydrological Sciences
Proceedings of the Anaheim Symposium, December 1976

FAULTING AND LAND SUBSIDENCE FROM GROUND-WATER AND HYDROCARBON PRODUCTION, HOUSTON-GALVESTON, TEXAS[1]

Charles W. Kreitler
Bureau of Economic Geology, The University of Texas at Austin
Austin, Texas, U.S.A. 78712

Abstract

Land subsidence in Harris and Galveston Counties, Texas, results from production of both ground water and hydrocarbon. Although ground-water withdrawal (over 2 million cubic meters) is the predominant cause of land subsidence, subsidence and faulting are also associated with at least six oil and gas fields: South Houston, Clinton, Mykawa, Blue Ridge, Goose Creek, and Webster fields.

The two-county area is interlaced with active surface faults with topographic escarpments and surface faults which control drainage patterns and create subtle photographic linear patterns, but exhibit no topographic escarpments.

Fluid production activates a given fault by differential compaction of the sediments on either side of the fault. The faults appear to be partial fluid barriers that compartmentalize land subsidence. The Texas City area is an example of a subsidence compartment where subsidence has been restricted by growth faults. Correlation of electric log data from boreholes across the faults indicates as much as 21 m of displacement of sand beds within the Chicot aquifer. This much offset of permeable beds is considered sufficient to create partial hydrologic barriers.

Introduction

Land subsidence in the Houston-Galveston area, Texas, U.S.A. has been attributed primarily to ground-water withdrawal (Gabrysch and Bonnet, 1975). Previous investigators (Weaver and Sheets, 1962; Winslow and Doyel, 1954; Winslow and Wood, 1959; Wood and Gabrysch, 1965; Jorgenson, 1975; Gabrysch and Bonnet, 1975) have mapped the subsidence surface and the piezometric surface as gently dipping, bowl-shaped depressions, centering on the Houston Ship Channel. These workers imply that major ground-water withdrawals from industrial complexes along the Ship Channel are causing much of the land subsidence in Harris County. Extensive hydrocarbon production from approximately 75 fields has also occurred in the two county area. As early as 1918 land subsidence and fault activation from hydrocarbon production was observed in the Goose Creek field, Baytown, Texas (Pratt and Johnson, 1926).

The Houston-Galveston area is interlaced with over 240 km of active faults exhibiting topographic escarpments as well as several hundred km of faults, not marked by escarpments, but do control drainage networks and coincide with photographic lineations. This paper describes the interrelationship of fault activation and ground-water and hydrocarbon production on land subsidence.

Structural Framework

Tertiary sediments of the Texas Gulf coast have been cut my many growth faults and faults associated with shallow-piercement and deep-seated salt domes. Many of the subsurface faults extend to land surface (either a Recent or Pleistocene surface). Most faults are either presently inactive,

[1] Publication authorized by Acting Director, Bureau of Economic Geology, The University of Texas at Austin.

or the rate of movement is so slow that no obvious topographic fault escarpment has developed. The surficial evidence that these faults do extend to land surface is subtle. Rectilinear drainage patterns indicate structural control. Aerial photographic lineations and streams commonly coincide with the surface traces of faults extrapolated from the subsurface (Kreitler, 1976).

Similarly, the active surface faults in the Houston area are not just surficial features, but are integrally related to subsurface structures. Many of the surface faults are coincident with the surface traces of faults extrapolated from the subsurface (Figure 1). Van Siclen (1967) described the continuity of the Addicks surface fault in western Houston to the subsurface fault which controls the location of the Addicks oil field.

The location of several streams and bayous in the Houston-Galveston area, such as Buffalo Bayou,Clear Creek, Highland Bayou, Dickinson Bayou, Brays Bayou, Cedar Bayou, Sims Bayou, and Greens Bayou, appear to be structurally controlled. These streams either are parallel to active faults and fault extrapolations or exhibit rectilinear drainage patterns indicating fault control (Figure 1).

Faulting and Subsidence from Ground-water Withdrawal

Even though many Tertiary faults in the Texas Coastal Zone extend upward to land surface, few show evidence of recent movement. However, in the areas of extensive fluid withdrawal (water, oil, or gas) these passive structural features become active faults. At least 240 km of active faults with topographic escarpments occur in Harris and Galveston Counties where over 2 million cubic meters of water per day are pumped.

Data from tilt meters across two active faults in western Houston show annual cyclic vertical movement that coincides with change of the piezometric surface of the Chicot aquifer (Figure 2). On the Long Point fault, vertical movement increased as the piezometric surface declined (May 1971 to October 1971). When the piezometric surface rose from October 1971 to March 1972, fault movement decreased. This cycle was repeated for the next year. Data from a tilt meter on the Eureka Heights fault show a better correlation of cumulative fault movement related to changes of the piezometric surface. A linear regression analysis between cumulative fault displacement and decline of the piezometric surface has a correlation coefficient of .98 and .99 from April 1971 to October 1971 and March 1972 to October 1972, respectively, indicating a very close statistical relationship. As the piezometric surface rose between October 1971 to March 1972 and October 1972 to March 1973, the downthrown side of the fault rebounded relative to the upthrown side.

Faults in the Houston-Galveston area appear to act as fluid barriers. Fluid production on one side of a fault causes pressure declines and aquifer or reservoir compaction on that side of the fault and not on the other. This differential sediment compaction is translated to the surface as differential land subsidence or fault movement.

Ground-water production is activating the Eureka Heights fault (Figure 2). The occurrence of rebound or reverse movement on the fault suggests that differential compaction is the principal mechanism of activation. This rebound of the downthrown side can be explained as differential elastic expansion of the aquifer. As the piezometric surface rose, a decrease in the vertical effective stress permitted a relaxation of the elastic component of aquifer compression. For the tilt meter to measure reverse movement on the fault, differential elastic rebound of the aquifer must occur since no surficial differential displacement will occur if an aquifer rebounds equally. This differential elastic rebound can be caused by a differential rise of the piezometric surface on either side of the fault,

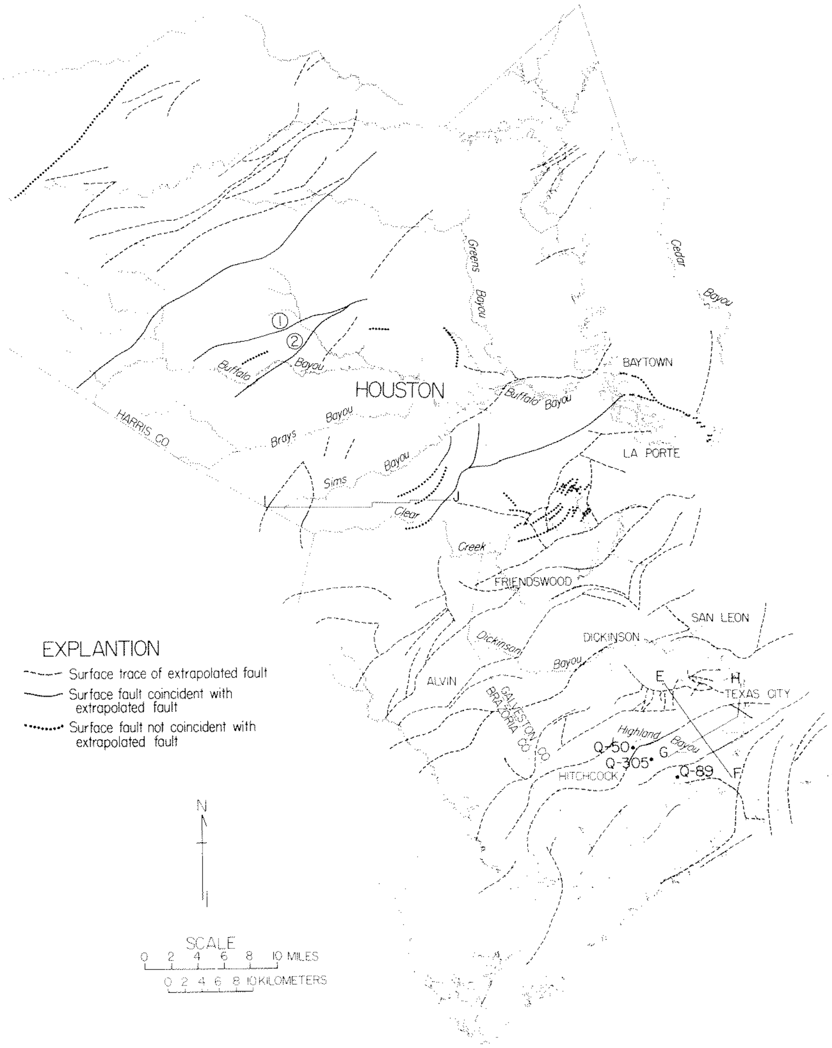

1. Active surface faults and surface traces of extrapolated subsurface faults, Harris and Galveston Counties, Texas. Surface traces were determined by extrapolating subsurface faults based on subsurface maps of Geomap Co. A fault plane of 45° or the dip calculated between two datum surfaces was used for the extrapolations.

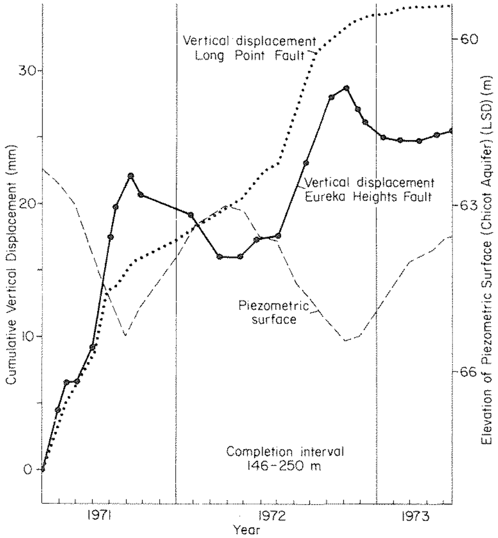

2. Cumulative vertical displacement on Long Point (1) and Eureka Heights (2) faults in the western part of Houston compared to elevation of piezometric surface of Chicot aquifer. Displacement data for April 1971 to April 1972 from Reid (1973); displacement data for May 1972 to May 1973 and drawdown data for Federal observation well L-J-65-13-408 from R. Gabrysch (personal communication, 1974). See figure 1 for meter locations.

suggesting that the fault acts as a partial hydrologic barrier. Fault movement, as recorded by the tilt meters, is not affected by precipitation. A linear regression analysis of fault movement and rainfall (International Airport, Houston, National Weather Service) for the same time periods has a correlation coefficient of 0.27 which indicates that shrinking and swelling of soils during dry and wet periods is not the cause of tilt-beam movement. The repetition of the fault movement cycle for the second year indicates that the meter boxes are not "settling in" to the soil, but are measuring real fault displacement.

In the Texas City area, Galveston County where heavy ground-water production has caused approximately 1.5 meters of subsidence, subsidence has been restricted to a limited area between faults on the northern and southern sides and another structural feature (reflected by Highland Bayou) on the western side. Ground-water production between the two faults and Highland Bayou is 12×10^6 cubic meters per year, whereas production north of the fault is 6.6×10^6 m^3/year and south of the fault there is no production (Harris-Galveston Coastal Subsidence District, 1976 permit applications). Sharp increases in subsidence coincide with the faults and the bayou (Figure 3). Electric log correlations across the two faults show significant displacements in the producing freshwater section of the Pleistocene sediments. Across the northern fault there are 21 m of throw at 150 m and across the southern fault there are 15 m of displacement at 200 m (Figure 4). On the southern fault, the downthrown side in the shallow subsurface is toward the coast. At the land surface, however, the fault scarp is facing inland, indicating a reversal in the direction of fault movement.

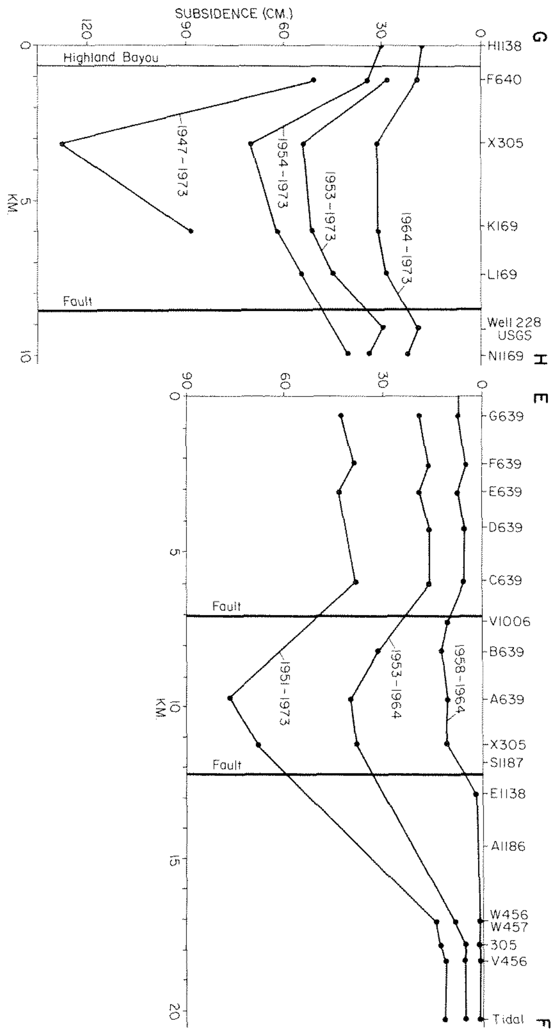

3. Fault control of subsidence, Texas City area, Galveston County. All subsidence data for all figures from adjusted NGS level lines. See Figure 1 for profile locations.

Growth faults in the Texas City area are being activated by ground-water withdrawal, as evidenced by the reversal in the direction of fault movement on the southern fault. Conversely, these faults are probably limiting the geographic extent of piezometric decline, aquifer compaction and subsequently land subsidence. The fault displacements, exhibited in the shallow subsurface are considered sufficient to cause hydrologic boundaries.

Sections of Buffalo Bayou which flows through the Pasadena-Channelview area (the area of maximum ground-water pumpage and maximum subsidence) coincide with traces of extrapolated faults and active surface faults.

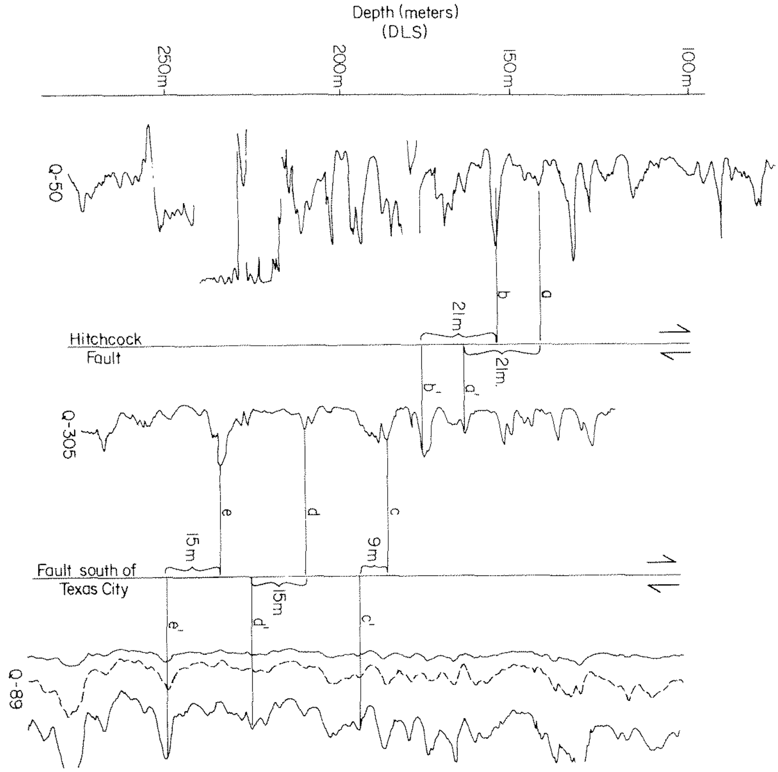

4. Fault displacement in shallow subsurface across the Hitchcock fault (21 m) and the fault south of Texas City (15 m). Well locations on Figure 1.

Other sections of the Bayou exhibit rectilinear drainage patterns. Relevelling data indicate that subsidence is much less at the bayou than 0.4 km away (Figure 5). A subsidence map for 1959-1964 demonstrates the relatively low rates of subsidence along Buffalo Bayou compared to the high rates of subsidence in the industralized areas of Pasadena and Channelview (Figure 5). Buffalo Bayou and the extrapolated fault bisect the large subsidence bowl contoured by Gabrysch and Bonnet (1975), Marshal (1973), and others into two separately subsiding basins. This demonstrates that there may be more subsidence on both sides of a fault than along the trace of the fault.

Faulting and Subsidence from Oil and Gas Production

Land subsidence and fault activation are also attributable to oil and gas production. The Saxet oil and gas field, though not in the Greater Houston area, but west of Corpus Christi, Texas, best demonstrates the interrelationship of oil and gas production with faulting and land subsidence in the Texas Coastal Zone.

In the Saxet field, a 2 m scarp has appeared along a segment of the surface extrapolation of a regional growth fault. The active segment of this fault lies almost exclusively within the Saxet oil and gas field. The topographic escarpment dies out along strike away from the field; natural, geologic activation, therefore, is not considered significant. Because there is no ground-water production in the area, ground-water withdrawals

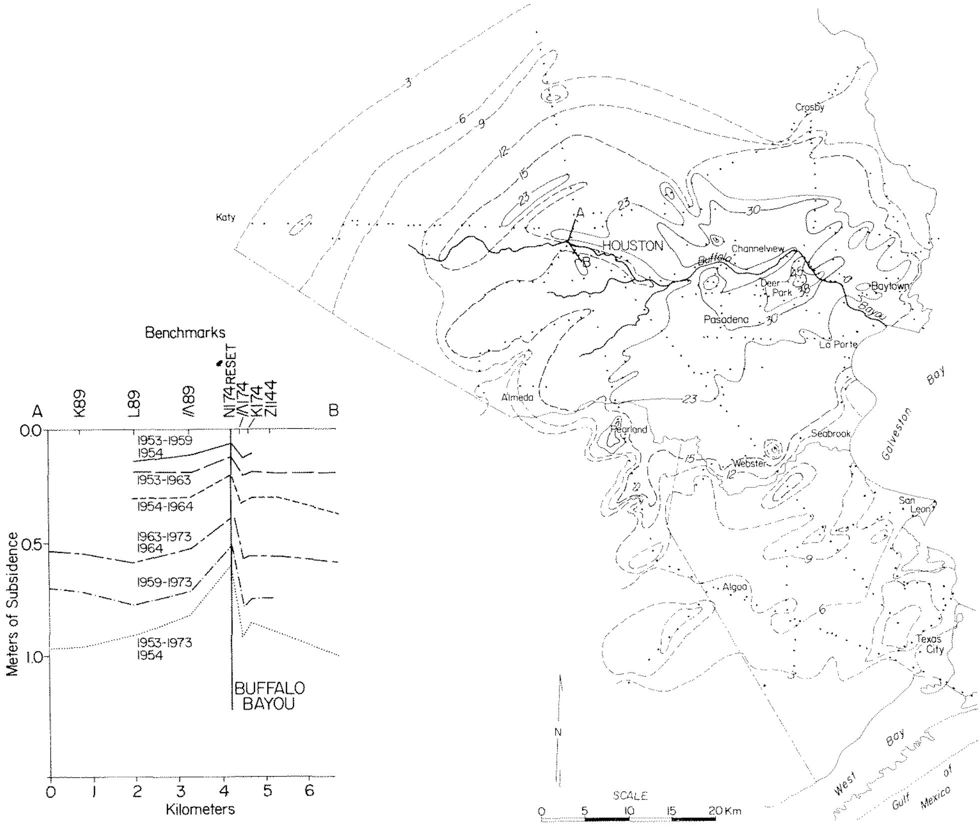

5. Subsidence map (1959 to 1964) for Harris and Galveston Counties. Note that Buffalo Bayou divides severe subsidence into two separately subsiding bowls. Subsidence profile across Bayou shows rapid increase of subsidence on both sides of Bayou. Subsidence contours in cm. Dots indicate data points.

cannot be responsible for the movement. Fault movement has occurred since the onset of oil and gas production (W.A. Price, personal communication, 1975). Leveling profiles across the Saxet field show sharp increases in subsidence at the fault (Figure 6). Subsidence rates from 1950 to 1959, 7 cm per year (0.22 ft per year), are approximately twice the rates from 1942-1950, 4 cm per year (0.14 ft per year). A rapid increase in gas production from shallow sands occurred from 1950 to 1959. Oil production, however, decreased during this period (Kreitler and Gustavson, 1976). Production of high-pressured gas may have led to the compaction of the shallow gas sands on the downthrown side of the Saxet fault and subsequent differential land subsidence and fault activation.

If oil and gas production in the Corpus Christi area causes subsidence and fault activation then these phenomena must also be considered for the Houston-Galveston area where there is extensive hydrocarbon production. In 1976, at least 6 producing fields have associated subsidence and faulting (Table 1). Detailed mapping of waterwell locations and approximate pumpage show minimal shallow ground-water production within the areas of these

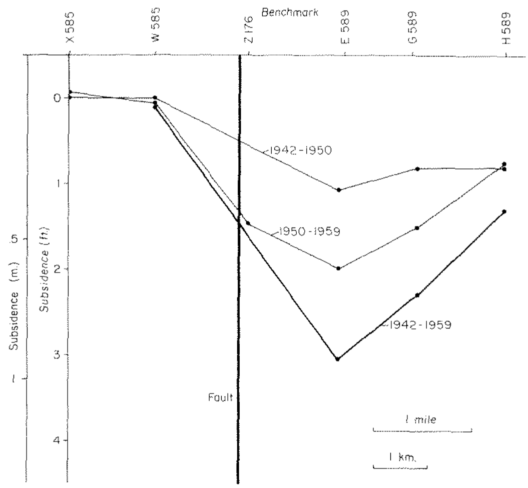

6. Land subsidence over Saxet oil and gas field, Corpus Christi, Texas. Note fault control of subsidence between benchmarks W585 and Z176.

fields; piezometric surface declines, resulting from local, shallow, ground-water production, therefore, are not considered a primary mechanism for field subsidence. Relevelling profiles across the Blue Ridge and Mykawa fields (Figure 7) show two components of subsidence. Below the dashed line is the localized component caused by hydrocarbon production. Above the dashed line is the regional component caused by ground-water production.

Fault Control of Subsidence

Fault control of subsidence similar to Figures 3, 6 and 7 is exhibited on 26 subsidence profiles in Harris, Galveston, and parts of Brazoria, Fort Bend, and Chamber Counties. The location, direction, and magnitude of 87 zones of differential subsidence (from the 26 subsidence profiles) that coincide with active surface faults, fault extrapolations, streams and

Table 1. Land subsidence and surface faulting associated with oil and gas fields, Harris Co., Texas.

Field No.	Field Name	Producing Horizon (m)	Total Production (10^6 bbl)	Subsidence (m)	Faulting (m)
1	South Houston	1,460[2]	39.3 (1974)[2]	0.3 (1942-1958)[4]	0.45 (1972)[5]
2	Clinton	915-2,134[2]	2.7 (1974)[2]	9	0.7 (1972)[5]
3	MyKawa	1,483-2,645[2]	4.1 (1974)[2]	0.5 (1942-1973)[4]	0.5 (1942-1973)[6]
4	Blue Ridge	1,420-2,381[2]	21.0 (1974)[2]	0.2 (1942-1973)[4]	0.15 (1966-1972)[5]
5	Webster	1,481-2,564[2]	41.3 (1974)[2]	9	0.45 (1942-1975)[7]
6	Goose Creek	1,490-1,310[8]	60.3 (1926)[8]	1.0 (1917-1926)[3]	0.43 (1917-1926)[3]

[1] See Figure 9 for field locations
[2] Texas Railroad Commission
[3] Pratt and Johnson (1926)
[4] National Geodetic Survey
[5] Reid (1973)
[6] Kreitler (1976)
[7] Clanton and Amsbury (1975)
[8] Minor (1926)
[9] not available

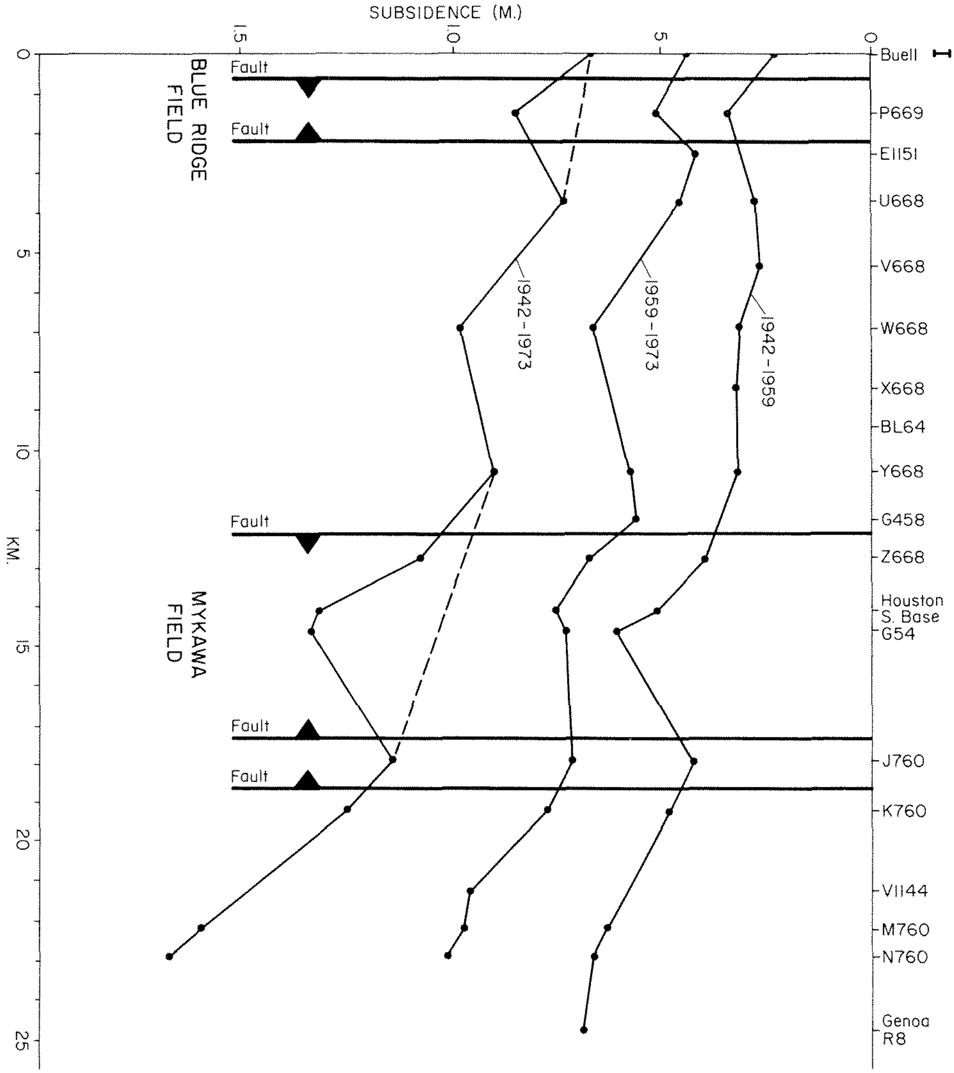

7. Subsidence over Blue Ridge and Mykawa oil fields. Note increased subsidence on both sides of surface faults east of Mykawa field. See Figure 1 for profile location.

bayous, and aerial photographic lineations are shown on Figure 8. Thirteen examples (Figure 8) show increased subsidence on both sides of a fault with the fault remaining in a zone of minimal subsidence. These faults may act as hydrologic barriers with ground-water production on both sides, or hydrocarbon production on one side and ground water on the other.

The areas with the greatest ground-water production and land subsidence are the South Houston-Pasadena-Baytown area and the Texas City area. In both areas, faults on the north and south sides restrict the area affected by severe subsidence.

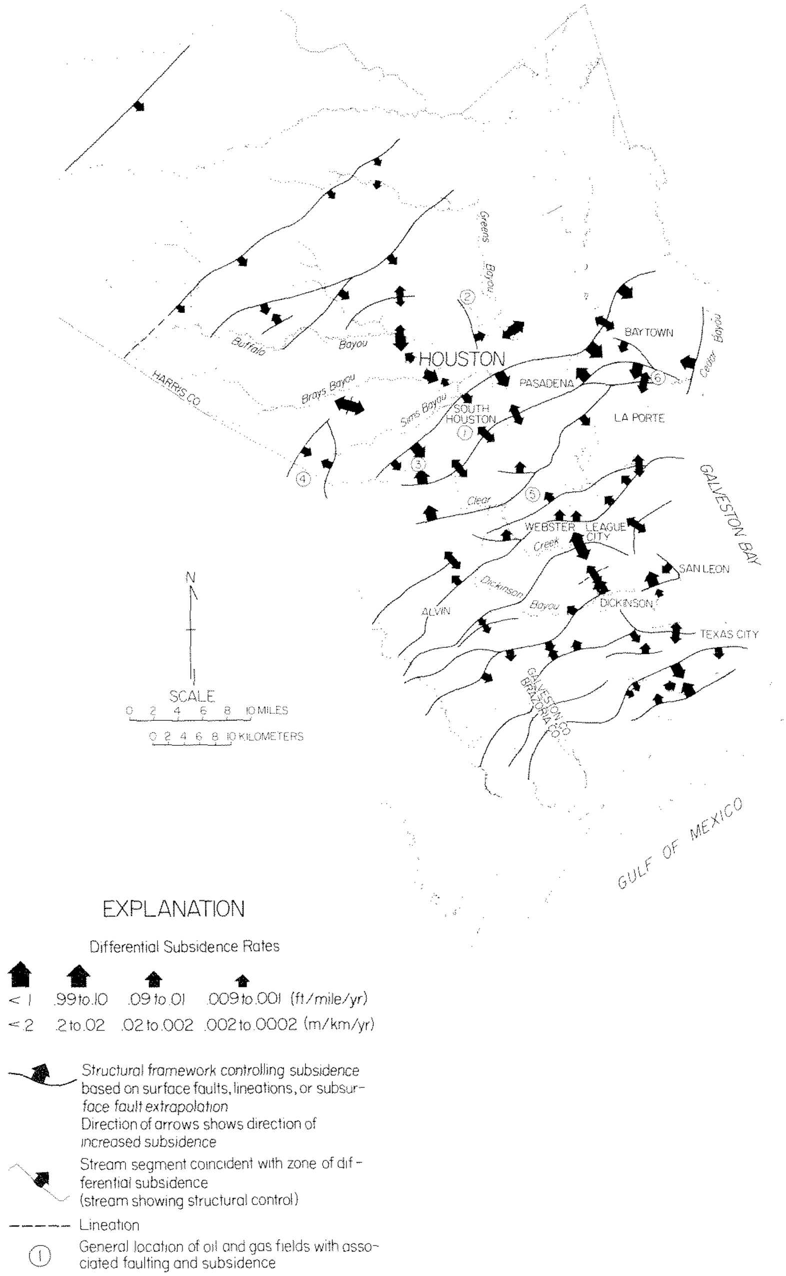

8. Coincidence of differential subsidence with active faults, surface traces of extrapolated subsurface faults, structurally controlled streams and aerial photographic lineations. Direction of arrow indicates the direction of increased subsidence. Size of arrow indicates the magnitude of differential subsidence.

The subsidence patterns exhibited in Figure 8 suggest that the producing aquifers and the associated subsidence are compartmentalized.

Summary

Subsidence in Harris and Galveston Counties is the result of both ground-water and hydrocarbon withdrawal. The structural elements (surface faults, extrapolated faults, faults expressed as drainage patterns) are the boundary conditions that limit the geographic extent of subsidence generated from either source of withdrawal. Ground-water production from one compartment causes sediment compaction and associated land subsidence within that compartment but may not adversely affect other areas of the aquifer.

Fault activation is the result of differential aquifer or reservoir compaction, as evidenced by the reversal in direction of fault movement on the fault south of Texas City and the tiltmeter data.

Acknowledgements

The author is indebted to Dawn McKalips for her geologic assistance and to R. A. Morton, L. J. Turk, W. R. Muehlberger, and E. G. Wermund for their critical review of this manuscript. This investigation was partially sponsored by the U.S. Geological Survey, Department of the Interior, under U.S.G.S. Grant number 14-08-0001-G-144 and U.S. Energy Research and Development Administration, Contract No. (40-1)-4900.

References

Clanton, U.S., and Amsbury, D.L., 1975, Active faults in southeastern Harris County, Texas: Environmental Geology, v. 1, p. 149-154.

Gabrysch, R. and Bonnet, C.W., 1975, Land-surface subsidence in the Houston-Galveston region, Texas: Texas Water Development Rept. 188, 19 p.

Jorgensen, D.G., 1975, Analog-model studies of ground-water hydrology in the Houston District, Texas: Texas Water Development Board Rept. 190, 84 p.

Kreitler, C. W., 1976, Lineations and faults in the Texas Coastal Zone: The University of Texas at Austin, Bureau of Economic Geology Report of Investigations 85, 32 p.

________, and Gustavson, T. C., 1976, Geothermal resources of the Texas Gulf Coast--Environmental concerns arising from the production and disposal of geothermal waters: The University of Texas at Austin, Second Geopressured Geothermal Energy Conference, Proceedings, volume 5, Legal, institutional and environmental, Report 3, 55 p.

Marshal, A.F., Jr. 1973, How much more will Houston sink: The Slide Rule, volume 33, number 2, 6 p.

Minor, H.E., 1926, Goose Creek oil field, Harris Co., Texas in Moore, R.C., ed.,Geology of salt dome oil fields: Am. Assoc. Petroleum Geologists, p. 546-557.

Pratt, W.E., and Johnson, D.W., 1926, Local subsidence of the Goose Creek oil field: Journal of Geology, volume 34, p. 577-590.

Reid, W.M., 1973, Active faults in Houston, Texas: The University of Texas at Austin, Ph.D. dissertation, 122 p. (unpublished).

Van Siclen, D., 1967, The Houston fault problem: Institute of Professional Geologists, Texas Section 3rd Annual Meeting, Proceedings, p. 9-31.

Weaver, P., and Sheets, M., 1962, Active faults, subsidence and foundation problems in the Houston, Texas, area, in Geology of the Gulf Coast and central Texas: Houston Geological Society Guidebook, p. 254-265.

Winslow, A.G., and Doyel, W.W., 1954, Land-surface subsidence and its relation to the withdrawal of ground water in the Houston-Galveston region, Texas: Economic Geology, volume 49, number 4, p. 413-422.

______, and Wood, L.A., 1959, Relation of land subsidence to ground-water withdrawals in the Upper Gulf Coast region, Texas: American Institute of Mining, Metallurgical and Petroleum Engineers, Transactions, volume 214, p. 1030-1034.

Wood, L.A., and Gabrysch, R.K., 1965, Analog model study of ground water in the Houston district: Texas Water Commission Bulletin 6508, 103 p.

Publication n°121 of the International Association of Hydrological Sciences
Proceedings of the Anaheim Symposium, December 1976

LAND SUBSIDENCE RESULTING FROM WITHDRAWAL OF GROUND WATER IN CARBONATE ROCKS

V. T. Stringfield and J. R. Rapp
U.S. Geological Survey
Reston, Virginia

Abstract

Land subsidence resulting from withdrawal of ground water in carbonate rocks may occur (1) where cavernous rocks are directly overlain by unconsolidated deposits, and (2) where old sinkholes are filled with unconsolidated deposits and the ground-water level is high enough to give some support to the unconsolidated deposits. When the water level is lowered, removing the support, the unconsolidated material can move downward into cavities and caverns in the underlying carbonate rocks. The resulting subsidence of the land surface may be gradual or it may occur suddenly.

In addition to lowering water levels and changing surface drainage, other man-imposed effects, such as seismic shocks (blasting), breaks in water mains and sewer pipes, or even over-watering in an irrigated area may result in surface subsidence or sinkholes. Subsidence or collapse may also be related to natural phenomena such as heavy rainfall, seasonal fluctuations in the water table, earthquakes, or other changes in the hydrologic regimen affecting the stability of the deposits overlying cavernous rock.

The dimensions of individual sinkholes range from a few centimeters to many meters. One of the largest sinks in Alabama resulting from withdrawal of water is about 145m long, 115m wide, and 50m deep.

Introduction

As stated by Poland and Davis, (1969, p. 187, 190) the principal causes of land subsidence are removal of solids or fluids from beneath the land surface, either naturally or artificially; solution; oxidation; compaction of soil or sediments under areas of surface flooding; vibration; or wetting; and tectonic movement. Fuller (1908,, p. 33) was the first investigator to suggest that withdrawal of fluids and decrease of fluid pressure cause sinking of the land surface due to removal of hydrostatic support.

Land subsidence has caused considerable damage in some areas. In some of these places, subsidence problems are being alleviated in one or more of several ways, including (1) cessation of withdrawal of fluids and (2) increase or restoration of fluid pressure by reduction of withdrawal, by artificial recharge, or by repressuring by injection of water.

The present paper discusses subsidence in carbonate rocks under natural conditions and subsidence caused by activities of man. One of the most recent reports on the early detection of sinkhole problems with a preliminary evaluation of remote sensing application is by Newton (1976, p. 8) who estimated that most of more than 4,000 man-induced sinkholes, areas of subsidence, and other related features in this category in carbonate rocks have occurred in Alabama since 1950. Newton divides the sinkholes into two types; those related to a decline in the water table and those related to construction. Newton's report includes a map of Alabama showing the areas in which sinkholes have occurred or could occur.

Aerial remote sensing has been used for (1) locating and monitoring sinkholes; (2) predicting potential collapse; (3) mapping fracture traces and lineaments of sinkholes; and (4) assisting general project planning (Warren and Wielchowsky, 1973). Gravity surveys have been used with fair accuracy in Far West Rand, South Africa, to determine sinkhole areas (Bezuidenhout and Enslin, 1970).

Special acknowledgements are due Messrs. Ren Jen Sun and Robert B. Anders, U.S. Geological Survey, for helpful discussions and suggestions regarding this manuscript.

Subsidence in Carbonate Rocks Under Natural Conditions

The development of natural sinkholes generally requires considerable geologic time and is not regarded as a serious environmental problem. However, sinkholes and related land subsidence due to activities of man that may cause serious problems occur only in areas where surface and subsurface solution and erosion have formed natural sinkholes and cavities, some of which are filled or overlain by unconsolidated deposits. Therefore, it is helpful to understand the conditions under which these natural features develop, and the areas in which they are present.

Bare carbonate rocks generally become indurated where they are exposed to weathering before the first stages of solution (karstification) have developed. Monroe (1966, p. 6) points out the importance of soil cover in the development of tropical karst features in Puerto Rico. Limestone hills without cover form caprock resistant to erosion. Soil resulting from weathering of the rocks is likely to be removed rapidly by surface erosion, especially on steep slopes (Flint and others, 1953, p. 1257-58). Such conditions are not favorable for subsurface solution of the rocks. The most favorable conditions for subsurface solution and the formation of sinkholes include some type of relatively less soluble cover through which meteoric water percolates to the underlying carbonate rocks. The cover may consist of (1) unconsolidated deposits, such as the blanket sand in Puerto Rico (Briggs, 1966), or (2) consolidated formations that include beds that are resistant to erosion, such as sandstone.

Where less soluble deposits overlying the carbonate rocks are unconsolidated and permeable, water percolates through the cover into joints and other openings in the carbonate rocks and forms a zone of saturation and a circulation system throughout the area as it moves underground to streams that cut through the cover. The circulation system forms solution channels in the upper part of the zone of saturation. As the zone of saturation is lowered, sinkholes will begin to form in the zone of aeration in the interstream areas.

Where less soluble formations covering the carbonate rocks contain resistant beds and where an agent of surface erosion, such as a stream, cuts through the cover into the underlying soluble rocks, meteoric water can then move downward from the less soluble beds into the carbonate rocks and out to a discharge area such as a surface stream at a lower elevation. These conditions initiate the circulation system in the carbonate rocks and result in the formation of a solution scarp. Recharge can occur along the solution scarp only where sinkholes and other solution features, such as vertical shafts, develop along the escarpment. These are later exposed on the surface of the carbonate rocks forming a sinkhole plain or plateau.

Where the less soluble formations overlying the carbonate rocks contain one or more resistant beds, such as the rocks of Pottsville age or the Cypress Sandstone in the Mammoth Cave region of Kentucky, one or more escarpments may form. In that area, the Pottsville escarpment has retreated ahead of the Dripping Springs escarpment. The sinkholes are the youngest along the escarpment and increase in age with increase in distance from the scarps. The Pennyroyal Plateau, a sinkhole plain adjacent to these escarpments, formed as the escarpments retreated. The distance to which the scarps retreat will depend in part on the dip of the formations. Where the dip is gentle, the distance will be greater than where it is steep.

Many of the sinkholes in some areas become clogged and filled with debris and unconsolidated deposits that accumulated on the plain as the less soluble resistant cover was removed by erosion. In some areas, as in the northern part of the Yucatan peninsula of Mexico, many of the cenote-type sinks remain open (Stringfield and LeGrand, 1974).

Under favorable conditions as many as 1,000 sinkholes may be present within an area of one square mile, as for example in Orange County, Indiana (Thornbury, 1954, p. 320).

In some regions where the carbonate rocks are approximately horizontal or gently dipping, the sinkhole pattern may be inherited by the underlying formations as the zone of saturation in the carbonate rocks is lowered with the lowering of base level. Under these conditions, sinkholes more than one hundred meters deep may develop, as in the Tertiary carbonate rocks in Florida, Puerto Rico, and Jamaica, W.I. Tres Pueblo sink in Puerto Rico is about 120m deep (Monroe, 1976). In Florida the base level was lowered more than 100m during the lowest stand of the Pleistocene sea. In Jamaica, W.I., the top of the zone of saturation in the carbonate rocks is as much as 300m below the part of the aquifer in which it stood when karstification began. In some areas of considerable topographic relief, as for example in the karst region between Mexico City and Monterrey, Mexico, sotanos, the cenote-type sinkhole, formed by upward stoping (collapse of limestone, bed by bed), may be more than 400m deep. Fish (1972, p. 37) reports El Sotano, Queretaro, Mexico, which is about 401m deep, is the deepest natural pit or shaft in the Americas.

Subsidence Due to Activities of Man

Sinkholes caused by activities of man are due chiefly to withdrawal of water from carbonate rocks in areas as described above, where (1) surface and subsurface solution and erosion have formed cavities and natural sinkholes which are covered or filled with unconsolidated deposits and (2) the ground-water level in the carbonate rocks is high enough to give some support to the unconsolidated deposits before the water level is lowered. When the water level is lowered, removing the support, the unconsolidated material can move downward into cavities and caverns in the underlying rocks, forming surface depressions or sinkholes. The subsidence may be gradual or sudden. This type of subsidence resembles that in some mining districts where removal of solids in the subsurface results in collapse of the roof of a mine.

In addition to withdrawal of water in carbonate rocks, other activities of man, such as changes in surface drainage, blasting, and breaks in sewer pipes may result in land subsidence or sinkholes. Subsidence or collapse may also be related to natural phenomena such as heavy rainfall, seasonal fluctuations of the water table, earthquakes and other stresses on the hydrologic system affecting the stability of the unconsolidated deposits overlying cavernous rocks.

The dimensions of the areas of subsidence or sinkholes range from a fraction of a meter to more than 100m. One of the largest sinkholes resulting from withdrawal of water from carbonate rocks in Alabama is about 145m long, 115m wide and 50m deep (LaMoreaux and Warren, 1973; Newton, 1976, p. 8). Foose (1966, p. 1045-1048) reported that in Far West Rand, Transvaal Republic, South Africa, lowering of water levels to dewater deep gold mines has reactivated old very deep natural sinkholes filled with unconsolidated sediments. Some of the new sinks are as much as 125m in diameter and 50m deep (Brink and Partridge, 1965).

Quinlan (1974, p. 161) reports that catastrophic collapses in the Transvaal have had the following effects; Thirty-four lives have been lost and about 35 million dollars have been spent on rebuilding, on application of safety measures, on research, and on compensation for damages including loss of water supplies.

The area of subsidence of individual sinkholes is relatively small in comparison with areas of subsidence due to compaction following withdrawal of water in unconsolidated deposits where subsidence may extend over many square kilometers. However, the maximum amount of subsidence may be only a few meters in comparison with subsidence of 100 or more meters in sinkholes.

In a few areas where a carbonate-rock aquifer under artesian pressure is overlain directly by a thick formation consisting of interbedded sand, clay, marl, and limestone, such as the Hawthorn Formation of Middle Miocene age in northeastern Florida and the coastal area of Georgia, a large decline of artesian pressure over a long period of time does not cause sinkholes, but may result in land subsidence due to compaction of unconsolidated or other compressible beds. The Hawthorn is as much as 150m thick in northeastern Florida and adjacent parts of Georgia, where it is a confining cover of the principal artesian aquifer of Tertiary age (known as the Florian aquifer in Florida). Although the formation is the confining cover, it contains zones of artesian water. In the Fernandina area in northeast Florida, a large decline in the artesian head in the carbonate-rock aquifer has reduced the head in the Hawthorn, indicating slow leakage into the underlying aquifer and possible land subsidence due to compaction of the Hawthorn Formation. The ratio of subsidence to artesian head, of course, would depend upon the thickness and lithologic character of compacting sediments.

In the Savannah area, Georgia, Davis and others (1963, p. 1-8) reported land subsidence of as much as 200mm at Savannah due to the decline of artesian pressure in the carbonate-rock aquifer which is overlain by the Hawthorn Formation. The ratio of subsidence to decline in head has been about 100mm of subsidence to 33m of head decline. During the period 1933-1955 subsidence exceeding 20mm occurred in an area of 80 square kilometers including the city of Savannah and extended 8 kilometers to the north and west. Poland and Davis, (1969, p. 230) concluded that the subsidence is due to compaction of the carbonate aquifer, and that compaction probably occurred chiefly in soft limestone and interbedded clay and marl which may be highly compressible.

In most, if not all of the areas of sinkholes in carbonate rocks in the United States, karstification and the present circulation system developed as a cover with resistant beds was removed by erosion. For example, karstification developed in Florida and Georgia where the covering Hawthorn Formation was encised by streams and then removed by erosion, exposing the underlying Tertiary limestone. The resistant beds of the Hawthorn formed scarps that retreated to their present positions by solution and erosion. Sinkholes occur where an appreciable thickness of the Hawthorn Formation has been removed by erosion.

Induced sinks must occur (1) where old sinkholes are filled with unconsolidated material and lowering of the water level in the limestone, causes reopening of the old sinkhole and (2) where cavernous limestone near the surface is overlain by unconsolidated deposits.

Surface depressions of the land surface may indicate where there are old sinks as in some parts of the Lake Region of Florida. However, in some areas there is no surface indication of an old sink or cavity below the surficial material; for example, in a stream valley or alluvial plain or terrace where the karst surface with old sinkholes or other solution cavities has been covered with alluvial deposits.

Stewart (1966, p. 6569) recorded 30 recent sinkholes in central Florida from 1953 to 1960. Nineteen of these sinks occurred in Polk County and eleven were in adjacent Hillsborough, Pasco, and Hernando Counties. All but six of the sinks in Polk County were closely associated with, or adjacent to, preexisting sinkhole areas. The land surface at 13 sites is about 21m or less above limestone; at 5 sites the depth to the limestone ranges from 30m to 70m.

Newton and Hyde (1971, p. 1, 17) reported that in the Birmingham area, Alabama, a major lowering of the water table, estimated to be as much as 45m, resulting from groundwater withdrawals, makes the area prone to the development of sinkholes. Until the water table recovers, sinkholes will continue to form with the greatest activity occurring during months of heavy rainfall. The decline of the water table results in a loss of support to the roofs of cavities in bedrock and to residual clay that overlies openings in bedrock which were filled with water prior to the decline of the water level. The removal of support can result in an immediate collapse or cause a downward migration of the clay through openings in underlying carbonate rocks. Migration or "spalling" of the clay into underlying openings results in the formation of cavities in the clay (pseudokarst) between bedrock and the land surface.

In the St. Louis area, Missouri, where the clastic cover consisting of formations of Pennsylvanian age has been removed from the underlying St. Louis Limestone of Mississippian age, and where karstified limestone is at or near the surface, there are numerous natural sinkholes. Although no new sinks are anticipated at the present time, the loss of soils through the old sinks is a problem where areas are developed for housing and other use. As described by Brucker (1970), the sinkholes may be classified as solution sinks and collapse sinks. The first class was developed by solution beneath the soil mantle without physical disturbance of the rocks. Generally as inwash of surface soil entered the sink through a swallow hole into an underground cavern, a funnel-shaped depression develops. The collapse-type sink was produced by collapse of rock into an underground cavern.

A method of treatment of the sinkholes, based upon the prevention of loss of soil into the underground drainage system in the limestone while still permitting surface water to escape into the underground drainage system, has been described by Brucker (1970).

Conclusion

Land subsidence due to natural sinkholes in carbonate-rock terranes generally requires considerable geologic time, and is not regarded as a serious environmental problem. However, sinkholes and related land subsidence that cause serious problems due to the activities of man, occur in areas where surface and subsurface solution and erosion formed natural sinkholes and cavities, some of which are filled or overlain by unconsolidated deposits. With adequate information on the hydrogeology and paleohydrology, the areas in which sinkholes may form due to the activities of man can be outlined.

Subsidence problems may be alleviated in one or more of several ways including, (1) cessation of withdrawal of water from carbonate rocks and (2) increase or restoration of water pressure by reduction of withdrawal, by artificial recharge, or by repressuring by injection of water.

References

Bezuidenhout, C. A., and Enslin, J. F., 1970, Surface subsidence and sinkholes in dolomitic areas of the Far West Rand, Transvaal Republic of South Africa, in Land Subsidence: Pub. No. 89, A.I.H.S. Unesco, p. 483-495.

Briggs, R. P., 1966, The blanket sands of northern Puerto Rico: 3rd Carribean Geol. Conf. Proc., p. 60-68.

Brink, A. B. A., and Partridge, T. C., 1965, Transvaal Karst, Some Considerations of development and Morphology with special reference to sinkholes and subsidence on the Far West, Rand, South African Geographical Journal, v. 47, p. 11-34.

Brucker, R. E., 1970, Geology and treatment of sinkholes in land development, St. Louis area, Missouri and Illinois: Missouri Industry News, v. 10, no. 7, p. 125-135.

Davis, G. H., Small, J. B., and Counts, H. B., 1963, Land subsidence related to decline of artesian pressure in the Ocala Limestone, at Savannah, Georgia, p. 1-8 in Trask, P. D. and Kiersek, G. A., Editors, Engineering Geology Case Histories, No. 4: Geol. Soc. America, 57 p.

Fish, John, 1972, Deep caves of Americas: Canadian Caves, v. 4, no. 1, 36 p.

Flint, D. E., Corwin, G., Dings, M. G., Fuller, W. P., MacNeil, F. S., and Saplis, R. A., 1953, Limestone walls of Okinawa: Geol. Soc. America Bull., v. 64, p. 1247-1260.

Foose, R. M., 1966, Sinkhole formation by ground-water withdrawals: Far West Rand, South Africa: Science, v. 157, no. 3792, p. 1045-1948.

Fuller, M. H., 1908, Summary of the controlling factors of artesian flows: U.S. Geol. Survey Bull. 319, 44 p.

La Moreaux, P. E., and Warren, W. M., 1973, Sinkhole: Geotimes, v. 18, no. 3, p. 15.

Monroe, W. H., 1966, Formation of tropical karst topography by limestone solution and reprecipitation: Carribean J. Sci. 6, nos. 1 and 2, p. 1-7.

______, 1976, Karst landforms in Puerto Rico: U.S. Geol. Survey Prof. Paper 899, fig. 7, (in press).

Newton, J. G., 1976, Early detection and correction of sinkhole problems in Alabama, with a preliminary evaluation of remote sensing applications: Alabama Highway Research, H.P.R. Report No. 76, 83 p.

Newton, J. G., and Hyde, L. W., 1971, Sinkhole problem in and near Roberts Industrial subdivision Birmingham, Alabama, A reconnaissance: Geol. Survey of Alabama, Circular 68, 42 p.

Poland, J. F., and Davis, G. H., 1969, Land subsidence due to withdrawal of fluids: Geological Society of America, Reprinted from reviews in Engineering Geology 2, p. 187-269.

Quinlan, J. T., 1974, Origin, distribution, and detection of development of two types of sinkholes in an anthropogenic karst, South Africa: Proceedings of 4th Conference, Karst geology and hydrology, West Virginia Geological and Economic Survey, p. 161.

Stewart, H. G., Jr., 1966, Ground-water resources of Polk County, (Florida): Florida Geol. Survey, Rept. of Investigations, No. 44, 170 p.

Stringfield, V. T., and LeGrand, H. E., 1974, Karst hydrogeology of Northern Yucatan Peninsula, Mexico: New Orleans Geological Society Field Trip 2, 1974, Annual meeting, Miami, Fla., Geological Society of America, p. 26-44.

Thornbury, W. D., 1954, Principles of Geomorphology: New York, John Wiley and sons, 618 p.

Warren, W. M., and Wielchowsky, C. C., 1973, Aerial remote sensing of carbonate terranes in Shelby County, Alabama: Geological Survey of Alabama, reprint series 26, 13 p. Reprinted from Ground Water, v. 11, Nov.-Dec. 1973.

Publication n°121 of the International Association of Hydrological Sciences
Proceedings of the Anaheim Symposium, December 1976

INDUCED SINKHOLES - A CONTINUING PROBLEM ALONG ALABAMA HIGHWAYS

J. G. Newton
U.S. Geological Survey
Tuscaloosa, Alabama

Abstract

Sinkholes are divided into two categories defined as "induced" and "natural." Induced sinkholes are those related to man's activities, whereas natural sinkholes are not. Damage from induced sinkholes far exceeds that resulting from natural sinkholes. An estimated 4,000 induced sinkholes or related features have formed in Alabama since 1900. In contrast, less than 50 natural collapses have been reported in Alabama and a significant number of these may have been related to man's activities.

Induced sinkholes are divided into two types: those resulting from a decline in the water table due to ground-water withdrawals and those resulting from construction. Almost all induced sinkholes occur where cavities develop in residual or other unconsolidated deposits overlying openings in carbonate rocks. The downward migration of the deposits into underlying openings in bedrock and the formation and collapse of resulting cavities are caused or accelerated by a decline in the water table that results in (1) loss of buoyant support, (2) increase in the velocity of movement of water, (3) water-level fluctuations at the base of unconsolidated deposits, and (4) induced recharge. Most sinkholes resulting from construction are due to the diversion of drainage over openings in bedrock.

INTRODUCTION

Recent sinkholes formed by collapses in the land surface have resulted in a variety of problems related to the maintenance and safety of man's structures and the pollution of existing and potential water supplies. In Alabama alone, costly damage has resulted from and numerous accidents have occurred or nearly occurred as a result of collapses beneath highways, streets, railroads, buildings, sewers, gas pipelines, vehicles, animals, and people.

In relation to their occurrence, sinkholes can be separated into two categories, even though most factors involved in their development are the same. In this report, these categories are defined as "induced" and "natural." Induced sinkholes are those that can be related to man's activities, whereas natural ones cannot. Induced sinkholes are the subject of this paper because damage to highways and other structures due to their development in Alabama far exceeds that attributable to natural sinkholes.

The purpose of this paper is to provide a description of forces involved in the development of induced sinkholes to aid in the recognition of active and potential areas of induced sinkhole development. Information included here is taken from a report on natural and induced sinkholes presented in Washington, D.C. in 1976 to the National Symposium on Subsidence sponsored by the Transportation Research Board, National Research Council. This paper represents a summary of findings resulting from investigations by the U.S. Geological Survey in cooperation with the Geological Survey of Alabama and the Bureau of Research and Development, Alabama Highway Department. Special recognition is due Dr. Philip E. LaMoreaux, former State Geologist, Geological Survey of Alabama, who, over a long period of time, has given repeated assistance and encouragement.

GEOLOGIC AND HYDROLOGIC SETTING

The terrane used to illustrate sinkhole development is a youthful basin underlain by carbonate rocks such as limestone and dolomite (fig. 1).

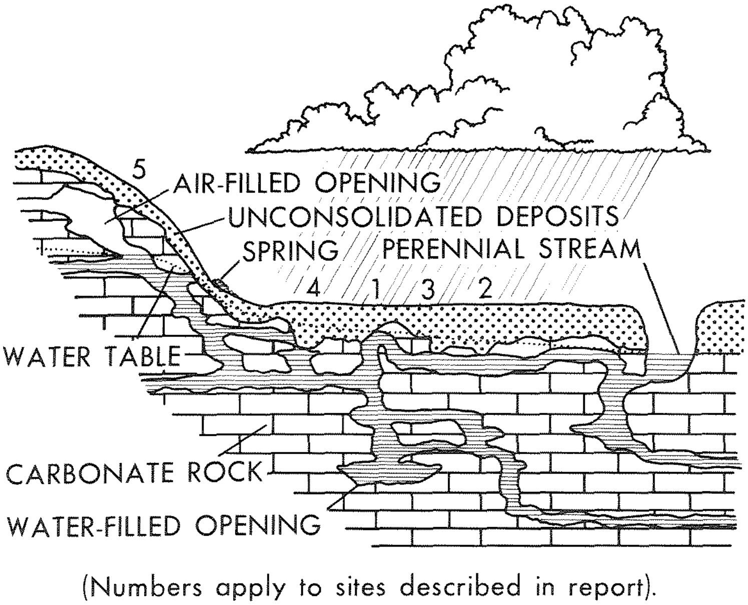

Figure 1. *Schematic cross-sectional diagram of basin showing geologic and hydrologic conditions.*

The basin contains a perennial or near-perennial stream. This particular terrane is used because it is very similar to that of 10 active areas of sinkhole development in Alabama that have been examined by the author. Factors related to the development of sinkholes that have been observed in these areas are generally applicable to other carbonate terranes. The terrane differs from those examined only in the inclination of beds, which is shown as horizontal for ease of illustration.

The development of sinkholes is primarily dependent on past and present relationships between carbonate rocks and water, climatic conditions, vegetation, and topography, and on the presence or absence of residual or other unconsolidated deposits overlying bedrock. The source of water associated with the development of sinkholes is precipitation which, in Alabama, generally exceeds 1270 mm annually. Part of the water runs off directly into streams, part replenishes soil moisture but is returned to the atmosphere by evaporation and transpiration, and the remainder percolates downward below the soil zone to ground-water reservoirs.

Water is stored in and moves through interconnected openings in carbonate rocks. Most of the openings were created, or existing openings along bedding planes, joints, fractures, and faults were enlarged by the solvent action of slightly acidic water coming in contact with the rocks. Water in the interconnected openings moves in response to gravity from higher to lower altitudes, generally toward a stream channel where it discharges and becomes a part of the streamflow.

Water in openings in carbonate rocks occurs under both water-table and artesian conditions; however, this study is concerned primarily with that occurring under water-table conditions. The water table is the unconfined upper surface of a zone in which all openings are filled with water. The configuration of the water table conforms somewhat to that of the overlying topography but is influenced by geologic structure, withdrawal of water, and variations in rainfall. The lowest altitude of the water level in a drainage basin containing a perennial stream occurs where the water level intersects the stream channel (fig. 1). Openings in bedrock underlying lower parts of the basin are water filled. This condition is maintained by recharge from precipitation in the basin. The water table underlying adjacent highland areas within the basin occurs at higher altitudes than the water table near the perennial stream. Openings in bedrock between the land surface and the underlying water table in highland areas are air filled (fig. 1). The progressive enlargement of these openings by solution has resulted in the formation of caves that are common in some parts of Alabama.

The general movement of water through openings in bedrock underlying the basin, even though the route may be circuitous, is toward the stream channel and downstream under a gentle gradient approximating that of the stream. Some water moving from higher to lower altitudes is discharged through springs along flanks of the basin because of the intersection of the land surface and the water table. The velocity of movement of water in openings underlying most of the lowland area is probably sluggish when compared to that in openings at higher altitudes.

A mantle of unconsolidated deposits consisting chiefly of residual clay (residuum), that has resulted from the solution of the underlying carbonate rocks, generally covers most of the bedrock in the typical basin described. Alluvial or other unconsolidated deposits often overlie the residual clay. The residuum commonly contains varying amounts of chert debris that are insoluble remnants of the underlying bedrock. Some unconsolidated deposits are carried by water into openings in bedrock. These deposits commonly fill solutionally enlarged joints, fractures, or other openings underlying the lowland areas. The buried contact between the residuum and the underlying bedrock, because of differential solution, can be highly irregular (fig. 1).

INDUCED SINKHOLES

It is estimated that more than 4,000 induced sinkholes, areas of subsidence, or other related features in this category have occurred in Alabama since 1900; most have occurred since 1950. During the same period, less than 50 new natural sinkholes have been reported. Induced sinkholes are divided into two types: those related to a decline in the water table, and those related to construction.

The following text, because this paper is cause oriented, is devoted to the description of the initial stage of development of induced sinkholes. Collapses forming new induced and natural sinkholes are similar in size. Recent collapses forming sinkholes in Alabama generally range from 1 to 90 m in diameter and from 0.3 to 30 m in depth. The largest collapse (fig. 2) occurred in a wooded area in Shelby County in December 1972. It apparently occurred in a matter of seconds. The collapse was about 90 m in diameter and 30 m deep.

Decline of Water Table

A relationship between the formation of sinkholes and high pumpage of water from new wells was recognized in Alabama as early as 1933 (Johnston, 1933). Subsequent studies in Alabama (Robinson and others, 1953; Powell and LaMoreaux, 1969; Newton and Hyde, 1971; Newton and others, 1975; Newton, 1976) have verified this relationship. Collapses, both observed and reported, have occurred in the immediate vicinities of 36 wells tapping limestone and dolomite in Alabama. The actual number of wells related to collapses probably far exceeds this figure because no inventory has been attempted. Three

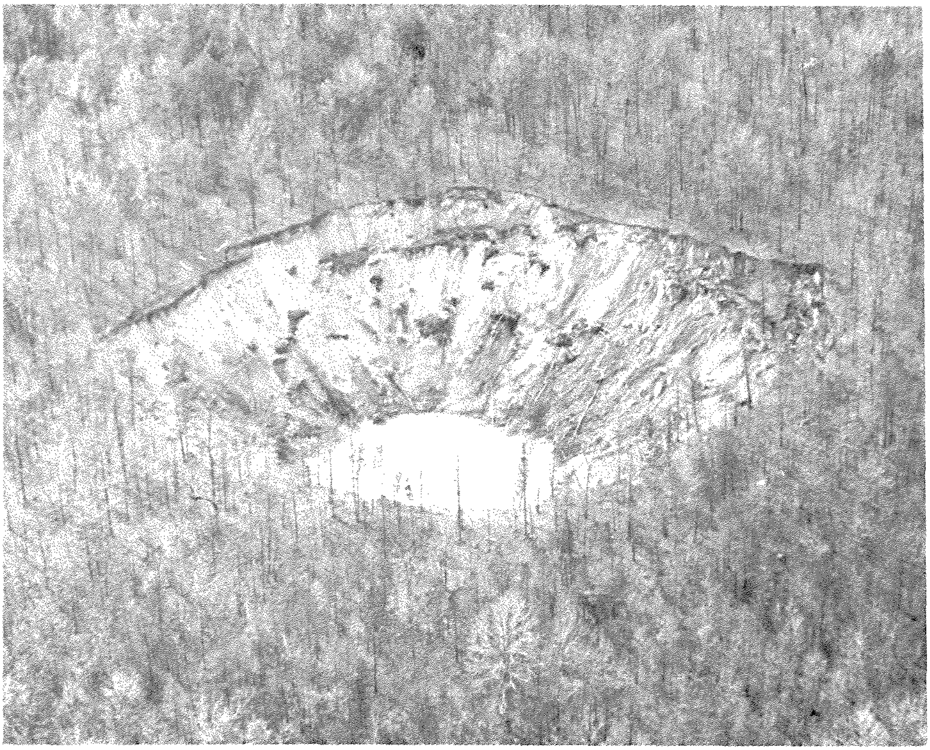

Figure 2. *Sinkhole resulting from collapse near Calera in Shelby County.*

collapses occurring during a pumping test of a new well in Birmingham in 1959 are excellent examples of sinkholes resulting from man-created forces (Newton and Hyde, 1971).

Dewatering or the continuous withdrawal of large quantities of water from carbonate rocks by wells, quarries, and mines in numerous other areas in Alabama is associated with extremely active sinkhole development. Numerous collapses in these areas contrast sharply with their lack of occurrence in adjacent geologically and hydrologically similar areas where withdrawals of water are minimal. For example, in five active sinkhole areas examined by the author, an estimated 1,700 collapses, areas of subsidence, or other associated features have formed in a total combined area of about 36 km^2. Recent collapses in adjacent areas underlain by the same geologic units are absent. This phenomenon is not unusual; the relationship of this type of sinkhole occurrence to cones of depression created by water withdrawals in Pennsylvania and Africa has been well established by Foose (1953, 1967).

Cause and development.--Two areas in Alabama in which intensive sinkhole development has occurred and is occurring have been studied in detail. Both areas were made prone to the development of sinkholes by major declines of the water table due to the withdrawal of ground water. The formation of sinkholes in both areas resulted from the creation and collapse of cavities in unconsolidated deposits caused by the declines (Newton and Hyde, 1971; Newton and others, 1973).

Cavities in unconsolidated deposits overlying carbonate rocks in areas where there have been water-table declines have also been described and explored in Africa and Pennsylvania (Donaldson, 1963; Jennings and others, 1965; Foose, 1967). The growth of one such cavity in Birmingham has been photographed through a small adjoining opening (Newton, 1976). The growth of the cavity resulted from the downward migration of clay into the two small openings in the top of bedrock.

Excellent reports prior to 1971 associated the development of sinkholes and subsidence with subsurface erosion caused by pumpage, the position of the water table, or a lowering of the water table due to withdrawals of ground water. Johnston (1933) noted that sinkholes appeared to be caused by the removal by moving ground water of residual clay filling fissures in limestone. He described the stoping action, surmised that water would have to be moving fast enough to erode clay and, because of this, stated that there appeared to be a causal relationship between this type sinkhole and high pumpage from new wells. Robinson and others (1953) attributed the development of sinkholes in a cone of depression to the increased velocity of ground water which caused the collapse of clay and rock-filled cavities in bedrock.

Foose (1953) associated the occurrence of recent sinkhole activity with pumping and a subsequent decline in the water table. He determined that their formation was confined to areas where a drastic lowering of the water table had occurred, that their occurrence ceased when the water table recovered, and that the shape of recent collapses indicated a lowering of the water table and withdrawal of its support.

Jennings and others (1965) associated development of sinkholes with pumpage and creation of cones of depression. They determined that sinkhole and subsidence problems increased where the water table was lowered and described the formation, enlargement, and collapse of cavities in unconsolidated deposits due to their downward migration. They also described geologic conditions necessary for the formation of the cavities. Foose (1967), in addition to his previous findings (1953), described the development of cavities in unconsolidated deposits in Africa and attributed them to the shrinkage of desiccated debris and the downward migration of the debris into bedrock openings. He also outlined geologic conditions related to their development and stated that a lowering of the water table initiated their formation.

Previous reports have described only indirectly or in part the hydrologic forces resulting from a decline in the water table that create or accelerate the growth of cavities that collapse and form sinkholes. These forces, based on studies in Alabama (Newton and Hyde, 1971; Newton and others, 1973) are (a) a loss of support to roofs of cavities in bedrock previously filled with water and to residual clay or other unconsolidated deposits overlying openings in bedrock, (b) an increase in the velocity of movement of ground water, (c) an increase in the amplitude of water-table fluctuations, and (d) the movement of water from the land surface to openings in underlying bedrock where recharge had previously been rejected because the openings were water filled.

The same forces creating cavities and subsequent collapses also result in subsidence. The movement of unconsolidated deposits into bedrock where the strength of the overlying material is not sufficient to maintain a cavity roof, will result in subsidence at the surface (Donaldson, 1963). Subsidence can also result from consolidation or compaction due to the draining of water from deposits previously located beneath the water table (Jennings, 1966). The former determination applies more to observations made in Alabama although the latter may be a contributing factor in some instances. Recognizable subsidence sometimes precedes a collapse (Newton and Hyde, 1971). This occurrence, where unconsolidated deposits are thin and consist chiefly of clay, indicates that the subsidence is due to a downward migration of the deposits rather than to compaction.

To demonstrate forces that result in the development of cavities and their eventual collapse, a schematic diagram is shown in figure 3 that

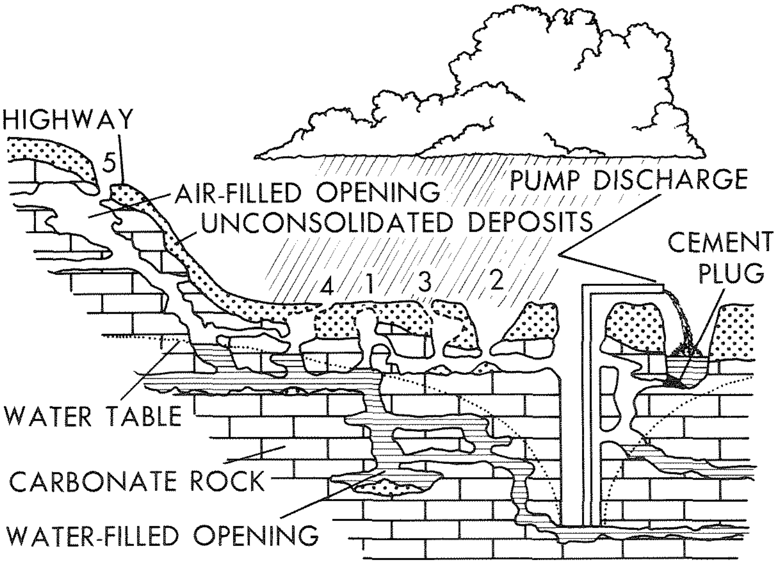

(Numbers apply to sites described in report).

Figure 3. *Schematic cross-sectional diagram of basin showing changes in geologic and hydrologic conditions resulting from water withdrawal.*

illustrates changes in natural geologic and hydrologic conditions previously described and shown in figure 1. A description of the forces triggered by a lowering of the water table follows. These forces or their effects are basic and can often be observed, measured, estimated, or computed in hydrologic work.

The loss of buoyant support following a decline in the water table can result in an immediate collapse of the roofs of openings in bedrock or can cause a downward migration of unconsolidated deposits overlying openings in bedrock. The buoyant support exerted by water on a solid (and hypothetically) unsaturated clay overlying an opening in bedrock for instance, would be equal to about 40 percent of its weight. This determination is based on the specific gravities of the constituents involved. Site 1 on figure 1 shows the unconsolidated deposit overlying a water-filled opening in bedrock. Site 1 on figure 3 shows the decline in the water table and the resulting cavity in the deposit formed by the downward migration of the unconsolidated deposit caused by the loss of support. The cavity may remain stable or it may enlarge upward by the spalling of the overlying deposit until the roof collapses.

The creation of a cone of depression in an area of water withdrawal results in an increased hydraulic gradient (slope of the water table) toward the point of discharge (fig. 3) and a corresponding increase in the velocity of movement of water. This force can result in the flushing out of the finer grained unconsolidated sediments that have accumulated in the interconnected solutionally enlarged openings. This movement also transports unconsolidated deposits migrating downward into bedrock openings to the point of discharge or to a point of storage in openings at lower altitudes.

The increase in the velocity of ground-water movement also plays an important role in the development of cavities in unconsolidated deposits. Erosion caused by the movement of water through unobstructed openings and against joints, fractures, faults, or other openings filled with clay or other unconsolidated sediments results in the creation of cavities that enlarge and eventually collapse (Johnston, 1933; Robinson and others, 1953). Collapses and subsidence due to erosion of clay-filled solutionally enlarged openings are occurring beneath and near Interstate Highway 59 in Birmingham, Ala.

Pumpage results in fluctuations in ground-water levels that are of greater magnitude than those occurring under natural conditions. The magnitude of these fluctuations depends principally on variations in water withdrawal and on fluctuations in natural recharge (precipitation). The repeated movement of water through openings in bedrock against overlying residuum or other unconsolidated sediments causes a repeated addition and subtraction of support to the sediments and repeated saturation and drying. This process might be best termed "erosion from below" because it results in the creation of cavities in unconsolidated deposits, their enlargement, and eventual collapse. Fluctuations of the water table against the roof of a cavity in unconsolidated deposits near Greenwood, Ala., have been observed and photographed through a small collapse in the center of the roof. These fluctuations, in conjunction with the movement of surface water into openings in the ground, resulted in the formation of the cavity and its collapse (Newton and others, 1973).

A drastic decline of the water table in a lowland area (fig. 3) in which all openings in the underlying carbonate rock were previously water filled (fig. 1) commonly results in induced recharge of surface water. This recharge was partly rejected prior to the decline because the underlying openings were water filled. The quantity of surface water available as recharge to such an area is generally large because of the runoff moving to and through it from areas at higher altitudes.

The inducement of surface water infiltration through openings in unconsolidated deposits interconnected with openings in underlying bedrock results in the creation of cavities where the material overlying the openings in bedrock is eroded to lower altitudes. Repeated rains result in the progressive enlargement of this type cavity. A corresponding thinning of the cavity roof due to this enlargement eventually results in a collapse. The position of the water table below unconsolidated deposits and openings in bedrock that is favorable to induced recharge is illustrated in figure 3. Sites 2, 3, and 4 on figure 3 illustrate a collapse and cavities in unconsolidated deposits that were formed primarily or in part by induced recharge. The creation and eventual collapse of cavities in unconsolidated deposits by induced recharge is the same process described by many authors as "piping" or "subsurface mechanical erosion" where it has been applied mainly to collapses occurring on noncarbonate rocks (Allen, 1969).

In an area of sinkhole development where a cone of depression is maintained by constant pumpage (fig. 3), all the forces described are in operation even though only one may be principally responsible for the creation of a cavity and its collapse. For instance, the inducement of recharge from the surface (site 2 on fig. 3) where the water table is maintained at depths well below the base of unconsolidated deposits, can be solely responsible for the development of cavities and their collapse. In contrast, a cavity resulting from a loss of support (site 1 on fig. 3) can be enlarged and collapsed by induced recharge if it has intersected openings interconnected with the surface. In an area near the outer margin of the cone (site 4 on fig. 3), the creation of a cavity and its collapse can result from all forces. The cavity can originate from a loss of support; can be enlarged by the continual addition and subtraction of support and the alternate wetting and drying resulting from water-level fluctuations; can be enlarged by the increased velocity of movement of water; and can be enlarged and collapsed by water induced from the surface.

Construction

Collapses resulting from construction are far less numerous than those due to a decline in the water table; however, they have resulted in extensive damage in Alabama. In this paper, the term "construction" applies not only to the erection of a structure, but also to any diversion of natural drainage and includes the clearing of timber in rural areas.

Cause and development.--The simplest cause of sinkholes or subsidence that can result from construction is loading. The emplacement of weight alone on unconsolidated deposits can result in compaction. The compaction can be irregular where the deposits overlie an uneven bedrock surface or openings in bedrock. Differential compaction and accompanying subsidence under these circumstances can result in foundation problems. The presence of natural or induced cavities in bedrock or unconsolidated deposits can result in a collapse when the overlying roof is subjected to loading.

Construction on unconsolidated deposits that overlie air-filled openings in bedrock (site 5 on fig. 1) can result in the formation of a sinkhole (site 5 on fig. 3). In construction, grading and the removal of trees creates new openings that connect the land surface with openings in bedrock. The concentration of surface runoff in drains or impoundments increases the downward movement of water. This downward movement sometimes erodes and transports unconsolidated deposits into underlying openings in bedrock forming a cavity in the deposits that eventually enlarges and collapses. This process is the same as that described under induced recharge (piping) where the water table has been lowered by pumping. It has also been described and illustrated in a carbonate terrane in Alabama where collapses have resulted in retention-basin failures (Warren, 1974).

The diversion of drainage and development of cavities and a tunnel in sand overlying carbonate rocks near Centreville, Ala. illustrates the "piping" process well. The grading of a timber trail resulted in the diversion and discharge of water into an opening at the surface (fig. 4) interconnected with an opening in the underlying bedrock. The water moved downward about 9 m, laterally about 15 m, and discharged downward. A cavity developed at this point (fig. 5) and, with continued subsurface erosion, the route along which the water moved enlarged backward toward the surface forming a tunnel (fig. 6). A second cavity formed as the erosion approached the surface and the collapse of its roof enlarged the opening into which water discharged (fig. 4).

The "piping" action can also apply to the development of sinkholes where water has been impounded on unconsolidated deposits that overlie carbonate rocks containing water-filled openings. On the floor of the impoundment, water moving through openings in the unconsolidated deposits to openings in carbonate rocks can form and collapse cavities in the deposits. This process generally occurs where there is considerable head or pressure exerted by the impounded water and where openings in the carbonate rocks have a discharge point outside of the impoundment at a lower altitude. The increase in the velocity of impounded water moving through unconsolidated deposits to underlying openings in bedrock will have an erosive capacity similar to that described previously in a cone of depression caused by pumpage. The saturation of previously unsaturated unconsolidated deposits by the impoundment will

Figure 4. *Opening into which water discharges.* (*Photograph by L. Lockett.*)

Figure 5. *Cavity resulting from subsurface erosion.* (*Photograph by L. Lockett.*)

Figure 6. *Tunnel resulting from subsurface erosion. (Photograph by L. Lockett.)*

also enhance the downward transport of the deposits. This action is probably responsible for the formation of sinkholes in the impoundment behind Logan Martin Dam on the Coosa River that reportedly resulted in the discharge of muddy water from an opening in the stream channel outside of the impoundment (John Winefordner, oral commun., 1973).

The most damaging collapse due to construction in Alabama involved Interstate Highway 59 near Attalla. A collapse about 3 m in diameter located in a drainage ditch along the highway allowed surface drainage to enter the ground. Based on a dye test, it was determined that the drainage discharged at a lower altitude beneath the fill of a lower lane. The lubrication of residual clay underlying the lane by this discharge and by some additional water from an unidentified source, resulted in a landslide and subsequent highway failure.

REFERENCES CITED

Allen, Alice S., 1969, Geologic settings of subsidence, *in* Reviews in engineering geology: Geol. Soc. America, v. 2, p. 305-342.

Donaldson, G. W., 1963, Sinkholes and subsidence caused by subsurface erosion: Regional Conf. for Africa on Soil Mechanics and Foundation Eng., 3rd, Salisbury, Southern Rhodesia 1963 Proc., p. 123-125.

Foose, R. M., 1953, Ground-water behavior in the Hershey Valley, Pennsylvania: Geol. Soc. America Bull. 64, p. 623-645.

_____1967, Sinkhole formation by ground-water withdrawal, Far West Rand, South Africa: Science, v. 157, p. 1045-1048.

Jennings, J. E., 1966, Building on dolomites in the Transvaal: The Civil Eng. in South Africa, v. 8, no. 2, p. 41-62.

Jennings, J. E., Brink, A. B. A., Louw, A., and Gowan, G. D., 1965, Sinkholes and subsidences in the Transvaal dolomites of South Africa: Internat. Conf. Soil Mechanics, 6th, 1965 Proc., p. 51-54.

Johnston, W. D., Jr., 1933, Ground water in the Paleozoic rocks of northern Alabama: Alabama Geol. Survey Spec. Rept. 16, 441 p.

Newton, J. G., 1976, Early detection and correction of sinkhole problems in Alabama, with a preliminary evaluation of remote sensing applications: Alabama Highway Dept., Bur. Research and Devel., Research Rept. No. HPR-76, 83 p.

Newton, J. G., and Hyde, L. W., 1971, Sinkhole problem in and near Roberts Industrial Subdivision, Birmingham, Alabama--a reconnaissance: Alabama Geol. Survey Circ. 68, 42 p.

Newton, J. G., Copeland, C. W., and Scarbrough, L. W., 1973, Sinkhole problem along proposed route of Interstate Highway 459 near Greenwood, Alabama: Alabama Geol. Survey Circ. 83, 53 p.

Powell, W. J., and LaMoreaux, P. E., 1969, A problem of subsidence in a limestone terrane at Columbiana, Alabama: Alabama Geol. Survey Circ. 56, 30 p.

Robinson, W. H., Ivey, J. B., and Billingsley, G. A., 1953, Water supply of the Birmingham area, Alabama: U.S. Geol. Survey Circ. 254, 53 p.

Warren, W. M., 1974, Retention basin failures in carbonate terranes: Water Resources Bull., v. 10, no. 1, p. 22-31.

Publication n°121 of the International Association of Hydrological Sciences
Proceedings of the Anaheim Symposium, December 1976

GEOPHYSICAL METHODS FOR LOCATION OF VOIDS AND CAVES

Roy J. Greenfield, Peter M. Lavin, and Richard R. Parizek
Dept. of Geosciences, The Pennsylvania State University
University Park, Pennsylvania

Abstract

The application of microgravimetric surveying, subsurface temperature measurements, electrical resistivity surveying, and seismic surface waves to the location of underground voids and caves will be discussed. Examples of field studies in carbonate terrains of central Pennsylvania, U.S.A., are presented. Microgravimetric procedures for determining soil thickness variations related to subsurface cavities as well as direct detection of cavities will be described. The existence of a cave may be inferred from subsurface temperature measurements at depths of 5 to 10 ft. Electrical resistivity measurements over fracture traces that delineate underlying zones of nearly vertical fracture concentration and caves show that these features give an anomaly. However, the anomaly can be either that for a resistive or conductive zone, depending on the time since a substantial rainfall. Theoretical results are presented for a resistive horizontal cylinder representing a dry cave. Use of seismic surface waves generated by harmonic or transient sources is discussed. Both a field study in an area of fractures and an ultrasonic seismic model study of a shallow cave show these features are detectable through changes in amplitudes and frequency content.

Introduction

For a number of years graduate students and staff at The Pennsylvania State University have been studying the geology and hydrology of carbonate terrains, with particular emphasis in central Pennsylvania. In the course of this work a number of studies have been conducted using geophysical methods to locate and to determine the extent of zones of fracture concentration revealed by fracture traces and lineaments, to locate caves, and to define the depth and configuration of the weathered top of bedrock below residual and transported soils. This paper contains a brief review of pertinent results of only some of these investigations using gravity, subsurface temperature, electrical resistivity, and seismic techniques.

Significance and Nature of the Problem

Detailed soils, subsurface geological and hydrological data are required to resolve land use planning, foundation engineering, geotechnical and environmental pollution control problems that arise within carbonate terrains in all regions. Test drilling is costly and there is a need to extrapolate results between boreholes and to define and isolate discontinuities not detected by test drilling. Carbonate terrains frequently display complex and rather abruptly varying subsurface conditions that are important in all kinds of foundation and resource exploration, evaluation and design work (see Parizek, 1977, in this volume). Of particular concern to some are the depth to and configuration of the bedrock surface. Weathering of carbonate bedrock is facilitated by joints, fractures, bedding plane partings, individual beds, faults, zones of fracture concentration, and related structures that are dispersed and that intersect in a difficult to predict manner (Parizek, 1977, in this volume).

Another class of problem includes the detection of sediment-filled and/or open voids in bedrock. These may be interconnected regionally and serve as major conduits to groundwater and pollutants, or they may be abandoned and located well above the seasonally high water table elevation.

Geophysical investigations can be helpful in addressing many of these data acquisition problems. New methods still need to be perfected to improve on the size and depth of features that can be detected which varies in importance depending on the problem at hand. This paper reports on four geophysical methods that have been found useful under Pennsylvania's geological conditions. Our research is continuing and we realize that there are limitations to our findings. Survey procedures applied and data requirements of others will not always be met using these techniques because of local geological difference and limitations of the methods.

Microgravimetric Methods

The success of gravimetric techniques in mapping near surface density changes due to buried stream valleys, bedrock topography, fracture zones and cavities (natural and man-made) is well established. Excellent reviews of procedures and results using standard gravimeters have been given by Neumann (1967) and Arzi (1975). A review of the application of "microgal" gravimeters to engineering problems was presented at the annual Meeting of the Transportation Research Board in 1975 by Omnes (1975). To review these "reviews" would do a disservice to the authors; therefore only certain aspects of microgravimetric methods that supplement these papers will be presented. No consideration will be given here to problems that are solvable using normal surveying procedures to detect anomalies on the order of 0.2 mGal or more (with station spacings of 300 ft or more) due to large caves (e.g., Colley, 1963) or buried stream valleys (e.g., Rankin and Lavin, 1970). Rather, we will concentrate on so-called high accuracy or microgravity surveying. Even this area requires breaking the discussion into two parts, dependent on whether standard gravimeters or "microgal" meters are employed.

Neumann (1967) and others have discussed the procedures and requirements for meaningful results using standard meters. The required accuracy of the surveys is dictated by the size of the expected anomalies. Numerous model studies have been made to study this aspect of the problem. Figure 1 is an example, showing the size of the anomaly as a function of the depth and size of the source for a sphere model.

Standard gravimeters have a reading precision of about 10 μGal; therefore, extreme care must be exercised in reading the instrument and correcting for its drift characteristics. Multiple readings at a given station and reoccupation of a single base station at approximately one-half hour intervals are often necessary. Corrections for elevation and position require careful (but easily attainable) surveys and should not produce significant errors with the possible exception in areas of considerable topographic relief where the choice of density to be used for the elevation and terrain corrections may be difficult. Study of the correlation between gravity anomalies and topography forms an important part of any analysis under these conditions. Neumann (1967) considers that it is quite feasible to detect anomalies as small as 30 μGals when sufficient care is exercised and station spacings are small enough so that the anomaly is defined by values at several stations.

Typically, the noise level of high accuracy surveys is high, often reaching levels on the order of the desired anomalies. Most of the sources of noise (such as near surface lateral density variations, changes in depth to bedrock, man-made structures) are inescapable. Thus, data enhancement techniques (such as downward continuation and vertical derivatives) are

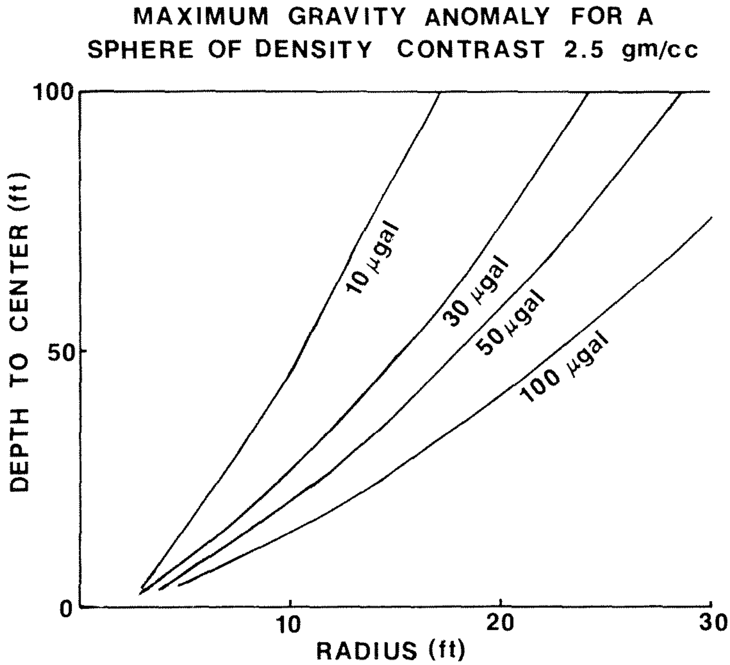

Figure 1

rarely called for. (In fact, one often has to low pass filter the data prior to attempting a quantitative interpretation, a point which will be demonstrated shortly.) Nevertheless, Fajklewicz (1976) proposes using measurements of the vertical gradient of gravity (over a distance of 1 yd) for detecting underground cavities and tunnels resulting from mining. The major effect of topography and the various sources of geologic and man-made noise on gradient measurements compared with that on gravity values limits the application of the gradient techniques to areas of small topographic variation and relatively homogeneous conditions.

Normal interpretation involves curve fitting procedures, usually using simple geometric models such as spheres, hemispheres, cylinders and slabs. Numerous examples are presented in the literature previously mentioned (and the many references cited in those works). A somewhat different approach will be presented here in order to illustrate the problems caused by "geologic noise."

A detailed gravity survey was run by Galiette (1974) in selected areas where well or seismic depth control was available as part of a study to determine soil thickness and bedrock competency for a sewage effluent spray irrigation program. The bedrock in the test area consisted of massive dolomite with interbedded sandstones. Variations in relief due to solution cavities and fracturing characterize the bedrock surface. The soil consists of thin layers of clay, silt and sand. An intermediate mixed zone of soil and large fragments of bedrock is common. Even though the area is complex, it was assumed that it could be modeled by a two-layer system with a density contrast of 1.0 g/cc (based on measured values).

Gravity readings were obtained at 20 ft intervals along selected profiles. A standard Worden gravimeter was used. Drift correction was based on reoccupation of the base station at 30 min intervals. Relief in the area was moderate (20 ft) so no terrain corrections were applied. The data were reproducible within ±0.05 mGal and the simple Bouguer anomaly was judged to be good to ±0.07 mGal.

The data were interpreted using a modified version of a method presented by Parasnis (1966) for the purpose of determining the minimum value of the maximum possible relief on the bedrock surface in a given region. In effect, the method is the equivalent stratum technique without downward continuation of the gravity data. The equivalent stratum method (Grant and West, 1965) relates the topographic relief h(x,y) on a surface at a mean depth, $\bar{h}$, to the observed gravity anomaly continued down to the mean surface, $\Delta g(x,y,\bar{h})$, by

$$h(x,y) = \frac{\Delta g(x,y,\bar{h})}{2\pi G\Delta\rho}$$

where G is the gravitational constant and $\Delta\rho=\rho_r-\rho_s$ is the density contrast across the surface (Figure 2). The procedure requires that the mean depth to the surface (as well as the density contrast) be known and that the relief be small compared to this mean depth.

Because of the high noise level of the data relative to the desired anomalies and the fact that the depth to bedrock (continuation distance) was only a few tens of feet, the gravity data were not continued downward prior to determining the variation of the bedrock surface. If the gravity difference (Δg) at the surface between two stations is used, it can be demonstrated that the relief (h) on the bedrock surface between the stations is

$$h > \frac{\Delta g}{2\pi G\Delta\rho}$$

Thus, the use of the values of the gravity anomaly between successive gravity stations gives a measure of the minimum relief on the bedrock between those stations. It requires that the depth to bedrock be known at one point in the survey area and that $\Delta\rho$ be known. Since the gravity anomaly is not downward continued, it is smoother and lower in magnitude than it would be if the equivalent stratum technique was used. Thus, the estimate

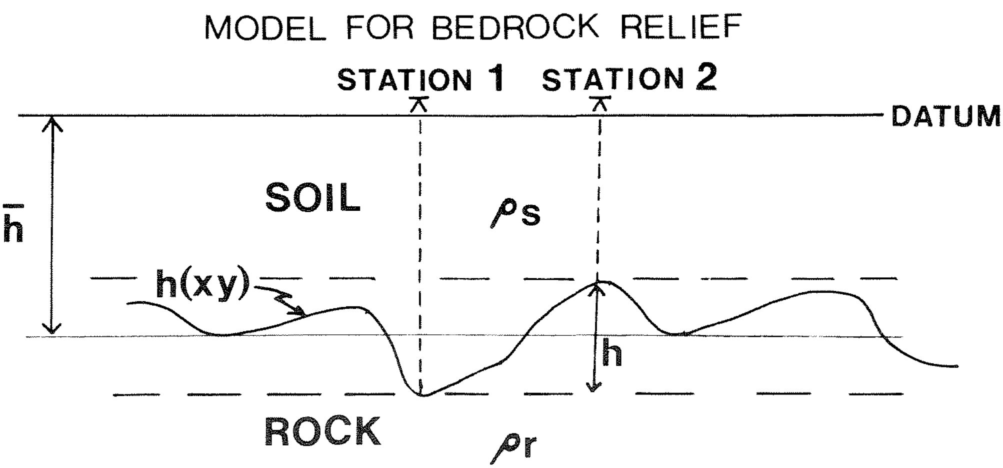

Figure 2

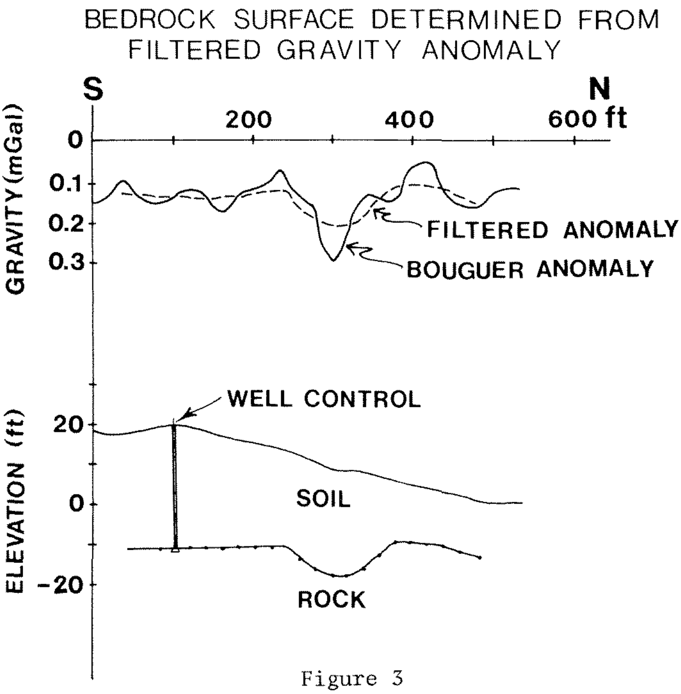

Figure 3

of the variation of h is smoother and smaller than the actual surface. This was not found to be a problem as long as the maximum depth to bedrock in the area was less than 100 ft.

Figure 3 shows the results from the work of Galiette (1974) for a typical profile in the test area. The Bouguer anomaly and filtered anomaly (using a 5 point operator with a cutoff of 0.005 cycles/ft) are shown in the upper graph. Use of the unfiltered data generally leads to an unstable solution as many of the short wavelength features (< 50 ft) are probably not related to the bedrock surface; they represent the "geologic noise" in this area. Using the known depth at the well, the values of gravity were converted into depth values (lower graph). The bedrock surface shows a depression (possibly a zone of concentrated weathered bedrock) with a lateral extent of 140 ft and a depth of 26 ft. There is a slight depression on the topographic surface directly above this feature. The calculated depth on the north end of the profile agrees closely with the depth at a nearby test well. Calculation of the theoretical gravity response due to the computed bedrock surface (using a two-dimensional polygon model) agrees well with the filtered anomaly.

In general, the interpretational method can be expected to give a smoother and shallower bedrock surface than is actually present. In the test area, depth values were no more than 20% too shallow as long as the bedrock interface was within 100 ft of the surface and the control depth was no greater than 50 ft. Choice of a density contrast (if not known) determines to some extent whether a minimum or maximum estimate of depth is obtained.

Turning now to the use of "microgal meters", it must be remembered that the limiting factor in gravity detection is not the sensitivity of the instrument (although problems of unstable operation are possible if the instrument is too sensitive). Rather, the limiting factor is the accuracy with which the corrections can be made and the degree of variation in local geology, topography and man-made sources of noise. In areas of small topographic relief with good maps and density control, anomalies as small as 30 μGal may be significant. In areas of rough topography anomalies would probably have to exceed several tenths of a milligal to be considered significant.

The reading precision of the microgal meters is about 2 to 5 μGal. Used with care, readings may be obtained faster than with standard meters as the need for repeating readings to achieve the desired accuracy is reduced (or eliminated).

The newsletter of the Franklin Institute in Philadelphia of November, 1959, reports on the use of a conventional Worden gravimeter, modified to have a sensitivity of about 4 μGal, to detect cavities under the city streets (Glenn, 1959). No corrections to the data were required as the effect of the cavities was very sharp compared with the "gradual" variations due to changes in elevation, position and "topography" (buildings). Cavities as small as 23 ft^3 were found.

A similar meter was tested and used by one of the authors (PML) in 1960. Figure 4 shows the drift-corrected readings over two known manholes in a street. The gradient is due primarily to the change in elevation along the profile. The absence of a major connection under the street between the manholes is indicated by the relative gravity high in the center of the profile. Further use of the instrument to search for small solution cavities ($\geq 60\ ft^3$) immediately below an airport runway met with limited success as the "noise" (due, in part, to variations in the thickness of the macadam and base courses) resulted in anomalies similar to those expected from the cavities.

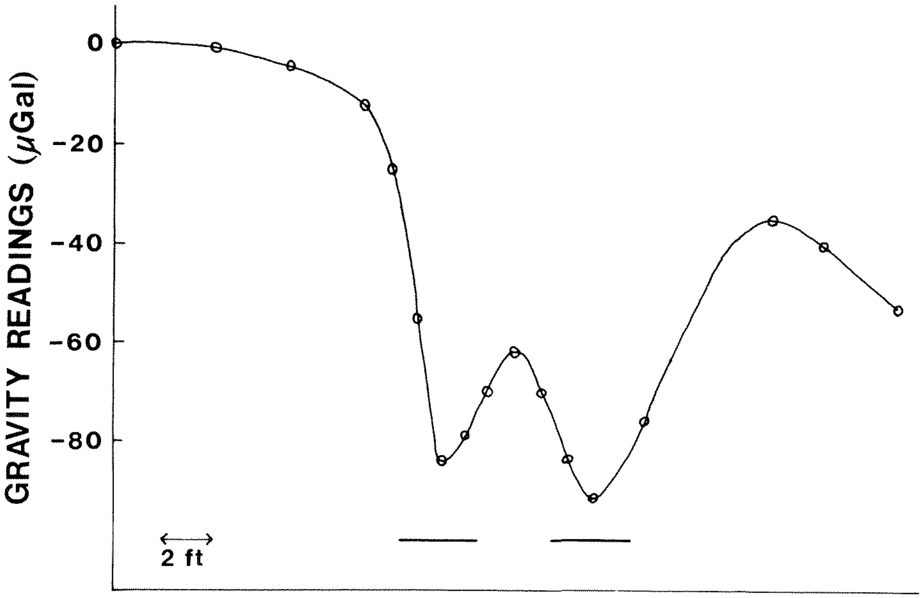

GRAVITY ANOMALY OVER MANHOLES

Figure 4

TEMPERATURE PROFILES
AT BOTTOM OF 6 FT HOLES

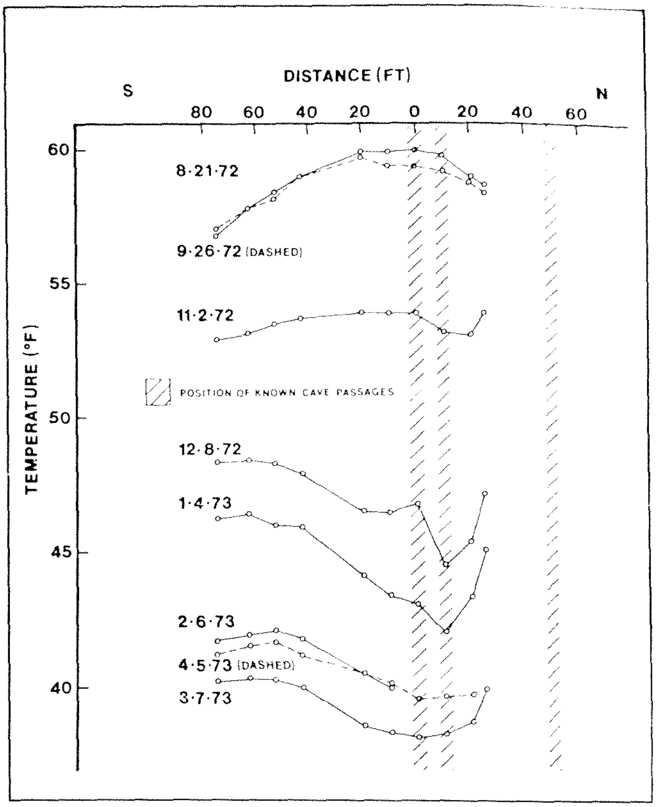

Figure 5

Starting in 1968, Compagnie Generale de Geophysique used a specially designed "Microgal" gravimeter (manufactured by LaCoste and Romberg, Inc.) for detection of cavities (Omnes, 1975). The reported "measuring accuracy" of about 5 μGal and the reduction of error by a factor of 5 in the results when compared with those obtained from a standard gravimeter led to a marked increase in the use of the tool to the point where it became their sole method used for detecting cavities for highway projects (Omnes, 1975). Some of the success of the gravity method is undoubtedly due to the fact that the observed anomalies are always larger than the theoretical anomalies based on the actual dimensions of the voids. This is due to the effect of the cavity on its surroundings (in terms of stress relief and increased fracturing and dissolutions). Several examples of this phenomenon are presented in the review by Omnes (1975).

Subsurface Temperature Measurements

Shallow subsurface temperature measurements have been used in the past to determine the location of aquifers (e.g. O'Brien, 1970; Cartwright, 1968; Bair, 1976). O'Brien (1970) used time averaged values to determine the spatial distribution of aquifer properties west of Schenectady, N.Y. Here the cool aquifer depressed the time average (mean) of the temperature at a 6 ft depth by several degrees. The spatial variation of the decrease of the average temperature was found to be an indicator of water transmissivity variations.

Work was done by Ebaugh (1973) and Ebaugh, Parizek and Greenfield (1974) to determine if soil temperature measurements could be used to locate caves or zones of fracture concentration in the folded and faulted carbonate areas in central Pennsylvania. Three sites were studied; we will discuss one of these, the Miller Cave site. Miller Cave is 1 to 10 ft wide and 15 ft high on the average. Its top is 30 ft below the surface. Temperature profiles at 6 ft depth taken perpendicular to the cave are shown in Figure 5. Note the higher 6 ft depth temperatures over the cave

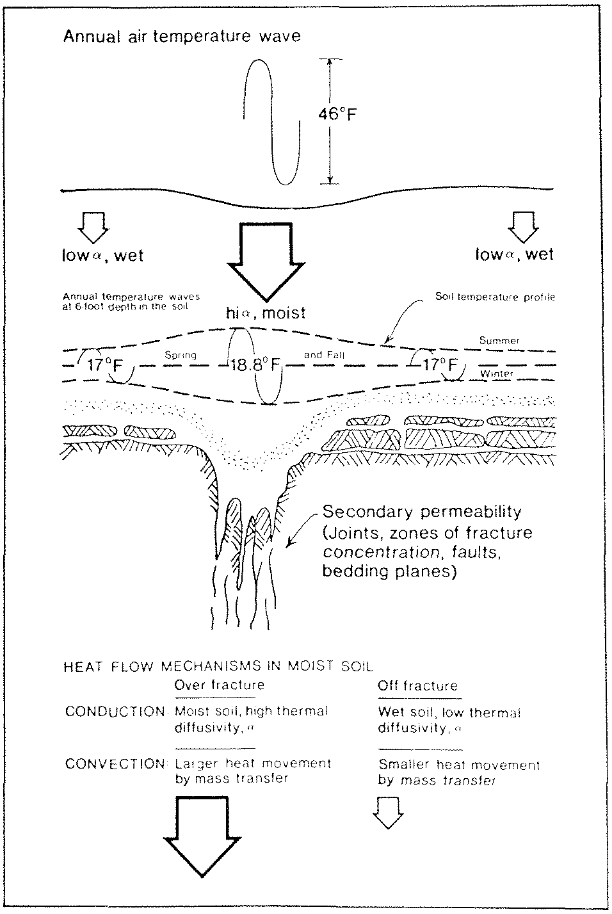

THEORETICAL ANNUAL SOIL TEMPERATURE VARIATION ABOVE AND ADJACENT TO FRACTURED BEDROCK

Figure 6

in the summer (e.g. 8-21-72 reading) compared to the summer temperature away from the cave. Also note that the winter temperatures are lower over the cave than the winter temperature away from the cave. Thus the measurements indicate a larger peak to peak amplitude for the annual temperature wave component over the cave (22°F) than at the portions of the profiles away from the cave (18°F). This larger amplitude may reflect a higher thermal diffusivity of the soil above the cave. Thermal diffusivity is dependent on the fractional volume of pore space filled by water; the value is maximum at approximately a 15% volume fraction (Bauer et al., 1972). Thus, if the cave and overlying zone of fracture concentration allow the soil above the cave to drain (moist soil) the thermal diffusivity would be higher than in areas with poorer drainage (wet soil). This leads to the greater observed amplitude for the annual component of 6 ft temperature fluctuations above the cave. This effect is shown diagramatically in Figure 6. The indication of drainage of the soil above Miller Cave is consistent with the drainage inferred from electrical resistivity measurements (see section on Electrical Resistivity). Figure 6 also shows how the added water flowing into the fracture above the cave could carry heat (by convection) downward in summer, and convect cold surface water in winter.

The question of whether the temperature in the cave could directly affect the 6 ft deep temperature values was examined theoretically. The effect being considered is similar to the lowering of the mean temperature, at 6 ft, by the cool aquifer noted by O'Brien (1970). In O'Brien's work the lateral extent of the aquifer was great enough so the heat flow was essentially vertical. However, it is more realistic to model a cave as an infinitely long horizontal cylinder, at a constant temperature which is different from the mean annual air temperature. The solution for the

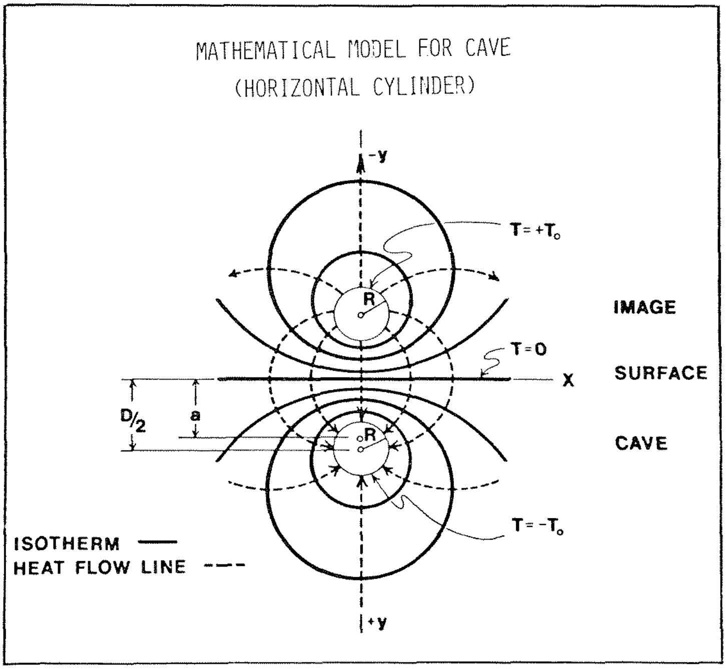

Figure 7

steady state temperature distribution for this cylinder model in a half-space (Figure 7) was evaluated by Ebaugh (1973). The solution was adapted, by analogy, from the electrostatic solution given by Smythe (1950, p. 76). The calculation gave the distribution of temperature about a cave whose mean annual temperature is different by two degrees from the mean annual air temperature, as is the case in the study area. Figure 8 shows the results for a model cave representative of the Miller Cave geometry. The theory predicts an anomaly, in the mean temperature, at a point directly above the cave, of 0.13°F at 3 ft depth and of 0.25°F at 6 ft depth. These values are too low to explain the measured anomaly. In general a cave will not give a measurable temperature anomaly by conduction of heat to the cave. As noted, however, a cave may be located by its effect on drainage of the overlying soil or, as pointed out by Ebaugh, Parizek and Greenfield (1974), by temperature variations noted in deeper boreholes or boreholes that pass near the cave.

Electrical Resistivity

Electrical resistivity surveys are used to define the subsurface resistivity structure. A general review of these methods is given by Van Nostrand and Cook (1966).

The most obvious application of electrical resistivity methods to subsidence monitoring is the location of caves or voids, since a cave or void has effectively infinite resistance unless filled with water or soil. The difficulty is that the cave will not be detectable if the depth to its top is greater than approximately one-fourth its height. Figure 9 shows the geometry for a Wenner array traverse over a horizontal cylinder model for a cave at four tenths of the cave radius below the surface. The apparent resistivity profile for this model is shown in Figure 10 for different ratios of "a" spacing to size of the cave (Yu, personal communication).

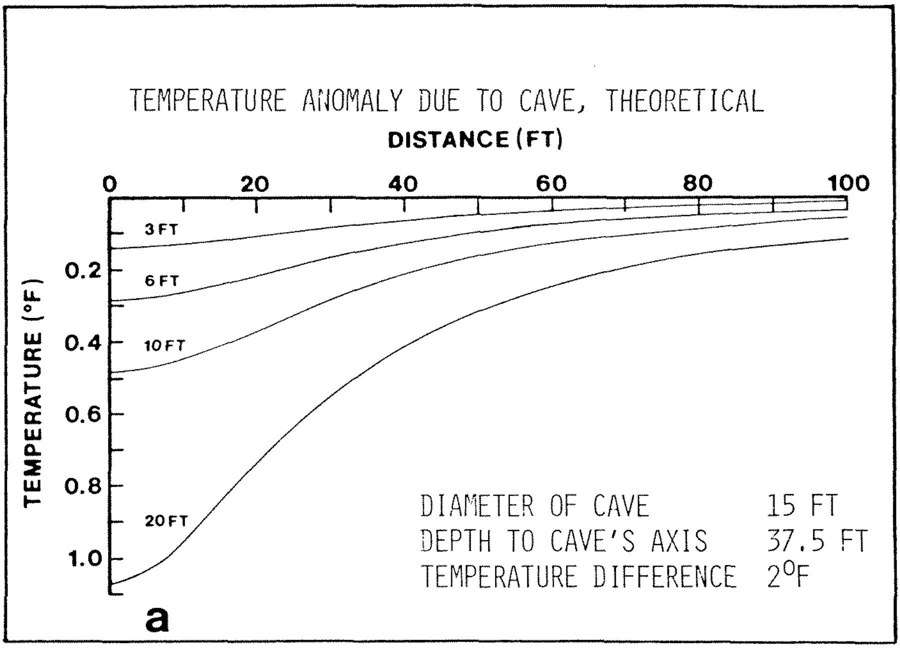

Figure 8

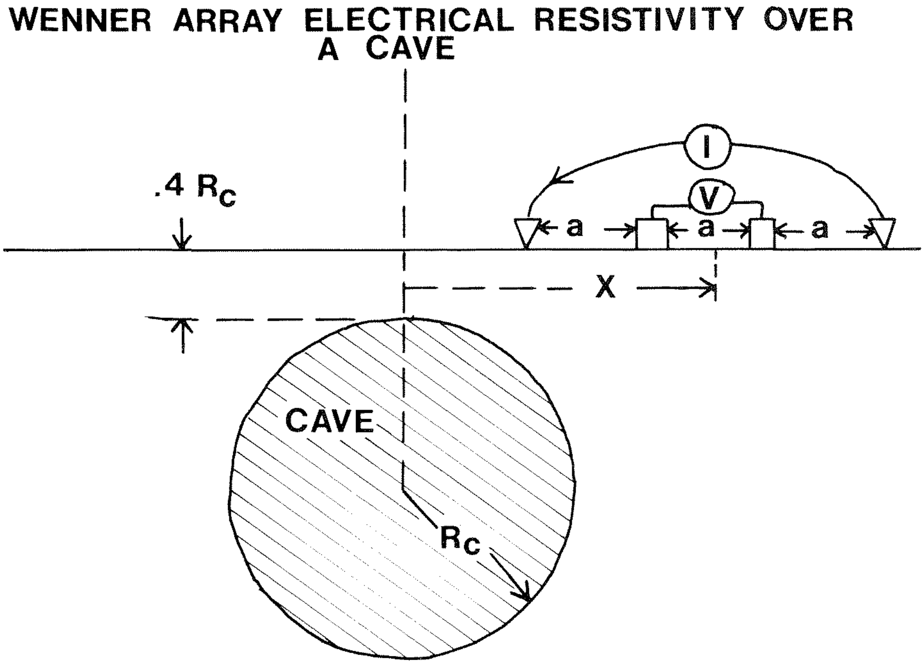

Figure 9

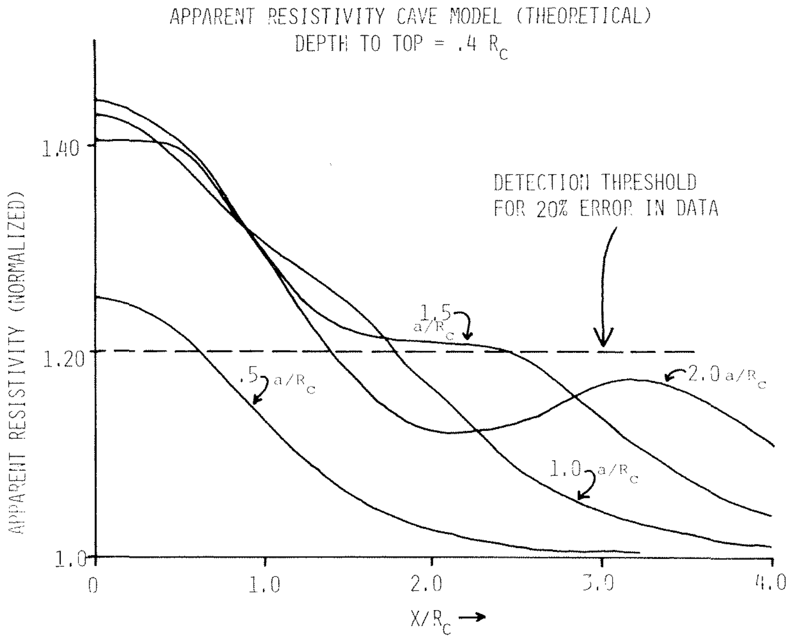

Figure 10

A 20% geologic noise level is probably the minimum to be expected due to changes in structure not related to the target cave. Thus if the size of the departure of the normalized apparent resistivity curve from 1.0 were much smaller than in Figure 10, the cave could not be detected. A deeper cave would, of course, give a smaller anomaly. Note that the maximum response occurs for an "a" spacing on the order of the depth (1.5 R_c) to the center of the cave. Similar results for a spherical cave model are given by Habberjam (1969).

The electrical resistivity method has been shown to respond to zones of fracture concentrations revealed by fracture traces mapped on aerial photographs in carbonate areas in Centre County, Pennsylvania. Kirk (1976) found a decrease of apparent resistivity over Miller Cave using a 10-ft spacing. This "a" spacing is too small to result in measurements which are influenced by the cave which is 30 to 40 ft below the surface. The observed response was attributed to the fracture zone above the cave and filling of the cracked rock zone with loose soil, which would be more conductive than the limestone.

Johnson (1966) ran Wenner profiles over several fracture traces. Results are shown in Figures 11 and 12 which show that in some cases the zone of fracture concentration below the fracture trace will give an increase in the apparent resistivity curve, while in other cases a decrease occurs. The increases tended to occur for profiles run during dry weather and the decreases for profiles run after rain when soil water content is high. The interpretation made was that after a rain, soil above the fracture zone will be wet for a period of time and will be electrically conductive. After a period of time the soil above the zone will have been

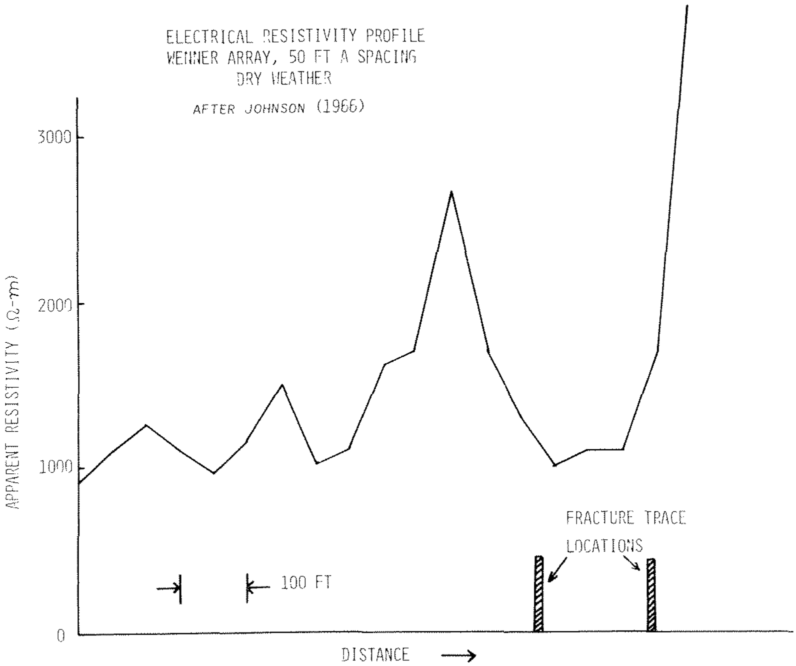

Figure 11

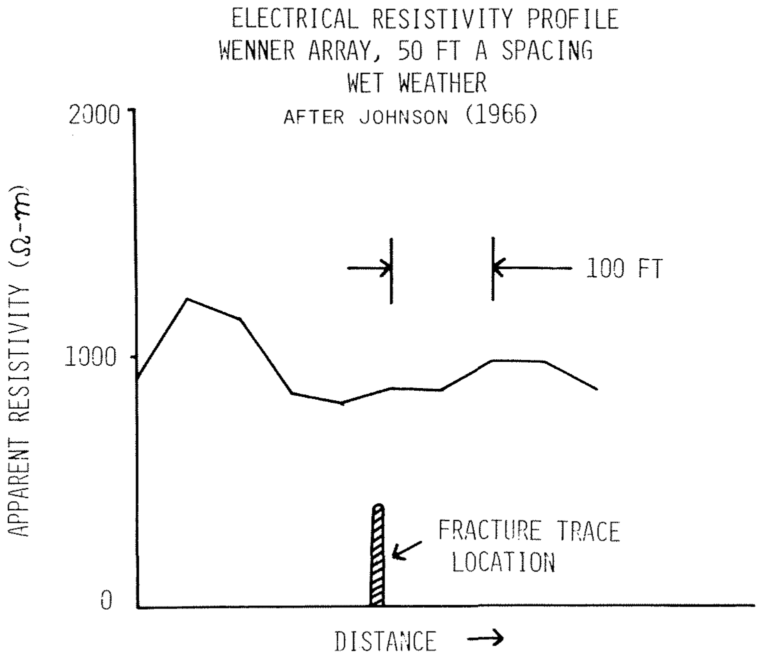

Figure 12

drained by seepage into the fracture system, leaving a dry electrically resistant soil. Unfortunately, Johnson (1966) did not repeat individual profiles several times to determine the period after a rain for which soils beneath fracture traces remain wet and conductive. His results do, however, point up the fact that the electrical resistivity method requires a good knowledge of the electrical characteristics of the area being monitored and how these characteristics change with rainfall history.

Electrical earth resistivity surveys, like geothermal surveys, are helpful in selecting which of many possible fracture traces mappable in a given area using air photographs delineate the most decomposed and permeable bedrock.

Seismic Methods

An obvious seismic method for detection of underground cavities would appear to be reflection seismology. Thus several attempts have been made to use seismic reflections to locate caves and tunnels. A discussion of this work is given by Dean (1975). None of the attempts have conclusively demonstrated that the method can be used to reliably detect a cavity. Cavities more than a few cavity diameters below the surface will not efficiently reflect low frequency seismic waves (wavelengths greater than the cavity diameter); high frequencies tend to be attenuated rapidly and thus the high frequency reflections will be small and lost in natural or source generated noise.

For cavities less than a cavity diameter below the surface, very high frequencies could be used. However, since the source and receiver must be close together, the source generated noise will probably make it impossible to see the reflection. Use of multiple geophone arrays may make it possible

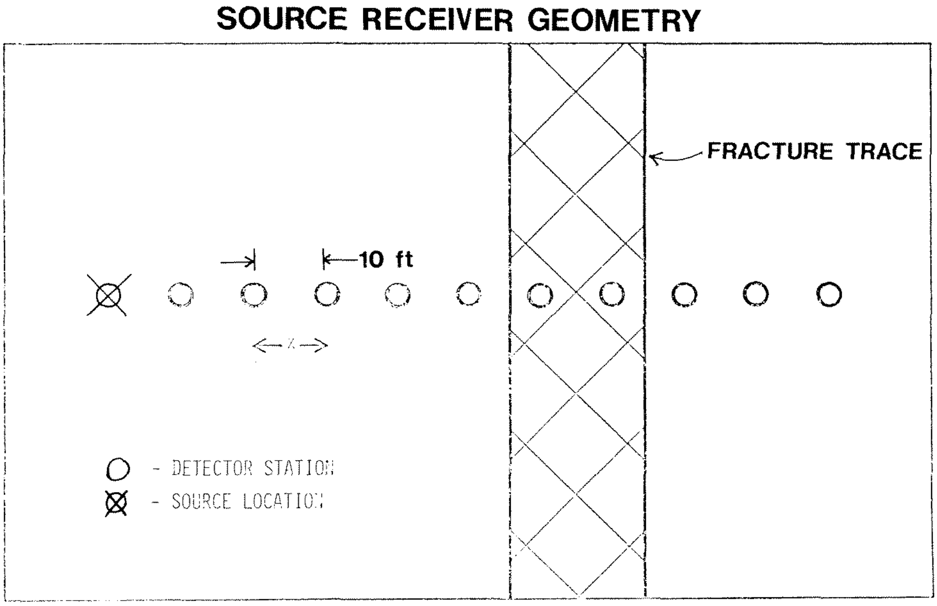

After Hawk (1972)

Figure 13

to see reflections from very shallow cavities. However, there are many problems associated with combining high frequency signals from an array of geophones. These problems are magnified when the reflector is very near both the source and the receivers.

Another method for near surface cavity detection was attempted by Watkins et al(1967). In this work observations were made which may have been due to a resonance of the cavity. The period of the resonance suggested is set by the time a Rayleigh-type wave takes to go around the circumference of the cavity.

Here we will discuss an alternative technique for locating either a cavity or a fractured zone. This approach requires the use of a source at a point removed from the cavity, which generates Rayleigh-type surface waves. The waves then propagate along the surface to the cavity where the presence of the cavity disrupts them.

A series of field measurements were made by Hawk (1972) around typical central Pennsylvania carbonate fracture zones. Figure 13 shows the source and a group of receivers in relation to a fracture trace. Two types of sources were employed; an impulsive source (a sledge hammer) and a harmonic wave source (a vibrating engine; seismic wave output was 25 Hz).

Figure 14 shows the ground amplitude versus receiver position for three profiles for the harmonic source. Notice the high amplitude that occurs over the fracture trace. This increase in amplitude over the trace was evident on the majority of profiles obtained by Hawk (1972). Thus a zone of high amplitude appears to be a good indicator of a fracture zone.

The transient source experiments also employed the source-receiver geometry of Figure 13. Two features of the seismic records (Figure 15) were indicative of the fracture zone. The first is the sudden disappear-

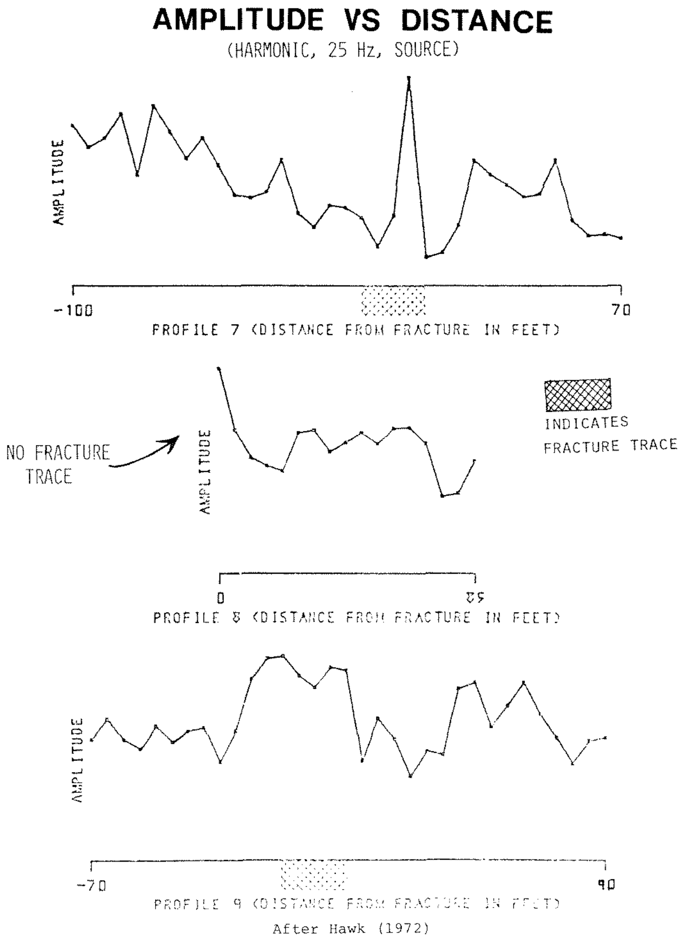

Figure 14

ance of the higher frequency energy for receiver positions at and beyond the fracture trace. The second feature is the greater time duration of the signal at receivers beyond the fracture trace compared to receivers between the source and the fracture trace.

The presence of the fracture zone may affect the Rayleigh wave in several ways. The soil in such a zone may have physical properties which are different from the soil over unfractured bedrock. Also, the bedrock will be fractured and have a lower strength than the unfractured bedrock. Travel-time studies (Lavin et al, 1972) have shown the seismic velocity to be lower in these zones. This lower velocity (thus lower elastic moduli) material can cause the increase in amplitude observed in the harmonic measurements.

The loss of the higher frequency waves in the transient experiments is due to one of two causes. First, the material within the fracture zone is less homogeneous than material adjacent to the fracture zone. This inhomogeneous material will cause loss of energy by scattering of energy out of the Rayleigh wave. This scattering is more effective in attenuating high rather than low frequency waves. The second possibility is that the material differences only extend to shallow depths below the surface. The short period surface wave amplitudes die off more rapidly with depth than the longer period waves. If the wave decay depth is much larger than the depth to which the material is altered by the fracture, the wave will pass with little effect. Thus the short period waves will be strongly affected while the longer period waves will not.

We prefer the scattering hypothesis as the mechanism for attenuating the short period component of the waves. In addition to decreasing the high frequency waves, scattering will cause a lengthening of the signal at receivers beyond the fracture zone (Dainty et al, 1974).

This method of using surface waves for detecting fracture zones might be extended to the detection of cavities. To examine this possibility we performed a seismic model experiment. The model setup is shown in Figure 16. Cavities of two sizes were cut into a Plexiglas sheet. The cavities are shown in Figure 17. The difference between cavities D and E is that cavity E comes within 0.5 cm of the surface and cavity D stops 2.0 cm below the surface. The amplitude decay depth of the Rayleigh waves used in the model experiment (∿15,000 Hz center frequency) was approximately

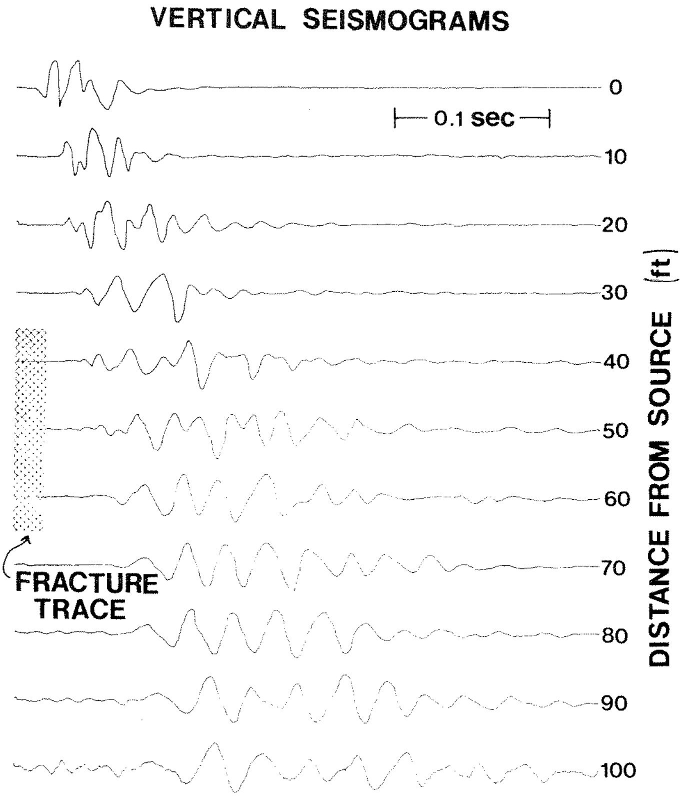

After Hawk (1972)

Figure 15

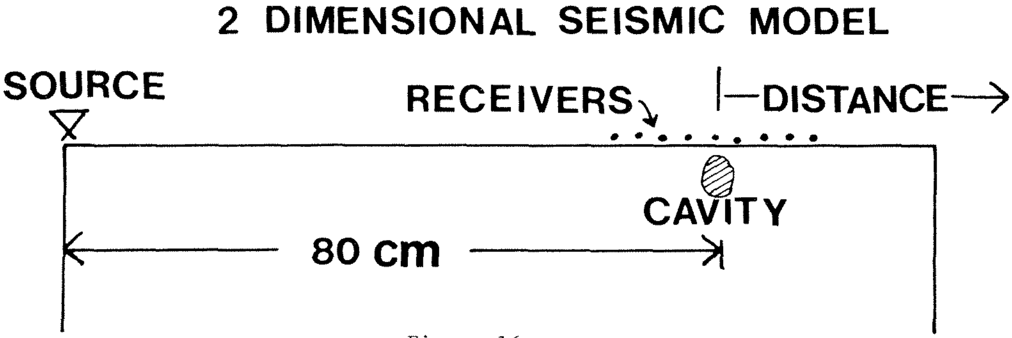

Figure 16

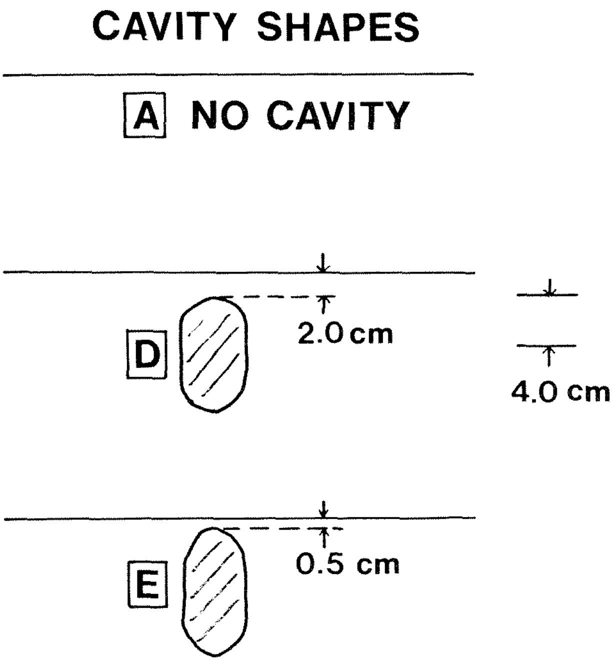

Figure 17

5 cm. Thus the bottoms of cavities D and E were deep enough to keep most surface waves energy from passing below the cavity. Therefore, the energy had to reach the receivers beyond the cavity by going between the top of the cavity and the surface. Figure 18 shows the vertical component wave amplitudes for surface receivers. Curve A is for no cavity present. The decay with distance for curve A is just due to natural attenuation of the Plexiglas and should be considered as the standard for comparison with curves D and E. Notice that for receivers located between the source and the cavity the amplitudes for curves A, D and E are similar. However, the

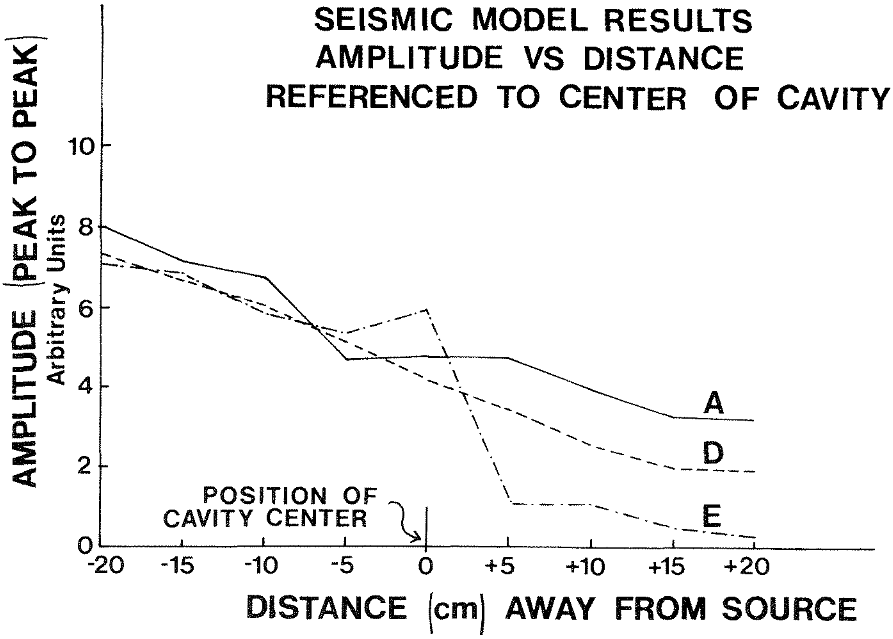

Figure 18

amplitude ratio of D to A is 0.6 and of E to A is 0.12 beyond the cavity, showing that the cavity will block the passage of the Rayleigh wave. Therefore, a sudden decrease in amplitude of the Rayleigh wave with distance from the source will be indicative of a shallow cavity.

Conclusions

Each of the four geophysical methods considered will, under favorable conditions, indicate the presence of a void or a fracture zone in carbonate bedrock. The gravitational method is probably the most likely to give an anomaly over the caverns. However, the electrical and seismic methods may allow large areas to be surveyed more rapidly than the gravitation method and may thus have an economic advantage.

In all four geophysical methods the anomaly indicating the presence of the cave or fracture zone is due, in a major degree, to changes in the soil and in its moisture content above the feature.

To make proper use of any of the geophysical methods it is necessary to have an understanding of the normal geophysical response of the area in question and to be able to predict the form of the geophysical anomaly due to the void or fracture. This is particularly true when dealing with high "noise" areas.

Further, where zones of fracture concentration control weathering of carbonate rocks, these features should first be mapped using conventional aerial photography (when mapping fracture traces) and LANDSAT, SKYLAB imagery or U-2 level photography (when mapping lineaments. Geophysical surveys may be planned following this initial work to narrow down points of interest or potential problem areas. Geophysical surveys may then be followed up with test borings that can be located to provide maximum information with the least amount of drilling expense. Photo and imagery analysis techniques are especially rapid and rather inexpensive, hence are a good starting point for planning most geophysical surveys in karst terrains. However, where modifications in land use have obscured the subtle evidence for fracture traces and aerial photographs that predate these changes do not exist, one will be forced back to a grid system application of geophysical surveying or a more random method of test drilling.

Acknowledgement

Much of the research described in this paper was supported by the Mineral Conservation Section, College of Earth and Mineral Sciences, The Pennsylvania State University. Computer results were done at the Computation Center of The Pennsylvania State University. The seismic analog model experiments were carried out by R. Christen.

References

Arzi, A. A., 1975, Microgravimetry for Engineering Applications: Geophysical Prospecting, v. 23, p. 408-425.

Bair, E. S., 1976, Permeability Distribution in Surficial Glacial Outwash Revealed by a Shallow Geothermal Prospecting Technique: M.S. Thesis, Dept. of Geosciences, Penn. State Univ., University Park, PA, 91 pp.

Bauer, L. D., W. H. Gardner, and W. R. Gardner, 1972, Soil Physics: John Wiley and Sons, Inc., New York, NY.

Cartwright, K., 1968, Thermal Prospecting for Groundwater: Water Resources Res., v. 4, p. 395-401.

Colley, G. C., 1963, The Detection of Caves by Gravity Measurements: Geophysical Prospecting, v. 11, p. 1-9.

Dainty, A. M., M. N. Toksöz, K. R. Anderson, P. J. Tines, Y. Nakamura, and G. Latham, 1974, Seismic Scattering and Shallow Structure of the Moon in Oceanus Procellarum: The Moon, v. 9, p. 11-29.

Dean, W. C., 1975, Tunnel Location by Magnetometer, Active Seismic, and Radon Decay Methods: Rpt. AL-75-1, Teledyne Geotech, Alexandria, VA.

Ebaugh, W. G., 1973, Temperature Patterns in Soil Above Caves and Fractures in Bedrock: M.S. Paper, Dept. of Geosciences, Penn. State Univ., University Park, PA.

Ebaugh, W. G., R. J. Greenfield, and R. R. Parizek, 1974, Temperature Patterns in Soil Above Caves and Fractures in Bedrock: Presented at Geolocigal Soc. Am., Cordilleran Section, Las Vegas, NV.

Fajklewicz, Z. J., 1976, Gravity Vertical Gradient Measurements for the Detection of Small Geologic and Anthropogenic Forms: Geophysics, v. 41, p. 1016-1030.

Galiette, S. J., 1974, The Use of the Gravity Surveying Technique in Studying Soil Thicknesses and Bedrock Topography: M.S. Paper, Dept. of Geosciences, Penn. State Univ., University Park, PA.

Glenn, N. S. (ed.), 1959, FIL Gravity Meter Detects Street Cavities: The Institute News, The Franklin Institute, Nov. 1959.

Grant, F. S., and G. S. West, 1965, Interpretation Theory in Applied Geophysics: McGraw Hill, New York, NY.

Habberjam, G. M., 1969, The Location of Spherical Cavities Using a Tripotential Resistivity Technique: Geophysics, v. 34, p. 780-784.

Hawk, J. H., 1972, Study of Seismic Methods in the Detection of Subsurface Fracture Zones: M.S. Paper, Dept. of Geosciences, Penn. State Univ., University Park, PA.

Johnson, P. W., 1966, Investigation of Photogeologic Fracture Traces by Electrical Processing Methods: M.S. Thesis, Dept. of Geol. and Geophys., Penn. State Univ., University Park, PA.

Kirk, K., 1976, Evaluation of the Tri-potential Technique in Locating Cavities, Fracture Zones, and Aquifers: M.S. Thesis, Geol. Dept., West Virginia Univ., Morgantown, WV.
Lavin, P. M., R. H. Merkel, S. S. Alexander, and R. J. Greenfield, 1972, Earth and Mineral Sciences, v. 41, p. 33-37, Penn. State Univ., University Park, PA.
Neumann, R., 1967, La Gravimétrie de Haute Précision - Application aux Recherches de Cavités: Geophysical Prospecting, v. 15, p. 116-134.
O'Brien, P. J., 1970, Aquifer Transmissivity Distribution as Reflected by Overlying Soil Temperature Patterns: Ph.D. Thesis, Dept. of Geol. and Geophys., Penn. State Univ., University Park, PA.
Omnes, G., 1975, Microgravity and its Application to Civil Engineering: Presented at Transportation Research Board, 54th Annual Meeting, Washington, D.C.
Parasnis, D. S., 1966, Mining Geophysics: Elsevier Publishing Co., New York, NY.
Rankin, W. E., and P. M. Lavin, 1970, Analysis of a Reconnaissance Gravity Survey for Drift Filled Valleys in the Mercer Quadrangle, Pennsylvania: J. of Hydrology, v. 10, p. 22-39.
Smythe, W. R., 1950, Static and Dynamic Electricity: McGraw Hill, New York, NY.
Van Nostrand, R. G., and K. L. Cook, 1966, Interpretation of Resistivity Data: U.S. Geol. Surv. Prof. Paper 499, U.S. Govt. Printing Office, Washington, D.C.
Watkins, J. S., R. H. Godson, and K. Watson, 1967, Seismic Detection of Near-surface Cavities: Geol. Surv. Prof. Paper 599-A, U.S. Govt. Printing Office, Washington, D.C.

Publication n°121 of the International Association of Hydrological Sciences
Proceedings of the Anaheim Symposium, December 1976

A GEOPHYSICAL METHOD OF INDICATING RELATIVE SINKHOLE SUSCEPTIBILITY

Charles Frederick Wall, P. E.
Pennsylvania Department of Transportation
Allentown, Pennsylvania

Abstract

This geophysical study involved a section of Interstate 78 in Lehigh County, Pennsylvania. The proposed roadway traversed carbonate rocks in an area affected by ground water withdrawal and where sinkholes are known to occur. A program set up to find the areas most susceptible to sinkhole formation combined electrical resistivity and shallow seismic refraction methods with air photo reconnaissance and drilling. The electrical resistivity methods used included both vertical sounding and horizontal traverses, as well as using the association parameter to group like soundings. The study showed the location of many areas susceptible to sinkhole formation and areas of incipient sinkhole activity. The exorbitant cost of fixing known sinkholes and the unknown factor of when an incipient sinkhole will collapse caused the alignment to be moved away from the affected area.

A corridor study of a proposed section of Interstate 78 in Lehigh County, Pennsylvania encountered the potentially critical problem of sinkhole formation aggravated by a condition of fluid withdrawal. A supplemental study was undertaken to discern the extent of the problem and to locate areas of instability.

The proposed roadway is located in the Saucon Valley, which is a small reentrant of the Great Valley Section of the Valley and Ridge Physiographic Province into the Reading Prong of the New England Upland Physiographic Province. The study area is entirely underlain by Ordovician carbonates. The North, West and South boundaries of the Valley consist of ridges of Pre-Cambrian gneiss and Cambrian sandstone and quartzite. The structure is extremely complex and is not completely understood at this time. (Fig. 1.) The regional trend parallels the Valley, which is Northeast-Southwest. Two faults roughly parallel the alignment. To the North is the Colesville Fault which dips to the South at 70^{o}; and to the south is the Saucon Fault, a thrust fault which dips to the south at an undetermined angle. A number of strike faults and cross-faults exist between the Colesville and Saucon Faults. Folding is extremely complex, with some beds overturned and recumbent. The major joints strike N 40^{o} - 60^{o} E and dip 75^{o} N. W. through vertical to steeply S. E. These fractures are deeply weathered and open as much as 4.5 meters. The open joints and faults provide the rock with a high secondary porosity. The primary porosity of most of the rock is practically zero. As an indication of this high porosity and high permeability, Callahan (1967) states that the pumping in the New Jersey Zinc Mine in the Saucon Valley is stabilized at 76 to 80 cubic meters per minute! As a consequence of this, the ground water level in the Valley is 122 to 152 meters below the surface. Most of the valley drainage is underground, with the only surface stream disappearing into a sinkhole at infrequent intervals.

The conditions prevalent in the Saucon Valley are not unique. The existence of a pumping operation causing ground water withdrawal and sinkhole formation in a carbonate terrain has been documented by others, including Brink

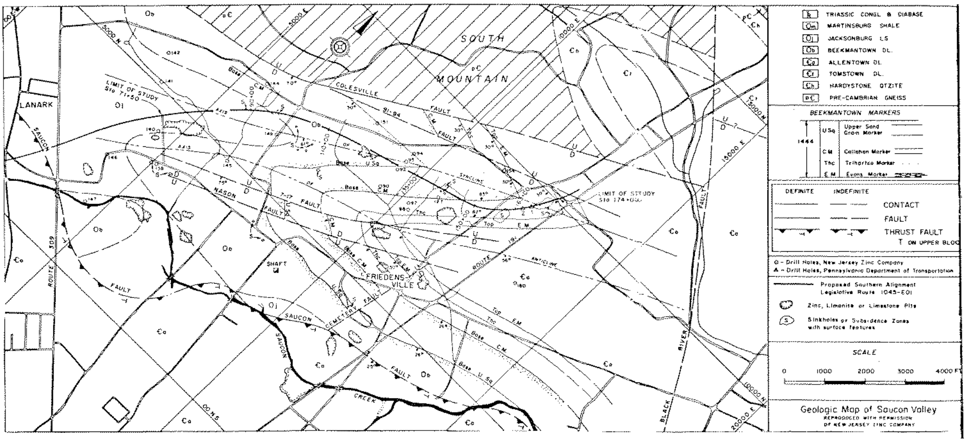

Fig. 1. Geologic map of Saucon Valley.

(1966), Foose (1953, 1969), Jennings (1966) and Jennings, et al (1965). Two types of sinkholes occur here. One is simply called a sinkhole, and is the result of the rapid collapse of the ground surface caused by the failure of a soil arch above a void. The other is known as compaction subsidence, and is the gradual subsidence of the ground surface. This type may occur when the weak zone is too large to form an arch, or the mechanism for transporting debris is absent, or the opening leading to the storage reservoir is clogged. In the Saucon Valley, the general cause for both types is the same; i.e., loss of buoyant support through a lowering of the water table, transportation of debris into a bedrock reservoir, upward migration of the void by roof spalling and, finally, roof collapse or continuous gradual subsidence. The final collapse is triggered by a disturbing agency. This may be excess percolating water in the arched material, causing loss of strength. Disturbing existing drainage patterns may produce this excess. Also, underground blasting causes earth tremors with vertical and lateral accelerations which induce stress in the soil arch. Other irregular ground movements that may cause the collapse of an arch are subsidences from mining operations and surface loading of a vibratory nature.

The soil in the valley is a glacial till originating from the local carbonates. The drill logs indicate an average thickness of 18 meters, with a range of 5 to 43 meters.

Color and color infra-red aerial photography at a scale of 1:4800 was used to locate sinkholes, linear features such as faults and joint systems, and to locate areas that have the geomorphic features likely to produce sinkholes. These features include closed basins, little surface drainage, a mottled ground appearance due to uneven moisture absorption, and a hummocky ground surface.

Exploratory diamond drill holes were put down by the mining company, and their drill logs were made available for this project. This information was used to correlate some of the electrical resistivity and shallow seismic work as well, so as to ascertain some of the rock contacts and the extremely fractured nature of the rock. The logs show intense weathering with openings and clay-filled joints as deep as 250 meters.

A multi-trace refraction seismograph was used to locate rock line, and also to differentiate between the fractured, weathered rock and the fresh rock below it.

The study was conducted in two phases. The first phase covered the mainline of Interstate 78 in the critical area; a distance of 3.1 kilometers. The second phase covered a proposed interchange between I-78 and Traffic Route 309.
The secondary sources of information and the corroborative methods have already been listed. The primary investigative method was electrical resistivity. Resistivity is a fundamental property of most materials, including soil and rock. The theory is based on the earth being a semi-infinite half space that is both homogeneous and isotropic. Since the earth is non-uniform, the quantity is called the apparent resistivity. The material that is encompassed by the electrical current is proportional to the distance between the electrodes. Therefore, the depth of penetration is also proportional to the inter-electrode distance or "a" spacing. There are many different methods available for using resistivity. The method used in this study involves inducing a direct current into the earth through two current electrodes and measuring the potential difference across two additional electrodes. The Wenner electrode array with the Lee modification was used. The Lee modification offers some protection against misinterpreting lateral variations as depth variations.

A number of different techniques were used to obtain the field data. The first method, called a vertical sounding, has the "a" spacing increasing by some constant over a fixed station. It is designed to provide information on the variation in subsurface conditions with depth. The Moore Cumulative Method is a manipulative method which uses the vertical sounding data and is successful in locating subsurface boundaries. This was used in conjunction with the vertical soundings, as were the Barnes Layer graphs. As the electrode separation is increased, a new incremental volume will affect the instrument readings. As the readings increase, the incremental volume becomes a smaller percentage of the total mass being measured. Thus, a small near-surface layer can have the same influence as a larger layer at depth. The Barnes Layer Method was devised by Barnes (1952) in order to reduce the magnitude of the problem by distinguishing the resistivity of each incremental layer. The vertical sounding, Moore's Cumulative and Barnes Layer data can all be contoured on a horizontal or vertical plane. The contour plots often show subsurface changes better than the individual sounding curves.

One of the principle methods used in indicating relative sinkhole susceptibility is Habberjam's (1970) association parameter. The output from the vertical soundings is used as the input data for the association parameter. The vertical soundings can be compared to one another by degree of likeness. Specifically, comparisons between soundings are based on curves with matched axes. Superposing the results of two soundings in this way, the differences between the dependent variable (apparent resistivity) at any spacing; i.e., $\log_{10} p\,(a_r, i) - \log_{10} p\,(a_r, j)$ can be taken as a measure of the departure between soundings at this spacing and as an overall measure of the difference between soundings. The variance of this quantity is:

$$A_{ij} = \frac{1}{n+1} \sum_{r=0}^{n} \left[\log_{10} p(a_r, i) - \log_{10} p(a_r, j) \right]^2$$

where Aij = association parameter,
$i\&j$ = sounding numbers,
p = apparent resistivity,
n = total number of soundings,
a_r = reading number.

This parameter has the obvious and important significance that it will be zero if the observed curves are perfectly alike, while in areas where apparent resistivities may vary by three orders of magnitude, Aij can range up to nine. In the field, soundings are limited to discrete spacings between the smallest a_o and the largest a_r; however, these limits may be narrowed to include only spacings from specific intervals of the sounding. In this way, the deeper part of the sounding may be isolated from the near-surface section.

Errors in observed resistivities at the one to two percent level will produce a value of Aij between otherwise like curves of less than 0.0001. However, the siting of large numbers of soundings in an area of even modest geologic complexity will mean that precisely equivalent sites are not occupied, and that a likeness search will be concerned with very much higher levels for the association parameter. For this study, an association parameter of 0.02 proved to be adequate.

With an association parameter selected as indicating a suitable degree of likeness, several methods of displaying the data are available. An association matrix can be assembled by arranging the soundings in geographical order and differentiating between soundings above and below the chosen association parameter. Geologic structure can sometimes be read from the geometric patterns displayed; however, the structure of the area under study proved to be too complex to do this.

An association profile was constructed with the Aij values on the ordinate and the sounding numbers on the abscissa. In this way, all soundings can be compared to each other and the profiles can be visually curve matched. In this study, a few master soundings were run over existing sinkholes and the remaining soundings compared to them. The results were encouraging and will be listed later.

The second basic method of obtaining electrical resistivity data is the horizontal traverse. Using one or more specific "a" spacings, the electrode array is moved along a line of traverse. Core borings are used to select the "a" spacings that will produce the most information. The spacing between traverse set ups is arbitrary, but should be chosen to reflect the complexity of the geologic structure. A computer was used to reduce all of the resistivity data. The output was in the form of data tabulations and the appropriate resistivity curves.

The following was accomplished in the first phase of the study of the main line of I-78. A horizontal traverse with "a" spacings of 9.1, 18.29 and 30.48 meters was run every 15.24 meters along the main line. Specific anomalus points were located on the traverse resistivity profile. Vertical soundings with a maximun "a" spacing of 31 meters were run at these points. These anomalus points represented incipient sinkholes or significant fracture zones. The vertical sounding data was used as the input for a series of association parameter profiles and matricies. Five of the 49 vertical soundings were run over existing sinkholes. One sounding was eliminated because of extreme backup The remaining soundings were grouped by curve matching the association profiles. Two sets of profiles were developed; one encompassing the entire range of "a" spacings, and the other using only the lower half of the "a" spacings. This process enabled us to see to what extent the likeness of the near surface material affected the groupings. Both sets resulted in groups with a high percentage of soundings (72%) associated with soundings taken over sinkholes. The other soundings not associated with sinkhole soundings could be reconciled with limey sandstone beds not susceptible to solution activity or with an argillaceous limestone formation that has not produced any sinkholes.

The Barnes Layer Values of a series of contiguous vertical soundings were used to produce a vertical cross section (Fig. 2).

Following is the interpretation for the section:

ohm-cm	Interpretation
0 - 15,000	Wet to moist clay and clay silt soils.
15,000 - 30,000	Moist silty and sandy soils.
30,000 - 100,000	Highly fractured rock with moist soil filling.
100,000 - 300,000	Slightly factured rock with dry to moist soil filling.
Over 300,000	Hard bedrock or dry, air-filled voids.

This section clearly shows the deep vertical chimneys in the rock. A comparison of this section and the air photos, drill logs and seismic sections with the sounding groups and horizontal traverses (Fig. 3) show that these areas associated with sinkholes have highly fractured bedrock and many incipient sinkholes at depth.

The following was accomplished in the second phase on the interchange of Interstate 78 and Traffic Route 309. A grid template (30.48 meters NE-SW x 60.96 meters NE-SE) was placed on a map of the interchange. An electrical resistivity vertical sounding was taken at every intersection of the grid. The soundings were carried to a depth of 34.38 meters. A total of 130 soundings were taken; 121 on the grid and 9 over known observable sinkholes. The vertical sounding readings at 9.1, 18.29 and 24.38 meters were taken from the data sheets and run through the computer as horizontal traverses. In addition to these nine traverses, one along each NE-SW grid line, a traverse was run along the proposed alignment of I-78. A Barnes Layer cross section was plotted along the middle line of the study area. Isopleth resistivity maps showing the values in plan view were developed for the interchange at the 10.67 and 22.86 meter vertical levels. The resistivity values for the vertical soundings were again used in an analysis using the association parameter. Diamond drilling and seismic sections were used to correlate the electrical resistivity work.

The resistivity traverse showed many broad fracture zones associated with known and incipient sinkholes. The traverse and the seismic spreads correlated well together and reconciled some extrapolated fault lines shown on the geologic map. A plan map of the interchange was overlayed with the isopleth resistivity maps, the association parameter groups and the geologic map. They supported the location of fracture zones as found with the horizontal traverses and seismic spreads. The association parameter groupings were divided into two subgroups; again, one using the full vertical sounding and one using the deeper half of the soundings. An average of 77% of the soundings were associated with soundings taken over sinkholes. An asso-

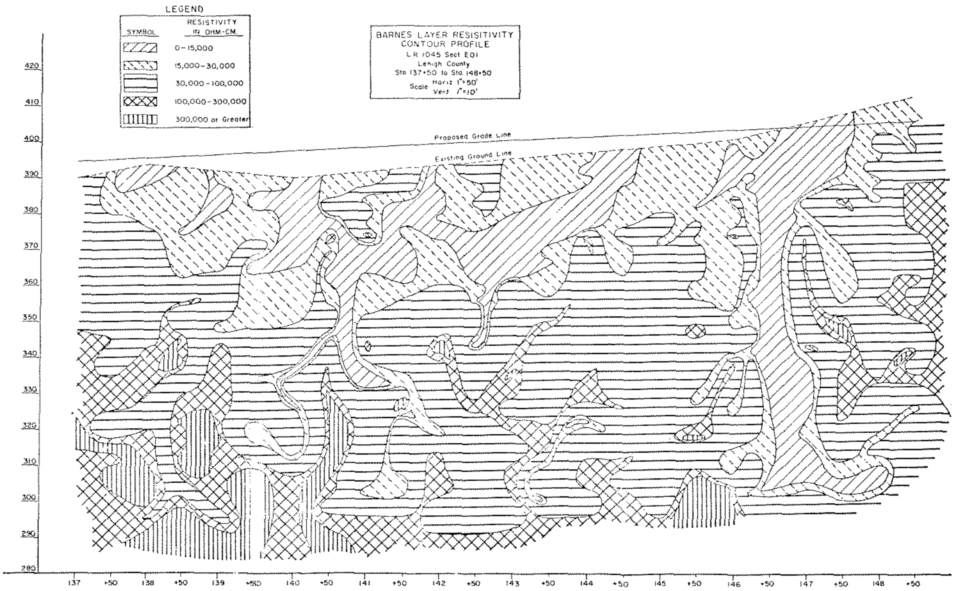

Fig. 2. Barnes Layer resistivity contour profile.

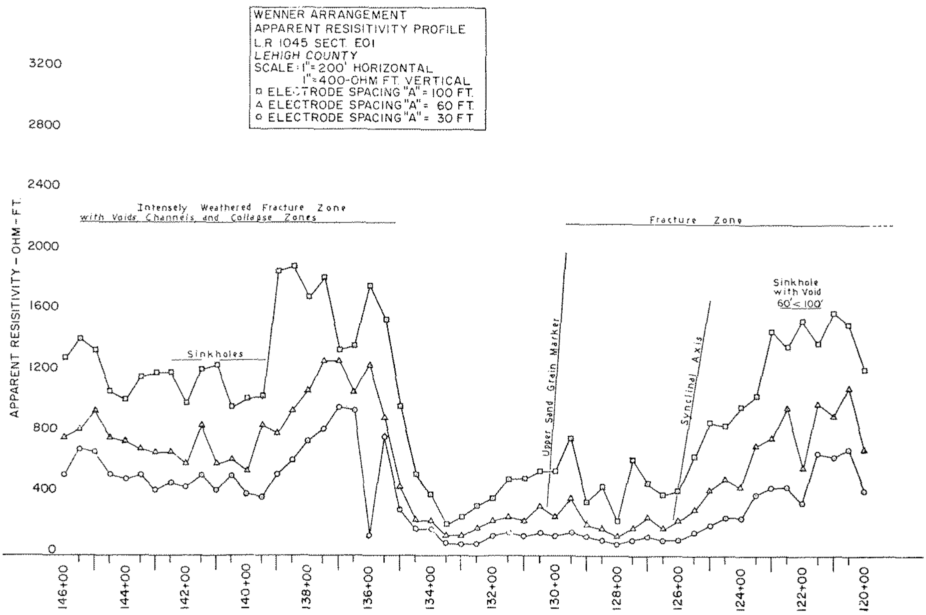

DIST 5-0

Fig. 3. Horizontal traverse resistivity profile.

ciation parameter of 0.02 was again considered to give a high degree of likeness in this geologic terrain.

The Barnes Layer cross section showed a number of air-filled voids at depth. These voids were accompanied, in some cases, by low resistivity values directly below them, indicating wet clay deposits on their floors.

Specific locations which were interpreted as incipient sinkholes or areas where sinkholes appeared on the surface numbered 21. This is a study area of 0.34 square kilometers.

All geophysical methods do not work in all cases. For this reason, many methods are used. Information bits found through the individual methods are associated one to another to obtain the maximum information available.

The main purpose of this study was to obtain a measure of relative sinkhole susceptibility--not to locate every incipient sinkhole in the area, although many were found. The information obtained was sufficient to convince those in authority that an alignment change was the most economical and safest of the alternatives offered. If the decision had been made to maintain the existing alignment, then a more intensive investigative program around the areas of incipient sinkhole activity would be undertaken. This phase would involve closer spacing of the resistivity traverses to obtain more resolution and more extensive use of diamond drilling.

References

Barnes, H. E., 1952. Soil Investigations Employing a New Method of Layer-Value Determination for Earth Resistivity Interpretation. Michigan State Highway Department Review; September.

Brink, A. B. A., 1966. Sinkholes in the Transvaal Dolomites. Safues, Vol. 1, No. 5.

Callahan, W. H., Geology of the Friedensville Zinc Mine, Lehigh County, Pennsylvania in Ore Deposits of the United States, 1933-67; The Graton-Sales Volume, John Ridge, Ed., American Institute of Mining, Metallurgical and Petroleum Engineers.

Cook, K. L., and VanNostrand, R. G., 1954. Interpretation of Resistivity Data Over Filled Sinks. Geophysics, Vol. 19, No. 4, pp. 761-770.

Dobrin, M. B., 1960. Introduction to Geophysical Prospecting. McGraw-Hill Book Co., Inc.

Drake, Jr., A. A., 1970. Structural Geology of the Reading Prong in Studies of Appalachian Geology - Central and Southern, John Wiley & Sons, Inc., pp. 271-291.

________________, Precambrian and Lower Paleozoic Geology of the Delaware Valley, New Jersey-Pennsylvania in Subitzky, S.,

1970. Geology of Selected Areas in New Jersey and Eastern Pennsylvania. Rutgers University Press.

Early, K. R. and Dyer, K. R., 1964. The Use of a Resistivity Survey on a Foundation Site Underlain by Karst Dolomite. Geotechnique, Vol. 14, pp. 341-348.

Foose, R. M., 1953. Ground-Water Behavior in the Hershey Valley, Pennsylvania. Bulletin of the Geological Society of America, Vol. 64, pp. 623-646.

______________________________, 1969. Mine Dewatering and Recharge in Carbonate Rocks near Hershey, Pennsylvania, in Kiersch, G. A. and Cleaves, A. B., 1969. Engineering Geology Case Histories Number 7. Geological Society of America.

______________________________, 1967. Sinkhole Formation by Groundwater: Far West Rand, South Africa. Science, Vol. 157, pp. 1045-1048.

Fountain, L. S., Herzog, F. X., and Owen, T. E., 1975. Detection of Subsurface Cavities by Surface Remote Sensing Techniques. Report No. FHWA-RD-75-80, Southwest Research Institute.

Goughnour, R. D., Anderson, R., and DiMaggio, J., 1976. Limestone Related Problems in Transportation Facilities. FHWA Paper presented at Symposium on Engineering, Construction and Maintenance Problems in Limestone Regions, Sponsored by Lehigh Valley Section of the American Society of Civil Engineers.

Habberjam, G. M., 1970. The Association of Resistivity Soundings. Geophysical Prospecting. Vol. 18, No. 2, pp. 199-214.

Henbest, O. J., & Erinakes, D. C., & Hixson, 1969. Seismic and Resistivity Methods of Geophysical Exploration. Technical Release No. 44, U. S. Department of Agriculture, Soil Conservation Service, Engineering Division.

Hobson, Jr., J. P., 1963. Stratigraphy of the Beekmantown Group in Southeastern Pennsylvania. General Geology Report G37, Pennsylvania Geological Survey.

Jakosky, J. J., 1950. Exploration Geophysics. Trija Publishing Co.

Jennings, J. E., 1966. Building on Dolomites in the Transvaal. The Civil Engineer in South Africa, Vol. 8, No. 2, pp. 41-62.

Jennings, J. E., & Brink, A. B. A., & Louw, A., & Gowan, G. D., 1965. Sinkholes and Subsidences in the Transvaal Dolomite of South Africa. Proceedings Sixth International Conference on Soil Mechanics.

Keller, G. V. and Frischknecht, F. C., 1966. Electrical Methods in Geophysical Prospecting: Oxford, Pergamon Press, 527 p.

Lehigh County, Pennsylvania, Soil Survey, 1963. United States and Pennsylvania Department of Agriculture and Pennsylvania State University.

Logan, O., 1954. Mapping Nearly Vertical Discontinuities by Earth Resistivities. Geophysics, Vol. 19, No. 4, pp. 739-760.

Love, C. L. A Geophysical Study of a Highway Problem in Limestone Terrain. State of California, Division of Highways.

Lueder, D. R., 1959. Aerial Photographic Interpretation. McGraw-Hill Book Co.

MD-I Instruction Manual for MD-1 Engineering Seismograph. Geophysical Specialties Co., Wayzata, Minnesota.

Miller, B. L., 1941. Lehigh County Geology and Geography. Pennsylvania Geological Survey, Bulletin C39.

Newton, J. G., 1976. Early Detection and Correction of Sinkhole Problems in Alabama, With a Preliminary Evaluation of Remote Sensing Applications. HPR Report No. 76, Project No. 930-070. Alabama Highway Research.

Pennsylvania Department of Transportation, 1970. Geophysical Survey Report for L. R. 1049, Section A02. Centre County.

Sowers, G. F., 1968. Settlement in Limestone Terrain. Presented at Geological Society of America Annual Meeting, Minneapolis, 1972.

Terzaghi, K., and Peck, R. B., 1948. Soil Mechanics in Engineering Practice. John Wiley & Sons, Inc.

Thornbury W. D., 1969. Principles of Geomorphology. John Wiley & Sons, Inc.

West, G. and Dumbleton, M. J., 1972. Some Observations on Swallow Holes and Mines in the Chalk. Quarterly Journal of Engineering Geology. Vol. 5, pp. 171-177.

Publication n°121 of the International Association of Hydrological Sciences
Proceedings of the Anaheim Symposium, December 1976

ARTIFICIAL RECHARGE OF DOLOMITIC GROUND-WATER COMPARTMENTS IN THE FAR WEST RAND GOLD FIELDS OF SOUTH AFRICA

by

J.F. Enslin, R.J. Kleywegt, J.H.T. Beukes and J.F. Gordon-Welsh
Geological Survey, Department of Mines, Pretoria
Republic of South Africa

ABSTRACT

The disposal of ground-water pumped to the surface by gold mines underlying the Dolomite Series on the Far West Rand in the past is outlined. The problem of selecting sites for boreholes capable of accepting large quantities of water for recharge purposes was solved after intensive gravity surveys and drilling had been conducted in compartments which had already been dewatered and as a result of which the dolomitic aquifer and its main conduits were better understood. A recharge case-history is included to illustrate the technique used.

RÉSUMÉ

On décrit l'élimination des eaux souterraines pompées à là surface par les mines d'or qui se developpent sous la Dolomie dans le "Far West Rand". Le problème du choix des emplacements de sondages d'injection a été résolu au moyen d'investigations gravimetriques détaillées et de sondages dans des comparitments qui ont été déja vidés. Il resulte de ces investigations que l'aquifère dolomitique et ses conduits Karstiques est mieux compris. Un exemple de recharge est présenté pour illustrer la technique employée.

I INTRODUCTION

The gold-bearing reefs of the Witwatersrand System, which are mined in the Far West Rand, underlie the 1 200 m thick Dolomitic Series of the Transvaal System (1) (fig. 1 and 2). The gold mines in the area, known as the West Wits Line, produced 24 per cent of the Free World's gold in 1975.

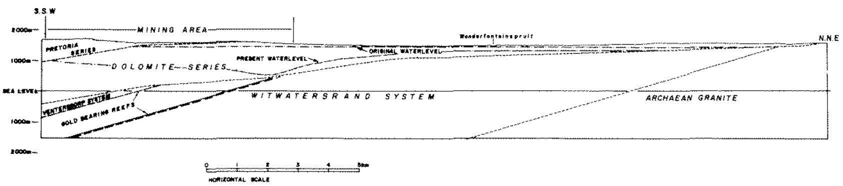

Figure 1. Typical geological profile through the Far West Rand.

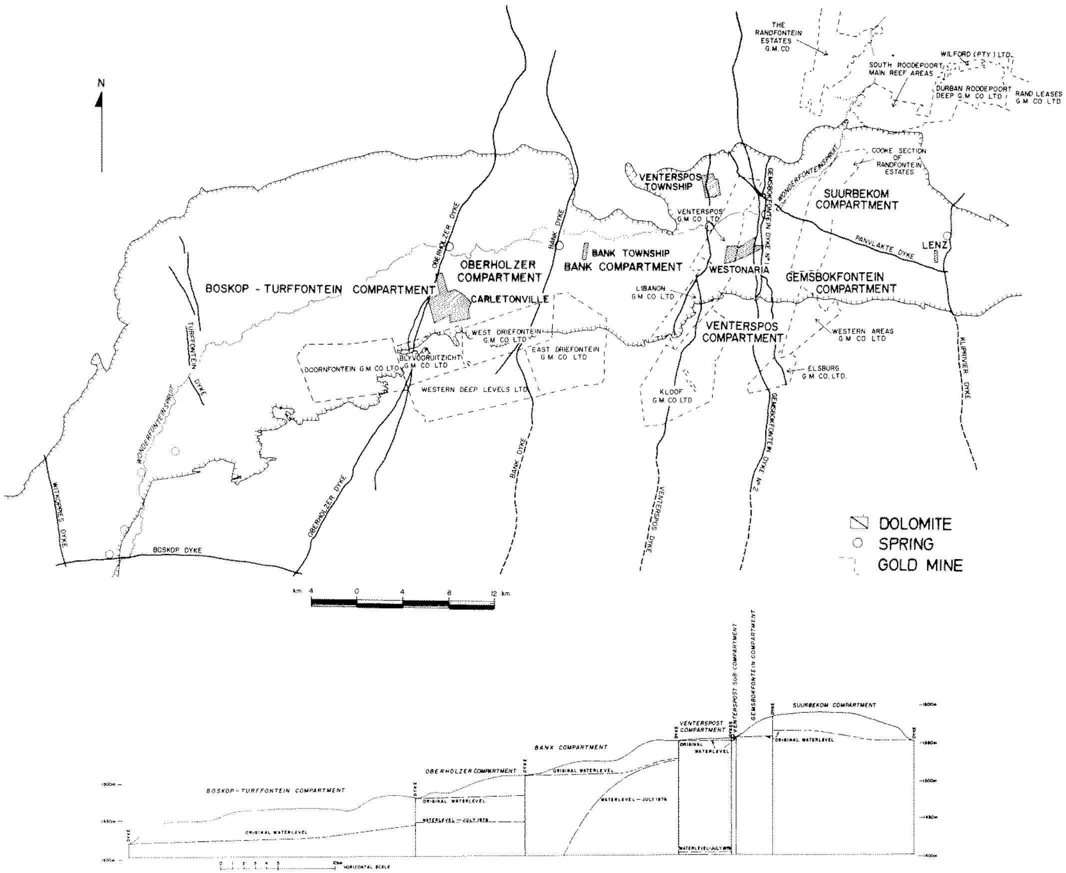

Figure 2. Dolomitic ground-water compartments in the Far West Rand.

Ground water stored in separate ground-water compartments in the dolomite (2), which is the most important aquifer in South Africa, flows into the mine workings at rates determined by the number of post-dolomite faults and associated fractures which are cut by the workings, the hydrological characteristics of the individual fault zones and the hydrostatic pressure of the water.

The ground water pumped to surface from the mine workings (fig. 3) has to be disposed of either by recharging the dolomitic ground-water compartment from which the water was derived, or by releasing the water outside the compartment, thus gradually dewatering it if the pumpage is more than the natural recharge.

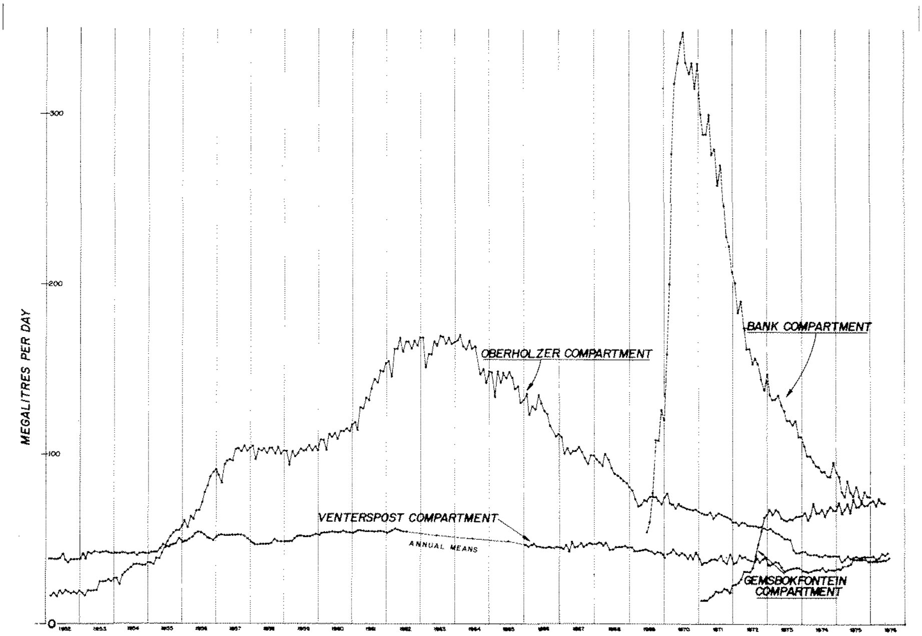

Figure 3. Pumping of dolomitic ground water entering mines for the various compartments on the Far West Rand.

The policy decision (3) as to which one of the above two methods has to be resorted to, for each compartment separately, depends on considerations of

(a) economic factors involved, namely the extent of damage due to subsidence and sinkholes caused by dewatering and the cost of replacement of the spring supplies weighed up against the additional pumping cost required for recirculation. The annual cost of pumping 100 Mℓ to the surface daily is of the order of U.S. $ 6×10^6 to U.S. $ 12×10^6, and

(b) safety factors, namely the danger to the miners of flooding of the mine by sudden inrushes of water at high pressure agains the danger to the population of the area of sinkholes caused by dewatering. Between 4 000 and 8 000 miners are underground during a shift on a typical gold mine on the Far West Rand. On 26th October 1968 an abnormally high inrush of 365 Mℓ/d occurred in the West Driefontein mine (4).

Recirculation of water in a particular compartment can only be considered and applied if it is possible to recharge the compartment at the rate of inflow of water into the mines in the compartment. This means that the total inflow into the mines (about 190 Mℓ/d in the Oberholzer Compartment and 56 Mℓ/d in the smaller Venterspost Compartment in 1962) under a pressure of about 1 000 metres or more of water has to be matched by artificial recharge at a pressure of usually less than 75 metres, depending on the depth of ground-water level below surface.

Furthermore, the demand on the water supply from the Vaal River for domestic, mining and industrial purposes in the Witwatersrand Area has been growing steadily. To provide for the future, other sources have to be developed and the existing supplies, which are stored in surface dams, have to be used more efficiently. Storage of some of the supply underground, free from evaporation, is one way of increasing the supply available. The dolomitic compartments on the Far West Rand could form an ideal underground storage for emergency supplies when the mines cease operating and this possibility has been investigated (5). For this purpose water will have to be pumped at rates of up to 500 Mℓ/d, and the recharge of the reservoirs will also have to be at a high rate when surplus water is available.

Recharge boreholes with large intake rates are, therefore, essential for recirculation of pumped mine water as well as for recharging the depleted emergency supplies stored underground.

II RECHARGE OF WATER IN OBERHOLZER COMPARTMENT (1952-1963)

When the inflow of water into the mines operating in the Oberholzer Compartment increased rapidly after 1952, the companies were faced with the problem of disposing of the water pumped to surface. By 1956 more than 90 Mℓ had to be pumped daily and was disposed of as follows:

(a) 40 Mℓ was spread on open ground draining towards the Wonderfontein River, about 8 km north of the mines. This drainage line is crossed by a railway line and two main roads. The recharge rate after saturation had been reached was less than the spreading rate, with the result that about 4 Mℓ reached the river, flowed across the dyke-barrier and was lost to the compartment.

(b) 22 $M\ell$ was recharged into a number of boreholes, spread over 15 km^2 and into two large sinkholes, one of which choked shortly after being put into operation.

(c) 28 $M\ell$ was used consumptively by the mines.

The recharge capacity was increased by drilling additional boreholes, and in 1962, when a total of 52 boreholes had been drilled, of which only a limited number could be used, a maximum daily rate of 30 $M\ell$ was maintained. Water spreading over the areas available to the mines had also reached its limit and a further increase would have been at the risk of flooding part of the Carletonville township, the railway line or the highways and the possible occurrence of sinkholes caused by the flooding. All increases were, therefore, discharged into a irrigation canal or into the river.

The difficulty of recharging the pumped water was one of the reasons for deciding in 1963 to dewater the Oberholzer Compartment.

III DEVELOPMENT OF TECHNIQUES FOR SITING BOREHOLES FOR RECHARGE ON A LARGE SCALE

In the early 1960's it was realised that the development of improved methods of siting recharge boreholes was essential to ensure the feasibility of recirculation in a compartment, should that be the preferred alternative in a particular mining situation or if the compartment should be required for storage of an emergency water supply.

Because at that time it was seldom possible to locate suitable boring sites particularly under a cover of Karoo sediments and aeolian soils, the Dolomite Series was still considered very speculative for drilling in and for developing strong permanent supplies of water.

An electromagnetic technique which had been developed for locating and tracing fissures and fault zones in hard rock formations was considered. The sensitivity of this method is low where the dolomite is covered by an appreciable thickness of younger rocks or rocks of low resistivity, and it is therefore seldom suitable for conditions on the Far West Rand (6).

(a) Gravity surveys for "unstable zones"

A solution to the problem of siting boreholes for large scale recharge or extraction of ground water in the dolomite of the Far West Rand became clear after extensive gravity surveys and intensive drilling had been undertaken to delineate "unstable zones", which are areas liable to subside or have sinkholes as a result of the dewatering (1), (7), (8). This work showed that

(i) the dolomitic bedrock normally occurs within about 15 m of the natural water table on the Far West Rand and is overlain by insoluble residual chert and wad and aeolian soils,

(ii) along fault and fracture zones leaching of the dolomite extends deeper than normal, sometimes to 100 m below the level of the natural water table, over the length of the structure and also laterally to yield honeycombed structures up to several hundred metres wide which tend to compact partially by slumping and settling over geological times,

(iii) these zones lying beneath the water table are thus not always very highly compacted and the lowermost parts are in fact cavernous, extremely porous and highly permeable,

(iv) in the compartments which were being dewatered these areas formed the "unstable zones" when the water level was lowered through the compacting material.

Furthermore, the dolomitic aquifer thus comprises the residual variably compacted material below the water table and its main conduits are the highly permeable deeper parts of these "unstable zones". LOCATING THESE UNSTABLE ZONES BY GRAVITY THUS ALSO ENABLES ONE TO SITE RECHARGE BOREHOLES.

(b) Interpretation of gravity surveys

For the interpretation of the gravity anomaly, the anomalous mass i.e. the deeply leached zone, is assumed to be almost rectangular in shape. This has been confirmed by drilling and by the locations of areas of highest differential ground subsidence where they were interpreted on the basis of such an assumption. The dimensions of the anomalous mass in these cases were determined by using Skeel's (9) curves for determining the depth to a two-dimensional rectangular prismatic body. The method is fast and has given very good results. Such an interpretation for the residual gravity profile through recharge borehole WAW2 is shown in figure 4. Where, for some reason or other, the cross-sectional shape of the anomalous mass is not rectangular an iterative technique based on that described by Bott (1960) is used with a starter model consisting of vertical rectangular prisms centred on the gravity stations or on interpolated residual gravity values. Where rocks of the Karoo System do not extend to beneath the level of the natural water table the mass deficiency below this level reflects the hydrological characteristics of the aquifer as the soluble carbonates have been removed. This holds even if minor compaction of the remaining residuum has taken place but could become less reliable for greater compaction or for cases where a greater percentage chert is present in the residuum.

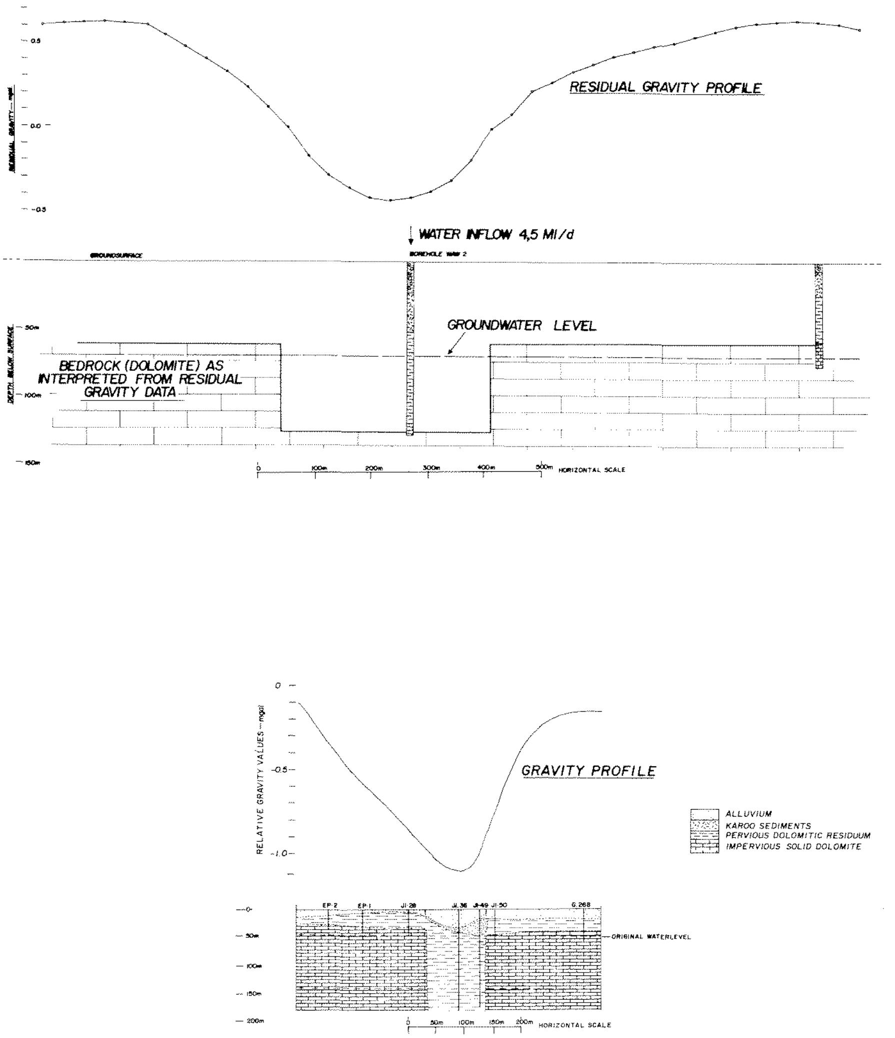

Figure 4. Interpreted gravity profile at recharge borehole WAW2 and a typical geological profile across an "unstable zone" in Carletonville.

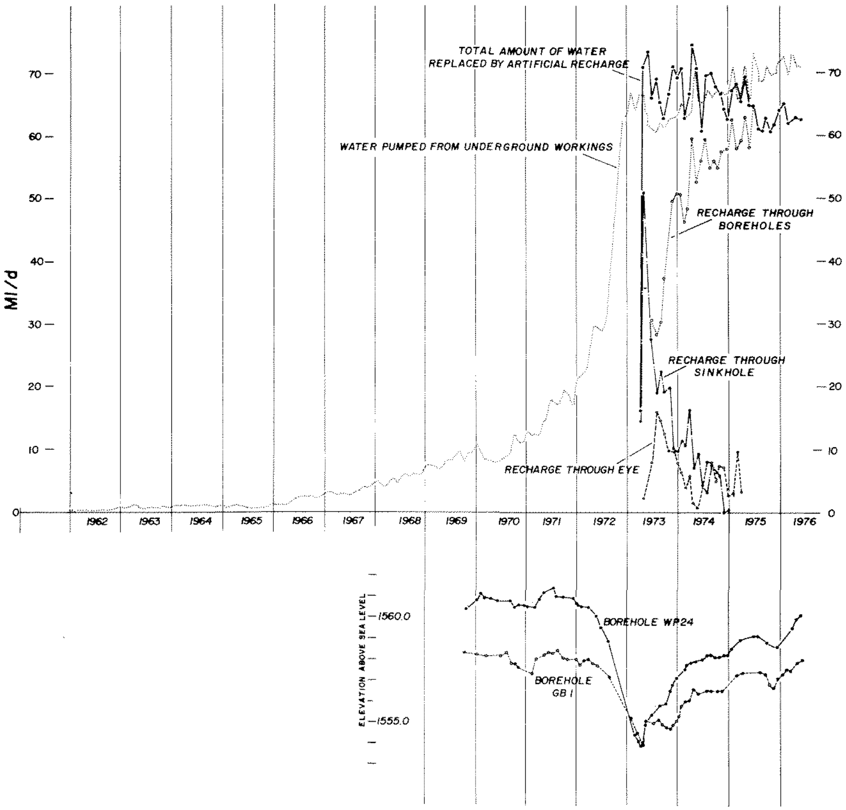

Figure 5. Water table response in the Gemsbokfontein Compartment as a result of water pumped to the surface by the mines and water recharged as indicated in figure 6.

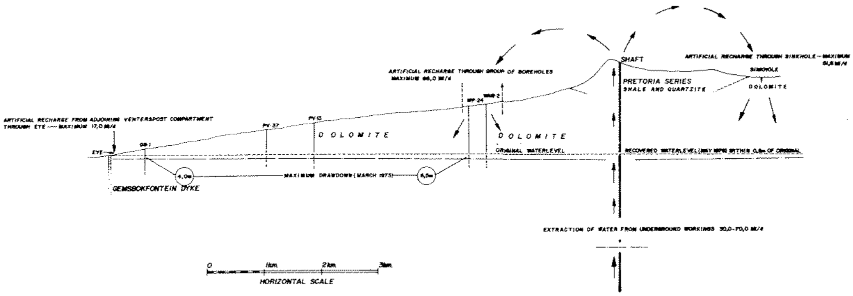

Figure 6. Schematic presentation of water extraction and recharge in the Gemsbokfontein Compartment.

IV RECHARGE OF THE GEMSBOKFONTEIN COMPARTMENT (1972--)

As can be seen on figure 5 there was a significant increase in the rate of water pumped and disposed outside the compartment from the Gemsbokfontein Compartment in the second half of 1971. Up to that time the loss from the compartment was matched by the natural recharge and no progressive long term lowering of the water table resulted. During 1972 the pumpage increased from 22 Mℓ/d to 65 Mℓ/d and as the water was not returned to the compartment, the water tables dropped sharply as shown in figure 5. When it became obvious that the sudden large inflow of water into the mine could not be controlled, the mine management decided to attempt to curtail the inflow of water into the mine by cementation of the water-bearing fissures and/or sealing off that part of the mine which was making large quantities of water and to keep the water-level static by recirculating the pumped water by recharging into a large sinkhole and into recharge boreholes which still had to be drilled (fig. 6). This was essential as the lowering of the water table was rapidly approaching the 6 m value which is considered to be the cut-off level at which sinkholes and subsidences could start to occur.

The recharge boreholes were developed on sites selected by the Geological Survey by using the gravity contour plan drawn up for determining the unstable zones in the Gemsbokfontein Compartment (fig. 7). These holes were fed with pumped mine water which was allowed to gravitate from a nearby hill.

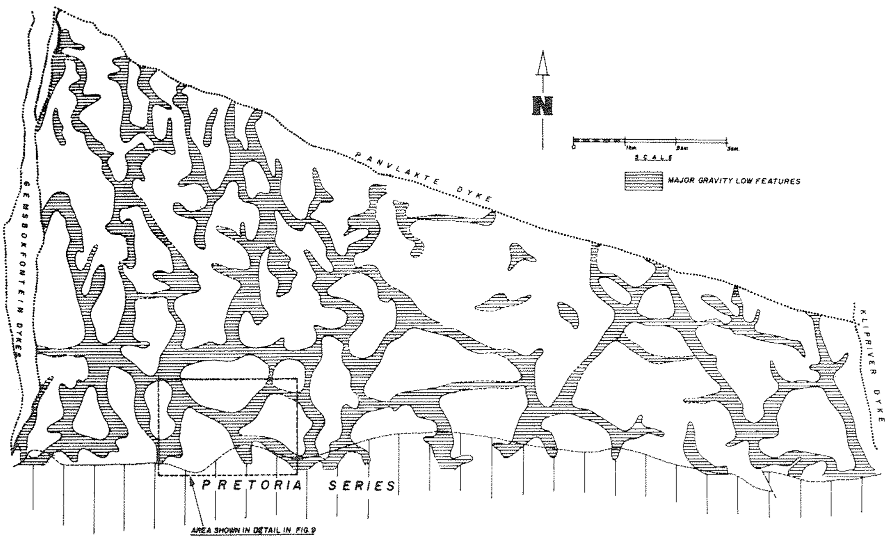

Figure 7. Leached fault and fracture zones in the Gemsbokfontein Compartment interpreted from gravity data. These zones comprise the main dolomitic aquifer and its conduit. With dewatering they form the "unstable zones".

A recharge test was done on the first hole to be completed and the results are shown on figure 8. The hole was recharged through 150 mm slotted casing which was inserted to the depth of solid dolomitic bedrock.

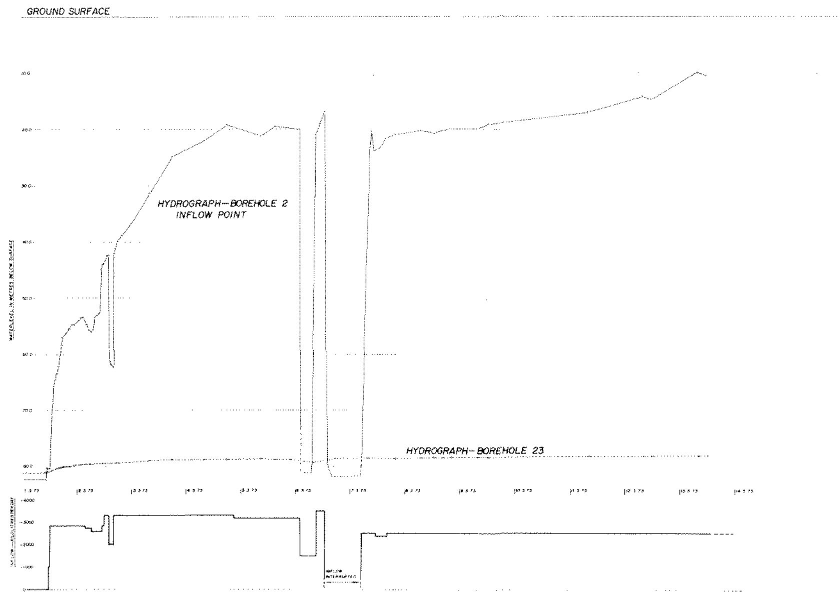

Figure 8. Recharge test performed on borehole WAW2 with observation hole WP23 75 m distant.

A prospecting borehole about 75 m away was monitored during the test. It seems obvious that the amount of water which could be fed into the subsurface formations was determined, within the limits of the experiment, by the slots in the casing and not by the ability of the medium to accept water. Since 1973 all the available pumped water has been returned to the compartment through ten boreholes (fig. 9) spread over an area of less than 1,0 km^2 at an average rate per borehole of approximately 6,3 Mℓ/d and a maximum rate of 9,2 Mℓ/d. This compares with average maximum recharge rates of 2-8 Mℓ/d per borehole in other countries. For a few months water taken from a mine in the neighbouring compartment was returned through the dry "eye" but when the rain season, which was better than normal, ensued this was discontinued. The total loss of water to date has almost been made up.

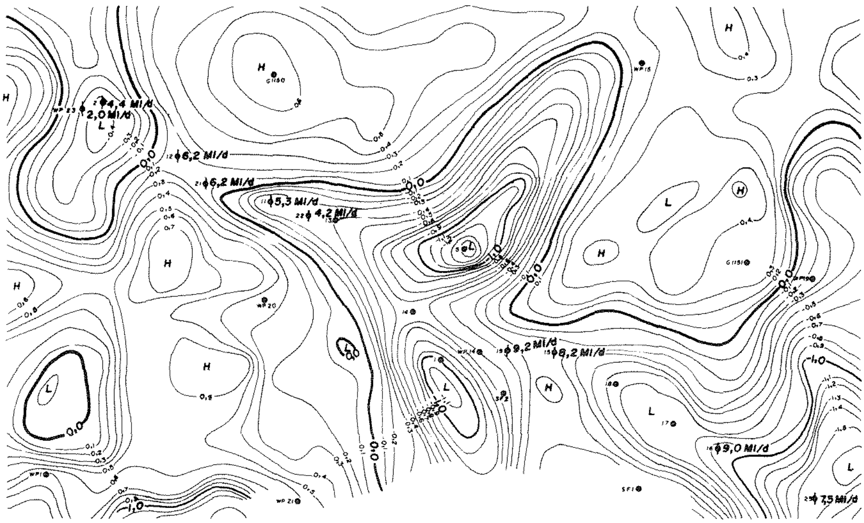

GRAVITY CONTOURS AT 0,1mgal INTERVALS

RECHARGE BOREHOLES

PROSPECTING AND INTERPRETATION BOREHOLES

Figure 9. Area of recharge through boreholes in the Gemsbokfontein Compartment.

V CONCLUSIONS

It has been shown that it is possible to recharge dolomitic ground-water compartments on the Far West Rand at a high rate for extended periods of time by developing borehole sited on the basis of gravity data in highly leached fault and fracture zones.

REFERENCES

1. DE KOCK, W.P. (1964). The geology and economic significance of the West Wits Line. pp 375-381. The dolomite water and its attendant problems. In The Geology of some Ore Deposits of Southern Africa, Vol. 1, 1964. Published by Geological Society of S.A.

2. ENSLIN, J.F. (1967). Dolomitic water supplies in the Transvaal, Republic of S.A.: Memoirs, Vol. VIII, AIH, Reunion Instanbul, pp 426-433.

3. BEZUIDENHOUT, C.A. and ENSLIN, J.F. (1969). Surface subsidence and sinkholes in the dolomitic area of the Far West Rand

Transvaal, Republic of South Africa. Published by the International Association of Hydrological Sciences.

4. CARTWRIGHT, A.P. (1969). West Driefontein - Ordeal by water. Published by Goldfields of S.A. Ltd. Printed by J.G. Ince and Son (Pty) Ltd, Johannesburg.

5. ENSLIN, J.F. and KRIEL, J.P. (1967). The assessment and possible future use of the dolomitic ground-water resources of the Far West Rand, Transvaal, Republic of South Africa. International Conference on Water for Peace, Washington, 1967.

6. ENSLIN, J.F. (1955). A new electromagnetic field technique. Geophysics, Vol. 20, pp 318-334.

7. JENNINGS, J.E., BRINK, A.B.A., LOUW, A. and GOWAN, G.D. (1965). Sinkholes and subsidences in the Transvaal dolomite of South Africa. Proc. 6th Intern. Conf. of Soil Mech. and Found. Eng., Montreal, 1965.

8. KLEYWEGT, R.J. and ENSLIN, J.F. (1973). The application of the gravity method to the problem of ground settlement and sinkhole formation in dolomite on the Far West Rand, South Africa. Proceedings of the IAEG Symposium on Sinkholes and Subsidence engineering - geological problems related to soluble rocks. Hannover, 1973. Published by Deutsche Gesellschaft für Erd- und Grundbau, Essen.

9. SKEELS, D.C. (1963). An approximate solution of the problem of maximum depth in gravity interpretation. Geophysics Vol. 28, pp 724-735.

Publication n°121 of the International Association of Hydrological Sciences
Proceedings of the Anaheim Symposium, December 1976

SOME ASPECTS OF THE SUBSIDENCES IN THE ROCKSALT DISTRICTS OF CHESHIRE, ENGLAND.

F. T. Howell and P. L. Jenkins
Department of Civil Engineering, The University of Manchester Institute of Science and Technology, Manchester M60 1QD, England.

Major and widespread subsidences occur in districts underlain by Triassic Rocksalt in Cheshire, England.

These deposits and their associated brines have been exploited by mining, "wild brine" and controlled pumping. The Authors consider that the primary mechanism of subsidence is the withdrawal of the protective interface of saturated brine from the saltbed, thereby permitting the solution of the rocksalt by undersaturated fluids. This effect can occur naturally, or as a result of the exploitation of the rocksalt and brines or of more distant freshwaters.

The magnitude and timing of the subsidences, which may severely damage surface structures, transport systems and agricultural land, are reviewed, and their possible relationships with certain geological variables are discussed. Supporting experimental data from models and statistical reviews of known subsidences are described.

Attempts to understand the nature and origins of these subsidences may, in the future, lead to prediction of further subsidence, but to date this has not been possible.

CERTAINS ASPECTS DE LA SUBSIDENCE DANS LES ZONES SALINES DU CHESHIRE, ANGLETERRE.

Des subsidences majeures et de grande étendue ont lieu dans les zones ayant des dépôts de sel-gemme d'origine triassique dans le Cheshire, Angleterre.

Ces dépôts ainsi que les saumures y présentes ont été exploités à la mine, à la "saumure-folle" et par le pompage contrôlé. Les Auteurs sont de l'avis que le mécanisme primaire de la subsidence est l'extraction de la face protectrice, que forme la saumure saturée, de la couche saline, permettant ainsi la dissolution du sel-gemme par les fluides sous-saturés. Cet effet peut avoir des causes naturelles, ou comme résultat de l'exploitation du sel-gemme et des saumures ou même de l'exploitation de l'eau douce plus éloignée.

L'importance des subsidences et le moment auquel elles se produisent, avec risque de sérieuses avaries des structures en surface, des réseaux de transport et des terrains agricoles, sont passés en revue, et leur rapport eventuel avec certaines variables géologiques discuté. Il est décrit les données expérimentales obtenues à partir de modèles et des revues statistiques de subsidences connues.

Les tentatives vers la compréhension de la nature et des origines de ces subsidences pourraient, dans l'avenir, mener à la prédiction d'autres subsidences, mais, jusqu'à ce jour ceci n'a pu être réalisé.

Introduction

The Cheshire Basin (Fig. 1) is part of North-west England and forms a synclinal structure some 50 miles (80 km) by 30 Miles (50 km) in extent containing some 3000 feet (920 m) of highly permeable sandstones, in turn overlain by some 3000 feet (920 m) of marls with rocksalt (Fig. 2).

At their maximum development the rocksalts are represented by an upper and lower sequence, respectively 1300 feet (400 m) and 625 feet (190 m) in thickness (Evans et al.1968). These rocks are mostly obscured by an unconformable veneer of unconsolidated gravels, sands, silts, clays and peat of Glacial and post Glacial age. This Drift can exceed 330 feet (100 m) in thickness where it conceals "fossil" valleys (Howell, 1973). No surface outcrops of rocksalt are known, for there is an upper zone where each saltbed is corroded, attenuated (the "wet rockhead"), or totally removed by solution (Fig. 3). In general, at depths down to 600 feet (180 m) below surface, these beds contain cavities with saturated or unsaturated brines under artesian heads, called "brine streams" or "brine runs". The brines are known as "wild" brines. At greater depths the rocksalts are usually intact, the "dry rockhead" condition.

The topography of the rocksalt districts is subdued and is generally lower than 330 feet (100 m) above sea level. The region is agriculturally rich and is crossed by important roads, railways, and canals. Towns with historical connections with the Salt trade, derived chemical industries, and engineering, form centres of population. Cheshire produces 82% of the United Kingdom's salt and estimated total reserves are some 400,000 million tons. Subsidences associated with the salt deposits have been reported for many years and, on occasion, are a costly and serious threat to surface structures.

The Rocksalt and Brine Industry

This industry is well described (Calvert, 1915) (Sherlock, 1921) (Wallwork, 1959) and dates back to pre-Roman times but the methods of extraction have changed in response to increasing demand and more specialist requirements.

Initial surface brines were evaporated in open pans. By the 19th century, shafts and wells were being sunk to tap the declining brine levels. Mining, which commenced in 1682, reached a peak in the industrial revolution but many mines were lost prematurely by inrushes of brine and water and now only a single, highly mechanised mine remains. The production of wild brine is declining but is offset by controlled brines derived by the orderly solution of large, regularly spaced cavities some 300 feet (90 m) in diameter from boreholes sunk in uncorroded salt beds. These cavities are finally preserved by flooding with saturated brine and no subsidence has been attributed to this technique.

In 1968 one million tons of rocksalt were mined and 500 million gallons (2.2 million m^3) of wild brine and 3900 million gallons (17.7 million m^3) of controlled brine extracted. Much of the rocksalt is for deicing roads. Some 75% of the brine goes directly to the chemical industry, the remainder is vacuum evaporated to form white salt. A levy is paid by the salt producers to offset some of the costs of salt subsidence and compensation is administered by the Cheshire Brine Subsidence Compensation Board (Collins 1971).

The Morphology and Classification of Topographic Subsidence in Rocksalt Districts of Cheshire

The solution of large volumes of rocksalt by natural processes usually leads to ground subsidence with a wide range of morphology. Many circular, crater-like depressions from 30 feet (10 m) to 650 feet (200 m) in diameter are reported (Plate 1.) Linear hollows up to 780 feet (240 m) in

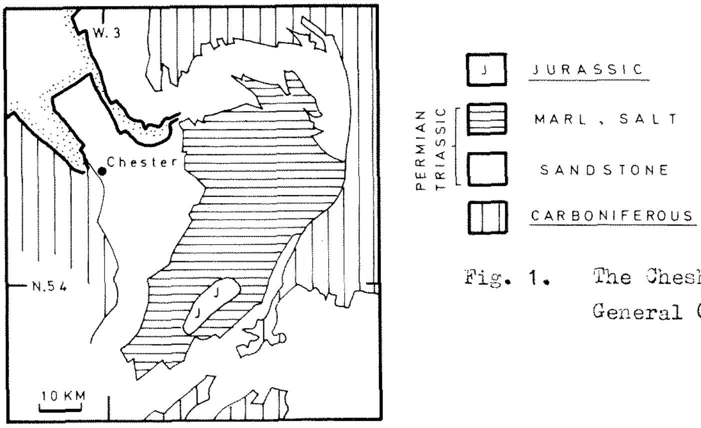

Fig. 1. The Cheshire Basin - General Geology.

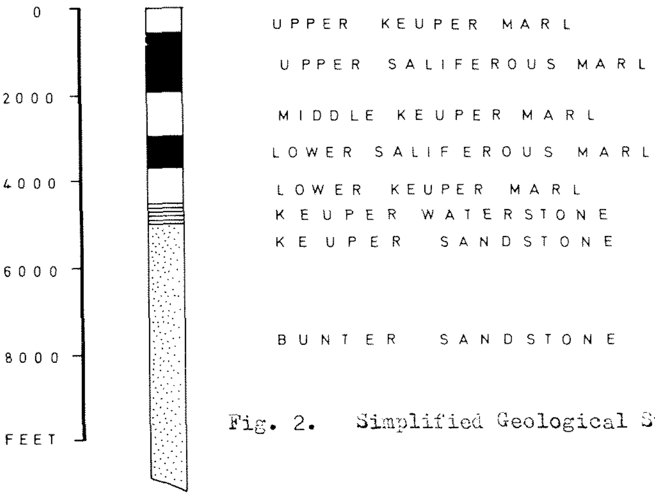

Fig. 2. Simplified Geological Succession.

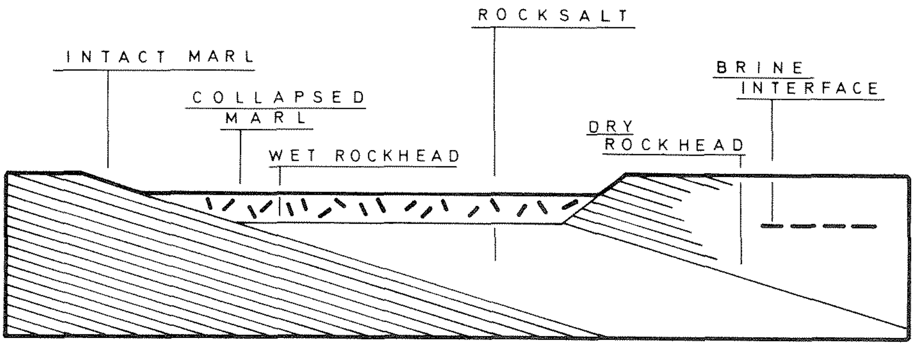

Fig. 3. Near-surface condition of rocksalt (after Evans et al.). Superficial deposits omitted.

Plate 1. Crater subsidence over interlayered sands and clays, 25 m diameter, 10 m deep, taking one week to develop. (Photo, authors.)

width and 5 miles (8 km) in length are known (Plate 2). These generally have a central trough-like section some 190 feet (60 m) wide bounded by convex slopes. Such hollows are related to the strike or dip of the salt-beds, or point radially towards a major centre of brine pumping. The craters tend to coalesce to form linear hollows which themselves may combine to form general depressions in excess of one square mile (2.5 km2) in extent.

Subsidences which result from the collapse of salt mine workings have forms specifically associated with the shape and extent of the mine. Where subsidences affect rivers, or reduce ground levels below the water table, ponds or lakes known as meres or flashes are formed. Care must be taken to differentiate between true salt subsidence features and other depressions such as kettle holes and ponds.

The Authors now propose an initial classification of landforms which are associated with rocksalt subsidence in Cheshire, based on their morphology. It recognises these landforms as stages in a geological cycle which is heavily dependent upon hydrogeological controls. We consider that each landform in the cycle has a general suite of properties in terms of dimensions, shape and rate of change (Table 1).

TABLE 1. PROGRESSION OF IDEALIZED SUBSIDENCE LANDFORMS

SUBSIDENCE DEVELOPMENT	SHAPE	DIMENSIONS (D) AND DEPTH (d) /metres/	SIDE ANGLE (Dependent on overlying strata properties)	RATE OF CHANGE	EFFECT
Subsurface pipes ↓ SURFACE PIT	CIRCULAR	$D = 10^0 - 10^1$ $d = < 5$	$> 70^\circ$	Appear without warning.	
↓ Down pipe Funnelling ↓ CRATER	CIRCULAR TO OVAL	$D = 10^1 - 10^2$ $d = 3 - 10$	$20^\circ - 35^\circ$	Rapid crater development — Craters may gradually expand by increments, joining other craters.	CATASTROPHIC
↓ Coalescing Craters ↓ LINEAR HOLLOW	ELONGATE TO LINEAR	$D = 10^2 - 10^3$ $d = 6 - 12$	Flanks up to 20°	Headward growth most rapid. Flanks almost stable.	VERY SEVERE
↓ Anastamosing ↓ REGIONAL LOWERING	WIDESPREAD DEPRESSION	$D = 10^3 - 10^5$ $d = 30+$	Variable	Anastamose, lowering intervening ground. Generally slow.	CHANGE OF ELEVATION MAY INDUCE FLOODING

Plate 2. View across partially flooded linear hollow. Note slip scars along flanks. Length of hollow in excess of 5 km. (Photo, authors.)

Thus the identification of a particular subsidence landform indicates the likely general progress of the subsidence at that location, although we stress that the detailed progression of each subsidence will differ considerably in response to local hydrogeological constraints. In the field we identify not only these subsidence stages but also remnants of previous cycles now containing sediments. Thus the present subsidence topography of Cheshire is an assemblage of landforms of differing ages and differing degrees of maturity.

Mechanism of Subsidence in the Rocksalt Districts of Cheshire

The basic mechanism is the formation of cavities in soluble strata by the attack of aggressive groundwaters. This loss of rock is eventually reflected at the surface by subsidences. The actual dimensions and timing of these subsidences are influenced by the nature of the soluble rocks, the adjacent and overlying strata, and the migrations of groundwaters. Although initially intact rocksalt and marl have very low permeabilities, minor dislocations due to crystallization and tectonics are present in the salt and these are selectively exploited by undersaturated groundwaters. Resulting collapses in the saltbed enhance the permeability of the overlying marls and any migration of fluids is accelerated.

The main constituents of the soluble evaporite beds of Cheshire are halite and gypsum with a scattering of mudstone (marl) pellets and thin marl partings. Halite usually forms 95% of the bed thickness, but the main evaporite beds may also be associated with thinner evaporite layers. Major beds of "marl" (mudstone, siltstone and fine sandstone) separate the evaporites (Calvert, 1915) (Evans et al.,1968).

Halite is extremely soluble when attacked by fresh or undersaturated brines at normal ambient temperatures (about $9^{o}C$). For a unit volume of salt to be dissolved, four unit volumes of freshwater must become fully saturated with salt. The rate of solution declines as the aggressive groundwater approaches saturation. Fully saturated brine has a relative density of 1.2 and freshwater floats on such brines with a well-defined interface, which in the field is often less than 33 feet (10 m) thick. Therefore solution of rocksalt depends not only upon the presence of freshwater or undersaturated brine, but also on the continual removal of any developing protective envelope of saturated brine. If these conditions do not occur then the solution process is effectively terminated, for the high density brines are not displaced. Diffusion processes across the interface are minimal.

We have constructed many laboratory tank models involving rocksalt and freshwater/brine interfaces. Without exception we have found that the location of the saturated brine interface is the crucial component to the limit of solution of the saltbeds.

In the field, because there are no surface exposures of rocksalt, the condition and distribution of the saltbeds and groundwaters can only be evaluated from boreholes and mining. The upper surfaces of one or more rocksalt beds in a given district are often corroded and the overlying strata may be seriously disturbed by this loss of support. If the roof of the collapse has not fully closed on to the corroded top of the saltbed, the resulting cavity normally contains brines under artesian conditions. These brine-streams tend to be interconnected and some of them, when pumped by boreholes or shafts, can yield continuously over 50,000 gallons/hour (227 m^3/hour) of saturated brine. Surface subsidence reflects subsurface changes in the rocksalt beds and, just as there is a sequence of subsidence landforms representing parts of the morphological cycle, so there must similarly be an evolutionary sequence of sub-surface events. We believe these to be:-

(a) Penetration by undersaturated groundwater along dislocations in the evaporites; for example through microfissures, joints and bedding plane separations.
The dislocations are attacked selectively by migrating aggressive groundwaters and their "random walk" systems become modified to form directional pathways in response to hydrogeological controls. At this stage the removal of rocksalt is small and little or no loss of support to overlying strata occurs, consequently no subsidence develops at the surface.

(b) In a dynamic groundwater environment solution can proceed, for the protective coating of saturated brine developed by the solution of strata is continually removed. Preferential flowpaths develop, further coalesce and widen sufficiently to cause collapses in the overlying strata. Crater-like depressions develop rapidly at the surface without prior warning. Evans et al.,1968, consider that craters are generally associated with thick sands. However, the superficial deposits are extremely complex and we note that craters develop over other materials (Table 2).

TABLE 2. NATURE OF STRATA IMMEDIATELY BELOW SUBSIDENCE (after I.G.S. 6" sheets 66, 75, 76, 85, 86)

	SANDS	CLAYS	PEATS
Percentage of Craters	43	54	3
Percentage of Linear Hollows	24	75	1

Laboratory tank models demonstrate that when minor roof falls obstruct simulated fissure systems they deflect migrating brines and the solution pathways are widened. A mechanism therefore exists for the selective widening of a brine run. Further experiments in the UMIST 100 G centrifuge on models of crater development show that considerable bulking of strata overlying the subsurface cavity takes place before any surface settlement occurs.Thus, in the field, large volumes of salt may be removed slowly without any corresponding subsidence. At a critical condition the bulking ceases and a rapid cascade of material into the underlying cavity occurs. A narrow, circular, vertical shaft (or "pipe") develops, which widens out to form a crater. The centrifuge experiments offer an explanation of the paradox in the field situation where, from hydrogeological considerations, the rate of removal of salt at a single location must be slow, but large craters, the consequence of a large loss of underlying strata, develop very rapidly. We are encouraged to accept the validity of the model, for although we ourselves have not observed the "pipe" phase of collapse in the field, it has been described by Ward, 1886.

(c) Fieldwork and observations based on reports, maps and air photographs show that the craters tend to develop in clusters, and eventually coalesce. They also herald the headwards or lateral extension of linear subsidences.

(d) The joining of craters produces linear hollows which develop a more precise shape as the directional and selective solution of path ways become established. Their orientation tends to be strike-dependent, presumably because of marl partings within the salt bed; dip-dependent, due to fracture control; or radial to pumping centres, due to selective solution within the hydraulic zone of the pump wells.

(e) In the field the width of linear hollows is restricted. In flow-tank models this effect is also observed and is thought to be caused by a balance between saturation and solution established at the slower moving edges of the brine run, coupled with less soluble strata boundaries.

(f) In some districts subsidences are widespread and represent either the anastamosing of "mature" linear hollows or a regional lowering of the protective saline interface. In the past, severe subsidences have been associated with the rapid collapse of saltmines when floodwaters dissolved their rocksalt supports, but these are special and easily reconciled circumstances (Calvert, 1915).

Probable Origins of Subsidence Features in the Rocksalt Districts of Cheshire

An assemblage of subsidence features has been described. These represent stages in natural geological processes compounded with man-made perturbations by pumping and mining on a local and regional scale.

In many areas brines exist at levels very much higher than present day corroded brine runs. Thus a major rise in the level of the protective brine must have occurred at some period after the formation of the brine run cavities, which themselves are the result of solution. Some subsidences have affected the general pattern of the Sub Drift Surface, post-Glacial peats and sediments are present in many hollows, and medieval land boundaries reflect the presence of ancient subsidence lines. The stable $^{16}O/^{18}O$ ratios in the wild brines differ from those of present day rainfall and are attributed to a cooler climate. These ratios are in contrast to those of connate Triassic and Carboniferous brines which indicate warm climatic origins, (Crook et al, 1973). Thus we attribute the development of the main brine runs to a lowering of the protective brine interface during the Pleistocene.

Today, in adjacent sandstone aquifers, a layer of up to 450 m of freshwater of similar cool climatic origins rests on connate brines. Crook and Howell (1973) demonstrate that for these freshwaters to have displaced connate saline waters, a major hydraulic imbalance was necessary. They show that this excess head would be present within the wet-base retreating phase of Pleistocene glaciers which covered the region on several occasions and which cut tunnel valleys (Howell, 1973). During this phase the underlying strata would not be frozen and would be permeable. We have constructed flowtank models of the saltfield overlain by a wetbase glacier made of ice chips. The hydraulic imbalance caused by a freshwater head within the glacier is sufficient to displace fully saturated brine to depths which are analagous to the observed field conditions (Fig. 4a). When the model glacier finally melts there is a rebound in the brine interface and saturated brine re-occupies corroded zones, an effect which is also observed in the field (Fig. 4b).

We believe that salt subsidences were occurring during Glacial and post-Glacial periods and that sediment-filled features represent an ancient cycle of landforms. After the glaciations a more quiescent phase, only

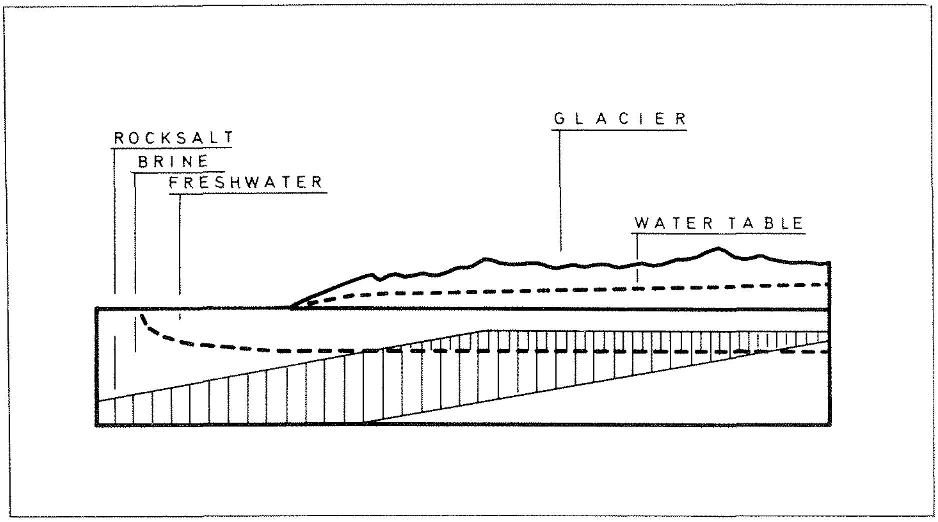

Fig. 4a. Emplacement of Glacial freshwater.

slightly disturbed by very slow regional migrations of groundwater, was established. This quiescence was interrupted by man-made disturbances in the groundwater regimes during the industrial revolution, when heavy pumping depleted reserves of brines in cavities in the saltbeds and marls. Undersaturated fluids replaced the brines, causing solution and collapse of the saltbeds. This pumping initiated a new phase of landform development as well as re-activating earlier quiescent landforms.

Although wild brine pumping was probably the largest single factor in disturbing the interface, other perturbations may occasionally occur by leakage below quarries, rivers and canal beds. No subsidence has yet been associated with controlled brine pumping and only one salt mine remains. Overpumping of adjacent aquifers, where rest water levels are below sea level in areas which are in hydraulic continuity with the saltfield, must also contribute to local problems, (Howell, 1965) (Bow et al., 1969) (Crook and Howell, 1970).

The Economic Consequence of Subsidence

When the ground subsides there is an interaction between the subsidence and any overlying or adjacent structure. The timing, magnitude and nature of the subsidences depend to a large extent upon the landform developing. Crater subsidences occur rapidly, for example one 25 m in diameter, 10 m deep, formed within a week. Settlements of over 1 m/year for 10 years are reported on a linear hollow, and subsidences of a few cms/year may occur over widespread areas. As well as the change of elevation resulting from subsidence, other factors are important - especially the severe strains which occur on the edges of subsidences.

Craters and linear hollows are capable of severely damaging building structures, roads, pipelines, canals, and railways (Plate 3). The more widespread regional subsidences do much less damage and may often go unnoticed except where sensitive structures are involved. Progressive reductions in ground level, even if no structural damage occurs, may ultim-

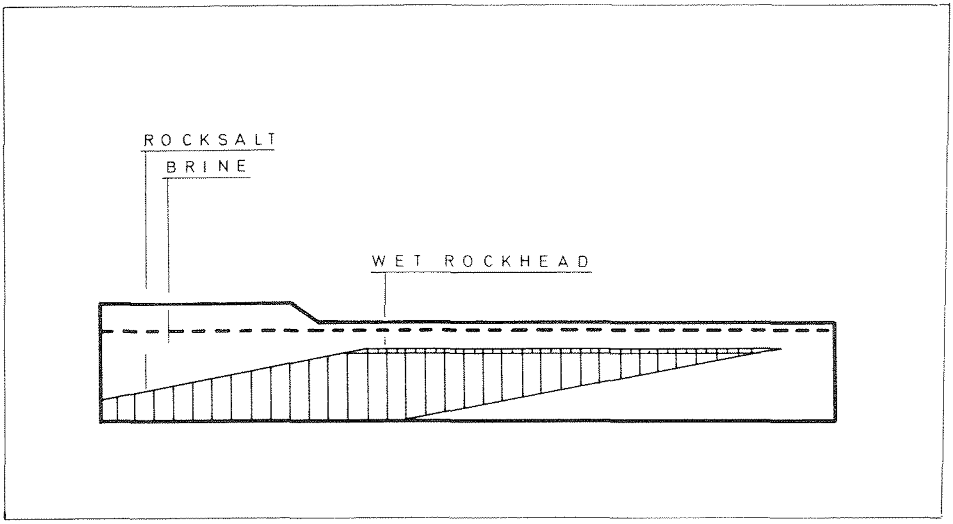

Fig. 4b. Post-Glacial rebound of saline interface.

ately give rise to new flooded areas (meres or flashes); railways, sewers and rivers changing gradients, and canals having to be rebanked. Agricultural land loses its quality as the ground sinks relative to the water table. Financial compensation is restricted and some structures, notably sewers, are exempted.

A proportion of costs associated with subsidence are indirect, others imponderable. Jacking points and extra reinforcement on civil engineering structures, and flexible and higher standard pipelines (Clarke,1968) raise the costs of construction. Severe speed restrictions on the railways impair inter-city high speed averages and developers give especial consideration to the possible consequences of building on the saltfield.

Future Trends and Outstanding Problems

The consequences of salt subsidence are such that it is important to predict, if at all possible, the nature and timing of subsidences. Since the prime cause is the removal of the protective interface of saturated brine from the saltbeds, prediction is dependent upon prediction of changes in the saline interface. A marked decrease in wild brine pumping is likely (Collins,1971) and, after some delay, related subsidences will cease. In addition, there are less severe regional movements of groundwater in response to natural hydraulic gradients. These may be expected to cause minor subsidences in the future. We suspect that some of the existing subsidence in the rocksalt areas near to the sandstone aquifers are the result of more intense migrations of groundwater induced by overpumping the freshwater in the sandstones, the extraction of freshwater in 1969 being in the order of 42,340 million galls/year (192 million m^3/year) (Crook and Howell,1970). The rate of aquifer pumping is unlikely to decline and the influence of freshwater extraction will continue. Local subsidences may form occasionally where the brine/freshwater interface has been disturbed by major civil engineering projects, quarrying, and by local peculiarities

Plate 3. Main line railway affected by subsidence. (Photo, authors. Courtesy British Rail.)

of the hydrogeology of the region, for example where rivers cross the saltbeds.

We are of the opinion that the major outstanding problem is still that of the prediction of the magnitude, timing, location and nature of the subsidences. It is particularly unfortunate that the onset of subsidence in districts hitherto free of movements is heralded by the sudden and dangerous crater collapses, or by headward subsidence of adjacent linear hollows. Our investigations with centrifuge models of such collapses give us some hope, for it does seem that important changes in the nature of the overlying strata and ground drainage must occur before any subsidence actually appears at the surface. Thus it may be possible for the significant changes in the fabric of the strata which precede subsidence to be detected by geophysical or remote sensing techniques. Since subsidences are landforms with a suite of properties growing in a well-established pattern of events, we feel that although we are nowhere near the refinement of prediction of subsidence trends available in coal mining, we can at least begin to make firmer, if only as yet descriptive, prediction of future events once subsidence has been noted. In the future, methods to ameliorate the subsidence by, for example, grouting, brine injection and deep sheet piling, may evolve from a better understanding of the nature of the subsidences.

Conclusions

Major subsidences in the Cheshire Basin are the result of groundwater migrations dissolving rocksalt beds. The characteristic landforms which result have a distinctive subsidence pattern.

Pleistocene injections of freshwater are considered to have initiated these landforms, which have been re-activated and supplemented by man-made perturbations in the groundwater regimes and are likely to continue well into the future.

Although predictions of the location, timing and magnitude of these subsidences cannot be made with any of the precision already possible in coal mining districts, we do not accept that rocksalt subsidence is totally capricious. Indeed, we consider that the recognition of mechanisms and some measure of order in the subsidence features forms a rational basis for future studies, which must be directed towards prediction and control.

Acknowledgement

The authors thank Professors Rowntree and Brotton, and the Department of Civil and Structural Engineering for their encouragement, and the Science Research Council for financial support.

Also the Royal Society for a travel grant to the U.S.A.

References

Bow, C. J., Howell, F. T., Payne, C. J. and Thompson, P. J., 1969, The lowering of the Water Table in the Permo-Triassic Rocks of South Lancashire: Water and Water Engineering, v. 73, no. 885, pp. 461-3.

Calvert, A. F., 1915, Salt in Cheshire: London.

Clarke, N. W. B., 1968, Buried Pipelines: Maclaren & Sons, London.

Collins, J. F. N., 1971, Salt: A policy for the control of salt extraction in Cheshire: Cheshire County Council.

Crook, J. M. and Howell, F. T., 1970, The Characteristics and Structure of

the Permo-Triassic Sandstone Aquifer of the Liverpool and Manchester Industrial Region of N. W. England: International Symposium on Groundwater, Palermo, pp. 217-25.
Crook, J. M. and Howell, F. T., 1973, Pleistocene Glaciers as the source of Fossil freshwaters encountered in the Permian and Triassic Sandstones of the Cheshire Basin, England: International Symposium on the Development of Groundwater resources, Madras, India, November, 1973.
Crook, J. M., Howell, F. T. and Sedgwick, R. D., 1973, Variation in Oxygen Stable Isotopes from Groundwater in the Cheshire Basin: Water and Water Engineering, June 1973, pp. 220-1.
Evans, W. B., Wilson, A. A., Taylor, B. J. and Price, D., 1968, Geology of the country around Macclesfield, Congleton, Crewe and Middlewich: Memoirs of the Geological Survey, G.B., H.M.S.O.
Howell, F. T., 1965, The Significance of the Ingress of Saline Waters into the Permo-Triassic Aquifers of South Lancashire: Water and Water Engineering, v. 69, no. 835, pp. 364-5.
Howell, F. T., 1973, The Sub Drift Surface of the Mersey and Weaver Catchment: Geological Journal, v. 8, pt. 2, pp. 285-96.
Sherlock, R. L., 1921, Rock Salt and Brine: Memoirs of the Geological Survey, Mineral Resources, G.B., Report 18.
Wallwork, K. L., 1959, The Mid Cheshire Salt Industry. Geography, v. 44, p. 171.
Ward, T., 1886, On the subsidences in the salt districts of Cheshire: their history and cause: Transactions of the Manchester Geological Society, v. 19, pp. 152-78.

Publication n°121 of the International Association of Hydrological Sciences
Proceedings of the Anaheim Symposium, December 1976

LAND SUBSIDENCE IN THE TOWN OF TUZLA DUE TO UNCONTROLLED SALT EXTRACTING THROUGH BOREHOLES

by

Prof. Dr. Muris Osmanagić, Mining Engineer
Dr Mr Ibrahim Jašarević, Civil Engineer, Assistant Professor
UNIVERSITY OF SARAJEVO

Abstract

Ground deformation, resulting from the ages-long extraction of salt water, caused serious damage in urban quarters of Tuzla in Yugoslavia. The progress of land subsidence in this locality is considered in the present paper, and the results of a long research with established regularities and the programme of future complex works aimed at an optimum adjustment of demands for economical production and protection of the community against the effects of salt mining.

1. Introduction

Disregarding the primitive mining by the old Illyrians, Romans and Turks, industrial production of salt water through deep wells in the township of Tuzla started in 1886 and has been increasingly continued ever since.

The rock salt deposit is extending in SE-NW direction and dipping to NW, covering an area of about 1,5 Sq.Km. More than 23o wells have been drilled in the deposit for test and production purposes, consequently, the deposit is defined except its NE margin.

The deposit is developed in four separate salt series of 2oo m total aparent thickness, but the depth of each of the series is variable and interbedded with significant marl strata by 3o per cent on average in the first series and by 5o per cent in the last salt series.

The rock salt deposit is overlain by banded and clayey marls with occasional sandstone intercalation. The uppermost salt series, about 15 m thick, which is almost exhausted, lies at the depth interval of 1oo m to 3oo m. The next underlying salt series about 6o m thick is being mined. Banded marl in the roof and the uppermost salt series form one aquifer which is recharged through salt deposit outcrops, especially on the eastern side from Solina River, and on southern side from the Jala River, generally along the zone of porous limestones and downward through a Tortonian schlieren. Ground water in the deposit is recharged by infiltration of rainwater at an average rate of q = 8.45 lit/sec and seepage of the Jala and Solina Rivers at q = 28.55 lit/sec on average. The proper drainage area of the aquifer is about 9.7 Sq.Km.

The extracting method used allows an inflow of fresh and brackish water from the upper salt series into deeper sections of the deposit. Salt solution at the bottom of deep wells with perforated tubes, which have the initial diameter 520 mm, is uncontrolled, resulting in a variable dynamic regime of ground water. The increased pumping of brackish water and an inadequate natural recharge have been noted to result in a rapid decline of ground water level, which fell by 107 m in period 1886-1972 (Fig. 1).

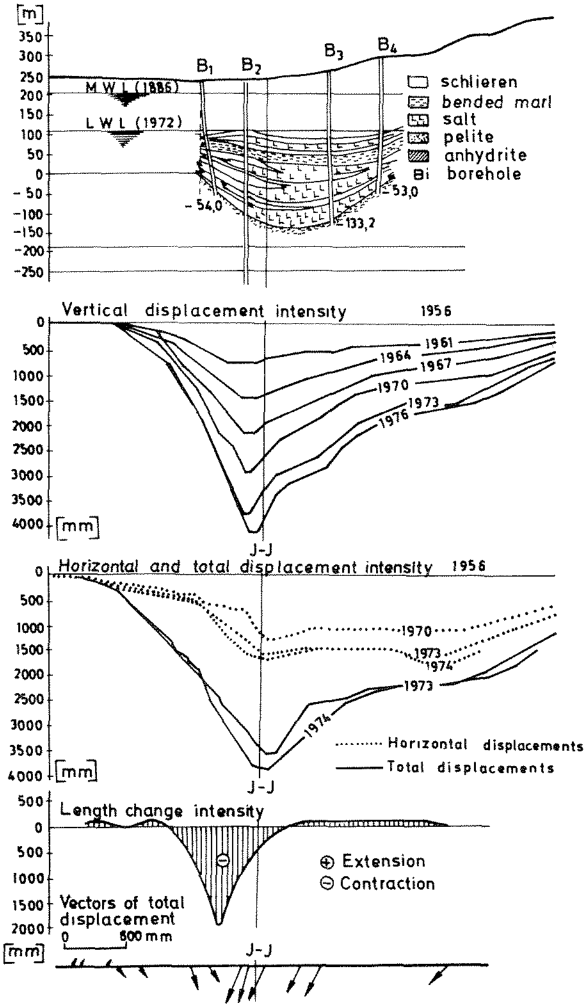

Fig.1

Parallel with the increased salt water pumping, the land subsidence and the damage of structures in the town have progressed. In last sixty years, the greatest subsidence recorded was 7.75 m. Figure 2 shows the development of vertical subsidence components and the extracting in dependence of time (Jašarević, 1975). Since 1956, permanent geodetic measurements in the detail triangulation, level and traverse networks have been carried out in the whole of the attacked area, with the goal of identifying typical land subsidence parameters of a continuous and uncontrolled salt extraction.

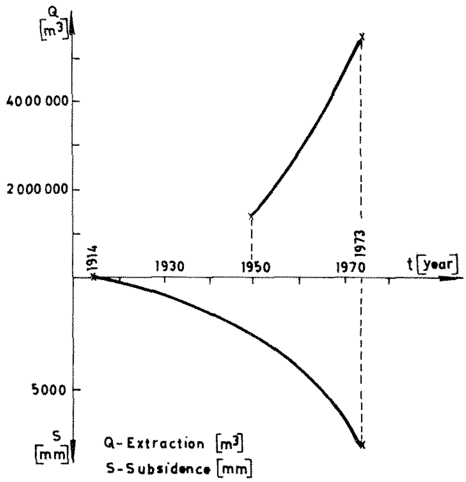

Fig. 2

2. Geodetic measurement results

The triangulation network covers an area of 8oo hectares, with the coordinates determining accuracy within $m_Y \approx m_X \leq$ 2o mm. The network of traverses includes 23o stations, which are determined with a mean error in length measuring of 4-5 mm. The level network includes 55o points, each measured with an accuracy of $m_h \leq 3$ mm. Triangulation and traverse stations are stabilized by reinforced-concrete posts, in form of truncated cone, with permanent vertical bench marks. Systematic geodetic measurements are taken once each summer and are used to prepare annual and summary plans of the area affected by land subsidence.

Maximum vertical subsidence in period 1956-1974 was 4281 mm near the measuring point 32 (Fig. 3). In the same point, annual subsidence for period 1973-1974 is estimated to 325 mm.

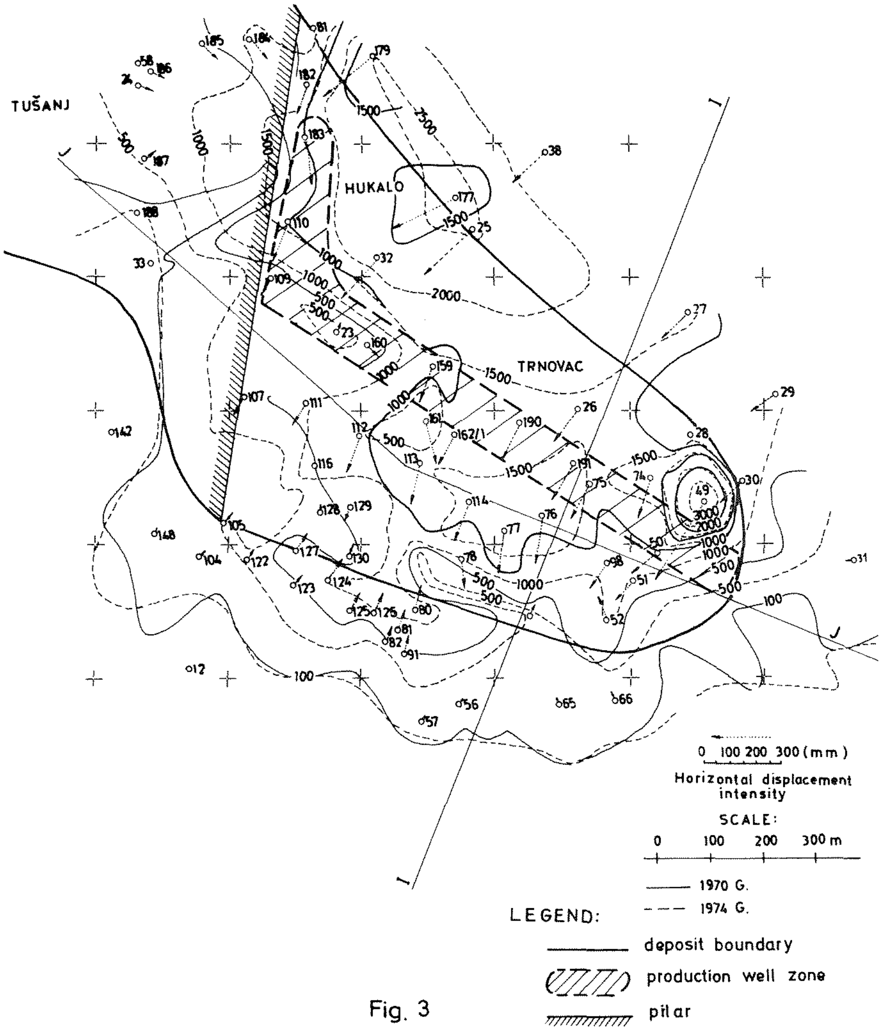

Fig. 3

The most intensive horizontal movement is noted on the northern side of the deposit, near point ⊙ 49, where a horizontal displacement of 3594 mm was registered in period 1956-1974 (Jašarević, 1974 and 1975).

3. Subsidence parameters depending on time, extraction and atmosphere's rainfalls

Analysing the geodetic measurements results, timedependent variation of average summary displacements (Up) in all observation points within the subsidence area in period 1956-1974 is established as

$$Up = a_o + a_1 t \quad \ldots\ldots\ldots\ldots\ldots \quad (1)$$

where,

a_o = 5o97,193

a_1 = 2,629

r = o,824 (correlation coefficient)

Similar procedure is used to set other equations of the future displacement forecast in various land subsidence points.

During the observation period 1956-1974, a quantity of 7,229.781 ton of pure salt was produced, and a subsidence of 2,964.61o m^3 in volume occurred. Dependence of subsidence volume (Z) on production (Q) is expressed by equation

$$Z = o.354\ Q^{1.454} \quad \ldots\ldots\ldots \quad (2)$$

with correlation coefficient r = o,8524.

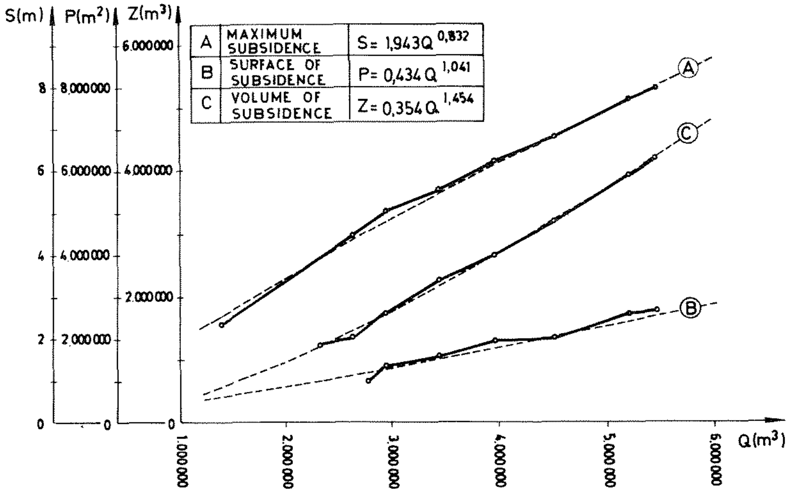

Fig. 4

Diagram (Fig.4) shows rating curves of maximum subsidence, area and volume of subsidence, and production (Jašarević 1974 and 1975, Osmanagić, 1975).

As illustrated by the curve in Fig. 5, the land subsidence volume difference is lately increasing. It is associated sidence volume difference is lately increasing. It is associated not only with the increased production, but also with atmosphere's rainfalls ascillation. Heavier rainfalls cause a rise of ground water level, decreasing the land subsidence, and vice versa.

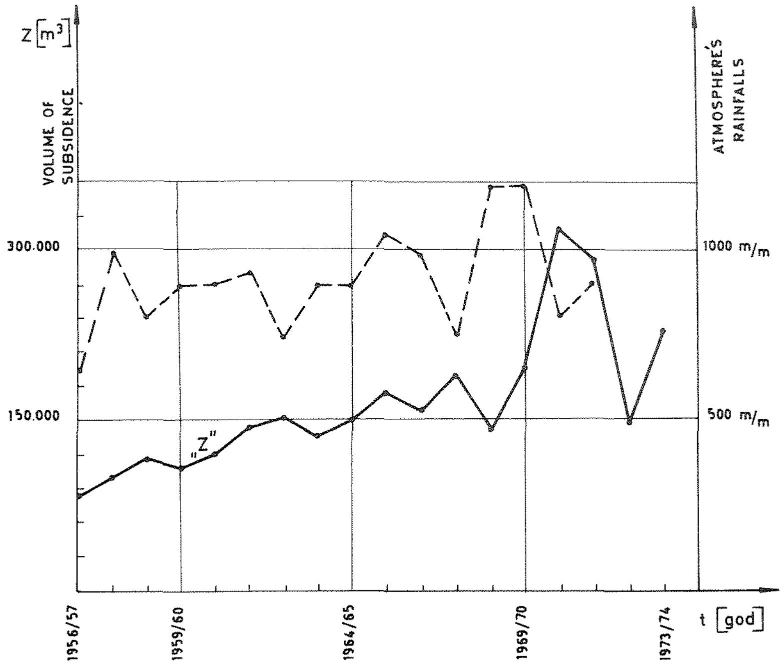

Fig. 5

4. Research in the pattern of rock failure process

It has been realized during the research, that geodetic measurements alone cannot give adequate data for a forecast of future subsidence, but that the system of internal processes of rock mass movement in mines must be mastered, this, however, calls for respective geomechanics laboratory and field investigations related to the pattern of rock failure process (Jašarević, 1975).

As regards the rock failure process, which develops under ground, respective parameters are tested in laboratory, such as shear strength, time-dependent deformability of overlying deposits, coefficient of porosity "e" (Fig.6). Time deposits compressibility is tested in laboratory in oedometer, a large apparatus of special construction, 5o cm in diameter and 1oo cm high, in which marl from the roof, of the grain size like that of the subsiding land, is built.

Void ratio "e" and discharging coefficient "g_g-1" can be derived from equations

$$e_o = \frac{\gamma_s - \gamma}{\gamma - 1}, \quad e = \frac{(h-h_s) - \varsigma}{h_s}$$

$$(g_g - 1) = \frac{\gamma (1 + e)}{\gamma_s + e} - 1, \quad h_s = \frac{h}{1 + e_o} \qquad \ldots \quad (3)$$

where,

γ_s = specific gravity,

γ = bulk density of material built in oedometer

h = height of material built in oedometer

ς = settlement in edometer at respective loading degree

Diagramatic representation of void ratio "e" is shown in Fig.6 as relative to stress in time "t"

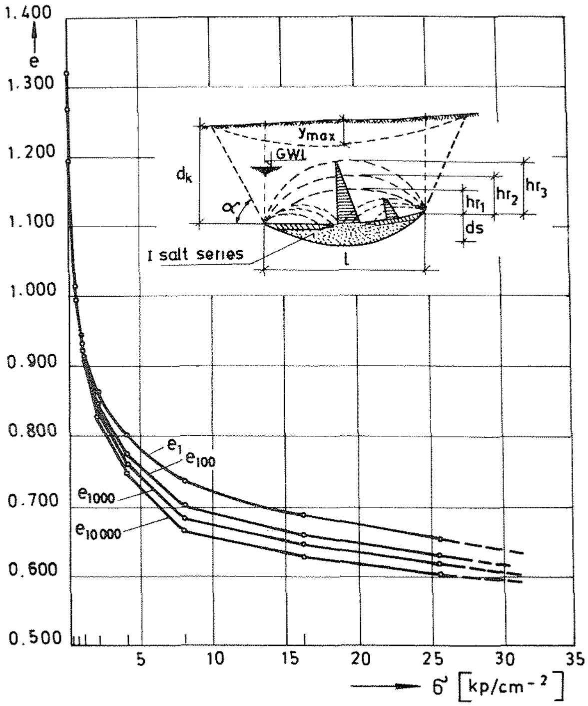

Fig. 6

The subsidence zone depth can be written in function of time, using the known equation:

$$h_r (t) = \frac{d_s}{(g_g - 1)} \quad \ldots\ldots\ldots \quad (4)$$

where,

d_s = thickness of respective salt series,

$h_r(t)$ = depth of rock failure zone.

Maximum sibsidence on surface, relative to thickness of the exhausted deposit, is determined by equation:

$$\frac{\Delta h}{h_r(t)} = \frac{\Delta \sigma}{M_s} \quad \ldots\ldots\ldots\ldots \quad (5)$$

where,

h = maximum subsidence,

$\Delta \sigma$ = difference in stress at consolidation.

Process of surface subsidence evolves parallel with consolidation of material in the rock failure zone, analytical results of subsidence obtained from equation (5) agree with results of the geodetic measurements (Jašarević, 1975).

5. Drawdown effect on land subsidence

Based on experimental data of a five-year period, an equation of ground water level (**S**) in wells relative to brine pumping (V) is set as following:

$$S = 0.86 \times 1o^{-5}\ V - o.22 \times 1o^{-1o}\ V^2 \quad \ldots\ldots\ldots\ldots \quad (6)$$

In 1956, we had **S** = 76 m and V = 988,664 m^3 , and in 1974, **S** = 1o7 m and V= 184,535 m^3, or an average drawdown of 3o m in last 18 years. However, groundwater level in wells has a variation range from 8 m to 32 m during a year (Osmanagić, 1975.).

Land subsidence Δh caused by drawdown is calculated from relation:

$$h = \frac{h_s}{M_s} \Delta \sigma \quad \ldots\ldots\ldots\ldots \quad (7)$$

where,

h_s = drawdown in a time period,

$\Delta \sigma$ = land stress change due to drawdown.

For h_s = 3o m, which was the drawdown from 1956 to 1974, Δh = 183 mm, in relation to average vertical subsidence in this period and in the well zone, comprised 8 per cent. This is not a high value in view of absolute subsidence values, but it may have great effect on structures where subsidence is different. Separation of the drawdown effect on the land subsidence and the effect of mass deficit (extracted salt) is checked in the depression cone zone, southwest in the deposit (protective pillar Hukalo), which is off the production works and where coincidence with the geodetically measured subsidence is high. Thus, the boundary angle was defined as $\alpha = 55^{\circ}$ (Fig.7) (Wohlrab, 1969, Boreli M, 1975, Osmanagić, 1975).

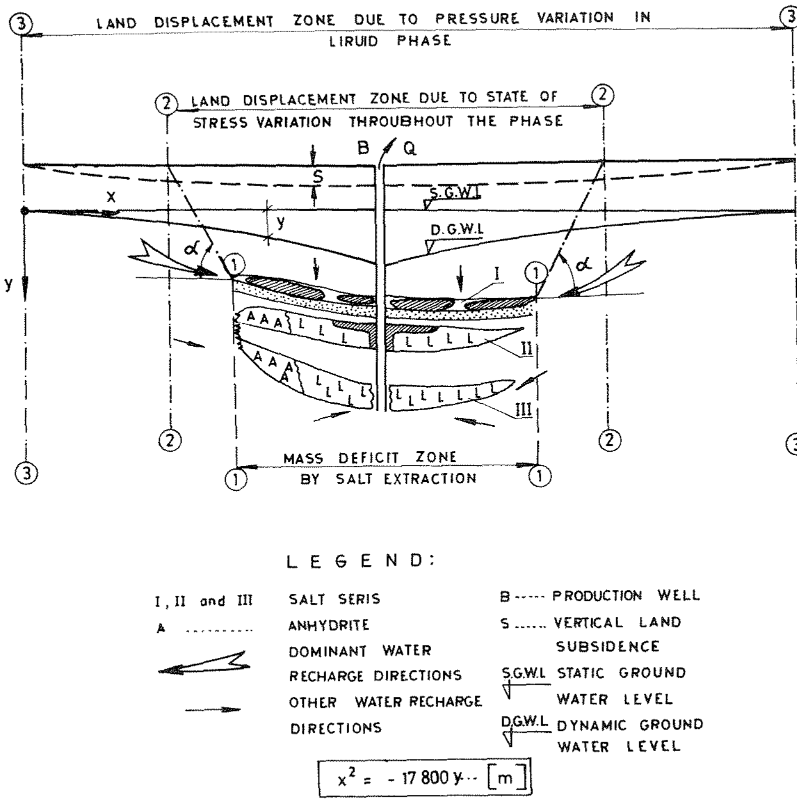

Fig.7

6. Use of numerical methods

Since analytical solutions in a closed form had many shortcomings, because time-dependent nonlinear states of stress and strain could not be introduced, it has been tried to use numerical methods.

The estimate was made for one cross section through the deposit and for plane state of strain, using the specific strain and stress relation which is nonlinear, established by laboratory tests

$$\varepsilon_i(\sigma_i, t) = \frac{\sigma_i}{E_i(\sigma_i)} \left\{ 1 + \varphi \left[1 - exp\left(- \frac{t}{T_{ret}} \right) \right] \right\} \quad \ldots (8)$$

where,

Ei = modulus of strain which is a function of total stresses,

of $Ei\ (\sigma i) = E_o\ exp\ (-a_1\ \sigma_i)$ .... (9)

φ = coefficient of flow

T_{ret} = time lag which is generally a complex function of stress and time

Taking the depth of rock failure zone h_r and the compressibility modulus of reconsolidated rock M_s, displacement in direction of coordinate axes U and V and stresses σv σh are established (Figs. 8 and 9).

Diagramatic representation of displacements U and V from individual movements of posts shows a high coincidence with the geodetically measured displacements on land surface. For stresses, however, certain local zones may be delineated in the studied section, where failure of roof and cracks may be expected (zone around point 82) as much as 1oo m deep. Moreover, local areas around points 1-1o and 61-7o are in a similar state (Vukelić, 1975).

7. Summary

In past research, regularities of land subsidence are established dependent on time, current salt extraction regime, drawdown and geomechanics characteristics of overlying deposits. Further investigations should be attempted at mastering the system of internal processes of rock mass movement, in order to adjust the salt mining method, which should cause the least land subsidence at the highest specific yield. Since analytical solutions in closed form are not possible, it should be tried to use numerical methods (FEM) with the introduction of all relevant factors which have some influence on the development of land subsidence and simulation methods by models of equivalnet materials.

The results obtained by numerical methods (FEM) will be checked through a comprehensive programme of geodetic measurements on land surface, which is already carried out and by stress and displacement measurements in rock mass through boreholes.

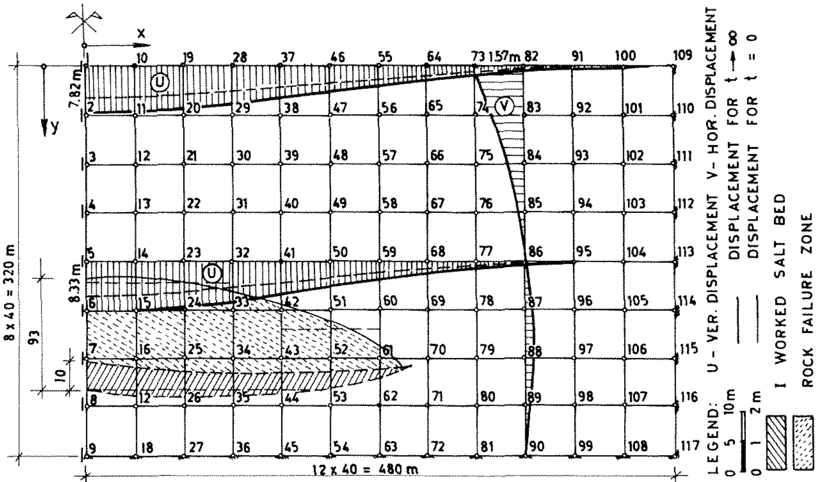

Fig. 8

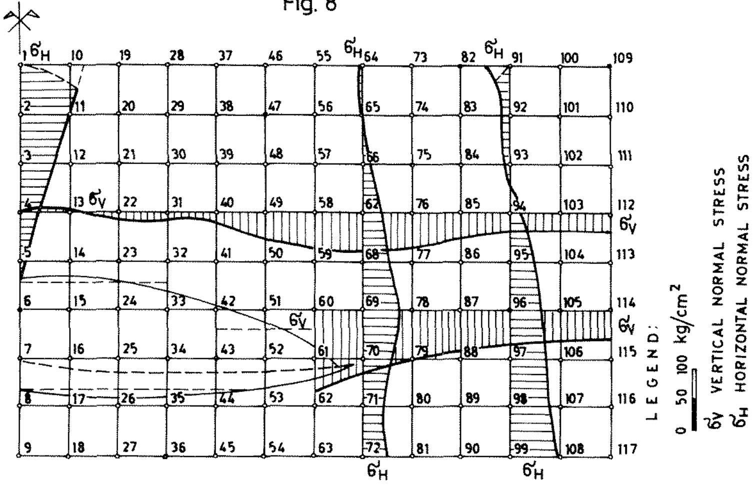

Fig. 9

References:

Boreli M, 1975 "Izvesne karakteristike strujanja podzemnih voda značajne za slijeganje terena u području ležišta kamene soli u Tuzli" (Certain Characteristics of Ground Vater Currents Significant for Land Subsidence in the Tuzla Rock Salt Deposit Area). Symposium on Enviroment Protection from the Hazards of Underground Workings), Tuzla

Jašarević I., M.Tatić, M.Redžepagić, P.Jovanović, 1975, "Istraživanje sheme procesa rušenja u masivu kod nekontrolisanog izluživanja ležišta kamene soli, kod nekontrolisanog izluživanja ležišta kamene soli, vezano sa prognozom deformacija terena na površini, sa ciljem sagledavanja mogućnosti izgradnje objekata" (Research in the Pattern of Rock Failure Process due to Uncontrolled Salt Extracting, Associated with the Land Subsidence Forecast, Aimed at an Elucidation of the Construction Feasibility) - Symposium on Environment Protection from the Hazards of Underground Workings (with Special Reference to Subsidence in Tuzla due to Uncontrolled Working of Salt Deposits), Tuzla.

Jašarević I, Tatić M, 1974, 1975. Studija geotehničkih karakteristika kamene soli i pratećih naslaga ležišta kamene soli u Tuzli sa prijedlogom metodologije za uspostavljanje medjuovisnosti eksploatacije slane vode putem sonih bunara i površinskih deformacija terena, Tuzla

Osmanagić M.1975 "Istraživanje uzoraka i procesa deformacija terena i metode podzemne eksploatacije radi smanjivanja štetnih posledica nastalih eksploatacijom mineralnih sirovina" (Investigation in the Causes and Processes of Land Subsidence and the Methods of Underaround Workings Aimed at a Minimization of Damages Resulting from Extraction of Mineral Ores) - Symposium on Environment Protection from the Hazards of Underground Workings, Tuzla.

Vukelić, S, 1975 "Jedan postupak proračuna slijeganja tla karakterističnog poprečnog profila na delu ležišta kamene soli u Tuzli " (A Land Subsidence Estimate Procedure for Typical Cross Section of Tuzla Rock Salt Deposit).
Symposium on Enviroment Protection from the Hazards of Underground Workings),Tuzla.

Wohlrab, B, 1969
"Effects of Mining Subsidences on the Ground Water and Remedial Measures", in: Proceedings of the Tokyo Symposium on Land Subsidence - IASH/AIHS - UNESCO.

Publication n°121 of the International Association of Hydrological Sciences
Proceedings of the Anaheim Symposium, December 1976

LAND SUBSIDENCE AND THE CALIFORNIA STATE WATER PROJECT

Clifford V. Lucas and Laurence B. James
California Department of Water Resources
Sacramento, California

Abstract

Construction of the multi-billion dollar water project required unique engineering solutions to complex subsidence-related problems. The California Aqueduct, the principal water conveyance facility of the project, crosses regions affected by four types of land deformation. These include subsidence related to ground water extraction, compaction of low density soils (partially hydrocompaction), production of oil or gas, and crustal movements due to tectonic activity. Large magnitudes of subsidence have affected design, construction, and operation of 200 miles (320 kilometres) of the aqueduct alignment. The aqueduct and its related facilities required unusual construction procedures, alignment studies, and structural features to mitigate the effects of subsidence.

INTRODUCTION

The California State Water Project, which is in the final stage of completion, consists of a complex of reservoirs and aqueducts for the purpose of capturing and storing surplus streamflow in Northern California and conveying it south to areas of deficient water supply. The construction of the initial facilities will include 25 dams and reservoirs, 8 power plants, 22 pumping plants, and 685 miles (1100 km) of aqueduct at a total cost of approximately $3 billion.

The California Aqueduct, the principal water conveyance facility of the project, and its related facilities (pumping plants, concrete-lined canal, check structures, and other minor structures) lies in part within subsidence regions. The location of the aqueduct with respect to these affected areas is shown in Figure 1.

The concrete-lined canal is the part of the system that is most vulnerable to damage from subsidence. This is primarily because of its sensitivity to vertical movement. The overall length of the Central Valley portion of the canal is 280 miles (450 km) with 200 miles (320 km) in areas of significant subsidence. Its average gradient is about .25 feet per mile (one metre of drop for each 20 km) of reach.

Four types of land deformation have been identified as occurring within regions crossed by the aqueduct. These include subsidence related to ground water extraction, hydrocompaction, and production of oil or gas and crustal movements due to tectonic activity.

As of 1970, an area of more than 13,500 square kilometres in the San Joaquin Valley was identified as having subsided at least 1 foot (0.3 metre) as a result of ground water extraction and hydrocompaction. Maximum subsidence has occurred southwest of Mendota in Fresno County and was determined to have exceeded 28 feet (8.5 metre) between 1926 and 1972. Selection of the aqueduct route through this depressed region involved a comparison of several alternative alignments to determine which could be constructed and maintained most economically.

Early in the investigation it was concluded that the only practical means of alleviating subsidence due to ground water extraction would be to reduce ground water production. The crops in the San Joaquin Valley dependent upon well irrigation are valued in millions of dollars. Therefore, a mandate restricting pumpage was recognized as economically and politically infeasible. However, it was reasoned that once in operation the aqueduct could provide irrigation water at a cost less than the cost of producing well water. As a consequence, curtailment of ground water production would result which in turn would lead to a reduction in subsidence. Thus the solution adopted for this problem was to let the problem take care of itself. Canal embankments and related structures were designed so that they could be raised to accommodate subsidence expected to occur during the period of transition from ground to surface water usage.

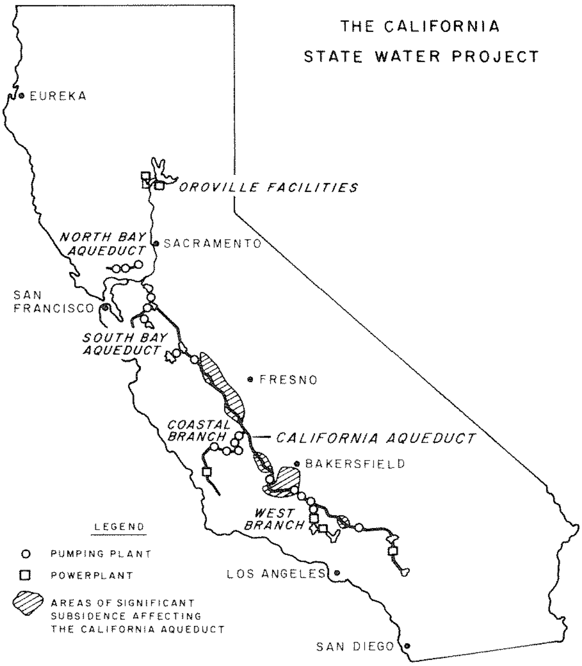

FIGURE 1

A major effort was focused on investigation of potential subsidence resulting from hydrocompaction. Geologic, soils, and engineering studies were conducted to identify susceptible areas and estimate expected future subsidence. A subsequent study concentrated on development of countermeasures for reducing post-construction subsidence to acceptable limits. A test facility was constructed near Mendota containing a section of prototype canal constructed in part in soils subject to hydrocompaction and in part in similar soil previously compacted by water ponding. Experiments were conducted with concrete-lined and heavy compacted earth-lined sections of this canal and with procedures for accelerating preconstruction hydrocompaction along the alignment of the future aqueduct. The techniques developed were subsequently employed successfully to presubside approximately 75 miles (120 km) of aqueduct right-of-way, along which the canal was subsequently excavated and lined with concrete.

Subsidence at 27 of the 493 oil fields located in California has ranged from 28 feet (8.5 metres) at Wilmington field near Los Angeles to a few centimeters at other affected fields. The California Aqueduct crosses six producing oil fields and passes within one mile of 11 others. No significant depression has been detected in any of these fields to date. The possibility of future subsidence has been discussed with the major California oil producers. They are aware of the potential effects on the canal and have stated their intentions to plan oil field operations accordingly. Monitoring of the aqueduct profile continues near oil fields by periodic leveling.

California is highly active seismically, and consequently an investigation of tectonic deformation near the aqueduct route was initiated during the early planning stage. Tiltmeters were installed at suspect locations; a statewide network of seismographs placed in operation; and sophisticated geodetic surveys undertaken to detect, monitor, and study any preceptible crustal deformations that might be occurring near the facilities.

DESIGN OF THE CALIFORNIA AQUEDUCT

The major effort in design of the California Aqueduct began in 1958. Planning and preliminary design studies to establish hydraulic gradient, dimensions, design criteria, and economical location of the aqueduct were being performed. Subsidence was recognized at that time as being a major problem which could not be ignored in solving other engineering problems.

From an engineering standpoint the subsidence could be separated into two general classifications. One affects a large area and continues over a long period of time. The other affects a small or localized area and its major effect occurs rapidly.

In this paper, we will refer to "deep subsidence" and "shallow subsidence". Deep subsidence is movement that takes place over large areas and for an extended period of time. This is primarily caused by the excessive extraction of ground water. Shallow subsidence is the movement that results from collapse of soil structure and compaction, this being primarily caused by "hydrocompaction" and a change in stress due to loading. Near surface soils are involved in this process and the effect tends to be localized and of relatively short duration.

Deep subsidence areas occurring near the aqueduct are shown on Figure 2. The large dark grey splotches in the valley are deep subsidence areas. The lighter splotches along the aqueduct alignment are shallow subsidence areas.

Deep subsidence affects the aqueduct in many ways. The economics of various alignments are considerably influenced. This subsidence occurs over an extended period of time. The subsidence forms a dish-shaped depression in the ground surface. If a depression were to develop along several miles of canal, embankments would have to be raised to maintain a specific water surface elevation. Structures crossing the canal would be raised or inundated, and the hydraulic characteristics of the channel would change. The canal capacity would change, with the canal section at the depression increasing in depth and width. Possibly, cracking of embankments would occur. Higher maintenance expenditures and more land would be required.

Preliminary design studies for the California Aqueduct considered several alignments. These alignments were partially affected by both deep and shallow subsidence. Figure 3 shows three alignments and an area of deep subsidence caused by ground water withdrawal. The Kern

Lake alignment crosses the subsidence area while the Buena Vista alignment partially goes around the west and south side and the Far West alignment skirts the edge. Figure 4 indicates the subsidence for the Kern Lake and Buena Vista alignments at various times in the future. The Far West alignment was assumed only to be slightly affected by deep subsidence.

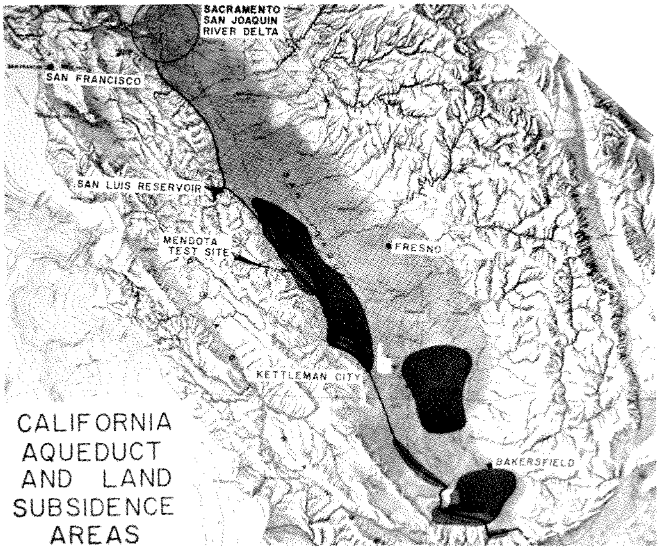

FIGURE 2

The design studies indicated that the Kern Lake alignment will subside 18 feet (5.5 metre) from 1970 to year 2000. The design studies for a trapezoidal-shaped canal built on this alignment in 1970 used a canal section with 2 to 1 side slopes, a 24-foot (7.3 metre) water depth, a bottom width of 24 feet (7.3 metre) and a top width of 120 feet (36.6 metre). In the year 2000, with the water surface elevation maintained the same as in 1970, the canal would be 42 feet (12.8 metre) deep and would have a top width of 192 feet (58.5 metre). It is obvious that the economics of this 25 miles (40 km) of alignment is drastically altered when subsidence is considered. The earthwork alone would be quadrupled, not to mention the concrete lining, structure raising, water quality, plant growth, sediment, seepage, and other problems.

The Buena Vista alignment is affected less by the deep subsidence. The profile shown in Figure 4 indicates the magnitude of subsidence from 1970 to 2000 to be a maximum of approximately 10 feet (3 metres). This alignment is 13 miles (21 km) longer (total length 38 miles)(61 km) than the Kern Lake alignment, but the costs related to subsidence are less significant.

The Far West alignment, assumed not to be affected by deep subsidence, has a length of 46 miles (74 km).

The economic comparison of these alignments indicated the Buena Vista alignment to be the most desirable. Deep subsidence makes the shorter Kern Lake alignment too costly. The length and other factors raised the cost of the Far West alignment above the cost for the Buena Vista alignment.

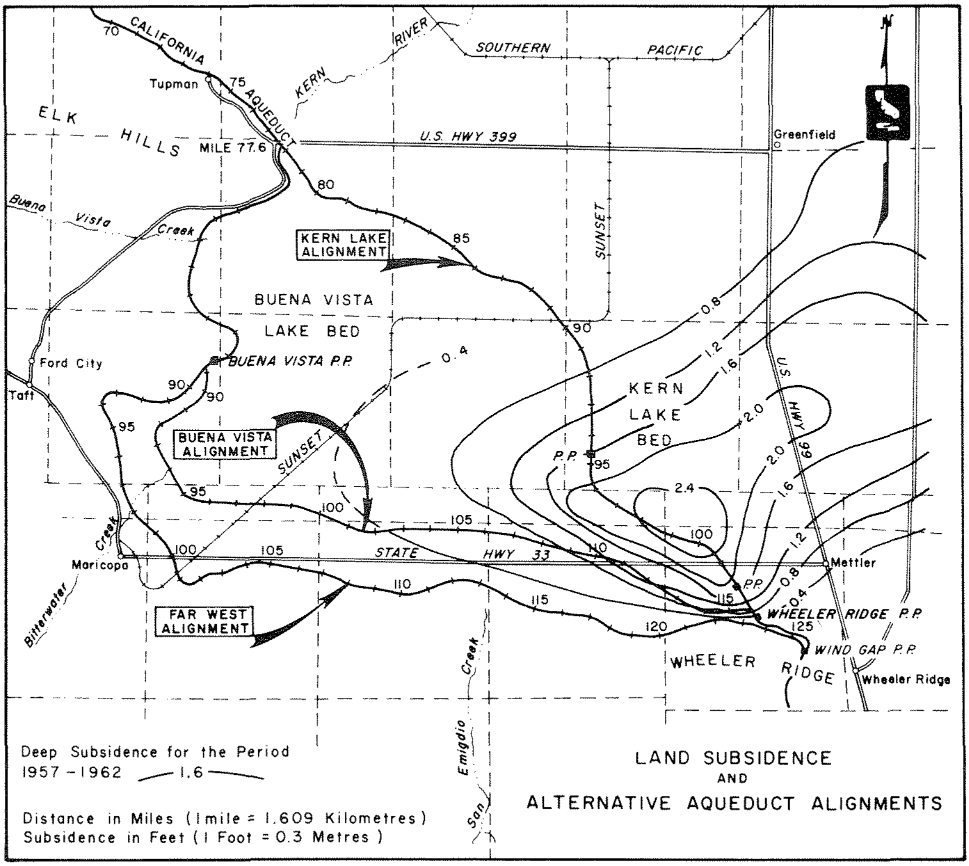

FIGURE 3

Approximately 20 (32 km) out of 38 miles (61 km) of the Buena Vista alignment will subside. The magnitude and the rate of subsidence will vary along this 20 miles (32 km). At Mile 97 (Figure 4) no subsidence is expected for the life of the project, while 14 miles (22 km) away at Mile 111 subsidence is expected to occur at an average annual rate of .3 to .4 foot (9 to 12 cm).

It was desirable that the initial investment for alleviation of subsidence effects be minimized, yet sufficient safeguards taken to assure that costly maintenance contracts would not be needed shortly after aqueduct completion.

The aqueduct was constructed with sufficient embankment freeboard and concrete canal lining freeboard for an estimated 10 years of continued deep subsidence. When the aqueduct subsides and the freeboard no longer exists, higher embankments and canal lining will be constructed.

Structures such as bridges, pipeline crossings, checks, siphons, and cross-drainage structures have been located such that they will not be affected by deep subsidence or they are designed to be raised. A pumping plant is located on Wheeler Ridge, at the edge of this deep subsidence area. Tilting of the pumping plant will occur. This will affect the mechanical equipment in the plant. Provisions have been made to counteract the tilting effect by adjusting the mechanical equipment.

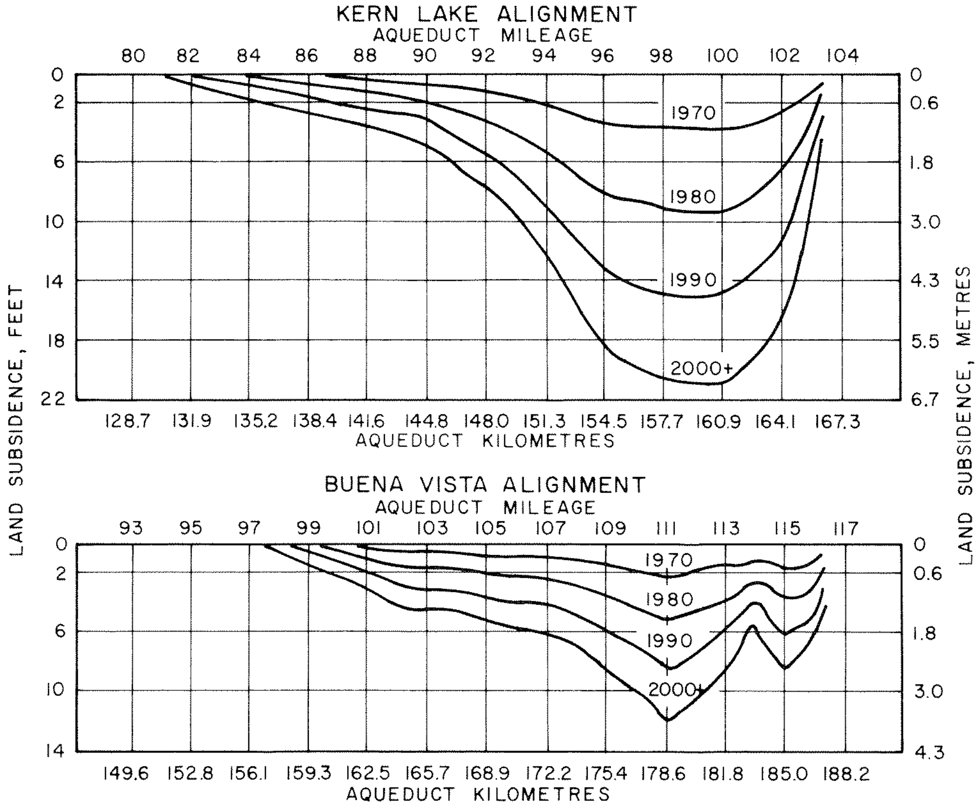

ESTIMATE FUTURE DEEP SUBSIDENCE FROM 1962 BASE ALONG ALTERNATIVE AQUEDUCT ALIGNMENTS IN BUENA VISTA LAKE-KERN LAKE AREA

FIGURE 4 COMPARISON OF DEEP SUBSIDENCE ON TWO AQUEDUCT ALIGNMENTS

Shallow subsidence has similar effects to those mentioned for deep subsidence. The economics are similar but not as significant when considering various alignments. This subsidence takes place rapidly. Using normal canal design and construction procedures, shallow subsidence would cause rupturing of canal embankments, collapse or cracking of canal lining, loss of water service through the canal, collapse of structures, and costly maintenance.

Although shallow subsidence affects many miles of aqueduct, it is confined to those areas where certain soil conditions exist and moisture is available. The magnitude of subsidence varies considerably over short distances. Figure 2 shows the areas along the aqueduct where hydrocompaction has or will occur.

The normal consolidation of saturated soils due to loading is not an unusual occurrence, and therefore requires no explanation of its localized effects. The soils along the aqueduct have a low density, and consolidation from small embankment loadings can produce several feet of subsidence.

Although shallow subsidence affects many miles of aqueduct, we consider its effects to be localized. Figure 5 is an example. This picture shows a small test plot through which water was applied. The small 8-foot (2.5 metre) diameter corrugated metal pipe was at the same elevation as the surrounding ground surface prior to putting water into the upended pipe. At the time this photograph was taken, the area near the pipe had subsided approximately 7 feet (2 metres). Figure 6 shows

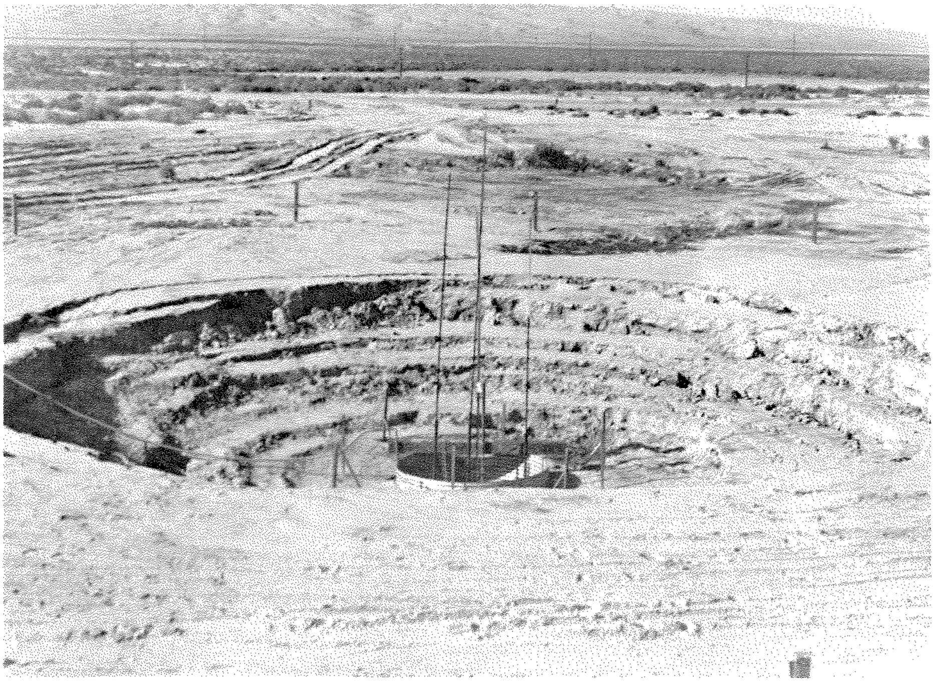

FIGURE 5 EXAMPLE OF LOCALIZED SHALLOW SUBSIDENCE

the localized effect on a canal. Moisture from the canal seeped into the foundation soils and hydrocompaction occurred. Subsidence of the compacted canal embankment followed the hydrocompaction of underlying soils. The cracking in the embankment next to the concrete lining is typical. Figure 7 is an example of what happens to a concrete canal lining. This picture was taken after approximately 2 feet (0.6 metre) of subsidence had occurred along 100 feet (30 metres) of canal embankment. Cracking of the canal lining had occurred with less than one foot of subsidence.

The lining did not buckle and collapse until more than one foot of subsidence had occurred. Subsidence from hydrocompaction would have affected approximately 70 miles (112 km) of the California Aqueduct in the San Joaquin Valley.

FIGURE 6 TYPICAL SUBSIDENCE EFFECT ON CANAL

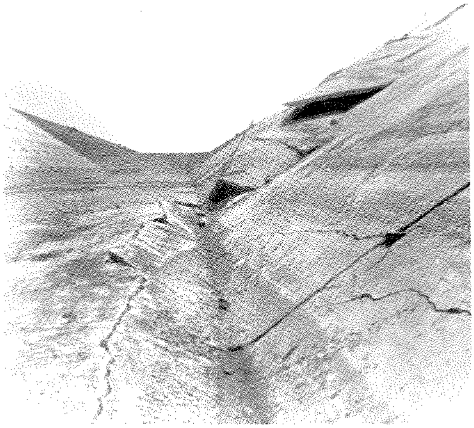

FIGURE 7 EXAMPLE OF SUBSIDENCE DAMAGE TO CANAL LINING

Preliminary design included alignment studies to avoid the subsidence areas. Location of the alignment was adjusted for the estimated subsidence that is expected to occur. During the preliminary design studies several questions arose. Would the foundation soils accumulate a sufficient quantity of water to start the hydrocompaction process? If hydrocompaction started, how rapidly would the ground subside?

It was determined that a watertight canal could not be constructed at a reasonable cost. The canal would form a natural barrier to agriculture drainage water and storm runoff water which could cause ponding and eventually subsidence would start.

Once hydrocompaction has started, it progresses rapidly until there is insufficient moisture to further lubricate the soil or the soils become normally consolidated. Figure 8 is an example of the rate of subsidence in a typical subsidence area. In this case, the soils subject to hydrocompaction were at various depths from the ground surface to 180 feet (55 metres) below. Water was applied at the ground surface and as it percolated downward, collapse of the soil structure occurred. After approximately 1000 days, hydrocompaction and normal consolidation was nearly complete. A surcharge consisting of a 10-foot (3 metre) embankment was then placed and its effect shown on Figure 8. Subsidence continued at this site at the rate of .01 foot (0.3 cm) per month. It has been assumed that this is a continuation of the normal consolidation process.

Since the foundation soils during or after construction of the aqueduct would get wet and the hydrocompaction started, it was decided that the soils along the canal alignment would be hydrocompacted prior to actual construction of the canal. This hydrocompaction has been accomplished by a series of ponds such as those shown in Figure 9.

Hydrocompaction from Kettleman City to the Tehachapi Mountains required approximately 140,000 acre-feet (172 x 10^6 cubic metres) of water and cost approximately $20,000,000.

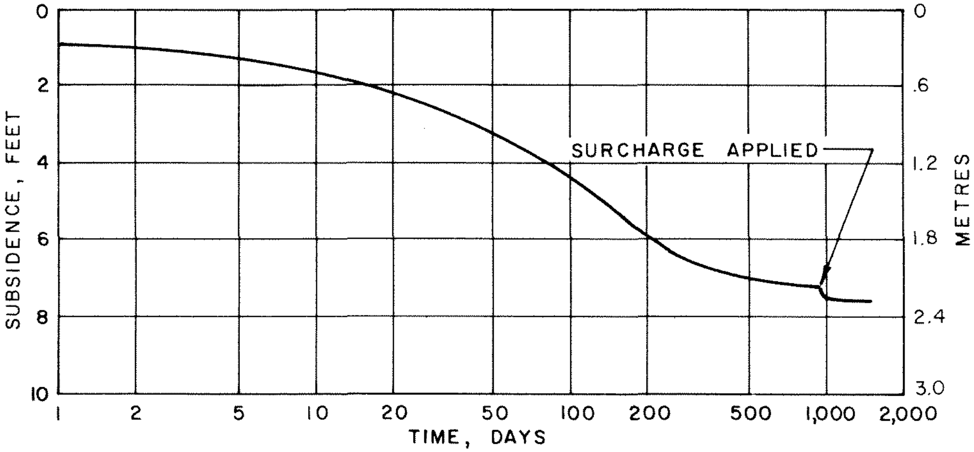

TYPICAL SUBSIDENCE - TIME RELATIONSHIP

FIGURE 8

A detailed study was performed to determine the extent and magnitude of subsidence along the canal alignment. There are areas where subsidence will definitely occur, areas where it is questionable, and areas where it will not occur.

FIGURE 9
HYDROCOMPACTION PONDS
ON
AQUEDUCT ALIGNMENT

Since the canal lining and embankments could only withstand a nominal magnitude of differential subsidence (approximately 1 foot in 100 feet) (.3 metre in 30 metres) without a major failure, the questionable areas were treated the same as those where subsidence would definitely occur. In most instances, it is not possible to define the magnitude of subsidence within an accuracy of ± 2 feet (0.6 metre) without performing an expensive and detailed subsurface exploration program. An example of the variation in subsidence magnitude over short distances is shown in Figure 10.

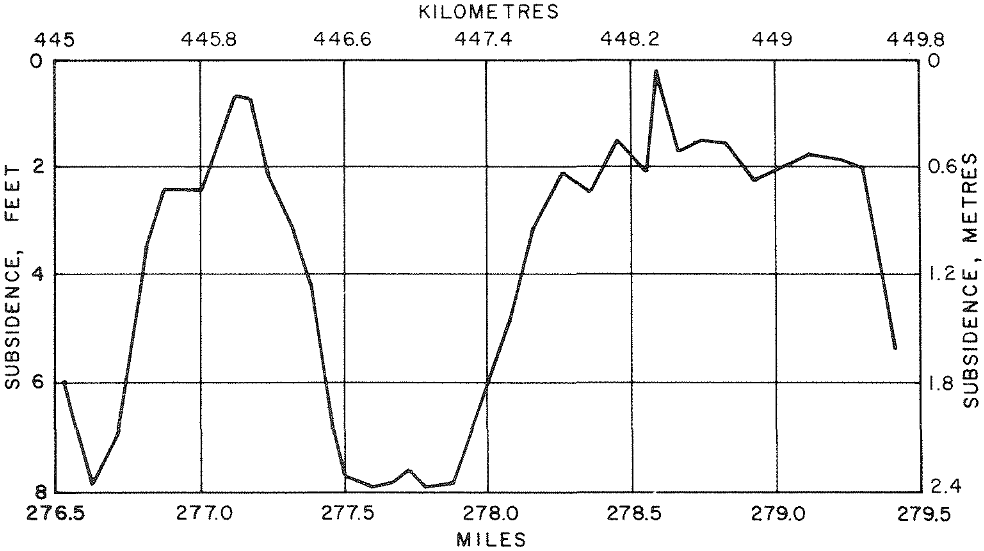

FIGURE 10 TYPICAL SHALLOW SUBSIDENCE MAGNITUDES ALONG AQUEDUCT

DESIGN OF CANAL SECTION

Design criteria for the canal is based on a 50-year life. The canal is designed for a maximum reliability over this period of time.

Hydrocompaction was accomplished for the full canal section. This includes the foundation soils for the compacted embankments on each side of the canal and at the turnouts. Operating roads and waste banks were placed on soils that have not been hydrocompacted.

An effort has been made to limit the differential movement that will occur after the canal lining has been constructed. Studies have indicated that a concrete lining with 10-foot (3 metre) joint spacing can accommodate approximately 1/4 to 1/2 inch (0.6 to 1.3 cm) of differential movement across a lining panel without cracking the lining. We have attempted to limit the differential movement after construction to approximately 1/4 inch (0.6 cm) per panel. Hydrocompaction and normal consolidation prior to lining the canal has reduced the differential movement to a tolerable amount.

FREEBOARD ALLOWANCES

There is a residual subsidence which continues after construction of the aqueduct. An allowance for this has been included in the canal lining freeboard. This allowance varies, depending on the location. A maximum of 2 feet (0.6 metre) has been constructed for residual shallow subsidence. The effect of residual shallow subsidence is similar to that of deep subsidence.

In areas where both shallow and deep subsidence occur, freeboard allowances for both have been included. As an example, on Figure 11 the normal freeboard from the water surface to the top of lining is 2.5 feet (0.76 metre). At one point on the canal a total lined freeboard of 8.5 feet (2.59 metre) was constructed; two and one-half feet normal freeboard, 2 feet (0.6 metre) for residual shallow subsidence, and 4 feet (1.2 metre) for deep subsidence. It is a design assumption that this will be adequate freeboard until 1980 or longer. It is probably adequate until 1985. When it becomes necessary, the embankments, structures, and concrete lining will be raised.

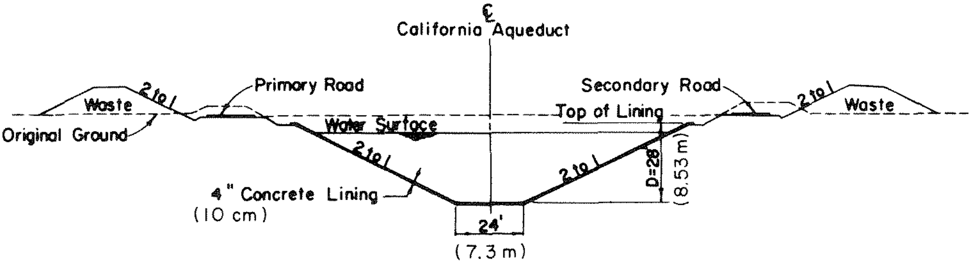

FIGURE 11 TYPICAL CANAL SECTION

SCHEDULING OF CONSTRUCTION

A major design problem was scheduling of construction. Items included in the schedule were, design and construction of hydrocompaction facilities, application of water for hydrocompaction, drying of area prior to canal construction, and canal construction. Water delivery dates had been established and the design and construction was to be completed within the time available. The schedule required that the hydrocompaction process be accelerated. In Figure 8 you will notice that the time required for most of the subsidence to occur was 500 days. Reduction of this time was accomplished by drilling and gravel packing infiltration wells within the ponded areas. Considering the horizontal and vertical permeability of the soil, the availability of water and the topography; the size of ponds and infiltration well depth and spacing were established. This was to accomplish the hydrocompaction at a specific location in 6 months instead of 500 days.

A drying period following hydrocompaction was essential to avoid excessive costs for dewatering during the canal construction. Approximately 4 to 6 months was allowed for this. The schedule worked out as planned, but there were a few areas where excess moisture was encountered when the canal was constructed.

Publication n°121 of the International Association of Hydrological Sciences
Proceedings of the Anaheim Symposium, December 1976

PREDICTION OF METASTABLE SOIL COLLAPSE

Jon L. Darwell and Bruce Denness,
Ocean Engineering,
School of Marine Technology,
University of Newcastle upon Tyne
and Bernard W. Conway,
Institute of Geological Sciences, London,
England.

Abstract

Many Pleistocene soils exhibit the characteristics of metastability, which is indicated by settlement caused by the addition of water under an effectively constant load. This settlement can range from slow subsidence to almost instantaneous collapse. The amount and rate of subsidence can be evaluated by simulating field conditions in the laboratory, but as the testing involved is specialised and time consuming, large scale investigations of particular areas can be expensive. Various methods of predicting metastable collapse from simple and rapidly-performed index tests have therefore been suggested by several workers in this field. This paper attempts to review the literature relating to collapse prediction for soils from a variety of depositional environments, and evolves a new method of graphical presentation of a collapse criterion that permits rapid prediction of metastability. This method has been proved to be the most reliable by correlation with laboratory oedometer tests, and uses inexpensive data. It is thus suitable for assessing large areas with a view to the siting of engineering works and the control of ground-water regimes.

Introduction

Many soils, from a wide variety of depositional environments or geneses, have been recognised as exhibiting the characteristic of metastability; that is, their structure becomes unstable under certain conditions and undergoes a measurable compression. The most ubiquitous potentially metastable soil is that generally known as loess, which occurs in large deposits on all continents; however, other metastable soils have been identified that either do not conform to the classical definition of loess or are of completely different origin, such as quick clays. Any general criterion for the prediction of structural collapse in soils must therefore take these soils into account.

Metastability in soils is concerned with settlement, or structural change, upon wetting; a truly metastable soil is in complete equilibrium with its surroundings until either the ambient loading or the water content of the soil is increased, whereupon settlement occurs either as subsidence (gradual settlement) or collapse (almost instantaneous settlement). In their natural, dry state most metastable soils form good foundation ground, retaining vertical slopes (Lofgren 1969) and are quite capable of bearing soil pressures up to 400 kN/m^2 (Lehr, 1967). However, on exposure to wetting, they undergo a sometimes catastrophic loss of strength, perhaps with an associated settlement of up to 20% of the soil volume (Knight and Dehlen, 1963). In view of the everincreasing construction occurring on metastable soil regions and the instantaneous and unforseeable nature of these settlements, a reliable and economic method of predicting areas of likely soil subsidence is of considerable importance.

A considerable amount of work has been performed in the past towards quantifying parameters that qualify settlements associated with metastability, particularly that concerned with an increase in soil water content; these include laboratory tests such as the double-oedometer test (Jennings and Knight 1956), triaxial tests (Grigorian, 1967), shear tests (Milovic, 1969) and in situ field tests of various types (Holtz and Hilf, 1961, Clevenger, 1956, Larionov, 1965). The main disadvantage with this type of collapse prediction is that it involves specialised and time-consuming testing; when applied as part of a large geotechnical investigation of a particular area, the time, cost and logistics of a testing programme based on this type of evaluation is uneconomic.

A method of predicting likely areas of subsidence from simple readily-available and cheap index parameters is therefore more appropriate. Several criteria for assessing soil stability have been put forward in the past: Denisov (1951) was amongst the first to recognise that the potential subsidence of soils is determined by their natural porosity and based his criterion on a consideration of the voids ratios at the natural moisture content and the liquid limit. Priklonskij (1952) and Feda (1966) introduced criteria involving the natural moisture content and both Atterberg Limits.

The method evolved here is an extension of Feda's criterion; it uses a graphical presentation so that once the basic index parameters for a particular soil are known, potential subsidence can be assessed simply from the graph expressing the criterion. This method is illustrated for metastable soils from very different depositional environments.

Review of Existing Criteria

Several criteria have been suggested by various researchers in the past for recognition of metastable soils. They are mostly inter-related since many of the parameters involved are interdependent, and all common criteria depend on comparisons between selected soil parameters at the liquid limit and the natural state.

Denisov (1951) was amongst the first to suggest that the porosity of a soil may be connected with metastability; a soil may be metastable if it is capable of absorbing enough water to take it up to or past the liquid limit. He therefore suggested that a soil may be metastable if:

$$\frac{e_L}{e_o} < 1$$

where e_L and e_o are void ratios at the liquid limit and natural moisture content respectively.

This criterion can be rewritten in terms of the natural dry density and the liquid limit, and as such was used by Gibbs and Holland (1960), Holtz and Hilf (1961) and Gibbs and Bara (1962) for presentation in graphical form:

$$e_o = W_o \cdot G = G\left\{\frac{\gamma_w}{\gamma_D} - \frac{1}{G}\right\}$$

and $e_L = W_L \cdot G$

so that Denisov's criterion becomes:

$$\frac{W_L}{\left\{\frac{\gamma_w}{\gamma_D} - \frac{1}{G}\right\}} < 1$$

where W_o, W_L are the moisture contents in the natural state and at the liquid limit, G is the specific gravity of the grains, γ_D is the natural dry density, and γ_w is the density of water.

The new Soviet Building Code criterion (Lehr, 1967, op.cit., Beles, Stanculescu and Schally, 1969) is similar to Denisov and related criteria in that it compares only parameters related to the porosity of a soil. The criterion states that metastability may be present if:

$$\frac{e_o - e_L}{1 + e_o} > - 0.1$$

This may be compared with the coefficient of subsidence (R) which is given by:

$$R = \frac{e_1 - e_2}{1 + e_1}$$

where e_1 and e_2 are the void ratios before and after wetting. The Soviet Code is valid if the natural degree of saturation (S_o) does not exceed 0.6.

Priklonskij (1952 op.cit.) was the first to suggest a criterion including parameters related to the strength of a soil, and his parameter (K_d) can be compared with the liquidity Index (I_L):

$$K_d = \frac{W_L - W_o}{W_L - W_P} < + 0.5 \quad \text{for subsidence}$$

and

$$I_L = \frac{W_o - W_P}{W_L - W_P}$$

$W_L - W_p = I_L$, where I_L is the plasticity index, and W_o, W_L and W_p are the moisture contents in the natural state and at the liquid and plastic limits respectively.

Feda (1966 op.cit.) produced probably the most comprehensive criterion and based his research on evolving a parameter related to the sensitivity of a soil. The sensitivity is defined as the ratio of the undisturbed and remoulded strengths under similar conditions so that a highly sensitive soil would therefore seem to be structurally unstable. Skempton and Northey(1952) established a relationship between sensitivity and the liquidity index, and accordingly Feda proposed that a soil is metastable if:

$$K_L = \frac{\frac{W_o}{S_o} - W_P}{I_P} > 0.85$$

where K_L is the subsidence index and W_o, S_o, W_P and I_P are as previously defined.

Feda imposed two constraints on the criterion, firstly that the soil should be sufficiently porous i.e. the natural porosity $n_o > 40\%$, and secondly that the soil should be subjected to a high enough external load for structural collapse to occur in wetting.

A New Interpretation

The criterion used by the authors and presented here is an adaptation of Feda's criterion. Given in the previous section, it can be rearranged to include values for the natural dry density (γ_D) and the specific gravity (G):

$$\frac{\frac{W_o - W_P}{S_o}}{W_L - W_P} > 0.85 \quad \text{for subsidence}$$

or:

$$\frac{e_o - e_P}{e_L - e_P} > 0.85$$

But
$$\frac{W_o}{S_o} = \frac{\gamma_w}{\gamma_D} - \frac{1}{G}$$

so $$\frac{\gamma_w}{\gamma_D} - \frac{1}{G} - W_P > 0.85\ (W_L - W_P)$$

or $$W_L + \frac{3}{17} W_P < \frac{1}{0.85} \left\{ \frac{\gamma_w}{\gamma_D} - \frac{1}{G} \right\}$$

for subsidence to be likely.

This expression can be represented as a series of parallel lines on a graph of liquid limit against plastic limit, each line being given by a unique combination of natural dry density (γ_D) and specific gravity (G). One particular line is illustrated in Figure 1. It runs from the upper boundary line where $W_L = W_P$ (i.e. $I_P = 0$) and the horizontal (liquid limit) axis where $W_P = 0$. The area shaded in Figure 1 between the three lines represents the inequality

$$W_L + \frac{3}{17} W_P < \frac{1}{0.85} \left\{ \frac{\gamma_w}{\gamma_D} - \frac{1}{G} \right\}$$

i.e. $$K_L = \frac{e_o - e_P}{e_L - e_P} > 0.85$$

Hence all points in this region represent cases where W_L and W_P are such that $K_L > 0.85$ for given values of γ_D and G, and thus any soil with indices located in this region should be metastable.

To allow for prediction of soils with a range of dry density and specific gravity, a series of lines is drawn. The effect of varying specific gravity with a constant dry density is shown in Figure 2: the central line is the case in which G = 2.65 and the outer two lines are for G = 2.55 and G = 2.75, for the same dry density. Any specific gravity can therefore be accommodated by interpolating between these three lines, or extrapolating outside them. The effect of varying the dry density produces a series of lines, as shown in Figure 3: each triplet of lines is for one dry density and the three values of specific gravity. Any dry density can thus be located by interpolating between the two relevant line triplets.

The procedure for evaluating the stability of a soil is as follows: the dry density and specific gravity of the soil are used to locate the particular line defined by these two values. If the point given by the liquid and plastic limits of the soil lies to the left of this line (the shaded area in Figure 1) the soil should be metastable since $K_L > 0.85$. Conversely, if it lies to the right, it should be stable. The complete graph is shown in Figure 4.

Evaluation of Prediction Criteria

Although a great deal has been written in the past on the properties and origins of metastable soils, their recognition and the prediction of their collapse, there has been comparatively little literature on the comparison of prediction criteria. The authors believe that Feda's criterion presents the most realistic parameter for predicting metastability and support this with their own studies of metastable soils and a review of published literature.

It can be shown that Feda's criterion is more conservative than that of Denisov, since when $W_L = W_O$, $K_L = 1$. Also compared with the Priklonskij parameter and the Soviet Building Code, Feda's criterion is more conserva-

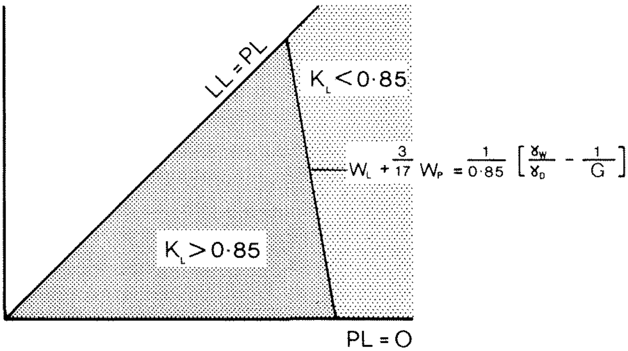

Fig. 2. Development of graphical interpretation.

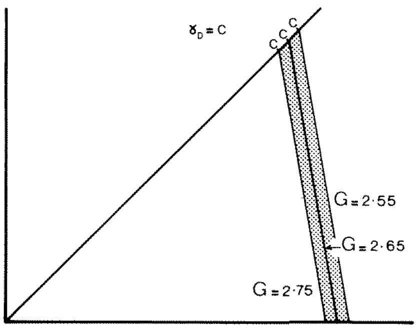

Fig. 1. Development of graphical interpretation.

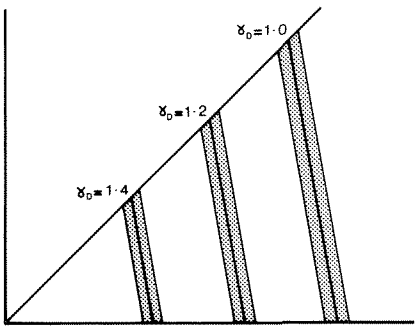

Fig. 3. Development of graphical interpretation.

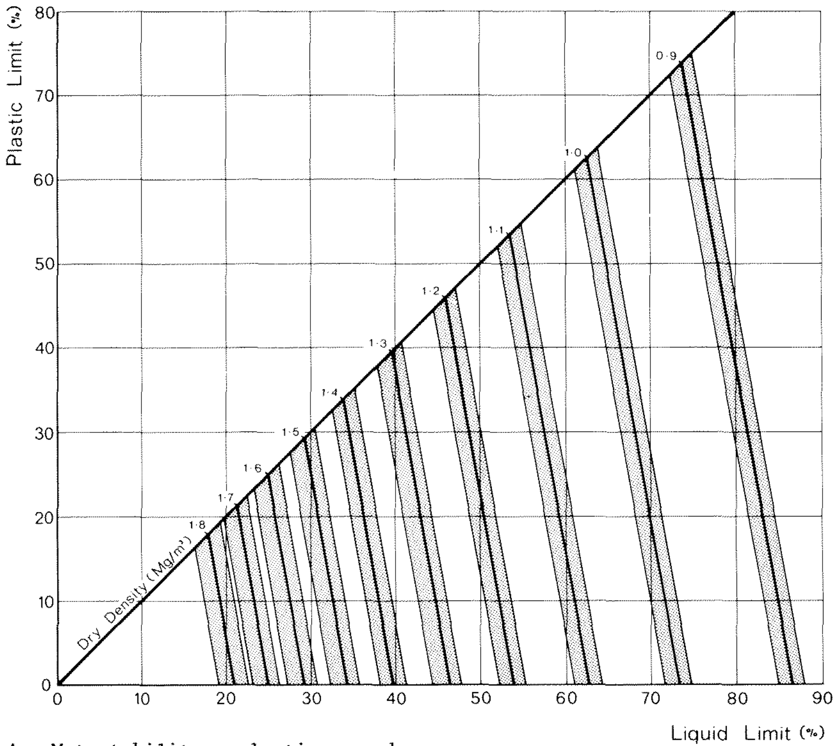

Fig. 4. Metastability evaluation graph.

tive than that of Prinklonskij, but not as conservative as the Soviet Code.

It is considered that the Soviet Code is too conservative and Feda's criterion is sufficiently sensitive to cover virtually all soils encountered. The Priklonskij and Denisov criteria on the other hand do not appear sufficiently sensitive to predict metastability in certain important cases, and this is supported by the data in Table 1 in which the applications of the metastability criteria reviewed here are listed for several soils of different depositional histories. The table includes two soils encountered by the authors, and others reported in the literature by previous researchers. The graphical approach to Feda's criterion using solely values for the Atterberg parameters, the specific gravity and the natural dry density is considered extremely tractable as it is quick and utilises data that is easily obtainable from field investigations as none of the parameters involved is sensitive to deterioration in storage during a survey.

The only disadvantage in the use of Feda's criterion occurs with soils for which the plastic limit is unobtainable: for such cases either the Soviet Building Code or the Denisov criterion should be used, depending on the degree of safety required.

Conclusions

1. Feda's creiterion is recommended as the most useful measure of potential soil metastability.

TABLE I

Soil Type	Source	Reference	Denisov (<1)	Feda (>0.85)	Soviet Code>-0.1	Priklonskij <0.5	R(typical)%
Calcareous aeolian silt (loess)	Praha-Dejvice	Feda (1966) No. 60M	1.04	0.93	+ 0.05	0.92	3
Pyroclastic Silt	Ecuador	Denness (1974)	1.06	0.87	- 0.03	0.89	3
Alluvial loams	South Essex	not published	1.02	0.90	- 0.01	1.70	2
"	"	"	1.05	0.85	- 0.02	1.89	2
Alluvial silt	San Joaquin	Hollz and Hilf (1961)	1.01	0.96	0.00	0.02	10
Silty loess	Pegwell Bay	Fookes and Best (1969)	1.01	0.99	- 0.01	2.7	5

2. The graphical approach to Feda's criterion presented here has proved extremely useful in rapid evaluation of metastable zones.

3. The use of easily produced index parameters has considerable advantages in site investigation.

4. The Soviet Building Code or the Denisov criterion are recommended in soils for which the plastic limit is unobtainable.

References and Bibliography

BALLY, R.J., ANTONESCU, I.P. and PERLEA, V.D. (1969) On Stress-Strain in highly compressible triphasic soils. Proc. 7th Int.Conf.SMFE. Vol.1 p.1-9.

BELES, A.A. and STANCULESCU, I.I. (1961) Settlements of Structures founded on highly porous soils. Proc. 5th Int.Conf.SMFE. Vol.1 p.587-594 (in French)

BELES, A.A., STANCULESCU, I.I. and SCHALLY, V.R. (1969) Prewetting of loess-soil foundation for hydraulic structures. Proc. 7th Int.Conf. SMFE. Vol.2 p.17-25.

BEREZANTZEV, V.G. et al (1969) On the strength of some soils. Proc. 7th Int. Conf. SMFE. Vol.2 p.11-19.

BOLOGNESI, A.J.L. and MORETTO, O. (1957) Properties and behaviour of silty soils originated from loess formation. Proc. 4th Int.Conf. SMFE 1/3 p.9-12

BRINK, A.B.A. and KANTEY, B.A. (1961) Collapsible grain structure of residual granite soils in Southern Africa. Proc. 5th Int.Conf.SMFE. Vol. 1 p.611-614

CASAGRANDE, A. (1932) The structure of day and its importance in foundation engineering. J.Boston Soc.Civ.Engrs. Vol.19(4) p.168-208.

CLEVENGER, W.A. (1956) Experiences with loess as foundation material. Proc.Am. Soc. Civ.Engrs. Vol.82 SM3 Paper 1025 pp.26.

CLOUGH, R.W. and WOODWARD, R.J. (1967) Analysis of embankment stresses and deformation. Proc.Am.Soc.Civ.Engrs. Vol. 93 SM4. p.529-549

DENISOV, N.Ya (1951) The engineering properties of loess and loess-like soils (in Russian) Moscow (Gosstroiizdat) p.133.

DENISOV, N.Ya. and RELTOV, B.F. (1961) The influence of certain processes on the strength of soils. Proc.5th Int.Conf.SMFE 1/12. p.75-78.

DENNESS, B. (1974) An assessment of the landslip hazard at the town of Guaranda, Ecuador. Inst.Geol.Sciences. EGU Report, IGS. 1019, 3/74.

DRANNIKOV, A.M. (1967) Construction on loess soils of small thickness. Proc. 3rd Asian Reg.Conf. SMFE 1/1 p.3-4.

FEDA, J. (1966) Structural stability of subsident loess soil from Praha-Dejvice. Eng.Geol. 1(3) p.201-219.

FINAEV, I.V. (1967) Bearing Capacity of piles in subsident loess soils. Proc. 3rd Asian Reg.Conf. SMFE 1/2 p.5-8.

FOOKES, P.G. and BEST, R. (1969) Consolidation Characteristics of some late Pleistocene periglacial metastable soils of east Kent. Q.J.Eng.Geol. Vol.2 p.103-128.

FOOKES, P.G. and KNILL, J.L. (1969) The application of engineering geology in the regional development of north and central Iran. Eng.Geol.3 p.81-120.

GIBBS, H.J. and BARA, J.P. (1962) Predicting surface subsidence from basic soils tests. ASTM Spec.Tech.Pub. 322 p.231-246.

GIBBS, H.J. and HOLLAND, W.Y. (1960) Petrographic and engineering properties of loess. Eng.Mono. No.28 (Denver Bur.Reclamation) p.1-37.

GRIGORIAN, A.A. (1967) Prediction of deformation of loess soils under building and structure foundations. Proc. 3rd Asian Reg.Conf. SMFE 1/3. p.9-12.

HOLTZ, W.G. and GIBBS, H.J. (1951) Consolidation and related properties of loessial soils. ASTM. Spec.Pub. 126. p.9-26.

HOLTZ, W.G. and HILF, J.W. (1961) Settlement of Soil Foundations due to saturation. Proc.5th Int.Conf. SMFE 3A/20. p.673-679.
JENNINGS, J.E.B. and BURLAND, J.B. (1962) Limitations to the use of effective stresses in partly saturated soils. Geotechnique Vol. 12. p.125-144
JENNINGS, J.E.B. and KNIGHT, K. (1957) The additional settlement of foundations due to collapse of structure of sandy subsoils on wetting. Proc. 4th Int.Conf.SMFE. 3a/12 p.316-319.
KASSIFF, G. and HENKIN, E.N. (1967) Engineering and physico-chemical properties affecting piping failure of loess dams in the Neger. Proc. 3rd Asian Reg.Conf.SMFE. 1/4 p.13-16.
KEZDI, A. (1969) Landslide in loess along bank of the Danube. Proc. 7th Int. Conf. SMFE. Vol.2 p.617-626.
KNIGHT, K. and DEHLEN, G.L. (1963) The failure of a road constructed on a collapsing soil. Proc. 3rd Reg.Conf. African SMFE. A.4 p.31-34.
KOLB, C.R. and SHOCKLEY, W.G. (1959) Engineering geology of the Mississipi Valley. Trans.Am.Soc.Civ.Engrs. Vol.124 p.633-656.
KRINITZSKY, E.L. and TURNBULL, W.J. (1967) Loess deposits of the Mississipi. Geol.Soc.Am. Spec.Paper No.94 pp.64.
LARIONOV, A.K. (1965) Structural characteristics of loess soils for evaluating their constructional properties. Proc. 6th Int.Conf.SMFE 1/14 p.64-68
LEHR, H. (1967) Foundation engineering problems in loess soils. Proc. 3rd Asian Reg. Conf.SMFE 1/6 p.20-24.
LITVINOV, I.M. et al (1961) Stabilization of soil for constructional purposes. Proc. 5th Int.Conf.SMFE. Vol. p.775-780
LOFGREN, B.E. (1969) Land subsidence due to the application of water. Reviews in Eng.Geol. II p.271-303.
MATALUCCI, R.C. et al (1970) Influence of microstructure of loess on triaxial shear strength. Eng.Geol. 4 p.341-351
MILOVIC, D.M. (1967) On some comparative studies of land loess and swamp loess. Proc. 3rd Asian Reg.Conf.SMFE. 1/7 p.25-28.
MUSTAFAEV, A.A. (1967) Infiltration and subsidence processes in loess soils Proc. 3rd Asian Reg.Conf.SMFE 4/7 p.155-158.
NORTHEY, R.D. (1969) Engineering Properties of loess and other collapsible soils. Spec.Session 5 7th Int.Conf. SMFE. p.445-452.
PILYUGIN, A.I. (1967) Settlement of loess foundations under canal embankments. Proc. 3rd Asian Reg.Conf.SMFE. 1/8 p.29-32.
PRINKLONSKIJ, V.A. Gruntovedenie. Vtoriaia Chast (Soil Science II) Gosgeolizdat, Moscow. pp.371 (in Russian). (1952)
ROSENQVIST, I.Th. (1953) Considerations on the sensitivity of Norwegian quick-clays. Geotechnique. Vol. 3. p.195-200.
RUSSELL, R.J. (1944) Lower Mississipi Valley loess. Bul.Geol.Soc.Am. Vol. 55 p.1-40.
SKEMPTON, A.W. and NORTHEY, R.D. (1952) The sensitivity of clays. Geotechnique Vol.3 p.30-53.
SMALLEY, I.J. (1966) Properties of glacial loess and the formation of loess deposits. Jour.Sed.Petr. Vol. 36 (3) p.669-676.
TURNBULL, W.J. (1948) Untility of loess as a construction material. Proc. 2nd Int.Conf.SMFE. 5/4d. p.97-103.

Publication n°121 of the International Association of Hydrological Sciences
Proceedings of the Anaheim Symposium, December 1976

FOUNDATION TREATMENT FOR SMALL EARTH DAMS ON SUBSIDING SOILS

Robert J. Fredrickson
USDA-Soil Conservation Service
Lincoln, Nebraska

Abstract

Embankments for small dams are subject to cracking and failure from differential settlements occurring in collapsible foundations. Soils involved are both alluvial and loessial in origin and are generally dry and low in natural density. Presented here is a method of using sand blankets and water to force consolidation to occur during construction rather than at some future and unknown time. Sand blankets are used to add water to foundation soils, weakening the dry-strength bonds, thus allowing the potential settlement to occur. Instrumentation is described which is used to monitor the effect of the sand blankets and embankment loading. Pertinent data from one earthfill dam 75 ft. (23 m) high, located in Frontier County, Nebraska, is used to illustrate the soil testing, plan, and results of the sand blanket method.

Large areas of Nebraska are covered by soils of alluvial and loessial origin which exhibit high dry strength but are subject to subsidence, collapse upon wetting and loading, and relatively high total settlements. These soils, of ML and CL classification, are usually deep enough that attempting to excavate a large enough quantity to solve the settlement problem causes the project to become economically unfeasible. In several cases, excavation of foundation soil would not have solved the problem of differential settlement and embankment cracking. Prewetting collapsible soils by sprinkling has not solved the problems because the foundation would not contain the water throughout the necessary length of the construction period. The method of sand blankets evolved as a result of devising and discarding ideas for introducing water to foundation soils before and during construction.

For collapsible foundations, the minimum embankment height is about 15 to 20 ft. (4.6 to 6.1 m), dependent on the dry strength bonding of the soil particles. The maximum height is not known, but the method has been used on foundations for earthfill dams in Nebraska where the maximum fill height was 80 ft. (24 m).

The proof that the collapsible soil exists is readily apparent by inspecting the e-log p and percent consolidation-log p curves. The results of several consolidation tests are shown on the attachments. Note that in each test the test sample was loaded, at natural moisture, in increments to 4000 psf (2 kg/cm^2), then saturated without changing the load. The test is then completed at the higher load increments.

The profile of the valley (see attachment) indicates the depth of the compressible soils. The alluvial and loessial soils lie above the Ogallala formation, which is considered incompressible for small earthfill dams. Deeply buried scarps usually occur in the Ogallala and contribute to the differential settlement problem. No water table was encountered within the depth of soil investigated.

The key to the method of sand blankets is shown on the attachment for the plan view of the dam. Four sand blankets are used on this site, each with a slot-perforated pipe located at the upper end. The blanket thickness varies from 1.5-2.0 ft. (45-60 cm) at the upper end to 1.0-1.5 ft. (30-45 cm) thick at the lower end depending on the length of blanket. The vegetation (native grass in this example) is burned off in the area to be occupied by the sand blankets. No vehicles are allowed on this surface in order to preserve the maximum available surface permeability. Piezometers at the lower end show that water reaches the lower end and indicates the head in the blanket to insure that the cover soil is not lifted up. Water meters are used to insure that an adequate volume is supplied to approach saturation in the volume of soil being considered. Water is introduced into the sand blankets through the filler pipes in sufficient quantity to saturate the required volume of foundation soil. Water is continually added during fill construction and is monitored by maintaining a head of 5-10 ft. (1.5-3 m) as measured by the piezometers. The project should be planned so that the entire fill height is attained without undue delay.

The settlement plates are the proof of the sand blanket method. The location of the plates are shown on the attachments and are positioned to indicate differential settlement, to compare actual settlement with computed settlement, and to show subsidence if any occurs. For Soil Conservation Service work, subsidence is settlement with water but without load. Settlement and collapse is a combination of water and loading. Computed vs. actual settlement is shown in the following table:

Settlement Plate No.	Station	Distance		Settlement			
		U.S.	D.S.	Computed		Actual	
				(ft)	(cm)	(ft)	(cm)
P1	8+80	-	20	0.7	21	2.2	67
P2	9+90	-	20	3.2	98	3.9	119
P3	9+85	25	-	3.2	98	3.3	101
P4	12+40	-	15	3.0	91	2.8	85
P5	13+20	-	15	5.0	152	4.0	122
P6	14+50	-	15	0.5	15	1.1	34
P7	13+20	40	-	5.1	155	3.6	110
P8	14+40	25	-	0.5	15	0.7	21

The embankment strains are accommodated by limiting the density of the fill and requiring that the in-place moisture be above optimum as determined by ASTM standard D-698. Compaction is obtained by controlled travel of loaded, rubber-tired hauling equipment; tamping rollers are seldom required.

Sectional embankments are used when the site lends itself to reducing differential settlements by causing settlement to occur in one area before the adjacent, and less compressible, foundation is loaded. In the example, the expected settlement for plates P4-P8 and the location of the Ogallala formation indicated that reduction of differential settlement was possible by use of the sectional fill.

To date, the method of sand blankets has been used on nine earthfill dams. No embankment cracks have been discovered and settlements have been obtained successfully. Variations from the computed settlements are believed to be due to the relative accuracy in obtaining undisturbed samples and applying test data to a large volume of foundation soil. The method should not be used without proper precautions for structure safety.

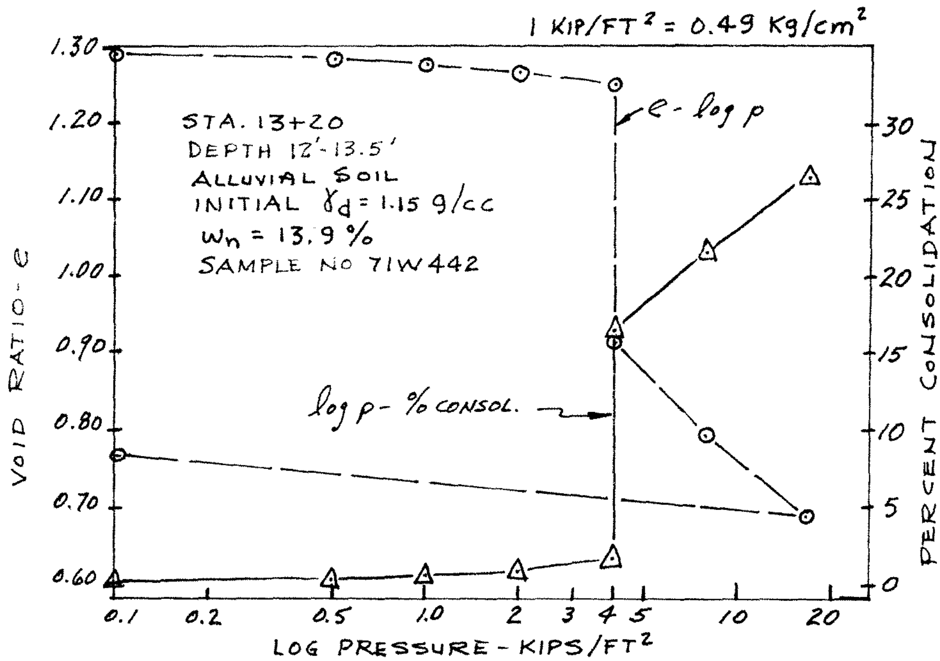
1 KIP/FT² = 0.49 Kg/cm²
STA. 13+20
DEPTH 12'-13.5'
ALLUVIAL SOIL
INITIAL γd = 1.15 g/cc
Wn = 13.9 %
SAMPLE NO 71W442
e - log p
log p - % CONSOL.
VOID RATIO - e
PERCENT CONSOLIDATION
1.30
1.20
1.10
1.00
0.90
0.80
0.70
0.60
30
25
20
15
10
5
0
0.1
0.2
0.5
1.0
2
3
4
5
10
20
LOG PRESSURE - KIPS/FT²

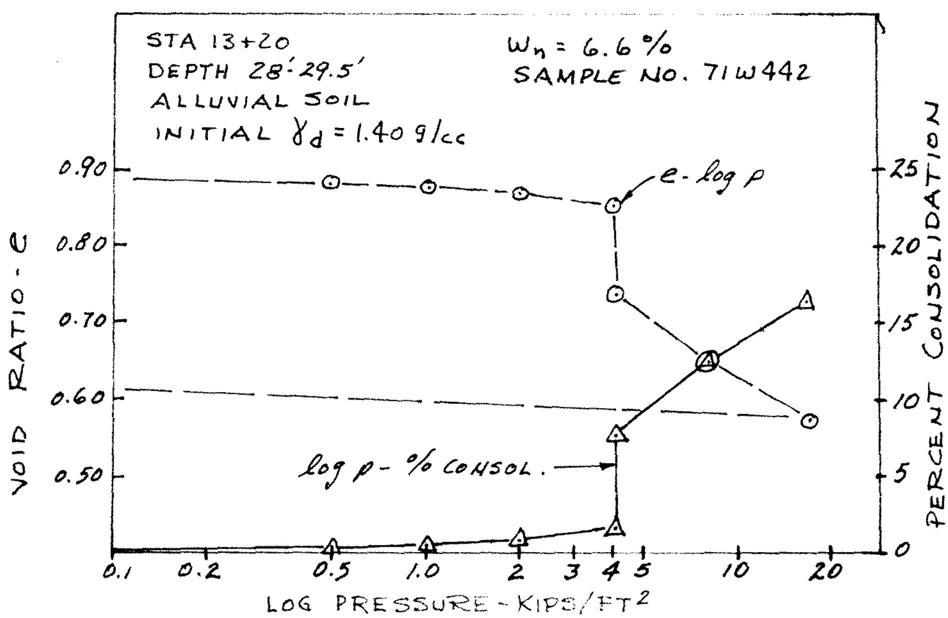
STA 13+20
DEPTH 28'-29.5'
ALLUVIAL SOIL
INITIAL γd = 1.40 g/cc
Wn = 6.6 %
SAMPLE NO. 71W442
e - log p
log p - % CONSOL.
VOID RATIO - e
PERCENT CONSOLIDATION
0.90
0.80
0.70
0.60
0.50
25
20
15
10
5
0
0.1
0.2
0.5
1.0
2
3
4
5
10
20
LOG PRESSURE - KIPS/FT²

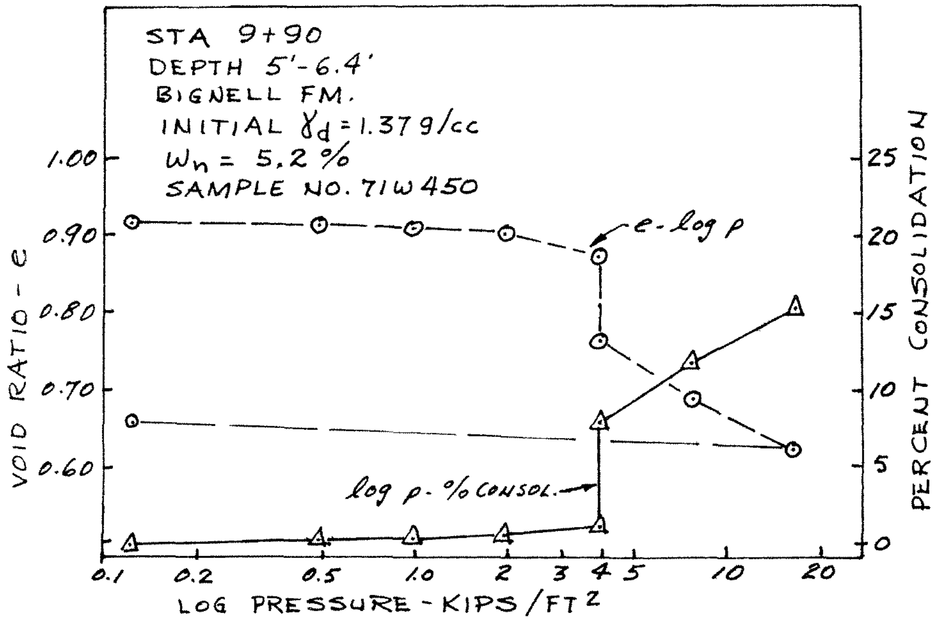
STA 9+90
DEPTH 5'-6.4'
BIGNELL FM.
INITIAL γ_d = 1.37 g/cc
W_n = 5.2 %
SAMPLE NO. 71W450
e-log p
log p-% CONSOL.
VOID RATIO - e
PERCENT CONSOLIDATION
LOG PRESSURE - KIPS/FT^2

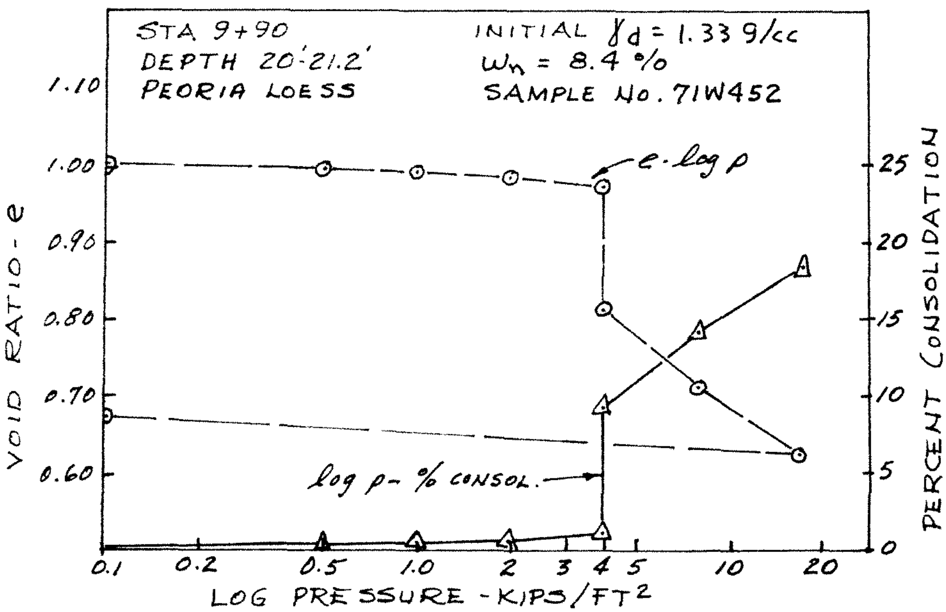
STA 9+90
DEPTH 20'-21.2'
PEORIA LOESS
INITIAL γ_d = 1.33 g/cc
W_n = 8.4 %
SAMPLE No. 71W452
e-log p
log p-% CONSOL.
VOID RATIO - e
PERCENT CONSOLIDATION
LOG PRESSURE - KIPS/FT^2

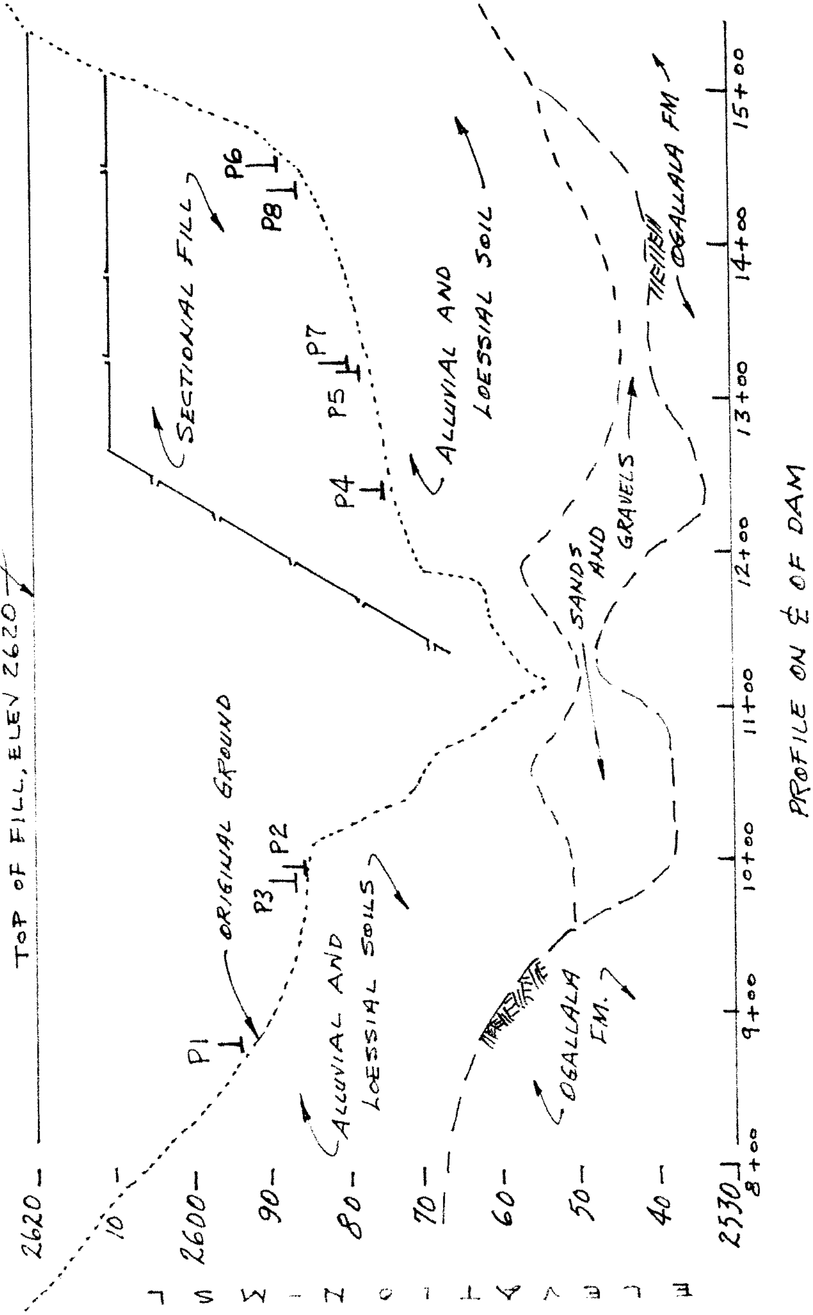
P1, ETC., = SETTLEMENT PLATE
TOP OF FILL, ELEV 2620
ORIGINAL GROUND
SECTIONAL FILL
ALLUVIAL AND LOESSIAL SOILS
ALLUVIAL AND LOESSIAL SOIL
SANDS AND GRAVELS
OGALLALA FM.
OGALLALA FM
P1
P2
P3
P4
P5
P6
P7
P8
ELEVATION - MSL
2620
10
2600
90
80
70
60
50
40
2530
8+00
9+00
10+00
11+00
12+00
13+00
14+00
15+00
PROFILE ON ℄ OF DAM

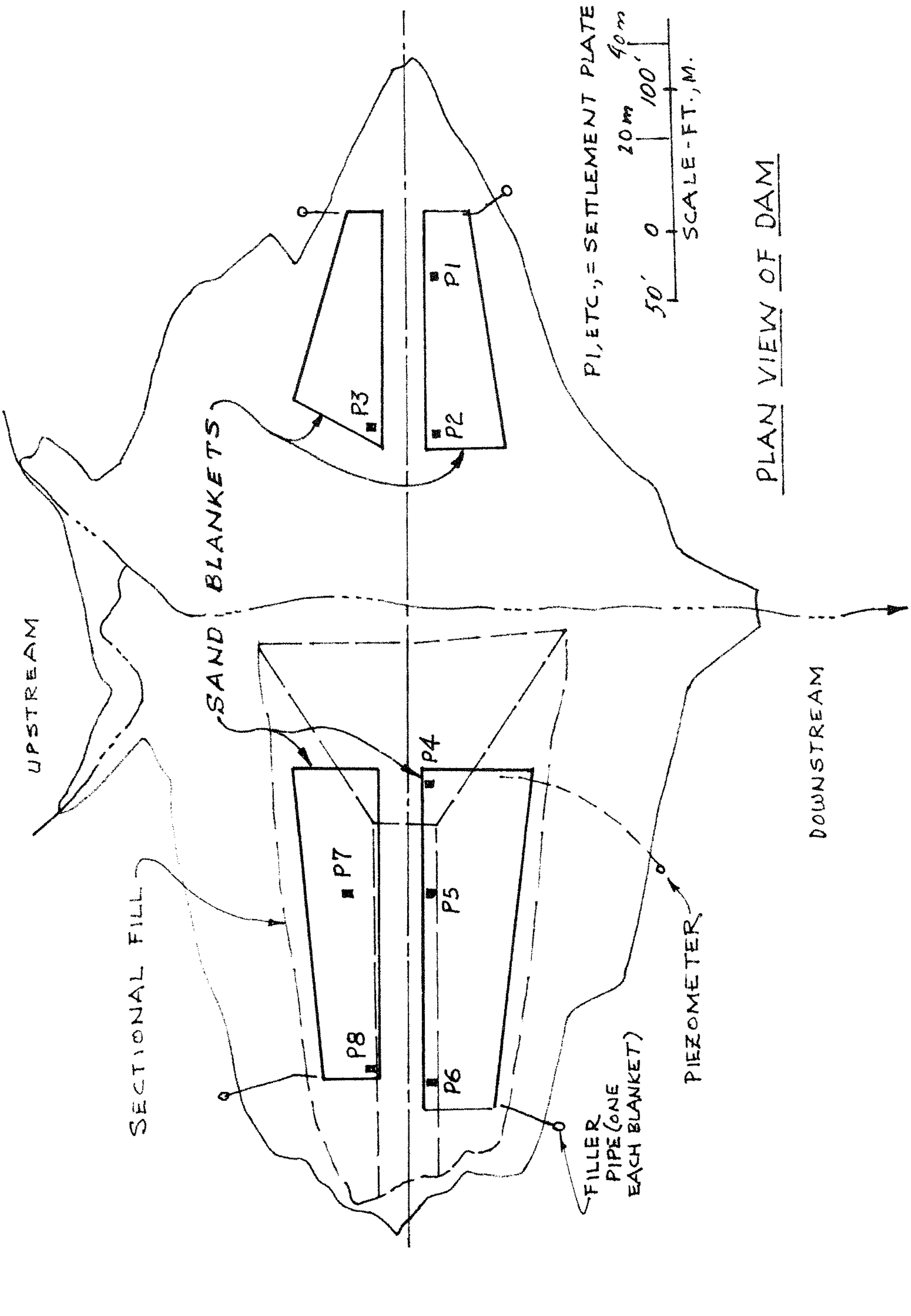
UPSTREAM
DOWNSTREAM
SAND BLANKETS
SECTIONAL FILL
PIEZOMETER
FILLER PIPE (ONE EACH BLANKET)
P1
P2
P3
P4
P5
P6
P7
P8
P1, ETC., = SETTLEMENT PLATE
0
20m
40m
50'
100'
SCALE - FT., M.
PLAN VIEW OF DAM

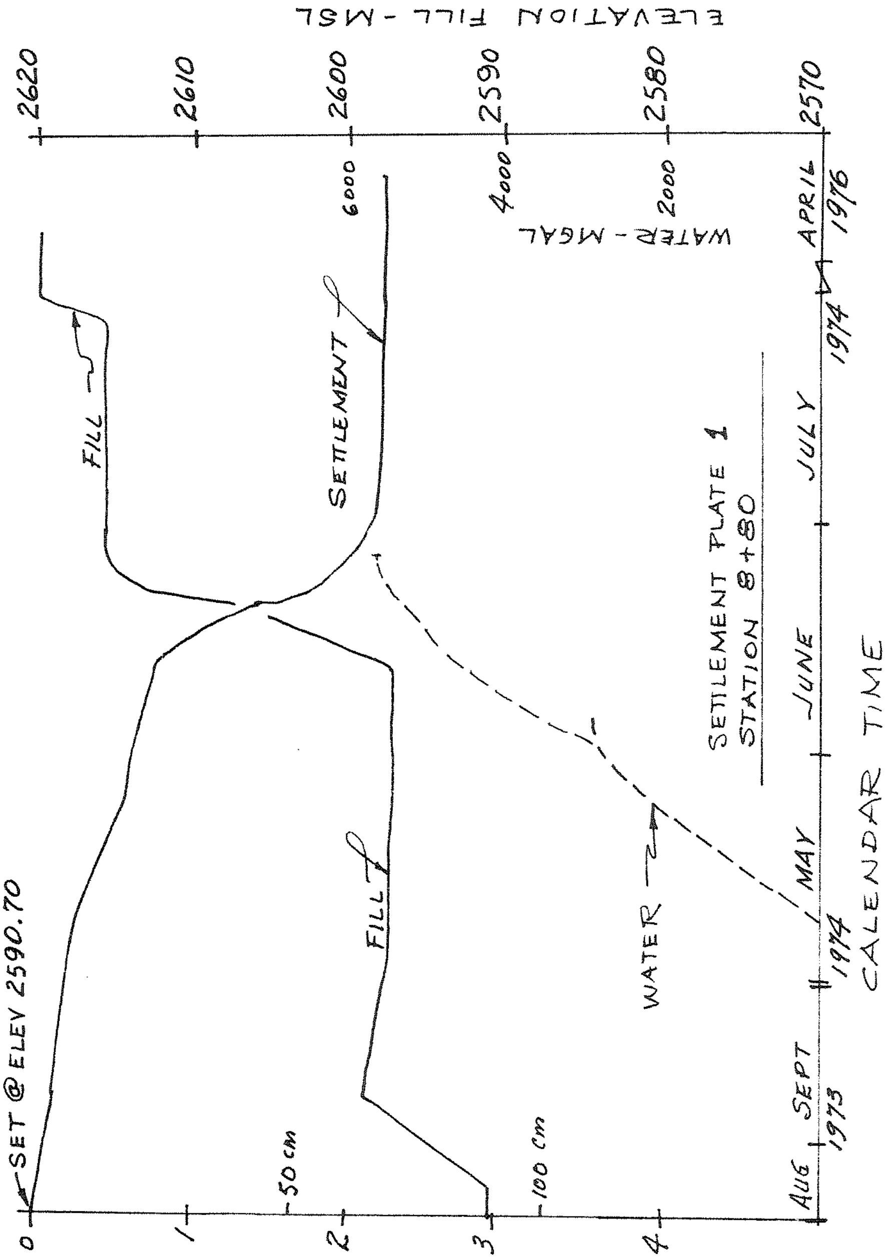
ELEVATION FILL - MSL
2620
2610
2600
2590
2580
2570
6000
4000
2000
WATER - MGAL
FILL
SETTLEMENT
SETTLEMENT PLATE 1
STATION 8+80
SET @ ELEV 2590.70
FILL
WATER
50 cm
100 cm
0
1
2
3
4
SETTLEMENT - FT.
AUG
SEPT
1973
1974
MAY
JUNE
JULY
1974
APRIL
1976
CALENDAR TIME

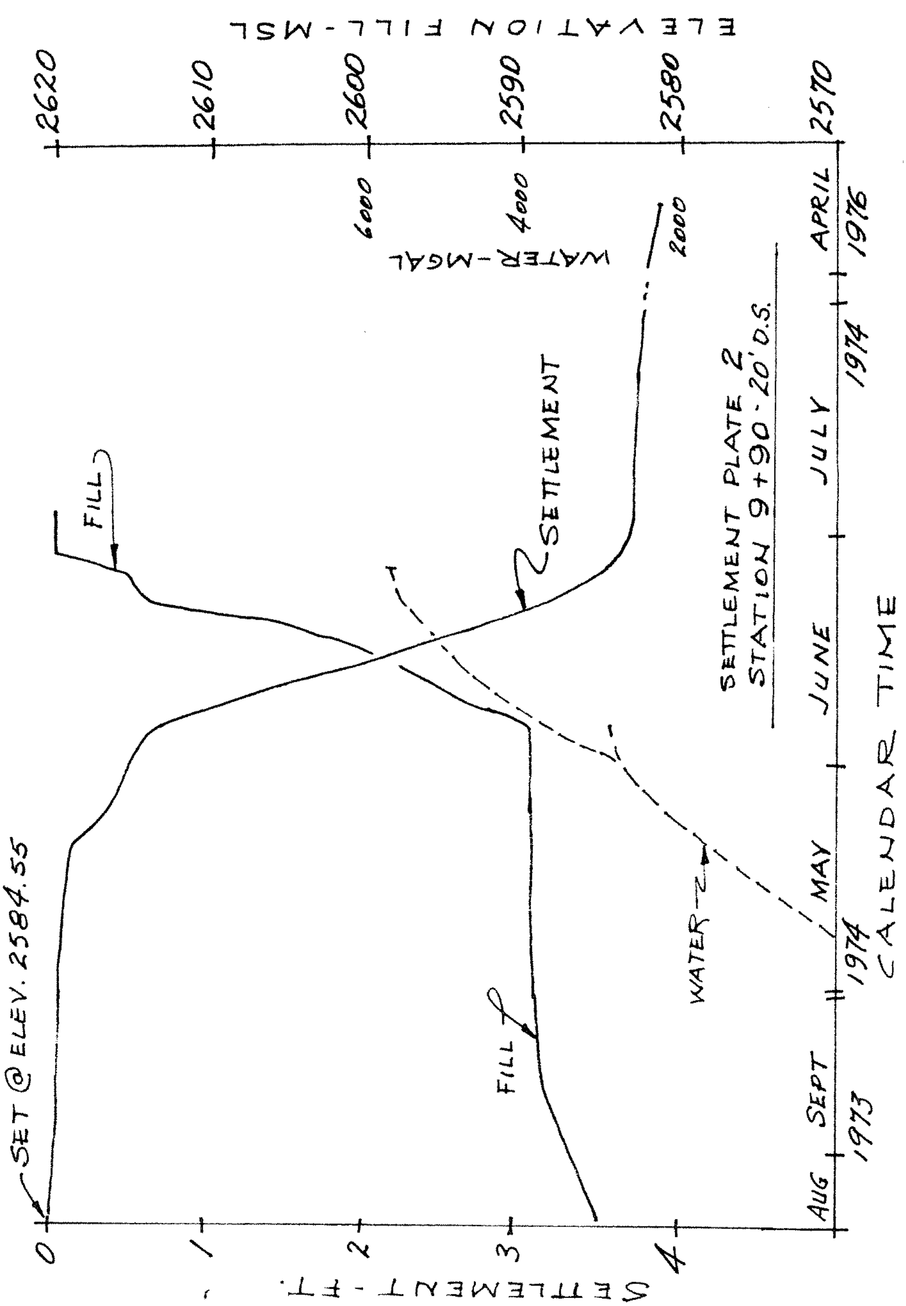
ELEVATION FILL - MSL
2620
2610
2600
2590
2580
2570
WATER-MGAL
6000
4000
2000
SET @ ELEV. 2584.55
FILL
SETTLEMENT
FILL
WATER
SETTLEMENT PLATE 2
STATION 9+90 · 20' O.S.
AUG
SEPT
1973
MAY
1974
JUNE
JULY
1974
APRIL
1976
CALENDAR TIME
0
1
2
3
4
SETTLEMENT - FT.

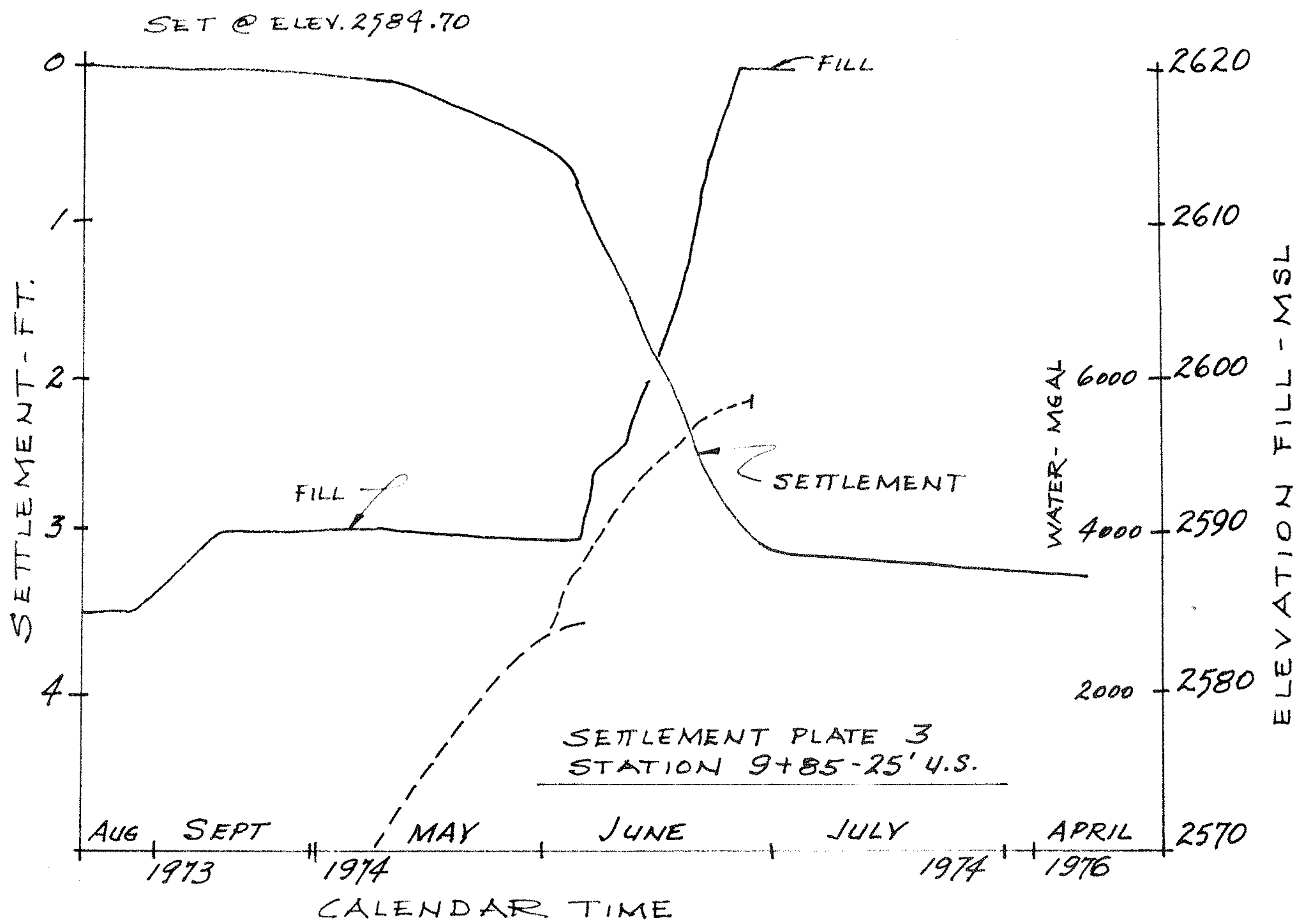
SET @ ELEV. 2584.70
SETTLEMENT - FT.
0
1
2
3
4
FILL
FILL
SETTLEMENT
WATER - MGAL
6000
4000
2000
ELEVATION FILL - MSL
2620
2610
2600
2590
2580
2570
SETTLEMENT PLATE 3
STATION 9+85-25' U.S.
AUG
SEPT
1973
1974
MAY
JUNE
JULY
1974
APRIL
1976
CALENDAR TIME

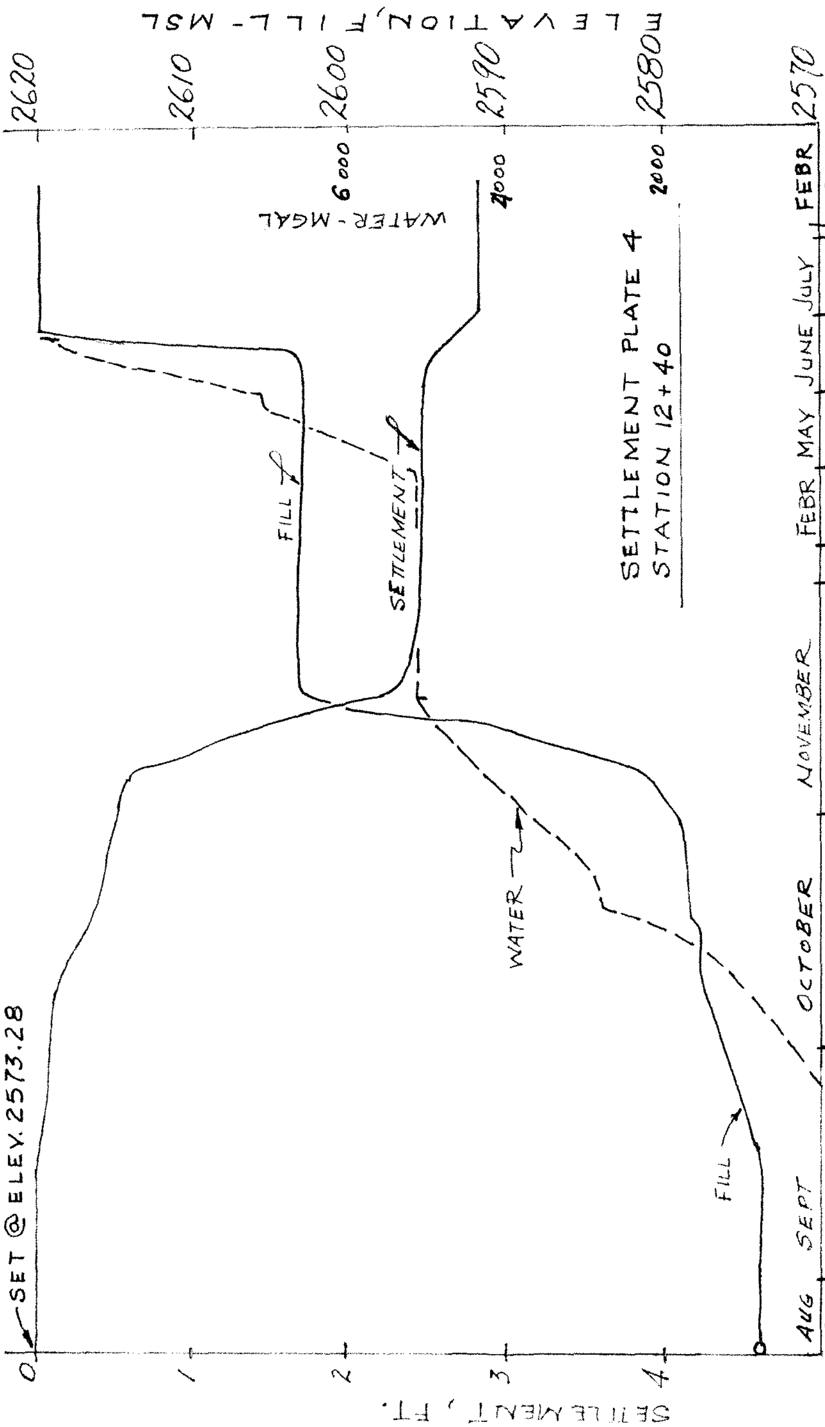
ELEVATION, FILL - MSL
SETTLEMENT, FT.
CALENDAR TIME
SETTLEMENT PLATE 4
STATION 12+40
SET @ ELEV. 2573.28
WATER - MGAL
FILL
SETTLEMENT
WATER
AUG 1973
SEPT
OCTOBER
NOVEMBER
1973
FEBR 1974
MAY
JUNE
JULY 1974
FEBR 1976
2620
2610
2600
2590
2580
2570
6000
4000
2000
0
1
2
3
4

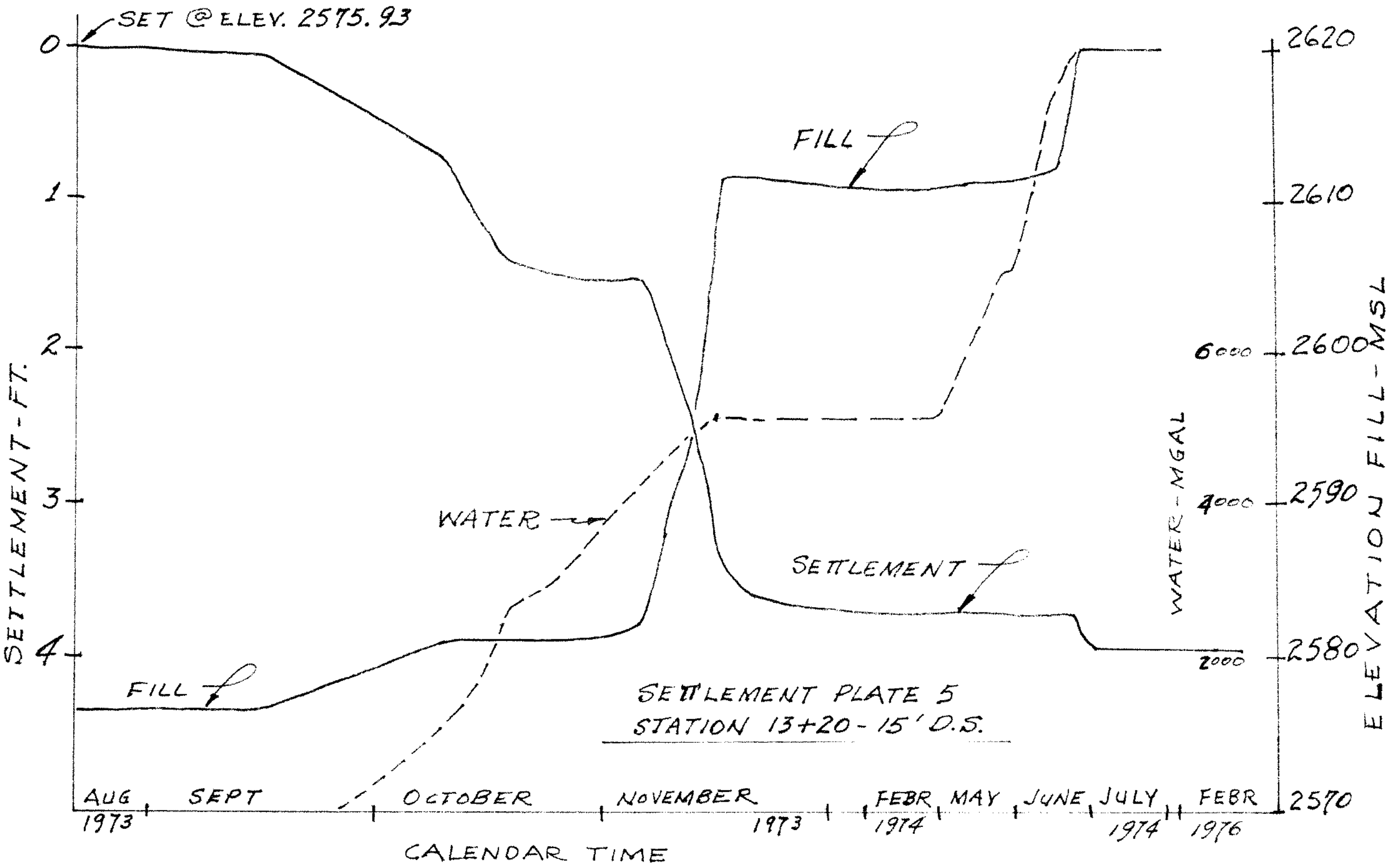
SET @ ELEV. 2575.93
SETTLEMENT - FT.
0
1
2
3
4
FILL
WATER
SETTLEMENT
ELEVATION FILL - MSL
2620
2610
2600
2590
2580
2570
WATER - MGAL
6000
4000
2000
SETTLEMENT PLATE 5
STATION 13+20 - 15' O.S.
AUG 1973
SEPT
OCTOBER
NOVEMBER
1973
FEBR 1974
MAY
JUNE
JULY 1974
FEBR 1976
CALENDAR TIME

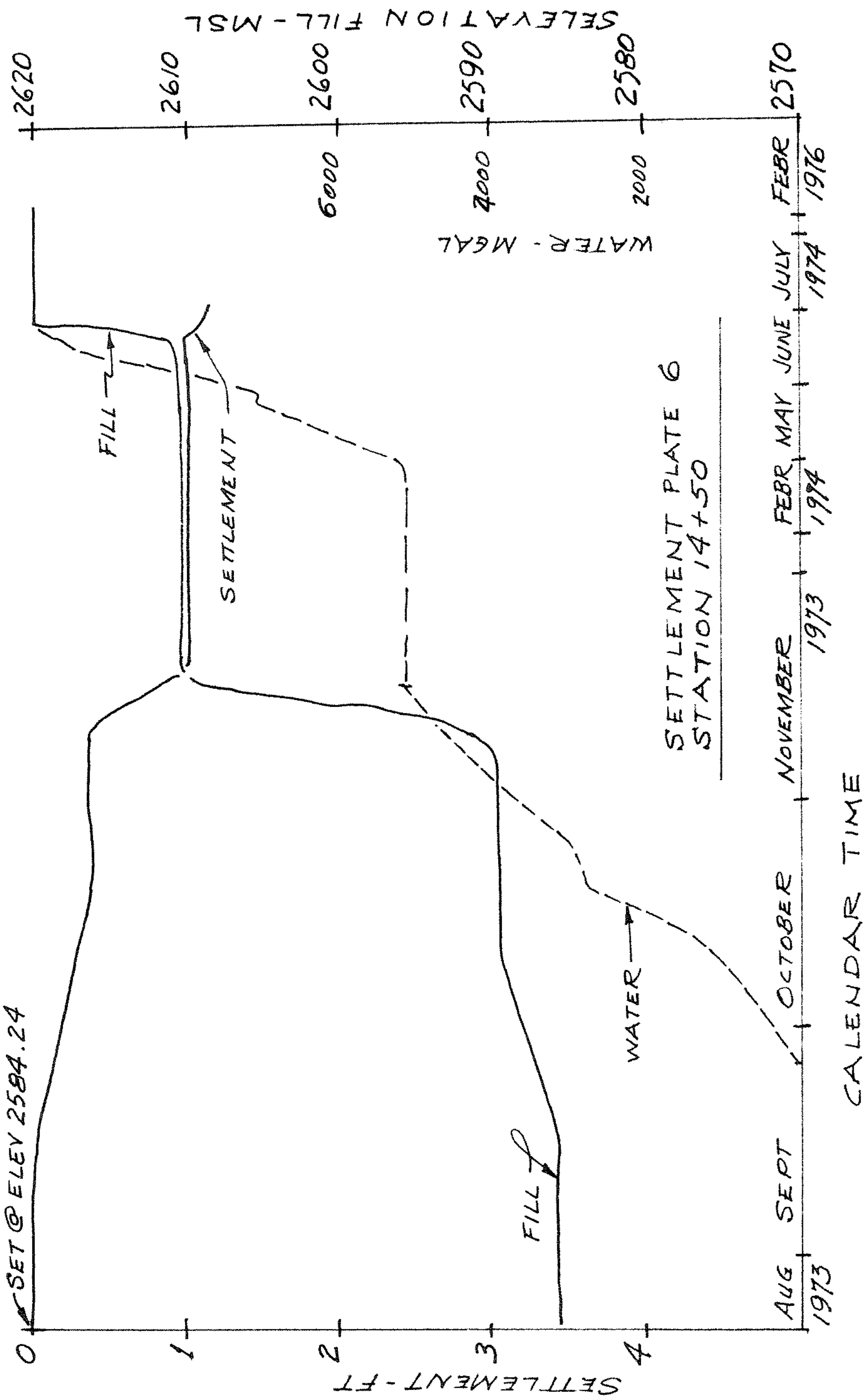
ELEVATION FILL - MSL
2620
2610
2600
2590
2580
2570
6000
4000
2000
WATER - MGAL
SETTLEMENT PLATE 6
STATION 14+50
FILL
SETTLEMENT
WATER
SET @ ELEV 2584.24
0
1
2
3
4
SETTLEMENT - FT
AUG 1973
SEPT
OCTOBER
NOVEMBER 1973
FEBR 1974
MAY
JUNE
JULY 1974
FEBR 1976
CALENDAR TIME

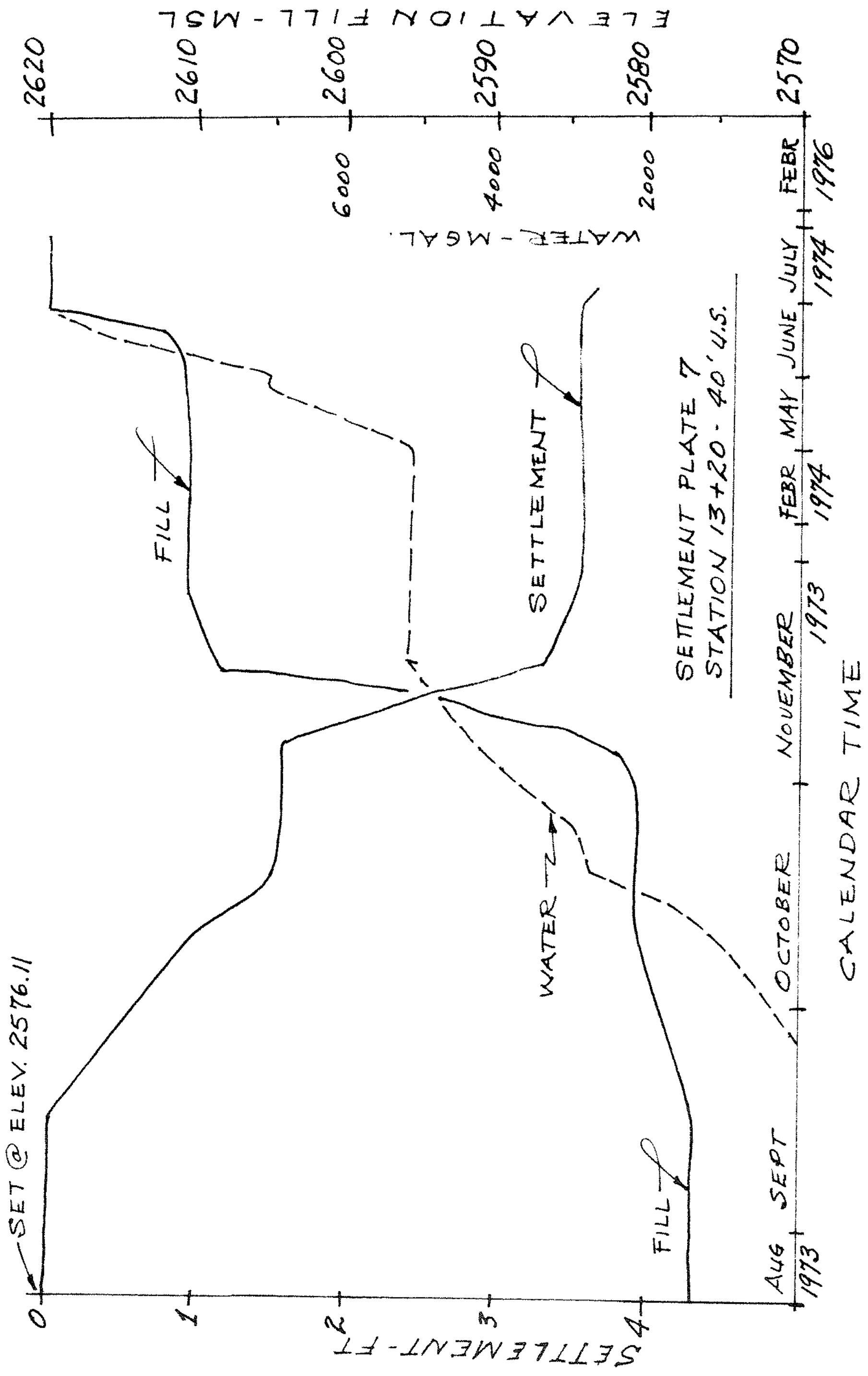

SETTLEMENT PLATE 7
STATION 13+20 - 40' U.S.
SET @ ELEV. 2576.11
FILL
SETTLEMENT
WATER
SETTLEMENT - FT
ELEVATION FILL - MSL
WATER - MGAL.
CALENDAR TIME
AUG 1973
SEPT
OCTOBER
NOVEMBER
1973
FEBR 1974
MAY
JUNE
JULY 1974
FEBR 1976
0
1
2
3
4
2620
2610
2600
2590
2580
2570
6000
4000
2000

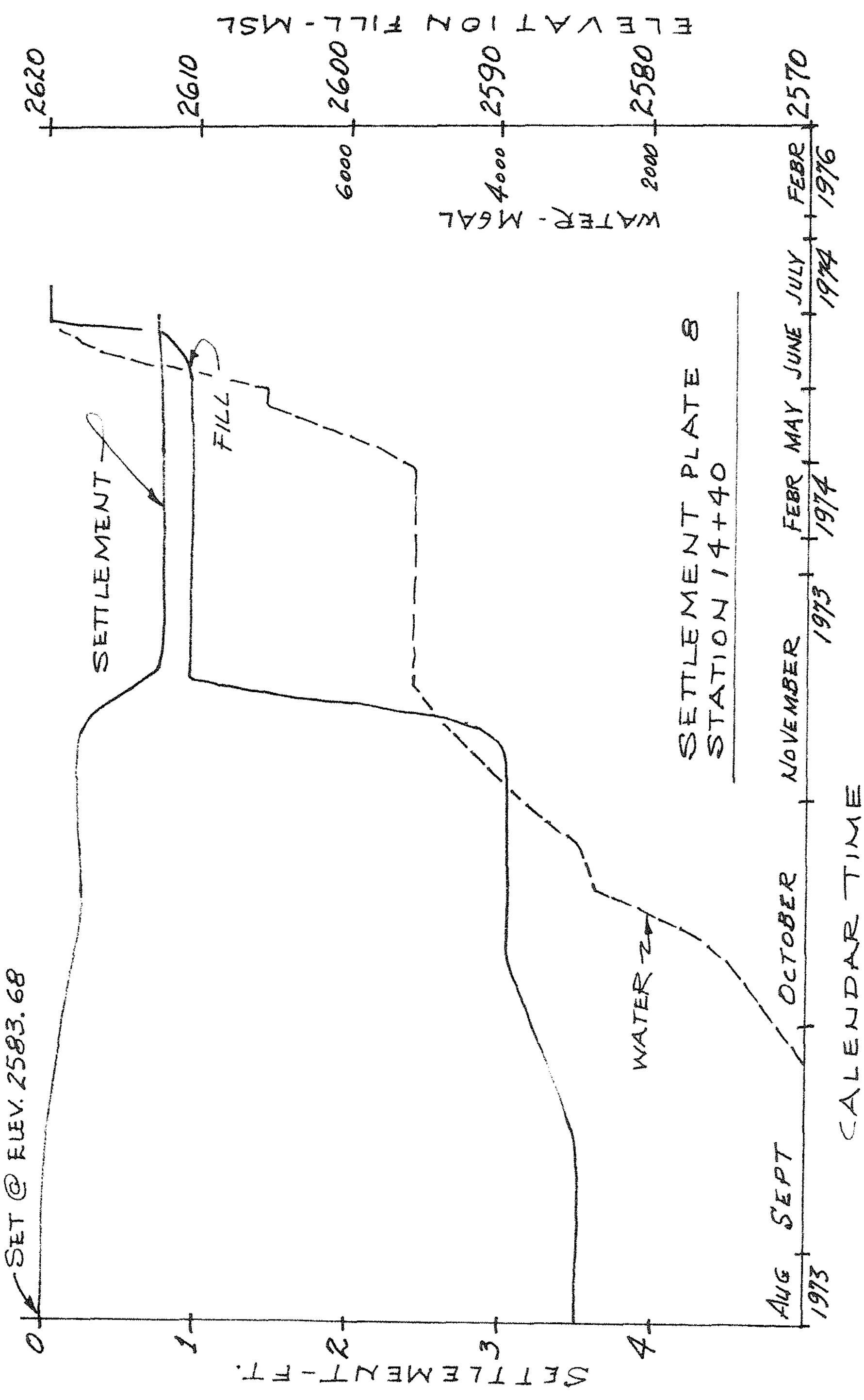
SETTLEMENT PLATE 8
STATION 14+40
SET @ ELEV. 2583.68
SETTLEMENT
FILL
WATER
SETTLEMENT - FT.
0
1
2
3
4
ELEVATION FILL - MSL
2620
2610
2600
2590
2580
2570
WATER - MGAL
6000
4000
2000
CALENDAR TIME
AUG 1973
SEPT
OCTOBER
NOVEMBER
1973
FEBR 1974
MAY
JUNE
JULY 1974
FEBR 1976

Publication n°121 of the International Association of Hydrological Sciences
Proceedings of the Anaheim Symposium, December 1976

THE APPLICATION OF CONSOLIDATION CONSTANTS, DERIVED FROM THE PORE SPACE, IN SUBSIDENCE CALCULATIONS

R.J. de Glopper
IJsselmeerpolders Development Authority
Lelystad, the Netherlands

Abstract

In the IJsselmeerpolders the soil profile consists of 1 to 8 m very soft Holocene sediments (pore spaces 60-85%), overlying a non-subsiding Pleistocene sand bed. Areas to be used for building purposes are raised by 1 m of sand, causing a subsidence of 0.2 to 1.5 m, depending on soil conditions.

Subsidence is calculated by form. 1. The need for undisturbed soil samples (costly) to determine the consolidation constants (time-consuming) is a disadvantage, as is the question of the representativeness of the very small samples.

A good relation was found between these constants and the pore space (Fig. 1). The last can be calculated from the easily and quickly determinable water contents (form. 2; fig. 2) in bigger and more representative samples (water saturated), which can be collected simply (a description of the procedure is given) and hence cheaply (Table 1).

The subsidence of a soft layer of 5 m was calculated at pore spaces of 60 through 90% with the mean value and the values at the upper and lower limit values of the 95% confidence range (Table 2). The deviations of the subsidence at the upper and lower limit values from the subsidence at the mean value were in the range of 10 cm, being quite acceptable.

During three years after loading at four sites the subsidence was both measured and calculated. Both values were not very well in agreement (Fig. 3), most probably due to the impossibility to determine the water overpressures accurately (Fig.1). Nevertheless, it could be made plausible that the use of the consolidation constants, derived from the pore space, gives a reliable approximation (Fig. 5).

The use of consolidation constants, derived from the pore space, will give more reliable results in subsidence calculations as a result of the wide scattering of the pore spaces in the small discs in which the consolidation constants are determined, so there is a great chance that these constants in such a sample are not representative (Table 3 and 4). In the determination of the pore space this chance is much smaller (more cores, larger samples).

Summarizing, the simple derivation of the consolidation constants from the easily determinable pore space is an attractive way of working, being quicker, cheaper and more reliable. Whether such relations also exist in sediments in other regions is not known so far, but it seems very likely.

Statement of the problem. In the IJsselmeerpolders the soil profile consists of a layer (1-8 m) of very soft (pore spaces 60-85%), water saturated Holocene sediments, overlying a non-subsiding Pleistocene sand bed. In areas, to be used for building new towns, such profiles are raised by 1 m of sand for various reasons. The consequence is a compaction of the soft layers (0.2-1.5 m), dependent on the soil conditions. Predictions on this subsidence are calculated by means of the Terzaghi-Keverling Buisman formula (Van der Veen, 1962), reading

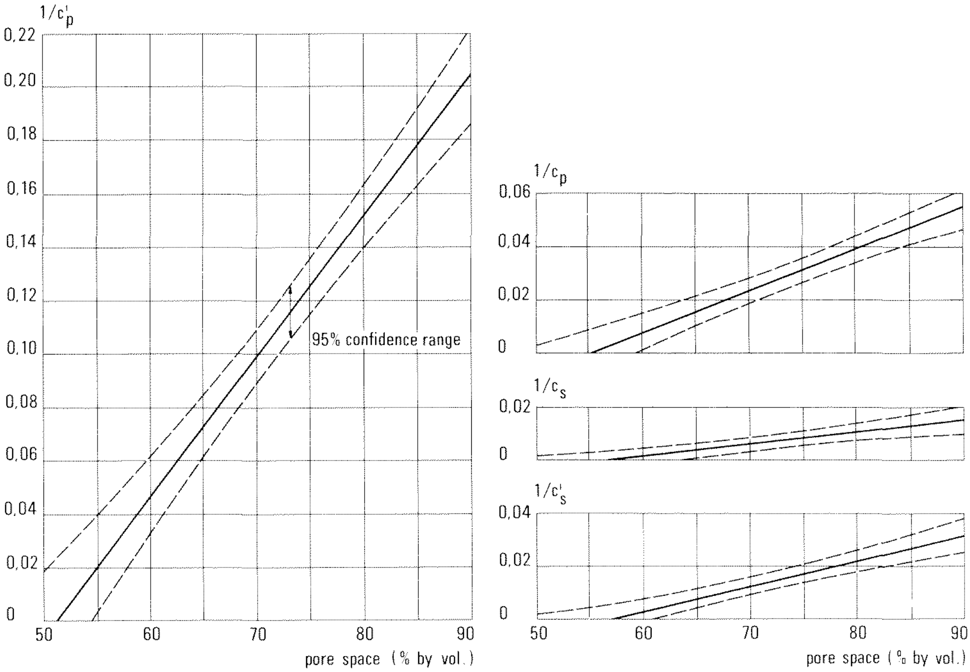

Fig. 1. The relation between the pore space and the consolidation constants and its 95% confidence range in sediments, occurring in the IJsselmeerpolders.

$$s = h \left\{ \left(\frac{1}{c_p} + \frac{1}{c_s} \log t \right) \ln \frac{p_g}{p_1} + \left(\frac{1}{c'_p} + \frac{1}{c'_s} \log t \right) \right\} \ln \frac{p_2}{p_g} \qquad (1)$$

where

s = subsidence	(m)	p_1 = grain press. before loading	($kg.dm^{-3}$)
h = original thickness of soft layer	(m)	p_g = boundary grain pressure	($kg.dm^{-3}$)
		p_2 = grain press. after loading	($kg.dm^{-3}$)
t = time	(days)	$\frac{1}{c_p}, \frac{1}{c_s}, \frac{1}{c'_p}, \frac{1}{c'_s}$ = consolidation constants	

In the application of the consolidation constants some problems are involved:

i. The collection of the necessary, undisturbed samples requires carefully operated, rather heavy and costly equipment (protection pipes, derrick and motor winch, bailer and samplers) as compared with most of the sampling techniques, common in soil science. Moreover, such sampling is time-consuming and hence expensive.

ii. The determination of these constants (in small discs; h = 2 cm; Ø = 6.4 cm) in the laboratory is also rather time-consuming and expensive.

iii. The representativeness of these discs is at least a doubtful matter in a heterogeneous material as soil is.

iv. The inaccuracy of the analysis of the consolidation constants itself is large. Standard deviations are in the range of 50% and even larger.

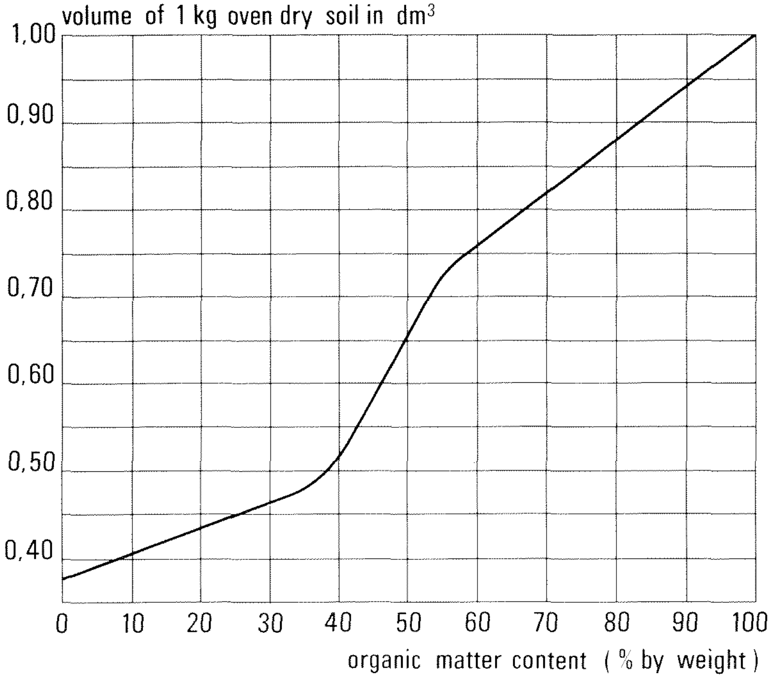

Fig. 2. The relation between the organic matter content (% by weight) and the volume of a unit weight of solid soil particles.

Therefore, a need has been felt for a simple, rapid and hence cheap, possibly more reliable method for the determination of the consolidation constants.

Relation between the consolidation constants and the pore space. Terzaghi stated as early as 1925 that the compressibility was related to the pore space. So the consolidation constants in water saturated soils were plotted against the pore space (Fig. 1). The relation appeared to be rather close. The correlation coefficients are high (0.75-0.93) and the 95% confidence range is rather narrow. In these diagrams soils are involved with widely varying characteristics, ranging from mineral soils with clay contents from 10 to 50% to soils, rich in organic matter and varying clay contents and peat soils. The data of all these different types of soil fit well in the diagrams. Whether such relations also exist in other regions and other types of sediment is not known so far, but it seems very likely.

In water saturated soils the pore space can easily be determined from the water content by

$$p.s. = \frac{V}{W + V} \times 100 \qquad (2)$$

where p.s. = pore space in % by volume out of the total volume
V = volume, taken up by 1 kg of oven dry soil (dm^3) and
W = volume of water (dm^3), calculated from the determined water content in % by weight, assuming the specific weight of water is 1.00 $kg.dm^{-3}$

In mineral soils the specific weight of the soil particles is 2.65 kg.

dm^{-3} *and hence* $V = 0{,}38\ dm^3$. *If organic matter is involved, the specific* weight of the soil particles decreases, due to the lower specific weight of the organic matter. Below 5% of organic matter, this can be left out of consideration. From 5 to 35% the specific weight of the organic matter is $1.50\ kg.dm^{-3}$ (De Glopper, 1973). Above contents of about 50% a value of $1.00\ kg.dm^{-3}$ is found. It is the most likely that this difference results from differences in the gas contents. The relation between the organic matter content and V is given in Fig. 2. Between 35 and 50% a transitional line is introduced.

In soils, not saturated with water, the pore space cannot be calculated by means of the water content, as part of the pores is filled by air. In that case, bulk weight samples have to be taken which is more laborious. It has not been checked yet, whether the type of relation of Fig. 1 then holds also, but it seems also very likely.

Sampling procedure. In water saturated, soft sediments the samples for the determination of the pore space can be taken by means of a simple soil auger, operated by two man by hand down to a depth of about 10 m below surface. The most suitable is a semi-circular gouge-auger (Ø 3.5 cm) with a working length of 1.5 m and extension pieces. Such an auger can also be applied in rather stiff soils, but then sampling takes more time and care. This type of auger does not disturb the soil, so no water is squeezed and the boundaries between possible different layers remain in place and can be recognized easily.

To avoid possible too large variations in the pore space in one sample, the height of each sample is restricted to 0.5 m. When the soil conditions change within this depth, the height of the sample has to be adapted to the easily visible boundaries between the different layers. At least ten cores make up a composite sample of each soil layer, by that giving representative data on the contents of water and, if necessary, the contents of organic matter and clay (Hofstee and Verhoeven, 1962). Next to the pore space, also the wet bulk weight, to be used for the calculation of the initial grain pressures (p_1 in form 1), can be calculated much more exactly by means of the water contents of these larger samples than from the very small discs, used in the conventional way of working.

Comparison of costs. The sampling to a depth of 5 to 8 m below surface by a gouge-auger takes 3 to 4 man-hours only. The collection of undisturbed samples for the determination of the consolidation constants to the same depth takes, due to the more complicated equipment and procedure, 35 to 50 man-hours or roughly ten times as much.

The determination of the contents of water, organic matter and clay takes some 10 to 14 days. When the water contents are determined only (suffices in mineral soils), already 2 days after sampling the analysis results can be available. This is much more rapid than the determination of the consolidation constants in the conventional way (over 6 weeks). In some cases, this can be a great advantage.

Apart from the less time-consuming and hence cheaper sampling procedure, the analysis costs for the determination of the pore space are remarkably lower, as can be seen from Table 1. The analysis costs, necessary for the

Table 1. Relative costs of various analyses

Type of analysis	Relative costs	Remarks
consolidation constants	100%	conventional method
water, org. matter, clay	34%	research purposes only
water, org. matter	23%	org. matter cont. over 5%
water	8%	org. matter cont. below 5%

determination of the pore space, are about 10 or 25% of those of the consolidation constants. The total costs of the determination of the consolidation constants by means of the pore space can be estimated at 10 to 15% of the costs of the determination of these constants in the conventional way (costs of equipment still left out of consideration).

Summarizing, it can be concluded that either the total costs are remarkably lower by applying the pore space/consolidation constant relationship or that at a given budget more detailed information can be collected.

Accuracy of the method. In order to check which inaccuracy results from the application of consolidation constants, derived from the pore space, the subsidence of a soft layer (5 m underneath a sand load of 1 m, a bulk weight of 1.70 $kg.dm^{-3}$ and a hydrostatical course of the waterpressures) was calculated at the mean value and at the 95% upper and lower limit values of the constants at various pore spaces. The results are in Table 2.

Table 2. Subsidence in cm of a soft layer of 5 m underneath a sand load of 1 m at various pore spaces at the upper and lower 95% confidence limits and the mean value of the consolidation constants (t in form. 1 is 10^4 days)

	Pore space in % by volume						
	60	65	70	75	80	85	90
upper limit	24 cm	36 cm	50 cm	69 cm	95 cm	131 cm	186 cm
mean value	12 cm	26 cm	41 cm	60 cm	83 cm	112 cm	158 cm
lower limit	-	16 cm	32 cm	50 cm	70 cm	94 cm	129 cm

At pore spaces, occurring the most frequently in the deposits in the IJsselmeerpolders (65-80%), the subsidence at the upper and lower limit values shows deviations from the subsidence at the mean value in the range of 9 to 12 cm. Hence, there is a chance of 95% that the actual subsidence deviates about 10 cm from the calculated subsidence. Such a deviation is quite acceptable. At higher values of the pore space the deviations are greater, but such values are rare (85% at the utmost).

At four observation sites, loaded by about 1.3 to 1.5 m of sand with a thickness of the soft layers, varying from 4.5 to 5.5 m, the actual subsidence was measured by regular leveling for the period from about three months till about three years after loading. The consolidation constants were determined in both ways and the subsidence was calculated from these constants at the same moments as the leveling.

The relation between the actual subsidence and

i. the subsidence calculated by determined consolidation constants is shown in Fig. 3A and

ii. the subsidence, calculated by consolidation constants, derived from the pore space, in Fig. 3B.

Theoretically, the calculated and measured subsidence should be equal. However, the actual relation deviates rather from this theoretical relation. Nevertheless, for each site apart there is a rather close relation between both values.

These deviations are most probably due to misassumptions of the water overpressures, taken into account in the calculations. These overpressures result from the sand load, supplied in a few days. As a consequence of the extremely low hydraulic conductivity of the soft layers (10^{-10} $m.day^{-1}$), the hydrodynamic period is very long. The water overpressures depend on the groundwater table in the sand load and the potential in the sand bed underneath the soft layers. As a result of the rather large variations in the

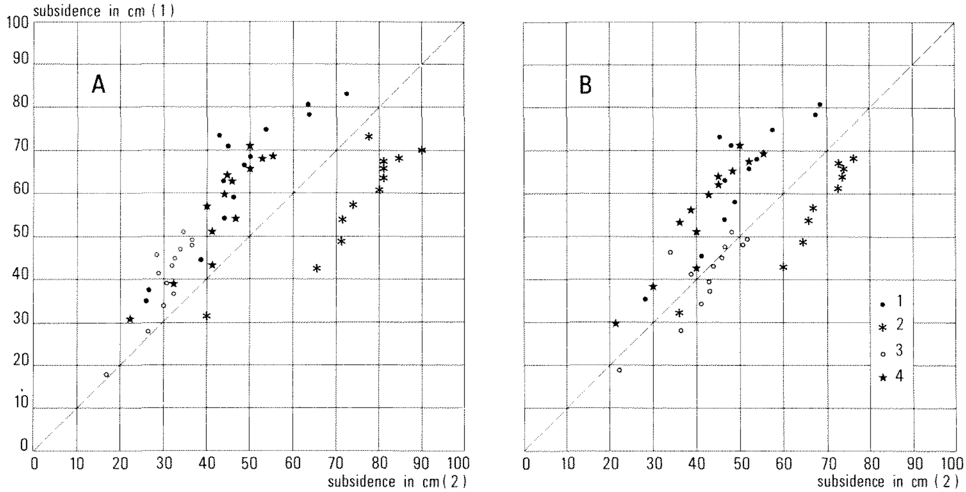

Fig. 3. The relation between the actual subsidence and A. the subsidence, calculated by determined consolidation constants (1 = measured; 2 = calculated) B. the subsidence, calculated by consolidation constants derived from the pore space (1 = measured; 2 = calculated).

groundwater table and also, though relatively small, variations in the potential in the underlying sand bed, an exact determination of the actual water overpressure at a given moment is impossible.

Evidently, the sometimes rather rapid changes in these overpressures do not influence the subsidence process essentially. The actual subsidence appears to be rectilinearly proportional to the logarithm of time (Fig. 4) which is in agreement with the theory. The calculated subsidence, considering the water overpressures, is on the contrary irregularly related to the logarithm of time and hence, less likely. In this case, the surface even rises sometimes which is very unlikely, of course.

In Fig. 5 the relation between the subsidence, calculated by determined consolidation constants and such constants, derived from the pore space, was plotted. Apart from site 3, the subsidence calculated in both ways is nearly equal. However, the determined constants at site 3 deviate from those, found in comparable layers at the other sites. Probably, the constants are determined in less representative discs out of the undisturbed samples. The subsidence values for a period of 10^4 days also fit well in these relations which confirms their reliability.

Lastly, the subsidence of a layer of 0.50 m, burdened by a sand layer of 1 m, a hydrostatical course of the water overpressures and varying pore spaces (mean 72.5%; s 3.3; extreme values 67.6 and 78.3) was calculated for layers of 2 cm and consolidation constants, derived from the pore space for each layer. Next to this, the subsidence was calculated for the whole layer of 0.50 m, applying the mean value of the pore space and the belonging constants. The total subsidence, calculated from layers of 2 cm was 7.48 cm and calculated for the layer as a whole 7.49 cm. Hence, the calculation by means of the mean constants of the whole layer (maximum 0.50 m) gives the same result as the subsidence, calculated by separate layers of 2 cm.

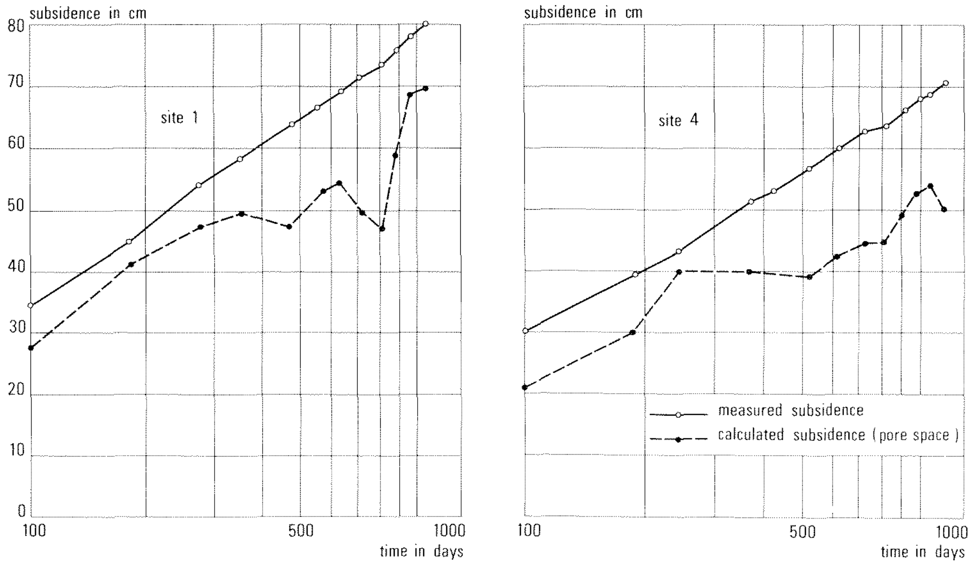

Fig. 4. The relation between the logarithm of time and 1. the actual subsidence and 2. the calculated subsidence at two sites of Fig. 3.

Summarizing, it can be concluded that the application of consolidation constants, derived from the pore space, gives reliable results in subsidence calculations.

Representativeness of both types of samples. The consolidation constants are determined in very small discs. In general, only one disc per metre depth is taken and considered to be representative for that metre, which is doubtful, at least. Moreover, in practice the analysis is done singular only.

The samples in which the pore spaces are determined, are more representative, as

- the sample is taken from the whole layer (max. thickness 0.50 m),
- it is composed of at least ten cores, so horizontal and accidental variations are ruled out and
- the analyses are performed in duplicate (Hofstee and Fien, 1971; when the results of the duplicate analysis differ too much according to statistical standards, the analyses are repeated).

As a consequence, the determination of the pore space is very accurate.

The pore space and hence, the consolidation constants may vary widely in a sediment. An impression of such variations is given in Table 3 (De Glopper, 1973). Undisturbed, tubular samples (h = 35-40 cm; Ø = 6.4 cm), four taken from a humose loam and six from a clayey loam, were subdivided into discs of 2 cm height in which the pore space was determined. The humose loam was visually very homogeneous, whereas the clayey loam was slightly laminated. The deviation of the pore space of each disc from the mean pore space per tubular sampler was calculated. From the frequency distribution in Table 3 it appears that the deviations are small and accidental in the humose loam. In the clayey loam these deviations are much larger and rather irregular.

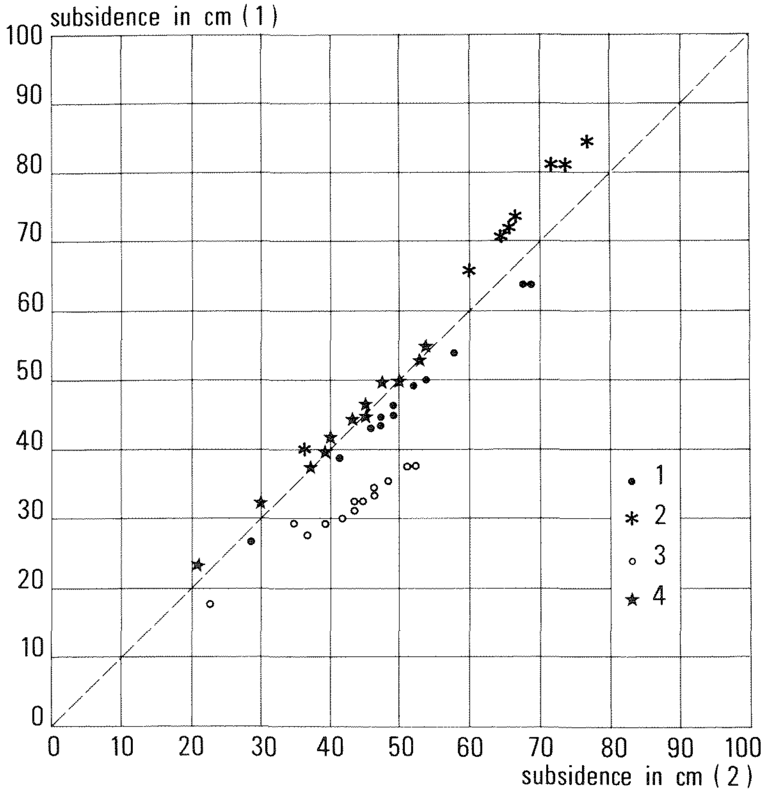

Fig. 5. The relation between the subsidence, calculated by determined consolidation constants and calculated by such constants, derived from the pore space, at the four sites of Fig. 3.

Table 3. Frequency distribution of the deviations of the pore space of discs (h = 2 cm; Ø = 6.4 cm) from the mean pore space of a sampler (h = 35-40 cm)

Deviation from the mean pore space per tubular sample	Number of discs	
	Humose loam	Clayey loam
0 - 1.0 vol.%	32	16
1.1 - 2.0 vol.%	18	12
2.1 - 3.0 vol.%	11	6
3.1 - 4.0 vol.%	2	12
4.1 - 5.0 vol.%	-	8
5.1 - 6.0 vol.%	-	5
6.1 - 7.0 vol.%	-	10
7.1 - 8.0 vol.%	-	10
8.1 - 9.0 vol.%	-	7
9.1 - 10.0 vol.%	-	5
>10.0 vol.%	-	12

It will be clear that in the clayey loam there is a great chance that the consolidation constants, determined in any of the discs, are not representative for the relative layer. In the humose loam the chance to arrive at representative values by analyzing any disc is much greater, of course.
In Table 4 the mean pore space and the mean consolidation constants of the same samples as in Table 3 are given, next to the standard deviations and the 95% confidence limits.

Table 4. Mean pore space (p.s.) and mean consolidation constants in undisturbed, tubular samples and the belonging standard deviations (a) and the 95% confidence range (b) of a slightly laminated clayey loam (sample 1-6) and a visually homogeneous humose loam (sample 7-10)

		p.s.	s	$1/c_p$	s	$1/c_s$	s	$1/c'_p$	s	$1/c'_p$	s
1	a	68.9	5.5	.0220	.0085	.0058	.0026	.0943	.0283	.0111	.0068
	b	79.5-	58.2	.0387-	.0053	.0109-	.0007	.1498-	.0388	.0244-	x
2	a	67.5	6.2	.0201	.0094	.0052	.0030	.0873	.0326	.0110	.0053
	b	73.7-	61.3	.0385-	.0017	.0111-	x	.1511-	.0234	.0214-	.0006
3	a	67.8	6.5	.0203	.0101	.0053	.0031	.0886	.0340	.0108	.0061
	b	80.6-	55.0	.0401-	.0005	.0114-	x	.1552-	.0220	.0228-	x
4	a	76.4	2.5	.0355	.0043	.0094	.0012	.1336	.0129	.0189	.0023
	b	81.3-	71.6	.0419-	.0251	.0118-	.0070	.1589-	.1083	.0234-	.0144
5	a	68.8	4.4	.0220	.0068	.0058	.0020	.0940	.0228	.0118	.0023
	b	77.4-	60.2	.0353-	.0087	.0097-	.0019	.1387-	.0493	.0163-	.0073
6	a	64.3	4.7	.0141	.0085	.0037	.0022	.0738	.0216	.0077	.0042
	b	73.5-	55.2	.0308-	x	.0080-	x	.1161-	.0315	.0159-	x
7	a	82.0	2.2	.0423	.0034	.0121	.0010	.1623	.0112	.0239	.0020
	b	86.2-	77.7	.0490-	.0346	.0141-	.0101	.1843-	.1403	.0278-	.0200
8	a	79.7	1.7	.0388	.0026	.0110	.0008	.1505	.0088	.0222	.0023
	b	83.1-	76.5	.0439-	.0377	.0126-	.0094	.1677-	.1333	.0267-	.0177
9	a	79.6	1.2	.0387	.0019	.0110	.0006	.1501	.0064	.0217	.0012
	b	82.0-	77.2	.0424-	.0350	.0122-	.0098	.1626-	.1376	.0241-	.0193
10	a	79.6	1.9	.0386	.0029	.0109	.0009	.1491	.0090	.0217	.0017
	b	83.2-	75.9	.0442-	.0329	.0127-	.0091	.1667-	.1315	.0250-	.0184

x = lower limit below 0 (impossible)

From Table 4 it can be seen that the standard deviations in the humose loam are small and hence the 95% confidence range narrow. No great inaccuracy will be introduced by applying constants, determined in any disc. In the clayey loam the standard deviations are large and by that the 95% confidence range wide. At the lower limit the values even drop below 0 sometimes which is impossible. So analyzing one disc only, the chance to arrive at non-representative constants is great. Constants, derived from the mean pore space of the much larger samples, in which this pore space is determined, will give a much more reliable approximation.

Despite of the visually only slight lamination of the clayey loam, yet the variations in pore space are wide and by that the chance to arrive at non-representative values. The greater this chance will be in actually laminated deposits. Hence, constants, derived from the large pore space samples, will give more reliable values and by that make possible a better estimate of the subsidence to be expected.

Conclusion. In the IJsselmeerpolders in water saturated sediments the application of consolidation constants, derived from the pore space, gives more reliable results in subsidence calculations than the application of such constants, determined conventionally. This is a consequence of the good representativeness of the relatively large samples in which the pore space is determined as compared with the small discs in which the constants are determined conventionally. Next to this greater reliability, the pore space can be determined easier, cheaper and more rapid.

It was not yet checked, whether such pore space/consolidation constants relations are also found in sediments not saturated with water or in other regions, though it seems very likely.

References

Glopper, R.J. de, 1973, Subsidence after drainage of the deposits in the former Zuyder Zee and in the brackish and marine forelands in The Netherlands: van Zee tot Land no. 50, Staatsuitgeverij, 's Gravenhage, Netherlands, 205 p.

Hofstee, J. and H.J. Fien, 1971, Analysemethoden voor grond, gewas, water en bodemvocht: Rijksdienst voor de IJsselmeerpolders, Lelystad, Netherlands, 193 p.

Hofstee, J. and B. Verhoeven, 1962, Gegevens betreffende de betrouwbaarheid van het grondonderzoek in het IJsselmeergebied: Flevobericht A no. 30, Rijksdienst voor de IJsselmeerpolders, Lelystad, Netherlands, 24 p.

Veen, C. van der, 1962, Grondmechanica: Uitgeversmij Kosmos, Amsterdam/ Antwerpen, 174 p.

Publication n°121 of the International Association of Hydrological Sciences
Proceedings of the Anaheim Symposium, December 1976

PREDICTION OF LAND SUBSIDENCE BY MEANS OF TIME SERIES ANALYSIS OF WATER LEVEL FLUCTUATION IN OBSERVATION WELL

Kuniaki Sato and Kunio Watanabe
Hydroscience and Geotechnology
Laboratory,Faculty of Engineering,
Saitama University,Urawa,Japan

Abstract

The land subsidence of this country has been one of important social problems causing by excessive ground water pumping and the natural gas exploitation in the past over thirty years. In this paper the authors advanced an estimation method of the land subsidence by means of the time series analysis of water level fluctuation from the statistical point of view in the observation well and also studied some statistical properties for the time series of water level and the subsidence being under influence of the pumping and other natural phenomena. By using the results the behavior of the ground water and the subsidence was examined in Osaka, Saitama and Chiba areas, and moreover the proposal concerned with just appreciation of pumping and the control of ground water based on the prediction of land subsidence was stated.

Introduction

As is well known, the land subsidence gives rise to such disasters as the failure of structure, the flood due to ill drainage in urban rivers and the salt intrusion in the coastal aquifers. To prevent the subsidence several regulation laws of ground water pumping with respect to the industrial and cooling water were executed since two decades in this country. Recently, our country meets with a stage of sharp demand of water and results in the water deficit in various districts. Accordingly, the ground water begins to be considered as a precious natural resource. It is not too much to say that the regulation of the pumping by laws is not always the best way under the circumstances. Now these days, it has been urgently desired to foreknow the appreciation of allowable pumping and the ground storage of water with due regard to the countermove of the subsidence in the basins.

Many observation wells are equipped to measure the ground water level and the subsidence under the background described above in big cities of this country. They are not enough made practical use to govern the ground water and the countermove of subsidence while a large amount of data are accumulated for a long term. For the benefit of practical use of those data it can be expected that the time series analysis may be available by computing some statistical quantities such as the correlation, the spectrum and the coherence. This study is aimed at the prediction of land subsidence and the control of ground water based on the results of time series analysis together with the geologic informations.

Observation Method and Location of Wells

Two ways have been used to investigate the land subsidence in this country. One is the leveling of land and the other is by the observation well in order to probe the ground shrinkage. Typical structure of well is shown in Fig.1. The equipment is composed of main parts of two well pipes, the beams and the automatic recorders. The observation of subsidence is done by a fixed arm at the top of inner well pipe and the ground water is measured by a float tied with the steel wire which is wound around the reel of the recorder.

The location of the observation stations used in the analysises is presented in Fig.3 by referring to Fig.2. Fig3.(a) is the stations in Osaka prefecture and those of Saitama and Chiba prefectures adjacent to Tokyo are given in Fig.3(b). The depth of wells and the sample size of time series analysises are indicated in Table 1 in accordance with the well numbers of Fig.3.

For the comparison of the daily time series four observed data of the ground water level and the subsidence are demonstrated for a year in Fig.4. It can be found clearly that the subsidence does occur in the summer as the ground water withdraws by the pumping and both the fluctuations include very small and random waves on the seasonal variations. On the other hand, the monthly time series in Saitama prefecture are illustrated from the beginning of the observation in Fig.5. The ground water withdrawn sharply with years in response to the water demand depended upon the economic growth of the country in an early stage and the land subsidence had been accelerated for years. The ground water level has been rising rapidly by the regulation laws of pumping since 1971, but the withdrawal area of ground water being accompanied with the subsidence sprawls to the rising cities by the urbanization today.

Table-1 Term of data, sample size, depth of well and well number of time series analysis

	Term of Data	Sample Size(day) by Blackman & Tukey	Sample Size(day) by MEM	Depth of Wells (m)	Well No.
Saitama	1975.4.1-	359	180	100	5-1
	"	365	"	150	7-2
	"	350	"	"	8-1
	"	365	"	700	10
	"	342	"	350	13
Chiba	1974.3.1-	296		70	2
Osaka	1972.12.1-	427		50	10
	"	"		"	11

Time Series Analysis

It may be said generally that we can regard the time series of observation as the sum of the trend, the cyclic and random components. For both cases of the ground water and the subsidence the secular trend is affected dominantly by the regulation of ground water pumping and the cyclic variation is closely related with the seasonal demand of ground water. The random component is very complicated because many factors like the natural phenomena and the artificial actions may intervene. It is to be supposed, however, that some characteristic factors governing the phenomena can be revealed by the time series analysis of the observed data.

In general the autocorrelation function for the steady time series of the ground water level H(t) and the subsidence S(t) can be defined by respectively

$$H(t) = H + h, \quad S(t) = S + s, \quad (1) \qquad \begin{aligned} C_h(\tau) &= \overline{h(t)h(t+\tau)}, \\ C_s(\tau) &= \overline{s(t)s(t+\tau)}, \end{aligned} \quad (2)$$

in which H;the trend of ground water level, S;the trend of subsidence, h and s;the steady random components, $C(\tau)$;the autocorrelation function, $\tau=n\Delta t$, $n=1,2,3,\cdot\cdot,M$, Δt;the time, ——;the time average, and the subscripts of h and s mean the ground water and the subsidence respectively. The two sided spectra as the Fourier transformation are given by

$$P_h(f) = \int_{-\infty}^{\infty} C_h(\tau) e^{-i2\pi f\tau} d\tau, (3) \quad P_s(\tau) = \int_{-\infty}^{\infty} C_s(\tau) e^{-i2\pi f\tau} d\tau, (4)$$

in which P(f);the spectrum and f;the frequency. The cross correlation function $C_{sh}(\tau)$ and the cross spectrum $P_{sh}(f)$ are given by

$$C_{sh}(\tau) = \overline{s(t)h(t+\tau)}, \ (5) \quad P_{sh}(f) = \int_{-\infty}^{\infty} C_{sh}(\tau) e^{-i2\pi f\tau} d\tau. \ (6)$$

The coherence concerned with the noise and the linearity in both time series is defined by

$$\gamma_{sh}^2(f) = \frac{|P_{sh}(f)|^2}{P_s(f)\cdot P_h(f)}, \qquad (7)$$

in which $\gamma_{sh}^2(f)$ is the coherence.

For the purpose of the analysis the steady time series should be used by introducing a proper trend filter. In this analysis the moving average of size length 31 days was adopted.

In order to compute the spectrum the Maximum Entropy Method (MEM) is used in addition to the Blackman-Tukey method, so the MEM has several advantages on the resolution of waves. The theory of MEM is based on the concept making the information entropy maximum under the condition of Eq.(8) by assuming that the time series for the time intervalτ are the Gaussian,

$$C(n) = \int_{-f_N}^{f_N} P(f) e^{i2\pi nf\Delta t} df, \qquad (-M\leq n\leq M) \qquad (8)$$

in which f_N;the Nyquist frequency(=$1/2\Delta t$), M;the maximum lag and C(n);the autocovariance function. For the analysis of the spectrum density function the final equations are obtained by introducing the concept of minimization of the error power to obtain the coefficients of the prediction error filter as follows,

$$P(f) = \frac{P_M}{2f_N}\left|1+\sum_{n=1}^{M} a_n e^{-i2\pi nf\Delta t}\right|^{-2}, \quad (9) \qquad \begin{bmatrix} C(0)C(1)\cdots C(M) \\ C(1)C(0)\cdots C(M-1) \\ \cdots\cdots\cdots \\ \cdots\cdots\cdots \\ C(M)\cdots C(1)C(0) \end{bmatrix} \cdot \begin{bmatrix} 1 \\ a_1 \\ \cdot \\ \cdot \\ a_M \end{bmatrix} = \begin{bmatrix} P_M \\ 0 \\ \cdot \\ \cdot \\ 0 \end{bmatrix}, \quad (10)$$

where $(a_1, a_2, \cdots, a_M)$ is the coefficients of prediction error filter and P_M the mean square of error for the term M. The spectrum can be computed from Eq.(9) if the coefficients and P_M are found by Eq.(10). In this study Burg's algorithm was used as a computation technique for the lag M=30 days (Andersen,N.,1974).

Results and Discussion

There is meaning in the comparison of the time series properties for different basins in view of the geological aspect. Several results of the correlograms are illustrated in Fig.6. Fig.6(a) is the correlograms of the monthly time series for the well number 6 and 10 in Osaka prefecture, and also the correlograms of the daily time series are shown in Fig.6(b), in which those of the well number 2 were computed by the time series in Chiba, the number 8-1 and 10 in Saitama and the number 10 and 11 in Osaka. Referring to the correlograms, we can find out that the periodicity of one year may be recognized for both the autocorrelation and the crosscorrelation by Fig.6(a) and on the other hand, the periodicity of the daily time series is hardly recognized in Fig.6(b). It is an interesting fact that the fluctuation scale of the ground water is larger than that of the subsidence and the scales are comparable even if the basins were different. By paying attention to the correlation value of the correlograms the monthly time series have high correlation between the ground water and the subsidence as compared with the case of the daily time series. It seems that the monthly time series depends on seasonal demand of ground water and the daily time series is not only related with the ground water pumping but also various random factors. When one does try to control systematically the subsidence by means of observed data of the ground water, the short time series is not always adequate and it is complicated in phenomena.

When the behavior and the fluctuation character of ground water are considered in a whole basin, it is very useful to study the wave structure of ground water fluctuations which may include many factors. The factors which may contribute to the ground water fluctuation in a basin are mainly classified into the meteorological phenomena (the rainfall, the atmospheric pressure, the temperature etc.), the hydraulic and hydrologic factors (the infiltration, the runoff, the seepage etc.), the geophysical phenomena (the tide, the earth tide, the earthquake etc.) and the artificial factors (the pumping, the regulation of pumping, the public works etc.). The structure of fluctuation waves including these factors for the daily time series are shown by the spectra in Fig.7, and the cross spectra of the ground water and the subsidence for the observation wells mentioned above are presented in Fig.8. In Fig.7(a) there are the predominant waves in the range of 0.02-0.05 cycle/day and 0.1-0.2 cycle/day at least.

On the other hand, the predominant waves can not be detected obviously as a whole except where they appear in the range of 0.04-0.07 cycle/day for well number 8-1 and 2, as shown in Fig. 7(b). It goes without saying that the similarity with respect to the structure of fluctuation waves in both the ground water and the subsidence does not exist notably for the daily time series. Generally speaking, the fluctuation of ground water level and that of the subsidence are not same, and the one is slow-moving and the other is high-moving. The cross spectra having both characters of the ground water and the subsidence are presented in Fig.8. From the cross spectra their predominant waves may be disclosed in two ranges of 0.03-0.04 cycle/day and 0.1-0.13 cycle/day. As the results of the spectrum analysis, the fluctuation of ground water accompanied with the land subsidence has a similar pattern on a whole, and that it will be bring with the monthly and weekly predominant periodicities even if the basins were different. It may be supposed as one of the reasons that the ground water movement in itself is affected by the ground water pumping over long term as well as the atmospheric and geological phenomena such as the atmospheric pressure and the earth tide.

For the sake of estimation of the linearity and the noise intervention in both time series the coherence is computed as shown in Fig.9. As referred to these values against the wave number, the coherences are high between 0.1-0.3 cycle/day for the well number 2,10 and 11, but those of the well number 8-1 and 10 are not so high over all range. It indicates a very interesting fact that the behavior of ground water in shallow wells may be very in response to the land subsidence, and on the contrary the subsidence may not depend the fluctuation of deep ground water. Accordingly, it may be difficult to predict the subsidence by using such short time series as the daily one for the deep well because the ground water level observed in deep well will differ probably with one of the subsidence layer in a short term. High frequency fluctuation of ground water is not, however, closely related with the subsidence even in shallow well.

Usually, it is said that MEM is better than Blackman-Tukey method in respect of the resolution for the spectrum analysis computation. In order to resolute the waves at high frequency the daily time series observed in Saitama were analyzed here by MEM with the lag time of 30 days. By these results as shown in Fig.10 there are the predominant waves near 0.14 and 0.3 cycle/day for the ground water and near 0.04-0.05 and 0.07-0.08 cycle/day for the subsidence at least. In this analysis long period waves are not enough resoluted because the sample size of 180 days is not so large as the long waves may be resoluted. It seems that it can not obtained to resolute the predominant waves of the subsidence series because of the complicacy in nature, although MEM were adopted.

In practice, to appreciate the correlation between the ground water and the subsidence in an area is important for the purpose of the prediction of subsidence and the control of ground water. Computed results of the correlation between the daily time series in Saitama prefecture are indicated in Fig.11 after making use of the moving average filter 31 days. These results present that all correlations $C_{sh}(\tau)$ at $\tau=0$ are not so large as those of both fluctuations may be recognized for the daily time series. According to some cases the maximum correlations accompanied with a few days of lag time were revealed. As described early, the correlation of daily time series is not appreciable wholly because of the random factors.

The cross correlation of the monthly time series for Osaka area is shown in Fig.12. For all computations the moving average filter of 13 months is used. So far as these results are concerned, the correlation values are appreciable compared with the case of the daily time series. By making practical application of the results the monthly amount of subsidence will be predicted by the time series of ground water level within the accuracy of analysis.

Conclusions

This study has been carried out with an object of the prediction of land subsidence and the control of ground water based on the results of time series analysis by computing some statistical quantities such as the correlation, the spectrum and the coherence. By the results following conclusions were obtained.

The time series of the ground water and the subsidence are composed of the secular trend, the seasonal variation and the irregular or random fluctuation by the observation data. The properties of time series are closely related with the artificial factors of ground water demand and the natural phenomena. It may be difficult to predict the subsidence by such short time series as the daily one because of the random components. But, the estimation of subsidence is possible by using the long time series like the monthly one. The ground water behaves properly by the predominant frequency in each basin.

It is not too much to say that the regulation of the ground water pumping by laws is not always the best way with a sharp demand of water resource. Recently, it has been urgently desired to foreknow the appreciation of allowable pumping and the ground storage of water with due regard to the countermeasure of the subsidence for various basins.

Acknowledgement

In this study the observation data were offered by Saitama, Chiba and Osaka prefectures. The authors wish to give thanks to the authorities concerned.

References

Andersen,N.,1974,On the calculation of filter coefficients for maximum entropy spectral analysis:Geophysics,Vol.39,no.1, p.69-72

Sato,K.,1974,On time series correlations between the ground water level and the subsidence:Proc.Natural Disaster Sciences Sym. in Japan,no.11,p.80-81(in Japanese)

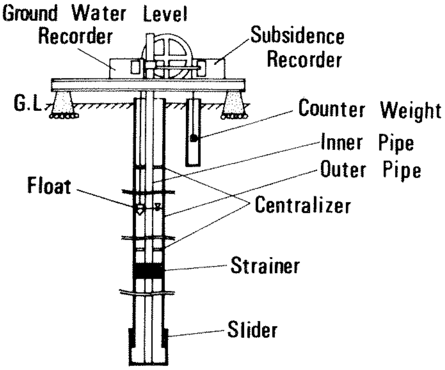

Fig.1 Structure of well

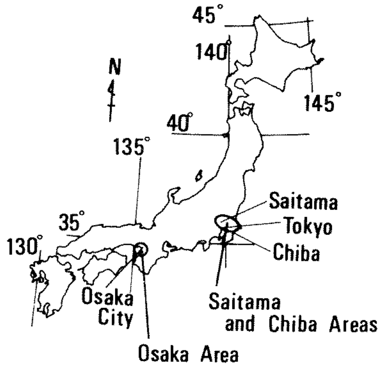

Fig.2 Location of study areas

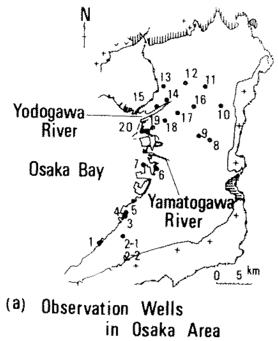

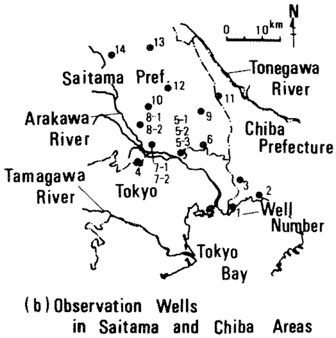

Fig.3 Observation stations

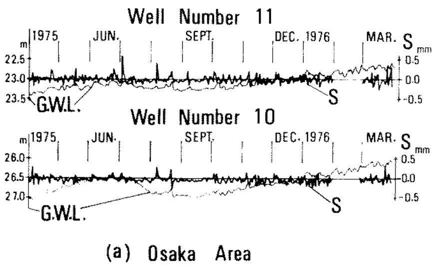

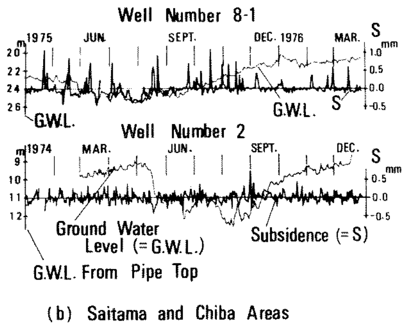

Fig.4 Daily time series of Osaka,Chiba and Saitama

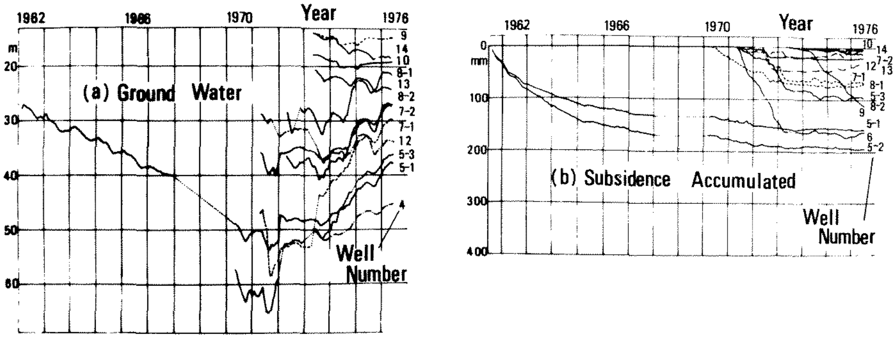

Fig.5 Annual variations of ground water level from well top and accumulated subsidence in Saitama

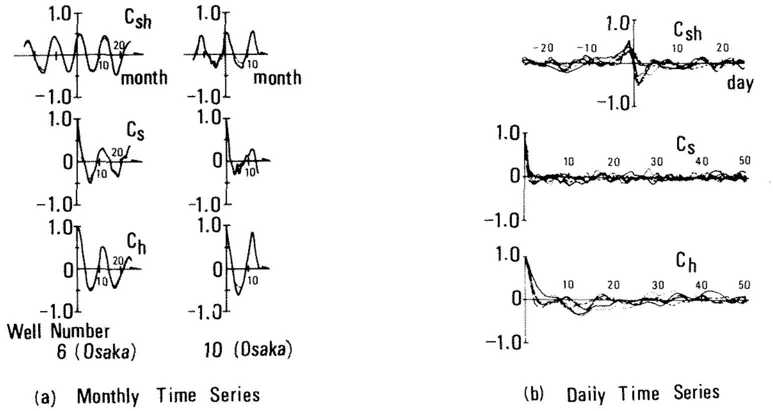

Fig.6 Correlograms of monthly time series and daily time series

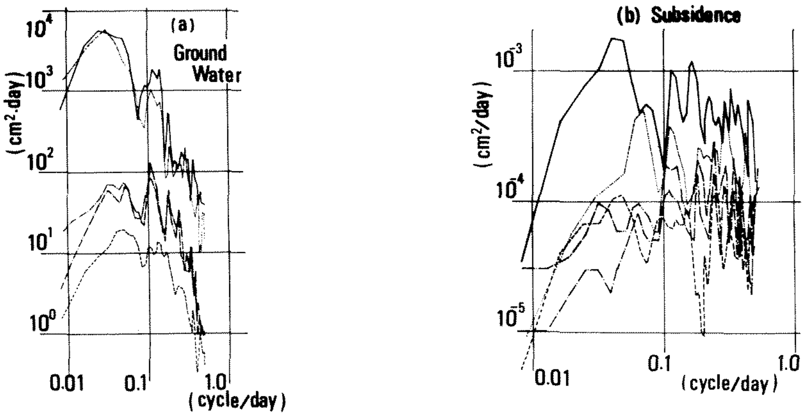

Fig.7 Spectra by Blackman-Tukey method

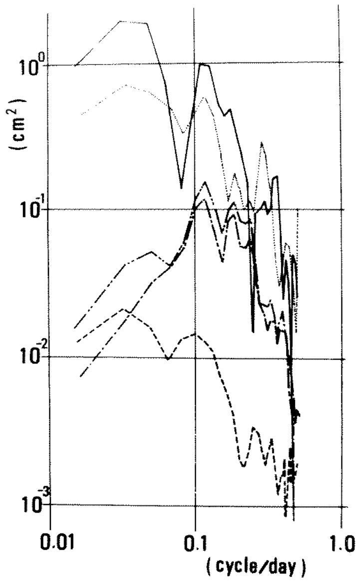

Fig.8 Cross spectra

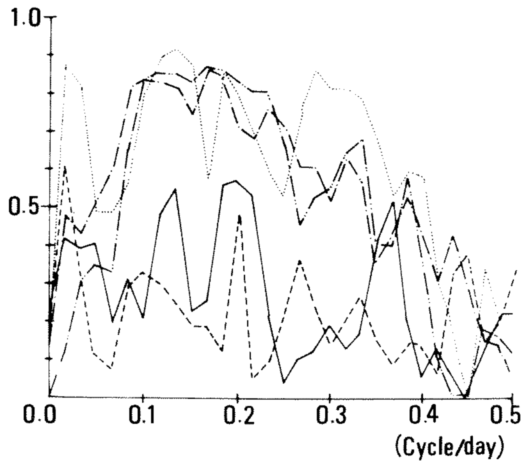

Fig.9 Coherences

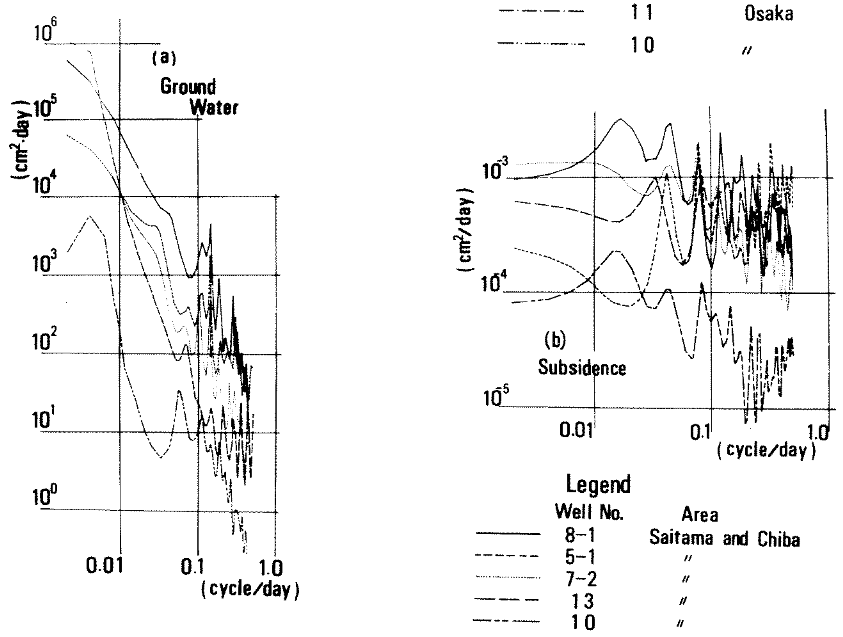

Fig.10 Spectra by MEM in Saitama

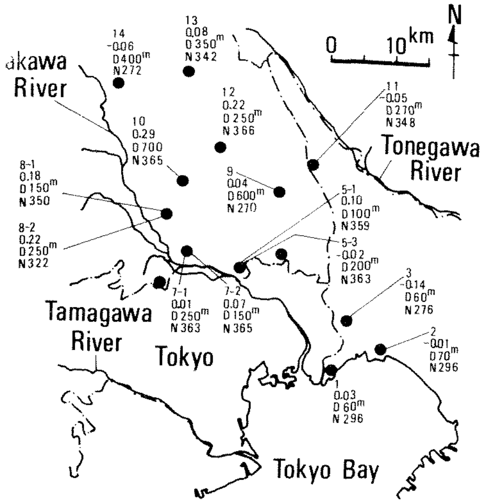

Fig.11 Cross correlations of Saitama and Chiba areas by daily time series ($C_{sh}(\tau)$ at $\tau=0$)

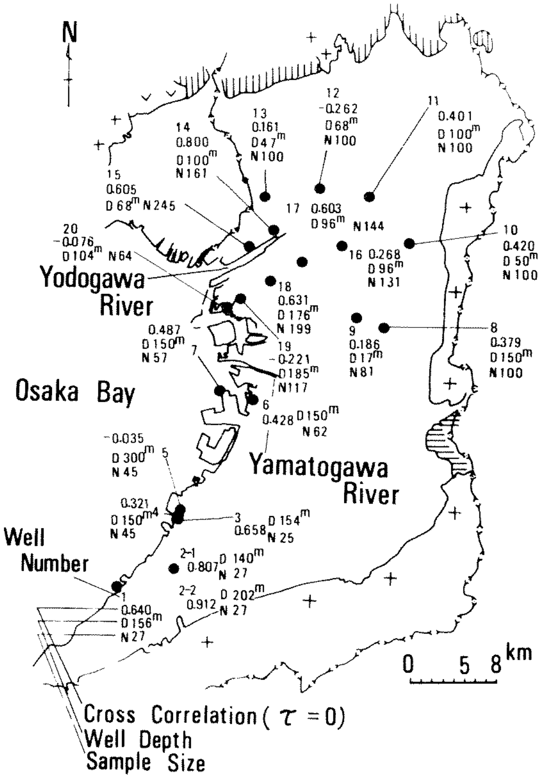

Fig.12 Cross correlations of Osaka by monthly time series ($C_{sh}(\tau)$ at $\tau=0$) (Sato,K.,'74)

Publication n°121 of the International Association of Hydrological Sciences
Proceedings of the Anaheim Symposium, December 1976

QUALITY OF PREDICTIONS OF LAND SUBSIDENCE ALONG DELTA-MENDOTA AND SAN LUIS CANALS IN CALIFORNIA, USA

Nikola P. Prokopovich
U.S. Bureau of Reclamation, Mid-Pacific Region,
2800 Cottage Way, Sacramento, California

Abstract

Some 64 km of the Delta-Mendota Canal and 144 km of San Luis Canal are affected by land subsidence caused by an irrigation overdraft of the confined sub-Corcoran aquifer system. The overdraft gradually diminshed or ceased with canal water deliveries. Subsidence during overdraft is designated as "active" and post-overdraft subsidence as "residual" subsidence.

Subsidence during construction and post-construction periods along Delta-Mendota Canal, recognized first in 1952 after canal completion, amounted to up to 2.4 m and resulted in overtopping of canal lining, bridges, and other structures. Ultimate amounts of residual subsidence after 1966 calculated mathematically in 1967, using changes of subsidence rates ranged from traces to 1.1 m. Subsequent levelings and new estimates confirm the good quality of the 1967 estimates. The estimates were used for current rehabilitation of the canal.

Preconstruction estimates of ultimate subsidence along the San Luis Canal were extrapolated empirically using mostly past subsidence rates. Estimated amounts of ultimate subsidence after January 1963 (beginning of construction) ranged from traces to about 4.25 m. These data were used for design purposes. Additional freeboard ranging from 0.3 to 2.1 m was provided in subsiding reaches to compensate for anticipated subsidence during construction and post-construction periods. Amounts of subsidence during the construction period, obtained from subsidence contour maps, and amounts of post-construction residual subsidence, were calculated semigraphically using changes of benchmark elevations. A comparison of these data indicates the satisfactory quality of estimates.

It appears that with experience and a little luck the ultimate amounts of subsidence can be reasonably estimated for design, construction, and rehabilitation purposes.

INTRODUCTION

Exogenic land subsidence (Prokopovich, 1972) is a well recognized worldwide geologic hazard (for example, Bolt et al, 1975) and is frequently related to various types of human activity. A future spread of such subsidence is anticipated with the rapid growth of world population and technological "know how" (Prokopovich, 1972). Particularly common is exogenic subsidence related to an overdraft of ground waters (Poland and Davis, 1969).

Damaging effects of such subsidence are especially notable and important for design, construction, and operation-maintenance of various canals, pumping plants and other structures which have to maintain design grades. Unfortunately, areas affected by such subsidence are frequently geographically associated with water conveyance systems (Prokopovich, 1972).

The importance of reliable predictions of ultimate amounts of a land subsidence for proper design and rehabilitation of various canals and other engineering structures cannot be overestimated. The following paper discusses the quality of predictions made by the author for two large USBR canals, the Delta-Mendota, and San Luis Canals in the California, San Joaquin Valley (fig. 1). The methods, theory, and technique of the predictions were previously described in several publications (Prokopovich, 1969 A, B, 1971, 1975) and are only briefly mentioned in the present text.

Original studies were made using "English measuring units." In this paper these values are converted into the metric system, except mileposts used for location along canals (1 mile = 1.609 km) and 0.2 foot contours on figure 4 (1 ft = 0.3048 m).

LOCATION AND ENGINEERING DATA

The Delta-Mendota and San Luis Canals are located on the western side of the semiarid San Joaquin Valley in the State of California, USA (fig. 1). Both canals are features of the Central Valley Project of the Federal Bureau of Reclamation (USBR, 1961, 1966).

The Delta-Mendota Canal, constructed in 1946-1951, was designed, constructed, and operated by the Bureau (USBR, 1959). The canal extends for about 182 km from the vicinity of Tracy in the Sacramento-San Joaquin Delta to the Mendota Pool on the San Joaquin River, some 50 km west of the city of Fresno. The upstream 153 km of the canal are concrete-lined, about 32.3 m wide at the top and 14.6 m wide at the bottom. The original designed depth of water varied from 5 to 4.3 m. The downstream 29 km of the canal are earth-lined, about 42 m wide at the top, 18-19 m wide at the bottom and 4.25 m deep. The canal is subdivided into individual pools by 21 check structures and the designed freeboard is about 1/2 m. The initial capacity of the canal is 130.3 m^3/sec. The designed canal gradient is 0.00005 (or 5 cm per one kilometer).

The San Luis Canal, constructed in 1963-1968, was designed and constructed by the Bureau (USBR, 1974) as a joint Federal-State Project operated by the California Department of Water Resources as a portion of the California Aqueduct. The 163.3 km long concrete-lined canal, with the maximum capacity of 371 m^3/sec, extends from the O'Neill Forebay Reservoir to the village of Kettleman City, 80 km south of Fresno. The canal is subdivided by the Dos Amigos Pumping Plant and eight check structures into nine individual pools. The bottom width of the canal ranges from 15.2 to 33.5 m, and the width at the top of the lining ranges from 48 to 78.4 m. Depth from the invert to the top of lining ranges from 8.2 to 11.2 m, and the designed canal gradient below the Dos Amigos Pumping Plant is 0.00004.

REGIONAL GEOLOGY

The San Joaquin Valley is a northwesterly trending structure trough (Bailey, 1966) between the Coast Ranges and the Sierra Nevada (fig. 1). It is about 370 km long and 60-100 km wide. The deformed, mostly marine, consolidated Tertiary and Cretaceous sediments of the trough are capped by unconsolidated, mostly alluvial, several hundred meters thick Quaternary overburden. The most prominent bed in the overburden is the Pleistocene buried lacustrian Corcoran clay. The clay creates a widespread confined "sub-Corcoran" aquifer system. This aquifer was the main source of irrigation water in the area and suffered from a severe overdraft prior to the construction of the canals (Bull and Miller, 1975). The historical piezometric decline along the Delta-Mendota Canal amounted to up to about 61 m and along the San Luis Canal about 145-160 m. Canal deliveries arrested the piezometric decline along the Delta-Mendota Canal in 1952-53 and along the San Luis Canal mostly in 1967. In the upstream portion of

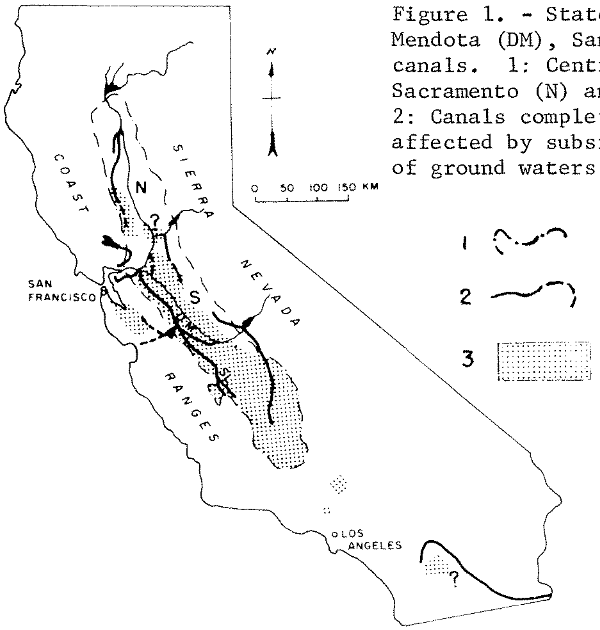

Figure 1. - State of California with Delta-Mendota (DM), San Luis (SL), and other USBR canals. 1: Central Valley composed of Sacramento (N) and San Joaquin (S) Valleys. 2: Canals completed and proposed. 3: Areas affected by subsidence due to an overdraft of ground waters.

the San Luis Canal piezometric decline was partially arrested prior to the completion of the canal by surface water deliveries by a local water district.

SUBSIDENCE

Decline of piezometric pressure due to an overdraft of confined ground water results in an increase of effective loading of overburden above the aquaclude and a compression of sediments within the aquifer system. The process, particularly in fine grained media, is slow.

Subsidence in which cause and effect are closely linked timewise is designated by USBR as "active subsidence." Subsidence which continues at diminishing rates for years after the end of stress increase is designated as "residual" (Prokopovich, 1969B, 1971). At any given time, subsidence caused by a continuous overdraft of ground water consists of the current increments of "active subsidence" plus the accumulation of continuing residual subsidence.

The San Joaquin Valley is one of the world's largest areas affected by land subsidence (Poland et al, 1975). Most of the subsidence here has been associated with overdraft of the sub-Corcoron aquifer system. The overdraft of other less important aquifers, however, has also contributed to some subsidence. Total historical maximum amounts of subsidence in the Valley are locally about 10 m. The phenomena has caused serious operational-maintenance and design construction problems, particularly for several canals.

Land subsidence is readily monitored by periodic levelings of a grid of benchmarks. Such levelings on the west side of San Joaquin Valley are complicated by the localized occurrence of an unusual geological process known as hydrocompaction or shallow subsidence, (Bull, 1964). Hydrocompaction is a peculiar property of some semiarid sediments leading to

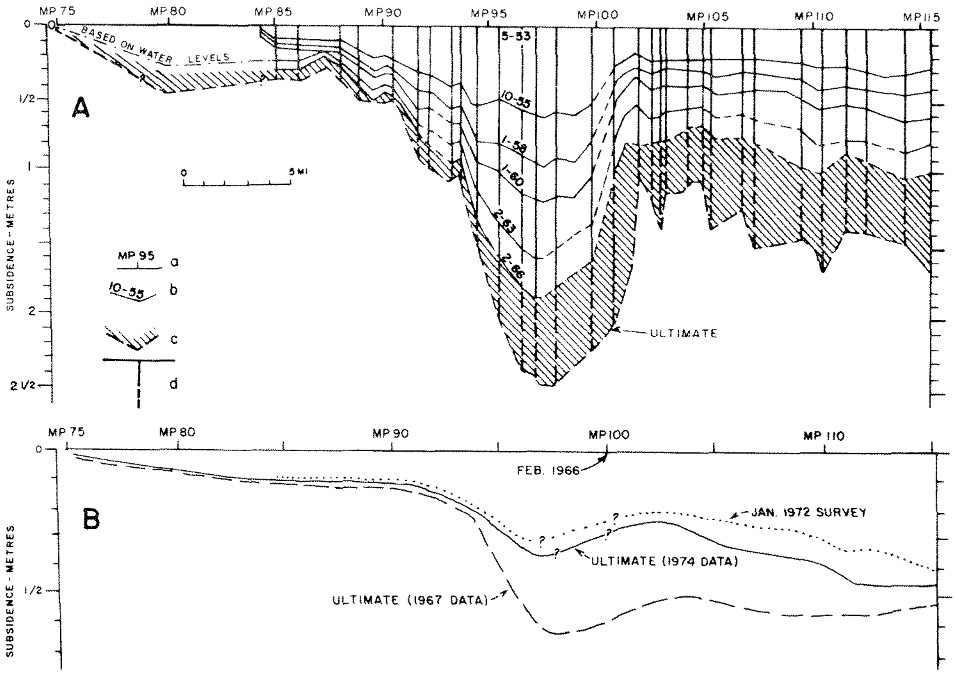

Figure 2. - A: Delta-Mendota Canal - post-construction subsidence along the downstream reaches and 1967 estimates of ultimate residual subsidence. a: milepost distance from intake; b: date of survey; c: predicted ultimate subsidence; d: benchmark data. B: A comparison of 1967 and 1974 estimates of residual subsidence.

spontaneous slumps, collapses, cracks, and settlements when wetted. In areas affected by hydrocompaction, benchmarks reflect cumulative results of 2 types of subsidence - regional, caused by an overdraft of ground waters, and hydrocompaction, caused by irrigation of local fields. Two such areas are known along the San Luis Canal.

Subsidence which took place during the construction of the San Luis Canal has been associated with an overdraft and is an example of "active subsidence."

Post construction subsidence along the Delta-Mendota and San Luis Canals are typical examples of residual subsidence associated with past overdraft of ground waters.

PREDICTIONS - DELTA-MENDOTA CANAL

The existence of land subsidence was not recognized during design and construction of the canal in 1946-1951. The concept of land subsidence was developed in 1952 and numerous benchmarks were established along the canal and periodically releveled thereafter downstream of "Mile Post" (MP) 85± in an area of notable subsidence. These levelings provide a good basis for predictions of ultimate residual subsidence. Some data on amounts of earlier subsidence were obtained by a comparison of 2 published sets of 7-1/2-minute topographic quadrangle maps surveyed in 1919-20 and 1955-56.

Additional data on post-construction subsidence above MP 85, i.e., upstream from the periodically surveyed reach, were obtained from water level measurements in the canal. These data and some sporadic levelings indicate that the entire canal alignment may be affected by subsidence.

Significant subsidence, however, is restricted to the downstream 42-47 miles of the alignment below MP 70-78 and affects both concrete- and earth-lined sections of the canal. Data on piezometric conditions along the canal obtained from a set of piezometric contour maps indicate a major piezometric decline between 1905-06 and 1953, and only minor fluctuations of stabilized piezometric levels after 1953, following delivery of canal water, and decrease of ground-water pumping.

Post-construction subsidence along the canal continued with decreasing rates (fig. 2) and caused serious operation-maintenance problems (fig. 3A-F). Maximum amounts of subsidence recorded by benchmark levelings after May 1953, were about 0.6 m in 1955; 1.25 m in 1960; 1.95 m in 1966; and 2.2 m in January 1972.

Two initial efforts to estimate ultimate subsidence along the canal based on laboratory one-dimensional consolidation tests of 20 samples of various sediments, particularly Corcoran clay, from a single test hole were made by Gibbs and Larcom (1956), and Gibbs (1959) and refined by Miller (1961). The Corcoran clay was identified as the main consolidating unit. This method could not be adopted to other areas because of lack of core holes to provide a sufficient number of samples for consolidation testing. Moreover, compaction recorder data at Ora Loma failed to identify any particular increase of compaction within the Corcoran clay.

Initial estimates of ultimate subsidence for rehabilitation purposes were made in 1967 (Prokopovich, 1969A, B), using time-subsidence graphs of individual benchmarks. It was assumed that such graphs for residual subsidence could be considered as "consolidation graphs" under a constant load and follow an exponential decay curve. The calculated values of subsidence after January 1966, using this approach, ranged from traces to 1.1 m (fig. 2).

The January 1972 leveling of canal benchmarks indicated, as predicted, a general decline of subsidence rates, which at the present trend, pose no major operational problems. The 1974 predictions of ultimate subsidence along the canal, based on this leveling, range from traces to 12 cm. Converted to the 1966 base, the predictions are rather close to the previous 1967 predictions (fig. 2); hence, the quality of prediction of residual subsidence seems to be high. In general, the 1974 estimates yield smaller amounts of ultimate subsidence than 1967 estimates. The difference is probably due to an improvement of regional piezometric conditions by surface water deliveries from the San Luis Canal to the neighboring Westlands area.

A general rehabilitation of the earth- and concrete-lined sections of the canal including embankments, lining, bridges, and other structures is now in progress (USBR, Specifications Nos. 200C-729, 200C-932, and 200C-933). The approximate cost of the rehabilitation is over $4 million.

PREDICTIONS - SAN LUIS CANAL

The existence of subsidence in the general vicinity of San Luis Canal was well-known prior to its design and attempts were made to neutralize its effects by providing some extra freeboard in critical reaches. However, the exact location of the alignment was not known initially and no permanent "leveling route" was available along the canal route. An interpretation of subsidence contour maps (fig. 4) based on periodic leveling of the established leveling network was used therefore for predictions.

The first "highly approximate" preconstruction estimates made in April 1961, were based on three assumptions: (1) currently available (from winter 1957-58 to winter 1959-60) subsidence rates would continue through construction; (2) the end of ground water overdraft and the termination of active

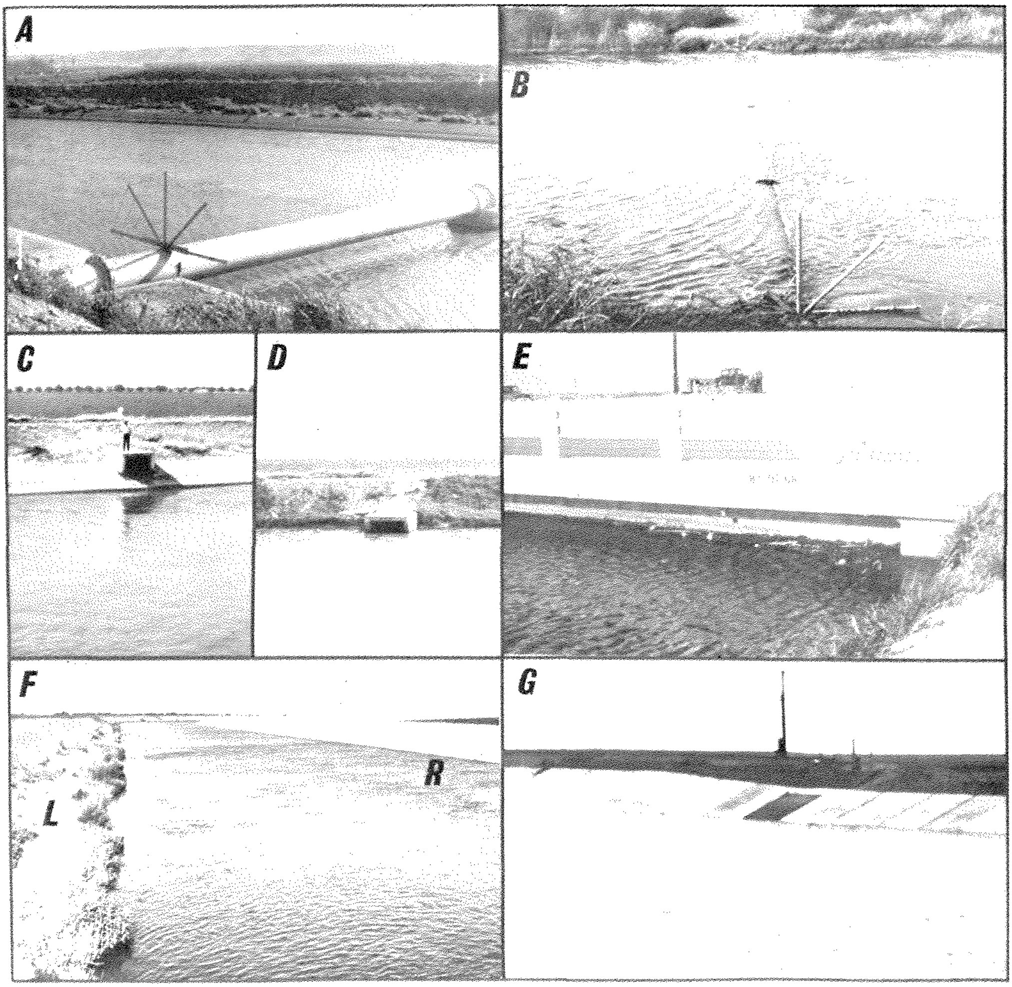

Figure 3. - Subsidence of Delta-Mendota (A-F) and San Luis Canals (G). A: Pipe crossing and concrete lining in a relatively stable area. B: The same in area affected by subsidence. Pipe and concrete lining are flooded. C & D: Drain outlets in stable (C) and subsiding (D) areas. E: Concrete bridge in subsiding area. Normal 1-meter clearance below bottom of the bridge is flooded. Bridge bottom is submerged. F: Rehabilitation of concrete-lined section of the canal in subsided area. Additional fill and extension of concrete lining on top of original lining are placed on the right bank (R). Left bank (L) is not rehabilitated. G: Designed raise of freeboard to compensate for future subsidence.

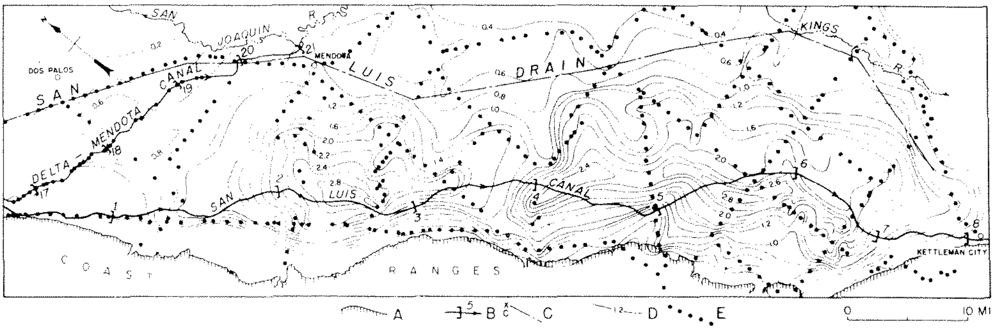

Figure 4. - An example of a subsidence contour map of the Los Banos-Kettleman City area showing total land subsidence between February 1963 and February 1966. Data based on USC&GS leveling of benchmarks. A: Edge of Coast Ranges; B: Canal and check with number; C: Contour lines of equal subsidence; contour interval 0.2 foot; (1 foot = 0.3048 m); D: Benchmarks located along leveling routes and used for contouring.

subsidence would take place at the end of construction in January 1968; and (3) residual post-construction subsidence would be equal to 5 years of subsidence at the "currently available" rates. Strip maps of the vicinity of canal alignment were prepared using the available published 7-1/2-minutes topographic maps surveyed in 1956. Subsidence rates were calculated from the latest available (1957-58 to 1959-60) subsidence contour maps for all section corners of the strip maps and the strip map topography was "updated" to show the "January 1963" (beginning of construction), "January 1968" (end of construction), and "ultimate topography" (fig. 5). No attempts were made to differentiate the "total" subsidence as shown on all subsidence contour maps (fig. 4) into deep subsidence caused by overdraft of ground water and "hydrocompaction." The latter, locally occurring along the canal, is caused by water application (Bull, 1964). The 1961 estimates of ultimate subsidence after beginning of the construction ("January 1963") showed three maximums and ranged from about 0.15 m to 4.15 m. Generalized predictions of ultimate subsidence along the canal alignment scaled from the 1961 strip maps are shown on figure 9.

The following, also "highly approximate", but hopefully somewhat improved estimates of ultimate subsidence completed in 1963 were made using two main approaches: (1) projection of the latest available subsidence rates of a few individual benchmarks near the canal alignment based on the winter 1959-60 and February 1963 levelings by USC&GS combined with compaction recorder data; and (2) ratios between piezometric decline and subsidence. The average rates of piezometric decline during a 10-year period (1951 to 1961) were adopted for predictions. The adaptability of "ratio approach" (strongly suggested by some authors) for the nearby located San Luis Drain has been questioned (Prokopovich, 1975, p. 15).

In the 1963 estimates, as an improvement, an attempt was made to minimize the effect of hydrocompaction on "available rates of subsidence" either (1) by graphic differentiation of subsidence into "deep" and hydrocompaction, or (2) by data obtained from a few compaction recorders.

In the 1963 estimates it was assumed that (1) active subsidence is caused by an overdraft of the sub-Corcoran aquifer system and that this overdraft and active subsidence will continue at constant rates until end

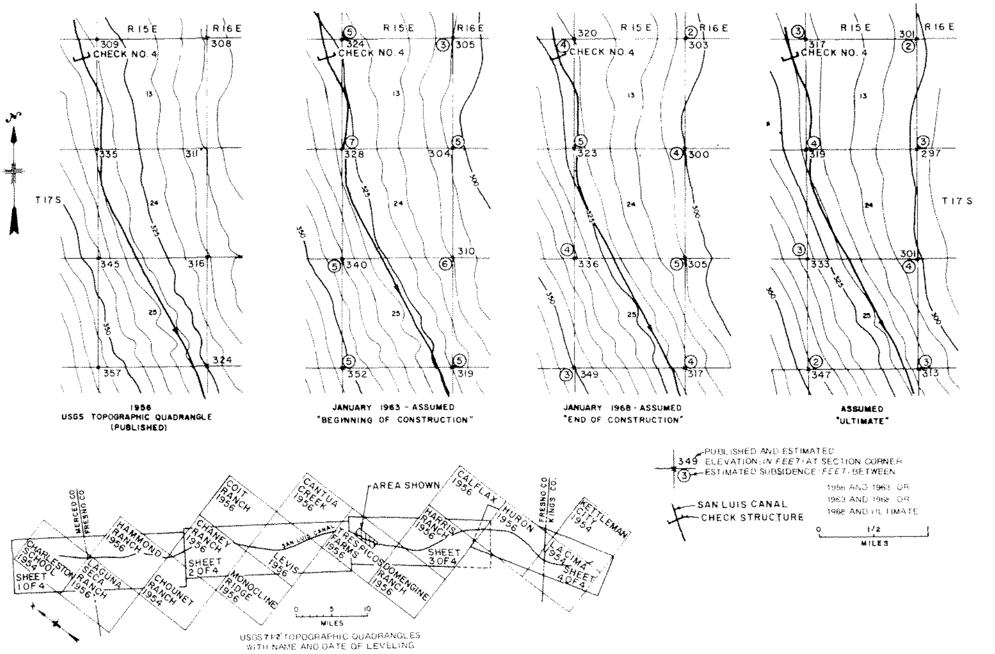

Figure 5. - San Luis Canal - An example of 1961 estimates of ultimate subsidence.

of ground-water overdraft, and (2) the subsequent residual subsidence would amount to about 10 percent of the total (past and future) active subsidence. Two datings of the end of overdraft (1968 and 1973) were considered because of the uncertainty of construction of the distribution system, changes of crop patterns, etc. The "1973" datum was assumed to duplicate ultimate conditions of the project.

Data obtained from the 1963 estimates (fig. 6) indicated that the estimates based on available subsidence rates ranged from 0.15 m to 4.5 m and were 0.25 to 1.5 m larger than the estimates based on the ratio between piezometric decline and subsidence. For design purposes both estimates and certain additional considerations were used to obtain some kind of "generalized values" of ultimate subsidence. These values followed between the two estimates downstream of milepost 130 and, in general, above the minimum values upstream of milepost 130 (fig. 6). The shift reflects considerations of (1) hydrocompaction, and (2) surface water deliveries by a local water district.

The generalized 1963 estimates were up to 1.4 m smaller than 1961 estimates upstream of milepost 139. Downstream of milepost 139 both estimates were, in general, rather close (fig. 9). The difference is caused probably by the effect of hydrocompaction and by the use of more up-to-date subsidence rates in 1963 estimates.

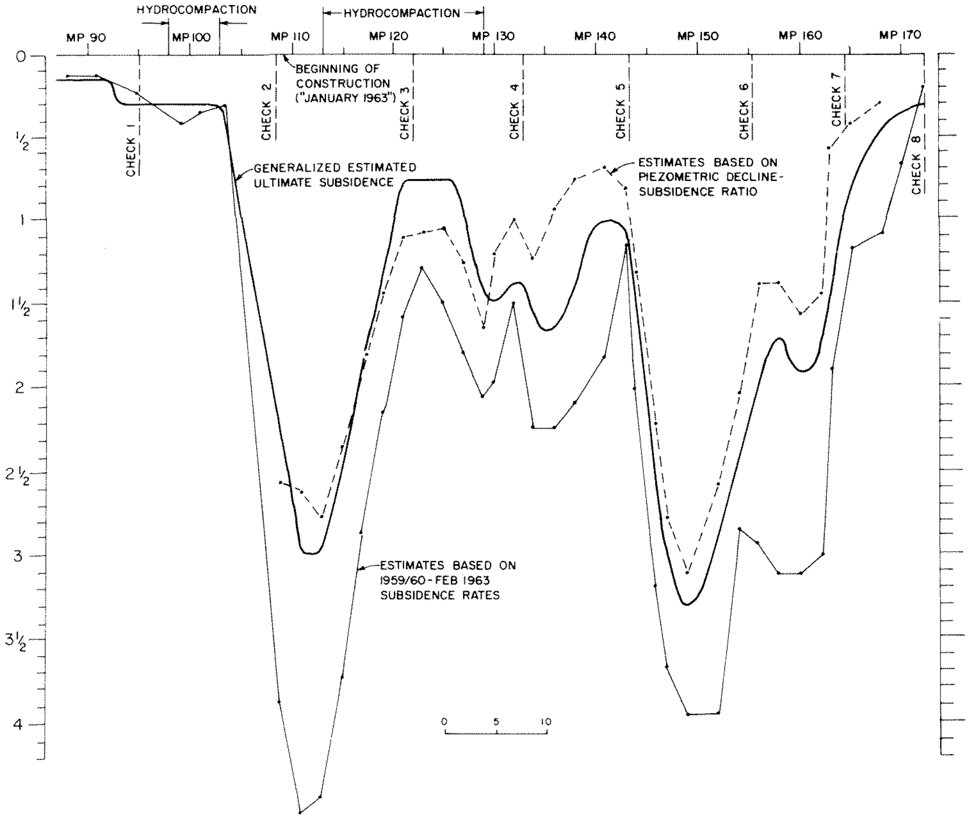

Figure 6. - San Luis Canal - 1963 estimates of ultimate subsidence. Simplified graphs.

The above estimates were used as guidelines by engineers in design of the canal by providing 0.3 to 2.7 m of extra freeboard on top of the normal 0.9 m freeboard (fig. 7). This additional freeboard was designed to compensate for the anticipated subsidence. In addition to this, in the area of maximum subsidence, the invert was placed 0.6 m above the designed grade for a distance of 3.27 miles between mileposts 109.90 and 113.17.

In general, the additional freeboard was sufficient to compensate for construction and post-construction subsidence. The notable deficiency of the extra freeboard occurred near check No. 4 with the designed freeboard of 1.8 m (including 0.9 m of "normal freeboard"). The total post-construction subsidence here, based on 1963 estimates, was 1.6 m. An additional freeboard ranging from about 0.9 to 1.2 m was added as required in this subreach at the end of construction.

No permanent benchmark net was established along the canal prior to or during its construction because of right-of-way and other technical reasons. Amounts of subsidence along the alignment during the construction as shown on figure 9 were therefore obtained graphically from an interpolation of subsidence contour maps. They range from about 0.05 m to 1.2 m.

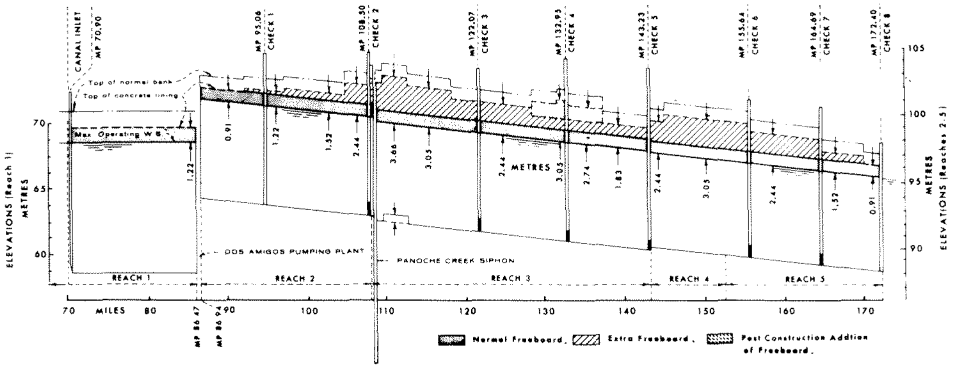

Figure 7. - San Luis Canal - Extra freeboard provided to compensate for anticipated subsidence.

The canal construction was carried on in 5 individual reaches from 1963 to 1968 and elevations of all reference and construction benchmarks within each of the reaches were "frozen" shortly before their construction. No subsidence was taken into account after such "freezing." Freezing dates for individual reaches were taken into account for estimates of freeboard lost during the construction period.

Partial delivery of canal water started in 1968, progressively increased with completion of the distribution system, gradually arrested overdraft of ground water, raised piezometric levels, and eventually stopped active subsidence. The changes were affected by delays in completion of distribution pipelines.

Some 570 benchmarks were established along the canal after its completion. Some of them have been periodically releveled. The levelings provided good data on residual subsidence along the canal. Several estimates of ultimate residual subsidence were made in 1970, 1972, and 1973 for up to 126 benchmarks using a specially developed rapid semigraphic method of calculation of ultimate amounts of residual subsidence (Prokopovich, 1971 and 1975). Generalized results of calculations ranged from traces to 0.3 m (fig. 8). Local conditions, for example, an excessive foundation settling at some bridges, are not included on the graph.

The latest available data indicate that subsidence rates along the canal have progressively declined and are now very small, generally less than 3 cm/yr. Such small and continuously declining rates probably will create no major operational problems. Minor tectonic (?) movements of reference benchmarks in the Coast Ranges interfere with adjustments of elevation of canal benchmarks and make any future recalculations of ultimate subsidence rather suspect.

A comparison of 1961, 1963, and 1972 estimates (fig. 9) indicates that: (1) the general trend of reaches of maximum and minimum subsidence was basically correct, (2) the 1963 estimates, except two reaches (MP 116-138 and 163-172) were generally higher than actual subsidence. The over-estimates are probably due to (1) an end of overdraft prior to the completion of the canal in its northern reach, (2) rapid post-construction recovery of piezometric levels (which diminished the effective loading and amounts of residual subsidence), and (3) interpretive character of subsidence contour maps. Regardless of these deficiencies, the estimates provided a reasonably good geologic background for designers, i.e., served their basic purpose.

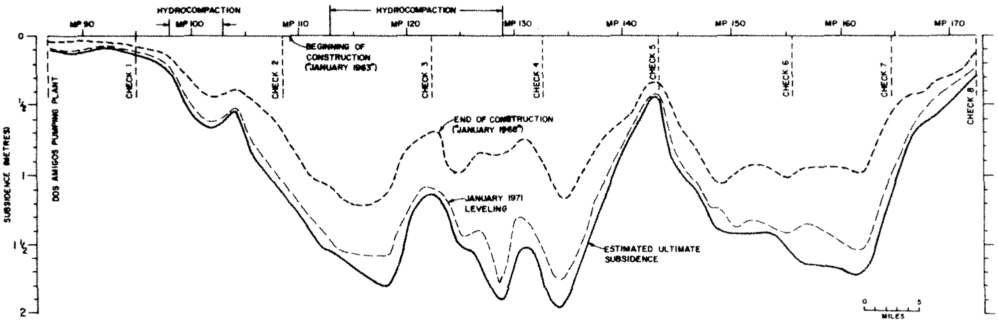

Figure 8. - San Luis Canal - Simplified graphs showing subsidence during and after construction. 1972 estimate.

DISCUSSION

Water is one of the most important natural resources on earth. The present great demand for water will increase in the future with growing population, agriculture, and industry. Future rapid development of ground water basins should be expected. Such development probably will lead to an increase of land subsidence (Prokopovich, 1972).

Many of the subsiding areas are or will be associated with existing or proposed water conveyance canals. The estimates of ultimate amounts of subsidence will be needed for proper rehabilitation of existing canals, pumping plants and other hydraulic structures, and for design of new structures. Bureau of Reclamation experience with two major canals in the San Joaquin Valley indicates that with proper historical data, particularly leveling records, supported by some experience and a little bit of "luck"

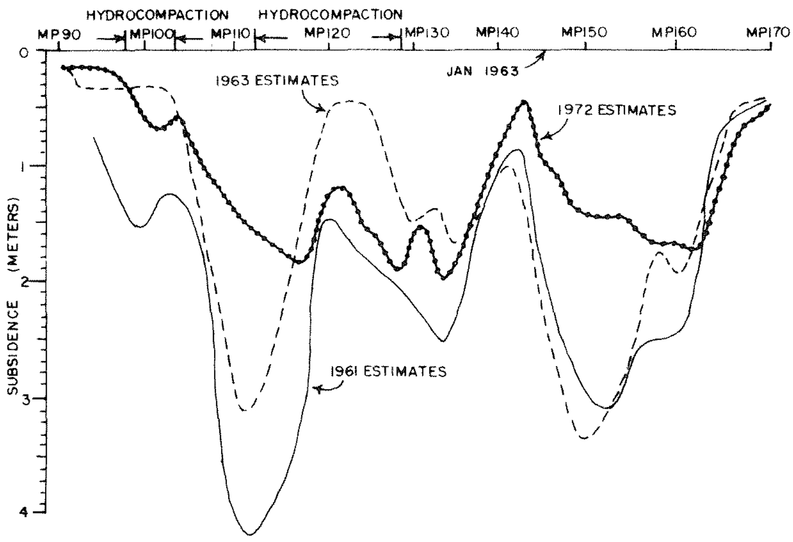

Figure 9. - San Luis Canal - A comparison of 1961, 1963, and 1972 ("final") generalized predictions of ultimate subsidence.

the ultimate amounts of subsidence can be reasonably estimated for design, construction, and rehabilitation purposes.

Calculations of "residual subsidence" provide acceptably accurate values, particularly for benchmarks with relatively large subsidence rates. Such calculations require at least three levelings. For benchmarks with small subsidence rates, the calculation may be "contaminated" by adjustment corrections, and other "noise" factors.

Estimates of ultimate "active subsidence" are less certain. Complicating factors are the future ground-water developments, particularly termination of overdraft and character of residual subsidence. Such estimates require a basic knowledge of local geology and the economic and political factors which control construction schedules. For example, ultimate water requirements are controlled by changes of crops, farming patterns, weather conditions and their periodic changes, cost of pumping, cost of farm products, etc. Historical data on past subsidence, changes of piezometric levels, and geographic spread of water usage could be particularly valuable for predictions.

References

Bailey, E. H., Editor, 1966, Geology of Northern California: California Division of Mines and Geology, Bull. 190, 507 p.

Bolt, B. A., W. L. Horn, G. A. MacDonald, and R. F. Scott, 1975, Geological hazards: Springer-Verlag, New York, Heidelberg, Berlin, 328 p.

Bull, W. B., 1964, Alluvial fans and near-surface subsidence in Western Fresno County, California: Studies of Land Subsidence, U.S. Geological Survey Professional Paper 437-A, p. A72.

Bull, W. B., and R. E. Miller, 1975, Land subsidence due to ground-water withdrawal in the Los Banos-Kettleman City area, California, Part 1: Changes in the hydrologic environment conducive to subsidence, U.S. Geological Survey Professional Paper 437-E, p. E71.

Gibbs, H. J., and F. B. Larcom, 1956, Report on a laboratory consolidation study for deep-seated land subsidence, San Joaquin Valley, California: Earth Laboratory Report EM-468, U.S. Department of the Interior, Bureau of Reclamation, Denver, Colorado, 11 p.

Gibbs, H. J., 1959, A laboratory testing study of land subsidence: Earth Laboratory Report No. EM-564 (mimeographed), U.S. Department of the Interior, Bureau of Reclamation, Denver, Colorado, 10 p.

Miller, R. E., 1961, Compaction of an aquifer system computed from consolidation tests and decline head: USGS Professional Paper 424B, p. B54-B58.

Poland, J. F., and G. H. Davis, 1969, Land subsidence due to withdrawal of fluids: Reviews in Engineering Geology II, Geological Society of America, Boulder, Colorado, p. 187-269.

Poland, J. F., B. E. Lofgren, R. L. Ireland, and R. G. Pugh, 1975, Land subsidence in the San Joaquin Valley, California, as of 1972: U.S. Geological Survey Professional Paper 437-H, p. H-78.

Prokopovich, N., 1969A, Prediction of future subsidence along Delta-Mendota and San Luis Canals, Western San Joaquin Valley, California: AIHS-UNESCO, Actes du Colloque de Tokyo, Affaissement du Sol, Association Internationale d'Hydrologie Scientifique, Publication 89, v.2, p. 600-610.

Prokopovich, N., 1969B, Land subsidence along Delta-Mendota Canal, California: Rock Mechanics, v.1, p. 134-144.

Prokopovich, N., 1971, Predictions of ultimate residual subsidence along San Luis Canal, California, Fourth Asian Regional Conference on Soil Mechanics and Foundation Engineering: Proceedings, Bangkok, Thailand, v.1, p. 67-73.

Prokopovich, N., 1972, Land Subsidence and population growth: 24th International Geological Congress, Canada, 1972, Section 13, Engineering Geology, Montreal, p. 44-54.

Prokopovich, N., 1975, Past and future subsidence along San Luis Drain, San Joaquin Valley, California: Association of Engineering Geologists Bulletin, Winter 1975, v.12, No. 1, p. 1-22.

U.S. Bureau of Reclamation, 1959, Delta-Mendota Canal, Technical record of design and construction: Department of the Interior, 180 p.

USBR, 1961, Central Valley Project: Reclamation Project Data, U.S. Government Printing Office, Washington, D.C., p. 92-112.

USBR, 1966, Central Valley Project - San Luis Unit: Reclamation Project Data (Supplement), U.S. Government Printing Office, Washington, D.C., p. 29-34.

USBR, 1974, San Luis Unit, Technical record of design and construction, v.1, History, general description and geology, U.S. Department of the Interior, Bureau of Reclamation: 164 p.

Publication n°121 of the International Association of Hydrological Sciences
Proceedings of the Anaheim Symposium, December 1976

PREDICTION AND NUMERICAL SIMULATION OF SUBSIDENCE ASSOCIATED WITH PROPOSED GROUNDWATER WITHDRAWAL IN THE TULAROSA BASIN, NEW MEXICO

J. R. MacMillan, R. L. Naff and L. W. Gelhar
Geoscience Department, New Mexico Institute of Mining and Technology
Socorro, New Mexico 87801

Abstract

Feasibility studies propose withdrawal of large volumes of saline groundwater in the Tularosa Basin, south-central New Mexico. The objective of this study is to numerically model the potential decline in elevation of the water table and land surface in a relatively undeveloped phreatic aquifer with little natural recharge.

We used an existing numerical flow model to predict drawdown; we developed a model equation to predict ultimate subsidence. The combined model equations require estimates of specific yield, average hydraulic conductivity, aquifer thickness, and compressibility and fraction of clay units in the aquifer as input. We also specify no flow boundaries to the aquifer and the pumped discharge per unit area required to meet assumed total water production. A computer program, using implicit finite difference representations of the governing equations, gives output in the form of maps of the predicted drawdown and subsidence at specified intervals of time.

Parameterization of the input variables is uncertain due to limited field data so that estimates of the magnitude of predicted drawdown and subsidence may be subject to significant error. However the pattern of drawdown and subsidence appears realistic and the significant aspect of the study is the quantitative treatment of land subsidence as a potential hazard. Numerical simulation of the combined model equations permits variable input, well field design or discharge and is a versatile tool to evaluate the effects of potential drawdown and subsidence prior to final decisions on site suitability.

Introduction

The Tularosa Basin in south-central New Mexico has recently been the site of feasibility studies which propose withdrawal of large volumes of saline groundwater. As a semi-arid climate keeps natural recharge of the basin-fill small, potential decline of the water table could be significant and land subsidence due to fluid withdrawal might become a substantial hazard.

The objective of this study is to numerically model the potential decline in elevation of the water table and land surface as a function of geographic position. A significant aspect of the study is the quantitative treatment of land subsidence as a potential hazard. Numerical simulations may be used to plan changes in well field design and discharge, to estimate drawdown and subsidence and to evaluate their effects on existing or planned structures prior to site selection. Due to low population density and generally poor water quality, groundwater resources in the Tularosa Basin are currently little utilized; thus a challenging aspect of this study is the parameterization of the hydrogeologic properties of the aquifer with limited field data.

Regional Hydrogeologic Setting

The Tularosa Basin is a north-south trending topographic and structural trough, typical in most respects of the Basin and Range Geomorphic Province of the southwestern United States. The average annual precipitation in the Tularosa Basin ranges from less than 25 cm (10 in.) at the basin center to over 63 cm (25 in.) in the adjacent mountains. The basin has closed interior drainage; surface runoff occurs mainly as intermittent flows associated with intense summer thunderstorms. A few perennial streams occur in the Sacramento Mountains on the east side of the basin.

The basin-fill ranges in age from Miocene to Recent; during this time high-angle, mostly normal faulting differentiated the region into a down-dropped, fault-trough basin and adjacent fault-block mountains. Playa lakes occupy the present basin floor (at an elevation of 1200 m, 4000 ft.) with eolian dunes on the east (downwind) side. The surfaces of individual and coallesced alluvial fans surround the basin floor and rise to 1500 m (5000 ft.) at the base of the mountains. Mountain escarpments, rising to 2400 m (8000 ft.), expose primarily Paleozoic and Mesozoic sedimentary rocks and late Mesozoic to middle Tertiary intrusive and extrusive igneous rocks. Near exposures of bedrock, alluvial fan deposits consist of coarse sand and gravel (braided channel and sheetflood deposits) interbedded with discontinuous, very poorly sorted, clay-rich debris flow deposits. The coarse-grained units tend to be porous and permeable; they serve as aquifers and well yields are as high as 6000 m^3/da. (1000 gpm; McLean, 1970). Lake bed deposits at the basin center contain nearly pure clay beds, are relatively impermeable and subject to compaction. Well yields in the basin center are generally less than 1600 m^3/da. (300 gpm; McLean, 1970). A gradation between these extremes in hydrogeologic characteristics occurs between the basin center and mountain front.

Most of these features are typical of basins in the southwestern United States, but the Tularosa Basin is somewhat unique because of the abundance of gypsum in the Paleozoic bedrock. The gypsum is recycled to the basin-fill by transportation as dissolved load and bedload from the mountains to sites of deposition in the basin.

The quality of the groundwater is controlled by the pattern of flow through the basin-fill. Recharge occurs near the mountain fronts so that good quality groundwater (dissolved solids <1000 mg/l) occupies a near surface, wedge-shaped zone thinning toward the basin center and underlain by more saline groundwater near the mountain front. The water table slopes toward the basin center; groundwater slowly migrates through the gypsiferous basin-fill, becoming more mineralized (dissolved solids >30,000 mg/l) toward the basin center where it is lost to evaporation. Consequently the playa lakes form (gypsum) salt-flats during dry periods and reworking by wind produces dunes composed of nearly pure gypsum--the "White Sands" of New Mexico.

<u>Flow and Subsidence Model</u>

We assumed the following sequence of water requirements:

Years 1 through 5	9.25×10^7 m^3/yr	(75,000 acre-ft/yr)
6 through 10	18.5×10^7 m^3/yr	(150,000 acre-ft/yr)
11 through 15	27.7×10^7 m^3/yr	(225,000 acre-ft/yr)
16 through 25	37.0×10^7 m^3/yr	(300,000 acre-ft/yr)

The well field, consisting of wells placed in a .63 km (1 mi) square grid pattern, would initially cover a 12.8 by 16 km (8 by 10 mi) area and expand southward by successively adding 12.8 by 16 km blocks to meet the increasing water requirements. Each well would pump about 3160 m^3/da. (580 gpm).

The aquifer flow model is based on the equation for nearly horizontal flow in a phreatic (water table) aquifer (e.g., Bear, 1972, p. 376)

$$\frac{\partial}{\partial x}\left(T\,\frac{\partial h}{\partial x}\right) + \frac{\partial}{\partial y}\left(T\,\frac{\partial h}{\partial y}\right) + N = S_y\,\frac{\partial h}{\partial t} \tag{1}$$

where h(x,y,t) is the water table elevation, (x,y) are horizontal coordi-

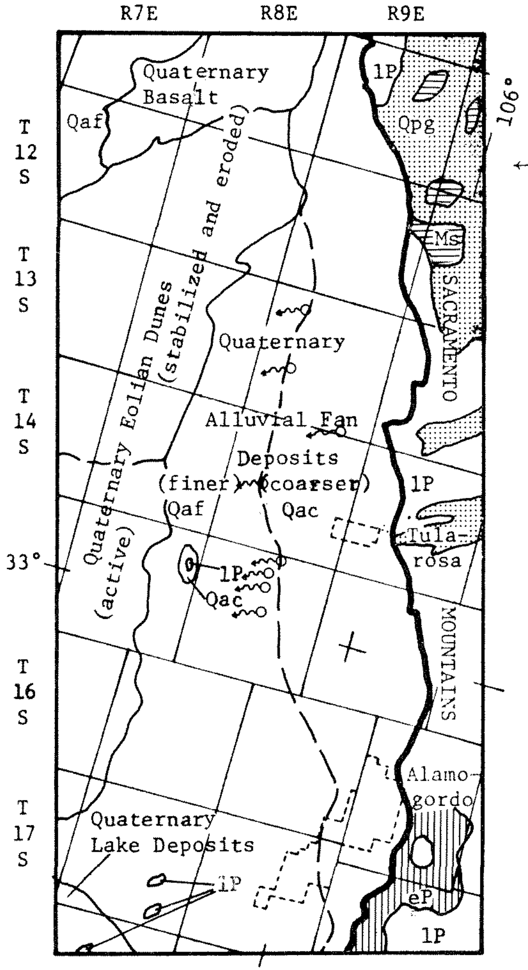

Figure 1
GENERALIZED SURFACE GEOLOGY

Qpg	Quaternary Pediment Gravel
Ms	Mesozoic Sedimentary Rocks
1P	late Paleozoic Rocks
eP	early Paleozoic Rocks
	Spring

Figure 2
THICKNESS OF UNCONFINED AQUIFER
Contours solid in areas of sufficient data, dashed where largely inferred.
Contours at:

0 ft	0 m
200 ft	60 m
700 ft	210 m
1350 ft	410 m

SCALE
Miles
0 2 4 6 8 10 12
0 4 8 12 16 20
Kilometers

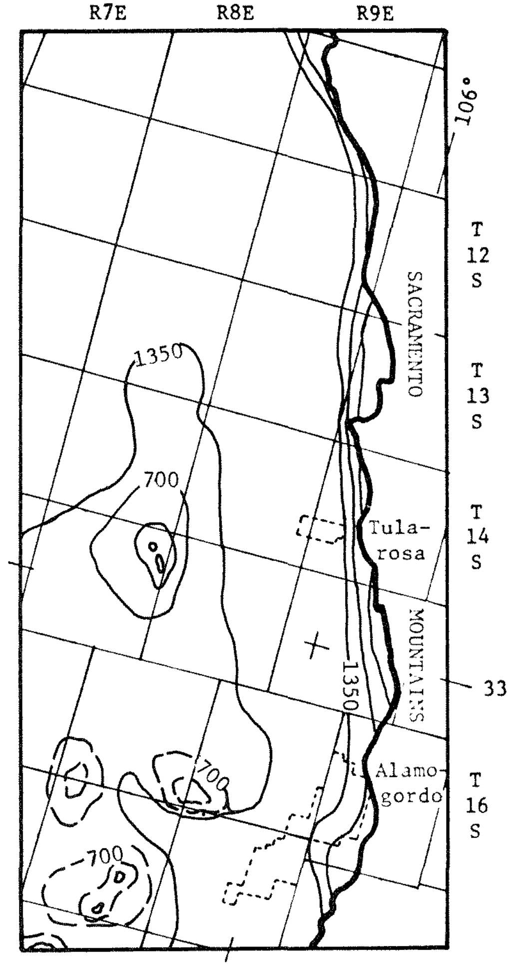

nates, t is time, T is transmissivity of the aquifer, S_y is specific yield, and N is rate of inflow to the aquifer. Transmissivity is the product of average hydraulic conductivity $\bar{K}$ and aquifer thickness m; for a phreatic aquifer the transmissivity is

$$T = \bar{K}m = \bar{K}(h-B) \tag{2}$$

where B is the elevation of the bottom of the aquifer. If the drawdown is small compared to aquifer thickness, the aquifer flow equation can be expressed in terms of the drawdown s from some initial ambient condition as

$$\frac{\partial}{\partial x}\left(T\frac{\partial s}{\partial x}\right) + \frac{\partial}{\partial y}\left(T\frac{\partial s}{\partial y}\right) + q = S_y\frac{\partial s}{\partial t} \tag{3}$$

where q is the pumped discharge per unit area of the well field. Equation 3 forms the basis for the drawdown model.

The aquifer model equation is solved using an implicit finite difference representation of the governing equation; a revised version of the computer program given by Pinder (1970) is used for the numerical simulations. The program is based on a rectangular array of nodal points at which $\bar{K}$, S_y, m and pumpage must be specified. Constant head or flow conditions can be specified at boundary nodes. From this input, the program computes the drawdown at each nodal point at a selected value of time.

Subsidence, as modelled in this study, is the result of an increase in effective stress on clay units within an aquifer system. The total stress within an aquifer system is regarded as equal to the sum of the effective stress and the fluid pressure (or neutral stress). Total stress is considered approximately constant for any point in the aquifer system; a decrease in pressure must result in a corresponding increase in effective stress. Average head declines obtained from the flow model allow prediction of increases in effective stress in the aquifer system which forces water from the pores of nearly pure clay units into more permeable units. The decrease in thickness of each clay unit, due to inelastic compression, is proportional to the volume of water forced from it, and the total (ultimate) subsidence of the land surface is approximately equal to the sum of the compressions of all clay units.

The basic subsidence prediction equation derived by Domenico and Mifflen (1965) and the effective stress relationship derived by Poland and Davis (in Varnes and Kiersch, 1969) for unconfined aquifers are used to obtain the following equation for ultimate subsidence:

$$\delta = \alpha\gamma(1 - S_y)\ C\ m\ s\ [1 - \frac{s}{2m}] \tag{4}$$

where δ is land-surface subsidence, α is compressibility of clay units, γ is unit weight of water, C is fraction clay material in the aquifer; other symbols are previously defined. The equation assumes complete communication of all permeable materials and an approximately uniform distribution of clay units in any vertical section, and neglects transient effects in the compaction process. Estimates of α and C are input; other variables are obtained from the flow model. This model equation is a rather simplified representation of the actual process but available subsurface data does not warrant further refinement.

Hydrogeology of the Study Area

The study area, located in the northeastern portion of the Tularosa Basin adjacent to the Sacramento Mountains, is rectangular, approximately 64 km (40 mi) by 32 km (20 mi). The long dimension trends north-northwest, parallel to the fault-controlled mountain front.

The surface geology of the study area (Fig. 1) displays the expected

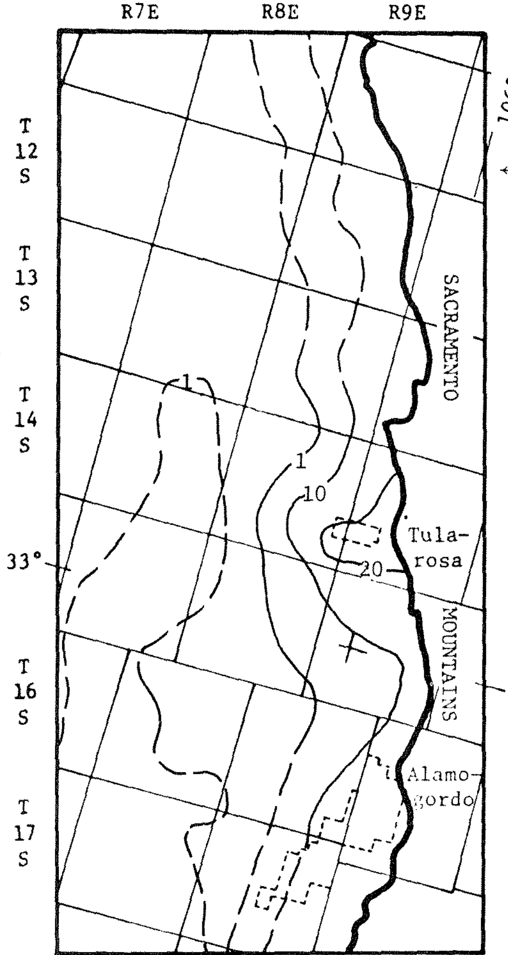

Figure 3
HYDRAULIC CONDUCTIVITY
(in upper 300 ft (90m) of aquifer)
Contours at:

1 ft/da	0.3 m/da
10 ft/da	3.0 m/da
20 ft/da	6.0 m/da

Figure 4
FACTION OF CLAY
(in upper 300 ft (90m) of aquifer)
Contours at:
0.2
0.4
0.6

SCALE
Miles
0 2 4 6 8 10 12
0 4 8 12 16 20
Kilometers

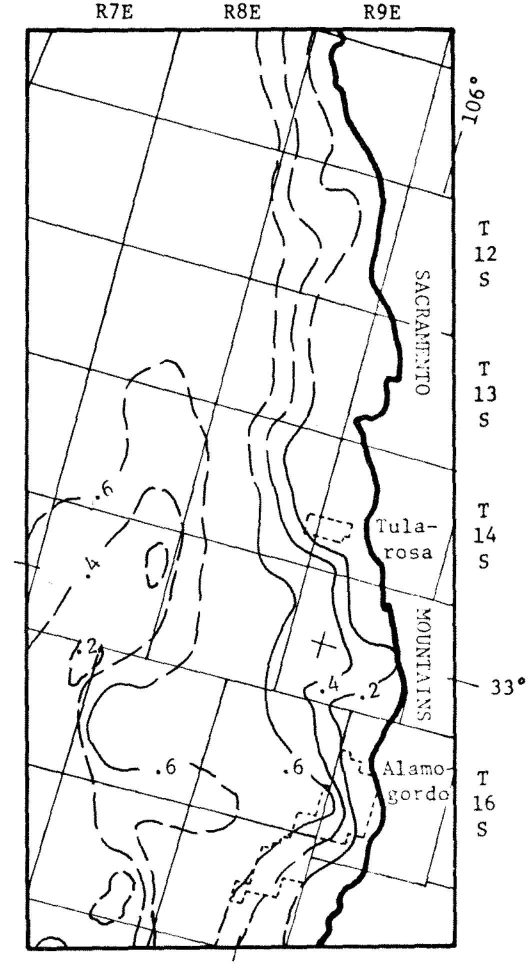

distribution of sediment types. A zone of alluvial fan deposits, which become finer-grained toward the basin center, is adjacent to the mountain front. A zone of eolian dune deposits separates alluvial fan deposits from lake bed deposits; the latter occur in the southwestern corner of Figure 1.

A few outcrops of Paleozoic bedrock, aligned north-south, occur approximately 16 km (10 mi) from the front of the Sacramento Mountains and interrupt this spatial distribution of sediment types. These outcrops indicate the occurrence of a subsurface ridge of bedrock. Both the outcrops and the subsurface ridge have supplied debris to the basin-fill as has the Sacramento Mountains, and consequently they are flanked by coarse-grained alluvial fan deposits.

It is apparent from Figure 1 that the hydrogeologic characteristics of the basin-fill vary rapidly as a function of geographic location. A similar lateral distribution of sediment types was probably deposited in the past. However, the location and areal extent of each sediment type have probably shifted laterally in time as a function of the balance between erosion and deposition, which in turn is controlled by the climatic and tectonic history of the region. Consequently, the subsurface arrangement of sediment types varies complexly.

Parameterization of Hydrogeologic Variables

The aquifer system is regarded as the saturated portion of the basin-fill above any laterally extensive clay unit in the subsurface. One of the few deep wells in the study area is located a few km southwest of Tularosa and penetrates 580 m (1900 ft) of basin-fill. Geophysical logs indicate the occurrence of several clay-rich, very low porosity units at depths greater than 410 m (1350 ft). We believe these units are lake-bed deposits which should be laterally extensive and confine deeper flow systems. Consequently we arbitrarily define the maximum thickness of the unconfined aquifer to be 410 m.

Using available drill hole, seismic refraction and gravity surveys, we constructed an isopach (thickness) map of the basin-fill in the study area. We also constructed a map of the water table, based on 1955 water level data, which defines the top of the unconfined aquifer. Using these maps and the arbitrarily defined maximum thickness, a map of the thickness of the unconfined aquifer can be constructed (Fig. 2).

Based on a method outlined by Logan (1964), hydraulic conductivities are estimated from specific capacity data obtained from pumping tests on several wells in the study area. Figure 3 shows the areal variability in conductivity. Most of these wells are located in the eastern portion of the study area and are shallow (90 m, 300 ft); we have of necessity assigned this distribution of conductivities to the entire thickness of the aquifer system.

Estimates of specific yield of the basin-fill are reported for well fields in or near the study area. Garza and McLean (1972) obtained an estimate of 8% for a well field near Tularosa by comparing the 1955 and 1969 cones of depression with estimated pumpage. Hood (1957) reported an average value of 8.5% based on individual well test methods in a field south of Alamogordo. These values are within the range of those reported for similar basin-fill deposits in the Southwest (Johnson, 1967). We selected a specific yield of 10% as a reasonable value and applied it to the entire aquifer in the study area.

We specify no flow boundaries to the model aquifer because the magnitude of the assumed pumpage from the well field is much greater than natural recharge, even along the range front boundary. Except for the eastern boundary, the margins of the well field are 8 km (5 mi) from the boundary nodes so that the effect of subsurface inflow to the study area would be

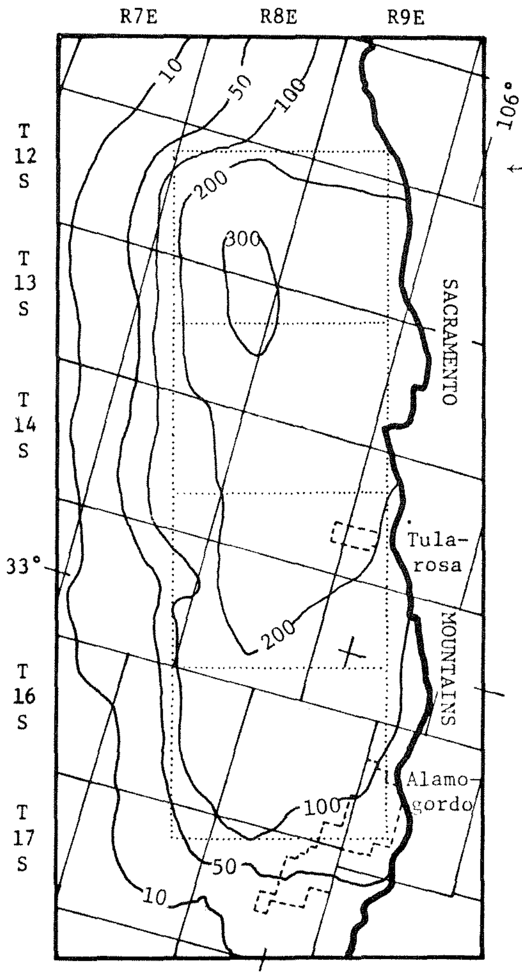

← Figure 5

PREDICTED DRAWDOWN AFTER 25 YEARS

Contours at:

10 ft	3 m
50 ft	15 m
100 ft	30 m
200 ft	60 m
300 ft	90 m

Dotted lines outline boundary of expanding well field

Figure 6 →

PREDICTED SUBSIDENCE AFTER 25 YEARS

Contours at:

1 ft	0.3 m
5 ft	1.5 m
10 ft	3.0 m
25 ft	7.5 m
35 ft	10.0 m

SCALE

Miles

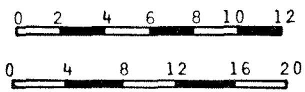

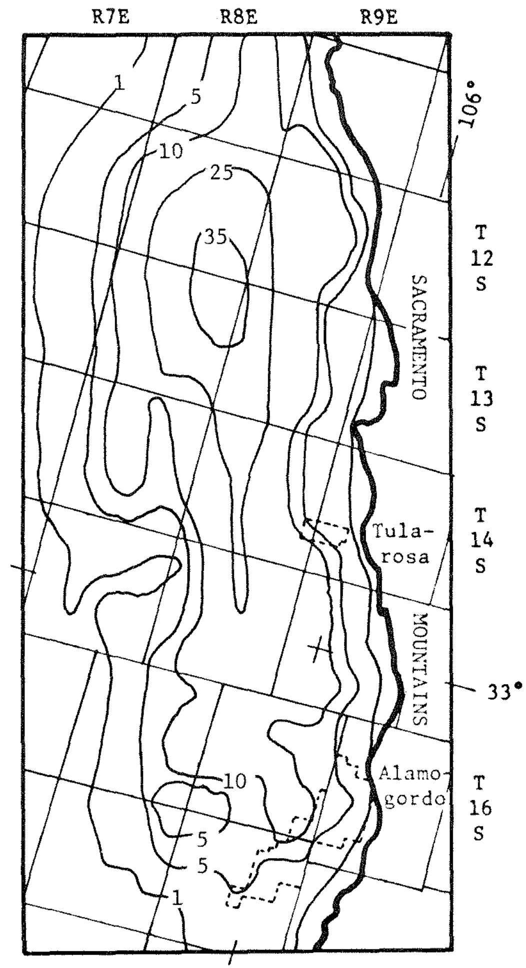

minimal compared to pumped discharge. The initial condition of the model aquifer equation (3) is one of no drawdown.

Additional variables required as input to the subsidence equation (4) is fraction of compressible (nearly pure clay) units in the aquifer and their compressibility. We processed driller's logs from the study area to obtain a map of fraction of the upper 90 m (300 ft) of the basin-fill which is reported as "clay" (Fig. 4). Few wells penetrated more than 90 m and of necessity we assigned the same spatial variability to the entire aquifer thickness.

We obtained the results of consolidation tests on shallow core samples of "silty clay" with formation water from the southwestern corner of the study area. We calculated strain-stress ratios in the stress range of 0.98 to 9.8 km/cm^2 (1 to 10 $tons/ft^2$) and obtained compressibilities ranging from 5.1×10^{-3} to 6.8×10^{-3} cm^2/kg (2.5×10^{-6} to 3.3×10^{-6} ft^2/lb) with a median of 5.9×10^{-3} (2.9×10^{-6}). This range of values is comparable to that encountered by Domenico (1972) near Las Vegas, Nevada; the median is close to the value used by Helm (1975) in model studies of the San Joaquin Valley, California. We assigned the median value to all clay units in the aquifer.

Results and Discussion

Figures 5 and 6 show the areal variability in predicted drawdown and subsidence, respectively, after 25 years of pumpage at the assumed rates. The marked asymmetry in the north-south direction of the pattern of drawdown and subsidence is primarily due to pumpage from the northern portion over the full 25 years versus only 10 years in the southern portion. The asymmetry in the east-west direction of drawdown (Fig. 5) is primarily due to the greater relative abundance of low conductivity, clay-rich units toward the west. Drawdown is large in areas where both pumpage and transmissivity are relatively large (though not necessarily at their individual maxima).

Subsidence (Fig. 6) is large where both drawdown and fraction of compressible (clay) units are relatively large. Asymmetry in the east-west direction of the areal distribution of subsidence is not marked because of the inverse spatial distribution of high drawdown and fraction of compressible units. That is, drawdown tends to be large near the mountain front where fraction of compressible clay units is low.

We regard the pattern of areal variability in drawdown and subsidence of these simulations as reasonable. However, the magnitude of the predicted drawdown and subsidence at a specific location may be subject to significant error because of the difficulty of parameterization of the input variables. Studies of observed subsidence attributed to fluid withdrawal in other basins in the Southwest suggest the predicted maximum subsidence, on the order of 12 m (40 ft), may be overestimated by a factor of up to 2, most likely due to an overestimate of fraction of compressible material in the aquifer. Additional simulations can be produced using reasonable ranges in input data. Moreover, simulations with variable well field design and pumpage as a function of time and space can be utilized to test whether the sites of maximum drawdown or subsidence or high gradients in subsidence can be shifted to areas where they would not pose a significant problem to existing or planned structures before a final decision on site suitability is made.

References

Bear, J., 1972, Dynamics of fluids in porous media: American Elsevier Pub. Co., Inc., New York, 764 p.

Domenico, P. A., 1972, Concepts and models in groundwater hydrology: McGraw-Hill Book Co., New York, 405 p.

Domenico, P. A., and Mifflen, M. D., 1965, Water from low-permeability sediments and land subsidence: Water Resources Research, v. 1, n. 4, 563-576.

Garza, S. and McLean, J. S., 1972, Fresh water resources of the east side of the Tularosa Basin, New Mexico: U.S. Geol. Surv., Openfile Rpt., 126 p.

Helm, D. C., 1975, One-dimensional simulation of aquifer system compaction near Pixley, California, 1. Constant parameters: Water Resources Research, v. 11, n. 3, 465-478.

Hood, J. W., 1957, Ground-water resources and related geology in the vicinity of Holloman Air Force Base, Otero County, New Mexico: U.S. Geol. Surv. Report to the U.S. Army Corps of Engineers, 397 p.

Johnson, A. I., 1967, Specific yield - compilation of specific yields for various materials: U.S. Geol. Surv., Water-Supply Paper 1662-D, 74 p.

Logan, J., 1964, Estimating transmissibilities from routine production tests of water wells: Ground Water, v. 2, n. 1, 35-37.

McLean, J. S., 1970, Saline ground-water resources of the Tularosa Basin, New Mexico: Office of Saline Water, Research and Development Progress Rpt. 561, 128 p.

Pinder, G. F., 1970, A digital model for aquifer evaluation: U.S. Geol. Surv. Techniques of Water Resources Investigations Series, Book 7, Chapt. C1, 18 p.

Varnes, D. J., and Kiersch, G., eds., 1969, Reviews in Engineering Geol. II: Geol. Soc. Am., 350 p.

Publication n°121 of the International Association of Hydrological Sciences
Proceedings of the Anaheim Symposium, December 1976

LEGAL IMPLICATIONS OF LAND SUBSIDENCE IN THE SAN JOAQUIN VALLEY

Rita Singer
Regional Solicitor's Office, Department of the Interior, Sacramento, California

Abstract

Land subsidence due to man's change of the natural hydrologic regime, recognized for the past couple of decades, has already caused disastrous environmental changes. In addition to technical methods by which to anticipate, ameliorate or repair these damages, consideration of legal means available to protect or rehabilitate the environment is perhaps overdue. Are the existing laws inadequate? If so, what kind of laws should be enacted? A difficult aspect of the problem is the fact that frequently the effects are not evident until considerable time has elapsed after the causative action occurred. Unforeseen legal and physical ramifications may occur because of the difficulty of identifying the causative factors and assigning responsibility to individuals. In California both the Federal and State governments have extensive interests in these questions.

Subsidence of the type related to activities of man might be subject to regulations. Should there, in addition, be pecuniary liability for causing damage to another's property? Should the injunctive process be available?

Land subsidence has an environmental impact and is recognized as a form of pollution. The State and Federal government have, in their respective environmental protection laws, required that adverse environmental impacts be taken into account before major activities are undertaken. If sufficient attention is paid to this problem, a great deal can be accomplished through this mechanism. Another available tool is the requirement to institute ground-water recharge in contracts for water service which are negotiated with local government agencies. Another indication of the Federal recognition of the subsidence problem is contained in the amendments to S. 586 and H.R. 3981, the Coastal Zone Management bills, which authorize loans and grants to states for planning and ameliorating or compensating for impacts due to oil and gas drilling. Perhaps similar State and local legislation is required to take care of the problems resulting from water withdrawals and hydrocompaction. A start has been made in southern California with State regulation of ground-water pumping. Los Angeles County has enacted ordinances requiring repressurizing of oil and gas fields. Since individual liability under the normal common-law tort rules would be difficult to apply, it is very likely that new statutory rules are needed to control the problem. The recognition of the extent of the damage both physical and monetary should make possible favorable consideration from Congress and the State Legislature on a broad basis.

Background

Land subsidence from uncontrolled pumping of water from the underground reservoirs for intensive agricultural purposes in the San Joaquin Valley has been occurring since the 1930's. (Poland, Lofgren, Ireland, and Pugh, 1975.) It is defined as the displacement of the ground surface arising from subsurface causes. (Bolt, Horn, Macdonald, Scott, 1975.) It can be observed as a bowl shaped downward surface displacement. It is primarily caused by man's activities at and below the earth's surface, in this case the withdrawal of water from subsurface rock layers. The extent to which the ground surface subsides depends on the amount by which the water level is lowered, the compressibility and depth of the layer from which the water is extracted, and the stiffness or rigidity of the overlying soil materials. (Bolt, Horn, Macdonald, Scott, 1975.) Once subsidence occurs as a result of pumping water from a confined aquifer, it is irreversible although the process can be retarded or halted.

For a relatively long time, the processes which lead to subsidence may be unobserved as they occur over periods measured in tens of years and because of the large areas affected. (Poland, Lofgren, Ireland, and Pugh, 1975.) The precise detection of the amount of subsidence in an area can be accurately determined only through a surveying and leveling network with the reference to bench marks or monuments outside the area affected by the subsidence. Frequently the subsidence is noticed only long after the process causing the subsidence was initiated.

Land subsidence can cause sharp economic and cultural losses. One writer has called exogenic (occurring near the earth's surface) subsidence a form of pollution because it degrades the environment by deteriorating the underlying aquifer system. Subsidence can also result in the intrusion of salty water into the aquifer, which in fact has probably occurred in the San Joaquin Valley. (N. Prokopovich, 1974.) Recently, a news article stated that settling of the ground beneath the California Aqueduct northwest of Los Banos was the cause of a rupture in that huge facility. (The Modesto Bee, July 6, 1976.) There is at least one positive effect caused by subsidence. It helps to preconsolidate the ground-water basin deposits to their historic low-water levels, thus permitting the basin to be managed for cyclic storage to those levels. Since more information has accumulated on the situation, steps are being taken to compensate for future subsidence problems. For example, when the Bureau of Reclamation built the San Luis Canal, a joint feature of the Central Valley Project and the California Aqueduct, additional freeboard was designed into it. But several years earlier when the Delta-Mendota Canal was being constructed, possible subsidence was not taken into account, and canal lining, bridges, pipe crossings and the like, have been partially or completely flooded due to land compaction and subsidence. (N. Prokopovich, 1972.) Many other undesirable effects may occur such as development of swamps, offsetting of drainage and stream patterns, soil cracking and slumping, as well as expensive damage to private property and loss of human life. (N. Prokopovich, 1972.)

Other cosmopolitan areas which have had notable ground subsidence problems due to extraction of water are Mexico City, Shanghai, and Venice so it would be fair to say the problem is worldwide. In addition to the San Joaquin Valley in California, there are several other areas which have suffered from land subsidence due to water extraction. They are Pleasant Valley, Sacramento Valley, and Santa Clara Valley. It is apparent that in this area, subsidence is more likely to occur in basins than in uplifted areas. (N. Prokopovich, 1972.) It is evident that the problem does not arise only in arid areas although in the United States, Texas, Arizona, Colorado and Nevada have suffered from the problem. Only in Japan to date have governmental controls been instituted to control water pumpage for industrial and domestic use in order to retard the adverse effects. (N. Prokopovich, 1972.) This paper will be limited to a discussion of the legal means of dealing with the problem as it occurs in the existing agricultural setting of the San Joaquin Valley, California, an area comprising the southern half of the great Central Valley, about 400 kilometers long and 65 to 100 kilometers wide. It is a large trough between the mountain range of the Sierra Nevada on the east and the Coast Range on the west. The geological composition of the soil is well-known. (N. Prokopovich, 1976.) Maps are available which show subsidence contours along certain leveling routes beginning with data for the year 1955. Some additional data is available by extrapolation for the period 1922-1932.

Although areas which have been subjected to subsidence resulting from removal of water from the underground aquifers cannot be brought back to their previous state, there are measures which can be taken to alleviate the situation and undoubtedly with more study in the future additional methods of control will be found. (J. F. Poland, 1972.) The major means to alleviate the problem in the San Joaquin Valley has been the importation of enormous amounts of water for agricultural use. This has dramatically reduced the need for groundwater pumpage and concurrently there has been a marked decrease in the subsidence rate and a rise in the artesian head in the zone. As of 1971, half of the historic head had been restored; half of the stress on the ground-water reservoir had been eliminated. United States Geological Survey records seem to support the view that subsidence can be permanently stopped if the artesian head can be raised and maintained at a sufficiently high level. (J. F. Poland, 1972.) Importing surface water to reduce or eliminate pumping affords the opportunity to achieve this objective. However, in most San Joaquin Valley areas it cannot be expected that the imported water will seep through the Soil Zone into the water table. In fact the buildup of the water table in the overlying soil is likely to increase the stress applied to the confined aquifer system. Frequently protective and remedial measures are costly. Poland notes that an estimate as of 1971 for the Santa Clara Valley area indicated that about $9 million of public funds had been spent on levee construction and other remedial work on stream channels to prevent flooding resulting from land subsidence. In addition Leslie Salt Company had spent an unknown but substantial amount to raise and maintain its salt pond levees. Several hundred water well casings had been ruptured by the compaction of the sediments; the repair or replacement cost of the damage was estimated as at least $4 million. (J. R. Roll, 1967.)

Legal Considerations

At common law (the principles and rules, originally derived from the English legal system, which are not authorized by a legislature), a landowner has the right to lateral support from the adjoining parcels. Wharam v. Investment Underwriters, 58 Cal. App. 2d 346, 136 P.2d 363 (1943). This is a natural right incident to ownership of land. Sargent v. Jaegling, 83 Cal. App. 485, 256 P. 1116 (1927). It is an absolute obligation to the owner of adjoining property. (California Real Estate Law and Practice, 1975.) Generally the issue arises in connection with excavation on one tract which causes the adjoining tract to collapse, such as commonly occurs in connection with underground mining. Additional discussions infra will cover the rules governing oil and gas extraction. The adjoining landowner may sue for and collect damages but the cause of action arises only after an actual subsidence has occurred. Empire Star Mines v. Butler, 62 Cal. App. 2d 466, 145 P.2d 49 (1944).

By statute, the common law rule has been relaxed in California as to liability for damage resulting from excavation under certain conditions, but it does not relieve the landowner from liability for his negligent actions. California Civil Code 832. In order to invoke the protection afforded by this law, the excavating landowner must show that he has given his neighbor the requisite notice. The statute also stipulates that damages may be assessed for injury to adjoining structures as well as for injury to the land in its natural state. California Civil Code § 832(4). If a public entity is the landowner which interferes with the lateral support owed its coterminous landowner, it may be liable on a theory of strict liability or inverse condemnation. Holtz v. Superior Court, 3 Cal.3d 296, 475 P.2d 441.

In addition to the remedy afforded by a suit for damages on a tort theory, the injured landowner may petition the court for an injunction. Similarly he may get relief only after damage has been caused or after it is apparent that he will be damaged by the action already taken. Empire Star Mines v. Butler, Op. Cit. A plaintiff has the choice of either suing for damages or for an injunction but not both. Rhodes v. San Mateo Inv. Co., 130 Cal. App. 2d 116, 278 P.2d 447 (1955). A separate cause of action arises from each occurrence of subsidence, not from the excavation itself. Bellman v. Contra Costa County, 54 Cal. 2d 363, 353 P.2d 300. In order to avoid the statute of limitations, suit must be brought within three years from the date of the injury. California Code of Civil Procedure 338(2).

It should be emphasized that all of the above rules and interpretations apply to a fact pattern that has little application to the land subsidence situation which exists as a result of water extraction from the underground as typically exemplified in the San Joaquin Valley. As heretofore pointed out, land subsidence of the nature we are concerned with here, ranges over an extended area and frequently results from causes far removed from the location of the subsided area. As a matter of fact it is very unlikely that with the present technical knowledge available a direct focal relationship could be established between a negligent water extractor on one tract and damage to the property of his neighbor.

Assuming that to be the case, the question arises as to what type of legislation or other regulation should be adopted to remedy this lacuna in the law? Most of us are familiar with the recent upsurge in the laws which have been passed at all levels of government to protect the environment. To name only two of the most prominent and publicized on the federal and state level, there are the National Environmental Policy Act of 1969 (Public Law 91-190, 83 Stat. 853, 42 U.S.C. 4332 et seq.) and California's Environmental Quality Act of 1970 (Public Resources Code §§ 21000-21165). These statutes set out a policy of heightened awareness of the importance of protecting against actions constituting adverse impacts on the natural and human environment. It is true, of course, that there is not a straight-line approach to attaining this goal since frequently economic and other social factors which appear to present conflicts are involved, but it is my view that we have irreversibly adopted as a state and a nation the principle of environmental protection even if this involves significant costs. Under these statutes it may well be that possible land subsidence impacts should be taken into account in assessing the desirability of undertaking certain activities. Under the federal statute, this would apply only to federal or federally assisted activities, but California's statute applies more broadly.

If we adopt the position that the type of land subsidence which we have been discussing is a form of environmental pollution, it is not difficult to move from that point to a recommendation that the kind of additional legislation which should be considered for enactment is a broad approach to the problem, one in which the federal or state government, or both, would participate prominently in financing grants and promoting research.

Several decades ago the city of Long Beach was faced with a similar crisis in connection with the development of the Wilmington Oil Field. Harbor engineers began to observe land subsidence in the port area. By 1945, the ground in some places had sunk 4 feet. By 1951, the subsidence was proceeding at the rate of 2.4 feet per year. By 1957, some subsidence had reached a depth of 24 feet. Long Beach realized that it was literally sinking in a sea of oil. (Report on Long Beach Custodianship of State Tideland Oil Operations. City of Long Beach, Dept. of Oil Properties.) Appeals were made to the State Legislature which responded in 1958 by passing a comprehensive and evidently satisfactory bill because to this day it has not been substantially amended. The adverse effects of the oil development program were turned around in a relatively short time so that not only was subsidence halted but to some extent there has been elevation gains or rebounds. (Department of Oil Properties Fiscal Annual Report for 1969-70.) The primary method to which this success was due is the injection of water into the oil fields. In order to do this efficiently it is necessary to do it on a fieldwide basis. The new law (California Public Resources Code §§ 3315-3347) authorized state action to require the owners and operators of the oil fields to unitize their repressurizing operations and established a means of financing the program. A subsidiary benefit is the increased efficiency which unitization achieved by eliminating unnecessary wells and the increased yield from the operating wells because of the repressurized soil. To cap the list of benefits, water produced with the oil, which in the past presented a disposal problem, now is used for the injection process after being treated. Recently, when the City decided to develop its offshore oil deposits, it delayed instituting the program until subsidence had been brought under control in the onshore operations. The proposal was put to a vote of the electorate, which approved a plan to require immediate repressuring as oil development takes place. The surface elevation and reservoir conditions are constantly monitored and correlations are made with oil production and water injection activities. At the end of 1970 there were 524 injection wells in operation in the Wilmington Field, with over 1.1 million barrels of water being injected daily.

Here is a splendid example of the State's recognition of a serious problem and the direct interest of the State in arresting and ameliorating it. (California Public Resources Code § 3315.) The first section of the act sets out that legislative policy "as necessary to safeguard life, health, property, and the public welfare." When it was tested in the courts, it was upheld. Long Beach v. Vickers, 10 Cal. Rptr. 359, 358 P.2d 687 (1961). The law sets out a series of regulations and guidelines to be administered by the State Oil and Gas Supervisor, who is empowered to enforce his orders by seeking an injunction or suing for damages. In addition, wilful violations of his orders can be penalized by a fine of up to $1,000.00 a day for each violation; nor will the payment of the penalty relieve the violator from liability for damages to any other person. Public Resources Code § 3343. More recently, additional environmental protective legislation has been enacted by the California Legislature "to prevent, as far as possible, damage to life, health, property and natural resources" in oil development areas. Public Resources Code § 3106. Tests and remedial work are now required to be undertaken by owners of oil wells to protect "neighboring property owners and the public." Public Resources Code § 3224. In 1973 a new chapter of the code was added to clean up or eliminate oil sumps for the protection of the State's wildlife resources. Public Resources Code §§ 3780-3787.

With the increased interest in geothermal development, the California Legislature saw fit to pass similar legislation to safeguard health, property and the public welfare in that field. The State's oil and gas supervisor was given the responsibility to see that these interests are protected and a Geothermal Resources Board was established to assist in this program. Public Resources Code §§ 3700-3776.

In the meantime, the federal government has also assumed an important role in protecting the environment with regard to the oil and gas development field, particularly as coastal zones are affected by offshore oil development. In 1972 (Public Law 92-583) and 1976 (Public Law 94-370) important legislation in this area was enacted which establishes a program of federal financial assistance to meet state and local needs resulting from increased energy production. The lead in the programs to be instituted is left to the individual states which are permitted to allocate portions of the funds to local agencies. (Coastal Zone Management Act, 16 U.S.C. 1451-64.) The federal government is also committed to a research and training program. As pointed out in Senate Report 94-277: "It is in the national interest that the Federal Government help to provide leadership and incentive for estuary preservation and restoration for the benefit of all the people." Paramount in the format which has been adopted is the federal consistency clause. This is intended to strengthen the ability of the states to cope with offshore oil development by insuring that such development in the federal jurisdiction is consistent with the adjoining state's coastal management program.

We can appreciate from the foregoing discussion that when the occasion arises, innovative and desirable legislation can be and is enacted to solve environmental problems of significant concern to our people. Laws are only a tool to serve as a support and supplement to adequate planning and research. We must recognize that the probability of land subsidence in susceptible areas should be taken into account in planning, designing and constructing projects. Comprehensive records are needed to delineate the hazardous areas so as to predict possible subsidence in undeveloped areas.

As it was so aptly put by Representative Leonor K. Sullivan in a letter to the Technology Assessment Board, dated September 18, 1974:

> "We ignore these potential problems at our peril, just as we have in the past. If, on the other hand, we attempt to understand them, it is possible that we may be able to develop methods of avoiding or minimizing their adverse impacts."

It was with that objective in mind that Congress enacted the Coastal Zone Management Act and its recent amendments.

Conclusion

Much more is now known of the causes of land subsidence due to water extraction than was known a few decades ago. We are beginning to recognize its deleterious scope and the need to take action to prevent its continued spread. Simply to deal with it on a one-to-one or individual basis seems to be out of the question. The old common law rules relating to lateral support just don't fit. Now that we have had successful experience in attacking the land subsidence problems resulting from oil and gas drilling, we should be optimistic that a similar solution to the subsidence problem resulting from water pumpage can also be found. It may be that the funding of research not only in the technology to be employed is desirable, but also in the legal means which should be instituted to insure compliance with the desired techniques on an areawide basis. Both the federal and state governments have a real stake in encouraging adequate solutions to this problem.

References

Bellman v. Contra Costa County, 54 Cal. 2d 363, 5 Cal. Rptr. 692, 353 P.2d 300 (1960).

Bolt, B.A., W.L. Horn, G.A. MacDonald, and R.F. Scott, 1975, Geological

Hazards: Springer-Verlag, New York, Heidelberg, Berlin, 328 pp.
California Real Estate Law and Practice, 1975, Hagman and Maxwell, Vol. 11, Part A-Lateral and Subjacent Support 32 pp.
City of Long Beach, Department of Oil Properties, Report on Long Beach Custodianship of State Tidelands Oil Operations, 29 pp.
City of Long Beach, Department of Oil Properties, Fiscal 1969-70 Annual Report, 27 pp.
City of Long Beach v. Vickers, 10 Cal. Rptr. 359, 358 P.2d 687 (1961).
Empire Star Mines v. Butler, 62 Cal. App. 2d. 466, 145 P.2d 49 (1944).
Holtz v. Superior Court, 3 Cal. 3d 296, 90 Cal. Rptr. 345, 475 P.2d 441 (1970).
Modesto Bee newspaper item, July 8, 1976, 1 p.
Poland, J.F., B.E. Lofgren, R.L. Ireland, and R.G. Pugh, 1975, Land Subsidence in the San Joaquin Valley, California, as of 1972: U.S. Geological Survey Professional Paper 437-H, prepared in cooperation with the Department of Water Resources, 78 pp.
Poland, J.F., 1972, Subsidence and its Control, American Association of Petroleum Geologists, Memoir No. 18, Underground Waste Management and Environmental Implications, 21 pp.
Prokopovich, N., 1972, Land Subsidence and Population Growth: 24th International Geological Congress, Canada, 1972, Section 13, Engineering Geology, Montreal, 10 pp.
Prokopovich, N., 1976, Some Geologic Factors Determining Land Subsidence: 25th International Geological Congress, Sydney, Australia, August 1976, Vol. 2, 23 pp.
Prokopovich, N., 1974, Land Subsidence and Pollution, Proceedings of the Second International Congress of the International Association of Engineering Geology, Sao Paulo, Brazil, Volume 1, Themes I - IV, 10 pp.
Rhodes v. San Mateo Investment Co., 130 Cal. App. 2d 116, 278 P.2d 447 (1955).
Roll, J.R., 1967, Effect of Subsidence on Well Fields, J. of Am. Waterworks Assoc., 59, No. 1, 8 pp.
Sargent v. Jaegling, 83 Cal. App. 485, 256 Pac. 1116 (1927).
United States Code Service, Lawyers Edition, 42 U.S.C.S., The Public Health and Welfare, 4 Vol.
United States Code Service, Lawyers Edition, 16 U.S.C.S., Conservation, 1 Vol.
United States Code, Congressional and Administrative News, 94th Congress, 2d Session, No. 7: Coastal Zone Management Act Amendments of 1976, Senate Report No. 94-277 (Commerce Committee) to accompany S. 586, 1975, 69 pp.
Wharam v. Investment Underwriters, 58 Cal. App. 2d 346, 136 P.2d 363 (1943).
West's Annotated California Civil Code, 8 Vol.
West's Annotated California Code of Civil Procedure, 13 Vol.
West's Annotated California Public Resources Code, 2 Vol.

Publication n°121 of the International Association of Hydrological Sciences
Proceedings of the Anaheim Symposium, December 1976

EXTERNAL COSTS OF SURFACE SUBSIDENCE: UPPER GALVESTON BAY, TEXAS*

Lonnie L. Jones**
Department of Agricultural Economics
Texas A&M University
College Station, Texas

Abstract

Land surface subsidence due to excessive groundwater withdrawal is a destructive force on Upper Galveston Bay, Texas. While pumping costs are relatively low, external costs associated with subsidence are extensive, increasing total groundwater costs. External costs of subsidence are estimated from a survey of damages and losses in property values and are used in a break-even analysis comparing costs of water from ground and surface sources. Surface water was least costly for the total study areas, suggesting economic feasibility for importing surface water to meet area needs and subsidence.

Land surface subsidence is a destructive force and a critical economic, political and legal issue on the Upper Galveston Bay of the Texas Gulf Coast. The subsidence phenomenon is caused by withdrawal of water from underground aquifers in excess of natural recharge. Municipalities and industries of the area pump groundwater from a relatively small portion of the Chicot and Evangeline aquifers. Geologic formations of these aquifers are composed of unconsolidated deposits of sand and clay. Excessive withdrawal of water decreases the hydraulic pressure that partially supports the overburden. Permanent compaction of clay strata and subsequent sinking of the land surface results [Gabrysch, 1969]. Subsidence of 7.5 feet (2.34 meters) has occurred at some locations since 1943. The area in which subsidence is one foot (0.3 meter) or more was 4,700 square miles (6,475 square kilometers) in 1973 [Gabrysch, 1975]. A major knowledge gap associated with subsidence in this region has been quantification of its external costs.

The magnitude of external costs associated with land subsidence is increased by the proximity of the affected area to tidewaters of Galveston Bay. Permanent inundation of property by normal tides and temporary flooding from storm tides have resulted in damages and losses to property values and, in some cases, abandonment of homes, commercial businesses and other property improvements.

Geologists and engineers who have studied the subsidence phenomenon agree that a rate of groundwater withdrawal exists at which the decline in water pressure, and thus, subsidence, would be stabilized. This

*Technical article 12897 of the Texas Agricultural Experiment Station. This research was supported in part by the Office of Water Research and Technology, Department of Interior, through the Texas Water Resources Institute. Guidance and assistance provided by Dr. Ron Lacewell, Dr. J.R. Runkles, Mr. James Larsen, Mr. John Warren and Dr. Wade Griffin in the many different phases of this study are gratefully acknowledged. Of course, any errors, omissions or misconceptions are the sole responsibility of the author.

**Associate Professor, Department of Agricultural Economics, Texas A&M University.

maximum acceptable withdrawal rate (MAWR) is expected to be equal to the rate of natural recharge of the aquifers, but its actual value for the affected area has not been established. The existence of MAWR is important because an alternative surface source of water exists to help meet area water needs, and conjunctive use of surface water and groundwater is physically feasible. However, internal cost differentials to the primary user have slowed the substitution of the alternative surface water for groundwater withdrawals.

The lack of knowledge of the extent of external costs associated with excessive withdrawals and consequent surface subsidence has hendered a direct comparison of total water costs to the area from the alternative sources.

The primary objective of this study was to identify and quantify these external costs. The specific objectives of this paper are to: (1) present estimates of external costs associated with subsidence of land surface on the Upper Galveston Bay of the Texas Gulf Coast and (2) use these external costs esimates in a comparative cost analysis of alternative sources of water supply for the subsiding area.

The Study Area

While the subsiding area of the Upper Galveston Bay covers some 4,000 square miles (6,475 square kilometers), subsidence related damage is most severe in a smaller area including portions of Harris, Brazoria, Galveston and Chambers counties. For the present study, a 945 square mile (2,448 square kilometer) area was delineated (Figure 1). This area encompasses cities such as Houston, Baytown, Pasadena, Seabrook, Kemah and Clear Lake. It is adjacent to Galveston Bay and is crossed by significant drainage ways such as Buffalo Bayou, Sims Bayou and Clear Creek.

The study area was further subdivided into three sub-areas and subsidence costs were estimated for each sub-area. Previous analyses show subsidence costs to be relatively intense for property located adjacent to waterfronts and subject to frequent inundation and temporary flooding [Warren, et al., 1974]. Hence, two of the sub-areas are composed chiefly of waterfront property.[1]

Data

Private damages and property losses associated with land subsidence were estimated separately for each of the sub-areas and then aggregated for the total study area. Square mile blocks were used as sampling frames and sample sizes of approximately ten percent in waterfront blocks and five percent in non-waterfront blocks were used as a data base. Personal interviews of residential and commercial property owners were conducted, using questionnaires designed for reporting the extent of damage, type of damage, date of occurrence and estimated loss in property value as a result of surface subsidence. A total of 1,051 private property questionnaires used in the analysis were completed by personal interview in 1974 and 1975.

Public costs were aggregated for the study area by the governmental entity incurring the cost (i.e., federal, state, county or municipal). Enumerators obtained these estimates from local, state and federal governmental officials.

---

[1] A complete description of the study area, method of data collection and analysis are presented by Jones and Larsen [1975].

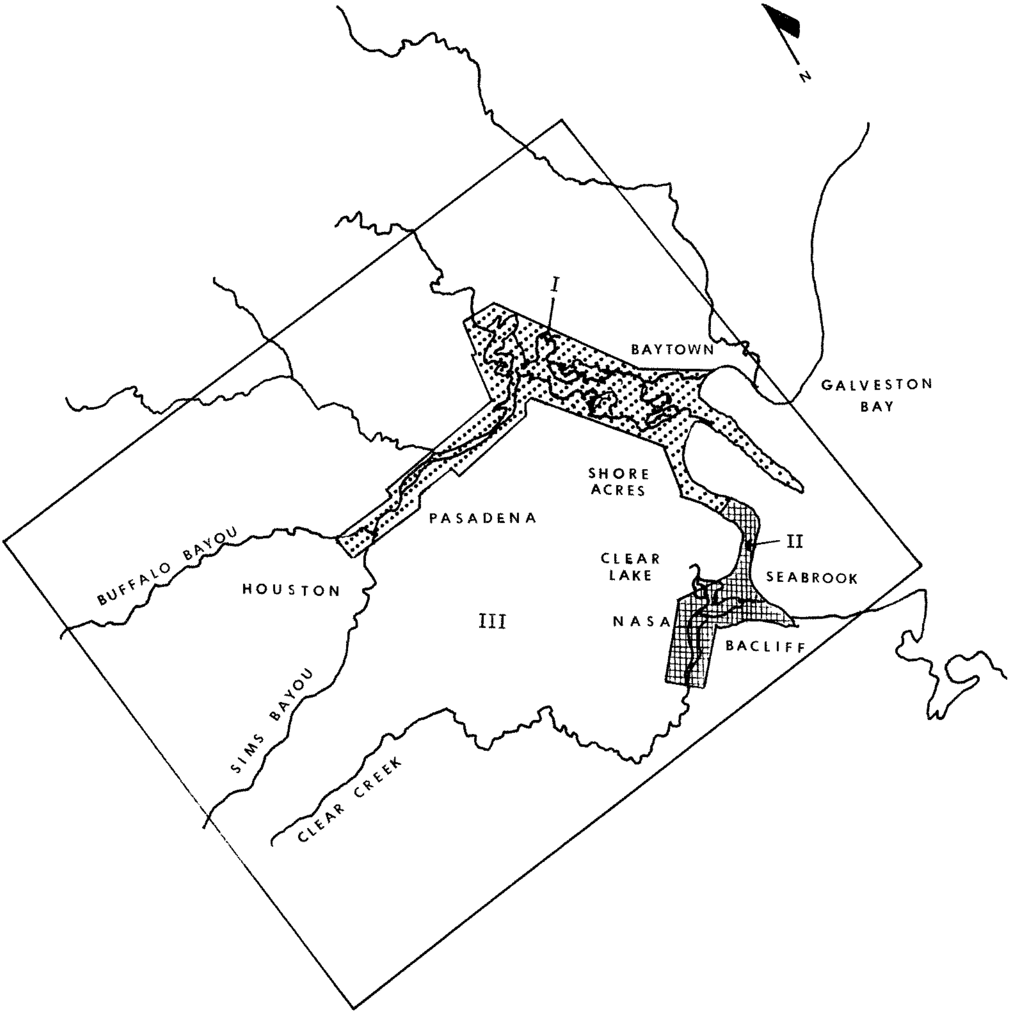

Figure 1. Approximate location of the study area and sub-areas I, II and III.

For the analysis of costs of water from alternative sources (ground and surface), information was obtained on current groundwater costs incurred by the various municipalities of the study area. Expected surface water costs were estimated from cost information currently being used in negotiations between municipalities and surface water suppliers.

Physical Effects of Subsidence

Physical effects of surface subsidence to real property are largely dependent upon location of the property. The most obvious problem caused by subsidence is the loss of land in low-lying tidal areas and the submergence of homes, buildings and structures located on the immediate coastline. Also damaging is the loss of surface elevation and the potential subjection of more land and property to the natural hazard of temporary flooding either from tidal surge or temporary runoff. This study revealed that these hazards (temporary tidal flooding and permanent inundation) account for most of the costs and losses in property value that have been associated historically with subsidence.[2]

In areas more remote from immediate coastlines, subsidence can result in changes in land slopes, stream gradients and stream drainage patterns. Such changes can cause problems in gravity transport systems, such as water and sewage lines [Brown, 1974]. Since the rate of subsidence is not uniform, temporary flooding from freshwater runoff has increased in some parts of the subsiding area. Gradual widening of streams and bayous, slow drainage and more frequent flooding was reported by numerous respondents remote from the coastline and at relatively high elevations.

Research by the Bureau of Economic Geology at the University of Texas found that subsidence activates and aggravates surface faults in the Upper Galveston Bay area [Brown, 1974]. This geologic research indicates a relationship between intensity of faulting and surface subsidence. Hence, structural damages to properties surveyed in this study were recorded and used in the analysis. These damages are manifested primarily as cracking, shifting and separation in residential and commercial structures and attachments such as sewer and waterlines. Along the water frontage, these costs constitute a relatively minor share of total subsidence costs.

Losses in property value arise primarily from two interrelated sources: (1) the actual total loss of the use of property and improvements, such as land, homes or commercial structures because of permanent or very frequent inundation as the property subsides and (2) property value reduction due to an increased incidence of flooding or other subsidence-related damages or a potential of such damages (e.g., deletion of the capitalized value of the expected [actual] increase in damages incurred through time). In either case, the dollar value of flood-prone property will be discounted to reflect expected damages, disutility and risk, resulting in a capital loss to owners of such property. In this study, losses in property value refer to the property owner's estimate of the value loss of improvements attributed to subsidence damages. As expected, such losses were highest in areas subject to frequent inundation and/or permanent inundation.

---

[2]Potential hazards from hurricanes and storm tides are clearly intensified by surface subsidence in areas adjacent to Galveston Bay. Estimates of historical costs contained in this paper are conservative since they include no estimate of costs of potential damages [Jones and Larsen, 1975].

Method of Comparing Water Costs

Externalities associated with land subsidence increase the total area cost of groundwater use. The alternative surface source of water has no negative externalities associated with its use,[3] but the internal unit costs are higher than for the common groundwater source.

The analysis presented in this paper concentrates on the least cost source of that quantity of water used to meet area needs above that which may be pumped without causing subsidence. This quantity is called the critical quantity of water, Q_c. Associated with Q_c are the external costs of subsidence. IF MAWR (maximum acceptable withdrawal rate or rate where no subsidence would occur), the per unit cost of groundwater, surface water and subsidence were known, the least-cost source of Q_c could be readily determined. But MAWR is unknown. Nevertheless, total subsidence costs are estimated and a break-even critical quantity of water Q_{be}, where the total cost of water would be equal regardless of source, is determined.

Since pumping quantities below MAWR, (i.e., $Q_c = 0$) causes no subsidence, the relevant analysis of water costs is confined to a comparison of the costs of obtaining the critical quantity of water, Q_c, from the two alternative sources.[4] It may be assumed that the area will pump MAWR quantity so long as internal pumping costs per unit are below surface water unit costs. Total costs of pumping Q_c quantity of water may be expressed as,

$$TC_s = (P_p \cdot Q_c) + (P_s \cdot Q_c) \tag{1}$$

where, TC_s is the total cost of pumping Q_c quantity of water, P_p is internal unit pumping cost and P_s is external unit cost of subsidence. Total costs of Q_c quantity of water obtained from the alternative source is,

$$TC_o = P_a \cdot Q_c \tag{2}$$

where, TC_o is the total cost of purchasing Q_c and P_a is the per unit cost of surface water. The least cost source of this critical quantity of water may be evaluated in terms of the relative magnitudes of TC_s and TC_o. If $TC_s < TC_o$, continued pumping would be the least-cost alternative for the area.

Since MAWR is unknown, Q_c is also unknown and values of TC_s and TC_o cannot be estimated directly. However, equations (1) and (2) provide the basis for estimating a break-even critical quantity of water, Q_{be} for which the total cost of obtaining Q_c is the same regardless of source. Rearranging equations (1) and (2) and equating TC_s and TC_o gives the following:

$$Q_{be} = \frac{P_s \cdot Q_c}{P_a - P_p} \tag{3}$$

---

[3]Reservoirs currently in place impound a sufficient quantity of water to adequately supply study area projected needs until the year 2000; thus, for this case, environmental and recreational issues of large reservoir construction are mute.

[4]Q_c is defined as Q_d - MAWR, where Q_d is total area water use. The complete model for estimating total costs of area water use is presented by Warren, et al., 1974. This report is an extension of the Warren report to a larger geographic area.

where, Q_{be} is the break-even critical quantity of water. $P_s \cdot Q_c$ is the total external cost associated with land subsidence (hereafter called TEC).

The estimation of Q_{be} is an important first step in minimizing total costs of water to the area, including subsidence costs. Once MAWR is estimated, a determination can be made as to the least cost source of acquiring Q_c quantity of water. For example, if Q_c, as estimated by engineers, is above (below) Q_{be}, continued pumping is justified (unjustified) since total cost of purchasing surface water would be more (less) than the total cost of pumping groundwater. If $Q_c = Q_{be}$, there would be indifference as to the source of the critical quantity of water, from the standpoint of total area costs.

The use of such a break-even analysis implies an underlying assumption of a linear relationship between unit water costs and water use level. This assumption may be an oversimplification although an examination of estimated annual subsidence costs does not reveal a significant departure from a linear relationship.

Estimated Subsidence Costs

Estimated subsidence related costs and property value losses for each sub-area are expressed on an average annual basis and presented in Table 1. Annual estimates for sub-area II (NASA-Clear Lake) are derived from the six-year period 1969-74 while the other areas (Pasadena-Baytown and Houston-other) are derived from the five-year period 1969-73. These costs represent only the reported costs over this period for which property owners had made expenditures. Hence, they should be considered a conservative estimate of subsidence-related damages and property value losses within each sub-area.

The estimates represent costs to property owners resulting from the day-to-day, gradual encroachment of saltwater and flooding from the weather pattern that occurred over the five or six-year period included in the study. The most damaging tropical storm to occur within the study area was Delia in 1972. Similar storms have an estimated return frequency of about five years [Bodine, 1974]. Not included are the 25, 50 or 100 year storms. Certainly sudsidence has increased property vulnerability to these large storm sizes. Expected damages from a large but infrequent storm would increase the average annual subsidence related cost estimates.[5]

Estimated annual costs and property value losses totaled over \$31.7 million for the study area as a whole. These were primarily costs to private property owners, but included just over \$.5 million per year in public costs.

Private property costs in the waterfront sub-areas (I and II) occurred chiefly as a result of temporary flooding and permanent inundation of improvements, or for remedial measures such as bulkheading and landfilling, raising piers, boat docks, loading docks for businesses and other construction. In the non-waterfront sub-area (III), highest costs were from temporary freshwater flooding and structural damages to property improvements. Respondents in this sub-area reported a gradual worsening of drainage problems in the recent years, primarily along creeks and bayous. In areas of low elevation, respondents reported increases in water encroachment and more frequent flooding.

---

[5] The increase in land area that would be affected by such storms has been estimated [Bureau of Economic Geology, 1970]. However, no attempt has been made to quantify expected annual costs of such occurrences.

Table 1. Estimated Average Annual Costs and Property Losses Associated With Land Subsidence, Upper Galveston Bay, Texas.

Sub-Area	Approximate Area Size		Estimated Average Annual Costs			
			Damages	Property Losses	Total	Percent of Total
	(sq. miles)	(km^2)	- - - -	$1000	- - - -	%
I (Pasadena-Baytown)[a]	83	215	3,926[d]	5,870	8,795	27.7
II (NASA-Clear Lake)[b]	25	65	2,108	2,900	5,009	15.8
III (Houston-other)[a]	837	2168	9,322	8,041	17,363	54.8
Public Costs[c]			538		538	1.7
TOTAL	945	2118	15,894	15,811	31,705	100

[a]Average annual costs and losses for the five-year period 1969-73.

[b]Average annual costs and losses for the six-year period 1969-74.

[c]Average annual costs for the five-year period 1969-73. This estimate includes actual expenditures only.

[d]Includes $37 thousand estimated costs to industry.

Highest costs were in sub-area III, with about $17.4 million total damages and property losses. Estimated costs for sub-areas I and II were over $8.79 million and $5 million, respectively. Although the totals are less than for sub-area III, these two sub-areas experienced a much higher intensity of subsidence costs. For instance, sub-area I makes up about 8.7 percent of the total study area and experienced 27.7 percent of the costs due to subsidence damages and property value losses. Sub-area II experienced 15.8 percent of total costs but occupies only about 3 percent of the total study area. Hence, subsidence damages and losses in property value are concentrated heavily in the areas in close proximity to the immediate coastline of Galveston Bay, Buffalo Bayou and Clear Lake. Other sections throughout the study area experienced damages and property losses but less frequently and less intensively.

Alternative Water Sources and Cost Comparisons

Since subsidence has been linked to groundwater withdrawal, one of the primary purposes in estimating costs associated with land subsidenc on Upper Galveston Bay is to provide information that may be used in evaluating alternative sources of water for municipal, industrial, agricultural and other uses.

Sources of Water

Average daily water use in the subsiding area was estimated at 347.3 mgd (15.2 cubic meters per second [m^3/s]) for the 1969-73 study period. Over half of this pumpage (198.8 mgd or 8.7 m^3/s) was for public supply uses, including households, commercial businesses and other municipal purposes. Industries within the area were the second largest users with an average daily use of 147.1 mgd (6.4 m^3/s) over the five-year period.

Two immediate sources of water are available to the subsiding area. One of these is the continued withdrawal of groundwater from the

Evangeline and Chicot aquifers. The other is surface water from several surface sources including Lakes Houston, Livingston and Conroe.

At present, as in the past, the subsiding area relies primarily on groundwater and withdrawals have increased in recent years. Total pumpage increased steadily up to 1972 when groundwater withdrawals reached 364.2 million gallons per day (mgd)(15.9 m^3/s). Pumpage in 1973 was somewhat lower at 353.9 mgd (15.5 m^3/s). Average daily withdrawals vary among years depending upon amounts of rainfall, season of rainfall and other factors [Gabrysch, 1972].

Surface water is currently used from Lake Houston and plans for delivery of water from Lake Livingston (Trinity River) via facilities under construction by the Coastal Industrial Water Authority are planned for completion in 1972 [Munson]. It is estimated that about 1.2 billion gallons per day (52.6 m^3/s) are available from Lakes Livingston, Houston, Conroe and other surface sources. The greater Houston water distribution systems completed or nearing completion have a total capacity of some 1.27 billion gallons per day (55.6 m^3/s) [Munson]. Lake Houston should not be considered a new source of surface water since the reservoir is already fully committed. Nevertheless, the addition of Lake Livingston surface water in 1976 and potential future supply from Lake Conroe and Wallisville reservoirs provides quantities of water well in excess of current needs within the subsiding area.

Comparison of Costs of Alternative Water Sources

The economic feasibility of importing surface water to substitute for groundwater may be analyzed by comparing the pumping (internal to the user) and subsidence-related (external to the user) costs of groundwater withdrawal to the cost associated with purchasing and conveying water from surface sources. The internal pumping costs of groundwater are low relative to the cost of acquiring and conveying surface water. Current estimates of costs within the subsidence area are about $.06 per thousand gallons ($.016 per cubic meter) for pumping groundwater and about $.22 per thousand gallons ($.058 per cubic meter) for purchase of surface water.[6] Hence, a user cost differential of approximately $.16 per thousand gallons ($.042 per cubic meter) in favor of groundwater exists between the two sources. However, since groundwater pumping results in additional costs due to surface subsidence that are not associated with surface water use, the external costs (damages and losses in property values) must be considered in the cost comparison.[7] The external, subsidence-related costs are estimated to be about $31.7 million per year (Table 1).

In this comparative analysis, a break-even equation is used to calculate the quantity of surface water that could be purchased at the internal cost differential of $.16 per thousand gallons ($13.7 per cubic meter) of water with $31.7 million of external costs associated with subsidence.

---

[6]The survey of public officials indicated that $.06 and $.22 were typical costs estimated for groundwater and surface water, respectively.

[7]The external costs from damages and losses in property values are incurred by groundwater users as well as non-users. Such costs are external in the sense that an individual within the areas cannot avoid the costs by varying the quantity of groundwater used. Avoidance of the external costs must be accomplished by collective action within the area.

This is a quantity of water that would just equate the total cost of surface water with the total cost (internal and external) of groundwater (Equation 3). The quantity of water (Q_{be}) calculated from equation 3 provides an estimate that may be compared directly with the critical quantity of water (Q_c).

As indicated, the subsidence-related external costs of groundwater pumping (TEC) were estimated at about \$31.7 million per year. Hence, Q_{be}, the break-even quantity of surface water, was estimated to be:

$$\frac{\$31,705,040}{\$.16} \text{ or } 542.89 \text{ mgd } (23.784 \text{ m}^3/\text{s}). \quad (4)$$

This indicates that with current water prices and the estimated subsicence-related costs, the purchase from surface sources of up to 543 mgd (23.784 m^3/s) would be economically justified. The magnitude of this break-even quantity is most significant when compared with average water use within the study area of 347.3 mgd (15.2 m^3/s); i.e., the annual average water use for the same five-year period over which external costs were estimated. This difference of 196 mgd (8.59 m^3/s) implies that, even if all groundwater pumping were displaced by imported surface water, the total costs for water in the area would be significantly reduced.

For example, assuming all water demands had been pumped from groundwater sources during the 1969-73 period at a cost of \$.06 per thousand gallons (\$.016 per cubic meter), total pumping cost would have been about \$7.6 million per year. Pumping costs plus annual external costs of \$31.7 million indicate a total cost of groundwater of \$39.3 million per year. Assuming the area's water use (347.3 mgd) had been supplied with purchased surface water at a cost of \$.22 per thousand gallons (\$.058 per cubic meter) total annual costs would have been about \$27.9 million, or a savings to the area of about \$11.4 million per year.

Since the total cost of acquiring surface water relative to groundwater pumping costs may vary from that used here ($P_s - P_p$ = \$.16), it is useful to consider estimates of break-even quantities of surface water at various cost differentials. Such estimates are presented in Figure 2. Given an estimated subsidence-related cost of \$31.7 million per year, the break-even quantity of surface water (Q_{be}) declines as the cost difference between surface and groundwater increases. However, for all cost differentials below \$.25 per thousand gallons the break-even quantity exceeds the average daily water use of 347.3 mgd in the study area. Assuming that no groundwater may be pumped without resultant subsidence (i.e., MAWR = 0) the values in Figure 2 imply that up to a price differential of \$.25 per thousand gallons could be paid to import surface water in order to reduce costs to the study area as a whole.

Implications

The implications of this study are dramatic and very clear. Damages and property value losses associated with land subsidence on the Upper Galveston Bay are high and extensive over a large portion of the coastal area. The resulting costs, as estimated in this study, are so high that continued pumping of groundwater at rates that cause subsidence cannot be justified. The pursuit of alternative sources of water to meet area needs and institutional measures for controlling subsidence are fully justified from a standpoint of reducing total costs to the area. Solutions to this problem lie in the creation of institutions that insure efficient conjunc-

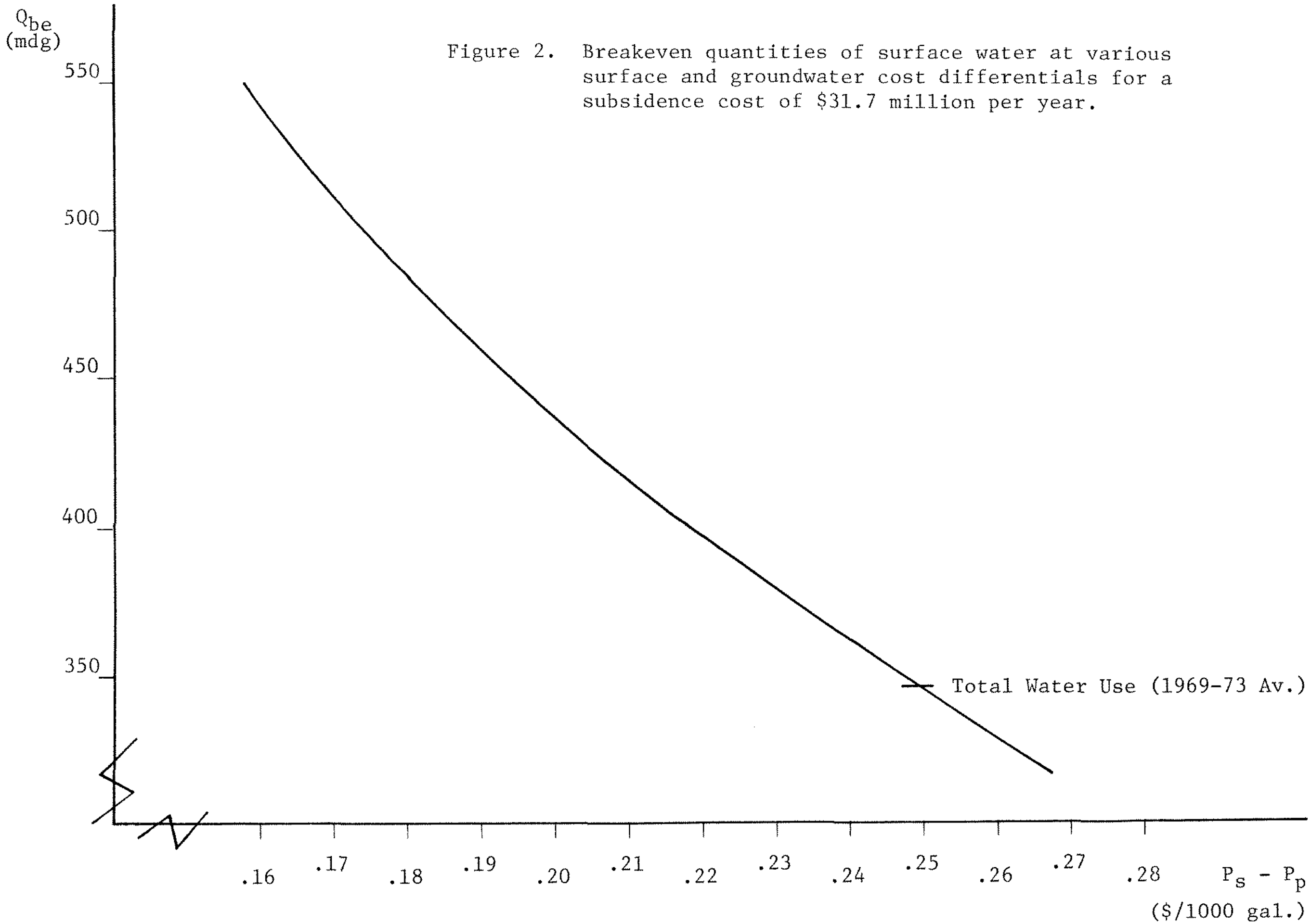

Figure 2. Breakeven quantities of surface water at various surface and groundwater cost differentials for a subsidence cost of $31.7 million per year.

tive use of surface and groundwater and equitable distribution of the benefits and costs of the change.

References

Bodine, B. R. 1974. Hurricane Surge Frequency Estimated for the Gulf Coast of Texas. U.S. Army Corps of Engineers Technical Memo 26.

Brown, L. F., et al. 1974. Natural Hazards of the Texas Coastal Zone. Bureau of Economic Geology, University of Texas.

Bureau of Economic Geology. 1970. Land Subsidence Amplifies Hurricane Dangers. The University of Texas, Austin.

Gabrysch, R. K. 1969. "Land Surface Subsidence in the Houston-Galveston Region, Texas." Proceedings of the International Symposium on Land Subsidence, Tokyo.

Gabrysch, R. K. 1972. Development of Groundwater in the Houston District 1966-1969. Texas Water Development Board Report 152, Austin.

Jones, Lonnie L. and James Larsen. 1975. Economic Effects of Land Subsidence Due to Excessive Groundwater Withdrawal in the Texas Gulf Coast Area. Texas Water Resources Institute Technical Report 67, College Station.

Munson, George P. 1973. Water on the Way. Coastal Industrial Water Authority, Houston.

Warren, John P., Lonnie L. Jones, Wade L. Griffin and Ronald D. Lacewell. 1974. Costs of Land Subsidence Due to Groundwater Withdrawal. Texas Water Resources Institute Technical Report 57, College Station.

Warren, John P., Lonnie L. Jones, Ronald D. Lacewell and Wade L. Griffin. 1975. "External Costs of Land Subsidence in the Houston-Baytown Area." American Journal of Agricultural Economics 57 (August): 450-455.

Publication n°121 of the International Association of Hydrological Sciences
Proceedings of the Anaheim Symposium, December 1976

SOME DATA POINTS ON SHORELINE RETREAT ATTRIBUTABLE TO COASTAL SUBSIDENCE

Edward B. Hands
U.S. Army Coastal Engineering Research Center
Fort Belvoir, VA 22060

Abstract

Coastal subsidence increases flooding in low lying coastal regions. Moreover, it disturbs the equilibrium profile, and allows waves to erode bluffs formerly above the reach of wave uprush. Ensuing adjustment of the profile drives the shoreline farther landward. Guidance is needed for obtaining quantitative estimates of the shore's response.

The mean surface elevation of Lake Michigan rose 0.5 m during a recent four year period. Concurrently, major elements of the submerged profile responded by building upward and migrating 26 m landward. Approximately 8 m of beach were lost due to submergence beneath the elevated lake surface; and an additional 6 to 7 m were lost due to erosion. The shoreline, however, lagged behind the rest of the profile in adjusting to the higher water levels.

Over a longer period, certain sections of Lake Michigan have undergone relative subsidence as a consequence of broad regional tilting of the earth's crust. It is estimated that during the last century the Lake Michigan basin tilted 0.06 to 0.09 m per 100 kilometers along its axis. Shore recession over the last century increased at a rate of 19 ± 10 m per 100 kilometers in the direction of greater subsidence.

Other coastal areas with similar geomorphology and wave exposure can be expected to recede at rates similar to those indicated above if subjected to the same subsidence. The initial response to rapid subsidence may be on the order of 50 units of retreat for each unit of subsidence. Profile retreat is, however, a non-linear, time-dependent function of subsidence, and for slower subsidence, shore-eroded sediments become spread over a broader profile, producing a larger ratio of shore retreat per unit of subsidence. Estimates of shore recession due to slow crustal motion of the Great Lakes basin indicate response ratios between 120:1 and 390:1. Furthermore, according to the concept of mass balance, the long term response ratio should also depend on the volume and size distribution of sediments being supplied to the nearshore profile by shore erosion. The lakeshore response was found to increase several fold where inadequate backshore deposits supplied less beach material per unit of recession.

I INTRODUCTION

1. Aim and Approach

Failure to consider the effects of subsidence may result in a serious error in projection of long term shore retreat at certain localities. Even moderate rates of subsidence can increase coastal erosion and submerge low lying coastal regions. Furthermore many conditions brought about by development of shore property, e.g., lowering of the water table accompanying ground water withdrawal, soil compaction in response to increased surface loads, vibrations associated with construction operations and later traffic, can, as documented by other papers in this symposium, contribute to subsidence; and thereby accelerate shore retreat. Estimates of potential shore erosion should, therefore, include allowances for the continuation of documented subsidence, and even for expected increases in the subsidence rate when the state-of-knowledge permits such predictions, based on development factors.

No guidance is available at present however, for estimating the amount of erosion which will result from a given rate of subsidence. More fundamental questions about coastal currents, waves, and the interactions of fluid and sediment, have yet to yield solutions; and in the absence of a theoretical understanding, empirical correlations between shore retreat and causative factors have assumed subsidence per se can be ignored (Caldwell, 1959; Richardson, 1976; and others). Usually the effects of subsidence on shore retreat rates are relatively small compared with the total variation in retreat rates. Moreover even where subsidence has a significant cumulative effect the shore damage will tend to be felt during the storm events. Thus the present uncertainty concerning the relationship between coastal subsidence and shore retreat should not be surprising.

Because subsidence is a minor variable among many affecting the rates of shore erosion, resolution of its contribution will depend on shore changes measured at sites of extreme subsidence, or over long periods of time. The purpose of this paper is to estimate the effects of coastal subsidence using first, data on Lake Michigan shore retreat during four years of rapidly rising lake levels; and secondly, using historic data on the 120 year retreat rate along sections of the Lake experiencing different rates of relative subsidence.

Figure 1. General Location Map

2. Terminology.

For the purpose of this paper, precise definitions have been formulated, that refine the meaning of several familiar words. *Submergence* will refer to the sinking of a coastal area relative to the mean water surface. Submergence may result from either land subsidence or elevation of the water surface. *Emergence* refers to the opposite relative displacement, and when expressed numerically, both will refer to lengths (L) measured in the vertical. Coastal planners and property owners are often more interested in the resulting horizontal change in shoreline position. *Transgression* (ant. *regression*) will refer to the horizontal distance that the shoreline moves in direct response to submergence (emergence). The *shoreline* is the intersection of the beach with the mean water surface, or some other specified datum such as low water (LWD) or mean high water (MHW). The shoreline divides the beach into *shore* (subaerial) and *nearshore* (submerged) zones.

Total lateral migration of the shoreline can be more or less than transgression (regression) depending on whether erosion or deposition prevails at the shoreline. Deposition refers to the accumulation of material on a surface (M/L^2 or L); erosion refers to its removal. The lateral migration of a specific contour will be referred to as *progradation* (L) if the contour moves toward the center of the basin and as *recession* if the contour moves away from the basin. *Shoreline retreat* (Fig. 2) will be the inclusive term referring to the total landward horizontal shift or the algebraic sum of *transgression* (a function of submergence) and *recession* (a function of subsequent erosion).

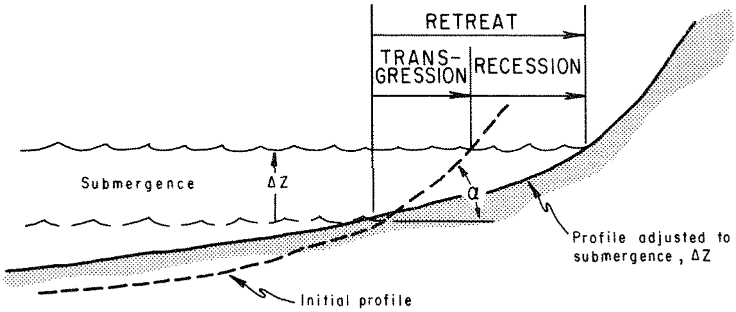

Figure 2. Terminology of Retreat
Transgression = $\Delta z \cot \alpha$
Retreat = transgression + recession

Shoreline retreat implies that there has been either local recession or transgression, but is unspecific as to which (or whether both) caused the landward shift in shoreline position. Figure 3 illustrates the meaning and heirarchy of the discussed terms.

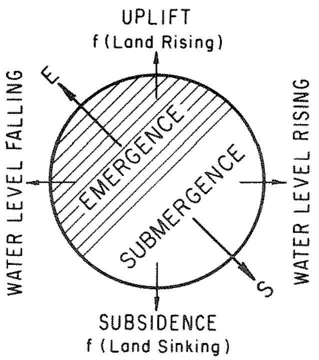

Figure 3a. Terminology of Vertical Processes

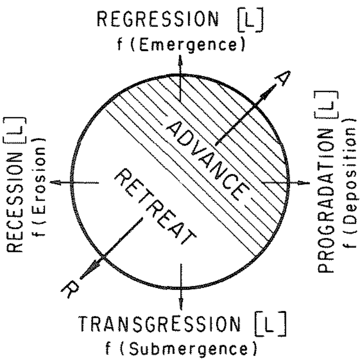

Figure 3b. Terminology of Horizontal Migration

II USE OF LAKE LEVEL FLUCTUATIONS TO MODEL SUBSIDENCE

1. Lake Level Fluctuations.

In terms of submergence and erosion, it is immaterial whether the land is sinking or the sea rising. Thus a stable or even uplifted shore can serve as a model if only the sea is rising facter than the land. Due to their distinctive hydrologic cycles, the Great Lakes can be used to model effects of subsidence on shore retreat.

The mean surface elevation of Lake Michigan has a definite annual cycle averaging about 15 cm in amplitude. This seasonal cycle is superimposed on *long term fluctuations* which, though not so regular as the seasonal cycle, are nevertheless clearly evident in the 115-year hydrograph of annual means (Fig. 4).

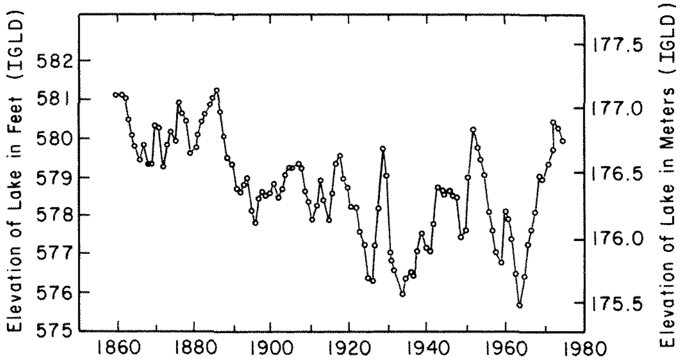

Figure 4. Annual Mean Surface Elevations of Lake Michigan (data from NOAA records)

Seasonal and long term lake level fluctuations are expressions of meterologic and climatic variations. As shown in Figure 4, the annual mean lake level generally increases for several years in succession before going into periods of decline. The cumulative effect has often been a considerable shift in annual mean lake levels, e.g., more than a meter between 1926 and 1929; 0.83 meters between 1950 and 1952; and 1.45 meters between 1964 and 1973. These long term lake level fluctuations are much more rapid (34, 41, and 16 cm/yr respectively) than trends in sea level which are typically on the scale several mm/yr. Runs of increasing lake level have rates more comparable to changes in relative sea level at sites of extreme local subsidence. This suggests using measurements made to determine the shore response to periods of rising lake levels, as input to a model for estimating the effects of coastal subsidence.

2. <u>Historic Data on Bluff Recession.</u>

Land surveys and aerial photographs have been used to document Lake Michigan bluff recession in excess of 300 meters (1116 feet) in 121 years (Powers, 1958). Average bluff recession rates shown in figure 5, represent nearly 1000 measurements compiled from various references reporting the position of bluffs at widely scattered sites around the lake shore. The height of each horizontal bar represents the recession rate obtained by averaging measurements from 9 to 100 different sites. The length of the bar indicates the various time spans, from 2 to 127 years, for which recession was calculated. In this format, measurements from localities having different degrees of exposure and resistance to erosive forces are lumped together, but two important features nevertheless stand out: first, the average lakeshore bluff is evidently subject to persistent long term retreat.

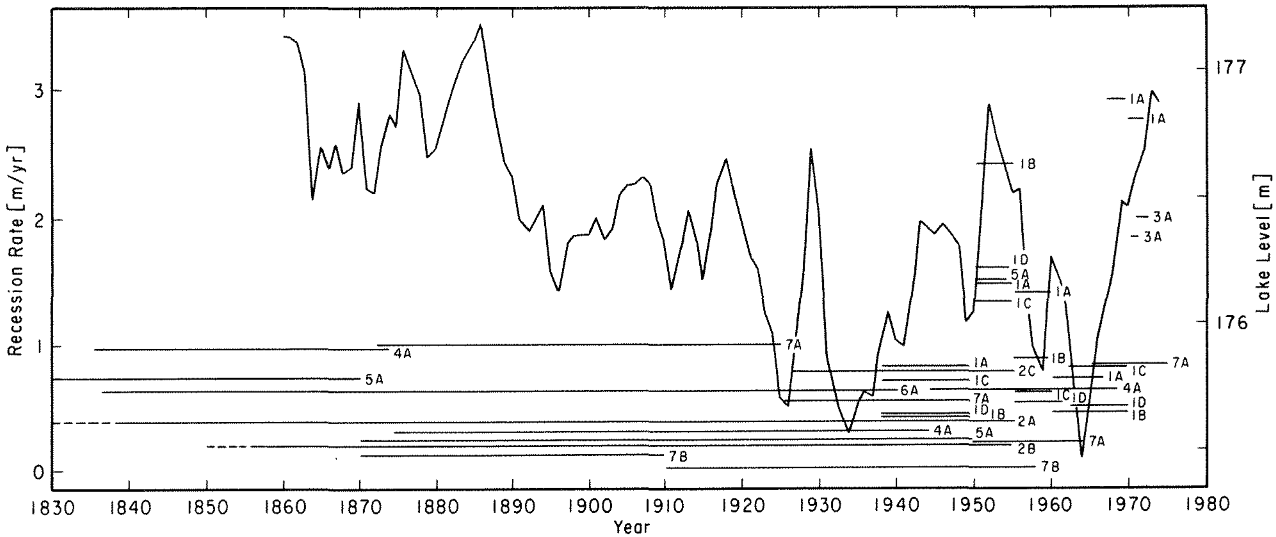

Figure 5. Mean lake level fluctuations (continuous jagged line) compared with changes in bluff recession rates (straight lines). Recession rates are averages of a number of measurements (see text) spanning a time indicated by the length of each line. To examine the change in recession with time, but holding the exposure and shore resistance constant, follow the rates by number/letter code. Numbers indicate sources: 1. Seibel (1972), 2. Powers, 1958, 3. Davis, et al. (1975), 4. Wisconsin Department of Natural Resources (1969), 5. U.S. Army Engineer District, Detroit (1956), 6. U.S. Congress (1946), and 7. Berg and Collinson (1976).

Secondly, rates of retreat are not uniform through time. During certain specific short periods, average recession rates increase significantly throughout the lake.

It has long been held that shore erosion was most rapid during periods of above average lake level. Evidence of this was presented by Seibel (1972) for Lake Michigan/Huron and by Berg and Duane (1968) for Lake Erie. Some investigators nevertheless still express doubt as to the validity of this relationship (Larsen, 1972; McKee, 1972). A comparison of the rates of recession shown in Figure 5 with the mean annual lake level (shown by the continuous jagged line) shows direct correlation between bluff recession rates and the mean elevation of the lake surface, in spite of the fact that the data collection periods, over which recession rates are averaged, were undesirably long and not ideally suited for resolving the effect of lake level changes. Consider for example, the change in recession at 1B in Figure 5. This average rate of recession is based on 40 point measurements along a specific length of shore. A 500% increase in average recession rate is noted between 1938-1950 and 1950-1955. The rate then decreased considerably as lake levels fell in the late 50's. Both lake level and recession decreased still further in the early sixties. Lake levels reached a record low in 1964. Recession was low but not below the long term average, which may reflect first the effect of available survey intervals; recession and lake levels were still moderately high in '60, '61, and '62, and then rose again rapidly in the closing years of that decade. A second possible reason for above average recession in the same decade in which levels dropped to a record low, is that the studies from which the 1B rates (as well as most of the other post 40's data) were taken, concentrated on the more critically eroding sections of the lake.

An estimate for the overall long term recession would be 0.37 m/yr (1.2 ft/yr) based on measurements at 94 stations selected from data presented by Powers (1958). Powers' data provides a good estimate of the overall historic recession because Powers chose his sites systematically, and the 94 sites used here were all originally surveyed between 1830 and 1838. Powers determined bluff recession by surveying, in 1956 and 1957, the distance of the shore bluff from township and range section-corners within 0.5 mile of the lake. Comparing his measurements with original government surveys, he found that the bluff had advanced at six of the 134 sites (average rate of advance 0.5 m/yr); and showed no change at four sites.

3. Profile Adjustment to a Single Period of Rapidly Rising Lake Levels.

The response of the beach to the most recently rising lake levels has been monitored at six stations in the vicinity of Pentwater Harbor about midway up the eastern shore of Lake Michigan. Study of profile changes has provided an estimate of the increase in shoreline retreat due to high lake levels, permitted the resolution of transgression and recession, and revealed changes across a broad submerged section of the profile which are also related to submergence. The dates of the four field seasons during which the six stations were reprofiled, together with the change in lake level between the field seasons (based on average daily means), and the mean monthly elevations during intervening periods are given in Figure 6.

a. Shore. The net retreat of the shoreline over the four year study period is shown in Table 1. In spite of a slightly higher lake level in the fall of 1969, the shoreline advanced between the spring and fall at two of the six profile stations (3 & 7) because a small coastal bar merged with the shore. Over the longer period from spring 1969 to 1971, a net retreat developed at all stations. The average retreat rate for the two year period was 4 m/yr, but there was still a considerable, random variation, in retreat among the different stations. Over the 1967-1971 (45 month period, longshore variations nearly vanished as all stations approached the average retreat rate of 4 m/yr.

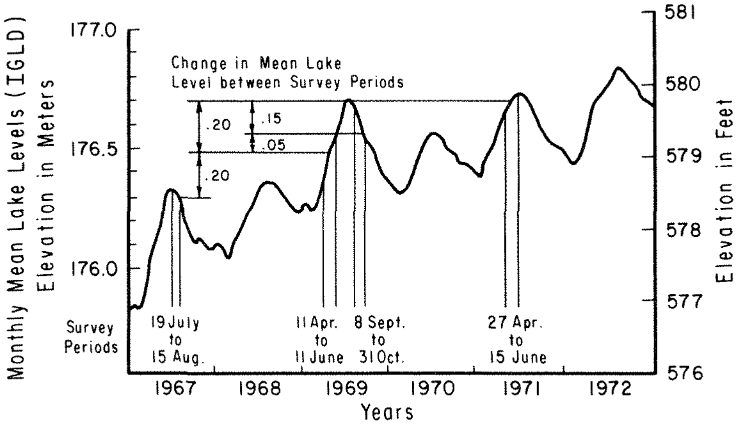

Figure 6. Lake Michigan Hydrograph Showing Differences in Mean Lake Levels Between the Various Survey Periods.

Table 1. Net shoreline retreat

Station number	Spring to Fall 1969	Spring 1969 to 1971	1967 to 1971
3	-1.5	1.5	13.4
4	1.5	12.0	16.7
5	2.5	10.7	14.6
6	3.3	7.5	15.2
7	-0.2	5.8	16.9
8	2.0	12.5	11.0
Avg. retreat (m)	1.3	8.3	14.6
Coefficient of variation (m)	1.4	0.51	0.15
Avg. retreat rate (m/yr)	3.3	4.1	3.9

A determination of the exact amount of *recession* depends on the elevation where the measurement is made. One convenient choice is at the elevation of lake surface in 1967. The average of daily means during the 1967 field season was 176.30 m (International Great Lakes Datum, IGLD, 1961) and the average for the whole year was slightly lower; 176.10. The positions of these two *shorelines* as well as the *LWD shoreline* (175.80) were calculated No datum higher than the 176.1 could be selected, however, because profiling was terminated at water's edge in 1967. If a datum lower than LWD had been selected, it would, by the time of the 1971 survey, have intersected the profile lakeward of a longshore bar. As can be seen in Figure 7, this bar was also migrating landward as lake level rose. A coastal bar migrating landward and upward can cause a sudden anomalous lakeward advance of some contours on an otherwise receding shore. Thus, measured recessions at the higher elevations are more reliable indices of shore retreat.

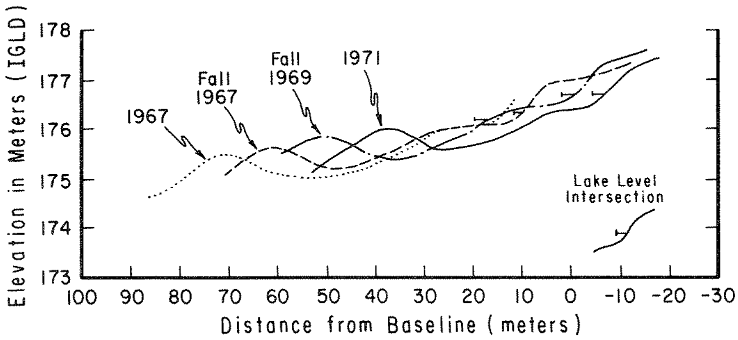

Fig. 7 Adjustments of the Upper Profile at Station 5.

Average recession (1967 to 1971) of the 176.30 m shoreline totaled 6.5 m. For this four year period transgression was responsible for more than 50% of the total shoreline retreat.

b. Nearshore. The nearshore profile is dominated, from near water's edge to a point approximately 500 m from shore, by a sequence of from four to five longshore bars. These bars are persistent year-round features, but are not stationary (Figure 8). On the north side of the harbor where four bars were persistent from year to year throughout the study, the inner three bars migrated an average of 26 m toward the shore, and rose in elevation about 0.5 m during the same four year period. The cross-sectional geometries, aerial relationships, and migration of multiple longshore bars are discussed in detail elsewhere for a larger region encompassing Pentwater Harbor (Hands, 1976).

4. Interpretation.

The 120 year rate of historic recession for a typical stretch of unconsolidated lake shore is about 0.37 m/yr (1.2 ft/yr). Rates of recession are not however constant; periods of accelerated recession occur during years of high lake level. If measurements of recession obtained during the recent episode of high water are divided into two nearly equal time intervals (1967 to 1969, 1969 to 1971), each reflecting equal submergence (0.2 m), then recession of the highest common *shoreline* (176.30 m) was about the same for both periods and totaled 6.5 m.

Total shoreline retreat exceeded recession by a factor of more than two. The difference between the total retreat (14.6 m) and recession (6.5) is transgression (8.1). In other words, in addition to 6.5 m lost by erosion, 8.1 m of shore has been lost by submergence beneath the elevated lake levels.

Figure 9 shows the total changes in average position of bar crests, bar troughs, and the 176.3 *shoreline* between 1967 and 1971. Changes in elevation of crests, troughs, and *shoreline* were essentially the same (0.55, 0.47, and 0.51 m respectively). Average horizontal changes were 25 m for the crests, 24 m for the troughs, but only 6.5 m for the 1967 *shoreline*.

An important question is whether the documented shoreline recession represents full or only partial adjustment to submergence. Per Bruun (1962) has hypothesized that there is an equilibrium form which beaches tend to adher to, and if sea-level rises, the equilibrium form will be shifted upward and landward. Lake Michigan bars moved up by an amount equal to the mean rise in lake level during the four year period. However, while maintaining a fixed depth, the bars encroached on the shoreline (Figures 8 and 9).

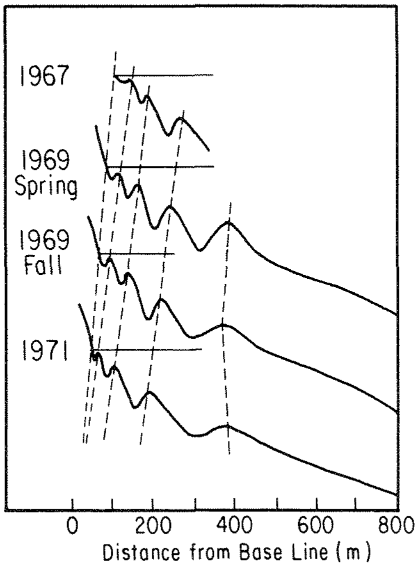

Figure 8. Landward Migration of Longshore Bars Over a Four Year Period of Rising Lake Levels.

If the 1967 profiles more nearly approximated the equilibrium form than did the later, steeper profiles, then considerable additional retreat must occur after lake levels stop rising, to flatten the profiles back to their 1967 configuration. The difference in bar and shoreline migration (25-15 = 10 m) is interpreted as a lag in the recession of the shoreface or upper beach. In order to adjust completely to the elevated lake surface, the upper part of the profile will probably recede farther landward by continued rapid erosion until it has increased, by roughly 10 m, its separation from the nearshore bars. Assuming shore erosion supplies a volume of sediment sufficient to readjust the nearshore profile, a crude sediment budget was calculated (Hands, 1975). The results were in substantial agreement with the preceding prediction inasmuch as mass balance provided an even larger estimate of the additional retreat necessary to re-establish equilibrium; the final ratio of recession to submergence was estimated to be about 60:1.

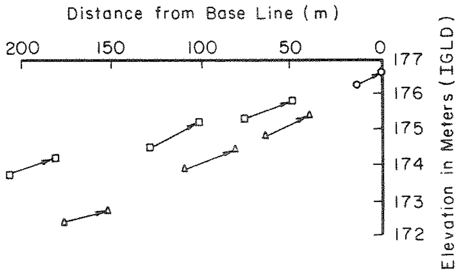

Figure 9. Migration of Bars and Shoreline (1967 to 1971). Migration of Bar Crests, □ , Trough Thalwegs, △ , and the Water's Edge, ○ , from their Mean Positions in 1967 to Their Mean Positions in 1971. Based on Profile Measurements at the Three Stations North of Pentwater Harbor.

Recently collected profile data provide more extensive coverage both along shore and offshore, and will thus provide a better basis for future refinements of the sediment budget.

III USE OF DIFFERENTIAL UPLIFT TO MODEL SUBSIDENCE

1. Regional Trends in Recession Rates.

By selecting from Powers' report those stations initially surveyed between 1830 and 1838 (94 in number) and then averaging them by county, evidence for an unreported regional trend in long term recession rates is obtained (Fig. 10). The relatively large variation in recession rate encountered as one moves from one station to the next along the shore, cautions against putting too much confidence in the mean rate derived for any given county. An average of only four sample rates isn't a very stable estimate of the true mean rate, and the number of measurements per county varies. Yet recurrent increases in recession rates toward the south on both sides of the lake support the hypothesis that a regional trend actually exists. Evidence of this trend has not been found in any other data on Lake Michigan shore recession, but no other data set has an area coverage and time span comparable to Powers'. The fact that Powers did not suggest a regional trend, and was apparently unaware of the evidence for one in his data, eliminates the possibility of even unconscious bias in the reduction of survey notes and compilation of recession rates. What then could be responsible for this regional trend in recession rates?

2. Possible Explanations.

The rate of bluff recession depends basically on: a) lake level behavior, b) erosive forces, c) resistance of the shore deposit, and d) the offshore profile. Waves are the primary source of energy needed to do the work of shore erosion, so the possibility that fetch and wind conditions might give rise to a trend in wave energy was examined. Visual wave observations have been taken for a number of years at various stations around Lake Michigan (LEO Data, unpubl.). The means of observed breaker heights for a three year period common to 24 stations were used to estimate the average wave power entering the surf zone at each station. Assuming the wave power delivered to the surf zone is proportional to the 5/2 power of the breaker height (CERC, 1973),

$$P_b \propto H_b^{5/2}$$

and furthermore assuming that the power of the average observed breaker is a good index of average breaker power, the distribution of $H_b^{5/2}$ around the lake was plotted (Fig. 11). Neither raw H_b, $H_b^{5/2}$, nor an index of breaker power gradient, $\Delta H_b^{5/2}/\Delta X$ (where ΔX is the shoreline distance between stations) suggested any regional trend in erosive forces.

The possibility that northern shores might benefit from a longer period of isolation from winter storm waves by pack ice, was eliminated by consulting an ice atlas (Rondy, 1969).

Essentially all the eastern shore of the lake can be described as alternating sections of sand dunes intersected by glacial moraines. Nothing in the distribution of shore types, height of the sand dunes, or morainal bluffs (Hands, 1970) suggest any regional trend in the shores' resistance to erosion. Although nearshore slopes do gradually flatten at the southern end of the lake, if the nearshore slope had any effect on recession rates, it would tend to decrease recession in the southern area rather than the reverse, which was observed.

The last independent variable considered is lake level. Annual and long term fluctuations in lake level affect all parts of the basin equally.

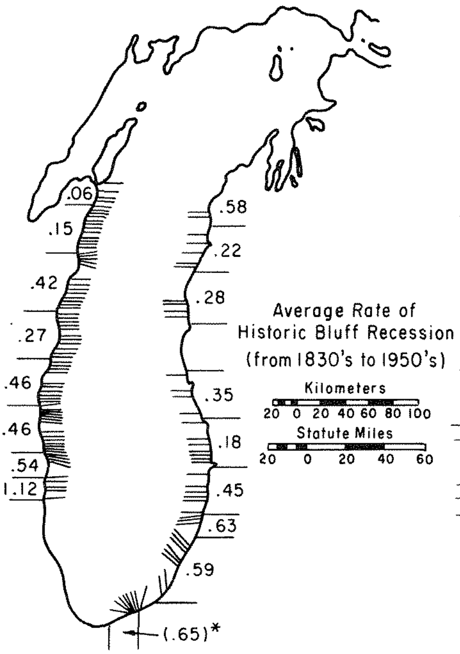

Figure 10. Rates of bluff recession [m/yr] averaged by counties. Tic marks indicate number and location of measurements. *For Porter Co., the average is for the period 1927 to 1957. All other averages are for the period 1830's to 1950's.

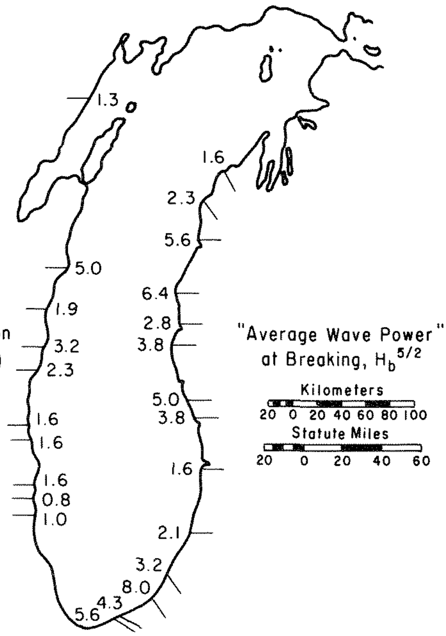

Figure 11. Distribution of "average wave power" based on visual observations of breaker height at 24 LEO* stations each reporting three years of data. *Littoral Environment Observation Program at the U.S. Army, Coastal Engineering Research Center.

Long term relative submergence would, thus, have to be a function of differential crustal motion.

3. Evidence of Differential Uplift of the Lake Michigan Basin.

Abandoned strandlines, relict from ancestral lakes, are particularly well developed in the Great Lakes basin above the elevation of present lake surfaces. Early geologists traced these abandoned shore features for hundreds of kilometers and found that they were not level, but rose in elevation toward the north. Assuming a given strandline formed approximately synchronously along its length, and was initially close to level, the observed tilt was interpreted as a measure of crustal uplift (Fig. 12). For instance in the northern Lake Michigan basin the Nipissing shoreline rises about 12 m in 200 km, indicating 12 m of differential uplift occurred since these features originally formed.

Water level records form a second and independent source of evidence for crustal motion. At a number of harbors on Lake Michigan, water level records extend back past the turn of the century. Differences in lake surface elevations recorded at separate locations vary with time, but the time series of differences should have a stationary mean if the two locations are not subject to differential crustal movement. Analysis of crustal movement using this approach goes back to Gilbert (1898). The total record of lake

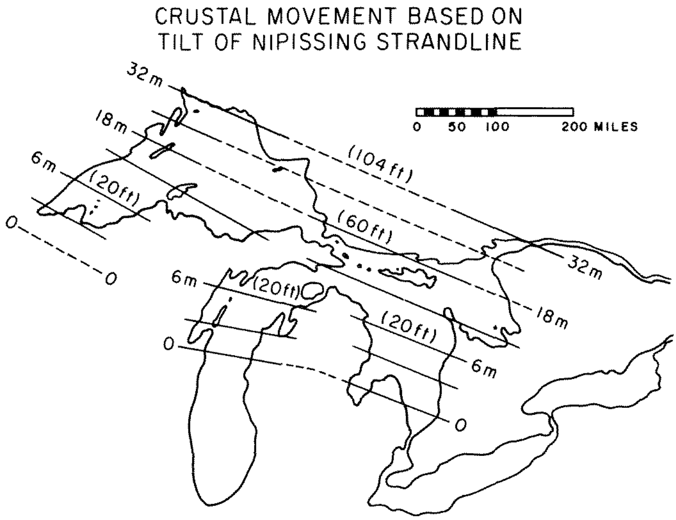

Figure 12. Geologic Evidence of Basin Tilt. Elevation of Ancient (3500 yr. B.P.) Strandline Features in Feet from Leverett and Taylor (1915).

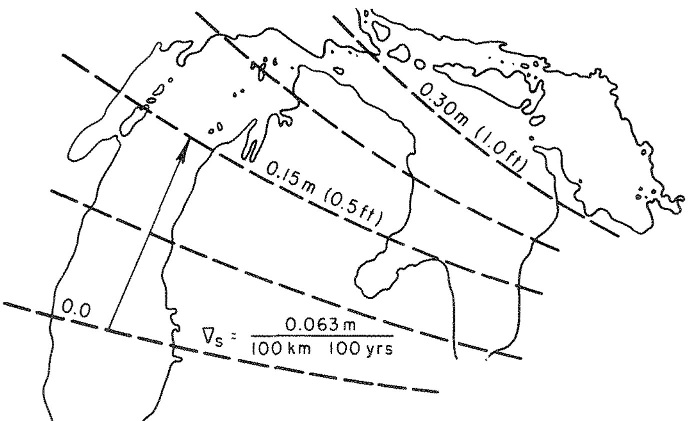

Figure 13. Regression of Lake Level Differences at Different Gages Indicate Basin Tilt (m/100 yrs); from Kite (1972).

level data has been recently reviewed, edited, adjusted, and analyzed by Kite (1972). His estimate of basin tilt, shown in Figure 13, is based on lake level records ranging from 35 to 110 years in length. Differences in water levels recorded at Milwaukee and Sturgeon Bay for example, increase over the 65 year period of common record. The increase is approximately linear with time, and at a rate of 2 mm/yr.

A third independent line of evidence for crustal movement comes from geodetic leveling. By comparing adjusted data obtained in 1929 and 1955 level surveys, Holdahl produced the unpublished map shown in Figure 14. Differences in measured elevations were found to increase along the level line running northwesterly from Chicago. By extrapolation the Lake Michigan basin is thought to have tilted 0.18 m in the 26 years between surveys. Between Milwaukee and Sturgeon Bay this would again be roughly equivalent to 2 mm/yr of differential uplift. These results were described

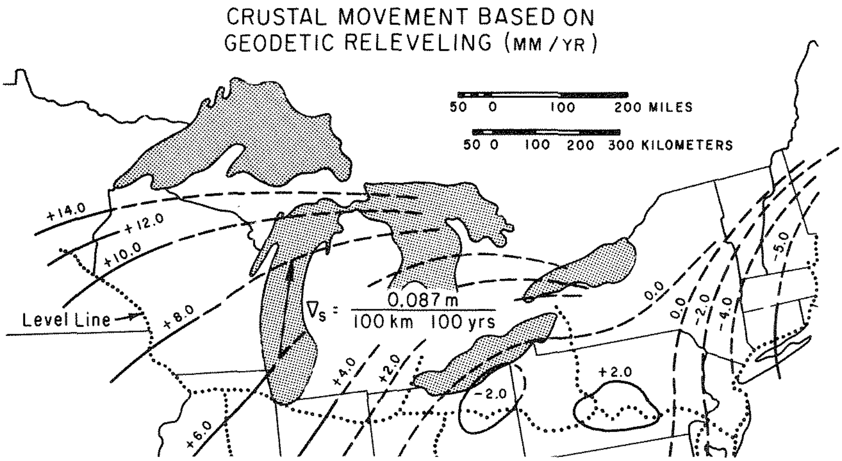

Figure 14. Comparison of First Order Level Net of 1929 with First Order Releveling in 1955 (Meade, 1972) indicates Basin Tilt.

(Meade, 1971) as tentative and subject to revision, but for present purposes they are more than adequate; the general pattern of an active regional tilt in the Lake Michigan basin is confirmed by the similarity of results from independent lines of investigation.

4. <u>Effect of Uplift on Long Term Recession Rates</u>.

Could the relative submergence of the southern end of the Lake Michigan basin explain the greater bluff recession that has occurred there? It is usually assumed that even if crustal uplift is an active process, it is too slow to be a significant factor in contemporary erosion problems. Given the uncertainties in computed rates of uplift and bluff recession, a possible relationship between the two should be examined in the simplest manner possible. In order to compare them quantitatively, both will be approximated by their linear trends. This is not meant to imply that recession is strictly a function of lakeshore position. As pointed out earlier there are many factors affecting recession. The attempt here is merely to obtain a quantitative estimate of how subsidence, taken by itself, affects recession. The regression coefficient is a good estimator of this effect as none of the other factors is thought to exert a regional control. The remaining scatter in Figure 15 illustrates the combined effect of these other variables, which as expected is considerable. The least square regression coefficient is 19 $\pm$ 10 ($\bar{x} \pm 2s$) m per century per 100 km along the lake axis; this trend is statistically significant even at the 1% level. From Figure 15 it seems that this trend may be an expression of a northerly decrease in an upper bound on recession, with low recession values distributed fairly uniformly up and down the lakeshore. Two low values near 60 and 80 km contribute heavily to this impression. It is speculated that greater investment in shore protection may explain the occurrence of some low recession values in the earlier settled southern portion of the basin.

The period of time covered by the water level records and by the bluff recession data discussed in Section 1 are roughly the same. The tilt of the basin estimated from Figure 13 and 14 would be .063 and .087 m per century per 100 km along the axis of the lake. Thus each centimeter of subsidence caused somewhere between one and four meters of recession if the trend in recession is to be attributed solely to subsidence.

It is noted that the longshore trend in recession rates is not so pronounced on the east shore as on the west. Nevertheless the hypothesis that the apparent trend might have arisen by chance ($H_0 : \beta = 0$) would still be rejected; under standard assumptions even if the test were applied to the east coast data taken by itself, $t = 2.4$, $n = 33$). With respect to the smaller increase in recession along the east shore, it is interesting to note that the east shore is backed by high dunes and glacial deposits rich in sand and gravel. Each meter of bluff retreat on the east shore would supply a greater volume of beach material than on the typically lower western shore.

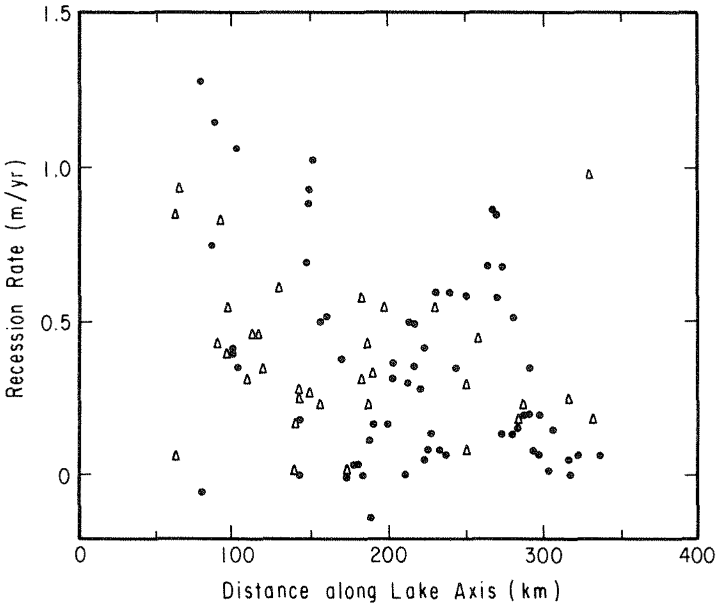

Figure 15. Long Term Rate of Recession Versus Position Measured Along Central Axis of the Lake. Values from the West Shore are Shown as •, East Shore as ▵.

IV CONCLUDING REMARKS

Subsidence increases the rate of erosion in unconsolidated deposits by allowing waves to reach bluffs that were formerly above the elevation of wave uprush. Moreover, waves lose less energy in passing over submerged offshore shoals. The increased erosion can be viewed as an adjustment of the beach to new conditions imposed by subsidence. The quantitative relationship between subsidence and the rate of shore retreat has however, received little attention. From the standpoint of shore protection there are many other over-riding variables that effect erosion. And in areas of extreme subsidence, there are many other damaging consequences: water supply, structural failures, etc. This study demonstrates that subsidence can have a measurable effect on shore retreat. The effect could have profound local impact - consider the resulting decrease in property value if a formerly stable barrier island where subjected to moderate subsidence over a fifty year period.

The shore of Lake Michigan retreated 15 m during a four year period in response to a 0.5 m increase in mean water elevation, and because a broad section of the submerged profile responded by moving 25 m landward, it appears that the shore was lagging behind in its adjustment to high lake levels. Total recession required to reestablish equilibrium after a 0.5 m coastal submergence in four years, extends years beyond the period of subsidence. Based on documented lake shore retreat, profile change, and a rough balancing of the sediment budget, it is estimated that 25 to 30 m of recession would be required to readjust the shore to the 0.5 m rise in lake level. This gives a ratio of expected recession to submergence of approximately 60 to 1.

The amount of shore retreat that would result from a much slower rate of subsidence was interpreted using records of long term bluff retreat and crustal motion. The Lake Michigan basin has been tilting upward toward the north. The 120-year mean recession rates show a similar trend; with recession rates increasing in the direction of greatest subsidence. Regional tilting seems to be the best explanation for the regional variation of recession. Under this assumption each cm of slow submergence would be responsible for from one to four m of shore recession; the ratio of recession to submergence would be between 100:1 and 400:1.

Shore retreat is a non-linear, time-dependent function, and so apparently is the relationship between recession and subsidence rates. Great Lakes studies suggest that long term subsidence may cause several times the recession that would result during a short period of equal, but rapid subsidence. It takes a number of years for the beach profiles to equilibrate. Moreover, slow, long term water level adjustments may permit littoral forces to spread shore eroded material across a wider submerged profile; and therefore, in the long term require a greater volume of shore eroded material to adjust to submergence.

Coastal areas with geomorphology, geology, and wave exposure similar to the study area may be expected to recede at rates roughly on the order of those measured if subjected to the same conditions of subsidence. Wherever possible, shore recession caused by subsidence should be determined along with measurements of subsidence. If enough additional data can be acquired, it may be feasible to establish some functional relationship between subsidence and shore recession that will be valid for a range of subsidence rates. Resulting relationships may then apply to broad classes of coastal conditions.

References

Berg, R.C. and Charles Collinson, 1976, Bluff Erosion, Recession Rates, and Volumetric Losses on the Lake Michigan Shore in Illinois: Environmental Geology Notes, No. 76, Illinois State Geological Survey.

Berg, D.W., and D.B. Duane, 1968, Effect of Particle Size and Distribution on Stability of Artificially Filled Beach, Presque Isle Peninsula, Pennsylvania: Proceedings 11th Conf. Great Lakes Research, p. 161-178.

Bruun, P., 1962, Sea-Level Rise as a Cause of Shore Erosion: Journal of the Waterways, Harbors, and Coastal Engineering Division, ASCE, Vol. 88, No. WW1, p. 117-130.

Caldwell, J.M., 1959, Shore Erosion by Storm Waves: MP 1-59, U.S. Army, Corps of Engineers, Beach Erosion Board, Washington, D.C.

Davis, R.A., Fingleton, W.G., and Pritchett, P.C., 1975, Beach Profile Changes, East Coast of Lake Michigan, 1970-1972: MP 10-75, U.S. Army, Corps of Engineers, Coastal Engineering Research Center, Fort Belvoir, VA.

Hands, Edward B., 1976, Observations of Barred Coastal Profiles Under the Influence of Rising Water Levels, Eastern Lake Michigan, 1967-71: TR 76-1, U.S. Army, Corps of Engineers, Coastal Engineering Research Center, Fort Belvoir, VA.

Hands, Edward B., 1975, Transgression and Recession on a Retreating Coastline: unpublished report, U.S. Army, Corps of Engineers, Coastal Engineering Research Center, Fort Belvoir, VA.

Hands, Edward B., 1970, A Geomorphic Map of Lake Michigan Shoreline: Proceedings of the 13th Conference on Great Lakes Research, p. 250-265.

IGLD, 1961, International Great Lakes Datum (1955): The Coordinating Committee on Great Lakes Basic Hydraulic and Hydrologic Data, 17 p.

Kite, G.W., 1972, An Engineering Study of Crustal Movement Around the Great Lakes: Technical Bulletin 63, Department of the Environment, Ottawa, Canada 57 p.

Larsen, C.E., 1972, The Culture Variable in Shore Erosion Along the Illinois Shore of Lake Michigan: a report supported by the Lake Michigan Federation, 20 p., 53 W. Jackson Blvd., Chicago, IL 60604.

Leverett, Frank and Frank B. Taylor, 1915, The Pleistocene of Indiana and Michigan and the History of the Great Lakes: Monograph Vol. LIII, U.S. Geological Survey, Washington, DC 523 p.

McKee, Edith, 1972, Evaluation of Beach Erosion Problem at Indiana Dunes National Lakeshore: unpublished report prepared for Leviton & Associates, 208 South LaSalle St., Chicago, IL 60604.

Meade, Buford K., unpublished, Report of the Sub-Commission on Recent Crustal Movements in North America: presented at the XV General Assembly of IVGG Moscow, USSR, August 1971.

Powers, W.E., 1958, Geomorphology of Lake Michigan Shoreline, ONR, final report on proj No. NR-387-015, Northwestern University, Evanston, IL.

Richardson, W.S., 1976, Forecasting Beach Erosion Along the Northeast Coast of the United States: Abstract, Northeastern/Southeastern Sectional Meeting, Arlington, VA.

Rondy, D.R., 1969, Great Lakes Ice Atlas: U.S. Lake Survey Research Rpt, 5-6, U.S. Lake Survey Center, Detroit, Michigan.

Seibel, Erwin, 1972, Shore Erosion at Selected Sites Along Lakes Michigan and Huron: University of Michigan PhD Thesis, 175 p.

U.S. Army, Corps of Engineers, Coastal Engineering Research Center, 1973, Shore Protection Manual: Stock No. 08022-00077, U.S. Government Printing Office, Washington, D.C., 160 p.

U.S. Army Engineer District, Detroit, 1956, Beach Erosion Control Berrien County, Michigan: unpublished.

U.S. Congress, 1946, Beach Erosion Study, Lake Michigan Shoreline of Milwaukee County, Wisconsin: House Doc. 526, 79th Congress, 2d session.

Wisconsin Department of Natural Resources, 1969, Survey Records of Milwaukee Co.: Exhibit #2, Public Works Hearing, H.R. 12712.

Acknowledgements.

The author wishes to express his appreciation to Dr. Craig H. Everts for his helpful review and to Drs. R.D. Hobson, William R. James, and R.K. Schwartz for many stimulating discussions.

EFFECT OF CLIMATE ON ORGANIC SOIL SUBSIDENCE

John C. Stephens and Ernest H. Stewart
Agricultural Research Service, U.S.D.A.
Ft. Lauderdale, Fla. and Ft. Pierce, Fla.

Abstract

A reliable estimate of the resultant subsidence rate is usually the most important need in determining the economic feasibility of draining organic soils. Subsidence of peat and muck soils when drained is due to either (a) oxidation, or (b) densification (compaction, desiccation, and loss of the buoyant force of groundwater). Initial subsidence is mainly due to densification. In warm climates, such as south Florida (U.S.A.), the greatest long-term losses, however, are caused by biochemical oxidation. Everglades organic soils are subsiding at rates ranging from 0.5 to 3 inches (1.3 to 7.7 cm) per year and averaging about 1.25 inches (4.2 cm) annually. Research studies demonstrate that biochemical oxidation, which has been responsible for 55 to 75% of total losses in Everglades agricultural soils, is accelerated by warm temperatures, low water tables, high pH, and high organic content.

Russian soil scientists found that compaction and desiccation were the major factors in the subsidence of similar soils near Minsk, Russia. Only 14% of the total subsidence for these soils was caused by biochemical oxidation, and it was suggested that the effects of biochemical oxidation may have been overstressed. By using the Q_{10} concept, where $Q_{10} = 2.0$, we found that measured soil temperature differences between the two regions accounted largely for the observed discrepant subsidence rates, thus providing engineers with a practical mathematical tool for transposing measured long-time subsidence rates from one climatic region to the other.

It has been recognized for 3 centuries that organic soils subside when drained. The history of drainage of the English Fens, which began in 1652, is largely a story of troubles caused by lowering of the land surface. The story of the Fenlands has been marked by alternate cycles of improved drainage with increased subsidence and consequent higher water tables. First, there was gravity drainage. This was followed by pumpage using windmills, then steam engines, and finally diesel engines. All of these methods greatly increased the rate of water removal but failed to provide a satisfactory solution to the problem of agricultural drainage. Frustratingly, the more the water table was lowered by more effective drainage, the more rapidly the peat surface continued to sink. Thus, the achievements of one generation became the problems of the next.

The renowned Holme Post, which was solidly imbedded into a firm foundation of underlying clay at Holme Fen, about 1848, is probably the oldest reliable record of subsidence in existence. By 1932, the soil around the post had dropped 3.25 m (Danby, 1956).

Numerous investigations have since shown that all bog-type organic soils subside with drainage to various degrees. In a paper given at the Tokyo Symposium (Stephens & Speir, 1969) we stated: "Investigators generally agree that subsidence rates for organic soils are positively correlated with groundwater depth - the higher the water table, the lower the subsidence rate. There is, however, no general agreement on the proper depth at which water tables should be held for good land management; or on the relative effect of each of the factors that cause subsidence. Most researchers in the U.S.A. and England believe that deep drainage of organic soil promotes destruction of organic matter, eventually leading to the loss of the organic bed. Several Russian researchers, however, regard deep drainage as a soil-forming process that improves fertility and transforms the underlying sub-soil layers into cultivable soil. We believe that both viewpoints are valid when local soil conditions, crop needs, and yield objectives are considered."

In the paper cited, the six causes of organic soil subsidence were listed as 1) shrinkage due to desiccation; 2) consolidation by loss of the bouyant force of groundwater, or loading, or both; 3) compaction, normally with tillage; 4) wind erosion; 5) burning; and 6) biochemical oxidation. The first three causes--drying, consolidation, and compaction--increase soil density only and do not cause the loss of soil mass. Such densification is largely a non-recurring phenomenon. Wind erosion and burning may occur periodically and can cause significant soil loss in certain bog deposits. Man can control wind erosion and burning, however. Oxidation, on the other hand, is a long-term process that continues as long as temperature, pH, and aeration are conducive to biochemical action. Thus, causes of subsidence can be divided into two main categories: a) physical, which increase soil density and reduce volume only; and b) chemical, which cause a loss in soil substance that can eventually lead to the loss of the bog deposit. Stephens and Speir (1969) compared subsidence rates and the percentage of the losses caused by physical and chemical changes at different world locations. Oxidation was held responsible for 65% of subsidence in the Florida Everglades, as compared with 20% in the Netherlands' polder Mastenbroek and 13% at the peat Bog Experiment Station, Minsk, Belorussia.

In this article, we offer an explanation for the difference in oxidative subsidence rates at different latitudes, in terms of chemical kinetics, and present a simple mathematical model that provides engineers with a tool for transposing long-time known subsidence rates from one climatic region to the other. A reliable estimate of the subsidence rate is usually the most important design need in determining the economic feasibility of draining and managing organic soils.

The kinetic theory gives a picture of how molecules behave and makes it possible to visualize the types of molecular interactions that cause chemical changes. The kinetic theory in its original form affords expressions only for the number of collisions taking place in unit time between gas molecules in unit volume. The fundamental idea of the theory has, however, been applied extensively to systems other than the gaseous system. The theory was found to apply to the kinetics of solutions in the early 1930's.

In brief, the random collision of molecules at high speed, computed from the Maxwell-Boltzmann curves and the laws of probability, form the basis of chemical kinetics. In 1878 J. J. Hood, and in 1887, S. A. Arrhenius, showed that the logarithm of the velocity coefficient, k, of a chemical reaction is linearly related to the reciprocal of the absolute temperature, T.

Expressing the rate of reaction change with temperature by the term Q_{10}, where Q_{10} represents the change in reaction rate for each 10°C temperature change, then from the Arrhenius law,

$$S_2 = S_1 (Q_{10})^x \tag{1}$$

where S_1 = the known oxidative subsidence rate at a known soil temp., T_1.

S_2 = corresponding oxidative subsidence rate at soil temperature T_2, and $x = \frac{T_2 - T_1}{10} = \frac{\Delta T}{10}$

Using the Arrhenius equation, reaction rates have been determined that range from 1 to 500. Rates of biochemical reactions affecting plant life,

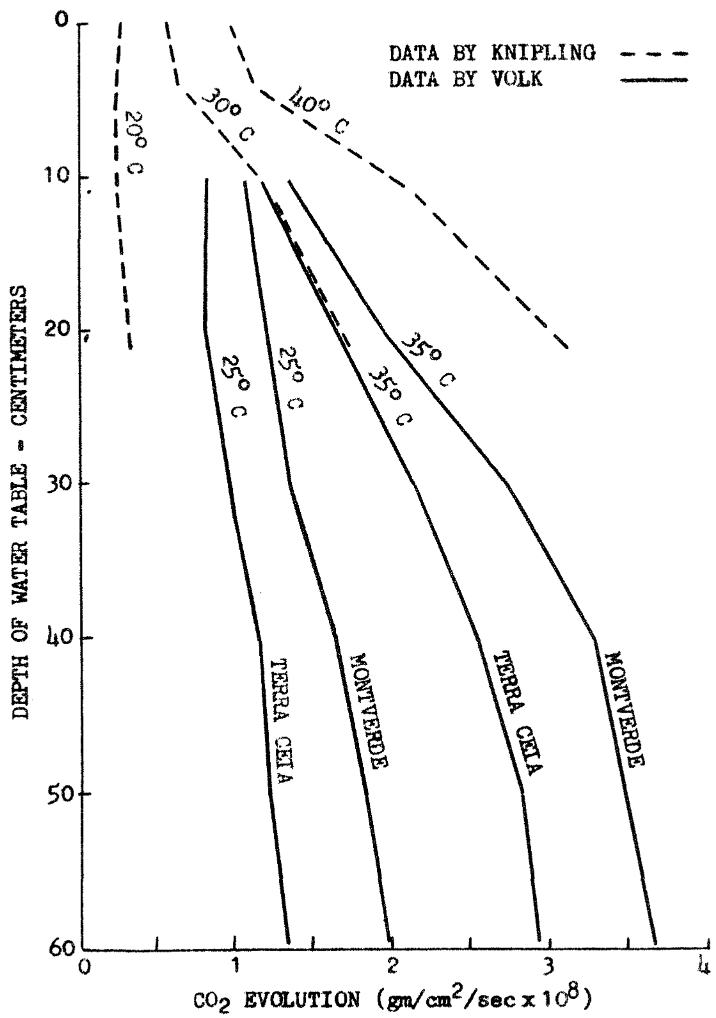

Figure 1. Carbon dioxide evolution rates from organic soil with various depths to the water table and at various temperatures.

however, are relatively stable. Most of these reactions have a Q_{10} value that ranges between 1.5 and 2.5 and averages approximately 2.0.

If, for example, where Q_{10} is known to be either 2.0 or 2.5, then from equation (1):

ΔT	x	$(2)^x$ and	$(2.5)^x$
5°	0.5	1.41	1.58
10	1.0	2.0	2.5
20	2.0	4.0	6.25
30	3.0	8.0	15.62
-10°	-1.0	0.50	0.40
-20	-2.0	0.25	0.16

Thus, where the value of Q_{10} can be ascertained and the biochemical sub-

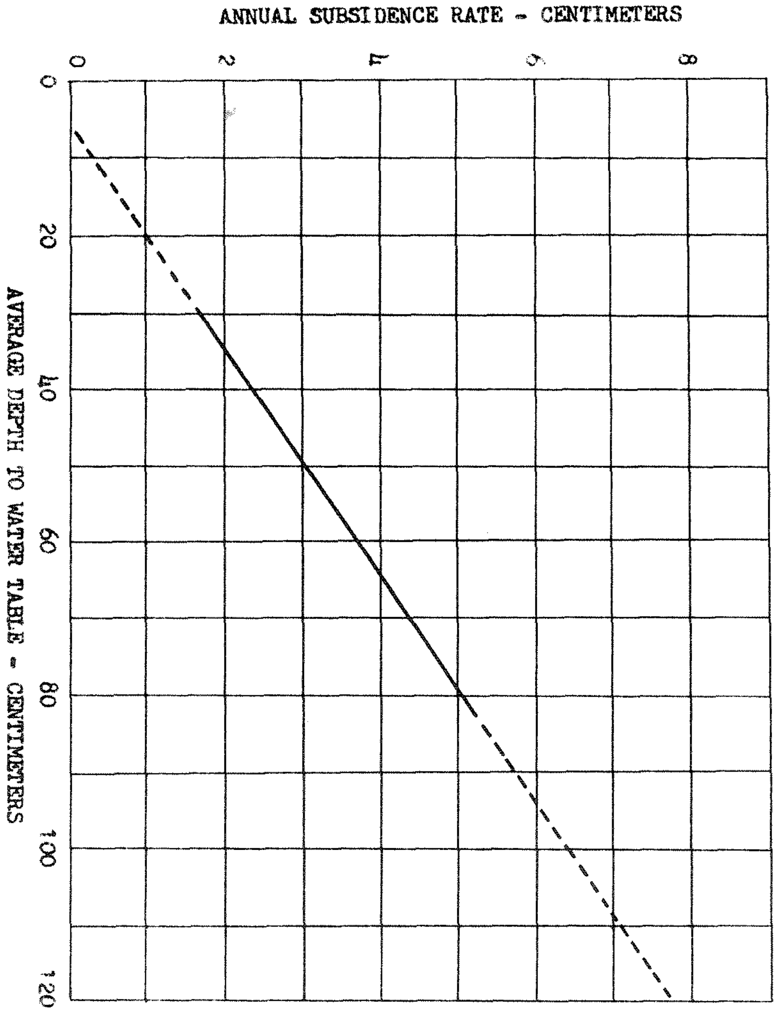

Figure 2. Subsidence rates in organic soils of Florida with various water table depths.

sidence rate S_1 is known for a location that has a soil temperature of T_1, then S_2 may be obtained for a different climatic region with a soil temperature of T_2. This can be done graphically, since the equation plots as a straight line of known slope on semi-log graph paper. Based on similar reactions and on laboratory results, a value of $Q_{10} = 2.0$ appears to be the proper rate for biochemical reactions in organic soils.

Knipling (1970) determined CO_2 evolution from a column of Okeechobee muck in a plexiglass cylinder. The CO_2 evolved was measured as the soil temperature was increased by 10°C increments from 10 to 60°C, and at four shallow watertable depths - 0, 4, 11, and 21 cm. The CO_2 evolution increased with watertable depth and with temperature. From 10 to 20°C the CO_2 changes were small, but generally doubled for each subsequent increase.

Volk (1973) estimated the subsidence rates of organic soils by measuring the CO_2 evolution from seven columns of three representative types of Everglades soil. He found that CO_2 losses were directly proportional to water table depth and temperature, and were a function of organic content and bulk density. Volk's tests were conducted at temperatures ranging from 5 to 45°C, with watertable depths from 5 to 60 cm, and with organic contents of 92.3% for Montverde, or Everglades peat, 90.5% for Terra Ceia, or Everglades peaty muck, and 33.3% for Torry, or Okeechobee muck. Each 10°C increase about doubled the CO_2 evolved at the intermediate temperatures. For a given temperature and watertable depth, the ash content and bulk density values were inversely proportional to the CO_2 evolved, i.e., the CO_2 evolution for Montverde > Terra Ceia > Torry. He ascribed the reduction in biochemical activity for mucks to the high mineral fraction of the soil that formed a clay-organic complex less accessible to the micro-population.

Knipling's results were computed on the basis of grams of CO_2 evolved per cm^2 area per sec. ($g/cm^2/sec$); and Volk's results as grams of C per cm^2 area per minute ($g/cm^2/min$). When converted to the same units, Knipling's results were comparable with Volk's for soils of near the same bulk density (Knipling: ash-12%, bulk density-0.23 g/cm^3; Volk: ash-7.7%, bulk density-0.18 g/cm^3). Figure 1 shows results from the two investigations at temperatures representative of organic soils in south Florida. Both results are plotted as g $CO_2/cm^2/sec \times 10^8$ vs. watertable depth, at the selected temperatures. Knipling's results agree closely with the results obtained by Volk for Montverde soil.

Corresponding subsidence rates for organic soils due to CO_2 evolved can be calculated by multiplying the C losses by the percentage soil C, by bulk density, and a time factor. For organic soils of the type used in Knipling's test, or for Volk's Montverde, approximately 1.20×10^{-8} g $CO_2/cm^2/sec$ evolved should produce an elevation loss of 1 cm annually.

Subsidence rates for plots with controlled water tables at the Florida Everglades Experiment Station are shown in Figure 2. The mean annual soil temperature for these plots was 25°C. The average soil bulk density for the plot with the 60-cm water table depth was 0.22 g/cm^3. From Figure 2, the subsidence rate of this plot is seen to be 3.76 cm/yr. From Figure 1, at 25°C the CO_2 evolution is approximately 1.9×10^{-8} $g/cm^2/sec$ for a similar density soil with this depth to water table. Thus the CO_2 evolution from the lab experiments computes to a subsidence loss of 2.28 cm/yr, or apparently accounts for 61% of the measured loss in elevation for the water table plots. However, the CO_2 evolution accounts only for the loss due to microbial respiration. It does not account for the loss of material hydrolyzed by microbial action, which is removed by leaching under field conditions. The fraction lost by leaching is unknown. It has been estimated as only a small percentage by some plant scientists and as high as 35% by others. For the water table plots, Neller (1944) found no increase in bulk density for 6 years. He stated, however, that his data were not based on enough replicated samples (duplicates only) to compensate for sample variation or for the errors of determination. He concluded, nevertheless, that only a small part of the subsidence could be attributed to compaction.

We reported at the First Symposium in 1969 that changes in bulk density had accounted for about 25% of the total subsidence in the Everglades since drainage began about 1913. This value was based on a field study near the experimental water table plots. Periodic leveling has shown that sinkage was the most severe immediately after drainage and during the first 5 years of tillage. This sinkage, due in large part to densification, wherein the top 18 inches of soil greatly increased in bulk density, took place long before the water table plot studies were begun in 1935. From this, we estimate that the increase in density during the years for which Neller reported (1935-41) did not exceed 10 to 15%. Thus, the loss of hydrolized material by microbial action, which is removed by leaching, would be 25 to 30% according to the experimental data cited. Whatever the exact contribution of the leachates from hydrolized organic material to biochemical subsidence, it is the same group of organisms that evolve CO_2 gas and thus they react in the same manner to a change in soil temperature.

In addition to ascertaining a Q_{10} value, one must determine the temperature at which the organisms become significantly active. Waksman (1929) found that microorganisms in organic soil were perceptibly active only above 5^oC. Significant, too, was his observation that despite differences in the nature and number of the microbial flora inhabiting virgin peats, that when these soils were limed, manured, and cultivated the micropopulation increased to about the same as that for Everglades peats under similar drainage.

From the evidence described we have assumed that the biochemical reactions responsible for the decomposition of peat have a Q_{10} value of 2.0, and that the base temperature at which decomposition becomes significant is $+5^oC$.

Although equation (1) and a graphical technique may be used to evaluate the soil temperature effects on the rate of organic soil decomposition, another, and probably better, evaluation procedure is to use algebraic equations.

The basic subsidence equation is,

$$S_T = (a + bD)\ e^{K\ (T-To)}, \text{ where} \tag{2}$$

S_T = biochemical subsidence rate at temperature, T.

D = depth of water table

e = base of the natural logarithm

K = reaction rate constant

To = base soil temperature (assumed as $+5^oC$)

a and b are constants

Using the empiricism that S_T multiplies to $Q_{10}.S_{(T+10)}$ for each 10^o rise in temperature, we have

$$S_{(T+10)} = Q_{10}.S_T = (a+bD)\ e^{K\ [(T+10)-To]}. \tag{3}$$

Dividing eq. (3) by eq. (2), we have

$$\frac{S_{(T+10)}}{S_T} = Q_{10} = e^{10K}, \tag{4}$$

By rewriting (3) to express K in terms of Q_{10}, we have

$$K = 1/10 \ln Q_{10}, \tag{5}$$

and substituting (5) into (2),

$$S_T = (a + bD)\ Q_{10}^{(T - To)/10}. \tag{6}$$

To determine values of a and b we use the data from Figure 2, where T is equal to 25^o; thus,

when D = 40 cm, S = 2.29 cm/yr,

and D = 80 cm, S = 5.00 cm/yr.

Substituting these values into (6) and solving the simultaneous equation to evaluate a and b, we get

$a = -0.1035$

$b = 0.0169.$

Then from (6) we have

$$S_x = (-0.1035 + 0.0169\ D)\ (2)^{(T_x - 5)/10} \qquad (7)$$

Equation (7) may thus be used to find the biochemical subsidence rate for lowmoor organic soils at location x where the annual average soil temperature at the 10-cm depth is T_x.

For example, equation (7) is used as follows to estimate the annual subsidence rate - exclusive of compaction or other bulk density change - at the Lullymore Experimental Station in the Irish Republic for the arable lowmoor soils, where the average annual soil temperature is 8.5° 1/ and the water table depth is held at 90 cm:

$$S_L = (-0.1035 + 0.0169 \times 90)\ (2)^{(8.5 - 5.0)/10} \qquad (8)$$

$$S_L = 1.4175 \times 2^{0.35}$$

$$S_L = 1.4175 \times 1.27 = 1.80\ \text{cm/yr}$$

This indicates that if the Everglades histosols were transposed to Lullymore, the rate of decomposition would be only 32% of the rate in south Florida where $T = 25^{\circ}$.

If the same soils were in a more tropical climate where the average soil temperature was 30°C, for example, again from (7)

$$S_x = (-0.1035 + 0.0169 \times 90)\ (2)^{(30-5)/10}$$

$$S_x = 8.02\ \text{cm/yr}$$

which is a rate 43% greater than the decomposition rate for south Florida.

For convenience in estimating S_x for any selected temperature, T_x, the results from equation (7) have been plotted at watertable depths, D, of 30, 60, 90, and 120 cm (Figure 3).

Obviously in the development of this model we have made certain simplifying assumptions. The assumption that $Q_{10} = 2.0$ and $To = 5^{\circ}$ is chosen according to the best information known to us. If, however, future studies indicate the values of Q_{10} and To to be somewhat different, the mathematical procedures for computations will still be valid. Only the constants for a and b will change. For instance, where $Q_{10} = 1.5$ and $To = 0^{\circ}$, then $a = -0.1523$ and $b = 0.0246$. We have assumed that values of Q_{10} and To are independent of water table depth, which is questionable. There is also lab evidence that the value of Q_{10} greatly exceeds 2.0 from To to about 10°C. In addition, there are inherent difficulties in using average annual soil temperatures to compute subsidence rates. It would be much better to compute the daily, or even monthly, integrated temperature values versus subsidence rates for the same time periods. Unfortunately, field subsidence rates cannot be accurately determined for such short time intervals.

In spite of the shortcomings of the model, its use would tend to err on the conservative side and we believe it is sufficiently accurate to justify field estimates of biochemical subsidence for engineering and

1/ Personal communication, Director, Lullymore Exp. Sta., Ireland, 1969.

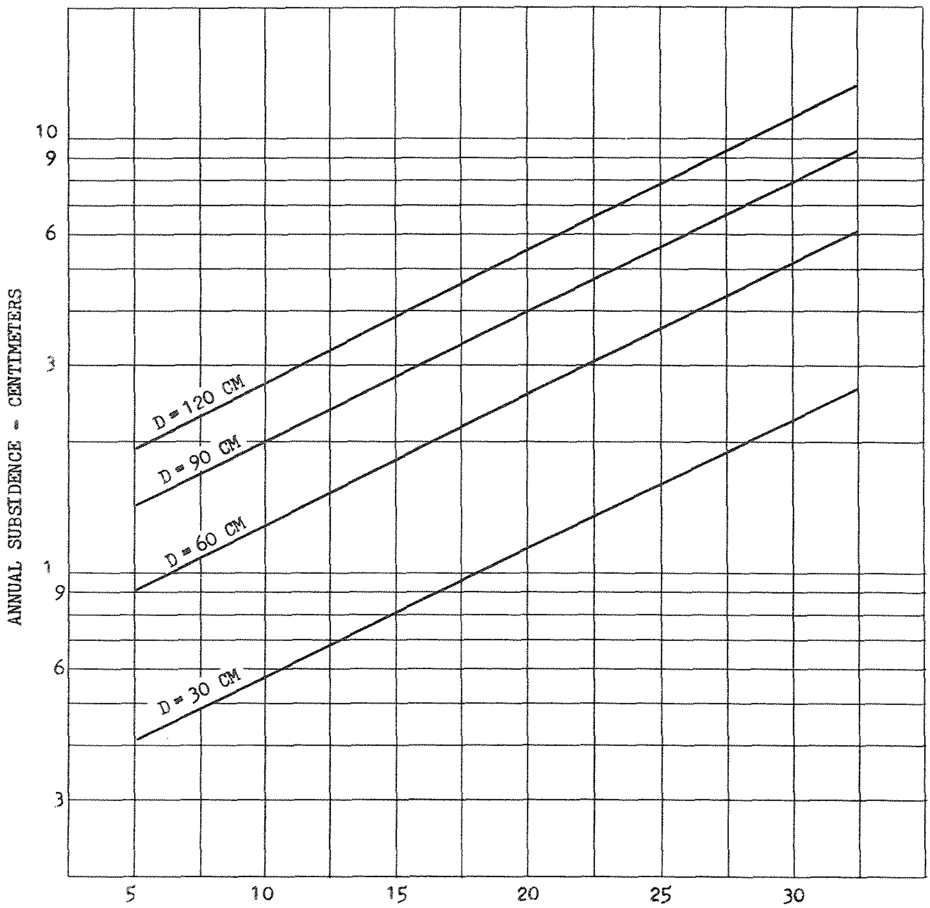

Figure 3. Annual subsidence of organic soils with various water table depths and soil temperatures.

economic predictions until better methods of computation are developed.

University of Florida Agricultural Experiment Station scientists have recently begun an intensive team effort of field, laboratory, and mathematical studies aimed at better defining the specific causes of biochemical subsidence and gaining better insights into the interrelationships of the causes. In connection with these studies, B. G. Volk and J. Browder[2] have evolved a sophisticated computerized mathematical model that simulates the interaction of climatologic and biologic factors on the biochemical oxidation of histosols following drainage. First runs, based in part on gross estimates of input data, have given results reasonably consistent with historical records. Hopefully, such studies will help researchers develop a better understanding of how the system works and to identify those factors that have the greatest impact on systems behavior so that additional research studies can be concentrated in these areas.

2/ Personal communication (Oct. 1976) Joan Browder and Robert G. Volk, preliminary memo. rpt., Systems Model of Carbon Transformation in Soil Subsidence.

Acknowledgments

The authors express their gratitude to Willard N. Snyder and William C. Mills, Hydraulic Engin., Athens, Ga.; and also Victor Chew, Biometrician, Gainesville, Fla.; all of A.R.S., for mathematical assistance.

References

Danby, H. C., 1956, The Drainage of the Fens: Cambridge Univ. Press, 2nd Ed.

Knipling, E. G., Schroeder, V. N., and Duncan, W. G., 1970, CO_2 Evolution from Florida Organic Soils: Soil & Crop Sci. Soc. Fla. Proc. Gainesville, Fla., Vol. 30, p. 320-326.

Neller, J. R., 1944, Oxidation Loss of Lowmoor Peat in Fields with Different Water Tables: Soil Sci., Vol. 57, no. 4, p. 275-280.

Stephens, John C., and Speir, W. H., 1969, Subsidence of Organic Soils in the U.S.A.: Assn. Intern. of Hydro. Sci., Colloque De Tokyo, Pub. 89.

Volk, B. G., 1973, Everglades Histosol Subsidence: 1. CO_2 Evolution as Affected by Soil Type, Temperature, and Moisture: Soil & Crop Sci. Soc. of Fla., Gainesville, Fla., Proc. Vol. 32, p. 132-135.

Waksman, S. A., and Stevens, R. K., 1929, Contributions to the Chemical Composition of Peat: V The Role of Micro-organisms in Peat Formation and Decomposition. Soil Sci., Vol. 38, no. 4, p. 315-340.

Publication n°121 of the International Association of Hydrological Sciences
Proceedings of the Anaheim Symposium, December 1976

NITRIFICATION IN EVERGLADES HISTOSOLS: A POTENTIAL ROLE IN SOIL SUBSIDENCE [1]

Robert L. Tate III
Agricultural Research and Education Center, P. O. Drawer A
Belle Glade, Florida

Abstract

Subsidence of the Everglades Histosols occurs at a rate of approximately 3 cm/year. The major cause of this loss of soil is the oxidation of the organic matter by the microbial community. One of the products of this microbial activity is inorganic nitrogen. Assuming an annual subsidence rate of 3 cm, approximately 1400 kg/ha of nitrogen is released per year. Much of this nitrogen accumulates in the soil as nitrate.

The microbial reaction sequence involved in the production of this nitrate is initiated by mineralization of the soil organic matter by the heterotrophic bacteria and fungi. The major nitrogenous product of this process is ammonium. This is the primary step involved in soil subsidence. The ammonium formed through the mineralization is then oxidized by the nitrifying bacteria to nitrate. Two groups of microorganisms are known to participate in this process, heterotrophic and autotrophic nitrifiers. Nitrate can be removed from the soil by denitrification, assimilation by the plant community or microbial community, or run off in the drainage waters.

Examination of the microbial community involved in nitrogen metabolism in Histosols suggests that the nitrate concentration found in the soil can be controlled through prudent control of the water table. Raising the water table would decrease the rate of soil subsidence, hence decreasing the amount of inorganic nitrogen formed, as well as inhibit nitrification and stimulate denitrification. Preservation of one natural resource, the organic soils, will help in the preservation of the surrounding lakes and streams.

The Everglades Histosols are subsiding at a rate of approximately 3 cm/year (Stephens and Speir, 1969). Among the reasons proposed for this loss of soil elevation are compaction, shrinkage due to drying, burning, wind erosion and microbial oxidation (Stephens and Speir, 1969). The primary cause must be considered to be microbial oxidation. This aerobic process which commenced upon drainage of the soil accounts for 58 to 73 percent of the observed subsidence (Volk, 1972). These values were obtained by comparing the amount of carbon dioxide produced by microbial oxidation of the soil with the known rate of subsidence of the soils in the field.

Among the products of this microbial oxidation of soil organic matter are the inorganic nitrogenous compounds nitrate and ammonium. With the soil organic nitrogen content of 3.5 percent (Davis and Lucas, 1959) in Everglades Histosols, approximately 1400 kg/ha inorganic nitrogen can be expected to be produced by the subsidence of 3 cm of soil. The accumulation of much of this nitrogen as nitrate was demonstrated by Neller (1944) when he observed nitrate accumulation in fallow soil and soil planted to corn. The nitrate concentration was measured in surface (0-15 cm) and subsurface (15-30 cm). Concentrations of 239 and 127 ppm nitrate-nitrogen (dry soil) were found in the surface and subsurface fallow soils, respectively. The growth of the corn resulted in a decrease in the nitrate in the surface soil to 145 ppm. No change was observed in the subsurface sample. Recent studies have demonstrated nitrate-

[1] Florida Agricultural Experiment Stations Journal Series No. 331

nitrogen concentrations in surface samples of fallow soil collected in January, 1976, of 320 ppm. In July, 1976, variation of the nitrate concentration with depth of Pahokee muck was examined. The nitrate concentration varied with depth with 456, 176, 149, and 83.6 ppm found at the 0-18, 18-28, 28-38 and 48-58 cm depths, respectively. The nitrate found deep in the profile was apparently in part formed *in situ* since nitrifying bacteria were found in high concentrations at these depths (Tate, unpublished data).

The moisture content of the soil has an effect on the observed nitrate content. Hortenstine and Forbes (1972) examined the nitrate content of soil water from a swampy area and an adjacent drained, newly cleared, unfertilized field. The nitrate-nitrogen concentration area was 8 fold higher in the drained area than in the swamp. Approximately 48 ppm nitrate-nitrogen was detected in the soil water at a 60 cm depth from the drained soil as compared to approximately 6 ppm from the swamp at a comparable depth. Neller (1944) also observed a decrease in nitrate with elevated water tables. With a water table of approximately 30 cm, 145 ppm nitrate-nitrogen was detected in the top 15 cm of soil. Lowering the water table to about 60 cm resulted in an increase in the nitrate concentration to 260 ppm. This indicates a direct relationship between subsidence rate and nitrate production. The rate of subsidence is inversely, linearly proportional to the depth to water table (Stephens, 1969). Thus, an increase in the depth to water table by 50 percent resulted in nearly a 50 percent increase in the nitrate detected.

This solubilization of the nitrogen as a result of subsidence is of great importance to the agriculturalist since it allows growth of crops on Histosols generally in the absence of exogenously added nitrogenous fertilizer. The environmentalist also finds an interest in this nitrate since it is produced in concentrations above those needed or used by the crop (Neller, 1944). Thus, a potential for nitrogenous enrichment of waters adjacent to and flowing from Histosols exists. As a result of the problems and benefits of this nitrogen, the microbial involvement in nitrogen metabolism in Histosols has been examined.

The microbial processes leading to and affecting the accumulation of nitrate in Histosols are presented in Fig. 1. The nitrogen is converted from the organic to the inorganic state by the process of mineralization. This is the step primarily relating to soil subsidence since the nitrogen is converted from an insoluble, chemically complexed form into a soluble form which can then be lost from the soil system. The primary product of this solubilization is ammonium. Some of this ammonium can be returned to the soil organic matter pool by the microbes and plants. These organisms use the ammonium in the synthesis of new cellular material. Upon the death of the organism the newly synthesized cellular material is cycled back into the soil organic matter. The ammonium formed from mineralization is further metabolized by the microcommunity to nitrate by a process called nitrification. Nitrite serves as an intermediate in this oxidative pathway. Since most of the organisms involved use ammonium as the primary substrate, one of the limiting factors in the formation of nitrate in the Histosol is the amount of ammonium available for oxidation. One exception to this will be discussed later. Nitrate can be removed from the soil by denitrification. In this process, the nitrate is reduced via nitrite to atmospheric nitrogen (dinitrogen). Because of the importance of the latter two processes, nitrification and denitrification, to the nitrate concentration found in the soil, they will be discussed in greater detail.

Nitrification: Nitrification is the biological oxidation of nitrogen from a reduced to a more oxidized state (Alexander, 1965). This aerobic process is primarily accomplished by the autotrophic nitrifier. These

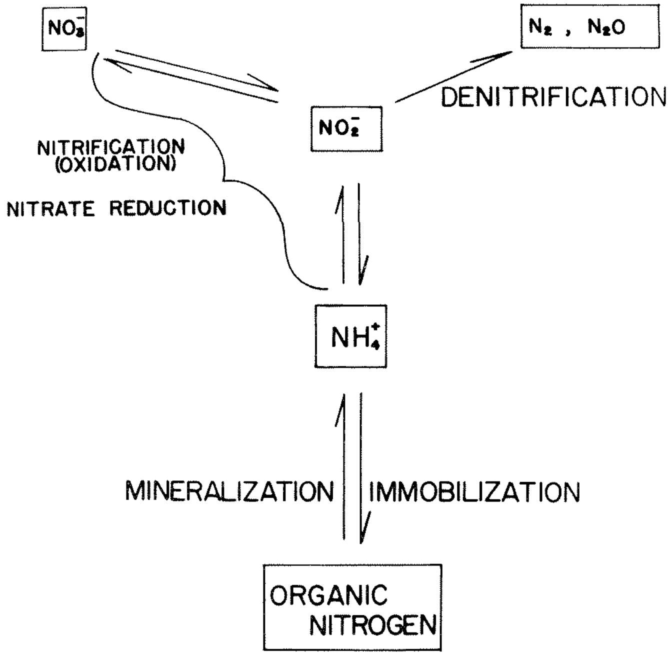

Fig. 1: Nitrogen Transformations in Histosols

organisms gain their energy from the oxidation of nitrogen, hence the name nitrifier, while using carbon dioxide as a carbon source. The microbes are classified as autotrophs since they only use inorganic compounds as their sources of carbon and energy. Since the oxidation of nitrogen is the sole source of energy for these organisms, their presence in the soil sample indicates that they are functioning in the production of nitrate (Alexander, 1965). The more prevalent autotrophic nitrifiers are classified in the bacterial genera Nitrobacter and Nitrosomonas. Nitrosomonas oxidize ammonium to nitrite while the Nitrobacter complete the oxidation by oxidizing the nitrite to nitrate. The energy yielded to the microorganism depends upon the portion of the reaction completed. Oxidation of ammonium to nitrite yields 65.2 to 84 kcal per mole of ammonium. The oxidation of nitrite yields 17.5 to 20.0 kcal per mole (Alexander, 1965). Based on the growth yields of Nitrosomonas europaea and Nitrobacter agilis in culture, Alexander et al. (1960) estimated that 2×10^8 Nitrosomonas and 4×10^7 Nitrobacter cells are needed to form 1.0 mg nitrate-nitrogen.

Likely, the most significant limiting factor for the functioning of these organisms in Histosols, aside from the existance of ammonium the primary substrate, is the presence of oxygen. These organisms are obligately aerobic and thus, would not be expected to be found in swampy soils or flooded muck. Herlihy (1973) found few Nitrobacter and no Nitrosomonas in undrained peat. After draining and cultivation, the number of Nitrosomonas and Nitrobacter increased to 1.3×10^6 and 3.3×10^7/g dry soil, respectively.

Recently, several heterotrophic bacteria and fungi have been shown to oxidize nitrogenous compounds, both inorganic and organic, to nitrite and/or nitrate (Eylar and Schmidt, 1959; Doxtander and Alexander, 1966; Gunner, 1963; Marshall and Alexander, 1962 and Odu and Adeoye, 1970). Verstraete and Alexander (1972) isolated an Arthrobacter sp. which oxidized ammonium to hydroxylamine, a bound hydroxylamine, a hydroxamic acid, a substance thought to be a primary nitro compound, as well as nitrite and nitrate. The bound hydroxylamine was identified as 1-nitrosoethanol. These workers also demonstrated that hydroxylamine, 1-nitrosoethanol, nitrite and nitrate were formed in samples of natural waters and soils amended with acetate and ammonium. This suggests that heterotrophic nitrification can occur in natural ecosystems (Verstraete and Alexander, 1973). Since these organisms gain most, if not all, of their energy from the oxidation of organic compounds, their existance in soil does not imply that they are nitrifying. Indeed, it has been shown that at least in culture the nitrate is formed in the culture after the growth of the microorganism. This suggests that the oxidation of ammonium is of no benefit to the heterotrophic nitrifier (Obaton et al., 1968).

Both types of nitrifier have been demonstrated in Pahokee muck (Tate, 1977). Samples of fallow muck collected in November, 1975, contained 3.3×10^4 Nitrobacter, 1.8×10^4 Nitrosomonas and 4.1×10^5 heterotrophic nitrifying arthrobacter/g dry soil. The nitrate concentration in the soil sample was 318 ppm. Considering the above relationship between population of nitrifiers and the amount of nitrate formed, the population of autotrophic nitrifiers found in this sample was less than 0.1 percent of that necessary to yield the measured quantity of nitrate. This suggests that other organisms were responsible for at least some of the nitrate formed. One potential candidate for the nitrification is the large population of heterotrophic nitrifiers.

As indicated previously, the presence of the heterotrophic nitrifier is not an indication of its being active in nitrification. Thus, several other studies were carried out to test this possibility (Tate, 1977). One indication of whether an organism is participating in a particular reaction is to observe the changes in the population when the substrate for the reaction is added. The population of an organism gaining benefit from the activity would be expected to increase. Thus, soil was amended with acetate and/or ammonium and the nitrifier population assayed. Ammonium stimulated the growth of the autotrophic nitrifier but not the heterotroph, whereas the addition of ammonium and acetate resulted in the same increase in the autotrophic nitrifiers accompanied by a four fold increase in the population of heterotrophic nitrifiers. Comparable concentrations of nitrate were produced with both treatments. In both cases, insufficient populations of autotrophic organisms were developed to account for the nitrate produced. As a further test of the function of the heterotrophic nitrifier, soil was amended with ammonium acetate plus sufficient 2-chloro-6-(trichloro-methyl) pyridine to inhibit nitrate formation but not prevent it. 2-Chloro-6-(trichloro-methyl) pyridine is a specific inhibitor of autotrophic nitrification (Goring, 1962). It was hoped that by partially inhibiting nitrate production it would be possible to determine if part of the nitrate formed resulted from the heterotrophs. The autotrophic nitrifier population was inhibited, as expected, while the heterotrophic organisms were totally uninhibited, again suggesting that the heterotrophs were indeed responsible for some of the nitrite found in the soil. A final test of this possibility involved the inoculation of sterile Pahokee muck with an Arthrobacter sp. isolated from muck. This organism produced nitrite but not nitrate when grown in culture. Nitrite was produced by this organism in natural soil and in soil amended with acetate and/or ammonium. This suggests that indeed the heterotrophic nitrifier is functioning in these soils.

The functioning of the heterotrophic nitrifier in these soils would have an impact on soil subsidence as well as water quality. These organisms could produce nitrate directly from the organic matter without having to rely on other microorganisms to produce the ammonium. Therefore the organisms would be participating directly in the process of soil subsidence. Another interesting side light to the function of the heterotroph in nitrification involves a public health problem. Verstraete and Alexander (1972) have demonstrated that one of the products of heterotrophic nitrification is 1-nitrosoethanol. Although the toxicological properties of this specific compound are not known, 1-nitrosoethanol is related to the carcinogenic N-nitrosamines which can be formed in nature (Ayanaba et al., 1973; Tate and Alexander, 1974).

Denitrification: Denitrification is the major natural biological process for removing nitrogen from these Histosols. For this discussion, denitrification will be defined as the biological reduction of nitrite and nitrate to volatile gases, dinitrogen and nitrous oxide. The microorganisms involved are heterotrophs which use the nitrogen as a terminal electron acceptor. The organisms are not obligatorily linked to the process; thus, the presence of denitrifiers in a soil sample, as it was with the heterotrophic nitrifier, does not indicate nitrifying activity. As a result of the basic nature of the process, two conditions would limit the extent of the reaction in Histosols. The first is the presence of oxygen. Broadbent and Stojanovic (1952) demonstrated that in mineral soils collected in New York denitrification was inversely proportional to the partial pressure of oxygen. They did though observe appreciable denitrification under fully aerobic conditions. The second limiting factor involves the source of electrons for the reductive step. The organism must have a source of metabolizable carbon for the denitrification to occur. Of the two conditions, oxygen is likely the major limiting factor in denitrification in Histosols.

Populations of 3.3×10^2 denitrifiers/g dry muck were found in surface (0-15 cm) muck. The muck samples were collected in November, 1975. Comparable populations were found in the subsurface samples (46-60 cm). This is interesting since it would be expected that as the depth increased the oxygen would become limiting, which would result in the stimulation of the denitrifier population. If some other factor such as carbon were limiting the population size, then a change in the oxygen supply, such as that expected by the increased depth in the soil, would not have an effect. To test this possibility the oxygen content of muck was decreased by flooding the soil. The Pahokee muck was flooded for two weeks prior to the measurement of the denitrifiers. A 100 fold increase in the denitrifiers in the flooded soil was observed. In control soil incubated under natural aerated conditions, no change in the population was observed. Thus, the limiting of oxygen content of the soil air resulted in a significant increase in the denitrifiers. This implies that oxygen was not decreased sufficiently in the samples from 46-60 cm listed above to induce the denitrifier population.

Further evidence that the denitrifiers were not active in these soils is the large concentrations of nitrate detected. Apparently, the denitrifiers are inhibited sufficiently to allow the nitrate to accumulate. The nitrate is then available to the plant community or to be washed into the surrounding waters.

Conclusions: Nitrate accumulation in Histosols is both beneficial and detrimental. The benefits to the agriculturalist are unquestioned. Unfortunately, the nitrate is produced by the soil microorganisms at a rate greater than is needed by the crop. This poses a potential threat to the regional water quality. Examination of the microorganisms responsible for this nitrate production suggests two means of limiting the accumulation. These are to decrease the subsidence rate, hence the amount of inorganic nitrogen produced, and to increase denitrification. Previous work has amply demonstrated that prudent control of the water table will decrease the subsidence rate. The characteristics of the microbial community suggest that elevated water table will also decrease nitrification and increase denitrification through the creation of an anaerobic environment. The nitrification will also be decreased through the reduction of the supply of the primary substrate, ammonium. Thus, the preservation of one resource, the organic soils, can lead to the protection of a second, or lakes and streams.

References

Alexander, M., 1965, Denitrifying Bacteria: in (C. A. Black, ed.) Methods of Soil Analysis, pt. 2. Chemical and Microbiological Properties: American Society of Agronomy. Madison, Wi., p. 1484-1486.

Alexander, M., 1965a, Nitrification: in (W. V. Bartholomew and F. E. Clark, ed.) Soil Nitrogen: American Society of Agronomy, Inc., Madison, Wi., p. 307-343.

Alexander, M., K. C. Marshall, and P. Hirsch, 1960, Autotrophy and Heterotrophy in Nitrification: Trans. Int. Congr. Soil Sci., 7th. v. 2, p. 586-591.

Ayanaba, A., W. Verstraete, and M. Alexander, 1973, Formation of Dimethylnitrosamine, a Carcinogen and Mutagen, in Soils Treated with Nitrogen Compounds: Soil Sci. Soc. Am. Proc. v. 37, p. 565-568.

Broadbent, F. E., and B. F. Stojanovic, 1952, The Effect of Partial Pressure of Oxygen on Some Nitrogen Transformations: Soil Sci. Soc. Am. Proc. v. 16, p. 359-363.

Davis, J. F., and R. E. Lucas, 1959, Organic Soils, Their Formation, Distribution, Utilization and Management: Special Bulletin 425, Michigan Ag. Exp. Sta., East Lansing, Mi.

Doxtander, K. G., and M. Alexander, 1966, Nitrification by Heterotrophic Soil Microorganisms: Soil Sci. Soc. Am. Proc. v. 30, p. 351-355.

Eylar, O. R., and E. L. Schmidt, 1959, A Survey of Heterotrophic Microorganisms from Soil for Ability to for Nitrite and Nitrate: J. Gen. Microbiol. v. 20, p. 473-481.

Goring, C. A. I., 1962, Control of Nitrification by 2-chloro-6-(trichloromethyl) pyridine: Soil Sci. v. 93, p. 211-218.

Gunner, H. B., 1963, Nitrification by Arthrobacter globiformis: Nature (London) v. 197, p. 1127-1128.

Hirlihy, M., 1973, Distribution of Nitrifying and Heterotrophic Microorganisms in Cutover Peats: Soil Biol. Biochem. v. 5, p. 621-628.

Hortenstine, C. C. and R. B. Forbes, 1972, Concentrations of Nitrogen, Phosphorus, Potassium and Total Soluble Salts in Soil Solution Samples from Fertilized and Unfertilized Histosols: J. Environ. Qual. v. 1, p. 446-449.

Marshall, K. C. and M. Alexander, 1962, Nitrification by Aspergillus flavus: J. Bacteriol. v. 83, p. 572-578.

Neller, J. R., 1944, Influence of Cropping, Rainfall, and Water Table on Nitrates in Everglades peat: Soil Sci. v. 57, p. 275-280.

Obaton, M., N. Amarger, and M. Alexander, 1968, Heterotrophic Nitrification by Pseudomonas aeruginosa: Arch. Microbiol. v. 63, p. 122-132.

Odu, C. T. I., and K. B. Adeoye, 1970, Heterotrophic Nitrification in Soils: A Preliminary Investigation: Soil Biol. Biochem. v. 2, p. 41-45.

Stephens, J. C., 1969, Peat and Muck Drainage Problems: J. Irrig. and Drainage Div. Paoc. Am. Soc. Civil Eng. v. 95, p. 285-305.

Stephens, J. C. and W. H. Speir, 1969, Subsidence of Organic Soils in the U. S. A.: Extrait de la Publication No. 89. Colloque de Tokyo. Assoc. Internationale D'Hydrologie Scientific p. 523-534.

Tate, R. L., 1977, Nitrification in Histosols: A Potential Role for the Heterotrophic Nitrifier: Submitted for Publication, Appl. Environ. Microbiol.

Tate, R. L. and M. Alexander, 1974, Formation of Dimethylamine and Diethylamine in Soil Treated with Pesticides: Soil Sci. v. 118, p. 317-321.

Verstraete, W., and M. Alexander, 1972, Heterotrophic Nitrification by Arthrobacter sp.: J. Bacteriol. v. 110, p. 955-961.

Verstraete, W., and M. Alexander, 1973, Heterotrophic Nitrification in Samples of Natural Ecosystems: Environ. Sci. Technol. v. 7, p. 39-52.

Volk, B. G., 1972, Everglades Histosol Subsidence 1. CO_2 Evolution as Affected by Soil Type, Temperature, and Moisture: Soil Crop Sci. Soc. Fl. Proc. v. 32, p. 132-135.

Waksman, S. A., and K. R. Stevens, 1929. Contribution to the Chemical Composition of Peat: V. The Role of Microorganisms in Peat Formation and Decomposition: Soil Sci. v. 28, p. 315-340.

Publication n°121 of the International Association of Hydrological Sciences
Proceedings of the Anaheim Symposium, December 1976

THE EARTH SURFACE SUBSIDENCE AT THE AREAS OF GAS AND OIL PUMPING OUT

A. S. Ilijn
Central Scientific Research Institute of Geodesy, Air Survey and Cartography

One of means for studying influence of technogenuos processes upon the Earth surface movements is the repeated leveling method.

The special geodetic polygones have been established in the USSR to analyze the technogenuos processes impact onto the Earth surface movement at area of working deposits of gas, oil, subsoil waters, and so on.

General procedure of geodetic polygone extension and geodetic surveying has been elaborated. Maximum settlement of the Earth surface has been found to be equal to :93 mm for 4 years at Sebelinskoje gas deposit with layer pressure lowering up to 40 atm: 60 mm for 3,5 years at Gazlinskoje gas deposit with layer pressure lowering up to 10 atm. Separate parts of Apseronskij peninsula sank up to 2,5 m for the period 1912-1962 due to oil pumping out. Maximum subsidence areals are related to the oil extracting regions. Irregular and fluctuable nature of the Earth surface movements due to intensity of deposit exploitation has been outlined in the paper.

References

Лилиенберг Д.А., Мещерский И.Н.., I968, "Современные тектонические движения Апшеронского полуострова".
Сборник. Современные движения земной коры, № 4, Москва

Успенский И.С., В.В.Гаревский, I969, "Об устойчивости реперов на территории эксплуатируемых газовых месторождений", "Геодезия и картография", № 9

Успенский М.С., Гаревский В.В., I970, "Об оседании земной поверхности в местах эксплуатации газовых месторождений", "Геодезия и картография", № 8.

Publication n°121 of the International Association of Hydrological Sciences
Proceedings of the Anaheim Symposium, December 1976

STUDIES OF ROCK STRATA SUBSIDENCE DUE TO DEEP WATER-LEVEL LOWERING IN MINING OPERATIONS IN THE USSR

V.A. Mironenko and E.P. Pisanets
Leningrad Mining Institute, Leningrad, USSR and USSR Ministry for Ferrous Metallurgy, Moscow, USSR.

Investigation of rock strata subsidence due to deep water-level lowering is gaining in practical importance in connection with both deformation of surface and subsurface structures and necessity of environmental protection. In mining, emphasis is placed upon studying shaft deformation due to deep water-level lowering, both ultimate subsidence values and subsidence rates being predicted.

The theoretical basis of subsidence studies *is the system of equations for flow in rheologic* media following from continuity equations for solid and liquid phases and equations of motion and state for the solid phase as the compression relationship of the hereditary creep theory. For the most important investigation stage, involving determining initial calculation parameters, this system of equations is advisable to simplify substantially by dividing the process under investigation into two stages /primary and secondary consolidation/.

The parameters of the ultimate consolidation stage, largely controlled by rheologic rock properties, are commonly determined with a sufficient reliability in laboratory compression tests. In contrast, the flow consolidation parameters may be estimated by laboratory methods only in rare cases on account of the effect of flow macroheterogeneity and fracturing of rock strata being compressed, role of the initial flow gradient and technical difficulties. Therefore with a long duration of the consolidation flow stage reliable prediction may be made only be test and test-development pumping accompanied by investigations using observation wells, pore pressure sensors, and surface and subsurface bench marks. Such observations combined with laboratory tests have allowed to predict subsidence in the Yuzhno-Belozersk mineral deposit area where land subsidence exceed 2.5 m. As a whole, this problem is of particular interest due to its complex /hydro-geomechanic/ nature. /Mironenko, V.A. and Shestakov, V.M., 1974/

References

Mironenko, V.A. and Shestakov, V.M., 1974, Principles of hydrogeomechanics, Nedra Publ., Moscow, 295 p. / in Russian/.

Publication n°121 of the International Association of Hydrological Sciences
Proceedings of the Anaheim Symposium, December 1976

ENGINEERING GEOLOGICAL PROBLEMS OF ANTHROPOGENE SURFACE SUBSIDENCE OF OIL AND GAS FIELDS IN WEST SIBERIA

Yu. F. Zakharov
Tyumen Branch of PNIIIS, Tyumen

Exploitation of oil fields in West Siberia is performed by keeping up a reservoir pressure in producing horizons by means of flooding within or outside of the producing limits of the fields. Water for injection is mainly taken out of shallow Apt-Conomanien or other aquifers. It is planned to extract some billions of m^3 (cubic meters) of underground water. Such a great amount of highly-concentrated and long-term withdrawal will end in a considerable decline of reservoir pressure in the aquifers causing the squeezing out of water and compaction of their argillaceous component. Irreversible deformation of argillaceous rocks results in warping of overlying layers or in subsidence of a ground surface over the area of withdrawal. Subsidence is speeded up by water transport of a significant amount of mineral particles out of the producing aquifers. Content of particles varies from 1 to 7,000 mg per litre of extracted water. Local subsidence of a sedimentary cover above the water-yielding beds and oil fields in West Siberia results in a water table rise commensurable with local subsidence or in flooding of the surficial deposits serving as foundations of structures or communication lines. At the majority of fields in West Siberia a ground-water table occurs at 0.5-2.0 m depth; thus subsidence may result in complete inundation of their lowered areas. Inferior foundation properties of West Siberian soils are even poorer when flooded; deformation and strength properties are lower, susceptibility for thixotropic softening rises; and the capacity for frosty upswell becomes apparent. Surface subsidence of the fields within a zone of permafrost soil will result in accumulation of temporary melt-waters or meteoric waters. The thermal effect of the ponded water may result in degradation of persistent frozen ground and in the deformation of those structures which were erected and depend on the conservation of frozen rocks at their foundations. Flooding speeds up corrosion and collapse of metal or reinforced concrete parts of structures which settle in the ground. Surface subsidence alters (usually for the worse) a number of geological processes, in the first place speeding up river-bank reworking and erosion of pipe lines trenches, and may cause resumption of fluvial drainage along numerous dead channels in the wide valleys of West Siberian rivers.

Forecasting of surface subsidence and accompanying flooding and other phenomena at the oil fields and water intakes areas in West Siberia is impeded by the short time of their operation, its high rate, and impetuous development of production forces in an extractive industry. Some parameters necessary for forecasting subsidence, with gasification of the Apt-Cenomanion aquifer as a possibility, are being studied. Based on these forecasts, the possibility of intensive remedial measures are suggested in the planning or operation of new fields—the putting of many structures of the fields on bases or abnormal hydroinsulation of their bottom parts, the increase of height of road embankments and the flattening of their slopes, and the reducing or, in highly dangerous cases (Samotlorskij field), the stopping of using Apt-Cenomanien waters for maintaining reservoir pressure. Especially intensive exploitation is foreseen for small fields in order to extract all the oil and gas before reaching the dangerous stage of subsidence.